FORESTS AND THEIR INTERACTIONS WITH THE ENVIRONMENT

EDITED BY: Sofia Valenzuela, Sanushka Naidoo and Amy Brunner

PUBLISHED IN: Frontiers in Plant Science and Frontiers in Microbiology

frontiers Research Topics

frontiers

ISSN 1664-8714
ISBN 978-2-88974-202-8
DOI 10.3389/978-2-88974-202-8

About Frontiers

Frontiers is more than just an open-access publisher of scholarly articles: it is a pioneering approach to the world of academia, radically improving the way scholarly research is managed. The grand vision of Frontiers is a world where all people have an equal opportunity to seek, share and generate knowledge. Frontiers provides immediate and permanent online open access to all its publications, but this alone is not enough to realize our grand goals.

Frontiers Journal Series

The Frontiers Journal Series is a multi-tier and interdisciplinary set of open-access, online journals, promising a paradigm shift from the current review, selection and dissemination processes in academic publishing. All Frontiers journals are driven by researchers for researchers; therefore, they constitute a service to the scholarly community. At the same time, the Frontiers Journal Series operates on a revolutionary invention, the tiered publishing system, initially addressing specific communities of scholars, and gradually climbing up to broader public understanding, thus serving the interests of the lay society, too.

Dedication to Quality

Each Frontiers article is a landmark of the highest quality, thanks to genuinely collaborative interactions between authors and review editors, who include some of the world's best academicians. Research must be certified by peers before entering a stream of knowledge that may eventually reach the public - and shape society; therefore, Frontiers only applies the most rigorous and unbiased reviews.
Frontiers revolutionizes research publishing by freely delivering the most outstanding research, evaluated with no bias from both the academic and social point of view. By applying the most advanced information technologies, Frontiers is catapulting scholarly publishing into a new generation.

What are Frontiers Research Topics?

Frontiers Research Topics are very popular trademarks of the Frontiers Journals Series: they are collections of at least ten articles, all centered on a particular subject. With their unique mix of varied contributions from Original Research to Review Articles, Frontiers Research Topics unify the most influential researchers, the latest key findings and historical advances in a hot research area! Find out more on how to host your own Frontiers Research Topic or contribute to one as an author by contacting the Frontiers Editorial Office: frontiersin.org/about/contact

FORESTS AND THEIR INTERACTIONS WITH THE ENVIRONMENT

Topic Editors:
Sofia Valenzuela, University of Concepcion, Chile
Sanushka Naidoo, University of Pretoria, South Africa
Amy Brunner, Virginia Tech, United States

Citation: Valenzuela, S., Naidoo, S., Brunner, A., eds. (2022). Forests and Their Interactions With the Environment. Lausanne: Frontiers Media SA.
doi: 10.3389/978-2-88974-202-8

Table of Contents

frontiers in Plant Science

ORIGINAL RESEARCH
published: 27 May 2020
doi: 10.3389/fpls.2020.00632

Identification of Quantitative Trait Loci for Altitude Adaptation of Tree Leaf Shape With *Populus szechuanica* in the Qinghai-Tibetan Plateau

Meixia Ye[1,2], *Xuli Zhu*[1,2], *Pan Gao*[1,2], *Libo Jiang*[1,2] *and Rongling Wu*[1,2,3]*

[1] *Beijing Advanced Innovation Center for Tree Breeding by Molecular Design, Beijing Forestry University, Beijing, China,*
[2] *Center for Computational Biology, College of Biological Sciences and Technology, Beijing Forestry University, Beijing, China,*
[3] *Center for Statistical Genetics, The Pennsylvania State University, Hershey, PA, United States*

As an important functional organ of plants, leaves alter their shapes in response to a changing environment. The variation of leaf shape has long been an important evolutionary and developmental force in plants. Despite an increasing amount of investigations into the genetic controls of leaf morphology, few have systematically studied the genetic architecture controlling shape differences among distinct altitudes. Altitude denotes a comprehensive complex of environmental factors affecting plant growth in many aspects, *e.g.*, UV-light radiation, temperature, and humidity. To reveal how plants alter ecological adaptation to altitude through genes, we used *Populus szechuanica* var. *tibetica* growing on the Qinghai-Tibetan plateau. F_{ST} between the low- and high- altitude population was 0.00748, Q_{ST} for leaf width, length and area were 0.00924, 0.1108, 0.00964 respectively. With the Elliptic Fourier-based morphometric model, association study of leaf shape was allowed, the dissection of the pleiotropic expression of genes mediating altitude-derived leaf shape variation was performed. For high and low altitudes, 130 and 131 significant single-nucleotide polymorphisms (SNPs) were identified. QTLs that affected leaf axis length and leaf width were expressed in both-altitude population, while QTLs regulating "leaf tip" and "leaf base" were expressed in low-altitude population. *Pkinase and PRR2* were common significant genes in both types of populations. Auxin-related and differentiation-related genes included *PIN1, CDK-like*, and *CAK1AT* at high altitude, whereas they included *NAP5, PIN-LIKES*, and *SCL1* at low altitude. The presence of *Stress-antifung* gene, *CIPK3* and *CRPK1* in high-altitude population suggested an interaction between genes and harsh environment in mediating leaf shape, while the senescence repression-related genes (*EIN2* and *JMJ18*) and *JMT* in jasmonic acid pathway in low-altitude population suggested their crucial roles in ecological adaptability. These data provide new information that strengthens the understanding of genetic control with respect to leaf shape and constitute an entirely novel perspective regarding leaf adaptation and development in plants.

Keywords: leaf shape, altitude, QTL, *Populus szechuanica*, Qinghai-Tibetan Plateau

OPEN ACCESS

Edited by:
Amy Brunner,
Virginia Tech, United States

Reviewed by:
Evandro Novaes,
Universidade Federal de Lavras, Brazil
Fangmin Cheng,
Zhejiang University, China

***Correspondence:**
Rongling Wu
rwu@bjfu.edu.cn

Specialty section:
This article was submitted to Plant Abiotic Stress, a section of the journal Frontiers in Plant Science

Received: *18 December 2019*
Accepted: *24 April 2020*
Published: *27 May 2020*

Citation:
Ye M, Zhu X, Gao P, Jiang L and Wu R (2020) Identification of Quantitative Trait Loci for Altitude Adaptation of Tree Leaf Shape With Populus szechuanica in the Qinghai-Tibetan Plateau. Front. Plant Sci. 11:632. doi: 10.3389/fpls.2020.00632

INTRODUCTION

Leaves are the site of plant photosynthesis and are important for both water balance and temperature adjustment. Considering these essential functions, leaf shape is an important factor by which plants maximize their survival (Nicotra et al., 2008; Moon and Hake, 2011). In response to varying geography and climate, plant genomes must undergo modification to develop favorable leaf shapes (Nicotra et al., 2011). As an influential environmental factor, altitude can significantly alter variation of plants' ecological adaptability and result in the change in leaf morphology (Milla and Reich, 2011), because it reflects a complex combination of factors (e.g., temperature, water, sunlight, and soil fertility). It has been widely accepted that altitude-determined morphogenetics are of great ecological and evolutionary importance for studying mechanisms of shape variation and biological adaptability (Klingenberg, 2010).

To compare the effects of altitude, using the oak metapopulation, Firmat et al. (2017) recently investigated the evolutionary, genetic, and environmental components of the timing of leaf unfolding and senescence along an elevation gradient. In seven successive elevation gradients on the Qinghai-Tibetan plateau, Lu (2017) revealed relationships among leaf characteristics in *Halenia elliptica*. The study revealed gradual alteration of leaf shape, which was accompanied by changes in photosynthetic pigment content, osmotic adjustment, and the anti-oxidation system, suggesting that an active stress response caused leaf shape alteration. Along global elevational gradients, Midolo et al. (2019) quantified changes in seven morpho-ecophysiological leaf traits in 109 plant species on four continents. Although altitude is presumed to influence leaf shape variation, the genetic mechanism mediating the effect of altitude on leaf shape has been elusive. Using molecular approaches, the respective leaf shape genes *ANGUSTIFOLIA* (*AN*), *ROTUNDIFOLIA3* (*ROT3*), and *REDUCED COMPLEXITY* (*RCO*) were revealed to regulate leaf width, length, and affect developing leaflets by repressing growth at their flanks respectively (Tsukaya, 2006; Bai et al., 2013; Vlad et al., 2014; Koyama et al., 2017). A module of auxin-*PIN1-CUC2* was discovered to affect function in patterning leaf margin (Bilsborough et al., 2011). However, the studies characterizing genes responsible for shape morphology have identified their roles in the context of development; thus, relationships between shape genes and elevation-caused ecological changes have not yet been established.

As one of the largest plateaus worldwide, the Qinghai-Tibetan plateau is a cradle of the planet's natural wealth on the earth. The high altitude of the Qinghai-Tibetan plateau has low temperatures, high UV radiation, and poor-quality soils, which combine to provide a unique natural laboratory for studying adaptability and evolution (Li and Fang, 1999). Trees growing on the Qinghai-Tibetan plateau face a variety of abiotic stresses; therefore, it is likely that they have been subjected to a series of adaptive or evolutionary changes. Genotypes are presumed to differ with altitude, including differences in leaf morphology. When performing genetic analyses, leaf shape is regarded as a quantitative phenotypic trait (Klingenberg, 2010). For quantitative genetic purposes, the characterization of leaf morphological variations at different altitudes is important for understanding a plant's long-term strategies for adaptation to environmental pressure (Miles and Ricklefs, 1994). The complex combination of climatic factors, as well as the extensive geographical diversity at different elevations, could have significant potential for the development of inheritable leaf morphological variation. Therefore, the association study was performed using natural populations from different altitudes in this study; this approach offers a compelling opportunity to dissect the genetic control of altitudinal expression on leaf morphology. This work can aid in elucidating connections among shape gene knowledge, ecological adaptation, and evolution.

For mapping leaf shape QTLs, leaf width, length, and angle were added to the conventional statistical model (Tian et al., 2011). To capture precise leaf shape information, leaf outlines were used based on the geometric morphometrics technique (Bookstein, 1991; Slice, 2007). The Procrustes alignment method is an accurate and lossless shape information method that filters out positional, sized, and rotational effects on leaf shape; it can fully encode all information that cumulatively influences leaf shape contouring. The radius-centroid-contour method uses the length curve of the radius from leaf centroid to all outline landmarks to obtain the minute contours of shape (Fu et al., 2013). A method uses the Elliptic Fourier (EF) series to enable accurate measurement of an object's outline had been developed recently, which has the inherent advantage of using sparse parameters to describe shape (Neto et al., 2006; Bo et al., 2014). The combination of genetic mapping and EF-based geometric morphometrics supported the development of "shape mapping," which led to the construction of *hp*QTL, a computational platform for mapping heterophylly QTL (Sun et al., 2018). The development of "shape mapping" has enabled genetic analysis of the effect of altitude on leaf shape.

To study the altitude-specific variation pattern of leaf morphology, this study used leaves from *Populus szechuanica var. tibetica*, a common indigenous tree species naturally distributed in the Qinghai-Tibetan plateau of China. The large elevation distribution on the Qinghai-Tibetan Plateau (ranging from 1100 to 4500 m, Shen et al., 2014), coupled with the distribution of *P. szechuanica* throughout, makes this species a useful model for studying ecological adaptability and leaf shape evolution. The objectives of this study were to (1) use the EF-based shape model to identify QTLs controlling the overall shape differences between low and high altitudes; (2) determine how altitude influences the genetic factors underlying leaf shape; and (3) establish a link between altitude and the expression of leaf shape QTLs. By analyzing leaf shape QTLs of *P. szechuanica* at different elevations, our work identified key QTLs that relate to leaf shape variation and ecological evolution; the results offer new opportunities and novel instrumentation for dissecting complex traits from the perspective of ecological evolutionary developmental biology.

MATERIALS AND METHODS

Mapping Population

Populus szechuanica, one of the *Cathay poplar* group of species in the genus *Populus*, is primarily distributed throughout the Qinghai-Tibetan Plateau, as well as the Sichuan and Yunnan Provinces in China. Leaves from trees representing different elevational populations of *P. szechuanica* were sampled in the Sejila mountain range, a provenance site in the Nyingchi prefecture of the Tibet Autonomous Region. A total of 119 individual trees from high altitude (2600–3090 m above sea level) and 141 individual trees from low altitude (2000–2300 m above sea level), as shown in **Supplementary Figure S1**, were sampled to construct the mapping population. In July 2012, 5–10 branches with vigorous growth and thick wood were cut from each tree and were stored in sand. After 2 years of extensive propagation in a common nursery (Dayi county, Sichuan Province), new cuttings of uniform length and diameter were planted in a common garden experiment in 2015. A mean of ≥10 clonal replicates were made for each tree from each population. This created a clonal line for each of the trees.

Phenotyping and Genotyping

For each clone from each original tree, one or two from each of the upper, middle, and lower sections of the crown of each clonal tree were sampled to measure leaf shapes. In total, 5,819 leaves from lines of the high-altitude group and 10,628 leaves from lines of the low-altitude group were collected and photographed to analyze their shapes. Digital images were taken of each leaf using a pose-fixed camera. The resulting RGB pictures of the leaves were converted to binary shape images, with white color representing the leaf area and black color denoting the image. Using a shape alignment method described by Fu et al. (2013), differences in the location and rotation of leaf position in the images, as well as differences in the effect scale due to leaf size, were removed using an orthogonal Procrustes method (Gower and Dijksterhuis, 2004). Differences in the shapes of leaves from clones in a given line could occur due to variations in the micro-environment (i.e., differences within nursery blocks) or due to heterophylly, which could cause leaves from different sections of the tree to have different shapes (Winn, 1999). To adjust for the potential influences of these factors, leaves from all sections of the clones in each line were used to derive an average shape by calculating the arithmetic average of each coordinate, along with several contour landmarks. The appropriate number of landmarks was determined using the Akaike Information Criterion for all 260 average shapes from plants of both altitude groups. The use of 70 landmarks had the lowest Akaike Information Criterion value. Therefore, coordinates of 70 landmarks along the boundary of each average leaf shape for each line, which had equal radii, were used as the phenotype for further mapping of leaf shape.

For all 260 lines, a genome-wide panel of single-nucleotide polymorphisms (SNPs) was sequenced by re-sequencing technology using an Illumina Hiseq^{TM}2000 platform. Each sample was deep sequenced to approximately 20-fold to generate a total of 13.71 billion raw paired-end reads. After removal of low-quality reads by filtering, the remaining clean reads were aligned against a reference genome of *Populus trichocarpa*,[1] deriving a total of approximately 12.76 million high-quality SNPs. After sequencing and the removal of low-quality sequence, workflow consisting of 3 major steps was employed: mapping, improvement and variant calling. For mapping, BWA-0.7.5[2] was firstly used to prepare the Burrows Wheeler Transform index for the reference using the index command, the MEM mode was applied to align reads to genome, with *-R* paramter designating the reference. SAMTOOLS-1.9 version[3] used command of fixmate and sort to order the mapped sequence into coordinate order within BAM file. For improvement step, all BAM files from each sample were merged and indexed respectively using the merge and index function. For the variant calling step, bcftools mpileup command was used to convert BAM into BCF file, which contained all genomic positions, using *-Ob -f -vmO z* parameter. Variant filtration was performed using bcftools filter to derive the final VCF file to recode the genotype at genome-wide level, parameter of *-s LOWQUAL -i '%QUAL>20'* were set to seperate true SNPs from error SNPs. Using Vcftools (Danecek et al., 2011), SNPs with a sequencing depth greater than 12, *p*-value of Hardy Weinberg equilibrium test greater than 0.05, minor allele frequency greater than 5%, and a missing rate and heterozygosity less than 10% were screened for further association studies. These criteria were satisfied by a set of 81,839 SNPs. For natural population, some SNPs segregated into 2 genotypes, still there were SNPs segregated into 3 genotypes, but their segregation ratio do not necessarily follow 1:1 or 1:2:1. Nonetheless, we use "testcross" and "intercross" to refer to these segregation types, but without considering the segregation ratio. SNPs of intercross type had 2 homozygous genotypes and 1 heterozygous genotype in natural population, while the testcross SNPs had 1 homozygous and 1 heterozygous genotype. All SNPs included 53,094 intercross markers and 28,745 testcross type of markers. The genotyping data in a format of VCF file were submitted to the European Variation Archive,[4] with a project ID of PRJEB36028.

Population Structure and Calculation of F_{ST} and Q_{ST}

FastStructure (Raj et al., 2014) was used to infer population structure from the large SNP dataset. Combining individual genotypes from both high- and low- altitude, this software identified $K = 2$ as the optimal group number for the whole population, as likelihood peak can be seen for $K = 2$ from **Supplementary Figure S2A**. All 260 genotypes can be divided into 2 subgroups. The high-altitude contained 97 and 22 genotypes, forming sub-population 1 and 2, the low-altitude population contailed 9 and 132 genotypes for sub-population 1 and 2 (**Supplementary Figure S2B**). Therefore, a total of 106

[1] https://ftp.ncbi.nlm.nih.gov/genomes/refseq/plant/Populus_trichocarpa/latest_assembly_versions/GCF_000002775.4_Pop_tri_v3/GCF_000002775.4_Pop_tri_v3_genomic.fna.gz

[2] http://bio-bwa.sourceforge.net/bwa.shtml

[3] http://www.htslib.org

[4] https://www.ebi.ac.uk/eva

and 154 genotypes constituted the "real high altitude population" and "real low altitude population," with the high- and low-altitude provenance occupying the ratio of 97/106 and 132/154. Further association study of shape was based on the two adjusted sub-populations.

With the normalized morphological shapes, we derived the detailed shape trait of leaf length, leaf width and leaf area using the home-made R script. Analysis of variance (ANOVA) were performed to calculate the within-deme variance (σ^2_{GW}) and between-deme variance (σ^2_{GB}) for each trait. Equation of $Q_{ST} = \sigma^2_{GB}/(\sigma^2_{GB} + 2\sigma^2_{GB})$ was employed to Q_{ST} values with the 3 traits (Raeymaekers et al., 2007). From all 81,839 SNPs, we selected 68867 neutral SNPs using their genomic position information, comprising 53063 SNPs locating at intergenic DNA sequence, 15575 SNPs residing at intron region, and 229 synonymous SNPs at exon region. Based on neutral SNPs, F_{ST} were calculated using the diveRsity package with R language (Keen et al., 2013).

ANOVA Analysis of Shape Traits

To test the significance effect of altitude, ANOVA analysis was performed using descriptor of shape, e.g., leaf length, leaf width and leaf area. For each of the trait, the phenotypic value for leaf l of genotype i from the altitude j from tree position k under block m is expressed as $y_{l|ijkm} = \mu + \alpha_i + g_{j|i} + p_k + \beta_m + GPI_{jk|i} + API_{ik} + \varepsilon_{ijklm\cdot}$ α_i is the ith altitude effect, $g_{j|i}$ is the genetic effect due to the jth progeny nested in altitude i, p_k is the position effect due to the kth position on the tree from upper to lower, β_m is the block effect due to the mth block within the filed of common garden. $GPI_{jk|i}$ is the interaction effect between the jth genotype and kth position given the ith altitude. API_{ik} is the interaction effect between the ith altitude and kth position. $\varepsilon_{ijklm\cdot}$is the residual. The ANOVA analysis was performed using *aov* function in R language.

Framework of the Shape Association

The overall population was presumed to contain n_H individuals from high altitude and n_L individuals from low altitude, all of which were genotyped for a panel of genome-wide SNPs. Based on geometric morphometrics, the x- and y-coordinate sequences of shape were used to represent the phenotypic data. The average shape for each line was calculated. For each average leaf, a total set of K landmarks were sampled clockwise at equal angle intervals along the margin. Let $(x_{Hi}, y_{Hi}) = (x_{Hi}(1), y_{Hi}(1); x_{Hi}(2), y_{Hi}(2); \ldots; x_{Hi}(K), y_{Hi}(K))$ denote the sequence of x- and y-coordinates of K landmarks for individual i in the high-altitude population. Let $(x_{Li}, y_{Li}) = (x_{Li}(1), y_{Li}(1); x_{Li}(2), y_{Li}(2); \ldots; x_{Li}(K), y_{Li}(K))$ denote x- and y-coordinates of K landmarks for individual i from the low-altitude population. For a given QTL carrying J genotypes, *e.g., QQ*, *qq*, and *Qq*, the set of landmarks enabled the construction of the likelihood using multivariate normal distribution. By referring to geometric methods (Bo et al., 2014), mean vector within density probability of multivariate normal distribution, equivalent to the shape descriptor, was modeled by Elliptic Fourier function, the order with which can be determined by an AIC criterion. The covariance matrix within the multivariate normal distribution was modeled by using an autoregressive model to structure the spatial (co)variance among all K outline landmarks (Zhao et al., 2005). In such framework, H_0 was proposed as no shape difference existed between genotypes, H_1 was proposed as the opposite. The test statistic for this hypothesis was calculated as the log-likelihood ratio (LR) of the null against the alternative model. The LR threshold was determined by an empirical approach based on 1,000 replications of permutation tests to derive significant SNPs (Churchill and Doerge, 1994). The model was implemented using R language, the code has been attached as an **Supplementary File S1** of **Presentation 1.ZIP**. The association of leaf area was performed using TASSEL software (Zhang et al., 2010).

RESULTS

Shape Phenotype

While it differed from the direct collection of leaves from trees in their natural growing environments, the design of a common garden plantation ensured a uniform environment and consistent management of plant growth. As a result of the homogeneous growth conditions in the plantation nursery, leaf shape diversity within the sample population reflected the intrinsic effect of genetic background on leaf shape. After calculation of average leaf shape, all Procrustes-aligned shapes (**Figures 1A,B**) had consistent orientations in both high-altitude and low-altitude populations. Leaf shape centroids with all 260 lines overlapped to the origin of the coordinate system. The absence of extraordinarily sized leaf shapes indicated a clear effect of Procrustes alignment in leaf shape association.

Among all samples, the average leaf shape varied from ovate-orbicular to ovate-lanceolate. As shown in **Figures 1A,B**, leaf shape variation for *P. szechuanica* was precisely confirmed based on leaf axis length, leaf width, length to width ratio, and the region where the broadest region of the leaf was located. For leaf axis length specifically, longer leaf shapes typically possessed a less-broad blade base. The broadest region of most leaves was approximately 1/4–1/3 of the length from the blade base. Relatively speaking, high-altitude plants yielded a slender and slightly narrowed blade base, whereas shorter leaves within the low-altitude population had greater width in the middle-lower section of the leaf shape (**Figure 1C**). Statistical analysis revealed that high-altitude leaves showed a leaf width variance of 0.00906 and leaf axis length variance of 0.000739. Low-altitude leaves showed a 1.386-fold change in width variance, compared with that from high-altitude leaves; the on-axis length variance was similar (0.000833).

ANOVA of Variation on Quantitative Morphology of Leaf

Outline points along leaf boundary for describing leaf morphology involve complex statistical issue in dissecting its variance source, therefore, we switch to use other descriptor of shape, e.g., leaf length, leaf width, leaf area. To test the significance effect of altitude, *F-value* (**Table 1**) for altitude effect was 105.834, 107.570, and 117.366 respectively for trait of leaf width, leaf length and leaf area, all of which had reached to the

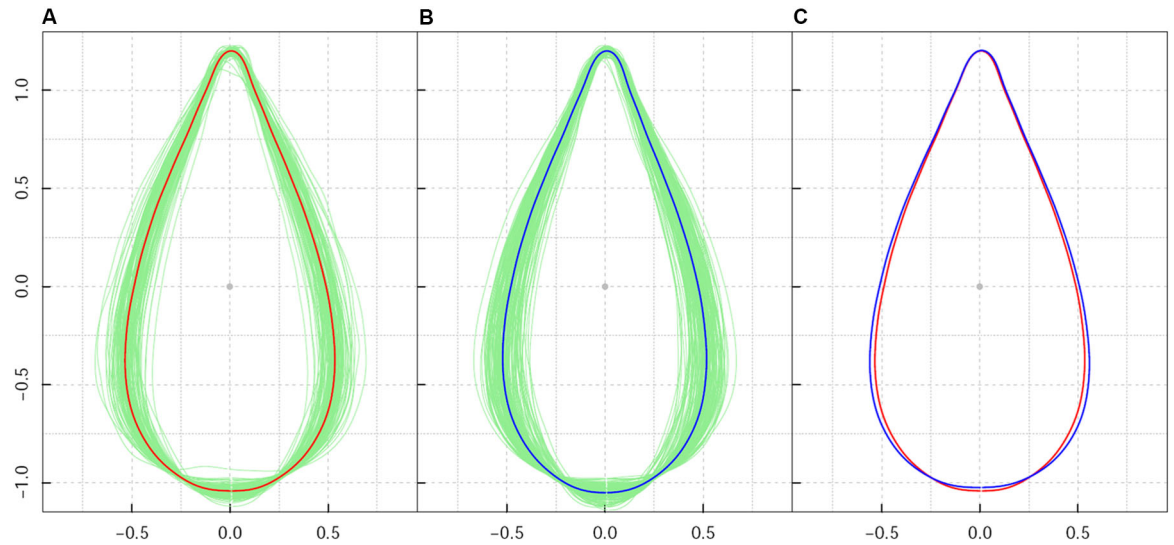

FIGURE 1 | Shape pattern of *Populus szechuanica* var. *tibetica* leaves sampled from high and low altitudes in the Qinghai-Tibetan plateau. **(A)** Denotes the mean shape of all 119 leaves from high-altitude populations; **(B)** denotes the mean shape of all 141 leaves from low-altitude populations; **(C)** shows the comparison of the mean shape of leaves at the population level. Both shapes from high- and low-altitude populations were corrected by Procrustes alignment.

extremely significant level. However, the statistics of *F-value* for altitude were smaller than that of leaf position of growth on the tree, suggesting the physiologically determined heterophylly of plant had larger effect than that caused by altitude.

Also, to test the overall genotype effect on leaf shape respectively nested in different altitude, the integrated model for dissecting the variance component resulted in an extremely significance of genotypic effect. Besides the similar result of significance with heterophylly effect, we observed that block had non-significant effect on shape, suggesting the clones for distinct genotype in the population didn't show a significant difference on shape development. Importantly, the 3 leaf traits had enlarged *F-value* of interaction effect between altitude and leaf position, than that of genotype-by-position, indicating the potential necessity to explore the force of high-and low- altitude in evolving ecological adaptation.

TABLE 1 | Analysis of variance for altitude and genotype effects on leaf shape.

Trait	Source	*F*	*p-value*
Leaf width	Altitude	105.834	<2e-16
	Genotype	52.807	<2e-16
	Block	0.815	0.367
	Leaf position	150.442	<2e-16
	Genotype × Position	0.987	0.617
	Altitude × Position	16.300	4.51e-16
Leaf length	Altitude	107.570	<2e-16
	Genotype	33.042	<2e-16
	Block	0.194	0.6596
	Leaf position	159.966	<2e-16
	Genotype × Position	1.060	0.0838
	Altitude × Position	14.514	3.24e-14
Leaf area	Altitude	117.366	<2e-16
	Genotype	46.323	<2e-16
	Block	0.217	0.6412
	Leaf position	141.837	<2e-16
	Genotype × Position	1.078	0.0373
	Altitude × Position	12.523	3.71e-12

F_{ST} Value, Q_{ST} Value and Their Comparison

Using the neutral SNPs from the genome-wide SNP panel, F_{ST} value for genetic divergence was calculated. F_{ST} result between the high- and low- altitude population was 0.007484551, showing a very low degree of genetic divergence due to the altitude (Pujol et al., 2008). Using F_{ST} value, we further derived a value of 33.152 with *Nm,* using the equation provided by Wright (1951) that *Nm = (1 - Fst)/(4Fst)*. This high measure had accounted for the important role of gene flow in replacing genetic drift for preventing population divergence. The combination of high gene flow and the low value of F_{ST} suggested that, altitude had not granted a geographical separation for population divergence along the mountain. Q_{ST} value for leaf width, leaf length and leaf area were calculated as 0.009243, 0.0110829, 0.009649 respectively. All Q_{ST} with the three traits were larger than the F_{ST} value, suggesting there might exist the local adaptation between the two sub-populations to cause the shape difference of leaf.

Mapping Shape QTLs in High- and Low-Altitude Populations

To determine the optimal number of EF harmonics, the goodness-of-fit of EF was analyzed for each harmonic order, ranging from 0 to 6. As shown in **Supplementary Figure S3**, with increased harmonic order, the superimposed ellipses improved

the goodness-of-fit with leaf shape. Harmonics 1–6 explained 53.7, 91.3, 94.9, 97.2, 98.4, and 98.8% of leaf shape information, respectively. Specifically, the 97.2% of total leaf shape variation explained by harmonic 4 exceeded 95%. Therefore, harmonic 4 was the optimal order to approach leaf shape vectors, as it was capable of providing sparse parameters for QTL mapping, laying a solid foundation for EF-based shape mapping.

Associations between each SNP and all average shapes provided a plot of log-likelihood ratios, reflecting the significance of association degree (**Figure 2A**). As a result of the segregation of different types with SNPs, we determined the threshold values for testcross and intercross SNPs by using a permutation test (Churchill and Doerge, 1994). One hundred and thirty SNPs were determined to significantly regulate leaf shape variation in the high-altitude population; these were sporadically distributed throughout the genome. Nine of 54 testcross SNPs and 28 of 76 intercross SNPs were annotated to functional genes. **Supplementary Table S1** lists detailed information regarding these SNPs, including their chromosomal position, segregation type, and functional annotation. Of the annotated SNPs, 6 highly linked SNPs that were collectively located at *LEUCINE RICH REPEAT* (*LRR*) *KINASE* genes on chromosome 4 were found to show association peaks. From chromosome 15, the SNPs within the *PIN-FORMED* (*PIN1*) gene and *CYCLIN-DEPENDENT KINASE* (*CDK*)-*LIKE* gene were found to be significant. Similar to the identification of the *CDK-LIKE* gene, one SNP

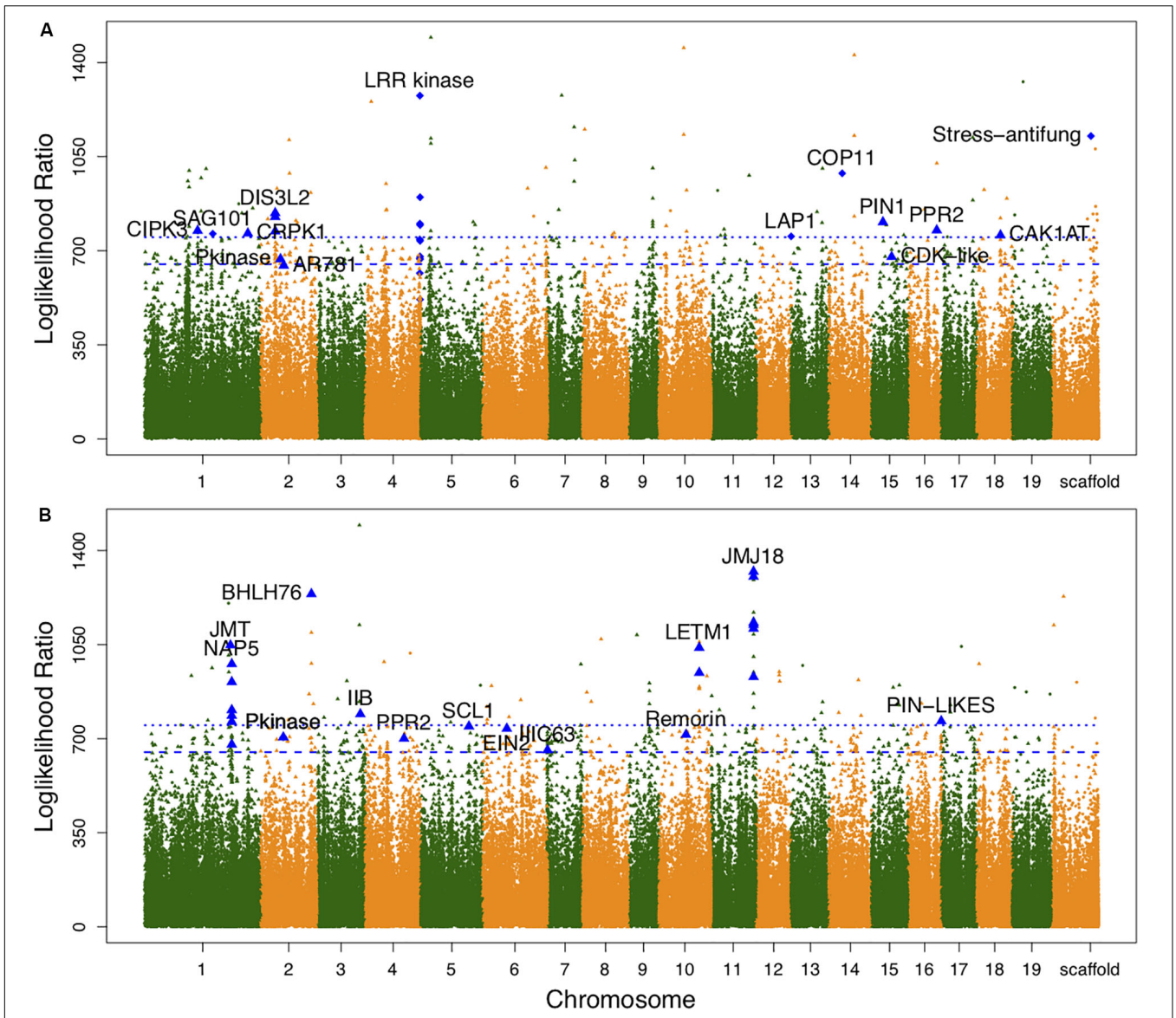

FIGURE 2 | Manhattan plots of leaf shape associations for high- and low-altitude populations. **(A,B)** Are results for high- and low-altitude populations, respectively. Diamond-shaped dots denote the testcross SNPs and triangle-shaped dots represent intercross SNPs. The broken line and dotted line indicate threshold values for testcross and intercross SNPs, respectively, which were determined by 1000 replicates of permutation tests.

within the *CDK-ACTIVATING KINASE* gene (*CAK1AT*) was mapped from chromosome 18. From chromosome 1, *CBL-INTERACTING PROTEIN KINASE 3* (CIPK3) and *COLD RESPONSIVE PROTEIN KINASE 1* (CRPK1) were identified. One significant SNP on chromosome 14 and on the scaffold were annotated as *COP11* and "Stress-antifung."

For the low-altitude population, the log-likelihood ratio plot showed 131 significant SNPs (**Figure 2B**). Based on their functional annotations (**Supplementary Table S2**), we determined common annotations of *Pkinase* and *PPR2*. Although the genomic positions of *PPR2* and *LETM1* differed between the high- and low-altitude populations, the co-occurrence of these genes in both populations suggests that they have similar roles in regulating leaf shape. For clustered distribution of significant SNPs at chromosomes 1 and 11, we identified *NON-INTRINSIC ABC PROTEIN 5 (NAP5)*, *JUMOJI DOMAIN-CONTAINING PROTEIN 18* (*JMJ18)*, and *JASMONIC ACID CARBOXYL METHYLTRANSFERASE* (*JMT)*. *BHLH76*, *IIB,* and *IIIC63* belonging to transcription factor genes also regulated leaf morphology at low altitude. The organ differentiation-related gene *SCARECROW-LIKE1* (*SCL1)*, auxin transport gene *PIN-LIKES*, and *ETHYLENE-INSENSITIVE PROTEIN* (*EIN2)* were also found to include significant SNPs. The large difference in annotation results revealed different genetic architecture controlling leaf morphology between the two altitudes.

Association of Leaf Area and Heritability

We also calculated the shape area by using the normalized leaf shapes among all 260 lines. The *Q+K* model for association analysis of leaf area for the combined population resulted in 279 significant SNPs. As shown in **Figure 3**, 130 out of them were annotated to 78 different genes. As compared to genes discovered in result of shape association, 5 genes overlaped with the two sets, e.g., the *SAG101*, *LRR kinase, EIN2*, *JMJ18*, *CAK1AT,* suggesting the overlapping role of shape in affecting area. Nevertheless, the rest genes labeled in the manhattan plot of area trait can further emphasize the other physiological regulation in determining leaf area.

From the variance component dissection with the association model, for significant SNPs, the cumulative heritability for leaf area was 6.916%. The maximum heritability value of single SNP was observed on 18786027 *bp* of chromosome 4, explaining 6.652% variance of the area variation. Similarly, the broad-sense heritability for leaf width and leaf length was 0.263 and 18.38%.

Types of QTL Expression

In high altitude population, by calculating leaf width, length, and area, we found 130 SNPs in the high-altitude population that showed an average change of 9.18% based on width between allelic genotypes; however, an allelic average change of 0.77% was revealed based on the axis of leaf length. A correlation of 0.9496 was identified between leaf area and leaf width—this indicated that the longitudinal expansion of leaves occurred allometrically against the latitudinal direction. For the same population, we found two different types of variation patterns with all 130 significant SNPs (**Figures 4A,B**); these showed that leaf shape differences were narrow vs. broad, and long-narrow vs. short-broad. For example, in comparison with *AA* and *AG*, the *GG* genotype at the SNP within the *PIN1* gene displayed the longest leaf axis and the narrowest leaf width (**Figure 4A**). The *TT*, *TG*, and *GG* genotypes with SNPs located at *CDK-like* genes only showed differences in width (**Figure 4B**). We classified these as "leaf length" and "leaf width" QTLs.

By dissecting shape pattern, along with the aforementioned "leaf length" QTL and "leaf width" QTL, two additional types of leaf shape divergence patterns were revealed in the low-altitude population (**Figures 4C,D**). Using the SNP at 7,547,290 bp of chromosome 1 as an example, with the segregating genotypes of

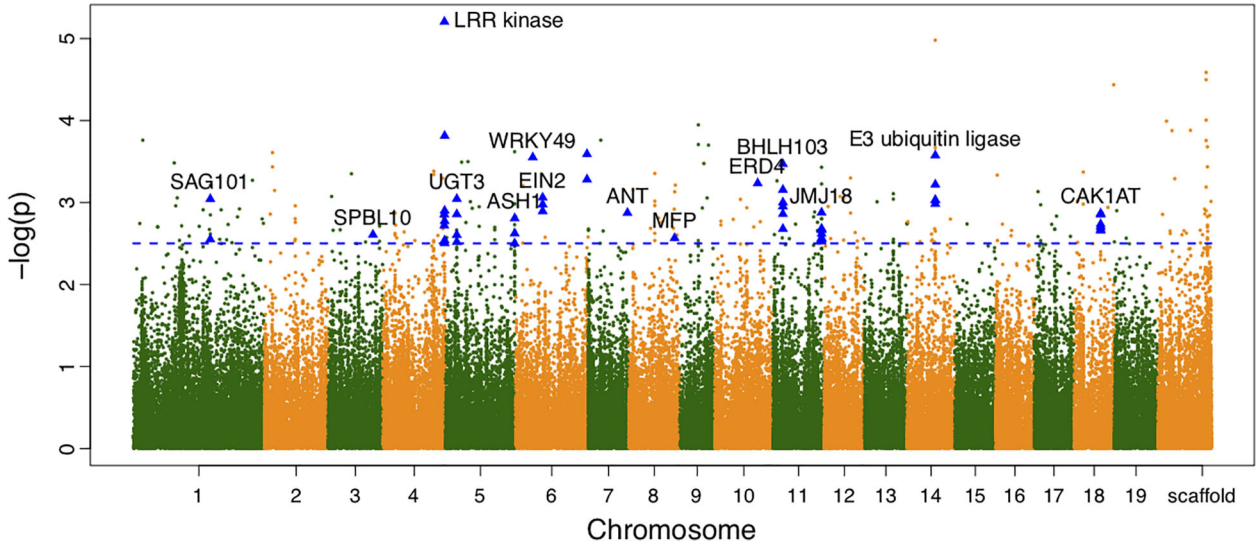

FIGURE 3 | Manhattan plots of leaf area associations for the combined population. Triangle-shaped dots represent significant SNPs within the functional important genes.

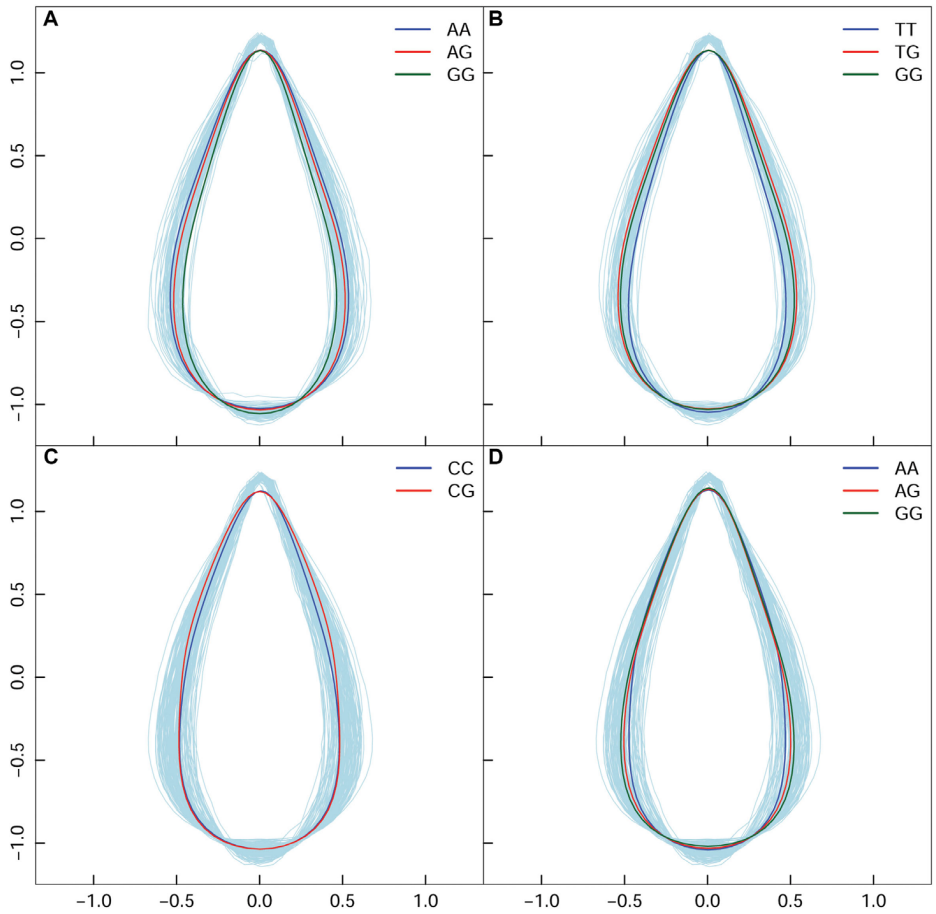

FIGURE 4 | Four QTL shape patterns in both high- and low-altitude populations. **(A,B)** Represent the high-altitude-specific "leaf length" and "leaf width" QTL. **(C,D)** Represent the low-altitude-specific "blade tip" and "blade base" QTL.

CC and *CG*, both were found to have an identical shape feature at the blade base, and an equal length of leaf axis. Nonetheless, *CG* showed an enlarged margin edge at the middle-upper section of the leaf (**Figure 4C**); therefore, the expression of the two genotypes resulted in the "blade tip" QTL. Because genotypes with the "tip" QTL also showed an identical length axis on the leaves, segregating genotypes shared the position where the broadest blade region was located. Traditional methods cannot identify this type of leaf shape QTL. For the intercross QTL peak within chromosome 16, the closely linked SNP collection that included the positions of 1,282,251, 1,282,300, 1,282,031, and 1,285,142 bp showed a "blade base" QTL (**Figure 4D**). Although the "blade base" QTL belonged to one class of the "width" QTL, it was characterized by a perfectly consistent contour of the blade tip and the differentiated outline of the leaf base among genotypes. The new identification of "blade tip" and "blade base" QTLs of low-altitude provenance differentiated and enriched the pool of shape morphology variation.

Altitudinal Expression of Shape QTL

In terms of a quantifiable leaf shape index, shape area and width, particular genotypes that incurred significant differences between the two populations are listed in **Supplementary Table S3**. From the union set of significant SNPs from the two altitude populations, 68 showed a change in leaf width of at least 10%, with maximum change of 24.52%. We used the SNP in the *PIN1* gene to explain the genetic effect of leaf shape pattern, because this SNP was significant at high altitude (**Figure 5A**), but was not significant at low altitude (**Figure 5B**). Both *AA* (**Figure 5C**) and *GA* (**Figure 5D**) tended to be stable and similar to each other, regardless of altitude; both dramatically differed from *GG* (**Figure 5E**). The reconstructed leaf shape that resulted from EF parameters enabled visualization of the components of leaf shape that differed among the three genotypes. Notably, comparison of leaf shape effects between high- and low-altitude populations revealed that *GG* considerably altered leaf shape; at low altitude, the width increase was 18.23% and the area increase was 16.40%. The expression difference with *GG* revealed that it caused 0.143% of heritability for controlling leaf shape at high altitude. Specifically, we identified reductions of leaf width and leaf area with the genes of *PIN1*, *CDK-like*, *IIIC63*, and *Protein kinase* at high altitude. For SNPs within other functional genes (*e.g., LRR kinase*, *NAP5*, *SCL1*, *BHLH76*), their genetic effects on shape are detailed in **Table 2**. Overall, there was a clear interaction between QTL and altitude.

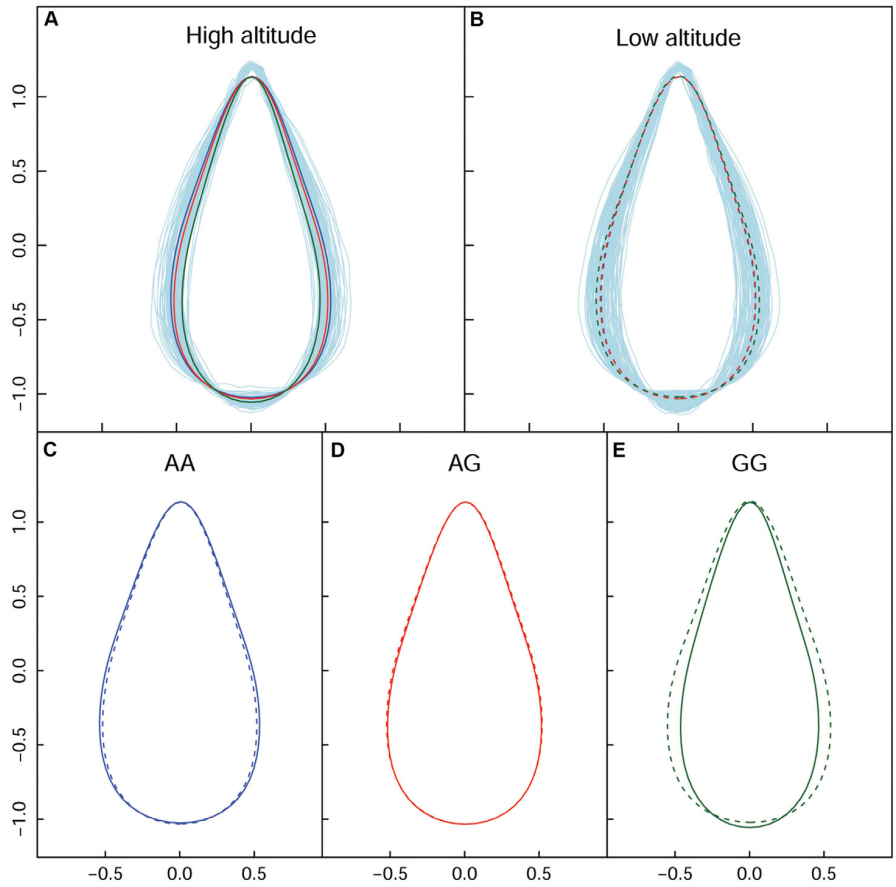

FIGURE 5 | Impact of allelic expression of QTL on the *PIN1* gene. **(A,B)** Are the shape difference showed by the three genotypes respectively in high and low altitude. **(C–E)** Are the genotype-specific shape comparison for the two altitudes. Solid and broken lines indicate shape from high and low altitude.

DISCUSSION

The morphology of a leaf constitutes a significant component of 'ideal plant type' (Mock and Pearce, 1975). In accordance with Fick's law, which specifies the substance diffusion rule, leaf shape affects substance exchange between the leaf and the outside world. Energy exchange on the blade surface can be equally affected by shape (Schuepp, 1993; Nicotra et al., 2008; Xu et al., 2009). This indicates that leaf shape plays an important role in maintaining plant function, as well as in the evolution of a plant's environmental adaptability. Changes in photo-protective strategies, physiology, photosynthetic metabolism, and anatomical structures of leaves have been studied with respect to altitude gradients over long periods (Tranquillini, 1964; Zhang et al., 2017). Because of the potential evolutionary forces contributing to speciation, the mechanisms by which altitude adaptation is altered through the genetic architecture of organ shape have become central issues in morphological biology (Chitwood and Sinha, 2016).

Altitude is an exceedingly important environmental factor that influences evolutionary changes. In this study, through common garden test, we investigated genetic effects on leaf morphology using natural population comprising high- and low-altitude samples. Q_{ST} – F_{ST} contrast showed three positive value with leaf length, leaf width and leaf area, suggesting the potential existence of local adaptation that *P. szechuanica* experienced, although F_{ST} revealed a very low degree of genetic divergence which can be ignored totally. Our results of shape dissection differed from studies of phenotypic plasticity, in which an organism alters its phenotype in response to environmental change (Schlichting, 1986). Given the two contrasting altitudes, the phenotypic variations we observed reflected the effects of the historical accumulation on leaf shape. It provides a new method to understand how altitude alters plant ecological adaptability to affect leaf shape through gene action and helps dissect the mechanisms of ecological adaptation in the context of ecological evolutionary developmental biology (Premoli et al., 2007).

Given on the accumulative heritability of shape area, width and length, the large difference between length and the other two traits (18.38% *versus* 6.916% and 0.263%) had suggested a stable expression of length on leaf axis, further indicating the easily changable trait of leaf width and leaf area relatively. Using the EF-based shape association model, our study successfully identified key genes for leaf shape in *P. szechuanica*. A total of 130 and 131 significant shape SNPs, respectively, for high- and low-altitude populations in the Qinghai-Tibetan plateau. Via

TABLE 2 | Genetic effects of SNPs within annotated genes.

Scaffold	Position	Gene	Full name	Gene ID	Allele	High-altitude population		Low-altitude population		Difference (%)	
						Area	Width	Area	Width	Area	Width
1	22082784	*CIPK3*	*CBL-INTERACTING PROTEIN KINASE 3*	POPTR_0019s08760	GG	1.677	1.107	1.598	1.054	4.96	5.05
1	28403445	*SAG101*	*SENESCENCE-ASSOCIATED CARBOXYLESTERASE 101*	POPTR_0001s29790	AG	1.760	1.169	1.644	1.085	7.04	7.72
1	43033561	*CRPK1*	*COLD-RESPONSIVE PROTEIN KINASE 1*	POPTR_0001s42950	AG	1.66	1.104	1.585	1.044	5.27	5.69
2	9660163	*AR781*	*AR781*	POPTR_0002s13000	TT	1.750	1.169	1.625	1.070	7.75	9.30
2	6092252	*DIS3L2*	*DIS3-like EXONUCLEASE 2*	POPTR_0002s08690	GG	1.823	1.212	1.598	1.051	14.08	15.33
4	22733081	*LRR kinase*	*LEUCINE RICH REPEAT kinase*	POPTR_0004s24030	TC	1.723	1.136	1.547	1.014	11.38	12.09
12	14701685	*LAP1*	*PROTEIN LAP1*	POPTR_0012s15030	CC	1.656	1.096	1.601	1.057	3.43	3.72
14	5416939	*COP11*	*COP9 signalosome complex subunit 1*	POPTR_0014s07160	AT	1.733	1.138	1.644	1.084	5.39	4.92
15	4747203	*PIN1*	*PIN-FORMED1*	POPTR_0015s04570	GG	1.468	0.964	1.610	1.075	9.64	11.46
15	8379891	*CDK-like*	*CYCLIN-DEPENDENT KINASE-LIKE*	POPTR_0015s07250	TT	1.475	0.970	1.530	1.007	3.75	3.90
18	9890878	*CAK1AT*	*CDK-ACTIVATING KINASE*	POPTR_0018s09000	TT	1.682	1.117	1.611	1.065	4.41	4.89
379	2531	*Stress-antifung*	*Salt stress response/antifungal*	POPTR_0379s00200	TC	1.701	1.129	1.615	1.069	5.33	5.64
1	36327299	*NAP5*	*NON-INTRINSIC ABC PROTEIN 5*	POPTR_0001s37340	TT	1.610	1.059	1.478	0.954	8.93	11.03
1	35770384	*JMT*	*JASMONIC ACID CARBOXYL METHYLTRANSFERASE*	POPTR_0001s36950	CC	1.619	1.063	1.444	0.942	12.05	12.90
2	21186580	*BHLH76*	*TRANSCRIPTION FACTOR BHLH76*	POPTR_0002s23650	TT	1.656	1.096	1.455	0.942	13.84	16.38
2	9487450	*Protein kinase*	*PROTEIN KINASE FAMILY PROTEIN*	POPTR_0002s12740	GG	1.656	1.096	1.455	0.942	13.84	16.38
3	18093953	*IIB*	*TRANSCRIPTION FACTOR IIB*	POPTR_0003s19330	GG	1.581	1.044	1.506	0.987	4.94	5.79
5	20022064	*SCL1*	*SCARECROW-LIKE1*	POPTR_0005s20890	CT	1.642	1.081	1.564	1.031	4.97	4.86
6	10067699	*EIN2*	*ETHYLENE-INSENSITIVE PROTEIN 2*	POPTR_0006s12900	AG	1.596	1.049	1.542	1.011	3.51	3.79
7	152674	*IIIC63*	*TRANSCRIPTION FACTOR IIIC63*	POPTR_0007s00430	TT	1.620	1.069	1.551	1.023	4.43	4.46
10	11244085	*Remorin*	*Remorin family protein*	POPTR_0010s10830	AA	1.609	1.058	1.402	0.902	14.74	17.28
11	17887288	*JMJ18*	*JUMOJI DOMAIN-CONTAINING PROTEIN 18*	POPTR_0011s15840	GG	1.633	1.080	1.523	0.999	7.22	8.03
16	13960977	*PIN-LIKES*	*PIN-FORMED LIKES*	POPTR_0016s14840	GG	1.642	1.086	1.517	1.001	8.23	8.48

annotation, *PIN1* was found as a known shape determination, its encoded auxin efflux carrier was involved in the maintenance of auxin gradients (Wenzel et al., 2010). *PIN-LIKES*, members within the same family, are similar to the *PIN* auxin transporter (Barbez et al., 2012). *NAP5*, the gene that encodes non-intrinsic ABC protein 5, is responsible for the transmembrane transport of auxin (Verrier et al., 2008). The exposures of these known shape genes and the class of auxin transporter gene contributed to the reliability of our leaf shape mapping results. Among them, *PPR2* and *Pkinase* were common regulatory genes, indicating that their shape regulation mechanism partially overlapped at both altitudes. Specific to low altitude, *EIN2* was found to negatively regulate miR164A, B, and C, thereby affecting leaf senescence in Kim et al. (2014) study. *JMJ18*, encoding a novel JmjC domain-containing histone H3K4 demethylase (a homologous member of *JMJ16* within the *JMJ* family), showed a leaf senescence repression role in *Arabidopsis* (Liu et al., 2019).

For the altitude-specific variation of leaf morphology, one possible explanation might involve the change of jasmonic acid (JA) regulated by senescence pathway. Since *JMJ18* and *JMT* were found in JA pathway to cause JA-mediated senescence, Wingler et al. (2015) reported a statistically significant negative correlation between higher JA and lower chlorophyll contents, but only when both temperature treatments were combined. Therefore, the connection between altitude and shape variation might be established through *JMJ* and *JMT* gene, because temperature is one of the main factor comprised in altitude. The significance of these leaf-senescence genes indicated that senescence-related physiology may contribute to the regulation of leaf shape at low altitude.

Interestingly, through the annotation of *Stress-antifung*, *CIPK3* and *CRPK1*, their importance with Stress-related functionality and expression in response to stress stimulation in high-altitude, *e.g.*, the role of the stress-antifung gene in mediating defense response, as well as the role of *LAP1*, which functions to alleviate stress-induced damage (Scranton et al., 2012). The role of *CIPK3* in response to abscisic acid, cold, drought, high salt and wounding condition might reflect its significance for plant growth in high-altitude, where these condition might co-existed (Sanyal et al., 2017). Similarly, the significant result with cold-stress responsive role of *CRPK1* might also represent one special defense to cause shape variation (Liu et al., 2017). *CAK1AT* was detected in the high-altitude population; this gene is annotated as a regulator of cell differentiation through control of CDK activity (Takatsuka et al., 2015). Similar to a *CDK-like* gene, *CAK1AT* was also included in the list of significant genes. Our identification of other cell-differentiation-related genes, such as *SCL1*, in the low-altitude population implied a potential interplay between two modules, *i.e.*, the organ-wide growth-reflecting differentiation and the local cell division involving leaf edge (Kierzkowski et al., 2019). Balance among these may generate the morphological diversity of leaves in high-altitude populations.

Through classification of "leaf length," "leaf width," "blade tip" and "blade base" genes, we discovered the exclusive expression of "blade tip" and "blade base" genes in the low-altitude population, which suggested that low altitude can assist a more tolerant environment for developing diversified leaf shapes. It also indicated the potential for greater plasticity among trees that grew in the low-altitude environment. Environmental factors in Qinghai-Tibetan plateau combines to form a unique case to study adaptive evolution (Li and Fang, 1999). By inspecting the impact of altitude on the allelic expression of leaf shape genes, the study revealed the complexity of the gene-by-altitude interaction, which denotes one of the G × E phenomena in a biological system (El-Soda et al., 2014). A comparison of the genotypic effect on leaf shape between distinct altitudes had minuted what shape aspects of QTLs that would be evolutionarily different. For instance, *GG* within the SNP of *PIN1* produce a longer leaf axis and narrower lamina for high-altitude populations, which was consistent with the need for narrower shapes in high-altitude populations to prevent water loss and to reduce allocation of leaf mass caused by high light intensity (Gregory-Wodzicki, 2000; Royer et al., 2009; Peppe et al., 2011). The combination of harsh environmental stresses in Qinghai-Tibetan plateau potentially subjects individuals to a series of adaptive changes. Thus, in the context of adaptation, the study provided the opportunity for in-depth exploration of the relationships between leaf shape diversity and biological adaptation; these aspects are linked through particular genes, metabolic clues, and biochemical pathways that underlie these fundamental issues of adaptation.

DATA AVAILABILITY STATEMENT

SNP typing data was uploaded to European Variation Archive (EVA) database, with a project ID of PRJEB36028. The web link is https://www.ebi.ac.uk/ena/data/view/PRJEB36028.

AUTHOR CONTRIBUTIONS

MY performed the data analyses and wrote the manuscript. LJ derived the model. PG and XZ participated in the field management of experimental materials and led the phenotype investigation and data collection. RW conceived of the idea of the overall investigation.

FUNDING

This work was supported by the Fundamental Research Funds for the Central Universities (No. 2015ZCQ-SW-06), the National Natural Science Foundation of China (No. 31600536), and the State Administration of Forestry of China (No. 201404102).

SUPPLEMENTARY MATERIAL

The Supplementary Material for this article can be found online at: https://www.frontiersin.org/articles/10.3389/fpls.2020.00632/full#supplementary-material

FIGURE S1 | Sampling sites, showing distributions of high- and low-altitude populations in Sejila mountain in the Qinghai-Tibetan plateau.

FIGURE S2 | Population structures for high- and low-altitude populations. **(A,B)** Represent the likelihood change over *K*s and population structures at high and low altitudes, respectively. Different colors denote distinct sub-populations; bar heights with different colors represent membership probabilities of individuals.

FIGURE S3 | Fitting of leaf shape using different harmonic orders of Elliptic Fourier (EF) parameters. Gray color denotes the true average leaf, while reconstructed shapes using EF parameters are shown with thick green lines.

TABLE S1 | Detailed annotations with identification of SNPs significant in the regulation of shape variation in high-altitude populations.

TABLE S2 | Detailed annotations with identification of SNPs significant in the regulation of shape variation in low-altitude populations.

TABLE S3 | Comparison of QTL expressions between high and low altitudes.

FILE S1 | The R script for GWAS of leaf shape.

REFERENCES

Bai, Y., Vaddepalli, P., Fulton, L., Bhasin, H., Hulskamp, M., and Schneitz, K. (2013). ANGUSTIFOLIA is a central component of tissue morphogenesis mediated by the atypical receptor-like kinase STRUBBELIG. *BMC Plant Biol.* 13:16. doi: 10.1186/1471-2229-13-16

Barbez, E., Kubes, M., Rolcik, J., Beziat, C., Pencik, A., Wang, B. J., et al. (2012). A novel putative auxin carrier family regulates intracellular auxin homeostasis in plants. *Nature* 485, 119–122. doi: 10.1038/nature11001

Bilsborough, G. D., Runions, A., Barkoulas, M., Jenkins, H. W., Hasson, A., Galinha, C., et al. (2011). Model for the regulation of *Arabidopsis thaliana* leaf margin development. *Proc. Natl. Acad. Sci. U.S.A.* 108, 3424–3429. doi: 10.1073/pnas.1015162108

Bo, W., Wang, Z., Xu, F., Fu, G., Sui, Y., Wu, W., et al. (2014). Shape mapping: genetic mapping meets geometric morphometrics. *Brief Bioinform.* 15, 571–581. doi: 10.1093/bib/bbt008

Bookstein, F. L. (1991). *Morphometric Tools for Landmark Data*. Cambridge: Cambridge University Press.

Chitwood, D. H., and Sinha, N. R. (2016). Evolutionary and environmental forces sculpting leaf development. *Curr. Biol.* 26, R297–R306. doi: 10.1016/j.cub.2016.02.033

Churchill, G. A., and Doerge, R. W. (1994). Empirical threshold values for quantitative trait mapping. *Genetics* 138, 963–971.

Danecek, P., Auton, A., Abecasis, G., Albers, C. A., Banks, E., DePristo, M. A., et al. (2011). The variant call format and VCFtools. *Bioinformatics* 27, 2156–2158. doi: 10.1093/bioinformatics/btr330

El-Soda, M., Malosetti, M., Zwaan, B. J., Koornneef, M., and Aarts, M. G. M. (2014). Genotype × environment interaction QTL mapping in plants: lessons from *Arabidopsis*. *Trends Plant Sci.* 19, 390–398. doi: 10.1016/j.tplants.2014.01.001

Firmat, C., Delzon, S., Louvet, J. M., Parmentier, J., and Kremer, A. (2017). Evolutionary dynamics of the leaf phenological cycle in an oak metapopulation along an elevation gradient. *J. Evol. Biol.* 30, 2116–2131. doi: 10.1111/jeb.13185

Fu, G., Bo, W., Pang, X., Wang, Z., Chen, L., Song, Y., et al. (2013). Mapping shape quantitative trait loci using a radius-centroid-contour model. *Heredity* 110, 511–519. doi: 10.1038/hdy.2012.97

Gower, J. C., and Dijksterhuis, G. B. (2004). *Procrustes Problems*. New York, NY: Oxford University Press.

Gregory-Wodzicki, K. M. (2000). Relationships between leaf morphology and climate, Bolivia: implications for estimating paleoclimate from fossil floras. *Paleobiology* 26, 668–688. doi: 10.1666/0094-83732000026<0668:RBLMAC<2.0.CO;2

Keen, K., McGinnity, P., Cross, T. F., Crozier, W. W., and Prodöhl, P. A. (2013). diveRsity: an R package for the estimation of population genetics parameters and their associated errors. *Methods Ecol. Evol.* 4, 782–788. doi: 10.1111/2041-210X.12067

Kierzkowski, D., Runions, A., Vuolo, F., Strauss, S., Lymbouridou, R., Routier-Kierzkowska, A. L., et al. (2019). A growth-based framework for leaf shape development and diversity. *Cell* 177, 1405–1418. doi: 10.1016/j.cell.2019.05.011

Kim, H. J., Hong, S. H., Kim, Y. W., Lee, I. H., Jun, J. H., Phee, B. K., et al. (2014). Gene regulatory cascade of senescence-associated NAC transcription factors activated by ETHYLENE-INSENSITIVE2-mediated leaf senescence signalling in *Arabidopsis*. *J. Exp. Bot.* 65, 4023–4036. doi: 10.1093/jxb/eru112

Klingenberg, P. C. (2010). Evolution and development of shape: integrating quantitative approaches. *Nat. Rev. Genet.* 11, 623–635.

Koyama, T., Sato, F., and Ohme-Takagi, M. (2017). Roles of miR319 and TCP transcription factors in leaf development. *Plant Physiol.* 175, 874–885. doi: 10.1104/pp.17.00732

Li, J., and Fang, X. (1999). Uplift of the Tibetan Plateau and environmental changes. *Chin. Sci. Bull.* 44, 2117–2124. doi: 10.1016/j.ympev.2012.08.004

Liu, P., Zhang, S. B., Zhou, B., Luo, X., Zhou, X. F., Cai, B., et al. (2019). The histone H3K4 demethylase JMJ16 represses leaf senescence in *Arabidopsis*. *Plant Cell* 31, 430–443. doi: 10.1105/tpc.18.00693

Liu, Z., Jia, Y., Ding, Y., Shi, Y., Li, Z., and Guo, Y. (2017). Plasma membrane CRPK1-mediated phosphorylation of 14-3-3 proteins induces their nuclear import to fine-tune CBF signaling during cold response. *Mol. Cell* 66, 117–128.e5. doi: 10.1016/j.molcel.2017.02.016

Lu, Y. (2017). *Study on the Adaptive Mechanism of Halenia elliptica in the Different Altitudinal Gradients*. Ph.D. thesis, Lanzhou University, Lanzhou.

Midolo, G., De Frenne, P., Holzel, N., and Wellstein, C. (2019). Global patterns of intraspecific leaf trait responses to elevation. *Glob. Chang. Biol.* 25, 2485–2498. doi: 10.1111/gcb.14646

Miles, D. B., and Ricklefs, R. E. (1994). *Ecological and Evolutionary Inferences from Shape: an Ecological Perspective*. Chicago, IL: University of Chicago Press.

Milla, R., and Reich, P. B. (2011). Multi-trait interactions, not phylogeny, fine-tune leaf size reduction with increasing altitude. *Ann. Bot.* 107, 455–465. doi: 10.1093/aob/mcq261

Mock, J. J., and Pearce, R. B. (1975). An ideotype of maize. *Euphitica* 24, 613–623.

Moon, J., and Hake, S. (2011). How a leaf gets its shape. *Curr. Opin. Plant Biol.* 14, 24–30. doi: 10.1016/j.pbi.2010.08.012

Neto, J. C., Meyer, G. E., Jones, D. D., and Samal, A. K. (2006). Plant species identification using Elliptic Fourier leaf shape analysis. *Comput. Electron Agr.* 50, 121–134. doi: 10.1016/j.compag.2005.09.004

Nicotra, A. B., Cosgrove, M. J., Cowling, A., Schlichting, C. D., and Jones, C. S. (2008). Leaf shape linked to photosynthetic rates and temperature optima in South African *Pelargonium* species. *Oecologia* 154, 625–635. doi: 10.1007/s00442-007-0865-1

Nicotra, A. B., Leigh, A., Boyce, C. K., Jones, C. S., Niklas, K. J., Royer, D. L., et al. (2011). The evolution and functional significance of leaf shape in the angiosperms. *Funct. Plant Biol.* 38, 535–552. doi: 10.1071/FP11057

Peppe, D. J., Royer, D. L., Cariglino, B., Oliver, S. Y., Newman, S., Leight, E., et al. (2011). Sensitivity of leaf size and shape to climate: global patterns and paleoclimatic applications. *New Phytol.* 190, 724–739. doi: 10.1111/j.1469-8137.2010.03615.x

Premoli, A. C., Raffaele, E., and Mathiasen, P. (2007). Morphological and phenological differences in *Nothofagus pumilio* from contrasting elevations: evidence from a common garden. *Austral Ecol.* 32, 515–523. doi: 10.1111/j.1442-9993.2007.01720.x

Pujol, B., Wilson, A. J., Ross, R. I. C., and Pannell, J. R. (2008). Are *Qst-Fst* comparisons for natural populations meaningful? *Mol. Ecol.* 17, 4782–4785. doi: 10.1111/j.1365-294X.2008.03958.x

Raeymaekers, J., Van Houdt, J., Larmuseau, M., Geldof, S., and Volckaert, F. (2007). Divergent selection as revealed by P_{ST} and QTL—based F_{ST} in three—spined stickleback (*Gasterosteus aculeatus*) populations along a coastal—inland gradient. *Mol. Ecol.* 16, 891–905. doi: 10.1111/j.1365-294X.2006.03190.x

Raj, A., Stephens, M., and Pritchard, J. K. (2014). fastSTRUCTURE: variational inference of population structure in large SNP data sets. *Genetics* 197, 573–589. doi: 10.1534/genetics.114.164350

Royer, D. L., Meyerson, L. A., Robertson, K. M., and Adams, J. M. (2009). Phenotypic plasticity of leaf shape along a temperature gradient in *Acer rubrum*. *PLoS One* 4:e7653. doi: 10.1371/journal.pone.0007653

Sanyal, S. K., Kanwar, P., Yadav, A. K., Sharma, C., Kumar, A., and Pandey, G. K. (2017). *Arabidopsis* CBL interacting protein kinase 3 interacts with ABR1, an APETALA2 domain transcription factor, to regulate ABA responses. *Plant Sci.* 254, 48–59. doi: 10.1016/j.plantsci.2016.11.004

Schlichting, C. D. (1986). The evolution of phenotypic plasticity in plants. *Ann. Rev. Ecol. Syst.* 17, 667–693.

Schuepp, P. H. (1993). Tansley review No. 59. Leaf boundary layers. *New Phytol.* 125, 477–507.

Scranton, M. A., Yee, A., Park, S. Y., and Walling, L. L. (2012). Plant leucine aminopeptidases moonlight as molecular chaperones to alleviate stress-induced damage. *J. Biol. Chem.* 287, 18408–18417. doi: 10.1074/jbc.M111.309500

Shen, D., Bo, W., Xu, F., and Wu, R. (2014). Genetic diversity and population structure of the Tibetan poplar (*Populus szechuanica var. tibetica*) along an altitude gradient. *BMC Genet.* 15:S11. doi: 10.1186/1471-2156-15-S1-S11

Slice, D. E. (2007). Geometric morphometrics. *Ann. Rev. Anthropol.* 36, 261–281. doi: 10.1146/annrev.anthro.34.081804.120613

Sun, L., Wang, J., Zhu, X., Jiang, L., Gosik, K., Sang, M., et al. (2018). HpQTL: a geometric morphometric platform to compute the genetic architecture of heterophylly. *Brief Bioinform.* 19, 603–612. doi: 10.1093/bib/bbx011

Takatsuka, H., Umeda-Hara, C., and Umeda, M. (2015). Cyclin-dependent kinase-activating kinases CDKD;1 and CDKD;3 are essential for preserving mitotic activity in *Arabidopsis thaliana*. *Plant J.* 82, 1004–1017. doi: 10.1111/tpj.12872

Tian, F., Bradbury, P. J., Brown, P. J., Hung, H., Sun, Q., Flint-Garcia, S., et al. (2011). Genome-wide association study of leaf architecture in the maize nested association mapping population. *Nat. Genet.* 43, 159–164. doi: 10.1038/ng.746

Tranquillini, W. (1964). The physiology of plants at high altitudes. *Ann. Rev. Plant Physiol.* 15, 345–362.

Tsukaya, H. (2006). Mechanism of leaf-shape determination. *Ann. Rev. Plant Biol.* 57, 477–496. doi: 10.1146/annurev.arplant.57.032905.105320

Verrier, P. J., Bird, D., Buria, B., Dassa, E., Forestier, C., Geisler, M., et al. (2008). Plant ABC proteins – a unified nomenclature and updated inventory. *Trends Plant Sci.* 13, 151–159. doi: 10.1016/j.tplants.2008.02.001

Vlad, D., Kierzkowski, D., Rast, M. I., Vuolo, F., Dello Ioio, R., Galinha, C., et al. (2014). Leaf shape evolution through duplication, regulatory diversification, and loss of a homeobox gene. *Science* 343, 780–783. doi: 10.1126/science.1248384

Wenzel, C. L., Schuetz, M., Yu, Q., and Mattsson, J. (2010). Dynamics of MONOPTEROS and PIN-FORMED1 expression during leaf vein pattern formation in *Arabidopsis thaliana*. *Plant J.* 49, 387–398. doi: 10.1111/j.1365-313X.2006.02977.x

Wingler, A., Juvany, M., Cuthbert, C., and Munne-Bosch, S. (2015). Adaptation to altitude affects the senescence response to chilling in the perennial plant *Arabis alpina*. *J. Exp. Bot.* 66, 355–367. doi: 10.1093/jxb/eru426

Winn, A. A. (1999). The functional significance and fitness consequences of heterophylly. *Int. J. Plant Sci.* 160, S113–S121. doi: 10.1086/314222

Wright, S. (1951). The genetic structure of populations. *Ann. Eugen* 15, 323–354.

Xu, F., Guo, W., Xu, W., Wei, Y., and Wang, R. (2009). Leaf morphology correlates with water and light availability: what consequences for simple and compound leaves? *Prog. Nat. Sci.Mater Int.* 19, 1789–1798. doi: 10.1016/j.pnsc.2009.10.001

Zhang, C., Zhang, D. W., Sun, Y. N., Arfan, M., Li, D. X., Yan, J. J., et al. (2017). Photo-protective mechanisms in reed canary grass to alleviate photo-inhibition of PSII on the Qinghai-Tibet Plateau. *J. Plant Physiol.* 215, 11–19. doi: 10.1016/j.jplph.2017.04.017

Zhang, Z., Ersoz, E., Lai, C.-Q., Todhunter, R. J., Tiwari, H. K., Gore, M. A., et al. (2010). Mixed linear model approach adapted for genome-wide association studies. *Nat. Genet.* 42, 355–360. doi: 10.1038/ng.546

Zhao, W., Chen, Y., Casella, G., Cheverud, J. M., and Wu, R. (2005). A non-stationary model for functional mapping of complex traits. *Bioinformatics* 21, 2469–2477. doi: 10.1093/bioinformatics/bti382

Conflict of Interest: The authors declare that the research was conducted in the absence of any commercial or financial relationships that could be construed as a potential conflict of interest.

frontiers in Plant Science

REVIEW
published: 22 July 2020
doi: 10.3389/fpls.2020.01126

CRISPR/Cas9 Gene Editing: An Unexplored Frontier for Forest Pathology

Erika N. Dort[1], *Philippe Tanguay*[2] *and Richard C. Hamelin*[1,3,4]*

[1] Department of Forest and Conservation Sciences, Faculty of Forestry, University of British Columbia, Vancouver, BC, Canada, [2] Laurentian Forestry Centre, Canadian Forest Service, Natural Resources Canada, Québec, QC, Canada, [3] Institut de Biologie Intégrative et des Systèmes (IBIS), Université Laval, Québec, QC, Canada, [4] Département des Sciences du bois et de la Forêt, Faculté de Foresterie et Géographie, Université Laval, Québec, QC, Canada

CRISPR/Cas9 gene editing technology has taken the scientific community by storm since its development in 2012. First discovered in 1987, CRISPR/Cas systems act as an adaptive immune response in archaea and bacteria that defends against invading bacteriophages and plasmids. CRISPR/Cas9 gene editing technology modifies this immune response to function in eukaryotic cells as a highly specific, RNA-guided complex that can edit almost any genetic target. This technology has applications in all biological fields, including plant pathology. However, examples of its use in forest pathology are essentially nonexistent. The aim of this review is to give researchers a deeper understanding of the native CRISPR/Cas systems and how they were adapted into the CRISPR/Cas9 technology used today in plant pathology—this information is crucial for researchers aiming to use this technology in the pathosystems they study. We review the current applications of CRISPR/Cas9 in plant pathology and propose future directions for research in forest pathosystems where this technology is currently underutilized.

Keywords: forest diseases, tree disease resistance, filamentous pathogens, poplar rust, Dutch elm disease (DED), sudden oak death (SOD), white pine blister rust (WPBR)

OPEN ACCESS

Edited by:
Sébastien Duplessis, INRA Centre Nancy-Lorraine, France

Reviewed by:
Jianqiang Miao, Northwest A&F University, China
Maria Andrea Ortega, University of Georgia, United States

***Correspondence:**
Richard C. Hamelin
richard.hamelin@ubc.ca

Specialty section:
This article was submitted to Plant Pathogen Interactions, a section of the journal Frontiers in Plant Science

Received: *03 June 2020*
Accepted: *08 July 2020*
Published: *22 July 2020*

Citation:
Dort EN, Tanguay P and Hamelin RC (2020) CRISPR/Cas9 Gene Editing: An Unexplored Frontier for Forest Pathology. Front. Plant Sci. 11:1126. doi: 10.3389/fpls.2020.01126

INTRODUCTION

Developed in 2012, CRISPR/Cas9 gene editing is relatively new, but research using this technology has expanded rapidly in most scientific fields with 7,105 publications in 2019 alone (Clarivate Analytics, 2020). Even though human health and medicine are the most prolific fields, researchers in plant sciences are also starting to explore the applications of CRISPR/Cas9. The use of CRISPR/Cas9 in plant breeding has sparked interest in the field of plant pathology where disease resistant plant cultivars are becoming increasingly important. The applications of CRISPR/Cas9 technology in plant pathology have already been reviewed, especially in the context of agriculture (Langner et al., 2018; Makarova et al., 2018; Das et al., 2019; Muñoz et al., 2019). However, literature addressing its applications in forestry is lacking, and we believe this is because CRISPR/Cas9 is currently underutilized in this field. The purpose of this review is to fill this literature gap while giving

forest pathologists a deeper understanding of CRISPR/Cas9 and its potential applications to better understand and manage tree diseases. We focus on how native CRISPR/Cas systems function as well as the mechanisms driving CRISPR/Cas9 gene editing technology as this information is crucial for implementation of this technology in forest pathosystems.

What Is CRISPR/Cas? A Primer for Understanding CRISPR/Cas9 Gene Editing

*C*lustered *r*egularly *i*nterspaced *s*hort *p*alindromic *r*epeats (CRISPRs) and CRISPR *as*sociated (Cas) proteins, or CRISPR/Cas, is a bacterial and archaeal DNA-based adaptive immune system that defends against bacteriophages, plasmids, and other mobile genetic invaders (Bhaya et al., 2011; Terns and Terns, 2011). The CRISPR/Cas system was first discovered by Japanese scientists in *Escherichia coli* (Ishino et al., 1987), but it has now been found in a large array of prokaryotic species. Among these species, CRISPR/Cas DNA loci exhibit extensive genetic diversity, but they all have a common underlying architecture comprising a CRISPR array composed of direct repeats interspaced with unique sequences called spacers, which are derived from foreign nucleic acids; this array is flanked by associated *cas* genes organized as an operon (Jansen et al., 2002; Bolotin et al., 2005; Pourcel et al., 2005) (**Figure 1A**). These elements of the CRISPR/Cas system work in concert to direct a three-stage defense response against invading phages and plasmids (Barrangou et al., 2007; van der Oost et al., 2009) (**Figure 1B**). Stage 1 (adaptation) occurs when the bacterial or archaeal host recognizes a fragment of DNA or RNA from an invader, named the protospacer (Deveau et al., 2008), and integrates it into the CRISPR array as a new spacer sequence (van der Oost et al., 2009). Protospacer selection is dictated by the presence of highly conserved 2–3 nucleotide regions near the protospacer sequence called 'protospacer-adjacent motifs', or PAMs (Marraffini and Sontheimer, 2010). Stage 2 (expression) involves the transcription of the CRISPR array into large RNA transcripts called precursor CRISPR-derived RNAs (pre-crRNAs), which are processed into smaller, mature crRNAs by Cas proteins that are transcribed from the *cas* genes (van der Oost et al., 2009). A mature crRNA contains a unique phage-derived spacer sequence flanked by fragments of its adjacent repeat sequences from the CRISPR array (Wiedenheft et al., 2012). Finally, Stage 3 (interference) takes place when a subsequent attack occurs by the same bacteriophage or plasmid; each crRNA associates with one or more Cas proteins to form a crRNA-protein effector complex, which conducts surveillance of the cell for invading DNA or RNA (Terns and Terns, 2011). The crRNA acts as a guide for the effector complex (guide RNA), directing it to create a double-stranded break (DSB) in the complementary protospacer sequence of the

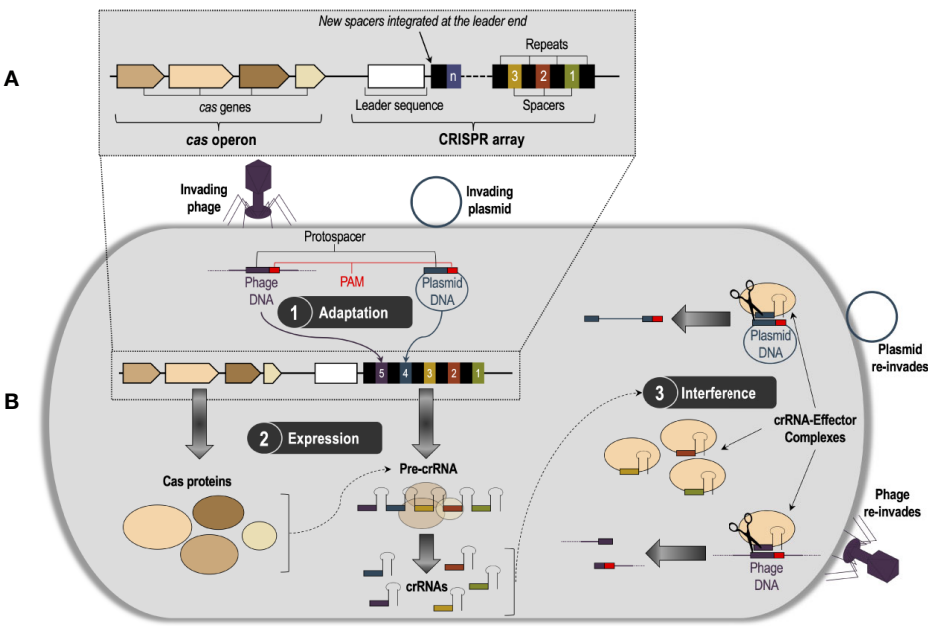

FIGURE 1 | (A) A generalized CRISPR/Cas system consisting of a CRISPR array and a *cas* operon. The CRISPR array is composed of a series of identical repeat sequences interspaced with unique sequences called spacers, which are derived from the genetic material of invading bacteriophages and plasmids. On the 5′ end of the spacer/repeat locus is an intraspecies-conserved leader sequence likely involved in transcription of the CRISPR array. Flanking the CRISPR array is the *cas* operon, which contains the CRISPR-associated (*cas*) genes that code for proteins involved in the CRISPR/Cas defense response. **(B)** The three-stage CRISPR/Cas defense response. Stage 1, adaptation, occurs when the bacterial or archaeal host recognizes a fragment of DNA or RNA from an invader, named the protospacer, and integrates it into the CRISPR array as a new spacer. New spacers are integrated at the leader end of the array. Stage 2, expression, involves the transcription of the *cas* genes into Cas proteins, and the CRISPR array into a precursor CRISPR RNA (pre-crRNA) molecule. The pre-crRNA molecule then gets processed by Cas proteins into smaller, mature CRISPR RNA (crRNA) molecules. In Stage 3, interference, the mature crRNAs associate with one or more Cas proteins to form crRNA-effector complexes, which survey the cell for foreign nucleic acids and subsequently cleave them *via* recognition of the protospacer-adjacent motif (PAM) sequence.

invader *via* recognition of the PAM (Terns and Terns, 2011). The fragmented DNA or RNA can no longer infect the host, thus completing successful defense by the CRISPR/Cas system. This highly adaptable nucleotide-based activity is what makes CRISPR/Cas gene editing technologies, which are designed from CRISPR/Cas systems, so effective.

How Does CRISPR/Cas9 Gene Editing Technology Work?

CRISPR/Cas9 gene editing technology is based on the Type II CRISPR/Cas system from the human pathogen *Streptococcus pyogenes* and was developed by an internationally collaborative research group headed by Jennifer Doudna and Emmanuelle Charpentier (Jinek et al., 2012). Type II systems are characterized by the multidomain protein Cas9 (Makarova et al., 2011; Makarova et al., 2015), which relies on two RNA molecules to guide it to its DNA target: a trans-activating crRNA (tracrRNA), and the usual crRNA (Deltcheva et al., 2011; Gottesman, 2011; Jinek et al., 2012). The tracrRNA is complementary to the repeat sequences in the corresponding pre-crRNA, and it base-pairs to those sequences facilitating Cas9 to process the pre-crRNA into a smaller mature crRNA molecule (Deltcheva et al., 2011). The tracrRNA, mature crRNA, and Cas9 endonuclease then form an effector complex and the two RNA molecules guide Cas9 to the target protospacer sequence of an invader (Jinek et al., 2012). Cas9 then uses the complementarity between the crRNA and the protospacer as well as the adjacent PAM to create a DSB in the target DNA (Jinek et al., 2012). The Doudna/Charpentier research group developed a single chimeric RNA molecule that combined the tracrRNA and crRNA, and they demonstrated that Cas9 can be programmed to cleave any target DNA by changing only a 20-nucleotide sequence in this single-guide RNA (sgRNA) (Jinek et al., 2012). Their results were immediately significant for the scientific community, allowing the editing of DNA in a broad range of organisms and caused a surge of research in all scientific fields that continues to this day. Additionally, the original chimeric *S. pyogenes* Cas9 technology has served as a model system from which many different CRISPR technologies have evolved.

CRISPR/Cas9 Exploits Cellular DNA Repair Mechanisms to Edit Genes

The success of nuclease-based technologies, including CRISPR/Cas9, as methods to edit genes relies on the highly conserved cellular DNA repair mechanisms present in all domains of life. Cas9 generates blunt-end DSBs at target DNA sites, and there are two main mechanisms that are triggered in eukaryotic cells in response to these DSBs: end-joining and homologous recombination, or homology-directed repair (HDR) (Ranjha et al., 2018). Both end-joining and HDR involve complex endogenous systems that can be divided into several sub-pathways that are triggered under different cellular conditions and generate very different repaired DNA products (Ceccaldi et al., 2016; Ranjha et al., 2018). There are two end-joining pathways, non-homologous end-joining (NHEJ) and microhomology-mediated end-joining (MMEJ), and neither require a DNA template for repair (Ranjha et al., 2018). These end-joining mechanisms are highly error prone, often resulting in insertions or deletions (indels) that create knockout mutants when they occur in the reading frame of a gene (Bortesi and Fischer, 2015; Ranjha et al., 2018). Conversely, repairs by the HDR pathways occur only in the presence of a donor DNA template containing regions homologous to the sequences surrounding the DSB induced by Cas9 (Bortesi and Fischer, 2015). The HDR pathway is more precise than the end-joining mechanisms, and thus can be used for highly specific gene modification or gene insertion. Eukaryotic organisms can use both homologous recombination and end-joining mechanisms to repair DNA damage in their cells, but the end-joining pathways are more frequent because they occur regardless of the presence of a donor DNA template and can therefore take place in any stage of the cell cycle (Ranjha et al., 2018). However, end-joining allows for less control in CRISPR/Cas9 gene editing due to the randomness of the mutations it induces (Langner et al., 2018). The less frequent HDR pathway allows for more control, but requires a homologous donor DNA template that, even when present, triggers HDR at a much lower rate than end-joining (Langner et al., 2018). Consequently, researchers wishing to activate the HDR pathway using CRISPR/Cas9 have the additional task of designing a homologous donor template that can be used for recombination at the target DNA site, and they will likely have to screen larger numbers of transformants to identify successful HDR candidates.

CRISPR/Cas9 Limitations

The major limitation of using the original *S. pyogenes* CRISPR/Cas9 (*Sp*Cas9) is the requirement of the PAM sequence adjacent to the protospacer DNA, which is used by the Cas9 complex in conjunction with the complementary sgRNA region to recognize and cleave the target DNA sequence (Jinek et al., 2012). The *Sp*Cas9 complex recognizes the PAM sequence 5′-NGG-3′, where N represents any of the four nucleotide bases (Jinek et al., 2012). This three-base-pair sequence is a common occurrence in most genomes, but its requirement limits the genes that can be targeted, especially when attempting to study genes involved in highly specific pathways of interest (Langner et al., 2018). Additionally, research has shown that CRISPR/Cas9 can recognize alternative PAM sequences, which increases the likelihood of off-target mutations (Zhang et al., 2014). In response to this limitation researchers have developed three new CRISPR/Cas9 systems from Cas9 orthologs in other bacterial species, each of which recognizes a unique PAM: *Sa*Cas9 from *Staphylococcus aureus*, *St*Cas9 from *Staphylococcus thermophilus*, and *Nm*Cas9 from *Neisseria meningitidis* (Kleinstiver et al., 2015). In addition, Cas9 protein variants are being engineered to recognize alternative PAMs (Agudelo et al., 2020). New CRISPR/Cas nucleases from other bacterial Type II systems have also been discovered: Cas12a, which targets DNA, and Cas13a, which targets single-stranded RNA (Shmakov et al., 2015; Burstein et al., 2017; Koonin et al., 2017). While bearing some similarities to Cas9, these two systems use slightly different mechanisms for cleaving target nucleic acid sequences and processing of pre-crRNA and

demonstrate advantages over Cas9 for certain applications, including within plant pathology (Langner et al., 2018).

Another limitation of any CRISPR/Cas technology is the occurrence of unwanted mutations (translocations, inversions, large deletions and insertions) resulting from the complex endogenous pathways that repair the double-stranded DNA breaks induced by Cas nucleases (Després et al., 2018; Kosicki et al., 2018). Additionally, Cas9-induced DSBs can be toxic to cells, inducing cell-death pathways and resulting in low transformation and editing efficiencies (Garst et al., 2017; Roy et al., 2018). To avoid these DSB-related limitations, nuclease-deficient Cas9 proteins have been engineered and fused to other proteins such as deaminases and recombinases to achieve base editing and site-specific recombination (Nishida et al., 2016; Standage-Beier et al., 2019). However, Cas9 continues to be the most commonly used CRISPR/Cas technology, has a number of applications in plant pathology, and is a valuable untapped resource for forest pathology; it is therefore the focus of the remainder of this review.

CURRENT APPLICATIONS OF CRISPR/CAS9 IN PLANT PATHOLOGY

Plant pathogenic viruses, bacteria, oomycetes, and fungi are natural components of healthy ecosystems, but globalization, climate change, and mismanagement have led many of these species to cause emerging infectious diseases (EIDs) that threaten natural and managed plant ecosystems (Anderson et al., 2004; Fisher et al., 2012). In the context of agriculture, plant EIDs are considered a threat to global food security (Pennisi, 2010), and in forestry they have significant impacts from both economic and biodiversity conservation perspectives (Anderson et al., 2004; Fisher et al., 2012). Chemical mitigation strategies using pesticides and fungicides have proven to be inadequate and environmentally destructive (Andolfo et al., 2016), so research has turned to genetic strategies: developing disease resistance in plants and/or engineering avirulent strains of pathogens. The development of CRISPR/Cas9 as an accurate and versatile gene editing technology increased the scope of such genetic strategies and has led plant pathologists to explore its disease-mitigation applications in both hosts and pathogens.

Using CRISPR/Cas9 to Engineer Disease Resistance in Plants

To date, most of the CRISPR/Cas9 research in plant pathology has focused on developing systems in the hosts, namely engineering disease resistance in agriculturally important plants. Not surprisingly, the first plants to be engineered using CRISPR/Cas9 were the model species *Arabidopsis thaliana* (Feng et al., 2013) and *Nicotiana benthamiana* (Nekrasov et al., 2013), but these were followed almost simultaneously by development in rice (Feng et al., 2013; Jiang et al., 2013; Miao et al., 2013), wheat (Wang et al., 2014), sorghum (Jiang et al., 2013), maize (Liang et al., 2014), and tomato (Brooks et al., 2014). The list of plant species engineered using CRISPR/Cas9 has expanded rapidly in the last six years, but it has remained in the realm of angiosperm species important in agriculture; use of this technology in forest species is largely absent in the literature, with the one exception of studies developing CRISPR/Cas9 systems in *Populus* species (Fan et al., 2015; Zhou et al., 2015).

The first CRISPR/Cas9 studies in plants were proof-of-concept experiments demonstrating the use of this technology in plants, but many of these species have now been engineered for resistance to viral, fungal, and bacterial diseases (Das et al., 2019). Engineering disease resistance in plants using CRISPR/Cas9 has generally been executed using one of two strategies: the pathogen–gene approach or the plant-gene approach. The former involves engineering an sgRNA into the plant chromosome that directs Cas9 to target a specific pathogen gene thereby impeding pathogenesis, whereas the latter uses an sgRNA that targets endogenous plant genes involved in pathogen interactions and modifies them to either boost the host immune response, or to interfere with the host-recognition pathway of the pathogen (Makarova et al., 2018).

Pathogen-Gene Approach

The pathogen-gene approach is best demonstrated with plant-virus pathosystems. CRISPR/Cas9-mediated virus resistance is most commonly tackled *via* a transgenic approach whereby a viral DNA sequence is used to design the sgRNA and is transformed into the plant genome with the CRISPR/Cas9 system (Ali et al., 2015; Ali et al., 2016; Zhang et al., 2018). This induces a response remarkably similar to that of the native CRISPR/Cas systems in that the plant is able to use its transgenic sgRNA-Cas9 system to target invading virus DNA, RNA, or mRNA. This approach has been primarily used in the model species *Nicotiana benthamiana* (Ali et al., 2015; Ali et al., 2016; Ji et al., 2018; Zhang et al., 2018) and *Arabidopsis thaliana* (Ji et al., 2018; Zhang et al., 2018), but it presents an intriguing paradigm for the use of CRISPR/Cas9 to fortify plant immune systems against invading pathogens.

Plant-Gene Approach

Engineering CRISPR/Cas9-mediated disease resistance using the plant-gene approach has mostly focused on targeting plant susceptibility (*S*) genes, a diverse group of genes with varying roles that ultimately render plants more susceptible to invading pathogens. The proteins encoded by *S* genes fall into two general categories: those that act as negative regulators of immunity, decreasing the plant immune response in certain contexts, and those that are part of plant development and regulatory pathways, which are targets for pathogen effector molecules (Langner et al., 2018). While traditional disease-resistance breeding has focused on disease resistance (*R*) genes that generally involve 'gene-for-gene' interactions with pathogens, it is thought that targeting *S* genes will yield more stable, broad-spectrum disease resistance (Pavan et al., 2009). Both *R*-gene- and *S*-gene-based resistance involve complex molecular pathways that interact with pathogens in different ways, and the details of these interactions have been reviewed elsewhere (Dangl and Jones, 2001; Jones and Dangl, 2006; Pavan et al., 2009; Lapin and Van den Ackerveken, 2013). Engineering

resistance to viruses with CRISPR/Cas9 using the plant-gene approach involves designing the sgRNA to target a region of the plant genome that is used by the virus for replication (Makarova et al., 2018). This method has been used for disrupting RNA viruses in both *Cucumis sativus* (cucumber) and *A. thaliana* by targeting the eukaryotic translation initiation factor gene *eIF4E* in the plant (Chandrasekaran et al., 2016; Pyott et al., 2016). However, the plant-gene approach is best demonstrated in pathosystems involving bacteria, oomycetes, and fungi in which the proteins encoded by plant *S* genes are relied upon by these pathogens for host recognition and immune suppression. Generating plant resistance in these systems has predominantly been focused on designing sgRNAs to target *S* genes, creating host knockout mutants that the pathogen effectors have difficulty recognizing (Langner et al., 2018; Das et al., 2019).

A well-studied *S* gene system is the mildew resistance locus O (*MLO*), which renders both monocot and dicot plant hosts susceptible to a variety of powdery mildew pathogens. The use of CRISPR/Cas9 to disrupt the *MLO* gene has proven to be effective for evading pathogen effector recognition and generating disease resistance in these systems. One of the best examples of this is a study by Nekrasov et al. who used CRISPR/Cas9 to generate 48 bp deletions in an *Mlo* gene in tomato plants (Nekrasov et al., 2017). The CRISPR/Cas9 mutants demonstrated resistance to the powdery mildew fungus *Oidium neolycopersici* without generating any other unwanted phenotypic effects (Nekrasov et al., 2017). Second-generation progeny (F1) were then cultivated by selfing the first-generation resistant mutants (F0), which resulted in the CRISPR/Cas9 transfer DNA plasmid being segregated away (Nekrasov et al., 2017). The F1 progeny also exhibited *O. neolycopersici* resistance, and whole-genome sequencing showed that no off-target mutations had occurred, and that no transgenic DNA was present (Nekrasov et al., 2017). A similar study by Wang et al. generated resistance in rice plants (*Oryza sativa*) to the rice blast pathogen *Magnaporthe oryzae* by using CRISPR/Cas9 to induce indels in an *S* gene that encodes proteins involved in sugar transport (SWEET proteins) (Wang et al., 2016). Wang et al. also used segregation to create non-transgenic, disease-resistant F1 progeny that exhibited all the desirable phenotypes from the wild-type plants (Wang et al., 2016). There are now a number of examples of CRISPR/Cas9 *S* gene mutants with enhanced disease resistance to various pathogens including: broad virus resistance in cucumber plants through disruption the eukaryotic translation initiation factor *eIF4E* (Chandrasekaran et al., 2016), resistance to bacteria and oomycete pathogens in tomato plants through deletions in a DMR6 gene (de Toledo Thomazella et al., 2016), bacterial canker-resistant Wanjincheng orange plants *via* mutations in the *CsLOB1* gene promoter (Peng et al., 2017), and powdery mildew resistance in wheat through Cas9-mediated mutations of the *TaEDR1* susceptibility gene (Zhang et al., 2017).

The above studies demonstrate the advantage of using the plant-gene approach in CRISPR/Cas9 research because the disruption of these genes with indels and the subsequent segregation of the transfer DNA results in disease-resistant plants that do not contain any transgenic material. However, the backcrossing required to segregate away the CRISPR/Cas9 plasmid DNA is only feasible in annual plants with short life cycles and is not suitable for perennial crop plants or forest species (Kanchiswamy et al., 2015). Non-transgenic CRISPR/Cas9 mutants can also be generated using a plasmid-free delivery system; this involves designing a pre-assembled enzymatic ribonucleoprotein (RNP) Cas9-sgRNA complex that is transfected directly into plant protoplasts. The Cas9-sgRNA RNP complex can modify the genomic target DNA but is subsequently degraded by the cell – this results in a disease-resistant plant mutant that contains no transgenic DNA (Makarova et al., 2018). These non-transgenic approaches are especially relevant in plant-based industries where the introduction of inter-specific transgenes generates public controversy around genetically modified organisms (GMOs) and initiates prohibitively strict regulations surrounding the use of such genetically modified plants. The ability of CRISPR/Cas9 to generate highly specific disease-resistant mutants that contain no foreign DNA allows for these plants to be used outside of the GMO regulatory framework (Kanchiswamy et al., 2015; Kanchiswamy, 2016; Makarova et al., 2018). It also allows specific genetic modifications to be made in the endogenous genomic context thereby avoiding the random insertion of transgenes from unrelated species and removing the risk of any unintended downstream effects from the presence of foreign DNA (Kim et al., 2014; Kanchiswamy et al., 2015; Kanchiswamy, 2016).

Using CRISPR/Cas9 to Target and Explore Genes in Filamentous Plant Pathogens

While the use of CRISPR/Cas9 to engineer pathogen resistance in plants is a promising approach to mitigating disease outbreaks, using CRISPR/Cas9 in pathogens is of equal interest both for the generation of avirulent strains and for increasing our understanding of how these species interact with their plant hosts to induce disease. So far, CRISPR/Cas9 research in plant pathogens has been far less prolific than research on plant disease resistance, and it has focused primarily on proof-of-concept experiments in filamentous fungi and oomycetes. The first successful demonstrations of CRISPR/Cas9 technology in filamentous fungi were independently published by four research groups in 2015, who all developed CRISPR/Cas9 systems in filamentous ascomycete species including *Neurospora crassa* (Matsu-ura et al., 2015), *Pyricularia oryzae* (Arazoe et al., 2015), *Trichoderma reesei* (Liu et al., 2015), and multiple *Aspergillus* species (Nødvig et al., 2015). These studies used Cas9 genes that were codon-optimized for filamentous fungi, endogenous promoters for expression of the sgRNA, and common fungal selection markers. More proof of concept studies followed and CRISPR/Cas9 was developed in a number of fungal species including important plant pathogens such as *Ustilago maydis* (corn smut: Schuster et al., 2016), *Fusarium graminearum* (Fusarium head blight of grain: Gardiner and Kazan, 2018), *F. oxysporum* (Fusarium wilt disease:

Wang et al., 2018), and *Sclerotinia sclerotiorum* (white mold: Li et al., 2018). The first CRISPR/Cas9 system in oomycetes was developed in the soybean pathogen *Phytophthora sojae*; the study used a Cas9 gene with human-optimized codons fused to the *P. sojae* nuclear localization signal (PsNLS) and driven by the oomycete Ham34 promoter (Fang and Tyler, 2016). CRISPR/Cas9 has now additionally been developed in *P. capsici* (Miao et al., 2018) and *P. palmivora* (Gumtow et al., 2018). A comprehensive review of the CRISPR/Cas9 techniques being used in filamentous fungi and oomycetes has been published by Schuster and Kahmann (2019); as with the plants, the CRISPR/Cas9 studies in filamentous pathogens have been focused on agriculturally important species, with no studies on forest pathogens reported in our literature search.

Targeting Pathogenicity Genes Using CRISPR/Cas9

The study on *S. sclerotiorum* by Li et al. (2018) is one of the few that has used CRISPR/Cas9 to generate pathogenicity mutants in a fungal plant pathogen. Their gene target was the oxalate biosynthesis gene *Ssoah1*, responsible for producing oxalic acid, which is involved in host tissue colonization by *S. sclerotiorum*. Li et al. generated DSBs at multiple *Ssoah1* target sites and found that fragments of their Cas9 transformation plasmid had been integrated into the *S. sclerotiorum* genome at the DSB sites; this demonstrated that the transformation plasmid was not only providing the Cas9 protein and sgRNA molecule, but also acting as a donor DNA molecule for the NHEJ pathway to repair the Cas9-induced DSB (Li et al., 2018). The Cas9-generated *S. sclerotiorum Ssoah1*-mutant strains exhibited significantly reduced oxalic acid production and reduced pathogenicity on soybean, Abyssinian cabbage, and tomato plants (Li et al., 2018). *Sclerotinia sclerotiorum* is a highly aggressive, necrotrophic phytopathogen with a very broad host range, so these results by Li et al. are very encouraging for the use of CRISPR/Cas9 as a tool for understanding the virulence of similar plant pathogens. Improved understanding of the specific modes of pathogenicity employed by different phytopathogens will subsequently improve management strategies for the diseases they cause.

An important group of pathogenicity genes are those encoding the effector proteins secreted by pathogens during host interactions. Effectors are an extremely diverse group of molecules and are found in some form in all groups of plant pathogens; they have a number of functions including facilitating infection, disrupting the plant immune response, and obtaining nutrients from host tissues (Toruño et al., 2016). Their ubiquity, as well as their dominant role in plant–pathogen interactions, makes them excellent candidates for CRISPR/Cas9 research. This was demonstrated by Fang and Tyler in the first study to develop a CRISPR/Cas9 system in oomycetes; they designed an sgRNA that targeted the RxLR effector gene *Avr4/6* in the soybean pathogen *Phytophthora sojae* (Fang and Tyler, 2016). RxLR effectors are widespread in oomycetes and can enter host cells and suppress effector-triggered immune responses (Jiang and Tyler, 2012). They can be detected by the receptors encoded by plant *R* genes (Jiang and Tyler, 2012); in soybeans the *R* genes involved in recognition of the Avr4/6 effector protein are *Rps*4 and *Rps*6 (Fang and Tyler, 2016). Fang and Tyler examined both the pathogen and host aspects of the *P. sojae* pathosystem: they used CRISPR/Cas9 to create five homozygous NHEJ *Avr4/6* mutants and two homozygous HDR *Avr4/6* mutants, and then assessed the interactions of the *P. sojae* mutants with soybean plants both with and without *Rps*4 or *Rps*6 resistance loci (Fang and Tyler, 2016). Their results showed that when inoculated with *P. sojae-Avr4/6* mutants, the *Rps4/Rps6* soybean plants were less able to defend themselves against infection, exhibiting an impaired immune response (Fang and Tyler, 2016).

The results from Fang and Tyler's 2016 study demonstrate the intricacy of plant–pathogen interactions and serve as a reminder for researchers wishing to use genetic engineering technologies to develop disease-resistant plants: using CRISPR/Cas9 to target an effector may impede the pathogen, but it might also have unintended consequences for the plant host depending on the recognition pathway associated with the effector. Systems that have coevolved for millions of years cannot be easily deconstructed, and if CRISPR/Cas9 is to be used as a tool for mitigating plant disease outbreaks the complexities of these systems must be considered. However, CRISPR/Cas9 provides a perfect opportunity to understand these complex pathosystems, and the study by Fang and Tyler is an excellent example of the use of CRISPR/Cas9 as a tool for elucidating the roles of pathogen genes *via* a functional genomics approach.

FUTURE PERSPECTIVES FOR CRISPR/CAS9 IN FOREST PATHOLOGY

Given the large number of studies on CRISPR/Cas9 in plant pathology and the promises for developing disease resistance, it is somewhat surprising that there is very little literature in the area of forest pathology (**Figure 2**). Forest pathogens are as devastating as their agricultural counterparts and can cause landscape level mortality that results in ecosystem-wide changes; well-known global examples include chestnut blight, Dutch elm disease, ash dieback, myrtle rust, white pine blister rust, and sudden oak death. However, disease management options are more limited in forestry than in agriculture; for example, the use of fungicides is generally confined to forest nurseries, with chemicals rarely being applied to trees once they have been planted. Disease resistance is one of the most promising avenues to combat forest pathogens, especially given the large geographical scales that these pathogens can affect. While there is recognition of the potential applications of CRISPR/Cas9 for forest ecosystems and a call for the use of this technology in these systems (Tsai and Xue, 2015; Fernandez i Marti and Dodd, 2018; Fritsche et al., 2018), no applied studies in forest pathosystems have been performed.

From the perspective of engineering plant disease resistance, this lack of CRISPR/Cas9 research in forest species is understandable for three major reasons. The first is that conifer species, which dominate forest ecosystems in the Northern Hemisphere, have significantly larger and more complex genomes than most agricultural angiosperms. Thus,

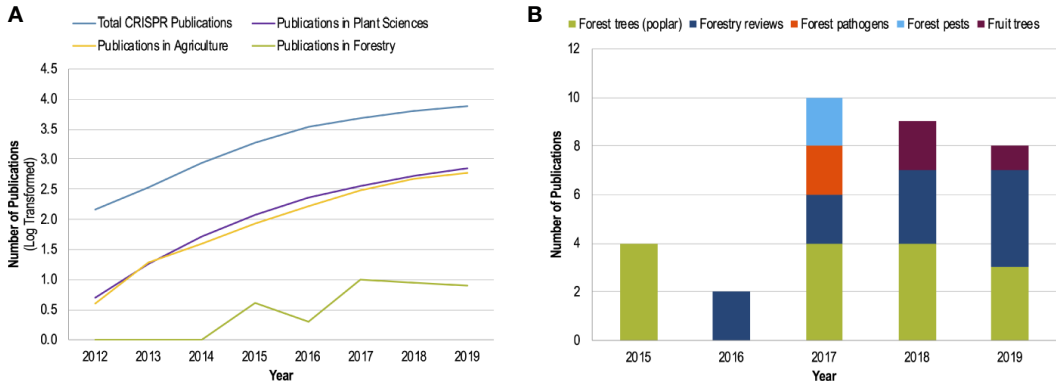

FIGURE 2 | The number of CRISPR publications by year since 2012 (development of CRISPR/Cas9 gene editing technology by Jinek et al.) obtained from a Web of Science topic search with the search parameters: 'CRISPR' or 'CRISPR-Cas*', or 'CRISPR/Cas*'. The 'Analyze Results' function of Web of Science was used to determine publication numbers by year and research area. **(A)** The log-transformed number of CRISPR publications by research area shows the common trend of increasing publications for CRISPR research for all areas except forestry. **(B)** A breakdown of the publication distribution by topic within forestry as determined by a manual search of the Web of Science search results.

there are far fewer whole genome sequences available (Nystedt et al., 2013; Neale et al., 2017)—a requirement for CRISPR/Cas9 gene editing in order to design effective sgRNAs and minimize off-target effects. The second reason is the increased difficulty of transformation protocols for forest tree species; this requires not only the transformation of DNA, but also the subsequent regeneration of the whole plant, which is a more time-consuming and complex process in woody perennial plants (Peña and Séguin, 2001; Fernandez i Marti and Dodd, 2018). The final reason is the controversy surrounding GMOs, which is shared with the agricultural sector, but is perhaps greater for woody forest species given their perennial nature and existence within semi-natural ecosystems; furthermore, the regulatory restrictions on genetically engineered trees are far stricter than those for agricultural crops (Strauss et al., 2009; Strauss et al., 2015; Strauss et al., 2016). Given these limitations, very few woody perennials have been successfully engineered with CRISPR/Cas9 relative to their annual counterparts, and the list of those that have is almost exclusively made up of agricultural species including *Coffea canephora* (coffee: Breitler et al., 2018), *Citrus sinensis* (sweet orange: Jia and Wang, 2014), *Citrus paradisi* (Duncan grapefruit: Jia et al., 2016), and *Malus* (apple: Malnoy et al., 2016; Nishitani et al., 2016). The only forest species for which CRISPR/Cas9 systems have been developed are those in the genus *Populus*: *P. tomentosa* (Fan et al., 2015; Jiang et al., 2017; Wan et al., 2017; Wang et al., 2017; Xu et al., 2017; Yang et al., 2017; Shen et al., 2018), *P. tremula* × *alba* (Zhou et al., 2015; Muhr et al., 2018), and *P. tremula* x *tremuloides* (Elorriaga et al., 2018). Only two of these studies used CRISPR/Cas9 to target genes involved in poplar disease resistance (Jiang et al., 2017; Wang et al., 2017).

Given the paucity of studies using CRISPR/Cas9 in forest tree species, it is not surprising that there are no published examples of the use of this technology in forest pathogens. However, there should be fewer obstacles for applying this approach to the pathogens since they are often taxonomically related to the oomycete and fungal species that cause disease on agricultural plants. The study by Fang and Tyler on *Phytophthora sojae* (2016) clearly demonstrated the power of CRISPR/Cas9 as a tool for gaining a deeper understanding of phytopathogens and how they interact with their plant hosts. Similar studies should be implemented in forest pathogens, and there are some forest pathosystems that are ideally suited for the use of CRISPR/Cas9 technology. Below, we give examples of four pathosystems that could be used to drive CRISPR/Cas9 research development in forest pathology (**Figure 3**): two using an approach of engineered resistance in the host, and two using an exploratory approach in the pathogen.

Proposed CRISPR/Cas9 Research in Four Forest Pathosystems

Engineering Disease Resistance in Poplars

While CRISPR/Cas9 research in poplars has already started, its focus has mainly been on modifying genes involved in growth, reproduction, and lignin development with the goal of improving *Populus* species for growth in plantations as well as use in the pulp and bio-refinery industries (Fan et al., 2015; Zhou et al., 2015; Wan et al., 2017; Xu et al., 2017; Yang et al., 2017; Elorriaga et al., 2018; Muhr et al., 2018; Shen et al., 2018; Chanoca et al., 2019). However, there are many potential applications for CRISPR/Cas9 technology for developing disease resistance, and perhaps the most promising application in forest pathology would be the genome editing of poplar species for resistance to their major pathogens, namely *Melampsora* and *Sphaerulina* species. In fact, the *Melampsora-Populus* pathosystems (**Figure 3A**) have previously been proposed as a model system to further our understanding of host–pathogen recognition mechanisms and the infection process (Feau et al., 2007) and would therefore be an excellent place to start CRISPR/Cas9 research in forest pathology.

Poplars are ecologically and economically valuable trees, playing important roles in both natural and managed forests,

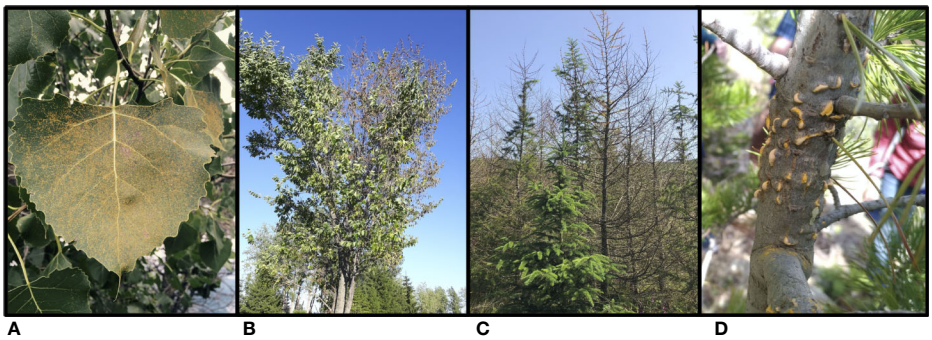

FIGURE 3 | The four forest pathosystems proposed for future CRISPR/Cas9 research: **(A)** uredinia of the poplar leaf rust pathogen *Melampsora medusae* f. sp. *deltoidis*, a basidiomycete fungus, on eastern cottonwood (*Populus deltoides*) leaves in Montréal, Quebec, CA (photo: Richard Hamelin, 2015); **(B)** flagging symptoms typical of Dutch elm disease, caused by the ascomycete fungal pathogen *Ophiostoma novo-ulmi*, on an American elm (*Ulmus americana*) in Québec, Quebec, CA (photo: Philippe Tanguay, 2016); **(C)** sudden larch death caused by the oomycete pathogen *Phytophthora ramorum* in a larch plantation in Galloway Forest Park, Scotland, GB (photo: Richard Hamelin, 2019); **(D)** aecia of the basidiomycete fungal pathogen *Cronartium ribicola*, causal agent of white pine blister rust, on a limber pine (*Pinus flexilis*) in Rocky Mountain National Park, Colorado, US (photo: Erika Dort, 2019).

and they have long been established as model species for molecular and genomic studies in forest trees (Bradshaw et al., 2000; Taylor, 2002; Wullschleger et al., 2002). Additionally, *Populus trichocarpa* was the first tree species to have its genome sequenced (Tuskan et al., 2006), which perfectly situates poplar pathosystems for study with CRISPR/Cas9. *Melampsora* leaf rusts and *Sphaerulina* leaf spot and stem canker pathogens are two of the most damaging groups of fungi affecting poplars in both natural stands and plantations, and they have major impacts on productivity and forest health. The barrier of entry for using CRISPR/Cas9 to engineer resistance to these pathogens is particularly low for two reasons, the first being that CRISPR/Cas9 protocols have already been established in *Populus* species (Fan et al., 2015; Zhou et al., 2015). The second reason is that candidate genes associated with resistance have already been identified for both *Melampsora* and *Sphaerulina* species (Yin et al., 2004; Duplessis et al., 2009; La Mantia et al., 2013; Muchero et al., 2018). As discussed previously, there have now been a number of studies using CRISPR/Cas9 in *Populus* species, and while two of these studies used CRISPR/Cas9 to explore the functions of genes in *Melampsora* resistance by creating knockout mutants (Jiang et al., 2017; Wang et al., 2017), none of them used CRISPR/Cas9 to directly engineer disease resistance.

Dutch Elm Disease

The possibility of using CRISPR/Cas9 to control the dominant Dutch elm disease (DED) pathogen *Ophiostoma novo-ulmi* (**Figure 3B**) is another exciting prospect. Genome sequencing and annotation of this pathogen has helped in identifying multiple candidate genes involved in the infection process (Forgetta et al., 2013; Khoshraftar et al., 2013; Comeau et al., 2015). Of particular interest are the genes involved in regulating the yeast-mycelial dimorphism exhibited by many *Ophiostoma* species. *Ophiostoma novo-ulmi* uses its budding yeast phase to travel rapidly through the tissues of its elm hosts but can also switch to a mycelial form that can penetrate xylem tissues and grow radially in the elm (Berrocal et al., 2012). This ability to switch between yeast and mycelial growth forms is thought to be involved in the pathogenicity of dimorphic fungi (Nadal et al., 2008), and has thus been explored in the DED pathogens for a number of years (Richards, 1994; Berrocal et al., 2012; Naruzawa and Bernier, 2014; Wedge et al., 2016). Transcriptomic analyses have identified candidate genes involved in this yeast-to-hypha transition (Nigg et al., 2015; Nigg and Bernier, 2016). These genes are excellent candidates for CRISPR/Cas9 gene editing: triggering the NHEJ pathway could create knockout mutants with reduced ability to switch to the yeast form thereby impeding translocation of the fungus throughout the elm tree.

Another group of interest as candidate genes involved in *O. novo-ulmi* pathogenicity are the secondary metabolite clusters. In plant pathogenic fungi, secondary metabolites such as host-selective toxins are well known to play an important role in disease development (Macheleidt et al., 2016). Bioinformatic annotations have identified *O. novo-ulmi* gene clusters putatively involved in biosynthesis of secondary metabolites, and interspecific comparative genomic analyses uncovered a fujikurin-like gene cluster (OpPKS8), found in the DED pathogens (*O. ulmi* and *O. novo-ulmi*) but absent in related non-phytopathogenic species (Sbaraini et al., 2017). According to phylogenetic analyses the authors suggested that this toxin-related cluster may have been horizontally acquired by DED pathogens (Sbaraini et al., 2017). Genes in the OpPKS8 cluster are good candidates for exploration with CRISPR/Cas9, which could be used as an additional tool to elucidate the functions of this secondary metabolite cluster and its potential role in pathogenicity.

Finally, a recent pangenomic analyses of a collection of strains from *O. ulmi* and *O. novo-ulmi* species showed that introgression has been the main driver of genomic diversity and has impacted fitness-related traits, with many of the introgressed regions containing genes involved in host–pathogen interactions and

eproduction (Hessenauer et al., 2020). Hessenauer et al. (2020) further demonstrated that the virulence of *O. novo-ulmi* was positively or negatively affected depending on the location of the introgressed genes in the genome. As with the secondary metabolites, CRISPR/Cas9 could be used as a means of exploring the functions of some of these introgressed genes that appear to play a role in virulence. Development of a CRISPR/Cas9 system in *O. novo-ulmi* has already begun (Tanguay, 2019), which makes implementing such pathogenicity-related strategies an impending reality.

Sudden Oak/Larch Death

Some filamentous plant pathogens exhibit virulence *via* their ability to suddenly switch lifestyles. This is the case in many fungal and oomycete species that are hemibiotrophs, meaning they can transition from an asymptomatic biotrophic phase to an aggressive necrotrophic phase in which they begin releasing toxins and killing host tissues (Lee and Rose, 2010; Koeck et al., 2011). The genes enabling this dual lifestyle could be effective targets for CRISPR/Cas9 in order to better understand how hemibiotrophic pathogens cause disease. Research in the oomycete pathogen, *Phytophthora infestans*, showed that effectors are the mediators of this lifestyle transition (Lee and Rose, 2010), which is not surprising given the dominant role these molecules play in plant–pathogen interactions. These results are very encouraging as CRISPR/Cas9 systems have already been developed in *P. sojae* (Fang et al., 2017), *P. capsici* (Miao et al., 2018), and *P. palmivora* (Gumtow et al., 2017), and it has proven successful in disrupting effector genes (Fang and Tyler, 2016; Gumtow et al., 2017). The invasive forest pathogen *Phytophthora ramorum* (**Figure 3C**), causal agent of sudden oak death in the United States (Rizzo et al., 2002a; Rizzo et al., 2002b) and sudden larch death in the United Kingdom (Webber et al., 2010), is another hemibiotrophic oomycete pathogen that causes devastating disease outbreaks in a broad range of woody hosts (Rizzo and Garbelotto, 2003). *Phytophthora ramorum* is classified as a highly aggressive pathogen given its ability to infect woody stems as well as foliar tissues, however, its hemibiotrophic nature allows it to remain asymptomatic anywhere from months to years before it transitions to its aggressive necrotrophic lifestyle (Rizzo and Garbelotto, 2003). It would therefore be an excellent candidate for CRISPR/Cas9 research exploring the role of effectors in mediating this lifestyle switch that influences virulence so significantly.

White Pine Blister Rust

White pine blister rust (WPBR), caused by the basidiomycete rust fungus *Cronartium ribicola* (**Figure 3D**), has severely affected North American populations of many economically and ecologically important pine species such as eastern and western white pines, sugar pine, and whitebark pine (Sniezko et al., 2014). In many white pine species both complete and partial resistance to WPBR have been detected. Complete resistance is mediated by a dominant *R* gene named *Cr*, which causes a hypersensitive response to *C. ribicola* and enables the pine host to survive by restricting the infection to the needles (Kinloch et al., 2003; Sniezko et al., 2014). Partial resistance appears to be a more complex response that is likely mediated by multiple genes, but the exact mechanisms driving this response are not yet known (Sniezko et al., 2014). While the *Cr* genes mediating complete resistance in white pines seem like the perfect candidates for CRISPR/Cas9-generated disease resistance, these *R* genes are likely not stable in the long-term because only a single mutation in a corresponding *C. ribicola* effector gene would be required to overcome this resistance (Sniezko et al., 2014). However, plant *R* gene immune receptors can be mutated to provide resistance to phylogenetically divergent pathogens (Segretin et al., 2014; Giannakopoulou et al., 2015), and CRISPR/Cas9 could be used to engineer such synthetic genes in tandem in order to create stable multi-resistance plant systems (Andolfo et al., 2016). Another option to obtain more durable long-term resistance in WPBR pathosystems is to focus CRISPR/Cas9 research on partial resistance. Cas9 can be co-expressed with many sgRNAs to simultaneously target multiple genes; this multiplex gene editing could facilitate the discovery of the genes involved in partial resistance, and it could also eventually be used to target those genes simultaneously in engineered WPBR-resistant pine populations. This partial resistance strategy may be less effective than complete resistance to a single *C. ribicola* strain, but it would be more stable in the long-term against a constantly evolving *C. ribicola* population exhibiting diverse mutations and could also protect pine hosts against other encroaching pathogen species.

The four suggestions above demonstrate the scope of utility of CRISPR/Cas9 gene editing technology and highlight how this tool has been underutilized in forest pathology. CRISPR/Cas9 is a relatively recent development, and there are clear obstacles to its use in forest pathosystems. However, given the large number of fungal and oomycete species for which CRISPR/Cas9 systems have now been established, the barrier of entry for pathologists studying filamentous forest pathogens has been lowered, and there is a generalized research pipeline that they can follow to implement this gene editing technology in their study organisms (**Figure 4**). This pipeline can comprise various approaches for developing a CRISPR/Cas9 system, including using different Cas9 delivery methods (RNP vs. plasmid) and genetic targets (DNA vs. RNA). **Figure 4** shows a generalized schematic of one such approach based on the CRISPR/Cas9 system being developed in the Dutch elm disease pathogen *Ophiostoma novo-ulmi* (Tanguay, 2019). We hope this gives forest pathologists a better understanding of the logistics involved in developing CRISPR/Cas9 systems in filamentous forest pathogens.

As sequencing technologies continue to improve and lower in cost, forest pathologists should aim to increase their exploration of the genetic basis of plant disease resistance *via* CRISPR/Cas9 gene editing. The power of this technology to aid our understanding of the intricacies of plant–pathogen interactions and generate effective strategies of disease resistance in forest pathosystems is much too great to ignore.

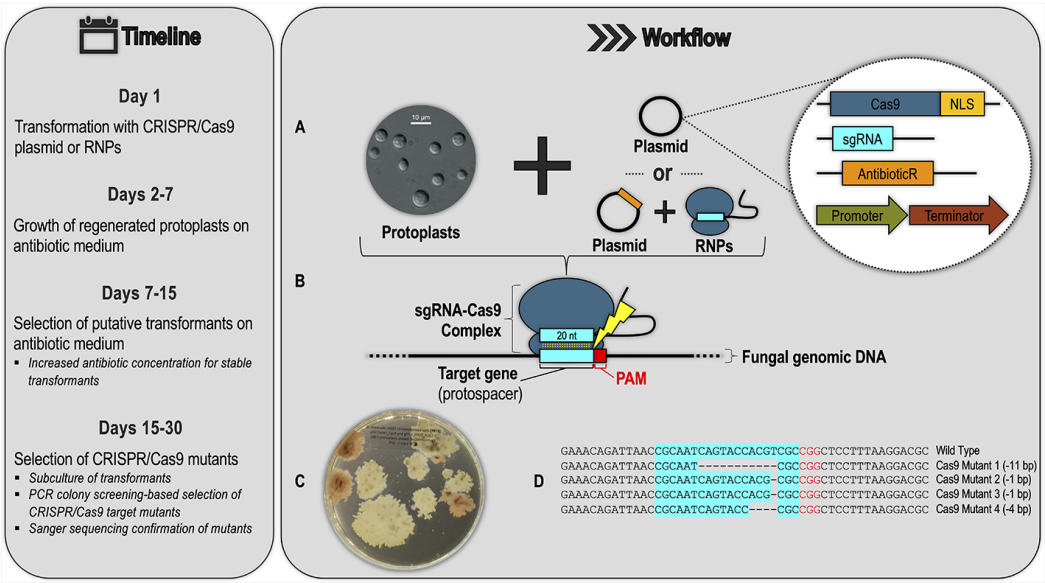

FIGURE 4 | Example of a generalized CRISPR/Cas9 workflow and timeline for a filamentous forest pathogen based on the protocol being developed for the Dutch elm disease pathogen *Ophiostoma novo-ulmi* (*Onu*). **(A)** Transformation of fungal protoplasts with a plasmid containing (see inset): a Cas9 gene fused to nuclear localization signal (NLS), a single-guide RNA (sgRNA) scaffold with a 20-nucleotide (nt) region designed to base-pair with the target genomic DNA, an antibiotic resistance gene for transformant selection, and gene promoters and terminators active in the target species. Alternatively, protoplasts can be co-transformed with a combination of Cas9-sgRNA ribonucleoprotein complexes (RNPs) and a plasmid for antibiotic transformant selection. **(B)** In successful transformants, Cas9 forms a complex with the sgRNA molecule, which guides the complex to the protospacer (a genomic DNA target in this example) with an adjacent PAM (protospacer adjacent motif) sequence. The sgRNA–Cas9 complex is analogous to the crRNA-effector complexes of native CRISPR/Cas systems, shown in **Figure 1** of this review. In the RNP approach, this sgRNA–Cas9 complex is pre-assembled and transfected directly into the protoplasts. **(C)** Transformants are selected by growth on antibiotic selective medium (picture shows *Onu* hygromycin-resistant transformants: pink colonies are CRISPR/Cas9 *ade2* mutants). **(D)** Successful CRISPR/Cas9 mutants are confirmed through sub-culture of the putative transformants from the previous step, PCR screening, and Sanger sequencing.

CONCLUSIONS

Since the discovery of CRISPR/Cas systems in 1987 (Ishino et al., 1987), our understanding of this adaptable immune response has come a long way, and the development of CRISPR/Cas9 gene editing technology in 2012 (Jinek et al., 2012) resulted in an explosion of research with wide-reaching implications for most biological systems. Despite the development of Cas9 tools in many pathosystems, there are still limitations to the use of CRISPR/Cas technology in plant pathology, especially concerning off-target effects. However, careful design of sgRNAs and modifications of the Cas proteins prevent most of these effects, and the use of RNP delivery systems has reduced off-target mutations to zero in many systems (Das et al., 2019). Additionally, the continued development of CRISPR/Cas technology in plant pathosystems will only improve efficiency as this technology is adapted to function in a diversity of organisms. To date, most CRISPR/Cas9 research in plant pathology has been focused on agricultural pathosystems, with little to no research in forest pathology. This is understandable given the availability of genomic resources for most major crops as well as the shorter generation times of crop plants relative to their forest counterparts, which makes for a quick feedback loop on any genetic modifications made with CRISPR/Cas9. However, forest pathogens are wreaking equal havoc in the forestry sector and represent a global threat to forest ecosystems that needs to be addressed immediately. The time is now to adopt CRISPR/Cas9 in forest pathology, at the very least to improve our understanding of host–pathogen interactions, but ideally to begin integrating it into forest improvement programs to generate more effective disease resistance strategies for long-term forest sustainability.

AUTHOR CONTRIBUTIONS

All authors listed have made a substantial, direct and intellectual contribution to the work, and approved it for publication.

FUNDING

This work was supported by Genome Canada's Large-Scale Applied Research Project (LSARP project #10106) with additional funding from Genome B.C., Genome Quebec, Canadian Food Inspection Agency, Natural Resources Canada and FPInnovations.

REFERENCES

Agudelo, D., Carter, S., Velimirovic, M., Duringer, A., Rivest, J.-F., Levesque, S., et al. (2020). Versatile and robust genome editing with *Streptococcus thermophilus* CRISPR1-Cas9. *Genome Res.* 30, 107–117. doi: 10.1101/gr.255414.119

Ali, Z., Abulfaraj, A., Idris, A., Ali, S., Tashkandi, M., and Mahfouz, M. M. (2015). CRISPR/Cas9-mediated viral interference in plants. *Genome Biol.* 16, 238. doi: 10.1186/s13059-015-0799-6

Ali, Z., Ali, S., Tashkandi, M., Zaidi, S. S.-A., and Mahfouz, M. M. (2016). CRISPR/Cas9-Mediated Immunity to Geminiviruses: Differential Interference and Evasion. *Sci. Rep.* 6, 26912. doi: 10.1038/srep26912

Anderson, P. K., Cunningham, A. A., Patel, N. G., Morales, F. J., Epstein, P. R., and Daszak, P. (2004). Emerging infectious diseases of plants: pathogen pollution, climate change and agrotechnology drivers. *Trends Ecol. Evol.* 19, 535–544. doi: 10.1016/j.tree.2004.07.021

Andolfo, G., Iovieno, P., Frusciante, L., and Ercolano, M. R. (2016). Genome-Editing Technologies for Enhancing Plant Disease Resistance. *Front. Plant Sci.* 7, 1813. doi: 10.3389/fpls.2016.01813

Arazoe, T., Miyoshi, K., Yamato, T., Ogawa, T., Ohsato, S., Arie, T., et al. (2015). Tailor-made CRISPR/Cas system for highly efficient targeted gene replacement in the rice blast fungus. *Biotechnol. Bioeng.* 112, 2543–2549. doi: 10.1002/bit.25662

Barrangou, R., Fremaux, C., Deveau, H., Richards, M., Boyaval, P., Moineau, S., et al. (2007). CRISPR Provides Acquired Resistance Against Viruses in Prokaryotes. *Science* 315, 1709–1712. doi: 10.1126/science.1138140

Berrocal, A., Navarrete, J., Oviedo, C., and Nickerson, K. W. (2012). Quorum sensing activity in *Ophiostoma ulmi*: effects of fusel oils and branched chain amino acids on yeast-mycelial dimorphism. *J. Appl. Microbiol.* 113, 126–134. doi: 10.1111/j.1365-2672.2012.05317.x

Bhaya, D., Davison, M., and Barrangou, R. (2011). CRISPR-Cas Systems in Bacteria and Archaea: Versatile Small RNAs for Adaptive Defense and Regulation. *Annu. Rev. Genet.* 45, 273–297. doi: 10.1146/annurev-genet-110410-132430

Bolotin, A., Quinquis, B., Sorokin, A., and Ehrlich, S. D. (2005). Clustered regularly interspaced short palindrome repeats (CRISPRs) have spacers of extrachromosomal origin. *Microbiology* 151, 2551–2561. doi: 10.1099/mic.0.28048-0

Bortesi, L., and Fischer, R. (2015). The CRISPR/Cas9 system for plant genome editing and beyond. *Biotechnol. Adv.* 33, 41–52. doi: 10.1016/j.biotechadv.2014.12.006

Bradshaw, H. D., Ceulemans, R., Davis, J., and Stettler, R. (2000). Emerging Model Systems in Plant Biology: Poplar (*Populus*) as A Model Forest Tree. *J. Plant Growth Regul.* 19, 306–313. doi: 10.1007/s003440000030

Breitler, J.-C., Dechamp, E., Campa, C., Zebral Rodrigues, L. A., Guyot, R., Marraccini, P., et al. (2018). CRISPR/Cas9-mediated efficient targeted mutagenesis has the potential to accelerate the domestication of *Coffea canephora*. *Plant Cell Tiss. Organ Cult.* 134, 383–394. doi: 10.1007/s11240-018-1429-2

Brooks, C., Nekrasov, V., Lippman, Z. B., and Van Eck, J. (2014). Efficient Gene Editing in Tomato in the First Generation Using the Clustered Regularly Interspaced Short Palindromic Repeats/CRISPR-Associated9 System. *Plant Physiol.* 166, 1292–1297. doi: 10.1104/pp.114.247577

Burstein, D., Harrington, L. B., Strutt, S. C., Probst, A. J., Anantharaman, K., Thomas, B. C., et al. (2017). New CRISPR–Cas systems from uncultivated microbes. *Nature* 542, 237–241. doi: 10.1038/nature21059

Ceccaldi, R., Rondinelli, B., and D'Andrea, A. D. (2016). Repair Pathway Choices and Consequences at the Double-Strand Break. *Trends Cell Biol.* 26, 52–64. doi: 10.1016/j.tcb.2015.07.009

Chandrasekaran, J., Brumin, M., Wolf, D., Leibman, D., Klap, C., Pearlsman, M., et al. (2016). Development of broad virus resistance in non-transgenic cucumber using CRISPR/Cas9 technology. *Mol. Plant Pathol.* 17, 1140–1153. doi: 10.1111/mpp.12375

Chanoca, A., de Vries, L., and Boerjan, W. (2019). Lignin Engineering in Forest Trees. *Front. Plant Sci.* 10, 912. doi: 10.3389/fpls.2019.00912

Clarivate Analytics (2020). Results Analysis Tool for Topic: "CRISPR." *Web Sci.*

Comeau, A. M., Dufour, J., Bouvet, G. F., Jacobi, V., Nigg, M., Henrissat, B., et al. (2015). Functional Annotation of the *Ophiostoma novo-ulmi* Genome: Insights into the Phytopathogenicity of the Fungal Agent of Dutch Elm Disease. *Genome Biol. Evol.* 7, 410–430. doi: 10.1093/gbe/evu281

Dangl, J. L., and Jones, J. D. G. (2001). Plant pathogens and integrated defence responses to infection. *Nature* 411, 826–833. doi: 10.1038/35081161

Das, A., Sharma, N., and Prasad, M. (2019). CRISPR/Cas9: A Novel Weapon in the Arsenal to Combat Plant Diseases. *Front. Plant Sci.* 9, 2008. doi: 10.3389/fpls.2018.02008

de Toledo Thomazella, D. P., Brail, Q., Dahlbeck, D., and Staskawicz, B. (2016). CRISPR-Cas9 mediated mutagenesis of a *DMR6* ortholog in tomato confers broad-spectrum disease resistance. *bioRxiv*. doi: 10.1101/064824

Deltcheva, E., Chylinski, K., Sharma, C. M., Gonzales, K., Chao, Y., Pirzada, Z. A., et al. (2011). CRISPR RNA maturation by *trans*-encoded small RNA and host factor RNase III. *Nature* 471, 602–607. doi: 10.1038/nature09886

Després, P. C., Dubé, A. K., Nielly-Thibault, L., Yachie, N., and Landry, C. R. (2018). Double Selection Enhances the Efficiency of Target-AID and Cas9-Based Genome Editing in Yeast. *G3: Genes Genomes Genet.* 8, 3163–3171. doi: 10.1534/g3.118.200461

Deveau, H., Barrangou, R., Garneau, J. E., Labonté, J., Fremaux, C., Boyaval, P., et al. (2008). Phage Response to CRISPR-Encoded Resistance in *Streptococcus thermophilus*. *J. Bacteriol.* 190, 1390–1400. doi: 10.1128/JB.01412-07

Duplessis, S., Major, I., Martin, F., and Séguin, A. (2009). Poplar and Pathogen Interactions: Insights from *Populus* Genome-Wide Analyses of Resistance and Defense Gene Families and Gene Expression Profiling. *Crit. Rev. Plant Sci.* 28, 309–334. doi: 10.1080/07352680903241063

Elorriaga, E., Klocko, A. L., Ma, C., and Strauss, S. H. (2018). Variation in Mutation Spectra Among CRISPR/Cas9 Mutagenized Poplars. *Front. Plant Sci.* 9, 594. doi: 10.3389/fpls.2018.00594

Fan, D., Liu, T., Li, C., Jiao, B., Li, S., Hou, Y., et al. (2015). Efficient CRISPR/Cas9-mediated Targeted Mutagenesis in Populus in the First Generation. *Sci. Rep.* 5, 12217. doi: 10.1038/srep12217

Fang, Y., and Tyler, B. M. (2016). Efficient disruption and replacement of an effector gene in the oomycete *Phytophthora sojae* using CRISPR/Cas9. *Mol. Plant Pathol.* 17, 127–139. doi: 10.1111/mpp.12318

Fang, Y., Cui, L., Gu, B., Arredondo, F., and Tyler, B. M. (2017). Efficient Genome Editing in the Oomycete *Phytophthora sojae* Using CRISPR/Cas9. *Curr. Protoc. Microbiol.* 44, 21A.1.1–21A.1.26. doi: 10.1002/cpmc.25

Feau, N., Joly, D. L., and Hamelin, R. C. (2007). Poplar leaf rusts: model pathogens for a model tree. *Can. J. Bot.* 85, 1127–1135. doi: 10.1139/B07-102

Feng, Z., Zhang, B., Ding, W., Liu, X., Yang, D.-L., Wei, P., et al. (2013). Efficient genome editing in plants using a CRISPR/Cas system. *Cell Res.* 23, 1229–1232. doi: 10.1038/cr.2013.114

Fernandez i Marti, A., and Dodd, R. S. (2018). Using CRISPR as a Gene Editing Tool for Validating Adaptive Gene Function in Tree Landscape Genomics. *Front. Ecol. Evol.* 6, 76. doi: 10.3389/fevo.2018.00076

Fisher, M. C., Henk, D. A., Briggs, C. J., Brownstein, J. S., Madoff, L. C., McCraw, S. L., et al. (2012). Emerging fungal threats to animal, plant and ecosystem health. *Nature* 484, 186–194. doi: 10.1038/nature10947

Forgetta, V., Leveque, G., Dias, J., Grove, D., Lyons, R., Genik, S., et al. (2013). Sequencing of the Dutch Elm Disease Fungus Genome Using the Roche/454 GS-FLX Titanium System in a Comparison of Multiple Genomics Core Facilities. *J. Biomol. Tech.* 24, 39–49. doi: 10.7171/jbt.12-2401-005

Fritsche, S., Poovaiah, C., MacRae, E., and Thorlby, G. (2018). A New Zealand Perspective on the Application and Regulation of Gene Editing. *Front. Plant Sci.* 9, 1323. doi: 10.3389/fpls.2018.01323

Gardiner, D. M., and Kazan, K. (2018). Selection is required for efficient Cas9-mediated genome editing in *Fusarium graminearum*. *Fungal Biol.* 122, 131–137. doi: 10.1016/j.funbio.2017.11.006

Garst, A. D., Bassalo, M. C., Pines, G., Lynch, S. A., Halweg-Edwards, A. L., Liu, R., et al. (2017). Genome-wide mapping of mutations at single-nucleotide resolution for protein, metabolic and genome engineering. *Nat. Biotechnol.* 35, 48–55. doi: 10.1038/nbt.3718

Giannakopoulou, A., Steele, J. F. C., Segretin, M. E., Bozkurt, T. O., Zhou, J., Robatzek, S., et al. (2015). Tomato I2 Immune Receptor Can Be Engineered to Confer Partial Resistance to the Oomycete *Phytophthora infestans* in Addition to the Fungus *Fusarium oxysporum*. *MPMI* 28, 1316–1329. doi: 10.1094/MPMI-07-15-0147-R

Gottesman, S. (2011). Dicing defence in bacteria. *Nature* 471, 588–589. doi: 10.1038/471588a

Gumtow, R., Wu, D., Uchida, J., and Tian, M. (2018). A *Phytophthora palmivora* Extracellular Cystatin-Like Protease Inhibitor Targets Papain to Contribute to Virulence on Papaya. *MPMI* 31, 363–373. doi: 10.1094/MPMI-06-17-0131-FI

Hessenauer, P., Fijarczyk, A., Martin, H., Prunier, J., Charron, G., Chapuis, J., et al. (2020). Hybridization and introgression drive genome evolution of Dutch elm disease pathogens. *Nat. Ecol. Evol.* 4, 626–638. doi: 10.1038/s41559-020-1133-6

Ishino, Y., Shinagawa, H., Makino, K., Amemura, M., and Nakata, A. (1987). Nucleotide sequence of the *iap* gene, responsible for alkaline phosphatase isozyme conversion in *Escherichia coli*, and identification of the gene product. *J. Bacteriol.* 169, 5429–5433. doi: 10.1128/jb.169.12.5429-5433.1987

Jansen, R., van Embden, J. D. A., Gaastra, W., and Schouls, L. M. (2002). Identification of genes that are associated with DNA repeats in prokaryotes. *Mol. Microbiol.* 43, 1565–1575. doi: 10.1046/j.1365-2958.2002.02839.x

Ji, X., Si, X., Zhang, Y., Zhang, H., Zhang, F., and Gao, C. (2018). Conferring DNA virus resistance with high specificity in plants using virus-inducible genome-editing system. *Genome Biol.* 19, 197. doi: 10.1186/s13059-018-1580-4

Jia, H., and Wang, N. (2014). Targeted Genome Editing of Sweet Orange Using Cas9/sgRNA. *PLoS One* 9, e93806. doi: 10.1371/journal.pone.0093806

Jia, H., Orbovic, V., Jones, J. B., and Wang, N. (2016). Modification of the PthA4 effector binding elements in Type I CsLOB1 promoter using Cas9/sgRNA to produce transgenic Duncan grapefruit alleviating XccΔpthA4:dCsLOB1.3 infection. *Plant Biotechnol. J.* 14, 1291–1301. doi: 10.1111/pbi.12495

Jiang, R. H. Y., and Tyler, B. M. (2012). Mechanisms and Evolution of Virulence in Oomycetes. *Annu. Rev. Phytopathol.* 50, 295–318. doi: 10.1146/annurev-phyto-081211-172912

Jiang, W., Zhou, H., Bi, H., Fromm, M., Yang, B., and Weeks, D. P. (2013). Demonstration of CRISPR/Cas9/sgRNA-mediated targeted gene modification in Arabidopsis, tobacco, sorghum and rice. *Nucleic Acids Res.* 41, e188. doi: 10.1093/nar/gkt780

Jiang, Y., Guo, L., Ma, X., Zhao, X., Jiao, B., Li, C., et al. (2017). The WRKY transcription factors PtrWRKY18 and PtrWRKY35 promote *Melampsora* resistance in *Populus*. *Tree Physiol.* 37, 665–675. doi: 10.1093/treephys/tpx008

Jinek, M., Chylinski, K., Fonfara, I., Hauer, M., Doudna, J. A., and Charpentier, E. (2012). A Programmable Dual-RNA–Guided DNA Endonuclease in Adaptive Bacterial Immunity. *Science* 337, 816–821. doi: 10.1126/science.1225829

Jones, J. D. G., and Dangl, J. L. (2006). The plant immune system. *Nature* 444, 323–329. doi: 10.1038/nature05286

Kanchiswamy, C. N., Malnoy, M., Velasco, R., Kim, J.-S., and Viola, R. (2015). Non-GMO genetically edited crop plants. *Trends Biotechnol.* 33, 489–491. doi: 10.1016/j.tibtech.2015.04.002

Kanchiswamy, C. N. (2016). DNA-free genome editing methods for targeted crop improvement. *Plant Cell Rep.* 35, 1469–1474. doi: 10.1007/s00299-016-1982-2

Khoshraftar, S., Hung, S., Khan, S., Gong, Y., Tyagi, V., Parkinson, J., et al. (2013). Sequencing and annotation of the *Ophiostoma ulmi* genome. *BMC Genomics* 14:162. doi: 10.1186/1471-2164-14-162

Kim, S., Kim, D., Cho, S. W., Kim, J., and Kim, J.-S. (2014). Highly efficient RNA-guided genome editing in human cells via delivery of purified Cas9 ribonucleoproteins. *Genome Res.* 24, 1012–1019. doi: 10.1101/gr.171322.113

Kinloch, B. B., Sniezko, R. A., and Dupper, G. E. (2003). Origin and Distribution of Cr2, a Gene for Resistance to White Pine Blister Rust in Natural Populations of Western White Pine. *Phytopathology* 93, 691–694. doi: 10.1094/PHYTO.2003.93.6.691

Kleinstiver, B. P., Prew, M. S., Tsai, S. Q., Topkar, V. V., Nguyen, N. T., Zheng, Z., et al. (2015). Engineered CRISPR-Cas9 nucleases with altered PAM specificities. *Nature* 523, 481–485. doi: 10.1038/nature14592

Koeck, M., Hardham, A. R., and Dodds, P. N. (2011). The role of effectors of biotrophic and hemibiotrophic fungi in infection. *Cell. Microbiol.* 13, 1849–1857. doi: 10.1111/j.1462-5822.2011.01665.x

Koonin, E. V., Makarova, K. S., and Zhang, F. (2017). Diversity, classification and evolution of CRISPR-Cas systems. *Curr. Opin. Microbiol.* 37, 67–78. doi: 10.1016/j.mib.2017.05.008

Kosicki, M., Tomberg, K., and Bradley, A. (2018). Repair of double-strand breaks induced by CRISPR–Cas9 leads to large deletions and complex rearrangements. *Nat. Biotechnol.* 36, 765–771. doi: 10.1038/nbt.4192

La Mantia, J., Klápště, J., El-Kassaby, Y. A., Azam, S., Guy, R. D., Douglas, C. J., et al. (2013). Association Analysis Identifies Melampsora ×columbiana Poplar Leaf Rust Resistance SNPs. *PLoS One* 8, e78423. doi: 10.1371/journal.pone.0078423

Langner, T., Kamoun, S., and Belhaj, K. (2018). CRISPR Crops: Plant Genome Editing Toward Disease Resistance. *Annu. Rev. Phytopathol.* 56, 479–512. doi: 10.1146/annurev-phyto-080417-050158

Lapin, D., and Van den Ackerveken, G. (2013). Susceptibility to plant disease: more than a failure of host immunity. *Trends Plant Sci.* 18, 546–554. doi: 10.1016/j.tplants.2013.05.005

Lee, S.-J., and Rose, J. K. C. (2010). Mediation of the transition from biotrophy to necrotrophy in hemibiotrophic plant pathogens by secreted effector proteins. *Plant Signaling Behav.* 5, 769–772. doi: 10.4161/psb.5.6.11778

Li, J., Zhang, Y., Zhang, Y., Yu, P.-L., Pan, H., and Rollins, J. A. (2018). Introduction of Large Sequence Inserts by CRISPR-Cas9 To Create Pathogenicity Mutants in the Multinucleate Filamentous Pathogen *Sclerotinia sclerotiorum*. *mBio* 9, e00567–e00518. doi: 10.1128/mBio.00567-18

Liang, Z., Zhang, K., Chen, K., and Gao, C. (2014). Targeted Mutagenesis in *Zea mays* Using TALENs and the CRISPR/Cas System. *J. Genet. Genomics* 41, 63–68. doi: 10.1016/j.jgg.2013.12.001

Liu, R., Chen, L., Jiang, Y., Zhou, Z., and Zou, G. (2015). Efficient genome editing in filamentous fungus *Trichoderma reesei* using the CRISPR/Cas9 system. *Cell Discovery* 1, 15007. doi: 10.1038/celldisc.2015.7

Macheleidt, J., Mattern, D. J., Fischer, J., Netzker, T., Weber, J., Schroeckh, V., et al. (2016). Regulation and Role of Fungal Secondary Metabolites. *Annu. Rev. Genet.* 50, 371–392. doi: 10.1146/annurev-genet-120215-035203

Makarova, K. S., Haft, D. H., Barrangou, R., Brouns, S. J. J., Charpentier, E., Horvath, P., et al. (2011). Evolution and classification of the CRISPR–Cas systems. *Nat. Rev. Microbiol.* 9, 467–477. doi: 10.1038/nrmicro2577

Makarova, K. S., Wolf, Y.II, Alkhnbashi, O. S., Costa, F., Shah, S. A., Saunders, S. J., et al. (2015). An updated evolutionary classification of CRISPR–Cas systems. *Nat. Rev. Microbiol.* 13, 722–736. doi: 10.1038/nrmicro3569

Makarova, S. S., Khromov, A. V., Spechenkova, N. A., Taliansky, M. E., and Kalinina, N. O. (2018). Application of the CRISPR/Cas System for Generation of Pathogen-Resistant Plants. *Biochem. Moscow* 83, 1552–1562. doi: 10.1134/S0006297918120131

Malnoy, M., Viola, R., Jung, M.-H., Koo, O.-J., Kim, S., Kim, J.-S., et al. (2016). DNA-Free Genetically Edited Grapevine and Apple Protoplast Using CRISPR/Cas9 Ribonucleoproteins. *Front. Plant Sci.* 7, 1904. doi: 10.3389/fpls.2016.01904

Marraffini, L. A., and Sontheimer, E. J. (2010). CRISPR interference: RNA-directed adaptive immunity in bacteria and archaea. *Nat. Rev. Genet.* 11, 181–190. doi: 10.1038/nrg2749

Matsu-ura, T., Baek, M., Kwon, J., and Hong, C. (2015). Efficient gene editing in Neurospora crassa with CRISPR technology. *Fungal Biol. Biotechnol.* 2, 4. doi: 10.1186/s40694-015-0015-1

Miao, J., Guo, D., Zhang, J., Huang, Q., Qin, G., Zhang, X., et al. (2013). Targeted mutagenesis in rice using CRISPR-Cas system. *Cell Res.* 23, 1233–1236. doi: 10.1038/cr.2013.123

Miao, J., Chi, Y., Lin, D., Tyler, B. M., and Liu, X. (2018). Mutations in ORP1 Conferring Oxathiapiprolin Resistance Confirmed by Genome Editing using CRISPR/Cas9 in *Phytophthora capsici* and *P. sojae*. *Phytopathology* 108, 1412–1419. doi: 10.1094/PHYTO-01-18-0010-R

Muchero, W., Sondreli, K. L., Chen, J.-G., Urbanowicz, B. R., Zhang, J., Singan, V., et al. (2018). Association mapping, transcriptomics, and transient expression identify candidate genes mediating plant–pathogen interactions in a tree. *PNAS* 115, 11573–11578. doi: 10.1073/pnas.1804428115

Muhr, M., Paulat, M., Awwanah, M., Brinkkötter, M., and Teichmann, T. (2018). CRISPR/Cas9-mediated knockout of *Populus* BRANCHED1 and BRANCHED2 orthologs reveals a major function in bud outgrowth control. *Tree Physiol.* 38, 1588–1597. doi: 10.1093/treephys/tpy088

Muñoz, I. V., Sarrocco, S., Malfatti, L., Baroncelli, R., and Vannacci, G. (2019). CRISPR-Cas for Fungal Genome Editing: A New Tool for the Management of Plant Diseases. *Front. Plant Sci.* 10, 135. doi: 10.3389/fpls.2019.00135

Nadal, M., García-Pedrajas, M. D., and Gold, S. E. (2008). Dimorphism in fungal plant pathogens. *FEMS Microbiol. Lett.* 284, 127–134. doi: 10.1111/j.1574-6968.2008.01173.x

Naruzawa, E. S., and Bernier, L. (2014). Control of yeast-mycelium dimorphism in vitro in Dutch elm disease fungi by manipulation of specific external stimuli. *Fungal Biol.* 118, 872–884. doi: 10.1016/j.funbio.2014.07.006

Neale, D. B., McGuire, P. E., Wheeler, N. C., Stevens, K. A., Crepeau, M. W., Cardeno, C., et al. (2017). The Douglas-Fir Genome Sequence Reveals

Specialization of the Photosynthetic Apparatus in Pinaceae. *G3: Genes Genomes Genet.* 7, 3157–3167. doi: 10.1534/g3.117.300078

Nekrasov, V., Staskawicz, B., Weigel, D., Jones, J. D. G., and Kamoun, S. (2013). Targeted mutagenesis in the model plant *Nicotiana benthamiana* using Cas9 RNA-guided endonuclease. *Nat. Biotechnol.* 31, 691–693. doi: 10.1038/nbt.2655

Nekrasov, V., Wang, C., Win, J., Lanz, C., Weigel, D., and Kamoun, S. (2017). Rapid generation of a transgene-free powdery mildew resistant tomato by genome deletion. *Sci. Rep.* 7, 482. doi: 10.1038/s41598-017-00578-x

Nigg, M., and Bernier, L. (2016). From yeast to hypha: defining transcriptomic signatures of the morphological switch in the dimorphic fungal pathogen *Ophiostoma novo-ulmi*. *BMC Genomics* 17, 920. doi: 10.1186/s12864-016-3251-8

Nigg, M., Laroche, J., Landry, C. R., and Bernier, L. (2015). RNAseq Analysis Highlights Specific Transcriptome Signatures of Yeast and Mycelial Growth Phases in the Dutch Elm Disease Fungus *Ophiostoma novo-ulmi*. *G3: Genes Genomes Genet.* 5, 2487–2495. doi: 10.1534/g3.115.021022

Nishida, K., Arazoe, T., Yachie, N., Banno, S., Kakimoto, M., Tabata, M., et al. (2016). Targeted nucleotide editing using hybrid prokaryotic and vertebrate adaptive immune systems. *Science* 353, aaf8729. doi: 10.1126/science.aaf8729

Nishitani, C., Hirai, N., Komori, S., Wada, M., Okada, K., Osakabe, K., et al. (2016). Efficient Genome Editing in Apple Using a CRISPR/Cas9 system. *Sci. Rep.* 6, 31481. doi: 10.1038/srep31481

Nødvig, C. S., Nielsen, J. B., Kogle, M. E., and Mortensen, U. H. (2015). A CRISPR-Cas9 System for Genetic Engineering of Filamentous Fungi. *PLoS One* 10, e0133085. doi: 10.1371/journal.pone.0133085

Nystedt, B., Street, N. R., Wetterbom, A., Zuccolo, A., Lin, Y.-C., Scofield, D. G., et al. (2013). The Norway spruce genome sequence and conifer genome evolution. *Nature* 497, 579–584. doi: 10.1038/nature12211

Pavan, S., Jacobsen, E., Visser, R. G. F., and Bai, Y. (2009). Loss of susceptibility as a novel breeding strategy for durable and broad-spectrum resistance. *Mol. Breed.* 25:1. doi: 10.1007/s11032-009-9323-6

Peña, L., and Séguin, A. (2001). Recent advances in the genetic transformation of trees. *Trends Biotechnol.* 19, 500–506. doi: 10.1016/S0167-7799(01)01815-7

Peng, A., Chen, S., Lei, T., Xu, L., He, Y., Wu, L., et al. (2017). Engineering canker-resistant plants through CRISPR/Cas9-targeted editing of the susceptibility gene CsLOB1 promoter in citrus. *Plant Biotechnol. J.* 15, 1509–1519. doi: 10.1111/pbi.12733

Pennisi, E. (2010). Armed and Dangerous. *Science* 327, 804–805. doi: 10.1126/science.327.5967.804

Pourcel, C., Salvignol, G., and Vergnaud, G. (2005). CRISPR elements in *Yersinia pestis* acquire new repeats by preferential uptake of bacteriophage DNA, and provide additional tools for evolutionary studies. *Microbiology* 151, 653–663. doi: 10.1099/mic.0.27437-0

Pyott, D. E., Sheehan, E., and Molnar, A. (2016). Engineering of CRISPR/Cas9-mediated potyvirus resistance in transgene-free *Arabidopsis* plants. *Mol. Plant Pathol.* 17, 1276–1288. doi: 10.1111/mpp.12417

Ranjha, L., Howard, S. M., and Cejka, P. (2018). Main steps in DNA double-strand break repair: an introduction to homologous recombination and related processes. *Chromosoma* 127, 187–214. doi: 10.1007/s00412-017-0658-1

Richards, W. C. (1994). Nonsporulation in the Dutch elm disease fungus *Ophiostoma ulmi*: evidence for control by a single nuclear gene. *Can. J. Bot.* 72, 461–467. doi: 10.1139/b94-061

Rizzo, D. M., and Garbelotto, M. (2003). Sudden oak death: endangering California and Oregon forest ecosystems. *Front. Ecol. Environ.* 1, 197–204. doi: 10.1890/1540-9295(2003)001[0197:SODECA]2.0.CO;2

Rizzo, D. M., Garbelotto, M., Davidson, J. M., Slaughter, G. W., and Koike, S. T. (2002a). *Phytophthora ramorum* as the Cause of Extensive Mortality of *Quercus* spp. and *Lithocarpus densiflorus* in California. *Plant Dis.* 86, 205–214. doi: 10.1094/PDIS.2002.86.3.205

Rizzo, D. M., Garbelotto, M., Davidson, J. M., Slaughter, W., and Koike, S. T. (2002b). *Phytophthora ramorum* and Sudden Oak Death in California: I. Host Relationships. In: R. B. Stanidord et al. *Proceedings of the Fifth Symposium on Oak Woodlands: Oaks in California's Challenging Landscape.* (USDA Forest Service Gen. Tech. Rep. PSW-GTR-184), 733–740.

Roy, K. R., Smith, J. D., Vonesch, S. C., Lin, G., Tu, C. S., Lederer, A. R., et al. (2018). Multiplexed precision genome editing with trackable genomic barcodes in yeast. *Nat. Biotechnol.* 36, 512–520. doi: 10.1038/nbt.4137

Sbaraini, N., Andreis, F. C., Thompson, C. E., Guedes, R. L. M., Junges, Â., Campos, T., et al. (2017). Genome-Wide Analysis of Secondary Metabolite Gene Clusters in *Ophiostoma ulmi* and *Ophiostoma novo-ulmi* Reveals a Fujikurin-Like Gene Cluster with a Putative Role in Infection. *Front. Microbiol.* 8, 1063. doi: 10.3389/fmicb.2017.01063

Schuster, M., and Kahmann, R. (2019). CRISPR-Cas9 genome editing approaches in filamentous fungi and oomycetes. *Fungal Genet. Biol.* 130, 43–53. doi: 10.1016/j.fgb.2019.04.016

Schuster, M., Schweizer, G., Reissmann, S., and Kahmann, R. (2016). Genome editing in *Ustilago maydis* using the CRISPR–Cas system. *Fungal Genet. Biol.* 89, 3–9. doi: 10.1016/j.fgb.2015.09.001

Segretin, M. E., Pais, M., Franceschetti, M., Chaparro-Garcia, A., Bos, J.II, Banfield, M. J., et al. (2014). Single Amino Acid Mutations in the Potato Immune Receptor R3a Expand Response to *Phytophthora* Effectors. *MPMI* 27, 624–637. doi: 10.1094/MPMI-02-14-0040-R

Shen, Y., Li, Y., Xu, D., Yang, C., Li, C., and Luo, K. (2018). Molecular cloning and characterization of a brassinosteriod biosynthesis-related gene *PtoDWF4* from *Populus tomentosa*. *Tree Physiol.* 38, 1424–1436. doi: 10.1093/treephys/tpy027

Shmakov, S., Abudayyeh, O. O., Makarova, K. S., Wolf, Y.II, Gootenberg, J. S., Semenova, E., et al. (2015). Discovery and Functional Characterization of Diverse Class 2 CRISPR-Cas Systems. *Mol. Cell* 60, 385–397. doi: 10.1016/j.molcel.2015.10.008

Sniezko, R. A., Smith, J., Liu, J.-J., and Hamelin, R. C. (2014). Genetic Resistance to Fusiform Rust in Southern Pines and White Pine Blister Rust in White Pines—A Contrasting Tale of Two Rust Pathosystems—Current Status and Future Prospects. *Forests* 5, 2050–2083. doi: 10.3390/f5092050

Standage-Beier, K., Brookhouser, N., Balachandran, P., Zhang, Q., Brafman, D. A., and Wang, X. (2019). RNA-Guided Recombinase-Cas9 Fusion Targets Genomic DNA Deletion and Integration. *CRISPR J.* 2, 209–222. doi: 10.1089/crispr.2019.0013

Strauss, S. H., Tan, H., Boerjan, W., and Sedjo, R. (2009). Strangled at birth? Forest biotech and the Convention on Biological Diversity. *Nat. Biotechnol.* 27, 519–527. doi: 10.1038/nbt0609-519

Strauss, S. H., Costanza, A., and Séguin, A. (2015). Genetically engineered trees: Paralysis from good intentions. *Science* 349, 794–795. doi: 10.1126/science.aab0493

Strauss, S. H., Ma, C., Ault, K., and Klocko, A. L. (2016). "Lessons from Two Decades of Field Trials with Genetically Modified Trees in the USA: Biology and Regulatory Compliance," in *Biosafety of Forest Transgenic Trees: Improving the Scientific Basis for Safe Tree Development and Implementation of EU Policy Directives Forestry Sciences*. Eds. C. Vettori, F. Gallardo, H. Häggman, V. Kazana, F. Migliacci, G. Pilate and M. Fladung (Dordrecht: Springer Netherlands), 101–124. doi: 10.1007/978-94-017-7531-1_5

Tanguay, P. (2019). CRISPR/Cas9 gene editing of the Dutch elm disease pathogen *Ophiostoma novo-ulmi*. *Can. J. Plant Pathol.* 41, 163–163. doi: 10.1080/0706066.12019.1519163

Taylor, G. (2002). *Populus*: Arabidopsis for Forestry. Do We Need a Model Tree? *Ann. Bot.* 90, 681–689. doi: 10.1093/aob/mcf255

Terns, M. P., and Terns, R. M. (2011). CRISPR-based adaptive immune systems. *Curr. Opin. Microbiol.* 14, 321–327. doi: 10.1016/j.mib.2011.03.005

Toruño, T. Y., Stergiopoulos, I., and Coaker, G. (2016). Plant-Pathogen Effectors: Cellular Probes Interfering with Plant Defenses in Spatial and Temporal Manners. *Annu. Rev. Phytopathol.* 54, 419–441. doi: 10.1146/annurev-phyto-080615-100204

Tsai, C.-J., and Xue, L.-J. (2015). CRISPRing into the woods. *GM Crops Food* 6, 206–215. doi: 10.1080/21645698.2015.1091553

Tuskan, G. A., DiFazio, S., Jansson, S., Bohlmann, J., Grigoriev, I., Hellsten, U., et al. (2006). The Genome of Black Cottonwood, *Populus trichocarpa* (Torr. & Gray). *Science* 313, 1596–1604. doi: 10.1126/science.1128691

van der Oost, J., Jore, M. M., Westra, E. R., Lundgren, M., and Brouns, S. J. J. (2009). CRISPR-based adaptive and heritable immunity in prokaryotes. *Trends Biochem. Sci.* 34, 401–407. doi: 10.1016/j.tibs.2009.05.002

Wan, S., Li, C., Ma, X., and Luo, K. (2017). PtrMYB57 contributes to the negative regulation of anthocyanin and proanthocyanidin biosynthesis in poplar. *Plant Cell Rep.* 36, 1263–1276. doi: 10.1007/s00299-017-2151-y

Wang, Y., Cheng, X., Shan, Q., Zhang, Y., Liu, J., Gao, C., et al. (2014). Simultaneous editing of three homoeoalleles in hexaploid bread wheat confers heritable resistance to powdery mildew. *Nat. Biotechnol.* 32, 947–951. doi: 10.1038/nbt.2969

Wang, F., Wang, C., Liu, P., Lei, C., Hao, W., Gao, Y., et al. (2016). Enhanced Rice Blast Resistance by CRISPR/Cas9-Targeted Mutagenesis of the ERF Transcription Factor Gene OsERF922. *PLoS One* 11, e0154027. doi: 10.1371/journal.pone.0154027

Wang, L., Ran, L., Hou, Y., Tian, Q., Li, C., Liu, R., et al. (2017). The transcription factor MYB115 contributes to the regulation of proanthocyanidin biosynthesis and enhances fungal resistance in poplar. *New Phytol.* 215, 351–367. doi: 10.1111/nph.14569

Wang, Q., Cobine, P. A., and Coleman, J. J. (2018). Efficient genome editing in *Fusarium oxysporum* based on CRISPR/Cas9 ribonucleoprotein complexes. *Fungal Genet. Biol.* 117, 21–29. doi: 10.1016/j.fgb.2018.05.003

Webber, J. F., Mullett, M., and Brasier, C. M. (2010). Dieback and mortality of plantation Japanese larch (*Larix kaempferi*) associated with infection by *Phytophthora ramorum*. *New Dis. Reps.* 22, 19. doi: 10.5197/j.2044-0588.2010.022.019

Wedge, M.-È., Naruzawa, E. S., Nigg, M., and Bernier, L. (2016). Diversity in yeast-mycelium dimorphism response of the Dutch elm disease pathogens: the inoculum size effect. *Can. J. Microbiol.* 62, 525–529. doi: 10.1139/cjm-2015-0795

Wiedenheft, B., Sternberg, S. H., and Doudna, J. A. (2012). RNA-guided genetic silencing systems in bacteria and archaea. *Nature* 482, 331–338. doi: 10.1038/nature10886

Wullschleger, S. D., Tuskan, G. A., and DiFazio, S. P. (2002). Genomics and the tree physiologist. *Tree Physiol.* 22, 1273–1276. doi: 10.1093/treephys/22.18.1273

Xu, C., Fu, X., Liu, R., Guo, L., Ran, L., Li, C., et al. (2017). PtoMYB170 positively regulates lignin deposition during wood formation in poplar and confers drought tolerance in transgenic Arabidopsis. *Tree Physiol.* 37, 1713–1726. doi: 10.1093/treephys/tpx093

Yang, L., Zhao, X., Ran, L., Li, C., Fan, D., and Luo, K. (2017). PtoMYB156 is involved in negative regulation of phenylpropanoid metabolism and secondary cell wall biosynthesis during wood formation in poplar. *Sci. Rep.* 7, 41209. doi: 10.1038/srep41209

Yin, T.-M., DiFazio, S. P., Gunter, L. E., Jawdy, S. S., Boerjan, W., and Tuskan, G. A. (2004). Genetic and physical mapping of *Melampsora* rust resistance genes in *Populus* and characterization of linkage disequilibrium and flanking genomic sequence. *New Phytol.* 164, 95–105. doi: 10.1111/j.1469-8137.2004.01161.x

Zhang, Y., Ge, X., Yang, F., Zhang, L., Zheng, J., Tan, X., et al. (2014). Comparison of non-canonical PAMs for CRISPR/Cas9-mediated DNA cleavage in human cells. *Sci. Rep.* 4, 5405. doi: 10.1038/srep05405

Zhang, Y., Bai, Y., Wu, G., Zou, S., Chen, Y., Gao, C., et al. (2017). Simultaneous modification of three homoeologs of *TaEDR 1* by genome editing enhances powdery mildew resistance in wheat. *Plant J.* 91, 714–724. doi: 10.1111/tpj.13599

Zhang, T., Zheng, Q., Yi, X., An, H., Zhao, Y., Ma, S., et al. (2018). Establishing RNA virus resistance in plants by harnessing CRISPR immune system. *Plant Biotechnol. J.* 16, 1415–1423. doi: 10.1111/pbi.12881

Zhou, X., Jacobs, T. B., Xue, L.-J., Harding, S. A., and Tsai, C.-J. (2015). Exploiting SNPs for biallelic CRISPR mutations in the outcrossing woody perennial *Populus* reveals 4-coumarate:CoA ligase specificity and redundancy. *New Phytol.* 208, 298–301. doi: 10.1111/nph.13

Conflict of Interest: The authors declare that the research was conducted in the absence of any commercial or financial relationships that could be construed as a potential conflict of interest.

frontiers in Microbiology

ORIGINAL RESEARCH
published: 08 September 2020
doi: 10.3389/fmicb.2020.02095

Metagenomics Reveal Correlations Between Microbial Organisms in Soils and the Health of *Populus euphratica*

Yu Tuo[1], Zhibao Dong[1]*, Xiping Wang[2], Beibei Gao[3], Chunming Zhu[1] and Fei Tuo[4]*

[1] School of Geography and Tourism, Shaanxi Normal University, Xi'an, China, [2] College of Horticulture, Northwest A&F University, Yangling, China, [3] Department of Pesticide Science, College of Plant Protection, Nanjing Agricultural University, State and Local Joint Engineering Research Center of Green Pesticide Invention and Application, Nanjing, China, [4] Greening Committee Office of Forestry Bureau of Yulin City, Yulin, China

OPEN ACCESS

Edited by:
Amy Brunner, Virginia Tech, United States

Reviewed by:
Muhammad Saleem, Alabama State University, United States
Victor Olalde, Unidad Irapuato (CINVESTAV), Mexico

***Correspondence:**
Yu Tuo
ytuo@snnu.edu.cn
Zhibao Dong
zbdong@snnu.edu.cn

Specialty section:
This article was submitted to Microbe and Virus Interactions with Plants, a section of the journal Frontiers in Microbiology

Received: *17 December 2019*
Accepted: *10 August 2020*
Published: *08 September 2020*

Citation:
Tuo Y, Dong Z, Wang X, Gao B, Zhu C and Tuo F (2020) Metagenomics Reveal Correlations Between Microbial Organisms in Soils and the Health of Populus euphratica. Front. Microbiol. 11:2095. doi: 10.3389/fmicb.2020.02095

Biological diversity plays an important role in the stability of ecosystems. The Mu Us Desert (MUD), located in Northern China, is an aeolian desert. Although it has been governed by a series of ecological restoration programs, the MUD still has limited biological diversity. *Populus euphratica* (*P. euphratica*), a xerophytic plant, has great potential to improve the biological diversity of the MUD. However, the survival rate of *P. euphratica* in the MUD has been very low. The current study tried to explore the mechanism of the high death rate of *P. euphratica* in the microbiome perspective. The correlation study between soil community composition and soil properties showed that water-filled pore space (WFPS), pH, EC, AP, NO_3^-, and NH_4^+ possess higher potential to change the bacterial community (18%) than the fungal community (9%). Principal coordinate analysis indicated that the composition of both bacteria (*Proteobacteria* and *Bacteroidetes*) and fungi (*Ascomycota*) in the root soil can be increased by *P. euphratica*. By systematically comparing between the fungal diversity in the root soil around *P. euphratica* and the pathogenic fungus extract from the pathogenic site of *P. euphratica*, we found that the high death rate of *P. euphratica* was associated with specific pathogenic fungus *Alternaria alternate* and *Didymella glomerata*. In addition, the microbiome composition analysis indicated that *P. euphratica* planting could also influence the portions of bacteria community, which also has great potential to lead to future infection. However, as the extraction and separation of bacteria from plants is challenging, the correlation between pathogenic bacteria and the high death rate of *P. euphratica* was not studied here and could be explored in future work.

Keywords: ***Populus euphratica*, Mu Us Desert, biological diversity, microbial communities, pathogen**

HIGHLIGHTS

- Soil microbiome can be influenced significantly by *Populus euphratica*.
- *A. alternate* and *D. glomerata* in soil can lead to the high death rate of *Populus euphratica*.
- Plant-pathogen interactions within bacteria and *Populus euphratica* death was observed.

INTRODUCTION

The Mu Us Desert (MUD) was once covered by 81 km^2 of sand dunes. Fortunately, after the efforts of several generations, its ecological environment has been greatly improved. Since 1978, the desert region in the MUD has been moved 400 km to the north (Feng et al., 2013; Li et al., 2013; Lai et al., 2016). The sand retreat was a great achievement and victory that made the MUD one of the most famous regional vegetation restorations (Li et al., 2019; Sun et al., 2019). However, the achievement of environmental management in the MUD is mainly attributed to the introduction of two kinds of plants: conifer pine and shrub. It is difficult for other conventional green plants to survive in the MUD due to the natural climate, and as a result, most of the restored areas were dominated by these two kinds of plants. Although proliferation of these species temporarily controlled the spread of the local desert and improved the local vegetation coverage, the limited biodiversity in the region renders the ecological environment fragile. The resulting risk of secondary desertification has always been an urgent problem for the ecological stability of the MUD region (Shu et al., 2018; Li et al., 2019).

YuLin (Yuyang District), located in the interior of the MUD, possesses 118.27 km^2 of grassland reclamation. YuLin is one of most typical vegetated areas of the MUD and has great potential as a pilot site due to its ecological stability (Li et al., 2019). *Populus euphratica*, a perennial woody plant with high salinity and aridity tolerance, is widely spread in Western China and adjacent Central Asian countries (Keram et al., 2019). Considering the growth habit of *P. euphratica*, the climatic and environmental conditions of the Yuyang District can be suitable for its growth (Shu et al., 2018). However, after several years of trying, the success of *P. euphratica*, which should be able to improve the ecological development in the MUD, has stagnated due to its high mortality rate. At the same time, some factors governing the success of *P. euphratica* have been discovered. After these *P. euphratica* trees were planted in the nursery garden, the survival rate was close to 100% within the first year. Once the *P. euphratica* trees were transferred outside, almost 50% of the saplings died within the second year. During the third year, less than 5% of these *P. euphratica* trees survived. Only 5% of these tested trees grew healthy after a probationary period of 3 years. By analyzing the dead plants, some typical symptoms, like stem cankers and rust disease, etc., were found. The symptoms identified in almost all of the dead *P. euphratica* were consistent. These fatal diseases seem to be a reliable reason for the high death rate of *P. euphratica*. At the same time, why was there such a large difference in the death rate among different growth periods? Where or how were the *P. euphratica* trees infected?

Previous studies indicated that, the plant-associated microbial communities could be affected by the tissue age of the plant, environmental conditions, and agronomical practices (Vorholt, 2012; Leff et al., 2015; Arrigoni et al., 2018). In this plant–pathogen interaction system, microbiome plays a vital role for the health of the plant. The microbiome transplanted by the soil could always predetermine future plant health (Wei et al., 2019). This study is focused on the bacterial and fungal community in the soil around *P. euphratica* and the endophyte pathogenic to *P. euphratica*. The biological diversity in different places at different periods was studied by high-throughput sequencing. In addition, the endophytes pathogenic to *P. euphratica* were extracted, isolated, and authenticated by DNA sequencing. We analyzed the correlations between microorganisms in soils and endophytes in the pathogenetic *P. euphratica*.

MATERIALS AND METHODS

Sampling Sites

According to the tree age, four different sampling sites were arranged: Sampling Site 1 (half year), the new development area of Yulin where *P. euphratica* had not been transplanted (XKWY, 38°9′37.7″N, 109°41′9.2″E) in the MUD, Yu Yang District, Northwest China; Sampling Site 2 (1 year), the new development area of Yunlin where *P. euphratica* were transplanted (XKY, 38°26′38.0″N, 109°35′38.2″E) in the MUD, Yu Yang District, Northwest China; Sampling Site 3 (2 years), the afforestation land (ZLD, 38°25′58.2″N, 109°37′18.7″E) in the MUD, Yu Yang District, Northwest China; Sampling Site 4 (3 years), Airport Road study site (JCL, 38°23′11.2″N, 109°37′11.78026″E) in the MUD, Yu Yang District, Northwest China. At the JCL study site, three types of different soils were investigated: JCLH, the soil around the surviving *P. euphratica* after 3 years of planting in JCL; JCLS, the soil around the dead *P. euphratica* after 3 years of planting in JCL; and JCLYLT, the soil in JCL without *P. euphratica* planting.

Collection of Soil and Plant Samples

Six replications were conducted at all sampling sites of the selected soil samples. Soil samples were collected surrounding the soil stem, approximately 20 cm in diameter, of *P. euphratica* at depths from 10 to 50 cm. After thoroughly mixing, 100 g of prepared soil samples was stored at −80°C for sequencing. Corresponding air-dried soil samples were sieved by a 2-mm mesh and stored at 4°C for the analysis of soil physicochemical properties. The diseased parts of *P. euphratica* at different study sites were imaged and collected by cutting off the target stem.

Isolation of Plant Endophytes

Twenty-four pathogenetic *P. euphratica* samples were collected from XKY, ZLD, and JCL. The collected samples were disinfected by 75% ethanol for 1 min and 10% NaClO for 5 min (surface treatment). After then, the disinfected samples were rinsed thoroughly by sterile water and then dried in aseptic fume

hood. Finally, the sterilized symptomatic stems were cultured by potato dextrose agar (PDA) culture medium, with antibiotic supplements (50 μg/ml of ampicillin and streptomycin sulfate), at 25°C. The characteristics of cultured mycelium on PDA were observed daily and isolated. The microscopic morphological characteristics of isolated colony were observed and recorded (Olympus, Tokyo, Japan). All the valuable biological materials have been protected, controlled, and accounted according the laboratory biosecurity guidance (WHO/CDS/EPR/2006.6) of World Health Organization (WHO).

DNA Extraction, Sequencing, and Analysis

Details of DNA extraction are shown in **Supplementary Text S1**. In brief, total DNA extraction of 36 soil samples was conducted (six groups with six repeats). DNA extraction of each sample possesses two technical replicates. The quality and concentration of extracted DNA were assessed. Samples were stored at −20°C before use. Details of bacteria 16S rRNA and fungi ITS gene amplicon sequencing are shown in **Supplementary Text S2**. Amplicon sequences were analyzed using the "DADA2" package in the R environment (version 3.6.1). Corresponding details are shown in **Supplementary Text S3**.

Statistical Analysis

The bacterial community composition differences among treatments were tested by PERMANOVA (adonis, transformed data by Bray–Curtis, permutation = 999), implemented in R version 3.6.1. The DESeq function of the "DESeq2" package (version 1.18.1) was employed to test for differentially abundant ASVs among treatments. Statistical significance was based on a value of $p < 0.05$ (with FDR < 5% under the Benjamini–Hochberg correction).

RESULTS

Correlation Between the Community Composition and Soil Properties

The correlation between the community composition and soil properties was statistically analyzed based on six different types of soil. These parameters, including water-filled pore space (WFPS), pH, EC, AP, NO_3^-, and NH_4^+, are shown in **Supplementary Table S1** and **Figure 1**. For the bacteria, the influence degree of the abovementioned parameters ranged as follows: pH > EC > WFPS > NO_3^- > AP > NH_4^+ (**Figure 1A**). These soil properties contributed to 18% of the change in the bacterial community (**Figure 1A**). According to the results of the correlation analysis, the influence of pH mainly affected *Massilia* and *Rhodococcus*, EC had a higher influence on *Devosia*; and NO_3^- on *Candidatus nitrososphaera*. For the fungi, the degree of influence of the abovementioned parameters ranged as follows: EC > pH > NO_3^- > WFPS > AP > NH_4^+ (**Figure 1C**). These soil properties contributed to 9% of the change in the fungal community (**Figure 1C**). In addition, the influence of EC mainly focused on *Psathyrella*, *Coprinellus*, *Mallocybe*, *Peziza*, and *Arcopilus*; NO_3^- mainly influenced *Psathyrella*, *Coprinellus*, *Mallocybe*, and *Arcopilus*; and WFPS mainly influenced *Psathyrella*.

Morphological Characteristics and Identification of Endophytic Fungi

To explore the correlations between stem pathogen infection and microbiome assemblage in the root soil, the endophytic fungi in the symptomatic segments were isolated and identified (**Figure 2**). A–D in **Figure 2** is four typical symptoms of diseased *P. euphratica* in XKY, ZLD, and JCL. Finally, a total of 10 types of endophytic fungi were isolated and identified. Among these fungi, *Epicoccum nigrum* can produce some colored pigments, which are antifungal agents against other pathogenic fungi (Brown et al., 1987; Sun et al., 2011; Radić and Štrukelj, 2012), and *Alternaria* species (*Alternaria alternate*, *Alternaria tenuissima*), whose killing power release depends on a high-humidity environment (Moral et al., 2018). *Phoma glomerata*, which has an excellent ecological plasticity, can be permitted by 90 different kinds of plants and normally can cause leaf spot (Dörr et al., 2011). *Trichoderma* is a widespread fungus that is considered as an opportunistic avirulent plant symbiont (Harman et al., 2004; Bae et al., 2011). Previously, reports of *Cladosporium oxysporum* indicated that it has pathogenic effects on tomato and some vegetables, while it normally causes leaf spot (Wilingham et al., 2002; Baiswar et al., 2011; Zheng et al., 2014). *Didymella glomerata* is within the *Didymellaceae* family, which can cause stem lesions or cankers (Chen et al., 2015; Basim et al., 2016; Yao et al., 2016; Donati et al., 2018). The *Valsa* genus (*Valsasordida*, *Valsanivea*, *Valsamalicola*, and *Valsamali*) belongs to the family of Valsaceae, which can cause trunk diseases. Additionally, trunk diseases possess great power to kill young poplar trees 2 or 3 years after infection (Yi and Chi, 2011; Ma et al., 2016; Aghdam et al., 2017; Liu et al., 2018; Yu et al., 2018).

Effects of *P. euphratica* on the Soil Microbial Community

According to the results of relative abundance analysis, for the bacteria, the most common phyla in the six types of soils were *Proteobacteria*, *Bacteroidetes*, *Acidobacteria*, *Actinobacteria*, and *Thaumarchaeota*. After *P. euphratica* planting, the relative abundance of *Proteobacteria* (dominant OTUs: OTU_12049, OTU_12644) (**Supplementary Figure S1**) and *Bacteroidetes* (dominant OTUs: OTU_13655, OTU_13821) (**Supplementary Figure S1**) increased (**Figure 3A**). However, the portions of *Actinobacteria* (dominant OTUs: OTU_22374) (**Supplementary Figure S1**) and *Thaumarchaeota* (dominant OTUs: OTU_5953, OTU_5954) (**Supplementary Figure S1**) were decreased (**Figure 3A**). At the same time, the fungi *Ascomycota* (dominant OTUs: OTU_3086, OTU_3548 and OTU_3550) (**Figure 6**) and *Basidiomycota* (dominant OTUs: OTU_2456) (**Figure 6**) were two of the most common fungal phyla. After *P. euphratica* planting, compared with the soil without *P. euphratica*, the relative abundance of *Ascomycota* in all the selected soils, except XKY, was increased (**Figure 3B**). However, the relative abundance of *Basidiomycota* was decreased in JCLH, JCLS,

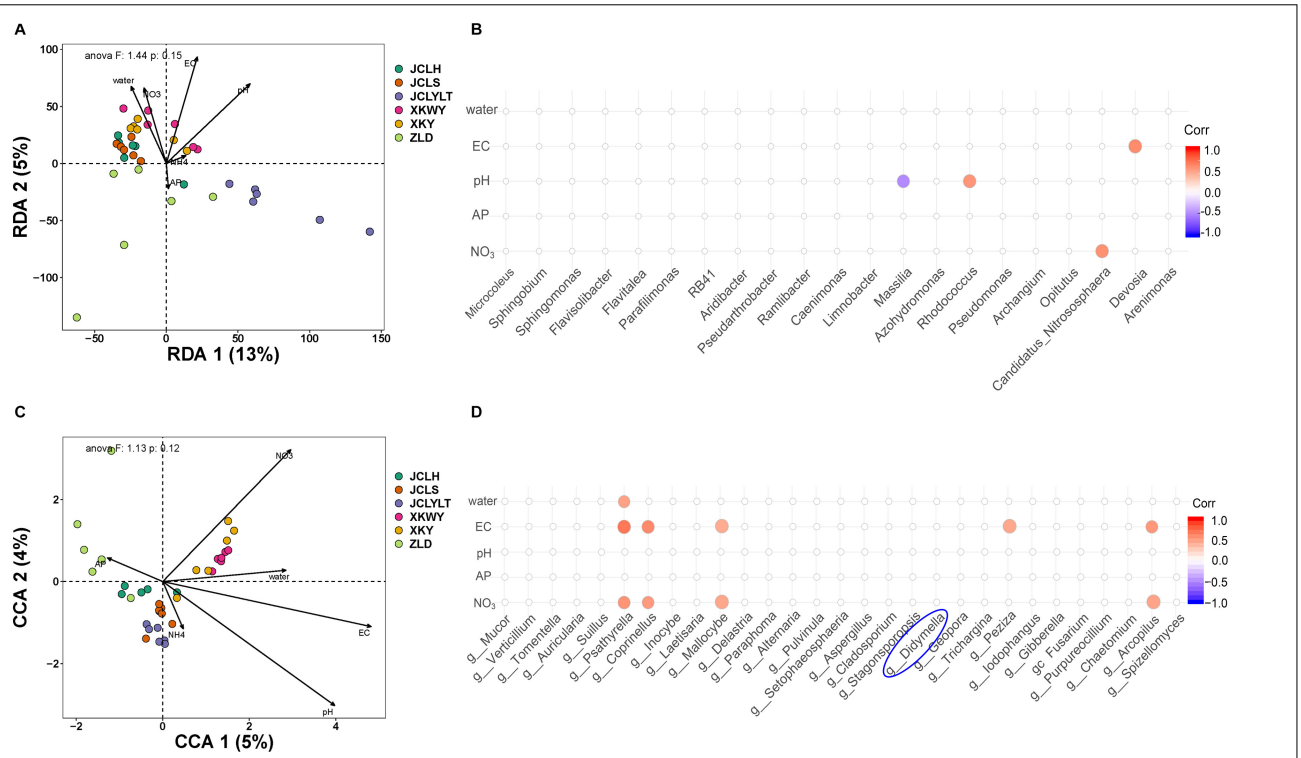

FIGURE 1 | The influence degree of soil properties to the **(A)** bacterial community, **(C)** fungal community, and corresponding correlations between soil properties and **(B)** bacteria and **(D)** fungi.

XKWY, and ZLD. Interestingly, XKY was the only exception (**Figure 3B**). By comparing the results of the relative abundance changing between the phyla level and the dominant OTUs level, we found that the relative abundance changing of similar trend dominant OTUs could meet with the phyla level well (**Figures 3**, **6** and **Supplementary Figure S1**).

α-Diversity

The results of the observed α-diversity are shown in **Figures 4A**, 5A, which indicated that *P. euphratica* planting could influence the community diversity of both bacteria and fungi significantly. Overall, the number of OTUs in the same soil sample was higher for bacteria than for fungi. For the bacteria, the community richness (**Figure 4A**, eveness Simpson) was increased after *P. euphratica* planting compared with JCLYLT. As for the species diversity (**Figure 4A**, Shannon), XKWY, XKY, and ZLD have higher species diversity than JCL. After *P. euphratica* planting, the species diversity difference of JCLH, JCLS, and JCLYL was not obvious. For the fungi, the community richness in JCLS was higher than that in other experimental sites (**Figure 5A**, eveness Simpson). Additionally, a similar tendency existed in the community diversity (**Figure 5A**, Shannon).

β-Diversity

For the bacterial community, the Bray–Curtis dissimilarity principal coordinate analysis (PCoA) results showed significant differences in the soils of JCL, XKWY, XKY, and ZLD (**Figure 4B**). In the JCL soils, after *P. euphratica* planting, both JCLS and JCLH showed pronounced differences compared to JCLYLT. The bacterial community between JCLS and JCLH was not completely separated. For the fungal community, the PCoA results indicated that the fungal community in the selected soil showed significant differences (**Figure 5B**). In the JCL soils, after *P. euphratica* planting, both JCLS and JCLH showed pronounced differences compared to JCLYLT. Similar to the bacterial community, the fungal community between JCLS and JCLH was not completely separated.

The differential abundance of bacteria and fungi of six selected soil sites are shown in **Figures 4C**, **5C**. The phyla with significant community differences from all the selected OTUs were presented.

The differential abundances of bacteria and fungi of six selected soil sites are shown in **Figures 4C**, **5C**. The phyla with significant community differences based on all the selected OTUs were presented.

DISCUSSION

The composition of soil microbiomes can be influenced by multiple environmental factors, and further interactions between pathogens and plants face the same situation (Xu et al., 2015; Wei et al., 2019). The results of this study indicated that soil physicochemical properties changed the composition of bacterial and fungal communities. Different parameters always possess, to some extent, a preference for specific phyla. For the bacteria,

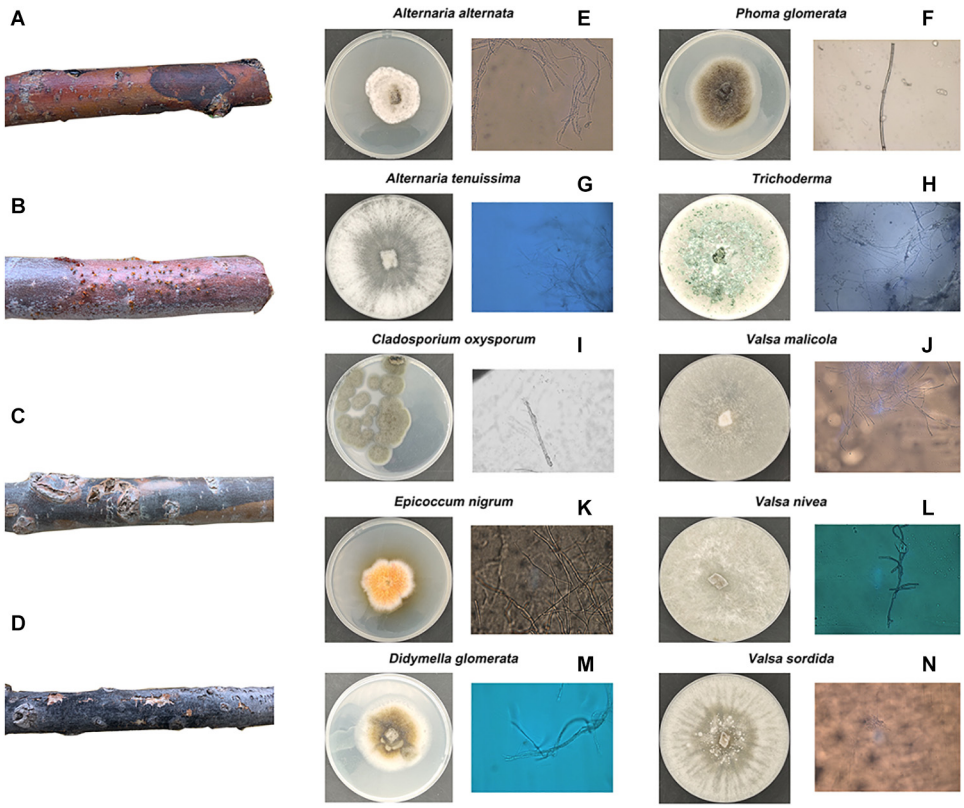

FIGURE 2 | Four kinds of common morphological characteristics of diseased *Populus euphrasae* in XKY, ZLD, and JCL are shown in **(A–D)**. The endophytic fungi isolated and identified from **(A–D)** are shown in **(E–N)**.

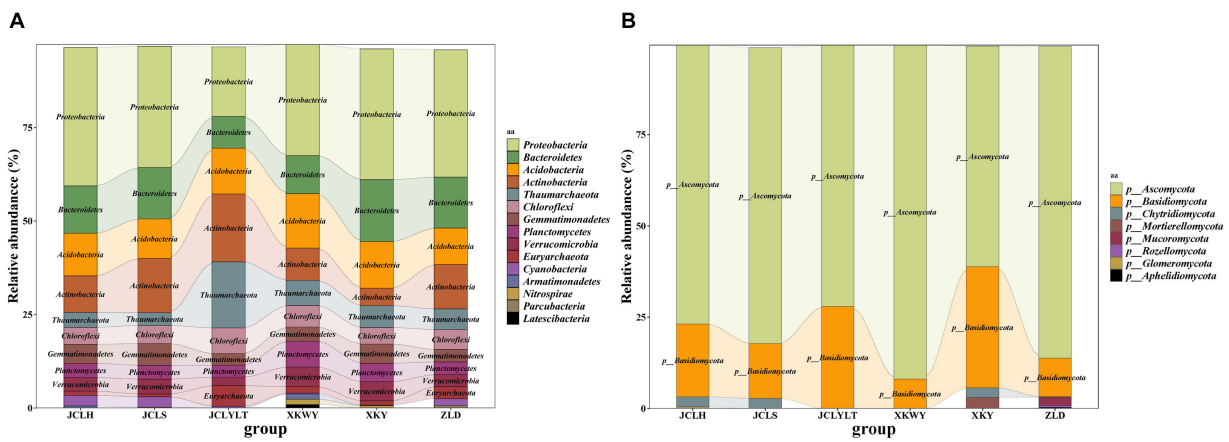

FIGURE 3 | The relative abundance of **(A)** bacterial community and **(B)** fungal community.

four different phyla were identified after taking the bacterial composition of all the sequenced soil samples into consideration. These affected phyla included *Massilia*, *Rhodococcus*, *Devosia*, and *Candidatus Nitrososphaera*. Previous studies have shown that most Rhodococcus species are benign (Mcleod et al., 2006). The genus *Massilia* possesses bacteria that are able to suppress pathogens for healthy plants. Studies of *Devosia* and *Candidatus Nitrososphaera* are scarce, and the pathogenicity of these genera remains unclear (Scola et al., 1998; Vannini et al., 2004; Zhalnina et al., 2014). For the fungi, EC, NO_3^-, and WFPS contributed some effect to five phyla, independent or synergistic. All the phyla had not been isolated and identified in symptomatic segments. Bacterial isolation and identification from infected segments were not studied here due to the large complexity.

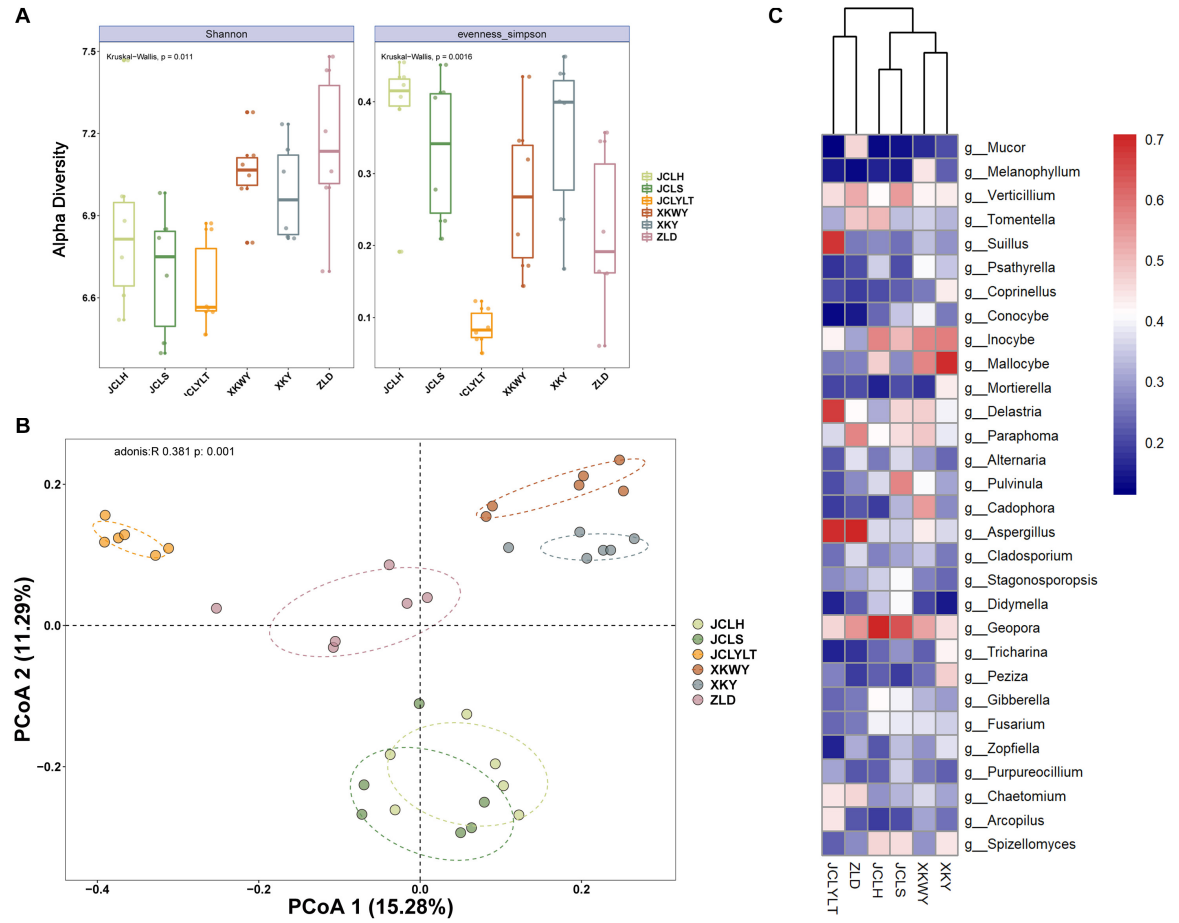

FIGURE 4 | (A) Alpha diversity analysis based on the OTUs account for the species richness using eveness Simpson index and species diversity using Shannon index. **(B)** The Bray–Curtis dissimilarity principal coordinate analysis (PCoA) of bacterial community structures in different soils. **(C)** Characteristic bacterial populations with significant community differences in different soils.

Figures 4B, **5B** show that the microbial community structure in the soils around the surviving *P. euphratica* is markedly different ($P < 0.001$). These results show the foundation difference of soil microbiome composition between different study sites. For the JCL sites, after *P. euphratica* planting, the microbiome community structures in both JCLH and JCLS were separated completely from JCLYLT ($P < 0.001$) (**Figures 4B**, **5B**). At the same time, the soil bacterial and fungal community structures between JCLH and JCLS almost clustered into two distinct groups but were not thoroughly separated ($P < 0.001$, accounting for 26.57% of the bacterial community and 28.86% of the fungal community). Early reports showed that variations in soil microbiome community structures and functions can affect target plants and determine whether the plants survived or succumbed to disease (Wei et al., 2019). In addition to composition, microbiome diversity level is also an important predictor for the soil health and plant growth (Saleem et al., 2019). Therefore, significant soil microbiome community structures have a great potential to lead to the high death rate of *P. euphratica*.

In this study, 10 types of endophytic fungi were isolated and identified. After systematic literature review, we found that *Alternaria* (*A. alternate*, *A. tenuissima*), *D. glomerata*, and the *Valsa* genus (*Valsa sordida*, *Valsa nivea*, *Valsa malicola*, *Valsa mali*) have great potential to participate in plant–pathogen interactions. Results showed that Ascomycota was the major fungal component in the selected soils with or without *P. euphratica* planting. Interestingly, *Alternaria*, *Didymella*, and *Valsa* all belong to the division of Ascomycota. By analyzing several characteristic fungal populations (the abundance of specific phyla in the studied soils that possess dramatic differences except *Valsa*, $p < 0.05$), we found that for the *Alternaria*, the relative abundance of *Alternaria* (OTU_3086, on behalf of *Alternaria alternate*) in JCLS was the highest within six selected soils (**Figure 6A**). The abundance of *Alternaria* in different studied sites followed an interesting rank: JCLS > ZLD > JCLH > XKWY ≈ XKY ≈ JCLYLT. The relative abundance of *Didymella* in JCLS was the highest. The abundance of *Didymella* (3,550 OTUs, on behalf of *D. glomerata*) in different studied sites followed an interesting

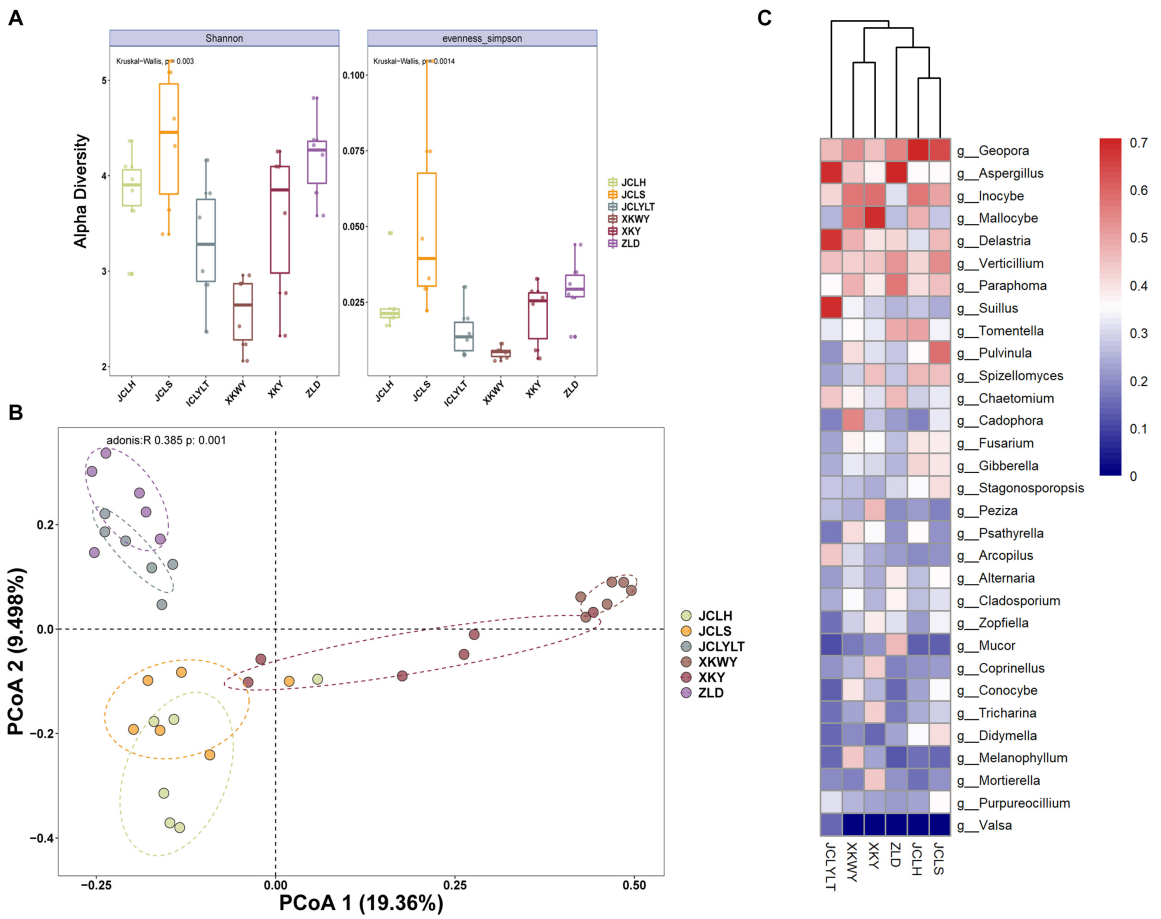

FIGURE 5 | (A) Alpha diversity analysis based on the OTUs account for the species richness using eveness Simpson index and species diversity using Shannon index. **(B)** Bray–Curtis dissimilarity principal coordinate analysis (PCoA) of fungal community structures in different soils. **(C)** Characteristic fungal populations with significant community differences in different soils.

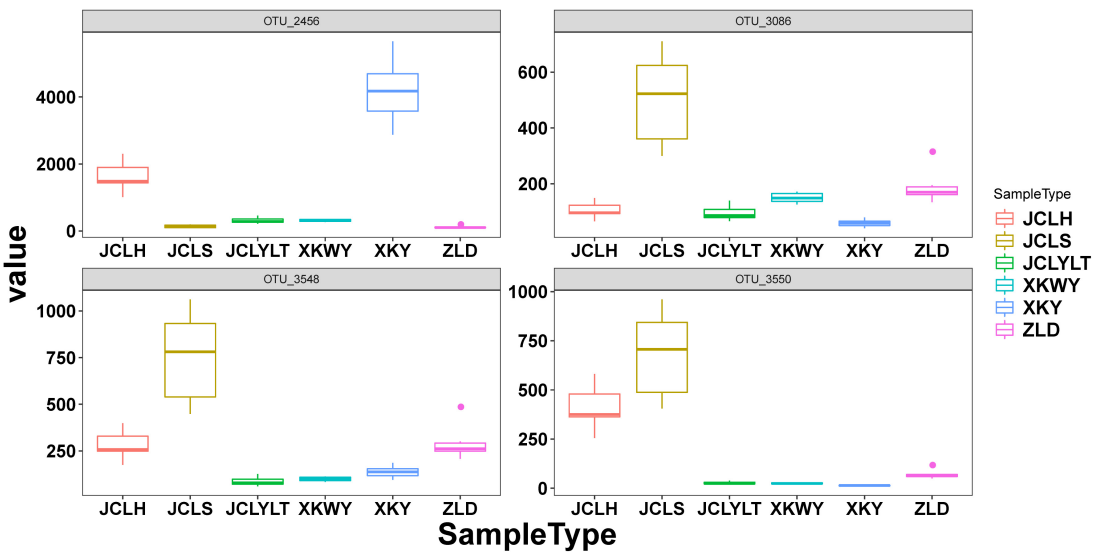

FIGURE 6 | The relative abundance of OTUs 2456, OTUs 3086, OTUs 3548, and OTUs 3550 in the studied soils.

rank: JCLS > JCLH > ZLD > XKWY ≈ XKY ≈ JCLYLT (**Figure 6B**). For the genus *Valsa*, there were almost no differences in the relative abundance among the selected soils. In this respect, the high death rate of *Populus* may be caused by *Alternaria alternate* and *D. glomerata*.

According to the plant–pathogen interactions discovered in the fungi perspective, we found that higher relative abundance of the target fungi in the *P. euphratica*-planted soil poses a high risk of infection. When we do a reasonable extrapolation of this result in the bacteria view, several candidate bacteria (OTU_12049 and OTU_12644, on behalf of JG34-KF-161 and *Sphingomonadaceae Sphingomonas*, respectively, within the *Proteobacteria* phyla) could be listed (**Supplementary Figure S1**). In addition, we should also pay attention to the relative abundance decrease of *Actinobacteria* (dominant OTUs: OTU_22374) (**Supplementary Figure S1**) and *Thaumarchaeota* (dominant OTUs: OTU_5953, OTU_5954) (**Supplementary Figure S1**) after *P. euphratica* planting. *Thaumarchaeota* has been regarded as the key player within the global nitrogen cycle (Shao et al., 2019). The phylogeny and the function of the class Actinobacteria remains controversial up to now (Ludwig et al., 2012; Sen et al., 2014). Its function within the plant–pathogen interaction system should be explored thoroughly. So, to do a further confirmation about this prediction will be a challenging, but meaningful, object in our future studies.

CONCLUSION

In conclusion, the results of the present study revealed deeper interactions between plant and pathogen. Increased attention on the presence of pathogens during tree planting will be a crucial factor in plant survival rates. Massart and Mark point out that in order to achieve a better biological control, we must combine as much potential factors together (e.g., host plants, host genotype, integrate microbial community, pathogen, biocontrol agents, molecules, etc.) (Massart et al., 2015; Mazzola and Gu, 2002). In addition, previous studies have indicated that the tolerance of plants to pathogens increases with increasing tree age and growth state (Mansfeld et al., 2017; Berendsen et al., 2018). Plant–pathogen interactions as a complicated dynamic equilibrium process warrant further study.

DATA AVAILABILITY STATEMENT

The data can be found in the NCBI database, with accession number – PRJNA597436.

AUTHOR CONTRIBUTIONS

YT puts forward the whole idea of this manuscript and implemented all the tasks. ZD had given several constructive instructions to this manuscript. XW and FT had given site instructions and integtate theory with practice. BG helped ZD with some interdisciplinary theories. CZ works as a assistant and made many contributions to this manuscript. All authors contributed to the article and approved the submitted version.

ACKNOWLEDGMENTS

We are grateful to Mr. Kailin Tian for the isolation of plant endophytes and Dr. Tao Wen for the DNA extraction and sequencing. We are also grateful to the American Journal Experts (T5LH6SVF) for their helpful efforts on the language edit of the manuscript.

SUPPLEMENTARY MATERIAL

The Supplementary Material for this article can be found online at: https://www.frontiersin.org/articles/10.3389/fmicb.2020.02095/full#supplementary-material

REFERENCES

Aghdam, A. R., Asadollah, B. A., Karimi, K., and Cryptosphaeria, M. A. (2017). Canker of populusnigra caused by cryptosphaeriapullmanensis, a new threat to poplar industry in Iran. *J. Phytopathol.* 165, 387–396. doi: 10.1111/jph.12572

Arrigoni, E., Antonielli, L., Pindo, M., Pertot, I., and Perazzolli, M. (2018). Tissue age and plant genotype affect the microbiota of apple and pear bark. *Microbiol. Res.* 211, 57–68. doi: 10.1016/j.micres.2018.04.002

Bae, H., Roberts, D. P., Lim, H. S., Strem, M. D., and Park, S. C. (2011). EndophyticTrichoderma isolates from tropical environments delay disease onset and induce resistance against *Phytophthora capsici* in hot pepper using multiple mechanisms. *Mol. Plant Microbe Interact.* 24, 336–351. doi: 10.1094/mpmi-09-10-0221

Baiswar, P., Chandra, S., Bag, T. K., Patel, R. K., and Ngachan, S. V. (2011). Cladosporiumoxysporum on *Prunusnepalensis* in India. *Australas. Plant Dis. Notes* 6, 3–6.

Basim, E., Basım, H., Abdulai, M., Baki, D., and Öztürka, N. (2016). Dentification and characterization of Didymellabryoniaecausing gummy stem blight disease of watermelon (*Citrullus lanatus*) in Turkey. *Crop. Prot.* 90, 150–156. doi: 10.1016/j.cropro.2016.08.026

Berendsen, R. L., Vismans, G., Yu, K., Song, Y., and Jonge, R. D. (2018). Disease-induced assemblage of a plant-beneficial bacterial consortium. *ISME J.* 12, 1496–1507. doi: 10.1038/s41396-018-0093-1

Brown, A. E., Finlay, R., and Ward, J. S. (1987). Antifungal compounds produced by Epicoccumpurpurascens against soil-borne plant pathogenic fungi. *Soil Biol. Biochem.* 19, 657–664. doi: 10.1016/0038-0717(87)90044-7

Chen, Q., Jiang, J. R., Zhang, G. Z., Cai, L., and Crous, P. W. (2015). Resolving the *Phoma* enigma. *Stud. Myco.* 82, 137–217. doi: 10.1016/j.simyco.2015.10.003

Donati, I., Cellini, A., Buriani, G., Mauri, S., and Kay, C. (2018). Pathways of flower infection and pollen-mediated dispersion of *Pseudomonas* syringaepv. actinidiae, the causal agent of kiwifruit bacterial canker. *Hortic. Res.* 5:56.

Dörr, A. J. M., Rodolfi, M., Scalici, M., Eliaa, A. C., and Garzoli, L. (2011). Phomaglomerata, a potential new threat to Italian inland waters. *J. Nat. Conserve.* 19, 370–373. doi: 10.1016/j.jnc.2011.06.006

Feng, X., Fu, B., Lu, N., Zeng, Y., and Wu, B. (2013). How ecological restoration alters ecosystem services: an analysis of carbon sequestration in China's loess Plateau. *Sci. Rep.* 3:2846.

Harman, G. E., Howell, C. R., Viterbo, A., Chet, I., and Lorito, M. (2004). Trichoderma species—opportunistic avirulent plant symbionts. *Nat. Rev. Microbiol.* 2, 43–56. doi: 10.1038/nrmicro797

Keram, A., Halik, Ü, Keyimu, M., Aishan, T., Mamat, Z., and Rouzi, A. (2019). Gap dynamics of natural *Populuseuphratica* floodplain forests affected by

hydrological alteration along the Tarim River: implications for restoration of the riparian forests. *For. Ecol. Manage.* 438, 103–113. doi: 10.1016/j.foreco.2019.02.009

Lai, Z., Zhang, Y., Liu, J., Wu, B., Qin, S., and Fa, K. (2016). Fine-root distribution, production, decomposition, and effect on soil organic carbon of three revegetation shrub species in northwest China. *For. Ecol. Manage.* 359, 381–388. doi: 10.1016/j.foreco.2015.04.025

Leff, J. W., Del Tredici, P., Friedman, W. E., and Fierer, N. (2015). Spatial structuring of bacterial communities within individual *Ginkgo biloba* trees. *Environ. Microbiol.* 17, 2352–2361. doi: 10.1111/1462-2920.12695

Li, S., Yan, C., Wang, T., and Du, H. Q. (2019). Monitoring grassland reclamation in the Mu us desert using remote sensing from 2010 to 2015. *Environ. Earth Sci.* 78:311.

Li, X. R., Zhang, Z. S., Huang, L., and Wang, X. (2013). Review of the ecohydrological processes and feedback mechanisms controlling sand-binding vegetation systems in sandy desert regions of China. *Chin. Sci. Bull.* 58, 1483–1496. doi: 10.1007/s11434-012-5662-5

Liu, P., Shi, Y. Y., and Zhu, L. W. (2018). Genetic variation in resistance to valsa canker is related to arbutin and gallic acid content in *Pyrus bretschneideri*. *Hortic. Plant J.* 4, 233–238. doi: 10.1016/j.hpj.2018.09.002

Ludwig, W., Euzéby, J., and Whitman, W. B. (2012). *Taxonomic Outline of the Phylum Actinobacteria. In Bergey's Manual§of Systematic Bacteriology*. New York, NY: Springer, 29–31.

Ma, R., Zhu, Y. F., Fan, X. L., and Tian, C. M. (2016). Canker disease of willow and poplar caused by Cryptosphaeriapullmanensis recorded in China. *Forest Pathol.* 46, 327–335. doi: 10.1111/efp.12261

Mansfeld, B. N., Colle, M., Kang, Y., Jones, A. D., and Grumet, R. (2017). Transcriptomic and metabolomic analyses of cucumber fruit peels reveal a developmental increase in terpenoid glycosides associated with age-related resistance to *Phytophthora.capsici*. *Hortic. Res.* 4:17022.

Massart, S., Martinez-Medina, M., and Jijakli, M. H. (2015). Biological control in the microbiome era: challenges and opportunities. *Biol. Control* 89, 98–108. doi: 10.1016/j.biocontrol.2015.06.003

Mazzola, M., and Gu, Y. H. (2002). Wheat genotype-specific induction of soil microbial communities suppressive to disease incited by *Rhizoctonia solani* anastomosis group (AG)-5 and AG-8. *Phytopathology* 92, 1300–1307. doi: 10.1094/phyto.2002.92.12.1300

McLeod, M. P., Warren, R. L., Hsiao, W. W., Araki, N., Myhre, M., Fernandes, C., et al. (2006). The complete genome of *Rhodococcus* sp. RHA1 provides insights into a catabolic powerhouse. *Proc. Natl. Acad. Sci. U.S.A.* 103, 15582–15587. doi: 10.1073/pnas.0607048103

Moral, J., Lichtemberg, P. S. F., Papagelis, A., Sherman, J., and Michailides, T. J. (2018). Didymellaglomeratacausing leaf blight on pistachio. *Eur. J. of Plant Pathol.* 151, 1095–1099. doi: 10.1007/s10658-018-1422-y

Radić, N., and Štrukelj, B. (2012). Endophytic fungi—The treasure chest of antibacterial substances. *Phytomedicine* 19, 1270–1284. doi: 10.1016/j.phymed.2012.09.007

Saleem, M., Hu, J., and Jousset, A. (2019). More than the sum of its parts: microbiome biodiversity as a driver of plant growth and soil health. *Annu. Rev. Ecol. Evol. Syst.* 50, 145–168. doi: 10.1146/annurev-ecolsys-110617-062605

Scola, L. B., Birtles, R. J., Mallet, M. N., and Raoult, D. (1998). Massiliatimonae gen. nov., sp. nov., isolated from blood of an immunocompromised patient with cerebellar lesions. *J. Clin. Microbiol.* 36, 2847–2852. doi: 10.1128/jcm.36.10.2847-2852.1998

Sen, A., Daubin, V., Abrouk, D., Gifford, I., Berry, A. M., and Normand, P. (2014). Phylogeny of the class Actinobacteria revisited in the light of complete genomes. The orders 'Frankiales' and Micrococcales should be split into coherent entities: proposal of Frankiales ord. nov., *Geodermatophilales* ord. nov., *Acidothermales* ord. nov. and *Nakamurellales* ord. nov. *Int. J. Syst. Evol. Micr.* 64, 3821–3832. doi: 10.1099/ijs.0.063966-0

Shao, K., Jiang, X., Hu, Y., Tang, X., and Gao, G. (2019). Thaumarchaeota affiliated with soil crenarchaeotic group are prevalent in the alkaline soil of an alpine grassland in northwestern China. *Ann. Microbiol.* 69, 867–870. doi: 10.1007/s13213-019-01492-5

Shu, P. X., Li, B. S., Wang, H., Qiu, Y. H., and Niu, D. F. (2018). Geochemical characteristics of surface dune sand in the Mu us desert, inner mongolia, and implications for reconstructing the paleoenvironment. *Quatern. Int.* 479, 106–116. doi: 10.1016/j.quaint.2017.05.053

Sun, H. H., Mao, W. J., Jiao, J. Y., Xu, J. C., and Li, H. Y. (2011). Structural characterization of extracellular polysaccharides produced by the marine fungus *Epicoccum nigrum* JJY-40 and their antioxidant activities. *Mar. Biotechnol.* 13, 1048–1055. doi: 10.1007/s10126-011-9368-5

Sun, Y., Zhang, Y., Feng, W., Qin, S. G., and Liu, Z. (2019). Revegetated shrub species recruit different soil fungal assemblages in a desert ecosystem. *Plant Soil* 435, 81–93. doi: 10.1007/s11104-018-3877-1

Vannini, C., Rosati, G., Verni, F., and Petroni, G. (2004). Identification of the bacterial endosymbionts of the marine ciliate Euplotesmagnicirratus (*Ciliophora*, *Hypotrichia*) and proposal of 'CandidatusDevosiaeuplotis'. *Int. J. Syst. Evol. Microbiol.* 54, 1151–1156. doi: 10.1099/ijs.0.02759-0

Vorholt, J. A. (2012). Microbial life in the phyllosphere. *Nat. Rev. Microbiol.* 10, 828–840. doi: 10.1038/nrmicro2910

Wei, Z., Gu, Y. A., Friman, V. P., Kowalchuk, G. A., and Xu, Y. C. (2019). Initial soil microbiome composition and functioning predetermine future plant health. *Sci. Adv.* 5:eaaw0759. doi: 10.1126/sciadv.aaw0759

Wilingham, S. L., Pegg, K. G., Langdon, P. W. B., Cooke, A. W., and Peasley, D. (2002). Combinations of strobilurin fungicides and acibenzolar (Bion) to reduce scab on passionfruit caused by *Cladosporium oxysporum*. *Australas. Plant Path.* 31, 333–336. doi: 10.1071/ap02036

Xu, X., Passey, T., Wei, F., Saville, R., and Harrison, R. J. (2015). Amplicon-based metagenomics identified candidate organisms in soils that caused yield decline in strawberry. *Hortic. Res.* 2:15022.

Yao, X. F., Li, P. F., Xu, J. H., Zhang, M., and Ren, R. S. (2016). Rapid and sensitive detection of *Didymella bryoniae* by visual loop-mediated isothermal amplification assay. *Front. Microbiol.* 7:1372. doi: 10.3389/fmicb.2016.01372

Yi, H. W., and Chi, Y. J. (2011). Biocontrol of Cytospora canker of poplar in northeast China with Trichodermalongibrachiatum. *Forest Pathol.* 41, 299–307. doi: 10.1111/j.1439-0329.2010.00704.x

Yu, C., Li, T., Shi, X., Saleem, M., Li, B., Liang, W., et al. (2018). Deletion of endo-β-1, 4-xylanase VmXyl1 impacts the virulence of Valsamali in apple tree. *Front. Plant Sci.* 9:663. doi: 10.3389/fpls.2018.00663

Zhalnina, K. V., Dias, R., Leonard, M. T., Quadros, P. D. D., and Camargo, F. A. O. (2014). Genome Sequence of candidatus nitrososphaera evergladensis from group I.1b enriched from everglades soil reveals novel genomic features of the ammonia-oxidizing archaea. *PLoS One* 9:e101648. doi: 10.1371/journal.pone.0101648

Zheng, C., Liu, Z. H., Tang, S. S., Lu, D., and Huang, X. Y. (2014). First report of leaf spot caused by cladosporiumoxysporum on greenhouse eggplant in China. *Plant Dis.* 98, 0191–2917.

Conflict of Interest: The authors declare that the research was conducted in the absence of any commercial or financial relationships that could be construed as a potential conflict of interest.

frontiers in Plant Science

ORIGINAL RESEARCH
published: 15 September 2020
doi: 10.3389/fpls.2020.557672

Association Mapping and Development of Marker-Assisted Selection Tools for the Resistance to White Pine Blister Rust in the Alberta Limber Pine Populations

Jun-Jun Liu[1], Richard A. Sniezko[2], Robert Sissons[3], Jodie Krakowski[4], Genoa Alger[3], Anna W. Schoettle[5], Holly Williams[1], Arezoo Zamany[1], Rachel A. Zitomer[2†] and Angelia Kegley[2]*

[1] Canadian Forest Service, Natural Resources Canada, Victoria, BC, Canada, [2] USDA Forest Service, Dorena Genetic Resource Center, Cottage Grove, OR, United States, [3] Parks Canada, Waterton Lakes National Park, Waterton Park, AB, Canada, [4] Alberta Agriculture and Forestry, Edmonton, AB, Canada, [5] USDA Forest Service, Rocky Mountain Research Station, Fort Collins, CO, United States

OPEN ACCESS

Edited by:
Sanushka Naidoo,
University of Pretoria, South Africa

Reviewed by:
Qingzhang Du,
Beijing Forestry University, China
Shouvik Das,
Indian Agricultural Research Institute (ICAR), India

***Correspondence:**
Jun-Jun Liu
jun-jun.liu@canada.ca

†Present address:
Rachel A. Zitomer,
Department of Forest Ecosystems and Society, Oregon State University, Corvallis, OR, United States

Specialty section:
This article was submitted to Plant Breeding, a section of the journal Frontiers in Plant Science

Received: 30 April 2020
Accepted: 25 August 2020
Published: 15 September 2020

Citation:
Liu J-J, Sniezko RA, Sissons R, Krakowski J, Alger G, Schoettle AW, Williams H, Zamany A, Zitomer RA and Kegley A (2020) Association Mapping and Development of Marker-Assisted Selection Tools for the Resistance to White Pine Blister Rust in the Alberta Limber Pine Populations. Front. Plant Sci. 11:557672. doi: 10.3389/fpls.2020.557672

Since its introduction to North America in the early 1900s, white pine blister rust (WPBR) caused by the fungal pathogen *Cronartium ribicola* has resulted in substantial economic losses and ecological damage to native North American five-needle pine species. The high susceptibility and mortality of these species, including limber pine (*Pinus flexilis*), creates an urgent need for the development and deployment of resistant germplasm to support recovery of impacted populations. Extensive screening for genetic resistance to WPBR has been underway for decades in some species but has only started recently in limber pine using seed families collected from wild parental trees in the USA and Canada. This study was conducted to characterize Alberta limber pine seed families for WPBR resistance and to develop reliable molecular tools for marker-assisted selection (MAS). Open-pollinated seed families were evaluated for host reaction following controlled infection using *C. ribicola* basidiospores. Phenotypic segregation for presence/absence of stem symptoms was observed in four seed families. The segregation ratios of these families were consistent with expression of major gene resistance (MGR) controlled by a dominant R locus. Based on linkage disequilibrium (LD)-based association mapping used to detect single nucleotide polymorphism (SNP) markers associated with MGR against *C. ribicola*, MGR in these seed families appears to be controlled by *Cr4* or other R genes in very close proximity to *Cr4*. These associated SNPs were located in genes involved in multiple molecular mechanisms potentially underlying limber pine MGR to *C. ribicola*, including NBS-LRR genes for recognition of *C. ribicola* effectors, signaling components, and a large set of defense-responsive genes with potential functions in plant effector-triggered immunity (ETI). Interactions of associated loci were identified for MGR selection in trees with complex genetic backgrounds. SNPs with tight Cr4-linkage were further converted to TaqMan assays to confirm their effectiveness as MAS tools. This work

demonstrates the successful translation and deployment of molecular genetic knowledge into specific MAS tools that can be easily applied in a selection or breeding program to efficiently screen MGR against WPBR in Alberta limber pine populations.

Keywords: association mapping, *Cronartium ribicola*, limber pine (*Pinus flexilis*), major gene resistance (MGR), marker-assisted selection (MAS), plant effector-triggered immunity (ETI), single nucleotide polymorphisms (SNPs), white pine blister rust (WPBR)

INTRODUCTION

Limber pine (*Pinus flexilis* James) is a native five-needle pine in western North America, naturally distributed from British Columbia and Alberta in Canada to southern California in the USA. Despite limited economic value, limber pine is a keystone species for high elevation montane ecosystems. Because of the species' high tolerance to drought, high winds, and exposure, individual trees can live for over 1,000 years in harsh environments where few other conifers are distributed. In these environments limber pine provides essential ecosystem services, including slope stabilization, headwater streamflow control, and subalpine tree island formation. They provide cover that allows less exposure-hardy plants to establish and grow and provide both shelter and a nutritious food source for wildlife such as birds, bears, and small mammals (Schoettle, 2004; Tomback and Achuff, 2010). They are highly valued by recreationalists for their unique windswept beauty (Government of Alberta, 2014) and, as one of the world's oldest living species, limber pine is also useful for dendrochronological studies (Millar et al., 2007).

Despite having a large geographic range, limber pine's status is precarious in portions of its distribution. It is threatened by invasion of the lethal non-native fungal pathogen *Cronartium ribicola* (J.C. Fisch), outbreaks of native mountain pine beetle (*Dendroctonus ponderosae* Hopkins), and habitat loss resulting from changes to fire regimes and climate change. *C. ribicola* causes white pine blister rust (WPBR) in five-needle pines all around the world. Because of its high susceptibility to *C. ribicola*, in environments suitable for the pathogen, over 60 percent of limber pine trees in Alberta were observed to be infected during 2009 surveys in Canada, and WPBR caused over 40 percent mortality in many regions (Smith et al., 2013). The Government of Alberta and the Committee on the Status of Endangered Wildlife in Canada have designated limber pine as an endangered species (COSEWIC, 2014; Government of Alberta, 2014).

A species recovery plan has been prepared and executed for limber pine conservation and restoration in Alberta (Alberta Whitebark and Limber Pine Recovery Team, 2014). Genetic resistance is considered essential to several key strategies for WPBR management and restoration of native five-needle pines in North America, and great progress has been made in conservation and tree improvement programs for several species since programs began in the 1960s (Sniezko et al., 2008; Sniezko et al., 2014; Sniezko et al., 2020). Over the past few years, limber pine seed families have been collected and assessed for resistance-related phenotypic traits in controlled seedling inoculation trials. Major gene resistance (MGR) and quantitative disease resistance (QDR) to WPBR have been identified in populations not yet invaded by WPBR as well as those with high pre-selection from natural infection. MGR to *C. ribicola* was first identified in limber pine seed families originating from southern Wyoming to southern Colorado, USA, and its genetic locus was designated as *Cr4* (Schoettle et al., 2014). Recently, MGR was also independently found in a limber pine parent from Alberta (Sniezko et al., 2016), in stands 400 km south of the northern limit of the species. Because the two regions where MGR has been documented in limber pine are more than 1,100 km apart geographically, it is important for selection and breeding programs to know whether the MGR found in the USA and Canada is controlled by the same R locus (*Cr4*).

Traditional breeding approaches are effective in selecting and testing for genetic resistance to WPBR, but they can take decades to identify sufficient numbers of resistant parent trees and reliably produce large cone crops. In addition, it can be difficult using conventional methods for tree breeders to capture and transfer genetic variability of a suite of complex traits together, such as host resistance to pathogens and pests and other related adaptive traits. Genetic dissection of complex phenotypic traits is thus still an obstacle in forest genetics. In recent years, genomic resources have been developed by next generation sequencing approaches in a few five-needle pine species, including genome-wide marker discovery (Liu et al., 2014; Syring et al., 2016), high-density genetic maps (Jermstad et al., 2011; Friedline et al., 2015; Liu et al., 2019), transcriptome profiles (Lorenz et al., 2012; Liu et al., 2013; Gonzalez-Ibeas et al., 2016; Liu et al., 2016; Baker et al., 2018), and whole genome sequences (Stevens et al., 2016). These genomics resources and tools open a completely new avenue for the capture and utilization of genome-wide variability in breeding programs (Falk et al., 2018; Weiss et al., 2020).

Genotyping a subset of in-silico SNPs anchored *Cr4* on the *Pinus* consensus linkage group 8 (LG8) (Liu et al., 2016). Genes with positive selection implied in disease resistance or drought tolerance were identified in limber pine and three other five-needle pines as potential targets for breeding and selection of these traits (Baker et al., 2018). Fine-scale genetic mapping revealed orthologous R loci co-positioned with members of the nucleotide-binding site leucine-rich repeat (NBS-LRR) gene family that reflected evolutionary pressure (Liu et al., 2019). These genomic studies facilitated further characterization and practical utilization of genetic diversity in breeding genetic resistance to WPBR in five-needle pines. However, the genomic information available so far is still too limited to

generate a sufficient foundation of knowledge required for genetic improvement of limber pine and other non-model forest conifers (Liu et al., 2016).

Here, we report an association study using unrelated open-pollinated limber pine seed families originating from Alberta to determine whether families expressing phenotypic signs of MGR have genotypic MGR markers. We also determine whether putatively resistant genotypes co-locate with previously identified *Cr4* known to occur in limber pine or whether they co-locate with other R genes. We aim to develop specific SNP markers that can be used for operational assays for MGR selection in breeding programs of limber pine to increase the frequency of WPBR-resistant genotypes.

MATERIALS AND METHODS

Plant Materials and Resistance Assessment

Ten Alberta open-pollinated seed families (**Supplementary Table S1**) were sown at Dorena Genetic Resource Center (DGRC) in spring of 2016, including one family (PB #2) previously reported with MGR segregation (Sniezko et al., 2016) and nine families with unknown resistance levels. Needle samples were collected from each seedling and stored at −20°C before DNA extraction.

Of the five spore stages of the *C. ribicola* life cycle, only basidiospores are able to infect needles of five-needle pine species. They develop on the underside of *Ribes* spp. leaves (pathogen's alternate host) during cool, wet weather conditions in late summer or early fall and infect the needles of five-needle pines. *Ribes* spp. leaves infected with a heterogenous mixture of *C. ribicola* genotypes were collected from multiple field locations in Oregon in the fall of 2016 and 2017. Since no virulent pathotype capable of overcoming limber pine MGR has yet been detected (Kinloch and Dupper, 2002), the *C. ribicola* sources used in these inoculations were assumed to be wild avirulent races.

Six and 18-month-old seedlings were inoculated in the fall of 2016 and 2017, respectively, using standard Dorena Genetic Resource Center protocols (Schoettle et al., 2014; Sniezko et al., 2016). Inoculation with *C. ribicola* basidiospores was performed in an inoculation room under controlled conditions at 18°C and 100% relative humidity. Study design was a randomized complete block, with 4 and 6 blocks for the 2016 and 2017 trials, respectively. Seedlings were transferred into the inoculation room two days prior to inoculation to acclimate to temperature and humidity conditions optimal for infection. Infected *Ribes* leaves were then placed on wire screens above the seedlings for the basidiospores to drop. Basidiospore shedding was monitored by checking microscope slides placed amongst the inoculation blocks. *Ribes* leaves were removed when basidiospore density reached a specific level (6000 or 3000 spores/cm^2 in the 2016 and 2017 trials, respectively). Basidiospore germination averaged 99% for the trials. Seedlings remained in the inoculation chamber for about 48 h to promote spore germination and needle infection. After removal from the inoculation room, seedlings from the 2016 inoculation were then transferred to a greenhouse for the duration of the trial, while the seedlings from the 2017 inoculation were subsequently planted outdoors in boxes.

Disease development in the 2016 trial was assessed a total of 7 times during the period from October 2016 to December 2017. Each seedling was evaluated for disease symptoms on needles and stems including presence/absence of needle spots (lesions), spot types and number, as well as necrotic or abscising needles, presence/absence of cankers, aecia, and spermatia. Resistant or susceptible phenotypes were determined based on stem canker development as described previously (Schoettle et al., 2014; Sniezko et al., 2016). For the seedlings inoculated in 2017, number of needle spots was assessed approximately 8 months after inoculation, and presence/absence of spots, and number, type, and severity of stem infections as well as vigor was assessed approximately one year following inoculation.

Consistency for MGR phenotypic expression was estimated using χ^2 tests by comparing phenotypic segregation of the same families inoculated in the two different years or with that from a previous report (Sniezko et al., 2016).

Linkage Group (LG) Wide Association Study of Resistance to *C. ribicola* in Alberta Seed Families

Genomic DNA was extracted from needle tissues using a QIAGEN DNeasy Plant Mini kit. Previous studies mapped *Cr4* in USA sources on the *Pinus* consensus LG8, which positioned 25 and 775 genes, respectively (Liu et al., 2016; Liu et al., 2019). Here the limber pine LG8 in USA sources (**Supplementary Table S2**) was updated by map integration using MergeMap software (Wu et al., 2011). To address the question of whether the MGR observed in the Alberta seed families was different from *Cr4* found in the Colorado and Wyoming populations, genes were selected throughout LG8 for SNP genotyping. Based on SNPs within their coding regions, Sequenom iPlex genotyping arrays were designed and used to genotype seedlings of seed families identified with MGR segregation. SNP genotyping was performed using the Sequenom iPlex MassARRAY platform (Sequenom, San Diego, CA, USA; Gabriel et al., 2009) at the Genome Quebec Innovation Centre, McGill University, Montreal, Quebec.

The extent of linkage disequilibrium (LD) was investigated along LG8, and a matrix of the squared allele frequency correlations (r^2) was constructed between all possible pairs of SNP loci with minor allele frequency (MAF) >5%. Association of markers with the resistant phenotype in the Alberta seed families was performed using a general linear model (GLM) and a mixed linear model (MLM) with the TASSEL software version 5.0 (Bradbury et al., 2007). In the GLM, *p*-values for marker effects were adjusted by 10^5 permutations (Churchill and Doerge, 1994). To avoid spurious marker-trait associations that might result from population stratification or relatedness (Yu et al., 2006; Euahsunthornwattana et al., 2014), the MLM included both fixed and random effect covariates which accounted for population structure and relatedness in genome-wide association studies (GWAS). In the MLM, proportions of individuals belonging to subpopulations were estimated as the Q matrix; average

relationship between individual seedlings was estimated by kinship (K) calculated from genotypes of the SNP loci. Manhattan plots and quantile-quantile (Q-Q) plots were used to graphically present the results of association tests. The R squared values of markers (r^2) were calculated and used to explain the proportion of phenotypic variation explained by each SNP locus. Associated SNPs and polymorphic genes were annotated based on their homologies to the available databases (NCBI-nr, PIR, KEGG, and GO) using BLAST2GO (Götz et al., 2008).

Genetic Interaction Modeling

Gene-gene interactions were detected by the generalized MDR (GMDR) approach using the GMDR software package (Winham and Motsinger-Reif, 2011; Hou et al., 2019) to study the genetic interaction effect on the limber pine MGR. A 10-fold cross-validation procedure and 10-time random seed number were used to minimize potential for false positives. The best model was selected through an exhaustive search based on maximizing cross-validation consistency, training balance accuracy, and testing balance accuracy at a significance $p < 0.05$.

Development of TaqMan Assays as MAS Tools

Based on results of the association analysis performed above, the top SNP loci with strong phenotypic association and potential R gene functional candidates were selected for design of TaqMan assays (**Table S3**). SNP genotyping was performed as described previously (Liu et al., 2020). TaqMan assays were first verified using genomic DNA extracted from megagametophyte tissues of at least one of the USA seed families previously used for genetic map construction (Liu et al., 2016), and then tested using the Alberta seedlings, including both the MGR-segregating and susceptible families identified in the present study. The genotype of each seedling was analyzed using the genotyping assays according to the manufacturer's instructions (Applied Biosystems). A 7500 Fast Real-Time PCR system (Applied Biosystems) was used to run quantitative PCR. PCR hot-start was activated at 94°C for 15 min, followed by 40 cycles at 94°C for 20 s and 60°C for 60 s. Genotypes at each SNP locus were called using the TaqMan Genotyper Software (Applied Biosystems). To assess the potential application of TaqMan assays as MAS tools, their accuracy for phenotypic selection was calculated as the ratio of the number of individual samples with agreement between genotypes and phenotype to the number of all individuals.

RESULTS

Phenotypic Segregation of Resistance Trait

Phenotypic segregation for cankered and stem symptom-free seedlings was observed in four seed families: PB #2, #7027, #6470, and #6665 (**Figure 1**, **Table S1**). These families fit with the expected Mendelian segregation ratios at either 1:1 for families #7027, #6470, and #6665 (χ^2 tested p values ranging from 0.68 to 1) or 3:1 for the family PB #2 (χ^2 tested $p = 0.13$) (**Supplementary Table S1**), indicating that those seed trees are putatively heterozygous for MGR. In contrast, 95% to 100% of the seedlings from the other six seed families were cankered, and they were identified as susceptible (**Figure S1**, **Table S1**). These tested seed families were selected from fields where the wild stand infection rates were in a range of 83%~95% (**Table S1**). Identification of multiple MGR families from disease-free trees in the field by our controlled trials indicates that natural selection tends to increase frequency of resistance alleles in the survivors.

In a comparison of the 2016 and 2017 inoculation trials with greenhouse and outdoor conditions respectively, segregation ratios were highly consistent for families #7027, #6470, and #6665 (χ^2 tested p values ranging from 0.29~0.62). PB #2 was not included in the 2017 inoculation trial, but its phenotypic segregation ratio from a 2014 inoculation (Sniezko et al., 2016) was also not significantly different from that of the 2016 trial (χ^2 tested $p = 0.80$). This consistency of MGR phenotypic segregation indicates that there was no obvious environmental interaction for MGR phenotypic expression across Alberta MGR seed families.

Linkage Disequilibrium (LD) of SNPs Along LG

Sequenom iPlex arrays were used for SNP genotype analysis across the four MGR-segregating seed families identified above. To reveal genetic correlations of SNP loci along LG, we first assessed LD levels between SNP loci using the r^2 statistic. As expected, high LD, or complete LD ($r^2 = 1$) was detected for the SNP pairs in the same genes or in different genes located at the same genetic position on LG8. Average r^2 between two SNP loci separated by distances less than 10 cM was 0.96 in the family PB #2 and 0.25 across the four families. The high average r^2 values at less than 10 cM indicate that the association mapping was powerful enough to detect causal loci at a relatively long distance in these limber pine populations using multiple seed families. A scatterplot of LD decay over genetic distance (cM) was generated to estimate the LD decay trend. Nonlinear regression revealed that LD decay was rapid as distances between the two markers increased (**Figure 2**), indicating that SNP markers with short-range LD likely have high reliability for MGR selection within limber pine seed families. When the distance between two SNP loci reached 25 cM, r^2 values decreased to 0.50 or 0.07 in the family PB #2 (**Figure 2A**) and across the four families (**Figure 2B**), respectively. Because a high mutation rate with frequent recombination events generally decreases LD, we further checked the *Cr4*-related LD across the four seed families and found that LD decay between the *Cr4* locus and SNP loci was faster than that between pairs of all SNP loci along the LG8, with the average r^2 value significantly lower (0.04 vs. 0.11, t-test $P < 0.001$) when the distance was over 25 cM (**Figure 2C**).

LG-Wide Association Study Identifies *Cr4* as the R Locus in Four Alberta Seed Families

In family PB #2, LG-wide association analysis using the general linear model (GLM) detected a total of 23 SNP loci (**Table S4**) in significant association with the resistant phenotype. r^2 for these 23 SNP markers ranged from 0.099 to 0.839 ($p < 0.05$ after correction by 1×10^5 permutations). The resistance-associated

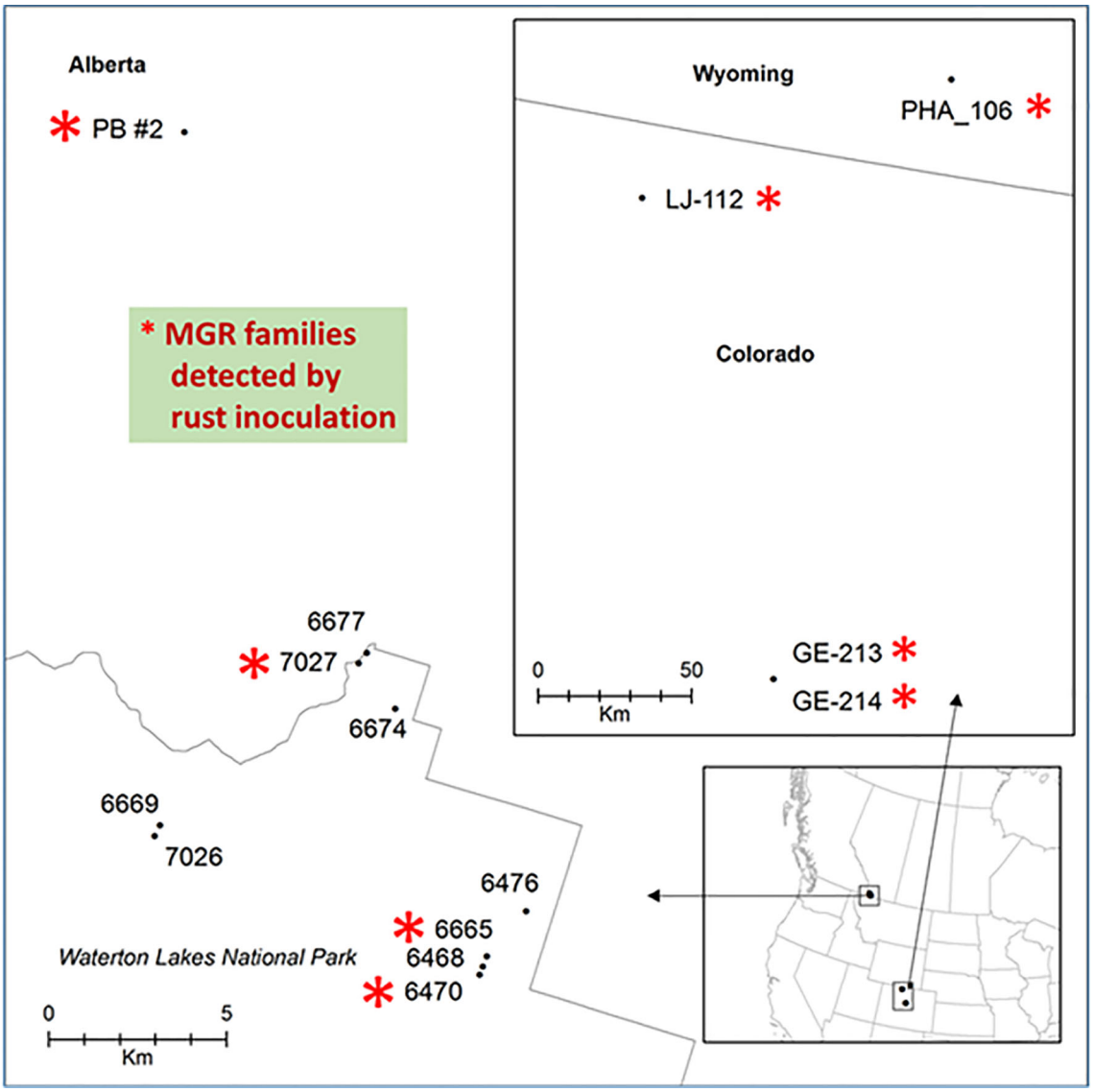

FIGURE 1 | Geographic locations of limber pine seed families used in this study. Families with major gene resistance from Alberta (this study and Sniezko et al., 2016) and a subset of those found from Wyoming and Colorado (Schoettle et al., 2014) that were used in this study are labeled with red stars.

SNPs were distributed in 17 genes localized on LG8 from positions 18.33 cM to 156.48 cM. Based on the LG8 genetic map updated in the present study (**Figure S1**, **Table S2**), M287456 was on one side and M304083 was on the other side of *Cr4* at 0.43 and 1.11 cM, respectively. The Manhattan plots of –Log10 (*p* values) or marker-Rsq (r^2 values) on a genome scale with marker positions (cM) across LG8 (**Figure 3A**, **Figure S2**) each had a single peak of significant marker-trait associations, near 126.80 cM where *Cr4* and its candidate genes were localized for MGR to *C. ribicola*. SNP M304083Y displayed the strongest association with the resistant phenotype ($r^2 = 0.839$), followed by M287456-634R and M287456-700R with $r^2 = 0.730$ (**Figure S2**).

Association analysis across all four open-pollinated seed families detected 18 SNP loci within 13 genes in significant association with the resistant phenotypes (**Figure 3B**, **Figure S2B**, and **Table S5**). These GLM-based results were well supported by an association analysis using a mixed linear model (MLM) (**Figures 3C, D**). As presented by Manhattan plots and quantile-quantile plots, MLM-based association tests detected 5 and 7 SNP loci with significant association with MGR in the PB #2 family and all seedlings across the four segregating families, respectively (**Figures 3E, F** and **Supplementary Table S5**). All association tests consistently showed co-localization of spikes of association with *Cr4*, indicating that the R locus was the

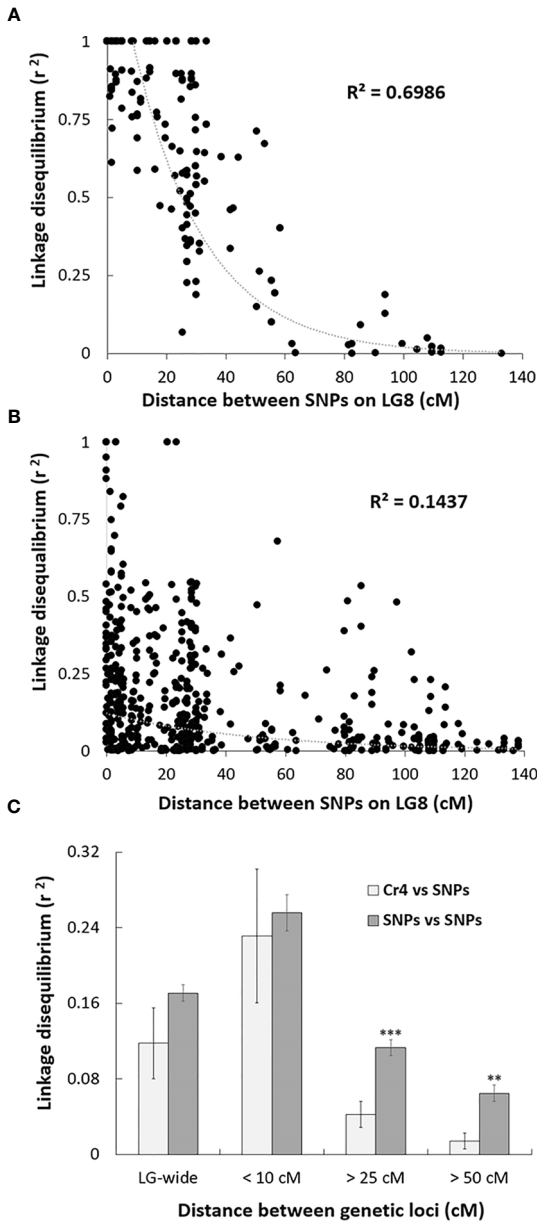

FIGURE 2 | Scatter plot of the estimates (r^2) of linkage disequilibrium (LD) decay for pairs of single-nucleotide polymorphisms (SNPs) in Alberta limber pine seed families with major gene resistance (MGR), with genetic distance in centimorgans (cM) within the Pinus consensus linkage group 8 (LG8). The curves are nonlinear regressions of LD decay (r^2) onto distance in cM. **(A)** LD decay detected in the progeny of family PB #2; **(B)** LD decay detected in the progeny of all four MGR Alberta seed families; **(C)** Comparison of the LD decay estimates (r^2) for pairs of SNPs and for pairs of *Cr4* coupling with one SNP locus. Pooled data from all surveyed SNPs were used to estimate LD decay based on distances between two loci at 10, 25, 50 cM, or LG-wide. Two and three stars indicate significant difference by t-test at $p < 0.01$, and $p < 0.001$, respectively.

same (*Cr4*) or very closely positioned in Canadian and USA seed families despite the large geographic distance between them.

SNP loci were further checked manually in each of four MGR-segregating open-pollinated seed families from Alberta, ranking a total of 12 SNPs, including M287456-700R and M304083Y as identified above by GLM and MLM, as the top SNPs with strong phenotypic association in at least one seed family (**Figure 4**). Most of them were positioned within 5 cM of *Cr4* (**Supplementary Figure S1**). Three and four SNPs co-segregated with resistant phenotypes in families #6665 (M124413Y, M304083Y, M286917Y, and M326511R) and #7027 (M118650W, M141475Y1, and M304083Y), respectively. Of these SNPs, M124413Y and M326511R were not detected by GLM and MLM runs across all four seed families due to the small sample size (34 seedlings) of seed family #6665.

Annotation of Polymorphic Genes Associated With MGR in Alberta Limber Pine Families

In total, 25 associated SNPs distributed across 19 unigenes were identified. Nine polymorphic genes were localized within 5-cM of *Cr4* (**Table S5**). All 19 associated unigenes showed significant homology hits in the Arabidopsis proteome by BLAST analysis (**Table S6**). Three genes had unknown function (M355530, M445775, and M124413), and 16 genes were assigned putative biological functions by BLAST-2-GO-based gene annotation. These included two R analogs of the NBS-LRR family (M463406 and M287456), two regulators for signal transduction pathways (M187937: RAB GTPase homolog G3D and M438219: little nuclei1-LINC1), three transcriptional factors (TFs; M296815: CCCH-type zinc finger protein with ARM repeat domain, M141475: GRAS family transcription factor, and M160798: Tesmin/TSO1-like CXC domain-containing protein). Five associated genes were involved in defense responses to biotic and abiotic stressors, including expansin-like B1 (M176778), galactinol synthase 1 (M204077), stress responsive α/β barrel domain protein (SRBP, M304083), pectin acetylesterase (PAE, M286987), and 6-phosphogluconate dehydrogenase (6PGDH, M259257). The remaining four genes were revealed to have functions involving ribosomal protein L12 (M444092), cytidine/deoxycytidylate deaminase (DCTD, M286987), nucleotide-diphospho-sugar transferase (M362778), and proline-rich spliceosome-associated (PSP) family protein (M118650).

Gene–Gene Interactions Associated With Limber Pine MGR

Modeling interactions between MGR-associated genes revealed three gene–gene models with the highest order. Consistent with results from the GLM and MLM-based association tests (above), a one-gene model was first identified with the SRBP gene (M304083Y) for MGR; it scored 10/10 for cross-validation consistency. A two-gene interaction was identified between SRBP (M304083Y) and DCTD (M286987Y), while a three-gene interaction was identified among SRBP (M304083Y), NBS-LRR (M287456-700R), and 6PGDH (M259257Y) which scored 9/10 and 7/10 for cross-validation consistency, respectively. The 10-fold cross validation for significance test showed all top tree models with $p = 0.001$ (**Table S7**).

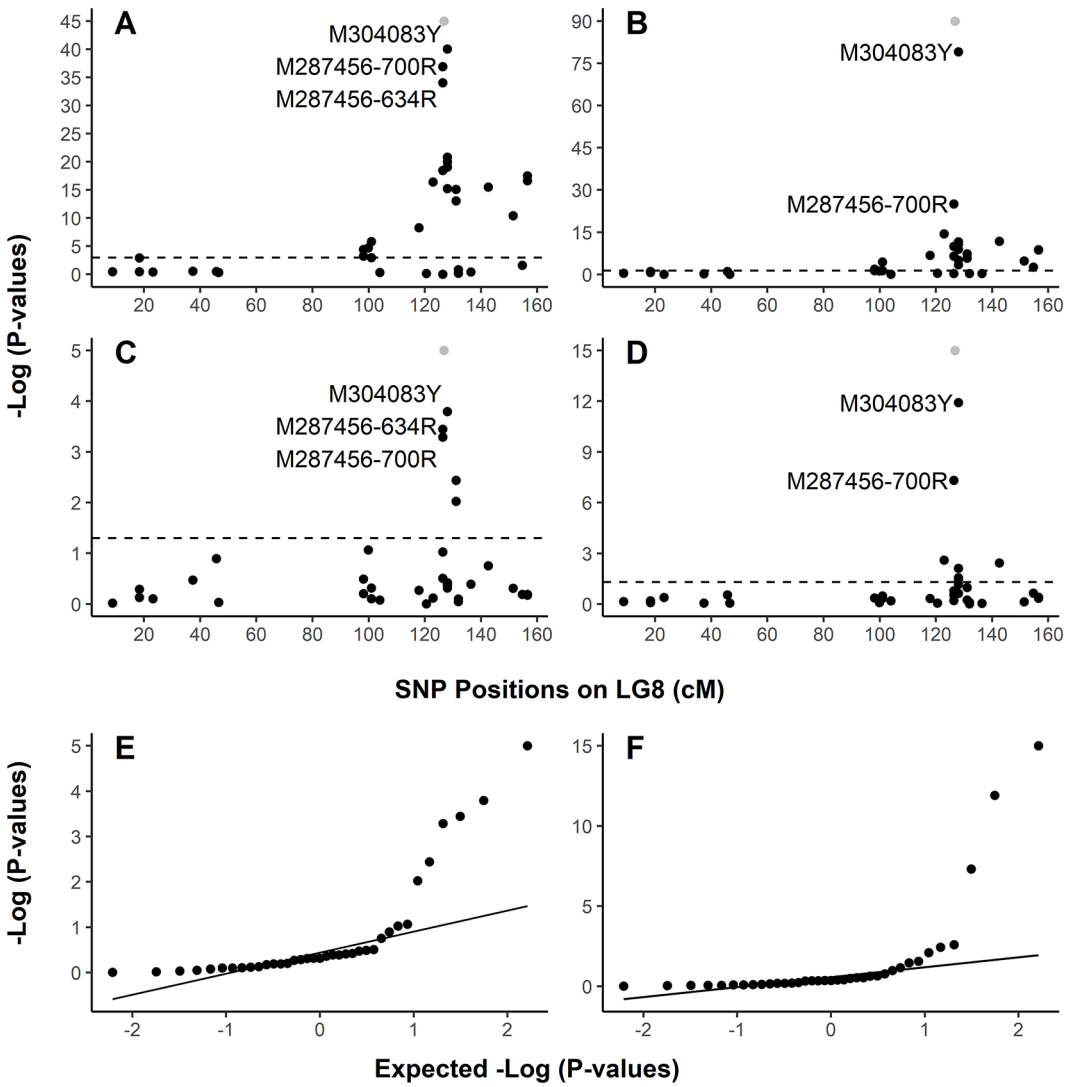

FIGURE 3 | Graphical representation of test results showing strong association of SNPs with resistance to *Cronartium ribicola*. The Manhattan plots for resistance show –log10 p-values from linkage group 8 (LG8)-wide scan in Alberta seed families plotted against positions around the putative *Cr4* locus. The x-axis represents SNP locations (cM) on LG8, and the y-axis represents –log10 p-values from genotypic associations with the resistance phenotype. The dash lines mark the threshold of p-values in Manhattan plotting. **(A)** Association test using GLM with family PB #2; **(B)** Association test using GLM with all samples of four Alberta seed families; **(C)** Association test using MLM with family PB #2; **(D)** Association test using MLM with all samples of four Alberta seed families. Quantile-quantile (Q-Q) plots showing the enrichment of association signals with observed p-values against the expected distribution under the null hypothesis. In the Manhattan plots **(A–D)**, Cr4 was included in grey dots to show its position on LG8. LG8 was updated by integrating genetic maps described previously (Liu et al., 2016; Liu et al., 2019). **(E)** Q-Q plot showing results of MLM run using family PB #2. **(F)** Q-Q plot showing results of MLM run using all samples of four Alberta seed families.

GMDR analysis calculated interactive variables in the score distributions, with a positive score for the MGR resistant group and a negative score for the susceptible group (**Figure S3**). The one-gene SRBP model detected uncertainty of MGR phenotypes for trees carrying SRBP genotypes (M304083-TC and CC) (**Figure S3A**). In the two-gene interactions of SRBP x DCTC, four genotypes in combinations of SRBP (M304083-TT and TC) and DCTD (M286987-CC and TC) were detected as the resistance interactive variables in the GMDR score distributions while seedlings with genotype SRBP (M304083-TC) in combinations with DCTD genotypes M286987-TC showed a higher potential to be susceptible than to be resistant (**Figure S3B**), decreasing false-positive diagnoses from the one-gene model. The uncertainty of MGR phenotypes resulting from SRBP genotype M304083-TC and CC was minimized in the three-gene model of SRBP, NBS-LRR and 6PGDH interactions (**Figure 3C**). SRBP genotype M304083-TC in combination with NBS-LRR genotype M287456-700AG was modulated to be susceptible (−0.6 vs. 0.0) while SRBP genotype M304083-CC in combination with 6PGDH genotype M259257CC was modulated to be resistant (0.4 vs. 0.0).

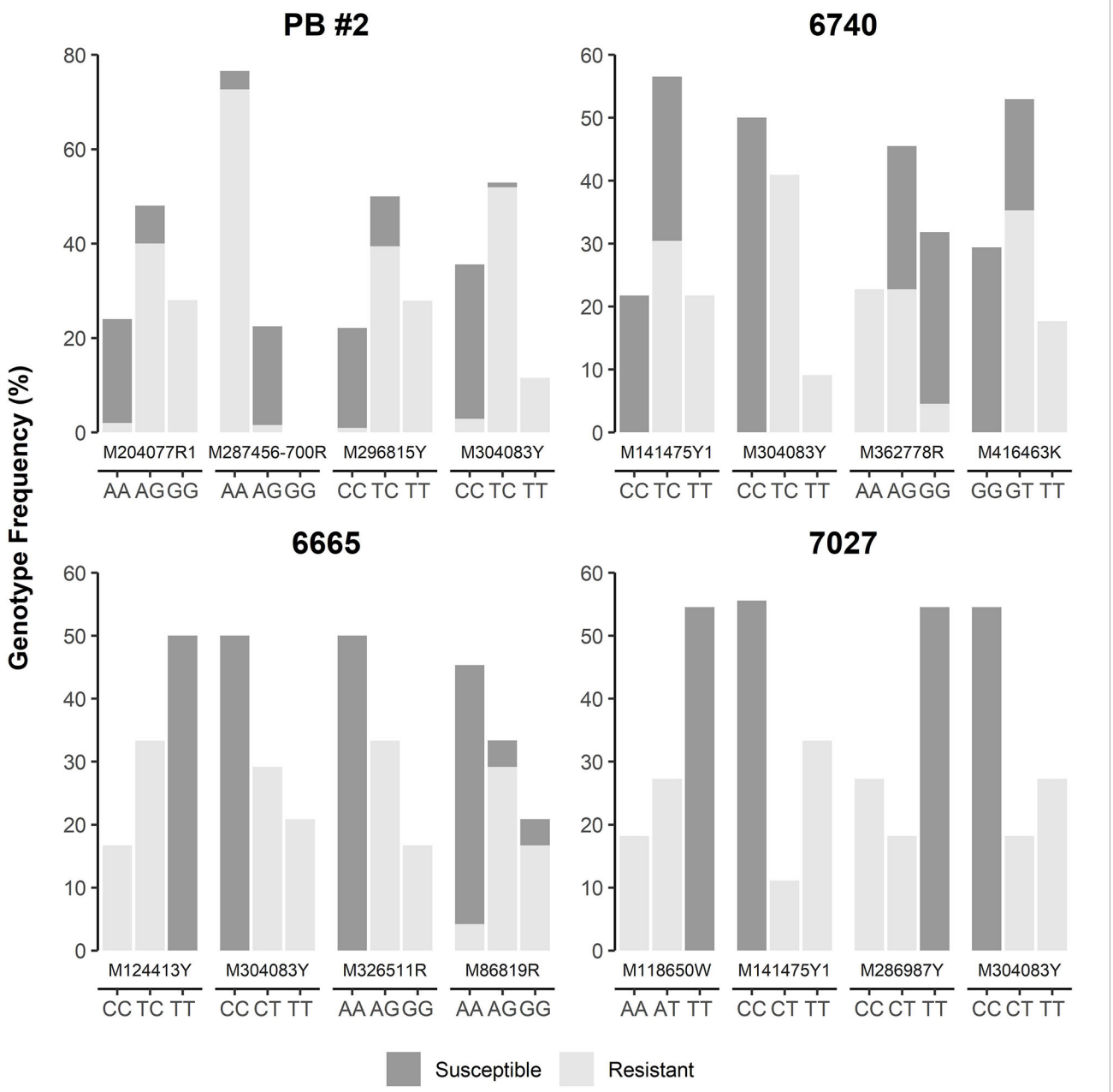

FIGURE 4 | Genotype frequency of the SNP loci that showed co-segregation or significant association with resistance to *Cronartium ribicola* in four Alberta open-pollinated seed families.

Development of TaqMan Arrays as MAS Tools for Breeding of Limber Pine Resistance

Because M304083Y had the highest marker-Rsq (r^2) across all four families and M287456 was a NBS-LRR candidate, SNP loci within both genes were selected to design TaqMan assays (**Table S4**). SNP genotypes detected using TaqMan assays and the Sequenom MassARRAY iPLEX platform were consistent, indicating that both technologies were highly reliable for SNP genotyping in limber pine. The TaqMan assays revealed genotypic segregation at the M304083-485Y locus in the progeny populations of four seed families, showing that the parent trees of all four MGR families have a T/C genotype at the M304083-485Y locus. In their progenies, T/T and T/C were linked to the resistant phenotype while C/C was linked to the susceptible phenotype. The genotype-phenotype matching rates

were 100% in the family #7027, 97.4% in the family PB #2, 97.1% in the family #6665, and 95.8% in the family #6470 (**Figure 4**), consistent with the results from the GLM and MLM-based association tests and GMDR modeling. Among parents of the six susceptible families (**Figure 1**, **Table S1**), five had the homozygous genotype C/C, and one had the heterozygous genotype C/T at the M304083-485Y locus. These results demonstrated that this TaqMan assay was an excellent MAS tool for MGR selection for the four Alberta MGR seed families. The TaqMan assay M287456-700R was valid with a genotype-phenotype matching rate of 95.4% in seed family PB #2, with A/A linked to the resistant phenotype and A/G linked to the susceptible phenotype. However, this locus was detected as a G/G genotype in the majority of progeny of the other three MGR seed families. Notably, the M304083 gene encoded a protein with unknown function and the gene M287456 was a *Cr4* candidate encoding a putative NBS-LRR protein (**Table S5**). Additional studies will be needed to confirm the functional contributions of these proteins to disease resistance in WPBR pathosystems.

DISCUSSION

Association Mapping in Limber Pine Open-Pollinated Populations

The present study documented MGR in three additional Alberta seed families as well as the previously identified PB #2, identifying new resistant germplasm to incorporate into the limber pine restoration program (Alberta Whitebark and Limber Pine Recovery Team, 2014). An association approach was used to map MGR because these four seed families originated in different areas and were open-pollinated with unknown pollen sources from natural stands. Because the presence of LD or allelic association is a prerequisite for association mapping, LD decay among SNPs using several Alberta open-pollinated limber pine families was examined. LD decay was detected with $r^2 = 0.5$ over 25 cM in the seed family PB #2, a similar level to biparental populations in other species (Flint-Garcia et al., 2003). We consistently found that the extent of LD was much higher in one open-pollinated family than that in the combined progeny of multiple parent trees in limber pine, indicating the latter had a greater genetic variability. Despite this high diversity, LD decay in a progeny population across four limber pine families (~10 cM at $r^2 > 0.1$) was much slower than in diversity panels as reported in other conifers (Plomion et al., 2014; Westbrook et al., 2015).

Association study results are commonly affected by the diversity of sampled individuals and population size. While previous studies assessed populations with <100 samples (Hart and Griffiths, 2015; Chang et al., 2016; Corwin et al., 2016), we sampled over 200 seedlings across four seed families; this allowed successful detection of SNPs associated with Alberta limber pine MGR. GWAS uses LD to identify markers associated with traits of interest that are segregating in target populations. Although unrelated populations are typically used in GWAS with case control designs, family-based GWAS designs are widely used to determine association between markers and traits within families. Compared to GWAS with case control designs using unrelated populations, GWAS with family-based designs is more powerful for detecting associated markers by avoiding artifacts of stratification at the population level (Lange et al., 2008). We used family-based populations without cryptic population structure, eliminating false positive marker-trait associations (Lipka et al., 2015). We conducted association analysis using both GLM and MLM. The latter assessed familial relatedness among individuals using a kinship matrix for family-based association studies of quantitative or binary traits (Eu-ahsunthornwattana et al., 2014; Hart and Griffiths, 2015). The MLM identified fewer SNPs with significant associations than did GLM, suggesting that MLM may be overly conservative (Wang et al., 2012). Our association study confirmed that the MGR in seed families from both the USA and Canada was controlled either by the same R gene (*Cr4*), or different R gene alleles positioned very close to each other.

Molecular Mechanisms Underlying Limber Pine Resistance *to C. ribicola*

Association of DNA variants with phenotypes facilitates elucidation of gene function and regulation as well as allelic architecture of complex traits (Neale and Savolainen, 2004). Based on the gene-for-gene model for plant disease resistance (Flor, 1971), we expected to identify limber pine R alleles that express host receptors interacting with effectors secreted by *C. ribicola* cells. Most well characterized R proteins in molecular plant-microbe interactions belong to the superfamilies of NBS-LRR and receptor-like protein kinases (RLK), acting either as intracellular or cell-surface receptors for reorganization of pathogenic effectors (Glazebrook, 2005). Of the two NBS-LRR genes associated with limber pine MGR, M287456 was mapped within a genetic distance < 0.5 cM of *Cr4*. Two M287456 SNPs were among the most significantly associated with the MGR phenotype. However, M287456 showed only limited similarity to its closest homologs in the sugar pine (*P. lambertiana* Dougl.) genome (Stevens et al., 2016) and western white pine (*P. monticola* ex D. Don) transcriptome (Liu et al., 2019), suggesting that it might have evolved recently, after diversification of the subgenus *Strobus*. This data supports our hypothesis that M287456 is the top R candidate for MGR against WPBR in Alberta seed families.

NBS-LRR proteins specifically target pathogenic effector proteins, initiating effector-triggered immunity (ETI) through signal transduction networks (Chisholm et al., 2006). A series of immune signaling components and TFs contribute to ETI downstream responses, including ion flux, oxidative reactive oxygen species (ROS) burst, activation of defense-responsive genes that facilitate syntheses of pathogenesis-related proteins, callose deposition, and hypersensitive response (HR)-related programmed cell death, which is a phenotypic expression of a typical resistance trait (Buscaill and Rivas, 2014). We identified two signaling components (homologs of RAB GTPase and LINC1) in association with MGR in Alberta limber pine. Small GTPases are well characterized as signaling components in activating defense responses through regulation of reactive oxygen species (ROS) during plant-microbe interactions (Rivero et al., 2019). For example, GTPase RabA4c overexpression

enhanced callose deposition at an early infection stage and caused complete penetration resistance to the virulent powdery mildew (Ellinger et al., 2014). Arabidopsis LINC1 is a positive PTI regulator and plays a key role in jasmonic acid signaling and glucosinolate biosynthesis; *linc1* mutants showed basal immunity towards *Pseudomonas syringae* and enhanced resistance to *Botrytis cinerea* infection (Jarad et al., 2020).

Among three MGR-associated TF genes in limber pine, the CCCH-type zinc finger proteins with ARM repeat domains constitute a TF family with multiple roles, including maintaining vegetative growth, enhancing stress tolerance, and stress-induced reproduction in response to several different stressors (Blanvillain et al., 2011). In western white pine, two CCCH-type zinc finger genes were upregulated in response to *C. ribicola* infection, including one exclusively responsive in the incompatible *Cr2-avcr2* interaction (Liu et al., 2013). In Arabidopsis, one family member (oxidative stress 2, OXS2) is required for salt tolerance by activating other downstream differentially expressed genes in the defense response (Jing et al., 2019). The GRAS TF family consists of multiple members that have different functions in plant development, signal transduction, and stress response. Several GRAS TFs are involved in regulation of cutin biosynthesis to promote mycorrhizal colonization (Xue et al., 2015). Induction of GRAS TF by fungal signals regulates the expression of downstream genes required for cell morphology changes during the host responses to obligate biotrophic fungi (Heck et al., 2016). Overall, the signaling and TF genes involved in limber pine MGR may imply the occurrence of cross-talk at different levels to integrate multiple signal pathways during white pine-blister rust (WP-BR) interactions.

Our study identified five associated genes involved in ETI downstream responses. Among them, a SNP of gene M304083, encoding a stress responsive α/β barrel domain protein, was most significantly associated with MGR, followed by four other genes with activities of expansin, galactinol synthase, PAE, and 6PGDH. The stress-response α/β barrel domain proteins have been known to be upregulated in response to salt stress (Gu et al., 2004; Zhan et al., 2019). The expansin superfamily, including expansin-like B, causes cell-wall loosening activity during cell expansion and other developmental events where cell-wall structures are modified (Sampedro and Cosgrove, 2005). The Arabidopsis expansin-like A2 (EXLA2) gene was identified by its down-regulation in response to infection by *Botrytis cinerea*, and its mutant showed enhanced resistance to necrotrophic fungi and hypersensitivity to abiotic stress (Abuqamar et al., 2013). Similarly, a western white pine expansin transcript was down-regulated in the early incompatible (*Cr2-avcr2*) WP-BR interactions (Liu et al., 2013). Galactinol synthase participates in the biosynthesis of oligosaccharides, promoting plant stress tolerance to heat, chilling, salinity and oxidative damage (Panikulangara et al., 2004; Nishizawa et al., 2008). In contrast to expansin, galactinol synthase was transcriptionally upregulated in the early incompatible (*Cr2-avcr2*) WP-BR interactions (Liu et al., 2013). PAEs catalyze the deacetylation of pectin, and decreased pectin acetylation results in increased resistance to microbial pathogens in transgenic plants (Pogorelko et al., 2013). As revealed by transcriptome analysis of mutants, Arabidopsis PAE9 activity affected transcript expression of 56 genes, mainly involved in oxidation-reduction reactions (Kloth et al., 2019). 6PGDH is the third enzyme of the pentose phosphate pathway and plays an essential role in oxidative stress defense (Hanau et al., 2013). 6PGDH was highly accumulated following pathogen infection in wheat, suggesting it is a key component in the activation of host defenses (Li et al., 2017). These reports provide further evidence to support the hypothesis that defense responsive genes play an important role in limber pine resistance. This large set of host genes works together to coordinate various molecular mechanisms underlying limber pine MGR. However, further studies are required to more fully characterize the related molecular mechanisms contributing to host resistance in WPBR pathosystems.

Development of MAS Tools for Limber Pine Resistance Screening

Major gene resistance to WPBR is an excellent case study for SNP development and validation of MAS tools because it is a well-studied trait in five-needle pine breeding programs (Sniezko et al., 2014). Of 25 associated markers that were mapped on LG8 in at least one of the USA MGR seed families (Liu et al., 2016; Liu et al., 2019), the SNP marker M304083Y showed a 97.5% genotype-phenotype matching rate across all tested seedlings from four Alberta families, and it was successfully converted into a TaqMan assay. Our modeling of gene-gene interactions revealed a potential to increase the selection accuracy of MAS tools by combining multiple genetic loci. Based on sensitivity, precision, specificity, design flexibility, and cost (Tajadini et al., 2014; Broccanello et al., 2018), the TaqMan SNP genotyping technology was selected for use in limber pine and other conifers (Liu et al., 2017; Liu et al., 2020). As a stress responsive α/β barrel domain protein, M304083 may only function in the PTI downstream response in the WPBR pathosystem. This gene provides an excellent genomic target for selective breeding of resistant individuals in related seed families.

The TaqMan assay developed from a SNP site of the NBS-LRR gene M287456 was revealed to be valid for MGR selection in only one of the tested seed families (PB #2). Due to low level expression of the NBS-LRR gene, only a partial fragment of M287456 was assembled in the limber pine transcriptome. Our previous exome-seq analysis mapped over 600 NBS-LRR gene sequences in limber pine and most of them were mapped in clusters throughout the genome. However, few NBS-LRR genes were mapped in the *Cr4* region (Liu et al., 2019). The NBS-LRR family is highly polymorphic and usually under diversifying selection pressure during plant genome evolution (Zhang et al., 2016). We also found that *Cr4*-related LD decay was much faster than the decay for all other pairs of the detected SNPs at >25 cM, suggesting more frequent recombination at this *R* locus. Availability of M287456 allowed fine dissection of the *R* locus by sequencing and mapping of its homologs. Further work is needed to explore nucleotide variations throughout the full M287456 gene and its homologs. Additional SNP sites within this NBS-LRR *Cr4*-candidate and its duplicated paralogs would have high potential for development of new MAS tools through high throughput technologies, such as

resistance gene enrichment sequencing (RenSeq) (Jupe et al., 2013). Coupled with QTL or GWAS studies for host resistance to WPBR, localizing all members of the NBS-LRR family across the genome would allow fine-scale genetic dissection of limber pine MGR and QDR to *C. ribicola*. As more novel genes are identified with strong phenotypic association, characterizing SNP loci within them for design of robust and deployable MAS tools will enhance limber pine improvement programs.

Selection of favorable alleles or allelic combinations is a lengthy process requiring breeding of outcrossing conifer species. In genotypic selection focused on a few genes with large phenotypic effects (such as MGR), application of MAS tools will enable shortened breeding cycles by allowing precise prediction of phenotypes for those genes. In limber pine breeding, ideal MAS tools will allow testing of needles of parent trees in the wild to determine if they have MGR, minimizing the need to wait to collect a viable seed crop, grow and inoculate seedlings, or at least reducing the number of seed families that must be tested to find MGR. Another important use of MAS tools for MGRs is for genotypic confirmation to support pyramiding of multiple resistance mechanisms. Some types of QDR may also exhibit stem symptom-free traits. Infection by virulent pathotypes may negate the MGR and allow observation of QDR among seedlings. Therefore, MAS tools may be applied to within-family selection for joint MGR and QDR as well as to forward selection in seed orchards when incorporating new parents that have both MGR and QDR genotypes.

MAS tools are too narrow for general use in more complex traits which are controlled by multiple genes. Although modeling of multiple gene interactions may expand the application of MAS tools to larger areas with more complex genetic backgrounds, genomic selection is a more attractive approach for breeders to select and predict complex traits with minor gene effects. Genetic characterization of genes or QTLs contributing to various complex traits of interest is an essential prerequisite for genomics-based breeding. GWAS and QTL identification for disease resistance are still relatively rare in five-needle pines. When SNPs underlying important quantitative traits are available from future GWAS and QTL mapping, their conversion into similar genotyping arrays will be useful for genomic selection in breeding programs. Our MAS tools and genotyping arrays, as well as previously reported genetic maps, offer valuable resources for future GWAS, QTL mapping, and genomic selection of these complex traits in limber pine and other related five-needle pines.

Future analysis aimed at assaying genetic variation across the whole genome is likely to facilitate a much more comprehensive elucidation of the genetic basis of phenotypic variation. Over 150 additional Alberta limber pine families from parents in heavily infected stands are currently under evaluation for WPBR resistance. As resistance related phenotypic data becomes available from conservation and breeding programs in the coming years, it would be interesting to expand the study to a wider geographical area where other resistance mechanisms may be present. Because the Sequenom-based SNP genotyping arrays developed here were verified for their application in association mapping of *Cr4*, these genotyping arrays can be applied to any limber pine families to search for additional R genes. Novel R genes will be confirmed in those families if all *Cr4*-linked SNPs of the genotyping arrays show no association with resistant phenotypes.

DATA AVAILABILITY STATEMENT

All relevant data is contained within the article. Gene sequence data for design of Sequenom iPLEX MassARRAY are shown in **Supplementary Material Table S4**.

AUTHOR CONTRIBUTIONS

J-JL, RAS, RS, and JK conceived the research. RS, GA, JK, and RAS provided the genetic materials. RAS, RZ, and AK conducted the disease ratings and analyzed phenotypic data. J-JL, HW, and AZ conducted SNP genotyping and analyzed genotypic data. AS shared SNP data and some genotypes of the limber pine species for the study. J-JL wrote the original draft with contributions from all authors. J-JL and RAS supervised the project. All authors contributed to the article and approved the submitted version.

FUNDING

This research was supported in part by the CFS-Pest Risk Management Program and funding from Waterton Lakes National Park of Canada.

ACKNOWLEDGMENTS

We would like to thank Gary Zhang and Gurp Thandi at CFS for bioinformatic analyses and data presentation, Bob Danchok, Emily Boes, and other colleagues at DGRC for sample collection and phenotype assessment; and colleagues at Waterton Lakes National Park for collection of the seed families used in this investigation.

SUPPLEMENTARY MATERIAL

The Supplementary Material for this article can be found online at: https://www.frontiersin.org/articles/10.3389/fpls.2020.557672/full#supplementary-material

SUPPLEMENTARY FIGURE 1 | Fine-scale genetic linkage map of the limber pine *Cr4* locus. Genetic distances between two adjacent loci are labeled in centimorgans (cM).

SUPPLEMENTARY FIGURE 2 | Scatter plot of the squared correlations of allele frequencies (r^2) versus distance in cM across Pinus consensus linkage group 8 (LG8). Each dot represents a SNP, with the X-axis showing their locations on LG8 and Y-axis showing the marker-Rsq values (r^2) squared for each SNP marker. The

putative *Cr4* gene was included with an expected r^2 value at 1. **(A)** Progeny of the seed family PB #2; **(B)** Progeny of all four Alberta seed families.

SUPPLEMENTARY FIGURE 3 | Gene-Gene interactions for association with major gene resistance detected by GMDR analysis. In each cell, the left bar represents a positive score for the resistant group and the right bar a negative score for the susceptible group. Resistant cells were indicated by dark shading, susceptible cells by light shading. For SRBP (M304083Y), 0 represents TT, 1 represents TC, and 2 represents CC genotype. For NBS-LRR (M287456-700R), 0 represents AA, 1 represents AG, and 2 represents GG genotype. For both DCTD (M286987Y) and 6PGDH (M259257Y), 0 represents CC, 1 represents TC, and 2 represents TT genotype. **(A)** one-gene model with SRBP (M304083Y); **(B)** two-gene model with SRBP (M304083Y) and DCTD (M286987Y); **(C)** three-gene model with SRBP (M304083Y), 6PGDH (M259257Y), and NBS-LRR (M287456-700R).

REFERENCES

Abuqamar, S., Ajeb, S., Sham, A., Enan, M. R., and Iratni, R. (2013). A mutation in the expansin-like A2 gene enhances resistance to necrotrophic fungi and hypersensitivity to abiotic stress in *Arabidopsis thaliana*. *Mol. Plant Pathol.* 14, 813–827. doi: 10.1111/mpp.12049

Alberta Whitebark and Limber Pine Recovery Team (2014). *Alberta limber pine recovery plan 2014-2019* (Edmonton, AB: Alberta Environment and Sustainable Resource Development. Alberta Species at Risk Recovery Plan No. 35).

Baker, E. A. G., Wegrzyn, J. L., Sezen, U. U., Falk, T., Maloney, P. E., Vogler, D. R., et al. (2018). Comparative transcriptomics among four white pine species. *G3: Genes Genomes Genet.* 8, 1461–1474. doi: 10.1534/g3.118.200257

Blanvillain, R., Wei, S., Wei, P., Kim, J. H., and Ow, D. W. (2011). Stress tolerance to stress escape in plants: role of the OXS2 zinc-finger transcription factor family. *EMBO J.* 30, 3812–3822. doi: 10.1038/emboj.2011.270

Bradbury, P. J., Zhang, Z., Kroon, D. E., Casstevens, T. M., Ramdoss, Y., and Buckler, E. S. (2007). TASSEL: software for association mapping of complex traits in diverse samples. *Bioinformatics* 23, 2633–2635. doi: 10.1093/bioinformatics/btm308

Broccanello, C., Chiodi, C., Funk, A., McGrath, J. M., Panella, L., and Stevanato, P. (2018). Comparison of three PCR-based assays for SNP genotyping in plants. *Plant Methods* 14, 28. doi: 10.1186/s13007-018-0295-6

Buscaill, P., and Rivas, S. (2014). Transcriptional control of plant defence responses. *Curr. Opin. Plant Biol.* 20, 35–46. doi: 10.1016/j.pbi.2014.04.004

Chang, H.-X., Lipka, A. E., Domier, L. L., and Hartman, G. L. (2016). Characterization of disease resistance loci in the USDA soybean germplasm collection using genome-wide associations. *Phytopathology* 106, 1139–1151. doi: 10.1094/PHYTO-01-16-0042-FI

Chisholm, S. T., Coaker, G., Day, B., and Staskawicz, B. J. (2006). Host-microbe interactions: shaping the evolution of the plant immune response. *Cell* 124, 803–814. doi: 10.1016/j.cell.2006.02.008

Churchill, G. A., and Doerge, R. W. (1994). Empirical threshold values for quantitative trait mapping. *Genetics* 138, 963–971.

Corwin, J. A., Copeland, D., Feusier, J., Subedy, A., Eshbaugh, R., Palmer, C., et al. (2016). The quantitative basis of the Arabidopsis innate immune system to endemic pathogens depends on pathogen genetics. *PLoS Genet.* 12, e1005789. doi: 10.1371/journal.pgen.1005789

COSEWIC (2014). *COSEWIC assessment and status report on the limber pine Pinus flexilis in Canada* (Ottawa: Committee on the Status of Endangered Wildlife in Canada).

Ellinger, D., Glöckner, A., Koch, J., Naumann, M., Stürtz, V., Schütt, K., et al. (2014). Interaction of the Arabidopsis GTPase RabA4c with its effector PMR4 results in complete penetration resistance to powdery mildew. *Plant Cell* 26, 3185–3200. doi: 10.1105/tpc.114.127779

Eu-ahsunthornwattana, J., Miller, E. N., Fakiola, M.Wellcome Trust Case Control Consortium 2, , Jeronimo, S. M. B., Blackwell, J. M., et al. (2014). Comparison of methods to account for relatedness in genome-wide association studies with family based data. *PLoS Genet.* 10, e1004445. doi: 10.1371/journal.pgen.1004445

Falk, T., Herndon, N., Grau, E., Buehler, S., Richter, P., Zaman, S., et al. (2018). Growing and cultivating the forest genomics database, TreeGenes. *Database* 2018, bay084. doi: 10.1093/database/bay084

Flint-Garcia, S. A., Thornsberry, J. M., and Buckler, E. S. (2003). Structure of linkage disequilibrium in plants. *Annu. Rev. Plant Biol.* 54, 357–374. doi: 10.1146/annurev.arplant.54.031902.134907

Flor, H. H. (1971). Current status of the gene-for-gene concept. *Annu. Rev. Phytopathol.* 9, 275–296. doi: 10.1146/annurev.py.09.090171.001423

Friedline, C. J., Lind, B. M., Hobson, E. M., Harwood, D. E., Mix, A. D., Maloney, P. E., et al. (2015). The genetic architecture of local adaptation I: the genomic landscape of foxtail pine (*Pinus balfouriana* Grev. & Balf.) as revealed from a high-density linkage map. *Tree Genet. Genomes* 11, 49. doi: 10.1007/s11295-015-0866-x

Gabriel, S., Ziaugra, L., and Tabbaa, D. (2009). SNP genotyping using the Sequenom MassARRAY iPLEX platform. *Curr. Protoc. Hum. Genet.* 60, 2.12.1–2.12.18. doi: 10.1002/0471142905.hg0212s60

Glazebrook, J. (2005). Contrasting mechanisms of defense against biotrophic and necrotrophic pathogens. *Annu. Rev. Phytopathol.* 43, 205–227. doi: 10.1146/annurev.phyto.43.040204.135923

Gonzalez-Ibeas, D., Martinez-Garcia, P. J., Famula, R. A., Delfino-Mix, A., Stevens, K. A., Loopstra, C. A., et al. (2016). Assessing the gene content of the megagenome: sugar pine (*Pinus lambertiana*). *G3: Genes Genomes Genet.* 6, 3787–3802. doi: 10.1534/g3.116.032805

Götz, S., García-Gómez, J. M., Terol, J., Williams, T. D., Nagaraj, S. H., Nueda, M. J., et al. (2008). High-throughput functional annotation and data mining with the Blast2GO suite. *Nucleic Acids Res.* 36, 3420–3435. doi: 10.1093/nar/gkn176

Government of Alberta (2014). *Species assessed by Alberta's endangered species conservation committee: short list* (Edmonton, AB, Canada).

Gu, R., Fonseca, S., Puskas, L. G., Hackler, L.Jr, Zvara, A., Dudits, D., et al. (2004). Transcript identification and profiling during salt stress and recovery of *Populus euphratica*. *Tree Physiol.* 24, 265–276. doi: 10.1093/treephys/24.3.265

Hanau, S., d'Empaire, L. P., Capone, I., Alberighi, S., Montioli, R., and Dallocchio, F. (2013). Evidence for dimer/tetramer equilibrium in *Trypanosoma brucei* 6-phosphogluconate dehydrogenase. *Biochim. Biophys. Acta* 1834, 2647–2652. doi: 10.1016/j.bbapap.2013.09.018

Hart, J. P., and Griffiths, P. D. (2015). Genotyping-by-sequencing enabled mapping and marker development for the By-2 Potyvirus resistance allele in common bean. *Plant Genome* 8, 1–14. doi: 10.3835/plantgenome2014.09.0058

Heck, C., Kuhn, H., Heidt, S., Walter, S., Rieger, N., and Requena, N. (2016). Symbiotic fungi control plant root cortex development through the novel GRAS transcription factor MIG1. *Curr. Biol.* 26, 2770–2778. doi: 10.1016/j.cub.2016.07.059

Hou, T. T., Lin, F., Bai, S., Cleves, M. A., Xu, H. M., and Lou, X. Y. (2019). Generalized multifactor dimensionality reduction approaches to identification of genetic interactions underlying ordinal traits. *Genet. Epidemiol.* 43, 24– 36. doi: 10.1002/gepi.22169

Jarad, M., Mariappan, K., Almeida-Trapp, M., Mette, M. F., Mithöfer, A., Rayapuram, N., et al. (2020). The lamin-like LITTLE NUCLEI 1 (LINC1) regulates pattern-triggered immunity and jasmonic acid signaling. *Front. Plant Sci.* 10, 1639. doi: 10.3389/fpls.2019.01639

Jermstad, K. D., Eckert, A. J., Wegrzyn, J. L., Delfino-Mix, A., Davis, D. A., Burton, D. C., et al. (2011). Comparative mapping in *Pinus*: sugar pine (*Pinus lambertiana* Dougl.) and loblolly pine (*Pinus taeda* L.). *Tree Genet. Genomes* 7, 457–468. doi: 10.1007/s11295-010-0347-1

Jing, Y., Shi, L., Li, X., Zheng, H., Gao, J., Wang, M., et al. (2019). OXS2 is required for salt tolerance mainly through associating with salt Inducible genes, CA1 and Araport11, in Arabidopsis. *Sci. Rep.* 9, 20341. doi: 10.1038/s41598-019-56456-1

Jupe, F., Witek, K., Verweij, W., Sliwka, J., Pritchard, L., Etherington, G. J., et al. (2013). Resistance gene enrichment sequencing (RenSeq) enables reannotation of the NB-LRR gene family from sequenced plant genomes and rapid mapping of resistance loci in segregating populations. *Plant J.* 76, 530–544. doi: 10.1111/tpj.12307

Kinloch, B. B., and Dupper, G. E. (2002). Genetic specificity in the white pine-blister rust pathosystem. *Phytopathol* 92, 278–280. doi: 10.1094/PHYTO.2002.92.3.278

Kloth, K. J., Abreu, I. N., Delhomme, N., Petřík, I., Villard, C., Ström, C., et al. (2019). PECTIN ACETYLESTERASE9 affects the transcriptome and metabolome and delays aphid feeding. *Plant Physiol.* 181, 1704–1720. doi: 10.1104/pp.19.00635

Lange, E. M., Sun, J., Lange, L. A., Zheng, S. L., Duggan, D., Carpten, J. D., et al. (2008). Family-based samples can play an important role in genetic association studies. *Cancer Epidemiol. Biomarkers Prev.* 17, 2208–2214. doi: 10.1158/1055-9965.EPI-08-0183

Li, J., Yang, X., Liu, X., Yu, H., Du, C., Li, M., et al. (2017). Proteomic analysis of the compatible interaction of wheat and powdery mildew (*Blumeria graminis* f. sp. tritici). *Plant Physiol. Biochem.* 111, 234–243. doi: 10.1016/j.plaphy.2016.12.006

Lipka, A. E., Kandianis, C. B., Hudson, M. E., Yu, J., Drnevich, J., Bradvury, P. J., et al. (2015). From association to prediction: Statistical methods for the dissection and selection of complex traits in plants. *Curr. Opin. Plant Biol.* 24, 110–118. doi: 10.1016/j.pbi.2015.02.010

Liu, J.-J., Sturrock, R. N., and Benton, R. (2013). Transcriptome analysis of *Pinus monticola* primary needles by RNA-seq provides novel insight into host resistance to *Cronartium ribicola*. *BMC Genomics* 14, 884. doi: 10.1186/1471-2164-14-884

Liu, J.-J., Sniezko, R. A., Sturrock, R. N., and Chen, H. (2014). Western white pine SNP discovery and high-throughput genotyping for breeding and conservation applications. *BMC Plant Biol.* 14, 380. doi: 10.1186/s12870-014-0380-6

Liu, J.-J., Schoettle, A. W., Sniezko, R. A., Sturrock, R. N., Zamany, A., Williams, H., et al. (2016). Genetic mapping of *Pinus flexilis* major gene (*Cr4*) for resistance to white pine blister rust using transcriptome-based SNP genotyping. *BMC Genomics* 17, 753. doi: 10.1186/s12864-016-3079-2

Liu, J.-J., Sniezko, R. A., Zamany, A., Williams, H., Wang, N., Kegley, A., et al. (2017). Saturated genic SNP mapping identified functional candidates and selection tools for the *Pinus monticola Cr2* locus controlling resistance to white pine blister rust. *Plant Biotechnol. J.* 15, 1149–1162. doi: 10.1111/pbi.12705

Liu, J.-J., Schoettle, A. W., Sniezko, R. A., Yao, F., Zamany, A., Williams, H., et al. (2019). Limber pine (*Pinus flexilis* James) genetic map constructed by exome-seq provides insight into evolution of disease resistance and a genomic resource for genomics-based breeding. *Plant J.* 98, 745–758. doi: 10.1111/tpj.14270

Liu, J.-J., Williams, H., Zamany, A., Li, X.-R., Gellner, S., and Sniezko, R. A. (2020). Development and application of marker-assisted selection (MAS) tools for breeding of western white pine (*Pinus monticola* Douglas ex D. Don) resistance to blister rust (*Cronartium ribicola* J.C. Fisch.) in British Columbia. *Can. J. Plant Pathol.* 42, 250–259. doi: 10.1080/07060661.2019.1638454

Lorenz, W. W., Ayyampalayam, S., Bordeaux, J. M., Howe, G. T., Jermstad, K. D., Neale, D. B., et al. (2012). Conifer DBMagic: a database housing multiple de novo transcriptome assemblies for 12 diverse conifer species. *Tree Genet. Genomes* 8, 1477–1485. doi: 10.1007/s11295-012-0547-y

Millar, C. I., Westfall, R. D., and Delany, D. L. (2007). Response of high-elevation limber pine (Pinus flexilis) to multiyear droughts and 20th-century warming, Sierra Nevada, California, USA. *Can. J. For Res.* 37, 2508–2520. doi: 10.1139/X07-097

Neale, D. B., and Savolainen, Q. (2004). Association genetics of complex traits in conifers. *Trends Plant Sci.* 9, 325–330. doi: 10.1016/j.tplants.2004.05.006

Nishizawa, A., Yabuta, Y., and Shigeoka, S. (2008). Galactinol and raffinose constitute a novel function to protect plants from oxidative damage. *Plant Physiol.* 147, 1251–1263. doi: 10.1104/pp.108.122465

Panikulangara, T. J., Eggers-Schumacher, G., Wunderlich, M., Stransky, H., and Schoeffl, F. (2004). Galactinol synthase1, a novel heat shock factor target gene responsible for heat-induced synthesis of raffinose family oligosaccharides in Arabidopsis. *Plant Physiol.* 136, 3148–3158. doi: 10.1104/pp.104.042606

Plomion, C., Chancerel, E., Endelman, J., Lamy, J. B., Mandrou, E., Lesur, I., et al. (2014). Genome-wide distribution of genetic diversity and linkage disequilibrium in a mass-selected population of maritime pine. *BMC Genomics* 15, 171. doi: 10.1186/1471-2164-15-171

Pogorelko, G., Lionetti, V., Fursova, O., Sundaram, R. M., Qi, M., Whitham, S. A., et al. (2013). Arabidopsis and Brachypodium transgenic plants expressing *A. nidulans* acetylesterases have decreased degree of polysaccharide acetylation and increased resistance to pathogens. *Plant Physiol.* 162, 9–23. doi: 10.1104/pp.113.214460

Rivero, C., Traubenik, S., Zanetti, M. E., and Blanco, F. A. (2019). Small GTPases in plant biotic interactions. *Small GTPases* 10, 350–360. doi: 10.1080/21541248.2017.1333557

Sampedro, J., and Cosgrove, D. J. (2005). The expansin superfamily. *Genome Biol.* 6, 242. doi: 10.1186/gb-2005-6-12-242

Schoettle, A. W., Sniezko, R. A., Kegley, A., and Burns, K. S. (2014). White pine blister rust resistance in limber pine: evidence for a major gene. *Phytopathol* 104, 163–173. doi: 10.1094/PHYTO-04-13-0092-R

Schoettle, A. W. (2004). Ecological roles of five-needle pine in Colorado: potential consequences of their loss. Breeding and genetic resources of five-needle pines: growth, adaptability and pest-resistance. *Proceedings RMRS-P-32.* (Fort Collins, CO, USA: USDA Forest Service, Rocky Mountain Research Station), 124–135.

Smith, C. M., Langor, D. W., Myrholm, C., Weber, J., Gillies, C., and Stuart-Smith, J. (2013). Changes in white pine blister rust infection and mortality in limber pine over time. *Can. J. For Res.* 43, 919–928. doi: 10.1139/cjfr-2013-0072

Sniezko, R. A., Kegley, A. J., and Danchok, R. (2008). White pine blister rust resistance in North American, Asian and European species - results from artificial inoculation trials in Oregon. *Ann. For Res.* 51, 53–66.

Sniezko, R., Smith, J., Liu, J.-J., and Hamelin, R. (2014). Genetic resistance to fusiform rust in southern pines and white pine blister rust in white pines—A contrasting tale of two rust pathosystems -Current status and future prospects. *Forests* 5, 2050–2083. doi: 10.3390/f5092050

Sniezko, R. A., Danchok, R., Savin, D. P., Liu, J.-J., and Kegley, A. (2016). Genetic resistance to white pine blister rust in limber pine (*Pinus flexilis*): major gene resistance in a northern population. *Can. J. For Res.* 46, 1173–1178. doi: 10.1139/cjfr-2016-0128

Sniezko, R. A., Johnson, J. S., and Savin, D. P. (2020). Assessing the durability, stability, and usability of genetic resistance to a non-native fungal pathogen in two pine species. *Plants People Planet.* 2, 57–68. doi: 10.1002/ppp3.49

Stevens, K. A., Wegrzyn, J. L., Zimin, A., Puiu, D., Crepeau, M., Cardeno, C., et al. (2016). Sequence of the sugar pine megagenome. *Genetics* 204, 1613–1626. doi: 10.1534/genetics.116.193227

Syring, J. V., Tennessen, J. A., Jennings, T. N., Wegrzyn, J., Scelfo-Dalbey, C., and Cronn, R. (2016). Targeted capture sequencing in whitebark pine reveals range-wide demographic and adaptive patterns despite challenges of a large, repetitive genome. *Front. Plant Sci.* 7, 484. doi: 10.3389/fpls.2016.00484

Tajadini, M., Panjehpour, M., and Javanmard, S. H. (2014). Comparison of SYBR Green and TaqMan methods in quantitative real-time polymerase chain reaction analysis of four adenosine receptor subtypes. *Adv. BioMed. Res.* 3, 85. doi: 10.4103/2277-9175.127998

Tomback, D. F., and Achuff, P. (2010). Blister rust and western forest biodiversity: Ecology, values, and outlook for white pines. *For Pathol.* 40, 186–225. doi: 10.1111/j.1439-0329.2010.00655.x

Wang, M., Jiang, N., Jia, T., Leach, L., Cockram, J., Waugh, R., et al. (2012). Genome-wide association mapping of agronomic and morphologic traits in highly structured populations of barley cultivars. *Theor. Appl. Genet.* 124, 233–246. doi: 10.1007/s00122-011-1697-2

Weiss, M., Sniezko, R. A., Puiu, D., Crepeau, M. W., Stevens, K., Salzberg, S. L., et al. (2020). Genomic basis of white pine blister rust quantitative disease resistance and its relationship with qualitative resistance. *Plant J.* doi: 10.1111/tpj.14928

Westbrook, J. W., Chhatre, V. E., Wu, L. S., Chamala, S., Neves, L. G., Muñoz, P., et al. (2015). A consensus genetic map for *Pinus taeda* and *Pinus elliottii* and extent of linkage disequilibrium in two genotype-phenotype discovery populations of *Pinus taeda*. *G3: Genes Genomes Genet.* 5, 1685–1694. doi: 10.1534/g3.115.019588

Winham, S. J., and Motsinger-Reif, A. A. (2011). An R package implementation of multifactor dimensionality reduction. *BioData Min.* 4, 24. doi: 10.1186/1756-0381-4-24

Wu, Y. H., Close, T. J., and Lonardi, S. (2011). Accurate construction of consensus genetic maps via integer linear programming. *IEEE ACM Trans. Comput. Biol. Bioinf.* 8, 381–394. doi: 10.1109/TCBB.2010.35

Xue, L., Cui, H., Buer, B., Vijayakumar, V., Delaux, P. M., Junkermann, S., et al. (2015). Network of GRAS transcription factors involved in the control of arbuscule development in *Lotus japonicus*. *Plant Physiol.* 167, 854–871. doi: 10.1104/pp.114.255430

Yu, J., Pressoir, G., Briggs, W. H., Vroh Bi, I., Yamasaki, M., Doebley, J. F., et al. (2006). A unified mixed-model method for association mapping that accounts for multiple levels of relatedness. *Nat. Genet.* 38, 203–208. doi: 10.1038/ng1702

Zhan, Y., Wu, Q., Chen, Y., Tang, M., Sun, C., Sun, J., et al. (2019). Comparative proteomic analysis of okra (*Abelmoschus esculentus* L.) seedlings under salt stress. *BMC Genomics* 20, 381. doi: 10.1186/s12864-019-5737-7

Zhang, Y., Xia, R., Kuang, H., and Meyers, B. C. (2016). The diversification of plant NBS-LRR defense genes directs the evolution of microRNAs that target them. *Mol. Biol. Evol.* 33, 2kaka692–2705. doi: 10.1093/molbev/msw154

Conflict of Interest: The authors declare that the research was conducted in the absence of any commercial or financial relationships that could be construed as a potential conflict of interest.

frontiers in Plant Science

ORIGINAL RESEARCH
published: 09 October 2020
doi: 10.3389/fpls.2020.546295

Effect of Drought on the Methylerythritol 4-Phosphate (MEP) Pathway in the Isoprene Emitting Conifer *Picea glauca*

Erica Perreca[1], Johann Rohwer[2], Diego González-Cabanelas[1], Francesco Loreto[3], Axel Schmidt[1], Jonathan Gershenzon[1] and Louwrance Peter Wright[1†]*

[1] Department of Biochemistry, Max Planck Institute for Chemical Ecology, Jena, Germany, [2] Laboratory for Molecular Systems Biology, Department of Biochemistry, Stellenbosch University, Stellenbosch, South Africa, [3] Consiglio Nazionale delle Ricerche, Dipartimento di Scienze Bio-Agroalimentari, Roma, Italy

OPEN ACCESS

Edited by:
Sanushka Naidoo, University of Pretoria, South Africa

Reviewed by:
Thomas D. Sharkey, Michigan State University, United States
Bjoern Hamberger, Michigan State University, United States

***Correspondence:**
Erica Perreca
eperreca@ice.mpg.de

†Present address:
Louwrance Peter Wright, Zeiselhof Research Farm, Pretoria, South Africa

Specialty section:
This article was submitted to Plant Abiotic Stress, a section of the journal Frontiers in Plant Science

Received: *27 March 2020*
Accepted: *17 September 2020*
Published: *09 October 2020*

Citation:
Perreca E, Rohwer J, González-Cabanelas D, Loreto F, Schmidt A, Gershenzon J and Wright LP (2020) Effect of Drought on the Methylerythritol 4-Phosphate (MEP) Pathway in the Isoprene Emitting Conifer Picea glauca. Front. Plant Sci. 11:546295. doi: 10.3389/fpls.2020.546295

The methylerythritol 4-phosphate (MEP) pathway of isoprenoid biosynthesis produces chlorophyll side chains and compounds that function in resistance to abiotic stresses, including carotenoids, and isoprene. Thus we investigated the effects of moderate and severe drought on MEP pathway function in the conifer *Picea glauca*, a boreal species at risk under global warming trends. Although moderate drought treatment reduced the photosynthetic rate by over 70%, metabolic flux through the MEP pathway was reduced by only 37%. The activity of the putative rate-limiting step, 1-deoxy-D-xylulose-5-phosphate synthase (DXS), was also reduced by about 50%, supporting the key role of this enzyme in regulating pathway metabolic flux. However, under severe drought, as flux declined below detectable levels, DXS activity showed no significant decrease, indicating a much-reduced role in controlling flux under these conditions. Both MEP pathway intermediates and the MEP pathway product isoprene incorporate administered $^{13}CO_2$ to high levels (75–85%) under well-watered control conditions indicating a close connection to photosynthesis. However, this incorporation declined precipitously under drought, demonstrating exploitation of alternative carbon sources. Despite the reductions in MEP pathway flux and intermediate pools, there was no detectable decline in most major MEP pathway products under drought (except for violaxanthin under moderate and severe stress and isoprene under severe stress) suggesting that the pathway is somehow buffered against this stress. The resilience of the MEP pathway under drought may be a consequence of the importance of the metabolites formed under these conditions.

Keywords: carotenoid, chlorophyll, DXS enzyme, metabolic flux, alternative carbon source, MVA pathway

INTRODUCTION

Nearly all members of the vast isoprenoid family of metabolites are produced from the two C_5 diphosphate intermediates, dimethylallyl diphosphate (DMADP) and its isomer isopentenyl diphosphate (IDP). These intermediates arise from two different pathways in plants, the mevalonate (MVA) pathway located in the cytosol, ER and peroxisomes, and the more recently identified

methylerythritol 4-phosphate (MEP) pathway localized in plastids (Hemmerlin et al., 2012). While C_5 units derived from the MVA pathway are used in the formation of compounds such as sesquiterpenes, sterols, brassinosteroids, triterpenes, dolichols and farnesylated proteins, C_5 units from the MEP pathway are used in the production of isoprene, monoterpenes, diterpenes, chlorophylls, and carotenoids as well as the gibberellin, strigolactone and abscisic acid hormones. The extent to which each of the two pathways contributes to the total DMADP/IDP pool under various conditions has not been completely elucidated. Eberl et al. (2018) suggested a contribution to the total DMADP/IDP intermediate pool size from the MVA pathway, under fungus infestation in poplar leaves. Dudareva et al. (2005) showed that the MEP pathway provides IDP precursors for both plastidial monoterpene and cytosolic sesquiterpenes synthesis in snapdragon flowers and pointed out the possibility of a cross talk between the two pathways. However, other studies showed that cross talk between both pathways is not capable of rescuing a pharmacological block in either pathway (Laule et al., 2003; Rodríguez-Concepción et al., 2004).

Isoprenoids have a wide variety of functions in plant growth, development, reproduction and defense. Among the MEP pathway products, several classes protect against oxidative stress, including carotenoids, tocopherols and isoprene. The formation of these compounds might be favored under conditions leading to oxidative stress, including high temperature, high light and low water supply. Experiments with high light and high temperature actually point to the possibility that metabolic flux through the MEP pathway is reduced in a number of plant species because of the inhibition of the two ultimate steps catalyzed by proteins with oxygen-sensitive 4Fe-4S clusters, leading to the accumulation of the intermediate 2-*C*-methyl-D-erythritol-2,4-cyclodiphosphate (MEcDP) (Rivasseau et al., 2009). However, little work has been done on the effects of drought in this context, and no comprehensive study has been performed on the MEP pathway in a conifer species. The effect of drought on plant metabolism in general has been studied for many years, but most attention has been focused on the increased synthesis of various osmolytes, such as quaternary ammonium compounds and polyhydric alcohols. There are also scattered reports on alterations in other pathways of primary and secondary metabolism (Selmar, 2008; Guo et al., 2018; Mundim and Pringle, 2018; Ahkami et al., 2019). Among isoprenoids, phytol and α-tocopherol in *Brachypodium distachyon* were reported to increase during early phases of drought vs. well-watered control plants, but declined during later drought phases (Ahkami et al., 2019). Meanwhile, secondary metabolite isoprenoids were shown in a meta-analysis to generally increase during drought (Mundim and Pringle, 2018), but the systematic investigation of drought effects on an isoprenoid pathway has not been undertaken.

Control of the MEP pathway is manifested at several different levels of organization. The first enzymatic step, 1-deoxy-D-xylulose-5-phosphate synthase (DXS), has been generally assumed to be rate limiting based on studies in which overexpression of the corresponding gene led to increases in MEP pathway products (Estévez et al., 2001; Enfissi et al., 2005). In *Arabidopsis thaliana*, DXS was shown to control approximately 80% of the metabolic flux through the MEP pathway in photosynthetic tissue by metabolic control analysis (Wright et al., 2014). DXS activity itself is regulated transcriptionally and post-transcriptionally (Rodríguez-Concepción, 2006; Banerjee and Sharkey, 2014). In particular, feedback inhibition of DMADP and IDP regulates DXS activity in some species (Banerjee et al., 2013). Other factors regulating the MEP pathway include the supply of the two initial substrates, glyceraldehyde-3-phosphate and pyruvate (Banerjee and Sharkey, 2014). Moreover, under certain conditions the intermediate MEcDP is subject to efflux from the pathway (Wright et al., 2014; González-Cabanelas et al., 2015), and appears to be the source of a plastid-to-nucleus signal that regulates salicylic acid signaling (Xiao et al., 2012; Onkokesung et al., 2019). Regulation of the MEP pathway has been well studied in angiosperms (Banerjee et al., 2013; Ghirardo et al., 2014), whereas information about gymnosperms, especially conifers, is very limited, especially under drought. Here we investigate the effect of drought on the MEP pathway in the widespread boreal conifer *Picea glauca*, one of the few conifers that emit both isoprene and monoterpenes (Loreto and Fineschi, 2015). As boreal forests are increasingly affected by global warming (Soja et al., 2007; Price et al., 2013), this study may help understand the consequences of drought on tree metabolism in a critical ecosystem.

We found drought to decrease metabolic flux through the MEP pathway in *P. glauca*, although this decline was considerably less than the declines in photosynthesis and transpiration observed, and there was no apparent decrease in the levels of most major MEP pathway products. Under moderate drought, decrease in pathway flux seemed to be modulated by the activity of DXS, but this enzyme had little contribution to the regulation of the MEP pathway under severe drought.

MATERIALS AND METHODS

Plant Material and Drought Treatment

Young trees of white spruce [*Picea glauca* (Moench) Voss], 3 years old, were purchased from a local nursery in Jena, Germany and grown outdoors at the Max Planck Institute of Chemical Ecology under natural conditions. At the end of May 2015, the trees were transferred inside a greenhouse with supplemental lighting. Relative humidity was maintained between 50 and 60%, light period was 14 h, and the temperature was 23°C:19°C, day: night. The experiment was performed in August after needles had fully expanded. Drought was applied by withholding water. At the beginning of the experiment, trees were irrigated and excess of water was allowed to drain for 2–3 h. Then the initial pot weight was measured using a digital balance to a precision of 1 g (model QS32A; Sartorius Instrumentation, Göttingen, Germany). Subsequently, pot weights were recorded daily. Each pot was enclosed with a bag to avoid soil evaporation. Therefore, loss of water was attributed to plant transpiration only. The experiment lasted 20 days. The availability of water under the different stress regimes, was described by the fraction of transpirable soil water (FTSW). The FTSW was calculated by

using the daily pot weight according to the formula (Sinclair and Ludlow, 1986; Ray and Sinclair, 1998):

$$\text{FTSW} = (\text{daily weight} - \text{final weight}) / (\text{initial weight} - \text{final weight})$$

The final pot weight was reached when soil water content no longer supports transpiration and corresponded to the FTSW endpoint (Sinclair and Ludlow, 1986). The relative transpiration rate (RTR) of the trees was calculated by their daily transpiration rate (TR), determined by daily pot weight loss, divided by the average transpiration rate (ATR) of a group of well-watered trees (Sinclair and Ludlow, 1986; Ray and Sinclair, 1998):

$$\text{RTR} = (\text{TR}/\text{ATR}) \times 100$$

Over the course of the experiment, these well-watered trees were irrigated daily until pot capacity and weighed. They were not used in any further measurements. Three treatments were performed: control, moderate drought and severe drought. We used five trees for each treatment, and the treatments were sampled at different times. The control trees were watered daily and sampled only at the end of the experiment. Stressed trees, from which water was completely withheld, were sampled when the target RTR (50% for moderate stress at FTSW12, 20% for severe stress at FTSW3) was achieved (**Supplementary Figure S1**). Sampling consisted of measuring from one twig the photosynthetic rate and isoprene emission, and labeling with $^{13}CO_2$ for 50 min. Afterward the same twig was harvested for metabolite analysis. This twig was always the youngest branch on the shoot, and had flushed in the current year. After sampling, trees were allowed to dry further until RTR was 10%, corresponding to the FTSW endpoint (Sinclair and Ludlow, 1986).

Sample Processing

After $^{13}CO_2$ labeling for 50 min (see details below), twigs were harvested, frozen immediately in liquid nitrogen, and transferred to a −80°C freezer. Only needles were used for biochemical analysis. After grinding, the total fresh weight was measured. Analysis of chlorophylls, carotenoids, β-cyclocitral, monoterpenes, and the DXS assay was carried out with fresh tissue, while analyses of MEP intermediate metabolites, sugars, and abscisic acid were carried out after freeze-drying. For each tree, 100 mg of fresh tissue were weighed before and after freeze-drying to determine fresh-to-dry weight conversion factors. Due to the differences in leaf water content between stressed and control trees all measurements were reported on a dry weight basis. Rates of photosynthesis and isoprene emission were also referenced to the dry weight of the needles.

Photosynthetic Rate Measurement

Photosynthesis was measured with a portable gas exchange system (LI-6400; LI-COR, Lincoln, NE, United States) using a chamber for measuring conifer needles supplied with the instrument. Measurements were performed between 10:00 and 14:00 under conditions of photosynthetic photon flux density (PPFD) (1000 μmol m^{-2} s^{-1}). Leaf temperature was set at 30°C, and the relative humidity in the cuvette ranged between 45 and 50%. After harvesting the measured tissue, *A*, the rate of carbon fixation, was calculated on a dry weight basis according to the LI-COR manual pages 16–51.

Abscisic Acid (ABA) Analysis

A 10 mg quantity of freeze-dried, ground leaf material was extracted with 1 ml methanol containing 40 ng ml^{-1} D_6-abscisic acid (Santa Cruz Biotechnology, Dallas, TX, United States) as an internal standard. The solution was incubated at 20°C for 30 min in a heating block shaking at 1000 rpm. After centrifugation at 18,000 × *g* at 4°C for 20 min, the supernatant was analyzed by using an Agilent 1260 Infinity high-performance liquid chromatography (HPLC) system (Agilent, Santa Clara, CA, United States) coupled to an API 5000 tandem mass spectrometer (AB Sciex, Framingham, MA, United States). A Zorbax Eclipse XDB-C18 column (50 × 4.6 mm, 1.8 μm) was used for the chromatographic separation with a formic acid (0.05% in water)/acetonitrile gradient (flow, 1.1 ml min^{-1}). ABA was detected via multiple reaction monitoring and quantified relative to the peak area of the standard.

Sugar Analysis

Freeze dried needles (5 mg) were extracted with 1 ml 80% MeOH. The solution was vortexed for 10 min at ambient temperature and centrifuged at 13,000 × *g* and 4°C for 5 min. The extracts were further diluted 1:10 with water before analysis on an Agilent 1260 Infinity HPLC system connected to an API 5000 triple quadrupole mass spectrometer. An external standard curve made with authentic standards (Sigma-Aldrich) at concentrations ranging between 1.25 and 20.0 μg ml^{-1} was used for quantification. Samples were analyzed directly by LC-MS/MS after a 1:20 (v/v) dilution in water. Separation was made via hydrophilic interaction chromatography on an apHera NH_2 polymer column (5 μm, 15 × 4.6 mm, Supelco, Bellefonte, PA, United States). Water and acetonitrile were used as mobile phases A and B, respectively. The elution profile was: 0–0.5 min, 80% B in A; 0.5–13 min, 80–55% B in A; 13–14 min, 55–80% B in A; and 14–18 min, 80% B in A. The ion spray voltage was maintained at −4500 eV. The turbo gas temperature was set at 600°C. Nebulizing gas was set at 50 psi, curtain gas at 20 psi, heating gas at 60 psi, and collision gas at 5 psi. Multiple reaction monitoring (MRM) was used to monitor isotopic composition of glucose and fructose by the following precursor ion → product ion reactions: *m/z* 178.8 → 58.7, *m/z* 179.8 → 58.7, *m/z* 179.8 → 59.7, *m/z* 180.8 → 58.7 *m/z* 180.8 → 59.7, and *m/z* 180.8 → 60.70. For sucrose, we used *m/z* 340.9 → 58.8, *m/z* 341.9 → 58.8, *m/z* 341.9 → 59.8, *m/z* 342.9 → 58.8 *m/z* 342.9 → 59.8, *m/z* 342.9 → 60.8, *m/z* 343.9 → 58.8, *m/z* 343.9 → 59.8, *m/z* 343.9 → 60.8, *m/z* 344.9 → 58.8, *m/z* 344 → 59.8, *m/z* 344.9 → 60.8, *m/z* 345.9 → 58.8, *m/z* 345.9 → 59.8, *m/z* 345.9 → 60.8, *m/z* 346.9 → 58.8, *m/z* 346.9 → 59.8, *m/z* 346.9 → 60.8, *m/z* 347.9 → 58.8, *m/z* 347.9 → 59.8, *m/z* 347.9 → 60.8, *m/z* 348.9 → 58.8, *m/z* 348.9 → 59.8, *m/z* 348.9 → 60.8, *m/z* 349.9 → 58.8, *m/z* 349.9 → 59.8, *m/z* 349.9 → 60.8, *m/z* 350.9 → 58.8, *m/z* 350.9 → 59.8, *m/z* 350.9 → 60.8, *m/z* 351.9 → 59.8, *m/z* 351.9 → 60.8, and *m/z* 352.9 → 60.8. The percentage of ^{13}C labeling in each metabolite after

50 min was calculated by summing all ^{13}C atoms incorporated in the sugar isotopes, and dividing this number by the overall sum of unlabeled and labeled C atoms.

Analysis of Methylerythritol 4-Phosphate (MEP) Pathway Intermediate Metabolites and ^{13}C-Labeling

To quantify the MEP pathway metabolites, 1-deoxy-D-xylulose 5-phosphate (DXP), 2-C-methyl-D-erythritol 4-phosphate (MEP), 4-diphosphocytidyl-2-C-methyl-D-erythritol (CDP-ME), 2-C-methyl-D-erythritol-2,4-cyclodiphosphate (MEcDP), isopentenyl diphosphate and dimethylallyl diphosphate (IDP + DMADP), samples of 5 mg dry weight were extracted twice with 250 µl of 50% acetonitrile containing 10 mM ammonium acetate, pH 9.0. After vortexing and centrifugation in a micro-centrifuge at 20,000 × *g* for 5 min, 200 µl of the supernatant from both extracts were combined, transferred into a new 1.5 ml tube and dried under a stream of nitrogen gas at 40°C. The residue was dissolved in 100 µl of 10 mM ammonium acetate, pH 9.0, and after vortexing, 100 µl of chloroform was added. The upper aqueous phase, separated by centrifugation at 20,000 × *g*, was transferred into a new tube and diluted with 1 volume of acetonitrile. To remove any precipitate, the supernatant was transferred to an HPLC vial after centrifugation at 20,000 × *g*.

Methylerythritol 4-phosphate pathway metabolites were analyzed on an Agilent 1260 Infinity HPLC system connected to an API 5000 triple quadrupole mass spectrometer. A 5 µl quantity of the extract was injected and the metabolites were separated on a hydrophobic interaction liquid chromatography (HILIC) XBridge Amide columns (150 × 2.1 mm, 3.5 µm; Waters, Milford, MA, United States) with a HILIC guard column containing the same sorbent (10 × 2.1 mm, 3.5 µm) and a SSI^{TM} high pressure pre-column filter (Sigma-Aldrich, St. Louis, MI, United States) using two solvents: 20 mM ammonium bicarbonate adjusted to pH 10.5 with LC-MS grade ammonium hydroxide (solvent A) and 80% acetonitrile containing 20 mM ammonium bicarbonate, pH 10.5 (solvent B). The solvent gradient profile started with 100% of solvent B, which decreased to 60% in the first 15 min, followed by an isocratic elution with 100% solvent B. Separation was performed at 25°C with a flow rate of 500 µl min^{-1}.

The mass spectrometer was used in the negative ionization mode with the following instrument settings: ion spray voltage −4500 V, turbo gas temperature 700°C, nebulizer gas 70 psi, heating gas 30 psi, curtain gas 30 psi, and collision gas 10 psi. DXP and its isotope distribution were monitored by the following precursor ion → product ion reactions: *m/z* 212.9 → 96.9, *m/z* 213.9 → 96.9, *m/z* 214.9 → 96.9, *m/z* 215.9 → 96.9, *m/z* 216.9 → 96.9, and *m/z* 217.9 → 96.9 [collision energy (CE), −16 V; declustering potential (DP), −60 V; and cell exit potential (CXP), −15 V]. MEcDP and its isotope distribution were monitored by the following precursor ion → product ion reactions: *m/z* 277.0 → 78.9, *m/z* 278.0 → 78.9, *m/z* 279.0 → 78.9, *m/z* 280.0 → 78.9, *m/z* 281.0 →7 8.9, and *m/z* 282.0 → 78.9 (CE, −38 V; DP, −50 V; CXP, −11 V). IDP/DMADP and their isotope distributions were monitored by the following precursor ion → product ion reactions: *m/z* 244.9 → 78.9, *m/z* 245.9 → 78.9, *m/z* 246.9 → 78.9, *m/z* 247.9 → 78.9, *m/z* 248.9 → 78.9, and *m/z* 249.9 → 78.9 (CE, −24 V; DP, −45 V; CXP, −11 V). Analyst 1.6 software (Applied Biosystems) was used for data acquisition and processing.

The metabolite concentrations were quantified by using external standard curves and were normalized to unlabeled standards added to each extract, after correction for natural ^{13}C abundance. Normalization to added unlabeled standards was accomplished by analyzing each sample twice, once with and once without the addition of 25 ng of DXP, 55 ng of MEcDP, and 24 ng of DMADP + IDP standards dissolved in 10 ml of water (Wright et al., 2014). Percentage of ^{13}C labeling in each metabolite after 50 min was calculated by summing all ^{13}C atoms incorporated in the various isotopologues, and dividing this number by the overall sum of unlabeled and labeled C atoms.

Measurement of Isoprene Emission and Incorporation of $^{13}CO_2$

Isoprene emission was analyzed when needles were in the cuvette for photosynthesis measurements. A proton transfer reaction mass spectrometer (PTR-MS; Ionicon, Innsbruck, Austria) (Lindinger et al., 1998) was employed with a Gas Calibration Unit (Ionicon) to generate precise flows of an isoprene standard for calibration. The PTR-MS was attached to the outflow of the LI-COR 6400 cuvette. The drift tube pressure was 2.2–2.3 mbar and the E/N ratio (electric field/particle density) was 130 Td (1 Td = 1 Townsend = 10^{-17} cm^2 V^{-1} s^{-1}). Isoprene was monitored with the mass signal *m/z* 69. The raw count-rate (cps) of the isoprene signal was normalized (ncps) to the sum of the primary ion and water cluster, and to the drift tube pressure. The average of the normalized signal during the steady state period was used to calculate the emission rate, after subtracting the background (empty chamber without needles). *In vivo* labeling was accomplished by replacing the $^{12}CO_2$ in the air entering the cuvette with $^{13}CO_2$ (0.99 atom% ^{13}C; Linde) at the same ambient concentration (380 µmol mol^{-1}). Labeling was performed for 50 min. The appearance of protonated masses of isoprene was followed in the PTR MS by monitoring *m/z* 70 ($^{13}C^{12}C_4H_9$), *m/z* 71 ($^{13}C_2{}^{12}C_3H_9$), *m/z* 72 ($^{13}C_3{}^{12}C_2H_9$), *m/z* 73 ($^{13}C_4{}^{12}CH_9$), and *m/z* 74 ($^{13}C_5H_9$). The percentage of ^{13}C labeling was calculated by summing all ^{13}C atoms incorporated in the isoprene isotopes, and dividing this number by the overall sum of unlabeled and labeled carbon atoms of isoprene (Schnitzler et al., 2004). Isoprene emission was normalized to the dry weight of the needles.

Preparation of Soluble Protein Extract and Measurement of DXS Activity

Freshly ground needles (200 mg) were immersed in 1 ml of extraction buffer containing 250 mM MOPSO (pH 6.8), 5 mM ascorbic acid, 5 mM sodium bisulfite, 5 mM dithiothreitol (DTT), 10 mM $MgCl_2$, 1 mM ethylenediaminetetraacetic acid (EDTA), 10% (v/v) glycerol, 1% (w/v) polyvinylpyrrolidone (PVP, M_r = 10,000), 4% (w/v) polyvinylpolypyrrolidone (PVPP), 4% (w/v) Amberlite XAD-4, and 0.1% (v/v) Tween 20. Extraction was

carried out in an 1.5 ml Eppendorf tube shaken in an Eppendorf Thermoshaker at 4°C and 1400 rpm. After centrifugation for 20 min at 4°C and 20,000 × *g*, the supernatant was passed through a 2 ml Zeba Spin desalting column with a 7 kDa molecular weight cut-off (Thermo Scientific, Rockford, IL, United States) to exchange the buffer to 50 mM Tris–HCl, pH 8.0, with 10% (v/v) glycerol and 10 mM $MgCl_2$. The total protein concentration was estimated by measuring absorbance at 280 nm using a NanoDrop 1000 UV-Vis spectrophotometer (Thermo Scientific).

The DXS enzyme assay was carried out in accord with a previous protocol (Wright and Phillips, 2014). Briefly, 30 μl from the total volume of enzyme extract was combined with 70 μl of assay buffer of 50 mM Tris–HCl, pH 8.0, with 10% (v/v) glycerol, 10 mM $MgCl_2$, 2.5 mM dithiothreitol, 1 mM thiamine pyrophosphate, 2 mM imidazole, 1 mM sodium fluoride, 1.15 mM molybdate, 1% (v/v) protease inhibitor cocktail, and 10 mM each of the substrates pyruvate and glyceraldehyde-3-phosphate. The final volume of 100 μl was incubated in a water bath at 25°C for 2 h. As a control for non-enzymatic conversion and the presence of assay product in the original plant extract, 30 μl of the enzyme extract were heated to 90°C for 10 min to deactivate the enzyme, and then combined with 70 μl of mixture assay and incubated for 2 h as well. The enzyme reaction was stopped by vigorously vortexing for 5 s with 100 μl of chloroform. After centrifugation in a microcentrifuge to complete phase separation, the upper aqueous phase, was transferred into a new tube and diluted with 1 volume of acetonitrile. As an internal standard, 25 ng of [$^{13}C_5$] DXP dissolved in water was added to the final solution dissolved in water.

The enzymatic end product DXP was quantified on an Agilent 1260 Infinity HPLC system connected to an API 5000 triple quadrupole mass spectrometer. DXP was separated via hydrophilic interaction liquid chromatography with the column and solvent system mentioned above for the analysis of MEP pathway metabolites. The flow rate was 1 ml min^{-1} with a column temperature of 25°C. The solvent profile started with a linear gradient from 0 to 16% A over 5 min and followed with an isocratic separation for 10 min. After a linear gradient from 16 to 40% A over 5 min, solvent A was returned to 0% over 15 min of equilibration. The mass spectrometer was used in the negative ionization mode with the following instrument settings: ion spray voltage −4500 V, turbo gas temperature 700°C, nebulizer gas 70 psi, heating gas 30 psi, curtain gas 30 psi, and collision gas 10 psi. DXP was monitored using the following precursor ion → product ion transition *m*/*z* 212.95 → 78.9 and DXP. The DXP produced by the DXS enzyme reaction was normalized to the [$^{13}C_5$] DXP internal standard monitored with the transition *m*/*z* 217.94 → 96.9.

Metabolic Flux Calculations

Plastidial concentrations of DXP, MEcDP and IDP + DMADP were estimated by assuming that IDP + DMADP only occurred in the chloroplast, and that only plastidial DXP and MEcDP pools would be labeled on the time-scale of the labeling experiment (50 min). Thus, the plastidial concentrations of DXP and MEcDP were estimated by calculating the ratio of their final ^{13}C-label incorporation to that of IDP + DMADP, and using these fractions to determine plastidial content. As isoprene labeling could be followed on-line instantaneously with the PTR-MS without the need for individual sampling, these measurements were taken as the instantaneous labeling state of the IDP + DMADP pool. This assumption was justified since isoprene is produced from DMADP in a single step, and the volatile isoprene gas escapes from the leaf. Moreover the assumption was verified experimentally by ensuring that the final label incorporation after 50 min in the isoprene and IDP + DMADP pools was identical (**Figure 5**). Following an approach similar to Yuan et al. (2008), the differential equations for label incorporation were integrated to obtain an analytical expression for the fractional labeling of the IDP + DMADP pool with time as a function of the pool sizes of DXP, MEcDP, and IDP + DMADP, as well as the flux through the pathway:

$$f(t) = m\left\{1 - \frac{A^2}{(A-B)(A-C)}\exp\left(-\frac{J}{A}t\right) - \frac{B^2}{(B-A)(B-C)}\exp\left(-\frac{J}{B}t\right) - \frac{C^2}{(C-A)(C-B)}\exp\left(-\frac{J}{C}t\right)\right\} \quad (1)$$

where *f(t)* is the fractional labeling of isoprene (which equates to the fractional labeling of IDP + DMADP) as a function of time, *m* is the maximal fractional labeling at the end of the run, *A, B,* and *C* are the pool sizes of DXP, MEcDP, and IDP + DMADP, respectively, *J* is the pathway flux and *t* is time. Equation (1) assumes that the pools of the other MEP pathway intermediates (MEP, ME-CDP, MEP-CDP, and HMBDP) are too small to significantly delay the label incorporation into downstream metabolites; these intermediates were below the limit of detection in the HPLC-MS analysis. To calculate the flux, Eq. (1) was fitted to isoprene labeling time-courses obtained from the PTR-MS [$f(t)$], with the plastidial pool sizes of DXP, MEcDP and IDP + DMADP entered as parameters *A*, *B*, and *C*, respectively (**Supplementary Figure S2**). The parameters *m* and *J* were obtained by minimizing the sum of squares of the differences between model and data with the Levenberg-Marquardt algorithm as implemented in the Python LMFIT module (Newville et al., 2014).

Chlorophyll and Carotenoid Analysis

After grinding the needles in liquid nitrogen, 50 mg were extracted in light-protected tubes with 1 ml of acetone by shaking for 6 h at 4°C in the dark. After centrifugation for 5 min at 2300 × *g* and 4°C, 800 μl of the extract was transferred into a light-protected tube and 200 μl of water was added. After centrifuging the samples for 1 min at 2300 × *g* and 4°C, they were transferred to brown glass vials for analysis on an HPLC Agilent 1100 Series with UV diode-array-detector. The detector was set at 445 nm for carotenoids and at 650 nm for the chlorophylls. These pigments were separated on a Supelcosil column LC-18 (7.5 cm × 4.6 mm, 3 μm; Sigma Aldrich) by using a gradient of acetone (solvent A) and 1 mM $NaHCO_3$ in

water (solvent B). The flow rate was 1.5 ml min^{-1}. The initial mobile phase consisted of 65/35% (v/v) solvent A/solvent B. Then, solvent A was linearly increased up to 90% in 12 min and to 100% in 8 min. 100% solvent A was kept for 2 min and then decreased to 65% in 3 min. Quantification was done using external standard curves. Authentic standards of chlorophylls and β-carotene (Santa Cruz Biotechnology) were analyzed in a range from 0.1 to 0.00625 mg ml^{-1}. Lutein, neoxanthin, and violaxanthin were considered to have the same response factors as β-carotene.

β-Cyclocitral Analysis

A 100 mg quantity of fresh tissue was extracted with 1 ml of methanol. The suspension was mixed by vortexing for 5 min and centrifuged for 20 min at 20, 000 × *g* and 4°C. The supernatant was centrifuged as above for 10 min, and 200 μl of the new supernatant were taken for the analysis using an Agilent 1260 Infinity high-performance liquid chromatography (HPLC) system coupled to an API 5000 tandem mass spectrometer. β-Cyclocitral was separated on an Zorbax Eclipse XDB-C18 column (50 × 4.6 mm, 1.8 μm) Chromatographic separation was performed by using a gradient of formic acid 0.05% in water, (solvent A) and acetonitrile (solvent B). The flow rate was set at 0.5 ml min^{-1}. The initial mobile phase consisted of 95/5% (v/v) solvent A/solvent B. Then, solvent A was decreased to 50% in 2 min and held for 3 min. After solvent A was decreased to 0% in 9 min and held for 11 min, it was raised again to 95%. β-Cyclocitral was monitored by following the precursor ion → product ion reaction: m/z 153.191 → 109.0. Quantification was done using an external standard curve made with an authentic standard of β-cyclocitral (Sigma-Aldrich).

Monoterpene Content Analysis

According to the procedure of Martin et al., 2002 fresh needles (100 mg) were immersed in 1.5 ml of tert-butyl methyl ether containing 150 μg ml^{-1} isobutylbenzene as internal standard, and shaken for 14 h at room temperature. The ethereal extract was transferred to a fresh vial and washed with 0.3 ml of 0.1 M $(NH_4)_2CO_3$ (pH 8.0) in order to purify the extracted terpenes from other organic acids. The sample was filtered through a Pasteur pipette column filled with silica gel (Sigma 60 Å) and anhydrous $MgSO_4$. Monoterpene analysis was performed by GC-MS with a Hewlett-Packard 6890 system, using a DB-WAX column (0.25 mm × 30 m, 0.25 μm, J&W Scientific, Folsom, CA, United States). Split injection was carried out at 220°C. Helium was used as carrier gas at a constant flow of 1 ml min^{-1}. The GC was programmed with an initial oven temperature of 40°C (3-minute hold), a ramp of 5°C min^{-1} until 80°C, then a ramp of 5°C min^{-1} until 200°C, followed by a final ramp of 60°C min^{-1} until 280°C (4-minute hold). For GC-FID analysis, the flame ionization detector operated at 300°C. GC-FID- and GC-MS-generated peaks were integrated using Hewlett-Packard Chemstation software. Identification of terpenes was based on comparison of retention times and mass spectra with those of authentic standards or with mass spectra in the Wiley library. In order to calculate needle monoterpene concentrations on a ng mg^{-1} dry weight basis, the residue of 100 mg extracted material of each trees was dried and weighed as described by Martin et al., 2002.

Statistics

The effect of drought treatment was tested using one-way ANOVA. When test results were significant, the means were compared using Tukey's *post hoc* test at $P < 0.05$. Normality was tested by the Shapiro-Wilk test.

RESULTS

Drought Treatment Reduces Photosynthesis and Increases Abscisic Acid (ABA) in White Spruce

By withholding water, two different drought treatments were imposed on young *Picea glauca* (white spruce) trees. In the moderate stress treatment, transpiration rate was reduced to 50% of that in well-watered trees, which occurred when the fraction of transpirable soil water (FTSW) was 12%. Under severe stress transpiration rate was reduced to 20% of that in well-watered trees, which occurred when the FTSW was 3% (**Supplementary Figure S1**). Photosynthesis decreased significantly under drought by an average of 70 and 96% under moderate and severe stress, respectively (**Figure 1**). At the same time, the hormone abscisic acid (ABA) increased by an average of 6.7- and 12.8-fold, respectively, under moderate and severe stress (**Figure 2**).

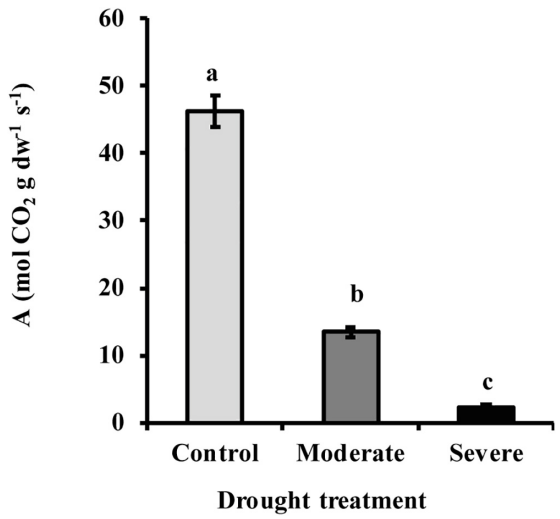

FIGURE 1 | Drought reduced the rate of photosynthesis *A* in white spruce (*Picea glauca*). Photosynthesis declined under moderate (transpiration rate 50% of well-watered control) and severe drought treatment (transpiration rate 20% of control). Data shown are means of five biological replicate ± SE. Different letters indicate significant differences at $P < 0.05$.

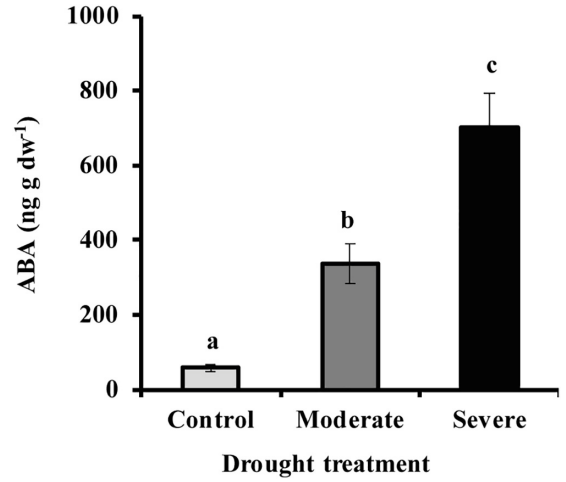

FIGURE 2 | Drought increased needle ABA content under moderate and severe drought conditions. Data shown are means of five biological replicate ± SE. Different letters indicate significant differences at $P < 0.05$.

Drought Treatment Reduces Photosynthetic Incorporation Into Sucrose in Needles, but Not Sucrose Content

To investigate the effect of drought on basic carbohydrate metabolism in white spruce needles, we measured $^{13}CO_2$ incorporation into glucose, fructose and sucrose. Incorporation into sucrose declined significantly by an average of 53 and 69% under moderate and severe stress, respectively, as a consequence of reduced photosynthesis, while incorporation into glucose and fructose was not affected (**Supplementary Figure S3**).

Drought Reduces Pools of Some MEP Pathway Intermediates and the Emission of the MEP Pathway Product Isoprene

The MEP pathway intermediates 1-deoxy-D-xylulose 5-phosphate (DXP) and 2-*C*-methyl-D-erythritol-2,4-cyclodiphosphate (MEcDP) declined significantly under moderate and severe drought stress in white spruce (**Figure 3**). By contrast, the pool of dimethylallyl diphosphate (DMADP) and isopentenyl diphosphate (IDP), present at less than half the level of the other intermediates measured, showed no change under both stress levels. Emission of isoprene, an immediate volatile product of the MEP pathway, was significantly reduced by over half only during severe stress (**Figure 4**).

Drought Reduces Relative Incorporation of $^{13}CO_2$ Into MEP Pathway Intermediates and Isoprene

During the 50 min time course of $^{13}CO_2$ labeling under control conditions, DXP and MEcDP were labeled to nearly 75% while labeling of DMADP + IDP and isoprene reached 87 and 85%, respectively (**Figure 5**). A typical pattern of isoprene labeling under all condition, is shown in **Supplementary Figure S4**. Among the isotopologues measured, the fully labeled molecule (*m/z* 74) was the most abundant at all time points after 20 min (**Supplementary Figure S5**). However, under moderate stress, labeling of DMADP + IDP and isoprene from $^{13}CO_2$ was 60%, and DXP and MEcDP still showed significantly lower incorporation than DMADP + IDP and isoprene. Under severe stress, incorporation into all MEP pathway intermediates and isoprene was only 10–20% (**Figure 5**). Considering isotopologues, the fully labeled molecule was only a minor component under both moderate and severe stress (**Supplementary Figure S5**). Thus increasing drought led to increased contribution of alternative carbon sources to the MEP pathway, rather than newly made products of photosynthesis.

Drought Decreases Metabolic Flux Through the MEP Pathway

Metabolic flux through the MEP pathway was calculated from the ^{13}C labeling of isoprene from $^{13}CO_2$ with time as a function of the pool sizes of the intermediates measured. The labeling of the pathway product isoprene was used since it could be conveniently assessed over the time course and was equivalent to the labeling of the final pathway intermediates, DMADP and IDP (**Figure 5**), as might be expected since isoprene is produced in a single enzymatic step from DMADP and released from the plant immediately as a volatile gas. Metabolic flux declined significantly (37%) under moderate drought (**Figure 6**). Under severe drought, metabolic flux could not be calculated because of the lack of sufficient incorporation of ^{13}C for accurate measurement.

Drought Reduces the Activity of 1-deoxy-D-xylulose 5-phosphate Synthase (DXS)

The first step of the MEP pathway, the condensation of pyruvate and glyceraldehyde 3-phosphate to form DXP, is catalyzed by DXP synthase (DXS). The activity of DXS measured *in vitro* in extracts of freshly ground needles was significantly reduced (50–55%) under both moderate and severe drought treatments, but no significant difference was observed between the two drought levels (**Figure 7**). This decline was similar to that observed for the product of the enzyme, DXP (**Figure 3**).

Drought Affects the Levels of Some Carotenoid Pigments and a Derivative, but Does Not Influence Chlorophyll Content

The decrease in metabolic flux through the MEP pathway might be expected to impact the levels of carotenoid and chlorophyll pigments since carotenoids are wholly derived from the MEP pathway while the C_{20} side chain of chlorophylls a and b is synthesized by the MEP pathway. However, the sum of chlorophyll a and chlorophyll b did not show any significant reduction with drought despite a declining trend (ANOVA one-way $P = 0.109$) (**Figure 8A**), even though photosynthesis itself

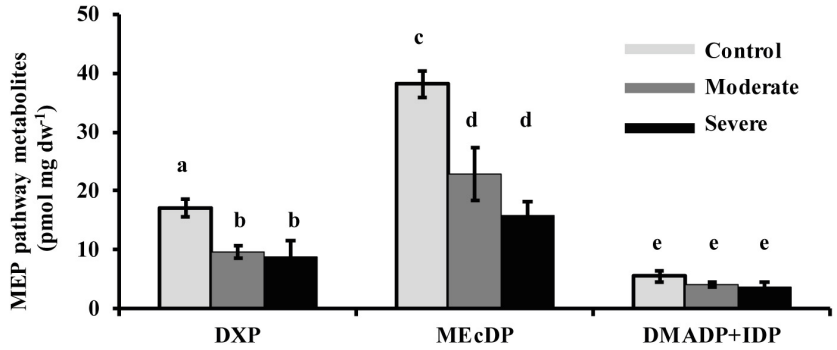

FIGURE 3 | Drought reduced the concentrations of the MEP pathway intermediates, DXP and MEcDP, but not DMADP + IDP in needles. Data shown are means of five biological replicate ± SE. Different letters indicate significant differences at $P < 0.05$.

was strongly reduced under both moderate and severe drought (**Figure 1**). Among the carotenoids, β-carotene (ANOVA one-way $P = 0.110$) and lutein (ANOVA one way $P = 0.449$) also did not decline significantly, although declining trends were evident (**Figures 8B,C**). By contrast, the xanthophyll violaxanthin showed a statistically significant reduction under both drought treatments (**Figure 8D**) while neoxanthin was reduced under severe drought (**Figure 8E**). An oxidized derivative of β-carotene, β-cyclocitral, that quenches oxidant species during oxidative stress (Ramel et al., 2012) increased under severe drought (**Figure 8F**).

Stored Monoterpene Content Is Not Influenced by Drought

Monoterpenes are major constituents of resins of *P. glauca* and other conifers, and are also produced by the MEP pathway.

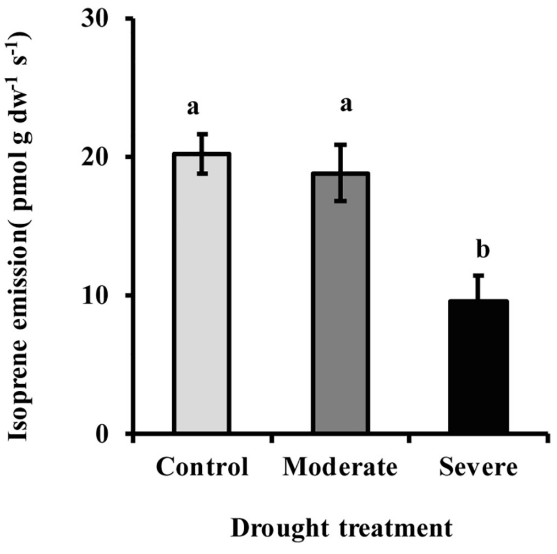

FIGURE 4 | Drought reduced isoprene emission from needles as measured with a PTR-MS. Data shown are means of five biological replicate ± SE. Different letters indicate significant differences at $P < 0.05$.

The pool size of stored monoterpenes in needles was not influenced by drought treatments, and the amounts of individual monoterpenes were also unaltered (**Supplementary Table S1**).

DISCUSSION

Decline in MEP Pathway Flux Under Drought Is Partially Mitigated by Use of Carbon Sources Other Than Photosynthesis

Drought treatment of young *Picea glauca* trees in our study caused a range of physiological and metabolic responses. A decline in transpiration rate, 50 and 80% under moderate and severe drought, respectively, coincided with a 72 and 96% decrease in photosynthetic rate, respectively (**Figure 1**). These changes were likely triggered by increased stomatal closure (Chaves, 1991; Cornic, 2000), induced by a sharp increase in ABA concentration, over 6- and 12-fold, respectively, under moderate and severe stress (**Figure 2**).

Despite the steep drop in carbon fixation, metabolic flux through the MEP pathway decreased by only 37% at moderate stress. Our $^{13}CO_2$ labeling data show that as the photosynthetic rate declined, reliance on alternative carbon sources increased to 40% under moderate stress and to 85–90% under severe stress for both the DMADP + IDP pool and the direct product isoprene (**Figure 5** and **Supplementary Figure S4**). Alternative carbon sources for isoprene have been suggested to include chloroplast starch deposits, CO_2 recycled by photorespiration and other respiratory processes, and glucose from xylem transport (Kreuzwieser et al., 2002; Loreto et al., 2004; Schnitzler et al., 2004; Jardine et al., 2014).

Based on the identical percentage of ^{13}C incorporated in DMADP + IDP and isoprene under all conditions, we assume that the same alternative carbon sources employed for isoprene are also used for the MEP pathway (**Figure 5**). The use of alternative carbon sources under drought is also suggested by changes in the relative labeling of MEP pathway intermediates from $^{13}CO_2$. Both DXP and MEcDP had significantly lower percentages of incorporated ^{13}C than

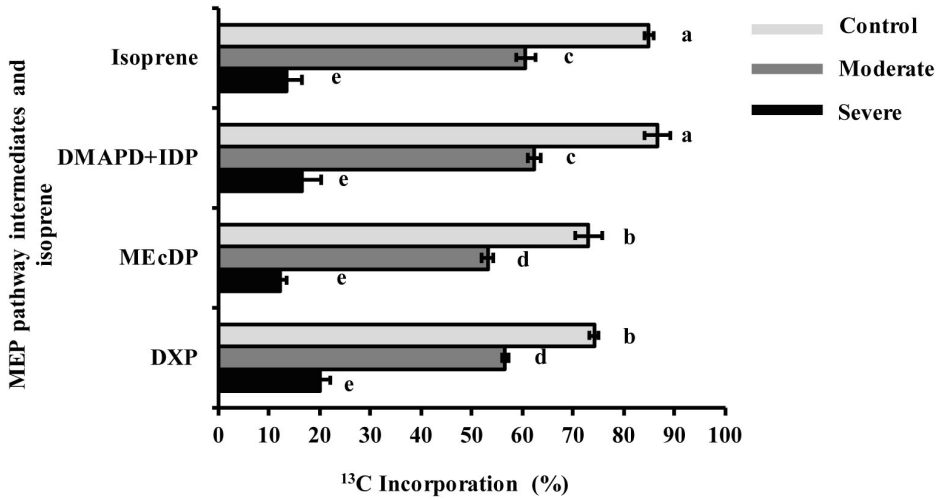

FIGURE 5 | Drought decreased ^{13}C incorporation from $^{13}CO_2$ into MEP pathway intermediates and isoprene under steady state conditions after 50 min labeling. Data shown are means of five biological replicate ± SE. Different letters indicate significant differences at $P < 0.05$.

DMADP + IDP and isoprene under both control conditions and moderate drought (**Figure 5**). These data indicate the presence of additional pools of these intermediates outside the chloroplast as previously measured in Arabidopsis for MEcDP (Wright et al., 2014). These additional pools may be located in the cytosol. The export of MEcDP from the plastid to the cytosol has been previously reported (Xiao et al., 2012; Zhou et al., 2012; González-Cabanelas et al., 2015), and this metabolite also participates in retrograde signaling processes from the plastid to the nucleus. Although an extra plastidic pool of DXP was never measured previously, plastidial uptake of exogenous DXP and its non-phosphorylated derivative was shown in *Eucalyptus globulus* and *Arabidopsis thaliana* (Wolfertz et al., 2003, 2004; Hemmerlin et al., 2006), and a plastidial transporter capable of accepting DXP was described in spinach (Flügge and Gao, 2005). Under severe drought DXP and MEcDP had similar ^{13}C labeling percentages as DMADP + IDP and isoprene (**Figure 5**), pointing to the disappearance of these additional pools and suggesting that the intermediates are now localized exclusively in the chloroplast. These additional quantities of MEP intermediates may help

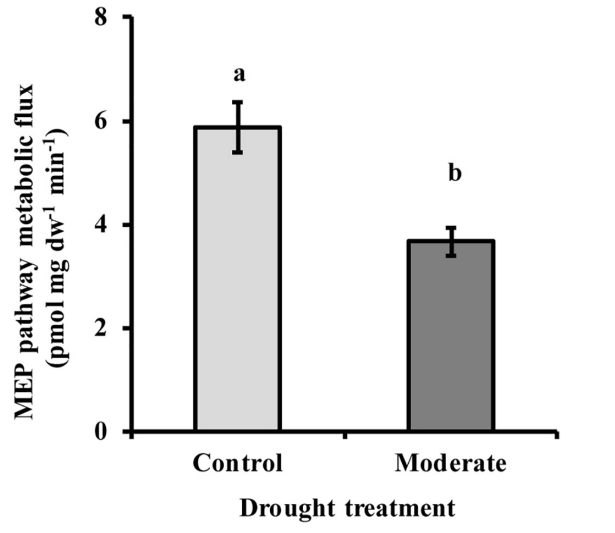

FIGURE 6 | Drought decreased MEP pathway metabolic flux under moderate stress conditions. Under severe stress metabolic flux was not detectable due to very low ^{13}C incorporation. Flux was calculated as described in the text. Data shown are means of three biological replicate ± SE. Different letters indicate significant differences at $P < 0.05$.

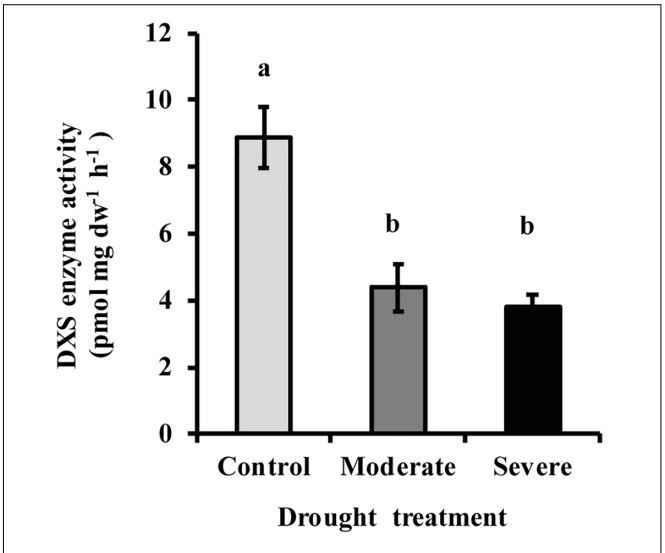

FIGURE 7 | Drought treatment caused a decline in the activity of DXS measured *in vitro* in extracts of white spruce needles. Data shown are means of three biological replicate ± SE. Different letters indicate significant differences at $P < 0.05$.

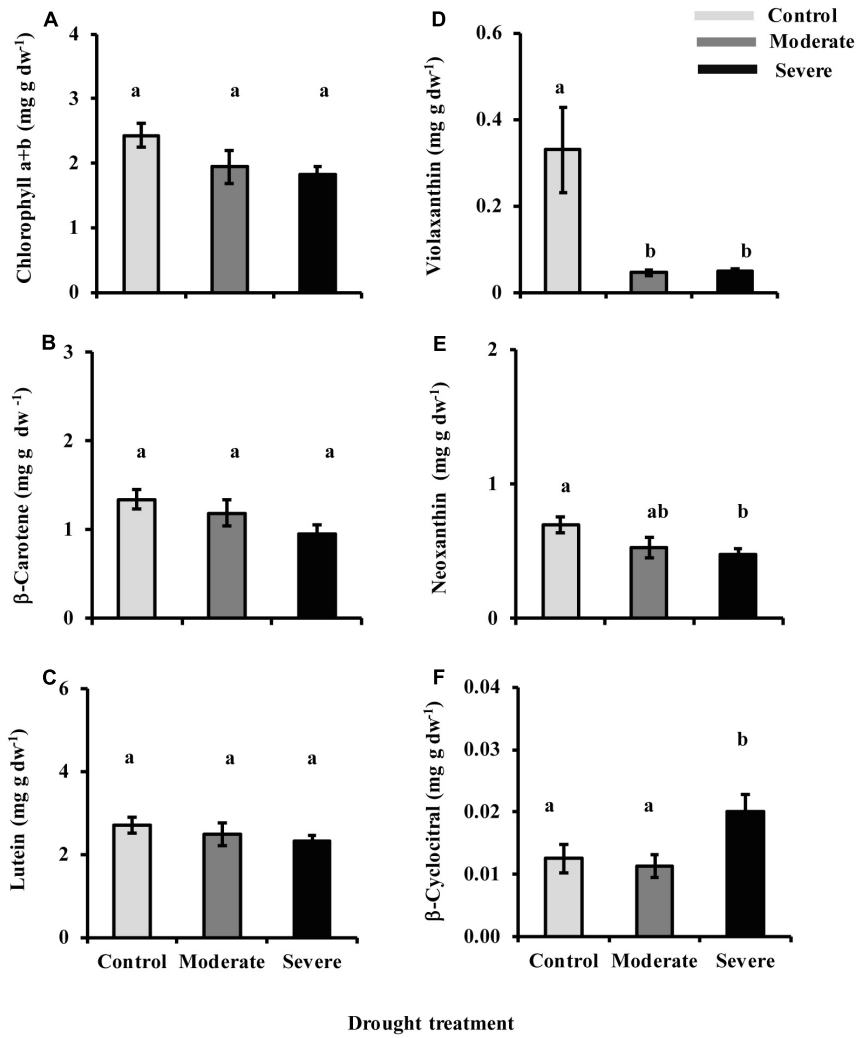

FIGURE 8 | Drought influences chlorophyll and carotenoid levels. Presented are data for **(A)** chlorophyll a and chlorophyll b, **(B)** β-carotene, **(C)** lutein, **(D)** violaxanthin, and **(E)** neoxanthin measured by HPLC-UV, and **(F)** β-cyclocitral measured by LC-MS. Data shown are means of five biological replicate ± SE. Different letters indicate significant differences at $P < 0.05$.

buffer the pathway against declines in metabolic flux under drought conditions caused by the decrease in photosynthetic rate. Further investigation on the intracellular trafficking of DXP and MEcDP may shed light on new mechanisms controlling the MEP pathway during stress.

The mevalonate (MVA) pathway of isoprenoid biosynthesis, localized in the cytosol, ER and peroxisomes, also produces DMADP and IDP. However, our data give no support to a role for products of the MVA pathway in supplying the MEP pathway under stress. Import of DMADP or IDP from outside the plastid would decrease ^{13}C incorporation in these diphosphate intermediates and in the DMADP product isoprene. Yet under drought there was no significant decline in ^{13}C labeling of either the DMADP + IDP pool or isoprene relative to the earlier MEP pathway intermediates, and sometimes even an increase (**Figure 5**). Thus the plastids did not import a supply of prenyl diphosphate intermediates under drought. Moreover, given that DMADP + IDP and isoprene always had the same ^{13}C incorporation percentage under all treatments, one can conclude that the only detectable pool of DMADP in the cell must serve as a precursor to isoprene synthesis, and therefore belongs to the MEP pathway and resides in the plastid where isoprene is made. This suggests that the MVA pathway is not operating at all under our experimental conditions, (see section "Materials and Methods" for details). Similar $^{13}CO_2$ measurements of the illuminated rosettes of *Arabidopsis thaliana* conducted by Wright et al., 2014 also found no evidence for measurable pools of DMADP outside the plastid that could be attributed to the MVA pathway. This previous study also found no evidence for labeling of MVA pathway intermediates from $^{13}CO_2$ in illuminated *A. thaliana* rosettes. The MVA pathway is also known from other studies to be less active during the day due to the negative effect of light on the transcription of pathway genes (Learned and Connolly, 1997; Rodríguez-Concepción, 2006; Vranová et al., 2013).

Down-Regulation of MEP Pathway Flux During Moderate Drought May Be Mediated by the Enzyme DXS

The down-regulation of the MEP pathway we observed under moderate drought was exhibited not only in the 37% decline of the metabolic flux (**Figure 6**), but also by declines of 40–50% in the levels of the key intermediates, DXP and MEcDP (**Figure 3**). In considering the mechanism for MEP pathway reduction, we focused on DXS, the first enzyme of the sequence. DXS was shown to be the principal rate-controlling step of the pathway in photosynthetic tissue of *Arabidopsis thaliana* based on metabolic control analysis (Wright et al., 2014). In addition, increases in *DXS* gene transcript levels were found to correlate with higher accumulation of MEP pathway end products (Estévez et al., 2001). Here we demonstrated that DXS activity was reduced by about 50–55% under moderate stress (**Figure 7**), very similar to the decline in metabolic flux, suggesting that this enzyme may well have modulated the down-regulation of the pathway seen under these conditions. Regulation of DXS activity also occurs post-transcriptionally (Rodríguez-Concepción, 2006; Hemmerlin, 2013; Banerjee and Sharkey, 2014). For example, DXS protein levels can be modulated by the casein lytic proteinase (CLP) complex (Pulido et al., 2016), which responds to changing environmental conditions. In particular, long term stress and drought, have been shown to increase some component of the CLP protein complex (Zheng et al., 2002; Demirevska et al., 2008), which could increase the removal of DXS during the process of protein quality control (Flores-Pérez et al., 2008). In addition, DXS activity can also be controlled by feedback inhibition of the MEP pathway by the end product DMADP (Banerjee et al., 2013; Ghirardo et al., 2014). Further work is needed to clarify the mechanism by which DXS catalysis is altered under drought conditions.

1-deoxy-D-xylulose-5-phosphate synthase does not appear to have a large role under severe drought since its activity did not significantly change between moderate and severe drought conditions (**Figure 7**), while the metabolic flux was reduced to a level that was not measurable. This result suggests that the MEP pathway is regulated in a very different manner under severe drought than under moderate drought. An enzyme one step beyond the MEP pathway that could also have a regulatory impact is isoprene synthase (Brilli et al., 2007). Inhibition of this reaction would reduce isoprene formation, as happened under severe drought in this study (**Figure 4**), and result in the allocation of DMADP to other MEP pathway products. Other pathway enzymes may also exert more control, such as 1-deoxy-D-xylulose 5-phosphate reductoisomerase (DXR) (Carretero-Paulet et al., 2006), 4-hydroxy-3-methylbut-2-en-1-yl diphosphate synthase (HDS) (Wang et al., 2019) and 4-hydroxy-3-methylbut-2-enyl diphosphate reductase, HDR.

Drought Effects on the Levels of MEP Pathway Products

Despite the substantial decline in MEP pathway flux under drought, we found no commensurate reduction in the major products of the MEP pathway produced in photosynthetic cells, the chlorophylls, lutein and β-carotene. Depending on the turnover rate of these pigments, it is possible that the drought treatment was not long enough to observe any net depletion. Some depletion of β-carotene is indicated by the sharp increase in β-cyclocitral, a β-carotene oxidation product (**Figure 8F**). However, the β-cyclocitral detected represents just a few percent of the total β-carotene pool. The decline in the carotenoid violaxanthin was considerable under both stress treatments but this is associated with the activation of the xanthophyll cycle to dissipate excess radiant energy via non-photochemical quenching and prevent the formation of reactive oxygen species (Demmig-Adams and Adams III, 1996). Other MEP pathway-derived products that we did not measure may have been reduced under drought, such as the tocopherols and the prenylquinones: plastoquinones, phylloquinones, and ubiquinones.

Under severe drought (but not under moderate drought), there was a very significant reduction (>50%) in the MEP pathway product isoprene. This may have diverted enough MEP pathway flux to chlorophyll and carotenoid formation to keep the pools of these pigments stable. However, transgenic silencing of isoprene formation in poplar led to only slight increases in the levels of chlorophylls and carotenoids (Behnke et al., 2007; Ghirardo et al., 2014), but the outcome could be different under severe drought. Under neither severe drought nor moderate drought was there any significant reduction in stored monoterpene formation. These findings are in agreement with previous reports about the general lack of monoterpene metabolism in conifer needles late in the growing season. For example, in *Picea abies*, the size of the stored pool of monoterpenes in current year needles did not change after the first 2 months of growth in July, and did not change in older needles at all over the entire growing season (Schönwitz et al., 1990). Our experiment was conducted in August. Exposing *Picea abies* to a low atmospheric CO_2 concentration (50 ppm) also did not change the amount of monoterpenes stored in current year needles (Huang et al., 2018).

Isoprene and Other MEP Pathway Products May Help Alleviate the Effects of Drought

The physiology and function of isoprene have been studied for many years since isoprene, produced especially in woody plants (Loreto and Fineschi, 2015), is the most abundant hydrocarbon released into the atmosphere from the earth's vegetation (Sharkey and Yeh, 2001). Knowledge of isoprene physiology and response to environment in conifers is not as large as in angiosperms. Here we monitored isoprene biosynthesis and emission in detail in white spruce under moderate and severe drought. After $^{13}CO_2$ incorporation, the percentage of isotopic label in isoprene was virtually identical to the percentage of labeling in the DMADP + IDP pool under all conditions (**Figure 5**), confirming that DMADP is the biosynthetic source of isoprene. Furthermore, isoprene is formed directly from DMADP by a single reaction catalyzed

by isoprene synthase and represents an efficient probe for the operation of the MEP pathway. The percentage of ^{13}C labeling in isoprene from $^{13}CO_2$ reached 85% after a 50 min time course under steady state conditions. The major role for photosynthesis in providing fixed carbon for isoprene biosynthesis, previously demonstrated in angiosperms (Brilli et al., 2007), is here demonstrated for a gymnosperm, *P. glauca*.

The continued production of isoprene under moderate drought suggests that its function is still needed despite the decline in photosynthetic carbon availability that occurs under these conditions. Isoprene has long been suggested to protect plants against high temperature and oxidative stress by various mechanisms (Singsaas et al., 1997; Vickers et al., 2009; Velikova et al., 2011; Pollastri et al., 2014), most recently by preserving thylakoid membrane stability and elasticity (Pollastri et al., 2019). However, a recent publication has suggested that isoprene may not be abundant enough to function in these ways and may instead act as a general signal for increased abiotic stress tolerance (Zuo et al., 2019). Regardless of function, isoprene formation and emission declined steeply under severe drought in our experiment, a pattern seen in angiosperms as well (Funk et al., 2004; Pegoraro et al., 2004; Brilli et al., 2007). Since continued emission under moderate stress, but abrupt decline at higher stress is widespread for isoprene emission in plants, further study of the causes behind this pattern may help to shed more light on isoprene function and MEP pathway regulation.

Changes in the levels of other isoprenoids under drought in this study may also help to alleviate stresses associated with low water supply. For example, the decline in the carotenoid violaxanthin is associated with the activation of the xanthophyll cycle. The increase in β-cyclocitral under severe drought may also help enhance tolerance toward oxidative stress after its conversion to β-cyclocitric acid (D'Alessandro et al., 2019). Although we did not measure tocopherols, these isoprenoid antioxidants could also reduce oxidative stress. Evidence for the alleviation of oxidative stress during drought comes from the lack of accumulation of MEcDP under these conditions. Previous studies showed an accumulation of MEcDP during high light as a consequence of the susceptibility to oxidative stress of the [4Fe–4S]-cluster contained in the following enzyme 4-hydroxy-3-methylbut-2-en-1-yl diphosphate synthase (HDS) (Rivasseau et al., 2009). By contrast, in our experiment the MEcDP pool size was not increased at all, but reduced. It is clear that the continued operation of the MEP pathway during drought may make a critical contribution to plant survival.

CONCLUSION

Under drought, white spruce trees significantly decrease their metabolic flux through the MEP pathway, but this decrease is not nearly as pronounced as the decrease in photosynthetic carbon fixation and transpiration rate. Reliance on alternative carbon sources besides photosynthesis is considerable under drought, and contributes to the continued operation of the MEP pathway. However, the other isoprenoid pathway (the MVA pathway) was not one of these alternative sources. More investigations are needed to determine how alternative carbon sources are recruited to the MEP pathway under stress and how this is regulated. The relative importance of the MEP pathway under drought may be a consequence of the number of pathway products shown to help protect against drought-associated oxidative stresses, including carotenoids, tocopherols and isoprene (Mattos and Moretti, 2015; Zuo et al., 2019). Control of MEP flux under moderate drought may be maintained by the well-known pathway regulator DXS. Under severe drought, when the DXS enzyme exerts a reduced role and isoprene emission drops, regulatory mechanisms could involve other MEP pathway enzymes. Further research is necessary to determine how a pathway that produces so many anti-oxidant metabolites is kept in service under drought. As the world's climate warms, such knowledge may be especially valuable for boreal tree species, such as the white spruce.

DATA AVAILABILITY STATEMENT

All datasets presented in this study are included in the article/**Supplementary Material**.

AUTHOR CONTRIBUTIONS

EP and LW designed the experiments. EP performed the experiments, analyzed the data, and wrote the manuscript. JR performed the calculation of the metabolic flux. JR, DG-C, FL, AS, JG, and LW supervised the study and complemented writing. All authors contributed to the article and approved the submitted version.

FUNDING

This study has been funded by the Max Planck Society and a Max Planck Society-Fraunhofer Society cooperation grant.

ACKNOWLEDGMENTS

We thank Almuth Hammerbacher for her helpful discussion on conifer tree physiology and Bettina Raguschke for assistance in the laboratory, Michael Reichelt for help with chemical analysis, and the gardeners of the MPI-CE for taking care of *Picea glauca* trees.

SUPPLEMENTARY MATERIAL

The Supplementary Material for this article can be found online at: https://www.frontiersin.org/articles/10.3389/fpls.2020.546295/full#supplementary-material

REFERENCES

Ahkami, A. H., Wang, W., Wietsma, T. W., Winkler, T., Lange, I., Jansson, C., et al. (2019). Metabolic shifts associated with drought-induced senescence in *Brachypodium*. *Plant Sci.* 289:110278. doi: 10.1016/j.plantsci.2019.110278

Banerjee, A., and Sharkey, T. (2014). Methylerythritol 4-phosphate (MEP) pathway metabolic regulation. *Nat. Prod. Rep* 31, 1043–1055. doi: 10.1039/c3np70124g

Banerjee, A., Wu, Y., Banerjee, R., Li, Y., Yan, H., and Sharkey, T. D. (2013). Feedback inhibition of deoxy-D-xylulose-5-phosphate synthase regulates the methylerythritol 4-phosphate pathway. *J. Biol. Chem.* 288, 16926–16936. doi: 10.1074/jbc.m113.464636

Behnke, K., Ehlting, B., Teuber, M., Bauerfeind, M., Louis, S., Hänsch, R., et al. (2007). Transgenic, non-isoprene emitting poplars don't like it hot. *Plant J.* 51, 485–499. doi: 10.1111/j.1365-313x.2007.03157.x

Brilli, F., Barta, C., Fortunati, A., Lerdau, M., Loreto, F., and Centritto, M. (2007). Response of isoprene emission and carbon metabolism to drought in white poplar (*Populus alba*) saplings. *New Phytol.* 175, 244–254. doi: 10.1111/j.1469-8137.2007.02094.x

Carretero-Paulet, L., Cairo, A., Botella-Pavía, P., Besumbes, O., Campos, N., Boronat, A., et al. (2006). Enhanced flux through the methylerythritol 4-phosphate pathway in Arabidopsis plants overexpressing deoxyxylulose 5-phosphate reductoisomerase. *Plant Mol. Biol.* 62, 683–695. doi: 10.1007/s11103-006-9051-9

Chaves, M. (1991). Effects of water deficits on carbon assimilation. *J. Exp. Bot.* 42, 1–16. doi: 10.1093/jxb/42.1.1

Cornic, G. (2000). Drought stress inhibits photosynthesis by decreasing stomatal aperture–not by affecting ATP synthesis. *Trends Plant Sci.* 5, 187–188. doi: 10.1016/s1360-1385(00)01625-3

D'Alessandro, S., Mizokami, Y., Legeret, B., and Havaux, M. (2019). The apocarotenoid β-cyclocitric acid elicits drought tolerance in plants. *Iscience* 19, 461–473. doi: 10.1016/j.isci.2019.08.003

Demirevska, K., Simova-Stoilova, L., Vassileva, V., and Feller, U. (2008). Rubisco and some chaperone protein responses to water stress and rewatering at early seedling growth of drought sensitive and tolerant wheat varieties. *Plant Growth Regul.* 56, 97–106. doi: 10.1007/s10725-008-9288-1

Demmig-Adams, B. and Adams III, W. W. (1996). The role of xanthophyll cycle carotenoids in the protection of photosynthesis. *Trends Plant Sci.* 1, 21–26. doi: 10.1016/S1360-1385(96)80019-7

Dudareva, N., Andersson, S., Orlova, I., Gatto, N., Reichelt, M., Rhodes, D., et al. (2005). The nonmevalonate pathway supports both monoterpene and sesquiterpene formation in snapdragon flowers. *Proc. Natl. Acad. Sci. U.S.A.* 102, 933–938. doi: 10.1073/pnas.0407360102

Eberl, F., Perreca, E., Vogel, H., Wright, L. P., Hammerbacher, A., Veit, D., et al. (2018). Rust infection of black poplar trees reduces photosynthesis but does not affect isoprene biosynthesis or emission. *Front. Plant Sci.* 9:1733. doi: 10.3389/fpls.2018.01733

Enfissi, E. M., Fraser, P. D., Lois, L. M., Boronat, A., Schuch, W., and Bramley, P. M. (2005). Metabolic engineering of the mevalonate and non-mevalonate isopentenyl diphosphate-forming pathways for the production of health-promoting isoprenoids in tomato. *Plant Biotechnol. J.* 3, 17–27. doi: 10.1111/j.1467-7652.2004.00091.x

Estévez, J. M., Cantero, A., Reindl, A., Reichler, S., and León, P. (2001). 1-Deoxy-D-xylulose-5-phosphate synthase, a limiting enzyme for plastidic isoprenoid biosynthesis in plants. *J. Biol. Chem.* 276, 22901–22909. doi: 10.1074/jbc.m100854200

Flores-Pérez, Ú, Sauret-Güeto, S., Gas, E., Jarvis, P., and Rodríguez-Concepción, M. (2008). A mutant impaired in the production of plastome-encoded proteins uncovers a mechanism for the homeostasis of isoprenoid biosynthetic enzymes in Arabidopsis plastids. *Plant Cell* 20, 1303–1315. doi: 10.1105/tpc.108.058768

Flügge, U.-I., and Gao, W. (2005). Transport of isoprenoid intermediates across chloroplast envelope membranes. *Plant Biol.* 7, 91–97. doi: 10.1055/s-2004-830446

Funk, J., Mak, J., and Lerdau, M. (2004). Stress-induced changes in carbon sources for isoprene production in *Populus deltoides*. *Plant Cell Environ.* 27, 747–755. doi: 10.1111/j.1365-3040.2004.01177.x

Ghirardo, A., Wright, L. P., Bi, Z., Rosenkranz, M., Pulido, P., Rodríguez-Concepción, M., et al. (2014). Metabolic flux analysis of plastidic isoprenoid biosynthesis in poplar leaves emitting and nonemitting isoprene. *Plant Physiol.* 165, 37–51. doi: 10.1104/pp.114.236018

González-Cabanelas, D., Wright, L. P., Paetz, C., Onkokesung, N., Gershenzon, J., Rodríguez-Concepción, M., et al. (2015). The diversion of 2-C-methyl-d-erythritol-2, 4-cyclodiphosphate from the 2-C-methyl-d-erythritol 4-phosphate pathway to hemiterpene glycosides mediates stress responses in *Arabidopsis thaliana*. *Plant J.* 82, 122–137. doi: 10.1111/tpj.12798

Guo, R., Shi, L., Jiao, Y., Li, M., Zhong, X., Gu, F., et al. (2018). Metabolic responses to drought stress in the tissues of drought-tolerant and drought-sensitive wheat genotype seedlings. *AoB Plants* 10:ly016.

Hemmerlin, A. (2013). Post-translational events and modifications regulating plant enzymes involved in isoprenoid precursor biosynthesis. *Plant Sci.* 203, 41–54. doi: 10.1016/j.plantsci.2012.12.008

Hemmerlin, A., Harwood, J. L., and Bach, T. J. (2012). A raison d'être for two distinct pathways in the early steps of plant isoprenoid biosynthesis? *Prog. Lipid Res.* 51, 95–148. doi: 10.1016/j.plipres.2011.12.001

Hemmerlin, A., Tritsch, D., Hartmann, M., Pacaud, K., Hoeffler, J.-F., van Dorsselaer, A., et al. (2006). A cytosolic Arabidopsis D-xylulose kinase catalyzes the phosphorylation of 1-deoxy-D-xylulose into a precursor of the plastidial isoprenoid pathway. *Plant Physiol.* 142, 441–457. doi: 10.1104/pp.106.086652

Huang, J., Hartmann, H., Hellén, H., Wisthaler, A., Perreca, E., Weinhold, A., et al. (2018). New perspectives on CO2, temperature, and light effects on BVOC emissions using online measurements by PTR-MS and cavity ring-down spectroscopy. *Environ. Sci. Technol.* 52, 13811–13823.

Jardine, K., Chambers, J., Alves, E. G., Teixeira, A., Garcia, S., Holm, J., et al. (2014). Dynamic balancing of isoprene carbon sources reflects photosynthetic and photorespiratory responses to temperature stress. *Plant Physiol.* 166, 2051–2064. doi: 10.1104/pp.114.247494

Kreuzwieser, J., Graus, M., Wisthaler, A., Hansel, A., Rennenberg, H., and Schnitzler, J. P. (2002). Xylem-transported glucose as an additional carbon source for leaf isoprene formation in Quercus robur. *New Phytol.* 156, 171–178. doi: 10.1046/j.1469-8137.2002.00516.x

Laule, O., Fürholz, A., Chang, H.-S., Zhu, T., Wang, X., Heifetz, P. B., et al. (2003). Crosstalk between cytosolic and plastidial pathways of isoprenoid biosynthesis in *Arabidopsis thaliana*. *Proc. Natl. Acad. Sci. U.S.A.* 100, 6866–6871. doi: 10.1073/pnas.1031755100

Learned, R. M., and Connolly, E. L. (1997). Light modulates the spatial patterns of 3-hydroxy-3-methylglutaryl coenzyme A reductase gene expression in *Arabidopsis thaliana*. *Plant J.* 11, 499–511. doi: 10.1046/j.1365-313x.1997.11030499.x

Lindinger, W., Hansel, A., and Jordan, A. (1998). On-line monitoring of volatile organic compounds at pptv levels by means of proton-transfer-reaction mass spectrometry (PTR-MS) medical applications, food control and environmental research. *Int. J. Mass Spectrom. Ion Process.* 173, 191–241. doi: 10.1016/s0168-1176(97)00281-4

Loreto, F., and Fineschi, S. (2015). Reconciling functions and evolution of isoprene emission in higher plants. *New Phytol.* 206, 578–582. doi: 10.1111/nph.13242

Loreto, F., Pinelli, P., Brancaleoni, E., and Ciccioli, P. (2004). 13C labeling reveals chloroplastic and extrachloroplastic pools of dimethylallyl pyrophosphate and their contribution to isoprene formation. *Plant Physiol.* 135, 1903–1907. doi: 10.1104/pp.104.039537

Martin, D., Tholl, D., Gershenzon, J., and Bohlmann, J. (2002). Methyl jasmonate induces traumatic resin ducts, terpenoid resin biosynthesis, and terpenoid accumulation in developing xylem of Norway spruce stems. *Plant Physiol.* 129, 1003–1018. doi: 10.1104/pp.011001

Mattos, L., and Moretti, C. (2015). Oxidative stress in plants under drought conditions and the role of different enzymes. *Enzym. Eng.* 5:136.

Mundim, F. M., and Pringle, E. G. (2018). Whole-plant metabolic allocation under water stress. *Front. Plant Sci.* 9:852. doi: 10.3389/fpls.2018.00852

Newville, M., Stensitzki, T., Allen, D., and Ingargiola, A. (2014). *LMFIT: Non-Linear Least-Square Minimization and Curve-Fitting for Python (Version 0.8.0)*. doi: 10.5281/zenodo.11813

Onkokesung, N., Reichelt, M., Wright, L. P., Phillips, M. A., Gershenzon, J., and Dicke, M. (2019). The plastidial metabolite 2-C-methyl-D-erythritol-2, 4-cyclodiphosphate modulates defence responses against aphids. *Plant Cell Environ.* 42, 2309–2323. doi: 10.1111/pce.13538

Pegoraro, E., Rey, A., Greenberg, J., Harley, P., Grace, J., Malhi, Y., et al. (2004). Effect of drought on isoprene emission rates from leaves of *Quercus virginiana* Mill. *Atmos. Environ.* 38, 6149–6156. doi: 10.1016/j.atmosenv.2004.07.028

Pollastri, S., Jorba, I., Hawkins, T. J., Llusià, J., Michelozzi, M., Navajas, D., et al. (2019). Leaves of isoprene-emitting tobacco plants maintain PSII stability at high temperatures. *New Phytol.* 223, 1307–1318. doi: 10.1111/nph.15847

Pollastri, S., Tsonev, T., and Loreto, F. (2014). Isoprene improves photochemical efficiency and enhances heat dissipation in plants at physiological temperatures. *J. Exp. Bot.* 65, 1565–1570. doi: 10.1093/jxb/eru033

Price, D. T., Alfaro, R., Brown, K., Flannigan, M., Fleming, R., Hogg, E., et al. (2013). Anticipating the consequences of climate change for Canada's boreal forest ecosystems. *Environ. Rev.* 21, 322–365. doi: 10.1139/er-2013-0042

Pulido, P., Llamas, E., Llorente, B., Ventura, S., Wright, L. P., and Rodríguez-Concepción, M. (2016). Specific Hsp100 chaperones determine the fate of the first enzyme of the plastidial isoprenoid pathway for either refolding or degradation by the stromal Clp protease in Arabidopsis. *PLoS Genet.* 12:e1005824. doi: 10.1371/journal.pgen.1005824

Ramel, F., Birtic, S., Cuiné, S., Triantaphylidès, C., Ravanat, J.-L., and Havaux, M. (2012). Chemical quenching of singlet oxygen by carotenoids in plants. *Plant Physiol.* 158, 1267–1278. doi: 10.1104/pp.111.182394

Ray, J. D., and Sinclair, T. R. (1998). The effect of pot size on growth and transpiration of maize and soybean during water deficit stress. *J. Exp. Bot.* 49, 1381–1386. doi: 10.1093/jxb/49.325.1381

Rivasseau, C., Seemann, M., Boisson, A. M., Streb, P., Gout, E., Douce, R., et al. (2009). Accumulation of 2-C-methyl-D-erythritol 2, 4-cyclodiphosphate in illuminated plant leaves at supraoptimal temperatures reveals a bottleneck of the prokaryotic methylerythritol 4-phosphate pathway of isoprenoid biosynthesis. *Plant Cell Environ.* 32, 82–92. doi: 10.1111/j.1365-3040.2008.01903.x

Rodríguez-Concepción, M. (2006). Early steps in isoprenoid biosynthesis: multilevel regulation of the supply of common precursors in plant cells. *Phytochem. Rev.* 5, 1–15. doi: 10.1007/s11101-005-3130-4

Rodríguez-Concepción, M., Forés, O., Martínez-García, J. F., González, V., Phillips, M. A., Ferrer, A., et al. (2004). Distinct light-mediated pathways regulate the biosynthesis and exchange of isoprenoid precursors during Arabidopsis seedling development. *Plant Cell* 16, 144–156. doi: 10.1105/tpc.016204

Schnitzler, J.-P., Graus, M., Kreuzwieser, J., Heizmann, U., Rennenberg, H., Wisthaler, A., et al. (2004). Contribution of different carbon sources to isoprene biosynthesis in poplar leaves. *Plant Physiol.* 135, 152–160. doi: 10.1104/pp.103.037374

Schönwitz, R., Lohwasser, K., Kloos, M., and Ziegler, H. (1990). Seasonal variation in the monoterpenes in needles of *Picea abies* (L.) *Karst*. *Trees* 4, 34–40.

Selmar, D. (2008). Potential of salt and drought stress to increase pharmaceutically significant secondary compounds in plants. *Landbauforschung Volkenrode* 58, 139–144.

Sharkey, T. D., and Yeh, S. (2001). Isoprene emission from plants. *Annu. Rev. Plant Biol.* 52, 407–436.

Sinclair, T., and Ludlow, M. (1986). Influence of soil water supply on the plant water balance of four tropical grain legumes. *Funct. Plant Biol.* 13, 329–341. doi: 10.1071/pp9860329

Singsaas, E. L., Lerdau, M., Winter, K., and Sharkey, T. D. (1997). Isoprene increases thermotolerance of isoprene-emitting species. *Plant Physiol.* 115, 1413–1420. doi: 10.1104/pp.115.4.1413

Soja, A. J., Tchebakova, N. M., French, N. H., Flannigan, M. D., Shugart, H. H., Stocks, B. J., et al. (2007). Climate-induced boreal forest change: predictions versus current observations. *Glob. Planet. Change* 56, 274–296. doi: 10.1016/j.gloplacha.2006.07.028

Velikova, V., Várkonyi, Z., Szabó, M., Maslenkova, L., Nogues, I., Kovács, L., et al. (2011). Increased thermostability of thylakoid membranes in isoprene-emitting leaves probed with three biophysical techniques. *Plant Physiol.* 157, 905–916. doi: 10.1104/pp.111.182519

Vickers, C. E., Gershenzon, J., Lerdau, M. T., and Loreto, F. (2009). A unified mechanism of action for volatile isoprenoids in plant abiotic stress. *Nat. Chem. Biol.* 5, 283–291. doi: 10.1038/nchembio.158

Vranová, E., Coman, D., and Gruissem, W. (2013). Network analysis of the MVA and MEP pathways for isoprenoid synthesis. *Annu. Rev. Plant Biol.* 64, 665–700. doi: 10.1146/annurev-arplant-050312-120116

Wang, J.-Z., Lei, Y., Xiao, Y., He, X., Liang, J., Jiang, J., et al. (2019). Uncovering the functional residues of Arabidopsis isoprenoid biosynthesis enzyme HDS. *Proc. Natl. Acad. Sci. U.S.A.* 117, 355–361. doi: 10.1073/pnas.1916434117

Wolfertz, M., Sharkey, T., Boland, W., Kühnemann, F., Yeh, S., and Weise, S. (2003). Biochemical regulation of isoprene emission. *Plant Cell Environ.* 26, 1357–1364. doi: 10.1046/j.0016-8025.2003.01059.x

Wolfertz, M., Sharkey, T. D., Boland, W., and Kühnemann, F. (2004). Rapid regulation of the methylerythritol 4-phosphate pathway during isoprene synthesis. *Plant Physiol.* 135, 1939–1945. doi: 10.1104/pp.104.043737

Wright, L. P., and Phillips, M. A. (2014). Measuring the activity of 1-deoxy-D-xylulose 5-phosphate synthase, the first enzyme in the MEP pathway, in plant extracts. *Methods Mol. Biol.* 1153, 9–20. doi: 10.1007/978-1-4939-0606-2_2

Wright, L. P., Rohwer, J. M., Ghirardo, A., Hammerbacher, A., Ortiz-Alcaide, M., Raguschke, B., et al. (2014). Deoxyxylulose 5-phosphate synthase controls flux through the methylerythritol 4-phosphate pathway in Arabidopsis. *Plant Physiol.* 165, 1488–1504. doi: 10.1104/pp.114.245191

Xiao, Y., Savchenko, T., Baidoo, E. E., Chehab, W. E., Hayden, D. M., Tolstikov, V., et al. (2012). Retrograde signaling by the plastidial metabolite MEcPP regulates expression of nuclear stress-response genes. *Cell* 149, 1525–1535. doi: 10.1016/j.cell.2012.04.038

Yuan, J., Bennett, B. D., and Rabinowitz, J. D. (2008). Kinetic flux profiling for quantitation of cellular metabolic fluxes. *Nat. Protoc.* 3, 1328–1340. doi: 10.1038/nprot.2008.131

Zheng, B., Halperin, T., Hruskova-Heidingsfeldova, O., Adam, Z., and Clarke, A. K. (2002). Characterization of chloroplast Clp proteins in Arabidopsis: localization, tissue specificity and stress responses. *Physiol. Plant.* 114, 92–101. doi: 10.1034/j.1399-3054.2002.1140113.x

Zhou, K., Zou, R., Stephanopoulos, G., and Too, H.-P. (2012). Metabolite profiling identified methylerythritol cyclodiphosphate efflux as a limiting step in microbial isoprenoid production. *PLoS One* 7:e47513. doi: 10.1371/journal.pone.0047513

Zuo, Z., Weraduwage, S. M., Lantz, A. T., Sanchez, L. M., Weise, S. E., Wang, J., et al. (2019). Isoprene acts as a signaling molecule in gene networks important for stress responses and plant growth. *Plant Physiol.* 180, 124–152. doi: 10.1104/pp.18.01391

Conflict of Interest: The authors declare that the research was conducted in the absence of any commercial or financial relationships that could be construed as a potential conflict of interest.

frontiers in Plant Science

ORIGINAL RESEARCH
published: 16 October 2020
doi: 10.3389/fpls.2020.580693

Hybrid Breeding for Restoration of Threatened Forest Trees: Evidence for Incorporating Disease Tolerance in *Juglans cinerea*

*Andrea N. Brennan[1], James R. McKenna[2], Sean M. Hoban[3] and Douglass F. Jacobs[1]**

[1]Department of Forestry and Natural Resources, Purdue University, West Lafayette, IN, United States, [2]USDA Forest Service, Northern Research Station, West Lafayette, IN, United States, [3]The Morton Arboretum, Lisle, IL, United States

Hybridization is a potential tool for incorporating stress tolerance in plants, particularly to pests and diseases, in support of restoration and conservation efforts. Butternut (*Juglans cinerea*) is a species for which hybridization has only recently begun being explored. This North American hardwood tree is threatened due to *Ophiognomonia clavigignenti-juglandacearum* (*Ocj*), the causal fungus of butternut canker disease (BCD), first observed in 1967. Observational evidence in some wild *J. cinerea* populations indicates that naturalized hybrids of *J. cinerea* with Japanese walnut (*Juglans ailantifolia*) may be more tolerant to BCD than non-admixed *J. cinerea*, but this has not been formally tested in a controlled trial. We aimed to examine potential BCD tolerance within and between *J. cinerea* and *J. cinerea* × *J. ailantifolia* hybrids and to determine if there is a difference in canker growth between BCD fungal isolates. Five-year-old *J. cinerea* and hybrid trees were inoculated with two *Ocj* fungal isolates collected from natural infections found in two different sites in Indiana, United States, and a blank control (agar only). Measurements of both artificially induced and naturally occurring cankers were taken at 8-, 12-, 20-, 24-, and 32-month post-inoculation. Differences in canker presence/absence and size were observed by fungal isolate, which could help explain some of the differences in BCD severity seen between *J. cinerea* populations. Smaller and fewer cankers and greater genetic gains were seen in hybrid families, demonstrating that hybrids warrant further evaluation as a possible breeding tool for developing BCD-resistant *J. cinerea* trees.

Keywords: butternut, *Ophiognomonia clavigignenti-juglandacearum*, fungal disease, inoculation, resistance breeding, Japanese walnut, conservation

OPEN ACCESS

Edited by:
Sofia Valenzuela, University of Concepcion, Chile

Reviewed by:
Radu E. Sestras, University of Agricultural Sciences and Veterinary Medicine of Cluj-Napoca, Romania
Dejun Li, Chinese Academy of Tropical Agricultural Sciences, China

****Correspondence:***
Douglass F. Jacobs
djacobs@purdue.edu

Specialty section:
This article was submitted to Plant Breeding, a section of the journal Frontiers in Plant Science

Received: *06 July 2020*
Accepted: *14 September 2020*
Published: *16 October 2020*

Citation:
Brennan AN, McKenna JR, Hoban SM and Jacobs DF (2020) Hybrid Breeding for Restoration of Threatened Forest Trees: Evidence for Incorporating Disease Tolerance in Juglans cinerea. Front. Plant Sci. 11:580693. doi: 10.3389/fpls.2020.580693

INTRODUCTION

Native and non-native diseases and pests are increasingly threatening ecosystems, especially forests, across the globe (Ennos, 2015; Early et al., 2016). This is driven in large part by anthropogenically driven activities, such as globalization and mass trade of plant material that inadvertently transports new pests and pathogens into novel environments (Early et al., 2016). Climate change compounds the problem by providing ideal environments for pests and pathogens (Dukes et al., 2009) and weakening host species, making the host species more vulnerable to

attack (Diez et al., 2012). Some species are not able to acclimate or adapt to these increased threats and are facing extinction (Thomas et al., 2004; Bellard et al., 2016).

Hybridization is currently under consideration as a possible tool to incorporate stress tolerance in support of restoration and conservation efforts (Hamilton and Miller, 2015). There are concerns that hybrids could be detrimental to both the target species and its ecosystem through potential invasion (Muhlfeld et al., 2014), outbreeding depression (genetic incompatibilities or reduced fitness; Allendorf et al., 2013), and genetic swamping (loss of local adaptations by genetic dominance from another species; Allendorf et al., 2013). However, desirable traits, such as disease and pest resistance conferred through hybridization, may be one of few remaining tools to save some species (Sniezko and Koch, 2017). Perhaps, the most notable example of using hybridization to support an endangered species is the American chestnut [*Castanea dentata* (Marsh.) Borkh.], which has been crossed with the Chinese chestnut (*Castanea mollissima* Blume) in pursuit of resistance to chestnut blight [*Cryphonectria parasitica* (Murrill) Barr.; Steiner et al., 2017; Clark et al., 2019; TACF, 2020]. The American Chestnut Foundation (TACF), one of the leading organizations in this effort, has been breeding and backcrossing *C. dentata* hybrids for three generations over 30 years and is currently trialing hybrids with increased resistance in several restoration sites in the eastern United States (TACF, 2020).

Another, lesser-known example where hybridization is being considered to save an endangered plant species, is butternut (*Juglans cinerea* L.), a North American hardwood tree species (Michler et al., 2006). While *J. cinerea* shares a native range in the eastern United States similar to black walnut (*Juglans nigra* L.), *J. cinerea* does not extend as far south and is one of few deciduous tree species in the far northern areas of the United States and southern Canada (Rink, 1990; Farrar, 2017). As a masting species, the tree is ecologically important for providing large, energy-rich nuts for both wildlife and humans (Schultz, 2003), but also holds economic importance through high quality wood products (Forest Products Laboratory, 2010). Culturally, *J. cinerea* has been used by Native Americans for a wide variety of purposes, including for medicine, food, dyes, and canoe construction (Moerman, 1998). Medicinally, *J. cinerea* has been documented to have a broader spectrum of antimicrobial activity compared to many other North American hardwood species (Omar et al., 2000).

Unfortunately, *J. cinerea* populations are now in severe decline due to butternut canker disease (BCD), caused by the fungus *Ophiognomonia clavigignenti-juglandacearum* (*Ocj*; Nair, Kostichka, & Kuntz; Broders and Boland, 2011). The disease, first reported in Wisconsin in 1967 (Relund, 1971), manifests as vertically oriented, elliptical cankers that develop on limbs and boles, often causing the surrounding outer bark to peel (Tisserat and Kuntz, 1984). Over time, the cankers multiply and coalesce, ultimately girdling and killing affected trees (Tisserat and Kuntz, 1984). The reduction in *J. cinerea* populations by BCD has nearly eliminated natural regeneration (Boraks and Broders, 2014), to the point that it is now considered endangered by the International Union for Conservation of Nature (Stritch and Barstow, 2019). *Juglans cinerea* is also listed under Canada's Species at Risk Act (Environment Canada, 2010) and in the United States; the species has a conservation status of either critically imperiled (S1), imperiled (S2), or vulnerable (S3) in 21 states (NatureServe, 2017).

Despite the sporadic occurrence of healthy *J. cinerea* trees in the wild, no durable resistance to BCD has been found in populations of *J. cinerea* to date, with all showing susceptibility upon further testing. For example, when Ostry and Moore (2008) inoculated grafted clones from 12 canker-free source trees with *Ocj*, all individuals displayed susceptibility to the disease. This has led to the concept of using hybridization to incorporate disease resistance into the species (Michler et al., 2006; McKenna et al., 2011; Boraks and Broders, 2014). *Juglans cinerea* does not hybridize with *J. nigra*, the only other *Juglans* conspecific in the eastern deciduous forest (Rink, 1990). However, *J. cinerea* does hybridize with the Japanese walnut (*Juglans ailantifolia* Carr.; Rink, 1990). A study of wild populations of both non-admixed *J. cinerea* and its naturalized hybrids with *J. ailantifolia* found possible tolerance in hybrids compared to its native progenitor, with *J. cinerea* exhibiting an average of 4.5 cankers per tree vs. an average of 2.5 for its hybrids (Boraks and Broders, 2014). However, there have been no controlled evaluations to formally test whether the hybrids hold increased BCD tolerance to *J. cinerea*.

The objectives of this study were to examine potential BCD tolerance within and between non-admixed *J. cinerea* ("*J. cinerea*") and *J. cinerea* × *J. ailantifolia* hybrids ("hybrids," unless otherwise noted) and to determine if there is a difference in canker growth between isolates of *Ocj*. Our hypotheses were as follows: (1) hybrids will have greater tolerance to BCD than *J. cinerea*; (2) some *J. cinerea* and hybrid families will show greater tolerance to BCD than other families; and (3) there will be a difference in canker infection by different *Ocj* isolates. To test these hypotheses, a multi-year field study was conducted using *J. cinerea*, and hybrid trees inoculated with two different isolates of *Ocj*.

MATERIALS AND METHODS

Plant Material

In the fall of 2002, seeds were collected from presumed *J. cinerea* trees in an open-pollinated clone bank in Rosemount, MN, United States originating from putatively resistant surviving trees in the wild (family accessions 709–750; **Table 1**; **Supplementary Table S1**). Seeds were also collected from six wild presumed *J. cinerea* trees in northern Indiana, United States (family accessions 702–708). The seeds were stratified in a cooler at 2.8°C through winter and germinated in a greenhouse in April 2003. The sprouted seeds were planted in a lowland field of Purdue University's Martell Forest (West Lafayette, IN, United States 40.4313991, −87.0389821) in May 2003. Approximately, 10 seedlings were planted per family (half-sib progenies sharing the same maternal parent) as two five-tree plots in a randomized row-block design with a spacing of 3.7 m between rows and 1.8 m within rows.

TABLE 1 | Best Linear Unbiased Predictors (BLUPs), accuracy estimates, breeding values (BVs), and genetic gains of families of *Juglans cinerea* and its hybrids with *Juglans ailantifolia* based on canker size (area).

Family	Species/hybrid	BLUP	Accuracy	BV	Gain (%)
707	Hybrid	−0.57	0.75	7.10	14
706	Hybrid	−0.46	0.67	7.32	11
711	Hybrid	−0.43	0.84	7.37	11
750	Hybrid	−0.37	0.81	7.49	9
704	Hybrid	−0.35	0.83	7.53	9
702	Hybrid	−0.34	0.81	7.57	8
748	Hybrid	−0.28	0.78	7.69	7
736	*Juglans cinerea*	−0.20	0.85	7.84	5
712	*Juglan cinerea*	−0.19	0.80	7.86	5
710	Hybrid	−0.12	0.83	8.00	3
713	*Juglan cinerea*	−0.09	0.76	8.06	2
717	*Juglan cinerea*	−0.08	0.81	8.07	2
730	*Juglan cinerea*	−0.08	0.85	8.07	2
709	*Juglan cinerea*	−0.08	0.86	8.08	2
731	Hybrid	−0.05	0.83	8.13	1
738	*Juglan cinerea*	−0.03	0.80	8.18	1
734	Hybrid	0.01	0.80	8.26	0
714	*Juglan cinerea*	0.03	0.84	8.29	−1
742	*Juglan cinerea*	0.06	0.80	8.36	−1
708	Hybrid	0.07	0.80	8.38	−2
728	*Juglan cinerea*	0.08	0.81	8.39	−2
722	*Juglan cinerea*	0.09	0.86	8.41	−2
732	Hybrid	0.09	0.81	8.42	−2
727	*Juglan cinerea*	0.12	0.83	8.48	−3
715	*Juglan cinerea*	0.13	0.76	8.50	−3
723	*Juglan cinerea*	0.19	0.84	8.61	−5
747	*Juglan cinerea*	0.20	0.86	8.63	−5
726	*Juglan cinerea*	0.20	0.80	8.63	−5
743	*Juglan cinerea*	0.21	0.84	8.65	−5
733	*Juglan cinerea*	0.22	0.85	8.67	−5
744	*Juglan cinerea*	0.26	0.82	8.75	−6
741	*Juglan cinerea*	0.27	0.81	8.78	−7
718	*Juglan cinerea*	0.33	0.87	8.90	−8
746	*Juglan cinerea*	0.33	0.85	8.90	−8
735	Hybrid	0.36	0.86	8.95	−9
716	*Juglan cinerea*	0.49	0.81	9.22	−12

Cankers were measured 32 months following inoculation with Ophiognomonia clavigignenti-juglandacearum (Ocj), the causal fungus of butternut canker disease (BCD). A positive genetic gain indicates a family with canker sizes smaller than the population mean, while a negative genetic gain indicates a family with canker sizes greater than the population mean.
Population mean = 8.237 (log transformed from mm^2).
Family variance = 0.098.

An initial visual screening of the seeds was conducted to exclude F1 hybrids at planting. Our original goal was to include only *J. cinerea* families and in particular, those from healthy wild trees that we considered as putatively resistant parents. However, by the third growing season in 2005, early genetic identification methods were being developed (Aradhya et al., 2006; Zhao and Woeste, 2011), and many *J. cinerea* × *J. ailantifolia* hybrids among our *J. cinerea* germplasm collection had been detected which allowed us to examine these "complex" hybrids for phenotypic differences in leaf size, twig color, and terminal and lateral bud characteristics to distinguish these from *J. cinerea*. For the families in the present study, the phenotypic traits of seedlings were rated in the fall of 2005 by two independent observers as 2 = *J. cinerea*, 1 = *J. cinerea* and hybrid mix, or 0 = hybrid, using the methods that ultimately became the basis for those of Woeste et al. (2009). We recognize that phenotypic assessment is imperfect, but Hoban and Romero-Severson (2011) found that nut growers only using their own personal experience and no key, were able to correctly identify their *J. cinerea* or hybrid trees 85% of the time. Therefore, we have high confidence that phenotypic methods used by expert foresters with long experience with these species should be able to make successful species designations in most cases. However, we also performed DNA tests on a subset of individuals from all families in 2009 using chloroplast markers (Aradhya et al., 2006; Zhao and Woeste, 2011), as well as ITS region, mitochondrial, and nuclear markers (Zhao and Woeste, 2011), which confirmed the initial phenotypic *J. cinerea* or hybrid genotype of each family. Further, a second subsample of 39 *J. cinerea* and hybrid trees from those included in the current study were also genetically analyzed in 2019 using the nuclear markers of Hoban et al. (2008) and chloroplast markers of McCleary et al. (2009). For the 31 samples that successfully amplified, the results of this genetic analysis subsample matched with the initial identification designations. From these analyses, we determined that seven of the Rosemount families and all six wild-collected Indiana families were *J. cinerea* × *J. ailantifolia* hybrids. Ultimately, 203 *J. cinerea* trees from 23 different families and 106 hybrid trees from 13 different families were included in the study.

Inoculations

Two different fungal isolates of *Ocj* were used for the inoculations. Both were collected from natural, spontaneous infections found in Indiana, the first from one of our seedlings in a breeding block at Martell Forest in West Lafayette (IN-1375-4A, "isolate 1") and the second from the Hoosier National Forest in southern Indiana (IN-1378-3, "isolate 2"). These were chosen in order to use isolates representative of the state in which the study was being conducted, and these specific isolates had already been collected and isolated by Michael Ostry and Melanie Moore (USDA Forest Service, Northern Research Station, St. Paul, MN, United States) and thus were readily available. Samples for initiating cultures were collected from cankered branches in early August 2008 and grown on malt agar in darkness at 20°C. Inoculum was prepared from sporulating cultures after 2 months. Inoculations were applied to the trees at 5 years old in 2008, from late September to early October, when trees have been shown to be most susceptible to infection from *Ocj* (Ostry and Moore, 2008). The inoculation application method was similar to that developed by Anagnostakis (1992) for screening chestnut trees (*Castanea* spp.) for tolerance to chestnut blight. Holes (6-mm diameter) were drilled into the main trunk at approximately breast height, through the bark and slightly into the sapwood. A 6-mm diameter plug of inoculum (agar with *Ocj*) was then inserted into each hole, with fungal hyphae facing inward, toward the cambium. A single layer of masking tape was then wrapped around each inoculation wound. Each hole was spaced 20 cm apart, running in a vertical line down the trunk. Each tree received five inoculation points in the following order: the first, top-most (apical) hole was plugged with a blank control (agar only);

the second and third holes with *Ocj* isolate 1; and the fourth and fifth holes with *Ocj* isolate 2.

Evaluation

Survival was recorded each time canker growth was measured. Cankers resulting from the inoculations were evaluated at 8, 12, 20, 24, and 32 months after the inoculations were applied. The maximum vertical lengths (l) and horizontal widths (w) of each canker were recorded. The canker length and width were used to calculate the area (A) of the inoculated canker, using the formula for an ellipse (oval):

$$A = \frac{l}{2} \times \frac{w}{2} \times \pi \ (\text{cm}^2) \quad (1)$$

Cankers occurring from natural *Ocj* infection (outside of inoculation areas) began appearing 4 years after planting in 2006, which was confirmed by isolation of the fungus from several samples of the naturally formed cankers in August 2008. Evaluations of the natural cankers were conducted concurrently with the artificially induced cankers at 8, 20, and 32 months following the inoculations. Natural cankers were rated for cumulative incidence and size using an ordinal scale. Incidence was rated from 0 to 3, where 0 = no natural cankers; 1 = 1 or 2 cankers; 2 = 3–5 cankers; and 3 = 6 or more cankers (McKenna et al., 2011). Size was based on the average size of the natural cankers (length × width), rated from 0 to 3, where 0 (none to very small) = less than ~30 × 10 mm; 1 (small) = ~30–59 × 10–19 mm; 2 (medium) = ~60–99 × 20–24 mm; and 3 (large) = ~100 × 25 mm or greater sized cankers (McKenna et al., 2011).

Data Analysis

All data was analyzed in R v. 3.5.3 (R Core Team, 2019). There was insufficient mortality by the conclusion of the study to conduct a valid statistical analysis of survival, so only survival percentages are reported. The control inoculations did not produce cankers and were not included in the statistical analyses. Canker growth for the remaining inoculations was analyzed at the species/hybrid level using a two-part model to account for the high level of zero growth instances in the early time points of the study. Both parts of the model were conducted using R package "lme4" (Bates et al., 2015). The first part used a linear mixed model to analyze the percent of individuals in each family with canker growth present over time. The second part evaluated canker area over time with linear mixed models only for inoculations where growth was present, using natural-log-transformed data to meet the assumption of normality of errors. For both parts, species/hybrid, fungal isolate, time, and block within the plot (three-level categorical variable) were considered fixed effects, and family was considered a random effect. Since the second part of the model evaluated at the individual level, individual tree was also included as random and nested within family. To facilitate breeding selection and evaluate variation at the family level, Best Linear Unbiased Predictors (BLUPs; Isik et al., 2017) were generated from a linear mixed model, as in the second part of the inoculated canker model. However, only a subset of the data was used to analyze canker area for inoculations where growth was present at the last time point (32-month post-inoculation), thus, time was not included in the analysis of this data subset. The BLUPs (random effects) for each family were taken from the model and estimates of accuracy were calculated for each BLUP based on its SE and the family variance (S) as (Mrode, 2014):

$$Accuracy = \sqrt{1 - \left(\frac{SE^2}{S}\right)} \quad (2)$$

Accuracy estimates are the correlation between true and predicted breeding values (BVs; Mrode, 2014) and are used in plant and animal breeding to evaluate confidence in predictions in lieu of the SE (Isik et al., 2017). The BLUPs were converted to BV by multiplying by two and adding the 32-month canker area population grand mean (μ). The BV was then converted to a percent gain relative to the population mean:

$$Genetic\ gain = \frac{\mu - BV}{\mu} \times 100 \quad (\%) \quad (3)$$

A positive genetic gain indicates a family with artificial canker sizes smaller than the population mean, while a negative genetic gain indicates a family with canker sizes greater than the population mean. The families were finally ranked in order of greatest to smallest gains to assist in family breeding selection. The incidence and size of naturally formed cankers were analyzed using cumulative link mixed models (also called ordinal regression or proportional odds models) with R package "ordinal" (Christensen, 2019). Species/hybrid, fungal isolate, time, and plot block were set as fixed effects. Individual tree nested within family were set as random effects.

RESULTS

Survival

By the conclusion of the study (32-month post-inoculation), there was 96 and 92% survival for *J. cinerea* and hybrid trees, respectively.

Artificially Induced Infection

The percent of individuals with canker growth present at the inoculation site strongly increased over time (χ^2 = 186.87, $p < 0.0001$; **Figure 1A**). There was no difference in the presence of canker growth following inoculation between *J. cinerea* and hybrid trees (χ^2 = 0.14, p = 0.713). However, there was a strong difference by fungal isolate (χ^2 = 421.48, $p < 0.0001$), with much greater presence of canker growth resulting from inoculations with isolate 1 than isolate 2. There was a moderate interaction between species and time (χ^2 = 5.74, p = 0.017), but there was no interaction evident between species/hybrid and fungal isolate (χ^2 = 2.94, p = 0.086); fungal isolate and

time (χ^2 = 0.13, p = 0.720); or species/hybrid, fungal isolate, and time (χ^2 = 0.20, p = 0.657).

The size of cankers resulting from the inoculations strongly increased over time (χ^2 = 1418.95, $p < 0.0001$; **Figure 1B**). Canker growth on the hybrids was smaller than on *J. cinerea* and by the final timepoint, the average inoculated canker area (non-zero) on hybrid trees was 41.9 (± 3.4) cm^2 compared to 61.8 (± 4.1) cm^2 on *J. cinerea* trees (χ^2 = 8.65, p = 0.003). There was also a difference in fungal isolate, with an average canker area of 48.3 (± 2.9) cm^2 for isolate 1 vs. 55.4 (± 4.7) cm^2 for isolate 2 by the final timepoint (χ^2 = 5.34, p = 0.021). A strong interaction was present between species/hybrid and time (χ^2 = 19.78, $p < 0.0001$), with canker growth increasing more rapidly in *J. cinerea* than the hybrids. However, there was no interaction evident between species/hybrid and fungal isolate (χ^2 = 0.31, p = 0.580); fungal isolate and time (χ^2 = 0.54, p = 0.463); or species/hybrid, fungal isolate, and time (χ^2 = 0.97, p = 0.325).

By the conclusion of the study at 32-month post-inoculation, genetic gains based on canker size ranged from −12 to 14% (**Table 1**). There was distinct separation of families by genetic gains based on canker size. In the top-ranking quarter (5–14% gains), seven of nine families were hybrids, while in the bottom quarter (−12 to −5% gains), eight of nine of families were *J. cinerea*.

Naturally Occurring Infection

Incidence of naturally occurring cankers increased strongly over time (χ^2 = 404.76, $p < 0.0001$; **Figure 2**). Species/hybrid was also an important predictor of natural canker incidence, with *J. cinerea* having a greater incidence of natural cankers than the hybrids at all timepoints (χ^2 = 24.53, $p < 0.0001$). As an example, by the final timepoint, 12 and 21% of *J. cinerea* had natural cankers in classes 0 (lowest incidence) and 3 (greatest incidence), respectively, compared to 42 and 5% in hybrids (**Figure 2**). There was no evidence of an interaction between species/hybrid and time for natural canker incidence (χ^2 = 2.67, p = 0.263).

The size of naturally occurring cankers increased greatly over time (χ^2 = 264.82, $p < 0.0001$; **Figure 2**). *Juglans cinerea* had larger natural cankers than the hybrids at all timepoints (χ^2 = 23.95, $p < 0.0001$). At the final timepoint, 12 and 11% of *J. cinerea* had cankers in size classes 0 (smallest) and 3 (largest), respectively, vs. 42 and 1% of hybrids (**Figure 2**). No evidence of an interaction between species/hybrid and time was found for the size of natural cankers (χ^2 = 2.62, p = 0.270).

DISCUSSION

Effect of Fungal Isolate

Supporting our hypothesis, the two *Ocj* isolates used for the inoculations in our study resulted in different levels of canker occurrence and size, which is consistent with studies by Ostry and Moore (2008) and Broders et al. (2012, 2015). In the current study, although the specific fungal isolate used in inoculations played a role in canker size, isolate played a much larger role in predicting the presence/absence of canker growth. This could indicate stronger variability in the ability of different *Ocj* isolates to initiate host infection. With differing levels of aggressiveness, the specific isolates present within a certain location may contribute, in part, to help explain why some areas experience more severe and sudden BCD outbreaks than others (Broders et al., 2015; Morin et al., 2017). However, it is likely that habitat and environment also play a strong role in determining occurrence of infection in these situations as well (Boraks and Broders, 2014; Labonte et al., 2015; Morin et al., 2017).

Tolerance of *Juglans cinerea* and Its Hybrids

Although there was no significant difference in inoculated canker absence/presence between *J. cinerea* and its hybrids, the hybrids did have smaller cankers (averaging nearly 1/3 smaller by the end of the study) that grew slower than those on the progenitor species. Further, hybrid families had the greatest genetic gains in terms of canker size by 32-month post-inoculation. When considering naturally occurring infection, the hybrids also had

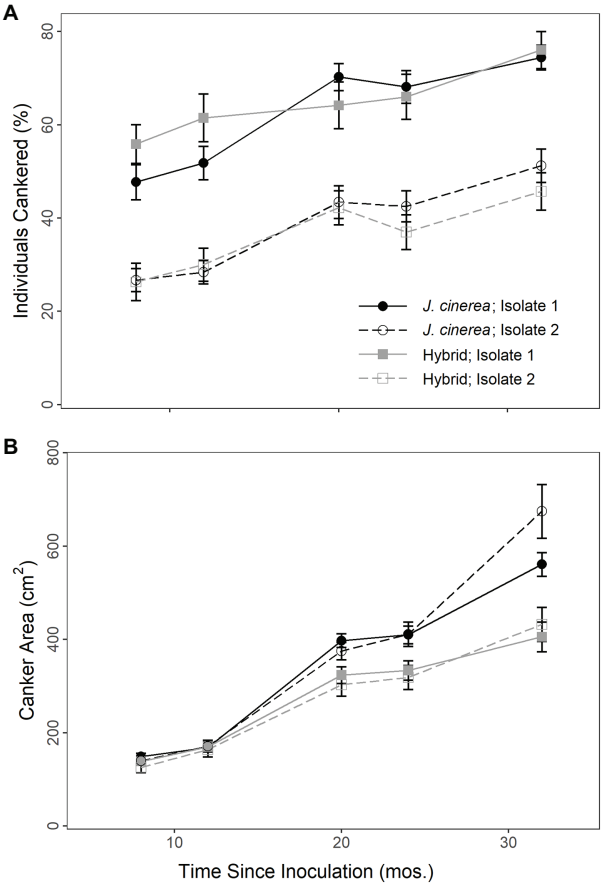

FIGURE 1 | Percent of individuals cankered **(A)** and canker area **(B)** over time on *J. cinerea* and its hybrids with *J. ailantifolia* following inoculation with two different isolates of *Ocj*, the causal fungus of butternut canker disease. Isolate significantly affected both percent of individuals cankered ($p < 0.0001$) and canker area (p = 0.021). Species/hybrid affected canker area (p = 0.003), but not percent of individuals cankered (p = 0.713).

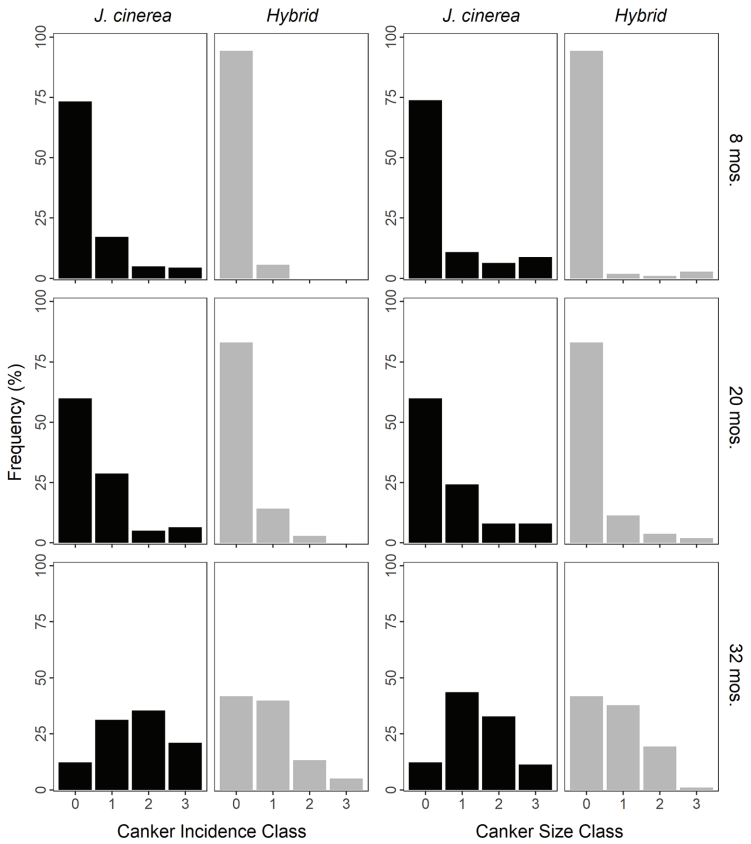

FIGURE 2 | Frequency of trees of *J. cinerea* and its hybrids with *J. ailantifolia* with naturally occurring cankers by different incidence and size classes over time since the initiation of the study. Cankers were formed by *Ocj*, the causal fungus of butternut canker disease. Incidence was rated from classes 0 (no natural cankers) up to 3 (6 or more cankers). Size was based on the average size of the natural cankers (length × width), rated from classes 0 (none to very small; less than ~30 × 10 mm) up to 3 (large; ~100 × 25 mm or greater). *Juglans cinerea* and hybrids were significantly different for both natural canker incidence and size at all timepoints ($p < 0.0001$ for all).

both fewer and smaller cankers than *J. cinerea*. Thus, our hypotheses that hybrids would show greater tolerance to BCD than *J. cinerea* was mostly supported. This trend was also seen in a study of populations of wild *J. cinerea* and naturalized hybrids in the northeastern United States, where the hybrids were found to be much less affected by the disease and had fewer cankers, less dieback, and greater vigor than trees of *J. cinerea* (Boraks and Broders, 2014). It should be noted, however, that while hybrids in the current study were more tolerant on average than *J. cinerea*, some hybrids performed worse than average and some *J. cinerea* performed better than average (**Table 1**).

Black and Neely (1978) reported that *J. cinerea* × *J. ailantifolia* hybrids also had greater tolerance than *J. cinerea* to another *Ophiognomonia* fungal species, anthracnose [*Ophiognomonia leptostyla* (Fr.) Sognov]. These results in *J. cinerea* can be compared to hybrids and other diseases in *Juglans*. In the aforementioned study, hybrids of *J. nigra* with four other *Juglans* species consistently showed greater anthracnose tolerance than their highly susceptible *J. nigra* parent (Black and Neely, 1978). Conversely, in another study, hybrids of Persian walnut (*Juglans regia* L.) and iron walnut (*Juglans sigllata* Dode) showed similar or even greater susceptibility to walnut bacterial blight (*Xanthomonas arboricola* pv. *juglandis* Pierce) than both their progenitors (Jiang et al., 2019). Heightened susceptibility to crown gall disease (*Agrobacterium tumefaciens* Smith & Townsend) has also been documented in hybrids of northern California black walnut [*Juglans hindsii* (Jeps.) Jeps. ex R.E. Sm.] and *J. regia* (McKenna and Epstein, 2003). Thus, disease tolerance in *Juglans* hybrids that is greater than one or both of the parents is not guaranteed and depends on the specific host-pathogen interaction for each disease. Further, in relation to pest resistance, *J. ailantifolia* and its hybrids with both *J. cinerea* and *J. nigra* have expressed greater susceptibility to butternut curculio (*Conotrachelus juglandis* LeConte) than the two native North American progenitors (Wilson and Corneil, 1978). This illustrates that in attempting to obtain BCD resistance in *J. cinerea*, it will be critical that increased susceptibility to native pests not also be inadvertently incorporated.

Interspecific hybrids have also been developed in other genera with the goal of incorporating disease resistance or tolerance into a susceptible and endangered native species. As discussed previously, *C. dentata* × *C. mollissima* hybrids backcrossed to *C. dentata* have been developed with increased resistance to chestnut blight compared to their susceptible *C. dentata* progenitor

(Steiner et al., 2017; Clark et al., 2019; TACF, 2020). After strong selection for *C. dentata*-specific traits and blight resistance, second (B_2) and third (B_3) backcross hybrid lines developed at TACF's Meadowview Research Farm (Meadowview, VA, United States) were found to have average blight areas (B_2) or blight ratings (B_3), significantly different and intermediate to their American and Chinese chestnut progenitors, but not different from those of the F_1 generation (Steiner et al., 2017). However, Clark et al. (2019) reported that blight resistance in *C. dentata*, *C. mollissima*, B_1, B_2, and B_3 Meadowview backcross hybrids ultimately varied when planted across different sites in the first natural forest field trials testing this resistance. While the *Castanea* hybrids held yearly resistance rankings that were intermediate to that of their progenitors in two of the sites (NC and VA), there was no significant difference between any of the progenitors or hybrids in a third site (TN). Given such genotype × environment variation, it is essential that future work test *J. cinerea* and hybrid families in common garden plots across multiple sites in order to assess the durability of possible BCD resistance. Efforts have also been pursued to develop Dutch elm disease (*Ophopstoma* spp.) resistant hybrids for restoring the endangered American elm (*Ulmus americana* L.) and several other *Ulmus* spp. affected by the disease (Brunet and Guries, 2016; Griffin et al., 2017; Martín et al., 2019). While progress has been made with promising hybrids and a few *U. americana* varieties (Brunet and Guries, 2016; Griffin et al., 2017; Martín et al., 2019), it has been slowed by incompatibility and ploidy barriers (Ager and Guries, 1982). These issues do not appear to be an issue with *J. cinerea* × *J. ailantifolia* hybrids given the large number of naturalized hybrids present in the landscape (Hoban et al., 2009).

Consistent with our second hypothesis, both *J. cinerea* and hybrid families separated out by genetic gains on 32-month canker size, with some families showing greater tolerance than others, indicating a possible genetic basis to disease tolerance (Isik et al., 2017). While hybrids tended to rank highest in genetic gains, some *J. cinerea* families, such as 736 and 712, had modest gains as well. However, the finding of a potential genetic basis to BCD tolerance in the current research must be compared to a heritability study of a wild population of *J. cinerea* in Wisconsin. Labonte et al. (2015) primarily concluded that genetic differences explained little of the variance in mortality, and that environmental and site differences were stronger predictors. It was also reported that while genetics was not correlated with survival, there were low, but significant correlations between genetics and canker-related traits, including canker number, which is consistent with the present study. The population assessed by Labonte et al. (2015) only contained non-admixed *J. cinerea* trees, which are believed to have originated from a small number of mother trees, limiting the genetic diversity. The present study, in contrast, included seeds propagated from long-term surviving selections collected from across a wide geographic range and inter-pollinated together in a grafted orchard, expanding the genetic diversity of our test families. Additionally, our study did not include environmental and site factors as in Labonte et al. (2015), so a comparison with the current study's results on heritability of BCD tolerance in hybrids is not entirely possible.

Survival, as assessed by Labonte et al. (2015), is likely a better measure in ultimately identifying the most BCD tolerant trees than the canker-related traits we evaluated in just under 3 years. However, the high survival (over 90%) for both *J. cinerea* and hybrid trees by the conclusion of the present study suggests that more than 32 months are required to understand the full potential of tolerance differences between the species and hybrids once *Ocj* infection begins. Further, the research of Labonte (2015), as well as Clark et al. (2019) with *C. dentata* (discussed earlier), both underscore the need for BCD tolerance screenings on multiple different sites to understand possible genotype × environment interactions. Sambaraju et al. (2018) reported that multiple factors, notably weather, influence *Ocj* epidemiology. It is likely that the successful restoration of *J. cinerea* will not be accomplished solely through the integration of genetic BCD resistance, but in combination with appropriate site selection and silvicultural practices (Jacobs et al., 2013).

Ultimately, beyond any increased disease tolerance or resistance that hybrids may hold compared to their progenitor species, it is essential to also consider how well such hybrids fill both the economic and ecological niches of the progenitor species they are intended to replace, including reproductive potential, physiology, invasiveness, and wood quality. These qualities have been evaluated to a moderate extent in *J. cinerea*, *J. ailantifolia*, and their hybrids. Crystal and Jacobs (2014) reported that the hybrids exhibited both intermediate drought and flood tolerance relative to their *J. cinerea* (more drought tolerant) and *J. ailantifolia* (more flood tolerant) progenitors. Phenotypically, Crystal et al. (2016) projected that most hybrids will tend more toward their *J. ailantifolia* progenitor, although some hybrids did occupy the same space as their *J. cinerea* progenitor. The concerns of dissimilar hybrid and *J. cinerea* phenotypes, along with the intermediate environmental tolerances of the hybrids, could limit their ability to act as a suitable replacement for *J. cinerea*, potentially changing the distribution of the species. However, in a phenotypical study of *C. dentata* hybrids and their progenitors, which are at a much more advanced breeding stage than *J. cinerea* hybrids, 96% of hybrid trees in the third backcross generation were distinctly different from their *C. mollissima* progenitor, and closely resembled *C. dentata* (Diskin et al., 2006). Thus, using *C. dentata* as an example threatened hardwood species for restoration (Jacobs et al., 2013); it may be possible to develop hybrids that are similar to *J. cinerea*, at least phenotypically, with careful selection and breeding.

Conclusions

Differences in canker occurrence and size by *Ocj* isolates were observed in this study, which may explain some of the differences in BCD severity reported among different *J. cinerea* populations. Hybrid families had smaller and fewer cankers and greater genetic gains compared to *J. cinerea* families, demonstrating that hybrids could be a possible breeding tool for developing BCD-resistant *J. cinerea* trees. Further, the genetic gain separation of families by canker size indicates potential heritability of BCD tolerance (under the timeframe of the current study). This is promising for the development of resistance breeding programs using hybrids, but possibly *J. cinerea* as well.

Hybridization in *J. cinerea* is one of just a few examples in plants where hybrids are being considered not only for preserving a species' economic value (timber and nut production), but also for ecological (restoration and conservation) and cultural purposes (ethnobotanical and medicinal). Thus, this study provides further evidence that hybrids represent a potentially effective tool for incorporating disease resistance to aid in restoration of threatened tree species.

DATA AVAILABILITY STATEMENT

The raw data supporting the conclusions of this article will be made available by the authors, without undue reservation.

AUTHOR CONTRIBUTIONS

AB analyzed the data, interpreted the results, and wrote the original manuscript. JM designed and executed the experiment, contributed to interpretation of the results, and revised the manuscript. SH and DJ contributed to interpretation of the results and revised the manuscript. All authors contributed to the article and approved the submitted version.

FUNDING

This work was supported by the USDA National Institute of Food and Agriculture, McIntire Stennis projects IND011535, the USDA Forest Service, and the Fred M. van Eck Foundation of the Hardwood Tree Improvement and Regeneration Center, Forestry and Natural Resources Department, Purdue University, USA.

ACKNOWLEDGMENTS

We express our appreciation to Melanie Moore and Dr. Michael Ostry of the USDA Forest Service for grafting seed orchards, harvesting seed, and isolating and culturing inoculum; and Bill Deeter of the Indiana Nut and Fruit Growers Association for sharing seed from Indiana trees. We thank Brian Beheler, Andrew Meier, Hector Midence, and Burk Thompson of Purdue University, Department of Forestry and Natural Resources, for technical assistance in the field. We would also grateful to Dr. Carolyn Pike (USDA Forest Service State and Private) for providing expertise on tree breeding and its statistical analysis. We thank James Warren (USDA Forest Service Northern Research Station) for providing tree accession information, maps, and field assistance. We would also like to thank Shiwei Liu (Purdue University), and the Purdue University Statistical Consulting Service for their statistical support.

SUPPLEMENTARY MATERIAL

The Supplementary Material for this article can be found online at: https://www.frontiersin.org/articles/10.3389/fpls.2020.580693/full#supplementary-material

REFERENCES

Ager, A. A., and Guries, R. P. (1982). Barriers to interspecific hybridization in *Ulmus american*. *Euphytica* 31, 909–920. doi: 10.1007/bf00039231

Allendorf, F. W., Luikart, G., and Aitken, S. N. (2013). "Hybridization" in *Conservation and the genetics of populations*. Chichester, UK: Wiley-Blackwell, 352–376.

Anagnostakis, S. L. (1992). Measuring resistance of chestnut trees to chestnut blight. *Can. J. For. Res.* 22, 568–571. doi: 10.1139/x92-075

Aradhya, M. K., Potter, D., and Simon, C. J. (2006). "Cladistic biogeography of *Juglans* (Juglandaceae) based on chloroplast DNA intergenic spacer sequences" in *Darwin's harvest: New approaches to the origins, evolution, and conservation of crops*. eds. T. Motley, N. Zerga and H. Cross (Columbia University Press: New York, NY), 143–170.

Bates, D., Maechler, M., Bolker, B. M., and Walker, S. C. (2015). Fitting linear mixed-effects models using lme4. *J. Stat. Softw.* 67, 1–48. doi: 10.18637/jss.v067.i01

Bellard, C., Cassey, P., and Blackburn, T. M. (2016). Alien species as a driver of recent extinctions. *Biol. Lett.* 12:20150623. doi: 10.1098/rsbl.2015.0623

Black, W. M., and Neely, D. (1978). Relative resistance of *Juglans* species and hybrids to walnut anthracnose [*Gnomonia leptostyla*]. *Plant Dis. Rep.* 62, 497–499.

Boraks, A., and Broders, K. D. (2014). Butternut (*Juglans cinerea*) health, hybridization, and recruitment in the northeastern United States. *Can. J. For. Res.* 44, 1244–1252. doi: 10.1139/cjfr-2014-0166

Broders, K. D., and Boland, G. J. (2011). Reclassification of the butternut canker fungus, *Sirococcus clavigignenti-juglandacearum*, into the genus *Ophiognomonia*. *Fungal Biol.* 115, 70–79. doi: 10.1016/j.funbio.2010.10.007

Broders, K., Boraks, A., Barbison, L., Brown, J., and Boland, G. J. (2015). Recent insights into the pandemic disease butternut canker caused by the invasive pathogen *Ophiognomonia clavigignenti-juglandacearum*. *For. Pathol.* 45, 1–8. doi: 10.1111/efp.12161

Broders, K. D., Boraks, A., Sanchez, A. M., and Boland, G. J. (2012). Population structure of the butternut canker fungus, *Ophiognomonia clavigignenti-juglandacearum*, in North American forests. *Ecol. Evol.* 2, 2114–2127. doi: 10.1002/ece3.332

Brunet, J., and Guries, R. P. (2016). "Elm genetic diversity and hybridization in the presence of Dutch elm disease." in *Proceedings of the American elm restoration workshop*. eds. C. Pinchot, K. S. Knight, L. M. Haugen, C. E. Flower, and J. M. Slavicek (Newton Square, PA: U.S. Department of Agriculture, Forest Service, Northern Research Station), 99–107.

Christensen, R. H. B. (2019). ordinal—Regression Models for Ordinal Data.

Clark, S. L., Schlarbaum, S. E., Saxton, A. M., and Baird, R. (2019). Eight-year blight (*Cryphonectria parasitica*) resistance of backcross-generation American chestnuts (*Castanea dentata*) planted in the southeastern United States. *For. Ecol. Manag.* 433, 153–161. doi: 10.1016/j.foreco.2018.10.060

Crystal, P. A., and Jacobs, D. F. (2014). Drought and flood stress tolerance of butternut (*Juglans cinerea*) and naturally occurring hybrids: implications for restoration. *Can. J. For. Res.* 44, 1206–1216. doi: 10.1139/cjfr-2014-0151

Crystal, P. A., Lichti, N. I., Woeste, K. E., and Jacobs, D. F. (2016). Vegetative and adaptive traits predict different outcomes for restoration using hybrids. *Front. Plant Sci.* 7:1741. doi: 10.3389/fpls.2016.01741

Diez, J. M., D'Antonio, C. M., Dukes, J. S., Grosholz, E. D., Olden, J. D., Sorte, C. J. B., et al. (2012). Will extreme climatic events facilitate biological invasions? *Front. Ecol. Environ.* 10, 249–257. doi: 10.1890/110137

Diskin, M., Steiner, K. C., and Hebard, F. V. (2006). Recovery of American chestnut characteristics following hybridization and backcross breeding to restore blight-ravaged Castanea dentata. *For. Ecol. Manag.* 223, 439–447. doi: 10.1016/j.foreco.2005.12.022

Dukes, J. S., Pontius, J., Orwig, D., Garnas, J. R., Rodgers, V. L., Brazee, N., et al. (2009). Responses of insect pests, pathogens, and invasive plant species to climate change in the forests of northeastern North America: what can we predict? *Can. J. For. Res.* 39, 231–248. doi: 10.1139/X08-171

Early, R., Bradley, B. A., Dukes, J. S., Lawler, J. J., Olden, J. D., Blumenthal, D. M., et al. (2016). Global threats from invasive alien species in the twenty-first century and national response capacities. *Nat. Commun.* 7:12485. doi: 10.1038/ncomms12485

Ennos, R. A. (2015). Resilience of forests to pathogens: an evolutionary ecology perspective. *Forestry* 88, 41–52. doi: 10.1093/forestry/cpu048

Environment Canada (2010). "Recovery strategy for the butternut (*Juglans cinerea*) in Canada," in Species at Risk Act Recovery Strategy Series (Ottawa, Canada: Environment Canada), 24. Available at: https://www.registrelep-sararegistry.gc.ca/virtual_sara/files/plans/rs_butternut_0910_e.pdf (Accessed May 21, 2020).

Farrar, J. L. (2017). *Trees in Canada*. Markham, Ontario: Fitzhenry and Whiteside Ltd.

Forest Products Laboratory (2010). Wood handbook: Wood as an engineering material. Madison, WI: USDA, Forest Service, Forest Products Laboratory. Available at: https://www.fpl.fs.fed.us/documnts/fplgtr/fpl_gtr190.pdf (Accessed June 26, 2020).

Griffin, J. J., Jacobi, W. R., McPherson, E. G., Sadof, C. S., McKenna, J. R., Gleason, M. L., et al. (2017). Ten-year performance of the United States National elm Trial. *Arboric. Urban For.* 43, 107–120.

Hamilton, J. A., and Miller, J. M. (2015). Adaptive introgression as a resource for management and genetic conservation in a changing climate. *Conserv. Biol.* 30, 33–41. doi: 10.1111/cobi.12574

Hoban, S., Anderson, R., McCleary, T., Schlarbaum, S., and Romero-Severson, J. (2008). Thirteen nuclear microsatellite loci for butternut (*Juglans cinerea* L.). *Mol. Ecol. Resour.* 8, 643–646. doi: 10.1111/j.1471-8286.2007.02030.x

Hoban, S. M., McCleary, T. S., Schlarbaum, S. E., and Romero-Severson, J. (2009). Geographically extensive hybridization between the forest trees American butternut and Japanese walnut. *Biol. Lett.* 5, 324–327. doi: 10.1098/rsbl.2009.0031

Hoban, S., and Romero-Severson, J. (2011). Homonymy, synonymy and hybrid misassignments in butternut (*Juglans cinerea*) and Japanese walnut (*Juglans ailantifolia*) nut cultivars. *Genet. Resour. Crop. Evol.* 59, 1397–1405. doi: 10.1007/s10722-011-9767-5

Isik, F., Holland, J., and Maltecca, C. (2017). *Genetic data analysis for plant and animal breeding*. Cham, Switzerland: Springer.

Jacobs, D. F., Dalgleish, H. J., and Nelson, C. D. (2013). A conceptual framework for restoration of threatened plants: the effective model of American chestnut (*Castanea dentata*) reintroduction. *New Phytol.* 197, 378–393. doi: 10.1111/nph.12020

Jiang, S., Han, S., He, D., Cao, G., Zhang, F., and Wan, X. (2019). Evaluating walnut (*Juglans* spp.) for resistance to walnut blight and comparisons between artificial inoculation assays and field studies. *Australas. Plant Pathol.* 48, 221–231. doi: 10.1007/s13313-019-0621-0

Labonte, N. R., Ostry, M. E., Ross-Davis, A., and Woeste, K. E. (2015). Estimating heritability of disease resistance and factors that contribute to long-term survival in butternut (*Juglans cinerea* L.). *Tree Genet. Genomes* 11, 1–12. doi: 10.1007/s11295-015-0884-8

Martín, J. A., Sobrino-Plata, J., Rodríguez-Calcerrada, J., Collada, C., and Gil, L. (2019). Breeding and scientific advances in the fight against Dutch elm disease: will they allow the use of elms in forest restoration? *New For.* 50, 183–215. doi: 10.1007/s11056-018-9640-x

McCleary, T. S., Robichaud, R. L., Nuanes, S., Anagnostakis, S. L., Schlarbaum, S. E., and Romero-Severson, J. (2009). Four cleaved amplified polymorphic sequence (CAPS) markers for the detection of the *Juglans ailantifolia* chloroplast in putatively native *J. cinerea populations*. *Mol. Ecol. Resour.* 9, 525–527. doi: 10.1111/j.1755-0998.2008.02465.x

McKenna, J. R., and Epstein, L. (2003). Susceptibility of Juglans species and interspecific hybrids to *Agrobacterium tumefaciens*. *HortScience* 38, 435–439. doi: 10.21273/HORTSCI.38.3.435

McKenna, J. R., Ostry, M. E., and Woeste, K. (2011). "Screening butternut and butternut hybrids for resistance to butternut canker." in *Proceedings of the 17th Central Hardwood Forest Conference*. eds. S. Fei, J. M. Lhotka, J. W. Stringer, K. W. Gottschalk, and G. W. Miller. April 5–7, 2010; (Lexington, KY: USDA Forest Service), 460–474.

Michler, C. H., Pijut, P. M., Jacobs, D. F., Meilan, R., Woeste, K. E., and Ostry, M. E. (2006). Improving disease resistance of butternut (*Juglans cinerea*), a threatened fine hardwood: a case for single-tree selection through genetic improvement and deployment. *Tree Physiol.* 26, 121–128. doi: 10.1093/treephys/26.1.121

Moerman, D. E. (1998). *Native American ethnobotany*. Portland, OR: Timber Press.

Morin, R. S., Gottschalk, K. W., Ostry, M. E., and Liebhold, A. M. (2017). Regional patterns of declining butternut (*Juglans cinerea* L.) suggest site characteristics for restoration. *Ecol. Evol.* 8, 546–559. doi: 10.1002/ece3.3641

Mrode, R. A. (2014). *Linear models for the prediction of animal breeding values*. *3rd Edn*. Oxfordshire, UK: CABI.

Muhlfeld, C. C., Kovach, R. P., Jones, L. A., Al-Chokhachy, R., Boyer, M. C., Leary, R. F., et al. (2014). Invasive hybridization in a threatened species is accelerated by climate change. *Nat. Clim. Chang.* 4, 620–624. doi: 10.1038/nclimate2252

NatureServe (2017). Data from: NatureServe explorer: an online encyclopedia of life. Version. 7.1. Available at: http://explorer.natureserve.org/index.htm (Accessed September 26, 2017).

Omar, S., Lemonnier, B., Jones, N., Ficker, C., Smith, M. L., Neema, C., et al. (2000). Antimicrobial activity of extracts of eastern North American hardwood trees and relation to traditional medicine. *J. Ethnopharmacol.* 73, 161–170. doi: 10.1016/S0378-8741(00)00294-4

Ostry, M. E., and Moore, M. (2008). Response of butternut selections to inoculation with *Sirococcus clavigignenti-juglandacearum*. *Plant Dis.* 92, 1336–1338. doi: 10.1094/PDIS-92-9-1336

R Core Team (2019). R: a language and environment for statistical computing. Vienna, Austria: R Foundation for Statistical Computing. Available at: https://www.r-project.org/ (Accessed December 30, 2019).

Relund, D. (1971). Forest pest conditions in Wisconsin. Madison, WI: Wisconsin Department of Natural Resources.

Rink, G. (1990). "*Juglans cinerea* L. butternut," in Silvics of North America, eds. R. Burns and B. Honkala (Washington, DC: USDA Forest Service Agricultural Handbook 654), 386–390. Available at: https://www.srs.fs.usda.gov/pubs/misc/ag_654/table_of_contents.htm (Accessed May 21, 2020).

Sambaraju, K. R., Desrochers, P., and Rioux, D. (2018). Factors influencing the regional dynamics of butternut canker. *Plant Dis.* 102, 743–752. doi: 10.1094/PDIS-08-17-1149-RE

Schultz, J. (2003). Conservation assessment for butternut or white walnut (*Juglans cinerea* L.). Milwaukee, WI: USDA Forest Service. Available at: https://www.fs.usda.gov/Internet/FSE_DOCUMENTS/fsm91_054130.pdf (Accessed May 21, 2020).

Sniezko, R. A., and Koch, J. (2017). Breeding trees resistant to insects and diseases: putting theory into application. *Biol. Invasions* 19, 3377–3400. doi: 10.1007/s10530-017-1482-5

Steiner, K. C., Westbrook, J. W., Hebard, F. V., Georgi, L. L., Powell, W. A., and Fitzsimmons, S. F. (2017). Rescue of American chestnut with extraspecific genes following its destruction by a naturalized pathogen. *New For.* 48, 317–336. doi: 10.1007/s11056-016-9561-5

Stritch, L., and Barstow, M. (2019). Data from: *Juglans cinerea*. IUCN Red List Threat. Species 2019.

TACF (2020). Breeding for blight resistance. American Chestnut Foundation. Available at: https://www.acf.org/science-strategies/tree-breeding/ (Accessed May 13, 2020).

Thomas, C. D., Cameron, A., Green, R. E., Bakkenes, M., Beaumont, L. J., Collingham, Y. C., et al. (2004). Extinction risk from climate change. *Nature* 427, 145–148. doi: 10.1038/nature02121

Tisserat, N., and Kuntz, J. (1984). Butternut canker: development on individual trees and increase within a plantation. *Plant Dis.* 68, 613–616. doi: 10.1094/PD-68-613

Wilson, L. F., and Corneil, J. A. (1978). "The butternut curculio on some hybrid walnuts in Michigan." in Walnut insects and diseases. eds. K. J. Kessler and B. C. Weber. June 13–14, 1978 (Carbondale, IL, USA: North Central Forest Experiment Station, Forest Service, US Department of Agriculture), 35–39.

Woeste, K., Farlee, L., Ostry, M., Mckenna, J., and Weeks, S. (2009). A forest manager's guide to butternut. *North. J. Appl. For.* 26, 9–14. doi: 10.1093/njaf/26.1.9

Zhao, P., and Woeste, K. E. (2011). DNA markers identify hybrids between butternut (*Juglans cinerea* L.) and Japanese walnut (*Juglans ailantifolia* Carr.). *Tree Genet. Genomes* 7, 511–533. doi: 10.1007/s11295-010-0352-4

Conflict of Interest: The authors declare that the research was conducted in the absence of any commercial or financial relationships that could be construed as a potential conflict of interest.

frontiers in Plant Science

MINI REVIEW
published: 21 October 2020
doi: 10.3389/fpls.2020.583323

Modern Strategies to Assess and Breed Forest Tree Adaptation to Changing Climate

Andrés J. Cortés[1,2], Manuela Restrepo-Montoya[2] and Larry E. Bedoya-Canas[2]*

[1] Corporación Colombiana de Investigación Agropecuaria AGROSAVIA, Rionegro, Colombia, [2] Departamento de Ciencias Forestales, Facultad de Ciencias Agrarias, Universidad Nacional de Colombia – Sede Medellín, Medellín, Colombia

Studying the genetics of adaptation to new environments in ecologically and industrially important tree species is currently a major research line in the fields of plant science and genetic improvement for tolerance to abiotic stress. Specifically, exploring the genomic basis of local adaptation is imperative for assessing the conditions under which trees will successfully adapt *in situ* to global climate change. However, this knowledge has scarcely been used in conservation and forest tree improvement because woody perennials face major research limitations such as their outcrossing reproductive systems, long juvenile phase, and huge genome sizes. Therefore, in this review we discuss predictive genomic approaches that promise increasing adaptive selection accuracy and shortening generation intervals. They may also assist the detection of novel allelic variants from tree germplasm, and disclose the genomic potential of adaptation to different environments. For instance, natural populations of tree species invite using tools from the population genomics field to study the signatures of local adaptation. Conventional genetic markers and whole genome sequencing both help identifying genes and markers that diverge between local populations more than expected under neutrality, and that exhibit unique signatures of diversity indicative of "selective sweeps." Ultimately, these efforts inform the conservation and breeding status capable of pivoting forest health, ecosystem services, and sustainable production. Key long-term perspectives include understanding how trees' phylogeographic history may affect the adaptive relevant genetic variation available for adaptation to environmental change. Encouraging "big data" approaches (machine learning—ML) capable of comprehensively merging heterogeneous genomic and ecological datasets is becoming imperative, too.

Keywords: genomics of adaptation, genomic prediction, genome-wide association studies, genome-wide selection scans, assisted gene flow, machine learning, big data

OPEN ACCESS

Edited by:
Sanushka Naidoo,
University of Pretoria, South Africa

Reviewed by:
Dejun Li,
Chinese Academy of Tropical Agricultural Sciences, China
Rodrigo J. Hasbun,
University of Concepcion, Chile

****Correspondence:***
Andrés J. Cortés
acortes@agrosavia.co

Specialty section:
This article was submitted to Plant Breeding, a section of the journal Frontiers in Plant Science

Received: *14 July 2020*
Accepted: *29 September 2020*
Published: *21 October 2020*

Citation:
Cortés AJ, Restrepo-Montoya M and Bedoya-Canas LE (2020) Modern Strategies to Assess and Breed Forest Tree Adaptation to Changing Climate. Front. Plant Sci. 11:583323. doi: 10.3389/fpls.2020.583323

INTRODUCTION

How trees will respond to climate change is a pressing question both in the contexts of natural forests and tree plantations (Kremer et al., 2014; Holliday et al., 2017; Isabel et al., 2020). Forests offer key ecological services, boosting significant resources of biodiversity in terms of species and habitats, while help mitigating the impact of excess air pollutants (Phillips et al., 2019; Pennisi, 2020). Trees also source natural renewable materials (i.e., wood itself, cellulose for the pulp industry,

and lignin and hemicelluloses for energy production), likely to increase in the future as sustainable alternatives to fossil fuels (Carlson et al., 2014).

Yet, forest tree species are being threatened by climate change (Sullivan et al., 2020) due to fluctuations in the frequency and intensity of heat, drought, salinity (Naidoo et al., 2019), and the incidence of pathogens and pests (Naidoo et al., 2014; Christie et al., 2015). Hence, now more than ever it is essential to explore changing abiotic (Chakhchar et al., 2017; Alcaide et al., 2019b) and biotic (Meyer et al., 2016) interactions. Rampant phenotypic plasticity (Berlin et al., 2017; Hallingback et al., 2019) to climate gradients is presumed in trees, arguing resilience to variability throughout their long lives. Still, forests adaptability should also be assessed in the light of spatially varying local environmental selective pressures (Savolainen et al., 2013), and trees' genetic and evolutionary potentials (Howe and Brunner, 2005). Both directly reflect and feedback overall adaptive genetic variation. Hence, understanding the genomic drivers that underpin adaptive trait variation becomes vital for conservation and industrial goals.

Developments in plant genomics (Brunner et al., 2007a; Neale and Kremer, 2011) have already disclosed the genetic basis of various useful traits (Khan and Korban, 2012; Tuskan et al., 2018). Yet, this information has limitedly been utilized in tree improvement and conservation (Flanagan et al., 2018), despite genetic gains (**Figure 1**) and optimized management are urgently required due to environmental issues (Scherer et al., 2020). Besides, breeding woody perennials is primarily bottlenecked by their outcrossing reproductive systems, prolonged juvenile phases (Grattapaglia et al., 2018), large genome sizes lacking elimination mechanisms of long-terminal transposons (Nystedt et al., 2013), and an excessive focus on productivity (Burdon and KlápšTě, 2019) that omits adaptive traits (**Table 1**; Li et al., 2019). Thus, here we discuss ways to side step these limitations by arguing how predictive genomics can increase selection accuracy and shorten generation intervals (Grattapaglia et al., 2018), assist the detection of exotic variants from tree germplasm (Migicovsky and Myles, 2017), and disclose the genomic potential of adaptation to different climates (Lind et al., 2018). These efforts will ultimately inform conservation and breeding to enhance forest health, ecosystem services, and sustainable production.

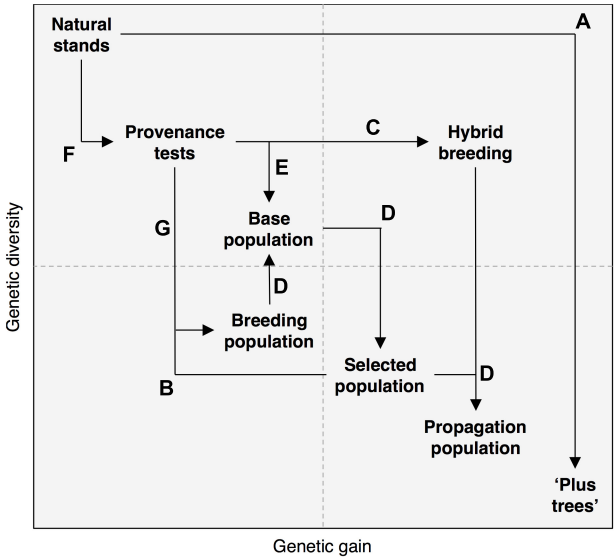

FIGURE 1 | Trans-disciplinary approaches (arrows) such as predictive breeding (GP) and machine learning (ML) promise supporting genome-wide marker-assisted (MAS) pre-breeding and breeding strategies for the selection of **(A)** "plus trees" in the wild, key **(B)** intra- and **(C)** inter- specific parental combinations, and **(D)** elite offspring from those parents. GP and ML should go beyond breeding and feedback **(E)** germplasm utilization and environmental niche classification (Cortés et al., 2013) and enviromics (Costa-Neto et al., 2020; Resende et al., 2020). Genomic-assisted characterizations, such as Genome-Wide Association Studies—GWAS (Neale and Savolainen, 2004), Genome–Environment Associations—GEA (Rellstab et al., 2015; Cortés and Blair, 2018; López-Hernández and Cortés, 2019) and Genome-Wide Selection Scans—GWSS (Zahn and Purnell, 2016), must also start considering more thoroughly **(F)** novel sources of local adaptation, **(G)** genetic-guided infusions and assisted gene flow (AGF), as well an overall systems genetics thinking (Ingvarsson et al., 2016; Myburg et al., 2019).

PREDICTIVE BREEDING PROMISES BOOSTING FOREST TREE GENETIC IMPROVEMENT

The aim of forest tree breeding is rarely to develop new varieties, but instead advance gradual population improvement through recurrent selection and testing (Neale and Kremer, 2011). Because of the long generation times of forest trees, their breeding has traditionally relied on phenotypic selection from natural stands by choosing "plus-trees" (**Figure 1A**). Their superior phenotype (primarily productivity and tree architecture, and seldom adaptability) is often measured *in situ* or in provenance trials. This starting pool of preferred trees constitutes the base population, an arboretum from which further selection is carried out to build a selected population with elite seed/scion donors. Their estimated combinatory ability is gathered from genetic tests such as progeny trials, and parental re-selection (**Figure 1B**) from top families and single trees (White et al., 2007). After three steps of selection (from the natural, base, and selected populations), eroded genetic diversity may jeopardize overall population's productivity and resilience due to inbreeding depression. In order to minimize this risk, a breeding population is established to increase genetic variability. Intermating may rely on infusions from external populations. Outbred multi-parental populations (Scott et al., 2020) hence become the base population of a second generation. A bottleneck of this approach is that each generation would last at least nine or 18 years, for seedling or elite clone identification, respectively, in a fast growing tree species such as *Eucalyptus* (Resende et al., 2012).

Shortcuts to speed up the traditional cycle of forest tree genetic improvement rely on hybrids and backcrossing. Hybrid breeding (**Figure 1C**) aims harnessing heterotic effects (hybrid vigor) due to dominance and over-dominance already existing in nature, capable of increasing yield and adaptability (Schilthuizen et al., 2004; Seehausen, 2004). Dominance refers to the masking of deleterious effects of recessive alleles as a consequence of the increased heterozygosity resulting from hybridization

TABLE 1 | Predictive breeding (genomic prediction—GP, also known as genomic selection—GS) studies in forest tree species published during the last years.

Species	Populations	Trait data	Genotyping data	GP algorithm	Key conclusions	References
Elaeis guineensis	162 individuals from the Deli and Group B populations	Seven oil yield components	262 SSRs	PBLUP, GBLUP	Genomic selection (GBLUP) calibrated according to conditions of the experiment showed higher trait precision when using pedigree-based model	Cros et al., 2015
Elaeis guineensis	A × B hybrid progeny tests with almost 500 crosses for training and 200 crosses for independent validation	Seven oil yield components	(>5,000 GBS-derived SNPs	GBLUP, PBLUP	Preselection for yield components using GBS is the first possible application of GS in oil palm.	Cros et al., 2017
Hevea brasilensis	332 clones from the F1 cross PB 260 × RRIM 600	Rubber production	332 SSRs on site 1 and 296 SSRs on site 2	RKHS, BLR_A, RR-BLUP-A, BLR_AD, RR-BLUP_AD	Mean between-site GS accuracy reached 0.561 when using the 125–200 SSRs with the highest Ho. The simulations showed that by applying a genomic preselection among 3,000 seedlings in the nursery there is a greater precision of selection of the genomic preselection compared to the phenotypic preselection. Statistical method had no effect on GS precision	Cros et al., 2019
Eucalyptus grandis × *E. urophylla* hybrids	999 individuals from 45 families	Cellulose content, composition of lignin monomer, total lignin, WD	33,398 SNP	ABLUP, GBLUP, ssGBLUP	ssGBLUP is a tool with a great projection for the improvement of the precision and the bias of the classic GBLUP for the genomic evaluation in the improvement of *Eucalyptus*	Cappa et al., 2019
Picea abies	1,370 controlled-pollinated individuals from 46 unrelated parents	Quality features of solid wood, pilodyn penetration, acoustic speed	116,765 SNP	ABLUP-A, ABLUP-AD, GBLUP-AD, GBLUD-ADE	GBLUP-AD is a model with great utility in production and propagation. Tree breeders can use it for seedling selection, or family and full-siblings selection	Chen et al., 2019
Eucalyptus globulus	646 individuals out of approximately 10 individuals per family	WD, branch quality, DBH, HT	14,442 SNP	BRR, Bayes C, HAP, HAP-SNP	In general, the BRR and Bayes C methods had a higher predictive capacity for most of the traits. In particular, genomic models that included the haplotype effect (either HAP or HAP SNP) significantly increased the AP of traits with low heritability.	Ballesta et al., 2019
Eucalyptus cladocalyx	1,470 individuals from 49 families	DBH, HT, BHT, WD, STR, SLD, FI	3.8 K Illumina Infinium EUChip60K SNPs	Bayes A, Bayes B, Bayes C, BRR	An GSq approach outperformed GS models in terms of predictive ability when the proportion of the variance explained by the significant marker-trait associations was higher than those explained by the polygenic background and non-significant markers	Ballesta et al., 2020
Eucalyptus clones of *E. urophylla* × *E. grandis*	1,130 clones of 69 full- sib families	Biomass production, WUE, wood properties	3,303 SNPs	GBLUP	The inclusion of wood δ13C in the selection process may lead to *Eucalyptus* varieties adapted to marginal zones still presenting good performance for biomass and wood chemical traits	Bouvet et al., 2020
Picea abies	726 trees of 40 families of complete siblings from two localities	Density, microfiber angle, wood stiffness	5,660 Infinium iSelect SNP matrix SNPs from exome capture and sequencing	Single-trait: GBLUP, BRR, GBLUP, TGBLUP, ABLUP. Multi-traits: GBLUP	Genomic prediction models showed similar results, but the multi-trait model stood out when weevil attacks were not available. Most of the results indicate that the weevil resistance genotypes were higher when there was a greater proportion of height to diameter and greater rigidity of the wood.	Lenz et al., 2020
Pinus radiata	457 POP2 descendants of 63 parents, and 524 POP3 descendants of 24 parents	Branching frequency, stem straightness, internal verification, and external bleeding	1,371,123 exome sequencing capture SNPs	GBLUP, ABLUP	An efficient way to improve non-key traits is through genomic selection with a pedigree corrected using SNP information	Li et al., 2019
Pseudotsuga menziesii	13,615 individuals	HT, 13 environmental variables	66,969 SNPs	ssGBLUP	GS-PA can be substantially improved using ECs to explain environmental heterogeneity and G × E effects. The ssGBLUP methodology allows historical genetic trials containing non-genotyped samples to contribute in genomic prediction, and, thus, effectively boosting training population size which is a critical step	Ratcliffe et al., 2019

(Continued)

TABLE 1 | Continued

Species	Populations	Trait data	Genotyping data	GP algorithm	Key conclusions	References
Shorea platyclados	356 individuals from a half-sib progeny population	Seven important traits, including growth, branching quality, wood quality traits	5,900 Illumina Hi-Seq X SNPs	rrBLUP	Selective breeding for these traits individually could be very effective, especially for increasing the diameter growth, branch diameter ratio and wood density simultaneously	Sawitri et al., 2020
Hevea brasiliensis	435 individual rubber trees at two sites. 252 F1 hybrids derived from a PR255 × PB217 cross, 146 F1 hybrids derived from a GT1 × RRIM701 cross, 37 genotypes from a GT1 × PB235 cross, and 4 testers (GT1, PB235, RRIM701, and RRIM600)	SC	30,546 GBS-derived SNPs	BLUP, SM, MM, MDs, Mde	Multi-environment models were superior to the single-environment genomic models. Methods in which GS is incorporated resulted in a fivefold increase in response to selection for SC with multi-environment GS (MM, MDe, or MDs)	Souza et al., 2019
Fraxinus excelsior	1,250 individuals	Tree health, ash dieback resistance	100–50,000 HiSeq X SNPs	RR-BLUP	Ash dieback resistance in *F. excelsior* is a polygenic trait that should respond well to both natural selection and breeding, which could be accelerated using genomic prediction	Stocks et al., 2019
Eucalyptus nitens	691 individuals	Solid wood production, height, DBH, stem straightness, WD, wood stiffness, wood shrinkage, growth strain	12,236 Illumina EUChip60K SNPs	BLUP, GBLUP	The greatest improvement in genetic parameters was obtained for tangential air-dry wood shrinkage and growth strain	Suontama et al., 2019
Pseudotsuga menziesii	A 38-year-old progeny test population (P1), selecting 37 of 165 families with complete siblings at random from 3 different settings. Validation population contained 247 descendants with controlled crosses from the 37 families	HT	Complete genotyping of exome capture	RR-BLUP, GRR, Byes-B	The validation of cross genomic selection of juvenile height in Douglas fir gave very similar results with the ABLUP predictive precision, but this precision may be linked to the relationship between training and validation conjugates	Thistlethwaite et al., 2019a
Pseudotsuga menziesii, *Picea glauca*, *P. engelmannii*	1,321 Douglas-fir trees, representing 37 full-sib F1 families and 1,126 interior spruce trees, representing 25 open-pollinated (half-sib) families	Mid-rotation height, WD	200–50,000 Illumina HiSeq 2000 SNPs	RR-BLUP	Reducing marker density cannot be recommended for carrying out GS in conifers. Significant LD between markers and putative causal variants was not detected using 50,000 SNPs	Thistlethwaite et al., 2020
Pinus contorta	Half- and full- sibs represented by 57 base parents and 42 full-sib families with an calculated effective population size of 92	Growth and wood quality	51,213 Illumina HiSeq SNPs	Bayes C, Bayes B, BLUP, GBLUP, ABLUP	The predictions of Marker-based models had accuracies that were equal to or better than pedigree-based models (ABLUP) when using several cross-validation scenarios and were better at ranking trees within families	Ukrainetz and Mansfield, 2020
Castanea dentate	7,173 descendants of BC3F3 from 346 "Clapper" mothers and 198 "Serious" mothers. For the BC3F2 progeny, a total of 1,134 "Clapper" and 1,042 "Graves" were sampled	*Cryphonectria parasitica* fungus severity (BC3F3) or presence/absence data (BC3F2)	Sequencing of a *C. dentata* clone in the PacBio Sequel platform	HBLUP, ABLUP, Bayes C	By means of genomic prediction and estimation of hybrid indices, a trade-off is between resistance and a proportion of inherited genome. The results found show that the genetic architecture underlying the heritability of resistance to blight is complex	Westbrook et al., 2020
Picea abies	484 progeny trees from 62 half-sib families	WD, MOE, MFA	130,269 Illumina HiSeq 2500 SNPs	ABLUP, GBLUP, rrBLUP, BayesB, RKHS	This study indicates standing tree-based measurements is a cost-effective alternative method for GS. Selection for density could be conducted at an earlier age than for MFA and MOE	Zhou et al. (2020)

For a comprehensive summary of previous studies not included here see Grattapaglia et al. (2018). Detailed abbreviations are shown at the end of the table. WUE, water use efficiency; SC, stem circumference; WD, wood density; MOE, modulus of elasticity; MFA, microfibril angle; DBH, diameter at breast height; HT, total tree height; BHT, first bifurcation height; STR, stem straightness; SLD, slenderness index; FI, flowering intensity; SNP, single nucleotide polymorphism; SSR, simple sequence repeat; GBS, genotyping by sequencing.

(i.e., an scape from inbreeding depression). On the other hand, over-dominance corresponds to the increase in aptitude as the result of the additive and epistatic effects of alleles that are naturally maintained by balancing selection and only coincide in hybrid genotypes. Hybrid breeding is nowadays widely used at operational plantations to maximize circumference at breast height (e.g., *E. grandis*× *E. nitens* and *Pinus elliotti* × *P. oocarpa*), height (e.g., *P. caribaea* × *P. tecunumanii*) and resistance to *Fusarium* spp. (i.e., *P. patula* × *P. tecunumanii*), among other potential uses (Burkhart et al., 2017). Backcrossing helps targeting the introgression of desired traits from exotic sources into elite populations, as has been done to transfer resistance to chestnut blight into American populations from Chinese wild donors (Cipollini et al., 2017).

Molecular breeding approaches (Badenes et al., 2016), in which genetic markers are used to assist selection, offer promising alternatives to speed up traditional tree breeding cycles, as well as hybrid and backcrossing schemes. Marker-Assisted Selection—MAS (Butcher and Southerton, 2007; Muranty et al., 2014) and Backcrossing—MAB (Herzog and Frisch, 2011) provide frameworks to pyramid target genetic variants of simple Mendelian traits, which are those regulated by few major genes (e.g., resistance to biotic stresses). Gene editing (Doudna and Charpentier, 2014; Dort et al., 2020) and transgenics (Campbell et al., 2003) can also transfer or silence allelic variants of major effects within a single generation (Pereira-Lorenzo et al., 2019). These may replicate the success of tolerant chestnuts (Alcaide et al., 2019a; Westbrook et al., 2019) and promote reproductive sterility (Meilan et al., 2001; Fritsche et al., 2018). Yet, molecular breeding via MAS, MAB and gene editing is often inefficient to trace quantitative traits as growth and adaptation to abiotic stresses. Adaptation is often polygenic (Cortés et al., 2018b; Barghi et al., 2020) due to many low-effect genes and their second-order interactions (Boyle et al., 2017).

A last-generation predictive breeding (**Figure 1D**) approach designed for quantitative polygenic traits is known as Genomic Prediction—GP (Desta and Ortiz, 2014; Crossa et al., 2017; Grattapaglia et al., 2018). GP standardizes infinitesimal marker-based additive predictive models by relying on historical phenotypic data (Meuwissen et al., 2001; Gianola et al., 2006; de los Campos et al., 2013). Trait data must be in Linkage Disequilibrium—LD or genetic auto-correlation (e.g., Kelleher et al., 2012), with the molecular markers or with the samples' genetic co-ancestry. GP utility has been demonstrated (**Table 1**) in model forest tree species such as *Eucalyptus* (Resende et al., 2012; Suontama et al., 2019), and conifers as *Pinus* (Resende M. F. et al., 2012; Li et al., 2019) and Douglas-fir (Thistlethwaite et al., 2017, 2019b), but also in non-model perennial crops such as coffee (Sousa et al., 2018), rubber (Cros et al., 2019; Souza et al., 2019) and oil palm (Cros et al., 2015). GP may even fit epigenetics (Roudbar et al., 2020), as well as multi-trait genomic models as was recently confirmed in Norway spruce for growth, wood quality and weevil resistance traits (Lenz et al., 2020). GP could also be coupled with somatic embryo-genesis for clonal propagation of elite genotypes by selecting elite zygotic embryos based on their genomic breeding value (Grattapaglia et al., 2018). GP has the potential to predict untested hybrid genotypes (Technow et al., 2014) in woody perennials (Cros et al., 2017; Tan et al., 2017) by genotyping potential parental lines and phenotyping few F1 hybrids. Prioritizing inter-specific combinations for field trials can speed up hybrid breeding. Meanwhile, like already envision for chestnut (Westbrook et al., 2020), Genomic-Assisted Backcrossing (GABC) will replace MAB as the strategy to assist introgression breeding into elite populations from exotic germplasm.

ASSISTING GENOMIC CHARACTERIZATION OF TREE GERMPLASM TO CAPTURE NOVEL VARIANTS

Exploiting tree wild populations for genomics-assisted breeding (**Figure 1E**) is key to broaden the genetic basis of woody perennial breeding programs (Migicovsky and Myles, 2017). Specifically, diverse seed bank collections and novel tree provenances might source (Ulian et al., 2020) exotic variation (e.g., unique wood quality properties). They also help avoiding genetic erosion (e.g., via infusions) and increasing long-term adaptability to climate change (e.g., making forests more tolerant to abiotic stresses such as drought and heat). For example, genomic diversity analyses helped capturing rare variants in *P. trichocarpa* germplasm (Piot et al., 2019) often missed by Genome-Wide Association Studies (GWAS) in the related species *P. tremula* (Khan and Korban, 2012). Expanded phylogenomic (Wang M. et al., 2020) and species (Wang et al., 2020) diversity may source novel alleles to support selective breeding, as in wood quality traits for improved bioenergy feedstock. In turn, GP might go beyond breeding, the focus of the previous section, and feedback seed bank characterization (Hickey et al., 2017)—e.g., by predicting seed traits (Kehel et al., 2020) and overall yield (Crossa et al., 2007, 2016) in diverse accessions that otherwise could not have been tested at once in genetic field trials. Although the use of GP for germplasm characterization is latent, it has not been fully explored in forest tree species, a main research gap to be filled in the oncoming years.

Tree species rich in evolutionary diversity (Shang et al., 2020) could leverage breeding. Hybridization (Nieto Feliner et al., 2020), introgression (Burgarella et al., 2019), and polyploidy (Mason and Wendel, 2020) have already pumped morphological novelty by testing more genetic compatibilities than humans ever will. Yet, genomics of adaptive radiations (Seehausen, 2004; Madriñán et al., 2013; Cortés et al., 2018a; Marques et al., 2019) are challenging (Schilthuizen et al., 2004; de la Harpe et al., 2017). Long-living oaks—*Quercus* (Plomion et al., 2018; Leroy et al., 2020b; Plomion and Martin, 2020) are a classical syngameon (Cannon and Petit, 2020) – a promiscuous network of weakly isolated species that has driven peerless historical (Crowl et al., 2020; Hipp et al., 2020; Leroy et al., 2020c) and current (Leroy et al., 2020a) adaptive introgression (Kremer and Hipp, 2020).

In short, marker-assisted schemes are liable to be implemented at various stages during pre-breeding—e.g., in the selection of

"plus trees" from the wild (De Dato et al., 2018), of target parental pairs (Blair et al., 2013), and of superior offspring (Galeano et al., 2012). These approaches also aid conservation (Martín et al., 2012; Mattioni et al., 2017) and germplasm tracing (Cortés et al., 2011; Blair et al., 2012; Chiocchini et al., 2016). Still, genomic-assisted studies of germplasm may risk focusing on productive traits and disregard locally adapted trait variation.

GENOMICS OF ADAPTATION TO DIFFERENT ENVIRONMENTS

Local genetic adaptation (**Figure 1F**) may prove useful in the reaction of forests to climate change (Savolainen et al., 2013; Lascoux et al., 2016), for instance via gene swamping of pre-adapted alleles (Kremer et al., 2014; de Visser et al., 2018). Nowadays there is a wide portfolio of genomic tools that appeal to environmental variables in order to infer the genetic basis of adaptation to abiotic stresses. Specifically, Genome-Wide Selection Scans—GWSS (Zahn and Purnell, 2016) and Genome–Environment Associations – GEA (Rellstab et al., 2015) aim detecting signatures of selection across environmental gradients by pinpointing sections in the genomes that correlate with habitat heterogeneity (Forester et al., 2016). These approaches have successfully been used to assess variation in bud-break phenology (McKown et al., 2018) and stomata patterning (McKown et al., 2014) as potential responses to climate warming in natural populations of *P. trichocarpa*. They have also allow comparing the likelihoods of adaptive reactions at continental (Holliday et al., 2011; Evans et al., 2014; Zhou et al., 2014; Stölting et al., 2015) and regional scales (Eckert et al., 2010; Holliday et al., 2016; Pluess et al., 2016; Ingvarsson and Bernhardsson, 2020) across phylogenetically diverse taxa (Yeaman et al., 2016). Currently there are even multi-scale approaches to detect widespread divergent selection in non-model tree species experiencing population decline (Mayol et al., 2020).

Local adaptation to climate change can be further enhanced (**Figure 1G**) via assisted gene flow—AGF (Aitken and Whitlock, 2013). AGF aims minimizing endogenous negative, while maximizing exogenous positive, selection by trans-locating pre-adapted individuals to facilitate adaptation of planted forests to climate change (Aitken and Bemmels, 2016). Management of local adaptation in a changing climate was recently examined in populations from lodgepole pine (*P. contorta*) across western Canada (Mahony et al., 2020). Yet, operational uses of genomic data to guide seed transfer or AGF are still lacking. Alternatively, genetic containment may be desired for transgenic trees (Brunner et al., 2007b; Klocko et al., 2016). The utility of these approaches in tropical forests remains to be explored. Tropical trees are more at risk from warming because they are closer to upper thermal limits (Freeman et al., 2020; Sentinella et al., 2020), as in montane (Cortés and Wheeler, 2018; Feeley et al., 2020; Tito et al., 2020) and alpine (Wheeler et al., 2014, 2016; Valencia et al., 2020) habitats. Disclosing the genetic, pan-genomic (Bayer et al., 2020), and epigenetic (Brautigam et al., 2013; Sow et al., 2018; Barrera-Redondo et al., 2020) bases of traits underlying adaptive responses in tree species will assist AGF, industrial milestones, and conservation priorities (Isabel et al., 2020) across meta-populations (Gonzalez et al., 2020), and even micro-habitats (Cortés et al., 2014; Abdelaziz et al., 2020).

CONCLUDING REMARKS

A major question in the interface between forests and their environments that genomics have the potential to assist is whether tree adaptation to the fast pace of climate change can happen despite their long generation times (Holliday et al., 2017). Specifically, GP offers a feasible way to predict adaptation from allele frequencies in many genes of low effects underlying polygenic traits (Isabel et al., 2020). This way, the role of adaptive responses can be balanced in relation with range shifts (i.e., migration) and extinction as possible climate change outcomes for tree populations (Aitken et al., 2008; Alberto et al., 2013). This question is equally insightful for domesticated and wild stands of forest trees, and must be coupled with reflections regarding the best propagation and conservation schemes. For instance, the factual consequences on genetic diversity of clonal and seedling forestry (Ingvarsson and Dahlberg, 2018), and of assisted gene flow (Aitken and Whitlock, 2013; Aitken and Bemmels, 2016), must be compiled.

Forest genomics tends focusing on economically important species. Yet, the power of population genomics must be further extended to comprehend neutral and adaptive processes in non-commercial species of ecological value in order to advance not just productivity, but also climate adaptation, forest health and conservation (Isabel et al., 2020). In this sense, GP is starting to permeate novel non-key traits other than growth and wood density, but still of interest for breeding, such as branching, stem straightness and external resin bleeding (Li et al., 2019). GP is also predicting adaptive trait variation for abiotic (Eckert et al., 2010) and biotic (Westbrook et al., 2020) stresses. In parallel to an enrichment of target traits, emerging genomic technologies might unlock woody plant trait diversity beyond the model tree species poplar, eucalyptus, willow, oak, chestnut and pecan (Tuskan et al., 2018).

There is currently a rich mosaic of alternative genetic methods to carry out both explicit (direct) and implied (indirect) selection on economic- (Burdon and KlápšTě, 2019) and ecological-worth (Holliday et al., 2017; Isabel et al., 2020) functions. These different traits can enlighten our understanding of the consequences of genetic divergence on the reaction of tree populations to climate change (Kremer et al., 2014). However, novel methodological developments should target more comprehensively complex trait–environment relationships (Bruelheide et al., 2018). They should also mingle between adaptive (Cortés et al., 2015b; Sedlacek et al., 2016) and range shift (Sedlacek et al., 2014; Wheeler et al., 2015) responses across altitudinal (Lenoir et al., 2008; Steinbauer et al., 2018), latitudinal (Chen et al., 2011) and micro-habitat (Sedlacek et al., 2015; Little et al., 2016) gradients.

PERSPECTIVES

Exploring natural adaptation to changing climate and genetic breeding for tolerance to abiotic stress in forest tree species has traditionally been assisted by GWAS, GWSS, GEA (Cortés et al., 2020), and AGF techniques. These approaches have allowed identifying and utilizing naturally available, locally adapted, variants. More recently, major developments in the field of predictive breeding (i.e., GP) promise to speed up selection from natural sources, as well as within the breeding cycle, by shortening the generation intervals and increasing the selection accuracy prior field trials. We have already identified and discussed major improvements in this line, such as multi-trait GP models (Lenz et al., 2020), coupled with integrative selection scores (Burdon and KlápšTě, 2019) on novel non-key (Li et al., 2019) and ecological-worth (Holliday et al., 2017; Isabel et al., 2020) traits. These innovations can capture multi-scale trait–environment relationships (Bruelheide et al., 2018) in non-model tree species (Mayol et al., 2020). Given the complexity and heterogeneity of trans-disciplinary data sources, Machine Learning (ML) offers a timely predictive and synthetizing approach capable of merging the highlights of the GWAS, GWSS, GEA, AGF and GP techniques.

"Supervised" ML typically utilizes "labeled" training datasets in order to cross-validate the "recall" rate of a target classification (e.g., selection). ML powerfully handles high-dimensional inputs of heterogeneous "features" without a joint probability distribution (Schrider and Kern, 2018). This way, algorithmically generated non-parametric models that avoid rejection sampling sidestep the "curse of dimensionality" and offer new ways to reveal complex systems (Myburg et al., 2019). ML has historically been utilized in functional genomics (Libbrecht and Noble, 2015) and ecological niche modeling (Phillips et al., 2017). Yet, it is now transitioning into GWAS-coupled MAS (Cortés et al., 2015a), GP (Crossa et al., 2019; Abdollahiarpanahi et al., 2020), GWSS (Schrider and Kern, 2018), and demographics—as when coupled with Approximate Bayesian Computation (Elleouet and Aitken, 2018; Liu et al., 2019).

We anticipate that ML techniques will brace GP predictions for various traits in multi-environment trials that aim disentangling the additive genetic variance and the genotype × environment components. Novel developments in the field of ML will further allow building more accurate predictions by merging environmental variables, microhabitat diversity, and genome-wide divergence, all within a tree-breeding context to pivot "plus tree" selection, hybrid breeding and GABC schemes, as well as in terms of adaptation to climate change in natural forests. Integrative assessments (Ingvarsson et al., 2016) via ML promise harnessing adaptive trait variation in forest tree species.

AUTHOR CONTRIBUTIONS

AC conceived this review. MR-M and LB-C collected literature and prepared summary tables. AC wrote the first draft of the review with later edits made by MR-M and LB-C.

FUNDING

Supported to AC during the early phases of this work was made through the grants 4.1-2016-00418 and BS2017-0036 from Vetenskapsrådet (VR) and from Kungliga Vetenskapsakademien (KVA), respectively. The editorial fund from the Colombian Corporation for Agricultural Research (AGROSAVIA) waged the publication of this review.

ACKNOWLEDGMENTS

This review homages C. Lexer R.I.P. (Fay and Palma-Silva, 2020; Karrenberg et al., 2020; Schloötterer, 2020) for his visionary contributions to the fields of forest tree genetics and population genomics, and for his exceptional enthusiasm while mentoring and welcoming pupils and colleagues at his affable research group. In particular, AC enormously appreciates his stimulating and supportive role as an inspiring doctoral co-advisor (2011–2015), and gratefully remembers his hospitality in Fribourg (Switzerland) during 2011–2013 through countless discussions, refreshing Fondue mealtimes, hikes and Pétanque contests. C. Lexer is also thanked for making possible exciting joint field trips with S. Humbert and Y. Naciri to Col du Sanetsch, Lac de Moiry and Lac des Autannes (Valais, Switzerland) in August 2011, and with S. Humbert and A. Tribsch to Hohe Tauern and Niedere Tauern (Austria) in July 2013, as well as for encouraging thought-provoking scientific discussions during the Swiss National Science Foundation (SNSF) Sinergia *Salix* Kickoff Meeting held in April 2011 at Davos (Graubünden, Switzerland), the European Society for Evolutionary Biology Congress held in August 2011 at Tubingen (Germany), the Swiss National Science Foundation (SNSF) Sinergia *Salix* Closure Meeting held in February 2013 at Fribourg (Switzerland), and the European Molecular Biology Organization (EMBO) workshop on Mechanisms of Plant Speciation (Lafon-Placette et al., 2016) held in June 2015 at Åkersberga (Sweden). Special recognition is additionally granted to S. Arenas, J.P. Jaramillo-Correa, F. López-Hernández and M.J. Torres-Urrego for debates while writing this review. Topic editors and reviewers are acknowledged for conceiving and pushing through a timely Research Topic on "Forests and Their Interactions with the Environment".

REFERENCES

Abdelaziz, M., Anderson, J. T., Rochford, M. E., Bemmels, J. B., Jameel, M. I., and Denney, D. A. (2020). Small spaces, big impacts: contributions of micro-environmental variation to population persistence under climate change. *AoB PLANTS* 12:plaa005. doi: 10.1093/aobpla/plaa005

Abdollahiarpanahi, R., Gianola, D., and Peñagaricano, F. (2020). Deep learning versus parametric and ensemble methods for genomic prediction of complex phenotypes. *Genet. Sel. Evol.* 52:12.

Aitken, S. N., and Bemmels, J. B. (2016). Time to get moving: assisted gene flow of forest trees. *Evol. Appl.* 9, 271–290. doi: 10.1111/eva.12293

Aitken, S. N., and Whitlock, M. C. (2013). Assisted gene flow to facilitate local adaptation to climate change. *Annu. Rev. Ecol. Evol. Syst.* 44, 367–388. doi: 10.1146/annurev-ecolsys-110512-135747

Aitken, S. N., Yeaman, S., Holliday, J. A., Wang, T., and Curtis-Mclane, S. (2008). Adaptation, migration or extirpation: climate change outcomes for tree populations. *Evol. Appl.* 1, 95–111. doi: 10.1111/j.1752-4571.2007.00013.x

Alberto, F. J., Aitken, S. N., Alia, R., Gonzalez-Martinez, S. C., Hanninen, H., Kremer, A., et al. (2013). Potential for evolutionary responses to climate change - evidence from tree populations. *Glob. Chang. Biol.* 19, 1645–1661. doi: 10.1111/gcb.12181

Alcaide, F., Solla, A., Cherubini, M., Mattioni, C., Cuenca, B., Camisón, Á., et al. (2019a). Adaptive evolution of chestnut forests to the impact of ink disease in Spain. *J. Syst. Evol.* 58, 504–516. doi: 10.1111/jse.12551

Alcaide, F., Solla, A., Mattioni, C., Castellana, S., and Martín, M. A. (2019b). Adaptive Diversity and drought tolerance in *Castanea Sativa* assessed through genic markers Est-Ssr. *Forestry* 92, 287–296. doi: 10.1093/forestry/cpz007

Badenes, M. L., Fernandez, I. M. A., Rios, G., and Rubio-Cabetas, M. J. (2016). Application of genomic technologies to the breeding of trees. *Front. Genet.* 7:198. doi: 10.3389/fgene.2016.00198

Ballesta, P., Bush, D., Silva, F. F., and Mora, F. (2020). Genomic predictions using low-density Snp markers, Pedigree and Gwas information: a case study with the non-model species *Eucalyptus Cladocalyx*. *Plants* 9:99. doi: 10.3390/plants9010099

Ballesta, P., Maldonado, C., Perez-Rodriguez, P., and Mora, F. (2019). Snp and Haplotype-based genomic selection of quantitative traits in *Eucalyptus Globulus*. *Plants* 8:331. doi: 10.3390/plants8090331

Barghi, N., Hermisson, J., and SchloöTterer, C. (2020). Polygenic adaptation: a unifying framework to understand positive selection. *Nat. Rev. Genet.* doi: 10.1038/s41576-020-0276-2 [Epub ahead of print].

Barrera-Redondo, J., Pinero, D., and Eguiarte, L. E. (2020). Genomic, transcriptomic and epigenomic tools to study the domestication of plants and animals: a field guide for beginners. *Front. Genet.* 11:742. doi: 10.3389/fgene.2020.00742

Bayer, P. E., Golicz, A. A., Scheben, A., Batley, J., and Edwards, D. (2020). Plant pan-genomes are the new reference. *Nat. Plants* 6, 914–920. doi: 10.1038/s41477-020-0733-0

Berlin, S., Hallingbäck, H. R., Beyer, F., Nordh, N. E., Weih, M., and Rönnberg-Wästljung, A. C. (2017). Genetics of phenotypic plasticity and biomass traits in hybrid willows across contrasting environments and years. *Ann. Bot.* 120, 87–100. doi: 10.1093/aob/mcx029

Blair, M. W., Cortés, A. J., Penmetsa, R. V., Farmer, A., Carrasquilla-Garcia, N., and Cook, D. R. (2013). A high-throughput Snp marker system for parental polymorphism screening, and diversity analysis in common bean (*Phaseolus Vulgaris* L.). *Theor. Appl. Genet.* 126, 535–548. doi: 10.1007/s00122-012-1999-z

Blair, M. W., Soler, A., and Cortés, A. J. (2012). Diversification and Population Structure in Common Beans (*Phaseolus vulgaris* L.). *PLoS One* 7:e49488. doi: 10.1371/journal.pone.0049488

Bouvet, J.-M., Makouanzi Ekomono, C. G., Brendel, O., Laclau, J.-P., Bouillet, J.-P., and Epron, D. (2020). Selecting for water use efficiency, wood chemical traits and biomass with genomic selection in a *Eucalyptus* breeding program. *For. Ecol. Manage.* 465:118092. doi: 10.1016/j.foreco.2020.118092

Boyle, E. A., Li, Y. I., and Pritchard, J. K. (2017). An expanded view of complex traits: from polygenic to omnigenic. *Cell* 169, 1177–1186. doi: 10.1016/j.cell.2017.05.038

Brautigam, K., Vining, K. J., Lafon-Placette, C., Fossdal, C. G., Mirouze, M., Marcos, J. G., et al. (2013). Epigenetic regulation of adaptive responses of forest tree species to the environment. *Ecol. Evol.* 3, 399–415. doi: 10.1002/ece3.461

Bruelheide, H., Dengler, J., Purschke, O., Lenoir, J., Jiménez-Alfaro, B., Hennekens, S. M., et al. (2018). Global trait–environment relationships of plant communities. *Nat. Ecol. Evol.* 2, 1906–1917.

Brunner, A. M., Difazio, S. P., and Groover, A. T. (2007a). Forest genomics grows up and branches out. *New Phytol.* 174, 707–710.

Brunner, A. M., Li, J., Difazio, S. P., Shevchenko, O., Montgomery, B. E., Mohamed, R., et al. (2007b). Genetic containment of forest plantations. *Tree Genet. Genomes* 3, 75–100. doi: 10.1007/s11295-006-0067-8

Burdon, R. D., and KlápšTě, J. (2019). Alternative selection methods and explicit or implied economic-worth functions for different traits in tree breeding. *Tree Genet. Genomes* 15:79.

Burgarella, C., Barnaud, A., Kane, N. A., Jankowski, F., Scarcelli, N., Billot, C., et al. (2019). Adaptive introgression: an untapped evolutionary mechanism for crop adaptation. *Front. Plant Sci.* 10:4. doi: 10.3389/fpls.2019.00004

Burkhart, H. E., Brunner, A. M., Stanton, B. J., Shuren, R. A., Amateis, R. L., and Creighton, J. L. (2017). An assessment of potential of hybrid poplar for planting in the Virginia Piedmont. *New Forests* 48, 479–490. doi: 10.1007/s11056-017-9576-6

Butcher, P., and Southerton, S. (2007). "Marker-Assisted Selection in Forestry Species," in *Marker-Assisted Selection – Current Status and Future Perspectives in Crops, Livestock, Forestry and Fish*, eds E. Guimarães, J. Ruane, B. Scherf, A. Sonnino, and J. Dargie (Rome: FAO).

Campbell, M. M., Brunner, A. M., Jones, H. M., and Strauss, S. H. (2003). Forestry's fertile crescent: the application of biotechnology to forest trees. *Plant Biotechnol. J.* 1, 141–154. doi: 10.1046/j.1467-7652.2003.00020.x

Cannon, C. H., and Petit, R. J. (2020). The oak syngameon: more than the sum of its parts. *New Phytol.* 226, 978–983. doi: 10.1111/nph.16091

Cappa, E. P., De Lima, B. M., Da Silva-Junior, O. B., Garcia, C. C., Mansfield, S. D., and Grattapaglia, D. (2019). Improving genomic prediction of growth and wood traits in *Eucalyptus* using phenotypes from non-genotyped trees by single-step Gblup. *Plant Sci.* 284, 9–15. doi: 10.1016/j.plantsci.2019.03.017

Carlson, C. H., Gouker, F. E., Serapiglia, M. J., Tang, H., Krishnakumar, V., Town, C. D., et al. (2014). "Annotation of the Salix purpurea L. genome and gene families important for biomass production," in *Proceedings of the Plant and Animal Genetics Conference XXII*, San Diego, CA.

Chakhchar, A., Haworth, M., El Modafar, C., Lauteri, M., Mattioni, C., Wahbi, S., et al. (2017). An assessment of genetic diversity and drought tolerance in Argan tree (*Argania Spinosa*) populations: potential for the development of improved drought tolerance. *Front. Plant Sci.* 8:276. doi: 10.3389/fpls.2017.00276

Chen, I. C., Hill, J. K., Ohlemuller, R., Roy, D. B., and Thomas, C. D. (2011). Rapid range shifts of species associated with high levels of climate warming. *Science* 333, 1024–1026. doi: 10.1126/science.1206432

Chen, Z. Q., Baison, J., Pan, J., Westin, J., Gil, M. R. G., and Wu, H. X. (2019). Increased prediction ability in Norway Spruce Trials marker X environment interaction and non-additive genomic selection model. *J. Hered.* 110, 830–843. doi: 10.1093/jhered/esz061

Chiocchini, F., Mattioni, C., Pollegioni, P., Lusini, I., Martín, M. A., Cherubini, M., et al. (2016). Mapping the genetic diversity of *Castanea Sativa*: exploiting spatial analysis for biogeography and conservation studies. *J. Geogr. Information Syst.* 08, 248–259. doi: 10.4236/jgis.2016.82022

Christie, N., Tobias, P. A., Naidoo, S., and Kulheim, C. (2015). The *Eucalyptus Grandis* Nbs-Lrr gene family: physical clustering and expression hotspots. *Front. Plant Sci.* 6:1238. doi: 10.3389/fpls.2015.01238

Cipollini, M., Dingley, N. R., Felch, P., and Maddox, C. (2017). Evaluation of phenotypic traits and blight-resistance in an American chestnut backcross orchard in Georgia. *Glob. Ecol. Conserv.* 10, 1–8. doi: 10.1016/j.gecco.2017.01.004

Cortés, A. J., and Blair, M. W. (2018). Genotyping by sequencing and genome – environment associations in wild common bean predict widespread divergent adaptation to drought. *Front. Plant Sci.* 9:128. doi: 10.3389/fpls.2018.00128

Cortés, A. J., Chavarro, M. C., and Blair, M. W. (2011). Snp marker diversity in common bean (*Phaseolus vulgaris* L.). *Theor. Appl. Genet.* 123, 827–845. doi: 10.1007/s00122-011-1630-8

Cortés, A. J., Garzón, L. N., Valencia, J. B., and Madriñán, S. (2018a). On the causes of rapid diversification in the Páramos: isolation by ecology and genomic divergence in *Espeletia*. *Front. Plant Sci.* 9:1700. doi: 10.3389/fpls.2018.01700

Cortés, A. J., Liu, X., Sedlacek, J., Wheeler, J. A., Lexer, C., and Karrenberg, S. (2015a). *Maintenance of Female-Bias in a Polygenic Sex Determination System is Consistent with Genomic Conflict. On the Big Challenges of a Small Shrub: Ecological Genetics of Salix Herbacea L.* (Uppsala: Acta Universitatis Upsaliensis).

Cortés, A. J., Monserrate, F., Ramírez-Villegas, J., Madriñán, S., and Blair, M. W. (2013). Drought tolerance in wild plant populations: the case of common beans (*Phaseolus vulgaris* L.). *PLoS One* 8:e62898. doi: 10.1371/journal.pone.0062898

Cortés, A. J., Skeen, P., Blair, M. W., and Chacón-Sánchez, M. I. (2018b). Does the genomic landscape of species divergence in phaseolus beans coerce parallel signatures of adaptation and domestication? *Front. Plant Sci.* 9:1816. doi: 10.3389/fpls.2018.01816

Cortés, A. J., Waeber, S., Lexer, C., Sedlacek, J., Wheeler, J. A., Van Kleunen, M., et al. (2014). Small-scale patterns in snowmelt timing affect gene flow and the distribution of genetic diversity in the alpine dwarf shrub *Salix Herbacea*. *Heredity* 113, 233–239. doi: 10.1038/hdy.2014.19

Cortés, A. J., and Wheeler, J. A. (2018). "The environmental heterogeneity of mountains at a fine scale in a changing world," in *Mountains, Climate, and Biodiversity*, eds C. Hoorn, A. Perrigo, and A. Antonelli (New York, NY: Wiley).

Cortés, A. J., Wheeler, J. A., Sedlacek, J., Lexer, C., and Karrenberg, S. (2015b). *Genome-Wide Patterns of Microhabitat-Driven Divergence in the Alpine Dwarf Shrub Salix Herbacea L. On the Big Challenges of a Small Shrub: Ecological Genetics of Salix Herbacea L.* (Uppsala: Acta Universitatis Upsaliensis).

Cortés, A. J., López-Hernández, F., and Osorio-Rodriguez, D. (2020). Predicting thermal adaptation by looking into populations' genomic past. *Front. Genet.* 11:564515. doi: 10.3389/fgene.2020.564515

Costa-Neto, G., Fritsche-Neto, R., and Crossa, J. (2020). Nonlinear kernels, dominance, and envirotyping data increase the accuracy of genome-based prediction in multi-environment trials. *Heredity* doi: 10.1038/s41437-020-00353-1

Cros, D., Bocs, S., Riou, V., Ortega-Abboud, E., Tisné, S., Argout, X., et al. (2017). Genomic preselection with genotyping-by- sequencing increases performance of commercial oil palm hybrid crosses. *BMC Genomics* 18:839. doi: 10.1186/s12864-017-4179-3

Cros, D., Denis, M., SaìNchez, L., Cochard, B., Flori, A., Durand-Gasselin, T., et al. (2015). Genomic selection prediction accuracy in a perennial crop: case study of oil palm (Elaeis Guineensis Jacq.). *Theor. Appl. Genet.* 128, 397–410. doi: 10.1007/s00122-014-2439-z

Cros, D., Mbo-Nkoulou, L., Bell, J. M., Oum, J., Masson, A., Soumahoro, M., et al. (2019). Within-family genomic selection in rubber tree (*Hevea brasiliensis*) increases genetic gain for rubber production. *Ind. Crops Prod.* 138:111464. doi: 10.1016/j.indcrop.2019.111464

Crossa, J., Burgueno, J., Dreisigacker, S., Vargas, M., Herrera-Foessel, S. A., Lillemo, M., et al. (2007). Association analysis of historical bread wheat germplasm using additive genetic covariance of relatives and population structure. *Genetics* 177, 1889–1913. doi: 10.1534/genetics.107.078659

Crossa, J., Jarquin, D., Franco, J., Perez-Rodriguez, P., Burgueno, J., Saint-Pierre, C., et al. (2016). Genomic prediction of gene bank wheat landraces. *G3* 6, 1819–1834. doi: 10.1534/g3.116.029637

Crossa, J., Martini, J. W. R., Gianola, D., Perez-Rodriguez, P., Jarquin, D., Juliana, P., et al. (2019). Deep kernel and deep learning for genome-based prediction of single traits in multienvironment breeding trials. *Front. Genet.* 10:1168. doi: 10.3389/fgene.2019.01168

Crossa, J., Perez-Rodriguez, P., Cuevas, J., Montesinos-Lopez, O., Jarquin, D., De Los Campos, G., et al. (2017). Genomic selection in plant breeding: methods, models, and perspectives. *Trends Plant Sci.* 22, 961–975.

Crowl, A. A., Manos, P. S., Mcvay, J. D., Lemmon, A. R., Lemmon, E. M., and Hipp, A. L. (2020). Uncovering the genomic signature of ancient introgression between white oak lineages (*Quercus*). *New Phytol.* 226, 1158–1170. doi: 10.1111/nph.15842

De Dato, G., Teani, A., Mattioni, C., Marchi, M., Monteverdi, M. C., and Ducci, F. (2018). Delineation of seed collection zones based on environmental and genetic characteristics for *Quercus Suber* L. in Sardinia, Italy. *iForest* 11, 651–659. doi: 10.3832/ifor2572-011

de la Harpe, M., Paris, M., Karger, D. N., Rolland, J., Kessler, M., Salamin, N., et al. (2017). Molecular ecology studies of species radiations: current research gaps, opportunities and challenges. *Mol. Ecol.* 26, 2608–2611. doi: 10.1111/mec.14110

de los Campos, G., Hickey, J. M., Pong-Wong, R., Daetwyler, H. D., and Calus, M. P. (2013). Whole-genome regression and prediction methods applied to plant and animal breeding. *Genetics* 193, 327–345. doi: 10.1534/genetics.112.143313

Desta, Z. A., and Ortiz, R. (2014). Genomic selection: genome-wide prediction in plant improvement. *Trends Plant Sci.* 19, 592–601. doi: 10.1016/j.tplants.2014.05.006

de Visser, J. A. G. M., Elena, S. F., Fragata, I. S., and Matuszewski, S. (2018). The utility of fitness landscapes and big data for predicting evolution. *Heredity* 121, 401–405. doi: 10.1038/s41437-018-0128-4

Dort, E. N., Tanguay, P., and Hamelin, R. C. (2020). Crispr/Cas9 gene editing: an unexplored frontier for forest pathology. *Front. Plant Sci.* 11:1126. doi: 10.3389/fpls.2020.01126

Doudna, J. A., and Charpentier, E. (2014). Genome editing. the new frontier of genome engineering with Crispr-Cas9. *Science* 346:1258096.

Eckert, A. J., Van Heerwaarden, J., Wegrzyn, J. L., Nelson, C. D., Ross-Ibarra, J., Gonzalez-Martinez, S. C., et al. (2010). Patterns of population structure and environmental associations to aridity across the range of loblolly pine (*Pinus Taeda* L., Pinaceae). *Genetics* 185, 969–982. doi: 10.1534/genetics.110.115543

Elleouet, J. S., and Aitken, S. N. (2018). Exploring approximate bayesian computation for inferring recent demographic history with genomic markers in nonmodel species. *Mol. Ecol. Resour.* 18, 525–540. doi: 10.1111/1755-0998.12758

Evans, L. M., Slavov, G. T., Rodgers-Melnick, E., Martin, J., Ranjan, P., Muchero, W., et al. (2014). Population genomics of *Populus trichocarpa* identifies signatures of selection and adaptive trait associations. *Nat. Genet.* 46, 1089–1096. doi: 10.1038/ng.3075

Fay, M. F., and Palma-Silva, C. (2020). Professor Christian Lexer (23.05.1971-15.12.2019). *Bot. J. Linn. Soc.* 192, 589–591. doi: 10.1093/botlinnean/boaa006

Feeley, K., Martinez-Villa, J., Perez, T., Silva Duque, A., Triviño Gonzalez, D., and Duque, A. (2020). The thermal tolerances, distributions, and performances of tropical montane tree species. *Front. For. Glob. Change* 3:25. doi: 10.3389/ffgc.2020.00025

Flanagan, S. P., Forester, B. R., Latch, E. K., Aitken, S. N., and Hoban, S. (2018). Guidelines for planning genomic assessment and monitoring of locally adaptive variation to inform species conservation. *Evol. Appl.* 11, 1035–1052. doi: 10.1111/eva.12569

Forester, B. R., Jones, M. R., Joost, S., Landguth, E. L., and Lasky, J. R. (2016). Detecting spatial genetic signatures of local adaptation in heterogeneous landscapes. *Mol. Ecol.* 25, 104–120. doi: 10.1111/mec.13476

Freeman, B. G., Song, Y., Feeley, K. J., and Zhu, K. (2020). Montane species and communities track recent warming more closely in the tropics. *bioRxiv* [Preprint]. doi: 10.1101/2020.05.18.102848

Fritsche, S., Klocko, A. L., Boron, A., Brunner, A. M., and Thorlby, G. (2018). Strategies for engineering reproductive sterility in plantation forests. *Front. Plant Sci.* 9:1671. doi: 10.3389/fpls.2018.01671

Galeano, C. H., Cortés, A. J., Fernandez, A. C., Soler, A., Franco-Herrera, N., Makunde, G., et al. (2012). Gene-based single nucleotide polymorphism markers for genetic and association mapping in common bean. *BMC Genet.* 13:48. doi: 10.1186/1471-2156-13-48

Gianola, D., Fernando, R. L., and Stella, A. (2006). Genomic-assisted prediction of genetic value with semiparametric procedures. *Genetics* 173, 1761–1776. doi: 10.1534/genetics.105.049510

Gonzalez, A., Germain, R. M., Srivastava, D. S., Filotas, E., Dee, L. E., Gravel, D., et al. (2020). Scaling-up biodiversity-ecosystem functioning research. *Ecol. Lett.* 23, 757–776.

Grattapaglia, D., Silva-Junior, O. B., Resende, R. T., Cappa, E. P., Muller, B. S. F., Tan, B., et al. (2018). Quantitative genetics and genomics converge to accelerate forest tree breeding. *Front. Plant Sci.* 9:1693. doi: 10.3389/fpls.2018.01693

Hallingback, H. R., Berlin, S., Nordh, N. E., Weih, M., and Ronnberg-Wastljung, A. C. (2019). Genome wide associations of growth, phenology, and plasticity traits in willow [*Salix Viminalis* (L.)]. *Front. Plant Sci.* 10:753. doi: 10.3389/fpls.2019.00753

Herzog, E., and Frisch, M. (2011). Selection strategies for marker-assisted backcrossing with high-throughput marker systems. *Theor. Appl. Genet.* 123, 251–260. doi: 10.1007/s00122-011-1581-0

Hickey, J. M., Chiurugwi, T., Mackay, I., Powell, W., and Implementing Genomic Selection in Cgiar Breeding Programs Workshop Participants (2017). Genomic prediction unifies animal and plant breeding programs to form platforms for biological discovery. *Nat. Genet.* 49, 1297–1303. doi: 10.1038/ng.3920

Hipp, A. L., Manos, P. S., Hahn, M., Avishai, M., Bodenes, C., Cavender-Bares, J., et al. (2020). Genomic landscape of the global oak phylogeny. *New Phytol.* 226, 1198–1212. doi: 10.1111/nph.16162

Holliday, J. A., Aitken, S. N., Cooke, J. E., Fady, B., González-Martínez, S. C., Heuertz, M., et al. (2017). Advances in ecological genomics in forest trees and applications to genetic resources conservation and breeding. *Mol. Ecol.* 26, 706–717. doi: 10.1111/mec.13963

Holliday, J. A., Suren, H., and Aitken, S. N. (2011). Divergent selection and heterogeneous migration rates across the range of sitka spruce (*Picea Sitchensis*). *Proc. Biol. Sci.* 279, 1675–1683. doi: 10.1098/rspb.2011.1805

Holliday, J. A., Zhou, L., Bawa, R., Zhang, M., and Oubida, R. W. (2016). Evidence for extensive parallelism but divergent genomic architecture of adaptation along

altitudinal and latitudinal gradients in *Populus trichocarpa*. *New Phytol.* 209, 1240–1251. doi: 10.1111/nph.13643

Howe, G. T., and Brunner, A. M. (2005). An evolving approach to understanding plant adaptation. *New Phytol.* 167, 1–5. doi: 10.1111/j.1469-8137.2005.01469.x

Ingvarsson, P. K., and Bernhardsson, C. (2020). Genome-wide signatures of environmental adaptation in European Aspen (*Populus Tremula*) under current and future climate conditions. *Evol. Appl.* 13, 132–142. doi: 10.1111/eva.12792

Ingvarsson, P. K., and Dahlberg, H. (2018). The effects of clonal forestry on genetic diversity in wild and domesticated stands of forest trees. *Scand. J. For. Res.* 34, 370–379. doi: 10.1080/02827581.2018.1469665

Ingvarsson, P. K., Hvidsten, T. R., and Street, N. R. (2016). Towards integration of population and comparative genomics in forest trees. *New Phytol.* 212, 338–344. doi: 10.1111/nph.14153

Isabel, N., Holliday, J. A., and Aitken, S. N. (2020). Forest genomics: advancing climate adaptation, forest health, productivity, and conservation. *Evol. Appl.* 13, 3–10. doi: 10.1111/eva.12902

Karrenberg, S., Buerkle, C. A., Field, D. L., and Savolainen, V. (2020). Dedication: Christian Lexer (1971-2019). *Philos. Trans. R. Soc. Lond. B Biol. Sci.* 375:20200232. doi: 10.1098/rstb.2020.0232

Kehel, Z., Sanchez-Garcia, M., El Baouchi, A., Aberkane, H., Tsivelikas, A., Charles, C., et al. (2020). Predictive characterization for seed morphometric traits for genebank accessions using genomic selection. *Front. Ecol. Evol.* 8:32. doi: 10.3389/fevo.2020.00032

Kelleher, C. T., Wilkin, J., Zhuang, J., Cortés, A. J., Quintero, ÁL. P., Gallagher, T. F., et al. (2012). Snp discovery, gene diversity, and linkage disequilibrium in wild populations of *Populus tremuloides*. *Tree Genet. Genomes* 821–829. doi: 10.1007/s11295-012-0467-x

Khan, M. A., and Korban, S. S. (2012). Association mapping in forest trees and fruit crops. *J. Exp. Bot.* 63, 4045–4060. doi: 10.1093/jxb/ers105

Klocko, A. L., Brunner, A. M., Huang, J., Meilan, R., Lu, H., Ma, C., et al. (2016). Containment of transgenic trees by suppression of leafy. *Nat. Biotechnol.* 34, 918–922. doi: 10.1038/nbt.3636

Kremer, A., and Hipp, A. L. (2020). Oaks: an evolutionary success story. *New Phytol.* 226, 987–1011. doi: 10.1111/nph.16274

Kremer, A., Potts, B. M., Delzon, S., and Bailey, J. (2014). Genetic divergence in forest trees: understanding the consequences of climate change. *Funct. Ecol.* 28, 22–36. doi: 10.1111/1365-2435.12169

Lafon-Placette, C., Vallejo-Marín, M., Parisod, C., Abbott, R. J., and Köhler, C. (2016). Current plant speciation research: unravelling the processes and mechanisms behind the evolution of reproductive isolation barriers. *New Phytol.* 209, 29–33. doi: 10.1111/nph.13756

Lascoux, M., Glémin, S., and Savolainen, O. (2016). Local adaptation in plants. *Encycl. Life Sci.* 0025270, 1–7. doi: 10.1002/9780470015902.a0025270

Lenoir, J., Gegout, J. C., Marquet, P. A., De Ruffray, P., and Brisse, H. (2008). A significant upward shift in plant species optimum elevation during the 20th century. *Science* 320, 1768–1771. doi: 10.1126/science.1156831

Lenz, P. R. N., Nadeau, S., Mottet, M. J., Perron, M., Isabel, N., Beaulieu, J., et al. (2020). Multi-trait genomic selection for weevil resistance, growth, and wood quality in Norway Spruce. *Evol. Appl.* 13, 76–94. doi: 10.1111/eva.12823

Leroy, T., Louvet, J. M., Lalanne, C., Le Provost, G., Labadie, K., Aury, J. M., et al. (2020a). Adaptive introgression as a driver of local adaptation to climate in European white oaks. *New Phytol.* 226, 1171–1182. doi: 10.1111/nph.16095

Leroy, T., Plomion, C., and Kremer, A. (2020b). Oak symbolism in the light of genomics. *New Phytol.* 226, 1012–1017. doi: 10.1111/nph.15987

Leroy, T., Rougemont, Q., Dupouey, J. L., Bodenes, C., Lalanne, C., Belser, C., et al. (2020c). Massive postglacial gene flow between European white oaks uncovered genes underlying species barriers. *New Phytol.* 226, 1183–1197. doi: 10.1111/nph.16039

Li, Y., Klápště, J., Telfer, E., Wilcox, P., Graham, N., Macdonald, L., et al. (2019). Genomic selection for non-key traits in radiata pine when the documented pedigree is corrected using DNA marker information. *BMC Genomics* 20:1026. doi: 10.1186/s12864-019-6420-8

Libbrecht, M. W., and Noble, W. S. (2015). Machine learning applications in genetics and genomics. *Nat. Rev. Genet.* 16, 321–332. doi: 10.1038/nrg3920

Lind, B. M., Menon, M., Bolte, C. E., Faske, T. M., and Eckert, A. J. (2018). The genomics of local adaptation in trees: are we out of the woods yet? *Tree Genet. Genomes* 14:29.

Little, C. J., Wheeler, J. A., Sedlacek, J., Cortés, A. J., and Rixen, C. (2016). Small-scale drivers: the importance of nutrient availability and snowmelt timing on performance of the alpine shrub *Salix Herbacea*. *Oecologia* 180, 1015–1024. doi: 10.1007/s00442-015-3394-3

Liu, S., Cornille, A., Decroocq, S., Tricon, D., Chague, A., Eyquard, J. P., et al. (2019). The complex evolutionary history of apricots: species divergence, gene flow and multiple domestication events. *Mol. Ecol.* 28, 5299–5314. doi: 10.1111/mec.15296

López-Hernández, F., and Cortés, A. J. (2019). Last-generation genome–environment associations reveal the genetic basis of heat tolerance in common bean (*Phaseolus vulgaris* L.). *Front. Genet.* 10:22. doi: 10.3389/fgene.2019.00954

Madriñán, S., Cortés, A. J., and Richardson, J. E. (2013). Páramo is the world's fastest evolving and coolest biodiversity hotspot. *Front. Genet.* 4:192. doi: 10.3389/fgene.2013.00192

Mahony, C. R., Maclachlan, I. R., Lind, B. M., Yoder, J. B., Wang, T., and Aitken, S. N. (2020). Evaluating genomic data for management of local adaptation in a changing climate: a lodgepole pine case study. *Evol. Appl.* 13, 116–131. doi: 10.1111/eva.12871

Marques, D. A., Meier, J. I., and Seehausen, O. (2019). A combinatorial view on speciation and adaptive radiation. *Trends Ecol. Evol.* 34, 531–544. doi: 10.1016/j.tree.2019.02.008

Martín, M. A., Herrera, M. A., and MartiìN, L. M. (2012). *In situ* conservation and landscape genetics in forest species. *J. Nat. Resour. Dev.* 2, 1–5.

Mason, A. S., and Wendel, J. F. (2020). Homoeologous exchanges, segmental allopolyploidy, and polyploid genome evolution. *Front. Genet.* 11:1014. doi: 10.3389/fgene.2020.01014

Mattioni, C., Martin, M. A., Chiocchini, F., Gaudet, M., Pollegioni, P., Velichkov, I., et al. (2017). Landscape genetics structure of european sweet chestnut (*Castanea Sativa* Mill): indications for conservation priorities. *Tree Genet. Genomes* 13:39.

Mayol, M., Riba, M., Cavers, S., Grivet, D., Vincenot, L., Cattonaro, F., et al. (2020). A multiscale approach to detect selection in nonmodel tree species: widespread adaptation despite population decline in *Taxus baccata* L. *Evol. Appl.* 13, 143–160. doi: 10.1111/eva.12838

McKown, A. D., Guy, R. D., Quamme, L., Klapste, J., La Mantia, J., Constabel, C. P., et al. (2014). Association genetics, geography and ecophysiology link stomatal patterning in *Populus trichocarpa* with carbon gain and disease resistance trade-offs. *Mol. Ecol.* 23, 5771–5790. doi: 10.1111/mec.12969

McKown, A. D., Klapste, J., Guy, R. D., El-Kassaby, Y. A., and Mansfield, S. D. (2018). Ecological genomics of variation in bud-break phenology and mechanisms of response to climate warming in *Populus trichocarpa*. *New Phytol.* 220, 300–316. doi: 10.1111/nph.15273

Meilan, R., Brunner, A. M., Skinnera, J. S., and Strauss, S. H. (2001). Modification of flowering in transgenic trees. *Prog. Biotechnol.* 18, 247–256.

Meuwissen, T. H. E., Hayes, B. J., and Goddard, M. E. (2001). Prediction of total genetic value using genome-wide dense marker maps. *Genetics* 157, 1819–1829.

Meyer, F. E., Shuey, L. S., Naidoo, S., Mamni, T., Berger, D. K., Myburg, A. A., et al. (2016). Dual Rna-sequencing of *Eucalyptus nitens* during *Phytophthora cinnamomi* challenge reveals pathogen and host factors influencing compatibility. *Front. Plant Sci.* 7:191. doi: 10.3389/fpls.2016.00191

Migicovsky, Z., and Myles, S. (2017). Exploiting wild relatives for genomics-assisted breeding of perennial crops. *Front. Plant Sci.* 8:460. doi: 10.3389/fpls.2017.00460

Muranty, H., Jorge, V., Bastien, C., Lepoittevin, C., Bouffier, L., and Sanchez, L. (2014). Potential for marker-assisted selection for forest tree breeding: lessons from 20 years of mas in crops. *Tree Genet. Genomes* 10, 1491–1510. doi: 10.1007/s11295-014-0790-5

Myburg, A. A., Hussey, S. G., Wang, J. P., Street, N. R., and Mizrachi, E. (2019). Systems and synthetic biology of forest trees: a bioengineering paradigm for Woody biomass feedstocks. *Front. Plant Sci.* 10:775. doi: 10.3389/fpls.2019.00775

Naidoo, S., Külheim, C., Zwart, L., Mangwanda, R., Oates, C. N., Visser, E. A., et al. (2014). Uncovering the defence responses of *Eucalyptus* to pests and pathogens in the genomics age. *Tree Physiol.* 34, 931–943. doi: 10.1093/treephys/tpu075

Naidoo, S., Slippers, B., Plett, J. M., Coles, D., and Oates, C. N. (2019). The road to resistance in forest trees. *Front. Plant Sci.* 10:273. doi: 10.3389/fpls.2019.00273

Neale, D. B., and Kremer, A. (2011). Forest tree genomics: growing resources and applications. *Nat. Rev. Genet.* 12, 111–122. doi: 10.1038/nrg2931

Neale, D. B., and Savolainen, O. (2004). Association genetics of complex traits in conifers. *Trends Plant Sci.* 9, 325–330. doi: 10.1016/j.tplants.2004.05.006

Nieto Feliner, G., Casacuberta, J., and Wendel, J. F. (2020). Genomics of evolutionary novelty in hybrids and polyploids. *Front. Genet.* 11:792. doi: 10.3389/fgene.2020.00792

Nystedt, B., Street, N. R., Wetterbom, A., Zuccolo, A., Lin, Y.-C., Scofield, D. G., et al. (2013). The Norway spruce genome sequence and conifer genome evolution. *Nature* 497, 579–584.

Pennisi, E. (2020). Tropical forests store carbon despite warming. *Science* 368:813. doi: 10.1126/science.368.6493.813

Pereira-Lorenzo, S., Ramos-Cabrer, A. M., Barreneche, T., Mattioni, C., Villani, F., Díaz-Hernández, B., et al. (2019). Instant domestication process of European chestnut cultivars. *Ann. Appl. Biol.* 174, 74–85. doi: 10.1111/aab.12474

Phillips, J., Ramirez, S., Wayson, C., and Duque, A. (2019). Differences in carbon stocks along an elevational gradient in tropical mountain forests of Colombia. *Biotropica* 51, 490–499. doi: 10.1111/btp.12675

Phillips, S. J., Anderson, R. P., Dudík, M., Schapire, R. E., and Blair, M. E. (2017). Opening the black box: an open-source release of maxent. *Ecography* 40, 887–893. doi: 10.1111/ecog.03049

Piot, A., Prunier, J., Isabel, N., Klapste, J., El-Kassaby, Y. A., Villarreal Aguilar, J. C., et al. (2019). Genomic diversity evaluation of *Populus trichocarpa* germplasm for rare variant genetic association studies. *Front. Genet.* 10:1384. doi: 10.3389/fgene.2019.01384

Plomion, C., Aury, J. M., Amselem, J., Leroy, T., Murat, F., Duplessis, S., et al. (2018). Oak genome reveals facets of long lifespan. *Nat. Plants* 4, 440–452.

Plomion, C., and Martin, F. (2020). Oak genomics is proving its worth. *New Phytol.* 226, 943–946. doi: 10.1111/nph.16560

Pluess, A. R., Frank, A., Heiri, C., Lalague, H., Vendramin, G. G., and Oddou-Muratorio, S. (2016). Genome-environment association study suggests local adaptation to climate at the regional scale in *Fagus sylvatica*. *New Phytol.* 210, 589–601. doi: 10.1111/nph.13809

Ratcliffe, B., Thistlethwaite, F., El-Dien, O. G., Cappa, E. P., Porth, I., Klápště, J., et al. (2019). Inter- and intra-generation genomic predictions for Douglas-Fir growth in unobserved environments. *bioRxiv* [Preprint]. doi: 10.1101/540765

Rellstab, C., Gugerli, F., Eckert, A. J., Hancock, A. M., and Holderegger, R. (2015). A practical guide to environmental association analysis in landscape genomics. *Mol. Ecol.* 24, 4348–4370. doi: 10.1111/mec.13322

Resende, M. D. V., Resende, M. F. R., Sansaloni, C. P., Petroli, C. D., Missiaggia, A. A., and Aguiar, A. M. (2012). Genomic selection for growth and wood quality in *Eucalyptus*: capturing the missing heritability and accelerating breeding for complex traits in forest trees. *New Phytol.* 194, 116–128. doi: 10.1111/j.1469-8137.2011.04038.x

Resende, M. F., Muñoz, P., Resende, M. D., Garrick, D. J., Fernando, R. L., Davis, J. M., et al. (2012). Accuracy of genomic selection methods in a standard data set of loblolly pine (*Pinus taeda* L.). *Genetics* 190, 1503–1510. doi: 10.1534/genetics.111.137026

Resende, R. T., Piepho, H. P., Rosa, G. J. M., Silva-Junior, O. B., Silva, F. F., Resende, M. D. V., et al. (2020). *Enviromics* in breeding: applications and perspectives on envirotypic-assisted selection. *Theor. Appl. Genet.* doi: 10.1007/s00122-020-03684-z

Roudbar, M. A., Momen, M., Mousavi, S. F., Ardestani, S. S., Lopes, F. B., Gianola, D., et al. (2020). Genome-wide methylation prediction of biological age using reproducing Kernel Hilbert spaces and Bayesian ridge regressions. *bioRxiv* [Preprint]. doi: 10.1101/2020.08.25.266924

Savolainen, O., Lascoux, M., and Merilä, J. (2013). Ecological genomics of local adaptation. *Nat. Rev. Genet.* 14, 807–820. doi: 10.1038/nrg3522

Sawitri, S., Tani, N., Na'iem, M., Widiyatno, Indrioko, S., Uchiyama, K., et al. (2020). Potential of genome-wide association studies and genomic selection to improve productivity and quality of commercial timber species in tropical rainforest, a case study of *Shorea platyclados*. *Forests* 11:239. doi: 10.3390/f11020239

Scherer, L., Svenning, J. C., Huang, J., Seymour, C. L., Sandel, B., Mueller, N., et al. (2020). Global priorities of environmental issues to combat food insecurity and biodiversity loss. *Sci. Total Environ.* 730:139096. doi: 10.1016/j.scitotenv.2020.139096

Schilthuizen, M., Hoekstra, R. F., and Gittenberger, E. (2004). Hybridization, rare alleles and adaptive radiation. *Trends Ecol. Evol.* 19, 404–405. doi: 10.1016/j.tree.2004.06.005

Schloötterer, C. (2020). Christian Lexer: a lifelong passion for trees. *Mol. Ecol.* 29, 443–444. doi: 10.1111/mec.15363

Schrider, D. R., and Kern, A. D. (2018). Supervised machine learning for population genetics: a new paradigm. *Trends Genet.* 34, 301–312. doi: 10.1016/j.tig.2017.12.005

Scott, M. F., Ladejobi, O., Amer, S., Bentley, A. R., Biernaskie, J., Boden, S. A., et al. (2020). Multi-parent populations in crops: a toolbox integrating genomics and genetic mapping with breeding. *Heredity.* doi: 10.1038/s41437-020-0336-6 [Epub ahead of print].

Sedlacek, J., Bossdorf, O., Cortés, A. J., Wheeler, J. A., and Van-Kleunen, M. (2014). What role do plant-soil interactions play in the habitat suitability and potential range expansion of the alpine dwarf shrub *Salix herbacea*? *Basic Appl. Ecol.* 15, 305–315. doi: 10.1016/j.baae.2014.05.006

Sedlacek, J., Cortés, A. J., Wheeler, J. A., Bossdorf, O., Hoch, G., Klapste, J., et al. (2016). Evolutionary potential in the alpine: trait heritabilities and performance variation of the dwarf willow *Salix herbacea* from different elevations and microhabitats. *Ecol. Evol.* 6, 3940–3952. doi: 10.1002/ece3.2171

Sedlacek, J., Wheeler, J. A., Cortés, A. J., Bossdorf, O., Hoch, G., Lexer, C., et al. (2015). The response of the alpine dwarf shrub *Salix herbacea* to altered snowmelt timing: lessons from a multi-site transplant experiment. *PLoS One* 10:e0122395. doi: 10.1371/journal.pone.0122395

Seehausen, O. (2004). Hybridization and adaptive radiation. *Trends Ecol. Evol.* 19, 198–207. doi: 10.1016/j.tree.2004.01.003

Sentinella, A. T., Warton, D. I., Sherwin, W. B., Offord, C. A., Moles, A. T., and Wang, Z. (2020). Tropical plants do not have narrower temperature tolerances, but are more at risk from warming because they are close to their upper thermal limits. *Glob. Ecol. Biogeogr.* 29, 1387–1398. doi: 10.1111/geb.13117

Shang, H., Hess, J., Pickup, M., Field, D. L., Ingvarsson, P. K., Liu, J., et al. (2020). Evolution of strong reproductive isolation in plants: broad-scale patterns and lessons from a perennial model group. *Philos. Trans. R. Soc. Lond. B Biol. Sci.* 375:20190544. doi: 10.1098/rstb.2019.0544

Sousa, T. V., Caixeta, E. T., Alkimim, E. R., Oliveira, A. C. B., Pereira, A. A., Sakiyama, N. S., et al. (2018). Early selection enabled by the implementation of genomic selection in *Coffea arabica* breeding. *Front. Plant Sci.* 9:1934. doi: 10.3389/fpls.2018.01934

Souza, L. M., Francisco, F. R., Goncalves, P. S., Scaloppi Junior, E. J., Le Guen, V., Fritsche-Neto, R., et al. (2019). Genomic selection in rubber tree breeding: a comparison of models and methods for managing GxE interactions. *Front. Plant Sci.* 10:1353. doi: 10.3389/fpls.2019.01353

Sow, M. D., Allona, I., Ambroise, C., Conde, D., Fichot, R., Gribkova, S., et al. (2018). Epigenetics in forest trees: state of the art and potential implications for breeding and management in a context of climate change. *Adv. Bot. Res.* 88, 387–453. doi: 10.1016/bs.abr.2018.09.003

Steinbauer, M. J., Grytnes, J. A., Jurasinski, G., Kulonen, A., Lenoir, J., Pauli, H., et al. (2018). Accelerated increase in plant species richness on mountain summits is linked to warming. *Nature* 556, 231–234.

Stocks, J. J., Metheringham, C. L., Plumb, W. J., Lee, S. J., Kelly, L. J., Nichols, R. A., et al. (2019). Genomic basis of European ash tree resistance to ash dieback fungus. *Nat. Ecol. Evol.* 3, 1686–1696. doi: 10.1038/s41559-019-1036-6

Stölting, K. N., Paris, M., Meier, C., Heinze, B., Castiglione, S., Bartha, D., et al. (2015). Genome-wide patterns of differentiation and spatially varying selection between postglacial recolonization lineages of *Populus Alba* (Salicaceae), a widespread forest tree. *New Phytol.* 207, 723–734. doi: 10.1111/nph.13392

Sullivan, M., Lewis, S. L., Affum-Baffoe, K., Castilho, C., Costa, F., Sanchez, A. C., et al. (2020). Long-term thermal sensitivity of earth's tropical forests. *Science* 368, 869–874.

Suontama, M., Klápště, J., Telfer, E., Graham, N., Stovold, T., Low, C., et al. (2019). Efficiency of genomic prediction across two *Eucalyptus nitens* seed orchards with different selection histories. *Heredity* 122, 370–379. doi: 10.1038/s41437-018-0119-5

Tan, B., Grattapaglia, D., Martins, G. S., Ferreira, K. Z., Sundberg, B. R., and Ingvarsson, P. R. K. (2017). Evaluating the accuracy of genomic prediction of growth and wood traits in two *Eucalyptus* species and their F1 hybrids. *BMC Plant Biol.* 17:110. doi: 10.1186/s12870-017-1059-6

Technow, F., Schrag, T. A., Schipprack, W., Bauer, E., Simianer, H., and Melchinger, A. E. (2014). Genome properties and prospects of genomic prediction of hybrid performance in a breeding program of maize. *Genetics* 197, 1343–1355. doi: 10.1534/genetics.114.165860

Thistlethwaite, F. R., Gamal El-Dien, O., Ratcliffe, B., Klapste, J., Porth, I., Chen, C., et al. (2020). Linkage Disequilibrium Vs. Pedigree: genomic selection prediction accuracy in conifer species. *PLoS One* 15:e0232201. doi: 10.1371/journal.pone.0232201

Thistlethwaite, F. R., Ratcliffe, B., Klápště, J., Porth, I., Chen, C., Stoehr, M. U., et al. (2017). Genomic prediction accuracies in space and time for height and wood density of Douglas-Fir using exome capture as the genotyping platform. *BMC Genomics* 18:930. doi: 10.1186/s12864-017-4258-5

Thistlethwaite, F. R., Ratcliffe, B., Klápště, J., Porth, I., Chen, C., Stoehr, M. U., et al. (2019a). Genomic selection of juvenile height across a single-generational gap in Douglas-Fir. *Heredity* 122, 848–863. doi: 10.1038/s41437-018-0172-0

Thistlethwaite, F. R., Ratcliffe, B., Klápště, J., Porth, I., Chen, C., Stoehr, M. U., et al. (2019b). Genomic selection of juvenile height across a single-generational gap in Douglas-Fir. *Heredity* 122, 848–863. doi: 10.1038/s41437-018-0172-0

Tito, R., Vasconcelos, H. L., and Feeley, K. J. (2020). Mountain ecosystems as natural laboratories for climate change experiments. *Front. For. Glob. Change* 3:38. doi: 10.3389/ffgc.2020.00038

Tuskan, G. A., Groover, A. T., Schmutz, J., Difazio, S. P., Myburg, A., Grattapaglia, D., et al. (2018). Hardwood tree genomics: unlocking woody plant biology. *Front. Plant Sci.* 9:1799. doi: 10.3389/fpls.2018.01799

Ukrainetz, N. K., and Mansfield, S. D. (2020). Assessing the sensitivities of genomic selection for growth and wood quality traits in lodgepole pine using Bayesian models. *Tree Genet. Genomes* 16:14.

Ulian, T., Diazgranados, M., Pironon, S., Padulosi, S., Liu, U., Davies, L., et al. (2020). Unlocking plant resources to support food security and promote sustainable agriculture. *Plants People Planet* 2, 421–445. doi: 10.1002/ppp3.10145

Valencia, J. B., Mesa, J., León, J. G., Madriñán, S., and Cortés, A. J. (2020). Climate vulnerability assessment of the *Espeletia* complex on PaìRamo sky islands in the Northern Andes. *Front. Ecol. Evol.* 8:565708. doi: 10.3389/fevo.2020.565708

Wang, J., Street, N. R., Park, E. J., Liu, J., and Ingvarsson, P. K. (2020). Evidence for widespread selection in shaping the genomic landscape during speciation of *Populus*. *Mol. Ecol.* 29, 1120–1136. doi: 10.1111/mec.15388

Wang, M., Zhang, L., Zhang, Z., Li, M., Wang, D., Zhang, X., et al. (2020). Phylogenomics of the genus *Populus* reveals extensive interspecific gene flow and balancing selection. *New Phytol.* 225, 1370–1382. doi: 10.1111/nph.16215

Westbrook, J. W., Holliday, J. A., Newhouse, A. E., and Powell, W. A. (2019). A plan to diversify a transgenic blight-tolerant American chestnut population using citizen science. *Plants People Planet* 2, 84–95. doi: 10.1002/ppp3.10061

Westbrook, J. W., Zhang, Q., Mandal, M. K., Jenkins, E. V., Barth, L. E., Jenkins, J. W., et al. (2020). Optimizing genomic selection for blight resistance in American chestnut backcross populations: a trade-off with American chestnut ancestry implies resistance is polygenic. *Evol. Appl.* 13, 31–47. doi: 10.1111/eva.12886

Wheeler, J. A., Cortés, A. J., Sedlacek, J., Karrenberg, S., Van Kleunen, M., Wipf, S., et al. (2016). The snow and the willows: accelerated spring snowmelt reduces performance in the low-lying alpine shrub *Salix herbacea*. *J. Ecol.* 104, 1041–1050. doi: 10.1111/1365-2745.12579

Wheeler, J. A., Hoch, G., Cortés, A. J., Sedlacek, J., Wipf, S., and Rixen, C. (2014). Increased spring freezing vulnerability for alpine shrubs under early snowmelt. *Oecologia* 175, 219–229. doi: 10.1007/s00442-013-2872-8

Wheeler, J. A., Schnider, F., Sedlacek, J., Cortés, A. J., Wipf, S., Hoch, G., et al. (2015). With a little help from my friends: community facilitation increases performance in the dwarf shrub *Salix herbacea*. *Basic Appl. Ecol.* 16, 202–209. doi: 10.1016/j.baae.2015.02.004

White, T., Adams, W., and Neale, D. (2007). *Forest Genetics*. New York, NY: CSIRO-CABI Publishing.

Yeaman, S., Hodgins, K. A., Lotterhos, K. E., Suren, H., Nadeau, S., Degner, J. C., et al. (2016). Convergent local adaptation to climate in distantly related conifers. *Science* 353, 1431–1433. doi: 10.1126/science.aaf7812

Zahn, L. M., and Purnell, B. A. (2016). Genes under pressure. *Science* 354:52. doi: 10.1126/science.354.6308.52

Zhou, L., Bawa, R., and Holliday, J. A. (2014). Exome resequencing reveals signatures of demographic and adaptive processes across the genome and range of black cottonwood (*Populus trichocarpa*). *Mol. Ecol.* 23, 2486–2499. doi: 10.1111/mec.12752

Zhou, L., Chen, Z., Olsson, L., Grahn, T., Karlsson, B., Wu, H. X., et al. (2020). Effect of number of annual rings and tree ages on genomic predictive ability for solid wood properties of Norway spruce. *BMC Genomics* 21:323. doi: 10.1186/s12864-020-6737-3

Conflict of Interest: The authors declare that the research was conducted in the absence of any commercial or financial relationships that could be construed as a potential conflict of interest.

frontiers in Plant Science

ORIGINAL RESEARCH
published: 22 October 2020
doi: 10.3389/fpls.2020.559697

Morphological Differences in *Pinus strobiformis* Across Latitudinal and Elevational Gradients

*Alejandro Leal-Sáenz[1], Kristen M. Waring[2], Mitra Menon[3], Samuel A. Cushman[4], Andrew Eckert[5], Lluvia Flores-Rentería[6], José Ciro Hernández-Díaz[7], Carlos Antonio López-Sánchez[8], José Hugo Martínez-Guerrero[9] and Christian Wehenkel[7]**

[1] Programa Institucional de Doctorado en Ciencias Agropecuarias y Forestales, Universidad Juárez del Estado de Durango, Durango, Mexico, [2] School of Forestry, Northern Arizona University, Flagstaff, AZ, United States, [3] Department of Evolution and Ecology, University of California, Davis, Davis, CA, United States, [4] USDA Forest Service, Flagstaff, AZ, United States, [5] Department of Biology, Virginia Commonwealth University, Richmond, VA, United States, [6] Department of Biology, San Diego State University, San Diego, CA, United States, [7] Instituto de Silvicultura e Industria de la Madera, Universidad Juárez del Estado de Durango, Durango, Mexico, [8] Department of Biology of Organisms and Systems, Mieres Polytechnic School, University of Oviedo, Campus Universitario de Mieres, C/Gonzalo Gutiérrez Quirós S/N, Mieres, Spain, [9] Facultad de Medicina Veterinaria y Zootecnia, Universidad Juárez del Estado de Durango, Durango, Mexico

OPEN ACCESS

Edited by:
Sofia Valenzuela, University of Concepcion, Chile

Reviewed by:
Santiago Ramírez Barahona, National Autonomous University of Mexico, Mexico
Alejandra Moreno-Letelier, National Autonomous University of Mexico, Mexico

***Correspondence:**
Christian Wehenkel
wehenkel@ujed.mx

Specialty section:
This article was submitted to Plant Abiotic Stress, a section of the journal Frontiers in Plant Science

Received: *16 June 2020*
Accepted: *28 September 2020*
Published: *22 October 2020*

Citation:
Leal-Sáenz A, Waring KM, Menon M, Cushman SA, Eckert A, Flores-Rentería L, Hernández-Díaz JC, López-Sánchez CA, Martínez-Guerrero JH and Wehenkel C (2020) Morphological Differences in Pinus strobiformis Across Latitudinal and Elevational Gradients. Front. Plant Sci. 11:559697. doi: 10.3389/fpls.2020.559697

The phenotype of trees is determined by the relationships and interactions among genetic and environmental influences. Understanding the patterns and processes that are responsible for phenotypic variation is facilitated by studying the relationships between phenotype and the environment among many individuals across broad ecological and climatic gradients. We used *Pinus strobiformis*, which has a wide latitudinal distribution, as a model species to: (a) estimate the relative importance of different environmental factors in predicting these morphological traits and (b) characterize the spatial patterns of standing phenotypic variation of cone and seed traits across the species' range. A large portion of the total variation in morphological characteristics was explained by ecological, climatic and geographical variables (54.7% collectively). The three climate, vegetation and geographical variable groups, each had similar total ability to explain morphological variation (43.4%, 43.8%, 51.5%, respectively), while the topographical variable group had somewhat lower total explanatory power (36.9%). The largest component of explained variance (33.6%) was the four-way interaction of all variable sets, suggesting that there is strong covariation in environmental, climate and geographical variables in their relationship to morphological traits of southwest white pine across its range. The regression results showed that populations in more humid and warmer climates expressed greater cone length and seed size. This may in part facilitate populations of *P. strobiformis* in warmer and wetter portions of its range growing in dense, shady forest stands, because larger seeds provide greater resources to germinants at the time of germination. Our models provide accurate predictions of morphological traits and important insights regarding the factors that contribute to their expression. Our results indicate that managers should be conservative during reforestation efforts to ensure match between ecotypic variation

in seed source populations. However, we also note that given projected large range shift due to climate change, managers will have to balance the match between current ecotypic variation and expected range shift and changes in local adaptive optima under future climate conditions.

Keywords: phenotypic variation, morphological traits, climate factors, redundancy analysis, multivariate canonical ordination, machine learning

INTRODUCTION

The interest of evolutionary ecologists has long been focused on patterns of phenotypic variation along environmental gradients (e.g., latitude, altitude and climate). However, this variation is also determined by the covariance between genetic and environmental influences (Conover et al., 2009). Studying patterns of phenotypic variation among many individuals along broad ecological and climatic gradients is a powerful framework to understand the patterns and processes that govern phenotypic expression and variation (Endler, 1986). Early ecologists frequently noted that phenotypes of many species change predictably along large-scale gradients of latitude, altitude and water depth, providing the basis for several so-called ecological rules (Bergmann, 1847; Atkinson and Sibly, 1997). Morphological traits are important characteristics (Violle et al., 2007) that help distinguish entities at all levels of biological organization, including life cycles, ecological and geographical distributions, and evolutionary and conservation status (Kaplan, 2001; Gregorius et al., 2003). For example, Delagrange et al. (2004) showed that the crown morphology of *Acer saccharum* and *Betula alleghaniensis* is influenced by light availability and tree size. Wahid et al. (2006) found that the morphology of *Pinus pinaster* cones and needles vary predictably along both latitudinal and altitudinal gradients and Gil et al. (2002) reported elevation-dependent cone and seed variation in *Pinus canariensis*.

Forest trees are often adapted to environmental gradients at multiple spatial scales (Morgenstern, 1996; Savolainen et al., 2007). The phenotype of an individual is influenced by their genotype, their environment and interactions between them (de Jong, 1990; Falconer and Mackay, 1996). The evolutionary response of a phenotypic trait to selection depends on genetic control of the trait, heritability of the trait and differential fitness of different morphotypes of the trait in different environmental conditions (Price, 1970). Quantifying morphological variation within a widely distributed species across a large spatial extent is often necessary to identify the relative importance of different environmental factors in relation to variation in intraspecific morphological traits (Boyd, 2002; Herrera et al., 2002; Franks et al., 2014; Ji et al., 2016). Such knowledge can then be applied to climate change adaptation, through strategies such as assisted migration and assisted gene flow (e.g., Aitken and Bemmels, 2016).

White pine species (subgenus *Strobus,* section *Quinquefoliae,* subsection *Strobus* (Gernandt et al., 2005)) are widespread in the temperate forest ecosystems of North America (Kral, 1993; Gernandt and Pérez-de la Rosa, 2014), making them a suitable focal group to investigate how the phenotype is influenced by environmental gradients. Members of subgenus *Strobus,* section *Quinquefoliae,* subsection *Strobus* have five needles per bundle, such that species in this group are commonly referred to as five-needle pines. Several white pines are also characterized by large cones (Farjon and Styles, 1997) and large seeds (Frankis, 2009). These include the southwestern white pine (*Pinus strobiformis* Engelm.), which has wide variation in cone length, 20–50 cm (Frankis, 2009), seed length, 1.2–1.8 cm (Farjon and Styles, 1997), seed weight of 0.140–0.411 g (Leal-Sáenz et al., 2020), and a geographical range that includes the Sierra Madre Occidental in Mexico and the southwestern United States (**Figure 1**). Southwestern white pine is of both commercial and ecological value. Commercial products include timber, cellulose, resin and pulp (Farjon and Styles, 1997; Villalobos-Arámbula et al., 2014).

Ecologically, *P. strobiformis* is an important tree species in the ecosystems it inhabits (Moreno-Letelier and Piñero, 2009; Bower et al., 2011; Looney and Waring, 2013). The large and nutritious seeds of white pines frequently form the foundation of large trophic networks and promote enhanced biodiversity (Keane and Cushman, 2018). Seeds are an important source of food for many birds and mammals, including corvids, parrots, mice, voles, chipmunks, squirrels and bears (Samano and Tomback, 2003; Tomback and Achuff, 2010; Looney and Waring, 2013). In addition to contributing to biodiversity, *P. strobiformis* also provides watershed protection and serves as a major floristic component of montane forest ecosystems (Wehenkel et al., 2014), and is a key element of mixed conifer forests across its range (Looney and Waring, 2013; Shirk et al., 2018).

Pinus strobiformis is highly susceptible to white pine blister rust (WPBR), an invasive tree disease caused by the fungus *Cronartium ribicola* (Geils and Vogler, 2011), as are all other white pine species (Hoff and Hagle, 1990; Sniezko et al., 2008). The dual threats of this non-native fungal pathogen and the projected warmer, drier climate have created an uncertain future for *P. strobiformis,* as well as other white pine species (Landguth et al., 2017; Keane and Cushman, 2018; Shirk et al., 2018). A contraction of more than 60% in the species range by 2080 is predicted under some scenarios of greenhouse gas emissions (Shirk et al., 2018), whereas other scenarios include a northerly shift of more than 1,000 km in the mean latitude and an increase of 500 m in the mean elevation of suitable habitat for the species.

Robust measurement of the degree to which morphological variation is determined by non-genetically controlled developmental responses to environmental gradients requires a statistical analysis that can jointly and simultaneously account for the ability of environmental factors to predict morphological characteristics. RDA is a multivariate direct ordination approach that is ideally suited to predicting multiple response variables as

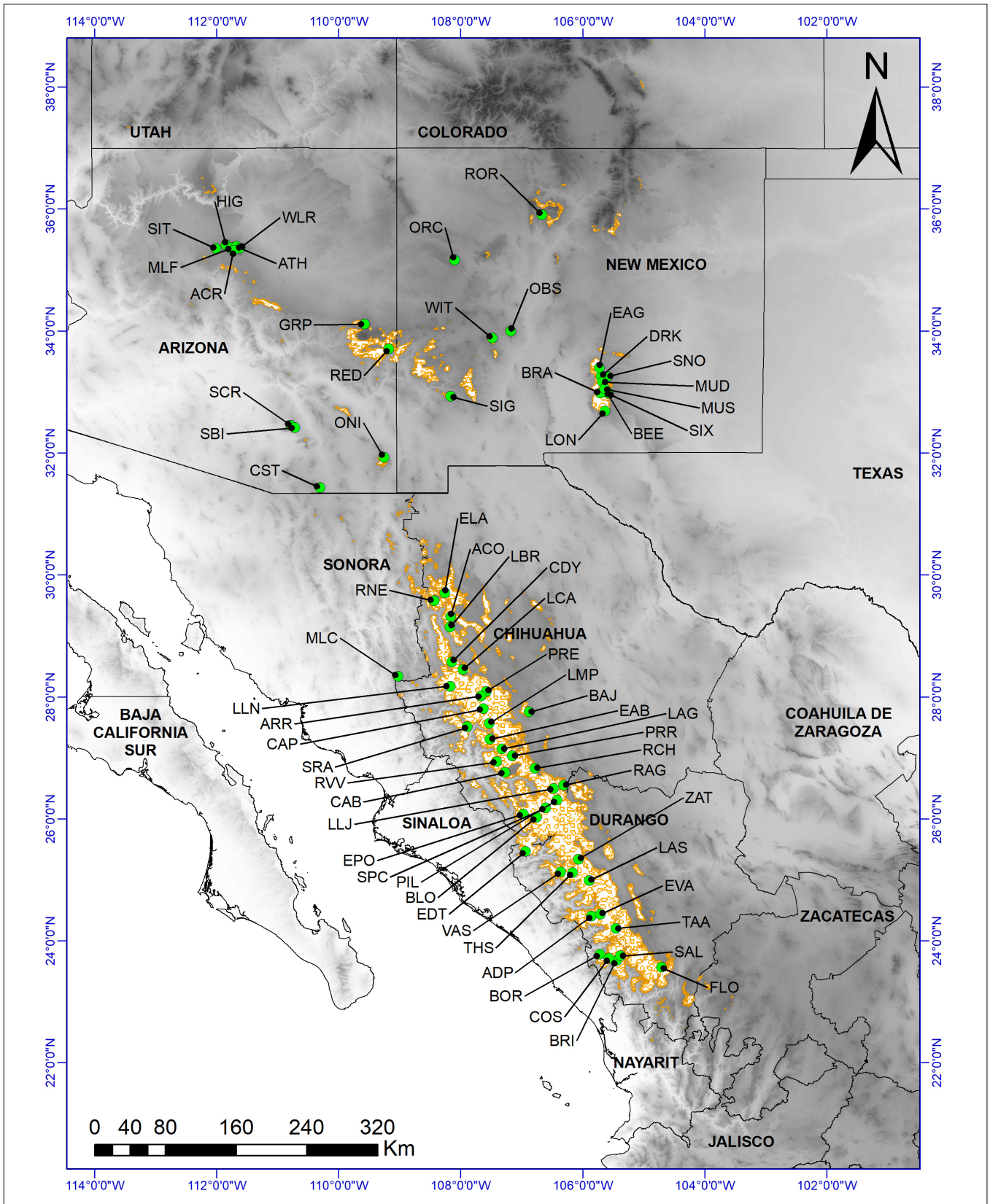

FIGURE 1 | Distribution of *Pinus strobiformis* (brown outlined areas, based on Shirk et al., 2018) and sample collection sites: 65 morphological data collection sites (green circles). Base digital elevation map was from Jarvis et al. (2008).

a function of multiple predictor variables and is the most well-known and trusted statistical method to conduct multivariate variance partitioning (Van Den Wollenberg, 1977; McGarigal et al., 2000). By implementing a series of partial redundancy analysis ordinations, the independent and joint effects of multiple sets of predictor variables can be separated (e.g., Borcard et al., 1992; Cushman and McGarigal, 2002, 2004). For instance, the proportion of morphological trait variance explained by pure effects of climatic data, spatial location or topography and the interaction between variables can be quantified. A series of partial redundancy analyses can then be used to identify environmental gradients correlated with phenotypic variation across the species range. This partitioning of the variance in morphological traits that can be explained independently and jointly by climatic and geographic factors is essential to understand the factors that drive morphological variation and the scales at which they operate.

Faced with an increasingly complex and rapidly changing future, forest managers need science-driven strategies to maintain tree species and forests. Given the ecological importance of *Pinus strobiformis* and the multiple challenges to future regeneration of the species, it is critical to understand factors underlying the morphological trait variation of reproductive structures (e.g., cones and seeds) in order to better manage reforestation and restoration efforts in the future. We used extensive sampling across the full range of *Pinus strobiformis,* to (a) estimate the relative importance of the effects of different environmental factors on these morphological traits and (b) characterize the spatial patterns of standing phenotypic variation of cone and seed morphological traits.

MATERIALS AND METHODS

Species and Study Sites

Pinus strobiformis is a widely distributed white pine, ranging from central and southern Arizona, New Mexico, western Texas, and southwestern Colorado in the United States, to the Sierra Madre Occidental in Mexico (**Figure 1**; Looney and Waring, 2013; Villagómez-Loza et al., 2014). According to the Mexican National Forest Inventory (2004–2009), performed by the Mexican National Forestry Commission (CONAFOR, 2009), *P. strobiformis* occurs within an area of about 2.3 million hectares in Mexico, mainly at elevations of between 2,500 and 3,000 m, although the suitable habitat is estimated to constitute a much larger area (Aguirre-Gutiérrez et al., 2015; but see Shirk et al., 2018). *P. strobiformis* occurs at elevations between 1,800 and 3,400 m in the southwestern United States (Looney and Waring, 2013) but occupies less than 2 % of the total forested area in Arizona (O'Brien, 2002).

In 2015, we collected cones and seeds from 65 *P. strobiformis* sites, located across a variety of abiotic conditions and a wide latitudinal gradient in Mexico and the United States and representing the current geographic distribution (**Figure 1**, **Supplementary Tables S1–S5**). Sites were selected based on accessibility and availability of ripe cones and seeds, with a minimum distance of 5.1 km between sites. All stands were situated in closed forests with minimal human disturbance (e.g., roads, cattle grazing, agriculture). Three to five trees with ripe cones were sampled at each site (a total of 297 trees). In each site, the sampled trees were separated by a minimum distance of 50 m, to minimize the chance of sampling the same genetic family.

Tree, Cone and Seed Morphology Data Collection

For each tree we recorded: Latitude, longitude and elevation (m), diameter at breast height (cm), total tree height (m), first live branch height (m), and crown length (m, obtained from the difference between total height and first live branch height) (**Supplementary Tables S1, S2**).

A minimum of 15 ripe cones with no signs of the presence of insects or diseases were collected from each tree, stored and transported in labeled bags (total 4,455 cones). These cones were allowed to dry at ambient temperature and humidity until they opened, and the seeds were then extracted. Empty seeds were separated from filled seeds, either manually or with a blower. The filled seeds were then weighed in 10-seed lots (g) on a balance (González-Ávalos et al., 2006; Iglesias et al., 2012).

Ten ripe cones were selected at random from the 15 cones (or more) harvested from each tree, for measurements. Total length (cm) and width (cm) of the widest part of each cone were recorded (the width was measured with the angle of the cone facing upward and taking care to avoid exerting pressure on the cone) (Bramlett et al., 1977; González-Ávalos et al., 2006; Iglesias et al., 2012; Prieto-Ruíz et al., 2014). The cone angle was measured with a 360° circular protractor, by placing the upper stem of the cone aligned with 0° (Forde, 1964; Wheeler and Guries, 1982).

Three of the ten cones per tree were randomly chosen for further measurements; three scales of the upper and three of the lower half of each cone were selected and removed. These scales were chosen from each third of the cone circumference, at angles of approximately 0°, 120°, and 240°. A total of 2,673 scales from the upper and 2,673 from the lower part of the cones were gotten from the 297 trees. The length and width of each scale was then measured with a digital caliper (mm). The length of the scale to the tip and the width at the widest part of the scale were recorded. The angle of each scale was measured using a circular protractor and aligning each scale to 90°. Cone specific trait means were calculated for each tree and site.

Environmental Factors and Hybrid Degree

For each site (**Figure 1**), the following abiotic and biotic factors were recorded to examine their impact on the morphological traits of *P. strobiformis*: geographical aspect (0° to 360°), slope (%), occurrence of *P. strobiformis* regeneration (presence), presence or not of *Ribes* spp. (an alternative host for the white pine blister rust pathogen) and presence or not of woody species in the neighborhood (**Supplementary Tables S4, S5**). We only recorded the presence of these species within a 20 m radius of each individual *P. strobiformis* tree and calculated the relative frequency of these species. The sampled trees were also examined for signs and symptoms of white pine blister rust, and the following rating system was applied when the disease was present: cankers present on branches (1), bole (2), or bole

and branches (3) (Arvanitis et al., 1984); these ratings were then transformed into frequency of occurrence prior to analyses (**Supplementary Table S2**). The climate data (20 temperature and precipitation variables) were downloaded from the PRISM database for the period from 1961 to 1990[1] (**Supplementary Table S3**). For further analysis, the geographical aspect (0° to 360°) was transformed into a cosine index – as 0° and 360° have the same zenithal aspect (Cushman and Wallin, 2002). Occurrence data were transformed into frequency of occurrence prior to analyses of the presence of trees and shrubs (**Supplementary Tables S4, S5**). We assumed that the presence of other tree species around *P. strobiformis* does not directly affect its morphological traits. However, this factor was used as additional proxy of other abiotic factors (such as soil traits) possibly influencing the morphological traits of *P. strobiformis* (Zhang et al., 2016).

Since *P. strobiformis* x *P. flexilis* hybrids, which were only reported in the US populations, could influence morphological traits, we also recorded the hybrid degree (the relative hybrid frequency or proportion of *P. strobiformis* to *P. flexilis* per stand) as predictor variable, following Menon et al. (2018) (**Supplementary Table S1**).

Statistical Analyses

Detecting Spatial Dependence in Morphological Traits by Ordinary Kriging Analysis

We conducted ordinary kriging (ordinary Gaussian process regression model) to spatially interpolate morphological traits, including a 10-fold point-by-point cross validation (Batista et al., 2016). The statistical software R (version 3.3.4) (R Development Core Team, 2017) and the Interpolation Kriging package (ArcGIS Desktop 10.5, 2016) were used to describe first-order variation in the spatial pattern of the morphological cone and seed traits, as well as the dasometric traits of the *P. strobiformis* sampled trees under study. We tested the following mathematical models for the semivariance: the spherical model, exponential model, Gaussian model and the Stein's parameterization. The corrected coefficient of determination between the observed and predicted values (R^2), the Unbiased Root Mean Squared Error of the residuals (URMSE), the mean squared error and the mean absolute error were used to assess the goodness-of-fit. Finally, the cone and seed traits with the best kriging model were selected for further regression models of morphological traits with respect to environmental variables. The modeling was carried out using the "*SP*" (Pebesma and Bivand, 2005) and "*automap*" packages (Hiemstra et al., 2009) including the *CRS, SpatialPixelsDataFrame*, *autoKrige, autoKrige.cv*, and *compare.cv* functions in R (version 3.3.4) (R Development Core Team, 2017).

Redundancy Analysis and Variance Partitioning

We implemented redundancy analysis with a multi-tiered variance partitioning method (e.g., Cushman and McGarigal, 2002), in the "*vegan*" R package (version 3.3.4) (Oksanen et al., 2010) to quantify the independent and joint ability of each set of environmental variables to predict the morphological characteristics of all sampled white pine individuals, and to measure the importance and joint interactive effects of the variables together. Importantly, this also enabled us to quantify the amount of morphological variation not explained by environmental variation in our data set. We computed a four-way partitioning among all climatic, vegetation, geographical and topographical variables. The spatial variables included the eigth spatial trend surface analysis terms (e.g., x, y, x^2, y^2, xy, x^2y, xy^2, and x^2y^2; Cushman and McGarigal, 2002).

Selection of Independent Environmental Factors Influencing Morphological Traits

Selection of appropriate independent variables is fundamental for achieving effective predictive models (Krzanowski, 1987; Gnanadesikan et al., 1995; Maronna et al., 2018). We tested for significant differences in the mean values of explanatory environmental variables across the 65 *P. strobiformis* stands with morphological data (**Supplementary Tables S1–S5**) to describe variation across populations. Many of our predictor variables were not normally distributed (the variables are listed in **Supplementary Tables S1–S5**). Due to the absence of normality, we used the non-parametric Kruskal-Wallis test (Kruskal and Wallis, 1952) to evaluate whether the observed median's differences in independent variables between *P. strobiformis* populations were statistically significant. All environmental variables for which we detected significant differences in median values of morphological traits ($\alpha = 0.01$) were included in further analysis.

Additionally, the most important environmental factors influencing morphological variation were also determined using partial least squares and area under the univariate receiver operator curve, using the "varImp" function applied to the results of univariate analysis with the machine learning algorithm, using Random Forest ["caret" package, function train, methods "rf," implemented in R (version 3.3.4; R Development Core Team, 2017)]. In each case, the unsupervised correlation filter was applied to the predictors prior to modeling (see details in the section "Regression techniques").

The variable-importance measure was determined using partial least squares (Kuhn, 2012), on the basis of the weighted sums of the absolute regression coefficients. The weights are a function of the reduction of the sums of squares across the number of partial least squares components and are computed separately for each outcome. The contributions of the coefficients are thus weighted proportionally to the reduction in the sums of squares. The trapezoidal rule was used to compute the area under the receiver operator curve, which was used as a measure of the variables importance (Kuhn, 2012).

Finally, we used the non-parametric Spearman's coefficient (r_s) to determine correlations between the variables and to estimate collinearity between important independent variables (selected by the Kruskal-Wallis test, partial least squares or receiver operator curve). When the r_s absolute value for the difference between two variables was greater than 0.70, only the

[1] http://forest.moscowfsl.wsu.edu/climate/

variable with the lowest p value in the Kruskal–Wallis test was included in the regression models (as reported by Salas et al., 2017 and Shirk et al., 2018). The relationships between the most important variables and two most spatially dependent cone and seed traits were represented graphically.

Modeling Spatially Dependent Cone and Seed Traits by Machine Learning Regression Methods

The number of variables was determined by the rule of ten events per variable (McGarigal et al., 2000; Vittinghoff and McCulloch, 2007, i.e., a maximum of the six most important variables for the 65 *P. strobiformis* stands were included in the models). Regression models, including 5-fold cross-validations, were used to predict the most spatially dependent *P. strobiformis* cone and seed traits for selected important, independent variables in each stand. Six machine learning algorithms were implemented in the "caret" package and function "train" models: (i) linear regression (method = "lm"), (ii) Random Forest (method = "rf"), (iii) Neural Network (method = "nnet"), (iv) Model Averaged Neural Network (method = "avNNet"), (v) Multi-Layer Perceptron (method = "mlpWeightDecay"), and (vi) Bayesian Regularized Neural Networks (method = "brnn") (Venables and Ripley, 1999; Williams et al., 2018, http://topepo.github.io/caret/index.html) in R (version 3.3.4) (R Development Core Team, 2017). The goodness-of-fit of the regression model was evaluated by using the (pseudo) coefficient of determination (R^2), root of the mean square error (RMSE), and mean squared error.

RESULTS

Detecting Spatial Dependence in Morphological Traits by Ordinary Kriging Analysis

The values of all studied morphological traits increased from the northern (United States) to the southern (Mexican) populations (e.g., cone length and seed weight were larger in southern populations; **Figure 2**; **Supplementary Figure S1**). The best kriging model for cone length used Stein's parameterization (R_k^2 = 0.89; *URMSE* = 1.72 cm; **Supplementary Table S6**). The goodness-of-fit values for the seed weight and scale top angle were slightly lower (R_k^2 = 0.75, *URMSE* = 0.04 g; R_k^2 = 0.74, *URMSE* = 3.04 mm). In general, the mean cone size, seed weight and scale angle were larger in the southern populations. The worst-performing spatial model was that for scale top width (R_k^2 = 0.05). There was a marginally positive relationship between latitude and DBH (R_k^2 = 0.06, p = 0.033), but there was no association between latitude and tree height (R_k^2 = 0.15, p = 0.38) (**Supplementary Table S6**).

Redundancy Analysis and Variance Partitioning

Collectively, vegetation, spatial, topographic, geographical, and climatic variables explained 54.7% of the total variation in the morphological characteristics among sampled trees (**Figure 3**). Of the marginal effects of these groups of variables, geographic variables showed the best ability to predict morphological characteristics, accounting for 51.5% of the variance (**Supplementary Table S7**), followed by vegetation variables (43.8%), climate variables (43.4%) and finally topographic variation (36.9%). There was very high covariation in the explanation among these different sets of variables, with no set explaining more than 6% (set geographic) of the variation in morphological traits independent of the other variable sets. The climate and topographic variable sets had very close to zero (0.004) independent explanatory power. The largest component of explained variance (33.6%) was the four way interaction of all four variable sets, suggesting that there is strong co-variation in environmental, climate and geographical variables in their relationship to morphological characteristics of *P. strobiformis* across its range. The second largest variance component was the three-way interaction between climate, vegetation and geographic variable sets. This shows that in total 39.6% of the variance in morphological traits across the range of southwestern white pine are jointly predicted by simultaneous variation in climate, vegetation and geographic variable sets (**Figure 3**).

Modeling Spatially Dependent Cone and Seed Traits Using Machine Learning Methods

For the 65 stands with morphological data, our modeling results indicated that growing season precipitation (GSP) was the most important independent variable for predicting both cone length and seed weight (**Supplementary Figures S2, S3**). However, the independent variables that together produced the best model of cone length of *P. strobiformis* were the GSP, winter precipitation (WINP), summer precipitation balance (SMRPB), frequency of occurrence of several overstory tree species (*Pseudotsuga menziesii* (Mirbel) Franco, *Pinus cooperi* C.E. Blanco and *Arbutus xalapensis* Kunth), yielding an RMSE of 1.75 cm using the Random Forest (rf) (**Table 1**; **Supplementary Figure S2**). The second-best model for cone length (RMSE = 1.83 cm) was produced by the Bayesian Regularized Neural Networks (brnn) and the same independent variables.

In contrast, the GSP, frequency of occurrence of *Pseudotsuga menziesii,* mean annual temperature (MAT), SMRPB, frequency of occurrence of *P. arizonica* Engelm. and *J. deppeana* Steud. in the same site, were the variables that together provided the best prediction of seed weight of *P. strobiformis* [with an RMSE of 0.039 g using linear regression, (lm)]. The second best model of seed weight (RMSE = 0.040 g) was produced using the variables GSP, MAT, frequency of occurrence of *Pseudotsuga menziesii,* frequency of occurrence of *P. strobiformis, P. arizonica* and SMRPB, the brnn approach (**Table 2**; **Supplementary Figures S3**). Higher GSP and SMRPB, lower frequency of occurrence of *Pseudotsuga menziesii*, corresponded to longer mean cone length (**Supplementary Table S8**). Higher GSP, MAT, higher frequency of occurrence of *P. arizonica* and *J. deppeana,* and lower frequency of occurrence of *P. menziesii* and earlier SMRPB were correlated with greater mean seed weights (**Supplementary Table S9**).

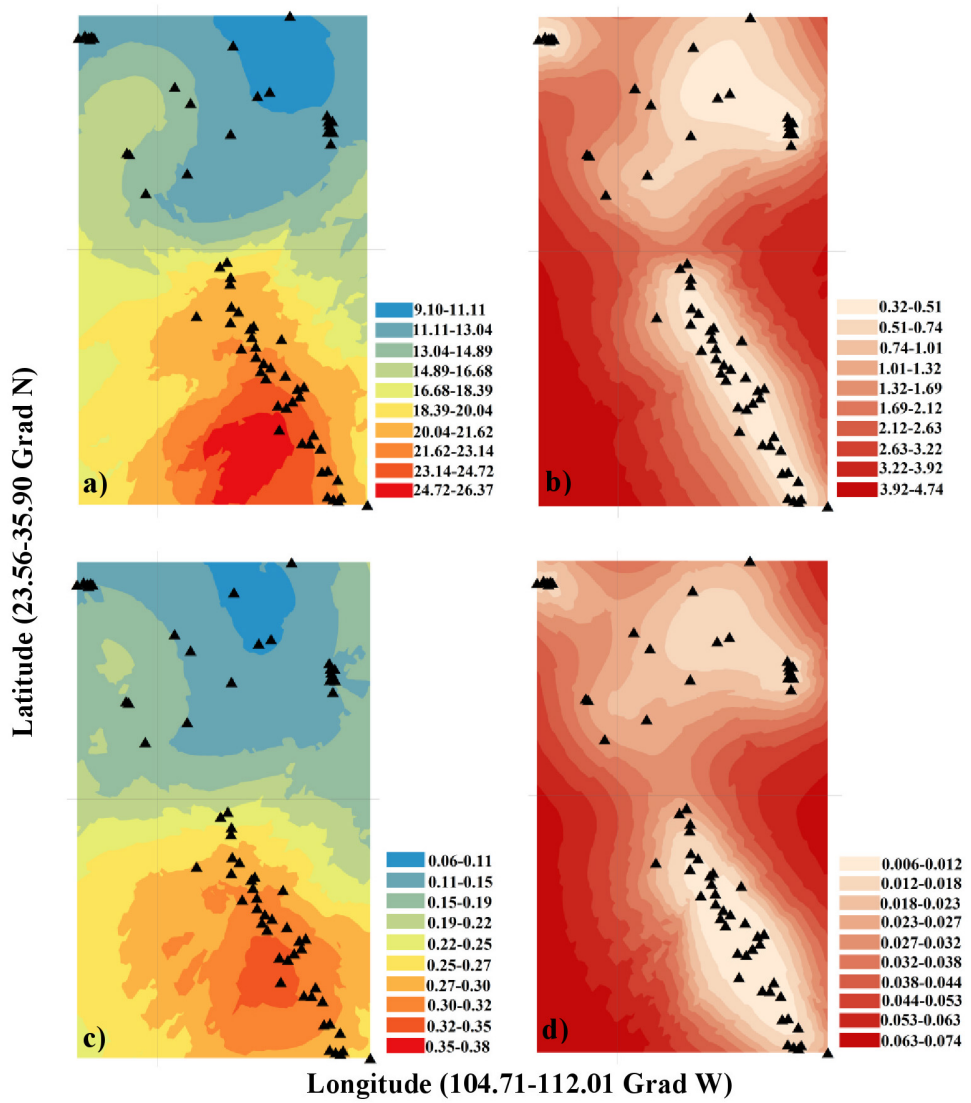

FIGURE 2 | Ordinary kriging model and its standard error (SE) for different morphological traits: **(a)** Cone length (cm), **(b)** SE of cone length (cm), **(c)** Seed weight (g), **(d)** SE of seed weight (g). The statistical software R (version 3.3.4) (R Development Core Team, 2017) and the Interpolation Kriging package (ArcGIS Desktop 10.5, 2016) were used to describe first-order variation in the spatial pattern.

Associations of Cone Length and Seed Weight With Tree Dimension and Hybrid Degree

The tree dimensions of DBH, total height and crown length were only marginally and non-significantly correlated with mean cone length (R^2 = 0.03, p = 0.15; R^2 = 0.02, p = 0.25; R^2 = 0.02, p = 0.25) and seed weight (R^2 = 0.07, p = 0.04; R^2 = 0.003, p = 0.67; R^2 = 0.03, p = 0.19), respectively. But, there was a moderately negative relationship between hybrid degree and both mean cone length and seed weight (R^2 = 0.30, p<0.00001), respectively.

Figure 4 shows the associations between mean cone length and seed weight and the most important variables: growing season precipitation (GSP), frequency of occurrence of *P. menziesii* in the neighborhood, and summer precipitation balance (SMRPB).

DISCUSSION

Modeling Spatially Dependent Cone and Seed Traits by Machine Learning Methods

The regression results also illustrated how environmental (GSP, SMRPB, WINP, and MAT) factors influenced the cone length and seed weight of *P. strobiformis*. The largest cones and heaviest seeds were found in more humid and temperate climates, which are located in the southern half of the Mexican Sierra Madre

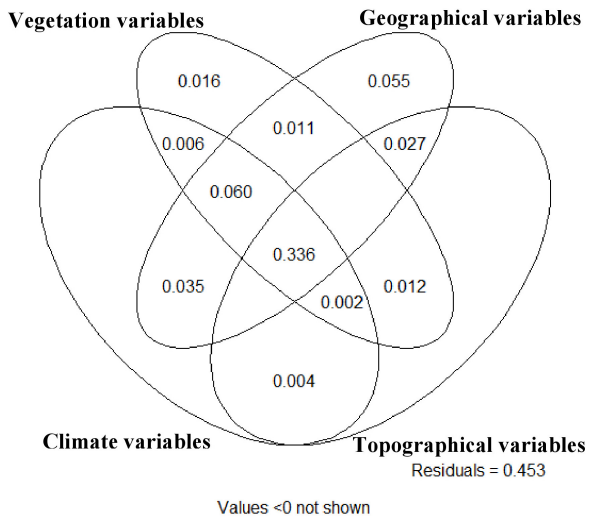

FIGURE 3 | Variance partitioning diagram from partial redundancy analysis among (1) climatic, (2) vegetation, (3) geographical, and (4) topographical variable groups. The total explained variance in morphological characteristics among all sampled individual trees is 54.7% and the numbers in each compartment of the diagram indicate the amount of variance explained by the variable sets overlapping in that compartment.

Occidental. This result is in contrast to earlier work in other tree species in the United States by Baker (1972); Schimpf (1977), Sorensen and Miles (1978) and Stromberg and Patten (1990) who found that seeds were larger in drier sites. This difference may reflect the much larger and broader sample of our study, which covered the entire species range and therefore provided a more complete picture of phenotypic variation across the entire distribution than was possible with more limited prior studies. Conversely, Mazer (1989) and Telenius and Torstensson (1991) found no significant association between seed weight and moisture availability; again, those studies were limited by the extent and size of sampling. Leishman and Westoby (1994b) reported that the comparative evidence of an association between large seeds and dry habitats is very limited, despite the general assumption made in the scientific literature. Our study resolves this issue by evaluating a larger, more representative and range-wide sample, and shows strong associations of seed weight and cone length with latitude and climate, with larger seeds and longer cones in the southern, wetter part of the species' range. However, hybridization with *P. flexilis* also leads to smaller cones and seeds of *P. strobiformis* at its northern border (Menon et al., 2018). Finally, hybridization effects with *P. ayacahuite* should not result in bigger seeds of *P. strobiformis* at the southern distribution border because seeds from *P. ayacahuite* are much smaller. However, hybridization with *P. ayacahuite* may lead to longer cones (Leal-Sáenz et al., 2020).

Redundancy Analysis and Variance Partitioning

The strong covariation between topographical, geographic, climatic, and vegetation in their relationship to morphological traits suggests that the major variation in the measured morphological traits is associated with the simultaneous and covarying influences of spatial, climatic and topographic factors. The dominant explanatory power of climate, vegetation and geographic variable sets suggest that these factors are particularly important in their relationship to morphological characteristics, while variables in the topographic group have relatively weaker association with morphological traits. The inability of this large empirical sample to statistically separate the effects of climate, vegetation and geographic groups suggests that it is difficult to identify which specific environmental, spatial or climatic factors may be driving observed morphological variation.

The results reported here, however, are useful in showing that a majority of the variability in *P. strobiformis* morphological traits is explainable by climatic, topographical, spatial and vegetation variables and the degree of hybridization with *P. flexilis*. There are strong patterns of morphological variation in this species that are largely explainable by the joint and simultaneous effects of multiple factors. It is not surprising that there is high and inseparable covariation among these factors, as climatic variables are known to change in predictable ways with geographical location (latitude) and topography (elevation). Thus, one hypothesis to explore in common garden experiments is that the variation in morphological traits across the species range are primarily local adaptations to climate, which covaries with elevation and other ecological variables, and that the high apparent relationship between morphology and topography, space and vegetation community are spurious correlations with the actual climatic drivers. A second, alternative, hypothesis could be that competition with other tree species drives the morphological differences across the range, and that the distribution of these competitors is associated with climatic gradients, leading to covariation of morphological traits with climate. Our evidence suggests that cone and seed morphology align with increasing hybridization with *P. flexilis,* resulting in shorter cones and smaller seeds (Steinhoff and Andresen, 1971). Hybridization occurs primarily in the United States populations to the north, creating complex interactions between morphology, climate and genetics (Menon et al., 2018).

Various studies have reported that seeds are often larger under competitive conditions due to the enhanced survival of larger seeds (Salisbury, 1942, 1974; Grime and Jeffrey, 1965; Hutchinson, 1967; Ng, 1978; Foster and Janson, 1985; Mazer, 1989; Leishman and Westoby, 1994a). Egli (2017) argued that variation in seed weight is mainly related to variation in the rate of seed growth during rapid seed filling. Decades of provenance trials in forest trees provide evidence for wide variation in several key ecological traits (Alberto et al., 2013; Lind et al., 2018). For instance, in whitebark pine (*Pinus albicaulis*), Bower and Aitken (2008) suggested that the phenotypic variation is due to genetic and geographic differentiation that reflects the long-term adaptive evolution from the last glacial maximum and from local environmental adaptation. *P. strobiformis* has a large north to south range that results in a gradient of increasing summer precipitation and temperature of the coldest month. The latitudinal climatic gradient along with other abiotic factors also influenced the presence of other tree species around

TABLE 1 | Best fit models of cone length (cm) based on 65 *Pinus strobiformis* stands in Mexico and United States.

Method of variable selection	Machine learning algorithm	Independent variable	RMSE	MAE	R^2
PLS	rf	GSP, WINP, SMRPB, *Pseudotsuga menziesii*, *P. cooperi*, *Arbutus xalapensis*	1.755	1.477	0.890
PLS	brnn	GSP, WINP, SMRPB, *Pseudotsuga menziesii*, *P. cooperi*, *Arbutus xalapensis*	1.832	1.514	0.867
ROC	lm	GSP, *Pseudotsuga menziesii*, MAT, SMRPB, *P. arizonica*, *J. deppeana*	1.939	1.536	0.865
PLS	mlpWeightDecay	GSP, WINP, SMRPB, *Pseudotsuga menziesii*, *P. cooperi*, *Arbutus xalapensis*	5.599	4.971	0.191
KW	avNNet	GSP, MAT, *Pseudotsuga menziesii*, *P. strobiformis, P. arizonica*, SMRPB	17.852	17.125	0.658
KW	nnet	GSP, MAT, *Pseudotsuga menziesii*, *P. strobiformis, P. arizonica*, SMRPB	17.856	17.128	0.621

PLS = Partial Least Squares, ROC = Receiver Operating Characteristic, KW = Kruskal Wallis, rf = Random Forest, brnn = Bayesian Regularized Neural Networks, lm = linear regression, mlpWeightDecay = Multi-Layer Perceptron, nnet = Neural Network, avNNet = Model Averaged Neural Network, RMSE = Root-mean-square error, MAE = Mean Absolute Error, R^2 = R squared, GSP = Growing season precipitation, April to September, Pseudotsuga menziesii = frequency of occurrence of Pseudotsuga menziesii in the neighborhood, SMRPB = Summer precipitation balance: (jul+aug+sep)/(apr+may+jun), Juniperus deppeana = frequency of occurrence of Juniperus deppeana in the neighborhood, P. arizonica = frequency of occurrence of P. arizonica in the neighborhood, P. strobiformis = frequency of occurrence of P. strobiformis in the neighborhood, P. cooperi = frequency of occurrence of P. cooperi in the neighborhood, Arbutus xalapensis = frequency of occurrence of Arbutus xalapensis, Arctostaphylos pungens = frequency of occurrence of Arctostaphylos pungens MAT = Mean annual temperature (degrees C), WINP = Winter precipitation: (nov+dec+jan+feb).

TABLE 2 | Best fit models of seed weight (g), based on 65 *Pinus strobiformis* stands in Mexico and United States.

Method of variable selection	Machine learning algorithm	Independent variables	RMSE	MAE	R^2
ROC	lm	GSP, *Pseudotsuga menziesii*, MAT, SMRPB, *P. arizonica, J. deppeana*	0.039	0.033	0.798
KW	brnn	GSP, MAT, *Pseudotsuga menziesii*, *P. strobiformis, P. arizonica*, SMRPB	0.040	0.031	0.780
KW	rf	GSP, MAT, *Pseudotsuga menziesii*, *P. strobiformis, P. arizonica*, SMRPB	0.041	0.033	0.752
PLS	avNNet	DD0, *Pseudotsuga menziesii*, *P. arizonica*, *Arctostaphylos pungens, Arbutus xalapensis,* SMRPB	0.043	0.037	0.769
PLS	nnet	DD0, *Pseudotsuga menziesii*, *P. arizonica*, *Arctostaphylos pungens, Arbutus xalapensis,* SMRPB	0.048	0.039	0.738
PLS	mlpWeightDecay	DD0, *Pseudotsuga menziesii*, *P. arizonica*, *Arctostaphylos pungens, Arbutus xalapensis,* SMRPB	0.075	0.061	0.468

PLS = Partial Least Squares, ROC = Receiver Operating Characteristic, KW = Kruskal Wallis, rf = Random Forest, brnn = Bayesian Regularized Neural Networks, lm = linear regression, mlpWeightDecay = Multi-Layer Perceptron, nnet = Neural Network, avNNet = Model Averaged Neural Network, RMSE = Root-mean-square error, MAE = Mean Absolute Error, R^2 = R squared, GSP = Growing season precipitation, April to September, Pseudotsuga menziesii = frequency of occurrence of Pseudotsuga menziesii in the neighborhood, SMRPB = Summer precipitation balance: (jul+aug+sep)/(apr+may+jun), Juniperus deppeana = frequency of occurrence of Juniperus deppeana in the neighborhood, P. arizonica = frequency of occurrence of P. arizonica in the neighborhood, Arbutus xalapensis = frequency of occurrence of Arbutus xalapensis in the neighborhood, Arctostaphylos pungens = frequency of occurrence of Arctostaphylos pungens in the neighborhood, MAT = Mean annual temperature (degrees C), P. strobiformis = frequency of occurrence of P. strobiformis in the neighborhood, DD0 = Degree-days < 0 degrees C (based on mean monthly temperature).

P. strobiformis. Therefore, the frequency of occurrence of these species corresponded to the cone length and seed weight as proxy of other abiotic and ecological factors of morphological traits (Zhang et al., 2016, Bañares-de-Dios et al., 2020). For example, we detected *Pseudotsuga menziesii* only in the United States sites, while *Juniperus deppeana, P. arizonica, P. cooperi*, and *A. xalapensis* were found only in the Mexico sites, and in the seed weight model the former species is associated with lower seed weights and the latter species with heavier average seed weights.

Many researchers have argued that variation in cone or seed size within species are closely associated with fitness and, therefore, with adaptive evolution (Roach, 1987; Winn, 1988; Biere, 1991; Platenkamp and Shaw, 1993; Ji et al., 2011). Seed size may also influence seed dispersal (Herrera et al., 1994; Jordano, 1995; Martínez et al., 2007; Shimada et al., 2015). Wang and Ives (2017) reported that seed weight affected almost all choices that rodents made in eating, removing and storing individual seeds. At the level of individual trees, larger seeds have improved probabilities of both predation and effective dispersal. Leslie et al. (2017) also reported that larger seeds were dispersed by animals while smaller seeds were dispersed by the wind and that the morphology of the cones is associated with the size of the seeds. Other studies have reported that latitude, genome size, forest structure, growth form and seed dispersal are related to differences in seed size (Salisbury, 1974; Lord et al., 1997; Leishman et al., 2000; Beaulieu et al., 2007). As the climate continues to shift, the morphological differences between the northern and southern *P. strobiformis* populations may result in differing reforestation patterns and affect management recommendations (Goodrich et al., 2018; Schoettle et al., 2018).

Common Gardens, Gradient Modeling and Simulation

Experimental common garden studies could separate these influences to some degree, by replicating species combinations across climatic gradients. Common garden experiments are important additionally to quantify the relative degree of phenotypic plasticity and, while they are unlikely to show local adaptation in action, they can show the signature of past local adaptation in the portion of the variance that is not ascribable to phenotypic plasticity. Ultimately, the observed morphological variation is a product of demographic history, local adaptation to climate and environment, phenotypic plasticity, and how these interact in the context of local environmental conditions. The importance of demographic history and genetic drift could be noted in the high explanatory power of geographic variables

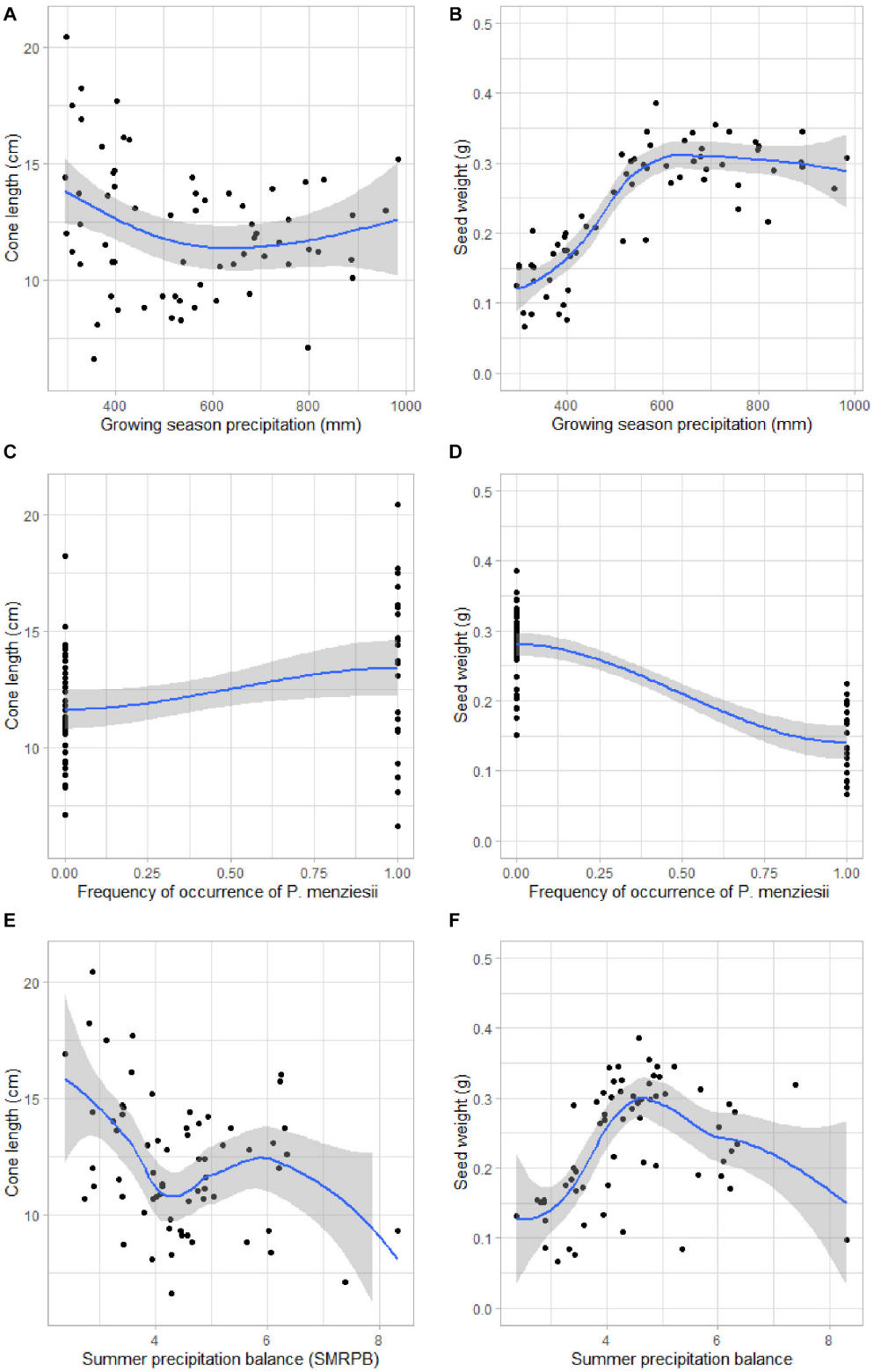

FIGURE 4 | Relationship between the important variables and cone length and seed weight of 65 study sites: **(A)** Cone length (cm) vs. growing season precipitation (mm), **(B)** Seed weight (g) vs. growing season precipitation (mm), **(C)** Cone length (cm) vs. frequency of occurrence of *Pseudotsuga menziesii* in the neighborhood, **(D)** Seed weight (g) vs. frequency of occurrence of *P. menziesii* in the neighborhood, **(E)** Cone length (cm) vs. summer precipitation balance, **(F)** Seed weight (g) vs. summer precipitation balance. The mean (black line) and standard deviation (gray area) is based on the GAM model.

even though several of them exhibited co-variation with climate and vegetation. To fully resolve the drivers of morphological variation, therefore, replicated and controlled common-garden experiments across the species range, representing combinations of all variable sets (e.g., topography, space, environment and genetics) are essential (Cushman, 2014). These common garden experiments should reciprocally transplant tree families from across the full range, and associate their expressed phenotypic variation with garden specific values of environmental variables, the values of these variables in the location of their maternal trees, and their individual genomic characteristics. Only through replicated and controlled experiments across ecological gradients that associate expressed variation with both environmental and genomic variability can we reliably identify and quantify the drivers of phenotypic variation (Sork et al., 2013).

In practice, however, such common garden studies may have limited practicality given the length of time needed for common garden plots to establish and mature to such a degree that they influence the expression or selection of morphological traits of long lived tree species. In addition, these gardens would have to be large to sufficiently represent forest stand conditions that would reflect competitive dynamics that drive selection or phenotypic plasticity. Finally, given that potentially a large amount of the variation in expressed phenotype is genetically controlled local adaptation, such common gardens would not necessarily show changes in phenotype in time frames feasible for experimentation, given multiple generations of selection are required to observe microevolutionary change in response to selection pressures related to competition or climate. Maintaining a large sample of spatially extensive gardens for many decades is a logistical and financial challenge.

Broad-scale sampling of genomic variation, morphological characteristics, and environmental variables across the species range provides another powerful framework to disentangle space, environment, climate, competition and genetic factors in influencing morphology (e.g., Cushman, 2014). Therefore, it is likely that the most effective way to separate the covarying influences of climate and competition on phenotypic variation will be through large-scale sampling of genomic variation across the population and association of this genomic variation with local environmental, climatic, and community conditions, and partitioning of the variance in morphological traits that are explainable by genomic variation vs. environmental variation. This would show the portion of morphological variation that is genetically correlated, which potentially indicates the degree of local adaptation. Specifically, while sampling standing variation in morphology and genomics across a species range does not enable experimental control necessary to isolate particular drivers with strong inferences, it does allow comparative mensurative designs that can trade space for time, and, critically, sample conditions in situ and at scales in both space and time that are operative and influential on the evolution and community dynamics of trees (McGarigal and Cushman, 2002). Thus we recommend future research combine and couple both broad-scale large-sample analysis of gene-environment gradients across the species range that can describe variation at broad scales and over long timer periods, with targeted, replicated and controlled common garden experiments that can isolate particular drivers of variation at small scales and over short times (Cushman, 2014).

Given the difficulty of reliably isolating drivers and apportioning explanatory variance among them with either observational or common garden experiments on long-lived tree species, we also recommend the use of simulation modeling (e.g., Landguth and Cushman, 2010; Landguth et al., 2017). Specifically, employing an individual-based, spatially explicit eco-evolutionary model (e.g., Landguth et al., 2020) to simulate the interactions of different degrees of gene flow, drift, environmental selection and phenotypic plasticity provides a unique means to explore the potential interactions of these factors and quantify the patterns of genomic and phenotypic variation that can be expected under these interactions (e.g., Cushman, 2015; Cushman and Landguth, 2016).

Implications for Management and Conservation

The ability of *P. strobiformis* to colonize its expected future range (Shirk et al., 2018) will be influenced by numerous factors, including colonization at the leading edge of the range shift, seed dispersal dynamics, resistance to white pine blister rust, competition with other species, introgression and hybridization (Menon et al., 2020), and genetic adaptation to local climate (Goodrich et al., 2016; Bucholz et al., 2020). Through our results, we have a better understanding of the environmental controls on cone and seed morphology, and we can more adequately evaluate seed provenances and transfer zones and provide better information for assisted migration strategies. Current best practices for seed transfer, such as (a) promoting a tight network of seed stands to prevent greater loss of local genetic variants and structure and (b) using the seeds to establish seedlings within a limited radius from each seed stand/provenance (Hernández-Velasco et al., 2017), are likely to exhibit continued success in the near future. Such practices are essential for current and near-future reforestation programs, including assisted migration or the establishment of new populations in areas that should be appropriate for specific species under expected climate change scenarios (Wehenkel et al., 2017). However, more innovative practices will be required under new climates not conducive to the reproductive success of local populations. This is particularly important given the large projected climate-driven range shift of *P. strobiformis* and predicted large climatic changes within the parts of the range that are likely to remain occupied (Shirk et al., 2018). We recommend a proactive approach, in which reforestation programs incorporate both local and regional seed sources and allow for assisted gene flow (Aitken and Bemmels, 2016). For example, a manager of *P. strobiformis* might include seed sources from the provenance that is most similar to the projected future climate of the planting location (given climate predictions for the species; Shirk et al., 2018) alongside local sources on sites of least aridity (Bucholz et al., 2020). Such a strategy promotes the local genetic structure while providing for adaptation to changing climates and allowing managers flexibility in determining seed sources most suitable

given other management considerations (e.g., white pine blister rust). As cone length and seed weight are probably also related to local/regional genetic adaptation (Rawat and Bakshi, 2011), these variables could be included in future climate-based seed transfer guidelines, providing suggestions for average cone lengths and seed weights most appropriate for a given site, including information on degree of hybridization present or desired for a planting site. Given the observed high covariation between climatic, community structure and geographic factors in this study, and the difficulty in separating them statistically or experimentally, there may be no silver bullet for managers to decide on the merits of different planting and assisted migration strategies. Again, given the difficulty of using observational or experimental data to guide these decisions, it may be useful to augment such studies with simulations that can control the interactions of these factors across large ranges of scale in both space and time to quantify the potential roles and influences of each factor in the context and interactions with the others (e.g., Landguth et al., 2017).

Scope and Limitations

Importantly, these results show that the pattern of morphological variation in *P. strobiformis* is highly predictable in relation to a combination of geographic, floristic, climatic and topographical variables. It is interesting to note that our analysis did not include several environmental variables that are known to strongly predict the distribution of *P. strobiformis* (e.g., soils; Shirk et al., 2018). Thus, it is likely that including a broader set of environmental variables that are limiting to *P. strobiformis* fitness at different scales and in different contexts would increase the amount of variance explained in morphological characteristics across the species range. Additionally, our analysis does not formally integrate observed genomic variation among individual trees in comparison to expressed phenotype across gradients of environmental, climatic and geographic gradients. Future work should therefore focus on collecting these factors simultaneously for a large number of trees across the full extent of the species range and ecological conditions to enable more rigorous evaluation of the degree to which genomic variation can explain observed phenotypic variation, and to what degree it is covarying and thus potentially controlled by selection along environmental gradients. Such studies would also be able to quantify the degree to which admixture with peripatric sister species (e.g., *P. flexilis*) confounds and contributes to observed variation in phenotypic characteristics along geographical and environmental gradients. Another area that would be valuable to integrate into analyses of relationships between phenotypic variation, geography, community structure and environmental gradients would be formal accounting of the influences of phylogeographic and demographic history. Phylogeographic and demographic history create non-stationary and non-equilibrium patterns of genetic structure across populations that are not linearly related to local adaptation or patterns of gene flow (e.g., Dyer et al., 2010). Developing and integrating methods that can account for this therefore is valuable. Again, simulation modeling (Cushman, 2015) may be the most powerful way to account for the interactions of gene flow, drift and selection within varying contexts of phylogeographic and demographic history, given their ability to stipulate and control all the factors that interact in a way that enables simulation experiments to robustly evaluate each factor and its interactions with others.

CONCLUSION

We showed that most variation in *P. strobiformis* morphological characteristics is strongly correlated with climatic gradients, suggesting selection for different morphological characteristics under different climatic contexts. However, we could not determine how much of the morphological variation is driven by climate independently of covarying topographical, ecological and spatial factors. In addition, our study does not quantify the degree to which observed morphological variation is genetically controlled, nor how much phenotypic plasticity there is. We advocate for replicated and controlled reciprocal transplant common garden experiments (e.g., Sork et al., 2013; Cushman, 2014) which can enable rigorous separation of the amount of phenotypic variance controlled by genotype, by the environment and by the interaction between genotype and environment. In addition, we suggest coupling such common garden studies to broad-scale gradient modeling of genomic and morphological variation across geographic, climatic and community gradients (Cushman, 2014). Simulation modeling, which can control all the potential factors driving covariation between genomic, phenotypic, geographical, and environmental factors at scales in space and time relevant to population responses are likely to be critical to rigorously quantify these relationships and untangle them. Ultimately a combination of common garden, gradient modeling and simulation studies provides the best means for advancing the important and challenge task of understanding and predicting eco-evolutionary dynamics across broad populations in complex and dynamic environments (Cushman, 2014). The results presented here, however, are useful and important in showing spatial range-wide patterns of phenotypic variation that are strongly associated with environmental gradients, and that a large portion of this variation is also associated with the joint effects of climate, topography, latitude and regional vegetation community composition.

The combination of variance partitioning and machine learning algorithms implemented here provides a clear demonstration of both the relative importance and independent effects of different climatic, geographic and environmental factors in driving morphological variation in *P. strobiformis*, but also identify the main patterns of this variation and the variables that are most strongly associated with them. We find that cone length, seed weight and cone morphology are strongly related to temperature and precipitation and increase in warmer and wetter parts of the species range. These results show that spatial modeling across a species range can yield accurate predictions of morphological traits as a function of environmental gradients. These models predict the considerable differences in geographical, topographical, climate, adaptive

and morphological variables in the species range and may help to distinguish the actual seed provenance of *P. strobiformis*.

DATA AVAILABILITY STATEMENT

The raw data supporting the conclusions of this article will be made available by the authors, without undue reservation.

AUTHOR CONTRIBUTIONS

CW and KW conceived and designed the experiments. KW, AL-S, and CW conducted sampling. AL-S, CW, and SC analyzed the data. ALS and CW prepared figures and tables and contributed reagents, materials, and analysis tools. AL-S, LF-R, and AE performed the experiments. CW, SC, KW, and AL-S wrote the manuscript. KW, CW, MM, SC, AE, LF-R, JH-D, CL-S, and JM-G reviewed drafts of the manuscript. All authors contributed to the article and approved the submitted version.

FUNDING

This material is based on work supported by the National Science Foundation under Grant Nos. EF-1442597 and EF-1442486. Cone and seed collections in the United States were partially financed by the USDA Forest Service Gene Conservation Program. We are also grateful to CONACYT for the financial support provided to AL-S.

ACKNOWLEDGMENTS

We appreciate the assistance of numerous field technicians who helped gather cones and field data and also thank Dr. Betsy Goodrich for her initial work on this project. Cone collections in Mexico were supported by the UJED Universidad Juarez del Estado de Durango. We are grateful to Sergio Leonel Simental-Rodríguez, Javier Hernández-Velasco, and Carlos Alonso Reyes-Murillo for assistance in collecting cones and field data. We also thank Cecilia Pulido-Díaz, Norberto Domínguez-Amaya, Adrian Silva-Cardoza, and David Hernández-Almaraz for their help with measuring cones, scales and seeds, and Samuel Ignacio Arroyo-Arroyo for his help with map construction.

SUPPLEMENTARY MATERIAL

The Supplementary Material for this article can be found online at: https://www.frontiersin.org/articles/10.3389/fpls.2020.559697/full#supplementary-material

REFERENCES

Aguirre-Gutiérrez, J., Serna-Chavez, H. M., Villalobos-Arambula, A. R., Pérez de la Rosa, J. A., and Raes, N. (2015). Similar but not equivalent: ecological niche comparison across closely related Mexican white pines. *Divers. Distribut.* 21, 245–257. doi: 10.1111/ddi.12268

Aitken, S. N., and Bemmels, J. B. (2016). Time to get moving: assisted gene flow of forest trees. *Evolut. Appl.* 9, 271–290. doi: 10.1111/eva.12293

Alberto, F. J., Aitken, S. N., Alía, R., González-Martínez, S. C., Hänninen, H., Kremer, A., et al. (2013). Potential for evolutionary responses to climate change–evidence from tree populations. *Glob. Change Biol.* 19, 1645–1661. doi: 10.1111/gcb.12181

ArcGIS Desktop 10.5 (2016). © 1999-2016. Version: 10.5.0.6491. Property of Environmental Systems Research Institute, Inc. (Esri) Inc., All Rights Reserved. Redlands, California, United States.

Arvanitis, L. G., Godbee, J. F., and Porta, I. (1984). Pitch canker impact on volume growth: a case study in slash pine plantations. *Southern J. Appl. For.* 8, 43–47. doi: 10.1093/sjaf/8.1.43

Atkinson, D., and Sibly, R. M. (1997). Why are organisms usually bigger in colder environments? Making sense of a life history puzzle. *Trends Ecol. Evol.* 12, 235–239. doi: 10.1016/S0169-5347(97)01058-6

Baker, H. G. (1972). Seed weight in relation to environmental conditions in California. *Ecology* 53, 997–1010. doi: 10.2307/1935413

Bañares-de-Dios, G., Macía, M. J., Granzow-de la Cerda, Í, Arnelas, I., de Carvalho, G. M., Espinosa, C. I., et al. (2020). Linking patterns and processes of tree community assembly across spatial scales in tropical montane forests. *Ecology* 101, 1–13. doi: 10.1002/ecy.3058

Batista, A. P. B., Mello, J. M. D., Raimundo, M. R., Scolforo, H. F., Reis, A. A. D., and Scolforo, J. R. S. (2016). Species richness and diversity in shrub savanna using ordinary kriging. *Pesquisa Agropecu. Brasil.* 51, 958–966. doi: 10.1590/S0100-204X2016000800008

Beaulieu, J. M., Moles, A. T., Leitch, I. J., Bennett, M. D., Dickie, J. B., and Knight, C. A. (2007). Correlated evolution of genome size and seed mass. *New Phytol.* 173, 422–437. doi: 10.1111/j.1469-8137.2006.01919.x

Bergmann, C. (1847). Über die Verhältnisse der Wärmeökonomie der Thiere zu ihrer Größe. *Gött. Stud.* 1, 595–708.

Biere, A. (1991). Parental effects in *Lychnis floscuculi*. I: seed size, germination and seedling performance in a controlled environment. *J. Evol. Biol.* 4, 447–465. doi: 10.1046/j.1420-9101.1991.4030447.x

Borcard, D., Legendre, P., and Drapeau, P. (1992). Partialling out the spatial component of ecological variation. *Ecology* 73, 1045–1055. doi: 10.2307/1940179

Bower, A. D., and Aitken, S. N. (2008). Ecological genetics and seed transfer guidelines for *Pinus albicaulis* (Pinaceae). *Am. J. Bot.* 95, 66–76. doi: 10.3732/ajb.95.1.66

Bower, A. D., McLane, S. C., Eckert, A., Jorgensen, S., Schoettle, A., and Aitken, S. (2011). "Conservation genetics of high elevation five-needle white pines," in *Proceedings of the High Five Symposium and RMRS-P-63 on The Future of High-Elevation, Five-Needle White Pines in Western North America*, eds R. E. Keane, D. F. Tomback, M. P. Murray, and C. M. Smith (Fort Collins, CO: U.S. Department of Agriculture, Forest Service, Rocky Mountain Research Station), 98–117.

Boyd, A. (2002). Morphological analysis of Sky island populations of *Macromeria viridiflora* (Boraginaceae). *Syst. Bot.* 27, 116–126. doi: 10.1043/0363-6445-27.1.116

Bramlett, D. L., Belcher, E. W. Jr., Debarr, G. L., Hertel, G. D., Karrfalt, R. P., Lantz, C. W., et al. (1977). *Cone Analysis of Southern Pines- A Guidebook. General Technical Report SE 13*. Asheville, NC: U.S. Department of Agriculture, Forest Service, Southeastern Forest Experiment Station.

Bucholz, E., Waring, K. M., Kolb, T. E., Swenson, J., and Whipple, A. (2020). Water relations and drought response of *Pinus strobiformis*. *Can. J. For. Res.* 50, 905–916. doi: 10.1139/cjfr-2019-0423

CONAFOR (2009). *Comisión Nacional Forestal*. México: National Forestry Commission of Mexico.

Conover, D. O., Duffy, T. A., and Hice, L. A. (2009). The covariance between genetic and environmental influences across ecological gradients. *Ann. N. Y. Acad. Sci.* 1168, 100–129. doi: 10.1111/j.1749-6632.2009.04575.x

Cushman, S. A. (2014). Grand challenges in evolutionary and population genetics: the importance of integrating epigenetics, genomics, modeling, and experimentation. *Front. Genet.* 5:197. doi: 10.3389/fgene.2014.00197

Cushman, S. A. (2015). Pushing the envelope in genetic analysis of species invasion. *Mol. Ecol.* 24, 259–262. doi: 10.1111/mec.13043

Cushman, S. A., and Landguth, E. L. (2016). Spatially heterogeneous environmental selection strengthens evolution of reproductively isolated populations in a Dobzhansky–muller system of hybrid incompatibility. *Front. Genet.* 7:209. doi: 10.3389/fgene.2016.00209

Cushman, S. A., and McGarigal, K. (2002). Hierarchical, multi-scale decomposition of species-environment relationships. *Landscape Ecol.* 17, 637–646. doi: 10.1023/A:1021571603605

Cushman, S. A., and McGarigal, K. (2004). Patterns in the species–environment relationship depend on both scale and choice of response variables. *Oikos* 105, 117–124. doi: 10.1111/j.0030-1299.2004.12524.x

Cushman, S. A., and Wallin, D. O. (2002). Separating the effects of environmental, spatial and disturbance factors on forest community structure in the Russian Far East. *For. Ecol. Manag.* 168, 201–215. doi: 10.1016/S0378-1127(01)00744-7

de Jong, G. (1990). Genotype-by-environment interaction and the genetic covariance between environments: multilocus genetics. *Genetica* 81, 171–177. doi: 10.1007/BF00360862

Delagrange, S., Messier, C., Lechowicz, M. J., and Dizengremel, P. (2004). Physiological, morphological and allocational plasticity in understory deciduous trees: importance of plant size and light availability. *Tree Physiol.* 24, 775–784. doi: 10.1093/treephys/24.7.775

Dyer, R. J., Nason, J. D., and Garrick, R. C. (2010). Landscape modelling of gene flow: improved power using conditional genetic distance derived from the topology of population networks. *Mol. Ecol.* 19, 3746–3759. doi: 10.1111/j.1365-294X.2010.04748.x

Egli, D. B. (2017). *Seed Biology and the Yield of Grain Crops*, 2nd Edn. Lexington, KY: University of Kentuchy.

Endler, J. A. (1986). *Natural Selection in the Wild. Monographs in Population Biology 21*. Princeton, NJ: Princeton University Press.

Falconer, D. S., and Mackay, T. F. C. (1996). *Introduction to quantitative genetics*, 4th Edn. London: Pearson Education Ltd.

Farjon, A., and Styles, B. T. (1997). *Pinus* (pinaceae). *Flora Neotropica. Monograph* 75. Bronx, NY: The New York Botanical Garden.

Forde, M. B. (1964). Variation in natural populations of *Pinus radiata* in California, New Zealand. *J. Bot.* 2, 459–485. doi: 10.1080/0028825X.1964.10428765

Foster, S., and Janson, C. H. (1985). The relationship between seed size and establishment conditions in tropical woody plants. *Ecology* 66, 773–780. doi: 10.2307/1940538

Frankis, M. (2009). *The High Altitude White Pines of Mexico and the Adjacent SW USA. (Pinus L. Subgenus Strobus Lemmon, Pinaceae)*. Available online at: http://pinetum.org/articles/Pinus/PNstylesiiFrankis2009.pdf (accessed August 19, 2019).

Franks, S. J., Weber, J. J., and Aitken, S. N. (2014). Evolutionary and plastic responses to climate change in terrestrial plant populations. *Evolut. Appl.* 7, 123–139. doi: 10.1111/eva.12112

Geils, B. W., and Vogler, D. R. (2011). "A natural history of *Cronartium ribicola*," in *The Future of High-Elevation, Five-Needle White Pines in Western North America*, eds R. E. Keane, D. F. Tomback, M. P. Murray, and C. M. Smith (Fort Collins, CO: US Department of Agriculture, Forest Service, Rocky Mountain Research Station), 210–217.

Gernandt, D. S., López, G. G., García, S. O., and Liston, A. (2005). Phylogeny and classification of *Pinus*. *Taxonomy* 54, 29–42.

Gernandt, D. S., and Pérez-de la Rosa, J. A. (2014). Biodiversidad de *Pinophyta* (coníferas) en México. *Rev. Mexic. Biodiver.* 85, 126–133. doi: 10.7550/rmb.32195

Gil, L., Climent, J., Nanos, N., Mutke, S., Ortiz, I., and Schiller, G. (2002). Cone morphology variation in *Pinus canariensis* Sm. *Plant Syst. Evol.* 235, 35–51. doi: 10.1007/s00606-002-0218-9

Gnanadesikan, R., Kettenring, J. R., and Tsao, S. L. (1995). Weighting and selection of variables for cluster analysis. *J. Classific.* 12, 113–136. doi: 10.1007/BF01202271

González-Ávalos, J., García-Moya, E., Vargas-Hernández, J. J., Trinidad-Santos, A., Romero-Manzanares, A., and Cetina-Alcalá, V. M. (2006). Evaluación de la producción y análisis de conos y semillas de *Pinus cembroides* Zucc. *Rev. Chapingo Ser. Cienc. Forest. Ambiente* 12, 133–138.

Goodrich, B. A., Waring, K. M., Auty, D., and Sánchez Meador, A. J. (2018). Interactions of management and white pine blister rust on *Pinus strobiformis* regeneration abundance in southwestern USA. *For. Int. J. For. Res.* 91, 492–505. doi: 10.1093/forestry/cpy009

Goodrich, B. A., Waring, K. M., and Kolb, T. E. (2016). Genetic variation in *Pinus strobiformis* growth and drought tolerance from southwestern US populations. *Tree Physiol.* 36, 1219–1235. doi: 10.1093/treephys/tpw052

Gregorius, H. R., Bergmann, F., and Wehenkel, C. (2003). Analysis of biodiversity across levels of biological organization: a problem of defining traits. *Perspect. Plant Ecol. Evol. Syst.* 5, 209–218. doi: 10.1078/1433-8319-00035

Grime, J. P., and Jeffrey, D. W. (1965). Seedling establishment in vertical gradients of sunlight. *J. Ecol.* 53, 621–642. doi: 10.2307/2257624

Hernández-Velasco, J., Hernández-Díaz, J. C., Fladung, M., Cañadas-López, Á, Prieto-Ruíz, J. Á, and Wehenkel, C. (2017). Spatial genetic structure in four *Pinus* species in the Sierra Madre Occidental, Durango, México. *Can. J. For. Res.* 47, 73–80. doi: 10.1139/cjfr-2016-0154

Herrera, C. M., Cerdá, X., García, M. B., Guitián, J., Medrano, M., Rey, P. J., et al. (2002). Floral integration, phenotypic covariance structure and pollinator variation in bumblebee-pollinated *Helleborus foetidus*. *J. Evol. Biol.* 15, 108–121. doi: 10.1046/j.1420-9101.2002.00365.x

Herrera, C. M., Jordano, P., Lopez-Soria, L., and Amat, J. A. (1994). Recruitment of a mast-fruiting, bird-dispersed tree: bridging frugivore activity and seedling establishment. *Ecol. Monogr.* 64, 315–344. doi: 10.2307/2937165

Hiemstra, P. H., Pebesma, E. J., Twenhöfel, C. J., and Heuvelink, G. B. (2009). Real-time automatic interpolation of ambient gamma dose rates from the Dutch radioactivity monitoring network. *Comput. Geosci.* 35, 1711–1721. doi: 10.1016/j.cageo.2008.10.011

Hoff, R., and Hagle, S. (1990). "Diseases of whitebark pine with special emphasis on white pine blister rust," in *Proceedings of the Symposium on Whitebark Pine Ecosystems: Ecology and Management of a High-Mountain Resource*, eds W. C. Schmidt and K. J. McDonald (Washington, DC: USDA), 179–190.

Hutchinson, T. C. (1967). Comparative studies of the ability of species to withstand prolonged periods of darkness. *J. Ecol.* 55, 291–299. doi: 10.2307/2257878

Iglesias, L. G., Solís-Ramos, L. Y., and Viveros-Viveros, H. (2012). Variación morfométrica en dos poblaciones naturales de *Pinus hartwegii* Lindl. del estado de Veracruz. *Rev. Int. Bot. Exp.* 81, 239–246.

Jarvis, A., Reuter, H. I., Nelson, A., and Guevara, E. (2008). *Hole-Filled SRTM for the GLOBE VERSION 4, Available from the CGIAR-CSI SRTM 90m Database*. Available online at: http://srtm.csi.cgiar.org (accessed August 26, 2019).

Ji, M., Deng, J., Yao, B., Chen, R., Fan, Z., Guan, J., et al. (2016). Ecogeographical variation of 12 morphological traits within *Pinus tabulaeformis*: the effects of environmental factors and demographic histories. *J. Plant Ecol.* 10, 386–396. doi: 10.1093/jpe/rtw033

Ji, M., Zhang, X., Wang, Z., Zhang, Q., and Deng, J. (2011). Intra-versus inter-population variation of cone and seed morphological traits of *Pinus tabulaeformis* Carr. in northern China: impact of climate-related conditions. *Polish J. Ecol.* 59, 717–727.

Jordano, P. (1995). Frugivore-mediated selection on fruit and seed size: birds and St. Lucie's cherry, *Prunus mahaleb*. *Ecology* 76, 2627–2639. doi: 10.2307/2265833

Kaplan, D. R. (2001). The science of plant morphology: definition, history, and role in modern biology. *Am. J. Bot.* 88, 1711–1741. doi: 10.2307/3558347

Keane, R. E., and Cushman, S. A. (2018). *Best Friends Forever: The Whitebark Pine and Clark's Nutcracker. The Wildlife Professional*. Washington, DC: USDA.

Kral, R. (1993). ""*Pinus*"," in *Flora of North America North of Mexico*, ed. Flora of North America Editorial Committee (New York, NY: Oxford University Press), 373–398.

Kruskal, W. H., and Wallis, W. A. (1952). Use of ranks in one-criterion variance analysis. *J. Am. Stat. Assoc.* 47, 583–621. doi: 10.1080/01621459.1952.10483441

Krzanowski, W. J. (1987). Selection of variables to preserve multivariate data structure, using principal components. *Appl. Stat.* 36, 22–33. doi: 10.2307/2347842

Kuhn, M. (2012). *Variable Importance Using the Caret Package*. Available online at: http://cran.cermin.lipi.go.id/web/packages/caret/vignettes/caretSelection.pdf (accessed September 25, 2019).

Landguth, E. L., and Cushman, S. A. (2010). CDPOP: a spatially explicit cost distance population genetics program. *Mol. Ecol. Resour.* 10, 156–161. doi: 10.1111/j.1755-0998.2009.02719.x

Landguth, E. L., Forester, B. R., Eckert, A. J., Shirk, A. J., Menon, M., Whipple, A., et al. (2020). Modelling multilocus selection in an individual-based, spatially-explicit landscape genetics framework. *Mol. Ecol. Resourc.* 20, 605–615. doi: 10.1111/1755-0998.13121

Landguth, E. L., Holden, Z. A., Mahalovich, M. F., and Cushman, S. A. (2017). Using landscape genetics simulations for planting blister rust resistant whitebark pine in the US Northern Rocky Mountains. *Front. Genet.* 8:1–12. doi: 10.3389/fgene.2017.00009

Leal-Sáenz, A., Waring, K. M., Sniezko, R., Menon, M., Hernández-Díaz, J. C., López-Sanchez, C. A., et al. (2020). Differences in cone and seed morphology of *Pinus strobiformis* and *Pinus ayacahuite*. *Southwest. Nat.* (in press).

Leishman, M. R., and Westoby, M. (1994b). The role of seed size in seedling establishment in dry soil conditions–experimental evidence from semi-arid species. *J. Ecol.* 82, 249–258. doi: 10.2307/2261293

Leishman, M. R., and Westoby, M. (1994a). The role of large seed size in shaded conditions: experimental evidence. *Funct. Ecol.* 8, 205–214. doi: 10.2307/2389903

Leishman, M. R., Wright, I. J., Moles, A. T., and Westoby, M. (2000). "Chapter 2: The evolutionary ecology of seed size," in *Seeds: the Ecology of Regeneration in Plant Communities*, 2nd Edn, ed. M. Fenner (Oxford: CABI Publishing), 31–57. doi: 10.1079/9780851994321.0031

Leslie, A. B., Beaulieu, J. M., and Mathews, S. (2017). Variation in seed size is structured by dispersal syndrome and cone morphology in conifers and other nonflowering seed plants. *New Phytol.* 216, 429–437. doi: 10.1111/nph.14456

Lind, B. M., Menon, M., Bolte, C. E., Faske, T. M., and Eckert, A. J. (2018). The genomics of local adaptation in trees: are we out of the woods yet? *Tree Genet. Genomes* 14:29. doi: 10.1007/s11295-017-1224-y

Looney, C. E., and Waring, K. M. (2013). Pinus strobiformis (southwestern white pine) stand dynamics, regeneration, and disturbance ecology: a review. *For. Ecol. Manag.* 287, 90–102. doi: 10.1016/j.foreco.2012.09.020

Lord, J., Egan, J., Clifford, T., Jurado, E., Leishman, M., Williams, D., et al. (1997). Larger seeds in tropical floras: consistent patterns independent of growth form and dispersal mode. *J. Biogeogr.* 24, 205–211. doi: 10.1046/j.1365-2699.1997.00126.x

Maronna, R. A., Martin, R. D., Yohai, V. J., and Salibián-Barrera, M. (2018). *Robust Statistics: Theory and Methods (with R)*. New York, NY: Wiley.

Martínez, I., García, D., and Obeso, J. R. (2007). Allometric allocation in fruit and seed packaging conditions the conflict among selective pressures on seed size. *Evol. Ecol.* 21, 517–533. doi: 10.1007/s10682-006-9132-x

Mazer, S. J. (1989). Ecological, taxonomic, and life history correlates of seed mass among indiana dune angiosperms: ecological archives M059-001. *Ecol. Monogr.* 59, 153–175. doi: 10.2307/2937284

McGarigal, K., Cushman, S., and Stafford, S. (2000). *Multivariate Statistics for Wildlife and Ecology Research*. New York: Springer Science.

McGarigal, K., and Cushman, S. A. (2002). Comparative evaluation of experimental approaches to the study of habitat fragmentation effects. *Ecol. Appl.* 12, 335–345. doi: 10.1890/1051-07612002012[0335:CEOEAT]2.0.CO;2

Menon, M., Bagley, J. C., Friedline, C. J., Whipple, A. V., Schoettle, A. W., Leal-Sàenz, A., et al. (2018). The role of hybridization during ecological divergence of southwestern white pine (*Pinus strobiformis*) and limber pine (*P. flexilis*). *Mol. Ecol.* 27, 1245–1260. doi: 10.1111/mec.14505

Menon, M., Landguth, E., Leal-Saenz, A., Bagley, J. C., Schoettle, A. W., Wehenkel, C., et al. (2020). Tracing the footprints of a moving hybrid zone under a demographic history of speciation with gene flow. *Evol. Appl.* 13, 195–209. doi: 10.1111/eva.12795

Moreno-Letelier, A., and Piñero, D. (2009). Phylogeographic structure of *Pinus strobiformis* Engelm. across the Chihuahuan Desert filter-barrier. *J. Biogeogr.* 36, 121–131. doi: 10.1111/j.1365-2699.2008.02001.x

Morgenstern, E. K. (1996). *Geographic Variation in Forest Trees. Genetics Basis and Application of Knowledge in Silviculture*. Vancouver, BC: UBC Press.

Ng, F. S. P. (1978). "Strategies of establishment in Malayan forest trees," in *Tropical Trees as Living Systems*, eds P. B. Tomlinson and M. H. Zimmerman (Cambridge: Cambridge University Press), 129–162.

O'Brien, R. A. (2002). *Arizona's Forest Resources, 1999. USDA Forest Service Resource Bulletin RMRS-RB*-2. Ogden, UT: USDA.

Oksanen, J., Blanchet, F. G., Kindt, R., Legendre, P., O'Hara, R. B., Simpson, G. L., et al. (2010). *Vegan: Community Ecology Package. R Package Version 1.17-4*.

Pebesma, E. J., and Bivand, R. S. (2005). Classes and methods for spatial data in R. *R News* 5, 9–13.

Platenkamp, G. A., and Shaw, R. G. (1993). Environmental and genetic maternal effects on seed characters in *Nemophila menziesii*. *Evolution* 47, 540–555. doi: 10.1111/j.1558-5646.1993.tb02112.x

Price, G. R. (1970). Selection and covariance. *Nature* 227, 520–521. doi: 10.1038/227520a0

Prieto-Ruíz, J. A., Bustamante-García, V., Muñoz-Flores, H. J., and Álvarez-Zagoya, R. (2014). "Capítulo 2. Análisis de conos y semillas en coníferas," in *Técnicas en el Manejo Sustentable de los Recursos Naturales. Cuerpo Académico "Manejo de Recursos Naturales y Sustentabilidad"*, eds F. Garza, O. J. A. Guevara, H. M. Villalón, and A. O. Carrillo (Monterrey: Impresión, Universidad Autónoma de Nuevo León), 27–44.

R Development Core Team (2017). *R: A Language and Environment for Statistical Computing*. Vienna: R Foundation for Statistical Computing.

Rawat, K., and Bakshi, M. (2011). Provenance variation in cone, seed and seedling characteristics in natural populations of *Pinus wallichiana* A.B. Jacks (Blue Pine) in India. *Ann. For. Res.* 54, 39–55.

Roach, D. A. (1987). Variation in seed and seedling size in *Anthoxanthum odoratum*. *Am. Midland Natural.* 117, 258–264. doi: 10.2307/2425967

Salas, E. A. L., Valdez, R., and Michel, S. (2017). Summer and winter habitat suitability of Marco Polo argali in southeastern Tajikistan: a modeling approach. *Heliyon* 3:e00445. doi: 10.1016/j.heliyon.2017.e00445

Salisbury, E. J. (1942). *The Reproductive Capacity Of Plants: Studies in Quantitative Biology*. London: G. Bell & Sons.

Salisbury, E. J. (1974). Seed size and mass in relation to environment. *Proc. R. Soc. Lond. Ser. B. Biol. Sci.* 186, 83–88. doi: 10.1098/rspb.1974.0039

Samano, S., and Tomback, D. F. (2003). Cone opening phenology, seed dispersal, and seed predation in southwestern white pine (*Pinus strobiformis*) in southern Colorado. *Écoscience* 10, 319–326. doi: 10.1080/11956860.2003.11682780

Savolainen, O., Pyhäjärvi, T., and Knürr, T. (2007). Gene flow and local adaptation in trees. *Annu. Rev. Ecol. Evol. Syst.* 38, 595–619. doi: 10.1146/annurev.ecolsys.38.091206.095646

Schimpf, D. J. (1977). Seed weight of *Amaranthus retroflexus* in relation to moisture and length of growing season. *Ecology* 58, 450–453. doi: 10.2307/1935621

Schoettle, A. W., Jacobi, W. R., Waring, K. M., and Burns, K. S. (2018). Regeneration for resilience framework to support regeneration decisions for species with populations at risk of extirpation by white pine blister rust. *New For.* 50, 89–114. doi: 10.1007/s11056-108-9679-8

Shimada, T., Takahashi, A., Shibata, M., and Yagihashi, T. (2015). Effects of within-plant variability in seed weight and tannin content on foraging behaviour of seed consumers. *Funct. Ecol.* 29, 1513–1521. doi: 10.1111/1365-2435.12464

Shirk, A. J., Cushman, S. A., Waring, K. M., Wehenkel, C., Leal-Sáenz, A., Toney, C., et al. (2018). Southwestern white pine (*Pinus strobiformis*) species distribution models project a large range shift and contraction due to regional climatic changes. *For. Ecol. Manag.* 411, 176–186. doi: 10.1016/j.foreco.2018.01.025

Sniezko, R. A., Kegley, A. J., and Danchok, R. (2008). White pine blister rust resistance in North American, Asian and European species - results from artificial inoculation trials in Oregon. *Ann. For. Res.* 51, 53–66.

Sorensen, F. C., and Miles, R. S. (1978). Cone and seed weight relationships in Douglas-fir from Western and Central Oregon. *Ecology* 59, 641–644. doi: 10.2307/1938763

Sork, V. L., Aitken, S. N., Dyer, R. J., Eckert, A. J., Legendre, P., and Neale, D. B. (2013). Putting the landscape into the genomics of trees: approaches for understanding local adaptation and population responses to changing climate. *Tree Genet. Genomes* 9, 901–911. doi: 10.1007/s11295-013-0596-x

Steinhoff, R. J., and Andresen, J. W. (1971). Geographic variation in *Pinus flexilis* and *Pinus strobiformis* and its bearing on their taxonomic status. *Silvae Genet.* 20, 159–167.

Stromberg, J. C., and Patten, D. T. (1990). Variation in seed size of a southwestern riparian tree, Arizona Walnut (*Juglans major*). *Am. Midland Natural.* 124, 269–277. doi: 10.2307/2426176

Telenius, A., and Torstensson, P. (1991). Seed wings in relation to seed size in the genus *Spergularia*. *Oikos* 61, 216–222. doi: 10.2307/3545339

Tomback, D. F., and Achuff, P. (2010). Blister rust and western forest biodiversity: ecology, values and outlook for white pines. *For. Pathol.* 40, 186–225. doi: 10.1111/j.1439-0329.2010.00655.x

Van Den Wollenberg, A. L. (1977). Redundancy analysis an alternative for canonical correlation analysis. *Psychometrika* 42, 207–219. doi: 10.1007/BF02294050

Venables, W. N., and Ripley, B. D. (1999). "Chapter 10: Tree-based methods," in *Modern Applied Statistics with S-PLUS*, 3rd Edn, eds J. Chambers, W. Eddy, W. Härdle, S. Sheather, and L. Tierney (New York, NY: Springer-Verlag Press), 303–327.

Villagómez-Loza, M. A., Bello-González, M. A., and Isarain-Chávez, E. (2014). *Pinus strobiformis* Engelmann: Nueva localidad para Guanajuato, México. *Agrociencia* 48, 615–625.

Villalobos-Arámbula, A. R., Pérez de la Rosa, J. P., Arias, A., and Rajora, O. P. (2014). Cross-species transferability of eastern white pine (*Pinus strobus*) nuclear microsatellite markers to five Mexican white pines. *Genet. Mol. Res.* 13, 7571–7576. doi: 10.4238/2014.september.12.24

Violle, C., Navas, M. L., Vile, D., Kazakou, E., Fortunel, C., Hummel, I., et al. (2007). Let the concept of trait be functional! *Oikos* 116, 882–892. doi: 10.1111/j.2007.0030-1299.15559.x

Vittinghoff, E., and McCulloch, C. E. (2007). Relaxing the rule of ten events per variable in logistic and Cox regression. *Am. J. Epidemiol.* 165, 710–718. doi: 10.1093/aje/kwk052

Wahid, N., González-Martínez, S. C., El Hadrami, I., and Boulli, A. (2006). Variation of morphological traits in natural populations of maritime pine (*Pinus pinaster* Ait.) in Morocco. *Ann. For. Sci.* 63, 83–92. doi: 10.1051/forest:20050100

Wang, B., and Ives, A. R. (2017). Tree-to-tree variation in seed size and its consequences for seed dispersal versus predation by rodents. *Oecologia* 183, 751–762. doi: 10.1007/s00442-016-3793-0

Wehenkel, C., Mariscal-Lucero, S. R., Jaramillo-Correa, J. P., López-Sánchez, C. A., Vargas-Hernández, J. J., and Sáenz-Romero, C. (2017). "Genetic diversity and conservation of Mexican forest trees," in *Biodiversity and Conservation of Woody Plants. Sustainable Development and Biodiversity*, Vol. 17, eds M. Ahuja and S. Jain (Cham: Springer), 37–67. doi: 10.1007/978-3-319-66426-2_2

Wehenkel, C., Quiñones-Pérez, C. Z., Hernández-Díaz, J. C., and López-Sánchez, C. A. (2014). "Ecology and Genetics of *Pinus strobiformis*," in *Proceedings of the IUFRO Joint Conference: Genetics of Five-Needle Pines, Rusts of Forest Trees, and Strobusphere*, eds A. W. Schoettle and R. A. Sniezko (Fort Collins, CO: US Department of Agriculture, Forest Service, Rocky Mountain Research Station), 1–6.

Wheeler, N. C., and Guries, R. P. (1982). Population structure, genic diversity, and morphological variation in *Pinus contorta* Dougl. *Can. J. For. Res.* 12, 595–606. doi: 10.1139/x82-091

Wickham, H., Chang, W., and Wickham, M. H. (2013). *Package 'ggplot2'. Computer Software Manual]*. Available online at: http://cran.r-project.org/web/packages/ggplot2/ggplot2.pdf (accessed September 4, 2019).

Williams, C. K., Engelhardt, A., Cooper, T., Mayer, Z., Ziem, A., Scrucca, L., et al. (2018). *Package 'caret', version 6.0-80. [Online]*. Available online at: https://cran.r-project.org/web/packages/caret/caret.pdf (accessed September 26, 2019).

Winn, A. A. (1988). Ecological and evolutionary consequences of seed size in *Prunella vulgaris*. *Ecology* 69, 1537–1544. doi: 10.2307/1941651

Zhang, C., Li, X., Chen, L., Xie, G., Liu, C., and Pei, S. (2016). Effects of topographical and edaphic factors on tree community structure and diversity of subtropical mountain forests in the lower lancang river basin. *Forests* 7:222. doi: 10.3390/f7100222

Conflict of Interest: The authors declare that the research was conducted in the absence of any commercial or financial relationships that could be construed as a potential conflict of interest.

frontiers in Plant Science

ORIGINAL RESEARCH
published: 11 November 2020
doi: 10.3389/fpls.2020.528550

Overexpression Levels of *LbDREB6* Differentially Affect Growth, Drought, and Disease Tolerance in Poplar

Jingli Yang[1†], Hanzeng Wang[1†], Shicheng Zhao[2], Xiao Liu[1], Xin Zhang[1], Weilin Wu[3] and Chenghao Li[1]*

[1] State Key Laboratory of Forest Genetics and Breeding, Northeast Forestry University, Harbin, China, [2] School of Pharmacy, Harbin University of Commerce, Harbin, China, [3] Agriculture College of Yanbian University, Yanji, China

The application of drought stress-regulating transcription factors (TFs) offers a credible way to improve drought tolerance in plants. However, many drought resistant TFs always showed unintended adverse effects on plant growth or other traits. Few studies have been conducted in trees to evaluate and overcome the pleiotropic effects of drought tolerance TFs. Here, we report the dose-dependent effect of the *Limonium bicolor LbDREB6* gene on its overexpression in *Populus ussurensis*. High- and moderate-level overexpression of *LbDREB6* significantly increased drought tolerance in a dose-dependent manner. However, the OE18 plants showed stunted growth under normal conditions, but they were also more sensitive to *Marssonina brunnea* infection than wild type (WT) and OE14 plants. While, OE14 showed normal growth, the pathogen tolerance of them was not significantly different from WT. Many stress-responsive genes were up-regulated in OE18 and OE14 compared to WT, especially for OE18 plants. Meanwhile, more pathogen tolerance related genes were down-regulated in OE18 compared to OE14 and WT plants. We achieved improved drought tolerance by adjusting the increased levels of exogenous *DREB* genes to avoid the occurrence of growth reduction and reduced disease tolerance.

Keywords: poplar, drought stress, dehydration responsive element binding transcription factor, dwarf, disease tolerance

OPEN ACCESS

Edited by:
Sanushka Naidoo,
University of Pretoria, South Africa

Reviewed by:
Ertugrul Filiz,
Duzce University, Turkey
Jiyi Zhang,
BASF, United States

****Correspondence:***
Chenghao Li
chli@nefu.edu.cn;
chli0@163.com

[†]These authors have contributed equally to this work

Specialty section:
This article was submitted to Plant Abiotic Stress, a section of the journal Frontiers in Plant Science

Received: *21 January 2020*
Accepted: *06 October 2020*
Published: *11 November 2020*

Citation:
Yang J, Wang H, Zhao S, Liu X, Zhang X, Wu W and Li C (2020) Overexpression Levels of LbDREB6 Differentially Affect Growth, Drought, and Disease Tolerance in Poplar. Front. Plant Sci. 11:528550. doi: 10.3389/fpls.2020.528550

INTRODUCTION

Drought is among the most serious environmental stressors resulting in substantial damage annually to the global agricultural and forestry industries (Kudo et al., 2017). Thus, improving drought tolerance of plants is urgently needed to stabilize the global productivity of crops. Vascular plants have evolved complex molecular strategies to cope with water deficit (Lata and Prasad, 2011; Li et al., 2014). In particular, vascular plants mediate some stress responses to drought via transcription factors (TFs), which serve as master regulators of many stress-response genes (Singh et al., 2002; Nakashima et al., 2014). Therefore, TFs may comprise critical targets for transgenic engineering to modify the tolerances of plants to abiotic stressors (Quan et al., 2010). However, the application of TFs to improve drought tolerance frequently comes at the cost of introducing undesired phenotypes, such as dwarfism, decreased pathogen tolerance, and decreased grain yield (Lata and Prasad, 2011; Bhargava and Sawant, 2013; Cabello et al., 2014; Shavrukov et al., 2016). These negative effects constrain the practical utilization of drought-resistant transgenic plants based

on TFs. Thus, to evaluate the drought tolerance conferred by TFs, it is necessary to simultaneously predict and avoid unintended effects in transgenic plants.

These TFs, especially the dehydration responsive element binding (DREB) factor family member, occur in many plant species and confer tolerance to abiotic stress (Lin et al., 2008; Liao et al., 2017). In *Arabidopsis thaliana* (L.) Heynh., the DREB subfamily is divided into six subgroups (A-1 to A-6) based on the structural characteristics of the proteins (Agarwal et al., 2017). Among the subgroups, A-1 and A-2 contain *DREB1* and *DREB2* TFs, which are known to be involved in stress responses to low temperature, drought, and high salt (Du et al., 2018). In *Arabidopsis*, *DREB2* positively regulates the expression of drought-response genes (Sakuma et al., 2006). Overexpression of Glycine max *DREB1* (*GmDREB1*) improved drought tolerance and responses to other abiotic stressors in transgenic *Arabidopsis* and wheat (Kidokoro et al., 2015; Zhou et al., 2020). Moreover, ectopic expression of *GhDREB1* from cotton yielded stronger tolerance to chilling in transgenic *Nicotiana tabacum* L. (tobacco) compared to the wild type (WT) (Shan et al., 2007).

DREBs of the A-6 subgroup have also been identified from several plant species, and their functions in stress responses and development have been characterized. For example, expression of *GhDBP2* is greatly up-regulated during drought, salt exposure, low temperature, and abscisic acid (ABA) treatments in the cotyledons of cotton plants (Huang et al., 2008), and overexpression of *CmDREB6* in chrysanthemum enhanced heat tolerance (Du et al., 2018). Similarly, *JcDREB*, an A-6 subgroup member from *Jatropha curcas* L., a biodiesel plant, was up-regulated by cold, salt, and drought stress, and overexpression of *JcDREB* in transgenic *Arabidopsis* enhanced salt and freezing tolerance (Tang et al., 2011). In tobacco, overexpression of *SsDREB*, an A-6 DREB from halophilic *Suaeda salsa* (L.) Pall., increased salt and drought tolerance compared to WT plants (Zhang et al., 2015).

Although DREBs of several subgroups are known to increase drought tolerance, they have also been shown to inhibit growth in transgenic plants (Huang et al., 2009). For example, *ZmDREB4.1* from maize, repressed cell division and constrained leaf extension and hypocotyl, petiole and stem elongation both natively in transgenic tobacco (Li et al., 2018). Likewise, overexpression of *AtDREB1A* in soybeans led to dwarfism and delayed flowering (Suo et al., 2016).

DREBs are also reported to be involved in the biotic stress signaling pathway. For example, the overexpression of *At DREB1* in *Solanum tuberosum* L. (potato) enhanced tolerance to the fungal pest, *Fusarium solani* (Mart.) Sacc. (1881) (Charfeddine et al., 2015). In contrast, in transgenic *Arabidopsis*, overexpression of *MsDREB2C* improved drought stress tolerance but caused greater sensitivity to the pathogenic bacterium, *Pst* DC3000 (*Pseudomonas syringae* Van Hall, 1904 pv. tomato DC3000), and to the pathogenic fungus, *Alternaria mali* Roberts (1914), compared to WT plants (Zhao et al., 2013). Therefore, a more comprehensive evaluation of DREBs is needed to assess their performance in transgenic plants under combined effects from abiotic and biotic stressors.

Although there are significant advances in our understanding of drought tolerance in trees, especially through model systems such as poplars, there remains a limited number of field-based studies on water stress in transgenic trees, particularly under natural conditions. With respect to DREBs specifically, there have been few studies on the A-6 subgroup in woody plants representing either model or non-model systems. In a study on apples, overexpression of an A-6 subfamily member, *MsDREB6.2*, was found to confer drought tolerance (Liao et al., 2017), similarly to its homolog in *Arabidopsis*, *RAP2.4* (Lin et al., 2008). This result suggests that A-6 DREBs may be involved in stress tolerance in woody plants as they are in herbaceous species. Nevertheless, data are largely lacking, and almost nothing is known about the negative effects of DREBs on growth in transgenic trees or the interactions of DREBs with the biotic stress response. Overall, more tree transgenesis is urgently needed to link physiology, systems biology, and field performance to the benefit of silviculture industries.

In the present study, we investigated the effect of different expression levels of *LbDREB6*, a DREB of the A-6 clade from *Limonium bicolor* (Bunge) Kuntze, on plant growth, drought tolerance, and pathogen susceptibility in transgenic *Populus ussuriensis* Komarov under natural water-deficient conditions. We found that moderate overexpression of *LbDREB6* increased drought tolerance but did not affect plant growth and pathogen susceptibility, while high levels of overexpression of *LbDREB6* caused stunted growth and increased sensitivity to pathogen infections compared to the WT. Our study provides a basis for using genetic modification to improve drought tolerance in poplar while avoiding other adverse traits such as growth inhibition and reduction of disease tolerance, which may have negative implications for woody crop plants.

MATERIALS AND METHODS

Plant Materials and Growth Conditions

Populus ussuriensis clone Donglin plants were grown *in vitro* on 1/2 MS semi-solid medium, with 0.6% w/v agar and 2% w/v sucrose, under irradiation of 16 h-light/8 h-dark cycles with PPFD of 46 μmol $m^{-2}{\cdot}s^{-1}$ at 25°C. The cuttings were subcultured at 4-week intervals.

Vector Construction and Populus Transformation

The coding region of *LbDREB6* (Ban et al., 2011) was fused into ProkII vector under the control of CaMV35S promoter. The binary vector ProkII carried the gene encoding neomycin phosphotransferase as a selection marker. The vector was introduced into *Agrobacterium* strain EHA105 prior to transformation by leaf discs using the method as described by Zhao et al., 2017. Transformants were selected on media containing 50 mg/L kanamycin. All transgenic plants were confirmed by genomic PCR and by mRNA qRT-PCR. qRT-PCR was used to quantify DREB6 transcripts using a conserved sequence (F: TAAGTGGGTGGCTGAGAT; R: CCTTCGGAACCGAATACTG). The *P. ussurensis PuActin*

gene (GeneBank accession number: MH644084) was used as the reference gene. All the primers are listed in **Supplementary Table 1**.

All regenerated WT and transgenic plantlets with well-developed leaf and root systems were transferred to the same size pots containing an autoclaved sand and soil mixture (1:3 v/v) at the same growth period. Potted plants were covered with transparent plastic to maintain high humidity and incubated in a growth chamber at 21°C under a 16 h photoperiod for 2 weeks, and then the cover was removed. The growth characterization was recorded after 3 months. The high-level *LbDREB6* overexpression lines (OE18, OE32, and OE35) and moderate-level *LbDREB6* overexpression lines (OE10, OE14, and OE30) plants were used in the following assay.

WESTERN BLOTTING ANALYSIS

Western blotting was performed as described by Chen et al. (2008). An anti-LbDREB6 polyclonal antibody (goat anti-mouse biotinylated immunoglobulin) was used to recognize LbDREB6. The antibody was prepared by the Institute of Genetics and Developmental Biology, Chinese Academy of Sciences. Immunoreactive polypeptides were visualized by using the Western ECL blotting substrate BeyoECL Moon (Beyotime, China). Imaging was performed using a LAS-4000 imaging system (Fijifilm Life Science, United States).

Growth Characteristics

Hand cut sections of the youngest fully developed leaves of WT, OE18, and OE14 plants that were cultured in a flask were cut transversely at the middle of the leaf and fixed with 4% formaldehyde in phosphate-buffered saline with 0.5% TritonX-100 for 4 h at 23°C in a tube roller. After three 10-min washes, sections were mounted in 0.1 mg·mL^{-1} Calcofluor White in water and imaged using Olympus microscopy (SZX7). Perimeters of leaf parenchyma cells were manually traced in Olympus Fluoview software and plotted. Using the same software, the area of hand cut sections of WT and transgenic plant stems was calculated. The same method was used for cross sections of the stems. For scanning electron microscopy (SEM), stem segments of 1-year-old plants grown in a greenhouse (OE18 and OE14) were glued onto aluminum stubs and placed on a chamber stage that had been precooled to −120°C. The samples were viewed using a VP-SEM instrument (S-3500N, Hitachi, Tokyo, Japan). After the regenerated plantlets were transferred to a greenhouse for 2 months, their height and leaf width of were investigated. Meanwhile, the gibberellic acid (GA) content of shoot tip samples was analyzed following the protocol instructions of the Plant Gibberellic Acid, GA, ELISA kit (San Diego, CA, United States). For GA treatment, plantlets transplanted for 2 months in a greenhouse under natural sunlight were sprayed daily with 100 μM GA_3 for 15 days. After 1 month, the height of WT, OE14, and OE18 plantlets was measured. For each experiment, 10 samples were used with three replicates. Data are presented as means of three biological replicates and error bars represent ±SD.

Drought Tolerance Assay

For plant growth analysis under drought stress, 6-month-old plants grown in pots in the greenhouse were used to conduct experiments. WT, OE14, and OE18 plants were grown under drought conditions for 2 weeks, and re-watered under normal conditions for a 2-week recovery period. The relative water content (RWC,%), chlorophyll content and gas exchange were investigated under drought stress. The growth height of WT and transgenic plant lines were also investigated after re-watering for 2 weeks. Additionally, we cultured the sterile cutting seedling in a flask under 7% PEG6000 treatment for 2 days. All the experiments were repeated three times.

Physiological and Biochemical Analysis

Before conducting the following experiments, plants were subjected to drought contains for 5 days in a greenhouse. Leaf RWC and chlorophyll were extracted and analyzed according to a previously published method (Wang et al., 2016). Leaf gas exchange was measured using a portable open gas exchange system (Li-6400; Li-Cor, Inc., Lincoln, NE, United States) equipped with a light source (Li-6200-02B LED; Li-Cor). The transpiration rate (Tr), stomatal conductance (Gs), and net CO_2 assimilation were measured in mature leaves between 0 and 5 days after drought stress. Environmental conditions in the leaf chamber consisted of a photosynthetic photon flux density of 1,400 μmol $m^{-2}·s^{-1}$, an air temperature of 25°C, and an ambient CO_2 concentration of 400 μmol mol^{-1}. Leaf malondialdehyde (MDA) content was determined as described by Chen et al. (2008). The electrolyte leakage (EL,%) was used to estimate cellular membrane stability, which was detected following the methods described by Gu et al. (2017). Leaf hydrogen peroxide levels were determined as described by Yin et al. (2010). The absorption of the supernatant was read at 390 nm, and the content of H_2O_2 was quantified based on the standard curve. All the experiments were repeated three times.

Inoculation of Poplar With Marssonina Brunnea

Individuals of approximately equal size from WT, OE10, OE14, OE30, OE18, OE32, and OE35 lines after transplantation for 2 months in a growth chamber (25°C temperature, 70% humidity, 16 h/8 h light/dark cycle) were used for inoculation experiments. Plants were inoculated by thoroughly spraying a spore suspension of *M. brunnea* (±10^5 spores mL^{-1}) onto the abaxial leaf surfaces according to the method used by Ullah et al. (2017). Immediately after spraying, each plant was covered with a polyethylene terephthalate bag to maintain high humidity; this was kept in the dark to facilitate spore germination. After 24 h, the bags were removed. Control seedlings were sprayed with distilled water. Leaf infection grade was set according to Zhao et al. (2017). All the experiments were repeated three times.

Transcriptome Analysis

We performed transcriptome analysis on two groups. One group was the fully expanded leaves, respectively, collected from WT and transgenic plant lines (OE14 and OE18) after

drought treatment for 7 days in a greenhouse, and the other group was the apical meristem with two unexpanded young leaves which were harvested from WT, OE14, and OE18 plants after being inoculated with the pathogen *M. brunnea*, for 2 days; samples were immediately frozen in liquid nitrogen for RNA extraction. For each sample, ∼20 μg total RNA of each sample was sent to Annoroad Gene Technology Co., Ltd., Beijing, China for high throughout Illumina HiSeq 4000 sequencing (Illumina, San Diego, CA, United States). Each sample was conducted with three biological replicates and three technical replicates. The clean reads were mapped to *P. trichocarpa* mRNA reference sequence using TopHat (ver. 2.0.9) software (Trapnell et al., 2009). Transcript expression level is measured as fragments per kilobase of transcript per million mapped reads by Cufflinks (Trapnell et al., 2010). The reads per kilobase million (RPKM) value was used as the threshold for judging whether the gene was expressed; $|\log_2 FC| > 1.0$, $P < 0.01$, and a false discovery rate (FDR) < 0.01 were used as a threshold for the differential expression of genes to screen for DEGs. The DEGs and their encoded proteins were annotated by comparing them against NCBI, the Swiss-Prot database, NCBI non-redundant nucleotide sequence database, and non-redundant protein database. Then, the DEGs were imported into the Blast2 GO program (Götz et al., 2008) to identify gene ontology (GO) terms. Singular enrichment analysis in agriGO database[1] was performed to identify significantly enriched GO terms. KEGG Orthology-Based Annotation System 2.0 (KOBAS, [2]) was utilized to identify significantly enriched pathways (Wu et al., 2006; Xie et al., 2011).

qRT-PCR Analysis

RNA was extracted from leaves of WT and transgenic lines of *Populus* exposed to drought stress for 7 days. Randomly selected 17 drought responsive genes in OE14 and OE18 compared to WT plants and six genes related to drought stress in OE18 compared to OE14 plants were verified by qRT-PCR, respectively. The primers used are listed in **Supplementary Table 1**. Furthermore, the selected 14 genes related to disease tolerance (*PP2C, LRR-1, RPS2, RPM1, PYL, ABP19a, WRKY49, WRKY9*, and *NR*) and *GA20ox1* were verified by qRT-PCR. All the experiments were repeated three times. The primer sets used in this study to validate transcriptome data are given in the **Supplementary Table 2**. The raw sequence data of drought stress and pathogen infection RNA-seq experiments have been deposited in the Gene Expression Omnibus with the accession numbers GSE139373 and GSE120118, respectively.

Data Analysis

Statistical testing was performed with IBM SPSS Statistics 21 (IBM Corporation, Armonk, NY, United States). The data were tested by Student's *t*-test ($^*P < 0.05$ or $^{**}P < 0.01$).

[1]http://bioinfo.cau.edu.cn/agriGO/analysis.php

[2]http://kobas.cbi.pku.edu.cn/program.run.do

RESULTS

Effect of High-Level and Moderate-Level LbDREB6 Overexpression on Growth in Transgenic Populus

A total of 11 independent *LbDREB6* overexpressing transgenic poplar lines were obtained by *Agrobacterium*-mediated genetic transformation and were analyzed through PCR. All lines had the expected 1,071 bp PCR product for the *LbDREB6* gene (**Supplementary Figure 1A**). The qRT-PCR results indicated that the expression levels of *LbDREB6* in transgenic plants were significantly higher than that in WT plants (**Figure 1A**). After transplantation for 2 months, the phenotyping experiment demonstrated that plants of most lines that had overexpression levels greater than 10 times that of WT plants were significantly shorter. In comparison, other transgenic lines with overexpression levels lower than 10 times that of the WT showed normal growth (**Figure 1B**). We chose three relatively moderate-level (OE10, OE14, and OE30) and three high-level (OE18, OE32, and OE35) *LbDREB6* overexpression lines to conduct the following assays (**Supplementary Figure 1B**). The western blotting analysis using an anti-LbDREB6 antibody revealed that OE18 had a high LbDREB6 protein expression compared to OE14, which was consistent with the RT-PCR result (**Supplementary Figure 1C**).

Leaf width of OE18 plants was significantly larger than that of WT plants (**Figure 1C**), while the leaf width was not considerably different between OE14 and WT plants (**Figure 1C**). Leaf and stem sizes are dependent on both the number and the size of cells in the organ (Zhou et al., 2013). Cross sections of stems revealed that the primary and secondary xylem rings of OE14 (**Figures 1D,G**) were not significantly different from WT plants (**Figures 1D,F**), while OE18 stems (**Figures 1D,H**) increased significantly compared to the WT plants (**Figures 1D,F**). As quantified by the cross-sectional area measurements, the leaf veins of OE14 (**Figures 1E,J**) was not significantly different from WT plants (**Figures 1E,I**), but the leaf veins of OE18 (**Figures 1E,K**) were 40∼50% larger than the WT plants (**Figures 1E,I**). SEM observation showed that cell walls of OE14 (**Figure 1M**) were not significantly different from WT plants (**Figure 1L**). However, the cell walls of OE18 (**Figure 1N**) were considerably thicker than WT plants (**Figure 1L**).

Comparison of High-Level and Moderate-Level LbDREB6 Overexpression on Drought Tolerance

We examined the effects of drought stress on WT and transgenic poplar plants after growth in a greenhouse for 6 months. Under well-watered conditions, performance did not differ between the WT and the transgenic lines. However, after 7 days of drought stress, leaves of WT plants exhibited extensive dehydration symptoms, but only slight wilting was observed in OE14 and no effect was seen in OE18 (**Figure 2A**). After 14 days of drought stress, most of the WT leaves were chlorotic, while OE14 plant lines had less damage compared to WT plants, and most of the

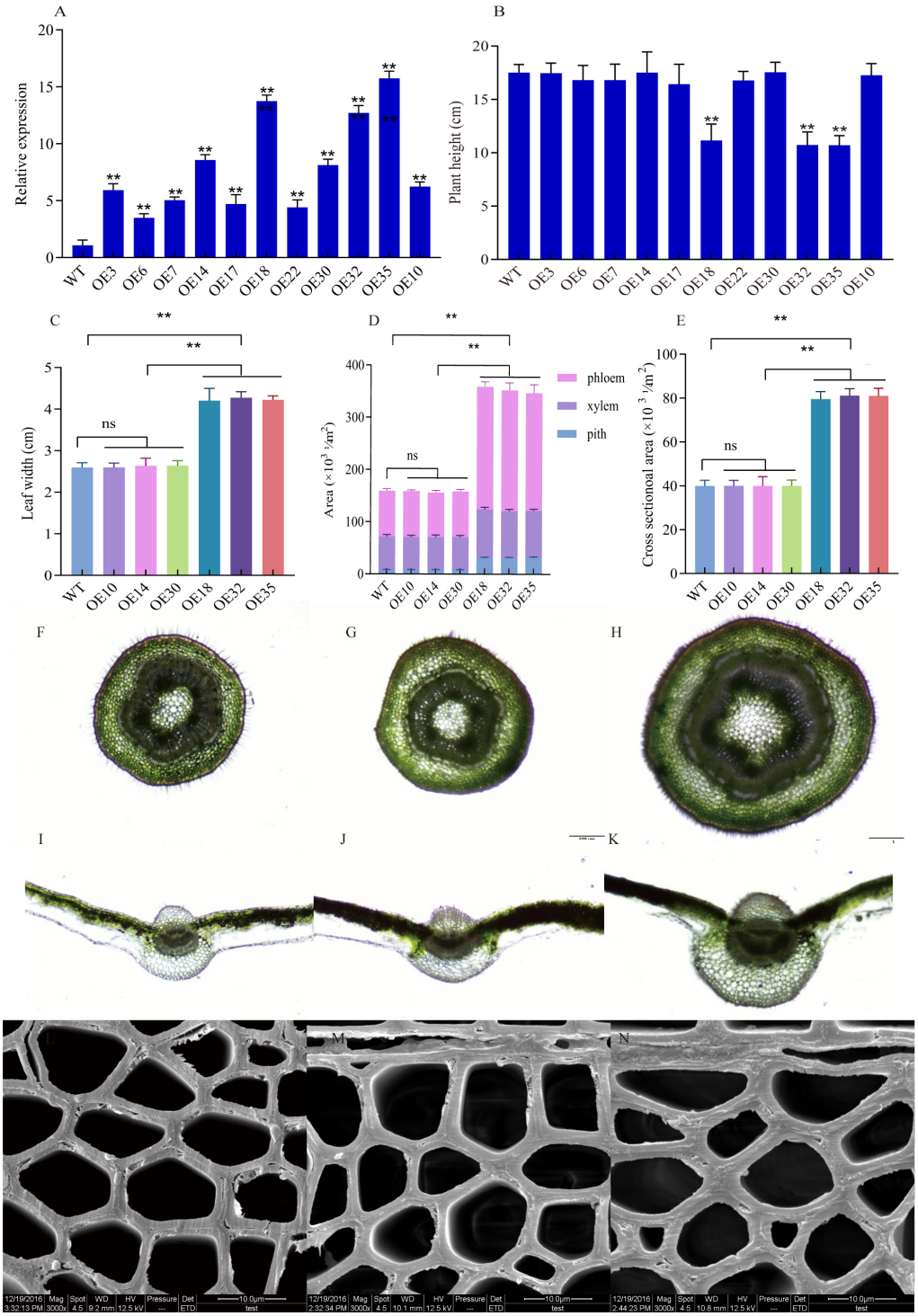

FIGURE 1 | Growth characteristics, cross-section, and scanning electron microscopy (SEM) observation of high-level (OE18) and moderate-level (OE14) *LbDREB6* overexpression lines and wild type (WT) *P. ussuriensis* plants. **(A)** qRT-PCR validations of OE18, OE14, and WT plants. *PtrActin* was used as an internal control. Data are presented as means of four biological replicates, and error bars represent ±SD. **(B)** Heights of OE18, OE14, and WT plants grown in greenhouse for 2 months. **(C)** Leaf widths of WT, OE18, and OE14 plants. **(D)** The quantification of sectioned areas representing bark, wood, and pith regions. **(E)** Midrib cross-sectional areas of WT, OE18, and OE14 plants. Samples were collected at 1 cm from the stem foundation. Cross-section of the stem in WT **(F)**, OE14 **(G)**, and OE18 **(H)** plants. Cross-section of the leaf midrib-xylem in WT **(I)**, OE14 **(J)**, and OE18 **(K)** plants. SEM observation of cell walls in WT **(L)**, OE14 **(M)**, and OE18 **(N)** plants. For **(B–E)**, each value represents the mean of 20 plants with three biological replicates, and error bars represent ±SD. Asterisks indicate significant differences, $^{*}P < 0.05$ and $^{**}P < 0.01$.

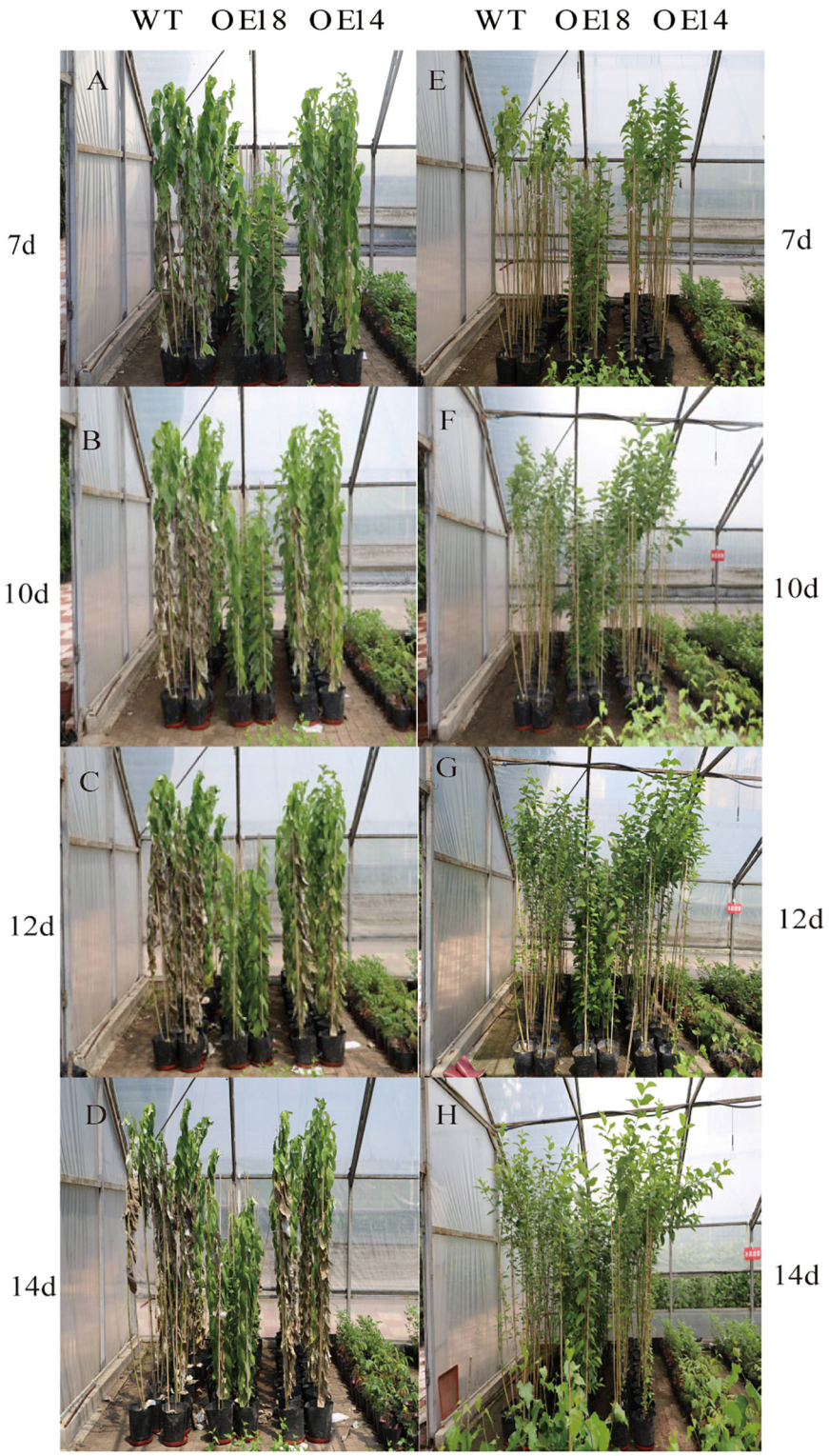

FIGURE 2 | Phenotypic observation of WT and transgenic plant lines under drought stress for **(A)** 7d, **(B)** 10d, **(C)** 12d, **(D)** 14d. Phenotypic observation of WT and transgenic plant lines re-watered for **(E)** 7d, **(F)** 10d, **(G)** 12d, **(H)** 14d.

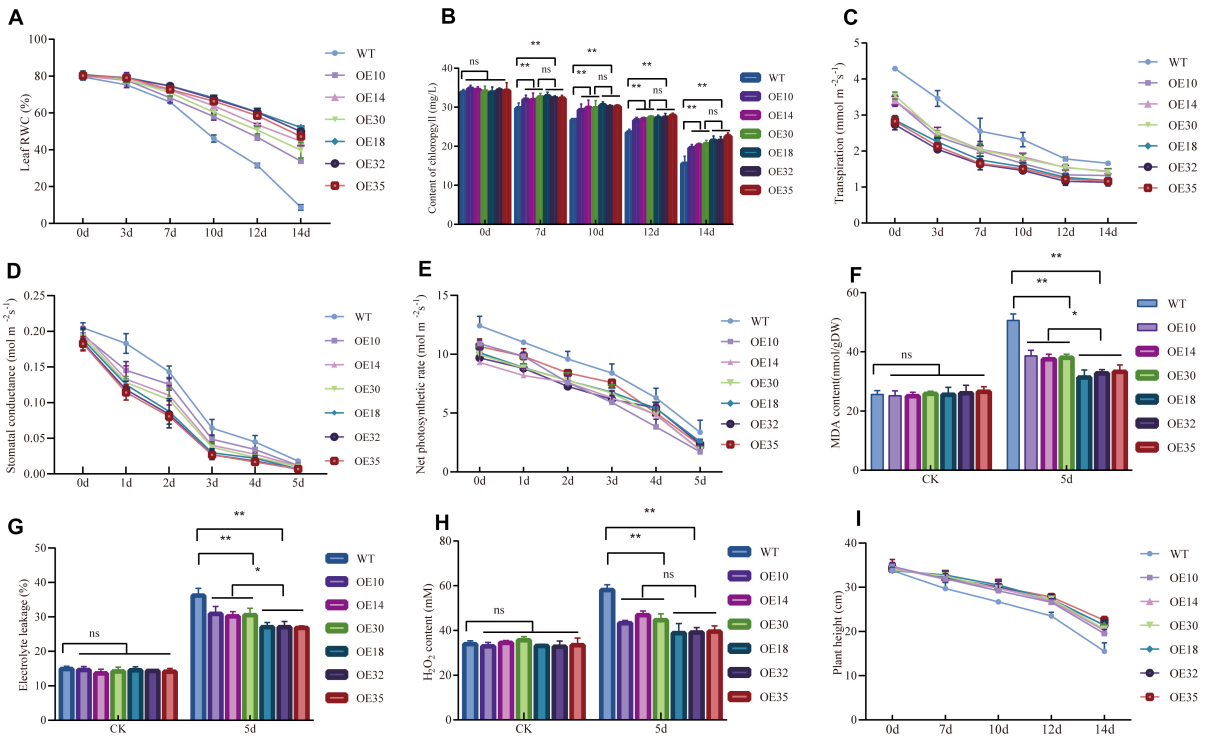

FIGURE 3 | Physiological analysis of *LbDREB6* overexpression lines and WT plants under drought stress. Measurement of leaf relative water content (RWC) **(A)**, chlorophyll content **(B)**, the transpiration **(C)**, stomatal conductance **(D)**, net CO_2 assimilation **(E)**, MDA content **(F)**, electrolyte leakage (EL) **(G)**, and H_2O_2 content **(H)**. **(I)** Plant height after being re-watered for 2 weeks. For **(I)**, each value represents the mean of 20 plants, and error bars represent ±SD. For **(A)** to **(H)**, data are presented as means of three biological replicates, and error bars represent ±SD. Asterisks indicate significant differences, $^*P < 0.05$ and $^{**}P < 0.01$.

OE18 lines were green and vigorous (**Figures 2B–D**). After re-watering for 10 days, OE14 plants recovered faster than the WT plants (**Figures 2E–H**).

During the drought period, the leaf RWC (%) showed a downward trend, especially for WT plants (**Figure 3A**). Furthermore, the chlorophyll level of the transgenic and WT plants also decreased, but the transgenic plants still had a higher chlorophyll content than WT plants (**Figure 3B**). Additionally, the transgenic and WT poplars had remarkable variations in transpiration rate (Tr), stomatal conductance (Gs), and net CO_2 assimilation during the 5 days of drought stress. The Tr and Gs in the transgenic and WT poplars showed an overall decreasing trend but they decreased faster in WT plants than that in transgenic poplars after 2 days of drought stress (**Figures 3C,D**). The net CO_2 assimilation in the transgenic and WT poplars both decreased, but the net CO_2 assimilation in WT poplars decreased much more rapidly than that in the transgenic poplars after drought treatment (**Figure 3E**).

The MDA content (**Figure 3F**) and relative electrical conductance (EL) (**Figure 3G**) of WT and transgenic plants considerably increased after drought treatment. Among them, the MDA content (**Figure 3F**) and EL (**Figure 3G**) in transgenic plants decreased compared with WT plants. Meanwhile, MDA, and EL in high-level *LbDREB6* overexpression plants were less than those in moderate-level *LbDREB6* overexpression plants. The H_2O_2 content in the leaves of WT and transgenic plants was not significantly different compared to that before the treatment (**Figure 3H**). The H_2O_2 content in transgenic plant leaves was lower than that in WT plants after drought treatment, although both showed an increased H_2O_2 content (**Figure 3H**). Moreover, the H_2O_2 content was less in OE18, OE32, and OE35 compared to OE10, OE14, and OE30. After re-watering, the transgenic plants grew vigorously, and the height of OE14 was significantly higher than the WT plants (**Figure 3I**), while, WT plants were affected much more seriously and grew slowly (**Figure 3I**). We also verified the result in the flask, after 7% PEG6000 treatment for 2 days, the leaves of the WT (**Supplementary Figure 2A**) were damaged early and seriously, but the OE14 (**Supplementary Figure 2B**) and OE18 (**Supplementary Figure 2C**) plants still grew normally. This result was consistent with that of the experiment conducted in the greenhouse. Altogether, the transgenic poplars had better tolerance to drought stress than WT plants and high expression levels of *LbDREB6* with less damage suffered from drought stress.

Expression Comparison of Downstream Target Genes Between OE14 and OE18 Leaf Transcriptomes in Response to Drought Stress

We used the Illumina sequencing platform to sequence the leaf transcriptomes of the WT and *LbDREB6*-transgenic plants

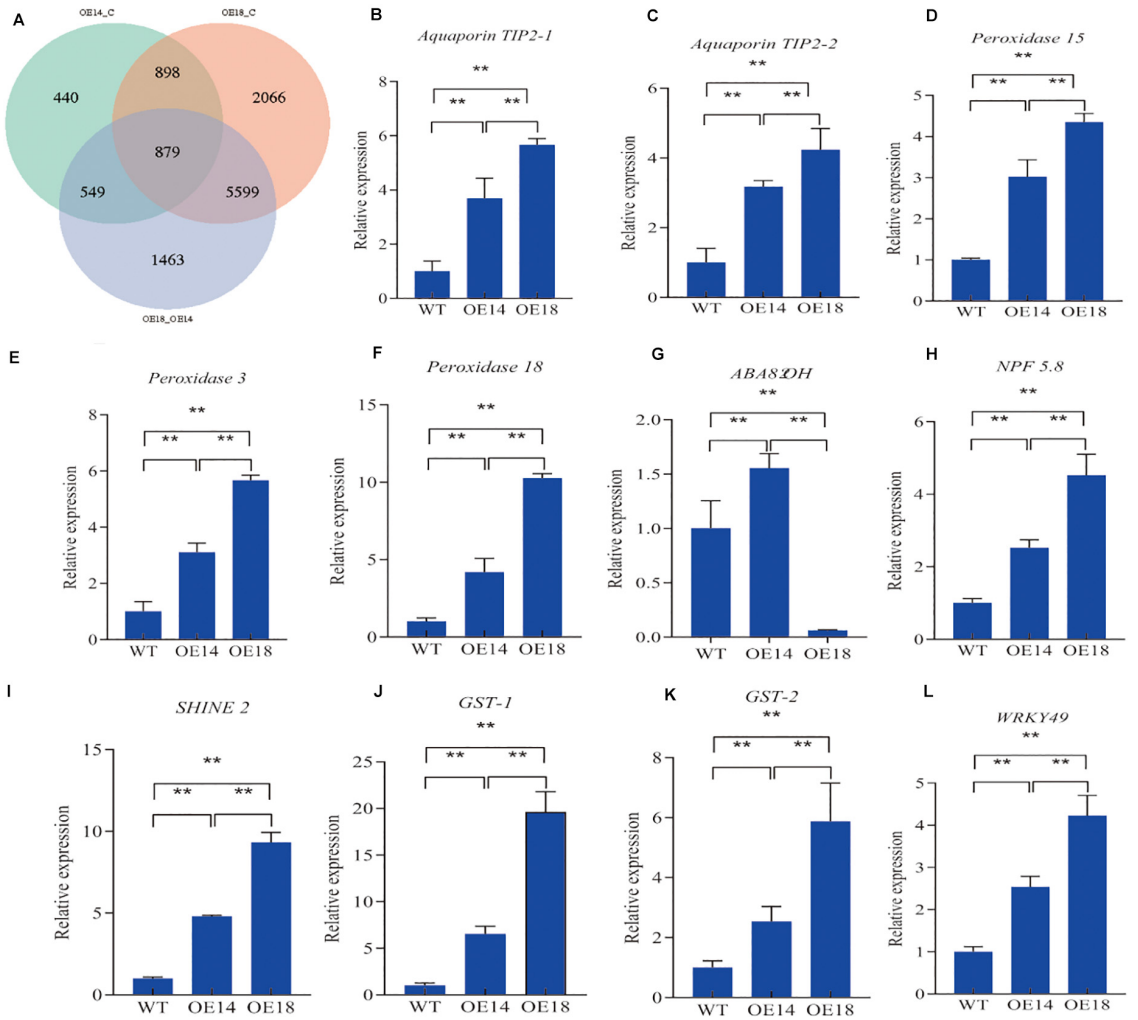

FIGURE 4 | Quantitative real-time PCR analyses of the transcript levels of eight selected DEGs co-up-regulated in high-level (OE18) and moderate-level (OE14) *LbDREB6* overexpression lines compared with WT plants under drought stress for 5 days. **(A)** Venn diagram among WT and OE14, WT and OE18, and OE14 and OE18 plants. Quantitative real-time PCR analyses of the transcript levels of **(B)** *Aquaporin TIP2-1*, **(C)** *Aquaporin TIP2-2*, **(D)** *Peroxidase 15*, **(E)** *Peroxidase 3*, **(F)** *Peroxidase 18*, **(G)** *ABA8'OH*, **(H)** *NPF 5.8*, **(I)** *SHINE2*, **(J)** *GST-1*, **(K)** *GST-2*, **(L)** *WRKY49*. Data are presented as means of three biological replicates, and error bars represent ±SD. Asterisks indicate significant differences, $^{*}P < 0.05$ and $^{**}P < 0.01$.

under drought stress for 7 days. We identified a total of 20698 differentially expressed genes (DEGs) during drought stress ($P < 0.05$ and FDR < 0.001). Among these DEGs, there were 2,766 (1,654 up, 1,112 down, **Supplementary Data 1**) in OE14 and 9,442 (5,862 up, 3,580 down, **Supplementary Data 2**) in OE18 compared to the WT, respectively, and 8,490 (5,213 up, 3,277 down, **Supplementary Data 3**) were identified in OE18 compared to OE14 plants. Finally, a total of 879 DEGs were common in three groups (**Supplementary Data 4** and **Figure 4A**). Of the common 879 DEGs, there were 707 up-regulated and 172 down-regulated genes; we found that multiple drought stress related downstream genes were differentially expressed, such as aquaporin (AQP) tonoplast intrinsic protein (TIP), glutathione S-transferase (*GST*), and some transcriptional factors. To verify the NGS data, the expression levels of eight genes were examined in WT, OE14, and OE18 plants with drought treatment by qRT-PCR (**Figures 4B–H**). It was found that the expression levels of all the genes tested were increased in the transgenic plants compared to the WT plants under drought treatment except *ABA8'OH* and *WRKY46* in OE18 (**Figure 4G**). Among them, the expression levels of seven genes were higher in OE18 than those in OE14 plants (**Figures 4B–F,H–L**), and there were no significant differences in expression levels of the five genes between OE14 and OE18 plants (**Supplementary Figures 4A–E**) except WRKY46 (**Supplementary Figure 4F**). It was likely that these DEGs resulted in drought resistance of OE18 and OE14 when compared to WT plants. In OE18, we also found some DEGs that were probably related to the drought tolerance phenotype when compared to OE14 plants (**Supplementary Data 3**). Most of these DEGs were

up-regulated, for example, major intrinsic protein (*MIP*) (Potri.003G050900, Potri.005G109300, and Potri.006G121700), cellulose synthase-like protein D5 (*CSLD5*) (Potri.014G125100), 2 galactinol synthase genes (*GolS*) (Potri.002G191600 and Potri.010G150400), and 5 late embryogenesis abundant (*LEA*) protein genes (Potri.018G052500, Potri.002G124600, Potri.009G003800, Potri.010G012100, and Potri.010G012100) responded to water deprivation; 2 peroxidase genes (Potri.007G122100 and Potri.018G015500), thioredoxin gene (Potri.001G028500), peptide methionine sulfoxide reductase B5 (*MSRB5*) (Potri.008G198600), L-ascorbate oxidase (Potri.004G010100), and peptide methionine sulfoxide reductase (MSRA) (Potri.T135400) respond to oxidative stress; 3 *ABP19a* (Potri.013G141900, Potri.001G169000, and Potri.003G065300), Metalloendoproteinase 2-MMP (Potri.019G073800), and 2 *GST* (Potri.011G140400 and Potri.011G140600) genes were involved in auxin-activated signaling pathways and development processes. We randomly selected some related genes to conduct qRT-PCR verification. The qRT-PCR analysis result showed that *ABP19a* (Potri.001G169000), *TIP2-1* (Potri.003G050900), *PIP2-8* (Potri.005G109300), *LEA* (Potri.018G052500), and *Peroxidase 18* (Potri.018G015500) were highly induced in OE18 compared to OE14 except *GolS* (Potri.010G15040) (**Supplementary Figure 5**). These results were consistent with the transcriptome data.

Effect of High- and Moderate-Level LbDREB6 Overexpression on Susceptibility to Marssonina Brunnea

After inoculation with the fungus *M. brunnea*, the OE14 line (**Figures 5B,D**) displayed no significant difference in phenotype compared to the WT (**Figures 5A,D**), while the lesion area on OE18 was larger than that of the WT (**Figures 5C,D**). This suggests that the enhanced expression level of *LbDREB6* affects the susceptibility of poplar to the fungus. The MDA content of WT, OE14, and OE18 lines considerably increased after pathogen treatment (**Figure 5E**); the MDA content in OE18 plants was greater than that in WT plants compared to OE14 plants (**Figure 5E**). In addition, the relative EL showed the same trend of change (**Figure 5F**), indicating the leaves of OE18 plants showed severe membrane damage compared to OE14 plants. Overall, the susceptibility to *M. brunnea* infection in OE18 increased and that in OE14 was not altered compared to WT plants.

Comparison of OE18 and OE14 on Expression of Genes Involved in Disease Tolerance Under Pathogen Infection

To determine the possible pathways of LbDREB6 in pathogen defense, we conducted transcriptomic sequencing of leaf inoculated with the pathogen *M. brunnea*, for two days, from which we obtained 53.20 Gb clean reads (18.2–24.7 million per library, Q30 $\geq$ 95.02%). Approximately 68.3–70.42% clean reads per library could be mapped to the *P. trichocarpa* genome (**Supplementary Table 3**). The quality of the assembled transcriptome was appropriate for functional annotation and further analysis compared with the WT.

Based on the transcriptome annotation, a total of 688 DEGs were identified in OE18 when compared to both the WT and OE14 plants (**Figure 6A** and **Supplementary Data 3**). In total, 58 DEGs related to disease tolerance were identified in OE18 plants including 41 up-regulated and 17 down-regulated genes (**Supplementary Data 3**). Plants have two different plant–pathogen interaction sub-pathways, pattern triggered immunity (PTI) and effector-triggered immunity (ETI) (He et al., 2015). In PTI, there were 17 genes differently expressed in OE18 when compared to both the WT and OE14 plants, including translated nucleotide-binding leucine-rich repeat (NB-LRR) kinase EFR, two WRKY TFs (WRKY49 and WRKY7), three ubiquitin E3 ligases, and some receptor-like proteins involved in immune response and regulating the expression downstream defense-related genes. In ETI, we found that two disease tolerance proteins RPM1 and one disease tolerance protein RPS2 were down-regulated. In addition, two nitrite reductase differentially induced genes were down-regulated in OE18 when compared to both the WT and OE14 plants. KEGG enrichment revealed that DEGs related to plant hormone signal transduction, followed by plant–pathogen interactions and biosynthesis of amino acids were enriched in OE18 plants when compared to both the WT and OE14 plants (**Figure 6B**); similarly, plant hormone signal transduction and plant–pathogen interactions were enriched in OE18 plants compared with both WT and OE14 plants (**Figure 6C**). In plant hormone pathways, one PYR/PYL family protein, two protein phosphatases 2C (PP2C), and two auxin-binding proteins ABP19a were also differentially expressed.

We selected some DEGs involved in plant–pathogen interaction pathways and ABA regulation to conduct qRT-PCR analysis. The result showed *PP2C-1, NB-LRR-1, NB-LRR-2, RPS2, RPM1-1, RPM1-2, PYL4, WRKY49*, and *NR* genes were down-regulated in OE18 plants when compared to both the WT and OE14 plants (**Figure 7**).

Effect of High-Level and Moderate-Level LbDREB6 Overexpression on GA20ox1 Gene Expression

We found that the *GA 20-oxidase 1* (*GA20ox1*) gene was down-regulated in OE18 plants when compared to both WT and OE14 plants from the shoot tip transcriptome dataset. The qRT-PCR results showed that the expression level of *GA20ox1* in OE18 was decreased to ∼50 and 49% when compared to the WT plants and OE14, respectively (**Figure 8A**). However, the expression of *GA20ox1* was not significantly different between the OE14 and WT plants (**Figure 8A**). To investigate if there is a difference in GA content between WT and transgenic plants, all samples of shoot tips were harvested after plants were transplanted into pots for 2 months. There was no significant difference between the WT or moderate-level *LbDREB6* overexpression plants, but GA in high-level *LbDREB6* overexpression plants was significantly lower, by ∼25%, when compared to the WT plants (**Figure 8B**). This was consistent with the gene expression pattern of *GA20ox1* in the samples (**Figure 8A**). To examine whether the dwarf phenotype was caused by GA deficiency, we cultivated WT and transgenic plantlets transplanted in a

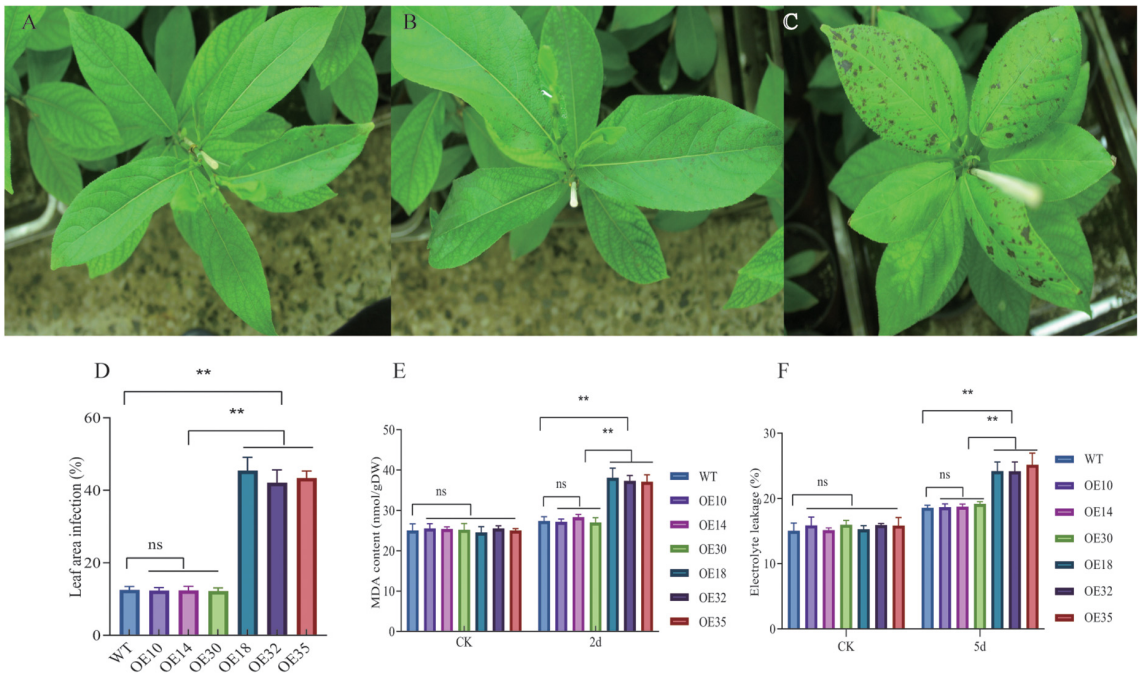

FIGURE 5 | Comparison of *LbDREB6* overexpression lines and WT leaves after *Marssonina brunnea* infection. The WT **(A)**, OE14 **(B)**, and OE18 **(C)** plants after being infected with *M. brunnea* for 2 days. Bar = 2cm. **(D)** Measurement of leaf disease indices. Each value represents the mean of 20 plants, and error bars represent ±SD. Measurement of MDA content **(E)** and electrolyte leakage (EL) **(F)** after being infected with *M. brunnea* for 2 days. Data are presented as means of three biological replicates, and error bars represent ±SD. Asterisks indicate significant differences, $^{*}P < 0.05$ and $^{**}P < 0.01$.

greenhouse under natural sunlight for 2 months and they were sprayed daily with 100 μM GA_3 for 15 days. Under these conditions, the height of the transgenic as well as the WT plants increased rapidly, especially for OE18 plants (**Supplementary Figure 3**). The increased ratio of OE18 plant height was higher than that of WT plants (**Supplementary Figure 3**). These results demonstrated that high-level overexpression of *LbDREB6* decreased growth rate, probably by inhibiting GA synthesis, while moderate overexpression of *LbDREB6* did not change the normal growth of transgenic *P. ussuriensis*.

DISCUSSION

Increasingly, numerous studies are showing that DREBs have crucial roles in regulating plant development and responses to both abiotic and biotic stresses. However, there have been only a few studies to date to investigate the multi-directional effects of DREBs in trees. In the present study, we overexpressed *LbDREB6* in poplar to investigate the role of this A-6 DREB TF in regulating plant growth, drought tolerance, and disease tolerance. We found that in the transgenic line of poplar with high levels of overexpression of *LbDREB6*, drought tolerance was greatly improved, but growth was inhibited, and there was a decreased tolerance to fungal pathogens. In contrast, in the plants having a moderate level of overexpression of *LbDREB6*, we observed drought tolerance along with normal growth and no effects on pathogen tolerance. Our study suggests that drought tolerance can be improved by carefully adjusting the levels of overexpression of DREB TF genes to avoid the occurrence of unfavorable effects.

The abilities of plants to respond to drought stress can sometimes be predicted by their varying capacities to modulate key physiological and biochemical responses at the cellular level, including changes in membrane integrity, internal water balance, and the accumulation of osmolytes and antioxidants (Kang et al., 2011). MDA, the final product of lipid-peroxidation, is one well-known marker of cell membrane injury (Taulavuori et al., 2001; Anjum et al., 2015), while accumulation of reactive oxygen species (ROS) can be scavenged by antioxidants (Royer and Noctor, 2003). Our results showed that the levels of MDA, H_2O_2, and ROS, in plants overexpressing *LbDREB6* under water deficit conditions were lower compared to WT plants. The lower levels of H_2O_2 may indicate that *LbDREB6* conferred enhanced protection from oxidative damage and a better ROS scavenging ability in the transgenic plants. Lower MDA levels seem to indicate that the transgenic plants had greater membrane integrity to withstand cellular-level effects of water loss. Our results were similar to observations in *35S:MsDREB6.2*-transgenic apple, which had improved tolerance to drought stress (Liao et al., 2017) and coincided with lower levels of ROS and MDA. Another measure of membrane integrity is EL (Gu et al., 2017). In this study, the lower rate of increase in EL in plants overexpressing *LbDREB6* suggests that less cell damage occurred from drought stress. This physiological change within the overexpression lines may account for the

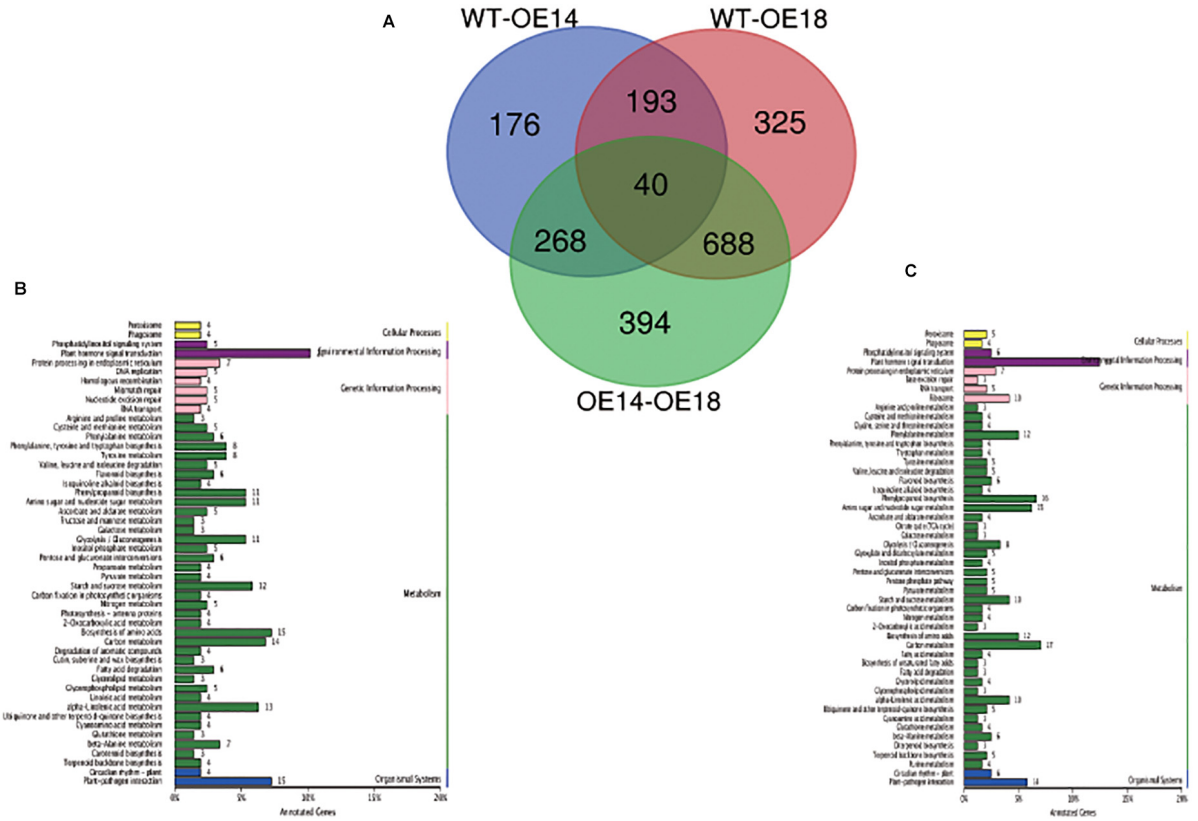

FIGURE 6 | Venn diagram and KEGG classification of the DEGs among high-level (OE18) and moderate-level (OE14) *LbDREB6* overexpression lines and WT *P. ussuriensis* plants after infection with *Marssonina brunnea*. **(A)** Venn diagram among WT and OE14, WT and OE18, and OE14, and OE18 plants. **(B)** KEGG classification of differentially expressed genes between WT and OE18 lines. **(C)** KEGG classification of differentially expressed genes between OE14 and OE18 lines.

higher RWC compared to WT plants under drought stress. These results indicate that the *LbDREB6*-overexpressing plants achieved better water balance to alleviate water deficiency and had higher drought tolerance compared to the non-transgenic WT plants. Additionally, both OE14 and OE18 showed better growth compared to WT plants under drought stress, though the OE18 line exhibited greater drought tolerance than OE14.

When the plants were subjected to drought stress, a large number of genes were differentially expressed compared to plants under normal growth conditions, and subsequently, many protein or metabolic products were generated to help protect the plant from drought stress. In this study, overexpression of *LbDREB6* yielded increased transcription of many downstream genes. This is expected because TFs like *LbDREB6* are significant upstream regulatory proteins, which play a major role in multiple pathways when plants are subjected to drought stress (Ning et al., 2011). Prior studies also revealed that transcription of downstream genes was increased when DREB TFs were up-regulated. For example, *MdSHINE2* from apple (a homolog of *AtSHINE2* in *Arabidopsis*), an A-6 DREB, conferred drought tolerance by regulating wax biosynthesis (Zhang et al., 2019). Similarly, *Arabidopsis* transformed with *GmWRKY54*, an A-6 DREB from soybean, conferred salt and drought tolerance, possibly through the regulation of *DREB2A* and *STZ/Zat10* (Zhou et al., 2008). Additionally, *RAP2.4* in *Arabidopsis* regulated the expression of the plasma membrane intrinsic protein (PIP) and TIP subfamilies of AQPs, which are integral membrane proteins, in response to drought stress (Rae et al., 2011). AQPs, especially PIP and TIP, are believed to play key roles in maintaining water homeostasis (Alexandersson et al., 2005; Rae et al., 2011).

In the current study, we found differential expression of several genes involved in drought response pathways between the transgenic lines and the WT. Notably, we found that two *GST* genes, which constitute part of an antioxidant defense system, were induced in transgenic *LbDREB6* overexpression lines. Activation of the GST antioxidant system occurred in response to ROS (Noctor et al., 2014; Fox et al., 2017) and indicates that the poplar trees were protected from ROS that resulted from drought. We also found that a key regulator of ABA catabolism, *ABA8'OH* (Potri.004G235400), was down-regulated in the OE18 line when compared to OE14. ABA is an important phytohormone that regulates plant water use, and thus, it is correlated with drought tolerance. While ABA can be applied exogenously to facilitate drought tolerance, this approach has limited utility because ABA is rapidly inactivated. Therefore, genes that regulate levels of endogenous ABA are of critical importance to develop drought resistant crops (Takeuchi et al., 2016). Down-regulation of

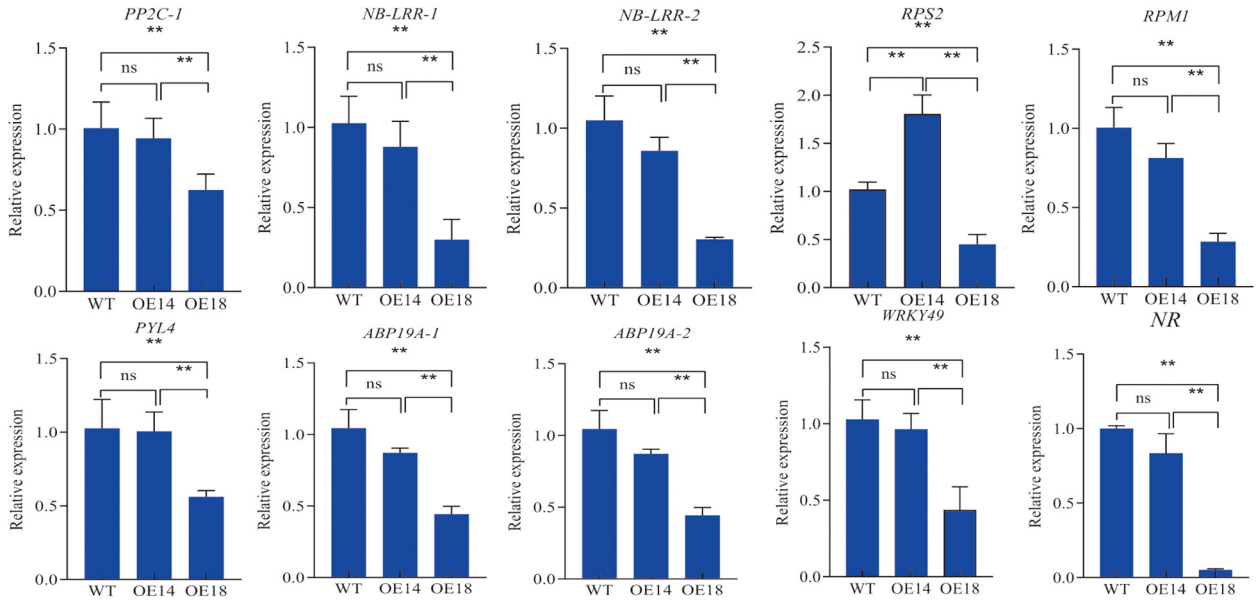

FIGURE 7 | Quantitative real-time PCR analyses of the transcript levels of disease tolerance related genes in leaves of high-level (OE18) and moderate-level (OE14) *LbDREB6* overexpression lines and WT *P. ussuriensis* plants under *M. brunnea* infection treatment. Data are presented as means of three biological replicates, and error bars represent ±SD. Asterisks indicate significant differences, $^{*}P < 0.05$ and $^{**}P < 0.01$.

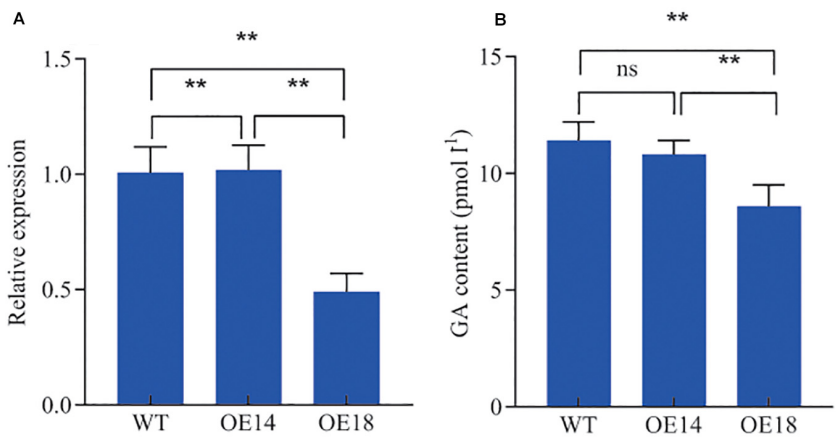

FIGURE 8 | Quantitative real-time PCR analyses of the transcript levels of the *GA20ox1* gene and GA content detection in leaves of high-level (OE18) and moderate-level (OE14) *LbDREB6* overexpression lines and WT *P. ussuriensis* plants. **(A)** qRT-PCR analysis of the *GA20ox1* gene. **(B)** GA content determination in leaves of WT and transgenic plants. Data are presented as means of three biological replicates, and error bars represent ±SD. Asterisks indicate significant differences, $^{*}P < 0.05$ and $^{**}P < 0.01$.

ABA8'OH should decrease catabolism of ABA, and therefore probably improves drought tolerance in the OE18 line. Taken together, these results suggest that *LbDREB6* can regulate large groups of stress-related genes, and subsequently, promote enhanced tolerance against drought stress.

Other genes known for their involvement in drought response, such as *MIP*, *TIP*, *GolS*, and *LEA*, showed a greater change in expression levels in the OE18 plants compared to OE14. *GolS* of *Arabidopsis*, *GolSAt2*, has been reported to confer drought tolerance and increase grain yield in transgenic rice (*Oryza sativa* L.) under dry field conditions (Selvaraj et al., 2017). *LEA* of wheat, *TaLEA3*, overexpressed in *Phellodendrons amurense* yielded tolerance to drought stress by rapid stomatal closure (Yang et al., 2018). Differential expression of homologs of these genes in OE18 may help to explain why this line is more drought resistant than OE14 at the transcriptional level.

Gibberellic acid, the most important hormone regulating shoot elongation, plays an important role in determining plant height (Richards et al., 2001). One critical gene family that participates in GA synthesis and degradation is *GA20ox*, an oxidase (Hedden and Phillips, 2000; Wuddineh et al., 2015). Decreasing the level of expression of *GA20ox* causes severe dwarf

phenotypes in some species due to reduced levels of active GAs. In tomato, *SlDREB* is known to act as a positive regulator in drought stress responses, but overexpression caused the dwarf phenotype via down-regulation of *GA20oxs* as well as ent-copalyl diphosphate synthase (*SlCPS*), another gene in the GA synthesis pathway (Li et al., 2012). The dwarf phenotype also affected *DREB1B/CBF1* transgenic tomato, which could be rescued by exogenous application of GA_3 (Hsieh et al., 2002). The expression levels of GA biosynthetic genes, including *OsGA20ox1*, were significantly reduced in rice plants overexpressing *JcDREB2* of *Jatropha curcas* (Tang et al., 2017). Similarly, here, we found that the expression level of *GA20ox1* in OE18 was decreased by ∼50% when compared to WT and OE14 plant lines, and OE18 showed lower GA content. The expression level of *GA20ox1* was not significantly different between the WT and OE14, which were also similar in height. Therefore, it appears that dwarfism due to overexpression of *LbDREB6* results from an interaction that down-regulates expression of the *GA20ox* gene family, and consequently, reduces the levels of GAs.

The poplar rust fungus, *Marssonina brunnea* (Ellis and Everh.) Magnus causes significant yield reduction and severe economic losses in commercial poplar plantations. In our study, OE18 was more sensitive to *M. brunnea* infection compared to both OE14 and WT plants, while we detected no difference between OE14 and WT plants. This suggests that tolerance to fungal infection was reduced by overexpression of *LbDREB6*. Briefly, plants have two tiers of responses to microbial and fungal pathogens: pattern triggered immunity (PTI) at epidermal layers in response to the pathogens themselves and effector triggered immunity (ETI), which responds to metabolites produced by pathogens after an infection is established (Boller and He, 2009). Both PTI and ETI recognize pathogen infection according to arrays of receptors that include kinases, TFs, and plant hormones (He et al., 2015). Additionally, pathogenic response in plants is mediated by plant hormones, such as salicylic acid, jasmonic acid, and ABA, which act as secondary messengers (Mauch-Mani and Mauch, 2005; He et al., 2015). We found that multiple pattern recognition receptors that participate in the PTI system, especially EF-Tu receptors (ETRs), were differentially expressed in the OE18 line, in which they were largely down-regulated compared to OE14 and WT plants. In particular, we observed that the ETRs, WRKY (WRKY49 and WRKY7), *RPM1, RPS2*, and *NOS* were down-regulated in OE18. WRKY TFs are known to play important roles in transcriptional reprogramming in response to various stressors including pathogen infection in plants. For example, in rice, *OsWRKY67* improved tolerance against two pathogens, *Magnaporthe oryzae* (T. T. Hebert) M. E. Barr and *Xanthomonas oryzae oryzae* (Vo et al., 2018). *NOS* genes regulate the production of nitric oxide, which is involved in the plant pathogenic response (Arasimowicz-Jelonek and Floryszak-Wieczorek, 2014). Thus, down-regulation of *NOS* in OE18 likely led to reduced nitric oxide, and therefore, decreased pathogen tolerance. Additionally, several genes affecting levels of ABA were also down-regulated in OE18. Specifically, we found that ABA receptors, including one *PYL4* and one *PP2C*, were down-regulated in OE18 as well as ABA responsive element binding factor (ABF), which encodes a basic leucine zipper TF. The PYR/PYL family of proteins positively regulate ABA response in various tissues by inhibiting the interaction of PP2C with a protein kinase, SnRK2 (Umezawa et al., 2009). Then, this complex stimulates the expression of ABF, which enhances tolerance to necrotrophic pathogens (Umezawa et al., 2009). Thus, we proposed that high levels of overexpression of *LbDREB6* yielded decreased tolerance to *M. brunnea* due to effects on the PTI system and actions of ABA. However, this behavior of *LbDREB6* merits further study.

CONCLUSION

In previous studies, the overexpression of DREBs in transgenic plants improved drought tolerance but with varying levels of growth inhibition under non-drought conditions. Our results show that the higher the overexpression level of the *LbDREB6* gene, the stronger the drought tolerance in *Populus ussuriensis*. However, under high levels of overexpression of *LbDREB6,* poplar trees exhibited growth inhibition and decreased tolerance to fungal infection. In contrast, under moderate levels of overexpression *LbDREB6,* poplar trees showed normal growth and no effect on fungal tolerance. These results provide novel insight into the regulation of plant growth by *LbDREB6* and its roles in diverse responses to biotic and abiotic stressors. Additionally, our study provides a method to achieve improved drought tolerance by adjusting the levels of overexpression of *DREB* genes to avoid the occurrence of unfavorable traits, such as decreased growth rate and reduced disease tolerance.

DATA AVAILABILITY STATEMENT

Publicly available datasets were analyzed in this study. This data can be found here: GSE139373 and GSE120118.

AUTHOR CONTRIBUTIONS

CL designed and conceived the experiments. JY and HW performed the experiments. SZ and XL analyzed the data. XZ and WW revised the manuscript. CL and JY wrote the manuscript. All authors reviewed and approved the manuscript.

FUNDING

This work was supported by the National Natural Science Foundation of China (31870649), the 111 Project (B16010), the Fundamental Research Funds for the Central Universities (2572016AA01), and Heilongjiang Touyan Innovation Team Program (Tree Genetics and Breeding Innovation Team).

ACKNOWLEDGMENTS

The authors acknowledge TopEdit (www.topeditsci.com) for the linguistic editing and proofreading during the preparation of this manuscript.

SUPPLEMENTARY MATERIAL

The Supplementary Material for this article can be found online at: https://www.frontiersin.org/articles/10.3389/fpls.2020.528550/full#supplementary-material

Supplementary Figure 1 | Generation and transplantation of *LbDREB6* transgenic *Populus ussuriensis* lines. **(A)** PCR validations on OE lines; M, DNA Marker DL2000; P, pROKII-GFP plasmid used as the positive control, N, gDNA of the wild type (WT) plant was utilized as the PCR templates for the negative control; lanes 4–12, gDNA of *LbDREB6* overexpression lines were utilized as the PCR templates for lane 4–7. **(B)** Transplantation of *in vitro* plants with well-developed leaf and root systems in pots containing autoclaved sand and soil mixture (1:3 v/v) for 3 months. Left: WT, middle: OE14 line, right: OE18 line. **(C)** Detection of the LbDREB6 protein in transformed *P. ussuriensis* by Western blotting.

Supplementary Figure 2 | Exogenous GA 3 effectively reverses the GA-deficiency phenotype. Data are presented as means of three biological replicates, and error bars represent ±SD. Asterisks indicate significant differences, $^{*}P < 0.05$ and $^{**}P < 0.01$.

Supplementary Figure 3 | Quantitative real-time PCR analyses of the transcript levels of eight selected DEGs co-up-regulated in high-level (OE18) and moderate-level (OE14) *LbDREB6* overexpression lines compared to WT plants under drought stress for 5 days. **(A)** *DREB2C*. **(B)** *Peroxidase 6*. **(C)** *ATHB-13*. **(D)** *MFYA*. **(E)** *WRKY40*. **(F)** *WRKY46*. Data are presented as means of three biological replicates, and error bars represent ±SD. Asterisks indicate significant differences, $^{*}P < 0.05$ and $^{**}P < 0.01$.

Supplementary Figure 4 | Quantitative real-time PCR analyses of the transcript levels of eight selected DEGs co-up-regulated in in high-level (OE18) and moderate-level (OE14) *LbDREB6* overexpression lines compared to WT plants under drought stress for 5 days. Data are presented as means of three biological replicates, and error bars represent ±SD. Asterisks indicate significant differences, $^{*}P < 0.05$ and $^{**}P < 0.01$.

Supplementary Table 1 | Primers used in qRT-PCR analysis for genes responsive to drought.

Supplementary Table 2 | Primers used in qRT-PCR analysis for disease tolerance related genes.

Supplementary Table 3 | Statistical analysis of sequencing.

Supplementary Data 1 | The differentially expressed genes in OE14 compared to the WT plant.

Supplementary Data 2 | The differentially expressed genes in OE18 compared to the WT plant.

Supplementary Data 3 | The differentially expressed genes in OE18 compared to the OE14 plant.

Supplementary Data 4 | Genes related to disease tolerance in OE18 line compared to the WT and OE14 lines.

REFERENCES

Agarwal, P. K., Gupta, K., Lopato, S., and Agarwal, P. (2017). Dehydration responsive element binding transcription factors and their applications for the engineering of stress tolerance. *J. Exp. Bot.* 68, 2135–2148. doi: 10.1093/jxb/erx118

Alexandersson, E., Fraysse, L., Sjovall-Larsen, S., Gustavsson, S., Fellert, M., Karlsson, M., et al. (2005). Whole gene family expression and drought stress regulation of aquaporins. *Plant Mol. Biol.* 59, 469–484. doi: 10.1007/s11103-005-0352-1

Anjum, N. A., Sofo, A., Scopa, A., Roychoudhury, A., and Gill, S. S. (2015). Lipids and proteins-major targets of oxidative modifications in abiotic stressed plants. *Environ. Sci. Pollut. R.* 22, 4099–4121. doi: 10.1007/s11356-014-3917-1

Arasimowicz-Jelonek, M., and Floryszak-Wieczorek, J. (2014). Nitric oxide: an effective weapon of the plant or the pathogen? *Mol. Plant. Pathol.* 15, 406–416. doi: 10.1111/mpp.12095

Ban, Q. Y., Liu, G. F., and Wang, Y. C. (2011). A *DREB* gene from *Limonium bicolor* mediates molecular and physiological responses to copper stress in transgenic tobacco. *J. Plant Physiol.* 168, 449–458. doi: 10.1016/j.jplph.2010.08.013

Bhargava, S., and Sawant, K. (2013). Drought stress adaption: metabolic adjustment and regulation of gene expression. *Plant Breed.* 132, 21–32. doi: 10.1111/pbr.12004

Boller, T., and He, S. Y. (2009). Innate immunity in plants: an arms race between pattern recognition receptors in plants and effectors in microbial pathogens. *Science* 324, 742–744. doi: 10.1126/science.1171647

Cabello, J. V., Lodeyro, A. F., and Zurbriggen, M. D. (2014). Novel perspectives for the engineering of abiotic stress tolerance in plants. *Curr. Opin. Biotech.* 26, 62–70. doi: 10.1016/j.copbio.2013.09.011

Charfeddine, M., Bouaziz, D., Charfeddine, S., Hammami, A., Ellouz, O. N., and Bouzid, R. G. (2015). Overexpression of dehydration-responsive element-binding 1 protein (DREB1) in transgenic *Solanum tuberosum* enhances tolerance to biotic stress. *Plant Biotechnol. Rep.* 9, 79–88. doi: 10.1007/s11816-015-0345-8

Chen, J. M., Gao, C., Shi, Q., Shan, B., Lei, Y. J., Dong, C. F., et al. (2008). Different expression patterns of CK2 subunits in the brains of experimental animals and patients with transmissible spongiform encephalopathies. *Arch. Virol.* 153, 1013–1020. doi: 10.1007/s00705-008-0084-z

Du, X., Li, W., Sheng, L., Deng, Y., Wang, Y., Zhang, W., et al. (2018). Over-expression of chrysanthemum CmDREB6 enhanced tolerance of chrysanthemum to heat stress. *BMC Plant Biol.* 18:178. doi: 10.1186/s12870-018-1400-8

Fox, H., Doron-Faigenboim, A., Ketty, G., Bourstein, R., Attia, Z., Zhou, J., et al. (2017). Transcriptome analysis of *Pinus halepensis* under drought stress and during recovery. *Tree Physiol.* 38, 423–441. doi: 10.1093/treephys/tpx137

Götz, S., García-Gomez, J. M., Terol, J., Williams, T. D., Nagaraj, S. H., Nueda, M. J., et al. (2008). High-throughput functional annotation and data mining with the Blast2GO suite. *Nucleic Acids Res.* 36, 3420–3435. doi: 10.1093/nar/gkn176

Gu, X. B., Gao, Z. H., Yan, Y. C., Wang, X. Y., Qiao, Y. S., and Chen, Y. H. (2017). *RdreB1BI* enhances drought tolerance by activating AQP-related genes in transgenic strawberry. *Plant Physiol. Biochy.* 119:33e42. doi: 10.1016/j.plaphy.2017.08.013

He, B., Gu, Y., Tao, X., Cheng, X., Wei, C., Fu, J., et al. (2015). *De novo* transcriptome sequencing of *Oryza officinalis* wall ex watt to identify disease-tolerance genes. *Int. J. Mol. Sci.* 16, 29482–29495. doi: 10.3390/ijms161226178

Hedden, P., and Phillips, A. L. (2000). Gibberellin metabolism: new insights revealed by the genes. *Trends Plant Sci.* 5, 523–530. doi: 10.1016/s1360-1385(00)01790-8

Hsieh, T. H., Lee, J. T., Yang, P. T., Chiu, L. H., Chamg, Y. Y., Wang, Y. C., et al. (2002). Heterology expression of the *Arabidopsis* C-repeat/dehydration response element binding factor 1 gene confers elevated tolerance to chiling and oxidative stresses in transgenic tomato. *Plant Physiol.* 129, 1086–1094. doi: 10.1104/pp.003442

Huang, B., Jin, L., and Liu, J. Y. (2008). Identification and characterization of the novel gene GhDBP2 encoding a DRE-binding peotein from cotton (*Gossypium hirsutum*). *J. Plant Physiol.* 165, 214–223. doi: 10.1016/j.jplph.2006.11.003

Huang, J. G., Yang, M., Liu, P., Yang, G. D., Wu, C. A., and Zheng, C. C. (2009). *GhDREB1* enhances abiotic stress tolerance, delays GA-mediated development and represses cytokinin signalling in transgenic *Arabidopsis*. *Plant Cell Environ.* 32, 1132–1145. doi: 10.1111/j.1365-3040.2009.01995.x

Kang, Y., Han, Y., Torres-Jerez, I., Wang, M., Tang, Y., Monteros, M., et al. (2011). System responses to long-term drought and re-watering of two contrasting alfalfa varieties. *Plant J.* 68:871e889. doi: 10.1111/j.1365-313X.2011.04738.x

Kidokoro, S., Watanabe, K., Ohori, T., Moriwaki, T., Maruyama, K., Mizoi, J., et al. (2015). Soybean DREB1/CBF-type transcription factors function in heat and drought as well as cold stress-responsive gene expression. *Plant J.* 81, 505–518. doi: 10.1111/tpj.12746

Kudo, M., Kidokoro, S., Yoshida, T., Mizoi, J., Todaka, D., Fernie, A. R., et al. (2017). Double overexpression of DREB and PIF transcription factors

improves drought stress tolerance and cell elongation in transgenic plants. *Plant Biotechnol. J.* 15, 458–471. doi: 10.1111/pbi.12644

Lata, C., and Prasad, M. (2011). Role of DREBs in regulation of abiotic stress responses in plants. *J. Exp. Bot.* 62, 4731–4748. doi: 10.1093/jxb/err210

Li, C., Yue, J., Wu, X., Xu, C., and Yu, J. (2014). An ABA-responsive DRE-binding protein gene from *Setaria italica*, *SiARDP*, the target gene of SiAREB, plays a critical role under drought stress. *J. Exp. Bot.* 65, 5415–5427. doi: 10.1093/jxb/eru302

Li, J., Sima, W., Ouyang, B., Wang, T., Ziaf, K., Luo, Z., et al. (2012). Tomato *SlDREB* gene restricts leaf expansion and internode elongation by downrefulatin key genes for gibberellin biosynthesis. *J. Exp. Bot.* 63, 6407–6420. doi: 10.1093/jxb/ers295

Li, S. X., Zhao, Q., Zhu, D. Y., and Yu, J. J. (2018). A DREB-like transcription factors from maize (*Zea mays*), ZmDREB4.1 plays a negative role in plant growth and development. *Front. Plant Sci.* 9:395. doi: 10.3389/fpls.2018.00395

Liao, X., Guo, X., Wang, Q., Wang, Y., Zhao, D., Yao, L., et al. (2017). Overexpression of *MsDREB6.2* results in cytokinin-deficient developmental phenotypes and enhances drought tolerance in transgenic apple plants. *Plant J.* 89, 510–526. doi: 10.1111/tpj.13401

Lin, R., Park, H., and Wang, H. (2008). Role of *Arabidopsis* RAP2.4 in regulating light- and ethylene-mediated developmental processes and drought stress tolerance. *Mol. Plant* 1, 42–57. doi: 10.1093/mp/ssm004

Mauch-Mani, B., and Mauch, F. (2005). The role of abscisic acid in plant–pathogen interactions. *Curr. Opin. Plant Biol.* 8, 409–414. doi: 10.1016/j.pbi.2005.05.015

Nakashima, K., Yamaguchi-Shinozaki, K., and Shinozaki, K. (2014). The transcriptional regulatory network in the drought response and its crosstalk in abiotic stress responses including drought, cold, and heat. *Front. Plant Sci.* 5:170. doi: 10.3389/fpls.2014.00170

Ning, Y., Jantasuriyarat, C., Zhao, Q., Zhang, H., Chen, S., Liu, J., et al. (2011). The SINA E3 ligase OsDIS1 negatively regulates drought response in rice. *Plant Physiol.* 157, 242–255. doi: 10.1104/pp.111.180893

Noctor, G., Mhamdi, A., and Foyer, C. H. (2014). The roles of reactive oxygen metabolism in drought: not so cut and dried. *Plant Physiol.* 164, 1636–1648. doi: 10.1104/pp.113.233478

Quan, R. D., Hu, S. J., Zhang, Z. L., Zhang, H. W., Zhang, Z. J., and Huang, R. F. (2010). Overexpression of an ERF transcription factor *TSRF1* improves rice drought tolerance. *Plant Biotechnol. J.* 8, 476–488. doi: 10.1111/j.1467-7652.2009.00492.x

Rae, L., Lao, N. T., and Kavanagh, T. A. (2011). Regulation of multiple aquaporin genes in *Arabidopsis* by a pair of recently duplicated DREB transcription factors. *Planta* 234, 429–444. doi: 10.1007/s00425-011-1414-z

Richards, D. E., King, K. E., Ait-Ali, T., and Harberd, N. P. (2001). How gibberellin regulates plant growth and development: a molecular genetic analysis of gibberellin signaling. *Annu. Rev. Plant Physiol. Plant Mol. Biol.* 52, 67–88. doi: 10.1146/annurev.arplant.52.1.67

Royer, C. H., and Noctor, G. (2003). Redox sensing and signaling associated with reactive oxygen in chloroplasts, peroxisomes and mitochondria. *Physiol. Planarum* 119, 355–364. doi: 10.1034/j.1399-3054.2003.00223.x

Sakuma, Y., Maruyama, K., Osakabe, Y., Qin, F., Seki, M., Shinozaki, K., et al. (2006). Functional analysis of an *Arabidopsis* transcription factor, DREB2A, involved in drought-responsive gene expression. *Plant Cell* 18, 1292–1309. doi: 10.1105/tpc.105.035881

Selvaraj, M. G., Ishizaki, T., Valencia, M., Ogawa, S., Dedicova, B., Ogata, T., et al. (2017). Overexpression of an *Arabidopsis thaliana* galactinol synthase gene improves drought tolerance in transgenic rice and increased grain yield in the field. *Plant Biotechnol. J.* 15, 1465–1477. doi: 10.1111/pbi.12731

Shan, D. P., Huang, J. G., Yang, Y. T., Guo, Y. H., Wu, C. A., Yang, G. D., et al. (2007). Cotton GhDREB1 increases plant tolerance to low temperature and is negatively regulated by gibberellic acid. *New Phytol.* 176, 70–81. doi: 10.1111/j.1469-8137.2007.02160.x

Shavrukov, Y., Baho, M., Lopato, S., and Langridge, P. (2016). The *TaDREB3* transgene transferred by conventional crossings to different genetic backgrounds of bread wheat improves drought tolerance. *Plant Biotechnol. J.* 14, 313–322. doi: 10.1111/pbi.12385

Singh, K. B., Foley, R. C., and Oñate-Sánchez, L. (2002). Transcription factors in plant defense and stress responses. *Curr. Opin. Plant Biol.* 5, 430–436. doi: 10.1016/s1369-5266(02)00289-3

Suo, H., Lü, J., Ma, Q., Yang, C., Zhang, X., Meng, X., et al. (2016). The AtDREB1A transcription factor up-regulates expression of a vernalization pathway gene, GmVRN1-like, delaying flowering in soybean. *Acta Physiol. Plant* 38:137. doi: 10.1007/s11738-016-2136-4

Takeuchi, J., Okamoto, M., Mega, R., Kanno, Y., Ohnishi, T., Seo, M., et al. (2016). Abscinazole-E3M, a practical inhinitor of abscisic acid 8'-hydroxylase for improvinig drought tolerance. *Sci. Rep.* 6:37060. doi: 10.1038/srep37060

Tang, M., Liu, X., Deng, H., and Shen, S. (2011). Over-expression of *JcDREB*, a putative AP2/EREBP domain-containing transcription factor gene in woody biodiesel plant *Jatropha curcas*, enhances salt and freezing tolerance in transgenic *Arabidopsis thaliana*. *Plant Sci.* 181, 623–631. doi: 10.1016/j.plantsci.2011.06.014

Tang, Y. H., Liu, K., Zhang, J., Li, X. L., Xu, K. D., Zhang, Y., et al. (2017). *JcDREB2*, a physic nut AP2/ERF gene, alters plant growth and salinity stress responses in transgenic rice. *Front. Plant Sci.* 8:306. doi: 10.3389/fpls.2017.00306

Taulavuori, E., Hellstrom, E. K., Taulavuori, K., and Laine, K. (2001). Comparison of two methods used to analyse lipid peroxidation from *Vaccinium myrtillus* (L.) during snow removal, reacclimation and cold acclimation. *J. Exp. Bot.* 52, 2375–2380. doi: 10.1093/jexbot/52.365.2375

Trapnell, C., Pachter, L., and Salzberg, S. L. (2009). TopHat: discovering splice junctions with RNA-Seq. *Bioinformatics* 25, 1105–1111. doi: 10.1093/bioinformatics/btp120

Trapnell, C., Williams, B. A., Pertea, G., Mortazavi, A., Kwan, G., van Baren, M. J., et al. (2010). Transcript assembly and quantification by RNA-Seq reveals unannotated transcripts and isoform switching during cell differentiation. *Nat. Biotechnol.* 28, 511–515. doi: 10.1038/nbt.1621

Ullah, C., Unsicker, S. B., Fellenberg, C., Constabel, C. P., Schmidt, A., and Gershenzon, J. A. (2017). Flavan-3-ols are an effective chemical defense against rust infection. *Plant Physiol.* 175, 1560–1578. doi: 10.1104/pp.17.00842

Umezawa, T., Sugiyama, N., Mizoguchi, M., Hayashi, S., Myouga, F., Yamaguchi-Shinozaki, K., et al. (2009). Type 2C protein phosphatases directly regulate abscisic acid-activated protein kinases in *Arabidopsis*. *Proc. Natl. Acad. Sci. U.S.A.* 106, 17588–17593. doi: 10.1073/pnas.0907095106

Vo, K. T. X., Kim, C. Y., Hoang, T. V., Lee, S. K., Shirsekar, G., Seo, Y. S., et al. (2018). *OsWRKY67* plays a positive role in basal and XA21-mediated tolerance in rice. *Front. Plant Sci.* 8:2220. doi: 10.3389/fpls.2017.02220

Wang, C., Liu, S., Dong, Y., Zhao, Y., Geng, A. K., Xia, X. L., et al. (2016). *PdEPF1* regulates water-use efficiency and drought tolerance by modulating stomatal density in poplar. *Plant Biotechnol. J.* 14, 849–860. doi: 10.1111/pbi.12434

Wu, J., Mao, X., Cai, T., Luo, J., and Wei, L. (2006). KOBAS server: a web-based platform for automated annotation and pathway identification. *Nucleic Acids Res.* 34, 720–724. doi: 10.1093/nar/gkl167

Wuddineh, W. A., Mazarrei, M., Zhang, J. Y., Poovaiah, C. R., Mann, D. G. J., Ziebell, A., et al. (2015). Identification and overexpression of *gibberellin 2-oxidase* (*GA2ox*) in switchgrass (*Panicum virgatum* L.) for improved plant architecture and reduced biomass recalcitrance. *Plant Biotechnol. J.* 13, 636–647. doi: 10.1111/pbi.12287

Xie, C., Mao, X., Huang, J., Ding, Y., Wu, J., Dong, S., et al. (2011). KOBAS 2.0: a web server for annotation and identification of enriched pathways and diseases. *Nucleic Acids Res.* 39, 316–322. doi: 10.1093/nar/gkr483

Yang, J., Zhao, S., Zhao, B., and Li, C. (2018). Overexpression of TaLEA3 induces rapid stomatal closure under drought stress in *Phellodendron amurense* Rupr. *Plant Sci.* 277, 100–109. doi: 10.1016/j.plantsci.2018.09.022

Yin, L., Wang, S., Eltayeb, A. E., Uddin, M. I., Yamamoto, Y., Tsuji, W., et al. (2010). Overexpression of dehydroascorbate reductase, but not monodehydroascorbate reductase, confers tolerance to aluminum stress in transgenic tobacco. *Planta* 231, 609–621. doi: 10.1007/s00425-009-1075-3

Zhang, X., Liu, X., Wu, L., Yu, G., Wang, X., and Ma, H. (2015). The SsDREB transcription factor from the succulent halophyte Suaeda salsa enhances abiotic stress tolerance in transgenic tobacco. *Int. J. Genomics* 2015, 1–13.

Zhang, Y. L., Zhang, C. L., Wang, G. L., Wang, Y. X., Qi, C. H., You, C. X., et al. (2019). Apple AP2/EREBP transcription factor MdSHINE2 confers drought resisitance by regulating wax biosynthesis. *Planta* 249, 1627–1643. doi: 10.1007/s00425-019-03115-4

Zhao, H., Jiang, J., Li, K. L., and Liu, G. F. (2017). *Populus simonii*× *Populus nigra* WRKY70 is involved in salt stress and leaf blight disease responses. *Tree Physiol.* 37, 1–18. doi: 10.1093/treephys/tpx020

Zhao, K., Shen, X. J., Yuan, H. Z., Liu, Y., Liao, X., Wang, Q., et al. (2013). Isolation and characterization of dehydration-responsive element-binding factor 2C (MsDREB2C) from *Malus sieversii* Roem. *Plant Cell Physiol.* 54, 1415–1430. doi: 10.1093/pcp/pct087

Zhou, M., Li, D., Li, Z., Hu, Q., Yang, C. H., Zhu, L. H., et al. (2013). Constitutive expresion of a *miR319* gene alters plant developemnt and enhances salt and drought tolerance in transgenic creeping bentgrass. *Plant Physiol.* 161, 1375–1391. doi: 10.1104/pp.112.208702

Zhou, Q. Y., Tian, A. G., Zou, H. F., Xie, Z. M., Li, G., Huang, J., et al. (2008). Soybean WRKY-type transcription factor genes, GmWRKY13, GmWRKY21, anf GmWRKY54, confer differential tolerance to abiotic stresses in transgenic *Arabidopsis* plants. *Plant Biotechnol. J.* 6, 486–503. doi: 10.1111/j.1467-7652.2008.00336.x

Zhou, Y., Chen, M., Guo, J., Wang, Y., Min, D., Jiang, Q., et al. (2020). Overexpression of soybean DREB1 enhances drought stress tolerance of transgenic wheat in the field. *J. Exp. Bot.* 71, 1842–1857. doi: 10.1093/jxb/erz569

Conflict of Interest: The authors declare that the research was conducted in the absence of any commercial or financial relationships that could be construed as a potential conflict of interest.

frontiers in Plant Science

ORIGINAL RESEARCH
published: 27 November 2020
doi: 10.3389/fpls.2020.580155

Phytohormones Regulate Both "Fish Scale" Galls and Cones on *Picea koraiensis*

*Mingyue Jia[1], Qilong Li[1], Juan Hua[1], Jiayi Liu[1], Wei Zhou[1], Bo Qu[1,2] and Shihong Luo[1,2]**

[1]College of Bioscience and Biotechnology, Shenyang Agricultural University, Shenyang, China, [2]Key Laboratory of Biological Invasions and Global Changes, Shenyang Agricultural University, Shenyang, China

The larch adelgid *Adelges laricis laricis* Vallot is a specialist insect parasite of *Picea koraiensis* (Korean spruce) and forms fish scale-like galls that damage the growth of the host plants. Our investigation reveals that both these galls and the fruits (cones) of *P. koraiensis* display lower concentrations of phytosynthetic pigments and accumulate anthocyanin cyanidin-3-*O*-glucoside and soluble sugars in the mature stages. Interestingly, high concentrations of 6-benzylaminopurine (BAP) both in the cauline gall tissues and in the larch adelgids themselves (4064.61 ± 167.83 and 3655.42 ± 210.29 ng/g FW, respectively), suggested that this vital phytohormone may be synthesized by the insects to control the development of gall tissues. These results indicate that the galls and cones are sink organs, and the development of gall tissues is possibly regulated by phytohormones in a way similar to that of the growth of cones. The concentrations of phytohormones related to growth [indole-3-acetic acid (IAA), cytokinins (CTK), and gibberellins (GAs)] and defense [salicylic acid (SA)], as well as SA-related phenolics [benzoic acid (BA) and *p*-hydroxybenzoic acid (*p*HBA)] in gall tissues were positively correlated with those in cones during the development stage. The levels of 1-aminocyclopropane-1-carboxylic acid (ACC) in the developmental stage of the cones correlates negatively with their concentrations in the gall tissues ($R = -0.92$, $p < 0.001$), suggesting that downregulation of ACC might be the reason why galls are not abscised after a year. Our results provide a new perspective on the potential mechanism of the development of cauline galls on *P. koraiensis*, which are regulated by phytohormones.

Keywords: plant-insect interactions, phytohormones, larch adelgid, sink organs, cauline gall

OPEN ACCESS

Edited by:
Sanushka Naidoo,
University of Pretoria, South Africa

Reviewed by:
Yoshihito Suzuki,
Ibaraki University, Japan
Makoto Tokuda,
Saga University, Japan

***Correspondence:**
Shihong Luo
luoshihong@syau.edu.cn

Specialty section:
This article was submitted to Plant Pathogen Interactions, a section of the journal Frontiers in Plant Science

Received: *28 July 2020*
Accepted: *09 November 2020*
Published: *27 November 2020*

Citation:
Jia M, Li Q, Hua J, Liu J, Zhou W, Qu B and Luo S (2020) Phytohormones Regulate Both "Fish Scale" Galls and Cones on Picea koraiensis. Front. Plant Sci. 11:580155. doi: 10.3389/fpls.2020.580155

INTRODUCTION

Herbivorous insects and plants are hugely important components of terrestrial communities and have coevolved over millions of years (Stahl et al., 2018). Damage caused by insect feeding on plants makes an important contribution to yield reductions across agricultural areas globally and is therefore responsible for considerable economic losses (Hilker and Fatouros, 2016). Insects are mobile and have evolved sophisticated and effective strategies to enable them to live on their host plants. Several different feeding habits are known and insects have evolved mouthparts that enable them to specialize in chewing, snipping, or sucking and have developed

chemical-molecular crosstalk to cope with plant defenses (Howe and Jander, 2008). An example of a strategy evolved by an insect to counter plant host defenses is that the salivary secretions of certain herbivorous insect caterpillars contain the enzyme glucose oxidase, which counteract the production of defensive metabolites induced by the caterpillar feeding on the plant (Musser et al., 2002). Furthermore, the digestive proteases in the guts of phytophagous insects are able to counter plant defense proteins (Zhu-Salzman and Zeng, 2015). The complex chemical networks involved in the interactions between plants and insects resulting from thousands of years of evolution remain a hot topic in research.

One fascinating research area in the field of plant-insect interactions is the interaction between galling insects and plants. Insect galls are tumor-like organs on plant tissues, which are stimulated by the feeding of galling insects that can induce accelerated division of the host cells (Hirano et al., 2020). Galls can function as shelters and feeding sites for the insects inside and can develop in almost every plant organ, including roots, stems, leaves, flowers, fruits, and seeds. Galls have a negative impact on their host plants, slow plant growth, and can reduce plant height, leaf area, and production of inflorescences (Fay et al., 1996). However, these organs represent a close and sophisticated association between the galling insects and their host plants (Kutsukake et al., 2019). It is well-known that plant defenses against herbivory are triggered by insect-specific elicitors (Howe and Jander, 2008). Meanwhile, the insects counter these strategies by triggering multiple effective defense pathways, which can counter the plant defenses (Zhu-Salzman and Zeng, 2015). Certain insects secrete effectors, which are injected physically into host cells to control the plant defenses (Cambier et al., 2019). It is possible that these effectors potentially act as mediators responsible for the formation of arthropod-induced plant galls (Oliveira et al., 2016). Moreover, gall-inducing insects can manipulate host plant cells and tissues and control the formation of galls accompany chemicals. Therefore, understanding the mechanisms by which these insects can offset plant defenses and manipulate plants in other ways is a key to explain the complicated relationships between plants and galling insects.

Gall formation occurs when plant cell growth is accelerated following a stimulus caused by the feeding of galling insects (Stone and Schonrogge, 2003). Gall tissues usually absorb the photoassimilates and can manipulate the source-sink relationships in plants, allowing the formation and growth of galls resemblance to plant other organs (Dorchin et al., 2006; Oliveira et al., 2017). An example of insect alteration of plant source-sink relationships is found in the galling aphid, *Pemphigus betae*. Galls induced by these aphids use plant sources to maintain their own growth and development in the same way as other organs of plants do, including increasing size through cell hypertrophy and tissue hyperplasia (Larson and Whitham, 1997). A favorable microenvironment for the development of their galls is ensured by gall-inducing wasps, *Trichilogaster signiventris*, which can alter the photosynthetic capacity of the gall tissues to induce a resource sink (Castro et al., 2012). However, although the changes in source-sink relationships can lead to striking resemblances between the gall organs and other plant organs in the processes of growth and development, there are few studies focusing on this phenomenon and the mechanisms remain unclear.

Phytohormones are considered to be the pivotal regulators in the manipulation of plant tissues to enable the formation and growth of galls (Li et al., 2017; Body et al., 2019). These hormones may be secreted by the gall-inducing insects themselves or by the host plants (Straka et al., 2010; Tooker and Helms, 2014). In certain cases, galling insects have the ability to regulate plant hormones. Cytokinins (CTK, in most cases iP and *t*Z) secreted by gall-inducing insects and cause the galls to become strong photosynthate sinks, meaning that the insects inside are continually supplied with nutrients (Naseem et al., 2014; Takei et al., 2015). Gibberellins (GAs) and abscisic acid (ABA) play key roles in the regulation of gall formation and in insect-induced defensive responses (Li et al., 2017). Meanwhile, jasmonates (JAs) and salicylic acid (SA) are the key defensive phytohormones that mediate plant responses to galling herbivores during gall initiation and development (Eitle et al., 2019). The regulation of phytohormones is therefore of crucial importance in the formation and development of galls.

The larch adelgid *Adelges laricis laricis* Vallot (Hemiptera, superfamily Phylloxeroidea, family Adelgidae) is polymorphic, commonly with a 2-year life cycle that involves different host plants (Yu et al., 1998). From field observations in Liaoning Province, China, *Picea koraiensis* (Korean spruce) was identified as a primary host plant for this adelgid. In the same area, the Japanese larch, *Larix kaempferi*, acts as a secondary host (**Figure 1**; Liu et al., 2011). Larch adelgids cause significant damage to young trees of *P. koraiensis*, affect the growth of stems and branches, and cause the formation of "fish scale" galls. On *L. kaempferi*, the larch adelgids suck the sap from the needles and shoots to produce large quantities of a white waxy secretion, resulting in dried and mildewed branches and seriously affecting tree growth (**Figure 1**; Yu et al., 1998; Liu et al., 2011). However, mechanism underlying gall formation in *P. koraiensis* is still poorly understood. In this study, we focus on exploring the dynamics of endogenous phytohormones in both galls and cones of *P. koraiensis* at different stages and investigate the roles of these hormones in the formation of galls. Our research contributes to a better understanding of the formation of gall tissues and supplies new insights into the potential mechanisms by which gall-inducing insects induce galls.

MATERIALS AND METHODS

Plant Materials and Galling Insects

Galls and normal branches without galls were collected in July 2019 from *Picea koraiensis* trees and were growing in Wan dianzi town (E: 125°13', N: 41°96'), Fushun city, Liaoning province. Plants were identified by Professor Bo Qu, and voucher specimens (SYNUBL013060–SYNUBL013065) were deposited at the College of Bioscience and Biotechnology, Shenyang Agricultural University. Based on morphology, the development of these cauline galls can be divided into five stages (**Figure 1**).

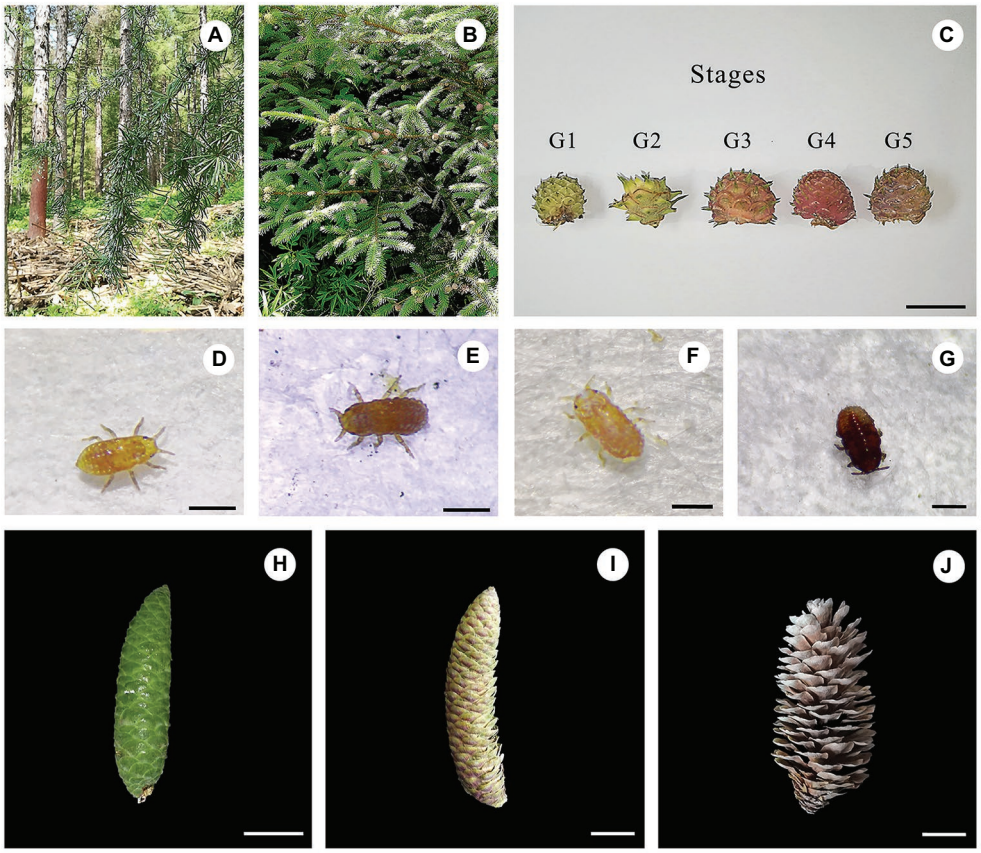

FIGURE 1 | Field and microscope observations of the larch adelges *Adelges laricis laricis* Vallot and the cones of *Picea koraiensis*. Cauline galls induced by *A. laricis laricis* Vallot on *P. koraiensis*. **(A)** Field habit of *Larix kaempferi*, a secondary host of *A. laricis laricis*. **(B)** Field habit of *P. koraiensis*, a first host of *A. laricis laricis*. **(C)** Morphological characteristics of cauline galls caused by *A. laricis laricis* on *P. koraiensis* at different developmental stages of G1–G5. **(D–G)** *A. laricis laricis* Vallot isolated from the gall tissues of *P. koraiensis*. **(H–J)** *P. koraiensis* cones at different developmental stages of F1–F3. Scale bars = 2 cm for **(C)** and **(H–J)**; 0.25 mm for **(D)** and **(E)**; 0.4 mm for **(F)**; 0.35 mm for **(G)**.

Galls at stage G1 were defined as those having gall tissues with white-green coloration. Stage G2 galls had deeper green coloration. Stages G1 and G2 together were defined as the "young" stage. The "mature" galls were divided into three stages of development, G3–G5, which are described by a gradual deepening of color from pale green to purple-black. The coloration of galls at stage G3 was turning from green to red. G4 galls were defined as completely red, and G5 galls were purple-black. The adelgid insects were almost totally absent from galls at stage G5. Cones were divided on the basis of morphology into three stages. Tender stage galls (green color, F1) were collected on July 1, 2019, mature stage galls (red, F2) were collected on September 1, 2019, and senescent stage galls (brown, F3) were collected on November 1, 2019.

Galls and cones were collected from five Korean spruce plants which were about 6 years old. Fifteen repeated gall and five repeated cones for each stage were collected. Galls were dissected in the laboratory to separate insects and gall tissues. Based on both morphological characters and molecular identification, the insects were identified as *Adelges laricis laricis* Vallot (larch adelgid) by Dr. Shouhui Sun, and voucher specimens (SYNUBC00045–SYNUBC00050) were deposited at the College of Bioscience and Biotechnology, Shenyang Agricultural University. Galls, adelgids, stems without galls, and cones were stored at −80°C for further analysis.

Quantification of Phytohormones

A total of 26 SA-related phenolics and phytohormones were assessed, including 6-benzylaminopurine (BAP), 6-(γ,γ-dimethylallylamino) purine (iP), *trans*-zeatin (*t*Z), gibberellins (GAs, GA_1, GA_3, GA_4, GA_7, GA_9, GA_{12}, GA_{19}, GA_{24}, and GA_{53}), indole-3-acetic acid (IAA), 3-indolepropionic acid (IPA), 1-aminocyclopropane-1-carboxylic acid (ACC), ABA, jasmonic acid (JA), salicylic acid (SA), methyl salicylate (MeSA), benzoic acid (BA), *p*-hydroxybenzoic acid (*p*HBA), *m*-hydroxybenzoic acid (*m*HBA), *p*-hydroxycinnamic acid (*p*HCA), *o*-hydroxycinnamic acid (*o*HCA), *m*-hydroxycinnamic acid (*m*HCA), and *trans*-cinnamic acid (*t*CA). The deuterated isotope-labeled compounds d_2-GA_1, d_2-GA_4, and d_6-ABA were used as internal standards, which were purchased from Tokyo Chemical Industry Co., Ltd. (TCI, Tokyo, Japan). The concentrations of phytohormones and SA-related phenolics were quantified by external standard

method. Phytohormones and SA-related phenolics were purchased from Tokyo Chemical Industry Co., Ltd. HPLC-grade solvents methanol (MeOH), formic acid, and acetonitrile were purchased from Merck. HLB and MCX solid-phase extraction cartridges were from Thermo (WondaSep HLB, MCX 60 mg/3 ml, 50EA/PKG).

The phytohormones with five biological replicates were extracted by following the previous descriptions with some slight modifications (Kojima et al., 2009). After removing larch adelgids from each gall chamber with a brush, the gall chambers (gall tissues) of each gall were prepared for a single sample. The cone and branches were chopped. After that, 500 mg fresh sample (gall tissues, branches, cones, or insects collected from the galls at stage G3) was homogenized using a precooled mortar pestle, and then ultrasonic-assisted extraction was conducted in 4 ml of extraction solution (methanol:water:formic acid = 15:4:1) for 45 min. After centrifugation at 12,000 rpm for 10 min, the supernatant was collected, the residue was ultrasonically reextracted and centrifuged by following the above method, and the extraction supernatants from both steps were combined. Samples and solutions were kept at 4°C throughout the extractions. HLB and MCX columns were preactivated with 2 ml methanol and 2 ml of 1 M formic acid. Every 2 ml of the supernatants loaded onto an HLB column and successively washed with 1 ml of the extraction solution. The eluates and washing solution were collected together and concentrated at 40°C under a rotary evaporator to get about 1 ml solution. This solution was passed through a MCX column eluting with 0.5 ml of 1 M formic acid and 2 ml methanol. And the methanol fraction was concentrated and redissolved in 0.2 ml of methanol. Then, the redissolved solutions were filtered through a 0.22 μm filter and transferred to 2 ml LC-MS glass bottles for UPLC-MS/MS analysis. The concentrations of GAs, IAA, IPA, ABA, JA, SA, MeSA, BA, *p*HBA, *m*HBA, *p*HCA, *o*HCA, *m*HCA, and *t*CA were analyzed. For analyses of BAP, iP, and *t*Z, the MCX column was sequentially eluted with 500 ml 0.35 M ammonia and 2 ml 0.35 M ammonia in 60% (v/v) methanol. The 0.35 M ammonia in 60% (v/v) methanol fraction was concentrated and redissolved in 0.2 ml of methanol for analysis of BAP, iP, and *t*Z using UPLC-MS/MS.

UPLC-MS/MS analyses were conducted using an UPLC-MS/MS system (Shimadzu LCMS-8050) with a Shim-pack GIST C_{18} (2 μm, 2.1 × 100 mm). The mobile phase consisted of 0.1% formic acid (A) and acetonitrile (B). The gradient elution was programed as follows: 0–2 min, 20–30% B; 2–8 min, 30% B; 8–12 min, 30–95% B; 12–14 min, 95% B; and 14–16 min, 95–20% B. A flow rate of 0.4 ml/min was used, and the injection volume was 10 μl. The column temperature was maintained at 40°C. The operating conditions of the electrospray ionization source (ESI) were as follows: gas flow 3 L/min; heating gas 10 L/min; dry gas flow 10 L/min; interface temperature, 300°C; and heating block temperature, 450°C. All the compounds were monitored using the multi reaction monitoring (MRM) mode, and the specific MRM parameters for each compound are given in **Supplementary Table S1**.

ACC was extracted as described previously (Ziegler et al., 2014). In short, the extract solutions and loading onto HLB columns were consistent with the methods of other phytohormones without MCX columns. The eluates of HLB column were evaporated to dryness at 37°C in a rotary evaporator. A total of 40 μl reaction buffer (anhydrous ethanol:water: triethylamine:PITC = 2:1:1:1) was added to the rotary evaporator bottle. After redissolving, the samples were left at room temperature for 20 min to react and were then evaporated to dryness as before. A further 50 μl 40% acetic acid was added and allowed to react at 90°C for 1 h. Then the reaction solution was evaporated and the residue redissolved in 500 μl methanol. The ACC was quantitatively analyzed using an UPLC-MS/MS system (Shimadzu LCMS-8050) with a Shim-pack GIST C_{18} (2 μm, 2.1 × 100 mm). The mobile phases were 0.1% formic acid (A) and acetonitrile (B). The gradient elution was conducted as follows: 0–13 min, 5–95% B. The flow rate was 0.4 ml/min and the volume of injection was 10 μl. The column temperature was maintained at 35°C. The electrospray ionization source (ESI) with multi reaction monitoring (MRM) mode was applied in MS detection (**Supplementary Table S2**).

Qualitative Analysis of Anthocyanins in Gall Tissues and Cones Using HPLC-DAD

After the insects inside the galls were removed, about 500 mg of the gall tissues (G3) or cones (F2) was ground into powder in liquid nitrogen and then suspended with 5 ml 80% methanol/water (*v*/*v*) with 2‰ formic acid in an ultrasonic bath for 45 min. The suspension was then centrifuged at 12,000 rpm for 5 min. After centrifugation, the supernatant was concentrated and evaporated to dryness. The supernatant was then suspended in 1 ml methanol and then analyzed using UPLC-MS/MS (UPLC-MS/MS 8050, Shimadzu Scientific Instruments, Inc., Tokyo, Japan) and HPLC-DAD (Agilent 1260). Samples were injected using an autosampler (SIL-30 AC; Shimadzu) into a mobile phase comprising acetonitrile (B) and 2% formic acid in water (D; 0–10 min: isocratic 15% B; 10–13 min, linear 15–95% B, 13–14 min, isocratic 95% B). The flow rate was 0.2 ml/min with injection volume of 10 μl. Cyanidin-3-*O*-glucoside was dissolved in methanol at 100 μg/ml and then analyzed by HPLC-DAD. At a flow rate of 1 ml/min, 10 μl of the sample was then injected into an Eclipse XDB-C_{18} column (5 μm, 4.6 × 250 mm), with the column temperature maintained at 30°C. The eluent was monitored at 200–600 nm. Mobile phases comprising (B) methanol and (D) 2% formic acid were used (0–30 min: linear 5–95% of B, 30–40 min, isocratic 95% of B).

Determination of the Concentrations of Photosynthetic Pigments in Gall Tissues and Cones

Pigments were extracted from fresh control branches, gall tissues (G1–G5), and cones (F1–F3) tissues. Each sample was treated with five biological replicates. After removing the galling insects, the fresh gall tissue or cone (200 mg) samples were suspended in 5 ml 80% acetone/water (*v*/*v*) and then ground with a pestle and mortar until all the tissues with

visible pigmentation had disappeared. A 3 ml aliquot of the extract was transferred to a cuvette for the determination of chlorophyll absorption using a spectrophotometer at 470, 646, and 663 nm. Absorption measurements were used to quantify the concentrations of chlorophylls *a*, and *b*, and of total carotenoids, based on the equations reported in previous publications (Wellburn, 1994).

Determination of the Concentrations of Soluble Sugars in Gall Tissues and Cones

Samples were prepared with five biological replicates as described above for the analyses of glucose, fructose, and sucrose (Guimarães et al., 2009). Briefly, 1 g of fresh gall tissues or cones were weighed and dried to a constant weight (105°C, 5 min and 80°C, 30 min). Dry gall tissues and cones were homogenized using a mortar pestle and transferred to the test tube. Then, samples were extracted in 80% aqueous ethanol for 40 min in the water bath at 80°C. The supernatant was collected, and the residue was reextracted two times under the same conditions. The supernatants from previous steps were combined. Samples with extraction solutions were shaken every 10 min throughout extractions. A total of 20 mg activated carbon was added and decolorized by shaking at 80°C for 30 min (shaking per 5 min). Further filtration with a funnel to rotary evaporator bottle was conducted and concentrated at 40°C under a reduced pressure and redissolved in 1 ml ultrapure water. Then, the redissolved solutions were filtered through a 0.22 μm filter for further HPLC (Agilent 1260) coupled to a refraction index detector (RID) analysis. The mobile phase consisted of the following linear gradients (flow rate, 1 ml/min; injection volume, 10 μl): 0–30 min, 20% A, 80% C (A was ultrapure water and C was acetonitrile). The column was Innovation NH_2 (Chrom-ma Trix Bio-Technology; 5 μm, 4.6 × 250 mm) and column temperature maintained at 35°C. Standard solutions of glucose, fructose, and sucrose were prepared in the range of 0.625–10 mg/ml. Furthermore, the calibration curves of glucose, fructose, and sucrose were y = 1E-05x−0.065 (t_R, 9.7 min; R^2 = 0.999), y = 1E-05x−0.027 (t_R, 8.4 min; R^2 = 0.996), and y = 2E-05x−0.017 (t_R, 13.8 min; R^2 = 0.991), respectively.

Statistical Analysis

The statistical analysis and graphics were conducted using ggstatplot (v 0.1.4). If the data followed a normal distribution, an independent-samples' *t*-test was used for comparison between the two groups, and the comparison among three or more groups was performed using one-way ANOVA with Tukey's test. If results of the *t*-test were significant and with the data were not normally distributed, a Mann-Whitney nonparametric test was used to compare two groups of data. Differences were considered to be statistically significant if $p \leq 0.05$. Corrplot and corrgram were used for the calculation of the correlation coefficient and for visualization. The R program (www.r-project.org) was used for statistical analysis and calculations.

RESULTS

Galls and Cones on *Picea koraiensis* Are Sink Organs

Based on morphological characters and DNA sequence analysis of DNA barcodes (*COI*), the gall insects in the stems of *Picea koraiensis* (Korean spruce) were identified as *Adelges laricis laricis* Vallot (Yu et al., 1998; Žurovcová et al., 2010).

Cones of Korean spruce are about 70–90 mm long and have a scaly surface. Each scale protects a seed. We split the development of the cones roughly into three stages: tender (F1), mature (F2), and senescent (F3). Galls caused by larch adelgids on *P. koraiensis* are about 15–20 mm both in length and width and also have a fish-scale like surface with strawberry shaped. The surface of the galls has a regular arrangement of cone-scale-like protuberances. Each protuberance has a split line and bundles of needles of varying lengths. The line of dehiscence appears white, orange-red, and finally pink before splitting. Each protuberance is in fact a highly organized and differentiated gall chamber, inhabited by the *A. laricis laricis* Vallot insects. Gall chambers are independent of each other and are irregularly arranged. Thus, from morphology, the larch adelgid galls resemble the cones of *P. koraiensis* (**Figure 1**).

Concentrations of glucose, fructose, and sucrose in fresh gall tissues and cones analyzed using HPLC-RID. The concentrations of these sugars increased throughout gall development. The higher concentrations of glucose, fructose, and sucrose in mature stage of gall tissues were observed than those of normal branches. Similarly, the higher concentrations of glucose and fructose exhibited in fresh mature cones (F2), with values of 1.56 ± 0.02 and 3.31 ± 0.22 mg/g FW, respectively (**Supplementary Figure S1**).

Concentrations of chlorophylls *a* and *b* and carotenoids were higher in normal branches than those in fresh gall tissues and cones, but there were no significant differences in the concentrations of these photosynthetic pigments between gall tissues and cones (**Figure 2**). The red coloration of the galls and cones of *P. koraiensis* is mainly due to the accumulation of anthocyanin pigments using HPLC-DAD analysis. Through the comparison with the standard, the main coloration in mature stage of gall tissues and cones was identified as cyanidin-3-*O*-glucoside (**Figure 3**). Thus, galls and cones are therefore both sink organs on the aerial parts of Korean spruce plants.

Growth Related Phytohormones in the Gall Tissues and Cones Throughout the Developmental Stages

The concentration of 6-benzylaminopurine (BAP) increased with the development of the gall tissues, reaching the value of 4064.61 ± 167.83 ng/g FW in the last stage. Furthermore, the concentration of BAP in the larch adelgids was 3655.42 ± 210.29 ng/g FW, which is four times higher than BAP concentrations in either normal branches or gall tissues at the related stage (G3, **Figures 4A**,**B**). Another cytokinin, 6-(γ,γ-dimethylallylamino) purine (iP), was found in the larch adelgids, but its concentration did not appear to be correlated

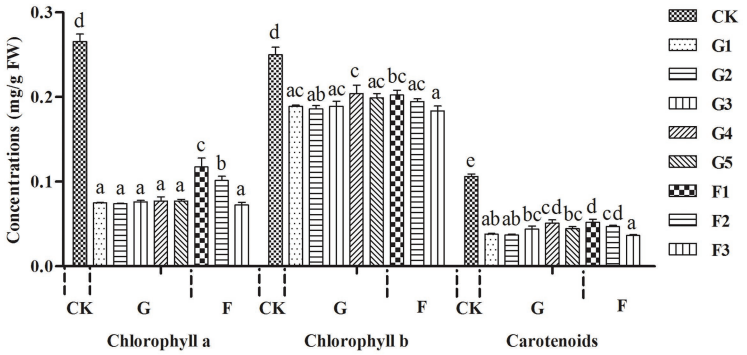

FIGURE 2 | Variations in concentration of photosynthetic pigments in galls tissues and the cones of *Picea koraiensis*. *CK* = normal branches. Data are presented in milligrams per gram of fresh weight (mg/g FW). G1–G5 represent the different developmental stages of gall tissues and F1–F3 represent different developmental stages of cones. G: gall tissues; F: cones. Mean differences were compared using one-way ANOVA with Tukey's test. The different small letters (a, b, c, and d) represent significant difference at 0.05 level. These results shown represent the average ± SD.

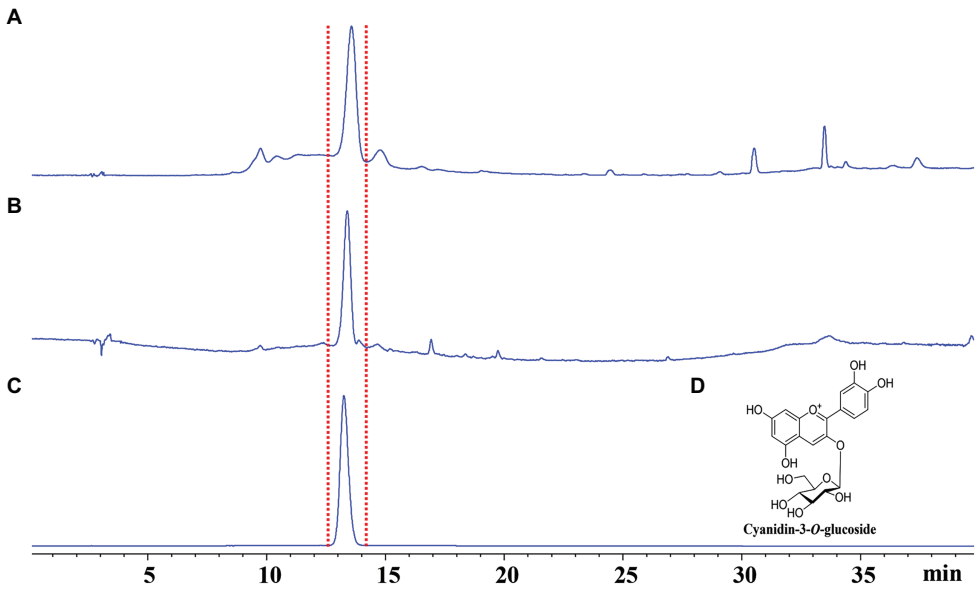

FIGURE 3 | Qualitative analyses of fresh gall tissues at stage G4 and cones of *Picea koraiensis* at stage F2 using HPLC-DAD at 520 nm. **(A)** HPLC analysis of gall tissues at stage G4; **(B)** HPLC analysis of cones of *Picea koraiensis* at stage F2; **(C)** HPLC analysis of cyanidin-3-*O*-glucoside (100 μg/ml); and **(D)** Chemical structures of cyanidin-3-*O*-rutinoside.

with the development of gall tissues or the cones in Korean spruce (**Figures 4C,D**). The concentrations of auxins (IAA and IPA) and gibberellins (GA_1, GA_3, and GA_4) were low in all treatments, except that there were higher concentrations of GA_1 in the normal branches of *P. koraiensis*, with concentrations of 223.03 ± 18.68 ng/g FW. Concentrations of GA_4 in gall tissues increased throughout development (**Figures 4E–N**). Thus, it is possible that the abnormal growth of the gall tissues might be stimulated by BAP synthesized by the larch adelgid insects.

Correlation analysis suggested that the concentrations of BAP were significantly and positively related to concentrations of iP ($R = 0.71$, $p < 0.01$), GA_1 ($R = 0.71$, $p < 0.01$), and GA_4 ($R = 0.74$, $p < 0.01$) in gall tissues, and furthermore that concentrations of iP were significantly and positively correlated with concentrations of GA_4 ($R = 0.95$, $p < 0.001$) in gall tissues. Moreover, there was a positive correlation between concentrations of GA_1 and GA_4 in gall tissues ($R = 0.52$, $p < 0.05$). In addition, there were negative correlations between concentrations of GA_3 and the other four growth related phytohormones in gall tissues, among which there was a significant negative correlation of GA_3 with GA_4 ($R = -0.66$, $p < 0.01$). There were negative correlations between concentrations of BAP and the other four growth related phytohormones during cone development. Concentrations of iP and GA_4 ($R = 0.82$, $p < 0.001$) were

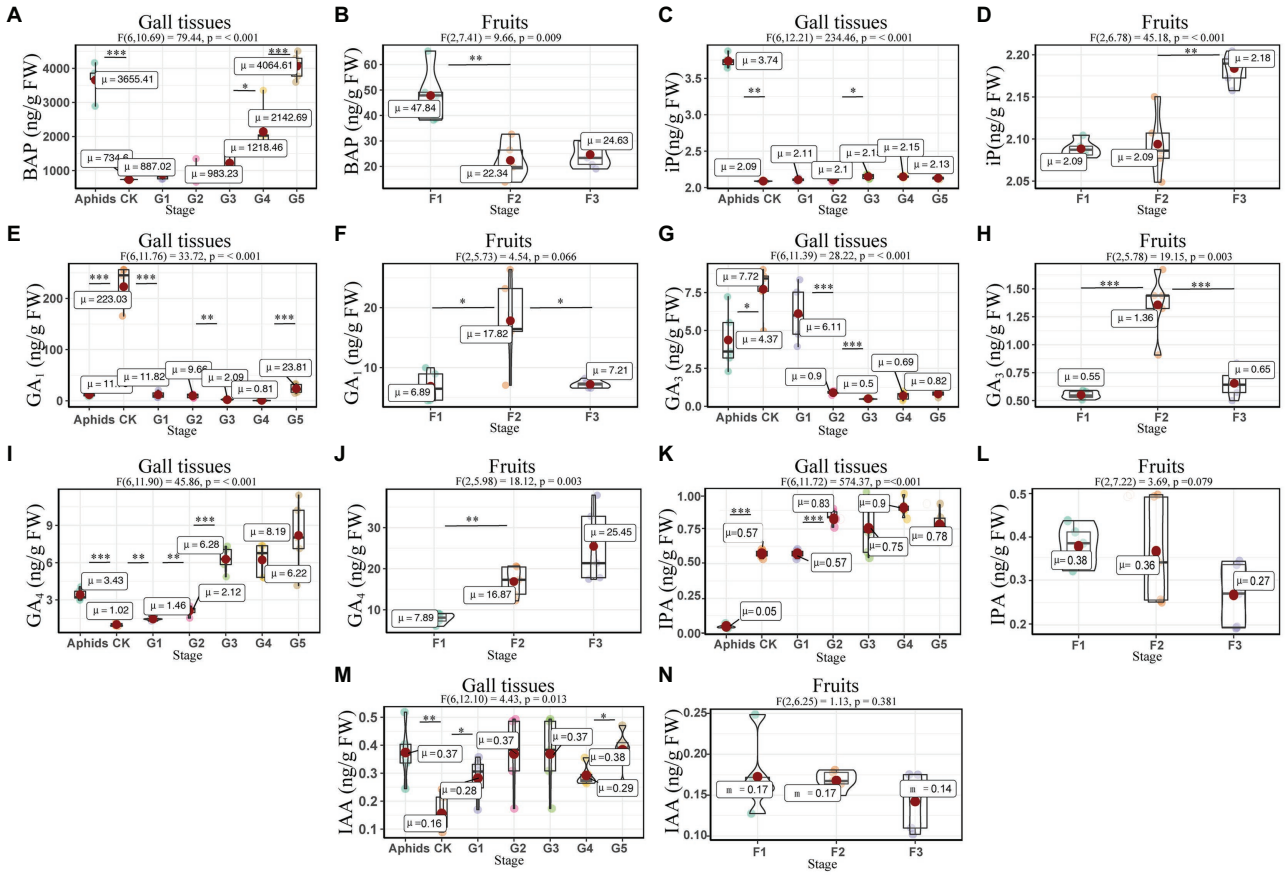

FIGURE 4 | Quantitative analysis of growth related phytohormones in the larch adelgids, gall tissues, and cones (fruits) of *P. koraiensis*. Quantitative analysis of 6-benzylaminopurine (BAP) in larch adelgids, gall tissues, normal branches **(A)**, and cones **(B)**. The level of 6-(γ,γ-dimethylallylamino) purine (iP) in gall tissues and normal branches **(C)** and cones **(D)**. The level of GA_1 in larch adelgids, gall tissues, and normal branches **(E)** and cones **(F)**. Quantitative analyses of GA_3 and GA_4 in larch adelgids, gall tissues, and normal branches (**G** and **I**), and cones (**H** and **J**), respectively. The Levels of IPA and IAA in larch adelgids, gall tissues, and normal branches (**K** and **M**), and cones (**L** and **N**), respectively. *CK* = normal branches. Data are presented in nanograms per gram of fresh weight (ng/g FW), and boxplots display the minimum, first quartile, median, third quartile, and maximum for each stage in the given tissues. G1–G5 represent the different developmental stages of gall tissues and F1–F3 represent different developmental stages of cones. Red point = mean value. Horizontal black line inside the box = median value. The shape of the boxplot indicates the distribution of results. Mean differences were compared using *t*-tests. *Denotes that the value of *p* is less than 0.05. **Denotes that the value of *p* is less than 0.01. ***Denotes that the value of *p* is less than 0.001. These results shown represent the average ± SD and performed one-way ANOVA test among three or more groups. ωp^2 = partial omega squared.

significantly and positively correlated. Concentrations of GA_1 were positively correlated with GA_3 (R = 0.93, p < 0.001) in cones. Furthermore, there was a positive, although not significant, correlation between GA_3 and GA_4 (**Figure 5**).

Defense Related Phytohormones in the Gall Tissues and Cones During the Developmental Stages

The concentrations of ABA and JA were affected by the developmental stage in both the gall tissues (ABA: F6, 12.13 = 27.82, P = <0.001; JA: F6, 11.64 = 145.24, P = <0.001) and Korean spruce cones. Similar expression patterns of ABA and JA in the developmental stages of the gall tissues were observed, in which the concentrations decreased throughout stages G2 and G3 and then increased again in stages G4 and G5 compared to stage G1 (**Figures 6A,C**). The normal gall-free branches of Korean spruce and cones at stage F1 showed the highest ABA concentrations, with values of 4967.60 ± 505.83 and 1574.46 ± 164.34 ng/g FW, respectively (**Figures 6A,B**). Concentrations of JA and ACC increased throughout cone development (**Figures 6D,F**). However, concentrations of ACC decreased throughout the developmental stages of the galls (**Figure 6E**).

The correlation analyses suggested that the concentrations of JA were positively correlated with those of ACC and ABA in gall tissues. During cone development, the concentrations of JA were significantly and negatively correlated with the ABA concentrations (R = -0.56, p < 0.05), and the concentrations of ABA were significantly and negatively correlated with those of ACC (R = −0.90, p < 0.001). In addition, there was a significant positive correlation between concentrations of JA and ACC (R = 0.83, p < 0.01). The concentrations of ACC and JA in the cones were negatively correlated with the

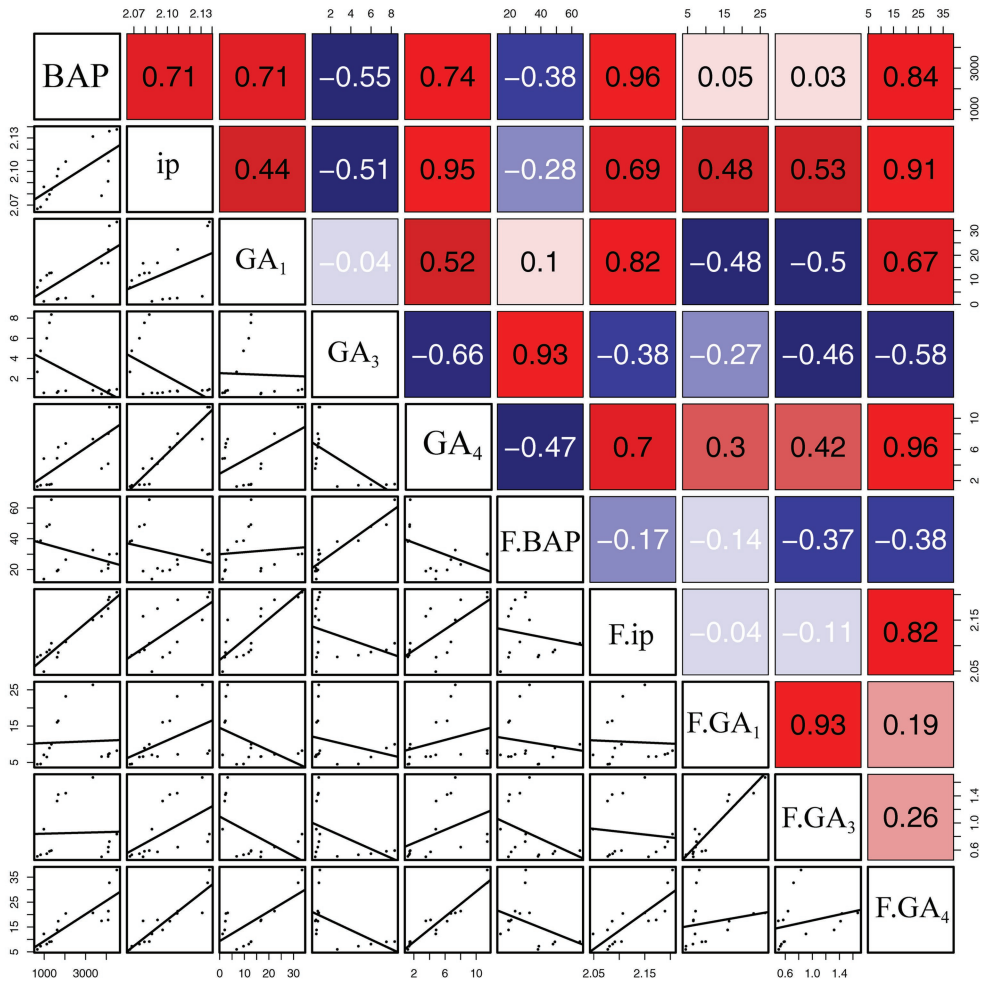

FIGURE 5 | Correlation of growth-related phytohormones between gall tissues and cones. The mean differences were compared using *t*-test ($p < 0.05$). BAP, iP, GA_1, GA_3, and GA_4 represent phytohormone levels in gall tissues; F.BAP, F.iP, F.GA_1, F.GA_3, and F.GA_4 represent phytohormone levels in cones. Red and blue squares represent positive and negative correlations, respectively.

corresponding phytohormones in the galls; however, only the concentrations of ACC showed a significant negative correlation between cones and galls ($R = -0.92$, $p < 0.001$). These results suggest that ACC cooperates with JA and ABA in the development of both galls and cones. Moreover, galls that do not abscize and can account for the downregulated ACC result in any current year. Upregulated ACC might therefore be triggered the abscission of the cones (**Figure 7**).

SA and SA-Related Phenolics in Gall Tissues and Cones Throughout the Developmental Stages

The concentrations of BA and *p*HBA were affected by developmental stage (gall tissues: BA: F6, 12.25 = 54.05, $p = <0.001$; *p*HBA: F6, 11.72 = 18.10, $p = <0.001$; cones: BA: F2, 6.24 = 19.13, $p = 0.002$; *p*HBA: F2, 5.51 = 33.82, $p = 0.001$). The BA in gall tissues exhibited the highest concentrations in the last stage of development, with a value of 9951.52 ± 1108.53 ng/g FW, which was four times that in the control branches and 13 times that in the mature cones (**Figure 8**). The highest concentrations of SA in the gall tissues were also observed in the last stage of gall development, with a value of 880.66 ± 98.05 ng/g FW, which was three times that in the control branches and 23 times that in mature cones. Interestingly, high concentrations of SA were also found in the larch adelgids, with values of 1195.92 ± 386.55 ng/g FW, indicating that the larch adelgids have the ability to store or transport SA. Compared with concentrations in gall tissues at other developmental stages, the upregulated concentrations of *t*CA and *p*HCA at stages G3 and G4 (**Figure 8**) were correlated with the concentration of anthocyanins at those stages, suggesting that *t*CA and *p*HCA are the key precursors in the biosynthesis of anthocyanins (**Scheme 1**). The concentrations of *t*CA, BA, and *p*HBA in the Korean spruce cones also increased with developmental stage.

The concentrations of BA in gall tissues were positively correlated with those of *p*HBA ($R = 0.96$, $p < 0.001$) and SA

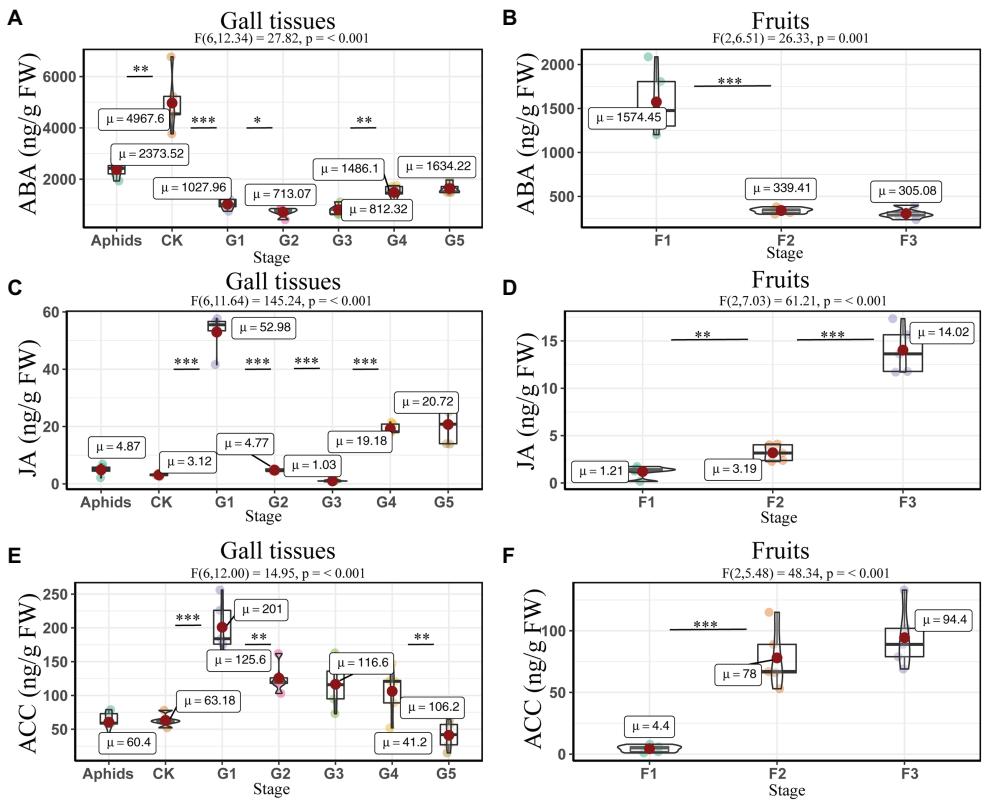

FIGURE 6 | Quantitative analysis of defense related phytohormones concentrations in larch adelgids, gall tissues, and cones of *P. koraiensis*. The abscisic acid (ABA), jasmonic acid (JA), and 1-aminocyclopropane-1-carboxylic acid (ACC) concentrations in gall tissues and normal branches **(A,C,E)** and cones **(B,D,F)**, respectively. *CK* = normal branches without gall. Data are presented in nanograms per gram of fresh weight (ng/g FW), and boxplots display the minimum, first quartile, median, third quartile, and maximum for each stage in the given tissues. Red point = mean value and horizontal black line inside the box = median value. The shape of the boxplots indicates distribution of results. The mean differences were compared using *t*-tests. *Indicates that the value of *p* is less than 0.05. **Indicates that the value of *p* is less than 0.01. ***Indicates that the value of *p* is less than 0.001. These results shown are the average ± SD and performed one-way ANOVA test among three or more groups. ωp^2 = partial omega squared.

($R = 0.76$, $p < 0.01$), and we also observed a significant positive correlation between the concentrations of *p*HBA and SA ($R = 0.66$, $p < 0.05$) in gall tissues. These results suggest that BA might be the precursor of *p*HBA and SA (**Scheme 1**). In addition, concentrations of *p*HCA in gall tissues were significantly and positively correlated with those of *t*CA ($R = 0.93$, $p < 0.001$) throughout the developmental stages. Similarly, throughout cone development, concentrations of BA were significantly and positively correlated with those of *p*HBA ($R = 0.98$, $p < 0.001$), *t*CA ($R = 0.97$, $p < 0.001$) and were also positively correlated with SA concentrations, although this relationship was not significant. In addition, there was a significant positive correlation between *p*HBA and *t*CA ($R = 0.99$, $p < 0.001$) in cones. The correlative patterns of *p*HBA, BA, and SA in cones were consistent with those in insect-induced galls. However, concentrations of *p*HCA and *t*CA in gall tissues were strongly and negatively correlated with those in cones. With the exception of *p*HCA and *t*CA, our results demonstrate that changes in the concentrations of SA-related phenolics during gall development are consistent with those during cone development (**Figure 9**).

DISCUSSION

Both Galls and Cones Are Sink Organs

Together with flowers, buds, stems, and roots, fruits are important natural plant sink organs that absorb photoassimilates from adjacent tissues to maintain their own normal growth and development (Dorchin et al., 2006; Samsone et al., 2011). The behavior of galls as assimilate sinks has been widely studied, and they compete with natural plant sink organs for the nutrient supply that supports their formation and growth (Yang et al., 2007; Huang et al., 2011, 2015). Galls can affect the carbon partitioning mechanisms within their host plant because they can alter the resource balance between source and sink tissues (Dorchin et al., 2006). The high level of sugars in the gall tissues evidenced that they can be sink organs on the stem of *P. koraiensis*. Consequently, galls have a negative impact on the growth and development of the host plant, leading to reductions in the production of flowers, fruits, seeds, or biomass (Oliveira et al., 2017). There is therefore a competitive relationship between the gall and fruit sinks. Based on close source-sink

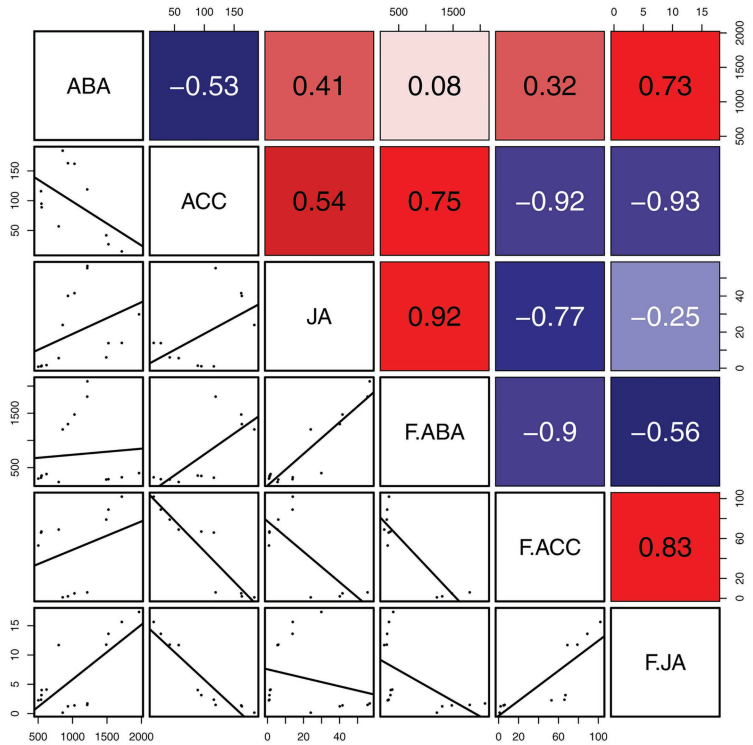

FIGURE 7 | Correlation of defense related phytohormones between gall tissues and cones. Mean differences were compared using *t*-tests ($p < 0.05$). Red and blue boxes represent positive and negative correlations, respectively.

relationships, the developmental processes of galls and fruit are similar. However, the mechanisms of this phenomenon are not fully understood.

6-Benzylaminopurine Stimulates the Development of the Gall Tissues

Endogenous 6-benzylaminopurine (BAP) and its derivatives have been detected in several plant species. Furthermore, BAP has been detected in many different parts of both the coconut palm (*Cocos nucifera* L.) and the Baikal skullcap (*Scutellaria baicalensis* Georgi; Nandi et al., 1989; Sáenz et al., 2003; Chernyad'ev, 2009). In our study, we found that the concentrations of the cytokinin BAP in the gall-inducing larch adelgids were significantly higher than those in either normal branches without galls or gall tissues at stages G1–G3. These results suggest that BAP is synthesized by the insects themselves to promote the formation of galls. Exogenous treatment with BAP will delay the leaf abscission of soybean (Kuang et al., 1992) indicated high level of BAP in last stage of gall tissues related to anti-abscission of the gall after a year. However, only the concentrations of BAP showed a little negative correlation between cones and gall tissues ($R = -0.38$; **Figure 5**). Thus, the anti-abscission of the *P. koraiensis* cones may be unrelated to the higher concentrations of BAP. Moreover, higher concentrations of iP and *t*Z have been found in gall-inducing insects (*Pontania* sp., *Eurosta solidaginis*, *Stenopsylla nigricornis*, and others) than in plant tissues (Mapes and Davies, 2001; Yamaguchi et al., 2012; Kai et al., 2017). It is therefore inferred that iP and *t*Z synthesized by the galling insects might manipulate host plants to facilitate the expansion of gall tissues (Mapes and Davies, 2001). However, in our experiments, the concentrations of iP and *t*Z in larch adelgids and in the gall tissues of *P. koraiensis* were relatively low, suggesting that they were not the key substances responsible for *A. laricis laricis* gall expansion on *P. koraiensis*.

The Accumulation of Anthocyanin Is Correlated to Sink Function of Gall Tissues

Anthocyanin acting as one of main coloring matters widely distributes in sink organs of plants (Wang et al., 2020). The red color observed in insect gall tissues is mainly caused by the presence of anthocyanins in those tissues (Gerchman et al., 2013). This has led to the possible connection between gall development and anthocyanins. Some researchers have found that this occur is due to the upregulation of the phenylpropanoid pathways by cytokinins in response to galler attack, which leads to anthocyanin accumulation in the galls (Connor et al., 2012). However, the upregulated phenylpropanoids may damage the photosynthetic system, which led to these tissues sensitive to UV radiation (Zhou et al., 2020). In order to reduce the

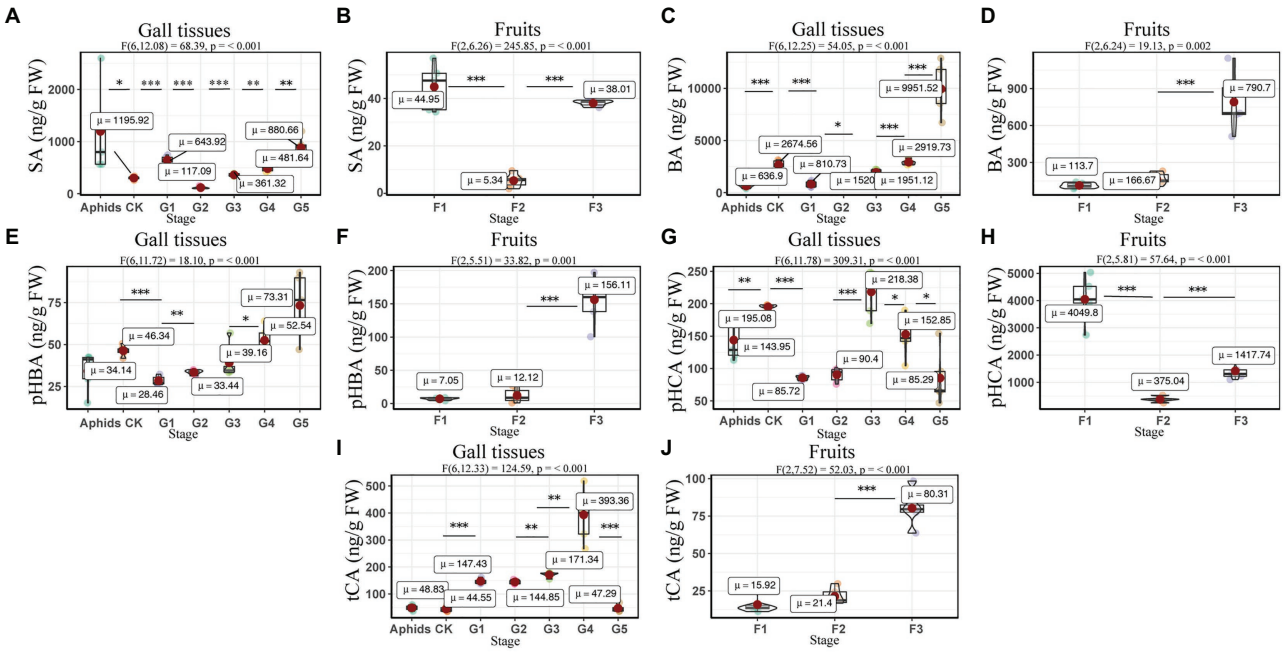

FIGURE 8 | Quantitative analysis of concentrations of SA and SA-related phenolics in larch adelgids, gall tissues, and *P. koraiensis* cones. Quantitative analysis of salicylic acid (SA), benzoic acid (BA), *p*-hydroxybenzoic acid (*p*HBA), *p*-hydroxycinnamic acid (*p*HCA), and *trans*-cinnamic acid (*t*CA) in gall tissues and normal branches **(A,C,E,G,I)** and cones **(B,D,F,H,J),** respectively. *CK* = normal branches. Data are presented in nanograms per gram of fresh weight (ng/g FW), and boxplots display the minimum, first quartile, median, third quartile, and maximum for each stage in the given tissues. Red point = mean value and horizontal black line inside the box = median value. Shape of boxplots indicates distribution of results. The mean differences were compared using *t*-tests. *indicates that the value of *p* is less than 0.05. **Indicates that the value of *p* is less than 0.01. ***Indicates that the value of *p* is less than 0.001. The results shown are an average ± SD and performed one-way ANOVA test among three or more groups. ωp^2 = partial omega squared.

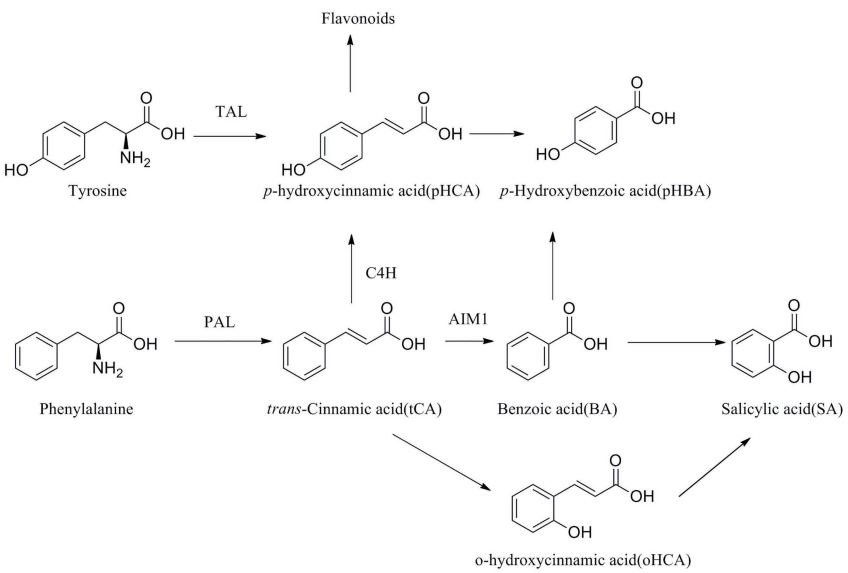

SCHEME 1 | Plausible biosynthesis pathway of SA-related phenolics.

damage of UV radiation, plants accumulate anthocyanins in these tissues (Connor et al., 2012). Moreover, the upregulation of anthocyanins may protect the galling aphids against UV radiation in peach species (Zhou et al., 2020). Totally, the accumulation of anthocyanins in gall tissues is correlated to their sink function.

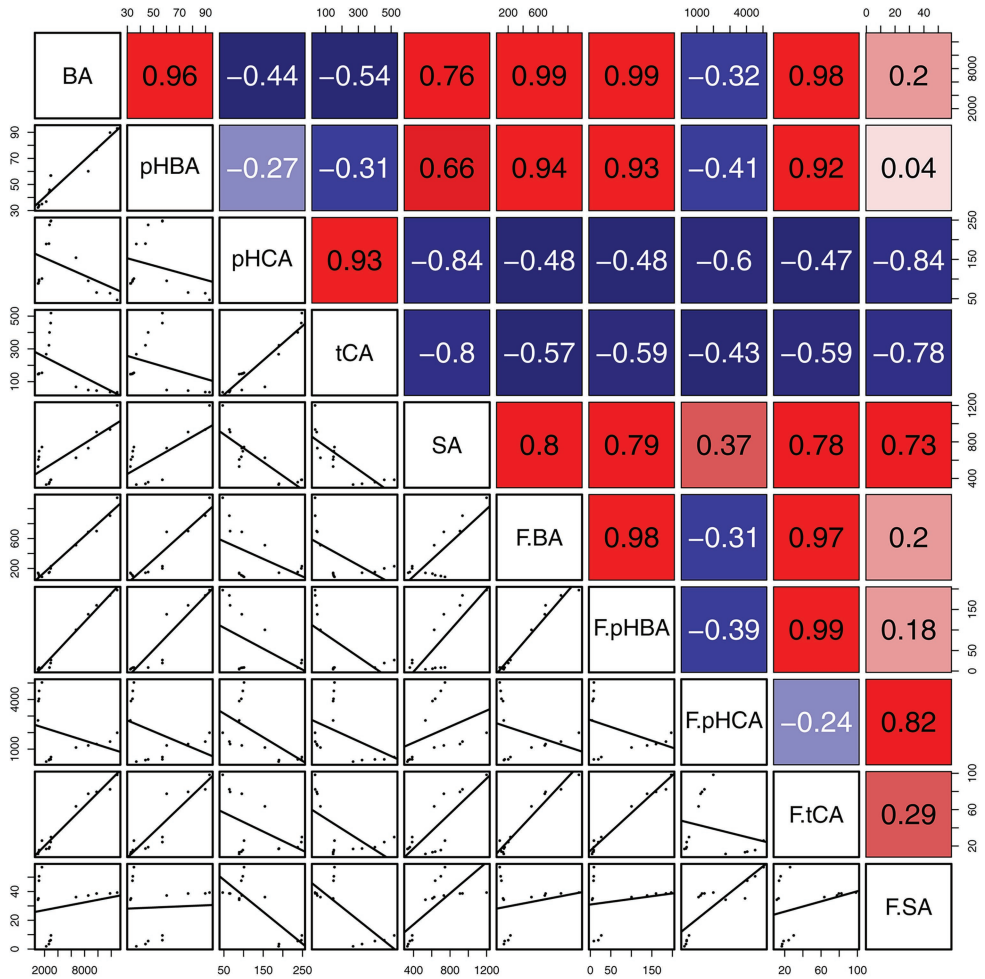

FIGURE 9 | Correlation of SA and SA-related phenolics between gall tissues and cones. The mean differences were compared using *t*-tests ($p < 0.05$). BA, *p*HBA, *p*HCA, *t*CA, and SA represent the levels of phytohormones in gall tissues; F.BA, F.*p*HBA, F.*p*HCA, F.*t*CA, and F.SA represent the phytohormone levels in cones. Red and blue boxes represent positive and negative correlations, respectively.

The Lack of Abscission of Galls Is Related to the Concentrations of 1-Aminocyclopropane-1-Carboxylic Acid

Fruit abscission is closely related to the regulation of plant hormones (Iqbal et al., 2017). The endogenous hormone ethylene has a major role in the process of fruit abscission, in which there is also crosstalk with the other hormones ABA, GAs, auxins, and CTK (Iqbal et al., 2017). The concentration of ACC is known to be positively correlated with to the fruit development and abscission (Samsone et al., 2012; McAtee et al., 2013). However, our observations of ACC in the *P. koraiensis* galls suggest that the concentrations of this phytohormone decrease with gall developmental stage. Furthermore, the galls on the stem of *P. koraiensis* do not abscise the year they form and can remain on the tree for at least 2 years. Hence, the lack of abscission of the *P. koraiensis* galls may related to the low concentrations of ACC.

The Functions of SA and SA-Related Phenolic Acids in Galls and Cones of Korean Spruce

SA and SA-related phenolic acids are broadly distributed throughout plant tissues and are closely related to the growth of plant (Eitle et al., 2019). The biosynthesis of these phenolic acids occurs *via* both the phenylalanine and the tyrosine pathway (Monica et al., 2016). In the phenylalanine pathway, phenylalanine is initially processed to *t*CA by phenylalanine ammonia lyase (PAL) and then to *p*HCA by cinnamate 4-hydroxylase (C4H), which leads on to the flavonoid pathway (**Scheme 1**). Different biosynthetic pathways are then employed to convert *t*CA to either *p*HBA or SA.

Phenolic acids are also important in plant responses to biotic and abiotic stresses, particularly against fungal infections (Firn, 1989). With the developmental stage of gall tissues, there is an increased risk of fungal infection with development of galls, because of the dehiscence (Amborabé et al., 2002). Therefore, it is speculated the higher concentrations of the phenolics BA and *p*HBA observed in galls may be related

to their role in defense against fungal attack. In addition, the phenolics *t*CA and *p*HCA are vital precursors of anthocyanin synthesis (Hilker and Fatouros, 2016). In *P. koraiensis* gall tissues, *t*CA and *p*HCA concentrations reached the highest levels at stages G4 and G3, respectively, where the gall tissues turn red, probably due to the accumulations of anthocyanins. This is similar to the accumulation of *t*CA throughout cone development, and the concentrations of *p*HCA in cone tissues were very high, which may also be associated with accumulation of anthocyanins and changes in color. Therefore, the role of anthocyanins in *P. koraiensis* galls and cones may be very similar.

CONCLUSION

All the present results suggest that phytohormones can act as the key regulators in the growth and development of both *P. koraiensis* galls and cones. This agrees with the results from the current study, which demonstrated that both galls and cones use a source-sink relationship for their own growth and development, resulting in similar appearance and morphology. In particular, BAP secreted by larch adelgids facilitates the formation of *P. koraiensis* galls. Our study provides further insights into gall formation and focuses on the potential mechanism by which the galling insects can induce gall tissues.

DATA AVAILABILITY STATEMENT

The raw data supporting the conclusions of this article will be made available by the authors, without undue reservation.

AUTHOR CONTRIBUTIONS

MJ, WZ, QL, JL, and SL designed the research and performed the experiments. MJ, WZ, JH, QL, and BQ analyzed the data. SL and MJ wrote the paper and conceived the project. All authors contributed to the article and approved the submitted version.

FUNDING

This research was financially supported by the National Key Research & Development Program of China (2017YFD0201400 and 2017YFD0201403), Liaoning Revitalization Talents Program (Grant No. XLYC1907151), the Scientific Research Foundation of Shenyang Agricultural University (Grant No. 880416055), and the Liaoning Agricultural Research and Industrialization Guidance Plan (2019JH8/10200017).

ACKNOWLEDGMENTS

We thank BQ for the help in identification of the plant materials and Shouhui Sun for the help in identification of the larch adelgid.

SUPPLEMENTARY MATERIAL

The Supplementary Material for this article can be found online at: https://www.frontiersin.org/articles/10.3389/fpls.2020.580155/full#supplementary-material

REFERENCES

Amborabé, B. E., Fleurat-Lessard, P., Chollet, J. -F., and Roblin, G. (2002). Antifungal effects of salicylic acid and other benzoic acid derivatives towards *Eutypa lata*: structure–activity relationship. *Plant Physiol. Biochem.* 40, 1051–1060. doi: 10.1016/S0981-9428(02)01470-5

Body, M. J. A., Zinkgraf, M. S., Whitham, T. G., Lin, C. H., Richardson, R. A., Appel, H. M., et al. (2019). Heritable phytohormone profiles of poplar genotypes vary in resistance to a galling aphid. *Mol. Plant-Microbe Interact.* 32, 654–672. doi: 10.1094/MPMI-11-18-0301-R

Cambier, S., Ginis, O., Moreau, S. J. M., Gayral, P., and Drezen, J. -M. (2019). Gall wasp transcriptomes unravel potential effectors involved in molecular dialogues with oak and rose. *Front. Physiol.* 10:926. doi: 10.3389/fphys.2019.00926

Castro, A. C., Oliveira, D. C., Moreira, A. S. F. P., Lemos-Filho, J. P., and Isaias, R. M. S. (2012). Source–sink relationship and photosynthesis in the horn-shaped gall and its host plant *Copaifera langsdorffii* Desf. (Fabaceae). *S. Afr. J. Bot.* 83, 121–126. doi: 10.1016/j.sajb.2012.08.007

Chernyad'ev, I. I. (2009). The protective action of cytokinins on the photosynthetic machinery and productivity of plants under stress (review). *Appl. Biochem. Microbiol.* 45, 351–362. doi: 10.1134/S0003683809040012

Connor, E. F., Bartlett, L., O'Toole, S., Byrd, S., Biskar, K., and Orozco, J. (2012). The mechanism of gall induction makes galls red. *Arthropod-Plant Inte.* 6, 489–495. doi: 10.1007/s11829-012-9210-7

Dorchin, N., Cramer, M. D., and Hoffmann, J. H. (2006). Photosynthesis and sink activity of wasp-induced galls in *Acacia pycnantha*. *Ecology* 87, 1781–1791. doi: 10.1890/0012-9658(2006)87[1781:PASAOW]2.0.CO;2

Eitle, M. W., Griesser, M., Vankova, R., Dobrev, P., Aberer, S., and Forneck, A. (2019). Grape phylloxera (*D. vitifoliae*) manipulates SA/JA concentrations and signalling pathways in root galls of *Vitis* spp. *Plant Physiol. Biochemist* 144, 85–91. doi: 10.1016/j.plaphy.2019.09.024

Fay, P. A., Hartnett, D. C., and Knapp, A. K. (1996). Plant tolerance of gall-insect attack and gall-insect performance. *Ecology* 77, 521–534. doi: 10.2307/2265627

Firn, R. D. (1989). Phenolic biosynthesis, leaf damage, and insect herbivory in birch (*Betula pendula*). *J. Chem. Ecol.* 15, 275–283. doi: 10.1007/BF02027789

Gerchman, Y., Lev-Yadun, S., and Inbar, M. (2013). Red gall pigmentation: cytokinin stimulation is not everything. *Arthropod-Plant Inte.* 7, 335–337. doi: 10.1007/s11829-013-9248-1

Guimarães, R., Barros, L., Carvalho, A. M., Sousa, M. J., Morais, J. S., and Ferreira, I. C. F. R. (2009). Aromatic plants as a source of important phytochemicals: vitamins, sugars and fatty acids in *Cistus ladanifer*, *Cupressus lusitanica* and *Eucalyptus gunnii* leaves. *Ind. Crop. Prod.* 30, 427–430. doi: 10.1016/j.indcrop.2009.08.002

Hilker, M., and Fatouros, N. E. (2016). Resisting the onset of herbivore attack: plants perceive and respond to insect eggs. *Curr. Opin. Plant Biol.* 32, 9–16. doi: 10.1016/j.pbi.2016.05.003

Hirano, T., Kimura, S., Sakamoto, T., Okamoto, A., Nakayama, T., Matsuura, T., et al. (2020). Reprogramming of the developmental program of *Rhus javanica* during initial stage of gall induction by *Schlechtendalia chinensis*. *Front. Plant Sci.* 11:471. doi: 10.3389/fpls.2020.00471

Howe, G. A., and Jander, G. (2008). Plant immunity to insect herbivores. *Annu. Rev. Plant Biol.* 59, 41–66. doi: 10.1146/annurev.arplant.59.032607.092825

Huang, M. Y., Huang, W. D., Chou, H. M., Chen, C. C., Chen, P. J., Chang, Y. T., et al. (2015). Structural, biochemical, and physiological characterization of photosynthesis in leaf-derived cup-shaped galls on *Litsea acuminata*. *BMC Plant Biol.* 15:61. doi: 10.1186/s12870-015-0446-0

Huang, M. Y., Lin, K. H., Yang, M. M., Chou, H. M., Yang, C. M., and Chang, Y. T. (2011). Chlorophyll fluorescence, spectral properties, and pigment composition of galls on leaves of *Machilus thunbergii*. *Int. J. Plant Sci.* 172, 323–329. doi: 10.1086/658157

Iqbal, N., Khan, N. A., Ferrante, A., Trivellini, A., Francini, A., and Khan, M. I. R. (2017). Ethylene role in plant growth, development and senescence: interaction with other phytohormones. *Front. Plant Sci.* 8:475. doi: 10.3389/fpls.2017.00475

Kai, S., Kumashiro, S., Adachi, S., Suzuki, Y., Shiomi, Y., Matsunaga, K., et al. (2017). Life history of *Stenopsylla nigricornis* (Hemiptera: Psylloidea: Triozidae) and phytohormones involved in its gall induction. *Arthropod-Plant Inte.* 11, 1–10. doi: 10.1007/s11829-016-9470-8

Kojima, M., Kamada-Nobusada, T., Komatsu, H., Takei, K., Kuroha, T., Mizutani, M., et al. (2009). Highly sensitive and high-throughput analysis of plant hormones using MS-probe modification and liquid chromatography–tandem mass spectrometry: an application for hormone profiling in *Oryza sativa*. *Plant Cell Physiol.* 50, 1201–1214. doi: 10.1093/pcp/pcp057

Kuang, A., Peterson, C. M., and Dute, R. R. (1992). Leaf abscission in soybean: cytochemical and ultrastructural changes following benzylaminopurine treatment. *J. Exp. Bot.* 43, 1611–1619. doi: 10.1093/jxb/43.12.1611

Kutsukake, M., Uematsu, K., and Fukatsu, T. (2019). Plant manipulation by gall-forming social aphids for waste management. *Front. Plant Sci.* 10:933. doi: 10.3389/fpls.2019.00933

Larson, K. C., and Whitham, T. G. (1997). Competition between gall aphids and natural plant sinks: plant architecture affects resistance to galling. *Oecologia* 109, 575–582. doi: 10.1007/s004420050119

Li, X. Q., Liu, Y. Z., Guo, W. F., Solanki, M. K., Yang, Z. D., Xiang, Y., et al. (2017). The gall wasp *Leptocybe invasa* (Hymenoptera: Eulophidae) stimulates different chemical and phytohormone responses in two *Eucalyptus varieties* that vary in susceptibility to galling. *Tree Physiol.* 37, 1208–1217. doi: 10.1093/treephys/tpx098

Liu, S. D., Ren, S., Zheng, J., Teng, S. J., Fan, H. J., and Dai, Y. Y. (2011). Study on distribution and rules of piercing-sucking insects in Jilin province (in Chinese). *Forest. Sci. Tech. Info.* 43, 9–11.

Mapes, C. C., and Davies, P. J. (2001). Cytokinins in the ball gall of *Solidago altissima* and in the gall forming larvae of *Eurosta solidaginis*. *New Phytol.* 151, 203–212. doi: 10.1046/j.1469-8137.2001.00158.x

McAtee, P., Karim, S., Schaffer, R., and David, K. (2013). A dynamic interplay between phytohormones is required for fruit development, maturation, and ripening. *Front. Plant Sci.* 4:79. doi: 10.3389/fpls.2013.00079

Monica, S., Rajat, S., Anuradha, S., Pankaj, K., Ankita, M., Sanjay, J., et al. (2016). Comparative analysis of phenolic compound characterization and their biosynthesis genes between two diverse bread wheat (*Triticum aestivum*) varieties differing for chapatti (unleavened flat bread) quality. *Front. Plant Sci.* 7:1870. doi: 10.3389/fpls.2016.01870

Musser, R. O., Hummusser, S. M., Eichenseer, H., Peiffer, M., Ervin, G., Murphy, J. B., et al. (2002). Herbivory: caterpillar saliva beats plant defences. *Nature* 416, 599–600. doi: 10.1038/416599a

Nandi, S. K., Letham, D. S., Palni, L. M. S., Wong, O. C., and Summons, R. E. (1989). 6-Benzylaminopurine and its glycoside as naturally occurring cytokinin. *Plant Sci.* 61, 189–196. doi: 10.1016/0168-9452(89)90223-9

Naseem, M., Wolfling, M., and Dandekar, T. (2014). Cytokinins for immunity beyond growth, galls and green islands. *Trends Plant Sci.* 19, 481–484. doi: 10.1016/j.tplants.2014.04.001

Oliveira, D. C., Isaias, R. M. S., Fernandes, G. W., Ferreira, B. G., Carneiro, R. G. S., and Fuzaro, L. (2016). Manipulation of host plant cells and tissues by gall-inducing insects and adaptive strategies used by different feeding guilds. *J. Insect Physiol.* 84, 103–113. doi: 10.1016/j.jinsphys.2015.11.012

Oliveira, D. C., Moreira, A., Isaias, R. M. S., Martini, V., and Rezende, U. C. (2017). Sink status and photosynthetic rate of the leaflet galls induced by *Bystracoccus mataybae* (Eriococcidae) on *Matayba guianensis* (Sapindaceae). *Front. Plant Sci.* 8:1249. doi: 10.3389/fpls.2017.01249

Sáenz, L., Jones, L. H., Oropeza, C., Vlácil, D., and Strnad, M. (2003). Endogenous isoprenoid and aromatic cytokinins in different plant parts of *Cocos nucifera* (L.). *Plant Growth Regul.* 39, 205–215. doi: 10.1023/A:1022851012878

Samsone, I., Andersone, U., and Ievinsh, G. (2011). Gall midge *Rhabdophaga rosaria*-induced rosette galls on *Salix*: morphology, photochemistry of photosynthesis and defense enzyme activity. *Env. Exp. Biol.* 9, 29–36.

Samsone, I., Andersone, U., and Ievinsh, G. (2012). Variable effect of arthropod-induced galls on photochemistry of photosynthesis, oxidative enzyme activity and ethylene production in tree leaf tissues. *Env. Exp. Biol.* 10, 15–26.

Stahl, E., Hilfiker, O., and Reymond, P. (2018). Plant-arthropod interactions: who is the winner? *Plant J.* 93, 703–728. doi: 10.1111/tpj.13773

Stone, G. N., and Schonrogge, K. (2003). The adaptive significance of insect gall morphology. *Trends Ecol. Evol.* 18, 512–522. doi: 10.1016/S0169-5347(03)00247-7

Straka, J. R., Hayward, A. R., and Emery, R. J. N. (2010). Gall-inducing *Pachypsylla celtidis* (Psyllidae) infiltrate hackberry trees with high concentrations of phytohormones. *J. Plant Interact.* 5, 197–203. doi: 10.1080/17429145.2010.484552

Takei, M., Yoshida, S., Kawai, T., Hasegawa, M., and Suzuki, Y. (2015). Adaptive significance of gall formation for a gall-inducing aphids on Japanese elm trees. *J. Insect Physiol.* 72, 43–51. doi: 10.1016/j.jinsphys.2014.11.006

Tooker, J. F., and Helms, A. M. (2014). Phytohormone dynamics associated with gall insects, and their potential role in the evolution of the gall-inducing habit. *J. Chem. Ecol.* 40, 742–753. doi: 10.1007/s10886-014-0457-6

Wang, F., Sha, J., Chen, Q., Xu, X., Zhu, Z., Ge, S., et al. (2020). Exogenous abscisic acid regulates distribution of ^{13}C and ^{15}N and anthocyanin synthesis in 'Red Fuji' apple fruit under high nitrogen supply. *Front. Plant Sci.* 10:1738. doi: 10.3389/fpls.2019.01738

Wellburn, A. R. (1994). The spectral determination of chlorophylls *a* and *b*, as well as total carotenoids, using various solvents with spectrophotometers of different resolution. *J. Plant Physiol.* 144, 307–313. doi: 10.1016/S0176-1617(11)81192-2

Yamaguchi, H., Tanaka, H., Hasegawa, M., Tokuda, M., Asami, T., and Suzuki, Y. (2012). Phytohormones and willow gall induction by a gall-inducing sawfly. *New Phytol.* 196, 586–595. doi: 10.1111/j.1469-8137.2012.04264.x

Yang, C. M., Yang, M. M., Huang, M. Y., Hsu, J. M., and Jane, W. N. (2007). Life time deficiency of photosynthetic pigment-protein complexes CP1, A1, AB1, and AB2 in two cecidomyiid galls derived from *Machilus thunbergii* leaves. *Photosynthetica* 45, 589–593. doi: 10.1007/s11099-007-0101-6

Yu, Z. J., Qi, H. A., Jiang, Z. l., and Li, G. W. (1998). Three-stage and sequential sampling techniques for the emigrant form of *Adelges laricis* Vall (in Chinese). *J. Beijing Forest. Uni.* 20, 47–51.

Zhou, W., Jia, M. Y., Zhang, G. C., Sun, J., Li, Q. L., Wang, X. L., et al. (2020). Up-regulation of phenylpropanoid biosynthesis system in peach species by peach aphids produces anthocyanins that protect the aphids against UVB and UVC radiation. *Tree Physiol.* doi: 10.1093/treephys/tpaa132 [Epub ahead of print]

Zhu-Salzman, K., and Zeng, R. S. (2015). Insect response to plant defensive protease inhibitors. *Annu. Rev. Entomol.* 60, 233–252. doi: 10.1146/annurev-ento-010814-020816

Ziegler, J., Qwegwer, J., Schubert, M., Erickson, J. L., Schattat, M., Burstenbinder, K., et al. (2014). Simultaneous analysis of apolar phytohormones and 1-aminocyclopropan-1-carboxylic acid by high performance liquid chromatography/electrospray negative ion tandem mass spectrometry via 9-fluorenylmethoxycarbonyl chloride derivatization. *J. Chromatogr. A* 1362, 102–109. doi: 10.1016/j.chroma.2014.08.029

Žurovcová, M., Havelka, J., Starý, P., VěChtová, P., Chundelová, D., Jarošová, A., et al. (2010). "DNA barcoding" is of limited value for identifying adelgids (Hemiptera: Adelgidae) but supports traditional morphological taxonomy. *Eur. J. Entomol.* 107, 147–156. doi: 10.14411/eje.2010.020

Conflict of Interest: The authors declare that the research was conducted in the absence of any commercial or financial relationships that could be construed as a potential conflict of interest.

frontiers in Plant Science

REVIEW
published: 30 November 2020
doi: 10.3389/fpls.2020.601009

The Threat of the Combined Effect of Biotic and Abiotic Stress Factors in Forestry Under a Changing Climate

*Demissew Tesfaye Teshome[1], Godfrey Elijah Zharare[2] and Sanushka Naidoo[1]**

[1]Department of Biochemistry, Genetics and Microbiology, Forestry and Agricultural Biotechnology Institute (FABI), University of Pretoria, Pretoria, South Africa, [2]Department of Agriculture, University of Zululand, KwaDlangezwa, South Africa

Plants encounter several biotic and abiotic stresses, usually in combination. This results in major economic losses in agriculture and forestry every year. Climate change aggravates the adverse effects of combined stresses and increases such losses. Trees suffer even more from the recurrence of biotic and abiotic stress combinations owing to their long lifecycle. Despite the effort to study the damage from individual stress factors, less attention has been given to the effect of the complex interactions between multiple biotic and abiotic stresses. In this review, we assess the importance, impact, and mitigation strategies of climate change driven interactions between biotic and abiotic stresses in forestry. The ecological and economic importance of biotic and abiotic stresses under different combinations is highlighted by their contribution to the decline of the global forest area through their direct and indirect roles in forest loss and to the decline of biodiversity resulting from local extinction of endangered species of trees, emission of biogenic volatile organic compounds, and reduction in the productivity and quality of forest products and services. The abiotic stress factors such as high temperature and drought increase forest disease and insect pest outbreaks, decrease the growth of trees, and cause tree mortality. Reports of massive tree mortality events caused by "hotter droughts" are increasing all over the world, affecting several genera of trees including some of the most important genera in plantation forests, such as Pine, Poplar, and *Eucalyptus*. While the biotic stress factors such as insect pests, pathogens, and parasitic plants have been reported to be associated with many of these mortality events, a considerable number of the reports have not taken into account the contribution of such biotic factors. The available mitigation strategies also tend to undermine the interactive effect under combined stresses. Thus, this discussion centers on mitigation strategies based on research and innovation, which build on models previously used to curb individual stresses.

Keywords: stress interaction, tree growth, tree mortality, forest disease, insect pests, economic impact, response, mitigation

OPEN ACCESS

Edited by:
Giorgio Gambino, Italian National Research Council, Italy

Reviewed by:
Prachi Pandey, National Institute of Plant Genome Research (NIPGR), India
Mahesh Patil, National Institute of Plant Genome Research (NIPGR), India
Tasir Sharief Per, Aligarh Muslim University, India

****Correspondence:***
Sanushka Naidoo
sanushka.naidoo@fabi.up.ac.za

Specialty section:
This article was submitted to Plant Pathogen Interactions, a section of the journal Frontiers in Plant Science

Received: *31 August 2020*
Accepted: *05 November 2020*
Published: *30 November 2020*

Citation:
Teshome DT, Zharare GE and Naidoo S (2020) The Threat of the Combined Effect of Biotic and Abiotic Stress Factors in Forestry Under a Changing Climate. Front. Plant Sci. 11:601009. doi: 10.3389/fpls.2020.601009

INTRODUCTION

Biotic and abiotic stress factors cause major economic losses by reducing yield and quality in agriculture and forestry. A global survey on the major food crops indicated that pathogens, insect pests (hereafter pests), and weeds cause average yield losses ranging from 17.2% in potato up to 30.0% in rice (Savary et al., 2019). Similarly, the major abiotic stresses such as

temperature extremes, drought, as well as the deficiency and toxicity of plant nutrients cause up to 51–82% annual loss of crop yield in the world (Oshunsanya et al., 2019). Despite the lack of similar comprehensive assessments of losses, there is sufficient evidence indicating that the forestry sector is similarly affected by these biotic and abiotic stresses (Phillips et al., 2009; Hurley et al., 2017; Graziosi et al., 2019; Schuldt et al., 2020). For example, Forest Resources Assessment (FRA-2015) revealed that the major biotic and abiotic stresses affected 141.6 million ha of forest in 75 reporting countries between 2003 and 2012 (van Lierop et al., 2015). Thus, biotic and abiotic stresses can negatively affect the "ecosystem services" of forests (Alcamo et al., 2003) and may contribute to the decline in the global forest area (Keenan et al., 2015).

The global forest area is expected to continue declining despite the recent decrease in the rate of annual forest loss (d'Annunzio et al., 2015; Keenan et al., 2015) and increase in planted forest area (Payn et al., 2015). According to FRA-2015, while the global forest area decreased from 4.12 to 3.99 billion ha from 1990 to 2015 (Keenan et al., 2015), planted forest area increased from 167.5 to 277.9 million ha during the same period (Payn et al., 2015). d'Annunzio et al. (2015) predicted that the global forest area will continue to decline in the current decade, though at a lower rate of loss. However, Song et al. (2018) found an increase in the overall area of global tree cover between 1982 and 2016. Yet, owing to the observed (Song et al., 2018) and predicted regional differences (d'Annunzio et al., 2015), it is expected that there will be areas, where forests will be lost at a very high rate.

The vulnerability of forests to biotic and abiotic stresses is increasing with climate change (Allen et al., 2015; Pureswaran et al., 2018) and global movement of pathogens and pests (Roy et al., 2014). All scenarios of global climate predictions indicate that the observed global change will continue and cause major changes in precipitation and temperature in different parts of the world (IPCC, 2018). Significant increase in temperature was observed on 76% of the global land area in the 20th century, and a further increase of 2.4–4°C is predicted to occur by 2100 (Gonzalez et al., 2010). Increasing frequency and intensity of droughts accompanied by global warming driven higher temperature, termed "hotter droughts" (Allen et al., 2015), are further witnesses of a changing climate (Crockett and Westerling, 2018). Global land area affected by prolonged heat waves increased from an average of less than 1% in the period from 1951 to 1980 to 10% in the period afterward, reaching as high as 22.21% in 2010 (Hansen et al., 2012) and is expected to increase throughout the 21st century (Wu et al., 2020). Such concerning changes are matched by the threat of forest pathogens and pests, which also continue to show increasing trends in different parts of the world (Roy et al., 2014; Deidda et al., 2016; Hurley et al., 2016; Nahrung and Carnegie, 2020).

Trees are often exposed to both simultaneous and sequential combinations of several biotic and abiotic stresses recurring throughout their long life. Thus, it is important to understand the complex interactions between multiple biotic and abiotic stresses (Anderegg et al., 2015) as it is difficult to predict the response of trees to multiple stress factors and the resulting damage from single stress studies (Pandey et al., 2015). This is particularly urgent in the context of global climate change, which may further complicate the interactions through increasing the frequency and severity of extreme weather events (IPCC, 2018). These events may increase the susceptibility of trees (Buotte et al., 2017), facilitate the spread, reproduction, and development of pathogens and pests (Matsuhashi et al., 2020), and weaken or destroy their natural enemies and competitors (Thurman et al., 2017). While climate change may also reduce damage by negatively affecting pests and pathogens (Zhan et al., 2018), more increased than decreased effects on tree growth and mortality have been observed (Creeden et al., 2014; Camarero et al., 2018).

Despite earlier focus on the dynamics and management of individual stresses in forest trees, research on combined biotic and abiotic stresses is increasing. Recent reviews focused on the mechanistic and theoretical foundations of some interactions (Cobb and Metz, 2017; Jactel et al., 2019; Simler-Williamson et al., 2019) estimated/predicted the effect of some of the interactions (Jactel et al., 2012; Gely et al., 2020), and documented regional impacts (Kolb et al., 2016). While a lot of studies focused on experimental stresses (Desprez-Loustau et al., 2006) and increased our understanding of the physiological and molecular mechanisms of tree responses, the more complex interactions in the field may have different outcomes (Huber and Bauerle, 2016). Most of the previous work focused on the impact of the gross "global change" which includes slight changes in temperature and moisture (Ayres and Lombardero, 2000; Weed et al., 2013; Pureswaran et al., 2018) and may affect the dynamics of forest pathogens and pests without necessarily causing physiological abiotic stresses on trees.

In this review, we discuss the importance and impact of climate change driven interactions between biotic and abiotic stresses in forestry. The damage biotic and abiotic stresses cause to trees could be the best indicator of impact (Jactel et al., 2012) because it is often difficult to partition the effect of individual stresses and their interactions under their combined occurrence (Calvão et al., 2019). Thus, using recent observations from forests in different parts of the world, we show how these interactions will shape the damage from forest disease and pest outbreaks, their effect on tree growth and mortality, as well as the resulting ecological and economic impacts. In addition to the effect of environmental factors under climate change such as variations in precipitation and temperature, we assess how these environmental factors at the level of an abiotic tree stressor will interact with the biotic stress factors and affect trees. We also discuss how the available mitigation strategies can be employed in this context. Despite the importance of the abiotic stresses such as nutrient toxicity and deficiencies, soil salinity and acidity, radiation extremes as well as the biotic stresses such as parasitic plants and mammalian herbivory, we limit our observations to the interactions of pests and pathogens with heat and drought stresses. These combinations represent the most important biotic-abiotic stress interactions inflicting the most damage (Breshears et al., 2005; Carnicer et al., 2011; Fettig et al., 2019; Gheitury et al., 2020), and their impact is increasing as they are strongly affected by global

climate change (McDowell et al., 2018). As a result, most of the studies also focus on these interactions (Desprez-Loustau et al., 2006). Furthermore, from the perspective of the physiological and molecular responses of plants, these interactions are generally representatives of many of the biotic-abiotic stress interactions (Wang et al., 2003; Kissoudis et al., 2014).

WEATHER EXTREMES AND FOREST DISEASE/PEST OUTBREAKS

Forest diseases and pests are significant threats to the forest sector. For example, diseases and pests respectively affected at least 12.5 and 85.5 million ha of forest in 75 countries reporting to FRA-2015 between 2003 and 2012 (van Lierop et al., 2015). They were found to be the most important causes of forest disturbance in the Northern Hemisphere affecting 43.9 million ha of forests every year (Kautz et al., 2017). Similarly, a recent study indicated that both pathogens and pests are among the major agents of disturbance in the temperate forests (Sommerfeld et al., 2018).

The interaction among plants, pathogens and pests, and the environment has been an important aspect of plant disease and pest outbreaks. With the increasing frequency and intensity of weather extremes due to global climate change, however, the environment is not just a matter of more or less "optimum" condition for biotic stress factors, rather it also comprises abiotic stress factors which affect the plants directly and indirectly. Similarly, extreme weather events may also affect pathogens and pests, further complicating the interaction. Apart from the weather extremes such as droughts and heat waves, mild variations in temperature and precipitation also affect the dynamics of disease and pest outbreaks (Ayres and Lombardero, 2000; Dukes et al., 2009; Weed et al., 2013).

The impacts of global climate change on forest pathogen and pest populations as well as the mechanisms and theoretical models behind their interaction with weather extremes have been studied using both experimental stresses and field observations (reviewed in Desprez-Loustau et al., 2006; Dukes et al., 2009; Cobb and Metz, 2017; Jactel et al., 2019; Simler-Williamson et al., 2019; Gely et al., 2020). Generally, changes in weather may affect both the host and the pathogen/pest either negatively or positively resulting in either an increase or a decrease in disease/pest outbreaks as well as the subsequent impacts on tree growth and mortality. Nevertheless, mechanistic models focusing on the pathogens and pests themselves indicate the possibilities of increased outbreak as the more likely scenario (Pureswaran et al., 2018; Jactel et al., 2019). It was also previously shown that most of the experimental drought-pathogen infection trials confirmed synergistic interaction (Desprez-Loustau et al., 2006). Similarly, a meta-analysis by Jactel et al. (2012) revealed an overall significant positive effect of drought on pathogen and pest damage. Thus, more rather than less damage can be expected from most of the biotic and abiotic stress combinations under climate change.

Furthermore, the change in the distribution and range of pathogens and pests due to climate change (Burgess et al., 2017; Pureswaran et al., 2018) may increase outbreaks in wider areas. Observed trends show that the area affected by diseases and pests increased from boreal to subtropical forests (Kautz et al., 2017). However, predictions show that climate warming may reverse this trend for some of the important pests and pathogens (Burgess et al., 2017). These changes may ultimately increase the area affected by outbreaks and the resulting damage at a global scale. In this section, we summarize the recent observed and predicted trends in forest disease and pest outbreaks using the damage to trees, except tree growth and mortality, which are discussed in the next sections, as an indicator to the outcome of the complex interactions between pathogens/pests and abiotic stresses (Jactel et al., 2012).

Forest Disease Outbreak

Variations in temperature and precipitation are observed to affect the prevalence and incidence of forest diseases and may lead to an outbreak (**Supplementary Table 1**). Several reports indicated that warming temperature increased the prevalence of diseases (Fabre et al., 2011; Brodde et al., 2019; Calvão et al., 2019). However, the effect of precipitation was less consistent showing negative (Calvão et al., 2019), positive (Fabre et al., 2011; Woods et al., 2016; Gao et al., 2019), and no correlation (Brodde et al., 2019; Thoma et al., 2019) with disease. This indicates that areas where an increase in temperature is predicted along with both decrease and increase in precipitation may possibly be exposed to future disease outbreaks. Indeed, Fabre et al. (2011), Bosso et al. (2017), and Matsuhashi et al. (2020) predicted future increases in disease outbreaks under these different scenarios (**Supplementary Table 1**). Thus, despite the contrasting observations, increased disease outbreaks are likely in many areas as climate predictions are equally contrasting in different regions of the world (IPCC, 2018).

There is also a possibility that changing climate may reduce or does not affect disease outbreak. A notable example for this is that a warming condition is found to be the major driver leading to local extinction of the fungal pathogen *Triphragmium ulmariae* (Zhan et al., 2018). Paap et al. (2017) reported that the incidence of *Phytophtora* spp. on *Corymbia calophylla* did not increase with temperature and only slightly increased with decreasing precipitation. Temperature increased infection of *Pinus albicaulis* by *Cronartium ribicola* only at high relative humidity and up to a certain threshold of 11°C (Thoma et al., 2019). Both extremely low and high temperatures did not favor crown rot disease caused by *Phytophthora alni* in alders (Aguayo et al., 2014) and pine wilt disease caused by pine wood nematode, *Bursaphelenchus xylophilus* (Gao et al., 2019) indicating that warming conditions may well reduce damage in some areas. However, a possible shift in the range of pathogens may cancel out this effect at a regional and global scale. For example, Burgess et al. (2017) predicted that global warming will increase the distribution of *Phytophthora cinnamomi* in cold areas, where it currently does not occur and decrease in warm areas, where it currently occurs. Moreover, observations of reduced impacts are rather scarce in the literature.

The changes in disease outbreaks observed or predicted under different scenarios of moderate and gradual changes in

temperature and precipitation regimes may differ under extreme conditions, such as heat and drought stresses. For example, Calvão et al. (2019) demonstrated that the mortality of *Pinus pinaster* under *B. xylophilus* infection is worsened by hotter and drier conditions indicating that these conditions may have enhanced infection. Previously, a review on the interaction of mainly experimental drought with different pathogens in trees revealed that drought and pathogen infection showed synergistic interaction in most of the cases (Desprez-Loustau et al., 2006). However, observations on the effect of heat waves, droughts, and hotter droughts on the incidence and severity of diseases seem to be scarce in the literature. Most of the previous studies focused on the resulting mortality, which will be discussed later.

The effect of drought and heat stresses may vary with the type of disease, the affected tissue, and the level of the abiotic stress (Desprez-Loustau et al., 2006; Jactel et al., 2012). Drought has been shown to significantly increase the damage caused by leaf pathogens and reduce that of root and stem pathogens (Jactel et al., 2012). Recent experimental studies have shown that drought increases the severity of diseases caused by necrotrophic pathogens in Pine and *Eucalyptus* (Sherwood et al., 2015; Barradas et al., 2018). Similarly, the resistance of *Eucalyptus marginata* clones to *P. cinnamomi* decreases with increasing temperature (Hüberli et al., 2002). However, we did not find other observations that support these results.

In general, the available information on the observed and predicted interactions between forest pathogens and changes in temperature and precipitation tend to show more damage than less. In cases where climate change reduces vulnerability to diseases, it is limited to specific pathogens and localities. Furthermore, such effects may be offset by possible new outbreaks related to range shift that can be enhanced by increased distribution of the pathogens due to globalization. This may result in a transitional period of a novel outbreak, which will be exotic to the trees, and is more damaging as has been seen in ash dieback (Marcais et al., 2017). Moreover, we only have limited knowledge on the interactions with the weather extremes such as drought and heat waves, which are predicted to increase in frequency and intensity.

Insect Pest Outbreak

Temperature is one of the most important drivers of forest pest outbreaks as shown in **Supplementary Table 1**. Rising temperatures have been associated with increased spruce budworm (*Choristoneura* spp.) outbreaks in North America (De Grandpré et al., 2019) and also increased infestation of *Picea abies* by *Ips typographus* in Europe (Marini et al., 2017; Mezei et al., 2017). This is consistent with the effect of warmer temperature in increasing the reproduction and survival of insects (Pureswaran et al., 2018). However, warming may not affect pest outbreak unless it is synchronized with the important phases of the insect's life cycle such as overwintering. In this regard, Gazol et al. (2019) showed that only warmer winters affect pine processionary moth, *Thaumetopoea pityocampa*, outbreak. According to these findings, while warming temperature may increase pest outbreaks, there are also possibilities that this may not always be the case.

While moderate warming has been associated with increased pest outbreak, extreme high temperature may have a different effect. For example, the enhancement of *I. typographus* infestation by warming declined at temperatures higher than a certain threshold (Mezei et al., 2017). It has been shown that extremely high temperatures such as heat waves may be lethal to the insects (Rouault et al., 2006). Thus, temperature which is not too high to kill the trees may reduce pest outbreak. Due to limited information on this aspect, there is a need for research to evaluate the temperature thresholds of the important pest species.

Drought has been strongly associated with historic pest outbreaks (Klein et al., 2019). However, its effect varies with the feeding guilds of insects, the substrate they feed on, and the intensity of drought (Jactel et al., 2012; Kolb et al., 2016; **Supplementary Table 1**). The outbreaks of bark beetles, wood borers, and sap suckers are often associated with drought. For example, drought increased bark beetle outbreaks in the United States (Kolb et al., 2016) and *Sirex noctilio* outbreak in Argentina (Lantschner et al., 2019). However, Jactel et al. (2012) also indicated that drought has a negative effect on sap suckers and wood borers. Yet, massive tree mortality events associated with the combined effect of droughts, and these groups of pests are increasing (see section Tree Mortality).

The effects of drought on defoliator pest outbreaks are not consistent in the literature. Drought decreased outbreaks of larch casebearer, *Coleophora laricella*, in the United States (Ward and Aukema, 2019). Similarly, insect and fungal pathogen caused defoliation decreased during severe drought in Southern European forests as defoliation and tree mortality caused by drought increased (Carnicer et al., 2011). The effect of drought on Western spruce budworm, *Choristoneura freeman*, outbreak varied during the different phases of the outbreak and had contrasting effect on drier and wetter areas. Although drought was a strong driver of outbreak initiation in wetter areas, it had no effect on the expansion of the area affected by the outbreak. In the drier areas, drought had no effect on outbreak initiation and only a small effect on the outbreak expansion (Xu et al., 2019). This indicates that drought stress may have a more important role in the initiation of pest outbreaks than their expansion. While the area affected by and intensity of pine caterpillar, *Dendrolimus* spp., outbreak clearly increased during drought years, the outbreak decreased with increasing precipitation (Bao et al., 2019). Overall, these results indicate that the effect of drought on the outbreak of defoliator insects may be weak, at least at the expansion phase.

From the foregoing discussion, it can be inferred that both drought and warming are associated with an increase in pest outbreak in many cases. However, their effects are not independent of each other. For example, the effect of temperature was observed to decrease with low rainfall (Marini et al., 2017). Several observations indicate that warmer and drier conditions favor outbreaks of many important bark beetles. Hotter droughts increased outbreaks of the mountain pine beetle *Dendroctonus ponderosae* in Western United States (Creeden et al., 2014; Buotte et al., 2017), the Eurasian spruce bark beetle *I. typographus* in Italy (Marini et al., 2012) and Austria (Netherer et al., 2019),

and the eastern larch beetle *Dendroctonus simplex* in United States (Ward and Aukema, 2019). Predictions also show that the trend of increased *D. ponderosae* outbreak will continue with increasing temperature and drought in Western United States until 2100 (Buotte et al., 2017). In line with these trends, such combinations have been important drivers of massive tree mortality.

Recent evidence revealed that Norway spruce stands in relatively wetter areas are more susceptible to bark beetle attack during drought seasons than stands in drier areas (Netherer et al., 2019) suggesting a possible acclimation by mild long term moisture deficit. A similar effect was observed in the initiation of Western spruce budworm outbreak (Xu et al., 2019). If this effect is further substantiated, it may give a choice to forest managers between minimizing risk from possible outbreaks and accepting some possible loss in productivity due to moisture deficit during normal times (Lévesque et al., 2014). Thus, further studies are needed on the extent of acclimation and the balance between predisposition and acclimation in different tree species (Bostock et al., 2014).

THE EFFECT OF COMBINED BIOTIC AND ABIOTIC STRESSES ON THE GROWTH AND MORTALITY OF FOREST TREES

Tree Growth

Although warmer weather may increase plant growth in wetter areas and currently colder areas such as boreal forests (Torzhkov et al., 2019), weather extremes such as drought and excessively high temperature are among the main tree growth limiting factors (Pichler and Oberhuber, 2007; Lévesque et al., 2014). Plant growth and reproduction are usually negatively correlated with these abiotic stresses (Blum, 2005). Similarly, in defense-growth trade-off, plants reduce growth and reproduction and allocate more resources in defending themselves against pathogens and pests (Jacquet et al., 2012; Huot et al., 2014). Plants may use different mechanisms to regulate this trade-off, which are also dependent on environmental factors (Kliebenstein, 2016; Karasov et al., 2017). Consequently, it is imperative to understand how combined biotic and abiotic stresses will shape this trade-off and affect the growth of forest trees.

The outcome of the interaction between different biotic and abiotic stresses with respect to tree growth varies with the type and level of the stresses and the species of trees. For example, the reduction in the growth of *P. abies* infected by the fungal pathogen *Heterobasidion annosum* was shown to be higher in drier and warmer locations (Gori et al., 2013) showing a synergistic interaction between the two stresses. Given that *H. annosum* is a root pathogen which may affect the transport of water, it can be hypothesized that pathogens which affect the vascular system of trees such as root rot and canker causing pathogens may have a similar effect. Infection by the fungal pathogen *Gremmeniella abietina* has been shown to reduce basal area increment by 26–58% in *Pinus sylvestris* stands (Sikström et al., 2011). Future studies may focus on determining whether drought will further reduce growth in such cases.

Defoliation by pests during drought has been thought to reduce evapotranspiration and hence water deficit stress, thus avoiding damage due to the interaction between pests and water deficit stress (Bouzidi et al., 2019). In support of this, the interaction between climatic moisture index and defoliation by pests enhanced the growth of surviving *Populus tremuloides* despite the negative effect on their survival (Cortini and Comeau, 2020). Even though combined defoliation by pine processionary moth, *T. pityocampa*, and mild drought reduced growth in *P. sylvestris*, this was matched by a similar level of recovery during non-drought years causing no overall loss in growth in the long term (Linares et al., 2014). Growth showed either a weak positive correlation or no correlation with the interaction between pest defoliation and mild drought in non-host and host trees, respectively (Itter et al., 2019). According to these observations, the risks of reduction in tree growth due to combined drought and pest defoliation might be minimal during relatively short term and mild droughts. Conversely, considerable damage due to insect defoliation in areas, where relatively longer and more intense droughts are predicted cannot be ruled out (Balducci et al., 2020).

The effect of either of drought and heat or pathogens and pests on the reduction of growth may be higher depending on the intensity of each of the stresses. The contribution of drought to growth decline was higher than that of insect outbreak in *P. tremuloides* (Chen et al., 2018). However, it was not indicated if there were any interactive effects. While leaf damage by the aspen leaf miner, *Phyllocnistis populiella*, reduced basal area index, variation in climatic moisture index and its interaction with defoliation had no effect on growth (Boyd et al., 2019). Nonetheless, the interaction of pest defoliation with severe drought may have a different impact on tree growth. For example, the growth of *P. tremuloides* decreased by 33% under the combined effect of hotter drought, defoliator, and wood boring pests between 1997 and 2014 in Canada (Hogg et al., 2008). These results indicate that the interactions of more severe abiotic stresses with pests and pathogens may cause more severe damage to tree growth.

Tree Mortality

Tree mortality is a natural phenomenon often caused by several contributing factors. Generally, it occurs at a very low rate in all forest populations without causing any considerable ecological and economic damage in the short term (Jimenez et al., 1985). Tree mortality events which affect relatively larger areas and a large number of trees have been mainly associated with rare catastrophic events, such as hurricanes, earthquakes, and landslides (Jimenez et al., 1985; Lugo and Scatena, 1996). However, recent evidences show that large scale tree mortality events, which are not associated with such rare catastrophes are increasing (Allen et al., 2010, 2015; Greenwood et al., 2017; McDowell et al., 2018) Here, we use the tree mortality classification given in Lugo and Scatena (1996) with the exception that the term "massive mortality" will be used to represent

the mortality events, which can be considered as both "catastrophic" and "extensive/massive."

The abiotic stresses such as the extremes of moisture and temperature as well as the biotic stresses such as pests and pathogens have been among the major drivers of massive mortality events (McDowell et al., 2018). It has long been known that tree mortality is a result of the contribution of several interacting causes that involve both biotic and abiotic factors (Franklin et al., 1987; Ciesla and Donaubauer, 1994). Thus, it can be expected that the different biotic and abiotic stresses are more likely to be acting in combination to cause the increasing massive mortality events. Indeed, there is an increasing number of observations in support of this (De Grandpré et al., 2019; Stephenson et al., 2019; Ward and Aukema, 2019). Even though these stress factors have always been problems in forestry and agriculture, the intensity and frequency of extreme weather events as well as forest disease and pest outbreaks have increased and will continue to increase due to climate change and global movement of pests and pathogens (Hansen et al., 2012; Roy et al., 2014; IPCC, 2018).

Reports of landscape level tree mortality events which can be considered to occur at both background and catastrophic rates (Lugo and Scatena, 1996) are increasing in different parts of the world (**Figure 1**; **Supplementary Table 2**). Combined biotic and abiotic stresses have been associated with many of these events, most of which are massive mortality events (**Figure 2**). This underlines that recent massive mortality events are more likely driven by combined biotic and abiotic stresses. This is in line with the "coupling" among various drivers and mechanisms of tree mortality hypothesized in McDowell et al. (2018), where drivers of tree mortality such as drought, high temperature, and biotic factors interact through the physiological mechanisms of tree death such as carbon starvation and hydraulic failure.

Hotter droughts have been associated with most of the massive mortality events, and both pathogens and pests have been reported in most of them (**Figure 3**). Some of the most severe recent mortality events are results of the combined effects of hotter droughts, bark beetles, and fungal pathogens (Worrall et al., 2008, 2010; Klockow et al., 2018; Gheitury et al., 2020). The combination between hotter droughts and bark beetles (Breshears et al., 2005; Floyd et al., 2009; Millar et al., 2012; de La Serrana et al., 2015; Kharuk et al., 2019) as well as hotter droughts and pathogens (Holuša et al., 2018; Wood et al., 2018) have also resulted in severe losses. These are considerable threats to forestry in the future as predictions show that hotter droughts (Crockett and Westerling, 2018) and associated tree mortality (Zhang et al., 2014b; Hember et al., 2017) have been increasing in different parts of the world and are expected to continue to increase (Allen et al., 2015; Wu et al., 2020).

Previously, Ciesla and Donaubauer (1994) established that abiotic stresses act as predisposing factors to biotic attacks which usually come out to be the inciting and contributing factors to tree death. A recent example for this was reported in Ward and Aukema (2019), where changes in temperature and precipitation predisposed eastern larch, *Larix laricina*, to defoliation by larch casebearer, *C. laricella*, and finally tree mortality occurs after eastern larch beetle, *D. simplex*, infestation. Furthermore, delayed mortality associated with pathogens and pests was observed after a severe drought indicating a possible predisposition by drought (Klockow et al., 2018). Thus, mortality events seemingly caused by a single biotic or abiotic stress may well have unreported biotic or abiotic predisposing/inciting factors. However, in some of the landscape level tree mortality events caused by droughts, biotic stress factors were not involved (**Figure 3**). Similarly, Kautz et al. (2017) estimated that biotic

FIGURE 1 | Map showing recent (1982–2020) landscape level tree mortality events associated with the biotic and abiotic stresses drought, heat, pests, pathogens, and their combinations reported in peer reviewed publications. The summary of the reports and the respective references are given in **Supplementary Table 2**. We searched on Google scholar using different combinations of the key words: "tree," "forest," "vegetation," "plantation," "massive," "mortality," "die-off," "die-back," and "decline." Reports from relevant reviews (Allen et al., 2010, 2015; McDowell et al., 2018) were also searched. Reports which do not indicate the spatial characteristics and intensity of mortality as well as those which include other exogenous mortality agents such as fire, flood, etc., were excluded. In addition, seedling mortality, mortality due to experimental stress, long term mortality analyses were not included. Then, reports which clearly describe individual mortality event/events and can be approximated as landscape scale according to the classification given in Lugo and Scatena (1996) were selected. Reports describing different aspects of the same mortality event at the same location were considered as single reports.

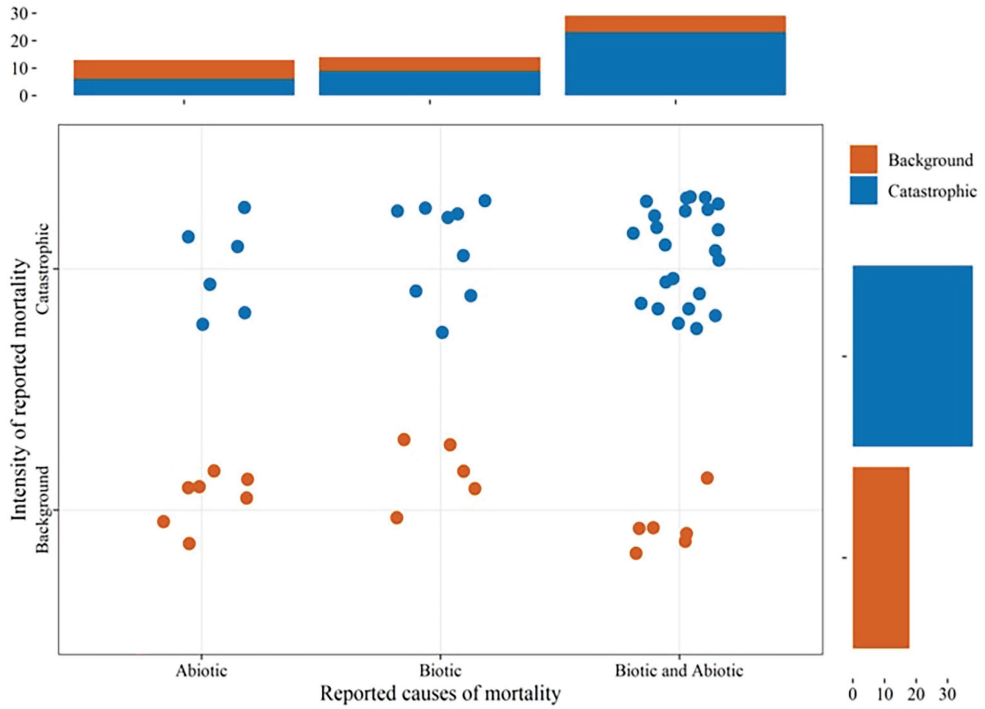

FIGURE 2 | The proportion of landscape level tree mortality events (**Figure 1**; **Supplementary Table 2**) reporting single or combined biotic and abiotic stresses as causes. The intensity of mortality events were approximated to background and catastrophic based on the classification given in Lugo and Scatena (1996).

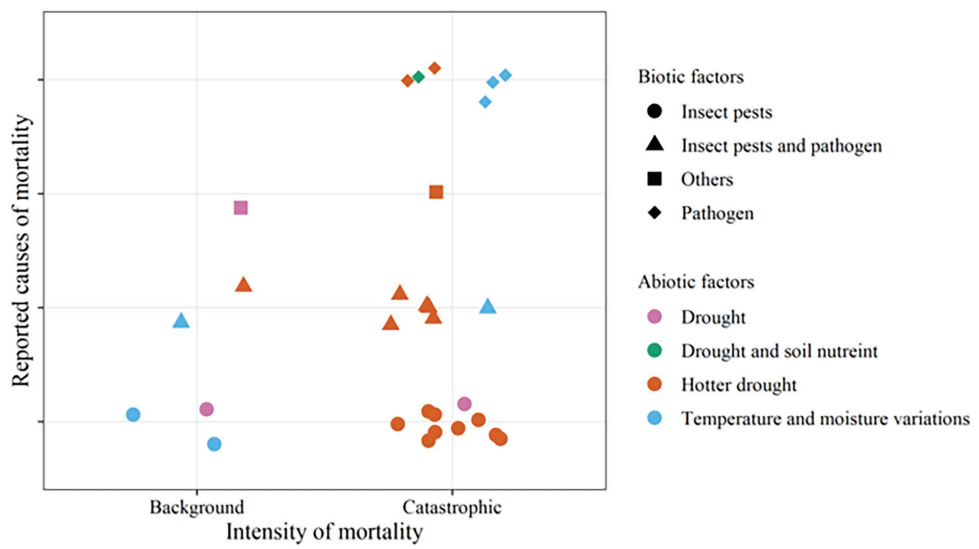

FIGURE 3 | The main biotic-abiotic stress combinations associated with recent landscape level tree mortality events caused by combined stress (**Figure 2**; **Supplementary Table 2**). Normal droughts are differentiated from hotter droughts, which refer to droughts accompanied by increased temperature as termed in Allen et al. (2015). "Others" refers to parasitic plants alone or with insect pests. The symbols/plot characters represent mortality events caused by combined stress. The shape and colors of the characters respectively represent the biotic and abiotic factors involved.

disturbances may cause up to 3.3 million ha tree mortality in the Northern Hemisphere per year without the involvement of abiotic stress factors. Re-examination of such mortality events will provide an insight in this regard. Future studies and prediction models should therefore consider both biotic and abiotic factors.

Parasitic plants and soil nutrients were reported to be associated with a few of the massive mortality events (**Figure 3**). Warming climate with lower precipitation increased tree mortality due to parasitic plants through decreasing the growth of trees and predisposing them to other drivers of mortality (Galiano et al., 2010; Bell et al., 2019). Increased infestation with insects and parasitic plants after severe drought was associated with a large increase in the annual tree mortality in pinyon pine (Flake and Weisberg, 2019). Soil nutrients, drought, and bacterial canker were found to cause massive poplar mortality in China (Ji et al., 2019). Thus, although these factors are beyond the scope of this review, they deserve to be explored in future research.

The reported landscape level mortality events (**Figure 1**) affected different species of trees belonging to several genera (**Figure 4**), including some of the most planted genera, such as *Pinus*, *Eucalyptus*, *Populus*, *Picea*, and *Abies* (Del Lungo et al., 2003; Brockerhoff et al., 2008). The genus *Pinus*, which covers the largest area of planted forests in the world (Del Lungo et al., 2003), is also the most highly affected genera (**Figure 4**). For example, mortality due to the combined effect of hotter drought and *Ips confuses* infestation in the United States was estimated to reach as high as 80% in *Pinus edulis* affecting more than 1.2 million ha forest during 2000–2003 (Breshears et al., 2005). Similarly, 89.6 and 48.1% of sampled *Pinus ponderosa* and *Pinus lambertiana* trees, respectively, were dead under the combined effect of *bark beetles* and the 2012–2015 hotter drought in California (Fettig et al., 2019). These mortality events clearly affected some species more severely than others (Suarez et al., 2004; Floyd et al., 2009; Fettig et al., 2019). Thus, forest tree genetic improvement programs and forest managers should consider selecting tree species that are tolerant to these combined stresses.

The effect of combined biotic and abiotic stresses on tree mortality is not limited to the extensive and catastrophic events on which we mainly focused here. There is evidence showing that the rate of gradual background tree mortality is also increasing with changing climate (van Mantgem et al., 2009; Taccoen et al., 2019). The biotic stress factors such as pests and pathogens have been identified as the major drivers of background tree mortality (Das et al., 2016). Therefore, it is reasonable to hypothesize that non-outbreak levels of pathogens and pests interacting with mild climate change driven abiotic stresses may be responsible for the increasing rate of background tree mortality. Recent evidence in support of this is that temperature and moisture variations indirectly affected pest and pathogen driven deaths of *Abies lasiocarpa* (Lalande et al., 2020).

ECONOMIC AND ECOLOGICAL IMPACTS OF COMBINED BIOTIC AND ABIOTIC STRESSES IN FORESTRY

The major causes of forest loss leading to the decline of the global forest area remain to be deforestation, shifting cultivation and wildfire (Curtis et al., 2018). While the direct contribution of biotic and abiotic stresses to such forest losses seems to

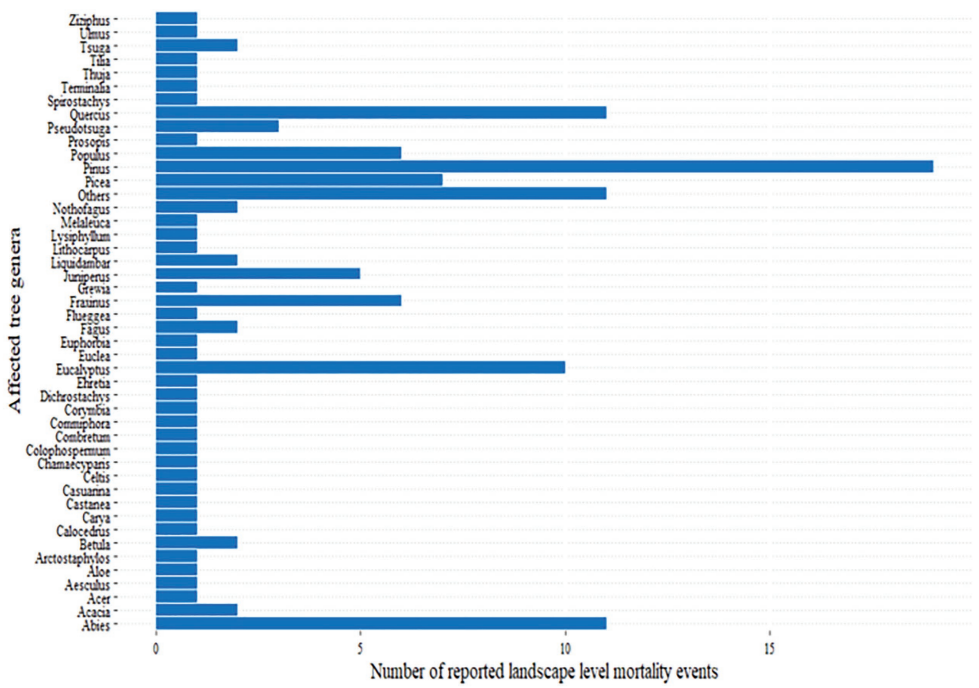

FIGURE 4 | The main genera of trees affected by landscape level tree mortality events across the world (**Figure 1**; **Supplementary Table 2**).

be relatively low (Curtis et al., 2018), their indirect role cannot be underestimated. For example, tree mortality caused by insect pest outbreaks, heat waves, and droughts are frequently associated with forest fires resulting in huge tree losses (Brando et al., 2014; Klein et al., 2019; Talucci and Krawchuk, 2019; Xie et al., 2020). In addition, the regional and temporal variation in the occurrence of biotic and abiotic stresses also highlights the importance of these factors. For example, pests were reported to cause 32% of the tree mortality in the Western United States compared with 18% loss caused by fire (Berner et al., 2017). Another study also indicated that biotic disturbances such as pathogens and pests are the most important causes of forest disturbance in the forests of the Northern Hemisphere (Kautz et al., 2017).

Apart from complete forest loss that leads to a change in land use, the economic and ecological impact of biotic and abiotic stresses operating in forestry can be viewed through their impact on the ecosystem services of trees (Alcamo et al., 2003). Previously, Boyd et al. (2013) used this framework to summarize the impact of pests and pathogens. The decline in forest productivity due to tree mortality and reduced growth resulting from combined biotic and abiotic stresses (section The Effect of Combined Biotic and Abiotic Stresses on the Growth and Mortality of Forest Trees) as well as reduced quality of products (Brodde et al., 2019) can affect the provisioning services and cause a direct revenue loss (Zwolinski et al., 1990; Aukema et al., 2011). Though controversial, it has been argued that climate change increases tree growth and hence forest productivity (Kirilenko and Sedjo, 2007; Reyer et al., 2017; Torzhkov et al., 2019; Ruiz-Pérez and Vico, 2020). However, even if there would be a possible increase, the impact of extreme weather interacting with increased pathogen and pest outbreaks will cause major losses and may even offset any gain in productivity (Reyer et al., 2017; Woods and Watts, 2019).

Increased tree mortality, crown die-back and defoliation caused by combined biotic and abiotic stresses may have a negative impact on human well-being by affecting the cultural and regulatory services of trees (Alcamo et al., 2003). The decrease in the density of forests and canopy cover of trees have been associated with increased human health problems stemming from respiratory diseases (Donovan et al., 2013) as well as increased temperature associated with the loss of canopy shade (Jones, 2019). Massive tree mortality may also have an impact on other components of the forest ecosystem, such as the micro and macro faunal and floral diversity. For example, massive ash (*Fraxinus* spp.) mortality caused by emerald ash borer (*Agrilus planipennis*) created canopy gap (Ulyshen et al., 2011) and accumulation of woody debris (Perry and Herms, 2017), which affect the activity and diversity of forest invertebrates. Massive tree mortality may also cause a decline in the population of coexisting organisms such as lichens, and may lead to local extinction (Jönsson and Thor, 2012; Lõhmus and Runnel, 2014).

Recent evidence indicates that biotic and abiotic stresses may contribute to the decline in the population of tree species and may even lead to extinction. A good example for this is the fungal pathogen *Austropuccinia psidii*, which has caused a rapid decline in *Rhodomyrtus psidioides* population in Australia since 2012 (Fensham et al., 2020). The coupling of biotic stresses with weather extremes may be beyond the capability of some species to adapt to a changing climate (Schaberg et al., 2008; Sáenz-Romero et al., 2020). This may result in a selective massive death of certain vulnerable species (Suarez et al., 2004) and may lead to local extirpations (Alfaro et al., 2014) and even extinction in the case of endemic species (Fensham et al., 2020). Thus, if the episodes of massive tree mortality caused by combined biotic and abiotic stresses (section The Effect of Combined Biotic and Abiotic Stresses on the Growth and Mortality of Forest Trees) continue even at current pace, the direct and indirect contribution of such stresses to the extinction of tree species may become a real threat at least to the already endangered species.

Biotic and abiotic stresses induce considerable emission of biogenic volatile organic compounds associated with the responses of stressed living trees (Faiola and Taipale, 2020) and decay of dead trees (Kurz et al., 2008; Phillips et al., 2009). Pest attack increased biogenic emissions of different compounds from trees and simultaneously occurring abiotic stresses such as heat and drought mostly further increased such emissions (Faiola and Taipale, 2020). Biotic and abiotic stresses negatively affect the global carbon pool by the loss of potential carbon sinks through reduced growth and death of trees as well as the addition of carbon sources for future emission from decaying dead trees (Kurz et al., 2008; Phillips et al., 2009). For example, hotter drought in the Amazon forest in 2005 caused the loss of 1.21–1.60 Pg potential carbon storage from reduced growth and tree mortality (Phillips et al., 2009). A severe drought in Texas, United States, caused the loss of 24–30 Tg C due to tree mortality (Moore et al., 2016). Similarly, a study in Canada estimated the loss of carbon storage due to pests to be 2.87 tone C ha^{-1} $year^{-1}$ (Zhang et al., 2014a). Furthermore, predictions also indicate that increased drought and associated pest outbreak will significantly affect the carbon balance in a similar fashion (Scheller et al., 2018). These examples are good indicators of the significance of combined biotic and abiotic stresses to environmental sustainability. However, in most of the cases, attempts to quantify these impacts are inadequate. Thus, further research on quantifying the emissions and their environmental impact will benefit environmental models for carbon balance (Faiola and Taipale, 2020).

It is difficult to attach an economic value to all kinds of damages caused by biotic and abiotic stresses. However, there were attempts to estimate the economic impacts from different perspectives (**Supplementary Table 3**). The economic loss due to tree death and reduced growth is a direct indicator of such impacts. However, dead trees, especially mature ones, can still be of economic value through "salvage logging" despite the undesirable ecological consequences due to the associated increase in harvest frequency (Thorn et al., 2018). An estimate of economic loss derived from predicted tree mortality (Waring et al., 2009; Ochuodho et al., 2012; Soliman et al., 2012), comparisons of the cost of protection to the possible loss (Watt et al., 2011; Cameron et al., 2018), and revenue loss due to downgraded products (Costanza et al., 2019) were used to

demonstrate possible damage from biotic and abiotic stresses. Government and household expenditures as well as losses in property value associated with tree mortality have also been estimated (Aukema et al., 2011). More holistic assessments included the economic loss from production, protection, tourism, and carbon sequestration (Notaro et al., 2009). However, only some of the studies (Waring et al., 2009; Ochuodho et al., 2012; Soliman et al., 2012) considered the combined effects of biotic and abiotic factors, which may result in an over- or under-estimation of loss. Because damages such as tree mortality are mostly the results of the combined effect of biotic and abiotic stresses, future studies should include these factors into their analyses. Moreover, as economic analysis is important for policy makers and forest managers, such information, which may be largely found in technical reports, should be systematically analyzed.

RESPONSES OF FOREST TREES TO COMBINED BIOTIC AND ABIOTIC STRESSES

The impact of combined biotic and abiotic stresses on the physiology of trees is different from that of individual stresses. Sequential or simultaneous combinations of biotic and abiotic stresses may have a negative or positive outcome on different morphological and physiological traits of forest trees depending on the species of trees, the type of biotic stress factors, and the duration and intensity of abiotic stresses (**Supplementary Table 4**). These changes may make trees either more susceptible or resistant to one or more of the co-occurring stresses.

Several individual biotic and abiotic stresses affect plant-water relations. For example, drought stress (McKiernan et al., 2017) and infection by fungal pathogens, which affect the vascular system (da Silva et al., 2018) influence the movement of water and reduce stem and leaf water potential. The simultaneous occurrence of these stresses may cause further reduction in water potential in plants. In support of this, it has been reported that infections by *Neofusicoccum eucalyptorum* in *Eucalyptus globulus* (Barradas et al., 2018) and *Obolarina persica* as well as *Biscogniauxia mediterranea* in *Quercus brantii* (Ghanbary et al., 2017) caused a further reduction in the stem water potential of drought stressed plants. However, this may not always be the case depending on the level of resistance to the involved pathogen as well as the intensity and duration of drought. For example, while both drought and infection by *Quambalaria coyrecup* reduced leaf water potential in *C. calophylla*, their combination did not result in a further reduction (Hossain et al., 2019). Similarly, while water potential decreased due to drought stress, no such reduction was observed due to infection by *Leptographium wingfieldii* in *P. sylvestris* (Croisé et al., 2001) and *P. cinnamomi* in *Quercus ilex* and *Quercus cerris* (Turco et al., 2004). Furthermore, priming with previous drought resulted in significantly higher leaf water potential as compared to non-primed plants under combined drought and *N. eucalyptorum* infection in *E. globulus* (Barradas et al., 2018). According to these observations, while drought stress strongly influences plant water-relations, the effect of fungal pathogens both as an individual stress and in combination with short term experimental drought seems to be moderate.

It is well-known that drought stress negatively affects photosynthetic gas exchange, however, some pathogens (da Silva et al., 2018) and their combination with drought (**Supplementary Table 4**) have also been reported to have a similar impact. Ghanbary et al. (2017) reported that drought and the pathogens *O. persica* and *B. mediterranea* significantly reduced stomatal conductance, photosynthetic rate, and maximum photochemical efficiency of photosystem II (Fv/Fm) in *Q. brantii*. Interestingly, the combination of both pathogens with drought caused further reduction in all of these parameters. Combined biotic and abiotic stresses may also negatively affect photosynthesis by reducing the concentration of photosynthetic pigments. For example, Ghanbary et al. (2018) reported that chlorophyll content decreased due to pathogen infection, drought, and their combination in *Q. brantii*. These findings indicate that the effect of combined biotic and abiotic stresses on photosynthesis may be worse than each of the individual stresses. This may be one of the reasons for the reduction in tree growth and increase in tree mortality associated with combined stresses.

Accumulation of osmolytes and soluble sugars are among the most common responses of plants to osmotic stress resulting from abiotic stresses such as drought. Such accumulations may increase due to pathogens and pests which affect plant-water relations. Sherwood et al. (2015) and Ghanbary et al. (2018) revealed that proline, which increased under both drought and pathogen infection, showed a further increase under the combination of both stresses. On the other hand, the accumulation of osmolytes and soluble sugars in response to abiotic stresses may create favorable condition for biotic stress factors such as fungal pathogens and wood boring pests thereby increasing the susceptibility of trees. In support of this, Caldeira et al. (2002) reported that a reduced bark moisture content and increased accumulation of glucose, fructose, and sucrose enhanced the survival and growth of *Phoracantha semipunctata* under drought conditions in *E. globulus*. Similarly, combined drought and pathogen infection increased soluble sugar concentration in *Q. brantii* (Ghanbary et al., 2018) resulting in increased susceptibility to pathogens (Ghanbary et al., 2017). These findings indicate that osmotic adjustment may represent a synergistic interaction between responses to biotic and abiotic stresses resulting in increased damage under multiple stress situations.

Metabolites such as phenolics and terpenoids, which are commonly involved in plant defense against pathogens and pests, may also be affected by co-occurring abiotic stress factors, such as heat and drought. Total phenol concentration increased under both drought and pathogen infection as individual stresses in *Q. brantii*, and a further increase was observed under their combination (Ghanbary et al., 2018). The interaction between drought and pine weevil, *Hylobius abietis*, attack respectively decreased and increased the accumulation of polyphenols and diterpins in *Pinus halepensis* (Suárez-Vidal et al., 2019). By doing so, moderate drought weakened basal defense and

significantly increased the susceptibility of seedlings to pest attack. However, there were also observations which revealed that combined stress did not have a significant effect on phenol and terpenoid concentrations. For example, a study in *C. calophylla* found that total phenols and total terpenes generally tended to increase due to *Q. coyrecup* infection while drought stress generally did not further increase their concentration (Hossain et al., 2019). Similarly, the concentration of total monoterpenes increased due to infection of *Pinus contorta* and *Pinus banksiana* by *Grosmannia clavigera* while drought stress had no effect (Lusebrink et al., 2016). These variations may be related to the tolerance/resistance of trees to each of the stresses.

Formation of reactive oxygen species (ROS) and their subsequent detoxification is a common response of plants to both biotic and abiotic stresses. Reactive oxygen species along with phytohormone signaling pathways have been considered to be two of the main "converging points" between responses to biotic and abiotic stresses in plants (Zhang and Sonnewald, 2017). Infection by *N. eucalyptorum* reduced the accumulation of Malondialdehyde (MDA) in drought primed *E. globulus* plants as compared to simultaneously infected ones (Barradas et al., 2018). However, this does not indicate improved resistance to the pathogen as lesion length was significantly longer in the drought-predisposed plants. Thus, it was hypothesized that the reduction in MDA may be the result of the pathogen's defense against pre-accumulated ROS. In agreement with this, despite the increase in MDA concentration due to drought stress, pathogen infection, and their combination in *Q. brantii*, both the highest MDA concentration and the largest lesion were recorded under combined stress (Ghanbary et al., 2017, 2018). Although H_2O_2, which increased due to drought stress, significantly decreased upon infection by *Diplodia sapinea* alone, and in combination with drought in *Pinus nigra*, this was not associated with an increased resistance to the pathogen (Sherwood et al., 2015). These results may indicate that the effect of combined biotic and abiotic stresses on the ROS signaling pathway tend to be synergistic resulting in increased damage to trees. However, as hypothesized in Sherwood et al. (2015), this may be limited to necrotrophic pathogens as ROS may affect biotrophs differently. The increased accumulation of ROS due to abiotic stresses may enhance hypersensitive response, which is an effective defense strategy against biotrophic pathogens unlike necrotrophic ones (Zhang and Sonnewald, 2017).

The involvement of phytohormones in modulating growth and responses to both biotic and abiotic stresses is well-known. A review by Zhang and Sonnewald (2017) hypothesized that Auxin may coordinate response to combined biotic and abiotic stresses. A study on *Lycopersicon esculentum* revealed that increased abscisic acid concentration due to drought stress did not cause susceptibility to infection by *Oidium neolycopersici* and *Botrytis cinerea* (Achuo et al., 2006). Similarly, the increased accumulation of jasmonic acid and salicylic acid, as well as unchanged concentration of abscisic acid due to prior drought stress resulted in improved resistance to infection by *Pseudomonas syringae* in *Arabidopsis thaliana* (Gupta et al., 2017). However, we did not find similar studies on forest trees.

The molecular response of plants to combined stress is generally different from their response to individual stresses. In addition to the molecular responses which are shared between the individual biotic and abiotic stresses that may be prioritized depending on the severity of stress, plants show molecular responses which are unique to combined stresses (Choudhary et al., 2016). A number of differentially expressed genes which were shared among the individual stresses and unique to combined stress have been identified in *Arabidopsis* (Gupta et al., 2016; Choudhary et al., 2017). Some of the uniquely regulated genes due to combined drought and pathogen infection in *Arabidopsis* include genes involved in fatty acid and amino acid metabolism, secondary metabolites, and photosynthesis pathways, as well as genes in the transcription factor families such as NAC, WRKY, and MYB (Gupta et al., 2016). However, to the best of our knowledge, there has been no study on the molecular changes due to combined biotic and abiotic stresses in forest trees.

Recent studies in *Arabidopsis* reported the identification of key genes which confer resistance to combined biotic and abiotic stresses. The transcription factor gene *G-Box Binding Factor 3* (*GBF3*), which regulates genes in the ABA signaling pathway (Dixit et al., 2019) and the micro-RNA gene *ath-miR164c*, which regulates genes involved in proline biosynthesis (Gupta et al., 2020), were found to confer tolerance to combined drought and infection by *P. syringae* in *A. thaliana*. Future studies should target the identification and characterization of more common regulators, while research in forest trees should prioritize the investigation of these genes.

MITIGATION STRATEGIES

Prevention strategies such as strict quarantine have been useful in minimizing the introduction of exotic pathogens and pests (Wingfield et al., 2015). In the case of combined biotic and abiotic stresses, prevention is still useful as it minimizes parts of the problem. Besides, it remains to be one of the most important ways to protect our natural forests where other strategies such as genetic improvement of tree resistance are not feasible. However, the possible risk of increased outbreaks of domestic pests and diseases due to climate change (section Weather Extremes and Forest Disease/Pest Outbreaks) calls for better coping mechanisms. Thus, *ex situ* conservation and selection of resistant trees should be considered for endangered species of vulnerable natural forests (Fensham et al., 2020; Sáenz-Romero et al., 2020).

Genetic improvement of tree resistance/tolerance to biotic and abiotic stresses through conventional breeding techniques and genetic engineering is a relatively longer term strategy (Wingfield et al., 2015; Naidoo et al., 2019). The vulnerability of trees to growth decline and massive mortality under the combined effect of biotic and abiotic stresses varied among species (Suarez et al., 2004; Floyd et al., 2009). Such genetic diversity is a valuable resource, not only for selective planting, but also for selective breeding and genetic engineering. The increasing availability of large multi-omics data, systems and

synthetic biology approaches as well as improved functional testing will allow us to integrate and complement conventional breeding, genetic engineering, and genome editing (Naidoo et al., 2019). Genetic improvement for combined biotic and abiotic stress tolerance may target either the regulators common to the different stresses or pyramiding of genes governing response to individual stresses (Kissoudis et al., 2014). Recent studies are shedding light on the possibilities of engineering plants for multiple traits (Cho et al., 2019). Thus, improving trees for resistance to combined biotic and abiotic stresses using these techniques may also become possible. Existing model systems that have been used to study biotic stresses such as those in *Eucalyptus* (Naidoo et al., 2013; Mangwanda et al., 2015; Visser et al., 2015), Pine (Visser et al., 2018), and Poplar (Feau et al., 2007; Hacquard et al., 2011) can be used to develop a workable approach in this regard. We propose the use of drought-pathogen interactions, which has been considered a model in annual crops (Pandey et al., 2017), to study combined biotic and abiotic stresses in forest trees. Owing to the representativeness of drought in several abiotic stresses (Wang et al., 2003) and the relative ease of manipulating pathogens in both field and green house studies, drought-pathogen interactions is a suitable model to study combined stress. In addition, as much as drought and pathogens are two of the most important stresses in agriculture and forestry, they have been studied as single and combined factors better than several others and their combinations (Desprez-Loustau et al., 2006; Pandey et al., 2017).

While genetic improvement of trees is a valuable strategy for plantation forestry, it is less feasible to natural forests, and it is also a long-term project which needs initial investment in research. Thus, the options of biological control of pests and pathogens (Hurley et al., 2012; Martín-García et al., 2019) and the use of microorganisms such as mycorrhiza and endophytes to alleviate abiotic stress tolerance (Liu et al., 2015; Khan et al., 2016; Ferus et al., 2019) should be explored. However, these biological agents have been used against single stresses under optimum environmental conditions (Slippers et al., 2012), and thus, may not function under multiple stress settings. For example, drought has been reported to negatively affect biological control using entomopathogenic nematodes (Hassani-Kakhki et al., 2019). Similarly, while severe drought increases *S. noctilio* outbreak (Lantschner et al., 2019), drought has the opposite effect on the biocontrol agent *Deladenus siricidicola* (Hurley et al., 2008). Thus, genetic

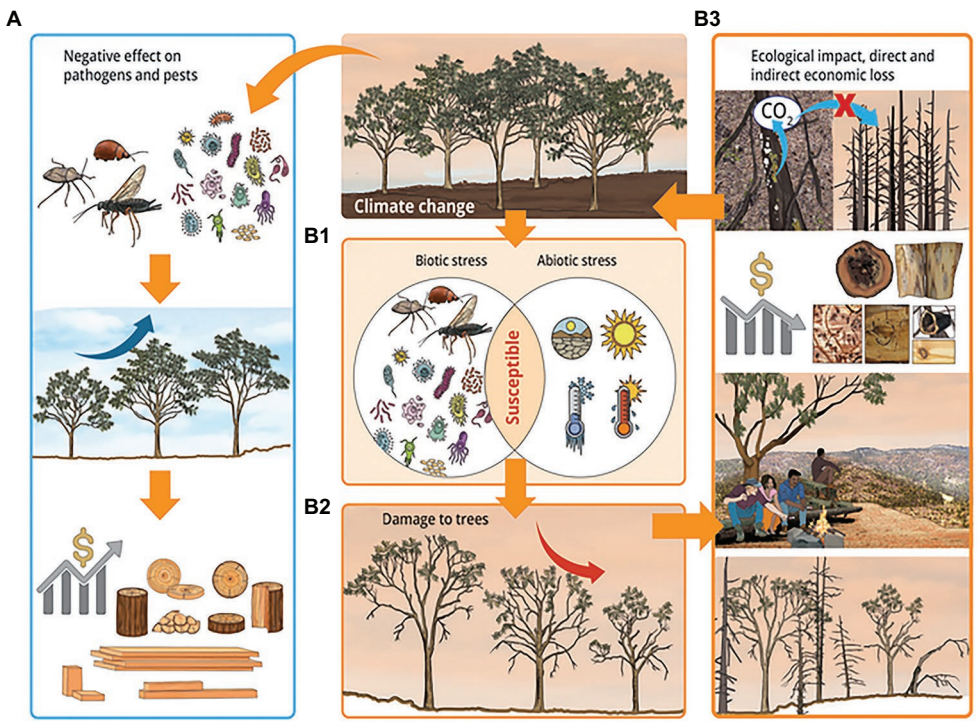

FIGURE 5 | A scheme showing the impact of combined biotic and abiotic stresses in forestry under the influence of climate change. Climate change may reduce damage from diseases and pests by negatively affecting pathogens and insect pests, increase tree growth, and result in beneficial economic and ecological impacts **(A)**. Climate change, along with increased global distribution of pathogens and pests due to globalization, may increase disease and pest outbreaks as well as the intensity and frequency of abiotic stresses. This increases the susceptibly of tress under combined biotic and abiotic stresses **(B1)**, and result in increased damage to trees, which includes decline in tree growth, increase in tree mortality, defoliation, and crown die-back **(B2)**. These damages negatively affect the ecosystem services of trees resulting in harmful economic and ecological impacts **(B3)**. The negative effect on the ecosystem services of forests include loss of potential carbon sinks and increased emission of biogenic volatile organic compounds, reduction in the quality and productivity of forest products, negative impact on human health and well-being, and loss of micro and macro faunal- and floral-diversities, which may in turn cause loss of indirect services from the forest. Yellow arrows indicate cause and effect relationships, and deep blue and red arrows indicate increase and decrease in tree growth, respectively.

improvement can and should also target biological control agents (Wang and Wang, 2017).

A number of forest management strategies can be deployed to mitigate the impacts of combined biotic and abiotic stresses. They include; thinning and reduction of the basal area of stands (Bradford and Bell, 2017; Restaino et al., 2019; Lalande et al., 2020), facilitating regeneration in advance of predicted hotter droughts (Redmond et al., 2018), shorter rotation age to minimize damage from bark beetle and droughts (Maclauchlan, 2016), and stand diversification such as "clonal composites" (Rezende et al., 2019). Accurate predictions of massive tree mortality and early warning on hot spots of combined biotic and abiotic stresses (Roux et al., 2015; Preisler et al., 2017; Rogers et al., 2018) will aid not only decision making by forest managers but also scientific interventions and priorities for *ex situ* conservation.

CONCLUSION

Biotic and abiotic stresses have always been important in agriculture and forestry. In recent years, their importance has increased as a result of climate change enhanced frequency and intensity of weather extremes as well as globalization which has increased the movement of pathogens and pests. Plants often face these biotic and abiotic stresses in combination, either simultaneously or sequentially. Forest trees are exposed to the recurrence of these combinations due to their long lifecycle. Plants show both shared and unique responses to combined biotic and abiotic stresses. As a result, it is difficult to predict both the response of plants to and damage due to combined stresses from single stress studies. In this context, we have shown the importance of combined biotic and abiotic stresses as drivers of forest disease and pest outbreaks (**Figure 5**). Indeed, observed and predicted evidences indicated that combined biotic and abiotic stresses are associated with reductions in tree growth and increasing episodes of massive tree mortality, which have huge economic and ecological implications.

Climate change driven abiotic stresses such as heat and drought may either increase or decrease pest and disease outbreaks depending on the species of trees, pests, pathogens, and forest biomes. Whether the increase or decrease is more likely at a global scale is a subject of continued debate, although the available evidences tend to show more increase in many cases. However, what is more important is that such changes along with the global movement of pathogens and pests will undoubtedly continue to bring in a new spatial and temporal trend of disease and pest outbreaks and the associated damage. This may also couple with weather extremes which are increasing in frequency and intensity.

The current studies and reviews, despite the inconsistency and contradiction of findings, underline two things. First, many of the studies used climatic variables rather than considering the physiological stress caused by weather extremes such as heat and drought. Particularly, while studies on warming showed considerable interaction with pathogens and pests, extreme heat and cold which cause physiological stress to both the trees and pathogens/pests might have an entirely different outcome. The more frequent heat waves and hotter droughts should thus be used as good opportunities to study such responses. Second, the interactions between host trees and pathogens/pests can be affected by climate change driven changes in the abiotic stresses in a complex manner, which can further be complicated by the interacting effect of the different abiotic factors. As a result, despite the global attention given to climate change and its impacts in forestry, we are far from fully understanding the constantly changing conditions. Thus, understanding all levels of interactions at least for the major stress combinations is important. In this regard, both experimental and observational studies using model systems can better equip us to respond to possible damages from combined biotic and abiotic stresses in the future.

AUTHOR CONTRIBUTIONS

SN and DT contributed to the conception of the review. DT wrote first draft. SN, DT, and GZ commented and revised the manuscript. All authors contributed to the article and approved the submitted version.

FUNDING

This work was supported by the South African National Research Foundation (NRF) Y-rated Grant to SN (UID105767). Opinions expressed and conclusion arrived at are those of the author(s) and are not necessarily to be attributed to the NRF. The authors acknowledge funding from the Technology Innovation Agency of South Africa through the Forest Molecular Genetics Cluster Program.

SUPPLEMENTARY MATERIAL

The Supplementary Material for this article can be found online at: https://www.frontiersin.org/articles/10.3389/fpls.2020.601009/full#supplementary-material

REFERENCES

Achuo, E., Prinsen, E., and Höfte, M. (2006). Influence of drought, salt stress and abscisic acid on the resistance of tomato to *Botrytis cinerea* and *Oidium neolycopersici*. *Plant Pathol.* 55, 178–186. doi: 10.1111/j.1365-3059.2006.01340.x

Aguayo, J., Elegbede, F., Husson, C., Saintonge, F. X., and Marçais, B. (2014). Modeling climate impact on an emerging disease, the *Phytophthora alni*-induced alder decline. *Glob. Chang. Biol.* 20, 3209–3221. doi: 10.1111/gcb.12601

Alcamo, J., Ash, N. J., Butler, C. D., Callicott, J. B., Capistrano, D., Carpenter, S. R., et al. (2003). *Millennium ecosystem assessment: Ecosystems and human well-being: A framework for assessment*. Washington, DC: Island Press.

Alfaro, R. I., Fady, B., Vendramin, G. G., Dawson, I. K., Fleming, R. A., Sáenz-Romero, C., et al. (2014). The role of forest genetic resources in responding to biotic and abiotic factors in the context of anthropogenic climate change. *For. Ecol. Manag.* 333, 76–87. doi: 10.1016/j.foreco.2014.04.006

Allen, C. D., Breshears, D. D., and McDowell, N. G. (2015). On underestimation of global vulnerability to tree mortality and forest die-off from hotter drought in the Anthropocene. *Ecosphere* 6:art129. doi: 10.1890/es15-00203.1

Allen, C. D., Macalady, A. K., Chenchouni, H., Bachelet, D., McDowell, N., Vennetier, M., et al. (2010). A global overview of drought and heat-induced tree mortality reveals emerging climate change risks for forests. *For. Ecol. Manag.* 259, 660–684. doi: 10.1016/j.foreco.2009.09.001

Anderegg, W. R., Hicke, J. A., Fisher, R. A., Allen, C. D., Aukema, J., Bentz, B., et al. (2015). Tree mortality from drought, insects, and their interactions in a changing climate. *New Phytol.* 208, 674–683. doi: 10.1111/nph.13477

Aukema, J. E., Leung, B., Kovacs, K., Chivers, C., Britton, K. O., Englin, J., et al. (2011). Economic impacts of non-native forest insects in the continental United States. *PLoS One* 6:e24587. doi: 10.1371/journal.pone.0024587

Ayres, M. P., and Lombardero, M. J. (2000). Assessing the consequences of global change for forest disturbance from herbivores and pathogens. *Sci. Total Environ.* 262, 263–286. doi: 10.1016/s0048-9697(00)00528-3

Balducci, L., Fierravanti, A., Rossi, S., Delzon, S., De Grandpré, L., Kneeshaw, D. D., et al. (2020). The paradox of defoliation: declining tree water status with increasing soil water content. *Agric. For. Meteorol.* 290:108025. doi: 10.1016/j.agrformet.2020.108025

Bao, Y., Wang, F., Tong, S., Na, L., Han, A., Zhang, J., et al. (2019). Effect of drought on outbreaks of major forest pests, pine caterpillars (*Dendrolimus* spp.), in Shandong Province, China. *Forests* 10:264. doi: 10.3390/f10030264

Barradas, C., Pinto, G., Correia, B., Castro, B., Phillips, A., and Alves, A. (2018). Drought× disease interaction in *Eucalyptus globulus* under *Neofusicoccum eucalyptorum* infection. *Plant Pathol.* 67, 87–96. doi: 10.1111/ppa.12703

Bell, D. M., Pabst, R. J., and Shaw, D. C. (2019). Tree growth declines and mortality associated with a parasitic plant increase during warm and dry climatic conditions in a temperate coniferous forest ecosystem. *Glob. Chang. Biol.* 26, 1714–1724. doi: 10.1111/gcb.14834

Berner, L. T., Law, B. E., Meddens, A. J., and Hicke, J. A. (2017). Tree mortality from fires, bark beetles, and timber harvest during a hot and dry decade in the western United States (2003–2012). *Environ. Res. Lett.* 12:065005. doi: 10.1088/1748-9326/aa6f94

Blum, A. (2005). Drought resistance, water-use efficiency, and yield potential—are they compatible, dissonant, or mutually exclusive? *Aust. J. Agric. Res.* 56, 1159–1168. doi: 10.1071/AR05069

Bosso, L., Luchi, N., Maresi, G., Cristinzio, G., Smeraldo, S., and Russo, D. (2017). Predicting current and future disease outbreaks of *Diplodia sapinea* shoot blight in Italy: species distribution models as a tool for forest management planning. *For. Ecol. Manag.* 400, 655–664. doi: 10.1016/j.foreco.2017.06.044

Bostock, R. M., Pye, M. F., and Roubtsova, T. V. (2014). Predisposition in plant disease: exploiting the nexus in abiotic and biotic stress perception and response. *Annu. Rev. Phytopathol.* 52, 517–549. doi: 10.1146/annurev-phyto-081211-172902

Bouzidi, H. A., Balducci, L., Mackay, J., and Deslauriers, A. (2019). Interactive effects of defoliation and water deficit on growth, water status, and mortality of black spruce (*Picea mariana* (Mill.) BSP). *Ann. For. Sci.* 76:21. doi: 10.1007/s13595-019-0809-z

Boyd, M. A., Berner, L. T., Doak, P., Goetz, S. J., Rogers, B. M., Wagner, D., et al. (2019). Impacts of climate and insect herbivory on productivity and physiology of trembling aspen (*Populus tremuloides*) in Alaskan boreal forests. *Environ. Res. Lett.* 14:085010. doi: 10.1088/1748-9326/ab215f

Boyd, I., Freer-Smith, P., Gilligan, C., and Godfray, H. (2013). The consequence of tree pests and diseases for ecosystem services. *Science* 342:1235773. doi: 10.1126/science.1235773

Bradford, J. B., and Bell, D. M. (2017). A window of opportunity for climate-change adaptation: easing tree mortality by reducing forest basal area. *Front. Ecol. Environ.* 15:1445. doi: 10.1002/fee.1445

Brando, P. M., Balch, J. K., Nepstad, D. C., Morton, D. C., Putz, F. E., Coe, M. T., et al. (2014). Abrupt increases in Amazonian tree mortality due to drought–fire interactions. *Proc. Natl. Acad. Sci. U. S. A.* 111, 6347–6352. doi: 10.1073/pnas.1305499111

Breshears, D. D., Cobb, N. S., Rich, P. M., Price, K. P., Allen, C. D., Balice, R. G., et al. (2005). Regional vegetation die-off in response to global-change-type drought. *Proc. Natl. Acad. Sci. U. S. A.* 102, 15144–15148. doi: 10.1073/pnas.0505734102

Brockerhoff, E. G., Jactel, H., Parrotta, J. A., Quine, C. P., and Sayer, J. (2008). Plantation forests and biodiversity: oxymoron or opportunity? *Biodivers. Conserv.* 17, 925–951. doi: 10.1007/s10531-008-9380-x

Brodde, L., Adamson, K., Julio Camarero, J., Castaño, C., Drenkhan, R., Lehtijärvi, A., et al. (2019). *Diplodia* tip blight on its way to the north: drivers of disease emergence in Northern Europe. *Front. Plant Sci.* 9:1818. doi: 10.3389/fpls.2018.01818

Buotte, P. C., Hicke, J. A., Preisler, H. K., Abatzoglou, J. T., Raffa, K. F., and Logan, J. A. (2017). Recent and future climate suitability for whitebark pine mortality from mountain pine beetles varies across the western US. *For. Ecol. Manag.* 399, 132–142. doi: 10.1016/j.foreco.2017.05.032

Burgess, T. I., Scott, J. K., Mcdougall, K. L., Stukely, M. J., Crane, C., Dunstan, W. A., et al. (2017). Current and projected global distribution of *Phytophthora cinnamomi*, one of the world's worst plant pathogens. *Glob. Chang. Biol.* 23, 1661–1674. doi: 10.1111/gcb.13492

Caldeira, M. C., Fernandéz, V., Tomé, J., and Pereira, J. S. (2002). Positive effect of drought on longicorn borer larval survivl and growth on *Eucalyptus* trunks. *Ann. For. Sci.* 59, 99–106. doi: 10.1051/forest:2001009

Calvão, T., Duarte, C. M., and Pimentel, C. S. (2019). Climate and landscape patterns of pine forest decline after invasion by the pinewood nematode. *For. Ecol. Manag.* 433, 43–51. doi: 10.1016/j.foreco.2018.10.039

Camarero, J. J., Álvarez-Taboada, F., Hevia, A., and Castedo-Dorado, F. (2018). Radial growth and wood density reflect the impacts and susceptibility to defoliation by gypsy moth and climate in radiata pine. *Front. Plant Sci.* 9:1582. doi: 10.3389/fpls.2018.01582

Cameron, N., Carnegie, A., Wardlaw, T., Lawson, S., and Venn, T. (2018). Economic appraisal of sirex wood wasp (*Sirex noctilio*) control in Australian pine plantations. *Aust. For.* 81, 37–45. doi: 10.1080/00049158.2018.1430436

Carnicer, J., Coll, M., Ninyerola, M., Pons, X., Sanchez, G., and Penuelas, J. (2011). Widespread crown condition decline, food web disruption, and amplified tree mortality with increased climate change-type drought. *Proc. Natl. Acad. Sci. U. S. A.* 108, 1474–1478. doi: 10.1073/pnas.1010070108

Chen, L., Huang, J. G., Dawson, A., Zhai, L., Stadt, K. J., Comeau, P. G., et al. (2018). Contributions of insects and droughts to growth decline of trembling aspen mixed boreal forest of western Canada. *Glob. Chang. Biol.* 24, 655–667. doi: 10.1111/gcb.13855

Cho, J. S., Jeon, H. W., Kim, M. H., Vo, T. K., Kim, J., Park, E. J., et al. (2019). Wood forming tissue-specific bicistronic expression of *Pd GA 20ox1* and *Ptr MYB 221* improves both the quality and quantity of woody biomass production in a hybrid poplar. *Plant Biotechnol. J.* 17, 1048–1057. doi: 10.1111/pbi.13036

Choudhary, A., Gupta, A., Ramegowda, V., and Senthil-Kumar, M. (2017). Transcriptomic changes under combined drought and nonhost bacteria reveal novel and robust defenses in *Arabidopsis thaliana*. *Environ. Exp. Bot.* 139, 152–164. doi: 10.1016/j.envexpbot.2017.05.005

Choudhary, A., Pandey, P., and Senthil-Kumar, M. (2016). "Tailored responses to simultaneous drought stress and pathogen infection in plants" in *Drought stress tolerance in plants. Vol. 1*. eds. M. A. Hossain, S. H. Wani, S. Bhattacharjee and L. P. Tran (Cham: Springer), 427–438.

Ciesla, W. M., and Donaubauer, E. (1994). *Decline and dieback of trees and forests: A global overview*. Rome: Food and Agriculture Organization.

Cobb, R. C., and Metz, M. R. (2017). Tree diseases as a cause and consequence of interacting forest disturbances. *Forests* 8:147. doi: 10.3390/f8050147

Cortini, F., and Comeau, P. G. (2020). Pests, climate and competition effects on survival and growth of trembling aspen in western Canada. *New For.* 51, 175–190. doi: 10.1007/s11056-019-09726-9

Costanza, K. K., Crandall, M. S., Rice, R. W., Livingston, W. H., Munck, I. A., and Lombard, K. (2019). Economic implications of a native tree disease, *Caliciopsis canker*, on the white pine (*Pinus strobus*) lumber industry in the northeastern United States. *Can. J. For. Res.* 49, 521–530. doi: 10.1139/cjfr-2018-0380

Creeden, E. P., Hicke, J. A., and Buotte, P. C. (2014). Climate, weather, and recent mountain pine beetle outbreaks in the western United States. *For. Ecol. Manag.* 312, 239–251. doi: 10.1016/j.foreco.2013.09.051

Crockett, J. L., and Westerling, A. L. (2018). Greater temperature and precipitation extremes intensify Western US droughts, wildfire severity, and Sierra Nevada tree mortality. *J. Clim.* 31, 341–354. doi: 10.1175/JCLI-D-17-0254.1

Croisé, L., Lieutier, F., Cochard, H., and Dreyer, E. (2001). Effects of drought stress and high density stem inoculations with *Leptographium wingfieldii*

on hydraulic properties of young scots pine trees. *Tree Physiol.* 21, 427–436. doi: 10.1093/treephys/21.7.427

Curtis, P. G., Slay, C. M., Harris, N. L., Tyukavina, A., and Hansen, M. C. (2018). Classifying drivers of global forest loss. *Science* 361, 1108–1111. doi: 10.1126/science.aau3445

d'Annunzio, R., Sandker, M., Finegold, Y., and Min, Z. (2015). Projecting global forest area towards 2030. *For. Ecol. Manag.* 352, 124–133. doi: 10.1016/j.foreco.2015.03.014

Das, T., Majumdar, M. H. D., Devi, R. T., and Rajesh, T. (2017). Climate change impacts on plant diseases. *SAARC J. Agric.* 14, 200–209. doi: 10.3329/sja.v14i2.31259

Das, A. J., Stephenson, N. L., and Davis, K. P. (2016). Why do trees die? Characterizing the drivers of background tree mortality. *Ecology* 97, 2616–2627. doi: 10.1002/ecy.1497

da Silva, A. C., de Oliveira Silva, F. M., Milagre, J. C., Omena-Garcia, R. P., Abreu, M. C., Mafia, R. G., et al. (2018). Eucalypt plants are physiologically and metabolically affected by infection with *Ceratocystis fimbriata*. *Plant Physiol. Biochem.* 123, 170–179. doi: 10.1016/j.plaphy.2017.12.002

De Grandpré, L., Kneeshaw, D. D., Perigon, S., Boucher, D., Marchand, M., Pureswaran, D., et al. (2019). Adverse climatic periods precede and amplify defoliator-induced tree mortality in eastern boreal North America. *J. Ecol.* 107, 452–467. doi: 10.1111/1365-2745.13012

Deidda, A., Buffa, F., Linaldeddu, B. T., Pinna, C., Scanu, B., Deiana, V., et al. (2016). Emerging pests and diseases threaten *Eucalyptus camaldulensis* plantations in Sardinia, Italy. *IForest* 9:883. doi: 10.3832/ifor1805-009

de La Serrana, R. G., Vilagrosa, A., and Alloza, J. (2015). Pine mortality in Southeast Spain after an extreme dry and warm year: interactions among drought stress, carbohydrates and bark beetle attack. *Trees* 29, 1791–1804. doi: 10.1007/s00468-015-1261-9

Del Lungo, A., Carle, J., and Varmola, M. (2003). "Planted forest database: analysis of annual planting trends and silvicultural parameters for commonly planted species" in *Planted Forest and Trees Working Papers, Working Paper 26*, Rome: Forest Resources Division, Food and Agriculture Organization of the United Nations, 60.

Desprez-Loustau, M. -L., Marçais, B., Nageleisen, L. -M., Piou, D., and Vannini, A. (2006). Interactive effects of drought and pathogens in forest trees. *Ann. For. Sci.* 63, 597–612. doi: 10.1051/forest:2006040

Dixit, S. K., Gupta, A., Fatima, U., and Senthil-Kumar, M. (2019). *AtGBF3* confers tolerance to *Arabidopsis thaliana* against combined drought and *Pseudomonas syringae* stress. *Environ. Exp. Bot.* 168:103881. doi: 10.1016/j.envexpbot.2019.103881

Donovan, G. H., Butry, D. T., Michael, Y. L., Prestemon, J. P., Liebhold, A. M., Gatziolis, D., et al. (2013). The relationship between trees and human health: evidence from the spread of the emerald ash borer. *Am. J. Prev. Med.* 44, 139–145. doi: 10.1016/j.amepre.2012.09.066

Dukes, J. S., Pontius, J., Orwig, D., Garnas, J. R., Rodgers, V. L., Brazee, N., et al. (2009). Responses of insect pests, pathogens, and invasive plant species to climate change in the forests of northeastern North America: what can we predict? *Can. J. For. Res.* 39, 231–248. doi: 10.1139/X08-171

Fabre, B., Piou, D., Desprez-Loustau, M. L., and Marcais, B. (2011). Can the emergence of pine *Diplodia* shoot blight in France be explained by changes in pathogen pressure linked to climate change? *Glob. Chang. Biol.* 17, 3218–3227. doi: 10.1111/j.1365-2486.2011.02428.x

Faiola, C., and Taipale, D. (2020). Impact of insect herbivory on plant stress volatile emissions from trees: a synthesis of quantitative measurements and recommendations for future research. *Atmos. Environ.* 5:100060. doi: 10.1016/j.aeaoa.2019.100060

Feau, N., Joly, D. L., and Hamelin, R. C. (2007). Poplar leaf rusts: model pathogens for a model tree. *Botany* 85, 1127–1135. doi: 10.1139/B07-102

Fensham, R. J., Carnegie, A. J., Laffineur, B., Makinson, R. O., Pegg, G. S., and Wills, J. (2020). Imminent extinction of Australian myrtaceae by fungal disease. *Trends Ecol. Evol.* 35, 554–557. doi: 10.1016/j.tree.2020.03.012

Ferus, P., Barta, M., and Konôpková, J. (2019). Endophytic fungus *Beauveria bassiana* can enhance drought tolerance in red oak seedlings. *Trees* 33, 1179–1186. doi: 10.1007/s00468-019-01854-1

Fettig, C. J., Mortenson, L. A., Bulaon, B. M., and Foulk, P. B. (2019). Tree mortality following drought in the central and southern Sierra Nevada, California, US. *For. Ecol. Manag.* 432, 164–178. doi: 10.1016/j.foreco.2018.09.006

Flake, S. W., and Weisberg, P. J. (2019). Fine-scale stand structure mediates drought-induced tree mortality in pinyon–juniper woodlands. *Ecol. Appl.* 29:e01831. doi: 10.1002/eap.1831

Floyd, M. L., Clifford, M., Cobb, N. S., Hanna, D., Delph, R., Ford, P., et al. (2009). Relationship of stand characteristics to drought-induced mortality in three Southwestern piñon–juniper woodlands. *Ecol. Appl.* 19, 1223–1230. doi: 10.1890/08-1265.1

Franklin, J. F., Shugart, H. H., and Harmon, M. E. (1987). Tree death as an ecological process. *Bioscience* 37, 550–556. doi: 10.2307/1310665

Galiano, L., Martínez-Vilalta, J., and Lloret, F. (2010). Drought-induced multifactor decline of scots pine in the Pyrenees and potential vegetation change by the expansion of co-occurring oak species. *Ecosystems* 13, 978–991. doi: 10.1007/s10021-010-9368-8

Gao, R., Wang, Z., Wang, H., Hao, Y., and Shi, J. (2019). Relationship between pine wilt disease outbreaks and climatic variables in the three gorges reservoir region. *Forests* 10:816. doi: 10.3390/f10090816

Gazol, A., Hernández-Alonso, R., and Camarero, J. J. (2019). Patterns and drivers of pine processionary moth defoliation in Mediterranean mountain forests. *Front. Ecol. Evol.* 7:458. doi: 10.3389/fevo.2019.00458

Gely, C., Laurance, S. G., and Stork, N. E. (2020). How do herbivorous insects respond to drought stress in trees? *Biol. Rev.* 95, 434–448. doi: 10.1111/brv.12571

Ghanbary, E., Kouchaksaraei, M. T., Guidi, L., Mirabolfathy, M., Etemad, V., Sanavi, S. A. M. M., et al. (2018). Change in biochemical parameters of Persian oak (*Quercus brantii* Lindl.) seedlings inoculated by pathogens of charcoal disease under water deficit conditions. *Trees* 32, 1595–1608. doi: 10.1007/s00468-018-1736-6

Ghanbary, E., Tabari Kouchaksaraei, M., Mirabolfathy, M., Modarres Sanavi, S., and Rahaie, M. (2017). Growth and physiological responses of *Quercus brantii* seedlings inoculated with *Biscogniauxia mediterranea* and *Obolarina persica* under drought stress. *For. Pathol.* 47:e12353. doi: 10.1111/efp.12353

Gheitury, M., Heshmati, M., Noroozi, A., Ahmadi, M., and Parvizi, Y. (2020). Monitoring mortality in a semiarid forest under the influence of prolonged drought in Zagros region. *Int. J. Environ. Sci. Technol.* 11, 4589–4600. doi: 10.1007/s13762-020-02638-8

Gonzalez, P., Neilson, R. P., Lenihan, J. M., and Drapek, R. J. (2010). Global patterns in the vulnerability of ecosystems to vegetation shifts due to climate change. *Glob. Ecol. Biogeogr.* 19, 755–768. doi: 10.1111/j.1466-8238.2010.00558.x

Gori, Y., Cherubini, P., Camin, F., and La Porta, N. (2013). Fungal root pathogen (*Heterobasidion parviporum*) increases drought stress in Norway spruce stand at low elevation in the Alps. *Eur. J. For. Res.* 132, 607–619. doi: 10.1007/s10342-013-0698-x

Graziosi, I., Tembo, M., Kuate, J., and Muchugi, A. (2019). Pests and diseases of trees in Africa: a growing continental emergency. *Plants People Planet* 2, 14–28. doi: 10.1002/ppp3.31

Greenwood, S., Ruiz-Benito, P., Martínez-Vilalta, J., Lloret, F., Kitzberger, T., Allen, C. D., et al. (2017). Tree mortality across biomes is promoted by drought intensity, lower wood density and higher specific leaf area. *Ecol. Lett.* 20, 539–553. doi: 10.1111/ele.12748

Gupta, A., Hisano, H., Hojo, Y., Matsuura, T., Ikeda, Y., Mori, I. C., et al. (2017). Global profiling of phytohormone dynamics during combined drought and pathogen stress in *Arabidopsis thaliana* reveals ABA and JA as major regulators. *Sci. Rep.* 7:4017. doi: 10.1038/s41598-017-03907-2

Gupta, A., Patil, M., Qamar, A., and Senthil-Kumar, M. (2020). *ath-mi*R164c influences plant responses to the combined stress of drought and bacterial infection by regulating proline metabolism. *Environ. Exp. Bot.* 172:103998. doi: 10.1016/j.envexpbot.2020.103998

Gupta, A., Sarkar, A. K., and Senthil-Kumar, M. (2016). Global transcriptional analysis reveals unique and shared responses in *Arabidopsis thaliana* exposed to combined drought and pathogen stress. *Front. Plant Sci.* 7:686. doi: 10.3389/fpls.2016.00686

Hacquard, S., Petre, B., Frey, P., Hecker, A., Rouhier, N., and Duplessis, S. (2011). The poplar-poplar rust interaction: insights from genomics and transcriptomics. *J. Pathog.* 2011:716041. doi: 10.4061/2011/716041

Hansen, J., Sato, M., and Ruedy, R. (2012). Perception of climate change. *Proc. Natl. Acad. Sci. U. S. A.* 109, E2415–E2423. doi: 10.1073/pnas.1205276109

Hassani-Kakhki, M., Karimi, J., El Borai, F., Killiny, N., Hosseini, M., Stelinski, L. L., et al. (2019). Drought stress impairs communication between *Solanum tuberosum* (Solanales: Solanaceae) and subterranean biological control agents. *Ann. Entomol. Soc. Am.* 113, 23–29. doi: 10.1093/aesa/saz050

Hember, R. A., Kurz, W. A., and Coops, N. C. (2017). Relationships between individual-tree mortality and water-balance variables indicate positive trends in water stress-induced tree mortality across North America. *Glob. Chang. Biol.* 23, 1691–1710. doi: 10.1111/gcb.13428

Hogg, E., Brandt, J., and Michaelian, M. (2008). Impacts of a regional drought on the productivity, dieback, and biomass of western Canadian aspen forests. *Can. J. For. Res.* 38, 1373–1384. doi: 10.1139/X08-001

Holuša, J., Lubojacký, J., Čurn, V., Tonka, T., Lukášová, K., and Horák, J. (2018). Combined effects of drought stress and *Armillaria* infection on tree mortality in Norway spruce plantations. *For. Ecol. Manag.* 427, 434–445. doi: 10.1016/j.foreco.2018.01.031

Hossain, M., Veneklaas, E. J., Hardy, G. E. S. J., and Poot, P. (2019). Tree host–pathogen interactions as influenced by drought timing: linking physiological performance, biochemical defence and disease severity. *Tree Physiol.* 39, 6–18. doi: 10.1093/treephys/tpy113

Huber, A. E., and Bauerle, T. L. (2016). Long-distance plant signaling pathways in response to multiple stressors: the gap in knowledge. *J. Exp. Bot.* 67, 2063–2079. doi: 10.1093/jxb/erw099

Hüberli, D., Tommerup, I. C., Colver, M. C., ColquhounC, I. J., and Hardy, G. E. S. J. (2002). Temperature and inoculation method influence disease phenotypes and mortality of *Eucalyptus marginata* clonal lines inoculated with *Phytophthora cinnamomi*. *Australas. Plant Pathol.* 31, 107–118. doi: 10.1071/AP01078

Huot, B., Yao, J., Montgomery, B. L., and He, S. Y. (2014). Growth–defense tradeoffs in plants: a balancing act to optimize fitness. *Mol. Plant* 7, 1267–1287. doi: 10.1093/mp/ssu049

Hurley, B. P., Croft, P., Verleur, M., Wingfield, M. J., and Slippers, B. (2012). "The control of the Sirex woodwasp in diverse environments: the south African experience" in *The sirex woodwasp and its fungal symbiont.* eds. B. Slippers, P. de Groot and M. J. Wingfield (Dordrecht: Springer), 247–264.

Hurley, B. P., Garnas, J., Wingfield, M. J., Branco, M., Richardson, D. M., and Slippers, B. (2016). Increasing numbers and intercontinental spread of invasive insects on eucalypts. *Biol. Invasions* 18, 921–933. doi: 10.1007/s10530-016-1081-x

Hurley, B. P., Slippers, B., Croft, P. K., Hatting, H. J., van der Linde, M., Morris, A. R., et al. (2008). Factors influencing parasitism of *Sirex noctilio* (Hymenoptera: Siricidae) by the nematode *Deladenus siricidicola* (Nematoda: Neotylenchidae) in summer rainfall areas of South Africa. *Biol. Control* 45, 450–459. doi: 10.1016/j.biocontrol.2008.02.010

Hurley, B. P., Slippers, B., Sathyapala, S., and Wingfield, M. J. (2017). Challenges to planted forest health in developing economies. *Biol. Invasions* 19, 3273–3285. doi: 10.1007/s10530-017-1488-z

IPCC (2018). "Summary for policymakers" in *Global Warming of 1.5°C. An IPCC Special Report on the impacts of global warming of 1.5°C above pre-industrial levels and related global greenhouse gas emission pathways, in the context of strengthening the global response to the threat of climate change, sustainable development, and efforts to eradicate poverty*. eds. V. Masson-Delmotte, P. Zhai, H. -O. Pörtner, D. Roberts, J. Skea, P. R. Shukla, et al.

Itter, M. S., D'Orangeville, L., Dawson, A., Kneeshaw, D., Duchesne, L., and Finley, A. O. (2019). Boreal tree growth exhibits decadal-scale ecological memory to drought and insect defoliation, but no negative response to their interaction. *J. Ecol.* 107, 1288–1301. doi: 10.1111/1365-2745.13087

Jacquet, J. -S., Orazio, C., and Jactel, H. (2012). Defoliation by processionary moth significantly reduces tree growth: a quantitative review. *Ann. For. Sci.* 69, 857–866. doi: 10.1007/s13595-012-0209-0

Jactel, H., Koricheva, J., and Castagneyrol, B. (2019). Responses of forest insect pests to climate change: not so simple. *Curr. Opin. Insect Sci.* 35, 103–108. doi: 10.1016/j.cois.2019.07.010

Jactel, H., Petit, J., Desprez-Loustau, M. L., Delzon, S., Piou, D., Battisti, A., et al. (2012). Drought effects on damage by forest insects and pathogens: a meta-analysis. *Glob. Chang. Biol.* 18, 267–276. doi: 10.1111/j.1365-2486.2011.02512.x

Ji, Y., Zhou, G., Li, Z., Wang, S., Zhou, H., and Song, X. (2019). Triggers of widespread dieback and mortality of poplar (*Populus* spp.) plantations across northern China. *J. Arid Environ.* 174:104076. doi: 10.1016/j.jaridenv.2019.104076

Jimenez, J. A., Lugo, A. E., and Cintron, G. (1985). Tree mortality in mangrove forests. *Biotropica* 17, 177–185. doi: 10.2307/2388214

Jones, B. A. (2019). Tree shade, temperature, and human health: evidence from invasive species-induced deforestation. *Ecol. Econ.* 156, 12–23. doi: 10.1016/j.ecolecon.2018.09.006

Jönsson, M. T., and Thor, G. (2012). Estimating coextinction risks from epidemic tree death: affiliate lichen communities among diseased host tree populations of *Fraxinus excelsior*. *PLoS One* 7:e45701. doi: 10.1371/journal.pone.0045701

Karasov, T. L., Chae, E., Herman, J. J., and Bergelson, J. (2017). Mechanisms to mitigate the trade-off between growth and defense. *Plant Cell* 29, 666–680. doi: 10.1105/tpc.16.00931

Kautz, M., Meddens, A. J., Hall, R. J., and Arneth, A. (2017). Biotic disturbances in Northern hemisphere forests–a synthesis of recent data, uncertainties and implications for forest monitoring and modelling. *Glob. Ecol. Biogeogr.* 26, 533–552. doi: 10.1111/geb.12558

Keenan, R. J., Reams, G. A., Achard, F., de Freitas, J. V., Grainger, A., and Lindquist, E. (2015). Dynamics of global forest area: results from the FAO Global Forest Resources Assessment 2015. *For. Ecol. Manag.* 352, 9–20. doi: 10.1016/j.foreco.2015.06.014

Khan, Z., Rho, H., Firrincieli, A., Hung, S. H., Luna, V., Masciarelli, O., et al. (2016). Growth enhancement and drought tolerance of hybrid poplar upon inoculation with endophyte consortia. *Curr. Plant Biol.* 6, 38–47. doi: 10.1016/j.cpb.2016.08.001

Kharuk, V., Shushpanov, A., Petrov, I., Demidko, D., Im, S., and Knorre, A. (2019). Fir (*Abies sibirica* Ledeb.) mortality in mountain forests of the Eastern sayan ridge. *Siberia Contem. Prob. Ecol.* 12, 299–309. doi: 10.1134/S199542551904005X

Kirilenko, A. P., and Sedjo, R. A. (2007). Climate change impacts on forestry. *Proc. Natl. Acad. Sci. U. S. A.* 104, 19697–19702. doi: 10.1073/pnas.0701424104

Kissoudis, C., van de Wiel, C., Visser, R. G., and van der Linden, G. (2014). Enhancing crop resilience to combined abiotic and biotic stress through the dissection of physiological and molecular crosstalk. *Front. Plant Sci.* 5:207. doi: 10.3389/fpls.2014.00207

Klein, T., Cahanovitc, R., Sprintsin, M., Herr, N., and Schiller, G. (2019). A nation-wide analysis of tree mortality under climate change: Forest loss and its causes in Israel 1948-2017. *For. Ecol. Manag.* 432, 840–849. doi: 10.1016/j.foreco.2018.10.020

Kliebenstein, D. J. (2016). False idolatry of the mythical growth versus immunity tradeoff in molecular systems plant pathology. *Physiol. Mol. Plant Pathol.* 95, 55–59. doi: 10.1016/j.pmpp.2016.02.004

Klockow, P. A., Vogel, J. G., Edgar, C. B., and Moore, G. W. (2018). Lagged mortality among tree species four years after an exceptional drought in East Texas. *Ecosphere* 9:e02455. doi: 10.1002/ecs2.2455

Kolb, T. E., Fettig, C. J., Ayres, M. P., Bentz, B. J., Hicke, J. A., Mathiasen, R., et al. (2016). Observed and anticipated impacts of drought on forest insects and diseases in the United States. *For. Ecol. Manag.* 380, 321–334. doi: 10.1016/j.foreco.2016.04.051

Kurz, W. A., Dymond, C., Stinson, G., Rampley, G., Neilson, E., Carroll, A., et al. (2008). Mountain pine beetle and forest carbon feedback to climate change. *Nature* 452:987. doi: 10.1038/nature06777

Lalande, B. M., Hughes, K., Jacobi, W. R., Tinkham, W. T., Reich, R., and Stewart, J. E. (2020). Subalpine fir mortality in Colorado is associated with stand density, warming climates and interactions among fungal diseases and the western balsam bark beetle. *For. Ecol. Manag.* 466:118133. doi: 10.1016/j.foreco.2020.118133

Lantschner, M. V., Aukema, B. H., and Corley, J. C. (2019). Droughts drive outbreak dynamics of an invasive forest insect on an exotic host. *For. Ecol. Manag.* 433, 762–770. doi: 10.1016/j.foreco.2018.11.044

Lévesque, M., Rigling, A., Bugmann, H., Weber, P., and Brang, P. (2014). Growth response of five co-occurring conifers to drought across a wide climatic gradient in Central Europe. *Agric. For. Meteorol.* 197, 1–12. doi: 10.1016/j.agrformet.2014.06.001

Linares, J. C., Senhadji, K., Herrero, A., and Hódar, J. A. (2014). Growth patterns at the southern range edge of scots pine: disentangling the effects of drought and defoliation by the pine processionary caterpillar. *For. Ecol. Manag.* 315, 129–137. doi: 10.1016/j.foreco.2013.12.029

Liu, T., Sheng, M., Wang, C., Chen, H., Li, Z., and Tang, M. (2015). Impact of arbuscular mycorrhizal fungi on the growth, water status, and photosynthesis of hybrid poplar under drought stress and recovery. *Photosynthetica* 53, 250–258. doi: 10.1007/s11099-015-0100-y

Lõhmus, A., and Runnel, K. (2014). Ash dieback can rapidly eradicate isolated epiphyte populations in production forests: a case study. *Biol. Conserv.* 169, 185–188. doi: 10.1016/j.biocon.2013.11.031

Lugo, A. E., and Scatena, F. N. (1996). Background and catastrophic tree mortality in tropical moist, wet, and rain forests. *Biotropica* 28, 585–599. doi: 10.2307/2389099

Lusebrink, I., Erbilgin, N., and Evenden, M. L. (2016). The effect of water limitation on volatile emission, tree defense response, and brood success of *Dendroctonus ponderosae* in two pine hosts, lodgepole, and jack pine. *Front. Ecol. Evol.* 4:2. doi: 10.3389/fevo.2016.00002

Maclauchlan, L. (2016). Quantification of *Dryocoetes confusus*-caused mortality in subalpine fir forests of southern British Columbia. *For. Ecol. Manag.* 359, 210–220. doi: 10.1016/j.foreco.2015.10.013

Mangwanda, R., Myburg, A. A., and Naidoo, S. (2015). Transcriptome and hormone profiling reveals *Eucalyptus grandis* defence responses against *Chrysoporthe austroafricana*. *BMC Genom.* 16:319. doi: 10.1186/s12864-015-1529-x

Marcais, B., Husson, C., Cael, O., Dowkiw, A., Saintonge, F. -X., Delahaye, L., et al. (2017). Estimation of ash mortality induced by *Hymenoscyphus fraxineus* in France and Belgium. *Balt. For.* 23, 159–167.

Marini, L., Ayres, M. P., Battisti, A., and Faccoli, M. (2012). Climate affects severity and altitudinal distribution of outbreaks in an eruptive bark beetle. *Clim. Chang.* 115, 327–341. doi: 10.1007/s10584-012-0463-z

Marini, L., Økland, B., Jönsson, A. M., Bentz, B., Carroll, A., Forster, B., et al. (2017). Climate drivers of bark beetle outbreak dynamics in Norway spruce forests. *Ecography* 40, 1426–1435. doi: 10.1111/ecog.02769

Martín-García, J., Zas, R., Solla, A., Woodward, S., Hantula, J., Vainio, E. J., et al. (2019). Environmentally friendly methods for controlling pine pitch canker. *Plant Pathol.* 68, 843–860. doi: 10.1111/ppa.13009

Matsuhashi, S., Hirata, A., Akiba, M., Nakamura, K., Oguro, M., Takano, K. T., et al. (2020). Developing a point process model for ecological risk assessment of pine wilt disease at multiple scales. *For. Ecol. Manag.* 463:118010. doi: 10.1016/j.foreco.2020.118010

McDowell, N., Allen, C. D., Anderson-Teixeira, K., Brando, P., Brienen, R., Chambers, J., et al. (2018). Drivers and mechanisms of tree mortality in moist tropical forests. *New Phytol.* 219, 851–869. doi: 10.1111/nph.15027

McKiernan, A. B., Potts, B. M., Hovenden, M. J., Brodribb, T. J., Davies, N. W., Rodemann, T., et al. (2017). A water availability gradient reveals the deficit level required to affect traits in potted juvenile *Eucalyptus globulus*. *Ann. Bot.* 119, 1043–1052. doi: 10.1093/aob/mcw266

Mezei, P., Jakuš, R., Pennerstorfer, J., Havašová, M., Škvarenina, J., Ferenčík, J., et al. (2017). Storms, temperature maxima and the Eurasian spruce bark beetle *Ips typographus*—an infernal trio in Norway spruce forests of the Central European High Tatra Mountains. *Agric. For. Meteorol.* 242, 85–95. doi: 10.1016/j.agrformet.2017.04.004

Millar, C. I., Westfall, R. D., Delany, D. L., Bokach, M. J., Flint, A. L., and Flint, L. E. (2012). Forest mortality in high-elevation whitebark pine (*Pinus albicaulis*) forests of eastern California, USA; influence of environmental context, bark beetles, climatic water deficit, and warming. *Can. J. For. Res.* 42, 749–765. doi: 10.1139/x2012-031

Moore, G. W., Edgar, C. B., Vogel, J. G., Washington-Allen, R. A., March, R. G., and Zehnder, R. (2016). Tree mortality from an exceptional drought spanning Mesic to semiarid ecoregions. *Ecol. Appl.* 26, 602–611. doi: 10.1890/15-0330

Nahrung, H. F., and Carnegie, A. J. (2020). Non-native forest insects and pathogens in Australia: establishment, spread and impact. *Front. For. Glob. Chang.* 3:37. doi: 10.3389/ffgc.2020.00037

Naidoo, R., Ferreira, L., Berger, D. K., Myburg, A. A., and Naidoo, S. (2013). The identification and differential expression of *Eucalyptus grandis* pathogenesis-related genes in response to salicylic acid and methyl jasmonate. *Front. Plant Sci.* 4:43. doi: 10.3389/fpls.2013.00043

Naidoo, S., Slippers, B., Plett, J. M., Coles, D., and Oates, C. N. (2019). The road to resistance in forest trees. *Front. Plant Sci.* 10:273. doi: 10.3389/fpls.2019.00273

Netherer, S., Panassiti, B., Pennerstorfer, J., and Matthews, B. (2019). Acute drought is an important driver of bark beetle infestation in Austrian Norway spruce stands. *Front. For. Glob. Chang.* 2:39. doi: 10.3389/ffgc.2019.00039

Notaro, S., Paletto, A., and Raffaelli, R. (2009). Economic impact of forest damage in an alpine environment. *Acta Silv. et Lignaria Hungarica* 5, 131–143.

Ochuodho, T. O., Lantz, V. A., Lloyd-Smith, P., and Benitez, P. (2012). Regional economic impacts of climate change and adaptation in Canadian forests: a CGE modeling analysis. *For. Policy Econ.* 25, 100–112. doi: 10.1016/j.forpol.2012.08.007

Oshunsanya, S. O., Nwosu, N. J., and Li, Y. (2019). "Abiotic stress in agricultural crops under climatic conditions" in *Sustainable agriculture, forest and environmental management*. eds. M. K. Jhariya, A. Banerjee and R. S. Meena (Singapore: Springer), 71–100.

Paap, T., Brouwers, N. C., Burgess, T. I., and Hardy, G. E. S. J. (2017). Importance of climate, anthropogenic disturbance and pathogens (*Quambalaria coyrecup* and *Phytophthora* spp.) on marri (*Corymbia calophylla*) tree health in Southwest Western Australia. *Ann. For. Sci.* 74:62. doi: 10.1007/s13595-017-0658-6

Pandey, P., Irulappan, V., Bagavathiannan, M. V., and Senthil-Kumar, M. (2017). Impact of combined abiotic and biotic stresses on plant growth and avenues for crop improvement by exploiting physio-morphological traits. *Front. Plant Sci.* 8:537. doi: 10.3389/fpls.2017.00537

Pandey, P., Ramegowda, V., and Senthil-Kumar, M. (2015). Shared and unique responses of plants to multiple individual stresses and stress combinations: physiological and molecular mechanisms. *Front. Plant Sci.* 6:723. doi: 10.3389/fpls.2015.00723

Payn, T., Carnus, J. -M., Freer-Smith, P., Kimberley, M., Kollert, W., Liu, S., et al. (2015). Changes in planted forests and future global implications. *For. Ecol. Manag.* 352, 57–67. doi: 10.1016/j.foreco.2015.06.021

Perry, K. I., and Herms, D. A. (2017). Effects of late stages of emerald ash borer (Coleoptera: Buprestidae)-induced ash mortality on forest floor invertebrate communities. *J. Insect Sci.* 17:119. doi: 10.1093/jisesa/iex093

Phillips, O. L., Aragão, L. E., Lewis, S. L., Fisher, J. B., Lloyd, J., López-González, G., et al. (2009). Drought sensitivity of the Amazon rainforest. *Science* 323, 1344–1347. doi: 10.1126/science.1164033

Pichler, P., and Oberhuber, W. (2007). Radial growth response of coniferous forest trees in an inner alpine environment to heat-wave in 2003. *For. Ecol. Manag.* 242, 688–699. doi: 10.1016/j.foreco.2007.02.007

Preisler, H. K., Grulke, N. E., Heath, Z., and Smith, S. L. (2017). Analysis and out-year forecast of beetle, borer, and drought-induced tree mortality in California. *For. Ecol. Manag.* 399, 166–178. doi: 10.1016/j.foreco.2017.05.039

Pureswaran, D. S., Roques, A., and Battisti, A. (2018). Forest insects and climate change. *Curr. Fores. Rep.* 4, 35–50. doi: 10.1007/s40725-018-0075-6

Redmond, M. D., Weisberg, P. J., Cobb, N. S., and Clifford, M. J. (2018). Woodland resilience to regional drought: dominant controls on tree regeneration following overstorey mortality. *J. Ecol.* 106, 625–639. doi: 10.1111/1365-2745.12880

Restaino, C., Young, D. J., Estes, B., Gross, S., Wuenschel, A., Meyer, M., et al. (2019). Forest structure and climate mediate drought-induced tree mortality in forests of the Sierra Nevada, USA. *Ecol. Appl.* 29:e01902. doi: 10.1002/eap.1902

Reyer, C. P., Bathgate, S., Blennow, K., Borges, J. G., Bugmann, H., Delzon, S., et al. (2017). Are forest disturbances amplifying or canceling out climate change-induced productivity changes in European forests? *Environ. Res. Lett.* 12:034027. doi: 10.1088/1748-9326/aa5ef1

Rezende, G. D. S. P., Lima, J. L., da Costa Dias, D., de Lima, B. M., Aguiar, A. M., Bertolucci, F. D. L. G., et al. (2019). Clonal composites: an alternative to improve the sustainability of production in eucalypt forests. *For. Ecol. Manag.* 449:117445. doi: 10.1016/j.foreco.2019.06.042

Rogers, B. M., Solvik, K., Hogg, E. H., Ju, J., Masek, J. G., Michaelian, M., et al. (2018). Detecting early warning signals of tree mortality in boreal North America using multiscale satellite data. *Glob. Chang. Biol.* 24, 2284–2304. doi: 10.1111/gcb.14107

Rouault, G., Candau, J. -N., Lieutier, F., Nageleisen, L. -M., Martin, J. -C., and Warzée, N. (2006). Effects of drought and heat on forest insect populations in relation to the 2003 drought in Western Europe. *Ann. For. Sci.* 63, 613–624. doi: 10.1051/forest:2006044

Roux, J., Germishuizen, I., Nadel, R., Lee, D., Wingfield, M., and Pegg, G. S. (2015). Risk assessment for *Puccinia psidii* becoming established in South Africa. *Plant Pathol.* 64, 1326–1335. doi: 10.1111/ppa.12380

Roy, B. A., Alexander, H. M., Davidson, J., Campbell, F. T., Burdon, J. J., Sniezko, R., et al. (2014). Increasing forest loss worldwide from invasive pests requires new trade regulations. *Front. Ecol. Manag.* 12, 457–465. doi: 10.1890/130240

Ruiz-Pérez, G., and Vico, G. (2020). Effects of temperature and water availability on Northern European boreal forests. *Front. For. Glob. Chang.* 3:34. doi: 10.3389/ffgc.2020.00034

Sáenz-Romero, C., Mendoza-Maya, E., Gómez-Pineda, E., Blanco-García, A., Endara-Agramont, A. R., Lindig-Cisneros, R., et al. (2020). Recent evidence of Mexican temperate forest decline and the need for ex situ conservation, assisted migration, and translocation of species ensembles as an adaptive

management to face projected climatic change impacts in a megabiodiverse country. *Can. J. For. Res.* 50, 843–854. doi: 10.1139/cjfr-2019-0329

Savary, S., Willocquet, L., Pethybridge, S. J., Esker, P., McRoberts, N., and Nelson, A. (2019). The global burden of pathogens and pests on major food crops. *Nat. Ecol. Evol.* 3:430. doi: 10.1038/s41559-018-0793-y

Schaberg, P. G., DeHayes, D. H., Hawley, G. J., and Nijensohn, S. E. (2008). Anthropogenic alterations of genetic diversity within tree populations: implications for forest ecosystem resilience. *For. Ecol. Manag.* 256, 855–862. doi: 10.1016/j.foreco.2008.06.038

Scheller, R. M., Kretchun, A. M., Loudermilk, E. L., Hurteau, M. D., Weisberg, P. J., and Skinner, C. (2018). Interactions among fuel management, species composition, bark beetles, and climate change and the potential effects on forests of the Lake Tahoe Basin. *Ecosystems* 21, 643–656. doi: 10.1007/s10021-017-0175-3

Schuldt, B., Buras, A., Arend, M., Vitasse, Y., Beierkuhnlein, C., Damm, A., et al. (2020). A first assessment of the impact of the extreme 2018 summer drought on Central European forests. *Basic Appl. Ecol.* 45, 86–103. doi: 10.1016/j.baae.2020.04.003

Sherwood, P., Villari, C., Capretti, P., and Bonello, P. (2015). Mechanisms of induced susceptibility to *Diplodia* tip blight in drought-stressed Austrian pine. *Tree Physiol.* 35, 549–562. doi: 10.1093/treephys/tpv026

Sikström, U., Jacobson, S., Pettersson, F., and Weslien, J. (2011). Crown transparency, tree mortality and stem growth of *Pinus sylvestris*, and colonization of *Tomicus piniperda* after an outbreak of *Gremmeniella abietina*. *For. Ecol. Manag.* 262, 2108–2119. doi: 10.1016/j.foreco.2011.07.034

Simler-Williamson, A. B., Rizzo, D. M., and Cobb, R. C. (2019). Interacting effects of global change on forest pest and pathogen dynamics. *Annu. Rev. Ecol. Evol. Syst.* 50, 381–403. doi: 10.1146/annurev-ecolsys-110218-024934

Slippers, B., Hurley, B. P., Mlonyeni, X. O., de Groot, P., and Wingfield, M. J. (2012). "Factors affecting the efficacy of *Deladenus siricidicola* in biological control systems" in *The sirex woodwasp and its fungal symbiont.* eds. B. Slippers, P. de Groot and M. J. Wingfield (Dordrecht: Springer), 119–133.

Soliman, T., Mourits, M. C., van der Werf, W., Hengeveld, G. M., Robinet, C., and Lansink, A. G. O. (2012). Framework for modelling economic impacts of invasive species, applied to pine wood nematode in Europe. *PLoS One* 7:e45505. doi: 10.1371/journal.pone.0045505

Sommerfeld, A., Senf, C., Buma, B., D'Amato, A. W., Després, T., Díaz-Hormazábal, I., et al. (2018). Patterns and drivers of recent disturbances across the temperate forest biome. *Nat. Commun.* 9, 1–9. doi: 10.1038/s41467-018-06788-9

Song, X. -P., Hansen, M. C., Stehman, S. V., Potapov, P. V., Tyukavina, A., Vermote, E. F., et al. (2018). Global land change from 1982 to 2016. *Nature* 560, 639–643. doi: 10.1038/s41586-018-0411-9

Stephenson, N. L., Das, A. J., Ampersee, N. J., Bulaon, B. M., and Yee, J. L. (2019). Which trees die during drought? The key role of insect host-tree selection. *J. Ecol.* 107, 2383–2401. doi: 10.1111/1365-2745.13176

Suarez, M. L., Ghermandi, L., and Kitzberger, T. (2004). Factors predisposing episodic drought-induced tree mortality in Nothofagus–site, climatic sensitivity and growth trends. *J. Ecol.* 92, 954–966. doi: 10.1111/j.1365-2745.2004.00941.x

Suárez-Vidal, E., Sampedro, L., Voltas, J., Serrano, L., Notivol, E., and Zas, R. (2019). Drought stress modifies early effective resistance and induced chemical defences of Aleppo pine against a chewing insect herbivore. *Environ. Exp. Bot.* 162, 550–559. doi: 10.1016/j.envexpbot.2019.04.002

Taccoen, A., Piedallu, C., Seynave, I., Perez, V., Gégout-Petit, A., Nageleisen, L. -M., et al. (2019). Background mortality drivers of European tree species: climate change matters. *Proc. Royal Soc. B* 286:20190386. doi: 10.1098/rspb.2019.0386

Talucci, A. C., and Krawchuk, M. A. (2019). Dead forests burning: the influence of beetle outbreaks on fire severity and legacy structure in sub-boreal forests. *Ecosphere* 10:e02744. doi: 10.1002/ecs2.2744

Thoma, D. P., Shanahan, E. K., and Irvine, K. M. (2019). Climatic correlates of white pine blister rust infection in whitebark pine in the greater yellowstone ecosystem. *Forests* 10:666. doi: 10.3390/f10080666

Thorn, S., Bässler, C., Brandl, R., Burton, P. J., Cahall, R., Campbell, J. L., et al. (2018). Impacts of salvage logging on biodiversity: a meta-analysis. *J. Appl. Ecol.* 55, 279–289. doi: 10.1111/1365-2664.12945

Thurman, J. H., Crowder, D. W., and Northfield, T. D. (2017). Biological control agents in the Anthropocene: current risks and future options. *Curr. Opin. Insect Sci.* 23, 59–64. doi: 10.1016/j.cois.2017.07.006

Torzhkov, I., Kushnir, E., Konstantinov, A., Koroleva, T., Efimov, S., and Shkolnik, I. (2019). "The economic consequences of future climate change in the forest sector of Russia" in *IOP Conference Series: Earth and Environmental Science*; October 23–24, 2019; Voronezh, Russia (IOP Publishing).

Turco, E., Close, T., Fenton, R., and Ragazzi, A. (2004). Synthesis of dehydrin-like proteins in *Quercus ilex* L. and *Quercus cerris* L. seedlings subjected to water stress and infection with *Phytophthora cinnamomi*. *Physiol. Mol. Plant Pathol.* 65, 137–144. doi: 10.1016/j.pmpp.2004.11.010

Ulyshen, M. D., Klooster, W. S., Barrington, W. T., and Herms, D. A. (2011). Impacts of emerald ash borer-induced tree mortality on leaf litter arthropods and exotic earthworms. *Pedobiologia* 54, 261–265. doi: 10.1016/j.pedobi.2011.05.001

van Lierop, P., Lindquist, E., Sathyapala, S., and Franceschini, G. (2015). Global forest area disturbance from fire, insect pests, diseases and severe weather events. *For. Ecol. Manag.* 352, 78–88. doi: 10.1016/j.foreco.2015.06.010

van Mantgem, P. J., Stephenson, N. L., Byrne, J. C., Daniels, L. D., Franklin, J. F., Fulé, P. Z., et al. (2009). Widespread increase of tree mortality rates in the western United States. *Science* 323, 521–524. doi: 10.1126/science.1165000

Visser, E. A., Mangwanda, R., Becker, J. V., Külheim, C., Foley, W., Myburg, A. A., et al. (2015). Foliar terpenoid levels and corresponding gene expression are systemically and differentially induced in *Eucalyptus grandis* clonal genotypes in response to *Chrysoporthe austroafricana* challenge. *Plant Pathol.* 64, 1320–1325. doi: 10.1111/ppa.12368

Visser, E. A., Wegrzyn, J. L., Myburg, A. A., and Naidoo, S. (2018). Defence transcriptome assembly and pathogenesis related gene family analysis in *Pinus tecunumanii* (low elevation). *BMC Genom.* 19:632. doi: 10.1186/s12864-018-5015-0

Wang, W., Vinocur, B., and Altman, A. (2003). Plant responses to drought, salinity and extreme temperatures: towards genetic engineering for stress tolerance. *Planta* 218, 1–14. doi: 10.1007/s00425-003-1105-5

Wang, C., and Wang, S. (2017). Insect pathogenic fungi: genomics, molecular interactions, and genetic improvements. *Annu. Rev. Entomol.* 62, 73–90. doi: 10.1146/annurev-ento-031616-035509

Ward, S. F., and Aukema, B. H. (2019). Anomalous outbreaks of an invasive defoliator and native bark beetle facilitated by warm temperatures, changes in precipitation and interspecific interactions. *Ecography* 42, 1068–1078. doi: 10.1111/ecog.04239

Waring, K. M., Reboletti, D. M., Mork, L. A., Huang, C. -H., Hofstetter, R. W., Garcia, A. M., et al. (2009). Modeling the impacts of two bark beetle species under a warming climate in the southwestern USA: ecological and economic consequences. *Environ. Manag.* 44, 824–835. doi: 10.1007/s00267-009-9342-4

Watt, M., Bulman, L., and Palmer, D. (2011). The economic cost of *Dothistroma* needle blight to the New Zealand forest industry. *N.Z. J. For.* 56, 20–22.

Weed, A. S., Ayres, M. P., and Hicke, J. A. (2013). Consequences of climate change for biotic disturbances in North American forests. *Ecol. Monogr.* 83, 441–470. doi: 10.1890/13-0160.1

Wingfield, M., Brockerhoff, E., Wingfield, B. D., and Slippers, B. (2015). Planted forest health: the need for a global strategy. *Science* 349, 832–836. doi: 10.1126/science.aac6674

Wood, J. D., Knapp, B. O., Muzika, R. -M., Stambaugh, M. C., and Gu, L. (2018). The importance of drought–pathogen interactions in driving oak mortality events in the Ozark border region. *Environ. Res. Lett.* 13:015004. doi: 10.1088/1748-9326/aa94fa

Woods, A., Martín-García, J., Bulman, L., Vasconcelos, M. W., Boberg, J., La Porta, N., et al. (2016). *Dothistroma* needle blight, weather and possible climatic triggers for the disease's recent emergence. *For. Pathol.* 46, 443–452. doi: 10.1111/efp.12248

Woods, A. J., and Watts, M. (2019). The extent to which an unforeseen biotic disturbance can challenge timber expectations. *For. Ecol. Manag.* 453:117558. doi: 10.1016/j.foreco.2019.117558

Worrall, J. J., Egeland, L., Eager, T., Mask, R. A., Johnson, E. W., Kemp, P. A., et al. (2008). Rapid mortality of *Populus tremuloides* in southwestern Colorado, USA. *For. Ecol. Manag.* 255, 686–696. doi: 10.1016/j.foreco.2007.09.071

Worrall, J. J., Marchetti, S. B., Egeland, L., Mask, R. A., Eager, T., and Howell, B. (2010). Effects and etiology of sudden aspen decline in southwestern Colorado, USA. *For. Ecol. Manag.* 260, 638–648. doi: 10.1016/j.foreco.2010.05.020

Wu, X., Hao, Z., Tang, Q., Singh, V. P., Zhang, X., and Hao, F. (2020). Projected increase in compound dry and hot events over global land areas. *Int. J. Climatol.* 40, 1–11. doi: 10.1002/joc.6626

Xie, H., Fawcett, J. E., and Wang, G. G. (2020). Fuel dynamics and its implication to fire behavior in loblolly pine-dominated stands after southern pine beetle outbreak. *For. Ecol. Manag.* 466:118130. doi: 10.1016/j.foreco.2020.118130

Xu, B., Hicke, J. A., and Abatzoglou, J. T. (2019). Drought and moisture availability and recent Western spruce budworm outbreaks in the Western United States. *Forests* 10:354. doi: 10.3390/f10040354

Zhan, J., Ericson, L., and Burdon, J. J. (2018). Climate change accelerates local disease extinction rates in a long-term wild host–pathogen association. *Glob. Chang. Biol.* 24, 3526–3536. doi: 10.1111/gcb.14111

Zhang, X., Lei, Y., Ma, Z., Kneeshaw, D., and Peng, C. (2014a). Insect-induced tree mortality of boreal forests in eastern Canada under a changing climate. *Ecol. Evol.* 4, 2384–2394. doi: 10.1002/ece3.988

Zhang, X., Lei, Y., Pang, Y., Liu, X., and Wang, J. (2014b). Tree mortality in response to climate change induced drought across Beijing, China. *Clim. Chang.* 124, 179–190. doi: 10.1007/s10584-014-1089-0

Zhang, H., and Sonnewald, U. (2017). Differences and commonalities of plant responses to single and combined stresses. *Plant J.* 90, 839–855. doi: 10.1111/tpj.13557

Zwolinski, J., Swart, W., and Wingfield, M. (1990). Economic impact of a post-hail outbreak of dieback induced by *Sphaeropsis sapinea*. *Eur. J. For. Pathol.* 20, 405–411. doi: 10.1111/j.1439-0329.1990.tb01155.x

Conflict of Interest: The authors declare that the research was conducted in the absence of any commercial or financial relationships that could be construed as a potential conflict of interest.

frontiers in Plant Science

ORIGINAL RESEARCH
published: 18 January 2021
doi: 10.3389/fpls.2020.606062

The BpMYB4 Transcription Factor From *Betula platyphylla* Contributes Toward Abiotic Stress Resistance and Secondary Cell Wall Biosynthesis

Ying Yu[1†], Huizi Liu[1†], Nan Zhang[1], Caiqiu Gao[1], Liwang Qi[2] and Chao Wang[1]**

[1] State Key Laboratory of Tree Genetics and Breeding, School of Forestry, Northeast Forestry University, Harbin, China, [2] Chinese Academy of Forestry, Beijing, China

OPEN ACCESS

Edited by:
Sanushka Naidoo,
University of Pretoria, South Africa

Reviewed by:
Qibin Ma,
South China Agricultural University, China
Kazuo Nakashima,
Japan International Research Center for Agricultural Sciences (JIRCAS), Japan

***Correspondence:**
Chao Wang
wangchao@nefu.edu.cn
Liwang Qi
lwqi@caf.ac.cn

[†] These authors have contributed equally to this work

Specialty section:
This article was submitted to Plant Abiotic Stress, a section of the journal Frontiers in Plant Science

Received: 14 September 2020
Accepted: 21 December 2020
Published: 18 January 2021

Citation:
Yu Y, Liu H, Zhang N, Gao C, Qi L and Wang C (2021) The BpMYB4 Transcription Factor From Betula platyphylla Contributes Toward Abiotic Stress Resistance and Secondary Cell Wall Biosynthesis. Front. Plant Sci. 11:606062. doi: 10.3389/fpls.2020.606062

The MYB (v-myb avian myeloblastosis viral oncogene homolog) family is one of the largest transcription factor families in plants, and is widely involved in the regulation of plant metabolism. In this study, we show that a MYB4 transcription factor, BpMYB4, identified from birch (*Betula platyphylla* Suk.) and homologous to EgMYB1 from *Eucalyptus robusta* Smith and ZmMYB31 from *Zea mays* L. is involved in secondary cell wall synthesis. The expression level of *BpMYB4* was higher in flowers relative to other tissues, and was induced by artificial bending and gravitational stimuli in developing xylem tissues. The expression of this gene was not enriched in the developing xylem during the active season, and showed higher transcript levels in xylem tissues around sprouting and near the dormant period. *BpMYB4* also was induced express by abiotic stress. Functional analysis indicated that expression of *BpMYB4* in transgenic Arabidopsis (*Arabidopsis thaliana*) plants could promote the growth of stems, and result in increased number of inflorescence stems and shoots. Anatomical observation of stem sections showed lower lignin deposition, and a chemical contents test also demonstrated increased cellulose and decreased lignin content in the transgenic plants. In addition, treatment with 100 mM NaCl and 200 mM mannitol resulted in the germination rate of the over-expressed lines being higher than that of the wild-type seeds. The proline content in transgenic plants was higher than that in WT, but MDA content was lower than that in WT. Further investigation in birch using transient transformation techniques indicated that overexpression of *BpMYB4* could scavenge hydrogen peroxide and $O_2^{\cdot -}$ and reduce cell damage, compared with the wild-type plants. Therefore, we believe that BpMYB4 promotes stem development and cellulose biosynthesis as an inhibitor of lignin biosynthesis, and has a function in abiotic stress resistance.

Keywords: BpMYB4 transcription factors, abiotic stress, secondary cell wall, functional analysis 2, *Betula platyphylla* Suk

INTRODUCTION

As a ubiquitous transcription factor in plants and animals, MYB proteins are widely involved in the regulation of developmental and metabolic changes in plants. The first *MYB* gene in plants, *ZmMYBC1*, was isolated from maize (Paz-ares et al., 1987). Subsequently, a large number of *MYB* functional genes were isolated and identified from various plants (Dubos et al., 2010). There are at least 196 *MYB* genes in Arabidopsis (*Arabidopsis thaliana*), at least 197 in Populus (*Populus trichocarpa*), and 124 in grapevine (*Vitis vinifera* L.) (Wilkins et al., 2009).

NAC-MYB-based transcriptional regulation of secondary cell wall biosynthesis in land plants is widely known. Plant secondary growth processes are affected by both MYB transcriptional activators and MYB transcriptional repressors, most of which belong to the fourth sub-group of the MYB family (Chen et al., 2002; Vannini et al., 2004). As transcriptional activators, AtMYB46 has been well-studied. Two highly homologous Arabidopsis genes, *AtMYB46* and *AtMYB83*, can be activated by *SND1* (SECONDARY WALL-ASSOCIATED NAC DOMAIN PROTEIN 1) and its homologous proteins, and its overexpression can activate the biosynthesis of lignin, cellulose and hemicellulose (Zhong et al., 2007; Mccarthy et al., 2009). *AtMYB26* regulates the synthesis of secondary cell walls through *NST1* (NAC SECONDARY WALL THICKENING PROMOTING FACTOR 1) and *NST2*, and its overexpression can lead to ectopic deposition of secondary cell walls (Mitsuda et al., 2005; Yang et al., 2007). *PtMYB4* from pine (*Pinus taeda*) and *EgMYB2* from eucalyptus (*Eucalyptus robusta Smith*) belong to the same phylogenetic group as *AtMYB46*. *PtMYB1* and *PtMYB4* can bind with AC elements and are expressed in developing wood, causing secondary wall thickening and lignin biosynthesis (Patzlaff et al., 2003b). Overexpression of *PtMYB4* in tobacco (*Nicotiana tabacum* L.) plants can induce the expression of some lignin biosynthesis genes and cause abnormal deposition of lignin and secondary wall thickening (Patzlaff et al., 2003a). *PtrMYB003* and *PtrMYB020* in Populus are homologous with Arabidopsis *AtMYB46* and are specifically expressed in secondary xylem; when overexpressed in Arabidopsis they activate the biosynthesis of cellulose, hemicellulose, and lignin (Mccarthy et al., 2010). Overexpression of *AtMYB58* and *AtMYB63* promoted the expression of lignin biosynthesis genes, resulting in ectopic deposition of lignin; in contrast, inhibiting their expression reduced the lignin content, resulting in secondary cell wall developmental defects (Zhong et al., 2008; Zhou et al., 2009). In addition, the MYB transcription factor regulates the synthesis of secondary walls by participating in other phenylpropanoid pathways. For example, AtMYB75 mainly regulates the biosynthesis of anthocyanins, but overexpression of this protein also leads to a slight increase in lignin accumulation, indicating that the protein is also involved in the regulation of lignin biosynthesis (Borevitz et al., 2000).

MYBs can also act as transcriptional inhibitors of lignin biosynthesis. For example, transfer of the Antirrhinum (*Antirrhinum majus* L.) *AmMYB308* gene into tobacco resulted in a significant decrease in the expression of C4H (cinnamate-4-hydroxylase), 4CL (4-coumarate:coenzyme A ligase) and CAD (cinnamyl alcohol dehydrogenase) genes, there by effectively inhibiting the biosynthesis of lignin. Transfer of *AmMYB300* into tobacco resulted in the inhibition of expression of 4CL (Tamagnone et al., 1998). In Arabidopsis, overexpression of the maize (*Zea mays* L.) transcriptional repressors ZmMYB31 and ZmMYB42 resulted in the inhibition of expression of *COMT* (caffeic acid 3-O-methyltransferase), thereby reducing lignin content (Fornalé et al., 2006). *EgMYB1* from eucalyptus is an inhibitor of lignin biosynthesis (Legay et al., 2007). Overexpression of *PvMYB4* in switchgrass (*Panicum virgatum*) inhibits lignin biosynthesis (Shen et al., 2011). Overexpression of *AtMYB32* causes anther distortion and affects the formation of anther cell walls (Preston et al., 2004). MYB189 negatively regulates secondary cell wall biosynthesis in Populus (Jiao et al., 2019). Given that there is a little information on the function of negative regulators in woody plants, the screening and identification of MYB transcription factors with transcriptional activation or transcriptional inhibition has broad research significance.

Following a stress stimulus, the expression of some transcription factors increases, resulting in signal amplification. Thus, the expression of downstream related genes are also regulated, so that overall stress resistance is improved to some extent. According to existing reports, MYB transcription factors are involved in a variety of plant stress responses and are key in regulating the cell's response to stress. Examples include a high temperature resistance gene *MYB68* (Feng et al., 2004); genes that respond to drought and salt stress, *GmMYB177* (Liao et al., 2008); genes that respond to drought and cold stress, *OsMYB4*; genes that respond to drought, salt and radiation stress, *OsMYB4* (Pasquali et al., 2008); genes that respond to cold, salt and drought stress, *AtMYB2* (Hoeren et al., 1998); and *OsMYB2* (Yang et al., 2012), to name a few.

Secondary growth and stress resistance are the important physiological processes for tree radial growth and wood formation. The properties of wood are determined by the composition and characteristics of xylem secondary cell wall. For pulping industry the lignin content in secondary cell wall is an important factor affecting pulping yield. The birch (*Betula platyphylla* Suk.) is one of the main pulpwood species. Therefore, it is of great significance to study the lignin biosynthesis and stress resistance for the genetic improvement of forest trees. In this study, a MYB transcription factor homologous to the genes inhibiting lignin synthesis was identified. The expression pattern of this gene in tissues, under artificial bending or abiotic stress treatment were analyzed. The functions related to secondary cell wall biosynthesis were identified by over-expressing *BpMYB4* in *Arabidopsis thaliana*. Besides, the function of this gene in abiotic stress tolerance was investigated through transient transformation in birch. The expression patterns of genes involved in abiotic stress response and cell wall biosynthesis in transgenic plants were analyzed. The results can help further understand the molecular mechanism of secondary growth processes and abiotic stress responses regulated by MYB transcription factors in woody plants.

MATERIALS AND METHODS

Plant Materials and Treatment

Under aseptic conditions, the epidermal cells of onion were torn and plated in 1/2 MS solid medium for sub-cellular localization studies (Wang et al., 2019).

The vernalized birch (*B. platyphylla*) seeds were washed with running water for 3 days and planted on the soil surface; the soil contained a mixture of perlite: vermiculite: soil (1: 1: 4). The plants were grown in a greenhouse under controlled conditions (16 h/8 h light/dark, 25°C, 70–75% relative humidity). Two-month-old seedlings were used to test the express levels between leaves, stems and roots. Developing xylem of 2-years-old birch seedlings were subjected to artificial bending experiments and temporal expression analysis (Wang et al., 2014). The birch seedlings were irrigated with 200 mM NaCl or 300 mM Mannitol solutions for 12 h, 24 h, and 48 h, and the birch irrigated with water was used as a control group for expression analysis under abiotic stress. Three biological replicates were performed.

Wild-type (WT) *Arabidopsis thaliana* (ecotype Col-0) seeds were surface-sterilized with 50% sodium hypochlorite for 6 min, washed six times with sterile distilled water, the seeds plated on solid 1/2 MS medium and incubated at 22°C under light. After growing the cotyledons, the seedlings were transferred to a mixture of perlite: vermiculite: soil (1: 1: 4) and grown in a greenhouse under controlled conditions (16 h/8 h light/dark, 25°C, 70–75% relative humidity). The plants were thoroughly watered every 5 days (Wen and Chang, 2002).

Gene Identification and Bioinformatics Analysis

A cDNA sequence (GenBank accession number KA257119.1) annotated as a MYB transcription factor was screened from birch tension wood transcriptome (Wang et al., 2014). The open reading frame (ORF) was determined using the NCBI blastX procedures[1]. The molecular weight and isoelectric point of the protein were predicted using Expasy[2]. The similarities in amino acid sequences were checked using BioEdit for multiple sequence alignments, and finally the MEGA version 4 software (Kubo et al., 1998) was used for phylogenetic tree analysis.

Sub-Cellular Localization

Total RNA of birch was extracted using CTAB method (Chang et al., 1993) and treated with DNase I to remove DNA contamination. Total RNA was reverse transcribed into cDNA using a PrimeScriptTMRT reagent Kit (Takara Bio Inc., Kusatsu, Shiga, Japan). *BpMYB4* CDS without a stop codon was fused to the N-terminus of green fluorescent protein (GFP) into the pROKII vector and driven by a CaMV 35S promoter. Vector construct primers are shown in **Supplementary Table 1**. The microcarriers (tungsten powder) embedded with the 35S: GFP plasmid and the 35S: gene-GFP plasmid were transformed into onion epidermal cells with high pressure helium gas using a PDS-1000 benchtop gene gun (Bio-Rad laboratories, Inc., Hercules, CA, United States). After 2 days of culture under dark conditions, the expression pattern was observed and captured using a LSM700 laser confocal microscope (Zeiss, Jena, Germany).

Real-Time PCR

Total RNA of plant was extracted by CTAB method for semi-quantitative RT-PCR and real-time RT-PCR analysis. Real-time RT-PCR was performed with a TransStart Top Green qPCR SuperMix kit (TransGen Biotech, Beijing, China) using the primer sequences listed in **Supplementary Table 2**. The amplification procedure was conducted using the following parameters: 94°C for 30 s; 45 cycles at 94°C for 12 s, 58°C for 30 s and 72°C for 45 s; and 79°C for 1 s for plate reading. The semi-quantitative PCR enzyme by rTaq (TaKaLa), which amplification procedure was conducted using the following parameters: 94°C for 2 min; 28 cycles at 94°C for 30 s, 58°C for 30 s and 72°C for 45 s. Three independent experiments were performed. The tubulin (GenBank accession number: FG067376) and ubiquitin (GenBank accession number: FG065618) genes were used as the internal controls. The relative expression level of each gene was calculated using the delta–delta CT method (Livak and Schmittgen, 2001).

Construction of Overexpression and Knock-Down Expression Vectors

The CDS of genes was inserted into the pROKII vector to construct the overexpression vector (OE) driven by a CaMV 35S promoter. A short sequence inverted repeat of 200 bp was inserted in the RNAi vector pFGC5941 to generate the RNAi-silencing knock down vector (SE). Vector construct primers are shown in **Supplementary Table 1**. The recombinant plasmids of the overexpression vector or the RNAi-silencing vector were transformed into *Agrobacterium tumefaciens* strain EHA105 using the freeze-thaw method (Zhang et al., 2018).

Transformation of Arabidopsis

For transformation, WT Arabidopsis was used at flowering time with the ripe pods removed. Transformation of 35S: MYB4-GFP into *A. thaliana* was performed using the Arabidopsis flower dipping method (Clough and Bent, 1998). The obtained seeds were screened for resistance with 1/2 MS solid medium containing 50 mg/L kanamycin, until T3 generation seeds were obtained. The semi-quantitative PCR was performed for expression identification of *BpMYB4* in transgenetic *Arabidopsis*. Primers are shown in **Supplementary Table 2**.

Histochemical Analysis

Transgenic *A. thaliana* growing for about 50 days was selected as the experimental group, and WT *A. thaliana* in the same growth cycle under the same environment was used as the control group. The mature stems of *A. thaliana* in the control group and the experimental group were sectioned by hand, and histochemically stained with a 1% phloroglucinol solution. The sections were observed with an optical microscope (Olympus BX53, Japan).

[1]https://blast.ncbi.nlm.nih.gov/Blast.cgi?PROGRAM~=~blastx&PAGE_TYPE~=~BlastSearch&LINK_LOC~=~blasthome

[2]http://www.expasy.org/tools

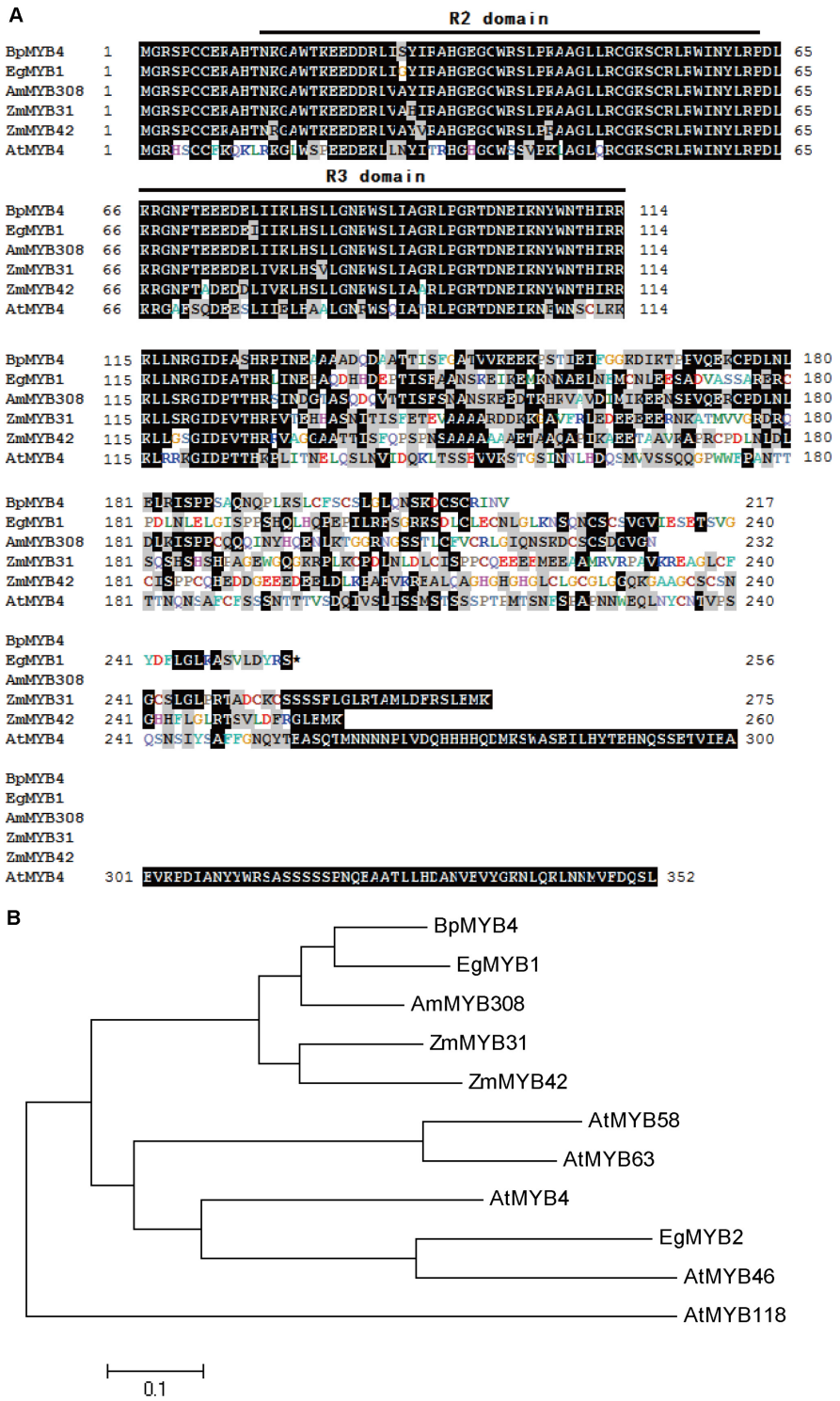

FIGURE 1 | Sequence analysis of BpMYB4. **(A)** ClustalW alignment of EgMYB1 and homologous proteins using BioEdit. Black and gray shadings represent identical and similar amino acids, respectively. The conserved regions R2 and R3 MYB DNA binding domains are indicated at the top. **(B)** Neighbor joining tree of BpMYB4 and homologous proteins (Bootstrap = 1000). Full-length amino acid sequences were used to construct the tree with the Mega 5.0 software. GenBank accession numbers: EgMYB1 (CAE09058), EgMYB2 (AJ576023), ZmMYB31 (CAJ42202), ZmMYB42 (CAJ42204), AmMYB308 (P81393), AtMYB4 (AF062860), AtMYB46 (NM121290), AtMYB58 (AF062893), AtMYB63 (AF062898), AtMYB118 (AF334817).

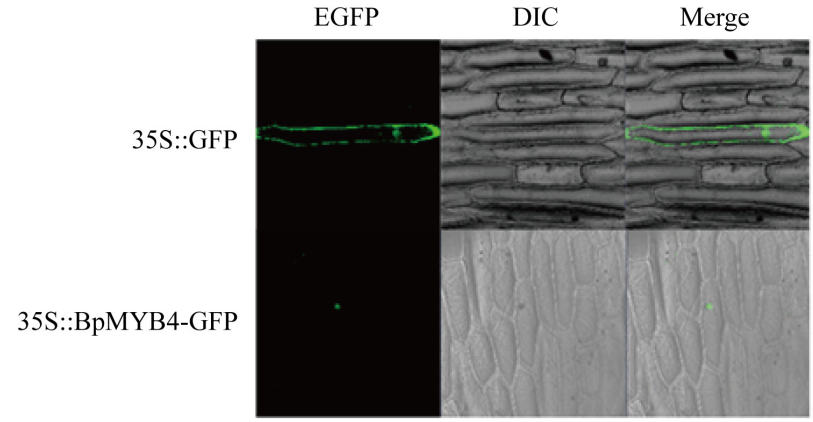

FIGURE 2 | Sub-cellular localization of BpMYB4 protein in onion epidermal cells. Onion epidermal cells were transiently transformed with constructs containing vector 35S: BpMYB4-GFP through particle bombardment method. Sub-cellular localization of 35S: BpMYB4-GFP fusion proteins were viewed using fluorescent confocal microscopy.

Chemical Analysis of Secondary Cell Wall

Lignin and cellulose content were determined by the Soxhlet extraction method (Thurbide and Hughes, 2000). The transgenic and WT Arabidopsis plants were harvested at about 50 days growth stage, dried in an oven at 105°C, pulverized, and bake to a constant weight at 55°C. A sample weight of exactly 0.5 g (weight to 0.0001 g) was used to determine the content of lignin in transgenic Arabidopsis, and a sample weight of exactly 1.0 g (weight to 0.0001 g) was used to determine the content of cellulose. Three technical replicas were made. All samples were wrapped with filter paper and tied with cotton thread.

Seed Germination Rate Under Abiotic Stress

Seeds of WT *A. thaliana* and from the overexpression lines of transgenic *A. thaliana* T3 generation (OE-7, OE-9, OE-25) were washed with sodium hypochlorite solution and sequentially sown on 1/2 MS, 1/2 MS + 100 mM NaCl, and 1/2 MS + 200 mM mannitol (Ji et al., 2013). The seeds were germinated in an artificial climate culture chamber for 10–15 days, and the germination rate was counted.

MDA and PRO Content Determination

Using PRO kit (Nanjing Jiancheng, China) to determine the content of L-proline (Pro) in plant materials under abiotic stress. Malondialdehyde (MDA) determination of plants under treatment was conducted by thiobarbituric acid method (Wang et al., 2010b). Three biological replicates were performed.

Transient Transformation in Birch and Treatment of Plants

Agrobacterium tumefaciens with pROKII, pFGC5941 empty vector, and the recombinant vectors were cultured to OD 600 value of 0.5, and the cells were collected and resuspended in 5% sucrose, 1.5 mg/L KT (6-Furfurylaminopurine), 0.5 mg/L NAA (1-naphthylacetic acid), 100 μM AS (acetosyringone) and 0.02% Tween 20 in 50 mL of 1/2 MS liquid medium (pH 5.6). Two month-old birch seedlings were soaked in the medium containing resuspended bacterial cells under 25°C, with constant shaking at 100 rpm for 2 h; the cultured birch seedlings were then washed 1–2 times with sterile deionized water, and the water on the birch seedlings was dried with sterile absorbent paper. The infected birch seedlings were transplanted into artificial nutrient soil (The ratio of soil, perlite and vermiculite was 5:3:2) and moisturized by mulching. The gene expression was detected by RT-PCR after culture at 25°C and light (approximately 150 μmol m^{-2} s^{-1}) for 3 days (Zhang et al., 2018).

The transiently transformed birch seedlings were replanted into the artificial nutrient soil in the greenhouse. After 3 days of culture, the transiently transformed birch and the untreated WT plants were treated with 100 mM NaCl and 200 mM mannitol for 24 h, respectively (Wang et al., 2019). Total RNA was extracted from birch seedlings under stress and transcribed into cDNA.

DAB, NBT, and Evan's Blue Staining

DAB (3-3'-diaminobenzidine), NBT (nitro blue tetrazolium) and Evan's Blue staining were performed on birch leaves after stress treatment (Zhang et al., 2018). The leaves were extracted and stained with DAB, NBT and Evan's Blue stains. At 37°C, tissues were stained with DAB overnight, stained with NBT for 4 h, and stained with Evan's Blue for 8 h. After staining, the stain was removed and decolorized. The solution (95% ethanol + 5% glycerol) was dehydrated in a boiling water bath.

RESULTS

BpMYB4 Is Homologous to Lignin Biosynthetic Inhibitory Factor

An mRNA sequence, KA257119.1, 4258 bp in length, from reaction wood of *B. platyphylla* was found in the Transcriptome Shotgun Assembly database (Wang et al., 2014). According to BLASTX and ORF analysis, a MYB transcription factor was

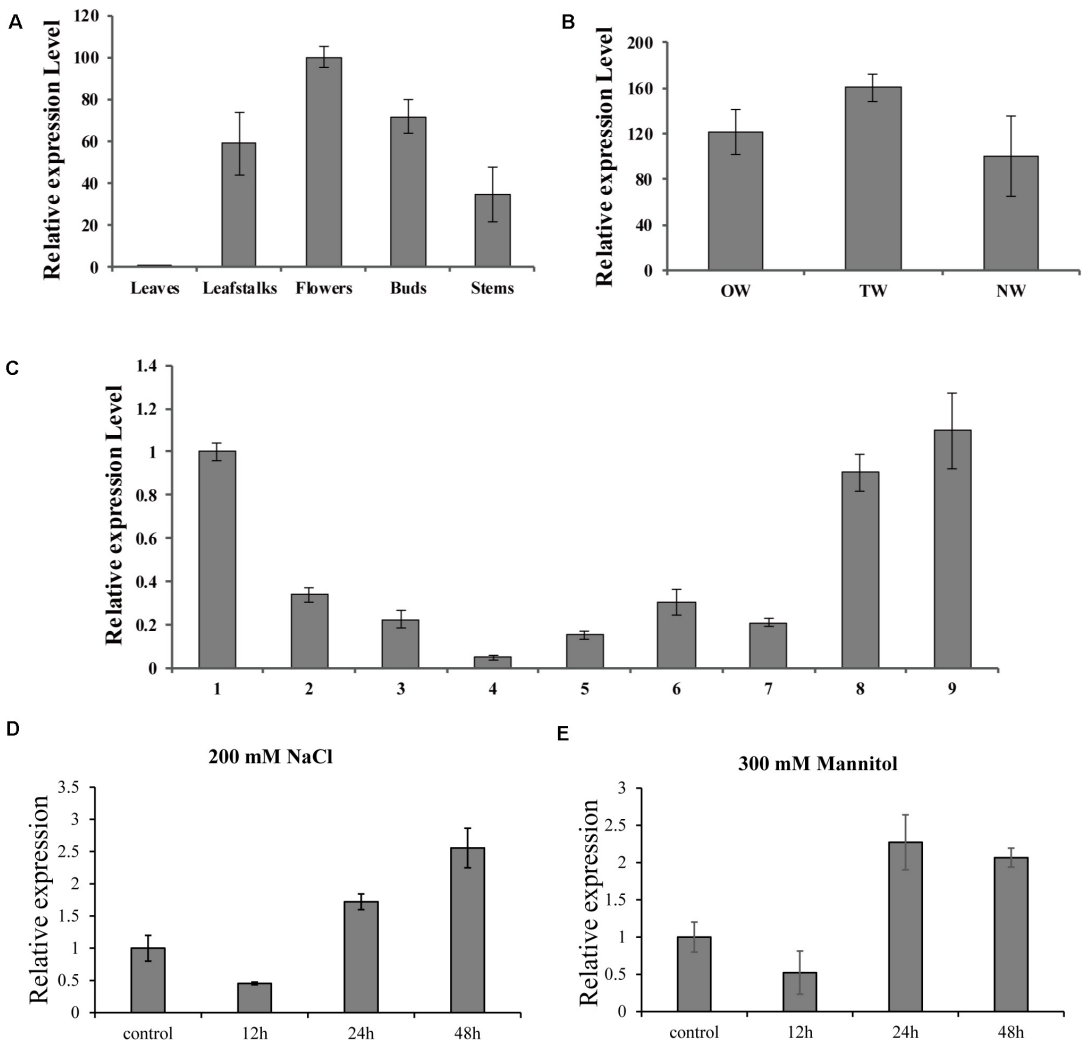

FIGURE 3 | Real-time RT-PCR expression analysis of BpMYB4. **(A)** Real-time RT-PCR analysis of BpMYB4 expression in different tissues. **(B)** Real-time RT-PCR expression analysis of BpMYB4 in OW (opposite wood), TW (tension wood) and NW (normal wood). **(C)** Real-time RT-PCR analysis of BpMYB4 expression in birch xylem at different growth stages (Numbers 1–9 indicate different months). **(D)** Real-time RT-PCR analysis of BpMYB4 expression in birch under different time stresses of 200 mM NaCl. **(E)** Real-time RT-PCR analysis of BpMYB4 expression in birch under different time stresses of 300 mM Mannitol. Error bars represent standard error for three replicates.

identified with an open reading region 654 bp in length, encoding a total of 217 amino acids. The molecular weight of this MYB protein is predicted to be approximately 53.661 kDa.

Multi-sequence alignment analysis demonstrated (Wang et al., 2018) that BpMYB4 has a typical R2R3 MYB TF signature. BpMYB4 protein is highly similar to AmMYB308 (P81393) (Tamagnone et al., 1998), ZmMYB42 (CAJ42204) (Fornalé et al., 2006), ZmMYB31 (CAJ42202) (Fornalé et al., 2010), and EgMYB1 (CAE09058) (Legay et al., 2007) across conserved domains (**Figure 1A**), with similarity reaching up to 80% using the full amino acid sequence and 95% in conserved domains. A phylogenetic tree (**Figure 1B**) analysis showed that BpMYB4 was more similar to EgMYB1, which is a inhibitory of lignin biosynthesis, compared with Antirrhinum AmMYB308 and maize ZmMYB31 and ZmMYB42.

Sub-Cellular Localization of BpMYB4

Recombinant plasmid 35S:MYB4-GFP was transfected into onion epidermal cells using the gene gun transformation technique, and the 35S: GFP plasmid was used as a positive control. Observations using a laser confocal microscope showed a green fluorescent signal in the nucleus of the onion epidermis, indicating that BpMYB4 is a nuclear protein (**Figure 2**).

Expression Analysis of BpMYB4 Gene

To further investigate the biological role of *BpMYB4* in secondary growth of birch, its gene expression pattern in different tissues, development stages in a growth season and during tension wood development, were analyzed using real-time quantitative PCR. The results (**Figure 3A**) showed that the expression level of *BpMYB4* was the highest in the inflorescence than other

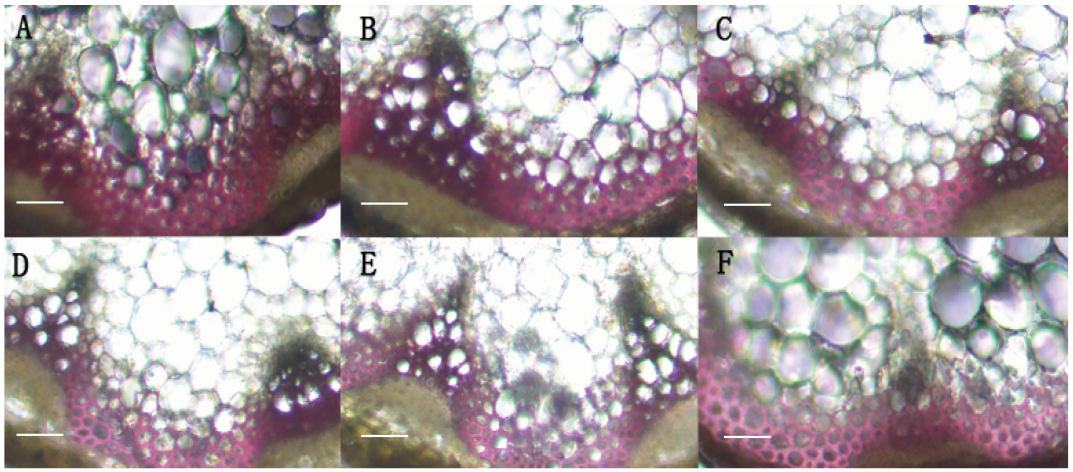

FIGURE 4 | Histological observation of transgenic Arabidopsis. **(A)** Histological observation of WT Arabidopsis. **(B–F)** Histological observation of transgenic Arabidopsis stems (**B:** line 2; **C:** line 3; **D:** line 7; **E:** line 9; **F:** line 25). scale bar represent 50 μm.

TABLE 1 | Determination of lignin and cellulose.

Number	Lignin%	Cellulose%
Line 2	12.08*	24.76*
Line 3	13.77*	25.01*
Line 7	12.81*	27.15*
Line 9	13.56*	27.81*
Line 25	13.75*	25.82*
WT	14.9	22.08

*Each experiment was replicated independently for at least three times. Asterisk indicates significant difference (*p < 0.05).*

tissues, followed by buds, petioles, stems and leaves of birch. Its expression level was nearly 100 times higher in inflorescence than that in leaves, and 40–60 times higher in petioles and stems, compared to leaves. In a growth season the expression level of *BpMYB4* was different in different stages of xylem development in birch (**Figure 3C**); its expression was abundant in late April and middle September, but decreased during active stages of cambium development. When the stems of birch were subjected to artificial bending and gravity stimulation, the transcript of *BpMYB4* was increased during tension wood (xylem formed above the area of the bending) development, compared to those in opposite wood (xylem formed below the area of the bending) and normal wood (xylem of the straight tree) (**Figure 3B**). Temporal expression patterns of the BpMYB4 gene were carried out to test BpMYB4 response to salt stress and drought stress using qRT-PCR. The results showed the expression of BpMYB4 were induced at 24 h after stress treatment (**Figures 3D,E**).

Phenotypic Analysis by Ectopic Expression of BpMYB4 in Transgenic Arabidopsis

In order to identify the function of *BpMYB4* in secondary growth, transgenic Arabidopsis plants overexpressing *BpMYB4* were generated. The semi-quantitative PCR was used to verify the expression of BpMYB4 gene in transgenic Arabidopsis, The results (**Supplementary Figure 1**) showed that *BpMYB4* gene were expressed in transgenic line 7, line 9 and line 25. The phenotypic observation showed the growth rate of the inflorescence stems of transgenic plants increased (**Supplementary Figure 2B**) compared with the WT. Transgenic Arabidopsis had a 10–15 day longer life cycle than WT. We further detected lignin deposition using anatomical observations (**Figure 4**). The stem sections stained with phloroglucinol-HCl showed decreased lignin deposition in transgenic plants with lighter red stain, compared to WT *A. thaliana*.

Analysis of Lignin and Cellulose Content in Transgenic *A. thaliana*

To verify the inhibitory role of *BpMYB4* in lignin biosynthesis, chemical analysis was performed to detect the changes in lignin and cellulose content of transgenic Arabidopsis. Chemical composition analysis suggested that the content of lignin in transgenic lines was reduced relative to WT, with decreasement of 3.85–8.23%. However, compared with WT, the content of cellulose in transgenic plants increased significantly ($P < 0.05$), with a averange increasment of 5.29–13.15% (**Table 1**). These results indicated that *BpMYB4* overexpression has a negative effect on lignin biosynthesis and deposition but a positive effect on cellulose content.

Analysis of Germination Rate in Response to Salt and Osmotic Stress

When the seeds of transgenic lines (OE-7, OE9, OE-25) and WT were exposed to salt or mannitol, it was found that *BpMYB4* overexpression conferred salt and osmotic stress tolerance to the seeds. There was no substantial difference in germination rates between transgenic Arabidopsis and WT lines under control conditions (**Figure 5**). Following 100 mM NaCl or 200 mM

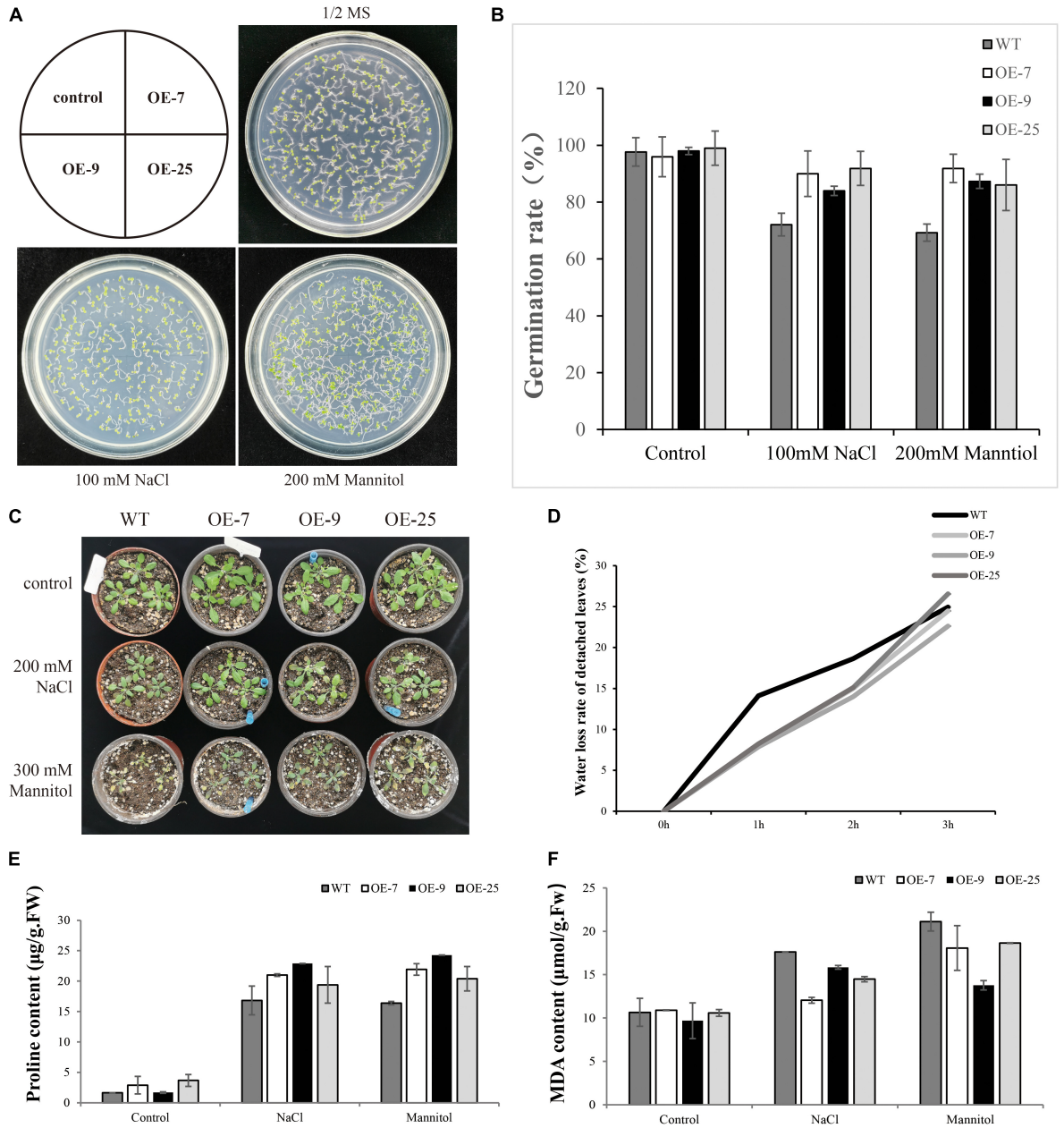

FIGURE 5 | Seed germination assays in mature seeds of WT (WT) and BpMYB4-OE lines (OE-7, OE-9, and OE-25). **(A)** Germination of WT, OE-7, OE-9 and OE-25 Arabidopsis seeds on 1/2 MS media, 100 mM NaCl + 1/2 MS and 200 mM mannitol + 1/2 MS. **(B)** Quantification of greening cotyledons on plates corresponding to **(A)**. **(C)** Growth phenotype of Arabidopsis plants. **(D)** Water loss rate of detached leaves. **(E)** Determination of Pro content in Arabidopsis plants. **(F)** Determination of MDA content in Arabidopsis plants.

mannitol treatment, compared with WT plants both OE-7, OE-9 and OE-25 lines displayed higher germination rates. These results suggest that *BpMYB4* overexpression improves abiotic stress tolerance in Arabidopsis.

MDA and PRO Content Determination

Malondialdehyde is the product of membrane lipid peroxidation in plant tissues subjected to oxidative stress under adversity, reflecting the degree of cell membrane lipid peroxidation and the strength of plant response to adversity (Ma et al., 2015). Pro plays an important role in osmotic regulation in plants. Under adversity conditions, the Pro content reflects the stress resistance of plants to a certain extent (Vendruscolo et al., 2007). We tested the content of MDA and Pro to study the resistance of *BpMYB4* transgenic plants to salt and drought stress. The WT and transgenic Arabidopsis were treated with 200 mM NaCl and 300 mM Mannitol solutions for 24 h, and the control plants were treated with water. Compared

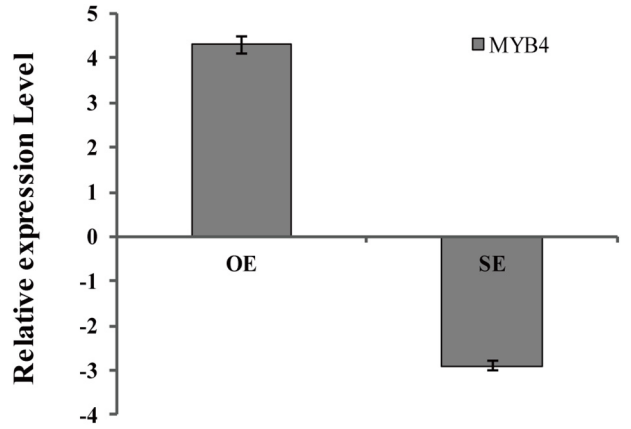

FIGURE 6 | Analysis of BpMYB4 expression in birch after transient transformation. The overexpression vector 35S: BpMYB4 (OE) and the inhibitory expression vector pFGC5941-BpMYB4 (SE) were transformed into birch seedlings by infection to make the vector transiently expressed in the plant, and the expression analysis of BpMYB4 was performed by real-time quantitative PCR.

with the control group, the content of MDA in transgenic Arabidopsis was reduced, and the content of Pro was increased. The above results indicate that the *BpMYB4* gene has certain stress resistance ability.

Generation of Transiently Transgenic Birch Plants With Knocked Down or Overexpressing BpMYB4

BpMYB4 was over-expressed or knocked down in birch using an *Agrobacterium*-mediated transient expression system, and the expression levels of *BpMYB4* in transgenic plants were detected by qRT-PCR (**Figure 6**). The results showed that expression of *BpMYB4* was highly up-regulated in the transiently transformed plants with 35S: MYB4 vectors, which was approximately 20-fold higher than that of the control, while expression of *BpMYB4* in the transiently transformed knock-down plants (pFGC5941: MYB4) was down-regulated, with only 1/4th of the transcripts present in the control. The results showed that *BpMYB4* was overexpressed or knocked down in the transiently transformed birch seedlings. These transformed lines were used in further functional analysis.

BpMYB4 Functions to Scavenge ROS and Maintain Cell Membrane Integrity in Transgenic Birch Subjected to Abiotic Stress

Abiotic stress can induce the generation of reactive oxygen species (ROS), such as hydrogen peroxide (H_2O_2) and superoxide anion $O_2^{\cdot -}$, and accumulation of ROS could damage cell membranes by oxidation of proteins, lipids and DNA (Mittler et al., 2004). To analyze the physiological mechanisms by which *BpMYB4* increases the ability to tolerate stress, birch plants were transformed transiently with 35S: BpMYB4, pROKII plasmid (control), pFGC5941: BpMYB4 or pFGC5941 plasmid (control), and WT as well as transgenic plants were irrigated with water (contro), 100 mM NaCl or 200 mM mannitol for 24 h. DAB staining in plants following abiotic stress have previously shown reduced hydrogen peroxide accumulation, leading to increased resistance (Sela et al., 2013). In the present results, DAB staining showed that under non-stress condition the over-expression (OE) plants, silencing expression (SE) plants, control plants and WT plants were not stained, with no obvious difference between them (**Figure 7A**). These results indicate that the content of hydrogen peroxide in these lines was similar in the controls. Under abiotic stress conditions, hydrogen peroxide accumulation in OE plants were at the lowest levels, and the hydrogen peroxide accumulation levels in the SE plants were the highest. This indicates that *BpMYB4* can reduce hydrogen peroxide accumulation in OE birch seedlings subjected to abiotic stress, and plays a role in stress tolerance of birch plants.

We performed NBT staining on the transiently transformed birch plants after abiotic stress treatment. Studies have shown that NBT staining can detect the accumulation of $O_2^{\cdot -}$ in cells under stress, thereby demonstrating the resistance ability of plants (Yu et al., 2018). The results are shown in **Figure 7B**. Following water treatment, there was no obvious color difference between OE plants, SE plants, control group and WT, indicating that $O_2^{\cdot -}$ content was basically the same. However, under NaCl or mannitol treatment, the level of $O_2^{\cdot -}$ in the OE plants was the lowest, and the level of $O_2^{\cdot -}$ in SE plants was the highest. This shows that the content of $O_2^{\cdot -}$ in the OE plants is smaller than that in WT and control group. Our results indicate that *BpMYB4* can reduce the accumulation of $O_2^{\cdot -}$ in birch trees under abiotic stress, further suggesting that *BpMYB4* plays a role in the stress resistance of birch trees.

Studies have shown that Evan's Blue staining can detect cell death and demonstrate the degree of stress resistance of plants (Singh and Upadhyay, 2014). Evan's Blue staining was performed on the transiently transformed birch plants after abiotic stress treatment. The results are shown in **Figure 7C**. Under the water treatment, there was no obvious color difference between OE plants, SE plants, the control group, and the WT, indicating that there was no remarkable difference in the degree of cell damage. However, under abiotic stress conditions, the damage of OE plant cell membranes was the lowest, and the damage of SE plant cell membranes was the highest. Our results indicate that *BpMYB4* can reduce the damage to cells in OE birch plants under abiotic stress. The Evan's Blue staining results again showed that *BpMYB4* has a certain function of stress resistance in birch.

BpMYB4 Regulates the Expression of Genes Related to Resistance and Cell Wall Biosynthesis

To analyze the genes regulated by BpMYB4 in stress resistance and cell well formation, we analyzed the expression levels of putative downstream resistance-related and cell wall biosynthesis-related genes in overexpressing and knock-out transgenic lines. The results in **Figure 8A** show that most resistance-related genes were highly up-regulated in

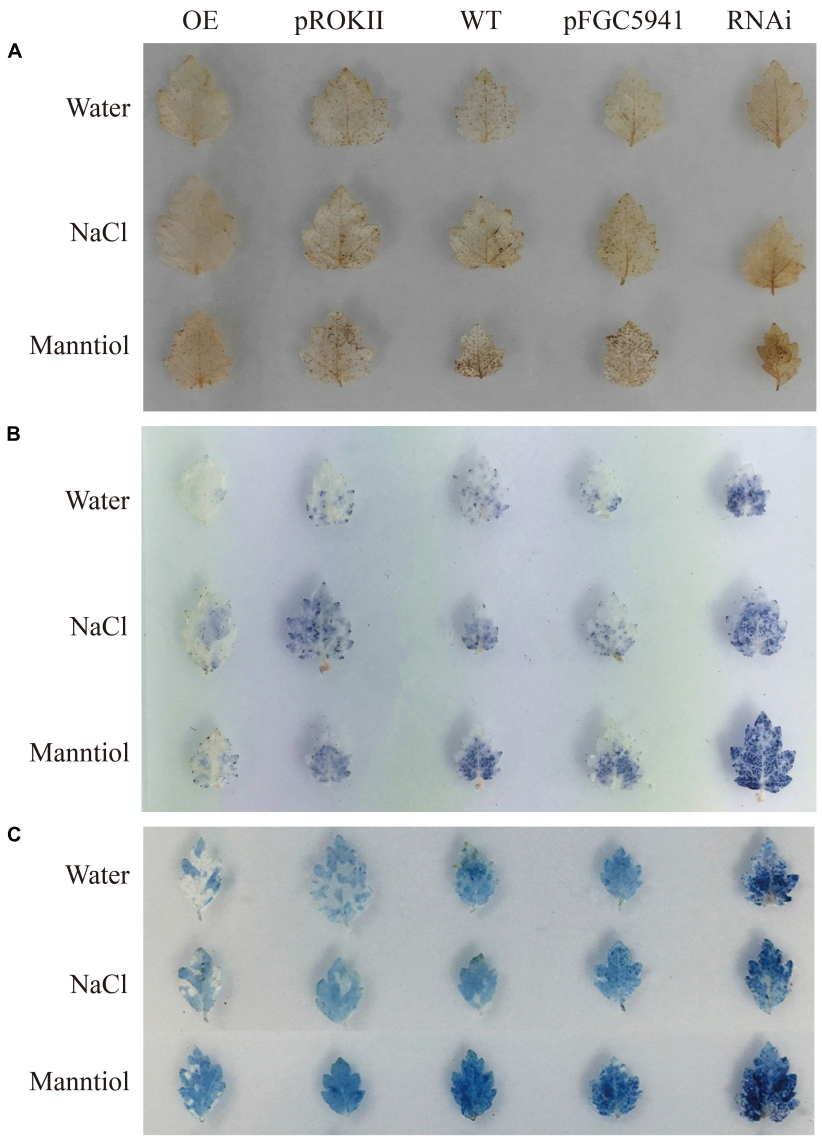

FIGURE 7 | Histochemical staining analysis of transiently transformed birch. The plants were stained with DAB **(A)** and NBT **(B)** to reveal the accumulation of $O_2^{\cdot-}$ and H_2O_2, respectively. **(C)** Analysis of cell death by Evan's Blue staining.

overexpressing lines (pROKII-*BpMYB4*) compared to the empty vector (pROK II) control line, including *SOD1, SOD2, SOD3, SOD4, SOD5, POD1, POD2, POD3 POD5, POD12, P5CDh1, P5CDh2,* and *P5CS2* genes. Among them, the maximum differential expression amount can reach as much as 27.4 fold, and the smallest is only about 1 flod. Therefore, most of the resistance-related genes were up-regulated in overexpressing lines, suggesting that overexpression of *BpMYB4* (pROKII-BpMYB4) can induce the expression of resistance-related genes. The results in **Figure 8B** show that most resistance genes are negatively regulated by the suppressed expression of *BpMYB4* (RNAi-BpMYB4), compared to the empty vector (RNAi) control line. Among them, *POD1, POD3, POD6, POD7, POD8, POD9, POD10, POD11, POD12, P5CDh1, P5CDh2, P5CS1,* and *P5CS2* expression were remarkably highly down-regulated. Among them, POD12 had the largest down-regulated expression level, and the down-regulated expression level could reach as much as 84.9 fold. These data indicate that knock-down expression of *BpMYB4* (RNAi-*BpMYB4*) can negatively affect the expression of resistance-related genes. The results in **Figure 9A** show that compared with the empty vector (pROKII) control line, in the OE lines (pROKII-*BpMYB4*), *CCO*, *CCR* and *C4H* genes which are the key regulator in lignin biosynthesis were down-regulated. *CESA* gene relate to cellulose biosynthesis was up-regulated, expression of *CAD* and *4CL* were also slight increased. Among them, the transcripts increase of *CESA* reached 3.61 fold, and the decreased expression level of *C4H* reached 8 fold. The results in **Figure 9B** show that compared with the RNAi empty vector

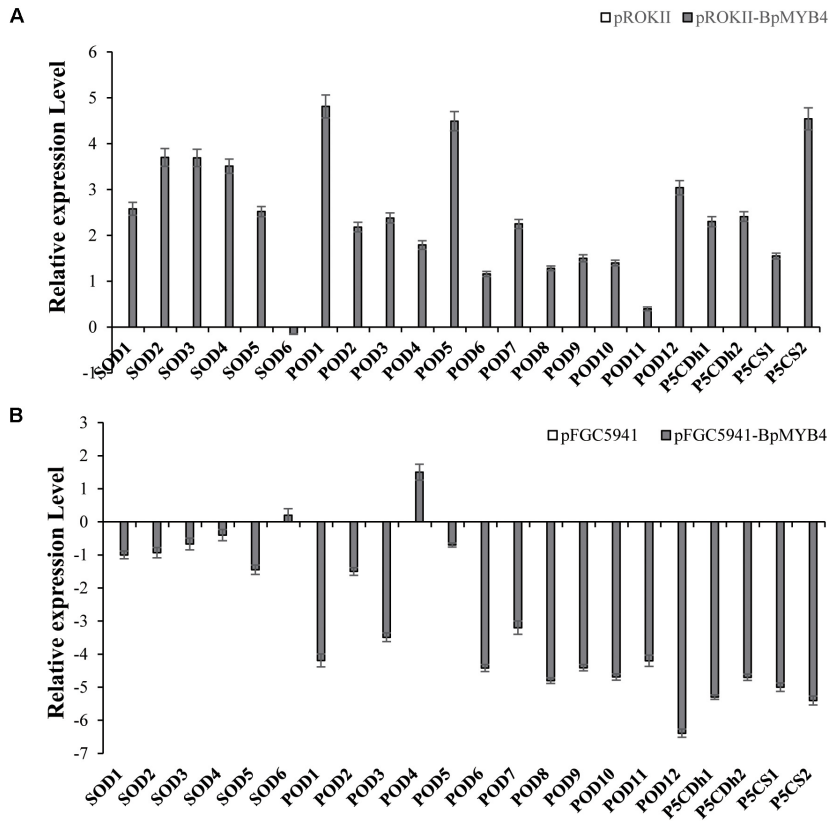

FIGURE 8 | The expression levels of resistance-related genes in overexpression and suppression of expression in birch. **(A)** Taking the empty vector strain (pROKII) as a control, the expression levels of resistance-related genes in overexpressing strains were monitored. **(B)** Taking the empty vector strain (RNAi) as a control, the expression levels of resistance-related genes in the suppressive expression line were monitored.

(pFGC5941) control line, in the suppressed expression lines (pFGC5941-*BpMYB4*), *CAD* and *C4H* genes were up-regulated, and *CCO*, *CESA* and *CCR* genes were down-regulated. Among them, the increased expression level of *CAD* reached 5.86 fold, and the transcripts decrease of *CESA* reached 30.27 flod. These data suggest that BpMYB4 transcript factor can negatively affect the expression of some lignin biosynthesis gene and positive regulate the cellulose biosynthesis gene in OE plants compare with the WT. Therefore, *BpMYB4* has a certain function in regulating the expression of cell wall biosynthesis-related and resistance-related genes.

DISCUSSION

Multiple sequence alignment and phylogenetic tree analysis demonstrated that BpMYB4 is similar to EgMYB1, AmMYB308, ZmMYB42 and ZmMYB31 at the amino acid level, all of which have been identified as lignin biosynthetic inhibitory factors (Tamagnone et al., 1998; Fornalé et al., 2006, 2010; Legay et al., 2007). Therefore, we speculated that BpMYB4 might also play a negative role in lignin biosynthesis in birch.

According to relevant reports, genes encoding transcription factors that inhibit vascular development are usually not highly or specifically expressed in vascular tissues (Zhao and Dixon, 2011). In this study *BpMYB4* was expressed at high levels in flowers, at levels higher than that seen in stems. In addition, *BpMYB4* was abundantly expressed during the dormancy seasons of April and September. This expression pattern was unlike that seen in some genes whose products are involved in secondary cell wall formation, which were highly expressed in June or July (Wang et al., 2010a), and might imply the role of inhibitors in secondary growth. *BpMYB4* transcript levels increased during tension wood development compared with those seen in opposite wood and normal wood. In tension wood of birch, the cellulose content was higher and lignin content was lower than those in opposite wood and normal wood (Wang et al., 2014). Together with the expression level changes and phylogenetic tree analysis, our results suggest that *BpMYB4* might be an inhibitor of lignin biosynthesis in birch.

Studies in populations of forest tree hybrids have shown that when the lignin content is greatly reduced and the cellulose content is increased in transgenic plants, the growth rate of roots and stems is significantly increased (Hu et al., 1999). There is a negative correlation between biomass growth and lignin content (Kirst et al., 2004; Novaes et al., 2009, 2010). In the present study, the inflorescence stems of the transgenic plants was higher than the WT. So we detected the secondary xylem development and lignin deposition using anatomical observations (**Figure 4**) and chemical analysis. The stem

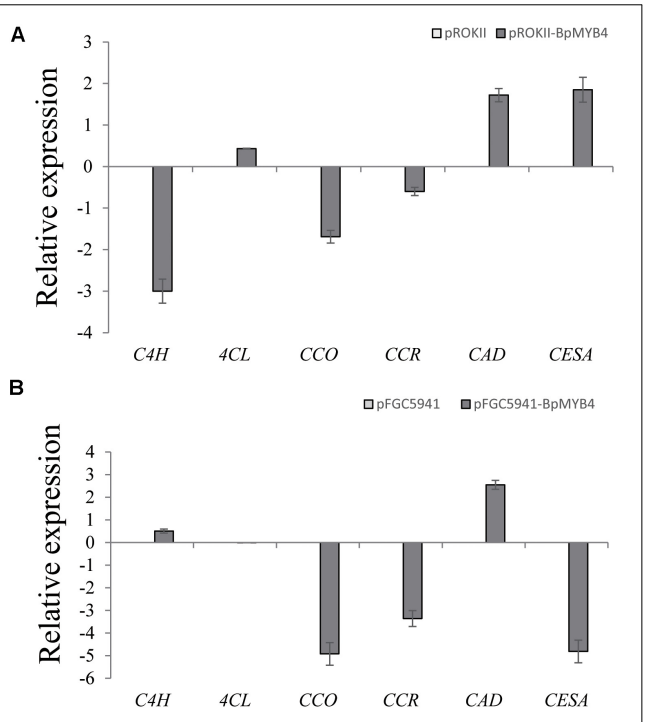

FIGURE 9 | The expression levels ofcell wall biosynthesis-related genes in overexpression and suppression of expression in birch. **(A)** Taking the empty vector strain (pROKII) as a control, the expression levels of cell wall biosynthesis-related genes in overexpressing strains were monitored. **(B)** Taking the empty vector strain (RNAi) as a control, the expression levels of cell wall biosynthesis-related genes in the suppressive expression line were monitored.

sections stained with phloroglucinol-HCl showed decreased lignin deposition in transgenic plants, relative to WT *A. thaliana*. The content of lignin in transgenic lines was reduced, but the content of cellulose in transgenic plants was increased relative to WT (**Table 1**). Therefore, we hypothesized that the reason of growth increase in stems of transgenic plants is that *BpMYB4* inhibited lignin biosynthesis. These results confirmed that *BpMYB4* has a negative effect on lignin biosynthesis and deposition but a positive effect on cellulose content. The express analysis of cell wall biosynthesis relate genes in transgenetic birch with *BpMYB4* transiently over-expressing suggested that BpMYB4 transcript factor can decreased the expression of some lignin biosynthesis gene and positive regulate the cellulose biosynthesis gene in OE plants compare with the WT. These data might explain the mechanism of cell wall components modification in transgenetic plants.

The transgenetic birch with *BpMYB4* transiently expression were used to investigate the resistance ability of *BpMYB4*. On the one hand, functional analysis in birch was used to verify the results of heterologous expression of *BpMYB4* in Arabidopsis experiment, on the other hand, it is convenient to analyze the genes that can be regulated in birch by BpMYB4. ROS are produced when plants face adverse conditions (Scandalios, 1993). Levels of H_2O_2 in plant cells may accumulate and cause oxidative damage when plants undergo stress (Larrigaudière et al., 2001). The amount of H_2O_2 released from the cells can be detected by the intensity of DAB staining. Previous studies have shown that reduced H_2O_2 accumulation (detected via DAB) following abiotic stress can increase stress resistance (Sela et al., 2013). In this study, after treatment with 100 mM NaCl or 200 mM mannitol, DAB staining showed that H_2O_2 accumulation in OE plants was lower than WT, but higher in SE plants compared to WT. This indicates that BpMYB4 can reduce H_2O_2 accumulation in OE birch seedlings subjected to abiotic stress. Another way ROS is produced in cells is via stress signaling, the cellular level of $O_2^{\cdot-}$ (Mittler et al., 2004). Staining with NBT indicates the activity of superoxide dismutase (Buc-Calderon and Roberfroid, 1988), which reflects the content of $O_2^{\cdot-}$ in cells (Yu et al., 2018). In the present study, under abiotic stress conditions, the levels of $O_2^{\cdot-}$ in OE plants were the lowest, and the levels of $O_2^{\cdot-}$ in SE plants were the highest. The results indicate that BpMYB4 can reduce the accumulation of $O_2^{\cdot-}$ in birch seedlings under abiotic stress. Accumulation of ROS may damage cell membranes by oxidation of proteins, lipids and DNA (Mittler et al., 2004). Studies have shown that Evan's Blue staining can detect cell death and demonstrate the degree of stress resistance of plants (Singh and Upadhyay, 2014). Therefore, we performed Evan's Blue staining on the transiently transformed birch plants after abiotic stress treatment. The results indicate that BpMYB4 can reduce the damage done by abiotic stress in OE lines of birch. BpMYB4 also induces the expression of most resistance-related genes. All the above results showed that BpMYB4 activates the metabolic pathway of ROS clearance by regulating the expression of resistance-related genes in transgenic birch trees subjected to abiotic stress, thereby reducing the level of ROS to maintain cell membrane integrity and playing a role in the resistance of birch trees.

CONCLUSION

In this study, we identified a *BpMYB4* gene which is homologous to other transcription factors that negatively regulate lignin biosynthesis. The expression analysis of *BpMYB4* in different tissues, under artificial bending treatment and at different stages in a growing season also imply that it might be an inhibitory transcription factor in secondary growth. Functional analysis in transgenic Arabidopsis further demonstrated that *BpMYB4* can promote height growth of inflorescence stems, increase cellulose and decrease lignin content in the transgenic plants. Analysis of the stable transformation of Arabidopsis and transiently transformed birch with BpMYB4 also indicated a certain stress resistance function. These results can be useful for further understanding the molecular mechanism of secondary growth procesess and abiotic stress responses regulated by MYB transcription factors.

DATA AVAILABILITY STATEMENT

The datasets presented in this study can be found in online repositories. The names of the repository/repositories

and accession number(s) can be found in the article/ **Supplementary Material**.

AUTHOR CONTRIBUTIONS

CW: conceptualization and methodology. HL and NZ: software. YY, HL, and NZ: formal analysis and investigation. YY and CW: writing—review and editing. YY: visualization. CW: funding acquisition. All authors contributed to the article and approved the submitted version.

FUNDING

This research was financially supported by "the Fundamental Research Funds for the Central Universities" (2572016DA01). The Overseas Expertise Introduction Project for Discipline Innovation (B16010). Heilongjiang Touyan Innovation Team Program (Tree Genetics and Breeding Innovation Team).

SUPPLEMENTARY MATERIAL

The Supplementary Material for this article can be found online at: https://www.frontiersin.org/articles/10.3389/fpls.2020.606062/full#supplementary-material

Supplementary Figure 1 | Semi-quantitative PCR analysis of *BpMYB4* Gene in transgenic Arabidopsis.

Supplementary Figure 2 | Observation of transgenic Arabidopsis phenotype. Comparison of transgenic Arabidopsis and WT at 1 week **(A)**, 4 weeks **(B)**, and 6 weeks **(C)**.

Supplementary Table 1 | Vector construction primer sequence.

Supplementary Table 2 | qRT-PCR primer sequence.

REFERENCES

Borevitz, J. O., Xia, Y., Blount, J., Dixon, R. A., and Lamb, C. (2000). Activation tagging identifies a conserved MYB regulator of phenylpropanoid biosynthesis. *Plant Cell* 12, 2383–2394. doi: 10.1105/tpc.12.12.2383

Buc-Calderon, P., and Roberfroid, M. (1988). Inhibition of O2.- and HO - mediated processes by a new class of free radical scavengers: the N-ACYL Dehydroalanines. *Free Radic. Res. Commun.* 5, 159–168. doi: 10.3109/10715768809066925

Chang, S. J., Puryear, J., and Cairney, J. (1993). A simple and efficient method for isolating RNA from pine trees. *Plant Mol. Biol. Rep.* 11, 113–116. doi: 10.1385/MB:19:2:201

Chen, W., Provart, N. J., Glazebrook, J., Katagiri, F., Chang, H. S., Eulgem, T., et al. (2002). Expression profile matrix of *Arabidopsis* transcription factor genes suggests their putative functions in response to environmental stresses. *Plant Cell* 14, 559–574. doi: 10.1105/tpc.010410

Clough, S. J., and Bent, A. F. (1998). Floral dip: a simplified method for Agrobacterium-mediated transformation of *Arabidopsis thaliana*. *Plant J.* 16, 735–743. doi: 10.1046/j.1365-313x.1998.00343.x

Dubos, C., Stracke, R., Grotewold, E., Weisshaar, B., Martin, C., and Lepiniec, L. (2010). MYB transcription factors in *Arabidopsis*. *Trends Plant Sci.* 15, 573–581. doi: 10.1016/j.tplants.2010.06.005

Feng, C. P., Andreasson, E., Maslak, A., Mock, H. P., Mattsson, O., and Mundy, J. (2004). *Arabidopsis MYB68* in development and responses to environmental cues. *Plant Sci.* 167, 1099–1107. doi: 10.1016/j.plantsci.2004.06.014

Fornalé, S., Shi, X. H., Chai, C. G., Encina, A., Irar, S., Capellades, M., et al. (2010). ZmMYB31 directly represses maize lignin genes and redirects the phenylpropanoid metabolic flux. *Plant J.* 64, 633–644. doi: 10.1111/j.1365-313X.2010.04363.x

Fornalé, S., Sonbol, F. M., Maes, T., Capellades, M., Puigdomenech, P., Rigau, J., et al. (2006). Down-regulation of the maize and *Arabidopsis thaliana* caffeic acid O-methyl-transferase genes by two new maize R2R3-MYB transcription factors. *Plant Mol. Biol.* 62, 809–823. doi: 10.1007/s11103-006-9058-2

Hoeren, F. U., Dolferus, R., Wu, Y., Peacock, W. J., and Dennis, E. S. (1998). Evidence for a role for AtMYB2 in the induction of the Arabidopsis alcohol dehydrogenase gene (ADH1) by low oxygen. *Genetics* 149, 479–490.

Hu, W. J., Harding, S. A., Lung, J., Popko, J. L., Ralph, J., Stokke, D. D., et al. (1999). Repression of lignin biosynthesis promotes cellulose accumulation and growth in transgenic trees. *Nat. Biotechnol.* 17, 808–812. doi: 10.1038/11758

Ji, X. Y., Liu, G. F., Liu, Y. J., Zheng, L., and Wang, Y. C. (2013). The bZIP protein from *Tamarix hispida, ThbZIP1*, is ACGT elements binding factor that enhances abiotic stress signaling in transgenic Arabidopsis. *Bmc Plant Biol.* 13:151. doi: 10.1186/1471-2229-13-151

Jiao, B., Zhao, X., Lu, W. X., Guo, L., and Luo, K. (2019). The R2R3 MYB transcription factor *MYB189* negatively regulates secondary cell wall biosynthesis in *Populus*. *Tree Physiol.* 39, 1187–1200. doi: 10.1093/treephys/tpz040

Kirst, M., Myburg, A. A., Leon, J. P. G. D., Kirst, M. E., Scott, J., and Sederoff, R. (2004). Coordinated genetic regulation of growth and lignin revealed by quantitative trait locus analysis of cDNA microarray data in an interspecific backcross of eucalyptus. *Plant Physiol.* 135, 2368–2378. doi: 10.1104/pp.103.037960

Kubo, K., Sakamoto, A., Kobayashi, A., Rybka, Z., Kanno, Y., Nakagawa, H., et al. (1998). Cys2/His2 zinc-finger protein family of petunia: evolution and general mechanism of target-sequencerecognition. *Nucleic Acids Res.* 26, 608–615. doi: 10.1093/nar/26.2.608

Larrigaudière, C., Lentheric, I., Pintó, E., and Vendrell, M. (2001). Short—term effects of air and controlled atmosphere storage on antioxidant metabolism in conference pears. *J. Plant Physiol.* 158, 1015–1022. doi: 10.1078/0176-1617-00114

Legay, S., Lacombe, E., Goicoechea, M., Brière, C., Séguin, A., Mackay, J., et al. (2007). Molecular characterization of *EgMYB1*, a putative transcriptional repressor of the lignin biosynthetic pathway. *Plant Sci.* 173, 542–549. doi: 10.1016/j.plantsci.2007.08.007

Liao, Y., Zou, H. F., Wang, H. W., Zhang, W. K., Ma, B., Zhang, J. S., et al. (2008). Soybean *GmMYB76, GmMYB92*, and *GmMYB177* genes confer stress tolerance intransgenic *Arabidopsis* plants. *Cell Res.* 18, 1047–1060. doi: 10.1038/cr.2008.280

Livak, K. J., and Schmittgen, T. D. (2001). Analysis of relative gene expression data using real-time quantitative PCR and the 2(-Delta Delta C(T)) Method. *Methods* 25:402. doi: 10.1006/meth.2001.1262

Ma, J., Du, G. Y., Li, X. H., Zhang, C. Y., and Guo, J. K. (2015). A major locus controlling malondialdehyde content under water stress is associated with *Fusarium* crown rot resistance in wheat. *Mol. Genet. Genomics Mgg.* 290, 1955–1962. doi: 10.1007/s00438-015-1053-3

Mccarthy, R. L., Zhong, R. Q., Fowler, S., Lyskowski, D., Piyasena, H., Carleton, K., et al. (2010). The poplar MYB transcription factors,*PtrMYB3* and *PtrMYB20*, are involved in the regulation of secondary wall biosynthesis. *Plant Cell Physiol.* 51, 1084–1090. doi: 10.1093/pcp/pcq064

Mccarthy, R. L., Zhong, R. Q., and Ye, Z. H. (2009). MYB83 is a direct target of SND1 and acts redundantly with *MYB46* in the regulation of secondary cell wall biosynthesis in *Arabidopsis*. *Plant Cell Physiol.* 50, 1950–1964. doi: 10.1093/pcp/pcp139

Mittler, R., Vanderauwera, S., Gollery, M., and Van Breusegem, F. (2004). Reactive oxygen gene network of plants. *Trends Plant Sci.* 9, 490–498. doi: 10.1016/j.tplants.2004.08.009

Mitsuda, N., Seki, M., Shinozaki, K., and Ohme-Takagi, M. (2005). The NAC transcription factors NST1 and NST2 of *Arabidopsis* regulates secondary wall thickening and are required for anther dehiscence. *Plant Cell* 17, 2993–3006. doi: 10.1105/tpc.105.036004

Novaes, E., Kirst, M., Chiang, V., Winter-Sederoff, H., and Sederoff, R. (2010). Lignin and biomass: a negative correlation for wood formation and lignin content in trees. *Plant Physiol.* 154, 555–561. doi: 10.1104/pp.110.161281

Novaes, E., Osorio, L., Drost, D. R., Miles, B. L., Boaventura-Novaes, C. R., Benedict, C., et al. (2009). Quantitative genetic analysis of biomass and wood chemistry of Populus under different nitrogen levels. *New Phytol.* 182, 878–890. doi: 10.1111/j.1469-8137.2009.02785.x

Pasquali, G., Biricolti, S., Locatelli, F., Baldoni, E., and Mattana, M. (2008). *Osmyb4* expressionimproves adaptive responses to drought and cold stress intransgenic apples. *Plant Cell Rep.* 27, 1677–1686. doi: 10.1007/s00299-008-0587-9

Patzlaff, A., McInnis, S., Courtenay, A., Surman, C., Newman, L. J., Smith, C., et al. (2003a). Characterisation of a pine MYB that regulates lignification. *Plant J.* 36, 743–754. doi: 10.1046/j.1365-313x.2003.01916.x

Patzlaff, A., Newman, L. J., Dubos, C., Whetten, R. W., Smith, C., McInnis, S., et al. (2003b). Characterization of PtMYB1, an R2R3-MYB from pine xylem. *Plant Mol. Biol.* 53, 597–608. doi: 10.1023/B:PLAN.0000019066.07933.d6

Paz-ares, J., Ghosal, D., Wienand, U., Peterson, P. A., and Saedler, H. (1987). The regulatory c1 locus of Zea mays encodes a protein with homology to myb proto-oncogene products and with structural similarities to transcriptional activators. *EMBO J.* 6, 3553–3558. doi: 10.1002/j.1460-2075.1987.tb02684.x

Preston, J., Wheeler, J., Heazlewood, J., Li, S. F., and Parish, R. W. (2004). *AtMYB32* is required for normal pollen development in *Arabidopsis* thaliana. *Plant J.* 40, 979–995. doi: 10.1111/j.1365-313X.2004.02280.x

Scandalios, J. G. (1993). Oxygen stress and superoxide dismutases. *Plant Physiol.* 101, 7–12. doi: 10.1104/pp.101.1.7

Sela, D., Buxdorf, K., Shi, J. X., Feldmesser, E., Schreiber, L., Aharoni, A., et al. (2013). Overexpression of AtSHN1/WIN1 provokes unique defense responses. *PLoS One* 8:e70146. doi: 10.1371/journal.pone.0070146

Shen, H., He, X. Z., Poovaiah, C. R., Wuddineh, W. A., Ma, J. Y., Mann, D. G. J., et al. (2011). Functional characterization of the switchgrass (*Panicum virgatum*) R2R3-MYB transcription factor *PvMYB4* for improvement of lignocellulosic feedstocks. *New Phytol.* 193, 121–136. doi: 10.1111/j.1469-8137.2011.03922.x

Singh, V. K., and Upadhyay, R. S. (2014). Fusaric acid induced cell death and changes in oxidative metabolism of *Solanum lycopersicum*L. *Bot. Stud.* 55:66. doi: 10.1186/s40529-014-0066-2

Tamagnone, L., Merida, A., Parr, A., Mackay, S., Culianez-Macia, F. A., Roberts, K., et al. (1998). The AmMYB308 and AmMYB330 transcription factors from Antirrhinum regulate phenylpropanoid and lignin biosynthesis in transgenic tobacco. *Plant Cell* 10, 135–154. doi: 10.1105/tpc.10.2.135

Thurbide, K. B., and Hughes, D. M. (2000). A rapid method for determining the extractives content of wood pulp. *Ind. Eng. Chem. Res.* 39, 3112–3115. 10.1021/ie0003178

Vannini, C., Locatelli, F., Bracale, M., Magnani, E., Marsoni, M., Osnato, M., et al. (2004). Overexpression of the rice *Osmyb4* gene increases chilling and freezing tolerance of *Arabidopsis thaliana* plants. *Plant J.* 37, 115–127. doi: 10.1046/j.1365-313x.2003.01938.x

Vendruscolo, E. C. G., Schuster, I., Pileggi, M., Scapim, C. A., Molinari, H. B. C., Marur, C. J., et al. (2007). Stress-induced synthesis of proline confers tolerance to water deficit in transgenic wheat. *J. Plant Physiol.* 164, 1367–1376. doi: 10.1016/j.jplph.2007.05.001

Wang, C., Wang, Y. C., Diao, G. P., Jiang, J., and Yang, C. P. (2010a). Isolation and characterization of expressed sequence tags (ESTs) from cambium tissue of birch (Betula platyphylla Suk.). *Plant Mol. Biol. Rep.* 28, 438–449. doi: 10.1007/s11105-009-0172-6

Wang, C., Zhang, N., Gao, C. Q., Cui, Z. Y., Sun, D., Yang, C. P., et al. (2014). Comprehensive transcriptome analysis of developing xylem responding to artificial bending and gravitational stimuli in *Betula platyphylla*. *PLoS one.* 9:e87566. doi: 10.1371/journal.pone.0087566

Wang, Y., Gao, C., Liang, Y., Wang, C., Yang, C., and Liu, G. (2010b). A novel bZIP gene from Tamarix hispida mediates physiological responses to salt stress in tobacco plants. *J. Plant Physiol.* 167, 222–230. doi: 10.1016/j.jplph.2009.09.008

Wang, Y. M., Wang, C., Guo, H. Y., and Wang, Y. C. (2019). BplMYB46 from *betula platyphylla* can form homodimers and heterodimers and is involved in salt and osmotic stresses. *Int. J. Mol. Sci.* 20:1171. doi: 10.3390/ijms20051171

Wang, S., Yang, C. P., Zhao, X. Y., Chen, S., and Qu, G. Z. (2018). Complete chloroplast genome sequence of *Betula Platyphylla*: gene organization, RNA editing, and comparative and phylogenetic analyses. *BMC Genomics* 19:950. doi: 10.1186/s12864-018-5346-x

Wen, C. K., and Chang, C. (2002). *Arabidopsis* rgl1 encodes a negative regulator of gibberellin responses. *Plant Cell Online* 14, 87–100. doi: 10.1105/tpc.010325

Wilkins, O., Nahal, H., Foong, J., Provart, N. J., and Campbell, M. M. (2009). Expansion and diversification of the *Populus* R2R3-MYB family of transcription factors. *Plant Physiol.* 149, 981–993. doi: 10.1104/pp.108.132795

Yang, A., Dai, X. Y., and Zhang, W. H. (2012). A R2R3-type MYB gene, OsMYB2, is involved in salt, cold, and dehydration tolerance inrice. *Exp. Bot.* 63, 2541–2556. doi: 10.1093/jxb/err431

Yang, C., Xu, Z., Song, J., Conner, K., Barrena, G. V., and Wilson, Z. A. (2007). Arabidopsis MYB26/MALE STERILE35 regulates secondary thickening in the endothecium and is essential for anther dehiscence. *Plant Cell* 19, 534–548. doi: 10.1105/tpc.106.046391

Yu, J. Q., Wang, J. H., Sun, C. H., Zhang, Q. Y., Hu, D. G., and Hao, Y. J. (2018). Ectopic expression of the apple nucleus-encoded thylakoid protein MdY3IP1 triggers early-flowering and enhanced salt-tolerance in *Arabidopsis thaliana*. *Bmc Plant Biol.* 18:18. doi: 10.1186/s12870-018-1232-6

Zhang, T., Zhao, Y., Wang, Y., Liu, Z., and Gao, C. (2018). Comprehensive analysis of MYB gene family and their expressions under abiotic stresses and hormone treatments in *tamarix hispida*. *Front. Plant Sci.* 9:1303. doi: 10.3389/fpls.2018.01303

Zhao, Q., and Dixon, R. A. (2011). Transcriptional networks for lignin biosynthesis: more complex than we thought. *Trends Plant Sci.* 16, 227–233. doi: 10.1016/j.tplants.2010.12.005

Zhong, R. Q., Lee, C. H., Zhou, J. L., McCarthy, R. L., and Ye, Z. H. (2008). A battery of transcription factors involved in the regulation of secondary cell wall biosynthesis in *Arabidopsis*. *Plant Cell* 20, 2763–2782. doi: 10.1105/tpc.108.061325

Zhong, R. Q., Richardson, E. A., and Ye, Z. H. (2007). The MYB46 transcription factor is a direct target of SND1 and regulates secondary wall biosynthesis in *Arabidopsis*. *Plant Cell* 19, 2776–2792. doi: 10.1105/tpc.107.053678

Zhou, J. L., Lee, C. H., Zhong, R. Q., and Ye, Z. H. (2009). MYB58 and MYB63 are transcriptional activators of the lignin biosynthetic pathway during secondary cell wall formation in *Arabidopsis*. *Plant Cell* 21, 248–266. doi: 10.1105/tpc.108.063321

Conflict of Interest: The authors declare that the research was conducted in the absence of any commercial or financial relationships that could be construed as a potential conflict of interest.

frontiers in Plant Science

ORIGINAL RESEARCH
published: 25 January 2021
doi: 10.3389/fpls.2020.578812

nifH Gene Sequencing Reveals the Effects of Successive Monoculture on the Soil Diazotrophic Microbial Community in *Casuarina equisetifolia* Plantations

Liuting Zhou[1†], Jianjuan Li[2†], Ganga Raj Pokhrel[3], Jun Chen[1], Yanlin Zhao[1], Ying Bai[1], Chen Zhang[1], Wenxiong Lin[1], Zeyan Wu[1,4,5] and Chengzhen Wu[2]*

[1] Fujian Agriculture and Forestry University, Fuzhou, China, [2] College of Forestry, Fujian Agriculture and Forestry University, Fuzhou, China, [3] Department of Chemistry, Birendra Multiple Campus, Tribhuvan University, Chitwan, Nepal, [4] Key Laboratory of Crop Ecology and Molecular Physiology, Fujian Agriculture and Forestry University, Fuzhou, China, [5] Fujian Provincial Key Laboratory of Agroecological Processing and Safety Monitoring, School of Life Sciences, Fujian Agriculture and Forestry University, Fuzhou, China

OPEN ACCESS

Edited by:
Sanushka Naidoo,
University of Pretoria, South Africa

Reviewed by:
Bing Yang,
Chengdu Institute of Biology, Chinese Academy of Sciences, China
Amit K. Jaiswal,
Purdue University, United States

***Correspondence:**
Zeyan Wu
wuzeyan0977@126.com

[†]These authors share first authorship

Specialty section:
This article was submitted to Plant Pathogen Interactions, a section of the journal Frontiers in Plant Science

Received: 01 July 2020
Accepted: 21 December 2020
Published: 25 January 2021

Citation:
Zhou L, Li J, Pokhrel GR, Chen J, Zhao Y, Bai Y, Zhang C, Lin W, Wu Z and Wu C (2021) nifH Gene Sequencing Reveals the Effects of Successive Monoculture on the Soil Diazotrophic Microbial Community in Casuarina equisetifolia Plantations. Front. Plant Sci. 11:578812. doi: 10.3389/fpls.2020.578812

The growth and productivity of *Casuarina equisetifolia* is negatively impacted by planting sickness under long-term monoculture regimes. In this study, Illumina MiSeq sequencing targeting *nifH* genes was used to assess variations in the rhizospheric soil diazotrophic community under long-term monoculture rotations. Principal component analysis and unweighted pair-group method with arithmetic means (UPGMA) clustering demonstrated distinct differences in diazotrophic community structure between uncultivated soil (CK), the first rotation plantation (FCP), the second rotation plantation (SCP), and the third rotation plantation (TCP). Taxonomic analysis showed that the phyla *Proteobacteria* increased while *Verrucomicrobia* decreased under the consecutive monoculture (SCP and TCP). The relative abundance of *Paraburkholderia*, *Rhodopseudomonas*, *Bradyrhizobium*, *Geobacter*, *Pseudodesulfovibrio*, and *Frankia* increased significantly while *Burkholderia*, *Rubrivivax*, and *Chlorobaculum* declined significantly at the genus level under consecutive monoculture (SCP and TCP). Redundancy analysis (RDA) showed that *Burkholderia, Rubrivivax*, and *Chlorobaculum* were positively correlated with total nitrogen and available nitrogen. In conclusion, continuous *C. equisetifolia* monoculture could change the structure of diazotrophic microbes in the rhizosphere, resulting in the imbalance of the diazotrophic bacteria population, which might be a crucial factor related to replanting disease in this cultivated tree species.

Keywords: *Casuarina equisetifolia*, monoculture rotations, *nifH* gene sequencing, diazotrophic microbial community, soil

INTRODUCTION

Casuarina equisetifolia Forst has covers over 300,000 ha in southeastern China. It is one of the preferred trees for forming shelterbelts in coastal areas, as it vegetates the coasts and contributes to stabilizing coastal sand and protecting against storms (Zhong et al., 2005; Karthikeyan et al., 2013). However, continuous monocultures of *C. equisetifolia* result in productivity decline and regeneration failure. This phenomenon is referred to as the consecutive monoculture problem (CMP) (Wardle et al., 2004). Replanting diseases are observed in many cultivated tree species, including Chinese fir, *Pinus elliottii*, *Picea abies*, and *Eucalyptus* spp. (Wu et al., 2017). The depletion in soil nutrients (Bennett et al., 2012), the autointoxication of root exudations (Araya et al., 2012), and the imbalance of rhizospheric microflora (Wu et al., 2016a) are thought to be the main reasons for CMP. Increasing the amount of chemical fertilizer does not alleviate this problem (Wardle et al., 2004). Root exudates not only directly inhibit the growth and reproduction of plants but also restrain rhizosphere microorganisms (Li et al., 2014; Arafat et al., 2017). Great attention has been paid to rhizospheric biological processes in recent years. Lu et al. (2017) indicated that soil microbial community compositions and theirs structures had distinct variations under Poplar monocultures. Similar results were found in Chinese fir, *Eucalyptus*, and *Pinus halepensis* (Fernandez et al., 2008; Jie et al., 2014; Wu et al., 2017).

Biological nitrogen fixation has attracted widespread attention due to its influential role in the nitrogen cycle. Hsu and Buckley (2009) investigated the diversity of nitrogen-fixing genes and their functional microbial communities through high-throughput MiSeq amplicon sequencing of *nifH* gene, which encodes a subunit of the nitrogenase enzyme complex related to nitrogen fixation efficiency. Penton et al. (2016) amplified *nifH* gene sequencing and found that permafrost thawing in Alaskan soil altered the N-fixing microbial community composition in soil as the depth of groundwater changed. Wang et al. (2017) found that long-term inorganic fertilization in acid soil altered the diazotrophic community structure and decreased the abundance of operational taxonomic units (OTUs). Biological nitrogen fixation has been recognized as a crucial source of nitrogen to support certain primary production (Zehr et al., 1998). N-fixation by diazotrophs is an important strategy by which most organisms regulate biological productivity (Li et al., 2018). Nevertheless, the relationship between the diazotrophic microbial community and monocultures of *C. equisetifolia* has received little attention. On the basis of the above facts, we hypothesized that diazotrophic microbial community structure might be altered by *C. equisetifolia* monocultures (Wu et al., 2016b; Chen et al., 2017; Zhou et al., 2019).

In this study, quantitative PCR (qPCR) assays and the MiSeq high-throughput sequencing technique were applied to assess the shifts in the abundance of *nifH* gene and diazotrophic community composition in rhizosphere soil, respectively, after *C. equisetifolia* monoculture. Meanwhile, correlation analyses were used to resolve the relationships between the diazotrophic microbial community and environmental parameters, including total nitrogen (TN), total phosphorus (TP), total potassium (TK), available nitrogen (AN), available phosphorus (AP), available potassium (AK), and pH. This research will help improve our understanding of the nitrogen-fixing microbial community structure in soil under CMP. It will provide effective scientific-based references on the molecular ecological mechanisms of soil restoration and improvement.

MATERIALS AND METHODS

Research Plot and Sample Collection

In this study, the plot was located at Chihu National Forest Center in Fujian Province, China (24°54′N and 118°55′E). Since the 1960s, the Chihu Forestry Farm cultivated a large-scale coastal windbreak and gradually established a settled coastal shelterbelt system. The annual mean temperature is 19.8°C (the extreme high and low temperatures are 35°C and 1°C, respectively), with a mean annual precipitation of 1,029 mm and a mean annual evaporation of 2,000 mm. There are three generations of *C. equisetifolia* plantation in the forest farm that were planted in 1987 (first rotation plantation, FCP), 2011 (second rotation plantation, SCP), and 2014 (third rotation plantation, TCP). Due to the long growth period of the arbor and field condition, the method of "space replacing time" is often applied in forestry research (Shi et al., 2018; Deng et al., 2019).

Three sampling positions (20 m × 20 m) were established at the FCP, SCP, and TCP on January 6, 2019. At the same time, a vacant area of soil in the forest farm with no *C. equisetifolia* cultivation was selected as a blank control, or CK. Each sampling position was set with three duplicate quadrats for a total of 12 quadrats. Soil samples were randomly collected from a depth of 0–20 cm at 12 quadrats. Twenty random replicated samples were taken from each quadrat. Soil samples from the FCP, SCP, and TCP were collected from the rhizosphere of *C. equisetifolia*. The field samplings were performed according to the method described by Zhou et al. (2019).

Determination of Soil Nutrients

Soil pH was measured using a glass electrode pH meter (1:2.5 soil–water suspensions) (Zhao et al., 2017). The available and total amounts of NPK were determined referring to the methods by Jackson (2005).

DNA Extraction

Soil DNA extractions were completed using a Power Soil DNA Isolation Kit (MoBio Laboratories, Carlsbad, CA, United States) following the manufacturer's specifications. The genomic DNA was confirmed using 1.2% agarose gels.

qPCR for *nifH*

Quantitative PCR was performed to quantify the relative abundance of the *nifH* gene in four individual rhizospheric soils with the primers *nifH*-F (AAAGGYGGWATCGGYAART CCACCAC) and *nifH*-R (TTGTTSGCSGCRTACATSGCCAT CAT) (Zhang et al., 2016). The reaction mixture (15 μl) for qPCR consisted of 7.5 μl 2 × SYBR green I Super Real Premix (TIANGEN, Beijing, China), 10 μM of each primer and 40 ng template DNA. The amplification conditions were 95°C for 30 s,

followed by 40 cycles of 95°C for 5 s, 60°C for 40 s. The standard curve equation was Y = −4.083X + 46.196 (R^2 = 0.99).

PCR Amplification and *nifH* Sequencing

High-throughput sequencing was used to explore the influences of successive monocultures of *C. equisetifolia* on rhizospheric soil diazotrophic microbial communities. For *nifH* gene sequencing, the primers *nifH*-F and *nifH*-R (the same as above) were applied to amplify the *nifH* gene. The PCR amplification was implemented on a Mastercycler Gradient (Eppendorf, Germany) with a 25 μl volume, including 12.5 μl 2 × Taq PCR MasterMix, 3 μl BSA (2 ng/μl), 2 μl Primer (5 μM), 2 μl template DNA, and 5.5 μl ddH_2O. Cycling parameters were 95°C for 5 min, followed by 32 cycles of 95°C for 45 s, 55°C for 50 s, and 72°C for 45 s with a final extension at 72°C for 10 min. The amplicons were purified with a QIAquick Gel Extraction Kit (QIAGEN, Germany), sequenced on the MiSeq PE300 platform at Allwegene Company, Beijing, China.

Data Analyses

The low-quality ($q < 20$) and short sequences (<200 bp) were removed *via* the Pear (v. 0.9.6). The final length of sequences was 400–420. The datasets were then analyzed using QIIME (v. 1.8.0, Caporaso et al., 2010). The qualified sequences were clustered into OTUs at a 97% identity threshold (Edgar, 2013). All effective tags were classified into different taxonomic groups using the Ribosomal Database Project (RDP) classifier (Cole et al., 2009). Alpha diversity indices were employed to identify the richness and diversity within samples (Xiong et al., 2015). In order to make the sequencing depth consistent, the abundances of OTUs were normalized. Alpha diversity indices were calculated by R software (v. 2.15.3, Caporaso et al., 2010) based on the normalized data (21,778 taxa). The principal component analysis (PCA), clustering analyses, and non-metric multidimensional scaling (NMDS) were carried out to assess the similarity and difference between individual samples (Wang et al., 2012). PCA and NMDS were implemented based on the R with vegan package (v. 3.0.2, Oksanen et al., 2009; Goossen et al., 2010). To compare the diazotrophic community compositions and structures in the rhizosphere, heat maps were applied within the top 20 most abundant OTUs using Mothur (Jami et al., 2013). Redundancy analysis (RDA) was performed to establish which environmental parameters played an important role in the variation of top 12 most abundant OTUs using Canoco 5.0. Statistical analysis was carried out by DPS 7.05 software, and analysis of variance (ANOVA) was applied to identify significance difference by LSD's test ($P < 0.05$).

RESULTS

Soil Physicochemical Data

The results of soil nutrient analysis showed that replanting soils had a lower level of pH under the extended *C. equisetifolia* monoculture regime. The TN content was higher in the FCP than in the SCP (significant, $P < 0.05$) and TCP (not significant, $P > 0.05$). AN was higher in the FCP than in the SCP and TCP ($P > 0.05$). In the FCP and SCP, TP was significantly higher than in the TCP ($P < 0.05$). No significant differences were observed in AP, TK, and AK (**Supplementary Table 1**).

Abundance of the *nifH* Gene

Figure 1 indicates that the quantity of the *nifH* gene changed significantly under monoculture regime ($p < 0.05$). The number of copies of the *nifH* gene was between 0.746 × 10^6 and 3.647 × 10^6/g soil, and the highest and lowest numbers were found in the SCP and CK, respectively. Compared with the CK, the number of copies in the FCP, SCP, and TCP were increased by 54.4, 388.9, and 127.6%, respectively.

OTU Clusters and Species Annotation

After filtration analysis, a sum of 656,599 high-quality tags (clean tags) was acquired from the CK, FCP, SCP, and TCP, with a mean of 54,717 effective sequences (**Supplementary Table 2**). Rarefaction curves indicated that the number of observed species was stable over 20,000 tags (**Supplementary Figure 1**). At the 97% similarity cut-off, effective tags from 12 soil samples were clustered into 4,610 OTUs. The average OTU numbers in the CK, FCP, SCP, and TCP were 272, 332, 375, and 559, respectively (**Supplementary Table 2**). The raw sequences data was deposited in NCBI (PRJNA666767).

Alpha Diversity Indices

In this research, the richness and diversity of diazotrophic microbial communities were obtained according to 21,778 taxa. **Table 1** exhibits the Chao1, Observed species, PD whole tree, and Shannon index of nitrogen-fixing microbial communities. The observed number of species was dramatically higher in the TCP than in the FCP and SCP ($p < 0.05$). The Shannon index was significantly higher in the TCP than in the FCP ($p < 0.05$) and it was also higher than in the SCP (not significant, $p > 0.05$). In the TCP, the soil nitrogen-fixing microbial communities showed significantly higher Chao1 and PD whole tree values than in the FCP and SCP ($p < 0.05$) (**Table 1**).

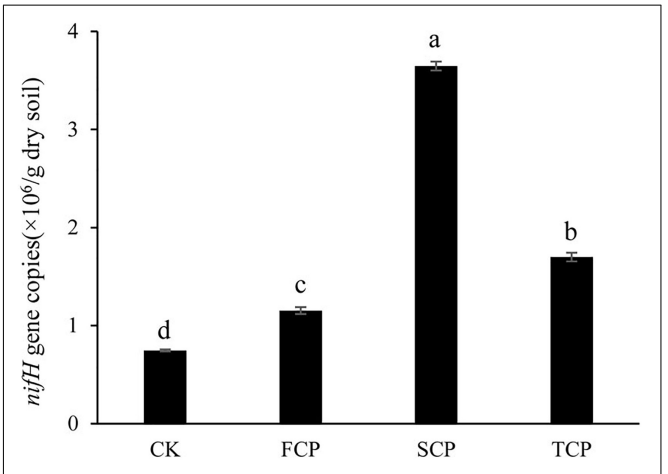

FIGURE 1 | Quantification of *nifH* gene in four different soil samples. Vertical bars show standard deviations. CK, FCP, SCP, and TCP represent the control with no *C. equisetifolia* cultivation, the first rotation plantation, the second rotation plantation and the third rotation plantation.

TABLE 1 | Calculations of Alpha diversity indices in CK, FCP, SCP, and TCP.

	Chao1	Observed species	PD whole tree	Shannon
CK	347.122 ± 3.529d	268.533 ± 9.411c	96.189 ± 4.781a	4.711 ± 0.086ab
FCP	501.560 ± 12.173b	353.267 ± 28.163b	34.525 ± 3.036d	4.461 ± 0.075b
SCP	439.649 ± 9.178c	350.867 ± 6.438b	54.372 ± 1.389c	4.738 ± 0.098ab
TCP	657.198 ± 11.229a	558.000 ± 5.667a	66.642 ± 2.091b	5.192 ± 0.406a

Different letters in each column indicate significant differences ($P \leq 0.05$ and $n = 3$).

PCA, UPGMA Clustering, NMDS, and PERMANOVA

The PCA analysis indicated obvious dissimilarities in the soil diazotrophic community structures among the four soil samples. The PCA plot completely accounted for 72.56% of the overall variation in the soil nitrogen-fixing microbial community. The PC1 explained 47.85% and the PC2 explained 24.71% of the microbial variation (**Supplementary Figure 2A**). When observing the unweighted pair-group method with arithmetic means (UPGMA) clustering, the figure showed that diazotrophic community structures clustered together from the SCP and TCP, whereas they were separated from the FCP, and the CK formed a separate group (**Supplementary Figure 2B**). The results of PCA and UPGMA clustering revealed that diazotrophic microbial community composition is different under monoculture regimes. Non-metric multidimensional scaling (NMDS) was applied to illustrate the differences in diazotrophic community composition and structure (Tibbits, 2008). Pairwise contrasts demonstrated that the CK, FCP, SCP, and TCP plots were significantly ($P < 0.05$) separated (**Figure 2**). The PERMANOVA analysis showed significant differences in the composition and distribution of the diazotrophic microbial community ($F = 26.7519$ and $P = 0.001$).

Venn Diagram Analysis

The shared and exclusive OTUs among the FCP, SCP, and TCP were explored through Venn analysis. **Supplementary Figure 3** indicates that the proportion of OTUs shared in the FCP, SCP and TCP was 30.9% (323 species). The proportion of OTUs found only in the FCP was 5.4% (57 species). The abundance of OTUs exclusively constructed in the SCP accounted for up to 13.4% (140 species). The percentage of OTUs constructed only in the TCP was 23.8% (249 species).

Abundance Change in the Diazotrophic Microbial Communities

Diazotrophic microbial OTUs consisted mostly of five phyla: *Proteobacteria*, *Verrucomicrobia*, *Chlorobi*, unidentified, and *Actinobacteria*. Among them, *Proteobacteria* was the dominant phylum, accounting for 85.7, 65.7, 94.4, and 85.5% of the total species in the CK, FCP, SCP, and TCP, respectively (**Supplementary Figure 4**).

At genus level, the *C. equisetifolia* monoculture regime generated a distinct enhancement in the relative abundance of *Paraburkholderia*, *Rhodopseudomonas*, *Bradyrhizobium*, *Geobacter*, *Pseudodesulfovibrio*, and *Frankia* and a distinct reduction in *Burkholderia*, *Rubrivivax*, and *Chlorobaculum* (**Table 2**). Compared with the FCP, the genus *Desulfovibrio* was slightly higher in the SCP but decreased in the TCP. The most common diazotrophic microbial communities of *C. equisetifolia* are listed in **Table 2**, including *Paraburkholderia*, *Bradyrhizobium*, *Burkholderia*, and *Frankia*.

It can be seen from the heat map analysis of the top 20 diazotrophic genera that distinct variations in diazotrophic community structure arose with the increase of CMP. Compared with the FCP, the discrepancy of community structures of diazotrophic bacteria increased within the extended monoculture regime, implying that diazotrophic community structure gradually changed under the CMP (**Figure 3**).

Linear discriminant analysis effect size (LEfSe) was applied to identify biomarkers (potential discriminating species in relative abundance between groups) from metagenome taxa (Xia et al., 2018). The LEfSe analysis revealed that there were 30 potential bacterial markers distinguishing the CK, FCP, SCP, and TCP with linear discriminant analysis (LDA) scores more than 3. In these tests, one phylum (unidentified), three classes (*Alphaproteobacteria*, *Gammaproteobacteria*, and unidentified), three orders (*Rhizobiales*, *Chromatiales*, and unidentified), and six families (*Bradyrhizobiaceae*, *Roseiarcaceae*, *Xanthobacteraceae*, *Alcaligenaceae*, *Ectothiorhodospiraceae*, and unidentified) were biomarkers for CK. Two phyla (*Chlorobi* and *Verrucomicrobia*), two classes (*Chlorobia* and *Opitutae*), two orders (*Chlorobiales* and *Opitutales*), and four families (*Chlorobiaceae*, *Methylocystaceae*, *Opitutaceae*, and unidentified) were significantly different in the FCP. In the SCP, biomarkers were mostly clustered in *Proteobacteria*, including *Deltaproteobacteria*, *Desulfuromonadales*, and *Geobacteraceae*. In the TCP, biomarkers were *Betaproteobacteria*, *Burkholderiales*, and *Burkholderiaceae* (**Figure 4**).

Correlation Analysis Between Diazotrophic Microbial Communities and Environmental Parameters

To detect the relationships between diazotrophic microbial communities and environmental parameters, RDA was performed based on the top 12 species of the diazotrophic microbial community and environmental parameters (**Figure 5**). The influence of environmental factors on the diazotrophic microbial community can be seen from the length of the arrow and the angle between the arrow and the microbe. RDA canonical axes 1 and 2, respectively, described 58.40 and 33.52% of the variation in the diazotrophic microbial community, suggesting a remarkable correlation between microbial communities and environmental parameters. As shown in **Figure 5**, the

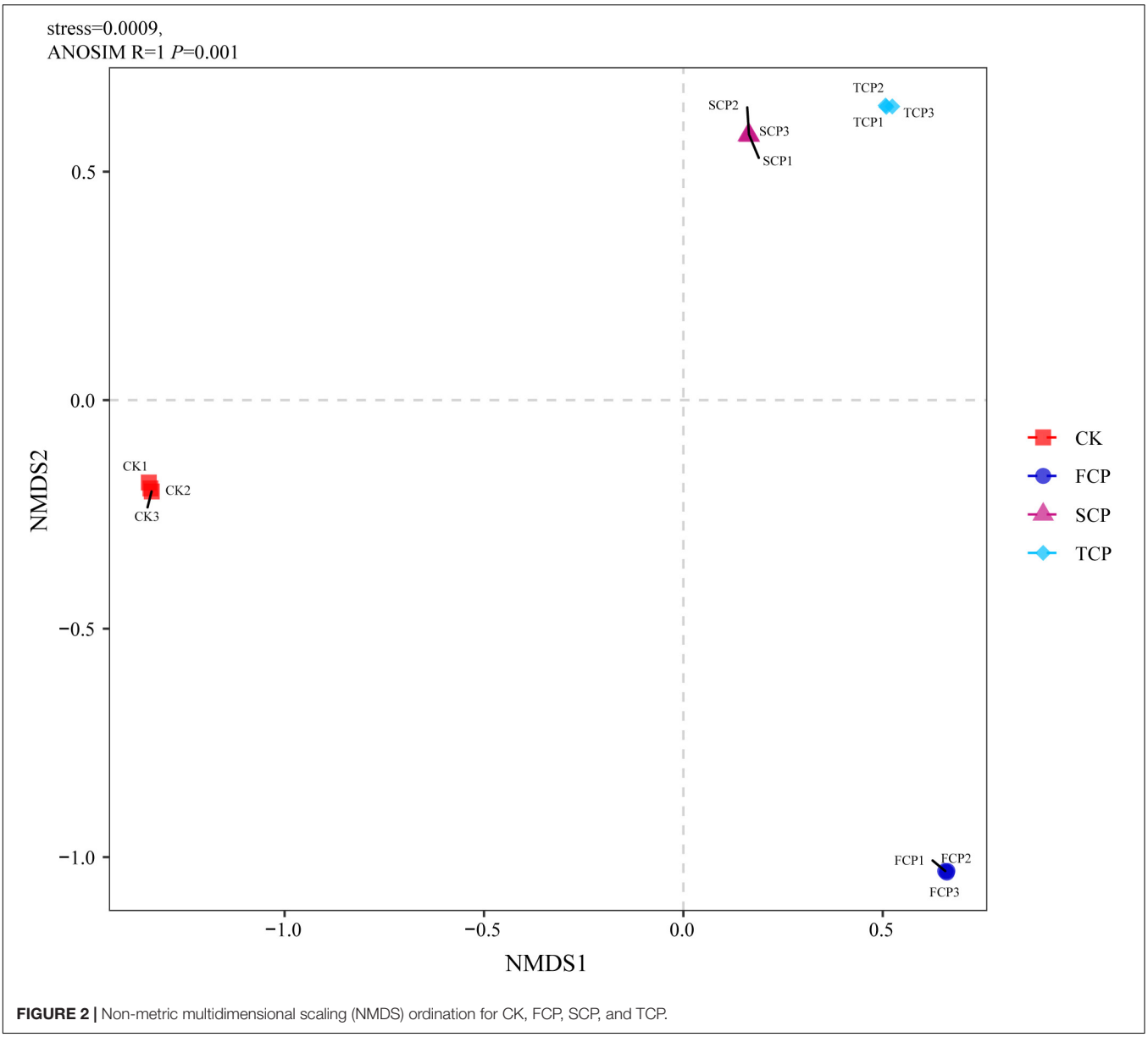

FIGURE 2 | Non-metric multidimensional scaling (NMDS) ordination for CK, FCP, SCP, and TCP.

TABLE 2 | Calculations of the top diazotrophic bacteria for four different soil samples at the genus level.

	CK	FCP	SCP	TCP
Paraburkholderia	0.50 ± 0.33b	6.05 ± 1.36b	29.58 ± 0.83a	40.18 ± 14.09a
Rhodopseudomonas	32.75 ± 3.34a	0.25 ± 0.04c	5.75 ± 1.50b	1.69 ± 1.39bc
Bradyrhizobium	8.04 ± 3.26b	1.87 ± 0.41c	21.24 ± 2.32a	8.21 ± 1.75b
Unidentified	10.23 ± 2.88b	18.52 ± 2.01a	3.87 ± 0.76c	4.91 ± 0.74c
Burkholderia	0.34 ± 0.49b	20.51 ± 3.52a	2.84 ± 0.34b	3.77 ± 0.34b
Geobacter	0.81 ± 0.22c	3.46 ± 0.77bc	11.64 ± 2.36a	7.71 ± 2.32ab
Rubrivivax	0.11 ± 0.07b	17.86 ± 3.07a	2.31 ± 0.11b	2.94 ± 0.54b
Halorhodospira	16.07 ± 1.42a	0.31 ± 0.12b	2.27 ± 0.35b	0.96 ± 0.61b
Desulfovibrio	2.39 ± 1.03c	6.02 ± 1.01ab	6.56 ± 1.16a	3.22 ± 1.26bc
Chlorobaculum	0.71 ± 0.83b	15.07 ± 1.97a	0.82 ± 0.16b	0.61 ± 0.12b
Pseudodesulfovibrio	2.46 ± 0.98ab	0.97 ± 0.34b	3.46 ± 0.85ab	5.89 ± 2.29a
Frankia	0.15 ± 0.10b	0.38 ± 0.32b	0.34 ± 0.14b	8.70 ± 2.77a

Different letters in each column indicate significant differences ($P \leq 0.05$ and $n = 3$).

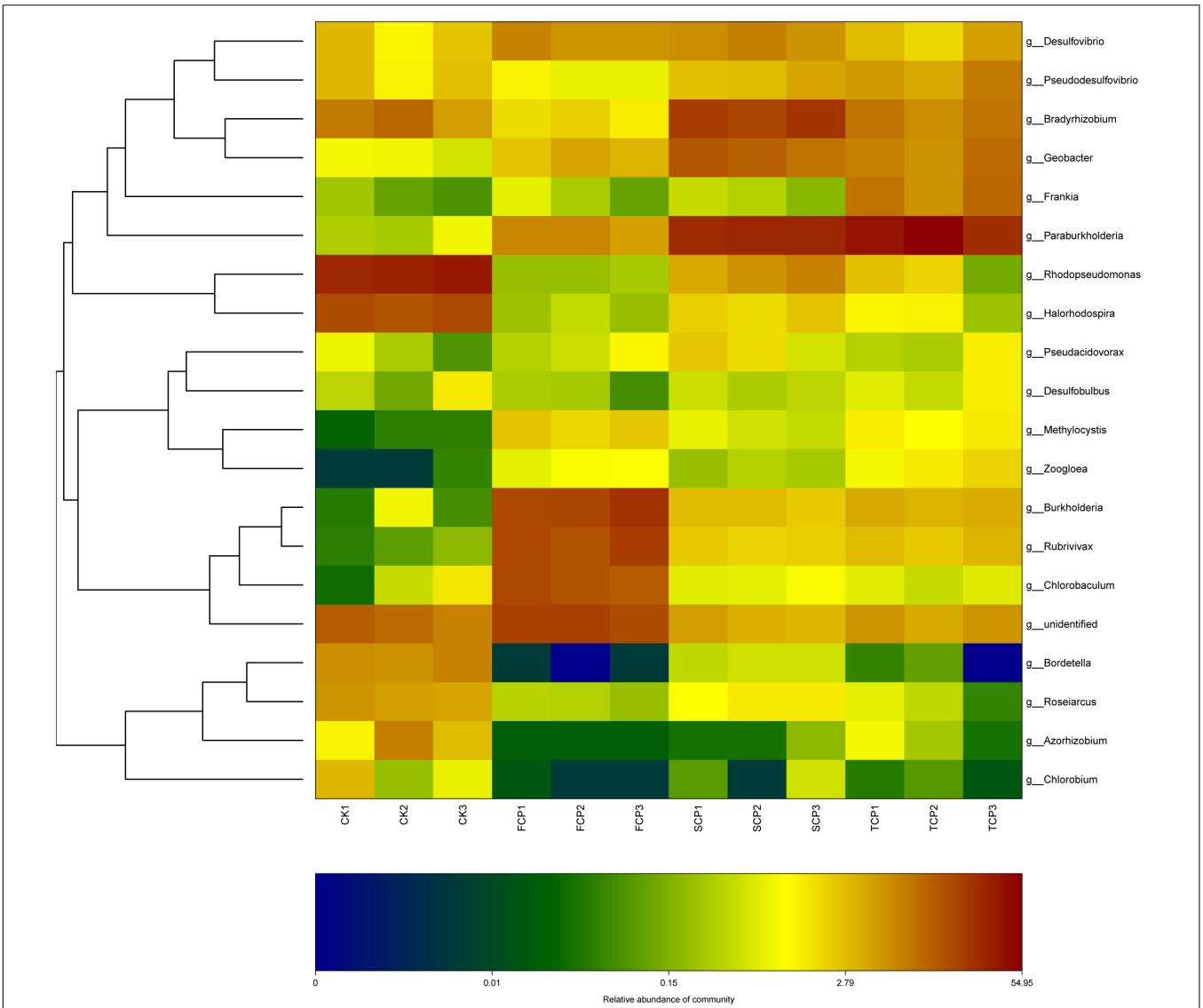

FIGURE 3 | Heat map analysis of the dominant diazotrophic genera in four individual soil samples.

SCP and TCP were clustered together and distributed at the negative end of RDA1, away from the CK and FCP, reflecting the significant shift of the diazotrophic microbial community under a monoculture regime. The results of RDA were consistent with the PCA results (**Supplementary Figure 2B**). In addition, from the results in **Figure 5**, it can be seen that *Burkholderia, Rubrivivax* and *Chlorobaculum* were positively correlated with the environmental parameters of TN, AN and TK, but negatively correlated with AK. However, the opposite was true for the *Bradyrhizobium* which was positively correlated with AK.

DISCUSSION

Consecutive monoculture problem, also known as soil sickness, has a severe impact on the growth and health of plants. It is a widespread and complex phenomenon in numerous cultivated tree species (Huang et al., 2013). Many factors are thought to contribute to the continuous cropping problem, including the physical and chemical properties of soil, the accumulation of allelochemicals, and changes in the soil microbial community (Wu et al., 2016a; Chen et al., 2018). In this study, we found that the contents of soil nitrogen (AN and TN) under monoculture regimes (SCP and TCP) were significantly lower than that in the FCP (**Supplementary Table 1**). The results indicated that soil physical and chemical properties may indirectly affect the healthy growth of *C. equisetifolia* through regulating the structure of the soil microbial community (Berendsen et al., 2012).

Recently, many studies have revealed that shifts in the soil microbial community are related to this soil sickness (Li et al., 2014; Liu et al., 2017). Soil microbes play a vital role in the growth and health of plants. Soil microbes are also known as the

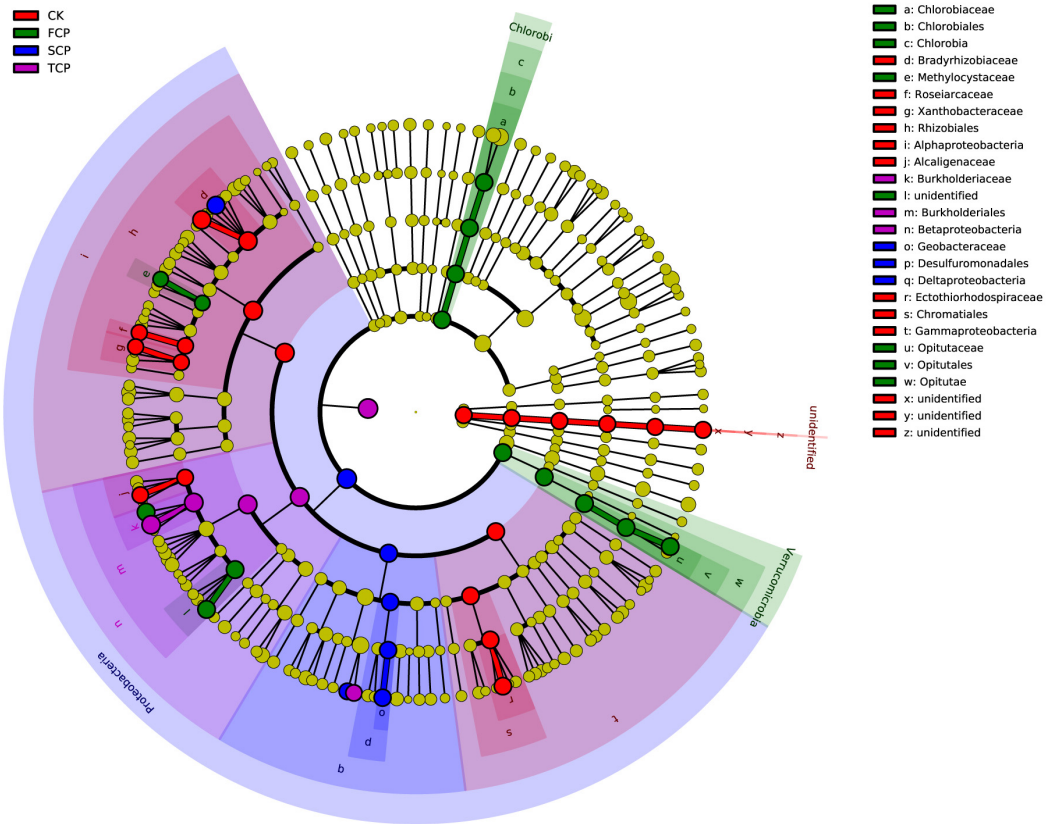

FIGURE 4 | Phylogenetic dendrogram of biomarkers in C. equisetifolia rhizospheric soil diazotrophic bacteria in CK, FCP, SCP, and TCP. The circles from inside to outside exhibit diazotrophic taxonomic levels from phylum to genus. Yellow dots mean that there is no significant difference in diazotrophic abundance among individual soil samples. The colors of the biomarkers are based on their corresponding class colors on the right.

second genome of plants (Berendsen et al., 2012; Berg et al., 2017). N-fixing organisms play a profound part in nitrogen cycling in forest ecosystems (Yousuf et al., 2014). In the present study, the *nifH* gene abundance in *C. equisetifolia* increased with the extension of monoculture. These results are contradictory to those of a previous study on a *Eucalyptus* successive plantation (Monteiro et al., 2020). Species diversity is a crucial factor for soil health (Chaparro et al., 2012). Wu et al. (2017) reported that the rhizosphere microbial diversity in Chinese fir was decreased after long-term successive rotations. In this study, most of the diversity indices were significantly lower in the FCP and in the SCP than TCP (**Table 1**). The differing results among these studies may be due to differences in factors including plant types, soil environments, and root chambers. The number of copies of the *nifH* gene increased under monoculture regime, while diversity indices were increased or decreased with monoculture. That is the diazotrophic community compositions and structures were changed under long-term monoculture *C. equisetifolia* plantations, indicating that our hypothesis was correct.

In recent years, more attention has been paid to the relationship between key rhizosphere microbes and plants, which is central to plant growth and development (Mendes et al., 2011; Chen et al., 2017). The *Proteobacteria* phylum is commonly explored in soil systems (Gaby and Buckley, 2011). In this study, the most predominant phylum present in the rhizosphere was *Proteobacteria*. The diazotrophic bacterial populations in the *C. equisetifolia* rhizospheric soil (**Supplementary Figure 4**) accounted for 85.69, 65.75, 94.40, and 85.54% of the total in the CK, FCP, SCP, and TCP, respectively, which was in accordance with the results found by Bazylinski et al. (2013). Taxonomic analysis (genus level) showed that continuous monoculture of *C. equisetifolia* increased the relative abundance of *Paraburkholderia*, *Rhodopseudomonas*, *Bradyrhizobium*, *Geobacter*, *Pseudodesulfovibrio*, and *Frankia*, whereas the abundance of *Burkholderia*, *Rubrivivax*, and *Chlorobaculum* decreased significantly (**Table 2**). Among these diazotrophs, compared with the FCP, the relative abundance of *Bradyrhizobium* increased by 1,135.83 and 439.04% in the SCP and TCP, respectively. *Bradyrhizobium* was the dominant diazotroph in soil systems due to strong persistence of diazotrophic bacteria across varying soil environmental conditions (Pereira et al., 2013). Relative to the FCP, the

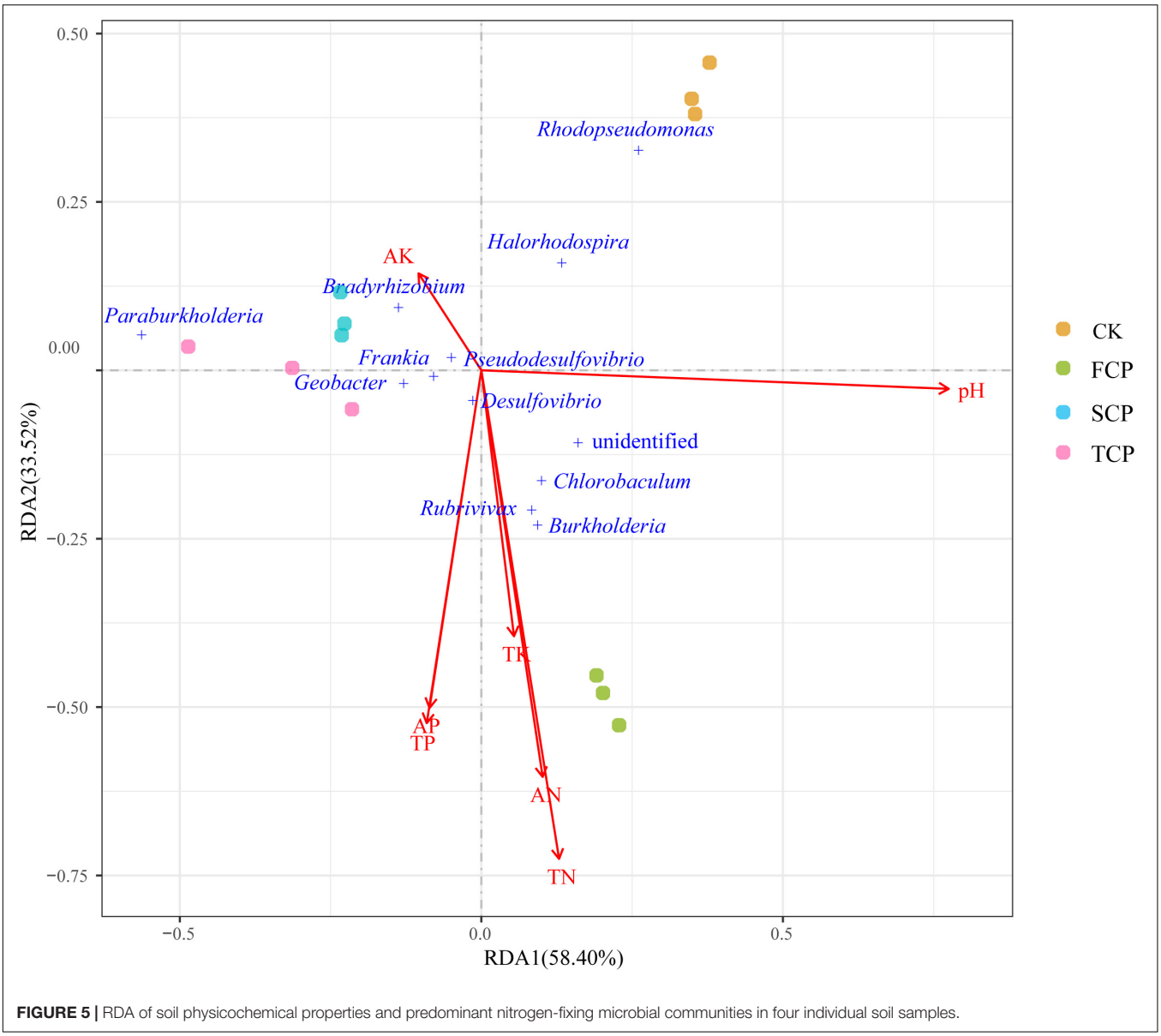

FIGURE 5 | RDA of soil physicochemical properties and predominant nitrogen-fixing microbial communities in four individual soil samples.

abundance of *Burkholderia* decreased by 722.18 and 544.03% in the SCP and TCP, respectively. *Burkholderia* can be used for biological control through such methods as promoting plant growth and bio-remediation. It has been reported that *Burkholderia* has the ability of nodulation and N-fixation in certain legume plants including *Burkholderia vietnamiensis*, *Burkholderia phymatum*, and *Burkholderia tuberum* (Coenye and Vandamme, 2003). Wu et al. (2016a) reported that monoculture of *Pseudostellaria heterophylla* led to a significant decline in the abundance of *Burkholderia*. Mendes et al. (2011) showed that the relative abundances of *Burkholderiaceae* was positively associated with disease suppression of sugar beet. Thus, certain species of diazotrophic bacteria found in this study were inhibited under *C. equisetifolia* monocultures (SCP and TCP) that might be key rhizosphere microbes or plant growth promoters. This issue should be studied in the future.

Many reports have indicated that soil microbial community composition was indirectly influenced by environmental parameters (Li and Wu, 2018; Zhang et al., 2019). In our study, RDA results showed that key rhizosphere microbes (*Burkholderia, Rubrivivax* and *Chlorobaculum*) were positively correlated with soil nitrogen (AN and TN). Therefore, based on their abundance (a significant decrease in SCP and TCP), soil nitrogen seems to play an important role in *C. equisetifolia* monocultures. The decline of *Burkholderia, Rubrivivax* and *Chlorobaculum* may be related to soil nitrogen under continuous planting. Their abundance may indicate an important role in plant-microbial interactions and soil function as well as nitrogen fixation. In addition, *Burkholderia* is considered a rhizospheric-plant promoting group (Zhao K. et al., 2014). It could play an important role in maintaining the stability of soil communities (Wakelin et al., 2017). The results of RDA suggested that the

diazotrophic microbial community may respond differently to environmental parameters, but this hypothesis should be further tested.

A growing number of researchers have reported that the imbalance of key rhizosphere microflora is considered to be the main cause of CMP. Zhao J. et al. (2014) revealed that *Eucalyptus* monocultures increased the abundance of fungi in rhizospheric soil. Successive rotations of *Cunninghamia lanceolata* generated imbalance in the soil microbial community. Most studies have reported that this phenomenon of imbalance resulted from alterations of the rhizospheric microflora induced by plant root exudations rather than direct allelopathy (Li et al., 2014; Wu et al., 2015). In this study, the continuous monoculture of *C. equisetifolia* shifted the structure of the diazotrophic population in rhizospheric soils. This shift may result in the imbalance of diazotrophic bacteria population structure, which might be a crucial factor in replanting disease of this cultivated tree species. Many previous studies have shown that root exudates restructure the plant-associated rhizospheric microbes and these microbes impact plants (Paterson et al., 2007; Haichar et al., 2008; Michalet et al., 2013). Therefore, further studies are required to analyze the effects of the *C. equisetifolia* root exudates to obtain precise knowledge of the soil nitrogen-fixing microorganism community structure.

CONCLUSION

Our result indicates that the continuous monoculture of *C. equisetifolia* distinctly influenced the diazotrophic community compositions and structures in the rhizosphere. The phyla *Proteobacteria* increased, whereas *Verrucomicrobia* decreased with increasing continuous monoculture. At the genus level, the relative abundance of *Paraburkholderia*, *Rhodopseudomonas*, *Bradyrhizobium*, *Geobacter*, *Pseudodesulfovibrio*, and *Frankia* increased significantly, while *Burkholderia*, *Rubrivivax*, and *Chlorobaculum* declined significantly. To more efficiently explore the causes of obstacles to continuous monoculture, the isolation of specific N-fixing organisms (i.e., *Bradyrhizobium* and *Burkholderia*) and their functions, which may be correlated with CMP, should be further studied. It is noteworthy that most specific N-fixing organisms appear to be highly sensitive to changes in the soil under monoculture regimes. This should be investigated further.

DATA AVAILABILITY STATEMENT

The data presented in the study are deposited in the (NCBI) repository, accession number (PRJNA666767; SRP286063).

AUTHOR CONTRIBUTIONS

ZW, WL, and LZ conceived the study. ZW, YZ, LZ, and WL designed all the experiments. JL, JC, YB, and CZ performed the experiments. LZ, CW, GP, and JL performed the statistical analyses. LZ and ZW wrote the manuscript with the assistance and approval of all authors.

FUNDING

This work was supported by the Chinese National Natural Science Foundation (31500443), Natural Science Foundation of Fujian Province, China (Grant No. 2018J01617), the Scientific Research Foundation of Fujian Agriculture and Forestry University (XJQ201718), the Fujian-Taiwan Joint Innovative Centre for Germplasm Resources and Cultivation of Crops (Grant No. 2015-75. FJ 2011 Program, China), and the Special Foundation of Science and Technology Innovation of Fujian Agriculture and Forestry University (CXZX2019051G).

ACKNOWLEDGMENTS

We thank LetPub (www.letpub.com) for its linguistic assistance during the preparation of this manuscript.

SUPPLEMENTARY MATERIAL

The Supplementary Material for this article can be found online at: https://www.frontiersin.org/articles/10.3389/fpls.2020.578812/full#supplementary-material

REFERENCES

Arafat, Y., Wei, X. Y., Jiang, Y. H., Chen, T., Saqib, H. S. A., Lin, S., et al. (2017).). Spatial distribution patterns of Root-Associated bacterial communities mediated by root exudates in different aged ratooning tea monoculture systems. *Int. J. Mol. Sci.* 18:1727. doi: 10.3390/ijms18081727

Araya, H., Otaka, J., Nishihara, E., and Fujii, Y. (2012). First isolation and identification of salicylate from Betula grossa var. *Ulmifolia - a potent root growth inhibitor*. *Allelopathy J.* 30, 153–158.

Bazylinski, D. A., Williams, T. J., Lefevre, C. T., Berg, R. J., Zhang, C. L., et al. (2013). Magnetococcus marinus gen. *Nov., Sp nov., A marine, magnetotactic bacterium that represents a novel lineage (Magnetococcaceae fam. Nov., Magnetococcales ord. Nov.) at the base of the Alphaproteobacteria*. *Int. J. Syst. Evol. Micr.* 63, 801–808. doi: 10.1099/ijs.0.038927-0

Bennett, A. J., Bending, G. D., Chandler, D., Hilton, S., and Mills, P. (2012). Meeting the demand for crop production: The challenge of yield decline in crops grown in short rotations. *Biol. Rev.* 87, 52–71. doi: 10.1111/j.1469-185X.2011.00184.x

Berendsen, R. L., Pieterse, C. M. J., and Bakker, P. A. H. M. (2012). The rhizosphere microbiome and plant health. *Trends Plant Sci.* 17, 478–486. doi: 10.1016/j.tplants.2012.04.001

Berg, G., Koeberl, M., Rybakova, D., Mueller, H., Grosch, R., Smalla, K., et al. (2017). Plant microbial diversity is suggested as the key to future biocontrol and health trends. *FEMS Microbiol. Ecol.* 93:fix050. doi: 10.1093/femsec/fix050

Caporaso, J. G., Kuczynski, J., Stombaugh, J., Bittinger, K., and Bushman, F. D. (2010). QIIME allows analysis of high-throughput community sequencing data. *Nat. Methods* 7, 335–336. doi: 10.1038/nmeth.f.303

Chaparro, J. M., Sheflin, A. M., Manter, D. K., and Vivanco, J. M. (2012). Manipulating the soil microbiome to increase soil health and plant fertility. *Biol. Fert. Soils* 48, 489–499. doi: 10.1007/s00374-012-0691-4

Chen, J., Wu, L. K., Xiao, Z. G., Wu, Y. H., Wu, H. M., Qin, X. J., et al. (2017). Assessment of the diversity of *Pseudomonas* spp. *and Fusarium spp. in Radix pseudostellariae rhizosphere under monoculture by combining DGGE and quantitative PCR. Front. Microbiol.* 8:1748. doi: 10.3389/fmicb.2017.01748

Chen, S. C., Yu, H. J., Zhou, X. G., and Wu, F. Z. (2018). Cucumber (*Cucumis sativus* L.) *Seedling Rhizosphere Trichoderma and Fusarium spp. Communities Altered by Vanillic Acid. Front. Microbiol.* 9:2195. doi: 10.3389/fmicb.2018.02195

Coenye, T., and Vandamme, P. (2003). Diversity and significance of *Burkholderia* species occupying diverse ecological niches. *Environ. Microbiol.* 5, 719–729. doi: 10.1046/j.1462-2920.2003.00471.x

Cole, J. R., Wang, Q., Cardenas, E., Fish, J., Chai, B., Farris, R. J., et al. (2009). The Ribosomal Database Project: Improved alignments and new tools for rRNA analysis. *Nucleic Acids Res.* 37, D141–D145. doi: 10.1093/nar/gkn879

Deng, C. H., Wu, L. L., Zhang, Y. T., Qiao, H., Liu, X. Y., Hu, Y. J., et al. (2019). The stoichiometry characteristics of soil and plant carbon, nitrogen, and phosphorus in different stand ages in *Camellia oleifera* plantation. *Acta Ecol. Sin.* 39, 9152–9161. doi: 10.5846/stxb201809202055

Edgar, R. C. (2013). UPARSE: Highly accurate OTU sequences from microbial amplicon reads. *Nat. Methods* 10:996. doi: 10.1038/NMETH.2604

Fernandez, C., Voiriot, S., Mévy, J., Vila, B., Orme, O. E., Dupouyet, S., et al. (2008). Regeneration failure of Pinus halepensis Mill.: *The role of autotoxicity and some abiotic environmental parameters. Forest Ecol. Manag.* 255, 2928–2936. doi: 10.1016/j.foreco.2008.01.072

Gaby, J. C., and Buckley, D. H. (2011). A global census of nitrogenase diversity. *Environ. Microbiol.* 13, 1790–1799. doi: 10.1111/j.1462-2920.2011.02488.x

Goossen, W. T. F., Epping, P. J. M. M., Heuvel, W. J. V. D., Feuth, T., and Hasman, A. (2010). Development of the Nursing Minimum Data Set for the Netherlands (NMDSN): Identification of categories and items. *J. Adv. Nurs.* 31, 536–547. doi: 10.1046/j.1365-2648.2000.01308.x

Haichar, F. Z., Marol, C., Berge, O., Rangel-Castro, J. I., and Prosser, J. I. (2008). Plant host habitat and root exudates shape soil bacterial community structure. *Isme. J.* 2, 1221–1230. doi: 10.1038/ismej.2008.80

Hsu, S., and Buckley, D. H. (2009). Evidence for the functional significance of diazotroph community structure in soil. *ISME J.* 3, 124–136. doi: 10.1038/ismej.2008.82

Huang, L. F., Song, L. X., Xia, X. J., Mao, W. H., Shi, K., Zhou, Y. H., et al. (2013). Plant-Soil feedbacks and soil sickness: From mechanisms to application in agriculture. *J. Chem. Ecol.* 39, 232–242. doi: 10.1007/s10886-013-0244-9

Jackson, M. L. (2005). *Soil Chemical Analysis: Advanced Course*. Madison, UW: Libraries Parallel Press, 432–433. doi: 10.1097/01.ss.0000223482.86664.14

Jami, E., Israel, A., Kotser, A., and Mizrahi, I. (2013). Exploring the bovine rumen bacterial community from birth to adulthood. *ISME J.* 7, 1069–1079. doi: 10.1038/ismej.2013.2

Jie, Z., Songze, W., Chenlu, Z., Zhanfeng, L., and Lixia, Z. (2014). Contributions of understory and/or overstory vegetations to soil microbial PLFA and nematode diversities in eucalyptus monocultures. *Plos One* 9:e85513.

Karthikeyan, A., Chandrasekaran, K., Geetha, M., and Kalaiselvi, R. (2013). Growth response of *Casuarina equisetifolia* Forst. *Rooted stem cuttings;to Frankia in nursery and field conditions. J. Biosci.* 38, 741–747. doi: 10.1007/s12038-013-9362-3

Li, S., and Wu, F. Z. (2018). Diversity and co-occurrence patterns of soil bacterial and fungal communities in seven intercropping systems. *Front. Microbiol.* 9:1521. doi: 10.3389/fmicb.2018.01521

Li, X. G., Ding, C. F., Hua, K., Zhang, T. L., Zhang, Y. N., Zhao, L., et al. (2014). Soil sickness of peanuts is attributable to modifications in soil microbes induced by peanut root exudates rather than to direct allelopathy. *Soil Biol. Biochem.* 78, 149–159. doi: 10.1016/j.soilbio.2014.07.019

Li, Y. Y., Chen, X. H., Xie, Z. X., Li, D. X., Wu, P. F., Kong, L. F., et al. (2018). Bacterial diversity and nitrogen utilization strategies in the upper layer of the northwestern pacific ocean. *Front. Microbiol.* 9:797. doi: 10.3389/fmicb.2018.00797

Liu, J. G., Li, X. G., Jia, Z. J., Zhang, T. L., and Wang, X. X. (2017). Effect of benzoic acid on soil microbial communities associated with soilborne peanut diseases. *Appl. Soil Ecol.* 110, 34–42. doi: 10.1016/j.apsoil.2016.11.001

Lu, Q., Zhang, J. C., and Chen, L. S. (2017). Impact of monoculture of poplar on the rhizosphere microbial communities over time. *Pedosphere* 30, 487–495. doi: 10.1016/S1002-0160(17)60416-8

Mendes, R., Kruijt, M., Bruijn, I., Dekkers, E., Voort, M., Schneider, J. H., et al. (2011). Deciphering the rhizosphere microbiome for disease-suppressive bacteria. *Science* 332, 1097–1100. doi: 10.1126/science.1203980

Michalet, S., Rohr, J., Warshan, D., Bardon, C., Roggy, J. C., Domenach, A. M., et al. (2013). Phytochemical analysis of mature tree root exudates in situ and their role in shaping soil microbial communities in relation to tree N-acquisition strategy. *Plant Physiol. Bioch.* 72, 169–177. doi: 10.1016/j.plaphy.2013.05.003

Monteiro, D. A., Fonseca, E. S., Rodrigues, R. D. A. R., Silva, J. J. N., Silva, E. P., Balieiro, F. C., et al. (2020). Structural and functional shifts of soil prokaryotic community due to *Eucalyptus* plantation and rotation phase. *Scient. Rep.* 10, 1–14.

Oksanen, J., Kindt, R., Legendre, P., O'Hara, B., Simpson, G. L., et al. (2009). *Vegan: Community Ecology Package. R. package. Version*. 15–12.

Paterson, E., Gebbing, T., Abel, C., Sim, A., and Telfer, G. (2007). Rhizodeposition shapes rhizosphere microbial community structure in organic soil. *New Phytol.* 173, 600–610. doi: 10.1111/j.1469-8137.2006.01931.x

Penton, C. R., Yang, C. Y., Wu, L. Y., Wang, Q., Zhang, J., Liu, F. F., et al. (2016). *nifH*-Harboring Bacterial Community Composition across an Alaskan Permafrost Thaw Gradient. *Front. Microbiol.* 7:1894. doi: 10.3389/fmicb.2016.01894

Pereira, E., Silva, M. C., Schloter-Hai, B., Schloter, M., van Elsas, J. D., and Salles, J. F. (2013). Temporal dynamics of abundance and composition of Nitrogen-Fixing communities across agricultural soils. *PLoS One.* 8:e74500. doi: 10.1371/journal.pone.0074500

Shi, D., Ni, J. P., Ni, C. S., and Liu, J. C. (2018). The effects of different restoration years on plant diversity in Wushan's alpine emigrant region. *Acta Ecol. Sin.* 39, 5584–5593. doi: 10.5846/stxb201802260392

Tibbits, K. J. (2008). Non-parametric multivariate comparisons of soil fungal composition: Sensitivity to thresholds and indications of structural redundancy in T-RFLP data. *Soil Biol. Biochem.* 40, 1601–1611. doi: 10.1016/j.soilbio.2008.01.008

Wakelin, S., Young, S., Gerard, E., Mander, C., and O'Callaghan, M. (2017). Isolation of root-associated *Pseudomonas* and *Burkholderia* spp. *with biocontrol and plant growth-promoting traits. Biocontrol. Sci. Techn.* 27, 139–143. doi: 10.1080/09583157.2016.1248899

Wang, C., Zheng, M., Song, W., Wen, S., and Wang, B. (2017). Impact of 25 years of inorganic fertilization on diazotrophic abundance and community structure in an acidic soil in southern China. *Soil Biol. Biochem.* 113, 240–249. doi: 10.1016/j.soilbio.2017.06.019

Wang, Y., Sheng, H. F., He, Y., Wu, J. Y., Jiang, Y. X., et al. (2012). Comparison of the levels of bacterial diversity in freshwater, intertidal wetland, and marine sediments by using millions of illumina tags. *Appl. Environ. Microb.* 78, 8264–8271. doi: 10.1128/AEM.01821-12

Wardle, D. A., Bardgett, R. D., Klironomos, J. N., Setala, H., Putten, W. H., and Wall, D. H. (2004). Ecological linkages between aboveground and belowground biota. *Science* 304, 1629–1633. doi: 10.1126/science.1094875

Wu, L. K., Chen, J., Wu, H. M., Qin, X. J., Wang, J. Y., Wu, Y. H., et al. (2016a). Insights into the Regulation of Rhizosphere Bacterial Communities by Application of Bio-organic Fertilizer in *Pseudostellaria heterophylla* Monoculture Regime. *Front. Microbiol.* 7:1788. doi: 10.3389/fmicb.2016.01788

Wu, L. K., Wang, J. Y., Huang, W. M., Wu, H. M., Chen, J., Yang, Y. Q., et al. (2015). Plant-microbe rhizosphere interactions mediated by *Rehmannia glutinosa* root exudates under consecutive monoculture. *Sci. Rep.* 5:15871. doi: 10.1038/srep15871

Wu, L. K., Wu, H. M., Chen, J., Wang, J. Y., and Lin, W. X. (2016b). Microbial community structure and its temporal changes in *Rehmannia glutinosa* rhizospheric soils monocultured for different years. *Eur. J. Soil Biol.* 72, 1–5. doi: 10.1016/j.ejsobi.2015.12.002

Wu, Z. Y., Li, J. J., Zheng, J., Liu, J. F., Liu, S. Y., Lin, W. X., et al. (2017). Soil microbial community structure and catabolic activity are significantly degenerated in successive rotations of Chinese fir plantations. *Sci. Rep.* 7:6691. doi: 10.1038/s41598-017-06768-x

Xia, Y., Lu, M. X., Chen, G., Cao, J. M., Gao, F. Y., Wang, M., et al. (2018). Effects of dietary *Lactobacillus rhamnosus* JCM1136 and *Lactococcus lactis* subsp *lactis* JCM5805 on the growth, intestinal microbiota, morphology, immune response

and disease resistance of juvenile Nile tilapia, *Oreochromis niloticus*. *Fish Shellfish Immun.* 76, 368–379. doi: 10.1016/j.fsi.2018.03.020

Xiong, W., Zhao, Q. Y., Zhao, J., Xun, W. B., Li, R., Zhang, R. F., et al. (2015). Different continuous cropping spans significantly affect microbial community membership and structure in a vanilla-grown soil as revealed by deep pyrosequencing. *Microbiol. Ecol.* 70, 1–10. doi: 10.1007/s00248-014-0516-0

Yousuf, B., Kumar, R., Mishra, A., and Jha, B. (2014). Differential distribution and abundance of diazotrophic bacterial communities across different soil niches using a gene-targeted clone library approach. *FEMS Microbiol. Lett.* 360, 117–125. doi: 10.1111/1574-6968.12593

Zehr, J. P., Mellon, M. T., and Zani, S. (1998). New Nitrogen-Fixing microorganisms detected in oligotrophic oceans by amplification of nitrogenase (*nifH*) genes. *Appl. Environ. Microbiol.* 64:3444. doi: 10.1002/(SICI)1097-0290(19980905)59:5

Zhang, L. N., Wang, D. C., Hu, Q., Dai, X. Q., Xie, Y. S., Li, Q., et al. (2019). Consortium of plant growth-promoting rhizobacteria strains suppresses sweet pepper disease by altering the rhizosphere microbiota. *Front. Microbiol.* 10:1668. doi: 10.3389/fmicb.2019.01668

Zhang, M. Y., Xu, Z. H., Teng, Y., Christie, P., Wang, J., Ren, W. J., et al. (2016). Non-target effects of repeated chlorothalonil application on soil nitrogen cycling: The key functional gene study. *Sci. Tot. Environ.* 543, 636–643. doi: 10.1016/j.scitotenv.2015.11.053

Zhao, J., Mei, Z., Zhang, X., Xue, C., Zhang, C. Z., Ma, T. F., et al. (2017). Suppression of Fusarium wilt of cucumber by ammonia gas fumigation via reduction of Fusarium population in the field. *Sci. Rep.* 7:43103. doi: 10.1038/srep43103

Zhao, J., Wan, S. Z., Zhang, C. L., Liu, Z. F., Zhou, L. X., Fu, S. L., et al. (2014). Contributions of understory and/or overstory vegetations to soil microbial PLFA and nematode diversities in *Eucalyptus* monocultures. *PLoS One.* 9:e85513. doi: 10.1371/journal.pone.0085513

Zhao, K., Penttinen, P., Zhang, X. P., Ao, X. L., Liu, M. K., Yu, X. M., et al. (2014). Maize rhizosphere in Sichuan, China, hosts plant growth promoting *Burkholderia cepacia* with phosphate solubilizing and antifungal abilities. *Microbiol. Res.* 169, 76–82. doi: 10.1016/j.micres.2013.07.003

Zhong, C. L., Bai, J. Y., and Zhang, Y. (2005). Introduction and conservation of casuarina trees in china. *Forest Res.* 18, 345–350. doi: 10.1360/biodiv.050121

Zhou, L. T., Li, J. J., Luo, Y., Liu, S. Y., Chen, J., Wang, J. Y., et al. (2019). Variation in soil fungal community structure during successive rotations of *Casuarina equisetifolia* plantations as determined by high-throughput sequencing analysis. *Plant Growth Regul.* 87, 445–453. doi: 10.1007/s10725-019-00483-5

Conflict of Interest: The authors declare that the research was conducted in the absence of any commercial or financial relationships that could be construed as a potential conflict of interest.

frontiers in Plant Science

ORIGINAL RESEARCH
published: 09 February 2021
doi: 10.3389/fpls.2021.588847

Gly Betaine Surpasses Melatonin to Improve Salt Tolerance in *Dalbergia odorifera*

El Hadji Malick Cisse, Ling-Feng Miao, Fan Yang, Jin-Fu Huang, Da-Dong Li and Juan Zhang*

School of Ecological and Environmental Sciences, Center for Eco-Environmental Restoration Engineering of Hainan Province, Key Laboratory of Agro-Forestry Environmental Processes and Ecological Regulation of Hainan Province, Hainan University, Haikou, China

Salinity is one of the most serious factors limiting plant growth which can provoke significant losses in agricultural crop production, particularly in arid and semi-arid areas. This study aimed to investigate whether melatonin (MT; 0.05 and 0.1 mM), which has pleiotropic roles, has a better effect than glycine betaine (GB; 10 and 50 mM) on providing salt tolerance in a woody plant *Dalbergia odorifera* T. Chen. Also, the alternative oxidase activity (AOX) in plant subjected to MT or GB under salinity (150 and 250 mM) was evaluated given that the effect of exogenous MT or GB on AOX has not been reported yet. The results showed that the exogenous application of GB on the seedlings of *D. odorifera* increased the plant growth parameters, relative water content, total of chlorophyll content, and carotenoid content compared with well-watered and MT treatments. Under severe salinity, the seedlings subjected to GB showed, a significant enhancement in water use efficiency, transpiration, and net photosynthetic rate regardless to MT-treated seedlings. The levels of proline and soluble sugar in the seedlings treated with MT or GB decreased significantly under mild and severe salinity correlated with those in salt-stressed seedlings. Furthermore, GB-treated plants exhibited a significant inhibition of malondialdehyde content compared with MT-treated plants. The concentration of thiols and phenolic compounds were significantly enhanced in the leaves of seedlings treated with MT compared with those treated with GB. Under salt stress condition, GB scavenged significantly higher levels of hydrogen peroxide than MT; while under severe salinity, plants subjected to MT showed better scavenging ability for hydroxyl radicals compared with GB-treated seedlings. The results demonstrated also an enhancement of the levels of superoxide dismutase (SOD), guaiacol peroxidase, and AOX activities in seedlings treated with GB or MT compared with salt-stressed plants. The catalase activity (CAT) was increased by 0.05 mM MT and 0.1 mM GB under mild salinity. Meanwhile, the AOX activity under severe salinity was enhanced only by GB 50 mM. The findings of this study suggested that GB-treated seedlings possessed a better salt tolerance in comparison with MT-treated seedlings.

Keywords: alternative oxidase, glycine betaine, melatonin, redox homeostasis, salt tolerance

OPEN ACCESS

Edited by:
Sanushka Naidoo,
University of Pretoria, South Africa

Reviewed by:
Magdi T. Abdelhamid,
National Research Centre, Egypt
Gholamreza Gohari,
University of Maragheh, Iran

****Correspondence:***
Fan Yang
yangfan@hainanu.edu.cn;
fanyangmlf6303@163.com

Specialty section:
This article was submitted to Plant Abiotic Stress, a section of the journal Frontiers in Plant Science

Received: *29 July 2020*
Accepted: *19 January 2021*
Published: *09 February 2021*

Citation:
Cisse EHM, Miao L-F, Yang F, Huang J-F, Li D-D and Zhang J (2021) Gly Betaine Surpasses Melatonin to Improve Salt Tolerance in Dalbergia odorifera. Front. Plant Sci. 12:588847. doi: 10.3389/fpls.2021.588847

HIGHLIGHTS

- GB and MT protect the homeostasis by decreasing the ROS, EL, and MDA.
- GB and MT promote the antioxidant activities including AOX.
- GB improves better salt tolerance compared to MT.

INTRODUCTION

Salinity is one of the most threatening abiotic stresses that can cause significant losses in agricultural crop production. Salinity can trigger an oxidative stress on plants at the sub-cellular level by overproduction and accumulation of reactive oxygen species (ROS), such as hydrogen peroxide (H_2O_2) and hydroxyl free radical (·OH) (Acosta-Motos et al., 2017; Hernández, 2019). Salt stress deprives plants to access soil water by increasing the osmotic strength of the soil solution. It can severely affect plant growth and photosynthetic apparatus by promoting ion toxicity and oxidative stress (Volkmar et al., 1998). There have been numerous studies to investigate the effect of exogenous application of melatonin (MT) or glycine betaine (GB) in plants under salt stress. Results showed that both of them can improve salt tolerance in various plant species. The glycine betaine, also named osmoprotectant (compatible solute) is belongs to the group of osmolytes that are present in all living organisms. GB (quaternary ammonium compound) is one the most well-known osmoprotectant and confers tolerance to abiotic stress in different plants (McNeil et al., 1999; Li et al., 2019). During abiotic stresses, GB can protect plant cells from oxidative stress by enhancing the antioxidant system (Demiral and Türkan, 2004; Malekzadeh, 2015). Meanwhile, the melatonin (N-acetyl-5-methoxytryptamine) plays also a vital role in plant stress tolerance. MT is an indolic compound derived from serotonin (5-hydroxytryptamine) and a multi-regulatory molecule that has many specific functions in plant physiology (Arnao and Hernández-Ruiz, 2019). Indeed, MT can improve homeostasis and photosynthesis and regulates gene expression in response to salt stress in plants (Szafrańska et al., 2016; Martinez et al., 2018). MT can activate the antioxidant systems in response to abiotic stresses, including salt stress. This phenomenon has been demonstrated by different authors in different species, such as soybean, rice, maize, radish, cucumber, papaya, and watermelon (Li et al., 2019). In rapeseed and cucumber, MT can significantly decrease the concentration of ROS induced by abiotic stress (Li et al., 2018). Furthermore, the literature review shows that the effect of salinity on woody plants is omnipresent and becomes disturbing with global climate change. Plants naturally establish diverse mechanisms to survive under certain salt concentrations in soil, which can be resulting in their death or growth inhibition (Flowers and Yeo, 1989).

Dalbergia odorifera T. Chen, a woody plant also named as fragrant rosewood, is a semi-deciduous perennial tree widely distributed in tropical areas, particularly in China. This plant is endemic to Hainan Island and belongs to the family of Leguminosae; this plant is threatened by habitat loss and overexploitation due to timber usage (Liu et al., 2019).

The demand for high-quality seedlings of fragrant rosewood in southern areas increases for use in forest establishment (Li et al., 2018). Many studies have investigated the positive effects of MT and GB on crop plants subjected to diverse abiotic stresses, but few works were conducted on woody plants. Thus, the overall goal of this present work was to investigate how *D. odorifera* seedlings respond to exogenous GB or MT. Moreover, the fact that MT might be considered as a phytohormone because of its structure and functions similar to auxin (IAA), it can improve the redox homeostasis and has a strong power to regulate plant growth (Arnao and Hernández-Ruiz, 2019). Meanwhile, GB promotes growth and survival of plants counteracting metabolic dysfunctions caused by stress (Annunziata et al., 2019). Thus, it is of interest to know which molecule is more effective to provide salt stress tolerance in plant. Hence, we hypothesized that MT might improve salt tolerance better than GB. Many studies have revealed that the alternative oxidase (AOX) gene expression is enhanced by different environmental stresses, including severe salinity. Furthermore, AOX is an antioxidant enzyme that has the same role as guaiacol peroxidase (POD) or superoxide dismutase (SOD) in regulating the synthesis of ROS, such as superoxide and H_2O_2. Considering that exogenous GB and MT increases the antioxidant enzyme activities in diverse species under abiotic stresses. In this study, we also hypothesized that the AOX activity would be enhanced by exogenous GB and MT application under salt stress.

MATERIALS AND METHODS

Plant Materials and Experimental Design

The layout of the trial was a factorial experiment in a completely randomized design using two factors and six replicates. The factors included (i) salinity level (Sodium chloride) (11.0 and 18.3 dS/m), (ii) MT and GB level (MT0.05 and 0.1 mM; GB 10 and 50 mM). The study was carried out in a greenhouse at Hainan University (20° 03′ 22.80″ N, 110° 19′ 10.20″ E) during April–June 2019. Six-month-old native seedlings of *D. odorifera* were collected in Ledong County (18° 44′ 52″ N, 109° 17′ 31″ E), Hainan province. The seedlings were transplanted in pots and grown under natural light conditions. The pots (10 cm in height and 12 cm in diameter) were filled with red soil mixed with 30% of sand. After a month of growth, healthy seedlings with approximately the same height and size of twig were selected. Treatments were designed as follows: (1) **CK:** control, well-watered conditions; (2) **M1**: 0.05 mM MT; (3) **M1S1**: 0.05 mM MT and 150 mM salt solution; (4) **M1S2**: 0.05 mM MT and 250 mM salt solution; (5) **M2**: 0.1 mM MT; (6) **M2S1**: 0.1 mM MT and 150 mM salt solution; (7) **M2S2**: 0.1 mM MT and 250 mM salt solution; (8) **G1**: 10 mM GB; (9) **G1S1**: 10 mM GB and 150 mM salt solution; (10) **G1S2**: 10 mM GB and 250 mM salt solution; (11) **G2**: 50 mM GB; (12) **G2S1**: 50 mM GB and 150 mM salt solution; (13) **G2S2**: 50 mM GB and 250 mM salt solution (14) **S1**: 150 mM salt solution; (15) **S2**: 250 mM salt solution. The treatments were selected on the basis of the articles published by

Ye et al. (2016), Kolář et al. (2003), and Wei et al. (2015). GB and MT solutions were applied first on the substrate (soil) and then sprayed on the leaves 5 days before the salinity treatment and every 2 days during the salt treatment (once in the morning). The seedlings were watered with clean water each day during the experiment to cope with high temperature and light condition in the greenhouse. The seedlings under well-watered and salt stress without MT or GB were sprayed with distilled water. After 25 days of treatment, leaves were harvested and cleaned with distilled water for physiological and biochemical analyses.

Growth Measurements

The leaf length and area were measured by a portable area meter LI-3000C (Li-COR, United States). Increments in leaf number, plant height, and stem diameter were recorded at the last treatment day. Data were collected from six seedlings in each treatment, and leaves were harvested and kept at −80°C. Relative water content, dew point water potential, and electrolyte leakage were measured on the harvest day.

Photosynthetic Parameter Measurement

Pigments content was determined in leaves by colorimetric method at absorbance of 663,646, and 470 nm with 80% acetone. Approximately 0.2 g leaf tissue was ground in 10 mL of 80% acetone (v/v), then the extract was centrifuged at 4,000 × *g* at 4°C for 10 min, and the supernatant was used for spectrophotometer readings. The concentration of pigments in each sample was calculated according to the following equations (Lichtenthaler and Wellburn, 1983):

$$\text{Chlorophyll } a = 12.21A663 - 2.81A646$$

$$\text{Chlorophyll } b = 20.13A646 - 5.03A663$$

$$\text{Carotenoid} = (1000A470 - 3.27\text{Chlorophyll } a - 104\text{Chlorophyll } b)/229$$

Net photosynthetic rate (Pn), intercellular carbon dioxide (Ci), stomatal conductance (Gs), transpiration rate (Trr), and water use efficiency (Wue) were measured with a TP-3051D photosynthetic apparatus (Zhejiang Top Instrument Co., Ltd.). Measurements were conducted on six seedlings (three leaves each seedling) in each treatment at 10:00–12:00 am according to Yang et al. (2010).

Determination of Osmolytes, Thiols, Phenols, and Proteins

Proline quantification was conducted by colorimetric method described by Bates et al. (1973) with some modifications. Sample of 500 mg leaves was grounded into liquid nitrogen and homogenized in 10 mL of 3% aqueous sulfosalicylic acid. About 2 mL of the filtered homogenate was mixed with acid-acetic ninhydrin reagent, and added to 2 mL of glacial acetic acid then incubated at 100°C for 1 h. The reaction was stopped by cooling the samples on ice. The chromophore-containing phase was extracted with 4 mL of toluene and the absorbance was measured at 520 nm. The proline concentration was determined using a standard curve.

Total soluble sugar content was determined by anthrone method (0.2% anthrone) according to Yemm and Willis (1954). About 2 mL of the reagent was added to 1 mL of the sample. Absorbance was read at 630 nm and a standard graph was used to calculate the concentration of soluble sugar in each sample.

Thiols react with 5, 5′-dithiobis (2-nitrobenzoic acid) DTNB to form 2-nitro-5-thiobenzoic acid (TNB), which turns yellow in alkaline medium and absorbs at 412 nm (Ellman, 1959).

A standard curve was used to determine the concentration of thiols. In brief, 0.5 M aqueous Tris solution (250 mL), DTNB aqueous solution (DTNB 10 mM; EDTA 20 mM for 25 mL), and 3% sulfosalicylic acid solution were prepared, and glutathione reduced aqueous solution 1 mM (50 mL) was prepared for the standard curve. About 1 mL of the standard solution or sample reacted with 50 μL of DTNB and the added with 1 mL of 0.5 M Tris. Absorbance was read at 412 nm after 30 min.

The total of phenol content was estimated according to the method of Swain and Hillis (1959), which was based on the Folin–Ciocalteu reagent. The oxidation of phenols reduces this reagent to a mixture of blue tungsten and molybdenum oxides. The intensity of the color is proportional to the rate of oxidized phenolic compounds. Leaves were crushed in 80% ethanol (v/v) and stirred hot (80°C) for 30 min. Ethanol was evaporated, and the residue was dissolved in 20 mL of distilled water. About 1 mL aliquot of the sample was added with 7.5 mL of distilled water and 0.5 mL of Folin's reagent and stirred vigorously. After 3 min, 1 mL of saturated Na_2CO_3 solution (40%) was added to the tube. After 1 h, absorbance was read at 725 nm, and the quantity of phenols was determined according to the following formula: A725 × V/Fw (V, volume; Fw, fresh weight).

Soluble protein content was determined by Bradford method; the reagent was prepared with 100 mg of Coomassie Brilliant Blue G-250 diluted in 50 mL of ethanol and 100 mL of 85% phosphoric acid was added. The final solution was completed with distilled water up to 1,000 mL and the reagent was filtered through Whatman filter paper. About 100 mg leaf samples were homogenized in 2 mL of phosphate buffer (pH 7.8). An aliquot of volume *v* (μL) was mixed with 1 mL of the reagent and absorbance was read at 595 nm.

Measurement of Malondialdehyde and ROS Accumulation

Malondialdehyde (MDA) was quantified by colorimetric method using 200 μL of samples with 800 μL of 20% (w/v) TCA containing 0.5% (w/v) 2-thiobarbituric acid in accordance with the method of Yang et al. (2010) with some modifications. About 200 mg of sample was homogenized in 5.0 mL of 5% (w/v) TCA and centrifuged at 12,000 × *g* for 10 min. About 4 mL of 20% trichloroacetic acid (TCA), containing 0.5% thiobarbituric acid (TBA), was mixed with 1 mL of the supernatant, incubated at 95°C for 30 min, cooled on ice, centrifuged at 8,000 × *g* for 15 min, and absorbance was read at 532 nm. Then absorbance was read at 532 nm and corrected by subtracting the value obtained at 600 nm (non-specific absorbance).

H_2O_2 was quantified according to the method of Yang et al. (2010). Approximately 200 mg of fresh leaves were grounded

and homogenized in 0.1% trichloroacetic acid then centrifuged at 6,000 × *g* for 15 min at 4°C. A volume of supernatant was incubated in the presence of potassium iodide added to 10 mM buffer solution. Absorbance was read at 390 nm, and the concentration of $H_2O_2$was estimated via a standard curve.

The concentration of ·OH was estimated with a colorimetric Hydroxyl Free Radical Scavenging Capacity Assay Kit (Nanjing Jiancheng Bioengineering Institute, China) based on the Fenton reaction, which is the most common chemical reaction that can produce ·OH. Approximately 100 mg of grounded leaf was mixed with 2 mL of potassium phosphate buffer (pH 7.8) and centrifuged at 8,000 × *g* for 10 min. Absorbance was recorded at 550 nm, and phosphate buffer solution was used as extraction solution.

Determination of Antioxidant Enzyme Activities

In brief, 1 g of fresh leaves were washed with distilled water, weighed and triturated in a mortar at 4°C by using 10 mL of 0.1 M phosphate buffer solution (pH 7.0) containing 0.1 mM EDTA, 0.1 mM ascorbate, and 1% polyvinylpolypyrrolidone (PVPP). The extract was centrifuged for 15 min at 12,000 × *g* and 4°C and used to assay the enzymatic activity of POD.

Peroxidase activity was measured following the method described by Fielding and Hall (1978) based on monitoring of guaiacol peroxidase scavenging activity by using guaiacol as hydrogen donor. The increase in absorption caused by guaiacol oxidation by H_2O_2 was measured at 470 nm. The reaction mixture contained 10 mM H_2O_2, 50 mM phosphate buffer, and 9 mM guaiacol in a total final volume of 3 mL with the sample.

Catalase activity (CAT) was measured by the procedure described by Aebi (1984). CAT activity was determined by colorimetric assay at 240 nm by measuring the decomposition of H_2O_2. The reaction mixture contained 100 mM phosphate buffer (pH 7.0), 30 mM H_2O_2, and 100 μL of crude extract in a total volume of 3.0 mL, CAT activity was measured and recorded by a decrease in absorbance until 0.5–3 min. CAT activity was calculated using a standard curve.

Ascorbate peroxidase (APX) and **SOD** were determined in accordance with the manufacturer's instructions and as described Yang et al. (2010, 2015). Fresh samples were weighed, then minced to small pieces in liquid nitrogen and homogenized with PBS (10 mg tissue to 100 μL PBS). After that, the particulates were removed by centrifugation (10,000 × *g* for 30 min at 4°C) and the assay was immediately performed with the aliquot and the rest of the samples were stored at −20°C. The supernatant was used for SOD and APX analysis by APX test kit and SOD assay kit based on hydroxylamine method (Nanjing Jiancheng Bioengineering Institute, China).

Alternative oxidase activity was evaluated using ELISA KIT (JL22749 Plant AOX ELISA KIT; 48T/96T). As one of the terminal oxidases of plant mitochondrial electron transport chain, AOX plays an important role in counterattacking salt stress. The reaction uses a purified plant AOX antibody to coat micro strip plate wells to make a solid-phase antibody. The addition of AOX and AOX antibody labeled with HRP to wells gives a complex antibody–antigen–antibody–enzyme complex. After washing completely, the system was added with 3, 3′, 5, 5′-tetramethylbenzidine (TMB) substrate solution. The TMB substrate becomes blue under HRP enzyme-catalyzed reaction. The reaction was terminated by adding sulfuric acid solution, and color change (yellow) was measured spectrophotometrically. For this assay, fresh leaves were collected, weighed, and homogenized with PBS (10 mg of tissues to 100 μL of PBS). The mixture was centrifuged at 1,000 × *g* for 20 min, and the supernatant was carefully collected. The assay was immediately conducted, and absorbance was read at 450 nm. A standard curve was used to estimate the level of AOX.

Statistical Analyses

The results were expressed as mean ± standard error, and Graph Pad prism 8.0.2 software was used to draw the graphs and analyze the data. All data were subjected to analysis of variance for a factorial experiment in a completely randomized design. Statistically significant differences between means were determined at $p \leq 0.05$ using Tukey's HSD (honestly significant difference) test. The principal component analysis was performed by Graph Pad prism 9.0.0. The heat-map was generated by using the 9 PCAs from loadings data.

RESULTS

Effect of GB and MT on Seedling Growth Under Salt Stress

Salt stress (150 and 250 mM) significantly decreased the plant height, leaf area, and the number of leaves ($p \leq 0.05$). The exogenous application of GB and MT enhanced the growth traits of *D. odorifera* under salt stress compared with the salt-stressed seedlings. In general, GB at all levels increased the plant height, leaf area, leaf length, and leaf number compared with the other treatments including the control (**Supplementary Figures 1–3** and **Table 1**). The application of GB and MT under salinity decreased significantly the electrolyte leakage and dew point water potential, and increased strongly the relative water content in leaves. Except for G1S1, GB treatments increased significantly the relative water content even under salt stress. The relative water content in control seedlings was 77.59%, and it were 82.43, 76.67, 78.86, 84.84, 81.42, and 77.67% for G1, G1S1, G1S2, G2, G2S1, and G2S2, respectively (**Table 1**).

Effect of GB and MT on Photosynthetic Parameters

As shown in **Figure 1**, salinity decreased the contents of chlorophyll a, chlorophyll b, and carotenoids in seedlings treated with salinity. The addition of GB during stress increased the concentration of these pigments. Seedlings exposed to G1 possessed significant increase in the content of chlorophyll a and b compared with control seedlings. The carotenoid content significantly increased when the seedlings were subjected to G2 and G2S1. The seedlings exposed to GB treatment showed a better salt tolerance than those subjected to MT treatments. In

TABLE 1 | Variations of plant height increment (PHI), number of leave increment (NLI), stem of diameter increment (SDI), relative water content(RWC), dew-point water potential (DWP), electrolyte leakage (EL), and leaf area (LA) in *D. odorifera* seedlings subjected to melatonin and glycine betaine under salinity (150 and 250 mM).

Treatment NaCl (mM)	GB/MT	PHI (cm)	NLI	SDI (mm)	RWC (%)	DPW (Mpa)	EL (%)	LA (cm^2)
0 mM	−MT/GB(Ck)	48.0 ± 2.82c	8 ± 1.82cde	0.3 ± 0.08bc	77.59 ± 1.62cd	−3.52 ± 0.80ab	25.61 ± 3.83h	18.29 ± 1.03c
	++M1	44.0 ± 2.58d	7 ± 0.81def	0.2 ± 0.07c	77.65 ± 2.83cd	−4.03 ± 0.18abc	26.71 ± 0.96g	18.40 ± 1.16c
	+M2	40.0 ± 1.44e	9 ± 1.80cd	0.4 ± 0.08ab	77.65 ± 2.47cd	−3.95 ± 2.83abc	28.90 ± 2.94ef	10.98 ± 1.08i
	+G1	52.5 ± 1.21b	12 ± 2.44ab	0.2 ± 0.08c	82.43 ± 1.64ab	−2.70 ± 0.69a	17.25 ± 0.80j	15.81 ± 1.02f
	+G2	51.0 ± 0.11b	10 ± 0.83cd	0.4 ± 0.11ab	84.84 ± 4.86a	−3.92 ± 3.81abc	26.71 ± 1.47g	12.52 ± 1.01h
150 mM	−MT/GB (S1)	37.0 ± 1.63f	6 ± 1.41efg	0.3 ± 0.01bc	70.90 ± 3.61e	−7.03 ± 1.63d	32.21 ± 4.13c	9.01 ± 1.44k
	+M1	35.5 ± 1.29fg	6 ± 1.41efg	0.3 ± 0.06bc	72.93 ± 1.63e	−6.45 ± 1.82cd	29.59 ± 6.28de	7.96 ± 1.11m
	+M2	46.5 ± 1.19cd	8 ± 0.81cde	0.4 ± 0.08ab	70.42 ± 6.09e	−5.36 ± 1.24bcd	29.12 ± 1.18def	22.85 ± 1.01b
	+G1	52.5 ± 1.73b	12 ± 2.44ab	0.3 ± 0.01bc	76.67 ± 3.26d	−4.32 ± 0.95abc	28.34 ± 0.73f	24.10 ± 1.01a
	+G2	41.0 ± 0.21e	13 ± 1.63a	0.5 ± 0.02a	81.42 ± 5.21abc	−3.63 ± 0.77ab	22.76 ± 0.97i	16.88 ± 2.14d
250 mM	−MT/GB (S2)	31.0 ± 1.36h	4 ± 0.71g	0.25 ± 0.01c	71.22 ± 2.12e	−14.98 ± 1.63f	36.28 ± 0.76a	8.30 ± 1.01l
	+M1	34.0 ± 0.81g	5 ± 0.91fg	0.3 ± 0.14bc	71.71 ± 1.72e	−11.44 ± 0.92e	36.02 ± 4.36a	6.68 ± 0.16n
	+M2	44.5 ± 1.29d	4 ± 0.84g	0.4 ± 0.08ab	72.81 ± 2.96e	−5.36 ± 5.27ab	36.14 ± 5.24a	12.93 ± 2.12g
	+G1	59.0 ± 0.95a	10 ± 2.16cd	0.4 ± 0.02ab	78.86 ± 1.75cd	−4.30 ± 3.97abc	29.92 ± 1.81d	16.21 ± 1.58e
	+G2	58.0 ± 1.63a	7 ± 1.82def	0.4 ± 0.09ab	77.67 ± 5.95cd	−5.90 ± 0.77bcd	34.06 ± 1.62b	9.94 ± 1.33j

Values are expressed as mean ± SD. The different letters indicate significant differences between treatments ($p < 0.05$) based on Tukey's multiple comparison test. The F-test between salinity factor and GB/MT: plant height increment $P < 0.0001$, number of leaf increment $P = 0.0236$, stem of diameter increment $P = 0.0716$, water content $P = 0.0012$, dew-point water $P < 0.0001$, electrolyte leakage $P < 0.0001$, and leaf area $P < 0.0001$.

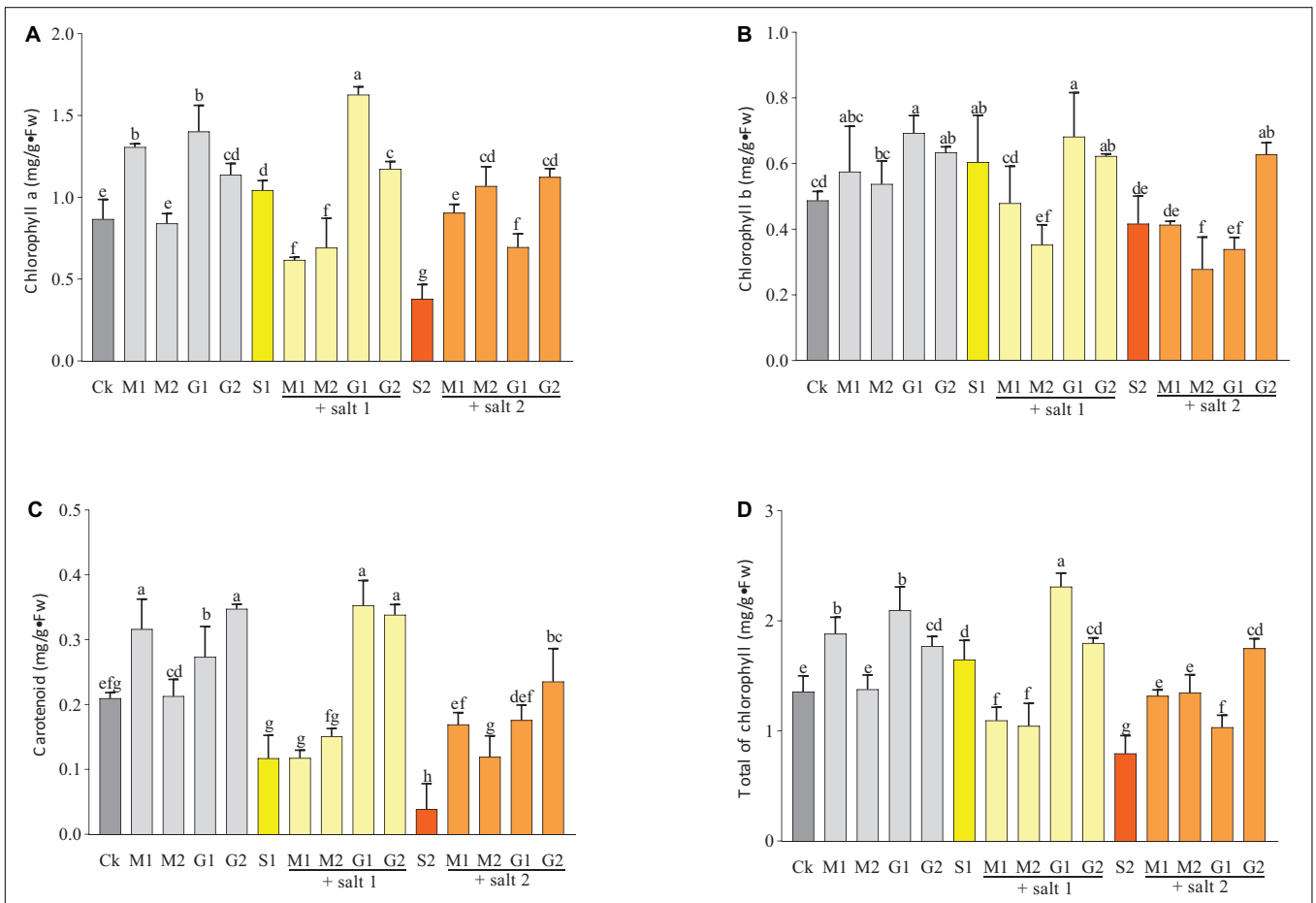

FIGURE 1 | Effects of melatonin and glycine betaine on chlorophyll a **(A)**, chlorophyll b **(B)**, carotenoids **(C)**, and the total of chlorophyll contents **(D)** under salt stress (150 and 250 mM). The bars on the top show SD, and different letters indicate significant differences according to Tukey's multiple comparison test ($p < 0.05$).

severe salt stress (250 mM), the MT treatments increased the total of chlorophyll and carotenoids contents in leaves.

Figure 2 showed that the Pn, Trr, Gs, and Wue in *D. odorifera* seedlings treated with GB or MT significantly increased under severe salt stress. Meanwhile, the Trr in seedlings treated with 0.1 mM MT decreased significantly compared with seedlings treated with S2. The Ci in leaves was reduced significantly when the seedlings were subjected to MT and GB under severe salinity. In mild salt stress (150 mM), the Trr, Pn, and Wue increased in seedlings treated with MT and GB compared with those in seedling treated with S1. Furthermore, treatment with 0.1 mM MT increased the Gs compared with S1. Seedlings that were not subjected to salt stress and treated with MT and GB showed an increase in the Wue and Pn. Based on the matrix table of Tukey's HSD, seedlings treated with GB showed a significant increase in the Wue, Trr, and Pn compared with seedlings treated with MT under severe salt stress. However, plants subjected to 0.1 mM MT exhibited increase in the Pn, Trr, Gs, and Wue compared with the seedlings treated with GB under mild salt stress (**Supplementary Table 1**).

TABLE 2 | Two factor ANOVA (Salinity and GB/MT) for all parameters studied of *Dalbergia odorifera* significance values.

	Salinity factor	GB/MT factor	Interactions between salinity and GB/MT
Plant height increment	<0. 0001****	<0.0001****	<0.0001****
Number of leaf increment	<0.0001****	<0.0001****	0.0236*
Stem of diameter increment	0.0455*	<0.0001****	0.0716 ns
Water content	<0.0001****	<0.0001****	0.0012**
Water potential	<0.0001****	<0.0001****	<0.0001****
Electrolyte leakage	<0.0001****	<0.0001****	<0.0001****
Leaf area	<0.0001****	<0.0001****	<0.0001****
Chlorophyll a	<0.0001****	<0.0001****	<0.0001****
Chlorophyll b	<0.0001****	<0.0001****	<0.0001****
Carotenoid	<0.0001****	<0.0001****	<0.0001****
Total Chlorophyll	<0.0001****	<0.0001****	<0.0001****
Pn	<0.0001****	<0.0001****	<0.0001****
Trr	<0.0001****	<0.0001****	<0.0001****
Gs	<0.0001****	<0.0001****	<0.0001****
Wue	<0.0001****	<0.0001****	<0.0001****
Ci	<0.0001****	<0.0001****	<0.0001****
Proline	<0.0001****	<0.0001****	<0.0001****
Soluble sugar	<0.0001****	<0.0001****	<0.0001****
Total of phenol	<0.0001****	<0.0001****	<0.0001****
Proteins	<0.0001****	<0.0001****	<0.0001****
Thiols	0.0011**	0.0106*	0.1133 ns
MDA	<0.0001****	<0.0001****	<0.0001****
H_2O_2	<0.0001****	<0.0001****	<0.0001****
·OH	<0.0001****	<0.0001****	<0.0001****
AOX	<0.0001****	<0.0001****	<0.0001****
POD	<0.0001****	<0.0001****	<0.0001****
CAT	<0.0001****	<0.0001****	<0.0001****
SOD	<0.0001****	<0.0001****	<0.0001****
APX	<0.0001****	0.0937 ns	0.0090**

*****p-value < 0.0001, **p-value < 0.01, *p-value < 0.05, ns P-value > 0.05, no significant.*

Accumulation of Osmolytes, Thiols, Phenols, and Proteins

Under well-watered conditions, the total of phenol content was increased by MT but decreased by treatment with 10 mM GB. Under mild and severe salt stress, only MT-treated seedlings showed a significant increase in the total of phenol content (**Figure 3**).

The concentration of thiols was decreased slightly by MT and GB treatments under salinity or without stress compared with the control. Under mild salinity, seedlings treated with MT or GB showed a similar concentration of thiols. However, under severe salt stress or well-watered condition, the concentration of thiols was significantly enhanced in the leaves of seedlings treated with MT compared with GB-treated seedlings (**Figure 4**).

As shown in **Figure 3**, the proline and soluble sugar contents in the leaves of *D. odorifera* seedlings treated with MT (M1S1, M2S1, M1S2, and M2S2) and GB (G1S1, G2S1, G1S2, and G2S2) decreased significantly under mild and severe salinity compared with those in seedlings that were only treated with salt solution. Meanwhile, the soluble sugar content in seedlings subjected to GB under mild salinity was significantly increased compared with that in seedlings treated with 150 mM salt solution. When the seedlings were treated with MT or GB under well-watered condition, the proline and soluble sugar contents in the leaves increased strongly compared with those in the control group, except for the leaves of seedlings exposed to 0.05 mM MT. At all levels of salinity and well-watered conditions, the MT treatments increased significantly the content of phenols compared with the GB treatments. A comparison with the control of severe salinity group showed that the plants treated with MT had higher concentration of phenols and their concentrations were significantly increased under well-watered conditions. In severe salinity, treatments with 0.05 mM MT and 50 mM GB significantly increased the protein content in seedlings of *D. odorifera* compared with the control group that was subjected to only 250 mM of salt solution. Under mild salinity, the protein content was strongly increased in seedlings treated with 0.05 mM MT or 50 mM GB. Under well-watered conditions, only the plants subjected to 0.05 mM MT showed significant increase in the protein content (**Figure 4**).

Reactive Oxygen Species and MDA Accumulation

Melatonin and GB decreased the ·OH content under salt stress, except in 10 mM GB-treated seedlings under severe salinity (**Figure 5**). GB significantly decreased the ·OH and H_2O_2 contents. Meanwhile the ·OH concentration in plants treated with 50 mM GB was similar to the control group. Seedlings submitted to mild salinity showed lower concentrations of ·OH and H_2O_2 when treated with GB or MT compared with the control group. Under mild and severe salinity treatments, the

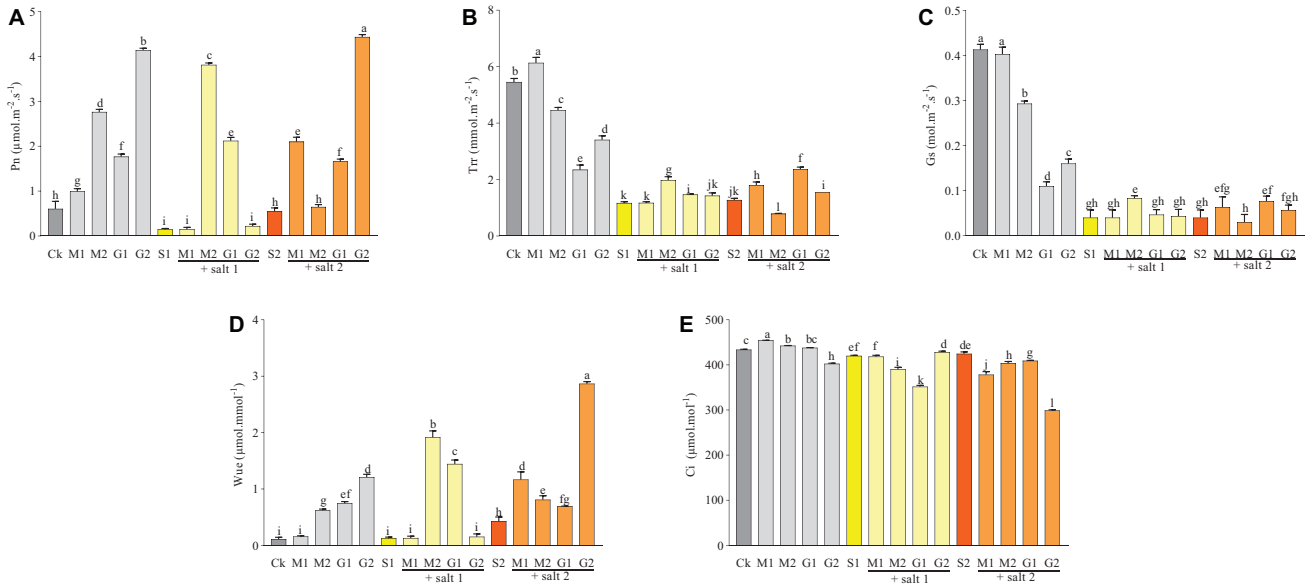

FIGURE 2 | Variations of Pn **(A)**, Trr **(B)**, Gs **(C)**, Wue **(D)**, and Ci **(E)** in *D. odorifera* subjected to melatonin and glycine betaine under salt stress (150 and 250 mM). The bars on the top show SD, and different letters indicate significant differences according to Tukey's multiple comparison test ($p < 0.05$).

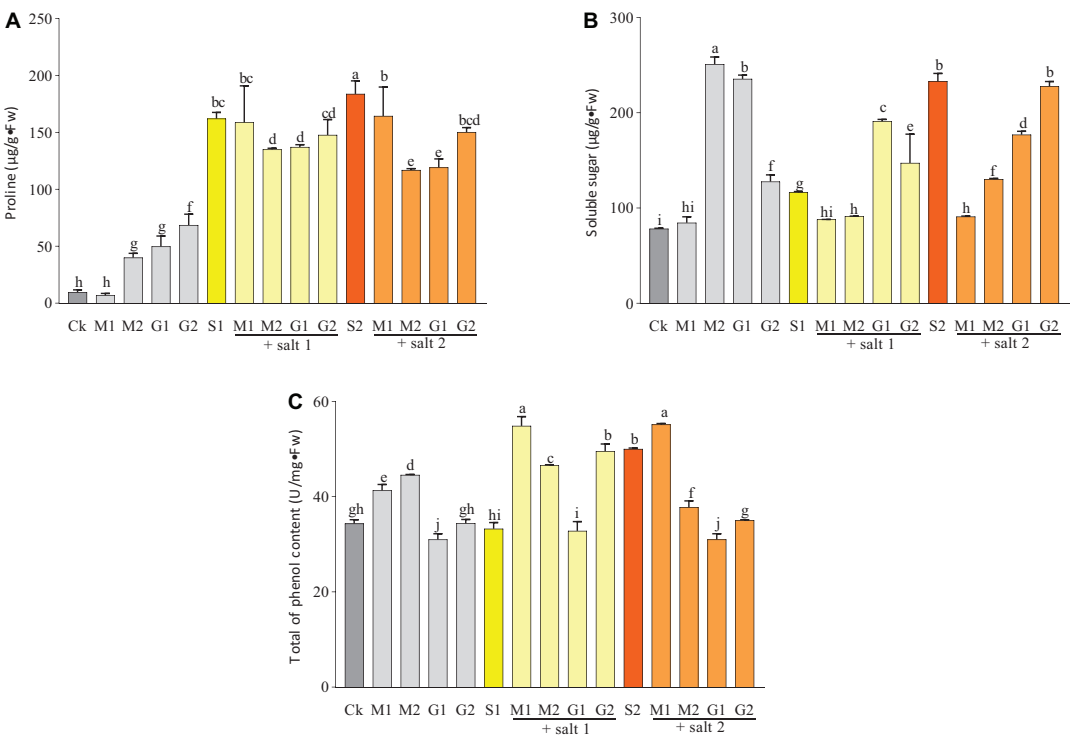

FIGURE 3 | Total of phenol **(A)**, proline **(B)**, and soluble sugar **(C)** contents in *D. odorifera* seedlings submitted to MT and GB under salinity (150 and 250 mM). The bars on the top show SD, and different letters indicate significant differences according to Tukey's multiple comparison test ($p < 0.05$).

matrix table of the Tukey's HSD test showed significant decrease in the H_2O_2 concentration by GB treatment in comparison with MT treatment. For 0.05 mM MT versus 50 mM GB under mild salinity, the P-value was equal to 0.008 (**Table 2** and **Supplementary Table 2**). When the MT treatment was increased to 0.1 mM, the table showed a similar effect on plants treated with 50 mM GB. Seedlings under severe salt stress and treated with MT (M1 and M2) and 10 mM GB showed strong

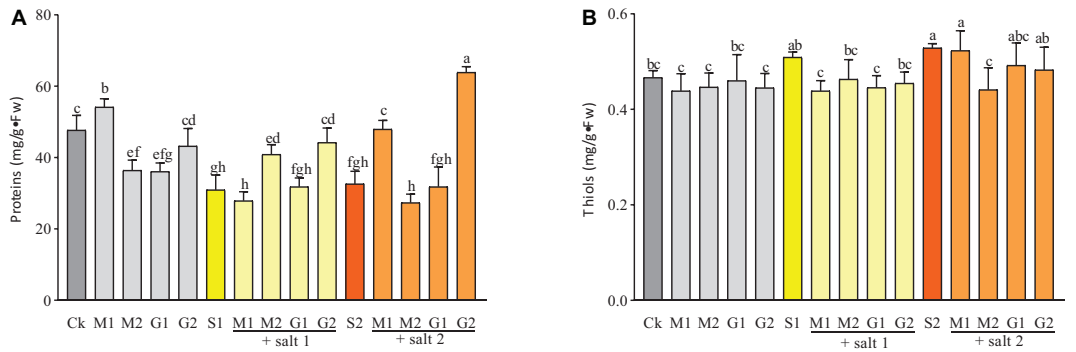

FIGURE 4 | Proteins **(A)** and thiols **(B)** contents in *D. odorifera* seedlings submitted to MT and GB under salinity (150 and 250 mM). The bars on the top show SD, and different letters indicate significant differences according to Tukey's multiple comparison test ($p < 0.05$).

reduction in the ·OH content compared with seedlings subjected to 50 mM GB. Under mild salinity, the MDA levels were similar among all treatments. However, for seedlings subjected to 10 mM GB, the MDA content decreased strongly compared with the control. Although treatments with MT and GB at all levels during severe salinity reduced the MDA content in *D. odorifera* seedlings, the matrix table of the Tukey's HDS concluded that GB treatments significantly decreased the MDA level in the seedlings compared with MT treatments under salinity (**Table 2** and **Supplementary Table 2**).

Antioxidant Activities

Glycine betaine and MT significantly increased the AOX and POD activities in *D. odorifera* seedlings under well-watered and mild salinity conditions compared with the control. However, in severe salinity, only plants subjected to 10 mM GB exhibited an increase in AOX activity compared with the control group (**Figure 6**). The POD activities in salt stressed plants treated with 10 mM GB or 0.1 mM MT were significantly elevated compared with those in the control group S2 and the other groups, where the POD activity was similar. Based on the matrix table of the Tukey's HDS (**Supplementary Table 3**), the AOX activity in plants subjected to 10 mM GB was better than that in plants treated with 0.05 mM MT under mild salinity. Furthermore, the 0.05 mM MT enhanced the AOX activity compared with 50 mM GB.

Mild salinity-treated plants showed a significant increase in the CAT and SOD activities when the seedlings were subjected to 0.05 mM MT and 10 mM GB compared with the control group (**Figure 6**). In severe salinity, only the SOD activity was enhanced by MT (M1 and M2) and GB at 50 mM. The seedlings of *D. odorifera* exhibited increased CAT activity under well-watered conditions and treatment with GB (G1 and G2) and MT at 0.1 mM compared with the control group. The SOD activity in seedlings treated with MT was similar to that in the control group but decreased significantly in plants treated with GB.

As shown in **Supplementary Table 3**, seedlings treated with MT increased the SOD activity under salt stress (p-value lower than 0.0001). However, seedlings treated with GB showed higher CAT activity compared with seedlings subjected to MT under mild salt stress (p-value equal to 0.0002). **Figure 6** shows an increase in the APX activity in the leaves of salt-treated seedlings compared with that in well-watered plants. However, under salinity, only 50 mM GB-treated seedlings showed an increase in the APX activity compared with S2.

Principal Component Analysis

The first nine PCAs from loadings are used to draw a heat map that showed the correlation between different measured parameters. The total cumulative proportion of variance of these nine factors corresponded to 78.09% and their eigenvalues were higher than 1. The proportion of variance of the first two principal components (PC1 and PC2) was 17.76 and 13.63% with eigenvalues equal to 5.15 and 3.95, respectively. Indeed, the most significant contribution to explain the correlation between the measured parameters comes from PC1 and PC2. Thus, each data from different parameters was plot with PC1 and PC2. The **Figure 7** showed a positive association between Leaf area, Gs and Trr; among the photosynthetic pigments excepted Chlorophyll a; between MDA, H_2O_2, proline, APX, and phenols content; amongst AOX, POD and EL; between relative water content and Ci as indicated by the small obtuse angle between their vectors. Based on the heat map, PC2 showed a better perceptible view of the system. Indeed, it exhibited a positive correlation between the plant height, relative water content, dew-point water potential, total of chlorophyll, Trr, Gs and leaf area. Meanwhile the correlation was negative between the plant height and the antioxidants enzymes, MDA or the H_2O_2. The positive correlation between plant height and relative water content or dew point water potential was significantly higher, 0.47 and 0.58, respectively (**Figure 7**).

DISCUSSION

Plants react to salinity over a variety of biochemical and molecular mechanisms, and the effects of salt on plant can be determined based on growth rate, metabolic status, photosynthetic parameters, and other indicators. Exogenous application of GB or MT confers strong salt stress tolerance to

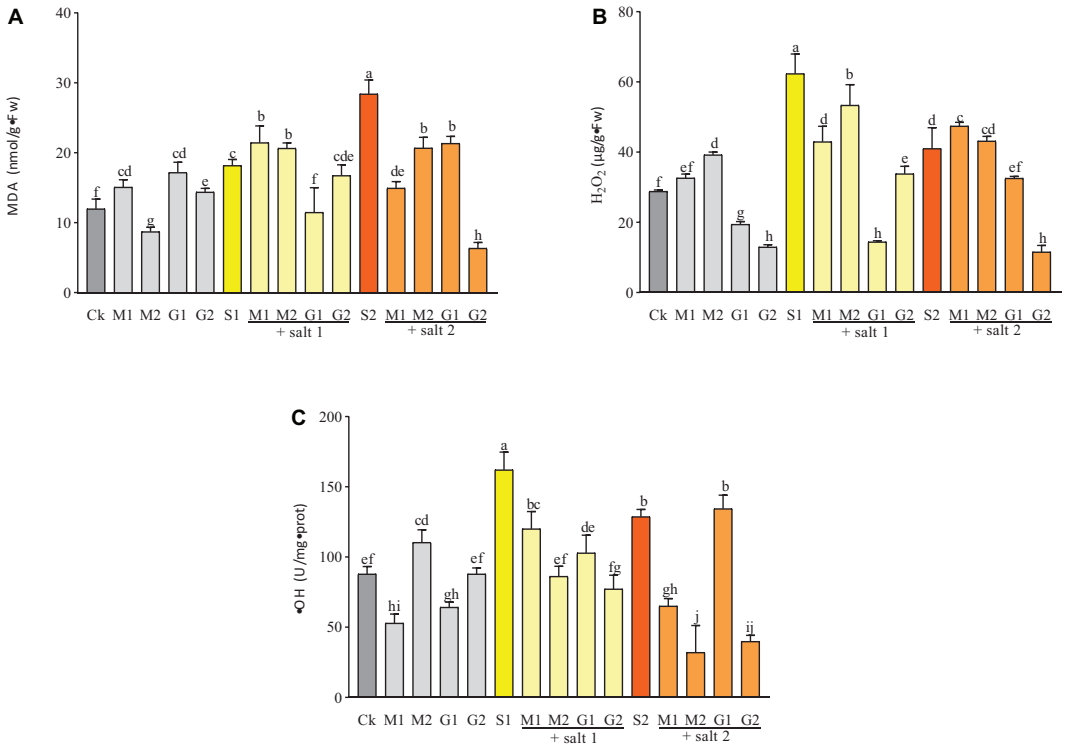

FIGURE 5 | ·OH **(A)**, H_2O_2 **(B)**, and MDA **(C)** contents in *D. odorifera* seedlings submitted to MT and GB under salinity (150 and 250 mM). The bars on the top show SD, and different letters indicate significant differences according to Tukey's multiple comparison test ($p < 0.05$).

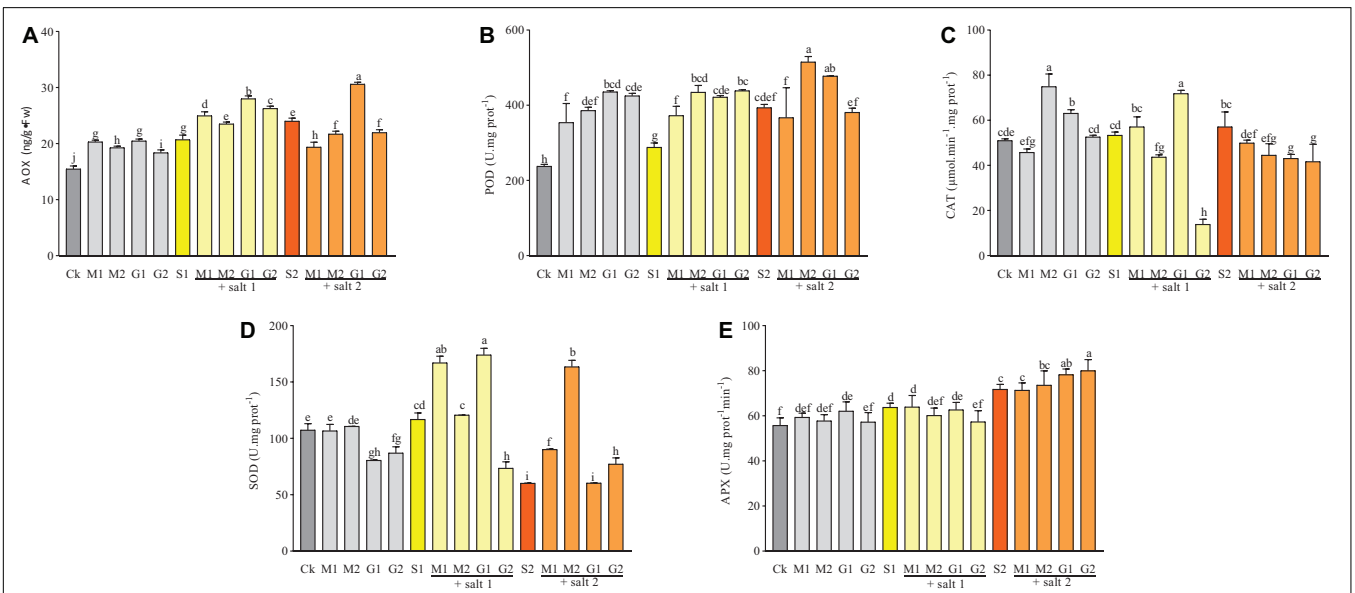

FIGURE 6 | The activities of AOX **(A)**, POD **(B)**, SOD **(C)**, CAT **(D)**, and APX **(E)** in *D. odorifera* seedlings subjected to MT and GB under salt stress (150 and 250 mM).The bars on the top show SD, and different letters indicate significant differences according to Tukey's multiple comparison test ($p < 0.05$).

plants in different mechanisms. GB or MT can affect positively the plant growth in diverse crop plants, such as in soybean (Malekzadeh, 2015; Wei et al., 2015). In this present work, under salt stress or not, seedlings treated with 0.05 mM MT did not show increase or decrease in the plant growth parameters compared with mild salt-stressed plants or well-watered seedlings. In a recent work, Zhong et al. (2020) concluded a benefit effect of 0.15 mM MT on grape seedling

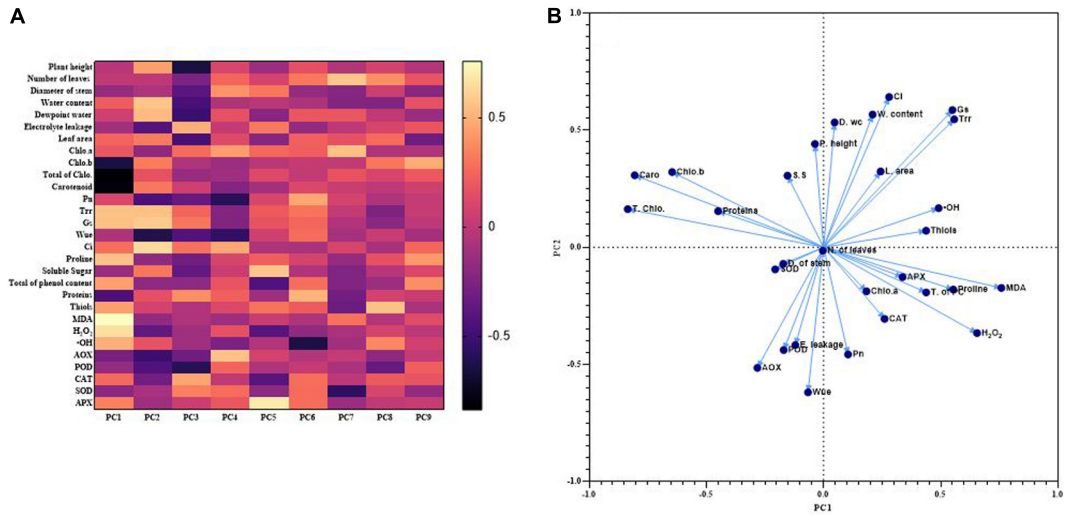

FIGURE 7 | Heat map of correlations among various measured parameters based on the loadings PCAs **(A)** and plot of the first two PCAs showing association between various measured parameters **(B)**.

growth. Seedlings treated with 0.1 mM MT showed better effect on the growth traits of *D. odorifera* seedlings compared with 0.05 mM MT-treated and well-watered plants. Indeed, the optimum concentration of MT that could promote plant growth differs according to the plants studied (Li et al., 2019). Salt stress has a negative effect on plant growth hormones, resulting in reduced growth to permit the plant to cope with stress. In this present study, GB showed better ability to increase plant growth than MT.

Exogenous application of MT and GB can protect and improve the activity of photosystem II. Under salt stress, MT and GB can enhance the biosynthesis of chlorophyll and slow the rate of its decomposition (Annunziata et al., 2019; Li et al., 2019). In this work, GB significantly increased the total of chlorophyll content compared with MT under salinity. One of the effects of salt stress on plants is to reduce water loss by closing the stomata. The variation in Gs manifested that under mild salinity, seedlings treated with MT and GB improved the reopening of stomata, thereby increasing the net photosynthesis rate.

Osmoprotectants, such as proline or soluble sugar, participate in regulating osmotic pressure in the cytoplasm and stabilizing proteins and membranes when plants face an abiotic stress. MT pre-treatment can increase the contents of proline and soluble protein under cold stress (Zhang et al., 2017) and can also limit cellular red-ox disruption by osmo-protection through the regulation of proline homeostasis (Antoniou et al., 2017). Based on recent studies, controversy exists with regard to how MT regulates soluble sugar content in plants. Pre-treatment of *Gossypium hirsutumm* L. seeds with 20 and 50 μM MT can increase the contents of proline, soluble proteins, and sugars (Chen et al., 2020). This present experiment showed a decrease in the proline and soluble sugar contents when the seedlings were subjected to GB and MT under severe salinity. Salinity is supposed to increase the concentrations of proline and soluble sugars to regulate homeostasis. The decrease in the concentrations of proline and soluble sugars is probably due to the adequate supply of GB and MT that are exogenously applied to plant cells. MT and GB can directly scavenge ROS and stabilize osmotic differences between the surroundings of the cell and the cytosol. Furthermore, salt stress affects negatively the concentration of proteins in plant cells. The results showed that GB increased the concentration of proteins better than MT in *D. odorifera* seedlings under saline conditions. Indeed one of the roles of GB is to safeguard proteins against different environmental stresses (Yancey, 1994). To face oxidative damages, the plant cell can use passive detoxification with different molecules, such as thiols, to scavenge the ROS. Zagorchev et al. (2013) reported that thiols are probably involved in plant response to almost all stress factors and are a key to plant stress tolerance. He also related that the leaves of tomato sprayed with 100 μM MT every 5 days showed protection of plant cells from ROS-induced damage by regulating 2-cysteine peroxiredoxin and biosynthesis of S-compounds. And in this present work, thiols were not affected by the supply of MT or GB. The phenolic compounds are other antioxidant molecules that can play a major role by scavenging the ROS. The antioxidant activity of phenolic composites allowed hyacinth bean plants to face oxidative stress caused by salinity. In *Hypericum pruinatum*, phenolic compounds show a significant physiological role in salinity (D'Souza and Devaraj, 2010; Caliskan et al., 2017). The results showed that the total of phenol content was significantly increased by MT and GB treatments under mild salinity.

Salt stress as abiotic stress can trigger an overproduction and accumulation of ROS, which are responsible for oxidative stress. Among ROS, ·OH and H_2O_2 are the protagonists of oxidative damages to proteins, nucleic acids, and lipid peroxidation in plants during stress. H_2O_2 is more stable than the other ROS, such as ·OH (1ns) (Sies, 1993), and is a suitable indicator for

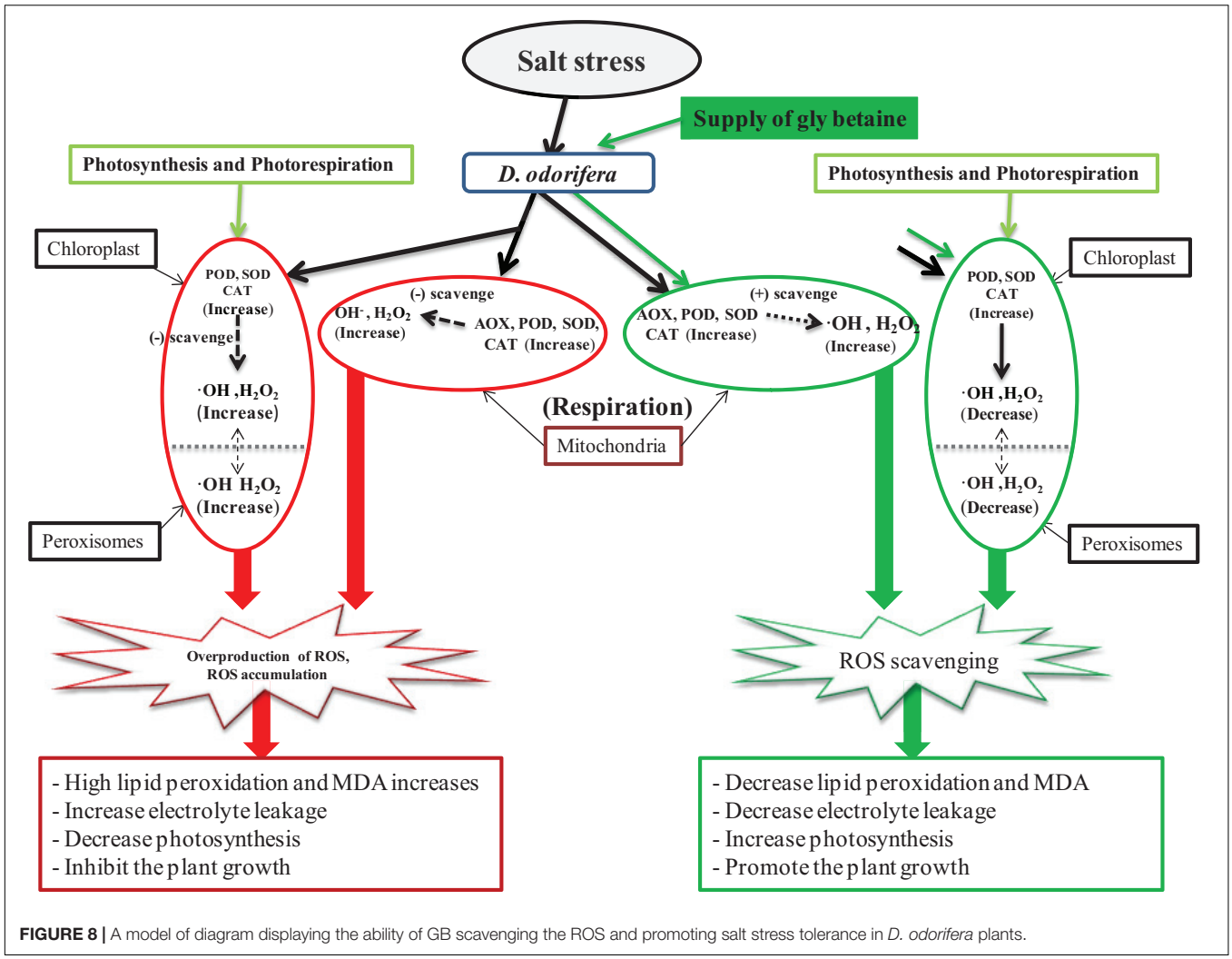

FIGURE 8 | A model of diagram displaying the ability of GB scavenging the ROS and promoting salt stress tolerance in *D. odorifera* plants.

evaluating oxidative stress in plant physiology. Several studies have indicated that exogenous MT application enhances stress tolerance by decreasing the ROS and MDA contents in *Avena nuda* under salt stress (Gao et al., 2019), in *Pisum sativum* against oxidative stress (Szafrańska et al., 2016), and in wheat plant under cadmium stress (Ni et al., 2018). In this present work, MT and GB effectively reduced the concentrations of ROS, MDA, and the EL in fragrant rosewood leaves under saline conditions. A previous report revealed that seeds under salt stress treated with 20 mM MT showed a significant decrease in the MDA and EL levels in cotton seeds (Chen et al., 2020). Under severe salinity, both concentrations 0.05 mM and 0.1 mM of MT were suitable to decrease the MDA and EL contents in *D. odorifera* seedlings. Based on the results, GB treated-seedlings showed higher decrease in the levels of MDA, EL, and ROS compared with MT-treated seedlings under salinity. This phenomenon may be explained by two possibilities: either the concentrations of MT used are insufficient or excessive compared with the concentrations of GB used; or either GB is more efficient to decrease and scavenge ROS and MDA in fragrant rosewood seedlings under salt stress compared with MT.

As one of the most threatening abiotic stresses in plants, salinity can cause perturbation in principal plant metabolic processes, such as photosynthesis, cellular respiration, and photorespiration, which stimulate the overproduction of ROS (Mittler et al., 2004). To counter the attack of the oxidative stress caused by overproduction and accumulation of ROS, plants can use enzymes, such as SOD, POD, CAT, APX, or AOX. These enzymes can scavenge ROS and protect the plant against oxidative damages. Several studies showed that exogenous application of MT or GB increases antioxidant enzyme activities under abiotic stress. In grape seedling leaves, exogenous MT treatment can significantly increase the CAT, SOD, and POD activities (Zhong et al., 2020). Exogenous application of GB can increase the activities of SOD, CAT, APX, or POD in wheat leaves against drought and salinity (Ma et al., 2006; Raza et al., 2007, 2014) as well as in *Glycine max* against salt stress (Malekzadeh, 2015). Furthermore, studies have proven that MT triggers the production of antioxidant enzymes in response to heat, salinity, and cold stress in *Lycopersicon esculemtum* (Martinez et al., 2018) and in tea (Li et al., 2018). In this present experiment, the results showed that exogenous application of GB and MT increased the

POD, SOD, and SOD activities. However, the APX activity was constant and was not affected by the supply of exogenous MT or GB. Seedlings treated with 10 mM GB showed an increase in the POD, SOD, and CAT activities under mild salinity and increase in the POD activity under severe salinity. This finding suggests that a supply of GB can better improve antioxidant enzyme activities in *D. odorifera* seedlings compared with the other treatments under salt stress. One of the peculiarities of this study is the evaluation of AOX activity, which appears in few or none studies concerning the effect of MT or GB on salinity. The AOX can indirectly regulate homeostasis by directly reducing oxygen to water (Saha et al., 2016), and it is induced by different environmental stress factors (Vanlerberghe and McIntosh, 1997). The results of the present work showed that GB and MT increased the AOX activity under mild salinity, but only GB improved the AOX activity in fragrant rosewood seedlings under severe salinity. To summarize, we showed how GB and MT improved salt tolerance in fragrant rosewood seedlings. According to the data, GB promoted better salt tolerance in *D. odorifera* compared with MT. GB enhanced photosynthesis, improved redox homeostasis, decreased MDA accumulation, and increased the antioxidant enzyme activities. GB also contributed to scavenge ROS, thereby alleviating oxidative damages caused by salt stress in *D. odorifera* (**Figure 8**).

CONCLUSION

Exogenous application of GB and MT efficiently relieved salinity damages in *D. odorifera* seedlings by scavenging ·OH, H_2O_2, and MDA. GB and MT promoted the growth parameters by enhancing photosynthetic and antioxidant activities and improved the salt stress tolerance by regulating antioxidant molecules, such as phenolic compounds, or osmolytes, such as proline and soluble sugar. The results confirmed the implication of exogenous MT and GB in improving AOX activity under salt stress. GB improved salt stress tolerance in *D. odorifera* seedlings better than MT. The synthesis of GB in plants has long been a target for engineering stress resistance. Hence, introducing the GB pathway might become a possibility for *D. odorifera* under saline stress.

DATA AVAILABILITY STATEMENT

The original contributions presented in the study are included in the article/**Supplementary Material**, further inquiries can be directed to the corresponding author.

AUTHOR CONTRIBUTIONS

All authors were engaged in this present work. EC and FY designed the experiment. EC performed most of the experiment and wrote the draft of the manuscript. L-FM, D-DL, J-FH, and JZ assist to carry the experiment in the greenhouse. J-FH assisted to perform the antioxidant enzymes analysis. FY provided funding, edited and revised the manuscript.

FUNDING

This work was sponsored by the Hainan Provincial Natural Science Foundation of China (320RC507 and 317052), the National Natural Science Foundation of China (Nos. 32060240 and 31660165), and the Scientific Research Starting Foundation of Hainan University to FY (kyqd1573).

ACKNOWLEDGMENTS

The authors are very grateful to the master degree students Yu-Jin Pu, Li-Jia Zhang, Hai-Bo Wang, and Lu-Yao Guo for their help during the experiment.

SUPPLEMENTARY MATERIAL

The Supplementary Material for this article can be found online at: https://www.frontiersin.org/articles/10.3389/fpls.2021.588847/full#supplementary-material

REFERENCES

Acosta-Motos, J., Ortuño, M., Bernal-Vicente, A., Diaz-Vivancos, P., Sanchez-Blanco, M., and Hernandez, J. (2017). Plant responses to salt stress: adaptive mechanisms. *Agronomy* 7:18. doi: 10.3390/agronomy7010018

Aebi, H. (1984). Catalase in vitro. *Method. Enzymol.* 105, 121–126. doi: 10.1016/S0076-6879(84)05016-3

Annunziata, M. G., Ciarmiello, L. F., Woodrow, P., Dell'Aversana, E., and Carillo, P. (2019). Spatial and temporal profile of glycine betaine accumulation in plants under abiotic stresses. *Front. Plant Sci.* 10:230. doi: 10.3389/fpls.2019.00230

Antoniou, C., Chatzimichail, G., Xenofontos, R., Pavlou, J. J., Panagiotou, E., Christou, A., et al. (2017). Melatonin systemically ameliorates drought stress-induced damage in Medicago sativa plants by modulating nitro-oxidative homeostasis and proline metabolism. *J. Pineal Res.* 62, 12401. doi: 10.1111/jpi.12401

Arnao, M. B., and Hernández-Ruiz, J. (2019). Melatonin: a new plant hormone and/or a plant master regulator? *Trends Plant Sci.* 24, 38–48. doi: 10.1016/j.tplants.2018.10.010

Bates, L. S., Waldren, R. P., and Teare, I. D. (1973). Rapid determination of free proline for water-stress studies. *Plant Soil* 39, 205–207. doi: 10.1007/BF00018060

Caliskan, O., Radusiene, J., Temizel, K. E., Staunis, Z., Cirak, C., Kurt, D., et al. (2017). The effects of salt and drought stress on phenolic accumulation in greenhouse-grown Hypericum pruinatum. *Ital. J. Agron.* 12, 271–275. doi: 10.4081/ija.2017.918

Chen, L., Liu, L., Lu, B., Ma, T., Jiang, D., Li, J., et al. (2020). Exogenous melatonin promotes seed germination and osmotic regulation under salt stress in cotton (*Gossypium hirsutum* L.). *PLoS One* 15:e0228241. doi: 10.1371/journal.pone.0228241

Demiral, T., and Türkan, I. (2004). Does exogenous glycinebetaine affect antioxidative system of rice seedlings under NaCl treatment? *J. Plant Physiol.* 161, 1089–1100. doi: 10.1016/j.jplph.2004.03.009

D'Souza, M. R., and Devaraj, V. R. (2010). Biochemical responses of Hyacinth bean (*Lablab purpureus*) to salinity stress. *Acta Physiol. Plant.* 32, 341–353. doi: 10.1007/s11738-009-0412-2

Ellman, G. L. (1959). Tissue sulfhydryl groups. *Arch. Biochem. Biophys.* 82, 70–77. doi: 10.1016/0003-9861(59)90090-6

Fielding, J. L., and Hall, J. L. (1978). A biochemical and cytochemical study of peroxidase activity in roots of *Pisum sativum*. *J. Exp. Bot.* 29, 983–991. doi: 10.1093/jxb/29.4.983

Flowers, T. S., and Yeo, A. R. (1989). "Effects of salinity on plant growth and crop yields," in *Environmental Stress in Plants*, ed. J. H. Cherry (Berlin: Springer), 101–119. doi: 10.1007/978-3-642-73163-1_11

Gao, W., Feng, Z., Bai, Q., He, J., and Wang, Y. (2019). Melatonin-mediated regulation of growth and antioxidant capacity in salt-tolerant naked oat under salt stress. *Int. J. Mol. Sci.* 20, 1176. doi: 10.3390/ijms20051176

Hernández, J. A. (2019). Salinity tolerance in plants: trends and perspectives. *Int. J. Mol. Sci.* 20, 2408. doi: 10.3390/ijms20102408

Kolář, J., Johnson, C. H., and Macháčková, I. (2003). Exogenously applied melatonin (N -acetyl-5-methoxytryptamine) affects flowering of the short-day plant *Chenopodium rubrum*. *Physiol. Plant.* 118, 605–612. doi: 10.1034/j.1399-3054.2003.00114.x

Li, J., Liu, J., Zhu, T., Zhao, C., Li, L., and Chen, M. (2019). The role of melatonin in salt Stress responses. *Int. J. Mol. Sci.* 20, 1735. doi: 10.3390/ijms20071735

Li, J., Zeng, L., Cheng, Y., Lu, G., Fu, G., Ma, H., et al. (2018). Exogenous melatonin alleviates damage from drought stress in *Brassica napus* L. (rapeseed) seedlings. *Acta Physiol. Plant.* 40:43. doi: 10.1007/s11738-017-2601-8

Li, X., Wei, J.-P., Scott, E., Liu, J.-W., Guo, S., Li, Y., et al. (2018). Exogenous melatonin alleviates cold stress by promoting antioxidant defense and redox homeostasis in *Camellia sinensis* L. *Molecules* 23, 165. doi: 10.3390/molecules23010165

Li, X.-W., Chen, Q.-X., Lei, H.-Q., Wang, J.-W., Yang, S., and Wei, H.-X. (2018). Nutrient uptake and utilization by fragrant rosewood (*Dalbergia odorifera*) seedlings cultured with oligosaccharide addition under different lighting spectra. *Forests* 9:29. doi: 10.3390/f9010029

Lichtenthaler, H. K., and Wellburn, A. R. (1983). Determinations of total carotenoids and chlorophylls a and b of leaf extracts in different solvents. *Biochem. Soc. T.* 11, 591–592. doi: 10.1042/bst0110591

Liu, F., Hong, Z., Xu, D., Jia, H., Zhang, N., Liu, X., et al. (2019). Genetic diversity of the endangered *Dalbergia odorifera* revealed by SSR markers. *Forests* 10:225. doi: 10.3390/f10030225

Ma, Q.-Q., Wang, W., Li, Y.-H., Li, D.-Q., and Zou, Q. (2006). Alleviation of photoinhibition in drought-stressed wheat (*Triticum aestivum*) by foliar-applied glycinebetaine. *J. Plant Physiol.* 163, 165–175. doi: 10.1016/j.jplph.2005.04.023

Malekzadeh, P. (2015). Influence of exogenous application of glycinebetaine on antioxidative system and growth of salt-stressed soybean seedlings (*Glycine max* L.). *Physiol. Mol. Biol. Plants* 21, 225–232. doi: 10.1007/s12298-015-0292-4

Martinez, V., Nieves-Cordones, M., Lopez-Delacalle, M., Rodenas, R., Mestre, T., Garcia-Sanchez, F., et al. (2018). Tolerance to stress combination in tomato plants: new insights in the protective role of melatonin. *Molecules* 23, 535. doi: 10.3390/molecules23030535

McNeil, S. D., Nuccio, M. L., and Hanson, A. D. (1999). Betaines and related osmoprotectants. Targets for metabolic engineering of stress resistance. *Plant Physiol.* 120, 945–949. doi: 10.1104/pp.120.4.945

Mittler, R., Vanderauwera, S., Gollery, M., and Van Breusegem, F. (2004). Reactive oxygen gene network of plants. *Trends Plant Sci.* 9, 490–498. doi: 10.1016/j.tplants.2004.08.009

Ni, J., Wang, Q., Shah, F., Liu, W., Wang, D., Huang, S., et al. (2018). Exogenous melatonin confers cadmium tolerance by counterbalancing the hydrogen peroxide homeostasis in wheat seedlings. *Molecules* 23, 799. doi: 10.3390/molecules23040799

Raza, M. A., Saleem, M., Shah, G., Khan, I., and Raza, A. (2014). Exogenous application of glycinebetaine and potassium for improving water relations and grain yield of wheat under drought. *J. Soil Sci. Plant Nutr.* 14, 348–364. doi: 10.4067/S0718-95162014005000028

Raza, S. H., Athar, H. R., Ashraf, M., and Hameed, A. (2007). Glycinebetaine-induced modulation of antioxidant enzymes activities and ion accumulation in two wheat cultivars differing in salt tolerance. *Environ. Exp. Bot.* 60, 368–376. doi: 10.1016/j.envexpbot.2006.12.009

Saha, B., Borovskii, G., and Panda, S. K. (2016). Alternative oxidase and plant stress tolerance. *Plant Signal. Behav.* 11, e125630. doi: 10.1080/15592324.2016.1256530

Sies, H. (1993). Strategies of antioxidant defense. *Eur. J. Biochem.* 215, 213–219. doi: 10.1111/j.1432-1033.1993.tb18025.x

Swain, T., and Hillis, W. E. (1959). The phenolic constituents of *Prunus domestica. I.* — The quantitative analysis of phenolic constituents. *J. Sci. Food Agr.* 10, 63–68. doi: 10.1002/jsfa.2740100110

Szafrańska, K., Reiter, R. J., and Posmyk, M. M. (2016). Melatonin application to pisum sativum L. seeds positively influences the function of the photosynthetic apparatus in growing seedlings during paraquat-induced oxidative stress. *Front. Plant Sci.* 7:1663. doi: 10.3389/fpls.2016.01663

Vanlerberghe, G. C., and McIntosh, L. (1997). Alternativeoxidase: from gene to function. *Annu. Rev. Plant Physiol. Plant Mol. Biol.* 48, 703–734. doi: 10.1146/annurev.arplant.48.1.703

Volkmar, K. M., Hu, Y., and Steppuhn, H. (1998). Physiological responses of plants to salinity: a review. *Can. J. Plant Sci.* 78, 19–27. doi: 10.4141/P97-020

Wei, W., Li, Q.-T., Chu, Y.-N., Reiter, R. J., Yu, X.-M., Zhu, D.-H., et al. (2015). Melatonin enhances plant growth and abiotic stress tolerance in soybean plants. *Journal of Experimental Botany* 66, 695–707. doi: 10.1093/jxb/eru392

Yancey, P. H. (1994). "Compatible and counteracting solutes," in *Cellular and Molecular Physiology of Cell Volume Regulation*, ed. K. Strange (Boca Raton, FL: CRC Press), 81–109. doi: 10.1201/9780367812140-7

Yang, F., Han, C., Li, Z., Guo, Y., and Chan, Z. (2015). Dissecting tissue- and species-specific responses of two Plantago species to waterlogging stress at physiological level. *Environ. Exp. Bot.* 109, 177–185. doi: 10.1016/j.envexpbot.2014.07.011

Yang, F., Wang, Y., and Miao, L.-F. (2010). Comparative physiological and proteomic responses to drought stress in two poplar species originating from different altitudes. *Physiol. Plant.* 139, 388–400. doi: 10.1111/j.1399-3054.2010.01375.x

Ye, J., Wang, S., Deng, X., Yin, L., Xiong, B., and Wang, X. (2016). Melatonin increased maize (*Zea mays* L.) seedling drought tolerance by alleviating drought-induced photosynthetic inhibition and oxidative damage. *Acta Physiol. Plant.* 38:48. https://doi.org/10.1007/s11738-015-2045-y

Yemm, E. W., and Willis, A. J. (1954). The estimation of carbohydrates in plant extracts by anthrone. *Biochem. J.* 57, 508—514. doi: 10.1042/bj0570508

Zagorchev, L., Seal, C., Kranner, I., and Odjakova, M. (2013). A central role for thiols in plant tolerance to abiotic stress. *Int. J. Mol. Sci.* 14, 7405–7432. doi: 10.3390/ijms14047405

Zhang, Y. P., Xu, S., Yang, S. J., and Chen, Y. Y. (2017). Melatonin alleviates cold-induced oxidative damage by regulation of ascorbate–glutathione and proline metabolism in melon seedlings (*Cucumis melo* L.). *J. Hortic. Sci. Biotechnol.* 92, 313–324. doi: 10.1080/14620316.2016.1266915

Zhong, L., Lin, L., Yang, L., Liao, M., Wang, X., Wang, J., et al. (2020). Exogenous melatonin promotes growth and sucrose metabolism of grape seedlings. *PLoS One* 15:e0232033. doi: 10.1371/journal.pone.0232033

Conflict of Interest: The authors declare that the research was conducted in the absence of any commercial or financial relationships that could be construed as a potential conflict of interest.

frontiers in Plant Science

MINI REVIEW
published: 19 March 2021
doi: 10.3389/fpls.2021.639769

Synergies and Entanglement in Secondary Cell Wall Development and Abiotic Stress Response in Trees

Heather D. Coleman[1], Amy M. Brunner[2] and Chung-Jui Tsai[3,4,5]*

[1]Department of Biology, Syracuse University, Syracuse, NY, United States, [2]Department of Forest Resources and Environmental Conservation, Virginia Tech, Blacksburg, VA, United States, [3]Department of Plant Biology, University of Georgia, Athens, GA, United States, [4]Department of Genetics, University of Georgia, Athens, GA, United States, [5]Warnell School of Forestry and Natural Resources, University of Georgia, Athens, GA, United States

A major challenge for sustainable food, fuel, and fiber production is simultaneous genetic improvement of yield, biomass quality, and resilience to episodic environmental stress and climate change. For *Populus* and other forest trees, quality traits involve alterations in the secondary cell wall (SCW) of wood for traditional uses, as well as for a growing diversity of biofuels and bioproducts. Alterations in wood properties that are desirable for specific end uses can have negative effects on growth and stress tolerance. Understanding of the diverse roles of SCW genes is necessary for the genetic improvement of fast-growing, short-rotation trees that face perennial challenges in their growth and development. Here, we review recent progress into the synergies and antagonisms of SCW development and abiotic stress responses, particularly, the roles of transcription factors, SCW biogenesis genes, and paralog evolution.

Keywords: abiotic stress, secondary cell wall, *Populus*, drought, nutrient stress, gene duplication

OPEN ACCESS

Edited by:
Paula Casati,
Centro de Estudios Fotosintéticos y Bioquímicos (CEFOBI), Argentina

Reviewed by:
Qingzhang Du,
Beijing Forestry University, China
Jin-Gui Chen,
Oak Ridge National Laboratory (DOE), United States

****Correspondence:***
Heather D. Coleman
hcoleman@syr.edu

Specialty section:
This article was submitted to Plant Abiotic Stress, a section of the journal Frontiers in Plant Science

Received: *09 December 2020*
Accepted: *01 March 2021*
Published: *19 March 2021*

Citation:
Coleman HD, Brunner AM and Tsai C-J (2021) Synergies and Entanglement in Secondary Cell Wall Development and Abiotic Stress Response in Trees. Front. Plant Sci. 12:639769. doi: 10.3389/fpls.2021.639769

INTRODUCTION

The plant secondary cell wall (SCW) plays important roles. In the stem, it participates in structure, form, and function, as a part of the water transport system. Throughout the plant, it is an important part of the defense system, as a barrier to attack, and in systematic response to biotic and abiotic stress. The cell wall acts as the first line of defense, and cell wall integrity sensing and maintenance are tightly integrated with biotic and abiotic stress signaling (Bacete et al., 2018). Cell wall plasticity is key to a plant's capacity to adjust to environmental conditions, such as water and nutrient availability, and adapt to specific climates (Landi and Esposito, 2017; Lee et al., 2017). The stress response role of the cell wall has been previously reviewed, particularly with regards to cell wall integrity as a mechanism for sensing and responding to stress (Novakovic et al., 2018; Vaahtera et al., 2019; Anderson and Kieber, 2020). Here, we focus on trees, highlighting examples of regulatory and SCW metabolism genes that indicate both synergy and antagonism in achieving multiple goals of improved stress resilience, biomass yield, and biomass quality.

The SCW consists of a complex network of cellulose, hemicellulose, and lignin (reviewed by Kumar et al., 2016; Meents et al., 2018; Zhong et al., 2019). Prior to maturity, production of this network is influenced by external factors. These interactions and their effect on biomass yield and quality traits are especially complex in trees where harvested wood is the result of a

multi-year history, from 2- to 3-year coppice cycles to decades of genotype × environment interactions. Optimum growth depends on developmental and physiological transitions being appropriately timed for the local climate (Cooke et al., 2012; Brunner et al., 2017). In temperate and boreal zones, this requires preparation for the cold and dehydration stresses of winter and subsequent reversal to allow resumption of growth with transitions occurring at seasonal times that avoid frost injury and optimally capture resources to support growth. Although photoperiod, prolonged chilling temperatures and accumulated exposure to warm temperature are primary signals for key phenological changes, other environmental factors modulate the timing and rate of these transitions (Cooke et al., 2012; Ding and Nilsson, 2016; Brunner et al., 2017; Maurya and Bhalerao, 2017). In temperate regions, water stress generally increases in mid to late summer, a trend thought to drive the transition from large vessel earlywood to dense, small vessel latewood (Plomion et al., 2001). In seasonally dry tropical climates, the intra-annual development of some tree taxa is characterized by distinct periods of rest and rapid shoot growth. Temperate taxa such as *Populus*, *Betula*, and many *Salix* species are free growing, a major factor for suitability as short rotation woody biomass crops. Their shoots have the capacity to continue to grow until a critical daylength threshold occurs; this capacity is limited by other factors, such as water and nutrient availability. Thus, achieving optimal woody biomass yield and quality requires increased understanding of the interplay among primary determinates of seasonal transitions and more episodic or site-specific stresses.

Not surprisingly, manipulation of SCW biosynthesis can result in widespread changes in both the metabolome and transcriptome that might lead to negative effects on growth and development (Xie et al., 2018b; Vanholme et al., 2019). Frequently, there are indications that altering SCW biosynthesis genes can have a direct or indirect impact on the plant's response to abiotic stress. There is also evidence that sub-functionalization or neo-functionalization of cell wall biosynthesis gene duplicates can have an impact on the relationship between stress-resistance and cell wall structure. Here, we examine the interaction between the SCW and abiotic stress responses, highlighting examples of transcription factors (TFs) and SCW biogenesis genes that directly impact both biomass and stress response, as well as the sub-/neo-functionalization of SCW biosynthesis gene paralogs in the plant response to abiotic stress.

TRANSCRIPTIONAL REGULATION OF SCW AND ABIOTIC STRESS

The intricate regulation of plant growth and stress response is directed in part by a large number of TFs, including MYB and NAC family members (Wilkins et al., 2009; Hu et al., 2010; Ye and Zhong, 2015; Chen et al., 2019). Dual roles of some TFs have been reported in both SCW formation and abiotic stress responses.

An ortholog of *Arabidopsis MYB46* (Zhong et al., 2007) from *Betula platyphylla* was overexpressed and silenced in birch (Guo et al., 2017). Overexpression lines showed improved growth under both salt and osmotic stress, while silenced lines were reduced in growth including above and below ground biomass, as well as chlorophyll content. Overexpression lines had increased levels of proline and reactive oxygen species (ROS) scavenging, attributed to increased expression of *Δ1-pyrroline-5-carboxylate synthetase* (*P5CS*), *superoxide dismutase* (*SOD*), and *peroxidase* (*POD*) genes. The overexpressing lines had increased lignin and cellulose levels and thicker fiber cell walls, but decreased hemicellulose relative to WT; silenced lines showed the opposite pattern. This was attributed to alterations in expression of a suite of lignin biosynthesis genes as well as *cellulose synthases* (*CesAs*), with increased expression in the overexpression lines, but reduced expression in silenced lines. Hemicellulose-related genes displayed the opposite pattern. ChIP-PCR supported interactions between BpMYB46 and promoters of the above-mentioned genes involved in ROS, proline, and SCW biosynthesis.

AtMYB61 induces ectopic lignification and dark photomorphogenesis in *Arabidopsis* (Newman et al., 2004). *AtMYB61* is also expressed in guard cells and its mis-expression has a direct impact on stomatal apertures, smaller in overexpressors and larger in knockout mutants relative to WT (Liang et al., 2005). The *Populus* ortholog PtoMYB170 positively regulates lignin biosynthetic genes, as evidenced by enhanced lignin deposition in PtoMYB170-overexpressing plants and reduced lignification in CRISPR-knockout (KO) lines (Xu et al., 2017). *PtoMYB170* is specifically expressed in guard cells and confers enhanced drought tolerance when overexpressed in *Arabidopsis* (Xu et al., 2017). This suggests that the dual functionality in SCW biogenesis and abiotic stress responses is evolutionarily conserved.

A dual role has also been reported for NAC secondary wall thickening promoting factor/secondary wall-associated NAC domain protein (NST/SND) orthologs in the regulation of SCW formation and abiotic stress resistance in both *Arabidopsis* and birch. *Arabidopsis snd1* mutants with impaired fiber SCW biogenesis (Zhong et al., 2006) were also shown to have reduced survival rate under salt stress (Jeong et al. 2018). Mutant lines had increased levels of ABA, which lends strength to the model that SND1 positively regulates MYB46 and lignin biosynthesis, and negatively regulates ABA signaling and biosynthesis (Jeong et al., 2018).

Hu et al. (2019) characterized the AtSND1 ortholog BpNAC012 in birch. BpNAC012 was expressed predominantly in stems and its expression in leaves increased in plants exposed to salt, osmotic, and drought stress. Silencing of BpNAC012 resulted in thinner fiber walls. While the cell wall thickness was unchanged in overexpression lines, these lines produced more biomass and were more tolerant to salt and osmotic stress, attributed to increased expression of *P5CS1* and *P5CS2* and increased SOD and POD activities. Multiple assays demonstrated interactions between BpNAC012 and the promoters of abiotic stress-responsive (SOD and POD) genes, as well as known lignin, cellulose, and hemicellulose biosynthesis genes and additional SCW TFs. The authors hypothesize a model in which BpNAC012 binds to the core sequence CGT[G/A] in regulation of genes associated with abiotic stress and binds

to the SNBE site in regulation of genes involved in SCW biosynthesis (Hu et al., 2019).

Additional examples of transcriptional co-regulation of growth, defense, and lignification in herbaceous species are discussed in a recent review (Xie et al., 2018b). In trees, the dual role of TFs in regulation of SCW formation and abiotic stress resistance is likely to involve responses to seasonal signals and dormancy-growth transitions, as well as reactions to sporadic stress events.

ROLES OF SCW BIOGENESIS GENES IN ABIOTIC STRESS RESPONSES

The effects of abiotic stresses on SCW biogenesis and wood formation have been covered in other reviews (Moura et al., 2010; Houston et al., 2016; Camargo et al., 2019; Eckert et al., 2019). Although few studies have investigated the role of SCW synthesis genes in stress responses in trees, many transcriptomic studies suggest roles for SCW biosynthesis in both seasonal adaptations and abiotic stress responses, with consequential effects on biomass utilization (Fox et al., 2017; Ployet et al., 2017; Wildhagen et al., 2017; Jokipii-Lukkari et al., 2018). For instance, drought-acclimated *Populus nigra* showed the expected reduction of cambial growth, with an unexpected increase of saccharification potential (Wildhagen et al., 2017). The increased sugar release was unrelated to lignin content but instead, was strongly associated with cell wall matrix polysaccharide biosynthesis and modification, based on gene coexpression network analysis (Wildhagen et al., 2017). Thus, besides well-documented effects of environmental stresses on lignin traits (Moura et al., 2010), the sensitivity of SCW polysaccharide biosynthesis to abiotic stresses also warrants attention.

A few studies show altered expression of stress-related genes in transgenics with modified wood characteristics. For instance, lignin-deficient poplars exhibited transcriptome reprogramming of genes associated with not only cell wall biogenesis and remodeling, but also ROS metabolism, detoxification, and response to various stimuli (Tsai et al., 2020). In particular, genes involved in the glutathione-ascorbate cycle, sulfate assimilation, and cadmium response were upregulated in lignin-reduced poplars. The patterns are in agreement with reported responses of cadmium-exposed plants, including poplars (Herbette et al., 2006; Van De Mortel et al., 2008; Elobeid et al., 2011; Ding et al., 2017), supporting a link between lignification and heavy metal-elicited oxidative stress responses.

Another study investigated tubulin genes encoding components of cortical microtubules that have long been thought to direct cellulose microfibril deposition during cell wall biogenesis (Baskin, 2001). Consistent with this role, several tubulin genes are among the most abundant transcripts in SCW-rich xylem (Hu et al., 2016). However, manipulation of tubulin genes can be lethal or result in abnormal development (Anthony et al., 1999; Burk et al., 2006; Ishida et al., 2007). In poplar, constitutive expression of xylem-biased tubulins led to abnormal vascular development, and plant regeneration was achieved only with post-translational modification mimics of tubulins (Swamy et al., 2015). Those plants showed tissue-dependent tubulin transgene expression, much higher in leaves than xylem, opposite to the expression of endogenous tubulins. No differences in major SCW constituents were detected in transgenic wood; however, extractability of lignin-bound pectin and xylan polysaccharides was increased, as was expression of genes encoding cell wall-modifying enzymes (Swamy et al., 2015). The authors suggest an association between pectin, xylan, and lignin during early stage of SCW biogenesis that is sensitive to subtle tubulin perturbation. In transgenic leaves with elevated expression of tubulin transgenes, pectin levels increased, while expression and activity of pectin methylesterase were reduced (Harding et al., 2018). Transgenic leaves also exhibited altered stomatal behavior, with delayed opening in response to light and delayed closure in response to drought (Swamy et al., 2015), consistent with microtubule involvement in guard cell dynamics. These studies add to the functional multiplicity of tubulins and microtubules in different phases of cell wall biogenesis, associated with both cellulosic and non-cellulosic polysaccharide assembly, and impacting both wood formation and stress responses.

Manipulation of SCW genes can cause tradeoffs between stress resistance and growth. Xyloglucan endotransglycosylase/hydrolase (XTH) acts in the relaxation of the cell wall, which is key in cell expansion during normal growth, and in cell wall remodeling during stress. XTH has been shown to allow or restrict cell wall expansion (Takeda et al., 2002), and to respond to drought stress (Iurlaro et al., 2016). In poplar, PtoXTH27 and PtoXTH34 were indicated to play a role in osmotic stress responses (Jiang et al., 2020).

Given the role of xylem in water transport (Rodriguez-Zaccaro and Groover, 2019), it is not surprising that alterations in wood composition often result in reduced water transport (Kitin et al., 2010). In *Arabidopsis*, this can be mitigated by restoring expression of SCW-related genes in vessels (De Meester et al., 2018). Hence, it will be interesting to test whether similar strategies can be an effective in improving wood quality and yield without negative effects on abiotic stress resilience.

SUB-FUNCTIONALIZATION OF DUPLICATED GENES

A largely unexplored area is the contribution of gene duplication and evolution to the integration or separation of genetic pathways involved in growth, stress resilience, and wood development. Members of the Salicaceae share a relatively recent WGD estimated to have occurred ~60 million years ago, and *Populus* retains ~8,000 Salicoid duplicate gene pairs (Tuskan et al., 2006; Rodgers-Melnick et al., 2012; Dai et al., 2014). Evidence of paralog regulatory divergence can be inferred from the growing wealth of RNA-seq datasets. Spatially-detailed expression profiling of the poplar secondary stem showed that Salicoid duplicates with peak expression during SCW deposition tended to exhibit highly-similar profiles, suggesting that many SCW-associated paralogs have functionally redundant roles (Sundell et al., 2017). However, increasing evidence supports a role for WGD in plant

environmental adaptation (Wu et al., 2020); thus, we compared published transcriptomic studies for evidence that paralogs showing highly-correlated expression in the *Populus* woody stem (Sundell et al., 2017) exhibit regulatory divergence in response to different abiotic stresses (Luo et al., 2015; Swamy et al., 2015; Xue et al., 2016; Lu et al., 2019; Yao et al., 2020), as well as to SCW modification (Tsai et al., 2020). Strikingly, in all these stress-tissue combinations, only one member of these paralog pairs was differentially expressed in response to the stress more often than both paralogs (**Figure 1**). Examples of functional diversification of gene duplicates with regards to SCW synthesis are provided below. With increasing efforts in functional characterization of gene duplicates, the expectation is that neo-/sub-functionalization of wood-expressed paralogs will continue to be identified as one of the mechanisms for tree adaptation to varying environment.

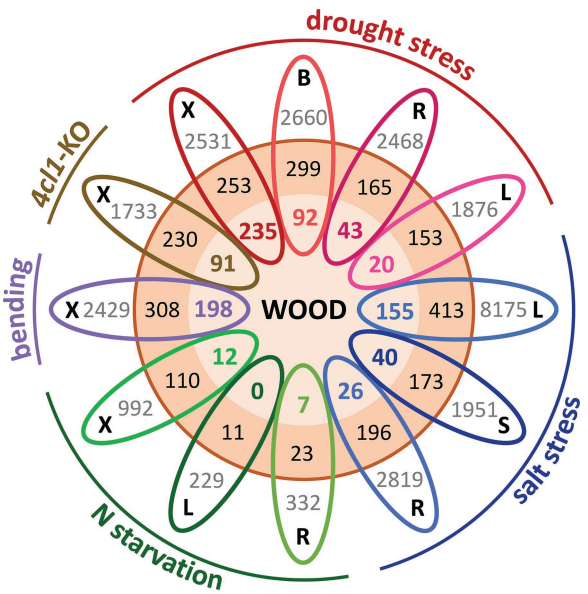

FIGURE 1 | Gene expression divergence in response to abiotic stress among *Populus* wood-expressed paralogs. Salicoid duplicates (3,428 genes or 1,714 paralogs pairs, orange circle) showing expression correlations of ≥0.75 across the secondary stem (Sundell et al., 2017) were interrogated for their responsiveness to different perturbations, including nitrogen (N) starvation in roots, leaves (Luo et al., 2015), and xylem (Lu et al., 2019), tension wood induction by bending (Swamy et al., 2015), drought-stressed xylem, bark, roots, and leaves (Xue et al., 2016), xylem of lignin-deficient trees (4CL1-KO; Tsai et al., 2020), and salt-stressed leaves, stem, and roots (Yao et al., 2020). Each oval represents one tissue (B, bark; L, leaf; R, root; S, stem; and X, xylem) from a given experiment, color-coded by perturbation type. Gray values indicate the total number of differentially expressed genes for the specific tissue-stress combination as reported in the source paper. Boldfaced color values (inner orange circle) indicate wood-expressed paralogous gene pairs where both members of the pair were differentially expressed in response to the indicated stress, whereas black values (outer orange circle) denote the number of cases where only one paralog of a pair showed differential expression. For clarity of illustration, each stress dataset was compared with the wood paralogs individually without considering overlapping gene responses across tissues or stress conditions.

One example is the poplar *5-enolpyruvylshikimiate 3-phosphate synthase* duplicate (Xie et al., 2018a); one encoding a classic EPSP synthase (PtrEPSP-SY) of the shikimate pathway, and the other harboring an extended N terminus with a helix-turn-helix DNA-binding motif (PtrEPSP-TF) with xylem-biased expression. Using linkage-disequilibrium based associate mapping, PtrEPSP-TF was found to exhibit associations with lignin content and syringyl-to-guaiacyl (S/G) ratio (Xie et al., 2018a). *PtrEPSP-TF* overexpression induces ectopic lignin and flavonoid biosynthesis through transcriptional repression of a hAT transposase PtrhAT. PtrhAT represses PtrMYB021, a MYB46 ortholog that regulates biosynthesis of SCW components, including lignin, cellulose, and xylan (Xie et al., 2018a). Neo-functionalization of a primary (shikimate) biosynthetic pathway gene with an additional role in transcriptional regulation of downstream secondary (phenylpropanoid) pathways represents an example of protein moonlighting conferring enhanced fitness of complex organisms (Copley, 2014).

A second example is the poplar paralogs of AtMYB61 involved in regulation of lignin biosynthesis and stomatal aperture noted above. While PtoMYB170 exhibits conserved dual functionality, guard cell expression was not detected for its Salicoid duplicate *PtoMYB216* (Xu et al., 2017). In this case, sub-functionalization might have resulted in more specific involvement of the poplar MYB216 in SCW biogenesis (Tian et al., 2013; Wei et al., 2019).

Another example concerns the poplar *4-coumarate:CoA ligase* (*4CL*) duplicates. In poplar, *4CL1* normally comprises ~90% of xylem *4CL* transcripts and encodes the predominant isoform involved in lignin biosynthesis (Hu et al., 1999; Voelker et al., 2010). *4CL1*-knockout led to ~20% lignin reduction and uniform wood discoloration (Zhou et al., 2015). Knockout of its Salicoid duplicate *4CL5*, the only other xylem-expressed *4CL* gene, has no effect on lignin accrual, suggesting a conditional role (Tsai et al., 2020). Nonetheless, the *4cl1* mutants maintain ~80% WT lignin levels, which must be sustained by *4CL5*. *4CL5* expression was not significantly changed in the *4cl1* mutants; however, *caffeoylshikimate esterase1* (*CSE1*) involved in caffeate biosynthesis and *caffeoyl-CoA O-methyltransferase1* (*CCoAOMT1*) that acts downstream of 4CL product caffeoyl-CoA were upregulated (Tsai et al., 2020). In contrast, the S lignin-specific *ferulate/coniferaldehyde 5-hydroxylases* were downregulated. These, along with elevated levels of caffeic acid in the mutant xylem hint at a novel mechanism for *in vivo* enhancement of 4CL5 function to sustain G lignin biosynthesis at the expense of S lignin (Tsai et al., 2020).

The preferential reductions of S lignin in the *4cl1* poplars (Zhou et al., 2015) contrasts with maize, sorghum, *Arabidopsis*, and switchgrass mutants where *4CL*-knockout led to strong G lignin reductions (Saballos et al., 2008; Van Acker et al., 2013; Park et al., 2017; Xiong et al., 2019). The molecular responses also differ between poplar and *Arabidopsis* mutants, with the latter showing upregulation of early pathway genes *phenylalanine ammonia-lyase2*, *cinnamate 4-hydroxylase*, and *4-coumaroylshikimate 3'-hydroxylase* (Vanholme et al., 2012). Gene coexpression network modeling revealed distinct associations between Salicoid paralogs of *4CL1/4CL5*, *CSE1/CSE2*, and *CCoAOMT1/CCoAOMT2* duplicates, with *4CL5*,

CSE1 and *CCoAOMT1* belonging to the same coexpression module in the *4cl1* mutant network (Tsai et al., 2020). The data provide evidence for coordinated subfunctionalization of multiple gene duplicates in the lignin pathway with conditional roles that may be key for lineage-specific adaptation.

CONCLUSION

To meet the grand challenge for sustainable food, fuel, and fiber under changing climate requires a holistic understanding of diverse roles of SCW genes during plant growth, development, and interactions with the environment. Expanding functional characterization efforts promise to provide additional insights into many of the hidden/conditional roles. This is especially important for woody perennials with a rich repertoire of gene duplicates, many of which likely have evolved *via* sub-/neo-functionalization. The specificity of CRISPR genome editing allows the dissection of functional redundancy vs. specificity of gene duplicates, and the targeted selection of genes and gene duplicates to better understand connections between SCW formation and abiotic stress resistance.

The necessity of exploring the largely unexamined, but clear intersectional implications of SCW development and abiotic stress responses, particularly in the face of changing climate, is clear. Trees present the challenge of integrating multi-year growth accumulation with recurring seasonal phenology and episodic stress events. Reflecting this diversity of environmental interactions, poplar transgenics with altered expression of lignin biosynthesis genes have shown phenotypic differences between greenhouse and field studies (reviewed in Chanoca et al., 2019). Although transgenic tree responses to stress and seasonal cues in controlled conditions provides insight, more field studies are needed to delineate gene functions in trees, and to advance genetic engineering for simultaneous improvement of wood yield, quality, and resilience to environmental stress and climate change.

AUTHOR CONTRIBUTIONS

All authors contributed equally to writing and editing of this manuscript.

FUNDING

This work was supported by the USDA National Institute of Food and Agriculture, McIntire Stennis project 1025004 (AB), the Department of Energy, Office of Biological and Environmental Research grants DE-SC0005140 (C-JT) and DE-SC0008470 (C-JT), and the Center for Bioenergy Innovation (C-JT).

REFERENCES

Anderson, C. T., and Kieber, J. J. (2020). Dynamic construction, perception, and remodeling of plant cell walls. *Annu. Rev. Plant Biol.* 71, 39–69. doi: 10.1146/annurev-arplant-081519-035846

Anthony, R. G., Reichelt, S., and Hussey, P. J. (1999). Dinitroaniline herbicide-resistant transgenic tobacco plants generated by co-overexpression of a mutant alpha-tubulin and a beta-tubulin. *Nat. Biotechnol.* 17, 712–716. doi: 10.1038/10931

Bacete, L., Mélida, H., Miedes, E., and Molina, A. (2018). Plant cell wall-mediated immunity: cell wall changes trigger disease resistance responses. *Plant J.* 93, 614–636. doi: 10.1111/tpj.13807

Baskin, T. I. (2001). On the alignment of cellulose microfibrils by cortical microtubules: a review and a model. *Protoplasma* 215, 150–171. doi: 10.1007/BF01280311

Brunner, A. M., Varkonyi-Gasic, E., and Jones, R. C. (2017). "Phase change and phenology in trees" in *Comparative and evolutionary genomics of angiosperm trees*. eds. A. Groover and Q. Cronk (Cham, Switzerland: Springer), 227–274.

Burk, D. H., Zhong, R. Q., Morrison, W. H., and Ye, Z. H. (2006). Disruption of cortical microtubules by overexpression of green fluorescent protein-tagged alpha-tubulin 6 causes a marked reduction in cell wall synthesis. *J. Integr. Plant Biol.* 48, 85–98. doi: 10.1111/j.1744-7909.2006.00202.x

Camargo, E. L. O., Ployet, R., Cassan-Wang, H., Mounet, F., and Grima-Pettenati, J. (2019). "Chapter seven - digging in wood: new insights in the regulation of wood formation in tree species" in *Advances in botanical research*. ed. F. M. Cánovas (Cambridge, MA, USA: Academic Press), 201–233.

Chanoca, A., de Vries, L., and Boerjan, W. (2019). Lignin engineering in forest trees. *Front. Plant Sci.* 10:912. doi: 10.3389/fpls.2019.00912

Chen, H., Wang, J. P., Liu, H., Li, H., Lin, Y.-C. J., Shi, R., et al. (2019). Hierarchical transcription factor and chromatin binding network for wood formation in *Populus trichocarpa*. *Plant Cell* 31, 602–626. doi: 10.1105/tpc.18.00620

Cooke, J. E. K., Eriksson, M. E., and Junttila, O. (2012). The dynamic nature of bud dormancy in trees: environmental control and molecular mechanisms. *Plant Cell Environ.* 35, 1707–1728. doi: 10.1111/j.1365-3040.2012.02552.x

Copley, S. D. (2014). An evolutionary perspective on protein moonlighting. *Biochem. Soc. Trans.* 42, 1684–1691. doi: 10.1042/BST20140245

Dai, X., Hu, Q., Cai, Q., Feng, K., Ye, N., Tuskan, G. A., et al. (2014). The willow genome and divergent evolution from poplar after the common genome duplication. *Cell Res.* 24, 1274–1277. doi: 10.1038/cr.2014.83

De Meester, B., De Vries, L., Ozparpucu, M., Gierlinger, N., Corneillie, S., Pallidis, A., et al. (2018). Vessel-specific reintroduction of CINNAMOYL-COA REDUCTASE1 (CCR1) in dwarfed ccr1 mutants restores vessel and xylary fiber integrity and increases biomass. *Plant Physiol.* 176, 611–633. doi: 10.1104/pp.17.01462

Ding, S., Ma, C., Shi, W., Liu, W., Lu, Y., Liu, Q., et al. (2017). Exogenous glutathione enhances cadmium accumulation and alleviates its toxicity in *Populus* × canescens. *Tree Physiol.* 37, 1697–1712. doi: 10.1093/treephys/tpx132

Ding, J. H., and Nilsson, O. (2016). Molecular regulation of phenology in trees - because the seasons they are a-changin'. *Curr. Opin. Plant Biol.* 29, 73–79. doi: 10.1016/j.pbi.2015.11.007

Eckert, C., Sharmin, S., Kogel, A., Yu, D., Kins, L., Strijkstra, G.-J., et al. (2019). What makes the wood? Exploring the molecular mechanisms of xylem acclimation in hardwoods to an ever-changing environment. *Forests* 10:358. doi: 10.3390/f10040358

Elobeid, M., Göbel, C., Feussner, I., and Polle, A. (2011). Cadmium interferes with auxin physiology and lignification in poplar. *J. Exp. Bot.* 63, 1413–1421. doi: 10.1093/jxb/err384

Fox, H., Doron-Faigenboim, A., Kelly, G., Bourstein, R., Attia, Z., Zhou, J., et al. (2017). Transcriptome analysis of *Pinus halepensis* under drought stress and during recovery. *Tree Physiol.* 38, 423–441. doi: 10.1093/treephys/tpx137

Guo, H., Wang, Y., Wang, L., Hu, P., Wang, Y., Jia, Y., et al. (2017). Expression of the MYB transcription factor gene BplMYB46 affects abiotic stress tolerance and secondary cell wall deposition in *Betula platyphylla*. *Plant Biotechnol. J.* 15, 107–121. doi: 10.1111/pbi.12595

Harding, S. A., Hu, H., Nyamdari, B., Xue, L.-J., Naran, R., and Tsai, C.-J. (2018). Tubulins, rhythms and cell walls in poplar leaves: it's all in the timing. *Tree Physiol.* 38, 397–408. doi: 10.1093/treephys/tpx104

Herbette, S., Taconnat, L., Hugouvieux, V., Piette, L., Magniette, M. L., Cuine, S., et al. (2006). Genome-wide transcriptome profiling of the early cadmium response of *Arabidopsis* roots and shoots. *Biochimie* 88, 1751–1765. doi: 10.1016/j.biochi.2006.04.018

Houston, K., Tucker, M. R., Chowdhury, J., Shirley, N., and Little, A. (2016). The plant cell wall: a complex and dynamic structure as revealed by the responses of genes under stress conditions. *Front. Plant Sci.* 7:984. doi: 10.3389/fpls.2016.00984

Hu, H., Gu, X., Xue, L.-J., Swamy, P. S., Harding, S. A., and Tsai, C.-J. (2016). Tubulin C-terminal post-translational modifications do not occur in wood forming tissue of *Populus*. *Front. Plant Sci.* 7:1493. doi: 10.3389/fpls.2016.01493

Hu, W. J., Harding, S. A., Lung, J., Popko, J. L., Ralph, J., Stokke, D. D., et al. (1999). Repression of lignin biosynthesis promotes cellulose accumulation and growth in transgenic trees. *Nat. Biotechnol.* 17, 808–812. doi: 10.1038/11758

Hu, R., Qi, G., Kong, Y., Kong, D., Gao, Q., and Zhou, G. (2010). Comprehensive analysis of NAC domain transcription factor gene family in *Populus trichocarpa*. *BMC Plant Biol.* 10:145. doi: 10.1186/1471-2229-10-145

Hu, P., Zhang, K., and Yang, C. (2019). BpNAC012 positively regulates abiotic stress responses and secondary wall biosynthesis. *Plant Physiol.* 179, 700–717. doi: 10.1104/pp.18.01167

Ishida, T., Kaneko, Y., Iwano, M., and Hashimoto, T. (2007). Helical microtubule arrays in a collection of twisting tubulin mutants of *Arabidopsis thaliana*. *Proc. Natl. Acad. Sci. U. S. A.* 104, 8544–8549. doi: 10.1073/pnas.0701224104

Iurlaro, A., De Caroli, M., Sabella, E., De Pascali, M., Rampino, P., De Bellis, L., et al. (2016). Drought and heat differentially affect XTH expression and XET activity and action in 3-day-old seedlings of durum wheat cultivars with different stress susceptibility. *Front. Plant Sci.* 7:1686. doi: 10.3389/fpls.2016.01686

Jeong, C. Y., Lee, W. J., Truong, H. A., Trinh, C. S., Jin, J. Y., Kim, S., et al. (2018). Dual role of SND1 facilitates efficient communication between abiotic stress signalling and normal growth in *Arabidopsis*. *Sci. Rep.* 8:10114. doi: 10.1038/s41598-018-28413-x

Jiang, Y., Li, Y., Lu, C., Tang, Y., Jiang, X., and Gai, Y. (2020). Isolation and characterization of *Populus* xyloglucan endotransglycosylase/hydrolase (XTH) involved in osmotic stress responses. *Int. J. Biol. Macromol.* 155, 1277–1287. doi: 10.1016/j.ijbiomac.2019.11.099

Jokipii-Lukkari, S., Delhomme, N., Schiffthaler, B., Mannapperuma, C., Prestele, J., Nilsson, O., et al. (2018). Transcriptional roadmap to seasonal variation in wood formation of Norway spruce. *Plant Physiol.* 176, 2851–2870. doi: 10.1104/pp.17.01590

Kitin, P., Voelker, S. L., Meinzer, F. C., Beeckman, H., Strauss, S. H., and Lachenbruch, B. (2010). Tyloses and phenolic deposits in xylem vessels impede water transport in low-lignin transgenic poplars: a study by cryo-fluorescence microscopy. *Plant Physiol.* 154, 887–898. doi: 10.1104/pp.110.156224

Kumar, M., Campbell, L., and Turner, S. (2016). Secondary cell walls: biosynthesis and manipulation. *J. Exp. Bot.* 67, 515–531. doi: 10.1093/jxb/erv533

Landi, S., and Esposito, S. (2017). Nitrate uptake affects cell wall synthesis and modeling. *Front. Plant Sci.* 8:1376. doi: 10.3389/fpls.2017.01376

Lee, Y., Karunakaran, C., Lahlali, R., Liu, X., Tanino, K. K., and Olsen, J. E. (2017). Photoperiodic regulation of growth-dormancy cycling through induction of multiple bud-shoot barriers preventing water transport into the winter buds of Norway spruce. *Front. Plant Sci.* 8:2109. doi: 10.3389/fpls.2017.02109

Liang, Y. K., Dubos, C., Dodd, I. C., Holroyd, G. H., Hetherington, A. M., and Campbell, M. M. (2005). AtMYB61, an R2R3-MYB transcription factor controlling stomatal aperture in *Arabidopsis thaliana*. *Curr. Biol.* 15, 1201–1206. doi: 10.1016/j.cub.2005.06.041

Lu, Y., Deng, S., Li, Z., Wu, J., Liu, Q., Liu, W., et al. (2019). Competing endogenous rna networks underlying anatomical and physiological characteristics of poplar wood in acclimation to low nitrogen availability. *Plant Cell Physiol.* 60, 2478–2495. doi: 10.1093/pcp/pcz146

Luo, J., Zhou, J., Li, H., Shi, W., Polle, A., Lu, M., et al. (2015). Global poplar root and leaf transcriptomes reveal links between growth and stress responses under nitrogen starvation and excess. *Tree Physiol.* 35, 1283–1302. doi: 10.1093/treephys/tpv091

Maurya, J. P., and Bhalerao, R. P. (2017). Photoperiod- and temperature-mediated control of growth cessation and dormancy in trees: a molecular perspective. *Ann. Bot.* 120, 351–360. doi: 10.1093/aob/mcx061

Meents, M. J., Watanabe, Y., and Samuels, A. L. (2018). The cell biology of secondary cell wall biosynthesis. *Ann. Bot.* 121, 1107–1125. doi: 10.1093/aob/mcy005

Moura, J. C. M. S., Bonine, C. A. V., De Oliveira Fernandes Viana, J., Dornelas, M. C., and Mazzafera, P. (2010). Abiotic and biotic stresses and changes in the lignin content and composition in plants. *J. Integr. Plant Biol.* 52, 360–376. doi: 10.1111/j.1744-7909.2010.00892.x

Newman, L. J., Perazza, D. E., Juda, L., and Campbell, M. M. (2004). Involvement of the R2R3-MYB, AtMYB61, in the ectopic lignification and dark-photomorphogenic components of the det3 mutant phenotype. *Plant J.* 37, 239–250. doi: 10.1046/j.1365-313X.2003.01953.x

Novakovic, L., Guo, T., Bacic, A., Sampathkumar, A., and Johnson, K. L. (2018). Hitting the wall-sensing and signaling pathways involved in plant cell wall remodeling in response to abiotic stress. *Plan. Theory* 7:89. doi: 10.3390/plants7040089

Park, J.-J., Yoo, C. G., Flanagan, A., Pu, Y., Debnath, S., Ge, Y., et al. (2017). Defined tetra-allelic gene disruption of the 4-coumarate:coenzyme a ligase 1 (Pv4CL1) gene by CRISPR/Cas9 in switchgrass results in lignin reduction and improved sugar release. *Biotechnol. Biofuels* 10:284. doi: 10.1186/s13068-017-0972-0

Plomion, C., Leprovost, G., and Stokes, A. (2001). Wood formation in trees. *Plant Physiol.* 127, 1513–1523. doi: 10.1104/pp.010816

Ployet, R., Soler, M., Carocha, V., Ladouce, N., Alves, A., Rodrigues, J.-C., et al. (2017). Long cold exposure induces transcriptional and biochemical remodelling of xylem secondary cell wall in Eucalyptus. *Tree Physiol.* 38, 409–422. doi: 10.1093/treephys/tpx062

Rodgers-Melnick, E., Mane, S. P., Dharmawardhana, P., Slavov, G. T., Crasta, O. R., Strauss, S. H., et al. (2012). Contrasting patterns of evolution following whole genome versus tandem duplication events in *Populus*. *Genome Res.* 22, 95–105. doi: 10.1101/gr.125146.111

Rodriguez-Zaccaro, F. D., and Groover, A. (2019). Wood and water: how trees modify wood development to cope with drought. *Plants, People, Planet* 1, 346–355. doi: 10.1002/ppp3.29

Saballos, A., Vermerris, W., Rivera, L., and Ejeta, G. (2008). Allelic association, chemical characterization and saccharification properties of brown midrib mutants of sorghum (*Sorghum bicolor* (L.) Moench). *Bioenergy Res.* 1, 193–204. doi: 10.1007/s12155-008-9025-7

Sundell, D., Street, N. R., Kumar, M., Mellerowicz, E. J., Kucukoglu, M., Johnsson, C., et al. (2017). AspWood: high-spatial-resolution transcriptome profiles reveal uncharacterized modularity of wood formation in *Populus tremula*. *Plant Cell* 29, 1585–1604. doi: 10.1105/tpc.17.00153

Swamy, P. S., Hu, H., Pattathil, S., Maloney, V. J., Xiao, H., Xue, L.-J., et al. (2015). Tubulin perturbation leads to unexpected cell wall modifications and affects stomatal behaviour in *Populus*. *J. Exp. Bot.* 66, 6507–6518. doi: 10.1093/jxb/erv383

Takeda, T., Furuta, Y., Awano, T., Mizuno, K., Mitsuishi, Y., and Hayashi, T. (2002). Suppression and acceleration of cell elongation by integration of xyloglucans in pea stem segments. *Proc. Natl. Acad. Sci. U. S. A.* 99, 9055–9060. doi: 10.1073/pnas.132080299

Tian, Q., Wang, X., Li, C., Lu, W., Yang, L., Jiang, Y., et al. (2013). Functional characterization of the poplar R2R3-MYB transcription factor PtoMYB216 involved in the regulation of lignin biosynthesis during wood formation. *PLoS One* 8:e76369. doi: 10.1371/journal.pone.0076369

Tsai, C. J., Xu, P., Xue, L. J., Hu, H., Nyamdari, B., Naran, R., et al. (2020). Compensatory guaiacyl lignin biosynthesis at the expense of syringyl lignin in 4CL1-knockout poplar. *Plant Physiol.* 183, 123–136. doi: 10.1104/pp.19.01550

Tuskan, G. A., Difazio, S., Jansson, S., Bohlmann, J., Grigoriev, I., Hellsten, U., et al. (2006). The genome of black cottonwood, *Populus trichocarpa* (Torr. & Gray). *Science* 313, 1596–1604. doi: 10.1126/science.1128691

Vaahtera, L., Schulz, J., and Hamann, T. (2019). Cell wall integrity maintenance during plant development and interaction with the environment. *Nat. Plants* 5, 924–932. doi: 10.1038/s41477-019-0502-0

Van Acker, R., Vanholme, R., Storme, V., Mortimer, J., Dupree, P., and Boerjan, W. (2013). Lignin biosynthesis perturbations affect secondary cell wall composition and saccharification yield in *Arabidopsis thaliana*. *Biotechnol. Biofuels* 6:46. doi: 10.1186/1754-6834-6-46

Van De Mortel, J. E., Schat, H., Moerland, P. D., Van Themaat, E. V. L., Van Der Ent, S., Blankestijn, H., et al. (2008). Expression differences for genes involved in lignin, glutathione and sulphate metabolism in response to cadmium in *Arabidopsis thaliana* and the related Zn/Cd-hyperaccumulator *Thlaspi caerulescens*. *Plant Cell Environ.* 31, 301–324. doi: 10.1111/j.1365-3040.2007.01764.x

Vanholme, R., De Meester, B., Ralph, J., and Boerjan, W. (2019). Lignin biosynthesis and its integration into metabolism. *Curr. Opin. Biotechnol.* 56, 230–239. doi: 10.1016/j.copbio.2019.02.018

Vanholme, R., Storme, V., Vanholme, B., Sundin, L., Christensen, J. H., Goeminne, G., et al. (2012). A systems biology view of responses to lignin biosynthesis perturbations in *Arabidopsis*. *Plant Cell* 24, 3506–3529. doi: 10.1105/tpc.112.102574

Voelker, S. L., Lachenbruch, B., Meinzer, F. C., Jourdes, M., Ki, C., Patten, A. M., et al. (2010). Antisense down-regulation of 4CL expression alters lignification, tree growth, and saccharification potential of field-grown poplar. *Plant Physiol.* 154, 874–886. doi: 10.1104/pp.110.159269

Wei, K., Zhao, Y., Zhou, H., Jiang, C., Zhang, B., Zhou, Y., et al. (2019). PagMYB216 is involved in the regulation of cellulose synthesis in *Populus*. *Mol. Breed.* 39:65. doi: 10.1007/s11032-019-0970-y

Wildhagen, H., Paul, S., Allwright, M., Smith, H. K., Malinowska, M., Schnabel, S. K., et al. (2017). Genes and gene clusters related to genotype and drought-induced variation in saccharification potential, lignin content and wood anatomical traits in *Populus nigra*. *Tree Physiol.* 38, 320–339. doi: 10.1093/treephys/tpx054

Wilkins, O., Nahal, H., Foong, J., Provart, N. J., and Campbell, M. M. (2009). Expansion and diversification of the *Populus* R2R3-MYB family of transcription factors. *Plant Physiol.* 149, 981–993. doi: 10.1104/pp.108.132795

Wu, S. D., Han, B. C., and Jiao, Y. N. (2020). Genetic contribution of paleopolyploidy to adaptive evolution in angiosperms. *Mol. Plant* 13, 59–71. doi: 10.1016/j.molp.2019.10.012

Xie, M., Muchero, W., Bryan, A. C., Yee, K., Guo, H. B., Zhang, J., et al. (2018a). A 5-enolpyruvylshikimate 3-phosphate synthase functions as a transcriptional repressor in *Populus*. *Plant Cell* 30, 1645–1660. doi: 10.1105/tpc.18.00168

Xie, M., Zhang, J., Tschaplinski, T. J., Tuskan, G. A., Chen, J.-G., and Muchero, W. (2018b). Regulation of lignin biosynthesis and its role in growth-defense tradeoffs. *Front. Plant Sci.* 9:1427. doi: 10.3389/fpls.2018.01427

Xiong, W., Wu, Z., Liu, Y., Li, Y., Su, K., Bai, Z., et al. (2019). Mutation of 4-coumarate: coenzyme A ligase 1 gene affects lignin biosynthesis and increases the cell wall digestibility in maize brown midrib5 mutants. *Biotechnol. Biofuels* 12:82. doi: 10.1186/s13068-019-1421-z

Xu, C., Fu, X., Liu, R., Guo, L., Ran, L., Li, C., et al. (2017). PtoMYB170 positively regulates lignin deposition during wood formation in poplar and confers drought tolerance in transgenic *Arabidopsis*. *Tree Physiol.* 37, 1713–1726. doi: 10.1093/treephys/tpx093

Xue, L.-J., Frost, C. J., Tsai, C.-J., and Harding, S. A. (2016). Drought response transcriptomics are altered in poplar with reduced tonoplast sucrose transporter expression. *Sci. Rep.* 6:33655. doi: 10.1038/srep33655

Yao, W., Li, C., Lin, S., Wang, J., Zhou, B., and Jiang, T. (2020). Transcriptome analysis of salt-responsive and wood-associated NACs in *Populus simonii* × *Populus nigra*. *BMC Plant Biol.* 20:317. doi: 10.1186/s12870-020-02507-z

Ye, Z.-H., and Zhong, R. (2015). Molecular control of wood formation in trees. *J. Exp. Bot.* 66, 4119–4131. doi: 10.1093/jxb/erv081

Zhong, R., Cui, D., and Ye, Z.-H. (2019). Secondary cell wall biosynthesis. *New Phytol.* 221, 1703–1723. doi: 10.1111/nph.15537

Zhong, R., Demura, T., and Ye, Z.-H. (2006). SND1, a NAC domain transcription factor, is a key regulator of secondary wall synthesis in fibers of *Arabidopsis*. *Plant Cell* 18, 3158–3170. doi: 10.1105/tpc.106.047399

Zhong, R., Richardson, E. A., and Ye, Z.-H. (2007). The MYB46 transcription factor is a direct target of SND1 and regulates secondary wall biosynthesis in *Arabidopsis*. *Plant Cell* 19, 2776–2792. doi: 10.1105/tpc.107.053678

Zhou, X., Jacobs, T. B., Xue, L.-J., Harding, S. A., and Tsai, C.-J. (2015). Exploiting SNPs for biallelic CRISPR mutations in the outcrossing woody perennial *Populus* reveals 4-coumarate:CoA ligase specificity and redundancy. *New Phytol.* 208, 298–301. doi: 10.1111/nph.13470

Conflict of Interest: The authors declare that the research was conducted in the absence of any commercial or financial relationships that could be construed as a potential conflict of interest.

frontiers in Plant Science

ORIGINAL RESEARCH
published: 08 April 2021
doi: 10.3389/fpls.2021.650616

Neighbors, Drought, and Nitrogen Application Affect the Root Morphological Plasticity of *Dalbergia odorifera*

*Li-Shan Xiang[1,2], Ling-Feng Miao[1,3] and Fan Yang[1,4,5]**

[1]School of Ecological and Environmental Sciences, Hainan University, Haikou, China, [2]School of Forestry, Hainan University, Haikou, China, [3]School of Plant Protection, Hainan University, Haikou, China, [4]Center for Eco-Environmental Restoration Engineering of Hainan Province, Haikou, China, [5]Key Laboratory of Agro-Forestry Environmental Processes and Ecological Regulation of Hainan Province, Haikou, China

In forest systems, neighbor-induced root morphological plasticity (RMP) is species specific and environment dependent. However, related studies on leguminous woody trees remain sparse. The objectives of this study were to evaluate the root morphological response of the leguminous woody *Dalbergia odorifera* T. Chen to different N-fixing niche neighbors under models of root system contact and isolation and to evaluate whether such response can be modified by drought or the application of nitrogen (N). The relationship between root morphology and the relative competitiveness of the whole *D. odorifera* plantlet was also assessed. *D. odorifera* plantlets from the woody Leguminosae family were used as target species and were grown with either identical N-fixing niche *D. odorifera*, the heterogeneous but con-leguminous *Delonix regia*, or the non-leguminous *Swietenia mahagoni*. All plants were grown under two water conditions (100% and 30% field capacity) and two N treatments (no N application and N application). Two planting models (root system contact in Experiment 1, root system isolation in Experiment 2) were applied to neighboring plantlets. The RMP of *D. odorifera* was assessed based on root morphology, root system classification, root nodules, and RMP-related indices. The growth of *D. odorifera* was estimated based on the relative growth ratio, net assimilation rate, and leaf N content. The relative competitiveness of the whole *D. odorifera* plantlet was evaluated through relative yield. The results of Experiment 1 showed that *D. odorifera* had different RMP responses to a different N-fixing niche neighbor with root system contact. The RMP of *D. odorifera* was promoted by a different N-fixing niche neighbor under conditions of drought or N deficiency. Drought improved the RMP of *D. odorifera* exposed to a different N-fixing niche neighbor. N application converted the promoting effect of *D. regia* on RMP to an inhibitory effect under well-watered conditions. Experiment 2 showed that belowground interaction with a different N-fixing niche neighbor may be the only way to influence RMP, as effects of aboveground interaction were negligible. Finally, correlation analysis showed that neighbor-induced RMP might predict the relative competitiveness of the whole *D. odorifera* plantlet under conditions of drought or N deficiency. These findings highlight the influences of neighbors, drought, and N

OPEN ACCESS

Edited by:
Sanushka Naidoo, University of Pretoria, South Africa

Reviewed by:
Luca Vitale, National Research Council of Italy (CNR), Italy
Agnieszka Piernik, Nicolaus Copernicus University in Toruń, Poland

***Correspondence:**
Fan Yang
yangfan@hainanu.edu.cn; fanyangmlf6303@163.com

Specialty section:
This article was submitted to Plant Abiotic Stress, a section of the journal Frontiers in Plant Science

Received: *07 January 2021*
Accepted: *16 March 2021*
Published: *08 April 2021*

Citation:
Xiang L-S, Miao L-F and Yang F (2021) Neighbors, Drought, and Nitrogen Application Affect the Root Morphological Plasticity of Dalbergia odorifera. Front. Plant Sci. 12:650616. doi: 10.3389/fpls.2021.650616

application on the RMP of *D. odorifera* and contribute to understanding neighbor-induced dynamic changes in the root traits of leguminous woody species in forest systems in the context of climate change.

Keywords: nitrogen contents, relative competitiveness, root morphological plasticity, root nodules, root system contact model, root system isolated model

INTRODUCTION

Water and nitrogen (N) are key resources that often determine individual growth, stand productivity, and dynamics of a community structure. Their low availability can induce belowground competition for resources. Roots, as the main organs that obtain soil resources and the first perceptual organs of belowground interaction, are sensitive to the availability of resources and the presence of neighbors and develop a series of adaptive responses in their presence. Root morphological plasticity (RMP) can be used to evaluate the advantages of resources and neighbors in terms of plant relative competitiveness and plant growth; such advantages can be assessed by root biomass distribution, root proliferation, root volume, root density, root length, specific root length (SRL), and mycorrhizal colonization (Lewis and Tanner, 2000; Bennett et al., 2012; Mou et al., 2012; Poorter et al., 2012; Goisser et al., 2016). With varying availability of resources, RMP may be modified and may influence the outcome of competition for resources (Mou et al., 2012; Ma et al., 2014).

Niche complementarity between species would explore a more exhaustive resource compared with niche similarity (Kahmen et al., 2006). Relevant resource-containing niches between belowground competitors determine the root competitive performance of target species (Zuppinger-Dingley et al., 2014). Compared with non-leguminous plants, N-fixing leguminous plants have extensive root systems and can acquire atmosphere-free N by symbiosis with N-fixing rhizobia in root nodules (Andrews and Andrews, 2017). Given the niche complementarity in N-fixing niches between leguminous and non-leguminous plants, leguminous trees have been widely used to facilitate productivity and to improve the tolerance of neighboring non-leguminous trees in mixed plantations (Lithourgidis et al., 2011; Yao et al., 2019). However, empirical evidence of the root plasticity of leguminous woody trees when interacting with different N-fixing niche neighbors is lacking.

Resource competition theory (Tilman, 1981, 1982, 1987), the stress gradient hypothesis (Bertness and Callaway, 1994), and related practices have confirmed that root competitive responses may be modified by the availability of soil resources (McNickle et al., 2014; Goisser et al., 2016; Guo et al., 2016). Previous studies on root responses to competition for resources have focused on either non-leguminous species in a forest ecosystem (Wang et al., 2018a) or leguminous herbaceous crops in an agroforestry ecosystem (Hauggaard-Nielsen et al., 2001; Wang et al., 2017). Leguminous woody species also play a key role in measuring the impact of external conditions on the dynamics of forestry systems (Wang et al., 2018b), especially in the context of climate change. Water and N as main inducers of competition for belowground resources directly affect outcomes of competition. The majority of leguminous species retain homeostasis after the addition of N because of the N absorbed from the soil and that from biological N fixation (Markham and Zekveld, 2007; Guo et al., 2017; Wang et al., 2018b). Conversely, some leguminous species are sensitive to N (Hansen et al., 1992) or water deficits (Sadras et al., 2016). However, the literature on whether the root competitive response of leguminous woody trees varies with drought and N deposition is still lacking, especially for mixed plantations of leguminous trees with different N-fixing niche neighbors.

Plants may detect and identify their neighbors through both aboveground and belowground mechanisms (Chen et al., 2012). The processes of aboveground and belowground competition are interactive and highly interdependent (e.g., on root structure; Bilbrough and Caldwell, 1995). Compared to belowground root competition for nutrients, plants subjected to a combination of aboveground and belowground competition allocate fewer resources to roots (Poorter et al., 2012). Accordingly, RMP is influenced by aboveground interaction (Gundel et al., 2014) and factors such as light and space (Mou et al., 1997). Therefore, we must consider whether the aboveground interaction among neighbors can affect RMP.

To capture more resources, plants can develop RMP to a heterogeneous distribution of nutrients that results from spatio-temporal heterogeneity in a natural soil environment or from resource depletion by neighbors (Mou et al., 1997, 2012; Wang et al., 2018a). The neighbor-induced RMP of a plant is generally estimated from some root-related indices, namely, the root response ratio (RRS) and root relative competition index (RRI; Li et al., 2013, 2018). In addition, foraging strategies based on root traits can be used to determine whole competitiveness (Semchenko et al., 2018). For example, in a mixture of two maize (*Zea mays* L.) genotypes (XY335 and HMY), the higher RRS (RRS > 0) of XY335 reflected a stronger RMP, which ultimately conferred a stronger competitive advantage on XY335 in a mixture of XY335 and HMY (Li et al., 2018). The majority of related studies also emphasize that plants with greater root proliferation can absorb nutrients more quickly under conditions of heterogeneous nutrients. Thus, plants with a higher RMP have a greater whole competitive advantage in a mixture (Semchenko et al., 2018). Traits may be required to predict plant performance and plant–plant interaction (Schroeder-Georgi et al., 2016). Therefore, RMP based on both the RRS and RRI may provide insights into

Abbreviations: NAR, Net assimilation rate; RGR, Relative growth ratio; RMP, Root morphological plasticity; RRI, Root relative competition index; RRS, Root response ratio; RY, Relative yield; SBD, Specific branching density; SRN, Specific root tip number; SRL, Specific root length.

the potential competitiveness of woody legumes with a different N-fixing niche neighbor.

Non-leguminous species in a forest ecosystem develop diverse RMP in response to the varying availability of resources and different resource-containing niche neighbors, especially in the context of climate change. However, most studies on leguminous species have focused on leguminous herbaceous crops in an agroforestry ecosystem. There is little knowledge of leguminous woody trees in a forestry system. N-fixing leguminous woody species have extensive root systems and play an essential role in measuring the impact of external conditions on the dynamics of forestry systems (Andrews and Andrews, 2017; Wang et al., 2018b). Thus, it is critical to understand the RMP of leguminous woody species when interacting with different N-fixing niche neighbors and test whether such RMP varies with drought and N deposition. This would help researchers evaluate neighbor-induced dynamic changes in the root traits of leguminous woody species in forest systems with the increase in extreme climatic events. *Dalbergia odorifera* is a precious leguminous woody tree with rhizobia in its root nodules. It has economic and medicinal value and is endemic to Hainan Island. *Delonix regia* and *Swietenia mahagoni* are tropical woody species with both economic and medicinal value; they are heterogeneous and belong to the same leguminous family as and a different family from *D. odorifera*, respectively. Thus, these three species belong to different N-fixing niches. The objectives of this study were to (1) characterize the effects of different N-fixing niche neighbors on the root morphology of leguminous woody *D. odorifera* with root system contact, (2) test whether the root morphology of *D. odorifera* is influenced by aboveground interaction with different neighbors with root system isolation, (3) determine whether this is influenced by drought and N application, and (4) evaluate whether the relative competitiveness of whole leguminous woody *D. odorifera* with different N-fixing niche neighbors can be predicted by RMP under a given environmental condition.

MATERIALS AND METHODS

One-year-old plantlets with approximately the same basal stem diameter and height were selected from a local nursery garden. No significant statistical differences between plantlets were observed. The experimental design was completely randomized, with three factors (water regime, N fertilization, and species competition). Two water conditions [well-watered: 95–100% field capacity (FC), drought: 25–30% FC] and two N treatments (N fertilization and no N fertilization) were set up after 4 weeks of growth. There were 24 treatments with five replicates per treatment in Experiment 1 (Exp1) and Experiment 2 (Exp2). In the well-watered and drought treatments, containers were weighed daily and rewatered to 95–100% FC and 25–30% FC, respectively, by replacing the amount of transpired water. NH_4NO_3 as N fertilizer was dissolved in water and then added to containers once a week at 0.4 g each time from April 2018 to July 2018. The experiment lasted 120 days.

Experiment 1: Interaction With Root System Contact

To assess the RMP of leguminous woody *D. odorifera* with different N-fixing niche neighbors under conditions of drought and N application with root system interaction, we performed a controlled greenhouse experiment. *D. odorifera* plantlets as leguminous woody target species were grown with *D. odorifera* of the same N-fixing niche (intraspecific competition [Do-Do]); *D. regia* that belonging to a heterogeneous but con-leguminous family (*D. odorifera* + *D. regia* [Do-Dr]); and a species from a different family (different N-fixing niche), *S. mahagoni* (*D. odorifera* + *S. mahagoni* [Do-Sm]). One-year-old plantlets were planted in plastic containers (50 × 21 × 16 cm, length × width × height) filled with 15 kg red soil and sand (1:2, v/v). The two individuals in each container were spaced approximately 25 cm apart, and belowground root contact was maintained.

Experiment 2: Interaction With Root System Isolation

Another experiment was simultaneously conducted to test the effects of aboveground interaction with different neighbors on *D. odorifera* root performance. Unlike in Experiment 1, we divided each container into two sections by placing a plastic partition in the middle of the container. The two plantlets were planted on either side of the plastic partition, and only aboveground interaction was allowed between them. The three planting models related to the N-fixing niche under these conditions of root isolation were one same N-fixing niche (*D. odorifera* + *D. odorifera* [Do/Do]) and two different N-fixing niches (*D. odorifera* + *D. regia* [Do/Dr] and *D. odorifera* + *S. mahagoni* [Do/Sm]). The water and N treatments were the same as those in Exp 1.

Harvesting and Analysis of Plant Growth

Five *D. odorifera* plantlets from each treatment were randomly selected for the measurement of plant leaf area with a portable area meter (Li-3000C, Li-Cor Inc., Lincoln, NE, United States) and then harvested after 120 days. All harvested *D. odorifera* individuals were separated into leaves, stems, and roots. The leaves and stems were oven-dried at 72°C for 72 h and then weighed. N concentration in the leaves was determined by the semi-micro Kjeldahl method (Mitchell, 1998).

The relative growth ratio (RGR; g g $^{-1}$ DM day $^{-1}$) and net assimilation rate (NAR) were used to evaluate the effects of neighbors on *D. odorifera* growth and understand the effects of the aboveground interaction of *D. odorifera* on root plasticity. RGR and NAR were calculated according to formulas described by Radford (1967) as follows:

$$\mathrm{RGR} = \frac{\left(\ln \mathrm{DM}_1 - \ln \mathrm{DM}_2\right)}{t_2 - t_1}$$

$$\mathrm{NAR} = \frac{\left(\mathrm{DM}_2 - \mathrm{DM}_1\right)\left(\ln \mathrm{lA}_2 - \ln \mathrm{lA}_1\right)}{\left(t_2 - t_1\right)\left(\mathrm{LA}_2 - \mathrm{LA}_1\right)},$$

where DM_1 and DM_2 are the total dry mass of *D. odorifera* at t_1 and t_2, respectively; LA_1 and LA_2 represent the leaf area

at t_1 and t_2, respectively; t_1 (days) and t_2 are the beginning and end of the experiment, respectively. The t_2–t_1 represents the duration of the experiment in days.

Relative yield (RY) was expected to account for the relative competitiveness of *D. odorifera* in the different planting models under a given environment. RY was calculated according to a formula described by De Wit (1960) as follows:

$$RY = Y_{ab} / Y_{aa}$$

Here Y_{aa} and Y_{ab} the are average biomass or nutrient content of the harvested organs of *D. odorifera* in the monoculture model (with the same N-fixing niche neighbor) and mixture model (with a different N-fixing niche neighbor), respectively. When RY > 1.0, *D. odorifera* is more stimulated by a different N-fixing niche neighbor than by the same one. That is, different N-fixing niche neighbors confer competitive advantages on *D. odorifera*. In addition, a greater value indicates a stronger effect on *D. odorifera* biomass from a different N-fixing niche neighbor.

Determination of Root Traits

Harvested *D. odorifera* roots were washed with running tap water and then carefully separated from neighboring roots. The total biomass of the intact root was measured and then scanned with a root scanner (Epson Perfection 1600 Pro, Model V700, Epson, Tokyo, Japan). Afterward, root length, root surface area, root diameter, root volume, root tips, branching number, and root classification (coarse roots, diameter ≥ 2 mm; fine roots, diameter < 2 mm) were analyzed with WinRHIZO (Regent Instruments, Quebec, Canada). Fresh nodules were carefully removed from *D. odorifera* roots and classified according to size as large (diameter ≥ 2 mm) or small (diameter < 2 mm). These nodules were then counted and weighed. Meanwhile, the ratio of nodule biomass to total root biomass (fresh weight) was calculated. The *D. odorifera* root samples were then collected, dried to a constant weight at 70°C, and weighted. In addition, SRL (the ratio of total root length to root dry weight), specific branching density (SBD; the ratio of root branching number to root dry weight), and specific root tip number (SRN; the ratio of root tip number to root dry weight) was calculated.

The RRI, which can be used as an indicator of neighbor-induced root investment, was calculated by a metric modified from Jolliffe (2000) as follows:

$$RRI = \left(RB_{ab} - RB_{aa}\right) / RB_{aa},$$

where RB_{aa} and RB_{ab} represent the root dry biomass of *D. odorifera* interacting with the same N-fixing niche neighbor or a different N-fixing niche neighbor, respectively, under a given environment. If the root dry biomass of *D. odorifera* interacting with the same N-fixing niche is the same as that of *D. odorifera* interacting with a different N-fixing niche neighbor, then RRI = 0. If RRI > 0, then *D. odorifera* benefits more from a different N-fixing niche neighbor than from the same N-fixing niche neighbor and invests more biomass to the root. If RRI < 0, the opposite is true. A higher RRI indicates greater promotion of root investment of *D. odorifera* from a different N-fixing niche neighbor.

The RRS was expected to explain the extent of root proliferation (coarse, fine, and total roots) to various neighbors under given water and N application conditions. RRS was calculated according to a formula modified from Li et al. (2013) as follows:

$$RRS_a = \Sigma\left[\left(RL_{ab} - RL_{aa}\right) / \left(RL_{ab} + RL_{aa}\right)\right] / n,$$

where RRS_a represents the RRS of *D. odorifera* to different neighbors; RL_{aa} and RL_{ab} are the root lengths of *D. odorifera* with conspecific competition (aa) and heterospecific competition (ab) under the given water and N application conditions, respectively; and n is the number of $(RL_{ab} - RL_{aa})/(RL_{ab} + RL_{aa})$ values. In this study, n equals 5, because five replicates (five random individuals) were set in each species competition treatment. The root proliferation of *D. odorifera* was expected to be promoted by competition with a heterogeneous neighbor when $RRS_a > 0$ and diametrically suppressed when $RRS_a < 0$. A greater RRS_a represents a stronger effect on the root proliferation of *D. odorifera* from a heterogeneous interaction.

Statistical Analysis

SPSS 19.0 was used for the statistical analysis. All data were tested for a normal distribution and homogeneity of variance before analyses. Multivariate analysis of variance was used to evaluate the effects of the interaction of water, N application, and competition. To estimate the correlations between the RY of the whole *D. odorifera* plantlet and RRI, RY of the roots, and RRS of total roots, we performed a correlation analysis. Differences were considered significant at $p < 0.05$.

RESULTS

Effects on Root Morphological Traits

In the root system contact model, the root length, root surface area, root diameter, root volume, and root branching number of *D. odorifera* plantlets exposed to interspecific competition (Do-Dr and Do-Sm) were higher than those of plantlets exposed to intraspecific competition (Do-Do) under both the 100% FC and 30% FC conditions (**Figure 1**). Drought-stressed *D. odorifera* plantlets showed significantly higher root length, root branching number, and root tips but smaller root diameter and root volume compared to the well-watered plantlets (**Figures 1A,C–F**). In addition, drought-stressed *D. odorifera* in the Do-Dr and Do-Sm models showed a greater increase in root length, root branching number, and root tips and a smaller decrease in root diameter and root volume compared to plantlets in the Do-Do model. N application decreased the root length, root surface area, root tips, and root branching number under the 100% FC condition (**Figures 1A,B,E,F**). Moreover, *D. odorifera* in the Do-Dr model showed the greatest decrease in these parameters. *D. odorifera* in the Do-Sm model showed the largest root diameter and root volume. The smallest values among the competition models were found in the Do-Dr model under the

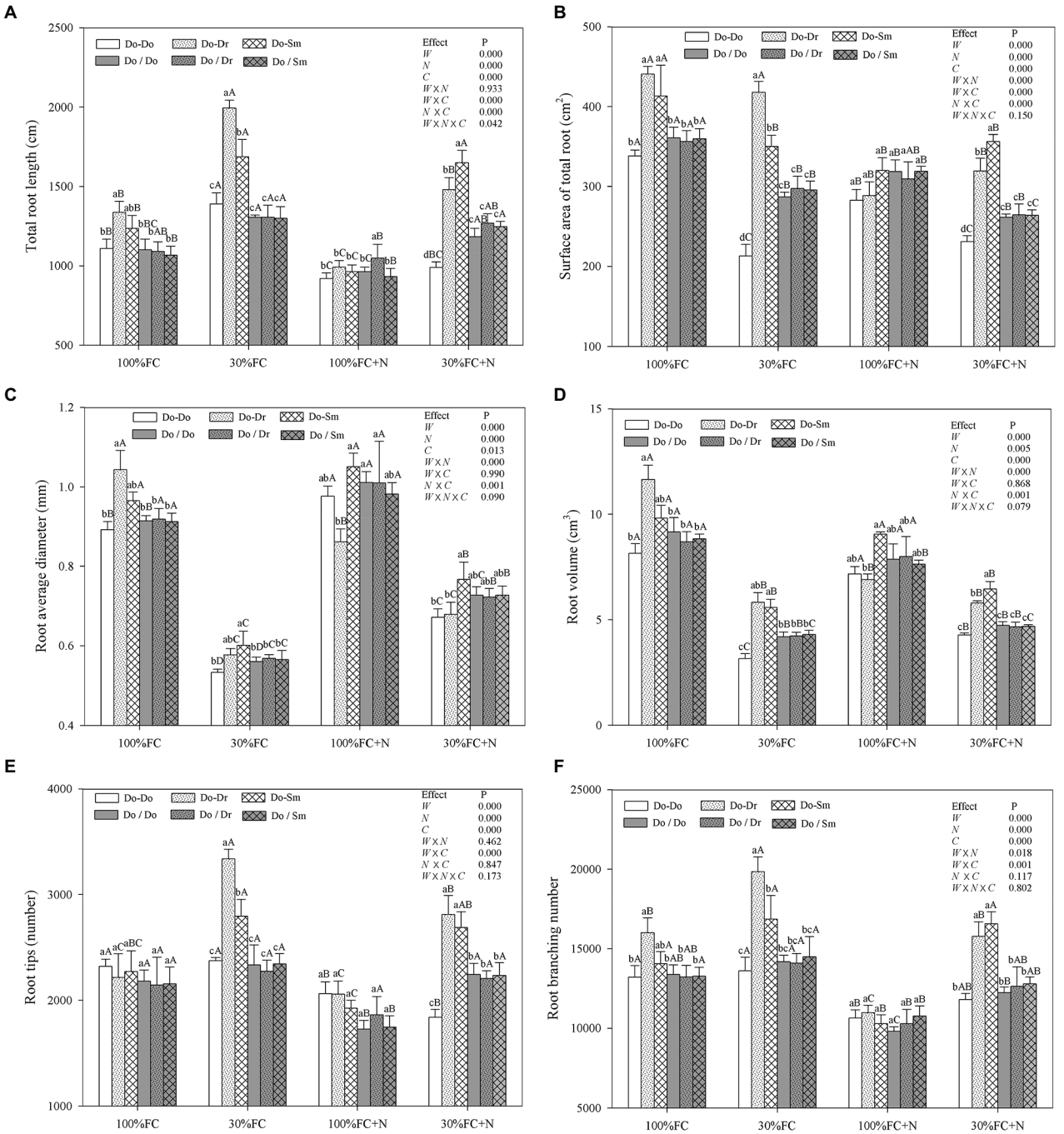

FIGURE 1 | Effects of water, N fertilization levels, and species competition models on total root length **(A)**, surface area of total root **(B)**, root diameter **(C)**, root volume **(D)**, root tips **(E)**, and root branching number **(F)** of *D. odorifera*. Means ± SEs, $n = 5$. Different lowercases in each graph indicate significant difference among different competitive models (competition between *D. odorifera* and various N-fixing niche neighbors) under the same water and N application according to Duncan's tests ($p < 0.05$). Different uppercases in each graph indicate significant difference among different water and N fertilization application in the same competitive models according to Duncan's tests. 100% FC, 100% field capacity; 30% FC, 30% field capacity; 100% FC+N, 100% field capacity and N fertilization treatment; 30% FC+N, 30% field capacity and N fertilization. Do-Do, Do-Dr, and Do-Sm indicate *D. odorifera* planted with *D. odorifera*, *D. regia,* and *S. mahagoni* in the root system contact models, respectively; Do/Do, Do/Dr, and Do/Sm indicate *D. odorifera* planted with *D. odorifera*, *D. regia* and *S. mahagoni* in the root system isolation models, respectively. W, water factor effect; N, nitrogen factor effect; C, species competition models factor effect; W × N, interaction effect of water and nitrogen factors; W × C, interaction effect of water and species competition models factors; N × C, interaction effect of nitrogen and species competition models factors; W × N × C, interaction effect of water, nitrogen, and species competition models factors. Multivariate analysis of variance (Multi-ANOVA) was conducted to evaluate the influence of different factors and their interaction effects.

100% FC+N condition with root system contact. N application increased the root diameter and root volume of *D. odorifera* in all competition models but decreased the root length, root surface area, root tips, and root branching number of plantlets under the 30% FC condition. In addition, a greater decrease in the root length, root surface area, root tips, and root branching number of *D. odorifera* was observed in the Do-Dr model compared to the Do-Do and Do-Sm models. *D. odorifera* in the Do-Sm and Do-Do models had the largest and smallest root length, root surface area, root diameter, root volume, root tips, and root branching number among all competition models under the 30% FC+N condition (**Figure 1**). Root morphological traits were significantly affected by water × N, water × competition, and N × competition interactions. The water × N × competition interaction significantly affected root length.

In the root system isolation model, few differences in root length, root surface area, root diameter, root volume, root tips, or root branching number among the competition models were found among the treatments (100% FC, 30% FC, 100% FC+N, 30% FC+N; **Figure 1**). Under the 100% FC and 30% FC conditions, the root length, root surface area, root diameter, root volume, and root branching number of *D. odorifera* plantlets with root system isolation were significantly lower than those of plantlets with root system contact in interspecific competition (Do/Dr vs. Do-Dr, Do/Sm vs. Do-Sm; **Figures 1A–D,F**). However, these parameters (except the insignificant difference in root length) were higher in *D. odorifera* plantlets with root system isolation than root system contact in the intraspecific competition (Do/Do vs. Do-Do). Under the 100% FC+N condition, *D. odorifera* in the Do/Dr and Do/Sm models had higher and lower root diameter and root volume in the root system isolation model than the root system contact model, respectively (Do-Dr, Do-Sm). Under the 30% FC+N condition, *D. odorifera* in the Do/Do model showed a higher root length, root surface area, root volume, root tips, and root branching number than in the Do-Do model, but lower values for these parameters than plants in interspecific competition (Do/Dr vs. Do-Dr, Do/Sm vs. Do-Sm) were found in the root system isolation model than in the root system contact model (**Figures 1A,B,D–F**).

In the root system contact model, drought stress increased the SRL, SBD, and SRN of *D. odorifera* in all competition models (**Figure 2**). These parameters showed a greater increase in the Do-Do model than in the Do-Dr and Do-Sm models. Moreover, drought-stressed *D. odorifera* in the Do-Do model exhibited the highest SRL, SBD, and SRN among all competition models. N application under well-watered conditions (100% FC) decreased the SBD and SRN of *D. odorifera* in all competition models, except the SRN in the Do-Dr model. Furthermore, *D. odorifera* in the Do-Sm model showed the lowest SRN among all competition models under the 100% FC+N condition. N application under drought stress decreased the SRL, SBD, and SRN of *D. odorifera* in the Do-Do and Do-Sm models; rare variations were found in the Do-Dr model. Moreover, *D. odorifera* in the Do-Sm model exhibited the lowest SBD and SRN among all competition models (**Figures 2B,C**). However, insignificant differences in the SRL, SBD, and SRN of *D. odorifera* among all competition models were observed in all treatments in the root system isolation model (**Figure 2**). Finally, water × N and N × competition interactions significantly affected the SRL.

Effects on Root System Classification

Under both the 100% FC and 30% FC conditions, *D. odorifera* plantlets showed a greater root length and surface area of both coarse and fine roots in the interspecific competition (Do-Dr and Do-Sm) than intraspecific competition (Do-Do) model with root system contact (**Figures 3A,B,D,E**). Compared to the well-watered condition, drought stress decreased both the root length and surface area of coarse roots, but it promoted the root length and surface area of fine roots, the root length ratio of fine root to coarse root, the surface area ratio of fine root to coarse root, and the volume ratio of fine root to coarse root (**Figure 3**). In addition, these parameters of *D. odorifera* showed a greater increase with interspecific competition (Do-Dr and Do-Sm) than intraspecific competition (Do-Do). N application promoted the coarse root length of *D. odorifera* in the Do-Do and Do-Sm models but decreased the root length and surface area of fine roots and the root length ratio of fine root to coarse root in all competition models under the well-watered condition. Under the 100% FC+N condition, *D. odorifera* plantlets in the Do-Sm model had the largest root length and surface area of coarse roots but the smallest root length ratio and surface area ratio of fine root to coarse root among all competition models in the root system contact model. However, the opposite was true in the Do-Dr model. N application decreased the root length and surface area of fine roots, the root length ratio, the surface area ratio, and the volume ratio of fine root to coarse root of plantlets in all competition models under drought stress. Moreover, under the 30% FC+N condition, *D. odorifera* plantlets from the Do-Sm model had larger root lengths and surface areas of both coarse and fine roots and a greater volume ratio of fine root to coarse root than those from the Do-Dr model; the values of these parameters in these two models were significantly higher than those in the Do-Do model. Water × competition and N × competition interactions significantly affected the surface area of fine roots. Water × N × competition interaction significantly affected the surface area of coarse roots and the surface area ratio of fine root to coarse root.

Similar to the aforementioned root morphological indicators, the root system classification of *D. odorifera* under the root system isolation model (Do/Do, Do/Dr, and Do/Sm) exhibited few differences by competition model (**Figure 3**). However, compared to the root contact model, *D. odorifera* in intraspecific competition under the root isolation model had larger root length and root surface area of both coarse and fine roots under the 100% FC, 30% FC, 30% FC+N conditions (**Figures 3A,B,D,E**). Under the 100% FC+N condition, *D. odorifera* plantlets in the Do/Dr model with root system isolation showed larger root length and root surface area of coarse roots but a smaller root length ratio and surface area ratio of fine root to coarse root compared to those in the root system contact model (Do/Dr vs. Do-Dr; **Figures 3A,C,D,F**).

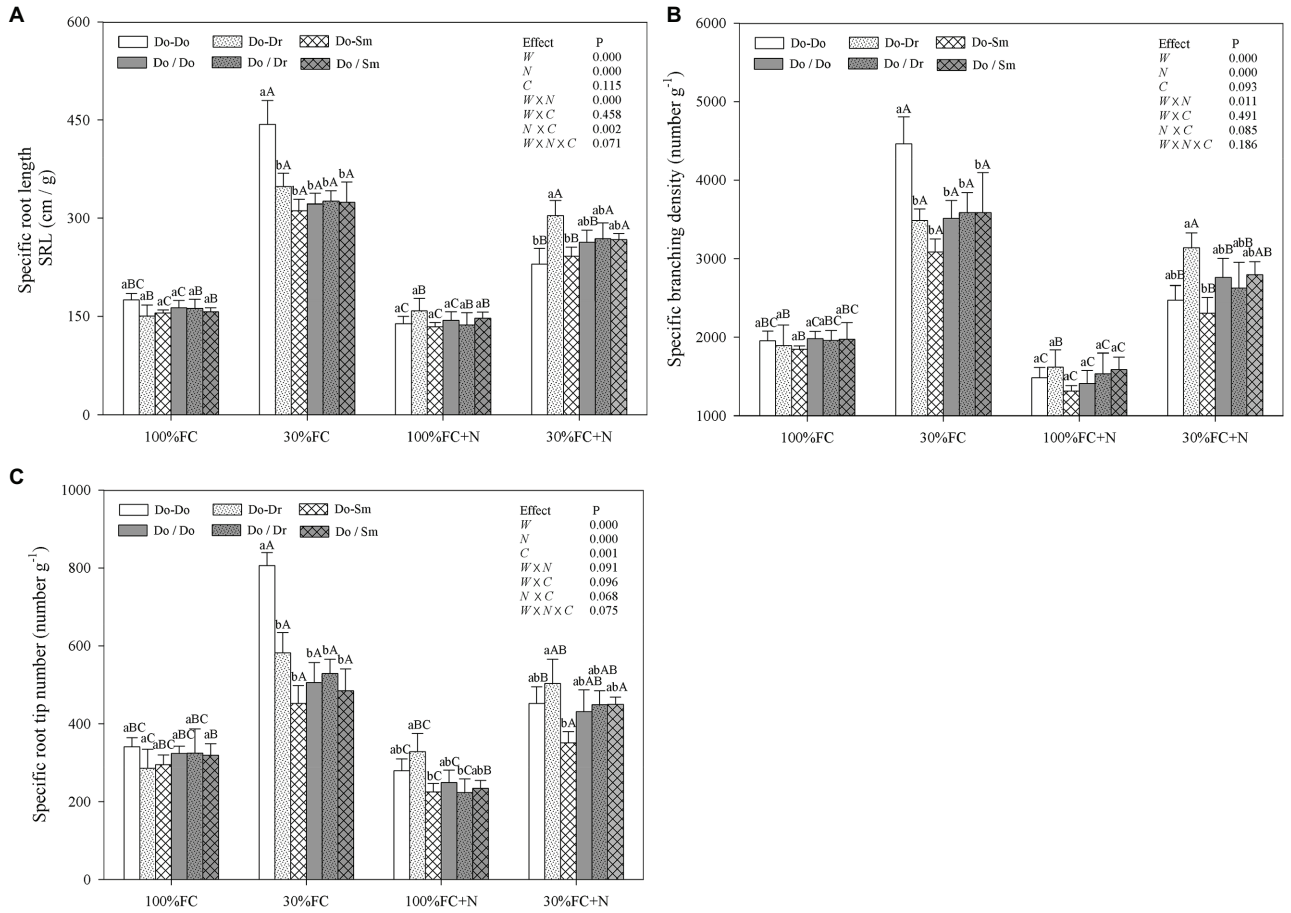

FIGURE 2 | Effects of water, N fertilization levels, and species competition models on specific root length **(A)**, specific branching density **(B)**, and specific root tip number **(C)** of *D. odorifera*. Different lowercases in each graph indicate significant difference among different competitive models (competition between *D. odorifera* and various N-fixing niche neighbors) under the same water and N application according to Duncan's tests ($p < 0.05$). Different uppercases in each graph indicate significant difference among different water and N fertilization application in the same competitive models according to Duncan's tests. For abbreviations explanation of treatments (species competition models, water, and N fertilization), data description, and statistics are the same as shown in **Figure 1**.

Effects on Root Nodules

Under the 100% FC condition, *D. odorifera* plantlets in the Do-Do model had the smallest number of large root nodules and total root nodules and the smallest fresh weight of root nodules. However, these parameters showed their highest values among the competition models in plantlets in the Do-Dr and Do-Sm models (**Figures 4A–C**). Drought stress decreased the number of large root nodules and total root nodules, the fresh weight of root nodules, and the ratio of nodule mass to total root mass (**Figure 4**). Drought-stressed *D. odorifera* in the Do-Do model showed the smallest number of large root nodules and total root nodules and the smallest fresh weight of root nodules. Although *D. odorifera* in the Do-Sm model had more large root nodules and a higher fresh weight of root nodules than in the Do-Dr model, plantlets in both models with root system contact exhibited a higher number and fresh weight of root nodules than those with root system isolation (Do-Dr vs. Do/Dr, Do-Sm vs. Do/Sm). N application under the 100% FC condition markedly decreased the number of large root nodules and total root nodules, the fresh weight of root nodules, and the ratio of nodule mass to total root mass in all competition models. In addition, *D. odorifera* in the Do-Sm model showed the greatest decreases in these parameters among all competition models. N application under the 30% FC condition markedly decreased the number of large root nodules, the fresh weight of root nodules, and the ratio of nodule mass to total root mass in all competition models (**Figures 4A,C,D**). Under the 30% FC+N condition, *D. odorifera* in the Do-Do and Do-Sm models had the most and least large root nodules and total root nodules and the highest and lowest fresh weight of root nodules among all competition models, respectively. However, the number of large root nodules and total root nodules, the fresh weight of root nodules, and the ratio of nodule mass to total root mass of *D. odorifera* differed little by treatment with root system isolation. Root nodules were significantly affected by water × N, water × competition, and N × competition interactions. The water × N × competition interaction significantly affected the number and fresh weight of root nodules.

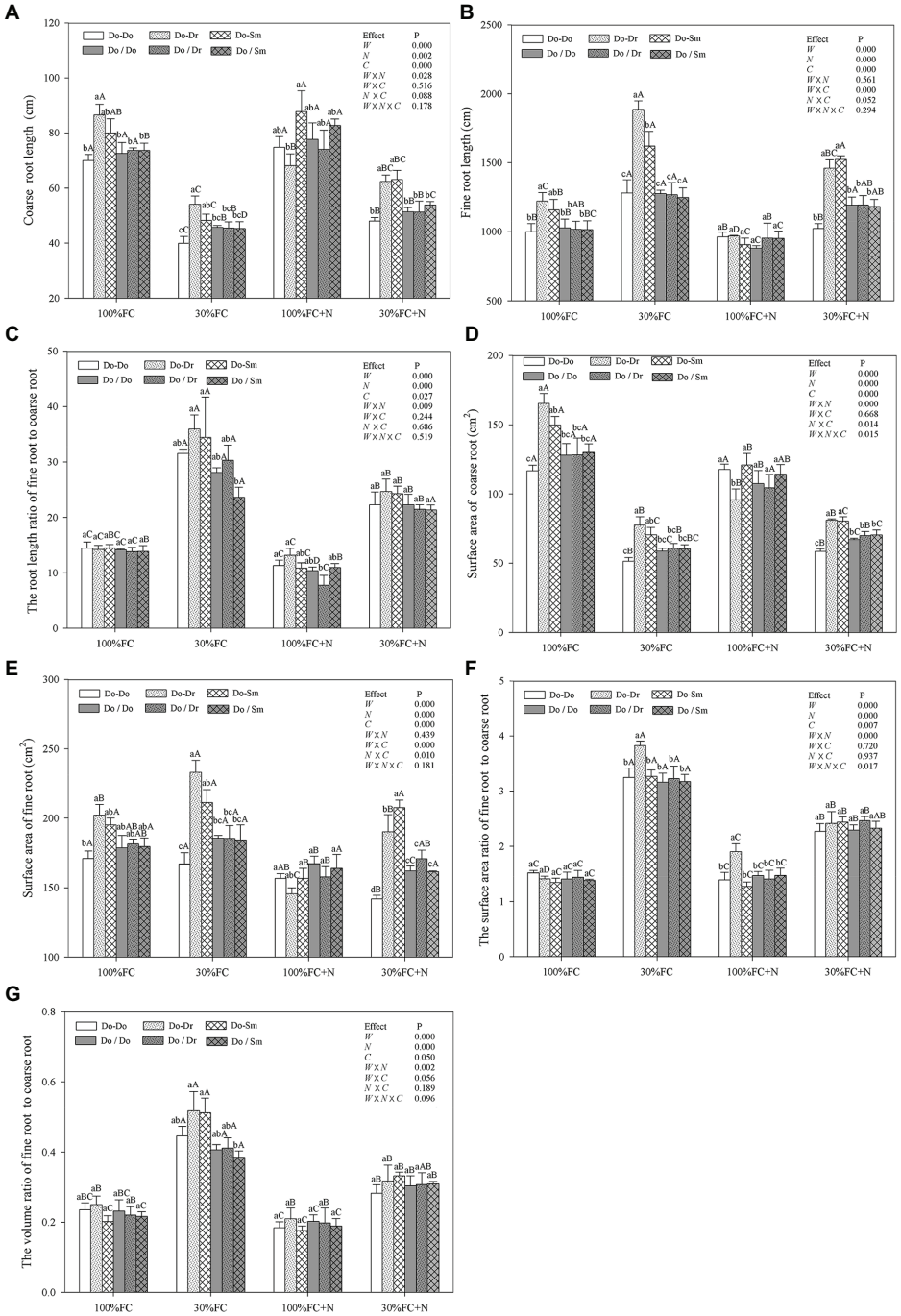

FIGURE 3 | Effects of water, N fertilization levels, and species competition models on coarse root length **(A)**, fine root length **(B)**, the root length ratio of fine root to coarse root **(C)**, coarse root surface area **(D)**, fine root surface area **(E)**, the root surface area ratio of fine root to coarse root **(F)**, and the root volume ratio of fine root to coarse root **(G)** of *D. odorifera*. Different lowercases in each graph indicate significant difference among different competitive models (competition between *D. odorifera* and various N-fixing niche neighbors) under the same water and N application according to Duncan's tests ($p < 0.05$). Different uppercases in each graph indicate significant difference among different water and N fertilization application in the same competitive models according to Duncan's tests. For abbreviations explanation of treatments (species competition models, water, and N fertilization), data description, and statistics are the same as shown in **Figure 1**.

Correlation Indices of RMP

Under the 100% FC and 30% FC conditions, insignificant differences in the RRI and RY of total roots and the RRS of both coarse and fine roots were observed between the Do-Dr and Do-Sm models, whereas the RRI and RRS exhibited positive values, and the RY of total roots was greater than 1.0 (**Figures 5, 6**).

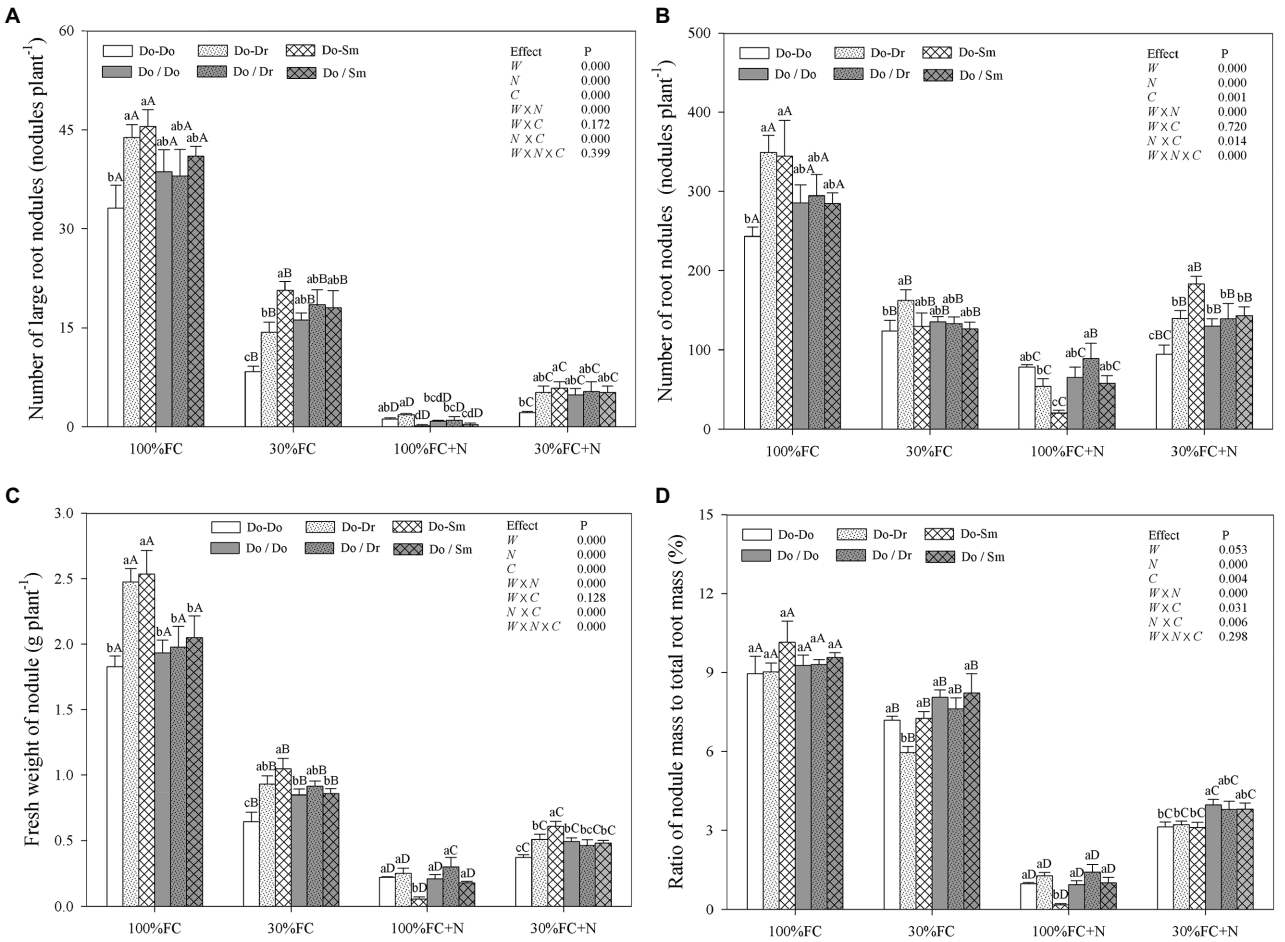

FIGURE 4 | Effects of water, N fertilization levels, and species competition models on large nodules number **(A)**, total nodules number **(B)**, fresh nodules weight **(C)**, and the ratio of nodules mass to root mass **(D)** of *D. odorifera*. Different lowercases in each graph indicate significant difference among different competitive models (competition between *D. odorifera* and various N-fixing niche neighbors) under the same water and N application according to Duncan's tests ($p < 0.05$). Different uppercases in each graph indicate significant difference among different water and N fertilization application in the same competitive models according to Duncan's tests. For abbreviations explanation of treatments (species competition models, water, and N fertilization), data description, and statistics are the same as shown in **Figure 1**.

Drought stress promoted the RRI and RY of total roots and the RRS of fine, coarse, and total roots in both the Do-Dr and Do-Sm models with root system contact. N application under the 100% FC condition decreased the RRI of total roots and the RRS of coarse and fine roots of *D. odorifera* in the Do-Dr model, whereas insignificant differences were found in plantlets in the Do-Sm model, except for a decreasing trend in the RRS of fine roots. The RRI of total roots and the RRS of coarse and total roots in the Do-Sm model were positive, whereas *D. odorifera* in the Do-Dr model showed a negative RRI of total roots and RRS of coarse roots under the 100% FC+N condition. N application under the 30% FC condition significantly decreased the RRI and RY of total roots in the Do-Dr model but increased the RRS of fine and total roots in the Do-Sm model (**Figures 5, 6**). Under the 30% FC+N condition, *D. odorifera* showed a significantly higher RRI and RY of total roots in the Do-Sm model than in the Do-Dr model (RRI, RRS > 0, RY > 1.0). Few differences in the RRI and RY of total roots and the RRS of coarse, fine, and total roots were observed among all competition models in all treatments with root system isolation.

Plant Growth and the Relative Competitiveness of the Whole *Dalbergia odorifera* Plantlet

Drought stress significantly decreased the RGR, NAR, and leaf N contents of *D. odorifera* plantlets but increased the RY of shoots and the whole plantlet in all competition models with root system contact (**Figure 7**). In addition, drought stress caused the greatest decrease in the RGR and NAR of plantlets in the Do-Do model. In contrast, plantlets in the Do-Do model had the smallest RGR, NAR, and leaf N content among all competition models under the 100% and 30% FC conditions; insignificant differences in these parameters were found between the Do-Do and Do-Dr models under the 100% FC condition. Moreover, the RYs of shoots, the whole plantlet, and leaf N content in

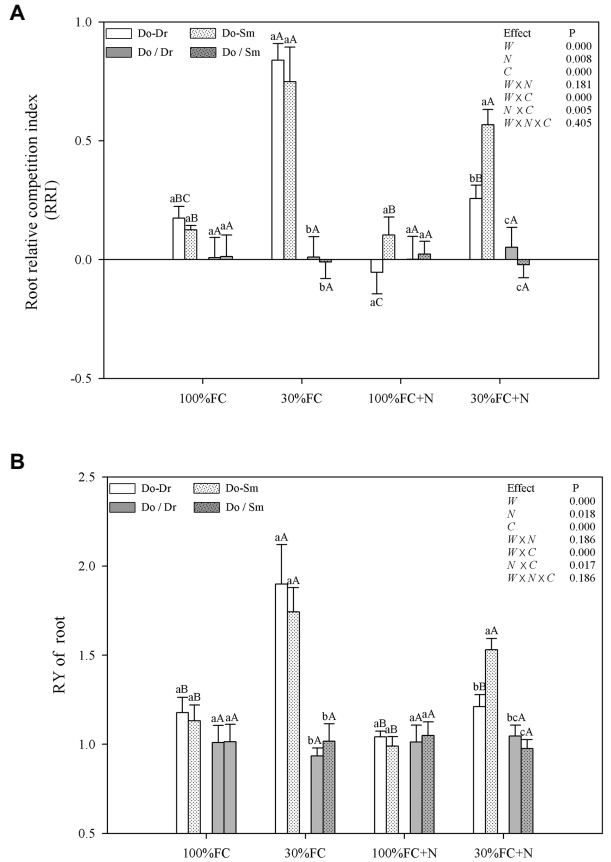

FIGURE 5 | Effects of water, N fertilization levels on RRI **(A)** and RY of root **(B)** in different species competition models. Means ± SEs, $n = 5$. Different lowercases in each graph indicate significant difference among different competitive models (competition between *D. odorifera* and various N-fixing niche neighbors) under the same water and N application according to Duncan's tests ($p < 0.05$). Different uppercases in each graph indicate significant difference among different water and N fertilization application in the same competitive models according to Duncan's tests. 100% FC, 100% field capacity; 30% FC, 30% field capacity; 100% FC + N, 100% field capacity and N fertilization; 30% FC + N, 30% field capacity and N fertilization. Do-Dr, Do-Sm indicate *D. odorifera* planting with *D. regia* (white bars) and *S. mahagoni* (white bars with dots) in the root system contact models, respectively; Do/Dr and Do/Sm indicate *D. odorifera* planting with *D. regia* (gray bars) and *S. mahagoni* (gray bars with dots) in the root system isolation models, respectively; W, water factor effect; N, nitrogen factor effect; C, species competition models factor effect; W × N, interaction effect of water and nitrogen factors; W × C, interaction effect of water and species competition models factors; N × C, interaction effect of nitrogen and species competition models factors; W × N × C, interaction effect of water, nitrogen and species competition models factors; Multivariate analysis of variance (Multi-ANOVA) was conducted to evaluate the influence of different factors and their interaction effects.

the Do-Dr and Do-Sm models were greater than 1.0. N application under both water conditions increased the RGR and leaf N content of *D. odorifera* in all competition models but decreased the RYs of shoots and the whole plantlet in the Do-Dr model. *D. odorifera* plantlets in the Do-Dr model had lower values for the RGR, NAR, and RYs of shoots and the whole plantlet than those in the Do-Sm model under the 100% FC+N and 30% FC+N conditions. Moreover, the RYs of shoots and the whole plantlet in the Do-Dr model were less than 1.0 under the 100% FC+N condition. N-applicated *D. odorifera* in the Do-Do and Do-Sm models showed a greater increase in the RGR than those in the Do-Dr model under the 30% FC condition. Moreover, plantlets in the Do-Do model showed the lowest RGR and NAR among all competition models. However, insignificant differences in RGR, NAR, leaf N content, the RY of shoots, the whole plantlet, and N content among the competition models were still observed in all treatments with root system isolation.

Relationships Between the Relative Competitive Advantage of Roots and the Relative Competitiveness of the Whole Plantlet (Exp1)

Under the 100% FC condition, the RY of the whole plantlet was significantly positively correlated with the RRI, RY, and RRS of total roots ($p < 0.05$; **Figure 8**). Moreover, drought stress significantly enhanced these positive correlations. However, N application under the 100% FC condition markedly decreased these correlations. In addition, although a significant correlation was found between the RY of the whole plantlet and the RRI of the roots, an insignificant correlation was observed between the RY of the whole plantlet and the RY and RRS of total roots under the 100% FC+N condition ($p < 0.05$). N application reduced the significant positive correlation between the RY of the whole plantlet and the RY of total roots. The RY of the whole plantlet was positively correlated with the RRI, RY, and RRS of total roots under the 30% FC condition.

DISCUSSION

Root Morphology and Plant Growth Respond Differently to Different N-Fixing Niche Neighbors in a Root System Contact Model (Exp1)

Root traits are key indicators of the relative competitiveness of a plant (Goisser et al., 2016), and root plasticity can reflect the utilization of available resources and the adaptability of plants to environmental stress through adjustments to root growth, morphology, and/or physiological activity (Huang and Eissenstat, 2000; Freschet et al., 2013). Thus, a higher RMP would imply a stronger advantage in terms of competition for resources (Huang and Eissenstat, 2000). In addition, roots may respond differently to neighbors (e.g., maximizing root length, root surface area, volume, or diameter) according to the availability of a common resource (Schenk, 2006; Craine et al., 2013). The higher root morphological traits (e.g., root length, root surface area, root diameter, root volume, root tips, root branching number, RRI, and RRS) of *D. odorifera* in interspecific competition compared to intraspecific competition under the 100% FC, 30% FC, and 30% FC+N conditions (**Figures 1, 5A, 6**) suggest that *D. odorifera* had stronger RMP in the presence of different N-fixing niche neighbors than in the presence of the same one. This finding is consistent with the niche partitioning hypothesis, which argues that plants may reduce root foraging behavior when faced with a niche-similar or equivalent neighboring root because of a similar

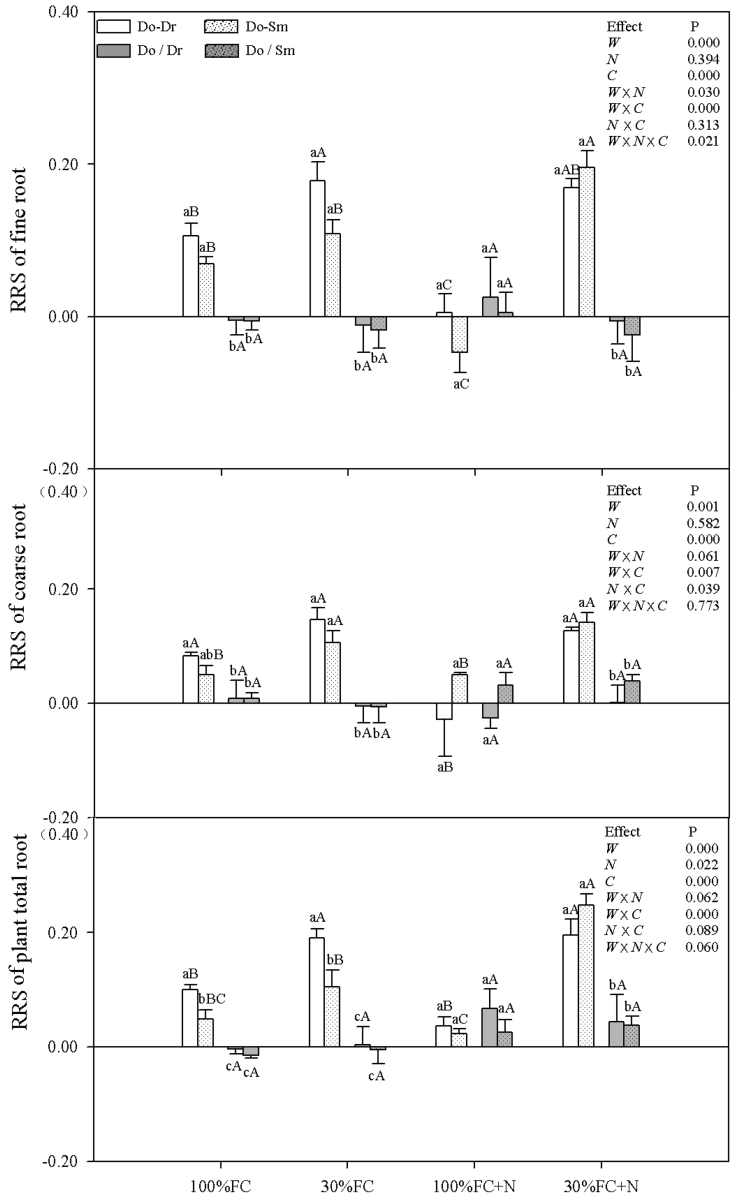

FIGURE 6 | Effects of water, N fertilization levels on RRS of *D. odorifera* in the total root, fine root, and coarse root in different species competition models. Different lowercases in each graph indicate significant difference among different competitive models (competition between *D. odorifera* and various N-fixing niche neighbors) under the same water and N application according to Duncan's tests ($p < 0.05$). Different uppercases in each graph indicate significant difference among different water and N fertilization application in the same competitive models according to Duncan's tests. For abbreviations explanation of treatments (species competition models, water, and N fertilization), data description, and statistics are the same as shown in **Figure 5**.

phenotype or nutrient demand (Macarthur and Levins, 1967; Cheplick and Kane, 2004). A higher RMP increases exploitation efficiency (Huang and Eissenstat, 2000; Richards et al., 2010). Therefore, different N-fixing niches *D. regia* and *S. mahagoni* can increase the exploitation efficiency of leguminous *D. odorifera* under drought stress or N deficiency. Under the 100% FC+N condition, *D. odorifera* planted with *S. mahagoni* had the highest root traits (root volume and diameter) among the three competing models (Do-Do, Do-Dr, and Do-Sm), whereas the lowest levels were observed in plantlets planted with *D. regia*. These findings demonstrate that root morphological traits of *D. odorifera* depend on its N-fixing niche neighbors.

Coarse and fine roots play different roles in function. Coarse roots predominantly store excess carbon, and fine roots absorb belowground resources (Guo et al., 2008). Moreover, fine roots are determinants of the acquisition of soil nutrients and water (Ma et al., 2018). In this study, competition with a heterogeneous neighbor markedly improved the root traits (e.g., root length, root surface area, and RRS) of both the coarse and fine roots of *D. odorifera* than the competition with a conspecific neighbor

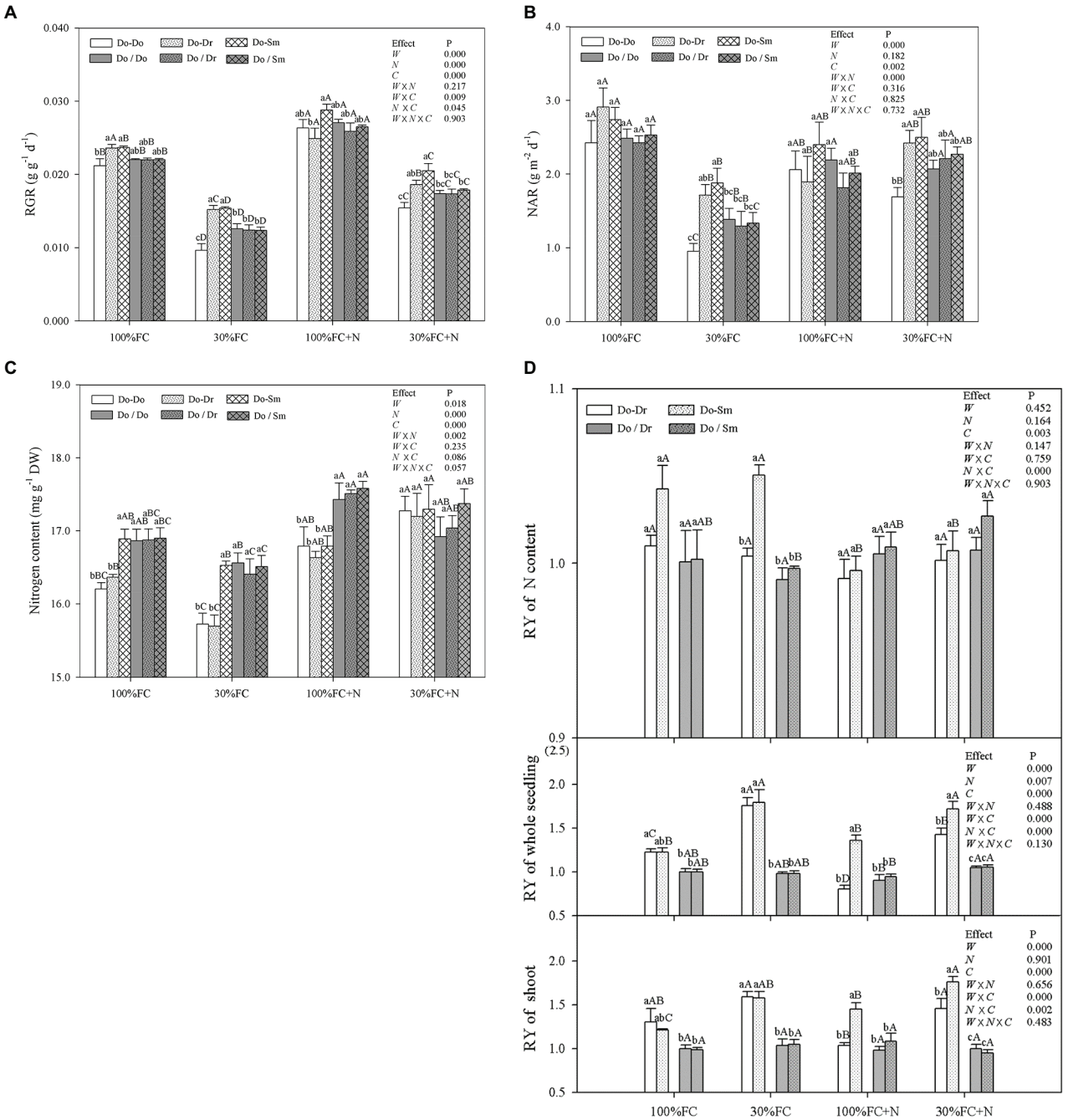

FIGURE 7 | Effects of water, N fertilization levels on RGR **(A)**, NAR **(B)**, leaf N content **(C)** of *D. odorifera*, and RY of the shoot, whole plantlet, and leaf N content **(D)** in different species competition models. Different lowercases in each graph indicate significant difference among different competitive models (competition between *D. odorifera* and various N-fixing niche neighbors) under the same water and N application according to Duncan's tests ($p < 0.05$). Different uppercases in each graph indicate significant difference among different water and N fertilization application in the same competitive models according to Duncan's tests. For abbreviations explanation of treatments (species competition models, water, and N fertilization), data description, and statistics are the same as shown in **Figure 5**.

under the 100% FC, 30% FC, and 30% FC+N conditions (**Figures 3A,B,D,E**). Moreover, the root length ratio and root surface area ratio of fine root to coarse root of *D. odorifera* benefitted slightly from a heterogeneous neighbor under the 30% FC condition (**Figures 3C,F**). A greater increase in the lateral fine roots (e.g., root length) of *Picea sitchensis* grown in a mixture with *P. sitchensis* compared to pure stands implies an improvement in exploitation efficiency (Richards et al., 2010). Therefore, the findings indicate that a neighbor with a different N-fixing niche induces more carbon storage in leguminous *D. odorifera* by increasing water

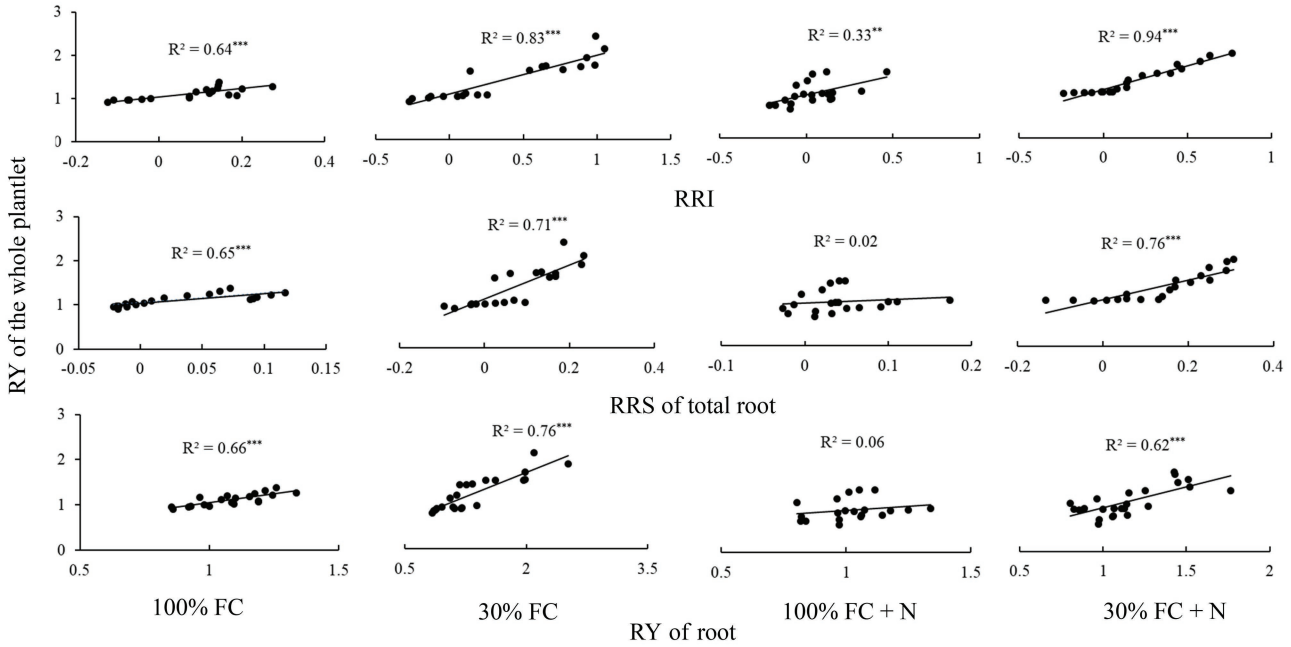

FIGURE 8 | The relationships between the RY of whole plantlet and RRI, RRS, and RY of total root, respectively. One point showed one sample. The solid lines represent the best-fit linear regressions. $^{**}p < 0.01$; $^{***}p < 0.001$. 100% FC, 100% field capacity; 30% FC, 30% field capacity; 100% FC+N, 100% field capacity and N fertilization; 30% FC+N, 30% field capacity and N fertilization.

and nutrient absorption in a harsh environment. In addition, *D. odorifera* planted with *S. mahagoni* had the largest coarse root length and surface area among all competition models under the 100% FC+N condition, whereas *D. odorifera* planted with *D. regia* had the smallest. These findings might highlight the fact that the resource forage ability and carbon storage of *D. odorifera* are enhanced by *S. mahagoni* but inhibited by *D. regia*.

N-fixing rhizobia are essential for the establishment of symbiotic N fixation in Leguminosae and may mediate competition (Bowsher et al., 2017). Previous studies have demonstrated that nodules can increase both root length and contact area with soil and alleviate soil resource limitations of plant growth by enhancing the acquisition of sparse water and nutrients (Richards et al., 2010). Our results show a higher number of nodules and weight of *D. odorifera* in the interspecific competition models compared to the intraspecific competition models under the 100% FC, 30% FC, and 30% FC+N conditions (**Figure 4**). These results suggest that the leguminous species in the mixture show greater nodulation than those in monoculture; similar results were observed in studies on an alfalfa–maize intercrop (Wang et al., 2019). Differences in root symbiosis and nutrient preferences between different species in the mixture may lead to greater soil nutrient capture and absorption than in a monoculture. Moreover, there is less competition for resources in mixed cultures (Richards et al., 2010). Therefore, the presence of different N-fixing niche neighbors may benefit the growth of nodules, promoting the absorption of water and nutrients in harsh environments. However, a large number of studies have shown that nodules depend on the availability of soil nutrients, and their distribution can be used to measure plant N fixation strategies (N fixation and soil N uptake; Wang et al., 2019). For example, symbiotic N fixation can be converted to soil N absorption with sufficient N application, thereby reducing rhizobium symbionts (Markham and Zekveld, 2007; Wang et al., 2019). The least number of nodules among all competition models was observed in *D. odorifera* planted with *S. mahagoni* under the 100% FC+N condition (**Figure 4**), which indicates that sufficient N decreases the number of nodules. The presence of the non-N-fixing niche *S. mahagoni* impacted the availability of soil resources due to differences in plant demand for nutrients and water, further aggravating the N sufficiency. Similar to observed modifications in root morphological traits, these findings emphasize that N-fixing nodules of the leguminous *D. odorifera* can be modulated by a different N-fixing niche neighbor.

Root and Plant Growth Respond Similarly to Different Niche Neighbors in a Root System Isolation Model (Exp2)

Through both aboveground mechanisms (e.g., light quality signals, volatile organic compounds) and belowground mechanisms (nutrient levels, soluble root exudates), plants can detect and identify their neighbors and estimate their impact on the availability of resources (Pierik et al., 2013). However, plants are exposed to multiple stressors and compete for above- and belowground resources simultaneously in nature. Thus, plant functional traits are changed by mechanisms of both aboveground and belowground interaction (Freschet et al., 2013). In the present study, under the 100% FC, 30% FC, and 30% FC+N conditions, *D. odorifera* in interspecific competition had weaker root plasticity (e.g., lower values for root length; surface area of the total, coarse, and fine roots; root

diameter; root volume; branching number) with root system isolation than with root system contact, but similar or stronger root plasticity was found for intraspecific competition (equal or higher values for the aforementioned indices). However, with root system isolation, root morphology and growth (RGR, NAR, leaf N content, and RY of shoots, the whole plantlet, and N content) responded similarly to intraspecific and interspecific competition under all conditions, which indicates that the RMP and growth of *D. odorifera* do not respond to interactions with different N-fixing niche neighbors. Our findings suggest that belowground interaction may be the only way to influence root interaction and the growth of *D. odorifera*, as the effects of aboveground interaction are negligible.

Effects of Drought and N Application on the RMP of *Dalbergia odorifera* in a Root System Contact Model (Exp1)

Many recent studies have indicated that climate change (e.g., drought and N deposition) can alter the competitive environment of target species through the performance of current competitors (Gilman et al., 2010; Calama et al., 2019). In the present study, drought stress promoted the RMP and root competitiveness of *D. odorifera* against different N-fixing niche neighbors (e.g., a greater increase in root length, root tips, and branching number). Similar responses have been found in other studies, such that facilitative effects of a neighboring plant became stronger under stress (Bertness and Ewanchuk, 2002; He et al., 2013). For example, in one study, the competitive effect of neighbors of *Arrhenatherum elatius* was transformed into a facilitative effect when the plants were exposed to drought (Grant et al., 2014). These results are consistent with the stress gradient hypothesis, which states that positive interaction becomes stronger as the severity of the environment increases (Callaway et al., 2002; Ulrich et al., 2018, 2019). Furthermore, studies have confirmed that severe resource limitations can convert negative interactions to positive ones (Maestre and Cortina, 2003; He et al., 2013; Grant et al., 2014). It is interesting that in this study N application under well-watered conditions converted the promoting effect of *D. regia* on *D. odorifera* RMP (RRI > 0) to an inhibitory effect (RRI < 0). Therefore, N application may alter the root interaction between *D. odorifera* and *D. regia* under well-watered conditions. However, N application under drought stress reduced the root foraging performance of leguminous *D. odorifera* (e.g., decreased the root length, root surface area, root tips, and root branching number). Furthermore, greater decreases in these parameters were observed in the Do-Dr model than in the Do-Do and Do-Sm models, which indicates that N application weakens the promoting effect of *D. regia* on RMP under drought stress. Taken together, these results suggest that drought stress and N application might change the RMP of *D. odorifera* exposed to a different N-fixing niche neighbor with root system contact.

Linking RMP to the Relative Competitiveness of the Whole Plantlet

The RGR and RY are two indicators of the competitive ability of a target species (Ravenek et al., 2016). Plants alter their NAR to improve their adaptability in response to aboveground and belowground competition (Marvel et al., 1992; Simon et al., 2014). *D. odorifera* had a higher RGR and NAR in interspecific competition than in intraspecific competition, and RY values for shoots, the whole plantlet, and leaf N content were greater than 1.0 (**Figures 7A,B,D**) under the 100% FC, 30% FC, and 30% FC+N conditions. These results suggest that the relative competitiveness of *D. odorifera* benefits from different N-fixing niche neighbors, in particular under conditions of drought, N deficiency, and combined drought and N deficiency.

A higher RRS and RRI can contribute to the effective capturing of water and nutrients, and both can be used to estimate neighbor-induced RMP and root competitive advantage (Li et al., 2013, 2018). *D. odorifera* in interspecific competition exhibited positive values for the RRI of total roots and the RRS of the total, coarse, and fine roots. Moreover, the RY of total roots was greater than 1.0 under the 100% FC, 30% FC, and 30% FC+N conditions (**Figures 5, 6**). This indicates that a different N-fixing niche neighbor induces stronger RMP compared to the same N-fixing niche neighbor under conditions of drought, N deficiency, and combined drought and N deficiency.

Many studies have documented the close functional coordination between belowground changes and the aboveground response (Belter and Cahill, 2015), and the functional traits of plants are associated with competitive dominance. Thus, traits can be used to predict individual performance and population interaction (Fort et al., 2014; Kraft et al., 2015). Root traits have a greater impact on plant performance than leaf traits and are the most important predictors of the population dynamics (Schroeder-Georgi et al., 2016). For instance, root traits can reflect a plant's competitive advantage (Li et al., 2018; Semchenko et al., 2018). In our study, we discovered a strong correlation between the RMP and the relative competitiveness of the whole *D. odorifera* plantlet. The fact that *D. odorifera* showed stronger relative competitiveness against a different N-fixing niche neighbor than the same N-fixing niche neighbor under the 100% FC, 30% FC, and 30% FC+N conditions is consistent with the trend toward a higher RMP. In addition, the RY of the whole plantlet was well correlated with the RRI, RRS, and RY of total roots under the 100% FC, 30% FC, and 30% FC+N conditions (**Figure 8**). Such correlations imply that RMP to different N-fixing niche neighbors might be useful for predicting the relative competitiveness of the whole plantlet in an environment of severe stress. This finding is consistent with a previous study, in which a significant correlation was found between root traits and species performance (Schroeder-Georgi et al., 2016). The finding can be explained by the stronger RMP of *D. odorifera* that resulted from having a complementary N-fixing niche neighbor, which aided in the capture of a large amount of available resources (Lambers et al., 2017; Erktan et al., 2018) and ultimately enhanced the relative competitiveness of the whole plantlet (Li et al., 2018; Semchenko et al., 2018).

CONCLUSION

The RMP of leguminous woody *D. odorifera* is promoted by a different N-fixing niche neighbor under conditions of drought,

N deficiency, and combined drought and N deficiency with root system contact. Drought stress improves the RMP of *D. odorifera* exposed to a different N-fixing niche neighbor. N application converts the promoting effect of *D. regia* on RMP to an inhibitory effect under well-watered conditions. Moreover, N application under drought stress weakens the promoting effect of *D. regia* on RMP. Belowground interaction with a different N-fixing niche neighbor may be the only way to influence the RMP of *D. odorifera*, as the effects of aboveground interaction are negligible. Furthermore, neighbor-induced RMP might predict the relative competitiveness of the whole *D. odorifera* plantlet under conditions of drought, N deficiency, and combined drought and N deficiency. These findings provide novel insights into neighbor-induced dynamic changes in the root traits of leguminous woody species in forest systems in the context of climate change.

DATA AVAILABILITY STATEMENT

The original contributions presented in the study are included in the article/supplementary material, further inquiries can be directed to the corresponding author.

AUTHOR CONTRIBUTIONS

L-SX, L-FM, and FY contributed to the present work. L-SX performed the experiment and wrote the draft manuscript. L-FM assisted to carry the experiment in the greenhouse. FY designed the experiment, provided funding, and edited and revised the manuscript. All authors contributed to the article and approved the submitted version.

FUNDING

This work was sponsored by the Hainan Provincial Natural Science Foundation of China (320RC507 and 317052), the National Natural Science Foundation of China (no. 32060240, 31660165), and the Scientific Research Starting Foundation of Hainan University to FY (kyqd1573).

ACKNOWLEDGMENTS

We are very grateful to master's degree students Yujin Pu, Lijia Zhang, Dadong Li, and Juan Zhang for their help during the experiment.

REFERENCES

Andrews, M., and Andrews, M. E. (2017). Specificity in legume-rhizobia symbioses. *Int. J. Mol. Sci.* 18:705. doi: 10.3390/ijms18040705

Belter, P. R., and Cahill, J. F. (2015). Disentangling root system responses to neighbors: identification of novel root behavioural strategies. *AoB Plants* 7:plv059. doi: 10.1093/aobpla/plv059

Bennett, E., Roberts, J. A., and Wagstaff, C. (2012). Manipulating resource allocation in plants. *J. Exp. Bot.* 63, 3391–3400. doi: 10.1093/jxb/err442

Bertness, M. D., and Callaway, R. (1994). Positive interactions in communities. *Trends Ecol. Evol.* 9, 191–193. doi: 10.1016/0169-5347(94)90088-4

Bertness, M. D., and Ewanchuk, P. J. (2002). Latitudinal and climate-driven variation in the strength and nature of biological interactions in New England salt marshes. *Oecologia* 132, 392–401. doi: 10.1007/s00442-002-0972-y

Bilbrough, C. J., and Caldwell, M. M. (1995). The effects of shading and N-status on root proliferation in nutrient patches by the perennial grass. *Oecologia* 103, 10–16. doi: 10.1007/BF00328419

Bowsher, A. W., Shetty, P., Anacker, B. L., Siefert, A., Strauss, S. Y., Friesen, M. L., et al. (2017). Transcriptomic responses to conspecific and congeneric competition in co-occurring *Trifolium*. *J. Ecol.* 105, 602–615. doi: 10.1111/1365-2745.12761

Calama, R., Conde, M., de-Dios-García, J., Madrigal, G., Vázquez-Piqué, J., Gordo, F. J., et al. (2019). Linking climate, annual growth and competition in a Mediterranean forest: *Pinus pinea* in the Spanish Northern Plateau. *Agric. For. Meteorol.* 264, 309–321. doi: 10.1016/j.agrformet.2018.10.017

Callaway, R. M., Brooker, R. W., Choler, P., Kikvidze, Z., Lortie, C. J., Michalet, R., et al. (2002). Positive interactions among alpine plants increase with stress. *Nature* 417, 844–848. doi: 10.1038/nature00812

Chen, B. J., During, H. J., and Anten, N. P. (2012). Detect thy neighbor: identity recognition at the root level in plants. *Plant Sci.* 195, 157–167. doi: 10.1016/j.plantsci.2012.07.006

Cheplick, G. P., and Kane, K. H. (2004). Genetic relatedness and competition in *Triplasis purpurea* (Poaceae): resource partitioning or kin selection? *Int. J. Plant Sci.* 165, 623–630. doi: 10.1086/386556

Craine, J. M., Dybzinski, R., and Robinson, D. (2013). Mechanisms of plant competition for nutrients, water and light. *Funct. Ecol.* 27, 833–840. doi: 10.1111/1365-2435.12081

De Wit, C. T. (1960). *On competition*. Netherlands: Wageningen.

Erktan, A., McCormack, M. L., and Roumet, C. (2018). Frontiers in root ecology: recent advances and future challenges. *Plant Soil* 424, 1–9. doi: 10.1007/s11104-018-3618-5

Fort, F., Cruz, P., Jouany, C., and Field, K. (2014). Hierarchy of root functional trait values and plasticity drive early-stage competition for water and phosphorus among grasses. *Funct. Ecol.* 28, 1030–1040. doi: 10.1111/1365-2435.12217

Freschet, G. T., Bellingham, P. J., Lyver, P. O., Bonner, K. I., and Wardle, D. A. (2013). Plasticity in above- and belowground resource acquisition traits in response to single and multiple environmental factors in three tree species. *Ecol. Evol.* 3, 1065–1078. doi: 10.1002/ece3.520

Gilman, S. E., Urban, M. C., Tewksbury, J. J., Gilchrist, G. W., and Holt, R. D. (2010). A framework for community interactions under climate change. *Trends Ecol. Evol.* 25, 325–331. doi: 10.1016/j.tree.2010.03.002

Goisser, M., Geppert, U., Rötzer, T., Paya, A., Huber, A., Kerner, R., et al. (2016). Does belowground interaction with *Fagus sylvatica* increase drought susceptibility of photosynthesis and stem growth in *Picea abies*? *Forest Ecol. Manag.* 375, 268–278. doi: 10.1016/j.foreco.2016.05.032

Grant, K., Kreyling, J., Heilmeier, H., Beierkuhnlein, C., and Jentsch, A. (2014). Extreme weather events and plant–plant interactions: shifts between competition and facilitation among grassland species in the face of drought and heavy rainfall. *Ecol. Res.* 29, 991–1001. doi: 10.1007/s11284-014-1187-5

Gundel, P. E., Pierik, R., Mommer, L., and Ballare, C. L. (2014). Competing neighbors: light perception and root function. *Oecologia* 176, 1–10. doi: 10.1007/s00442-014-2983-x

Guo, Q. X., Li, J. Y., Zhang, Y. X., Zhang, J. X., Lu, D. L., Korpelainen, H., et al. (2016). Species-specific competition and N fertilization regulate non-structural carbohydrate contents in two Larix species. *Forest Ecol. Manag.* 364, 60–69. doi: 10.1016/j.foreco.2016.01.007

Guo, D. L., Xia, M. X., Wei, X., Chang, W. J., Liu, Y., and Wang, Z. Q. (2008). Anatomical traits associated with absorption and mycorrhizal colonization are linked to root branch order in twenty-three Chinese temperate tree species. *New Phytol.* 180, 673–683. doi: 10.1111/j.1469-8137.2008.02573.x

Guo, Y. P., Yang, X., Schob, C., Jiang, Y. X., and Tang, Z. Y. (2017). Legume shrubs are more nitrogen-homeostatic than non-legume shrubs. *Front. Plant Sci.* 8:1662. doi: 10.3389/fpls.2017.01662

Hansen, A., Martin, P., Buttery, B., and Park, S. (1992). Nitrate inhibition of N_2 fixation in *Phaseolus vulgar* is L. cv. OAC Rico and a supernodulating mutant. *New Phytol.* 122, 611–615. doi: 10.1111/j.1469-8137.1992.tb00088.x

Hauggaard-Nielsen, H., Ambus, P., and Jensen, E. S. (2001). Temporal and spatial distribution of roots and competition for nitrogen in pea-barley intercrops – a field study employing ^{32}P technique. *Plant Soil* 236, 63–74. doi: 10.1023/A:1011909414400

He, Q., Bertness, M. D., and Altieri, A. H. (2013). Global shifts towards positive species interactions with increasing environmental stress. *Ecol. Lett.* 16, 695–706. doi: 10.1111/ele.12080

Huang, B., and Eissenstat, D. M. (2000). "Root plasticity in exploiting water and nutrient heterogeneity" in *Plant-environment interactions*. ed. R. Wilkinson (Boca Raton, FL: CRC Press), 111–132.

Jolliffe, P. A. (2000). The replacement series. *J. Ecol.* 88, 371–385. doi: 10.1046/j.1365-2745.2000.00470.x

Kahmen, A., Renker, C., Unsicker, S. B., and Buchmann, N. (2006). Niche complementarity for nitrogen an explanation for the biodiversity and ecosystem functioning relationship? *Ecology* 87, 1244–1255. doi: 10.1890/0012-9658(2006)87[1244,NCFNAE]2.0.CO;2

Kraft, N. J., Godoy, O., and Levine, J. M. (2015). Plant functional traits and the multidimensional nature of species coexistence. *Proc. Natl. Acad. Sci. U. S. A.* 112, 797–802. doi: 10.1073/pnas.1413650112

Lambers, H., Albornoz, F., Kotula, L., Laliberté, E., Ranathunge, K., Teste, F. P., et al. (2017). How belowground interactions contribute to the coexistence of mycorrhizal and non-mycorrhizal species in severely phosphorus-impoverished hyperdiverse ecosystems. *Plant Soil* 424, 11–33. doi: 10.1007/s11104-017-3427-2

Lewis, S., and Tanner, E. (2000). Effects of above- and belowground competition on growth and survival of rain forest tree seedlings. *Ecology* 81, 2525–2538. doi: 10.1890/0012-9658(2000)081[2525:EOAABC]2.0.CO;2

Li, H. B., Ma, Q. H., Li, H. G., Zhang, F. S., Rengel, Z., and Shen, J. B. (2013). Root morphological responses to localized nutrient supply differ among crop species with contrasting root traits. *Plant Soil* 376, 151–163. doi: 10.1007/s11104-013-1965-9

Li, H. B., Zhang, D. S., Wang, X. X., Li, H. G., Rengel, Z., and Shen, J. B. (2018). Competition between *Zea mays* genotypes with different root morphological and physiological traits is dependent on phosphorus forms and supply patterns. *Plant Soil* 434, 125–137. doi: 10.1007/s11104-018-3616-7

Lithourgidis, A. S., Dordas, C. A., Damalas, C. A., and Vlachostergios, D. N. (2011). Annual intercrops: an alternative pathway for sustainable agriculture. *Aust. J. Crop. Sci.* 5, 396–410. doi: 10.1016/j.agwat.2011.01.017

Ma, Z. Q., Guo, D. L., Xu, X. L., Lu, M. Z., Bardgett, R. D., Eissenstat, D. M., et al. (2018). Evolutionary history resolves global organization of root functional traits. *Nature* 555, 94–97. doi: 10.1038/nature25783

Ma, Q. H., Wang, X., Li, H. B., Li, H. G., Cheng, L. Y., Zhang, F. S., et al. (2014). Localized application of $NH4^+$-N plus P enhances zinc and iron accumulation in maize via modifying root traits and rhizosphere processes. *Field Crop Res.* 164, 107–116. doi: 10.1016/j.fcr.2014.05.017

Macarthur, R., and Levins, R. (1967). The limiting similarity, convergence, and divergence of coexisting species. *Am. Nat.* 101, 377–385. doi: 10.1086/282505

Maestre, F. T., and Cortina, B. J. (2003). Positive, negative, and net effects in grass-shrub interactions in Mediterranean semiarid grasslands. *Ecology* 84, 3186–3197. doi: 10.1890/02-0635

Markham, J. H., and Zekveld, C. (2007). Nitrogen fixation makes biomass allocation to roots independent of soil nitrogen supply. *Can. J. Bot.* 85, 787–793. doi: 10.1139/B07-075

Marvel, J., Beyrouty, C., and Gbur, E. (1992). Response of soybean growth to root and canopy competition. *Crop Sci.* 32, 797–801. doi: 10.2135/cropsci1992.0011183X003200030044x

McNickle, G. G., Brown, J. S., and Schwinning, S. (2014). An ideal free distribution explains the root production of plants that do not engage in a tragedy of the commons game. *J. Ecol.* 102, 963–971. doi: 10.1111/1365-2745.12259

Mitchell, A. K. (1998). Acclimation of pacific yew (*Taxus brevifolia*) foliage to sun and shade. *Tree Physiol.* 18, 749–757. doi: 10.1093/treephys/18.11.749

Mou, P., Jones, R. H., Tan, Z. Q., Bao, Z., and Chen, H. M. (2012). Morphological and physiological plasticity of plant roots when nutrients are both spatially and temporally heterogeneous. *Plant Soil* 364, 373–384. doi: 10.1007/s11104-012-1336-y

Mou, P., Mitchell, R. J., and Jones, R. H. (1997). Root distribution of two tree species under a heterogeneous nutrient environment. *J. Appl. Ecol.* 34, 645. doi: 10.2307/2404913

Pierik, R., Mommer, L., Voesenek, L. A. C. J., and Robinson, D. (2013). Molecular mechanisms of plant competition: neighbor detection and response strategies. *Funct. Ecol.* 27, 841–853. doi: 10.1111/1365-2435.12010

Poorter, H., Niklas, K. J., Reich, P. B., Oleksyn, J., Poot, P., and Mommer, L. (2012). Biomass allocation to leaves, stems and roots: meta-analyses of interspecific variation and environmental control. *New Phytol.* 193, 30–50. doi: 10.1111/j.1469-8137.2011.03952.x

Radford, P. J. (1967). Growth analysis formulae - their use and abuse1. *Crop Sci.* 7:171. doi: 10.2135/cropsci1967.0011183X000700030001x

Ravenek, J. M., Mommer, L., Visser, E., Ruijven, J., Paauw, J., Smit-Tiekstra, A., et al. (2016). Linking root traits and competitive success in grassland species. *Plant Soil* 407, 39–53. doi: 10.1007/s11104-016-2843-z

Richards, A. E., Forrester, D. I., Bauhus, J., and Scherer-Lorenzen, M. (2010). The influence of mixed tree plantations on the nutrition of individual species: a review. *Tree Physiol.* 30, 1192–1208. doi: 10.1093/treephys/tpq035

Sadras, V., Lake, L., Li, Y., Farquharson, E. A., and Sutton, T. (2016). Phenotypic plasticity and its genetic regulation for yield, nitrogen fixation and $\delta\ ^{13}C$ in chickpea crops under varying water regimes. *J. Exp. Bot.* 67, 4339–4351. doi: 10.1093/jxb/erw221

Schenk, H. J. (2006). Root competition: beyond resource depletion. *J. Ecol.* 94, 725–739. doi: 10.1111/j.1365-2745.2006.01124.x

Schroeder-Georgi, T., Wirth, C., Nadrowski, K., Meyer, S. T., Mommer, L., Weigelt, A., et al. (2016). From pots to plots: hierarchical trait-based prediction of plant performance in a mesic grassland. *J. Ecol.* 104, 206–218. doi: 10.1111/1365-2745.12489

Semchenko, M., Lepik, A., Abakumova, M., and Zobel, K. (2018). Different sets of belowground traits predict the ability of plant species to suppress and tolerate their competitors. *Plant Soil* 424, 157–169. doi: 10.1007/s11104-017-3282-1

Simon, J., Li, X. Y., and Rennenberg, H. (2014). Competition for nitrogen between European beech and sycamore maple shifts in favour of beech with decreasing light availability. *Tree Physiol.* 34, 49–60. doi: 10.1093/treephys/tpt112

Tilman, D. (1981). Tests of resource competition theory using four species of Lake Michigan Algae. *Ecology* 62, 802–815. doi: 10.2307/1937747

Tilman, D. (1982). *Resource competition and community structure*. Princeton: Princeton University Press.

Tilman, D. (1987). On the meaning of competition and the mechanisms of competitive superiority. *Funct. Ecol.* 1, 304–315. doi: 10.2307/2389785

Ulrich, W., Hulisz, P., Mantilla-Contreras, J., Elvisto, T., and Piernik, A. (2019). Compensatory effects stabilize the functioning of Baltic brackish and salt marsh plant communities. *Estuar. Coast. Shelf Sci.* 231:106480. doi: 10.1016/j.ecss.2019.106480

Ulrich, W., Kubota, Y., Piernik, A., and Gotelli, N. J. (2018). Functional traits and environmental characteristics drive the degree of competitive intransitivity in European saltmarsh plant communities. *J. Ecol.* 106, 865–876. doi: 10.1111/1365-2745.12958

Wang, X. Y., Gao, Y. Z., Zhang, H. L., Shao, Z. Q., Sun, B. R., and Gao, Q. (2019). Enhancement of rhizosphere citric acid and decrease of $NO3^-$/$NH4^+$ ratio by root interactions facilitate N fixation and transfer. *Plant Soil* 447, 169–182. doi: 10.1007/s11104-018-03918-6

Wang, X., Guo, X., Yu, Y., Cui, H., Wang, R. Q., and Guo, W. H. (2018b). Increased nitrogen supply promoted the growth of non-N-fixing woody legume species but not the growth of N-fixing *Robinia pseudoacacia*. *Sci. Rep.* 8:17896. doi: 10.1038/s41598-018-35972-6

Wang, P., Shu, M., Mou, P., and Weiner, J. (2018a). Fine root responses to temporal nutrient heterogeneity and competition in seedlings of two tree species with different rooting strategies. *Ecol. Evol.* 8, 3367–3375. doi: 10.1002/ece3.3794

Wang, L., Zhu, Y., Zhao, Y., Yin, W., and Chai, Q. (2017). Response of nitrogen utilization to root interaction and plant density in barley-pea intercropping system. *Chin. J. Eco-Agric.* 25, 200–210. doi: 10.13930/j.cnki.cjea.160530

Yao, X. Y., Li, Y. F., Liao, L. N., Sun, G., Wang, H. X., and Ye, S. M. (2019). Enhancement of nutrient absorption and interspecific nitrogen transfer in a *Eucalyptus urophylla* × *eucalyptus grandis* and *Dalbergia odorifera* mixed plantation. *Forest Ecol. Manag.* 449:117465. doi: 10.1016/j.foreco.2019.117465

Zuppinger-Dingley, D., Schmid, B., Petermann, J. S., Yadav, V., De Deyn, G. B., and Flynn, D. F. (2014). Selection for niche differentiation in plant communities increases biodiversity effects. *Nature* 515, 108–111. doi: 10.1038/nature13869

Conflict of Interest: The authors declare that the research was conducted in the absence of any commercial or financial relationships that could be construed as a potential conflict of interest.

frontiers in Plant Science

ORIGINAL RESEARCH
published: 29 April 2021
doi: 10.3389/fpls.2021.658880

Role of Mixed-Species Stands in Attenuating the Vulnerability of Boreal Forests to Climate Change and Insect Epidemics

Raphaël D. Chavardès[1,2], Fabio Gennaretti[1,2], Pierre Grondin[3], Xavier Cavard[1], Hubert Morin[4] and Yves Bergeron[1,5]*

[1]*Institut de Recherche sur les Forêts, Université du Québec en Abitibi-Témiscamingue, Rouyn-Noranda, QC, Canada,* [2]*Groupe de Recherche en Écologie de la MRC-Abitibi, Université du Québec en Abitibi-Témiscamingue, Amos, QC, Canada,* [3]*Direction de la Recherche Forestière, Ministère des Forêts, de la Faune et des Parcs, Québec, QC, Canada,* [4]*Département des Sciences Fondamentales, Université du Québec à Chicoutimi, Saguenay, QC, Canada,* [5]*Université du Québec à Montréal, Montréal, QC, Canada*

OPEN ACCESS

Edited by:
Sanushka Naidoo, University of Pretoria, South Africa

Reviewed by:
Agnieszka Piernik, Nicolaus Copernicus University in Toruń, Poland
Slobodanka Pajevic, University of Novi Sad, Serbia

***Correspondence:**
Fabio Gennaretti
fabio.gennaretti@uqat.ca

Specialty section:
This article was submitted to Plant Abiotic Stress, a section of the journal Frontiers in Plant Science

Received: *26 January 2021*
Accepted: *07 April 2021*
Published: *29 April 2021*

Citation:
Chavardès RD, Gennaretti F, Grondin P, Cavard X, Morin H and Bergeron Y (2021) Role of Mixed-Species Stands in Attenuating the Vulnerability of Boreal Forests to Climate Change and Insect Epidemics. Front. Plant Sci. 12:658880. doi: 10.3389/fpls.2021.658880

We investigated whether stand species mixture can attenuate the vulnerability of eastern Canada's boreal forests to climate change and insect epidemics. For this, we focused on two dominant boreal species, black spruce [*Picea mariana* (Mill.) BSP] and trembling aspen (*Populus tremuloides* Michx.), in stands dominated by black spruce or trembling aspen ("pure stands"), and mixed stands (M) composed of both species within a 36 km^2 study area in the Nord-du-Québec region. For each species in each stand composition type, we tested climate-growth relations and assessed the impacts on growth by recorded insect epidemics of a black spruce defoliator, the spruce budworm (SBW) [*Choristoneura fumiferana* (Clem.)], and a trembling aspen defoliator, the forest tent caterpillar (FTC; *Malacosoma disstria* Hübn.). We implemented linear models in a Bayesian framework to explain baseline and long-term trends in tree growth for each species according to stand composition type and to differentiate the influences of climate and insect epidemics on tree growth. Overall, we found climate vulnerability was lower for black spruce in mixed stands than in pure stands, while trembling aspen was less sensitive to climate than spruce, and aspen did not present differences in responses based on stand mixture. We did not find any reduction of vulnerability for mixed stands to insect epidemics in the host species, but the non-host species in mixed stands could respond positively to epidemics affecting the host species, thus contributing to stabilize ecosystem-scale growth over time. Our findings partially support boreal forest management strategies including stand species mixture to foster forests that are resilient to climate change and insect epidemics.

Keywords: Forest tent caterpillar (*Malacosoma disstria*), spruce budworm [Choristoneura fumiferana (Clem.)], summer heat stress, growing season length, climate-growth relations, trembling aspen (*Populus tremuloides* Michx.), *Picea mariana* (Mill) B.S.P, stand mixture

INTRODUCTION

The boreal forest is the second largest biome on Earth, providing humans with ecosystem services that include sustainably harvested wood, carbon storage, and freshwater resources (Gauthier et al., 2015). Yet, there are growing concerns for the boreal forest about climate change affecting ecosystem services through direct and indirect impacts on stand dynamics and disturbances (Seidl et al., 2016). To address these concerns, landscape managers are encouraged to follow a suite of strategies to minimize vulnerabilities to climate change and reduce potential losses in stand productivity and commercial species abundance (Gauthier et al., 2014). Among the suggested strategies is the promotion of tree species mixture within stands, i.e., mixed-species stands (Felton et al., 2016).

The role of species mixture was investigated in reviews that compile a suite of findings identifying the beneficial effects of mixed-species stands over single-species stands including increased stand-level biodiversity and productivity (e.g., carbon sequestration, nutrient cycling, and water-use efficiency), decreased risk of damage caused by some disturbances (e.g., pathogens, pests, and windthrow), and diversified forestry production over time (Lilles and Coates, 2013; Felton et al., 2016; Liu et al., 2018). However, these reviews also mention challenges and disadvantages for the promotion of mixed-species stands relative to single-species stands. Specifically, the beneficial effects of species mixture may be confounded in research studies with the influences of site type, density, and tree age (Lilles and Coates, 2013). Species mixture may also bring some disadvantages, such as increased risks to browsing, higher logging costs, and less management simplicity (Felton et al., 2016). More importantly, studies that focus on understanding the dynamics in mixed-species stands and how these compare with single-species stands remain few, and thus limit our assessments of the benefits and disadvantages of these stands with respect to climate change and its impacts (Liu et al., 2018).

Species mixture interacts with the effects of climate change, which is influencing the growth of trees in boreal forests of Canada in several direct and indirect ways. For example, higher temperatures promote longer growing seasons and shoot elongation (Bronson et al., 2009); whereas increased summer heat stress and reductions in water availability result in growth suppressions and physiological stresses (Deslauriers et al., 2014; Girardin et al., 2016a,b; Puchi et al., 2020). Yet, while many studies investigated how climate may directly affect the growth of boreal species (e.g., Jarvis and Linder, 2000; Girardin et al., 2008; Price et al., 2013; Girardin et al., 2014; Chen et al., 2016; D'Orangeville et al., 2016, 2018a,b; Hember et al., 2017; Chaste et al., 2019), these rarely assess given species' growth responses to climate as a function of whether a stand is dominated by a single species or a mixture of species (hereafter, "pure stands" and "mixed stands," respectively). Apart from direct influences on tree growth, climate change can also indirectly influence the growth of trees by accelerating and magnifying disturbances such as insect epidemics that increased in frequency and severity in some boreal forests of Canada (e.g., Chen et al., 2018; Navarro et al., 2018). Insect development, survival, fecundity, and dispersion, as well as host-tree susceptibility *via* drought for example can all be influenced by climate change (Jactel et al., 2019). Nonetheless, only few studies investigated how insect epidemics affect pure vs. mixed stands.

In our study, the objective was to assess how climate and insect epidemics impact the growth of given boreal tree species in mixed and pure stands of eastern Canada. We focused on two regionally dominant tree species, black spruce [*Picea mariana* (Mill.) Britton, Sterns, & Poggenburg] and trembling aspen (*Populus tremuloides* Michx.), in mixed stands and stands dominated by one species [i.e., pure black spruce stands (PBS) and pure trembling aspen stands (PTA), respectively]. We compared stand attributes, developed species, and stand specific basal area increment (BAI) chronologies to test climate-growth relations, and compared tree growth during epidemics of a black spruce defoliator, the spruce budworm (SBW; *Choristoneura fumiferana* Clemens), and a trembling aspen defoliator, the forest tent caterpillar (FTC; *Malacosoma disstria* Hübn.). Although generally SBW has been associated with low mortality of black spruce relative to other species, studies suggest it could become a more privileged species of the spruce budworm diet in the future (Lavoie et al., 2019). Furthermore, we developed a model to jointly evaluate the influence of climate attributes, namely growing season length and summer heat stress, and insect epidemics, on the growth of a given tree-species and stand composition type. We hypothesized that black spruce and trembling aspen in mixed stands have greater average growth than in pure stands, and that these species are less vulnerable to climate change and insect epidemics in mixed- relative to pure stands. Ultimately, our research provides information on the potential role of species mixture in attenuating the vulnerability of eastern Canadian to climate change and insect epidemics.

MATERIALS AND METHODS

Study Area

The 36 km^2 study area extends from 49°08'–49°11'N to 78°46'–78°53'W (**Figure 1**) in the clay belt of the black spruce-feather moss bioclimatic domain of western Quebec (Saucier et al., 2011). Though black spruce dominates in most forests of the study area, trembling aspen can also dominate in some stands or compose mixed stands with black spruce, particularly on clay surficial deposits (Ministère des Forêts, de la Faune et des Parcs, 2020a). Most stands within the study area originated from the same fire that occurred in 1916 (Légaré et al., 2005). The climate normals from 1971 to 2000 for the nearest weather station at La Sarre (48°47'N, 79°13'W, and 244 m.a.s.l., Environment Canada, 2020a) show mean annual air temperature is 0.7°C, with mean monthly temperatures of 16.9°C and −18.2°C for July and January, respectively. Total annual precipitation averages 889.8 mm,

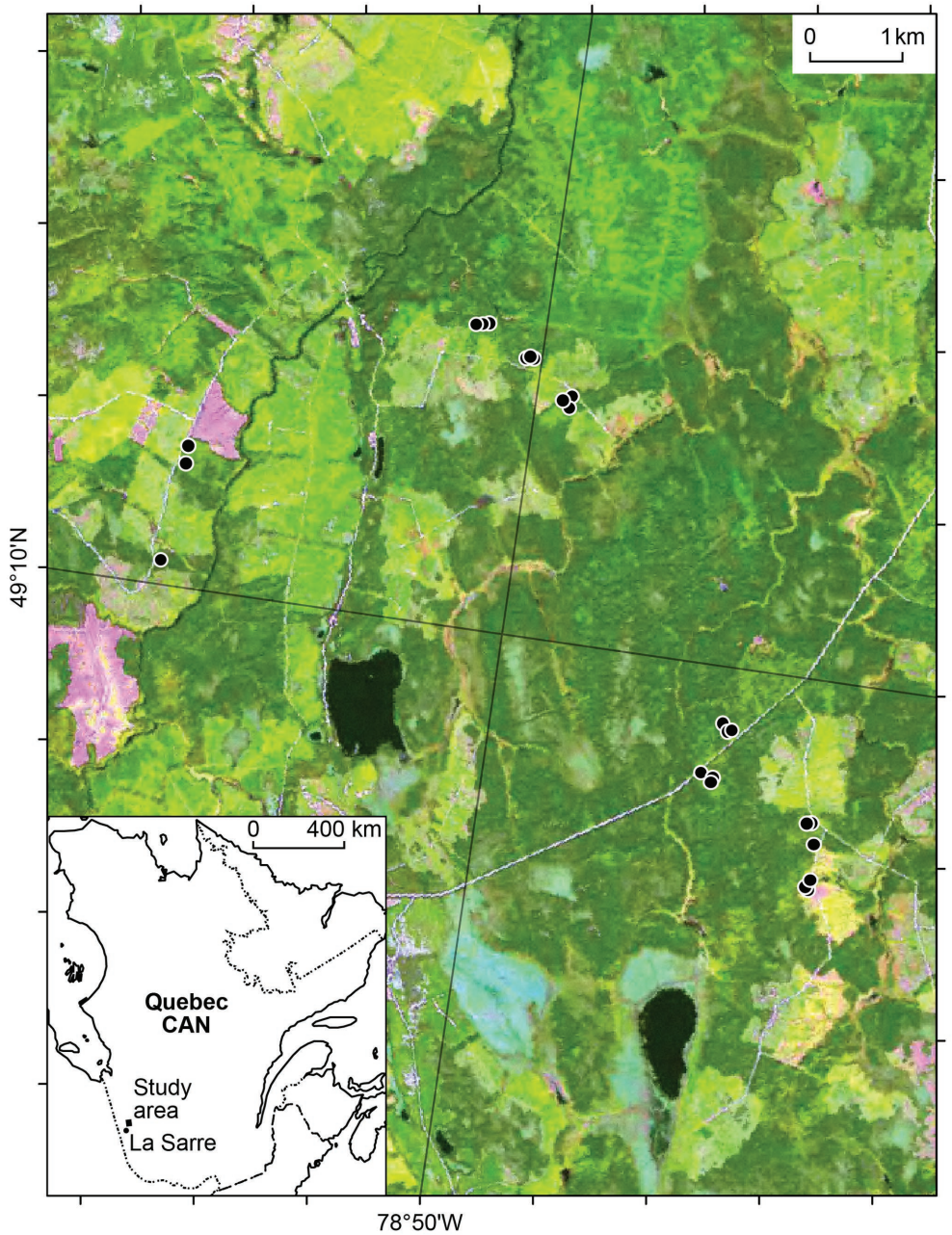

FIGURE 1 | Map of the study area with the 24 sites (black dots) located in boreal forests of western Quebec, Canada (CAN). The inset map shows the study area relative to the La Sarre weather station.

with 473.6 mm (53%) occurring as rain from May to September (Environment Canada, 2020a).

Stand and Tree-Ring Data

We used stand and tree-ring data from Cavard et al. (2010). On similar clay deposits and drainage, Cavard et al. (2010) established 24 circular 400 m^2 plots in eight blocks. At each plot, 20–40 trees were cored, and the diameter at breast height (DBH; 1.3 m above ground) and the species of each tree ≥5 cm DBH were recorded. In each block, three forest composition types were sampled: pure black spruce, pure trembling aspen, and mixed stands containing both species. Pure stands were defined as containing >75% of the dominant species in relative basal area, whereas mixed stands were mostly comprised of black spruce and trembling aspen but had no single species comprising more than 60% of the basal area (Cavard et al., 2010). For each core (n = 784), ring-width series were measured using a sliding-stage micrometer (Cavard et al., 2010).

We recovered the 784 ring-width series and reanalyzed them using CDendro version 9.0.1 (Larsson, 2017) and COFECHA

to develop five chronologies with high inter-series correlations (>0.40) and using trees with pith or inner rings dating from before 1950. These five chronologies were for black spruce and trembling aspen in different composition types: (1) black spruce in PBS, (2) trembling aspen in PTA, (3) suppressed to intermediate black spruce in PTA, (4) trembling aspen in mixed stands, and (5) black spruce in mixed stands. Altogether, 197 ring-width series satisfied the chronology development criteria (n = 164 for black spruce and n = 33 for trembling aspen). For each series, we estimated the distance to pith (after Duncan, 1989) to calculate five chronologies of mean basal area increments (BAIs) using the R package "dplr" (Bunn, 2008). To exclude juvenile growth in the chronologies for following analyses over 1950–2005, we retained a minimum cambial age of 15 years.

To compare stand attributes across composition types, we assessed stand basal area and tree density, and basal area of individual trees according to their age. To test for significant differences across stand basal area and tree density, we conducted Kruskal-Wallis one-way ANOVA on ranks with *post hoc* Tukey tests. To assess significant differences in mean basal area according to tree age, we compared the uncertainty intervals defined by the SEM.

Climate-Growth Relations

To test climate-growth relations, we required continuous monthly climate records. The nearest weather station at La Sarre had missing values between 1951 and 2004 (Environment Canada, 2020b). We therefore generated climate data, including monthly maximum, average, and minimum temperatures and monthly total precipitation from 1950 to 2005 for the study area with ClimateNA (Wang et al., 2016). Using the climate data and the mean BAI chronologies, we calculated correlations functions using the R package "treeclim" (Zang and Biondi, 2015). Specifically, we calculated Pearson's Product moment correlations with their 95% CIs derived from 1,000 random bootstrapped samples (Efron and Tibshirani, 1993). In each analysis, we assessed a 17-month window from April of the previous year through September of the year of ring formation. We also assessed the early and late months of the growing season and the summer months by calculating mean values for April and September, and from June to August, respectively. This allowed us to examine the influences of growing season length and summer heat stress, which were identified in previous research as variables impacting tree growth in boreal forests near our study area (e.g., Hofgaard et al., 1999; Drobyshev et al., 2013), and resulted in significant correlations in our analyses. As the correlations in our analyses were weak to moderate during the previous year of ring formation, we only provide results for the year of ring formation.

Influence of Specific Epidemic Years on Host and Non-host Species

We assessed if recorded SBW and FTC epidemic years within the region were associated to relevant growth anomalies for black spruce and trembling aspen in pure or mixed stands. Recorded epidemic years occurred in the 1970s for SBW (Ministère des Forêts, de la Faune et des Parcs, 2020b), and 1980, 2000, and 2001 for FTC (Bergeron et al., 2002; Ministère des Forêts, de la Faune et des Parcs, 2020c). We ranked mean BAI increases and decreases from 1 year to the next for the five chronologies between 1950 and 2005 (i.e., first-differenced chronologies), and we verified if the largest anomalies were simultaneous to epidemic years.

Interactions Among Tree Growth, Species Mixture, Climate, and Insect Epidemics

We implemented linear models in a Bayesian framework using Markov Chain Monte Carlo (MCMC) sampling with Metropolis-Hastings steps (Gelman et al., 2014) to explain the mean BAI chronologies for each species and stand composition type as a function of climate and the occurrence of insect epidemics. The models simultaneously accounted for the impact of climate and epidemics to disentangle their effects. In the models, we tested the influence of (1) baseline mean BAI growth and mean BAI long-term linear trend for each chronology, (2) April and September average temperature anomalies as a proxy of growing season length, (3) June–August average temperature anomalies as a proxy of average summer heat stress, and (4) the presence of recorded SBW and FTC epidemics. We modeled predicted mean BAI for a specific year t and a specific chronology y as:

$$\begin{aligned} \boldsymbol{BAI_{t,y} = \alpha\_Baseline_y + Trend_t \cdot \alpha\_Tr_y + SeasonLength_t \cdot} \\ \boldsymbol{\alpha\_SL_y + SummerHeat_t \cdot \alpha\_SH_y + Budworm_t \cdot} \\ \boldsymbol{\alpha\_SB_y + Caterpillar_t \cdot \alpha\_TC_y} \end{aligned}$$

Where each α is an estimated parameter depicting the effect of a given factor on the mean BAI chronologies, *α_Baseline* represents the predicted baseline mean BAI of a chronology over the period 1950–2005 (units: cm^2), *Trend* is an incremental number varying from −27 (1950) to +28 (2005) and thus *α_Tr* represents the coefficient of a long-term linear trend for a chronology linked to forest demography and dynamics (units: cm^2/year), *SeasonLength* is the mean temperature anomaly for April and September (departures from the mean), *SummerHeat* is the June–August mean temperature anomaly (departures from the mean), *Budworm* is the SBW epidemic intensity, and *Caterpillar* is the FTC epidemic intensity. We used uniform priors for each α, and a Jeffreys prior for the SD of departures between the models and the observations (σ). Model posterior probability over iterations of the MCMC (60,000 iterations with the first 10,000 rejected) was then computed with the product between the model likelihood $\left(\prod_{t=1950}^{2005} N\left(BAI_{t,y};\, \mu = SimBAI_{t,y}, \sigma_y\right)\right)$ and priors of the hyperparameter vector $\left(p\left(\psi_y\right)\right)$.

The SBW epidemic intensity was identified as suggested by Rossi et al. (2018) with a 9-year triangular impact (0.2, 0.4, 0.6, 0.8, 1, 0.8, 0.6, 0.4, and 0.2) centered on 1974 (value = 1), the most widespread epidemic year during the 1970s in our study area (Ministère des Forêts, de la Faune et des Parcs, 2020b). The FTC epidemic intensity was assigned to 1 for the

years 1980 and 2001 and to 0.5 for the year 2000 according to recorded epidemics (Bergeron et al., 2002; Ministère des Forêts, de la Faune et des Parcs, 2020c).

We plotted posterior distributions of the Bayesian model parameters (the six α for each model), including baseline mean BAI, mean BAI long-term linear trend, growing season length, summer heat, SBW impact, and FTC impact. We also implemented simpler models with subsets of the explanatory variables; however, we only present the full model because results were consistent among models. We considered that an overlap <10% across parameter posterior distributions for specific models was evidence of significant differences.

RESULTS

Chronology and Stands Attributes

The five tree-ring chronologies had series intercorrelations ranging from 0.56 to 0.71, indicating robust crossdating and a similar response of trees within stands to climate and environmental variation (**Table 1**). Stand median densities were significantly higher in PBS than in PTA, whereas median basal areas were significantly larger in PTA than in PBS (**Table 2**). Mixed stands had average densities and basal areas. Based on cambial age, black spruce grew significantly faster in mixed stands than in pure black spruce or trembling aspen stands (**Supplementary Figure 1**). In PTA, black spruce was suppressed by aspen. For trembling aspen, the difference in growth according to cambial age was not significant, although aspen in pure stands revealed larger mean basal areas.

Climate-Growth Relations

Mean BAI was positively correlated with higher temperatures in the early months of spring (March–April) for black spruce regardless of stand mixture, and in September for black spruce in PTA (**Figure 2**; **Supplementary Figures 2, 3**). Combined, April and September temperatures were positively correlated with mean BAI for black spruce regardless of stand mixture, indicating that black spruce may respond positively to longer growing seasons. Compared to black spruce, trembling aspen had no significant correlations between mean BAI and April and September temperatures.

Mean BAI was negatively correlated with higher temperatures in June and July for black spruce in pure black spruce and mixed stands, and in August for trembling aspen, suggesting that both species may be negatively impacted by summer heat stress. During winter months (January and February), increased precipitation was negatively correlated with mean BAI for black spruce in pure spruce stands (**Figure 3**), and for the same stands positive correlations with August precipitation were detected, indicating some hydric limitations in the late summer. For trembling aspen, no significant correlations with precipitation were detected.

Influence of Specific Epidemic Years on Host and Non-host Species

SBW and FTC epidemics revealed distinct impacts on growth depending on composition type (**Figure 4**; **Supplementary Table 1**). The SBW epidemic recorded in the 1970s coincided with decreases in mean BAI from 1 year to the next for black spruce in 1970, 1973, and 1974 across PBS (5th, 22nd, and 6th largest decreases, respectively), mixed stands (3rd, 7th, and 8th largest decreases, respectively), and PTA (2nd, 9th, and 14th largest decreases, respectively).

Forest tent caterpillar epidemics recorded in 1980, 2000, and 2001 coincided with decreases in mean BAI from 1 year to the next for trembling aspen across PTA (1st, 10th, and 2nd largest decreases, respectively) and mixed stands (1st, 15th, and 13th largest decreases, respectively). For black spruce in mixed and PTA, 1980 corresponded to large

TABLE 2 | Summary of stand attributes per composition type (mean value and range in parentheses).

Stand composition type	Mean basal area (m^2 ha^{-1})	Mean tree density (no. of stems ha^{-1})
Pure black spruce	45 (31–56)^{a}	3731 (1800–5275)^{b}
Mixed	54 (40–64)^{ab}	1916 (1125–2650)^{ab}
Pure trembling aspen	58 (42–73)^{b}	1313 (825–2025)^{a}

Pure stands were defined as containing >75% of the dominant species in relative basal area, whereas mixed stands had ≤75% of one species in relative basal area. Stems with diameter at breast height ≥5 cm were used. Different letters represent significant differences between median values ($p < 0.05$); the order of the letter marks is ascending.

TABLE 1 | Statistical characteristics of the black spruce and trembling aspen chronologies by stand composition type.

Species	Black spruce			Trembling aspen	
Composition type	Pure black spruce	Mixed	Pure trembling aspen	Pure trembling aspen	Mixed
No. of trees (radii)	61	73	30	22	11
Mean ring width (mm)	0.82	0.81	0.73	1.39	1.53
Mean sensitivity	0.16	0.21	0.22	0.32	0.27
SD (mm)	0.29	0.38	0.29	0.65	0.63
1st order autocorrelation	0.79	0.79	0.71	0.64	0.65
Series intercorrelation	0.56	0.58	0.63	0.71	0.63
Mean BAI (cm^2)	2.5	3.0	2.2	9.3	8.8
Chronology length (calendar yrs)	1928–2005	1925–2005	1929–2005	1921–2005	1926–2005

All characteristics, except chronology length, were computed over the period of analysis spanning from 1950 to 2005. BAI, basal area increments.

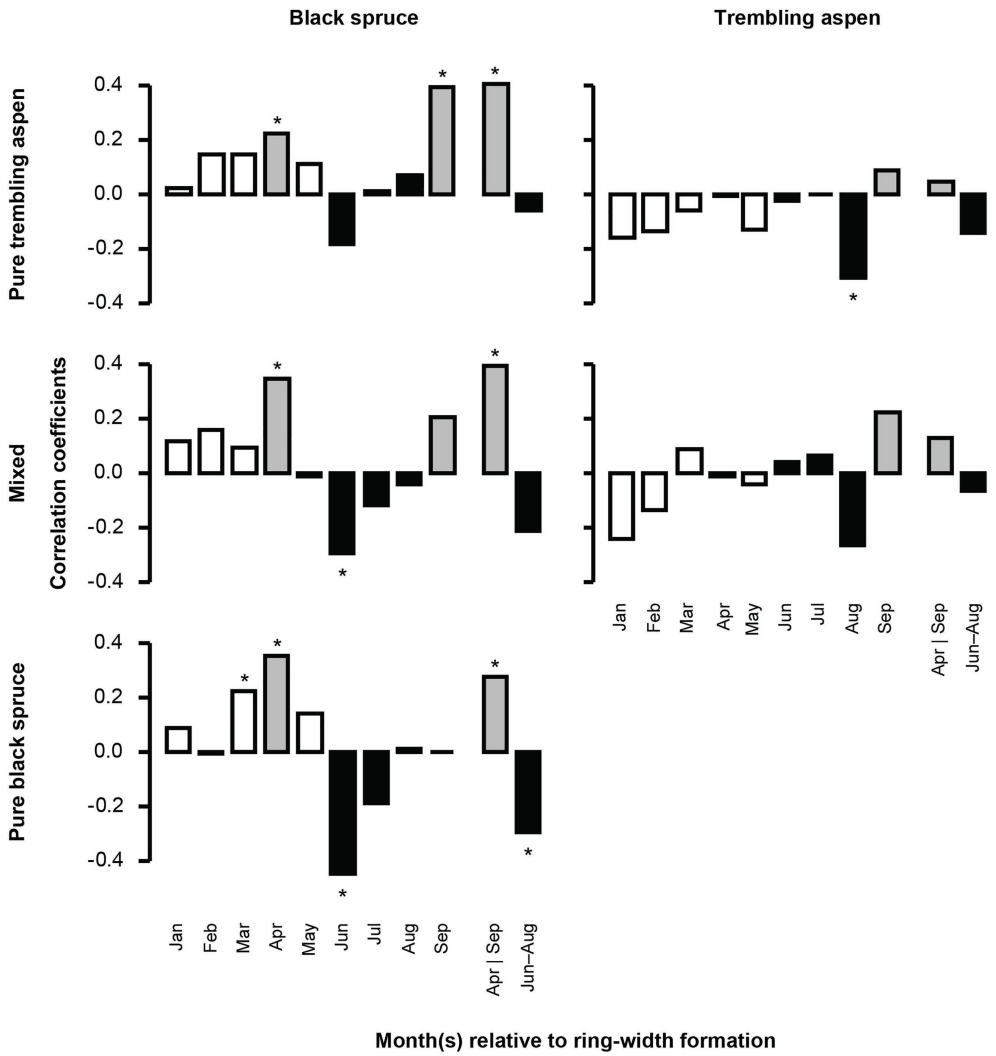

FIGURE 2 | Correlation between monthly average temperature and mean basal area increment (BAI) chronologies of black spruce and trembling aspen in pure and mixed stands from 1950 to 2005. April and September, important months for growing season length, are in gray; June–August, determining summer conditions, are in black. Stars represent significant correlation coefficients ($p < 0.05$). In each analysis, a 9-month window from January to September, and the mean values for April and September, and June–August of the year of ring formation were evaluated.

increases in mean BAI from 1 year to the next (3rd and 1st largest increases, respectively). This suggests that black spruce benefitted from an opening of the canopy due to FTC epidemics.

Interactions Among Tree Growth, Species Mixture, Climate, and Insect Epidemics

The linear Bayesian models summarized the growth responses of specific mean BAI chronologies to site conditions, climate, and insect epidemics. The models explained moderate to high proportions of BAI variability (R^2 = 28–67%; **Supplementary Figure 4**). No convergence issues in parameter selection were detected based on unimodal distributions of parameter posterior probabilities, shrinking of these probabilities relative to prior ranges, and stability of parameter values over MCMC chains (**Supplementary Figures 5–13**; **Supplementary Table 2**).

Most significant differences across posterior distributions were for black spruce in its three stand composition types. Black spruce average growth, indicated by baseline mean BAI, was significantly greater in mixed stands than in pure stands, and significantly greater in PBS than in PTA (**Figure 5A**). Mean BAI long term-linear trends were negative for black spruce in mixed stands and positive for PTA (**Figure 5B**). Regardless of composition type, black spruce responded positively to longer growing seasons and negatively to higher summer heat stress. Although differences among stand composition types were not significant, spruce in mixed stands benefitted most from longer growing seasons (**Figure 5C**) and was least vulnerable to summer heat stress (**Figure 5D**). Black spruce in mixed and pure aspen stands was more vulnerable to SBW epidemics (**Figure 5E**); however, these spruce trees benefitted from the negative impact of FTC epidemics on aspen (**Figure 5F**).

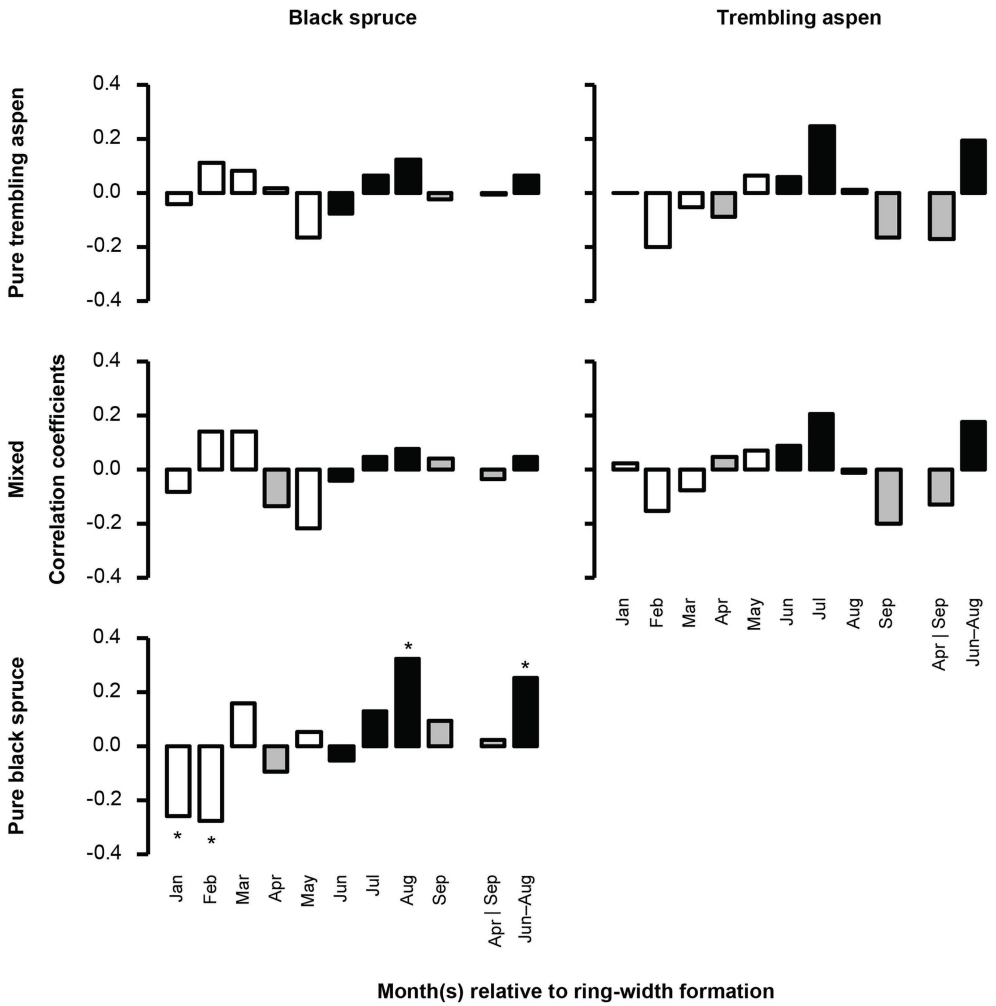

FIGURE 3 | Correlation between total monthly precipitation and mean BAI chronologies of black spruce and trembling aspen in pure and mixed stands from 1950 to 2005. April and September, important months for growing season length, are in gray; June–August, determining summer conditions, are in black. Stars represent significant correlation coefficients ($p < 0.05$). In each analysis, a 9-month window from January to September, and the mean values for April and September, and June–August of the year of ring formation were evaluated.

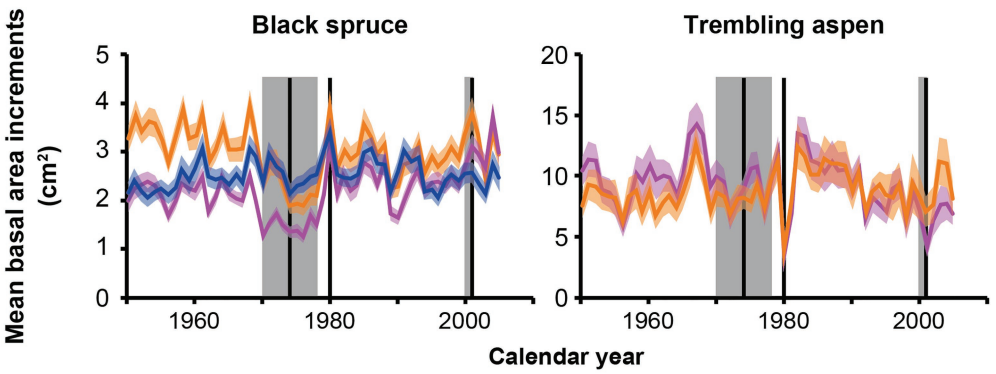

FIGURE 4 | Mean BAIs for black spruce and trembling aspen from 1950 to 2005. The blue curve represents mean BAI in pure black spruce stands (PBS), the orange curves represent mean BAI in mixed stands, and the purple curves represent mean BAI in pure trembling aspen stands (PTA). The colored areas represent ±1 SEM. The gray areas and black vertical lines correspond to the spruce budworm epidemic centered around 1974, and the forest tent caterpillar (FTC) epidemics of 1980 and 2000–2001 (Bergeron et al., 2002; Ministère des Forêts, de la Faune et des Parcs, 2020c).

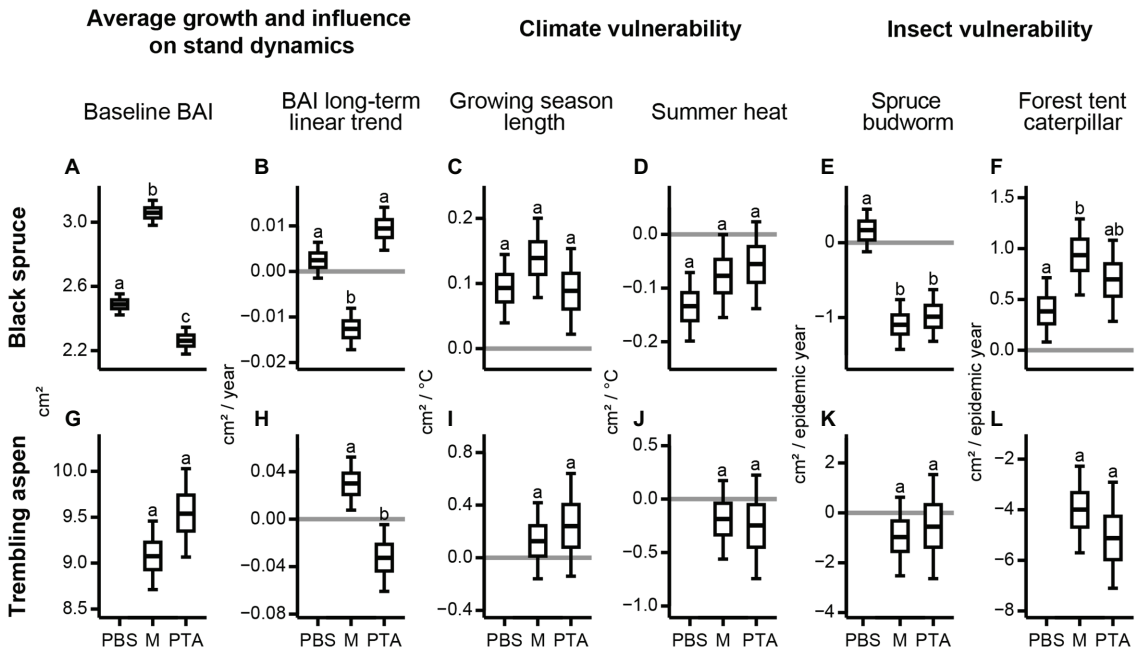

FIGURE 5 | Posterior distributions for parameters of the linear Bayesian models used to explain mean BAI chronologies for specific composition type as a function of climate and occurrence of insect epidemics. Boxplots compare the parameters for black spruce and trembling aspen in PBS, mixed stands (M), and PTA. Different letters represent posterior distributions with <10% overlap. We show the posterior distributions for **(A,G)** baseline BAI, **(B,H)** BAI long-term linear trend, **(C,I)** growing season length, **(D,J)** summer heat, **(E,K)** spruce budworm, and **(F,L)** forest tent caterpillar according to species and composition type.

TABLE 3 | Summary of the effects of species mixture on responses of black spruce and trembling aspen based on the results of the linear Bayesian models (**Figure 5**).

	Responses of		
	Black spruce in mixed vs. pure black spruce stands	**Black spruce in pure trembling aspen vs. pure black spruce stands**	**Trembling aspen in mixed vs. pure trembling aspen stands**
Average growth and influence on stand dynamics			
Baseline BAI	Higher*	Lower*	Lower‖
BAI long-term linear trend	Lower*	Higher‖	Higher*
Climate vulnerability			
Growing season length	Positive response‖	Null	Null
Summer heat	Lower vulnerability‖	Lower vulnerability‖	Null
Insect vulnerability			
Insect epidemic (SBW for spruce; FTC for aspen)	Higher vulnerability*	Higher vulnerability*	Null
Insect epidemic on the companion species	Positive response*	Positive response‖	Null

*For example, we compared the posterior distributions of baseline mean BAIs among mixed and pure stands to determine the result (i.e., higher or lower baseline mean BAI values). We identified with *responses that had overlaps between posterior distributions <10%, and with ‖responses with non-overlapping interquartile ranges between posterior distributions. SBW, spruce budworm; FTC, forest tent caterpillar.*

Compared to black spruce, trembling aspen did not reveal significant differences across its two stand composition types (**Figures 5G,I–L**), except for the mean BAI long-term linear trend, which was significantly greater in mixed stands (**Figure 5H**). Both aspen chronologies were negatively affected by the FTC epidemics, which halved mean BAI during epidemic years (**Figure 5L**).

DISCUSSION

We aimed to assess how climate and insect epidemics impact the growth of boreal tree species in mixed and pure stands of eastern Canada because species mixture may be a potential strategy to promote resilience of boreal forests in the context of global change by increasing tree growth (Hisano et al., 2019), reducing tree climate vulnerability to extreme events, and attenuating the impact of insect epidemics (Drobyshev et al., 2013). Here, we verify if some of these potential beneficial effects are visible in the mean BAI values of key boreal tree species in mixed and pure stands of eastern Canada: black spruce and trembling aspen. The results of our study are summarized in **Table 3**, and **Figure 5**, which is used to organize the following discussion.

Average vs. Long-Term Growth as Function of Composition Type

Our study provided evidence that trees in mixed stands can yield high mean BAI values and be less vulnerable to predicted warming in the region due to climate change. Black spruce

trees in mixed stands had high baseline mean BAI relative to spruce in pure stands (**Figure 5A**), but their long-term growth trend was impacted by the SBW epidemic in the 1970s, which coincided with several years of above average summer drought within the region (Environment Canada, 2020b; **Figure 5B**). Higher average growth of black spruce in mixed stands with aspen may be due to lower stand densities than in PBS, although mixed stands had higher basal areas (**Table 3**), and due to niche partitioning and type of leaf litter (Cavard et al., 2011). Black spruce in mixed stands may exploit a complementary crown packaging with trembling aspen (Burns and Honkala, 1990a,b; Cavard et al., 2011), a partitioning of the soil profile between the different root systems (Mekontchou et al., 2020), and higher nutrient availability due to aspen litterfall, which is less acidic and decomposes faster than black spruce needle litter (Légaré et al., 2005; Laganière et al., 2010). These beneficial effects were reduced following the SBW epidemic and dry conditions during the 1970s, resulting in a negative mean BAI long-term linear trend for spruce in mixed stands (**Figures 4, 5B**) and in a positive trend for aspen in the same stands (**Figure 5H**), although aspen showed a growth decline after the mid-1980s (**Figure 4**; **Supplementary Figure 4**). The aspen growth decline after the mid-1980s was more evident in pure stands likely because intraspecific competition for aspen in pure stands increased over time as these trees grew to large sizes more rapidly than in mixed stands (**Figure 5G**). Consequently, spruce trees in pure aspen stands showed a growth suppression until the mid-1980s and a suppression release afterward, resulting in a positive mean BAI long-term linear trend (**Figures 4, 5B**).

Climate-Growth Relations as a Function of Composition Type

We found black spruce was slightly less vulnerable to climate warming in mixed stands (**Figures 5C,D**). Although longer growing seasons and cooler summers benefitted the growth of black spruce regardless of stand mixture, black spruce in mixed stands responded more positively to longer growing seasons and was less vulnerable to summer heat stress. With warmer springs that hasten snowmelt, growth can start earlier for black spruce (Rossi et al., 2011). Growing seasons can also end later with warmer autumns, which favor the growth of black spruce especially in PTA and mixed stands. Black spruce endures less competition for water, light, and nutrients in mixed stands as aspen loses its foliage at the end of dry summers and in early fall (Constabel and Lieffers, 1996). During summer, higher temperatures lead to higher heat stress and increase moisture evaporation from shallow soils in which spruce roots grow (Way et al., 2013). These processes were attenuated in mixed stands because of niche partitioning and potential hydraulic lift from deeper rooted trembling aspen. We also found that increased precipitation as snow during winter months decreases the growth of black spruce in pure stands only. Dense PBS produce more shading, and snowmelt is delayed, especially when snow accumulation is high during cold winters. This process likely delays the beginning of the growing season for black spruce in pure spruce stands.

Compared to black spruce, trembling aspen revealed less sensitivity to climate and stand mixture (**Figures 5I,J**). The weak responses to climate during the year of ring formation for trembling aspen, are consistent with some other studies analyzing climate-growth relations in eastern Canadian boreal forests (e.g., Huang et al., 2010; D'Orangeville et al., 2018a), but contrast with Drobyshev et al. (2013) who found that trembling aspen responded positively to warmer and drier climate within the region.

Vulnerability to Insect Epidemics as a Function of Composition Type

Our study highlights significant interactions of species mixture with forest responses to insect epidemics. Although black spruce is a potential host for SBW (Blais, 1957), we found spruce in mixed stands and pure aspen stands showed a greater decrease in mean BAI and thus higher vulnerability to the 1970s SBW epidemic than in pure spruce stands (**Figure 5E**). The presence of aspen as a non-host species did not decrease the vulnerability to SBW of the host species as found in other studies within eastern Canada (e.g., Bergeron et al., 1995; Cappuccino et al., 1998; Campbell et al., 2008). However, these studies focused their analyses on balsam fir [*Abies balsamea* (L.) Mill.], the preferred diet of SBW (Hennigar et al., 2008). Two potential explanations may be proposed for this unexpected result. First, within the study area, Nagati et al. (2019) found a spatial association between balsam fir and trembling aspen linked to higher litter nutrient availability, which supports mycorrhizal communities associated with balsam fir. In our plots, we noticed the presence of balsam fir regeneration mainly in aspen dominated stands and we hypothesized that this presence may have contributed to the concentration of SBW on the nearby available spruce trees. Second, studies reporting a positive effect of species mixture on the attenuation of SBW impact analyzed species composition at the landscape/regional level (e.g., Campbell et al., 2008). In the region encompassing our study area, black spruce stands tend to dominate the landscape. The effect of species mixture in this condition may be less relevant than in a patchier landscape limiting SBW diffusion.

Conversely, the FTC epidemics in 1980 and 2000–2001 affected aspen trees severely, with a similar magnitude across mixture categories (**Figure 5L**), while black spruce in mixed and pure aspen stands had simultaneous and significant positive responses in growth, likely linked to higher light and water availability (**Figure 5F**). This implies that stand mixture may contribute to the stabilization of biomass increments over time at the ecosystem level, even when one species is affected by growth depletions in particular years. Similar findings on tree biomass stabilization in mixed stands of temperate and boreal forests of eastern Canada were reported by Aussenac et al. (2016). Differing growth responses between species associated with climatic fluctuations and insect epidemics could compensate thereby attenuating negative impacts on stand biomass accumulation (Aussenac et al., 2016).

CONCLUSION

In boreal forests of eastern Canada, stand species mixture offered several benefits against vulnerability to climate change and insect epidemics. Specifically, we found that black spruce in mixed stands had on average higher tree biomass accumulation than in pure stands; although, the long-term growth trend in mixed stands was negative due to stand dynamics and the 1970s SBW epidemic. In mixed stands, black spruce was less vulnerable to summer heat stress than in pure stands and benefitted from longer growing seasons. In contrast, trembling aspen was overall less sensitive to climate than black spruce, regardless of stand mixture. Within mixed relative to pure stands, both spruce and aspen did not show any reduction of vulnerability to insect epidemics as a host species, but spruce responded positively to FTC epidemics affecting aspen.

Our findings revealed the complex interactions of tree species in mixed stands and provide partial support toward forest management strategies that promote species mixture to decrease forest vulnerability to climate change and insect epidemics. For example, tree species responses to insect epidemics seemed to be affected by multiple interactions at stand and study area scales masking the effect of species mixture; although, contrasting growth responses between host and non-host tree species could stabilize carbon accumulation of mixed stands over time. Clearly, further research is warranted to disentangle the strength and direction of these interactions for boreal tree species in different mixtures and potentially other environmental conditions.

DATA AVAILABILITY STATEMENT

The original contributions presented in the study are included in the article/**Supplementary Material**, further inquiries can be directed to the corresponding author.

AUTHOR CONTRIBUTIONS

XC: data curation. RC and FG: formal analysis, methodology, visualization, and writing— original draft. RC, FG, and YB: investigation. YB and FG: resources and supervision. RC, FG, YB, XC, PG, and HM: writing – review and editing. All authors contributed to the article and approved the submitted version.

FUNDING

Funding was provided by the International Research Network on Cold Forests, the Ministère des Forêts, de la Faune et des Parcs (MFFP; contract number 142332177-D), and the Natural Sciences and Engineering Research Council of Canada (Alliance Grant number ALLRP 557148-20, obtained in partnership with the MFFP and Resolute Forest Products).

ACKNOWLEDGMENTS

We thank Philippe Marchand for statistical advice, Alain Leduc, Lorena Balducci, Miguel Montoro Girona, and Sergio Rossi for technical advice, and Danielle Charron, Ari Kainelainen, and Théo Châtellier for field and laboratory support. We also thank the two reviewers who made comments that improved the manuscript.

SUPPLEMENTARY MATERIAL

The Supplementary Material for this article can be found online at: https://www.frontiersin.org/articles/10.3389/fpls.2021.658880/full#supplementary-material

REFERENCES

Aussenac, R., Bergeron, Y., Mekontchou, C. G., Gravel, D., Pilch, K., and Drobyshev, I. (2016). Intraspecific variability in growth response to environmental fluctuations modulates the stabilizing effect of species diversity on forest growth. *J. Ecol.* 105, 1010–1020. doi: 10.1111/1365-2745.12728

Bergeron, Y., Denneler, B., Charron, D., and Girardin, M. P. (2002). Using dendrochronology to reconstruct disturbance and forest dynamics around Lake Duparquet, northwestern Quebec. *Dendrochronologia* 20, 175–189. doi: 10.1078/1125-7865-00015

Bergeron, Y., Leduc, A., Joyal, C., and Morin, H. (1995). Balsam fir mortality following the last spruce budworm outbreak in northwestern Quebec. *Can. J. For. Res.* 25, 1375–1384. doi: 10.1139/x95-150

Blais, J. R. (1957). Some relationships of the spruce budworm, *Choristoneura fumiferana* (Clem.) to black spruce, *Picea mariana* (Moench) Voss. *Forest. Chron.* 33, 364–372. doi: 10.5558/tfc33364-4

Bronson, D. R., Gower, S. T., Tanner, M., and Van Herk, I. (2009). Effect of ecosystem warming on boreal black spruce bud burst and shoot growth. *Glob. Chang. Biol.* 15, 1534–1543. doi: 10.1111/j.1365-2486.2009.01845.x

Bunn, A. G. (2008). A dendrochronology program library in R (dplR). *Dendrochronologia* 26, 115–124. doi: 10.1016/j.dendro.2008.01.002

Burns, R. M., and Honkala, B. H. (1990a). *Silvics of North America: Volume 1. Conifers*. United States Department of Agriculture, Forest Service. Washington, DC, United States of America. Available at: https://www.srs.fs.usda.gov/pubs/misc/ag_654_vol1.pdf (Accessed April 19, 2021).

Burns, R. M., and Honkala, B. H. (1990b). *Silvics of North America: Volume 2 Hardwoods*. United States Department of Agriculture, Forest Service. Washington, DC, United States of America. Available at: https://www.srs.fs.usda.gov/pubs/misc/ag_654_vol2.pdf (Accessed April 19, 2021).

Campbell, E. M., MacLean, D. A., and Bergeron, Y. (2008). The severity of budworm-caused growth reductions in balsam fir/spruce stands varies with the hardwood content of surrounding forest landscapes. *For. Sci.* 54, 195–205. doi: 10.1093/forestscience/54.2.195

Cappuccino, N., Lavertu, D., Bergeron, Y., and Régnière, J. (1998). Spruce budworm impact, abundance and parasitism rate in a patchy landscape. *Oecologia* 114, 236–242. doi: 10.1007/s004420050441

Cavard, X., Bergeron, Y., Chen, H. Y. H., and Paré, D. (2010). Mixed-species effect on tree aboveground carbon pools in the east-central boreal forests. *Can. J. For. Res.* 4, 37–47. doi: 10.1139/x09-171

Cavard, X., Bergeron, Y., Chen, H. Y. H., Paré, D., Laganière, J., and Brassard, B. (2011). Competition and facilitation between tree species change with stand development. *Oikos* 120, 1683–1695. doi: 10.1111/j.1600-0706.2011.19294.x

Chaste, E., Girardin, M. P., Kaplan, J. O., Bergeron, Y., and Hély, C. (2019). Increases in heat-induced tree mortality could drive reductions of biomass resources in Canada's managed boreal forest. *Landsc. Ecol.* 34, 403–426. doi: 10.1007/s10980-019-00780-4

Chen, L., Huang, J. G., Dawson, A., Zhai, L. H., Stadt, K. J., Comeau, P. G., et al. (2018). Contributions of insects and droughts to growth decline of trembling aspen mixed boreal forest of western Canada. *Glob. Chang. Biol.* 24, 655–667. doi: 10.1111/gcb.13855

Chen, H. Y. H., Luo, Y., Reich, P. B., Searle, E. B., and Biswas, S. R. (2016). Climate change-associated trends in net biomass change are age dependent in western boreal forests of Canada. *Ecol. Lett.* 19, 1150–1158. doi: 10.1111/ele.12653

Constabel, A. J., and Lieffers, V. J. (1996). Seasonal patterns of light transmission through boreal mixewood canopies. *Can. J. For. Res.* 26, 1008–1014. doi: 10.1139/x26-111

Deslauriers, A., Beaulieu, M., Balducci, L., Giovannelli, A., Gagnon, M. J., and Rossi, S. (2014). Impact of warming and drought on carbon balance related to wood formation in black spruce. *Ann. Bot. London* 114, 335–345. doi: 10.1093/aob/mcu111

D'Orangeville, L., Duchesne, L., Houle, D., Kneeshaw, D., Côté, B., and Pederson, N. (2016). Northeastern North America as a potential refugium for boreal forests in a warming climate. *Science* 352, 1452–1455. doi: 10.1126/science.aaf4951

D'Orangeville, L., Houle, D., Duchesne, L., Philippe, R. P., Bergeron, Y., and Kneeshaw, D. (2018a). Beneficial effects of climate warming on boreal tree growth may be transitory. *Nat. Commun.* 9, 1–10. doi: 10.1038/s41467-018-05705-4

D'Orangeville, L., Maxwell, J., Kneeshaw, D., Pederson, N., Duchesne, L., Logan, T., et al. (2018b). Drought timing and local climate determine the sensitivity of eastern temperate forests to drought. *Glob. Chang. Biol.* 24, 2339–2351. doi: 10.1111/gcb.14096

Drobyshev, I., Gewehr, S., Berninger, F., and Bergeron, Y. (2013). Species specific growth responses of black spruce and trembling aspen may enhance resilience of boreal forest to climate change. *J. Ecol.* 101, 231–242. doi: 10.1111/1365-2745.12007

Duncan, R. P. (1989). An evaluation of errors in tree age estimates based on increment coes in kahikatea (*Dacrycarpus dacrydioides*). *N. Z. Nat. Sci.* 16, 31–37.

Efron, B., and Tibshirani, R. (1993). *An Introduction to the Bootstrap*. New York: Chapman & Hall, Inc.

Environment Canada (2020a). *Canadian Climate Normals 1971–2000: La Sarre, Québec*. National Climate Data and Information Archive. Ottawa, Ontario, Canada. Available at: https://climate.weather.gc.ca/climate_normals/index_e.html (Accessed April 19, 2021).

Environment Canada (2020b). *Canadian Daily Climate Data*. National Climate Data and Information Archive. Ottawa, Ontario, Canada. Available at: https://climate.weather.gc.ca/historical_data/search_historic_data_e.html (Accessed April 19, 2021).

Felton, A., Nilsson, U., Sonesson, J., Felton, A. M., Roberge, J. M., Ranius, T., et al. (2016). Replacing monocultures with mixed-species stands: ecosystem service implications of two production forest alternatives in Sweden. *Ambio* 45, S124–S139. doi: 10.1007/s13280-015-0749-2

Gauthier, S., Bernier, P., Burton, P. J., Edwards, J., Isaac, K., Isabel, N., et al. (2014). Climate change vulnerability and adaptation in the managed Canadian boreal forest. *Environ. Rev.* 22, 256–285. doi: 10.1139/er-2013-0064

Gauthier, S., Bernier, P., Kuuluvainen, T., Shvidenko, A. Z., and Schepaschenko, D. G. (2015). Boreal forest health and global change. *Science* 21, 819–822. doi: 10.1126/science.aaa9092

Gelman, A., Carlin, J. B., Stern, H. S., Dunson, D. B., Vehtari, A., and Rubin, D. B. (2014). *Bayesian Data Analysis*. Boca Raton: Chapman & Hall_CRC.

Girardin, M. P., Bouriaud, O., Hogg, E. H., Kurz, W., Zimmermann, N. E., Metsaranta, J. M., et al. (2016a). No growth stimulation of Canada's boreal forest under half-century of combined warming and CO2 fertilization. *Proc. Natl. Acad. Sci. U.S.A.* 113, E8406–E8414. doi: 10.1073/pnas.1610156113

Girardin, M. P., Guo, X. J., De Jong, R., Kinnard, C., Bernier, P., and Raulier, F. (2014). Unusual forest growth decline in boreal North America covaries with the retreat of Arctic sea ice. *Glob. Chang. Biol.* 20, 851–866. doi: 10.1111/gcb.12400

Girardin, M. P., Hogg, E. H., Bernier, P. Y., Kurz, W. A., Guo, X. J., and Cyr, G. (2016b). Negative impacts of high temperatures on growth of black spruce forests intensify with the anticipated climate warming. *Glob. Chang. Biol.* 22, 627–643. doi: 10.1111/gcb.13072

Girardin, M. P., Raulier, F., Bernier, P. Y., and Tardif, J. C. (2008). Response of tree growth to a changing climate in boreal Central Canada: a comparison of empirical, process-based, and hybrid modelling approaches. *Ecol. Model.* 213, 209–228. doi: 10.1016/j.ecolmodel.2007.12.010

Hember, R. A., Kurz, W. A., and Coops, N. C. (2017). Increasing net ecosystem biomass production of Canada's boreal and temperate forests despite decline in dry climates. *Global Biogeochem. Cy.* 31, 134–158. doi: 10.1002/2016GB005459

Hennigar, C. R., MacLean, D. A., Quiring, D. T., and Kershaw, J. A. (2008). Differences in spruce budworm defoliation among balsam fir and white, red, and black spruce. *For. Sci.* 54, 158–166. doi: 10.1093/forestscience/54.2.158

Hisano, M., Chen, H. Y. H., Searle, E. B., and Reich, P. B. (2019). Species-rich boreal forests grew more and suffered less mortality than species-poor forests under the environmental change of the past half-century. *Ecol. Lett.* 22, 999–1008. doi: 10.1111/ele.13259

Hofgaard, A., Tardif, J., and Bergeron, Y. (1999). Dendroclimatic response of Picea mariana and *Pinus banksiana* along a latitudinal gradient in the eastern Canadian boreal forest. *Can. J. For. Res.* 29, 1333–1346. doi: 10.1139/x99-073

Huang, J. G., Tardif, J. C., Bergeron, Y., Denneler, B., Berninger, F., and Girardin, M. P. (2010). Radial growth response of four dominant boreal tree species to climate along a latitudinal gradient in the eastern Canadian boreal forest. *Glob. Chang. Biol.* 16, 711–731. doi: 10.1111/j.1365-2486.2009.01990.x

Jactel, H., Koricheva, J., and Castagneyrol, B. (2019). Responses of forest insect pests to climate change: not so simple. *Curr. Opin. Insect Sci.* 35, 103–108. doi: 10.1016/j.cois.2019.07.010

Jarvis, P., and Linder, S. (2000). Constraints to growth of boreal forests. *Nature* 405, 904–905. doi: 10.1038/35016154

Laganière, J., Paré, D., and Bradley, R. L. (2010). How does a tree species influence litter decomposition? Separating the relative contribution of litter quality, litter mixing, and forest floor conditions. *Can. J. For. Res.* 40, 465–475. doi: 10.1139/X09-208

Larsson, L. (2017). CDendro package version 9.0.1. Cybis Elektronik & Data AB. Available at: http://www.cybis.se (Accessed April 19, 2021).

Lavoie, J., Montoro Girona, M., and Morin, H. (2019). Vulnerability of conifer regeneration to spruce budworm outbreaks in the eastern Canadian boreal Forest. *Forests* 10, 1–14. doi: 10.3390/f10100850

Légaré, S., Paré, D., and Bergeron, Y. (2005). Influence of aspen on forest floor properties in black sprue-dominated stands. *Plant Soil* 274, 207–220. doi: 10.1007/s11104-005-1482-6

Lilles, E. B., and Coates, K. D. (2013). An evaluation of the main factors affecting yield differences between single- and mixed-species stands. *J. Ecosyst. Manage.* 14, 1–14.

Liu, C. L., Kuchma, O., and Krutovsky, K. V. (2018). Mixed-species versus monocultures in plantation forestry: development, benefits, ecosystem services and perspectives for the future. *Glob. Ecol. Conserv.* 15, 1–13. doi: 10.1016/j.gecco.2018.e00419

Mekontchou, C. G., Houle, D., Bergeron, Y., and Drobyshev, I. (2020) Contrasting root system structure and belowground interactions between black spruce (*Picea mariana* (Mill.) B.S.P) and trembling aspen (*Populus tremuloides* Michx) in boreal mixedwoods of eastern Canada. *Forests* 11, 1–19. doi: 10.3390/f11020127

Ministère des Forêts, de la Faune et des Parcs (2020a). Data from: Cartographie du 5e inventaire écoforestier du Québec méridional – Méthodes et données associées. Ministère des Forêts, de la Faune et des Parcs, Direction des Inventaires Forestiers, Québec, Canada. Available at: https://www.donneesquebec.ca/recherche/fr/dataset/resultats-d-inventaire-et-carte-ecoforestiere/resource/1ea8bc6b-18e9-4676-8aba-c1f3edbcbc0e (Accessed April 19, 2021).

Ministère des Forêts, de la Faune et des Parcs (2020b). Data from: Données sur les perturbations naturelles – Insecte: Tordeuse des bourgeons de l'épinette. Ministère des Forêts, de la Faune et des Parcs, Direction de la Protection des Forêts, Québec, Canada. Available at: https://www.donneesquebec.ca/recherche/dataset/donnees-sur-les-perturbations-naturelles-insecte-tordeuse-des-bourgeons-de-lepinette (Accessed April 19, 2021).

Ministère des Forêts, de la Faune et des Parcs (2020c). Data from: Données sur les perturbations naturelles – Insecte: Livrée des forêts. Ministère des Forêts, de la Faune et des Parcs, Direction de la Protection des Forêts, Québec, Canada. Available at: https://www.donneesquebec.ca/recherche/dataset/

donnees-sur-les-perturbations-naturelles-insecte-livree-des-forets (Accessed April 19, 2021).

Nagati, M., Roy, M., Desrochers, A., Manzi, S., Bergeron, Y., and Gardes, M. (2019). Facilitation of balsam fir by trembling aspen in the boreal forest: do ectomycorrhizal communities matter? *Front. Plant Sci.* 10:932. doi: 10.3389/fpls.2019.00932

Navarro, L., Morin, H., Bergeron, Y., and Montoro Girona, M. (2018). Changes in spatiotemporal patterns of 20th century spruce budworm outbreaks in eastern Canadian boreal forests. *Front. Plant Sci.* 9:1905. doi: 10.3389/fpls.2018.01905

Price, D. T., Alfaro, R. I., Brown, K. J., Flannigan, M. D., Fleming, R. A., Hogg, E. H., et al. (2013). Anticipating the consequences of climate change for Canada's boreal forest ecosystems. *Environ. Rev.* 21, 322–365. doi: 10.1139/er-2013-0042

Puchi, P. F., Castagneri, D., Rossi, S., and Carrer, M. (2020). Wood anatomical traits in black spruce reveal latent water constraints on the boreal forest. *Glob. Chang. Biol.* 26, 1767–1777. doi: 10.1111/gcb.14906

Rossi, S., Morin, H., and Deslauriers, A. (2011). Multi-scale influence of snowmelt on xylogenesis of black spruce. *Arct. Antarct. Alp. Res.* 43, 457–464. doi: 10.1657/1938-4246-43.3.457

Rossi, S., Plourde, P. Y., and Krause, C. (2018). Does a spruce budworm outbreak affect the growth response of black spruce to a subsequent thinning? *Front. Plant Sci.* 9:1061. doi: 10.3389/fpls.2018.01061

Saucier, J. P., Robitaille, A., Grondin, P., Bergeron, Y., and Gosselin, J. (2011). *Les régions écologiques du Québec méridional*. Quebec: Ministère des Ressources Naturelles et de la Faune, Direction des Inventaire Forestiers.

Seidl, R., Spies, T. A., Peterson, D. L., Stephens, S. L., and Hicke, J. A. (2016). Searching for resilience: addressing the impacts of changing disturbance regimes on forest ecosystem services. *J. Appl. Ecol.* 53, 120–129. doi: 10.1111/1365-2664.12511

Wang, T. L., Hamann, A., and Spittlehouse, and D., Carroll, C., (2016). Locally downscaled and spatially customizable climate data for historical and future periods for North America. *PLoS One* 11:e0156720. doi: 10.1371/journal.pone.0156720

Way, D. A., Crawley, C., and Sage, R. F. (2013). A hot and dry future: warming effects on boreal tree drought tolerance. *Tree Physiol.* 33, 1003–1005. doi: 10.1093/treephys/tpt092

Zang, C., and Biondi, F. (2015). treeclim: an R package for the numerical calibration of proxy-climate relationships. *Ecography* 38, 431–436. doi: 10.1111/ecog.01335

Conflict of Interest: The authors declare that the research was conducted in the absence of any commercial or financial relationships that could be construed as a potential conflict of interest.

frontiers in Plant Science

REVIEW
published: 30 April 2021
doi: 10.3389/fpls.2021.606908

Breeding for Climate Change Resilience: A Case Study of Loblolly Pine (*Pinus taeda* L.) in North America

Lilian P. Matallana-Ramirez[1], Ross W. Whetten[1], Georgina M. Sanchez[2] and Kitt G. Payn[1]*

[1] Department of Forestry and Environmental Resources, North Carolina State University, Raleigh, Raleigh, NC, United States, [2] Center for Geospatial Analytics, North Carolina State University, Raleigh, Raleigh, NC, United States

Earth's atmosphere is warming and the effects of climate change are becoming evident. A key observation is that both the average levels and the variability of temperature and precipitation are changing. Information and data from new technologies are developing in parallel to provide multidisciplinary opportunities to address and overcome the consequences of these changes in forest ecosystems. Changes in temperature and water availability impose multidimensional environmental constraints that trigger changes from the molecular to the forest stand level. These can represent a threat for the normal development of the tree from early seedling recruitment to adulthood both through direct mortality, and by increasing susceptibility to pathogens, insect attack, and fire damage. This review summarizes the strengths and shortcomings of previous work in the areas of genetic variation related to cold and drought stress in forest species with particular emphasis on loblolly pine (*Pinus taeda* L.), the most-planted tree species in North America. We describe and discuss the implementation of management and breeding strategies to increase resilience and adaptation, and discuss how new technologies in the areas of engineering and genomics are shaping the future of phenotype-genotype studies. Lessons learned from the study of species important in intensively-managed forest ecosystems may also prove to be of value in helping less-intensively managed forest ecosystems adapt to climate change, thereby increasing the sustainability and resilience of forestlands for the future.

Keywords: abiotic stress, drought, cold, loblolly pine, tree breeding, tree physiology, conifer genomics, climate change

OPEN ACCESS

Edited by:
Amy Brunner, Virginia Tech, United States

Reviewed by:
Jean Beaulieu, Laval University, Canada
Thomas Kolb, Northern Arizona University, United States

***Correspondence:**
Ross W. Whetten
ross_whetten@ncsu.edu

Specialty section:
This article was submitted to Plant Abiotic Stress, a section of the journal Frontiers in Plant Science

Received: *16 September 2020*
Accepted: *08 April 2021*
Published: *30 April 2021*

Citation:
Matallana-Ramirez LP, Whetten RW, Sanchez GM and Payn KG (2021) Breeding for Climate Change Resilience: A Case Study of Loblolly Pine (Pinus taeda L.) in North America. Front. Plant Sci. 12:606908. doi: 10.3389/fpls.2021.606908

INTRODUCTION

Plants experience stress when they receive any type of stimulus that disrupts metabolic homeostasis and affects growth, development, and productivity. During the first phases of the stress event, the plant will use energy to find a new equilibrium by adjusting metabolic pathways, thereby increasing the probability of survival in a process that is usually referred to as acclimation or physiological adaptation.

Two general mechanisms of dealing with stress are avoidance and tolerance. Avoidance implies that plants evade the stressful condition by preventing or reducing the exposure to its deleterious effects, whereas tolerance consists of responses that enable plants to endure or withstand the adverse conditions (McDowell et al., 2008; Schulze et al., 2020). These mechanisms need not be mutually exclusive; different plant species can lie at various points along a continual spectrum of response. Failure to acclimate to stress due to insufficient avoidance or tolerance mechanisms can result in a number of deleterious events, which in the extreme can lead to death. Plant tolerance of stressful conditions can be due to physiological mechanisms of resistance or resilience. Resistance in this context means maintenance of growth, development, and productivity under stressful conditions, while resilience means that plants show reduced rates of growth or productivity under stressful conditions, with some degree of increase either to the pre-disturbance level or to a new stable condition, after the stress condition is past. Plant resilience can vary both in how quickly the plant will be able to return to the pre-disturbance condition (Holling, 1973; Lloret et al., 2011; Eilmann and Rigling, 2012) or in the difference between the pre-disturbance condition and the new stable state (Ingrisch and Bahn, 2018). In the particular case of forest species, studies are often motivated by how to enhance productivity and define the level of tolerance or resistance by the maintenance of stem growth and wood production (e.g., Orwig and Abrams, 1997; Eilmann et al., 2010). Nevertheless, the levels of stress-response and survival rates depend to a great extent on the initial plant condition (e.g., type of species, age), the plant history (e.g., priming, or acclimation to previous stressful events), and the level and extension of the disruption.

This is particularly interesting in the case of cultivated forest tree species for which genetic improvement programs exist and provide a significant fraction of planting stock for reforestation. In these species, breeders have typically focused on selection of trees with improved productivity and quality traits under climate conditions that were expected to vary little over time. Unfortunately, climate change is associated with increases in both the variability and the average levels of temperature and water availability, leading to extreme variability of weather events recently called "weather whiplash." This phenomenon has been highlighted as a major issue that will affect the way plants and animals will mitigate and adapt to future climate conditions (Swain et al., 2018; Casson et al., 2019). These changes have the potential to degrade the productivity of cultivated forest species, so tree breeders will need to incorporate some measures of tolerance or resistance to these disturbances into their breeding and selection programs as soon as possible in order to minimize negative impacts on productivity of forest plantations in the latter half of this century.

Managed agricultural and forest ecosystems can be modified both through changes in management practices and by choice of resilient and well-adapted planting stock, but stress response plasticity and the genetic differences that underline tolerance and resistance are still largely unknown in conifers. The combination of new phenotyping technologies and genomic tools has allowed major advances in understanding of the genetic basis of abiotic stress response in Populus species (e.g., Georgii et al., 2019), particularly Populus trichocarpa (e.g., Weighill et al., 2019a,b). These new technologies in the areas of engineering and genomics are beginning to be applied to phenotype-genotype studies in conifers as well (D'Odorico et al., 2020; Depardieu et al., 2020). Continued advances in acquisition and analysis of data using sensing technologies such as hyperspectral imaging must be combined with advances in genomic tools and resources to better understand the role of genetic and epigenetic mechanisms in conifer responses to drought and cold stress, and find new paths forward in forest tree breeding.

Loblolly pine (*Pinus taeda* L.) is the most-planted forest tree species in North America (McKeand et al., 2021), and will be the species on which our review is focused. We begin by introducing the extensive geographic variation observed for loblolly pine and the importance of selecting an appropriate seed source to ensure good survival and optimal productivity. We then introduce a general timeline of loblolly pine seed production and plantation establishment, and highlight the stages most vulnerable to extremes of temperature and drought. This is followed by a review of the physiological changes that have been described as adaptation strategies adopted by plants to cope with drought and cold stress. This topic offers a perfect transition into the molecular level and a relatively new area of research that studies the cross-talk between stress responses and the potential to use this information to identify trees with increased adaptation and resilience. We conclude with a discussion of the potential of high-throughput phenotype data collection and genomic analyses to enable new approaches to improving resistance or resilience of forest trees to drought and cold stress. Considerable progress has been made in this area with angiosperm forest trees (Tuskan et al., 2018), but much less is known about conifers due to their much larger and more complex genomes; our focus will be on conifers in general and loblolly pine in particular.

LOBLOLLY PINE BREEDING AND PRODUCTION

Natural Range and Geographic Variation

Loblolly pine is the most widely planted timber species in the southeastern United States (Schultz, 1997). The greatest productivity of planted pine is achieved through the practice of intensive silviculture, where superior genotypes are selected to match the site and subsequent silvicultural treatments are directed at alleviating resource limitations (Allen et al., 2005; McKeand et al., 2006; Fox et al., 2007). Loblolly pine naturally inhabits a diverse range of environments, extending from Delaware to central Florida and west to eastern Texas (Schultz, 1997). The distribution is mostly continuous (**Figure 1**), with a major discontinuity at the Mississippi River Valley and a few small disjunct populations in Texas collectively known as the "lost pines." In general, the natural range of loblolly pine is limited to the north by low temperature and to the west by low precipitation (Schmidtling, 2001). Given the wide geographic

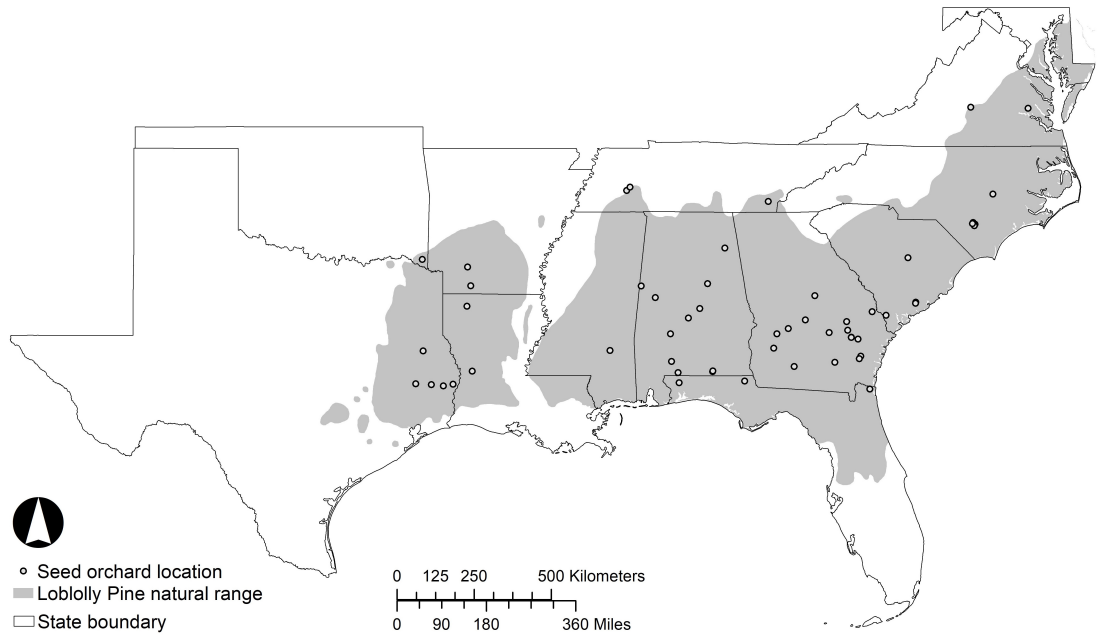

FIGURE 1 | The inset shows the southeastern region of the United States, and the shaded area of the figure shows the natural range of loblolly pine within the region. Dots indicate the approximate locations of active loblolly pine seed orchards.

range with differing climates and photoperiods, this species has extensive geographic variation.

Research shows that the selection of an appropriate seed source of loblolly pine is crucial to ensuring good survival and optimal productivity. A pioneering study involving the establishment of a loblolly pine provenance test in 1927 in eastern Louisiana (Wakeley, 1944; Wakeley and Bercaw, 1965) highlighted the existence of genetic variation across a wide geographical distribution. In the study, the trees grown from the local seed source of Livingston Parish, LA produced approximately twice the volume of wood per hectare as those grown from seeds sourced from Arkansas, Georgia, and Texas. The general conclusion was drawn that local seed sources are best, although the study was planted in only a single location. A number of studies have expanded on this work to characterize patterns of geographic variation in the southern pines, including the Southwide Southern Pine Seed Source Study (SSPSSS) initiated in 1951 (Wells and Wakeley, 1966; Wells, 1983). The results of the SSPSSS indicated that while the Livingston Parish provenance was indeed superior on many sites, it is not always true that local seed sources are superior for economically important traits compared to more distant sources. For example, seed sources from warmer regions tended to grow faster than local sources, providing the difference in the average minimum winter temperature between the source and planting location was not too great (Schmidtling, 2001).

Average minimum winter temperature is commonly used by horticulturalists to guide seed transfers (Pike et al., 2020), and forms the basis of the USDA Plant Hardiness Zones (USDA Plant Hardiness Zone Map, 2012). These zones are based on increments of 5° to 10° F (2.8–5.4 C) for the convenience of US gardeners. Analysis of a variety of provenance and seed source studies led to the conclusion that loblolly pine seed sources can be planted in an area having an average minimum winter temperature up to 5° F (2.8°C) below that found at the seed source, and will typically result in an increase in productivity relative to seeds local to the planting area with minimal risk of cold damage (Schmidtling, 2001; Lambeth et al., 2005). However, these authors caution that the transfer of seed northward or inland to a planting site with winter minimum temperature colder by more than 10 °F (5.4°C) can result in an elevated risk of cold damage. With the prospect of warmer temperatures as a result of climate change, the economic advantage of moving loblolly pine from seed sources of warmer regions to colder planting sites approaching a temperature differential of 10 °F (5.4°C) or more, will need to be balanced with the risk of cold damage during extreme freeze events.

Important observations regarding the movement of seed longitudinally were also brought to light by the SSPSSS. Possibly the most important observation was that seed sources from west of the Mississippi River were more drought tolerant and disease resistant to fusiform rust disease (caused by the fungus *Cronartium quercuum* f. sp. *fusiforme*) compared to eastern sources but that the western sources generally grew slower (Wells, 1985; Schmidtling, 2001). The presence of this variation is likely rooted in the Pleistocene geologic era, as it is postulated that loblolly pine survived the Pleistocene glaciation of North America in two separate refugia, one in southeast Texas and or northeast Mexico, and the other in south Florida and or Caribbean (Wells et al., 1991; Schmidtling et al., 1999; Schmidtling, 2003). The appreciation of these patterns of

geographic variation was an important first step in the genetic improvement of loblolly pine.

Tree improvement programs in the southern United States have structured the genetic resource of loblolly pine into breeding populations that broadly represent the different geographic regions of the species. Tree breeders have primarily focused on improving volume growth, tree form, disease resistance, and wood quality (Zobel and Talbert, 1984). In the 1950s, several large tree improvement programs were initiated at land grant universities and at the USDA Forest Service in order to meet the growing needs of plantation forestry in the southern United States (Zobel and Sprague, 1993). Improved seed from first-generation seed orchards became available in the 1960s and early 1970s, and produced 7–12% more volume per hectare at harvest than trees grown from wild seed (Li et al., 1999). Over time, tree improvement programs in the region have transitioned to the second, third, and fourth cycles of improved material (McKeand and Bridgwater, 1998). Aspinwall et al. (2012) estimated the realized gain in productivity from planting genetically-improved loblolly pine was 17% for the period from 1968 to 2007. Currently, approximately 80% of the more than 12 million planted hectares in the southern United States are loblolly pine, with upwards of 700 million seedlings deployed annually (McKeand et al., 2015) from Virginia in the north, south to Florida and west to Texas. Numerous cases of operational plantations have demonstrated large realized genetic gains from using non-local seed sources, delivering benefits that include increased growth, reduction in fusiform rust disease, improved cold or drought tolerance, and better stem form and wood quality (Lambeth et al., 2005). However, the establishment of non-local provenances does come with risks associated with biotic and abiotic stress, particularly cold or drought damage. Hence, thorough testing of improved genetic material remains important to ensure the successful establishment and desired productivity of planted forests.

Climate Change and Its Impact on the Production and Deployment of Loblolly Pine

The typical cycle of planted loblolly pine forests commences in the seed orchards where improved seed is produced and made available to nurseries that grow seedlings for plantation establishment. During each of these stages there is the potential for cold and/or drought events (**Figure 2**). The ability of planting stock to withstand extremes of temperature and water availability at different times of the year or at different stages of the life cycle is important to quantify and manage in both the seed orchard and deployment environment.

Loblolly pine seed orchards are established throughout much of the southeastern United States with a high concentration in the southern regions of the states of Georgia and Alabama (**Figure 1**), but all within the natural range of loblolly pine. Seed orchard managers often select sites in a less harsh environment than the seed source origin with respect to minimum winter temperature, with the major concern being the detrimental effects of extreme cold events on strobilus development and survival. Abundant survival of female strobili is a prerequisite for a plentiful cone crop. In loblolly pine, strobilus primordia develop rapidly when spring temperatures begin to rise in mid-to-late February and early March (Schultz, 1997). Pollination typically occurs from February to April, with the window of pollen shed and female receptivity shifting from south to north along the species distribution as warmer temperatures move northward. Female strobili are most susceptible to spring freeze events during the time of female receptivity and post-pollination pollen tube

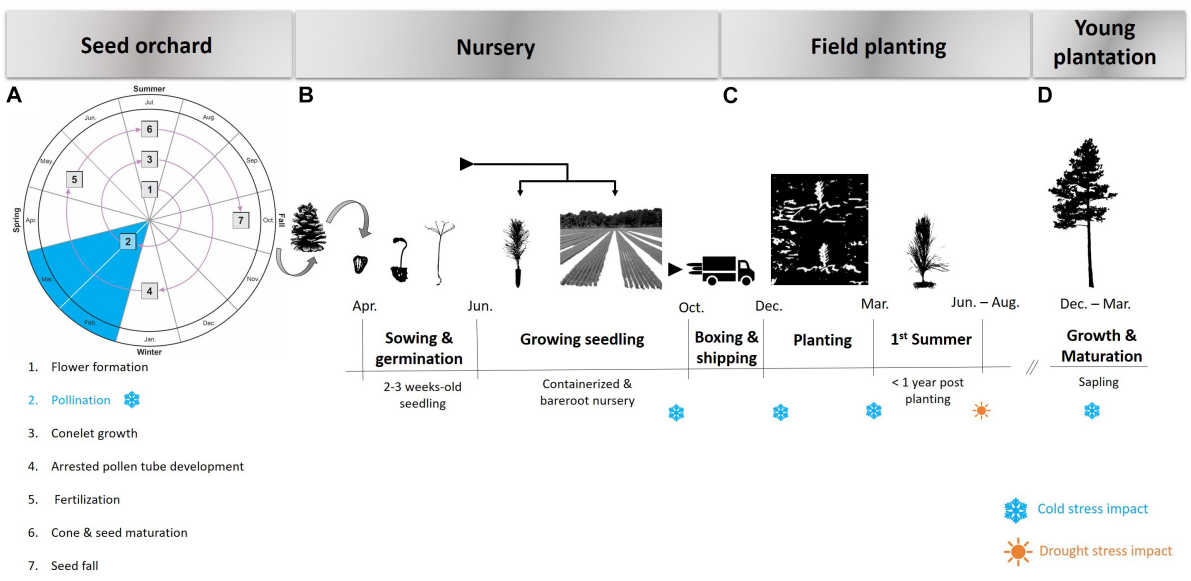

FIGURE 2 | Process flow of loblolly pine seed production (Adapted from Bramlett et al., 1978) **(A)**, nursery raising **(B)**, field planting **(C)**, and early growth **(D)**. The possible occurrence of cold and drought events resulting in an elevated risk of stress is indicated in blue and orange respectively.

growth (**Figure 2A**). Fertilization occurs over a year later, once the pollen tube reaches the archegonium in the summer of the year following pollination. The effect of temperature and other external variables on pollen- development, kinetics and dynamics is highly unexplored in loblolly pine. Thus, improvement of pollen-collection practices and pollen-viability tests could be part of future studies. Mature cones are harvested in October, approximately 4 months after fertilization and eighteen months after pollination.

Knowledge of the molecular mechanisms controlling reproductive processes in conifers is limited, so the potential for improving the resilience or resistance of loblolly pine seed production is unclear. Some genes related to male strobilus and pollen development have been characterized, including MADS-box genes (Sundström and Engström, 2002; Katahata et al., 2014), FT (FLOWERING LOCUS T)-like genes (Klintenäs et al., 2012), gibberellin metabolism genes (Niu et al., 2014), and putative LEAFY homologs (Dornelas and Rodriguez, 2005; Shiokawa et al., 2008). A few reports of transcriptome analyses of conifer reproductive tissues have been reported (Niu et al., 2016; Ma et al., 2020), and as the quality of conifer genome assemblies and annotation is improved, these data may contribute to understanding of molecular mechanisms that will enable better management of abiotic stress effects in conifer seed production.

Seed harvested from pine orchards are typically sown in forest tree nurseries, and the seedlings are cultivated as field-grown bareroot stock or seedlings grown in containers. Irrigation systems ensure that water stress is mitigated in the seedling nursery setting. However, the degree of control over factors affecting freeze injury of open grown seedlings in the nursery is more challenging. At a macro scale, nurseries should be located in a cold hardiness zone that is appropriate for the level of cold adaptability of the seed source. For example, an increased likelihood of freeze injury may occur if seed sources of southern pines from hardiness Zone 8 are sown in nurseries located in Zones 6 or 7a (South, 2007). Seeds are typically sown after the risk of frost is past in the location of each nursery, so the first significant risk of cold exposure comes in the fall when the seedlings are 5- to 6 months old (**Figure 2B**). The topography of the nursery site also impacts the level of exposure of seedlings to freezing temperatures. Obstruction of cold air drainage by land, buildings, or vegetation can result in the ponding of cold air and greater risk of freeze damage (Colombo et al., 2001). The gradual cold hardening process is triggered in the fall by shortening photoperiods and lowered temperatures (Weiser, 1970; Aronsson, 1975; Greer and Warrington, 1982). Conversely, lengthening photoperiods and, in particular, increased temperatures provide cues for rapid dehardening (Greer and Stanley, 1985; Leinonen et al., 1997). The greatest risk of cold damage is caused by unseasonal frosts in the fall while the plants are still hardening, and in the spring when plants are dehardening (Bannister and Neuner, 2001). A freeze event preceded by unseasonably warm temperatures is likely to increase the risk of freeze injury. South (2006) provided a summary of historical freeze events that occurred in the southeastern United States and their impact on pine seedlings grown in nurseries across the region. The findings show a trend that unusually high minimum temperatures for several days prior to a hard freeze increases the likelihood of seedling cold damage, compared to freeze events preceded by seasonally typical (lower) temperatures. Consequently, a future of warming temperatures and increased climate variability may adversely affect levels of cold hardiness and render conifers more susceptible to injury brought about by freeze events (Bansal et al., 2015).

For planted forests, it is during the first year following field establishment that the crop is most vulnerable to cold and drought stress (**Figure 2C**). At this stage, plants are small and have relatively undeveloped root structures with limited access to water and nutrients, which exacerbates their susceptibility to stress factors. Prolonged dry periods during the summer months following planting are particularly challenging in excessively drained and shallow soils that accentuate the effects of drought. Numerous climate models predict future drier conditions in much of North America, including the southeastern United States (Dai, 2013; Cook et al., 2014). For loblolly pine, provenances in the western portion of the natural range have evolved in more xeric climates and have likely responded to natural selection for drought resistance (Schmidtling, 2001, 2003). The results of long-term field trials established on relatively dry sites in Texas showed that local Texas seed sources were on average more productive than non-local seed sources (Long, 1980). Studies of tree mortality after a severe drought in Texas in 2011 reported that mature loblolly pine trees showed lower mortality than other pine or angiosperm tree species in the region (Klockow et al., 2018, 2020). Two long-term trials in southern Arkansas, where water availability is less limiting, showed that loblolly seed sources from east of the Mississippi provided significantly more volume growth compared to local seed sources (Wells and Lambeth, 1983). An example of the successful movement of seed sources from east to west for commercial operations involved the planting of North Carolina loblolly pine in Arkansas and Oklahoma (Lambeth et al., 1984). In those operations, the risk of drought damage was reduced by planting the non-local planting stock on sites deemed to have an appropriate soil profile to ensure water availability. The successful transfer of faster growing seed sources from east to west on suitable soils will likely continue, although the potential for decreased rainfall due to climate change suggests this practice should be pursued with caution.

PHYSIOLOGICAL RESPONSES TO WATER DEFICIT AND COLD STRESS

Among the abiotic stresses that affect plants, suboptimal temperature and water deficit are particularly critical for determining plant survival. The two major mechanistic hypotheses to account for drought-induced tree death are hydraulic failure and carbon starvation. During hydraulic failure tree death is largely explained as a result of dysfunctional water transport caused by xylem embolism, whereas during carbon starvation death is caused by shortages of carbohydrate reserves resulting from a decline in photosynthesis (McDowell, 2011; Sevanto et al., 2014). The precise manner in which these

carbon and water relations play out during extreme drought, especially under field conditions, remains unclear. As a result, new studies have reframed our understanding of plant hydraulics by introducing the interactions between a tree's physiological strategies within a local environment (Sperry and Love, 2015; Feng et al., 2017), their phenotypic characteristics (Couvreur et al., 2018), phenotypic plasticity, and the dynamic spatial interactions of these variables (Manzoni et al., 2014). The introduction of multidimensional models to understand tree water management has opened opportunities to obtain a more accurate understanding of how trees in natural and managed forests respond to restricted water availability and the variation of this response in a future climate change. Among these topics, researchers have studied more carefully the interactions between carbon metabolism and hydraulics (McDowell et al., 2008; McDowell, 2011), the negative legacy of drought on tree stem growth (Anderegg et al., 2015), the implications of the use of storage water to reduce fluctuations in xylem tension (Skelton, 2019), and the extent to which xylem refilling may contribute to the reversibility of loss in xylem hydraulic conductance over longer timescales (McCulloh and Meinzer, 2015; Trifilò et al., 2015). Two major physiological strategies plants use to mitigate the stress of water deficit are avoidance and resistance. Avoidance, in the context of plant response to water deficit, could be defined as the ability to maintain fundamental normal physiological processes under mild or moderate drought stress conditions by reducing water loss (e.g., rapid stomatal closure), enhancing water uptake ability (e.g., changes in root morphology), and modifying vegetative and reproductive growth. On the other hand, drought resistance refers to the ability to maintain physiological activities under severe drought conditions by increasing osmoregulatory molecules in the cells, and adjusting enzymatic pathways to reduce the accumulation of hazardous substances (Fang and Xiong, 2015).

Iso/Anisohydric: A Complex Hydraulic Trait

Trees, like other terrestrial plants, transpire most of the water extracted from the soil in exchange for CO_2 in the atmosphere to convert solar energy, CO_2, and water into organic matter and oxygen. A sophisticated hydraulic arrangement allows the long-distance transportation of water that relies on the maintenance of water potentials along the root-trunk-branch-leaf continuum and the interaction soil-plant-atmosphere (Feng et al., 2017). The terms isohydric and anisohydric refer to water management strategies that plants use to maintain optimal water capacity by the control of stomatal aperture. This helps plants to maintain a basic tradeoff between carbon gain and water loss and has been linked to plant vulnerability to hydraulic failure (e.g., embolism) or carbon starvation. The terms have been re-evaluated over the last two decades as understanding plant water-relations has grown in connection with studies of the mechanisms that triggered massive numbers of tree deaths in different ecosystems globally (Allen, 2009; O'Brien et al., 2017). The anisohydric/isohydric dichotomy has proven to be insufficient to explain the multifunctionality of hydraulic traits that trees use under stress conditions and cannot be used as a unique indicator of drought-induced vulnerability or mortality between or within species (Klein, 2014; Martinez-Vilalta and Garcia-Forner, 2017). For example, in conifers, relatively isohydric species like *Pinus radiata* (Mitchell et al., 2017) rely on high levels of the hormone abscisic acid (ABA) to maintain stomata closed during sustained water stress. In loblolly pine and *Pinus edulis* (Plaut et al., 2012), other relatively isohydric species, drought-induced mortality has been hypothesized to be the product of long-term stomatal closure rather than hydraulic failure from cavitation itself (McDowell et al., 2008), while other conifers have xylem tissues with extreme resistance to embolism allowing leaves to dehydrate (Brodribb et al., 2014). Furthermore, researchers have found that trees can also exhibit differences of those traits in different organs (Domec et al., 2009; McCulloh and Meinzer, 2015), despite the observation that forest ecosystems around the globe have a tendency to maintain similar margins for water potentials (Sperry and Love, 2015) and hydraulic conductivity and capacitance (McCulloh et al., 2013) as mechanisms to avoid stem dieback and death. However, as Rodríguez-Gamir et al. (2016) state, there is inconsistent information on the contribution of different plant organs to the total hydraulic conductance and respiration.

Phenotypic plasticity in water−use traits and evidence of the strong impact of environmental conditions on drought-stress responses have been documented for loblolly pine. In one of these studies, genetically related and even-aged loblolly pine trees were exposed to different water constraints imposed by different soils. The trees that grew in soils of lower water availability (i.e., sand), had longer root systems and were more prone to xylem cavitation (Hacke et al., 2000). Another group investigated the effects of changes in CO_2 and nitrogen on water transport traits, long distance water transport, and drought tolerance in loblolly pine trees in a plantation on low clay loam. The study revealed that loblolly pine trees required a structural change of the hydraulic pathway to produce stomatal closure under elevated CO_2 and nitrogen, attributing these changes, at least partially, to the development of conducting tissue with different hydraulic characteristics. Interestingly, they also demonstrated that under certain circumstances trees that grew under elevated CO_2 conditions showed less reduction in stomatal conductance than trees that grew under normal CO_2, similar to the response observed in broadleaf trees. This could imply that measurable changes might be correlated to the time of exposure and acclimation to elevated CO_2 by the alteration of the anatomy of loblolly pine needles (Domec et al., 2009, 2016). Other studies in 2-year-old loblolly pine saplings were focused on the correlation between temperature and the regulation of stomatal adjustment. Elevated CO_2 caused a decline in stomatal conductance, as it was observed before by Domec et al. (2009), whereas an increase in leaf temperature had the opposite effect. Nevertheless, the increase in the level of CO_2 did not fully mitigate the increased stomatal opening when both temperature and CO_2 concentration increased. Surprisingly, when comparing the response of loblolly pine with poplar, a species that uses a completely different management strategy for water loss, both species increased stomatal conductance under

elevated temperatures, suggesting that the regulation of stomatal activity did not depend exclusively on the rate of transpiration. The inability of loblolly pine to maintain strict control over water loss by transpiration when temperatures increased may have a negative impact on survival and productivity under a hotter future climate but more such studies must be performed in the field to obtain more accurate predictions (Carnicer et al., 2013; Urban et al., 2017).

Embolism and the Complex Dynamic for Hydraulic Capacity Recovery

Cavitation is a phenomenon that occurs in xylem of vascular plants when the pressure of the water phase falls below its vapor pressure and changes from liquid to gas creating a bubble that fills the vessels or the tracheids. The blocking of a xylem vessel or tracheid by a bubble is called embolism. There are two known environmental causes of xylem cavitation: water stress (drought) and freeze-thaw cycles (frost drought) (Tyree and Sperry, 1989). In the case of water stress, the evidence indicates that critical low xylem pressures aspirate bubbles into the functional xylem conduits through pit membranes communicating with previously embolized conduits (Jarbeau et al., 1995) while in freezing, the air bubbles can form *in situ* because gases are insoluble in ice (Ewers, 1985). Despite the unanimous agreement in the relationship between drought-induced mortality and resistance to xylem embolism (Adams et al., 2017; Choat et al., 2018), a debate has arisen regarding the ability of some techniques to measure and discern between the capacity of a plant to resist embolism (Brodribb et al., 2010; Delzon and Cochard, 2014; Choat et al., 2016), and the ability to recover by use of other strategies. A recent publication exemplified this controversy by rebutting a well-known theory about the high vulnerability to embolism and embolism repair mechanisms in laurel (*Lauris nobilis* L.) (Salleo et al., 1996; Tyree et al., 1999; Trifilò et al., 2014, 2015). The authors used a direct, non-invasive method and concluded that this species is not only highly resistant to xylem embolism but that in absence of extreme drought events, it will maintain a positive hydraulic safety margin, and daily cycles of embolism formation and refilling are unlikely to occur (Knipfer et al., 2015, 2016; Lamarque et al., 2018). This common disagreement lies, at least partially, in our limited ability to observe *in vivo* the functional status of xylem conduits (Klein et al., 2018). The idea that trees can establish the positive pressure required to remove emboli in transpiring tissues many meters above the soil surface has been deemed unlikely by some authors, making refilling under sustained tension within the current theoretical framework thermodynamically untenable (Zwieniecki and Holbrook, 2009; Brodersen and McElrone, 2013).

Evergreen conifers suffer frost drought when the ice in soil, roots and frozen trunk parts prevent water uptake for months, while needles can reach substantially higher temperatures than the air during sunny winter days causing relevant water losses (Mayr et al., 2003, 2006). Recent publications have provided more evidence of these mechanisms in evergreen conifers. Mayr et al. (2019) analyzed the loss of hydraulic conductivity in a 10-year dataset, and correlated winter embolism to climate parameters. They demonstrated that *Picea abies* is able to survive winter embolism based on periodic xylem refilling during spring. On the other hand, Hammond et al. (2019) were interested in identification of a lethal threshold for hydraulic failure when portions of the xylem were still functional but the conductivity was reduced below a threshold for sufficient survival even when water became available. As a result, they found that the point of no return for 2-year-old loblolly pine saplings was a threshold at 80% loss of hydraulic conductivity, although certain trees were able to survive even when more than 90% of their xylem conductivity were lost. This threshold was much higher than what has been reported for other conifers (Brodribb and Cochard, 2009). The authors discussed that the possible cause for this extreme survival-trait could be attributed to a non-gradual re-watering during drought relief because in the field, rewatering usually never happened at once and in a continuous way. They also concluded that as long as there was supply of water to the vascular cambium, and xylem tension was able to relax before complete hydraulic failure, there was a chance for survival. Finally, the generated function for calculating mortality could be directly input to vegetation models, although the authors suggested more studies to standardize the analysis across different developmental stages and species. It is important to notice that vulnerability to cavitation does not determine drought tolerance itself. The establishment of the critical threshold and the time to reach it, are the results of the interaction of a number of associated physiological, morphological and environmental factors and therefore, further experimental studies are required to confirm the processes involved in drought-recovery (Choat et al., 2018).

The Paradox: Water Use Efficiency and Fertilization

For loblolly pine plantations, productivity has been the result of years of intensive management and silviculture advancements that have enabled a higher profitably for a variety of uses in very short rotations (8–12 years) (Coyle et al., 2016; D'Amato et al., 2017). The strategy of the plantations is to increase leaf area or water availability, while stem growth is often predicted by leaf area index. In the southeastern United States the major limitation to loblolly pine production is site fertility, specifically related to available nitrogen and phosphorus, even on excessively drained soils (Fox et al., 2007). Mid-rotation fertilization has been an increasingly common practice to provide the nutrients to redirect growth from roots to leaves and stems (Albaugh et al., 2004). Recent studies in loblolly pine have focused on unraveling how fertilization and water availability affect growth, and water use efficiency to predict tree and stand growth but have found very contrasting results. Samuelson et al. (2014) reported no effects of fertilization or throughfall reduction on growth efficiency of a 7-year-old loblolly pine plantation in Georgia. In contrast, a study conducted in a well-drained loblolly pine plantation in Virginia, when the trees were in their 8th and 9th growing seasons, concluded that during the growing season, the combination of fertilization and a reduction

of throughfall caused the most consistent decrease in canopy-averaged stomatal conductance and canopy transpiration but apparently did not limit photosynthesis, causing a significant increase in stem volume (Ward et al., 2015). Interestingly, according to these authors, the leaf area index (LAI) did not increase with fertilization and they suggested that this could be related to the stand having not reached the point at which its nutrient demand exceeded the current supply. They also suggested that the largest changes might occur in the hydraulic system structure, specifically in the root system. This was in agreement with Ewers et al. (2000) who concluded that fertilized stands reduced the safety margins to avoid hydraulic failure and the reduction in the root system made loblolly pine more susceptible to drought-induced mortality. Maggard et al. (2017) found that fertilization increased LAI in the two first years of their study but it was not significant in the third one, attributing the result to a weakening effect of the one-time fertilizer treatment 3 years after application. They also found a negative effect of throughfall reduction on LAI, in contrast with no effect on LAI found after ∼30% reduction on a 7-year-old loblolly pine plantation in Georgia (Samuelson et al., 2014), and over the 2 years for a 9-year-old loblolly pine plantation in Virginia (Ward et al., 2015). Despite these findings supporting negative impacts in loblolly pine plantations due to water scarcity, the current models seem to be affected by local variables and stand traits that should be evaluated before inferring direct effects on productivity.

Theory Interplay: Carbon Starvation and Hydraulic Failure

Plant carbon starvation is the physiological result of an imbalance that occurs when carbon supply from photosynthesis, non-structural carbohydrates (carbon storage compounds) and metabolites from autophagy are not enough to maintain the carbon demands for respiration, growth and defense (McDowell, 2011). Maintaining a positive carbon balance during drought conditions is often considered a major challenge for trees (Galiano et al., 2011; Mitchell et al., 2013) but even during prolonged drought there is more than one way for trees to maintain a positive carbon balance (Klein, 2014; McDowell et al., 2016). To maintain this balance, trees must control stomatal aperture. Although a reduction in the stomatal conductance has been proven to be insufficient to explain mortality directly, theory and evidence point that a reduction in hydraulic function and photosynthesis caused by a decline in stomatal conductance, are primary drivers of death (McDowell, 2011; McDowell et al., 2013). Results from different studies provided clear evidence of partial and complete plant mortality associated with hydraulic failure in both isohydric and anisohydric species, however, no tests of hydraulic failure have excluded carbon starvation or other processes as mechanisms involved in mortality (McDowell, 2011). Furthermore, woody plants exhibit a continuum of hydraulic strategies, rather than a clear distinction between two contrasting alternatives (Sevanto et al., 2014), as well as intraspecific variability in water-use strategies to either resist or recover from different levels of drought stress (Poyatos et al., 2013; Hentschel et al., 2014; Klein, 2014; Garcia-Forner et al., 2017; Petrucco et al., 2017). A large number of recent experiments have proven that hydraulic failure and carbon starvation are interconnected processes (Savi et al., 2016; Yoshimura et al., 2016; Petrucco et al., 2017; Tomasella et al., 2017) and attempts to underline their interplay depends on the intensity and the duration of the drought event (McDowell et al., 2016). Drought duration is important because stored carbohydrates may act temporarily as a buffer that could supply carbon to continue with basic physiological processes even under severe drought events, but extended droughts can increase pest vulnerability (McDowell et al., 2008, 2016) and this could be an additional variable that could affect tree mortality.

Allocation of carbon is a mechanism that plants used to adapt to changes in the environment (Chaves et al., 2002). The distribution of carbon among the plant under stress conditions is correlated to the production of recent photosynthates and the carbon stores and their accessibility. Recently, new research is providing the first steps toward quantifying response thresholds for carbon allocation in different species including evergreen trees under stress conditions (Blessing et al., 2015; Eziz et al., 2017). Bradley and Will (2017) explored biomass distribution and its correlation with transpiration rates for shortleaf pine (*Pinus echinata*), loblolly pine, and their hybrids under limited water conditions. Drought tolerance is linked to survival in the first years of planting and therefore to long-term productivity, and "shortleaf pine is presumed to be more drought tolerant than loblolly pine" (Bradley and Will, 2017), so the authors wanted to determine drought hardiness in the hybrid while unraveling biomass partitioning. The authors found that shortleaf and the hybrid pines had a greater allocation of carbon in the roots, and speculated that this could lead to better performance by shortleaf and hybrid pines under drought conditions. It is interesting to note that an analysis of tree mortality across 5 years after a severe drought in east Texas in 2011 reported that loblolly pine showed significantly lower mortality than shortleaf pine in years three, four and five (Klockow et al., 2018). Despite the large list of publications on this topic, the minimum carbohydrate threshold that determines plant survival, as well as the responses to the co-occurrence of carbon starvation and hydraulic failure processes is unknown.

PHENOTYPIC PLASTICITY AND SIGNALING CROSSTALK UNDER STRESS

Phenotypic plasticity is an incredible evolutionary tool that confers any organism the ability to adapt to and cope with changes in its environment. Plastic responses depend on changes in gene expression and protein function and guarantee the maintenance of metabolic homeostasis, foraging for resources, and defense (Aphalo et al., 1999). Therefore, they are expressed over a variety of time scales, from the molecular level during short-term acclimation, to changes at the morphophysiological

level that may take several years to develop. For generations, traditional tree breeders have been able to improve traits that have an economic and environmental impact based on the selection of phenotypes since they reflect the interactions between the genome and a complex network of responses to the micro- and mega- environments. Nevertheless, fast and unpredictable changes in climate to which some species may be unable to rapidly adapt, and the physiological nature of woody species, are slowing the development of effective tools for tree improvement. Genes that are important in establishing stress responses are being identified thanks to the rapid growth of genomics. In recent years, reduced sequencing cost and high throughput systems have increased the available transcriptome datasets and the number of scientists who attempt to sequence and assemble complex tree genomes. Reference genome sequence assemblies have been published for ten species of gymnosperms: *Picea abies* (Norway spruce) (Nystedt et al., 2013), *Picea glauca* (white spruce) (Birol et al., 2013; Warren et al., 2015), *Pinus taeda* (loblolly pine) (Neale et al., 2014; Wegrzyn et al., 2014; Zimin et al., 2014), *Pinus lambertiana* (sugar pine) (Stevens et al., 2016), *Ginkgo biloba* (ginkgo) (Guan et al., 2016), *Pseudotsuga menziesii* (Douglas fir) (Neale et al., 2017), *Gnetum montanum* (Wan et al., 2018), *Larix sibirica* (Siberian larch) (Kuzmin et al., 2019), *Abies alba* (European silver fir) (Mosca et al., 2019), and *Sequoiadendron giganteum* (giant sequoia) (Scott et al., 2020). The long term goal of plant genomic studies is to accelerate our understanding of the networks involved in both the normal- and the stress- functioning of the organisms, thus accelerating the breeding process. In this genomic era, new methods to accelerate breeding, improve resistance, and increase genetic gain have promised to be the future for agriculture. This includes whole-genome based selection and even customized genotypes by the use of editing techniques like CRISPR/Cas9. In order to achieve this goal in conifers, scientists need to overcome two major limitations. First, the sequencing of conifer megagenomes requires large investments that most public and private investors are not willing to pay. This is, to some extent, related to the second limitation, in that once the DNA sequence data are in hand, the assemblies are often highly fragmented. Many of the assemblies listed above contain over a million scaffolds (Gonzalez-Ibeas et al., 2016; Mosca et al., 2019). A large investment of time and computational resources will be required to improve these fragmented assemblies. The one exception to this is the genome of *Sequoiadendron giganteum* or giant redwood; Scott et al., 2020 reported assembly of eleven chromosome-scale contiguous sequences totaling 8.125 Gb (the expected haploid genome size). The combination of sequencing technologies and assembly methods used for this project may be the guide for future efforts to improve the quality of other conifer genome assemblies.

According to Knight and Knight (2001), cross-talk is defined as the convergent result from different stressors while specificity is referred to as any part of a signaling pathway that enables the distinction between two or more possible outcomes. During cross-talk different pathways could achieve the same response, or interact with other pathways, each affecting the other's outcome. The perception and response to stress signals occur via secondary messengers including cyclic nucleotides, lipid molecules, reactive oxygen species, H_2O_2, nitric oxide and Ca^{2+}(Zhou et al., 2019). Since they also play important roles in the maintenance of homeostasis, changes in their production, balance, use, and elimination are commonly related to stress signaling. Then, the transcription factors and their co-regulators are the key nuclear effector proteins responsible for translating cellular inputs created by the secondary messengers to target and control dosage of gene expression. This can be achieved by post-transcriptional modifications of the transcription factors and their co-regulators. Finally, the activation or suppression of stress-responsive genes can change the levels of proteins that have either metabolic or regulatory roles, such as those involved in detoxification, osmolyte biosynthesis, proteolysis of cellular substrates, water channels, ion transporters, and heat shock proteins (Joshi et al., 2016). Only recently have researchers started to pay more attention to the molecular mechanisms that occur when the stressors appear almost simultaneously, decreasing the time that plants require for adjustment and recovery (Hussain et al., 2018). Simple strategies for improving the performance of trees in water-limited environments do not exist, mainly because the responses are the results of multiple tolerance and avoidance mechanisms (Polle et al., 2019). Among the reviewed literature [Polle et al., 2019; see Li X. et al. (2019); Estravis-Barcala et al., 2020], authors agreed that the identification of the genes expressed or inactivated during stressful events, that are also common features of different stress-response pathways, could play a key role in enhancing tree tolerance to multiple harsh environments. However, the inference and extrapolation of information from genomic studies in model plants to the analysis of molecular events in trees must be done cautiously, not only because of the multiple variables during the performance of the experiments but also because of the fragmented nature of the current tree genomes. Furthermore, a unanimous conclusion was found in all studies, the imperative necessity to characterize stress responses in large-scale experimental field studies in different environments and among different developmental stages.

POST-TRANSCRIPTIONAL REGULATION AND STRESS MEMORY

Alternative Splicing and Alternative Polyadenylation

Transcribed RNA is modified by the addition of a 5' cap structure, transformation into a mature messenger RNA (mRNA) by splicing, and the addition of a 3' polyA tail by polyadenylation. Plant studies have shown that alternative splicing (AS) and alternative polyadenylation (APA) are important mechanisms involved in the regulation of the proteome, but there is only a limited knowledge of the interaction between these mechanisms and their interplay during transcriptional and post-transcriptional regulation in plants. During AS, multiple messenger RNA (mRNA) isoforms are produced from a single gene enhancing the functional diversity of the proteome during

development (Szakonyi and Duque, 2018) and under stress conditions (Marquez et al., 2012; Chamala et al., 2015; Thatcher et al., 2016; Mei et al., 2017). APA, confers a gene the capacity to generate transcripts with multiple polyadenylation sites and differential usage of these sites can lead to the formation of distinct mRNA isoforms (Edwalds-Gilbert et al., 1997; Barabino and Keller, 1999). Natural genetic and phenotypic variations that occur in crop plants constitute the main resources for modern breeding strategies. In several crops, AS has shown to be an efficient tool to improve stress-resistance and to have a direct effect on yield and growth (Panahi et al., 2014; Mei et al., 2017; Wei et al., 2017). Due to cost and technological limitations, the number of studies that have been successful at producing high-quality genome references is still smaller than the constantly growing number of transcriptome studies. High throughput sequencing can be applied in species with and without reference genomes but detection of AS and APA events depend on the accurate prediction of transcript sequences, hence depending on the ability to reconstruct full-length isoforms and high-quality transcriptome annotations. Unfortunately, for many plant species including gymnosperms, the knowledge of which parts of genomes constitute genes and their isoforms remains unclear. This has been a notorious bottleneck in the study of AS and APA in non-model plants, particularly woody species with complex genomes. Chen et al. (2020) compiled recent publications focused on AS studies in different tree species at various stages of development and in response to various stresses. The group, highlighted major contributions in the study of AS in woody species that have been focused on development and stress-responses, including fruit ripening (Mica et al., 2010; Gupta et al., 2015), flower morphogenesis (Ai et al., 2012), wood formation (Xu et al., 2014), drought stress (Guo et al., 2017; Ding et al., 2020), and cold stress (Xiao and Nassuth, 2006; Rahman et al., 2014; Li et al., 2020). Strategies to advance in the functional analysis of AS in woody species have been proposed (Chen et al., 2020). These are some examples of the applicability of these methods in angiosperms: phylogenetic analysis and spatial expression analysis to unravel functional conserved genes and *cis*-elements involved in AS (Li et al., 2017; Liu et al., 2017); identification of regulatory genes in signaling cascades that exhibit AS in specific stress-depend patterns (Li Z. et al., 2019) specifically induced by temperature stress (cold and heat) (Palusa et al., 2007). The potential of these methods relies entirely on the completeness of the genome-wide references, the accuracy of the genome annotations and proper bioinformatics tools. Therefore, we are still far from being able to use them in gymnosperms. For some woody species, there is already a substantial amount of transcriptome data delivered from methods focused on measuring gene expression (e.g., RNA-seq). Other methods (e.g., ATAC-seq, DNase- and MNase- seq) that have the potential to provide information about accessible DNA and its correlation with active regions of the genome involved in adaptation to climate changes could be applied to conifers. In parallel with the advance in the applications of these methodologies, new bioinformatics tools have become available to identify APA (Ha et al., 2018) and allele-specific AS from large populations (Demirdjian et al., 2020) in transcriptome data, however, they need to be implemented for analysis in gymnosperms.

Epigenetics and Stress Memory

In the cells, transcription selects and doses gene activity by following the DNA blueprint while chromatin provides the platform that is necessary for the interaction between transcription factors, co-regulators and polymerase activity. Despite the terms epigenetics has been used for more than 50 years, the nature of the concept has jointly evolved with the advances of the omics era and has been recently reevaluated in the light of its impact on stress responses in both animals and plants. The epigenome can be defined as all the chemical compounds that are "on or attached" to DNA and cause modification in its function without altering the sequence (Riggs et al., 1996). An increasing number of publications provide evidence of mitotically and/or meiotically heritable traits in gene function attributed to epigenetic mechanisms and associated with changes in the environmental conditions (Vyse et al., 2020). The environmental cues experienced by parent trees during the reproductive process can affect growth and adaptive traits of their progeny as a result of epigenetic changes. In forest trees, this phenomenon was initially described as seed orchard "aftereffects" (Bjørnstad, 1981; Johnsen, 1989a,b), after being observed in conifers when northern selections of Norway spruce [*Picea abies* (L.) Karst.] were moved to a southern seed orchard location in order to enhance seed production. Bud set in full-sib progeny produced by the cloned northern selections located in the southern orchard (lat. 58° N) environment were delayed up to 3 weeks compared to their half-sibs from the same mother trees growing in the northern (63° N – 66° N) natural stand (Bjørnstad, 1981). The orchard progeny were also more susceptible to frost damage compared to their natural-stand counterparts when subjected to low temperatures in a phytotron (Johnsen, 1989a). When field tested on a northern site, the phenology and extended height growth of the orchard progeny resembled that of southern ecotypes (Johnsen, 1989b). Similar epigenetic effects have since been observed in other conifer species, including white spruce (*Picea glauca*) (Stoehr et al., 1998), Scots pine (*Pinus sylvestris*) (Dormling and Johnsen, 1992), and *Larix* spp. (Greenwood and Hutchison, 1996).

It follows that an adaptive epigenetic memory may have important implications for seed production sites in the southeastern United States. According to Schmidtling (1987), locating southern pine seed orchards south of the origin of selected trees can result in improved flowering and seed production. The hypothesis that the parental environment in the orchard could alter progeny performance of southern pines in the Southeast was tested in shortleaf pine (*Pinus echinata* Mill.). Ramets of 22 shortleaf pine clones were established in two diverse environments, one located in central Arkansas, United States (34.6° N), near the source of the ortets, and the second site located in south Mississippi (30.5° N) (Schmidtling and Hipkins, 2004). Thirteen identical controlled crosses (full-sib families) were made at each location, and the resulting seedlings were planted at the two locations where the seed was produced. After four growing seasons, trees from seed produced in the

two environments differed significantly in height, with families produced in the warmer (southern) environment generally being taller at both planting locations. The reproductive environment × family interaction was also significant, indicating that the effect depended upon the genetic background of the parent trees. By age 9 years, the reproductive environment effect was no longer statistically significant (Schmidtling and Hipkins, 2004). In the study by Schmidtling and Hipkins (2004), there was no reference of cold damage at the time of planting or during the immediate winters that followed, but major ice storm damage in the northern planting was reported following the eighth growing season. The ice-damage was quantified using a six point (0–5) categorical scoring system. The mean ice-damage score for trees produced in the northern reproductive environment was 2.38 vs 2.62 for those produced in the southern reproductive environment. The difference, though small, was statistically significant ($P = 0.018$). The authors concluded that after-effects of reproductive environment do exist in shortleaf pine for growth and adaptive traits but are not as clear-cut nor at the same scale as that reported by Johnsen (1989a,b) in the Norway spruce studies. According to Schmidtling and Hipkins (2004), one explanation is that the north–south distance between the shortleaf seed sources amounts to only 4.1 degrees latitude rather than the 5–8 degrees latitude difference in the Norway spruce studies. In the case of loblolly pine, most seed orchards are located in the central and southern portion of the species distribution. A similar level of epigenetic effects to those reported for shortleaf pine might be expected for loblolly pine, given the vast majority of planted areas of loblolly pine in the southeastern United States are within 5 degrees latitude of the seed orchard locations.

WORKING TOWARD NEXT-GENERATION BREEDING

Phenomics and High-Throughput Phenotyping

The current major goal of biological sciences is to generate functional models that integrate genome and phenome, allowing a multidimensional knowledge of the biology of organisms and the prediction of how they will behave under future scenarios. Several emerging global technologies (e.g., genomics, proteomics, metabolomics) are identifying and measuring changes in the molecular components under a broad set of experimental conditions including several abiotic and biotic stresses. On the other hand, next-generation phenomics measures changes in the physical attributes on a genome-wide scale that an organism overcomes during its lifespan. Both data and analytical pipelines have grown exponentially by the application of high-throughput systems. Advances in these areas are creating the next-generation breeding techniques that will reshape the way we have done agriculture until now (revised in Chen et al., 2014; Esposito et al., 2019; Yang et al., 2020). Recently, molecular breeding techniques that center the attention in DNA-features that are tightly linked to phenotypic traits, seem to be growing faster than the methods that allow the characterization of those traits in the field, and that are key components for measuring and validation of the level of improvement during selection.

The introduction of a number of highly user−friendly (and portable) chlorophyll fluorometers as well as more sophisticated high throughput hyperspectral imaging have enhanced not only the accuracy of chlorophyll measurements but also the implementation of large phenotyping platforms with the automatic control and data analysis system, which allows performing parallel studies of a large amount of plants during long cycles of growth under constant monitoring and different environments (Yao et al., 2018). Light energy absorbed by chlorophyll molecules in a leaf can undergo one of three fates: it can be used to drive photosynthesis (photochemistry), excess energy can be dissipated as heat or it can be re−emitted as light, which is observed as chlorophyll fluorescence (Maxwell and Johnson, 2000). The radiation reflected from a surface as a function of the wavelength is called the spectral signature. The spectral signature of a plant is related to its biochemical constituents, of which leaf chlorophyll content is both sensitive to environmental conditions and has a strong influence on leaf optical properties and canopy albedo (Blackburn and Pitman, 1999; Baltzer and Thomas, 2005). Therefore, chlorophyll fluorescence provides a powerful tool to infer information related to the photosynthetic apparatus and its associated metabolism (Humplík et al., 2015; Cen et al., 2017). Hyperspectral data can be used to detect subtle features across the entire visible and near-infrared regions of the electromagnetic spectrum, which correlate especially well with major leaf pigments such as the leaf chlorophyll content (Zhang et al., 2008). This could be particularly helpful under current climate change because healthy and stress vegetation present difference reflectance features in the green peak and along the red edge due to changes in pigment levels (Rock et al., 1988; Belanger et al., 1995; Gitelson and Merzlyak, 1996). Some of the commonly used physiological indicators to assess plant water conditions include stomatal conductance (Zhou et al., 2013), leaf water potential (Dzikiti et al., 2010; Zhou et al., 2013), leaf equivalent water thickness (Danson et al., 1992), and relative water content (Hunt et al., 1987; Maki et al., 2004). By obtaining complete reflectance curves at high spatial and spectral resolutions, specific plant chemical traits, including leaf water content, can be modeled and extracted at fairly high accuracies and used as phenotypes to describe plant stress (Lowe et al., 2017).

During the last 20 years researchers have advanced in the development of high throughput plant phenomics studies in controlled environments like growth chambers and greenhouses by the implementation of imaging systems, pipelines for analysis and interpretation models that would enable the use of genotypic data and novel gene discovery in a more efficient way, moving these systems toward a real optimization of plant breeding. There are limitations for predicting the performance of commercial plant varieties under field conditions based on plant phenotyping in controlled environments, but these systems are particularly useful in studying how plant phenotypes vary among different genotypes in response to controlled stress conditions. Furthermore, the control over different parameters serve to study the interactions between genetic and environmental factors that

can produce unanticipated phenotypic responses (Ge et al., 2016). Previous studies have used hyperspectral imaging to determine and quantify early signs of drought stress of maize (Ge et al., 2016; Pandey et al., 2017) and cereals (Behmann et al., 2014); however, there remains a lack of targeted experiments for measuring drought indicators in loblolly pine. In pines, the content of pigments could be markedly affected by growing conditions, plant age, needle age and origin of the seed source (Linder, 1972). Because hyperspectral imaging captures spatial and spectral information that is usually processed by traditional automated image processing tools and interactive analytical approaches derived from spectroscopy, the first step in the investigation and improvement of these methods to assess drought stress in the greenhouse, is to explore more approaches to handle the plant material in different phenotypic stages and to create models that ultimately will help to increase the sensitivity and accuracy of the detection of early signs.

Integrating Microbiome Effects

Multiple reports have described significant effects on plant drought response of growing plants in soil from a region with less precipitation than is typical of the natural range of the species in question (O'Brien et al., 2018; Allsup and Lankau, 2019; Ulrich et al., 2020). O'Brien et al. (2018) tested effects of different soil microbiota and water availability levels on three species: *Trifolium stellatum*, *Lagarus ovatus*, and *Sisymbrium erysimoides*, a legume, a grass, and a forb respectively. Under conditions of limited water availability, the grass and the forb species both produced more biomass when grown in soil from a drier site than in soil from a region with higher average precipitation. Allsup and Lankau (2019) grew seedlings of *Ostrya virginiana* (American hop hornbeam) and *Betula nigra* (river birch), both angiosperm tree species native to eastern North America, in sterilized soil from different regions inoculated with soil microbiome samples from different regions. They found that microbial inoculum from regions with lower precipitation supported greater seedling biomass production under water-limited growth conditions than the inoculum from regions with higher precipitation, regardless of the soil source. Ulrich et al. (2020) compared chlorophyll fluorescence parameters among loblolly pine families from the western (drier) and eastern (wetter) extremes of the natural range of loblolly pine, for both control seedlings grown in sterile sand and treated seedlings grown in sterile sand inoculated with soil from New Mexico, which is west of, and much drier than, the natural range of loblolly pine. They reported that control and inoculated seedlings from the eastern "wet" family showed no difference in the rate of decline of the Fv/Fm ratio of chlorophyll fluorescence in a time series of measurements taken over 4 weeks after they stopped providing water to the seedlings. In contrast, control seedlings of the western "dry" family showed a slower rate of decline in the Fv/Fm ratio than inoculated seedlings of the "dry" family, suggesting that the inoculated soil had a negative effect on the "dry" family but not on the "wet" family. Both Ulrich et al. (2020) and Allsup and Lankau (2019) speculated that the use of soil inocula from regions drier than the climate region from which the experimental plants were drawn contributed to the observed effects of inoculation in their respective studies. An alternative hypothesis is that the effects are due to the presence of novel species of soil microorganisms to which the plants had not been previously exposed.

A meta-analysis of data from 126 papers (Karst et al., 2018) presented evidence that interactions between 59 host tree species and 52 genera of ectomycorrhizal fungi tend to have positive effects on average, and the degree of positive effect was generally larger when the host and fungal species used came from allopatric rather than sympatric ranges. In other words, the response to inoculation tended to be larger when the host plant and fungal inoculum came from regions farther apart. This effect was detected both when using only data from studies with species of pines (the genus with greatest representation among all the studies examined), or using data from all studies except those on pines, so the results are not driven by any unique response of the most-studied plant genus. The question of whether this effect might account for some fraction of the differences in plant drought responses attributed to inoculation with soil microbiota from drier regions (O'Brien et al., 2018; Allsup and Lankau, 2019; Ulrich et al., 2020) remains to be determined. Future experiments to test the effects of inoculation with soil microbiota from dry regions on plant drought responses should include control inoculations with soil microbiota from regions equally distant from the native range of the host plant, but with similar water availability, to test the hypothesis that specific effects on drought responses are related to the water availability in the region from which the microbial inoculum was obtained, rather than simply the distance from the host plant range.

FUTURE DIRECTIONS

Climate models suggest that the southeastern United States is likely to show significant changes over the next 50 years in the length of the frost-free growing season and the average late-winter (March) minimum temperature (**Figure 3** and **Supplementary Table 1**), and in the average length of summer "dry periods" between rainfall events and the average July maximum temperatures (**Figure 4** and **Supplementary Table 1**). The current projected duration of a cycle of loblolly pine breeding is 14 years (Isik and McKeand, 2019), so in the absence of revolutionary changes, two breeding cycles can be completed for loblolly pine by 2050. The 30-year time period used for **Figures 3**, **4** climate factors is typically sufficient for a loblolly pine plantation to grow from establishment to harvest, so trees planted by 2051 will generally be harvested by 2080. Projected differences in the number of frost-free days and March minimum temperatures (**Figure 3**) do not highlight obvious risks for pollination, seedling production, or plantation growth, although these plots do not show the risk of "weather whiplash." Projected changes in the maximum number of days between rainfall events and in the average maximum July temperature (**Figure 4**) do suggest that tolerance (resistance, resilience, or both) of higher temperatures and lower water availability will be a valuable trait for loblolly pine planting stock.

Intra-specific genetic variation for drought tolerance has been observed in many species, including genera such as

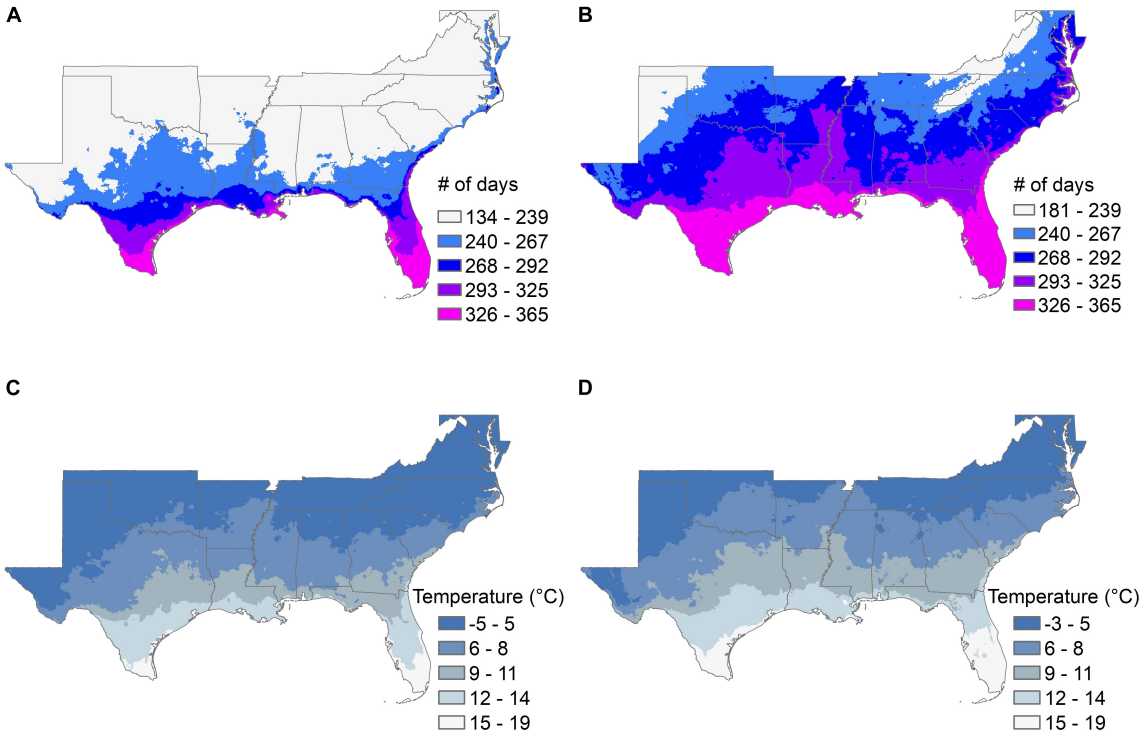

FIGURE 3 | The average number of frost-free days in the growing season **(A,B)** and the average March minimum temperature **(C,D)** are shown for the southeastern United States for the 30-year historical record from 1976 to 2005 **(A,C)**, and from 2051 to 2080 **(B,D)**. The color scales in the legends are the same for both time periods, but the lowest category for frost-free days and for average March minimum temperatures are slightly different because the lower limits are higher in the projections for 2051 to 2080.

Picea, *Pinus*, *Abies*, and *Cryptomeria*. Several early studies with loblolly pine reported genetic variation both among loblolly pine provenances and among families within provenances (Zobel, 1955; Cech and Goddard, 1957). The observation of existing genetic variation for drought tolerance suggests that breeders could select for improved drought responses, either resistance or resilience or both, provided that cost-effective methods for testing could be developed to allow collection of appropriate phenotypic data for enough individuals. Breeders working to improve loblolly pine often are interested in comparing the performance of dozens to hundreds of different individuals, and depending on the nature of experimental designs used, this can mean measuring phenotypes of hundreds to thousands of plants. By reviewing publications about physiological responses to water and cold stress, we identified some studies that would provide valuable information about how loblolly pine is adapting to changes in climate at the cellular and physiological levels. This includes research on ABA-stomatal control and application of micro-computed tomography to detect embolism and conduct refilling. However, these detailed physiological assessments are often impractical for such large numbers of individual plants, so past efforts to measure drought responses in loblolly pine for breeding purposes have often relied on common-garden field trials where seedlings grown from seed collected in different parts of the natural range of loblolly pine are planted together in trials, often in multiple locations. A recent analysis that looked for time-course trends over the last 20 years in six top impact factor journals, revealed that the fraction of papers that represented the interaction between the topics "omics" x ecophysiology represented <4% on average compared with papers on both terms in 2017 (Flexas and Gago, 2018). This could be an opportunity for ecophysiologists and omics-researchers to look for multidisciplinary projects and focus on the improvement of robust predictive models for breeding.

Two key questions for breeders are what phenotypes to measure, and which trees to select. The answer will be different for different species, because the sensitivity to drought and the hazard from drought will vary across regions and species. For loblolly pine in the southeastern United States, the initial stage of plantation establishment is particularly important in terms of drought. The first year after seedlings are planted in the field is the most critical time in terms of water availability, because the root systems are still small and unable to reach water in deeper soil horizons. Selection for the ability of pine seedlings to survive a period of limited water availability during the first year could reduce the risk of plantation failure, and should also be a relatively easy trait to measure under controlled conditions. An additional advantage of working with seedlings at this age may be that the physiological or genetic mechanisms of resistance need not be identified in advance, provided that screening methods mimic as closely as possible the kind of drought stress to which resistance

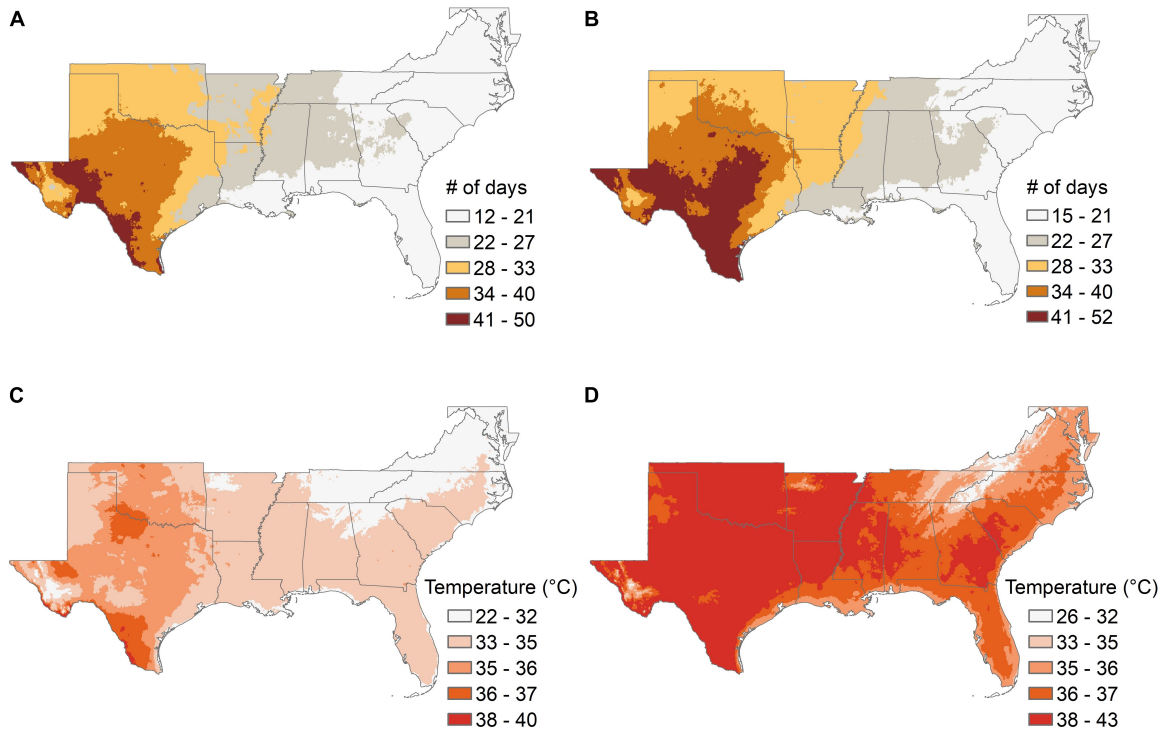

FIGURE 4 | The average number of days without precipitation during summer months **(A,B)** and the average July maximum temperatures **(C,D)** are shown for the southeastern United States for the 30-year historical record from 1976 to 2005, and from ensemble climate model projections using the RCP 8.5 scenario for the period from 2051 to 2080. The boundaries of the lowest and highest categories for both pairs of maps are slightly different between the maps showing the historical record and those showing projected future conditions because the minimum and maximum values increased in the future projections, but the color scales are the same for both time periods.

is desired. Projections from ensemble climate models (**Figure 4B**) suggest that the ability to survive a period of 3–4 weeks without rainfall during the first summer after planting is likely to be a valuable trait to increase the likelihood of successful plantation establishment in much of the southeastern United States by mid-century. Seedlings can be exposed to such stresses under controlled conditions now, either in greenhouse studies with controlled delivery of water (Marchin et al., 2020), or by field planting seedlings in regions with little to no summer rainfall and providing supplemental irrigation during spring growth and then withdrawing irrigation to impose the desired drought stress during the summer. The latter method could also have the additional feature of imposing higher summer temperatures than are currently common in the natural range of loblolly pine, but may become common in the future (**Figure 4D**).

Integrative studies that combine surveys of genetic variation across the natural range with analyses of gene expression, high-throughput phenotyping data, and analyses of replicated test plantings derived either from experimental crosses or from accessions collected from natural populations, have provided new insights into mechanisms of drought tolerance and other complex phenotypes in some non-model species (Lovell et al., 2018; Weighill et al., 2019a,b). Some efforts toward this kind of analysis have been made in conifers (De La Torre et al., 2019; Lu et al., 2019a,b; Mahony et al., 2020), but they are constrained by the lack of high-quality sequenced genomes and annotation for most conifers, as previously discussed. The current (v2.01) loblolly pine assembly allowed mapping of fewer than half the SNPs associated with polymorphisms in a recent genome-wide association study onto scaffolds anchored to linkage groups in the genetic map (De La Torre et al., 2019). More than half of the trait-associated SNPs were in non-coding regions, and the relationship between those variants and any genes whose expression levels or tissue-specificity might be affected by the variant locus cannot be determined given the current fragmented assembly (Zimin et al., 2017).

Genomic approaches to understand and improve drought responses in trees have been reviewed (Hamanishi and Campbell, 2011; Moran et al., 2017; Isabel et al., 2020), and additional reports of association studies in conifers have been published since then (Trujillo-Moya et al., 2018; De La Torre et al., 2019; Lu et al., 2019b; Mahony et al., 2020). Associations can be identified between genotypes and phenotypes, an approach common in crop and model plant species as well as animal genetics and human biomedical research, or between genotypes and environmental variables for samples collected from across the range of a species (Rellstab et al., 2015). A common theme to the results of such studies in loblolly pine has been that individual single-nucleotide polymorphisms (SNPs) associated with drought response or environmental variables

related to water availability or aridity typically explain a relatively small proportion of the observed variation. Many of the SNPs associated with phenotypic or environmental variation also show low minor-allele frequency in the population, suggesting that many such loci would have to be genotyped in many individual trees in order to have enough power to model phenotypic variation for breeding purposes. Multivariate methods that analyze multiple SNP alleles (sometimes grouped by functional categories such as the genes in which those SNPs occur) and multiple phenotypes in parallel have shown improved power to detect associations of genotypes with environmental variables (Rellstab et al., 2015; Forester et al., 2018) and with phenotypic variation (Kaakinen et al., 2017; Luo et al., 2020). Genomic selection is another approach to parallel analysis of many SNP loci with phenotypic information, and considerable interest has been shown in applying this method to forest tree breeding (reviewed by Lebedev et al., 2020).

Most conifer breeding programs work with families of progeny as the genetic entries in field tests, because inbred lines are typically not available. The most advanced breeding programs in loblolly pine are only five to eight generations from trees selected from wild populations, but pedigree records showing the relationships across multiple generations are available for many individuals in the advanced-generation breeding populations (Isik and McKeand, 2019). These family-based structured breeding populations will be suitable for haplotype-based analyses, which have been shown to have greater sensitivity for detection of the genetic basis of complex clinical phenotypes in human populations (Howard et al., 2017). A key requirement for such analyses, however, is the ability to detect "haplotype blocks," or groups of variant alleles that are on the same chromosome homolog and are inherited together through multiple generations. Biomedical researchers have been working for the past two decades to collect data on the haplotype structure of the human genome (Gabriel et al., 2002; The International HapMap Consortium, 2003; Altshuler et al., 2005). Across the human population as a whole, these haplotype blocks are an imperfect representation of linkage disequilibrium among SNP alleles (Wall and Pritchard, 2003), but within groups of individuals that are related by descent from a common ancestor, population haplotype data can be used to detect haplotypes that are "identical-by-descent" (IBD) from a common ancestor (Browning, 2008; Gusev et al., 2011).

Patterns of linkage disequilibrium in the loblolly pine genome are very different from those found in human populations (Brown et al., 2004; Lu et al., 2016; Acosta et al., 2019), so a population-based "haplotype map" will only be possible for a group of related trees descended from a relatively small number of founding parents. This strategy is similar to that used in Multi-parent Advanced Generation InterCross (MAGIC) populations in crop breeding and model plant and animal studies (Cavanagh et al., 2008; Kover et al., 2009; Threadgill et al., 2011). When a high-quality genome assembly and annotation are available for loblolly pine, long-read DNA sequencing methods (Oxford Nanopore or Pacific Biosciences) can be used to detect long-range linkages among SNP alleles to identify parental haplotypes, followed by SNP array-based or sequence-based genotyping of progeny to impute the entire complexity of the parental genome sequences to the progeny. This approach would enable a combination of haplotype-based methods for associating phenotypic variation to specific chromosome haplotypes with RNA-seq-based analysis of gene expression, AS, and APA sites usage to collect comprehensive genomic datasets for multivariate analysis. Conducting such analyses in parallel with several MAGIC populations, each composed of crosses among loblolly pine parents from different parts of the natural range and planted in replicated field trials in multiple environments, would provide a valuable resource for the dissection of genetic variation controlling complex phenotypes in pine. Phenotypes in such test plantings could be measured using high-throughput methods such as hyperspectral imaging for phenological differences (D'Odorico et al., 2020), acoustic stress wave and drill resistance methods for wood properties (Walker et al., 2019), and terrestrial LIDAR (Liang et al., 2016). Integrative analysis of large datasets with multiple phenotypes and genomic data sources would be a powerful tool in helping tree breeders better understand and work with the natural genetic variation so abundant in loblolly pine populations. Accelerating breeding progress will be essential for meeting social needs for forest products in the second half of the 21st century.

AUTHOR CONTRIBUTIONS

RW and LM-R conceived the idea of the review and prepared the initial outline. LM-R contributed **Figure 2**. RW, LM-R, and KP gathered the literature for all sections. GS contributed the analysis of climate change models and **Figures 1**, **3**, **4**. All authors contributed to revising and editing the draft sections, and approved the content of the final manuscript.

FUNDING

Funding has been provided by USDA NIFA (awards #2011-68002-30185 and #2018-67013-27573), USDA Specialty Crops Research Initiative (award #2012-51181-19940), USDA McIntire-Stennis funds (award # NCZ04214), the NC State University Cooperative Tree Improvement Program.

ACKNOWLEDGMENTS

The authors thank Dr. J. B. Jett, Dr. Steven McKeand, and Dr. Fred Raley for contributing information on seed orchard locations for **Figure 1**, and Mr. Austin Heine for helpful discussions on the management of loblolly pine seed production.

SUPPLEMENTARY MATERIAL

The Supplementary Material for this article can be found online at: https://www.frontiersin.org/articles/10.3389/fpls.2021.606908/full#supplementary-material

REFERENCES

Acosta, J. J., Fahrenkrog, A. M., Neves, L. G., Resende, M. F. R., Dervinis, C., Davis, J. M., et al. (2019). Exome resequencing reveals evolutionary history, genomic diversity, and targets of selection in the conifers *Pinus taeda* and *Pinus elliottii*. *Genome Biol. Evol.* 11, 508–520. doi: 10.1093/gbe/evz016

Adams, H. D., Zeppel, M. J. B., Anderegg, W. R. L., Hartmann, H., Landhäusser, S. M., Tissue, D. T., et al. (2017). A multi-species synthesis of physiological mechanisms in drought-induced tree mortality. *Nat. Ecol. Evol.* 1, 1285–1291. doi: 10.1038/s41559-017-0248-x

Ai, X.-Y., Lin, G., Sun, L.-M., Hu, C.-G., Guo, W.-W., Deng, X.-X., et al. (2012). A global view of gene activity at the flowering transition phase in precocious trifoliate orange and its wild-type [*Poncirus trifoliata* (L.) Raf.] by transcriptome and proteome analysis. *Gene* 510, 47–58. doi: 10.1016/j.gene.2012.07.090

Albaugh, T. J., Allen, H. L., Dougherty, P. M., and Johnsen, K. H. (2004). Long term growth responses of loblolly pine to optimal nutrient and water resource availability. *For. Ecol. Manag.* 192, 3–19. doi: 10.1016/j.foreco.2004.01.002

Allen, C. D. (2009). Climate-induced forest dieback: an escalating global phenomenon? *Unasylva* 60, 43–49.

Allen, H. L., Fox, T. R., and Campbell, R. G. (2005). What is ahead for intensive pine plantation silviculture in the South? *South. J. Appl. For.* 29, 62–69. doi: 10.1093/sjaf/29.2.62

Allsup, C., and Lankau, R. (2019). Migration of soil microbes may promote tree seedling tolerance to drying conditions. *Ecology* 100:e02729. doi: 10.1002/ecy.2729

Altshuler, D., Donnelly, P., The International and HapMap Consortium (2005). A haplotype map of the human genome. *Nature* 437, 1299–1320. doi: 10.1038/nature04226

Anderegg, W. R. L., Flint, A., Huang, C.-Y., Flint, L., Berry, J. A., Davis, F. W., et al. (2015). Tree mortality predicted from drought-induced vascular damage. *Nat. Geosci.* 8, 367–371. doi: 10.1038/ngeo2400

Aphalo, P. J., Ballaré, C. L., and Scopel, A. L. (1999). Plant-plant signaling, the shade-avoidance response and competition. *J. Exp. Bot.* 50, 1629–1634. doi: 10.1093/jxb/50.340.1629

Aronsson, A. (1975). *Influence of Photo- and Thermoperiod on the Initial Stages of Frost Hardening and Dehardening of Phytotron-Grown Seedlings of Scots Pine* (*Pinus silvestris* L.) *and Norway spruce* (*Picea abies* (L.) Karst.*). Technical Report*. Stockholm: Royal School of Forestry, Sveriges lantbruksuniversitet, 128.

Aspinwall, M. J., McKeand, S. E., and King, J. S. (2012). Carbon sequestration from 40 years of planting genetically improved loblolly pine across the southeast United States. *For. Sci.* 58, 446–456. doi: 10.5849/forsci.11-058

Baltzer, J. L., and Thomas, S. C. (2005). Leaf optical responses to light and soil nutrient availability in temperate deciduous trees. *Am. J. Bot.* 92, 214–223. doi: 10.3732/ajb.92.2.214

Bannister, P., and Neuner, G. (2001). "Frost resistance and the distribution of conifers," in *Conifer Cold Hardiness*, eds F. J. Bigras and S. J. Colombo (Dordrecht: Kluwer Academic Publishers), 3–22. doi: 10.1007/978-94-015-9650-3_1

Bansal, Sheel, St Clair, J. B., Harrington, C. A., and Gould, P. J. (2015). Impact of climate change on cold hardiness of Douglas-fir (*Pseudotsuga menziesii*): environmental and genetic considerations. *Glob. Change Biol.* 21, 3814–3826. doi: 10.1111/gcb.12958

Barabino, S. M. L., and Keller, W. (1999). Last but not least: regulated poly(A) tail formation. *Cell* 99, 9–11. doi: 10.1016/S0092-8674(00)80057-4

Behmann, J., Schmitter, P., Steinrücken, J., and Plümer, L. (2014). Ordinal classification for efficient plant stress prediction in hyperspectral data. *Int. Arch. Photogramm.* 7, 29–36. doi: 10.5194/isprsarchives-XL-7-29-2014

Belanger, M. J., Miller, J. R., and Boyer, M. G. (1995). Comparative relationships between some red edge parameters and seasonal leaf chlorophyll concentrations. *Can. J. Remote Sens.* 21, 16–21. doi: 10.1080/07038992.1995.10874592

Birol, I., Raymond, A., Jackman, S. D., Pleasance, S., Coope, R., Taylor, G. A., et al. (2013). Assembling the 20 Gb white spruce (*Picea glauca*) genome from whole-genome shotgun sequencing data. *Bioinformatics* 29, 1492–1497. doi: 10.1093/bioinformatics/btt178

Bjørnstad, A. (1981). Photoperiodical after-effects of parent plant environment in Norway spruce (*Picea abies* (L) Karst.) seedlings. *Rep. Norw. For. Res. Inst.* 36, 4–30.

Blackburn, G. A., and Pitman, J. I. (1999). Biophysical controls on the directional spectral reflectance properties of bracken (*Pteridium aquilinum*) canopies: results of a field experiment. *Int. J. Remote Sens.* 20, 2265–2282. doi: 10.1080/014311699212245

Blessing, C. H., Werner, R. A., Siegwolf, R., and Buchmann, N. (2015). Allocation dynamics of recently fixed carbon in beech saplings in response to increased temperatures and drought. *Tree Physiol.* 35, 585–598. doi: 10.1093/treephys/tpv024

Bradley, J. C., and Will, R. E. (2017). Comparison of biomass partitioning and transpiration for water-stressed shortleaf, loblolly, and shortleaf × loblolly pine hybrid seedlings. *Can. J. For. Res.* 47, 1364–1371. doi: 10.1139/cjfr-2017-0167

Bramlett, D. L., Belcher, E. W. Jr., DeBarr, G. L., Hertel, G. D., Karrfalt, R. P., Lantz, C. W., et al. (1978). "Cone analysis of southern pines: a guidebook," in *Gen. Tech. Rep.* (Asheville, NC: U.S. Department of Agriculture, Forest Service, Southeastern Forest Experiment Station) SE-13: 28.

Brodersen, C. R., and McElrone, A. J. (2013). Maintenance of xylem network transport capacity: a review of embolism repair in vascular plants. *Front. Plant Sci.* 4:108. doi: 10.3389/fpls.2013.00108

Brodribb, T. J., and Cochard, H. (2009). Hydraulic failure defines the recovery and point of death in water-stressed conifers. *Plant Physiol.* 149, 575–584. doi: 10.1104/pp.108.129783

Brodribb, T. J., Bowman, D. J. M. S., Nichols, S., Delzon, S., and Burlett, R. (2010). Xylem function and growth rate interact to determine recovery rates after exposure to extreme water deficit. *New Phytol.* 188, 533–542. doi: 10.1111/j.1469-8137.2010.03393.x

Brodribb, T. J., McAdam, S. A. M., Jordan, G. J., and Martins, S. C. V. (2014). Conifer species adapt to low-rainfall climates by following one of two divergent pathways. *Proc. Natl. Acad. Sci. U.S.A.* 111, 14489–14493. doi: 10.1073/pnas.1407930111

Brown, G. R., Gill, G. P., Kuntz, R. J., Langley, C. H., and Neale, D. B. (2004). Nucleotide diversity and linkage disequilibrium in loblolly pine. *Proc. Natl. Acad. Sci. U.S.A.* 101, 15255–15260. doi: 10.1073/pnas.0404231101

Browning, S. R. (2008). Estimation of pairwise identity by descent from dense genetic marker data in a population sample of haplotypes. *Genetics* 178, 2123–2132. doi: 10.1534/genetics.107.084624

Carnicer, J., Barbeta, A., Sperlich, D., Coll, M., and Peñuelas, J. (2013). Contrasting trait syndromes in angiosperms and conifers are associated with different responses of tree growth to temperature on a large scale. *Front. Plant Sci.* 4:409. doi: 10.3389/fpls.2013.00409

Casson, N. J., Contosta, A. R., Burakowski, E. A., Campbell, J. L., Crandall, M. S., Creed, I. F., et al. (2019). Winter weather whiplash: impacts of meteorological events misaligned with natural and human systems in seasonally snow−covered regions. *Earth's Fut.* 7, 1434–1450. doi: 10.1029/2019EF001224

Cavanagh, C., Morell, M., Mackay, I., and Powell, W. (2008). From mutations to MAGIC: resources for gene discovery, validation and delivery in crop plants. *Curr. Opin. Plant Biol.* 11, 215–221. doi: 10.1016/j.pbi.2008.01.002

Cech, F. C., and Goddard, R. E. (1957). "Selecting drouth resistant loblolly pine in Texas," in *Proceedings of the 4th Southern Forest Tree Improvement Conference*, Athens, 4.

Cen, H., Weng, H., Yao, J., He, M., Lv, J., Hua, S., et al. (2017). Chlorophyll fluorescence imaging uncovers photosynthetic fingerprint of citrus huanglongbing. *Front. Plant Sci.* 8:1509. doi: 10.3389/fpls.2017.01509

Chamala, S., Feng, G., Chavarro, C., and Barbazuk, W. B. (2015). Genome-wide identification of evolutionarily conserved alternative splicing events in flowering plants. *Front. Bioeng. Biotechnol.* 3:33. doi: 10.3389/fbioe.2015.00033

Chaves, M. M., Pereira, J. S., Maroco, J., Rodrigues, M. L., Ricardo, C. P. P., Osório, M. L., et al. (2002). How plants cope with water stress in the field? Photosynthesis and growth. *Ann. Bot.* 89, 907–916. doi: 10.1093/aob/mcf105

Chen, D., Chen, M., Altmann, T., and Klukas, C. (2014). "Bridging genomics and phenomics," in *Approaches in Integrative Bioinformatics: Towards the Virtual Cell*, eds M. Chen and R. Hofestädt (Berlin: Springer), 299–333. doi: 10.1007/978-3-642-41281-3_11

Chen, X., Castro, S. A., Liu, Q., Hu, W., and Zhang, S. (2020). Practical considerations on performing and analyzing CLIP-seq experiments to identify transcriptomic-wide RNA protein interactions. *Methods* 155, 49–57. doi: 10.1016/j.ymeth.2018.12.002

Choat, B., Badel, E., Burlett, R., Delzon, S., Cochard, H., and Jansen, S. (2016). Noninvasive measurement of vulnerability to drought-induced embolism by X-ray microtomography. *Plant Physiol.* 170, 273–282. doi: 10.1104/pp.15.00732

Choat, B., Brodribb, T. J., Brodersen, C. R., Duursma, R. A., López, R., and Medlyn, B. E. (2018). Triggers of tree mortality under drought. *Nature* 558, 531–539. doi: 10.1038/s41586-018-0240-x

Colombo, S. J., Menzies, M. I., and O'Reilly, C. (2001). "Influence of nursery cultural practices on cold hardiness of coniferous forest tree seedlings," in *Conifer Cold Hardiness*, Vol. 1, eds F. J. Bigras and S. J. Colombo (Dordrecht: Springer Netherlands), 223–252. doi: 10.1007/978-94-015-9650-3_9

Cook, B. I., Smerdon, J. E., Seager, R., and Coats, S. (2014). Global warming and 21st century drying. *Clim. Dyn.* 43, 2607–2627. doi: 10.1007/s00382-014-2075-y

Couvreur, V., Faget, M., Lobet, G., Javaux, M., Chaumont, F., and Draye, X. (2018). Going with the flow: multiscale insights into the composite nature of water transport in roots. *Plant Physiol.* 178, 1689–1703. doi: 10.1104/pp.18.01006

Coyle, D. R., Green, G. T., Barnes, B. F., Klepzig, K., Nowak, J. T., and Gandhi, J. K. (2016). Landowner and manager awareness and perceptions of pine health issues and southern pine management activities in the southeastern United States. *J. For.* 114, 541–551. doi: 10.5849/jof.15-093

D'Amato, A. W., Jokela, E. J., O'Hara, K. L., and Long, J. N. (2017). Silviculture in the United States: an amazing period of change over the past 30 years. *J. For.* 116, 55–67. doi: 10.5849/JOF-2016-035

D'Odorico, P., Besik, A., Wong, C. Y. S., Isabel, N., and Ensminger, I. (2020). High-throughput drone-based remote sensing reliably tracks phenology in thousands of conifer seedlings. *New Phytol.* 226, 1667–1681. doi: 10.1111/nph.16488

Dai, A. (2013). Increasing drought under global warming in observations and models. *Nat. Clim. Change* 3, 52–58. doi: 10.1038/nclimate1633

Danson, F. M., Steven, M. D., Malthus, T. J., and Clark, J. A. (1992). High-spectral resolution data for determining leaf water content. *Int. J. Remote Sens.* 13, 461–470. doi: 10.1080/01431169208904049

De La Torre, A. R., Wilhite, B., and Neale, D. B. (2019). Environmental genome-wide association reveals climate adaptation is shaped by subtle to moderate allele frequency shifts in loblolly pine. *Genome Biol. Evol.* 11, 2976–2989. doi: 10.1093/gbe/evz220

Delzon, S., and Cochard, H. (2014). Recent advances in tree hydraulics highlight the ecological significance of the hydraulic safety margin. *New Phytol.* 203, 355–358. doi: 10.1111/nph.12798

Demirdjian, L., Xu, Y., Bahrami-Samani, E., Pan, Y., Stein, S., Xie, Z., et al. (2020). Detecting allele-specific alternative splicing from population-scale RNA-seq data. *Am. J. Hum. Genet.* 107, 461–472. doi: 10.1016/j.ajhg.2020.07.005

Depardieu, C., Girardin, M. P., Nadeau, S., Lenz, P., Bousquet, J., and Isabel, N. (2020). Adaptive genetic variation to drought in a widely distributed conifer suggests a potential for increasing forest resilience in a drying climate. *New Phytol.* 227, 427–439. doi: 10.1111/nph.16551

Ding, Y., Wang, Y., Qiu, C., Qian, W., Xie, H., and Ding, Z. (2020). Alternative splicing in tea plants was extensively triggered by drought, heat and their combined stresses. *PeerJ* 8:e8258. doi: 10.7717/peerj.8258

Domec, J.-C., Palmroth, S., and Oren, R. (2016). Effects of *Pinus taeda* leaf anatomy on vascular and extravascular leaf hydraulic conductance as influenced by N-fertilization and elevated CO_2. *J. Plant Hydraul.* 3:e007. doi: 10.20870/jph.2016.e007

Domec, J.-C., Palmroth, S., Ward, E., Maier, C. A., Thérézien, M., and Oren, R. (2009). Acclimation of leaf hydraulic conductance and stomatal conductance of *Pinus taeda* (loblolly pine) to long-term growth in elevated CO_2 free-air CO_2 enrichment) and N-fertilization. *Plant Cell Environ.* 32, 1500–1512. doi: 10.1111/j.1365-3040.2009.02014.x

Dormling, I., and Johnsen, Ø (1992). Effects of the parental environment on full-sib families of *Pinus sylvestris*. *Can. J. For. Res.* 22, 88–100. doi: 10.1139/x92-013

Dornelas, M. C., and Rodriguez, A. P. M. (2005). A FLORICAULA/LEAFY gene homolog is preferentially expressed in developing female cones of the tropical pine *Pinus caribaea* var. *caribaea*.". *Genet. Mol. Biol.* 28, 299–307. doi: 10.1590/S1415-47572005000200021

Dzikiti, S., Verreynne, J. S., Stuckens, J., Strever, A., Verstraeten, W. W., Swennen, R., et al. (2010). Determining the water status of Satsuma mandarin trees [*Citrus unshiu* Marcovitch] using spectral indices and by combining hyperspectral and physiological data. *Agric. For. Meteorol.* 150, 369–379. doi: 10.1016/j.agrformet.2009.12.005

Edwalds-Gilbert, G., Veraldi, K. L., and Milcarek, C. (1997). Alternative poly(A) site selection in complex transcription units: means to an end? *Nucleic Acids Res.* 25, 2547–2561. doi: 10.1093/nar/25.13.2547

Eilmann, B., and Rigling, A. (2012). Tree-growth analyses to estimate tree species' drought tolerance. *Tree Physiol.* 32, 178–187. doi: 10.1093/treephys/tps004

Eilmann, B., Buchmann, N., Siegwolf, R., Saurer, M., Cherubini, P., and Rigling, A. (2010). Fast response of scots pine to improved water availability reflected in tree-ring width and Δ13C. *Plant Cell Environ.* 33, 1351–1360. doi: 10.1111/j.1365-3040.2010.02153.x

Esposito, S., Carputo, D., Cardi, T., and Tripodi, P. (2019). Applications and trends of machine learning in genomics and phenomics for next-generation breeding. *Plants* 9:34. doi: 10.3390/plants9010034

Estravis-Barcala, M., Mattera, M. G., Soliani, C., Bellora, N., Opgenoorth, L., Heer, K., et al. (2020). Molecular bases of responses to abiotic stress in trees. *J. Exp. Bot.* 71, 3765–3779. doi: 10.1093/jxb/erz532

Ewers, B. E., Oren, R., Albaugh, T. J., and Dougherty, P. M. (2000). Carry-over effects of water and nutrient supply on water use of *Pinus taeda*. *Ecol. Appl.* 9, 513–525. doi: 10.1890/1051-07611999009[0513:COEOWA]2.0.CO;2

Ewers, F. W. (1985). Xylem structure and water conduction in conifer trees, dicot trees, and lianas. *IAWA Bull.* 6, 309–317. doi: 10.1163/22941932-90000959

Eziz, A., Yan, Z., Tian, D., Han, W., Tang, Z., and Fang, J. (2017). Drought effect on plant biomass allocation: a meta-analysis. *Ecol. Evol.* 7, 11002–11010. doi: 10.1002/ece3.3630

Fang, Y., and Xiong, L. (2015). General mechanisms of drought response and their application in drought resistance improvement in plants. *Cell. Mol. Life Sci.* 72, 673–689. doi: 10.1007/s00018-014-1767-0

Feng, X., Dawson, T. E., Ackerly, D. D., Santiago, L. S., and Thompson, S. E. (2017). Reconciling seasonal hydraulic risk and plant water use through probabilistic soil–plant dynamics. *Glob. Change Biol.* 23, 3758–3769. doi: 10.1111/gcb.13640

Flexas, J., and Gago, J. (2018). A role for ecophysiology in the "omics" era. *Plant J. Cell Mol. Biol.* 96, 251–259. doi: 10.1111/tpj.14059

Forester, B. R., Lasky, J. R., Wagner, H. H., and Urban, D. L. (2018). Comparing methods for detecting multilocus adaptation with multivariate genotype–environment associations. *Mol. Ecol.* 27, 2215–2233. doi: 10.1111/mec.14584

Fox, T. R., Jokela, E. J., and Allen, H. L. (2007). The development of pine plantation silviculture in the southern United States. *J. For.* 105, 337–347. doi: 10.1093/jof/105.7.337

Gabriel, S. B., Schaffner, S. F., Nguyen, H., Moore, J. M., Roy, J., Blumenstiel, B., et al. (2002). The structure of haplotype blocks in the human genome. *Science* 296, 2225–2229. doi: 10.1126/science.1069424

Galiano, L., Martínez-Vilalta, J., and Lloret, F. (2011). Carbon reserves and canopy defoliation determine the recovery of Scots pine 4 yr after a drought episode. *New Phytol.* 190, 750–759. doi: 10.1111/j.1469-8137.2010.03628.x

Garcia-Forner, N., Biel, C., Savé, R., and Martínez-Vilalta, J. (2017). Isohydric species are not necessarily more carbon limited than anisohydric species during drought. *Tree Physiol.* 37, 441–455. doi: 10.1093/treephys/tpw109

Ge, Y., Bai, G., Stoerger, V., and Schnable, J. C. (2016). Temporal dynamics of maize plant growth, water use, and leaf water content using automated high throughput RGB and hyperspectral imaging. *Comp. Electron. Agric.* 127, 625–632. doi: 10.1016/j.compag.2016.07.028

Georgii, E., Kugler, K., Pfeifer, M., Vanzo, E., Block, K., Domagalska, M. A., et al. (2019). The systems architecture of molecular memory in poplar after abiotic stress. *Plant Cell* 31, 346–367. doi: 10.1105/tpc.18.00431

Gitelson, A. A., and Merzlyak, M. N. (1996). Signature analysis of leaf reflectance spectra: algorithm development for remote sensing of chlorophyll. *J. Plant Physiol.* 148, 494–500. doi: 10.1016/S0176-1617(96)80284-7

Gonzalez-Ibeas, D., Martinez-Garcia, P. J., Famula, R. A., Delfino-Mix, A., Stevens, K. A., Loopstra, C. A., et al. (2016). Assessing the gene content of the megagenome: sugar pine (*Pinus lambertiana*). *G3 Genes Genomes Genet.* 6, 3787–3802. doi: 10.1534/g3.116.032805

Greenwood, M. S., and Hutchison, K. W. (1996). "Genetic aftereffects of increased temperature in *Larix*," in *Proceedings 1995 Meeting of the Northern Global Change Program; Gen. Tech. Rep. NE-214*, eds H. John, B. Richard, and O. Kelly

(Radnor, PA: U. S. Department of Agriculture, Forest Service, Northeastern Forest Experiment Station).

Greer, D. H., and Stanley, C. J. (1985). Regulation of the loss of frost hardiness in *Pinus radiata* by photoperiod and temperature. *Plant Cell Environ.* 8, 111–116. doi: 10.1111/j.1365-3040.1985.tb01217.x

Greer, D. H., and Warrington, I. J. (1982). Effect of photoperiod, night temperature, and frost incidence on development of frost hardiness in *Pinus radiata*. *Aust. J. Plant Physiol.* 9, 333–342. doi: 10.1071/pp9820333

Guan, R., Zhao, Y., Zhang, H., Fan, G., Liu, X., Zhou, W., et al. (2016). Draft genome of the living fossil *Ginkgo biloba*. *GigaScience* 5:49. doi: 10.1186/s13742-016-0154-1

Guo, Y., Pang, C., Jia, X., Ma, Q., Dou, L., Zhao, F., et al. (2017). A NAM domain gene, GhNAC79, improves resistance to drought stress in upland cotton. *Front. Plant Sci.* 8:1657. doi: 10.3389/fpls.2017.01657

Gupta, V., Estrada, A. D., Blakley, I., Reid, R., Patel, K., Meyer, M. D., et al. (2015). RNA-seq analysis and annotation of a draft blueberry genome assembly identifies candidate genes involved in fruit ripening, biosynthesis of bioactive compounds, and stage-specific alternative splicing. *GigaScience* 4:5. doi: 10.1186/s13742-015-0046-9

Gusev, A., Kenny, E. E., Lowe, J. K., Salit, J., Saxena, R., Kathiresan, S., et al. (2011). DASH: a method for identical-by-descent haplotype mapping uncovers association with recent variation. *Am. J. Hum. Genet.* 88, 706–717. doi: 10.1016/j.ajhg.2011.04.023

Ha, K. C. H., Blencowe, B. J., and Morris, Q. (2018). QAPA: a new method for the systematic analysis of alternative polyadenylation from RNA-seq data. *Genome Biol.* 19:45. doi: 10.1186/s13059-018-1414-4

Hacke, U. G., Sperry, J. S., Ewers, B. E., Ellsworth, D. S., Schäfer, K. V. R., and Oren, R. (2000). Influence of soil porosity on water use in *Pinus taeda*. *Oecologia* 124, 495–505. doi: 10.1007/pl00008875

Hamanishi, E. T., and Campbell, M. M. (2011). Genome-wide responses to drought in forest trees. *Forestry* 84, 273–283. doi: 10.1093/forestry/cpr012

Hammond, W. M., Yu, K., Wilson, L. A., Will, R. E., Anderegg, W. R. L., and Adams, H. D. (2019). Dead or dying? Quantifying the point of no return from hydraulic failure in drought-induced tree mortality.". *New Phytol.* 223, 1834–1843. doi: 10.1111/nph.15922

Hentschel, R., Rosner, S., Kayler, Z. E., Andreassen, K., Børja, I., Solberg, S., et al. (2014). Norway spruce physiological and anatomical predisposition to dieback. *For. Ecol. Manag.* 322, 27–36. doi: 10.1016/j.foreco.2014.03.007

Holling, C. S. (1973). Resilience and stability of ecological systems. *Ann. Rev. Ecol. Syst*. 4, 1–23. doi: 10.1146/annurev.es.04.110173.000245

Howard, D. M., Hall, L. S., Hafferty, J. D., Zeng, Y., Adams, M. J., Clarke, T.-K., et al. (2017). Genome-wide haplotype-based association analysis of major depressive disorder in Generation Scotland and UK Biobank. *Transl. Psychiatry* 7, 1–9. doi: 10.1038/s41398-017-0010-9

Humplík, J. F., Lazár, D., Fürst, T., Husičková, A., Hýbl, M., and Spíchal, L. (2015). Automated integrative high-throughput phenotyping of plant shoots: a case study of the cold-tolerance of pea (*Pisum sativum* L.). *Plant Methods* 11:20. doi: 10.1186/s13007-015-0063-9

Hunt, R. E., Rock, B. N., and Nobel, P. S. (1987). Measurement of leaf relative water content by infrared reflectance. *Remote Sens. Environ.* 22, 429–435. doi: 10.1016/0034-4257(87)90094-0

Hussain, H. A., Hussain, S., Khaliq, A., Ashraf, U., Anjum, S. A., Men, S., et al. (2018). Chilling and drought stresses in crop plants: implications, cross talk, and potential management opportunities. *Front. Plant Sci.* 9:393. doi: 10.3389/fpls.2018.00393

Ingrisch, J., and Bahn, M. (2018). Towards a comparable quantification of resilience. *Trends Ecol. Evol.* 33, 251–259. doi: 10.1016/j.tree.2018.01.013

Isabel, N., Holliday, J. A., and Aitken, S. N. (2020). Forest genomics: advancing climate adaptation, forest health, productivity, and conservation. *Evol. Appl.* 13, 3–10. doi: 10.1111/eva.12902

Isik, F., and McKeand, S. E. (2019). Fourth cycle breeding and testing strategy for *Pinus taeda* in the NC State University cooperative tree improvement program. *Tree Genet. Genomes* 15:70. doi: 10.1007/s11295-019-1377-y

Jarbeau, J. A., Ewers, F. W., and Davis, S. D. (1995). The mechanism of water-stress-induced embolism in two species of chaparral shrubs. *Plant Cell Environ.* 18, 189–196. doi: 10.1111/j.1365-3040.1995.tb00352.x

Johnsen, Ø (1989a). Phenotypic changes in progenies of northern clones of *Picea abies* (L) Karst. grown in a southern seed orchard. I. Frost hardiness in a phytotron experiment. *Scand. J. For. Res.* 4, 317–330. doi: 10.1080/02827588909382569

Johnsen, Ø (1989b). Phenotypic changes in progenies of northern clones of *Picea abies* (L.) Karst. grown in a southern seed orchard: II. Seasonal growth rhythm and height in field trials. *Scand. J. For. Res.* 4, 331–341. doi: 10.1080/02827588909382570

Joshi, R., Wani, S. H., Singh, B., Bohra, A., Dar, Z. A., Lone, A. A., et al. (2016). Transcription factors and plants response to drought stress: current understanding and future directions. *Front. Plant Sci.* 7:1029. doi: 10.3389/fpls.2016.01029

Kaakinen, M., Mägi, R., Fischer, K., Heikkinen, J., Järvelin, M.-R., Morris, A. P., et al. (2017). MARV: a tool for genome-wide multi-phenotype analysis of rare variants. *BMC Bioinform.* 18:110. doi: 10.1186/s12859-017-1530-2

Karst, J., Burns, C., Cale, J. A., Antunes, P. M., Woods, M., Lamit, L. J., et al. (2018). Tree species with limited geographical ranges show extreme responses to ectomycorrhizas. *Glob. Ecol. Biogeogr.* 27, 839–848. doi: 10.1111/geb.12745

Katahata, S.-I., Futamura, N., Igasaki, T., and Shinohara, K. (2014). Functional analysis of SOC1-like and AGL6-like MADS-box genes of the gymnosperm *Cryptomeria japonica*. *Tree Genet. Genomes* 10, 317–327. doi: 10.1007/s11295-013-0686-9

Klein, T. (2014). The variability of stomatal sensitivity to leaf water potential across tree species indicates a continuum between isohydric and anisohydric behaviours. *Func. Ecol.* 28, 1313–1320. doi: 10.1111/1365-2435.12289

Klein, T., Zeppel, M. J. B., Anderegg, W. R. L., Bloemen, J., De Kauwe, M. G., Hudson, P., et al. (2018). Xylem embolism refilling and resilience against drought-induced mortality in woody plants: processes and trade-offs. *Ecol. Res.* 33, 839–855. doi: 10.1007/s11284-018-1588-y

Klintenäs, M., Pin, P. A., Benlloch, R., Ingvarsson, P. K., and Nilsson, O. (2012). Analysis of conifer FLOWERING LOCUS T/TERMINAL FLOWER1-like genes provides evidence for dramatic biochemical evolution in the angiosperm FT lineage. *New Phytol.* 196, 1260–1273. doi: 10.1111/j.1469-8137.2012.04332.x

Klockow, P. A., Edgar, C. B., Moore, G. W., and Vogel, J. G. (2020). Southern pines are resistant to mortality from an exceptional drought in east Texas. *Front. For. Glob. Change* 3:23. doi: 10.3389/ffgc.2020.00023

Klockow, P. A., Vogel, J. G., Edgar, C. B., and Moore, G. W. (2018). Lagged mortality among tree species four years after an exceptional drought in east Texas. *Ecosphere* 9:e02455. doi: 10.1002/ecs2.2455

Knight, H., and Knight, M. R. (2001). Abiotic stress signaling pathways: specificity and cross-talk. *Trends Plant Sci.* 6, 262–267. doi: 10.1016/s1360-1385(01)01946-x

Knipfer, T., Cuneo, I. F., Brodersen, C. R., and McElrone, A. J. (2016). In situ visualization of the dynamics in xylem embolism formation and removal in the absence of root pressure: a study on excised grapevine stems. *Plant Physiol.* 171, 1024–1036. doi: 10.1104/pp.16.00136

Knipfer, T., Eustis, A., Brodersen, C., Walker, A. M., and McElrone, A. J. (2015). Grapevine species from varied native habitats exhibit differences in embolism formation/repair associated with leaf gas exchange and root pressure. *Plant Cell Environ.* 38, 1503–1513. doi: 10.1111/pce.12497

Kover, P. X., Valdar, W., Trakalo, J., Scarcelli, N., Ehrenreich, I. M., Purugganan, M. D., et al. (2009). A multiparent advanced generation inter-cross to fine-map quantitative traits in *Arabidopsis thaliana*. *PLoS Genet.* 5:e1000551. doi: 10.1371/journal.pgen.1000551

Kuzmin, D. A., Feranchuk, S. I., Sharov, V. V., Cybin, A. N., Makolov, S. V., Putintseva, Y. A., et al. (2019). Stepwise large genome assembly approach: a case of Siberian larch (*Larix sibirica* Ledeb). *BMC Bioinform.* 20:35–46. doi: 10.1186/s12859-018-2570-y

Lamarque, L. J., Corso, D., Torres-Ruiz, J. M., Badel, E., Brodribb, T. J., Burlett, R., et al. (2018). An inconvenient truth about xylem resistance to embolism in the model species for refilling *Laurus nobilis* L.". *Ann. For. Sci.* 75:88. doi: 10.1007/s13595-018-0768-9

Lambeth, C. C., Dougherty, P. M., Gladstone, W. T., McCullough, R. B., and Wells, O. O. (1984). Large-scale planting of North Carolina loblolly pine in Arkansas and Oklahoma: a case of gain versus risk. *J. For.* 82, 736–741. doi: 10.1093/jof/82.12.736

Lambeth, C., McKeand, S. E., Rousseau, R., and Schmidtling, R. (2005). Planting nonlocal seed sources of loblolly pine – managing benefits and risks. *South. J. Appl. For*. 29, 96–104. doi: 10.1093/sjaf/29.2.96

Lebedev, V. G., Lebedeva, T. N., Chernodubov, A. I., and Shestibratov, K. A. (2020). Genomic selection for forest tree improvement: methods, achievements and perspectives. *Forests* 11:1190. doi: 10.3390/f11111190

Leinonen, I., Repo, T., and Hänninen, H. (1997). Changing environmental effects on frost hardiness of scots pine during dehardening. *Ann. Bot.* 79, 133–137. doi: 10.1006/anbo.1996.0321

Li, B., McKeand, S. E., and Weir, R. (1999). Tree improvement and sustainable forestry - impact of two cycles of loblolly pine breeding in the USA.". *For. Genet.* 6, 229–234.

Li, J.-X., Hou, X.-J., Zhu, J., Zhou, J.-J., Huang, H.-B., Yue, J.-Q., et al. (2017). Identification of genes associated with lemon floral transition and flower development during floral inductive water deficits: a hypothetical model. *Front. Plant Sci.* 8:1013. doi: 10.3389/fpls.2017.01013

Li, X., Li, M., Zhou, B., Yang, Y., Wei, Q., and Zhang, J. (2019). Transcriptome analysis provides insights into the stress response crosstalk in apple (*Malus* × *domestica*) subjected to drought, cold and high salinity. *Sci. Rep.* 9:9071. doi: 10.1038/s41598-019-45266-0

Li, Y., Mi, X., Zhao, S., Zhu, J., Guo, R., Xia, X., et al. (2020). Comprehensive profiling of alternative splicing landscape during cold acclimation in tea plant. *BMC Genomics* 21:65. doi: 10.1186/s12864-020-6491-6

Li, Z., Shen, J., and Liang, J. (2019). Genome-wide identification, expression profile, and alternative splicing analysis of the brassinosteroid-signaling kinase (BSK) family genes in *Arabidopsis*. *Int. J. Mol. Sci.* 20:1138. doi: 10.3390/ijms20051138

Liang, X., Kankare, V., Hyyppä, J., Wang, Y., Kukko, A., Haggrén, H., et al. (2016). Terrestrial laser scanning in forest inventories. *Int. J. Photogramm. Remote Sens.* 115, 63–77. doi: 10.1016/j.isprsjprs.2016.01.006

Linder, S. (1972). *Seasonal Variation of Pigments in Needles, a Study of Scots Pine and Norway Spruce Seedlings Grown Under Different Nursery Conditions*. Stockholm: Studia Forestalia Suecica, 100.

Liu, Z., Yuan, G., Liu, S., Jia, J., Cheng, L., Qi, D., et al. (2017). Identified of a novel cis -element regulating the alternative splicing of LcDREB2. *Sci. Rep.* 7:46106. doi: 10.1038/srep46106

Lloret, F., Keeling, E. G., and Sala, A. (2011). Components of tree resilience: effects of successive low−growth episodes in old ponderosa pine forests. *Oikos* 12, 1909–1920. doi: 10.1111/j.1600-0706.2011.19372.x

Long, E. M. (1980). Texas and Louisiana lobolly pine study confirms importance of local seed sources. *South. J. Appl. For.* 4, 127–132. doi: 10.1093/sjaf/4.3.127

Lovell, J. T., Jenkins, J., Lowry, D. B., Mamidi, S., Sreedasyam, A., Weng, X., et al. (2018). The genomic landscape of molecular responses to natural drought stress in *Panicum hallii*. *Nat. Commun.* 9:5213. doi: 10.1038/s41467-018-07669-x

Lowe, A., Harrison, N., and French, A. P. (2017). Hyperspectral image analysis techniques for the detection and classification of the early onset of plant disease and stress. *Plant Methods* 13, 1–12.

Lu, M., Krutovsky, K. V., and Loopstra, C. A. (2019a). Predicting adaptive genetic variation of loblolly pine (*Pinus taeda* L.) populations under projected future climates based on multivariate models. *J. Hered.* 110, 857–865. doi: 10.1093/jhered/esz065

Lu, M., Krutovsky, K. V., Nelson, C. D., Koralewski, T. E., Byram, T. D., and Loopstra, C. A. (2016). Exome genotyping, linkage disequilibrium and population structure in loblolly pine (*Pinus taeda* L.). *BMC Genomics* 17:730. doi: 10.1186/s12864-016-3081-8

Lu, M., Loopstra, C. A., and Krutovsky, K. V. (2019b). Detecting the genetic basis of local adaptation in loblolly pine (*Pinus taeda* L.) using whole exome−wide genotyping and an integrative landscape genomics analysis approach. *Ecol. Evol.* 9, 6798–6809. doi: 10.1002/ece3.5225

Luo, L., Shen, J., Zhang, H., Chhibber, A., Mehrotra, D. V., and Tang, Z.-Z. (2020). Multi-trait analysis of rare-variant association summary statistics using MTAR. *Nat. Commun.* 11:2850. doi: 10.1038/s41467-020-16591-0

Ma, J.-J., Liu, S.-W., Han, F.-X., Li, W., Li, Y., and Niu, S.-H. (2020). Comparative transcriptome analyses reveal two distinct transcriptional modules associated with pollen shedding time in pine. *BMC Genomics* 21:504. doi: 10.1186/s12864-020-06880-9

Maggard, A. O., Will, R. E., Wilson, D. S., Meek, C. R., and Vogel, J. G. (2017). Fertilization can compensate for decreased water availability by increasing the efficiency of stem volume production per unit of leaf area for loblolly pine (*Pinus taeda*) stands.". *Can. J. For. Res.* 47, 445–457. doi: 10.1139/cjfr-2016-0422

Mahony, C. R., MacLachlan, I. R., Lind, B. M., Yoder, J. B., Wang, T., and Aitken, S. N. (2020). Evaluating genomic data for management of local adaptation in a changing climate: a lodgepole pine case study. *Evol. Appl.* 13, 116–131. doi: 10.1111/eva.12871

Maki, M., Ishiahra, M., and Tamura, M. (2004). Estimation of leaf water status to monitor the risk of forest fires by using remotely sensed data. *Remote Sens. Environ.* 90, 441–450. doi: 10.1016/j.rse.2004.02.002

Manzoni, S., Katul, G., and Porporato, A. (2014). A dynamical system perspective on plant hydraulic failure. *Water Resour. Res.* 50, 5170–5183. doi: 10.1002/2013WR015236

Marchin, R. M., Ossola, A., Leishman, M. R., and Ellsworth, D. S. (2020). A simple method for simulating drought effects on plants. *Front. Plant Sci.* 10:1715. doi: 10.3389/fpls.2019.01715

Marquez, Y., Brown, J. W. S., Simpson, C., Barta, A., and Kalyna, M. (2012). Transcriptome survey reveals increased complexity of the alternative splicing landscape in *Arabidopsis*. *Genome Res.* 22, 1184–1195. doi: 10.1101/gr.134106.111

Martinez-Vilalta, J., and Garcia-Forner, N. (2017). Water potential regulation, stomatal behaviour and hydraulic transport under drought: deconstructing the iso/anisohydric concept. *Plant Cell Environ.* 40, 962–976. doi: 10.1111/pce.12846

Maxwell, K., and Johnson, G. N. (2000). Chlorophyll fluorescence—a practical guide. *J. Exp. Bot.* 51, 659–668. doi: 10.1093/jexbot/51.345.659

Mayr, S., Hacke, U., Schmid, P., Schwienbacher, F., and Gruber, A. (2006). Frost drought in conifers at the alpine timberline: xylem dysfunction and adaptations. *Ecology* 87, 3175–3185. doi: 10.1890/0012-9658200687[3175:FDICAT]2.0.CO;2

Mayr, S., Schmid, P., Beikircher, B., Feng, F., and Badel, E. (2019). Die hard: timberline conifers survive annual winter embolism. *New Phytol.* 226, 13–20. doi: 10.1111/nph.16304

Mayr, S., Schwienbacher, F., and Bauer, H. (2003). Winter at the alpine timberline. Why does embolism occur in Norway spruce but not in stone pine? *Plant Physiol.* 131, 780–792. doi: 10.1104/pp.011452

McCulloh, K. A., and Meinzer, F. C. (2015). Further evidence that some plants can lose and regain hydraulic function daily. *Tree Physiol.* 35, 691–693. doi: 10.1093/treephys/tpv066

McCulloh, K. A., Johnson, D. A., Meinzer, F. C., and Woodruff, D. R. (2013). The dynamic pipeline: hydraulic capacitance and xylem hydraulic safety in four tall conifer species. *Plant Cell Environ.* 37, 1171–1183. doi: 10.1111/pce.12225

McDowell, N. G. (2011). Mechanisms linking drought, hydraulics, carbon metabolism, and vegetation mortality. *Plant Physiol.* 155, 1051–1059. doi: 10.1104/pp.110.170704

McDowell, N. G., Fisher, R. A., Xu, C., Domec, J.-C., Hölttä, T., Mackay, D. S., et al. (2013). Evaluating theories of drought-induced vegetation mortality using a multimodel-experiment framework. *New Phytol.* 200, 304–321. doi: 10.1111/nph.12465

McDowell, N. G., Williams, A. P., Xu, C., Pockman, W. T., Dickman, L. T., Sevanto, S., et al. (2016). Multi-scale predictions of massive conifer mortality due to chronic temperature rise. *Nat. Clim. Change* 6, 295–300. doi: 10.1038/nclimate2873

McDowell, N., Pockman, W. T., Allen, C. D., Breshears, D. D., Cobb, N., Kolb, T., et al. (2008). Mechanisms of plant survival and mortality during drought: why do some plants survive while others succumb to drought? *New Phytol.* 178, 719–739. doi: 10.1111/j.1469-8137.2008.02436.x

McKeand, S. E., and Bridgwater, F. E. (1998). A strategy for the third breeding cycle of loblolly pine in the Southeastern U.S. *Silvae Genet.* 47, 223–234.

McKeand, S. E., Jokela, E. J., Huber, D. A., Byram, T. D., Allen, H. L., Li, B., et al. (2006). Performance of improved genotypes of loblolly pine across different soils, climates, and silvicultural inputs. *For. Ecol. Manag.* 227, 178–184. doi: 10.1016/j.foreco.2006.02.016

McKeand, S. E., Payn, K. G., Heine, A. J., and Abt, R. C. (2021). Economic significance of continued improvement of loblolly pine genetics and its efficient deployment to landowners in the southern United States. *J. For.* 119, 62–72. doi: 10.1093/jofore/fvaa044

McKeand, S. E., Peter, G. F., and Byram, T. (2015). "Trends in deployment of advanced loblolly pine germplasm," in *PINEMAP Year 4 Annual Report*, ed E. Sommer (Washington, DC: USDA), 59.

Mei, W., Liu, S., Schnable, J. C., Yeh, C.-T., Springer, N. M., Schnable, P. S., et al. (2017). A comprehensive analysis of alternative splicing in paleopolyploid maize. *Front. Plant Sci.* 8:694. doi: 10.3389/fpls.2017.00694

Mica, E., Piccolo, V., Delledonne, M., Ferrarini, A., Pezzotti, M., Casati, C., et al. (2010). High throughput approaches reveal splicing of primary microRNA transcripts and tissue specific expression of mature microRNAs in *Vitis vinifera*. *BMC Genomics* 10:558. doi: 10.1186/1471-2164-10-558

Mitchell, P. J., McAdam, S. A. M., Pinkard, E. A., and Brodribb, T. J. (2017). Significant contribution from foliaged-derived ABA in regulating gas exchange in *Pinus radiata*. *Tree Physiol.* 37, 236–245. doi: 10.1093/treephys/tpw092

Mitchell, P. J., O'Grady, A. P., Tissue, D. T., White, D. A., Ottenschlaeger, M. L., and Pinkard, E. A. (2013). Drought response strategies define the relative contributions of hydraulic dysfunction and carbohydrate depletion during tree mortality. *New Phytol.* 197, 862–872. doi: 10.1111/nph.12064

Moran, E., Lauder, J., Musser, C., Stathos, A., and Shu, M. (2017). The genetics of drought tolerance in conifers. *New Phytol.* 216, 1034–1048. doi: 10.1111/nph.14774

Mosca, E., Cruz, F., Gómez-Garrido, J., Bianco, L., Rellstab, C., Brodbeck, S., et al. (2019). A reference genome sequence for the European silver fir (*Abies alba* Mill.): a community-generated genomic resource. *G3 Genes Genomes Genet.* 9, 2039–2049. doi: 10.1534/g3.119.400083

Neale, D. B., McGuire, P. E., Wheeler, N. C., Stevens, K. A., Crepeau, M. W., Cardeno, C., et al. (2017). The Douglas-fir genome sequence reveals specialization of the photosynthetic apparatus in Pinaceae. *G3 Genes Genet. Genomes* 7, 3157–3167. doi: 10.1534/g3.117.300078

Neale, D. B., Wegrzyn, J. L., Stevens, K. A., Zimin, A. V., Puiu, D., Crepeau, M. W., et al. (2014). Decoding the massive genome of loblolly pine using haploid DNA and novel assembly strategies. *Genome Biol.* 15:R59. doi: 10.1186/gb-2014-15-3-r59

Niu, S., Yuan, H., Sun, X., Porth, I., Li, Y., El-Kassaby, Y. A., et al. (2016). A transcriptomics investigation into pine reproductive organ development. *New Phytol.* 209, 1278–1289. doi: 10.1111/nph.13680

Niu, S., Yuan, L., Zhang, Y., Chen, X., and Li, W. (2014). Isolation and expression profiles of gibberellin metabolism genes in developing male and female cones of *Pinus tabuliformis*. *Funct. Integ. Genome* 14, 697–705. doi: 10.1007/s10142-014-0387-y

Nystedt, B., Street, N. R., Wetterbom, A., Zuccolo, A., Lin, Y.-C., Scofield, D. G., et al. (2013). The Norway spruce genome sequence and conifer genome evolution. *Nature* 497, 579–584. doi: 10.1038/nature12211

O'Brien, M. J., Engelbrecht, B. M. J., Joswig, J., Pereyra, G., Schuldt, B., Jansen, S., et al. (2017). A synthesis of tree functional traits related to drought-induced mortality in forests across climatic zones. *J. Appl. Ecol.* 54, 1669–1686. doi: 10.1111/1365-2664.12874

O'Brien, M. J., Pugnaire, F. I., Rodríguez-Echeverría, S., Morillo, J. A., Martín-Usero, F., López-Escoriza, A., et al. (2018). Mimicking a rainfall gradient to test the role of soil microbiota for mediating plant responses to drier conditions. *Oikos* 127, 1776–1786. doi: 10.1111/oik.05443

Orwig, D. A., and Abrams, M. D. (1997). Variation in radial growth responses to drought among species, site, and canopy strata. *Trees* 11, 474–484. doi: 10.1007/s004680050110

Palusa, S. G., Ali, G. S., and Reddy, A. S. N. (2007). Alternative splicing of pre-mRNAs of *Arabidopsis serine*/arginine-rich proteins: regulation by hormones and stresses. *Plant J.* 49, 1091–1107. doi: 10.1111/j.1365-313X.2006.03020.x

Panahi, B., Abbaszadeh, B., Taghizadeghan, M., and Ebrahimie, E. (2014). Genome-wide survey of alternative splicing in *Sorghum bicolor*. *Physiol. Mol. Biol. Plants* 20, 323–329. doi: 10.1007/s12298-014-0245-3

Pandey, P., Ge, Y., Stoerger, V., and Schnable, J. C. (2017). High throughput in vivo analysis of plant leaf chemical properties using hyperspectral imaging. *Front. Plant Sci.* 8:1348. doi: 10.3389/fpls.2017.01348

Petrucco, L., Nardini, A., von Arx, G., Saurer, M., and Cherubini, P. (2017). Isotope signals and anatomical features in tree rings suggest a role for hydraulic strategies in diffuse drought-induced die-back of *Pinus nigra*. *Tree Physiol.* 37, 523–535. doi: 10.1093/treephys/tpx031

Pike, C., Potter, K. M., Berrang, P., Crane, B., Baggs, J., Leites, L., et al. (2020). New seed-collection zones for the eastern United States: the eastern seed zone forum. *J. For.* 118, 444–451. doi: 10.1093/jofore/fvaa013

Plaut, J. A., Yepez, E. A., Hill, J., Pangle, R., Sperry, J. S., Pockman, W. T., et al. (2012). Hydraulic limits preceding mortality in a piñon–juniper woodland under experimental drought. *Plant Cell Environ.* 35, 1601–1617. doi: 10.1111/j.1365-3040.2012.02512.x

Polle, A., Chen, S. L., Eckert, C., and Harfouche, A. (2019). Engineering drought resistance in forest trees. *Front. Plant Sci.* 9:1875. doi: 10.3389/fpls.2018.01875

Poyatos, R., Aguadé, D., Galiano, L., Mencuccini, M., and Martínez-Vilalta, J. (2013). Drought-induced defoliation and long periods of near-zero gas exchange play a key role in accentuating metabolic decline of Scots pine. *New Phytol.* 200, 388–401. doi: 10.1111/nph.12278

Rahman, M. A., Moody, M. A., and Nassuth, A. (2014). Grape contains 4 ICE genes whose expression includes alternative polyadenylation, leading to transcripts encoding at least 7 different ICE proteins. *Environ. Exp. Bot.* 106, 70–78. doi: 10.1016/j.envexpbot.2014.01.003

Rellstab, C., Gugerli, F., Eckert, A. J., Hancock, A. M., and Holderegger, R. (2015). A practical guide to environmental association analysis in landscape genomics. *Mol. Ecol.* 24, 4348–4370. doi: 10.1111/mec.13322

Riggs, A. D., Russo, V. E. A., and Martienssen, R. A. (1996). *Epigenetic Mechanisms of Gene Regulation*. Plainview, NY: Cold Spring Harbor Laboratory Press.

Rock, B. N., Hoshizaki, T., and Miller, J. R. (1988). Comparison of in situ and airborne spectral measurements of the blue shift associated with forest decline. *Remote Sens. Environ.* 24, 109–127. doi: 10.1016/0034-4257(88)90008-9

Rodríguez-Gamir, J., Primo-Millo, E., and Forner-Giner, M. Á (2016). An integrated view of whole-tree hydraulic architecture. Does stomatal or hydraulic conductance determine whole tree transpiration? *PLoS One* 11:e0155246. doi: 10.1371/journal.pone.0155246

Salleo, S., Lo Gullo, M. A., De Paoli, D., and Zippo, M. (1996). Xylem recovery from cavitation-induced embolism in young plants of *Laurus nobilis*: a possible mechanism. *New Phytol.* 132, 47–56. doi: 10.1111/j.1469-8137.1996.tb04507.x

Samuelson, L. J., Pell, C. J., Stokes, T. A., Bartkowiak, S. M., Akers, M. K., Kane, M., et al. (2014). Two-year throughfall and fertilization effects on leaf physiology and growth of loblolly pine in the Georgia Piedmont. *For. Ecol. Manag.* 330, 29–37. doi: 10.1016/j.foreco.2014.06.030

Savi, T., Casolo, V., Luglio, J., Bertuzzi, S., Trifilò, P., Lo Gullo, M. A., et al. (2016). Species-specific reversal of stem xylem embolism after a prolonged drought correlates to endpoint concentration of soluble sugars. *Plant Physiol. Biochem.* 106, 198–207. doi: 10.1016/j.plaphy.2016.04.051

Schmidtling, R. C. (1987). Locating pine seed orchards in warmer climates: benefits and risks. *For. Ecol. Manag.* 19, 273–283. doi: 10.1016/0378-1127(87)90037-5

Schmidtling, R. C. (2001). *Southern Pine Seed Sources. General Technical Report SRS-44*. Asheville, NC: U.S. Department of Agriculture, Forest Service, Southern Research Station, 25.

Schmidtling, R. C. (2003). The southern pines during the Pleistocene. *Acta Hortic.* 615, 203–209. doi: 10.17660/actahortic.2003.615.19

Schmidtling, R. C., and Hipkins, V. (2004). The after-effects of reproductive environment in shortleaf pine. *Forestry* 77, 287–295. doi: 10.1093/forestry/77.4.287

Schmidtling, R. C., Carroll, E., and LaFarge, T. (1999). Allozyme diversity of selected and natural loblolly pine populations. *Silvae Genet.* 48, 35–45.

Schultz, R. P. (1997). *Loblolly Pine: The Ecology and Culture of Loblolly Pine (Pinus taeda* L.). Washington, DC: U.S. Department of Agriculture, Forest Service, 493.

Schulze, E. D., Beck, E., Buchmann, N., Clemens, S., Müller-Hohenstein, K., and Scherer-Lorenzen, M. (2020). *Plant Ecology*. Berlin: Springer-Verlag GmbH.

Scott, A. D., Zimin, A. V., Puiu, D., Workman, R., Britton, M., Zaman, S., et al. (2020). A reference genome sequence for giant sequoia. *G3* 10, 3907–3919. doi: 10.1534/g3.120.401612

Sevanto, S., Mcdowell, N. G., Turin, L., Dickman, R. P., and Pockman, W. T. (2014). How do trees die? A test of the hydraulic failure and carbon starvation hypotheses. *Plant Cell Environ.* 37, 153–161. doi: 10.1111/pce.12141

Shiokawa, T., Yamada, S., Futamura, N., Osanai, K., Murasugi, D., Shinohara, K., et al. (2008). Isolation and functional analysis of the CjNdly gene, a homolog in

Cryptomeria japonica of FLORICAULA/LEAFY genes. *Tree Physiol.* 28, 21–28. doi: 10.1093/treephys/28.1.21

Skelton, R. (2019). Of storage and stems: examining the role of stem water storage in plant water balance. *Plant Physiol.* 179, 1433–1434. doi: 10.1104/pp.19.00057

South, D. B. (2006). *Freeze Injury to Southern Pine Seedlings in Gen. Tech. Rep. SRS-92*. Asheville, NC: U.S. Department of Agriculture, Forest Service, Southern Research Station, 441–447.

South, D. B. (2007). Freeze injury to roots of southern pine seedlings in the USA. *South. Hemis. For. J.* 69, 151–156. doi: 10.2989/SHFJ.2007.69.3.3.353

Sperry, J. S., and Love, D. M. (2015). What plant hydraulics can tell us about responses to climate-change droughts. *New Phytol.* 207, 14–27. doi: 10.1111/nph.13354

Stevens, K. A., Wegrzyn, J. L., Zimin, A., Puiu, D., Crepeau, M., Cardeno, C., et al. (2016). Sequence of the sugar pine megagenome. *Genetics* 204, 1613–1626. doi: 10.1534/genetics.116.193227

Stoehr, M. U., L'Hirondelle, S. J., Binder, W. D., and Webber, J. E. (1998). Parental environment aftereffects on germination, growth, and adaptive traits in selected white spruce families. *Can. J. For. Res.* 28, 418–426. doi: 10.1139/x98-012

Sundström, J., and Engström, P. (2002). Conifer reproductive development involves B-type MADS-box genes with distinct and different activities in male organ primordia. *Plant J.* 31, 161–169. doi: 10.1046/j.1365-313X.2002.01343.x

Swain, D. L., Langenbrunner, B., Neelin, J. D., and Hall, A. (2018). Increasing precipitation volatility in twenty-first-century California. *Nat. Clim. Change* 8, 427–433. doi: 10.1038/s41558-018-0140-y

Szakonyi, D., and Duque, P. (2018). Alternative splicing as a regulator of early plant development. *Front. Plant Sci.* 9:1174. doi: 10.3389/fpls.2018.01174

Thatcher, S. R., Danilevskaya, O. N., Meng, X., Beatty, M., Zastrow-Hayes, G., Harris, C., et al. (2016). Genome-wide analysis of alternative splicing during development and drought stress in maize. *Plant Physiol.* 170, 586–599. doi: 10.1104/pp.15.01267

The International HapMap Consortium (2003). The international HapMap project. *Nature* 426, 789–796. doi: 10.1038/nature02168

Threadgill, D. W., Miller, D. R., Churchill, G. A., and de Villena, F. P.-M. (2011). The collaborative cross: a recombinant inbred mouse population for the systems genetic era. *ILAR J.* 52, 24–31. doi: 10.1093/ilar.52.1.24

Tomasella, M., Häberle, K.-H., Nardini, A., Hesse, B., Machlet, A., and Matyssek, R. (2017). Post-drought hydraulic recovery is accompanied by non-structural carbohydrate depletion in the stem wood of Norway spruce saplings. *Sci. Rep.* 7:14308. doi: 10.1038/s41598-017-14645-w

Trifilò, P., Barbera, P. M., Raimondo, F., Nardini, A., and Lo Gullo, M. A. (2014). Coping with drought-induced xylem cavitation: coordination of embolism repair and ionic effects in three Mediterranean evergreens. *Tree Physiol.* 34, 109–122. doi: 10.1093/treephys/tpt119

Trifilò, P., Nardini, A., Lo Gullo, M. A., Barbera, P. M., Savi, T., and Raimondo, F. (2015). Diurnal changes in embolism rate in nine dry forest trees: relationships with species-specific xylem vulnerability, hydraulic strategy and wood traits. *Tree Physiol.* 35, 694–705. doi: 10.1093/treephys/tpv049

Trujillo-Moya, C., George, J.-P., Fluch, S., Geburek, T., Grabner, M., Karanitsch-Ackerl, S., et al. (2018). Drought sensitivity of Norway spruce at the species' warmest fringe: quantitative and molecular analysis reveals high genetic variation among and within provenances. *G3 Genes Genomes Genet.* 8, 1225–1245. doi: 10.1534/g3.117.300524

Tuskan, G. A., Groover, A. T., Schmutz, J., DiFazio, S. P., Myburg, A., Grattapaglia, D., et al. (2018). Hardwood tree genomics: unlocking woody plant biology. *Front. Plant Sci.* 9:1799. doi: 10.3389/fpls.2018.01799

Tyree, M. T., and Sperry, J. S. (1989). Vulnerability of xylem to cavitation and embolism. *Ann. Rev. Plant Physiol. Plant Mol. Biol.* 40, 19–36. doi: 10.1146/annurev.pp.40.060189.000315

Tyree, M. T., Salleo, S., Nardini, A., Lo Gullo, M. A., and Mosca, R. (1999). Refilling of embolized vessels in young stems of laurel. Do we need a new paradigm? *Plant Physiol.* 120, 11–22. doi: 10.1104/pp.120.1.11

Ulrich, D. E. M., Sevanto, S., Peterson, S., Ryan, M., and Dunbar, J. (2020). Effects of soil microbes on functional traits of loblolly pine (*Pinus taeda*) seedling families from contrasting climates. *Front. Plant Sci.* 10:1643. doi: 10.3389/fpls.2019.01643

Urban, J., Ingwers, M. W., McGuire, M. A., and Teskey, R. O. (2017). Increase in leaf temperature opens stomata and decouples net photosynthesis from stomatal conductance in *Pinus taeda* and *Populus deltoides* x *nigra*. *J. Exp. Bot.* 68, 1757–1767. doi: 10.1093/jxb/erx052

USDA Plant Hardiness Zone Map (2012). *Agricultural Research Service*. Washington, DC: USDA.

Vyse, K., Faivre, L., Romich, M., Pagter, M., Schubert, D., Hincha, D. K., et al. (2020). Transcriptional and post-transcriptional regulation and transcriptional memory of chromatin regulators in response to low temperature. *Front. Plant Sci.* 11:39. doi: 10.3389/fpls.2020.00039

Wakeley, P. C. (1944). Geographic source of loblolly pine seed. *J. For.* 42, 23–32.

Wakeley, P. C., and Bercaw, T. E. (1965). Loblolly pine provenance test at age 35. *J. For.* 63, 168–174.

Walker, T. D., Isik, F., and McKeand, S. E. (2019). Genetic variation in acoustic time of flight and drill resistance of juvenile wood in a large loblolly pine breeding population. *For. Sci.* 65, 469–482. doi: 10.1093/forsci/fxz002

Wall, J. D., and Pritchard, J. K. (2003). Assessing the performance of the haplotype block model of linkage disequilibrium. *Am. J. Hum. Genet.* 73, 502–515. doi: 10.1086/378099

Wan, T., Liu, Z.-M., Li, L.-F., Leitch, A. R., Leitch, I. J., Lohaus, R., et al. (2018). A genome for gnetophytes and early evolution of seed plants. *Nat. Plants* 4, 82–89. doi: 10.1038/s41477-017-0097-2

Ward, E. J., Domec, J.-C., Laviner, M. A., Fox, T. R., Sun, G., McNulty, S., et al. (2015). Fertilization intensifies drought stress: water use and stomatal conductance of *Pinus taeda* in a midrotation fertilization and throughfall reduction experiment. *For. Ecol. Manag.* 355, 72–82. doi: 10.1016/j.foreco.2015.04.009

Warren, R. L., Keeling, C. I., Saint Yuen, M. M., Raymond, A., Taylor, G. A., Vandervalk, B. P., et al. (2015). Improved white spruce (*Picea glauca*) genome assemblies and annotation of large gene families of conifer terpenoid and phenolic defense metabolism. *Plant J.* 83, 189–212. doi: 10.1111/tpj.12886

Wegrzyn, J. L., Liechty, J. D., Stevens, K. A., Wu, L.-S., Loopstra, C. A., Vasquez-Gross, H. A., et al. (2014). Unique features of the loblolly pine (Pinus taeda L.) megagenome revealed through sequence annotation. *Genetics* 196, 891–909. doi: 10.1534/genetics.113.159996

Wei, H., Lou, Q., Xu, K., Yan, M., Xia, H., Ma, X., et al. (2017). Alternative splicing complexity contributes to genetic improvement of drought resistance in the rice maintainer HuHan2B. *Sci. Rep.* 7:11686. doi: 10.1038/s41598-017-12020-3

Weighill, D., Jones, P., Bleker, C., Ranjan, P., Shah, M., Zhao, N., et al. (2019a). Multi-phenotype association decomposition: unraveling complex gene-phenotype relationships. *Front. Genet.* 10:417. doi: 10.3389/fgene.2019.00417

Weighill, D., Tschaplinski, T. J., Tuskan, G. A., and Jacobson, D. (2019b). Data integration in poplar: 'omics layers and integration strategies. *Front. Genet.* 10:874. doi: 10.3389/fgene.2019.00874

Weiser, C. J. (1970). Cold resistance and acclimation in woody plants. *HortScience* 5, 403–410.

Wells, O. O. (1983). Southwide pine seed source study—loblolly pine at 25 years. *South. J. Appl. For.* 7, 63–71. doi: 10.1093/sjaf/7.2.63

Wells, O. O. (1985). Use of Livingston Parish, Louisiana loblolly pine by forest products industries in the southeast. *South. J. Appl. For.* 9, 180–185. doi: 10.1093/sjaf/9.3.180

Wells, O. O., and Lambeth, C. C. (1983). Loblolly pine provenance test in southern Arkansas: 25th year results. *South. J. Appl. For.* 7, 71–75. doi: 10.1093/sjaf/7.2.71

Wells, O. O., and Wakeley, P. C. (1966). Geographic variation in survival, growth, and fusiform-rust infection of planted loblolly pine. *For. Sci. Monogr.* 11:40.

Wells, O. O., Switzer, G. L., and Schmidtling, R. C. (1991). Geographic variation in Mississippi loblolly pine and sweetgum. *Silvae Genet.* 40, 105–119.

Xiao, H., and Nassuth, A. (2006). Stress- and development-induced expression of spliced and unspliced transcripts from two highly similar dehydrin 1 genes in *V. riparia* and *V. vinifera*. *Plant Cell Rep.* 25, 968–977. doi: 10.1007/s00299-006-0151-4

Xu, P., Kong, Y., Song, D., Huang, C., Li, X., and Li, L. (2014). Conservation and functional influence of alternative splicing in wood formation of *Populus* and *Eucalyptus*. *BMC Genomics* 15:780. doi: 10.1186/1471-2164-15-780

Yang, W., Feng, H., Zhang, X., Zhang, J., Doonan, J. H., Batchelor, W. D., et al. (2020). Crop phenomics and high-throughput phenotyping: past decades, current challenges, and future perspectives. *Mol. Plant* 13, 187–214. doi: 10.1016/j.molp.2020.01.008

Yao, J., Sun, D., Cen, H., Xu, H., Weng, H., Yuan, F., et al. (2018). Phenotyping of *Arabidopsis* drought stress response using kinetic chlorophyll fluorescence and multicolor fluorescence imaging. *Front. Plant Sci.* 9:603. doi: 10.3389/fpls.2018.00603

Yoshimura, K., Saiki, S.-T., Yazaki, K., Ogasa, M. Y., Shirai, M., Nakano, T., et al. (2016). The dynamics of carbon stored in xylem sapwood to drought-induced hydraulic stress in mature trees. *Sci. Rep.* 6:24513. doi: 10.1038/srep24513

Zhang, Y., Chen, J., Miller, J., and Noland, T. (2008). Retrieving chlorophyll content in conifer needles from hyperspectral measurements. *Can. J. Remote Sens.* 34, 296–310.

Zhou, D. R., Eid, R., Miller, K. A., Boucher, E., Mandato, C. A., and Greenwood, M. T. (2019). Intracellular second messengers mediate stress inducible hormesis and programmed cell death: a review. *Biochim. Biophys. Acta Mol. Cell Res.* 1866, 773–792. doi: 10.1016/j.bbamcr.2019.01.016

Zhou, S., Duursma, R. A., Medlyn, B. E., Kelly, J. W. G., and Prentice, I. C. (2013). How should we model plant responses to drought? An analysis of stomatal and non-stomatal responses to water stress. *Agric. For. Meteorol.* 182–183, 204–214. doi: 10.1016/j.agrformet.2013.05.009

Zimin, A. V., Stevens, K. A., Crepeau, M. W., Puiu, D., Wegrzyn, J. L., Yorke, J. A., et al. (2017). An improved assembly of the loblolly pine mega-genome using long-read single-molecule sequencing. *GigaScience* 6, 1–4. doi: 10.1093/gigascience/giw016

Zimin, A., Stevens, K. A., Crepeau, M. W., Holtz-Morris, A., Koriabine, M., Marçais, G., et al. (2014). Sequencing and assembly of the 22-Gb loblolly pine genome. *Genetics* 196, 875–890. doi: 10.1534/genetics.113.159715

Zobel, B. (1955). "Drought hardy tests of loblolly pines," in *Proceedings of the 3rd Southern Forest Tree Improvement Conference*, New Orleans, 3.

Zobel, B. J., and Sprague, J. R. (1993). *A Forestry Revolution: The History of Tree Improvement in the Southern United States*. Durham: Carolina Academic Press.

Zobel, B., and Talbert, J. (1984). *Applied Forest Tree Improvement*. Caldwell NJ: The Blackburn Press.

Zwieniecki, M. A., and Holbrook, N. M. (2009). Confronting Maxwell's demon: biophysics of xylem embolism repair. *Trends Plant Sci.* 14, 530–534. doi: 10.1016/j.tplants.2009.07.002

Conflict of Interest: KP is Director of the Cooperative Tree Improvement Program at NC State University, a public-private partnership founded in 1956 that receives funding from stakeholders in the forestry sector including landowners, seed producers, seedling nurseries, and timberland management organizations.

The remaining authors declare that the research was conducted in the absence of any commercial or financial relationships that could be construed as a potential conflict of interest.

frontiers in Plant Science

ORIGINAL RESEARCH
published: 21 May 2021
doi: 10.3389/fpls.2021.575090

Floodwater Depth Causes Different Physiological Responses During Post-flooding in Willows

*Irina Mozo, María E. Rodríguez, Silvia Monteoliva and Virginia M. C. Luquez**

Instituto de Fisiología Vegetal (INFIVE), UNLP–CONICET, La Plata, Argentina

Willows are widely planted in areas under risk of flooding. The physiological responses of willows to flooding have been characterized, but little is known about their responses during the post-flooding period. After the end of the stress episode, plants may modify some traits to compensate for the biomass loss during flooding. The aim of this work was to analyze the post-flooding physiological responses of willow under two different depths of stagnant floodwater. Cuttings of *Salix matsudana* NZ692 clone were planted in pots in a greenhouse. The experiment started when the plants were 2 months old with the following treatments: Control plants (watered to field capacity); plants partially flooded 10 cm above soil level (F10) and plants partially flooded 40 cm above soil level (F40). The flooding episode lasted 35 days and was followed by a recovery period of 28 days (post-flooding period). After the flooding period, height, diameter and total biomass were higher in F10, while F40 plants showed an increase in plant adventitious root production and leaf nitrogen content. During the post-flooding period, the photosynthetic rate, nitrogen, chlorophyll and soluble sugar contents were significantly higher in leaves of F40 than in Control and F10 treatments. Stomatal conductance and specific leaf area were higher in the previously flooded plants compared to Control treatment. Plants from F10 treatments showed a higher growth in height, root-to-shoot ratio, and carbon isotope discrimination than F40, while the opposite occurred for growth in diameter, vessel size and leaf area. We conclude that depth of floodwater not only causes different responses during flooding, but that its effects are also present in the post-flooding recovery period, affecting the growth and physiology of willows once the stress episode has ended. Even when flooding impacted growth negatively in F40, in the post-flooding period these plants compensated by increasing the photosynthetic rate, plant leaf area and xylem vessel size. Willows endurance to flooding is the result of both responses during flooding, and plastic responses during post-flooding.

Keywords: ***Salix matsudana*** **Koidz, photosynthetic rate, stomatal conductance, chlorophyll, vessels**

OPEN ACCESS

Edited by:
Sanushka Naidoo,
University of Pretoria, South Africa

Reviewed by:
Keisuke Nagai,
Nagoya University, Japan
Daniel Adriaan Weits,
Sant'Anna School of Advanced Studies, Italy

***Correspondence:**
Virginia M. C. Luquez
vluquez@agro.unlp.edu.ar

Specialty section:
This article was submitted to Plant Abiotic Stress, a section of the journal Frontiers in Plant Science

Received: *22 June 2020*
Accepted: *26 April 2021*
Published: *21 May 2021*

Citation:
Mozo I, Rodríguez ME, Monteoliva S and Luquez VMC (2021) Floodwater Depth Causes Different Physiological Responses During Post-flooding in Willows. Front. Plant Sci. 12:575090. doi: 10.3389/fpls.2021.575090

INTRODUCTION

The natural habitat of willows (*Salix* spp.) is floodplain areas, and they are adapted not only to endure, but also to use periodic flooding disturbances for sexual reproduction and seed dispersal (Karrenberg et al., 2002). Being a pioneer species, they have a rapid growth, and the capability of asexual reproduction through wood cuttings facilitates the development of clonal

plantations with various aims, such as bioenergy, paper, timber, and wood panels, among others (Kuzovkina and Volk, 2009). In addition, willow plantations provide significant environment-protection services, like erosion control, wind and snow breaks, shelterbelts and phytoremediation (Kuzovkina and Volk, 2009).

Willows are widely planted in areas under risk of experiencing flooding episodes, and the occurrence of this stress is likely to increase due to climate change, in several areas of the world (Kreuzwieser and Rennenberg, 2014; Voesenek and Bailey-Serres, 2015). The main challenge flooding poses to plants is the energy crisis caused by the decrease in oxygen availability (Voesenek and Sasidharan, 2013; Fukao et al., 2019). Among the plant responses to flooding are changes in root-to-shoot ratio (Markus-Michalczyk et al., 2016); development of adventitious roots with aerenchyma (Li et al., 2006; Steffens and Rasmussen, 2016); a reduction in photosynthetic capacity because of stomatal and non-stomatal limitations (Kreuzwieser et al., 2002; Herrera et al., 2008a), changes in photosynthetic pigments, and carbon and nitrogen metabolism (Kreuzwieser et al., 2002; Voesenek and Bailey-Serres, 2015), and changes in leaf size, specific leaf area and leaf nitrogen content (Doffo et al., 2018; Rodríguez et al., 2018). In waterlogged seedlings, N uptake and photosynthesis were less affected in tolerant species (poplar and oak) and more in the flood sensitive beech (Kreuzwieser et al., 2002). In some species, flooding alters xylem hydraulic conductivity (Herrera et al., 2008b), and xylem vessel size and number (Copini et al., 2016; Doffo et al., 2017). These responses can also vary according to flooding duration, floodwater depth, if the water is stagnant or moving, and the age of the plant (Kozlowski, 1997; Glenz et al., 2006). In several flood-tolerant species, two extreme responses have been characterized: LOES (Low Oxygen Escape Syndrome) and LOQS (Low Oxygen Quiescence Syndrome, Voesenek and Bailey-Serres, 2015). LOES occurs in response to partial flooding and implies an increased growth response that keeps the plant above water. LOQS occurs when plants suffer a prolonged complete submergence, reducing metabolism to save energy (Voesenek and Bailey-Serres, 2015). These responses imply different signaling pathways, and also have different post-flooding responses (Voesenek and Bailey-Serres, 2015). When completely submerged, several trees, including willows, show an LOQS-type response (Iwanaga et al., 2015; Rodríguez et al., 2018).

The physiological responses of willows to partial flooding have been characterized (Li et al., 2004; Rodríguez et al., 2018), but little is known about their responses during the post-flooding period. After the end of the stress episode, plants may modify some traits to compensate for biomass loss during flooding. The aim of this work was to analyze the physiological responses to flooding and, mainly, post-flooding of willow under two different depths of stagnant floodwater. The hypotheses were: (1) Floodwater depth will have a differential impact during the post-flooding period on dry matter partitioning, photosynthetic activity, plant leaf area, vessel size and stem hydraulic conductivity; (2) Leaves expanded during and after flooding will have different morphological and biochemical characteristics that could affect their photosynthetic activity in the post-flooding period.

MATERIALS AND METHODS

Plant Material, Growing Conditions, and Treatments

One-year-old, 20 cm long cuttings of *Salix matsudana* NZ692 clone were planted in 5 L plastic pots with a 50:50 mixture of sand and garden soil. One cutting per pot was planted on August 4, 2017. The pots were placed in a greenhouse in the city of La Plata (34° 59′ 09″ S; 57° 59′ 42″ W), with natural photoperiod and irradiance (maximum irradiance: 2,050 mmoles m^{-2} s^{-1}). Until the start of the treatment, the pots were watered whenever necessary to keep them at field capacity. Sprouting occurred between August 29 and September 3, 2017. To avoid damage caused by insects, the plants were sprayed every 2 weeks with insecticide. Before the start of the treatment, cuttings were pruned and only one shoot per plant was kept, to minimize the variability in plant size induced by a different number of shoots per tree. The experiment started on October 23, 2017 with the following treatments: Control plants watered to field capacity (C); plants flooded 10 cm above soil level (F10), and plants flooded 40 cm above soil level (F40). There were 22 plants per treatment, arranged in a completely randomized design. Flooding for F10 treatment was induced by placing the pots with the trees into a sealed 10 L pot filled with tap water up to 10 cm above soil level; water was added when necessary to keep this level. For F40 treatment, plants were placed in 100 L plastic tanks filled with water that partially covered the plants 40 cm above soil level. The treatment lasted 35 days, after that, an intermediate sampling was carried out. The rest of the plants were taken out of flooding and watered daily to field capacity for 28 days (see the outline of the experiment in **Supplementary Figure 1**). During the post-flooding period, the plants were fertilized with 50 mL of complete Hoagland solution once a week to ensure an adequate nutrient availability.

Growth Measurements

Total shoot height (H) was measured with a graduate stick. For each plant, the height values were plotted vs. time, and a linear function was adjusted. The growth rate in height (GRH) was determined as the slope of the adjusted straight line (Rodríguez et al., 2020). The basal diameter (D) of the shoot was measured with a digital caliper, and the growth rate in diameter (GRD) was determined as described for GRH. The dry weight of leaves, stems and roots was determined after drying them at 65°C to constant weight. The total leaf area (TLA) was measured with a LICOR LI 3100 Area Meter (Lincoln, Nebraska, United States), discriminating between the area developed during the flooding and post-flooding periods. The specific leaf area (SLA) was determined as the ratio between the leaf area and the dry weight of the leaves expanded in each period (flooding and post-flooding).

Gas Exchange and Carbon Isotopic Discrimination

At the beginning of the flooding treatment, a 2 cm long leaf was tagged with typing corrector (Luquez et al., 2012). This leaf

was named L1 and completed its expansion during flooding. Similarly, another leaf was tagged at the beginning of the post-flooding treatment (L2). On these leaves, photosynthetic rate (A), stomatal conductance (gs) and transpiration (E) were measured with an IRGA CIRAS 2, during the post-flooding period. Measurements were performed between 10 and 13 h, with an irradiance of 1,500 mmoles m^{-2} s^{-1} and a CO_2 concentration of 360 ppm.

After gas exchange measurements, leaf discs were frozen for chlorophyll determination (see below) and the rest of the leaf was dried at 35°C until constant weight for carbon isotopic discrimination (Δ). To determine Δ, the leaf was grounded to powder with mortar and pestle. The determination of the carbon isotopic composition of the leaf (δC_{13leaf}) was carried out at the INGEIS Laboratory (Instituto de Geocronología y Geología Isotópica [Geochronology and Isotope Geology Institute]) (CONICET-UBA, Buenos Aires, Argentina). The carbon isotopic composition of the air (δC_{13air}) was assumed to be −8‰. Δ was calculated according to Farquhar et al. (1989):

$$\Delta = (\delta C_{13air} - \delta C_{13leaf})/(1 + (\delta C_{13leaf}/1,000))(‰)$$

Biochemical Determinations

Leaf discs from leaves L1 and L2 were stored at −80°C until measurements were performed. Chlorophyll content was determined using N,N dimethylformamide according to the methods described by Inskeep and Bloom (1985).

Sugar content was determined on fully expanded leaves that were frozen and kept at -80°C until the determinations. Insoluble and soluble reducing sugar content was determined using the Somogy Nelson method (Southgate, 1976). Frozen leaves (0.15 g) were crushed with mortar and pestle, and homogenized twice with 1 mL of 96% ethanol (v/v). The extract was centrifuged at 9,000 × g for 5 min at 4°C. The supernatant was used for analysis of soluble reducing sugars. The pellet obtained after centrifugation was hydrolyzed with 1.5 mL of 1.1% HCl at 100°C for 30 min. After cooling the suspension obtained, it was centrifuged at 9,000 × g for 5 min at 4°C and the supernatant was used to analyze insoluble sugars. After the Somogy Nelson reaction, the absorbance was measured at 520 nm. Glucose was used as standard.

Total leaf nitrogen was determined on fully expanded leaves that were dried at 60°C. The leaves were ground to powder with a hand mill and the total nitrogen content determined on 0.25 g of material according to the Kjeldahl method (Kirk, 1950).

Hydraulic Conductivity Measurements

Hydraulic conductivity was measured in four plants of each treatment at the end of the post-flooding period, as described in Doffo et al. (2017). Measurements were performed on a segment of the basal part of the main stem. The values of the hydraulic conductivity per unit stem length (kh), the specific hydraulic conductivity per unit of xylem area (ks) and the specific hydraulic conductivity per unit leaf area (kl) were calculated according to the modified Poiseuille's law (Cruiziat et al., 2002).

Anatomical Analysis

The xylem anatomical analysis was carried out on a 10 cm basal segment of the main stem, just below the segment used for hydraulic conductivity measurements. At the start and end of the flooding period, small marks were made with a scalpel on the stem to injury the cambium, in order to distinguish the xylem formed in the pre-flooding, flooding and post-flooding periods (**Figure 6D**, Grièar et al., 2007; Monteoliva et al., 2020). The entire cross-sections of stem segments were cut using a sliding microtome, then stained with safranin (1%), and photographed with a microscope (Olympus CX30, Japan) and a digital camera (Infinity, Lumenera, Canada). The captured images were analyzed for the following parameters: vessel lumen diameter (μm), vessel area (VA, μm^2), and vessel number (VN, mm^{-2}). The analysis was performed with the image analysis software ImagePro Plus v.6.3 (Media Cybernetics, United States). The vessel's lumen fraction (LM) was estimated as the product between vessel area and number for each period, and was expressed as the percentage of the total stem area of the plant.

To determine stomatal density, a fully expanded leaf was fixed in FAA (formaldehyde alcohol acetic acid 10:50:5%). The leaves were cleared for the observation of stomata, placing them for 3 days in a 50:50 mix of 5% sodium hydroxide and 5% commercial bleach. Once decolored, the material was cleaned with distilled water and kept for 48 h in a 5% chloralhydrate solution. After that, the leaves were cleaned with distilled water, stained with 1% safranin and mounted in gelatin-glycerin for observation (Arambarri, 2018). To determine stomatal density, ten fields per sample were counted at 400×.

The material for the anatomical analysis of adventitious roots and hypertrophied lenticels was fixed in FAA. Afterward, the samples were dehydrated in an alcoholic series to absolute alcohol and acetone. Samples were included in Epoxi resin for 36 h under mild vacuum at 35, 50, and 60°C to allow polymerization. The thin sections were stained with toluidine blue and photographed at 10×.

Statistical Analysis

The data were analyzed with a one-way ANOVA followed with a *post-hoc* mean comparison with the Tukey test ($p < 0.05$).

RESULTS

Flooding triggered the formation of hypertrophied lenticels (**Figures 1A,B,C** and **Supplementary Figure 2**) and adventitious roots (**Figures 1B,C,E**) in the stem parts covered by water. After 4 days of flooding, plants of both flooding treatments (F10 and F40) started to develop hypertrophied lenticels (**Figures 1B,C** and **Supplementary Figure 2A**). After 7 days of flooding, adventitious roots appeared in both flooding treatments (**Figures 1B,C,2A** and **Supplementary Figure 2A**). The adventitious roots developed in the stems under water; in consequence we called them aquatic roots. The aquatic roots had aerenchyma in both F10 and F40 (**Figures 1D,E**). At the end of the 35-day flooding period, the development of aquatic roots was profuse in F40, representing 42% of the total root

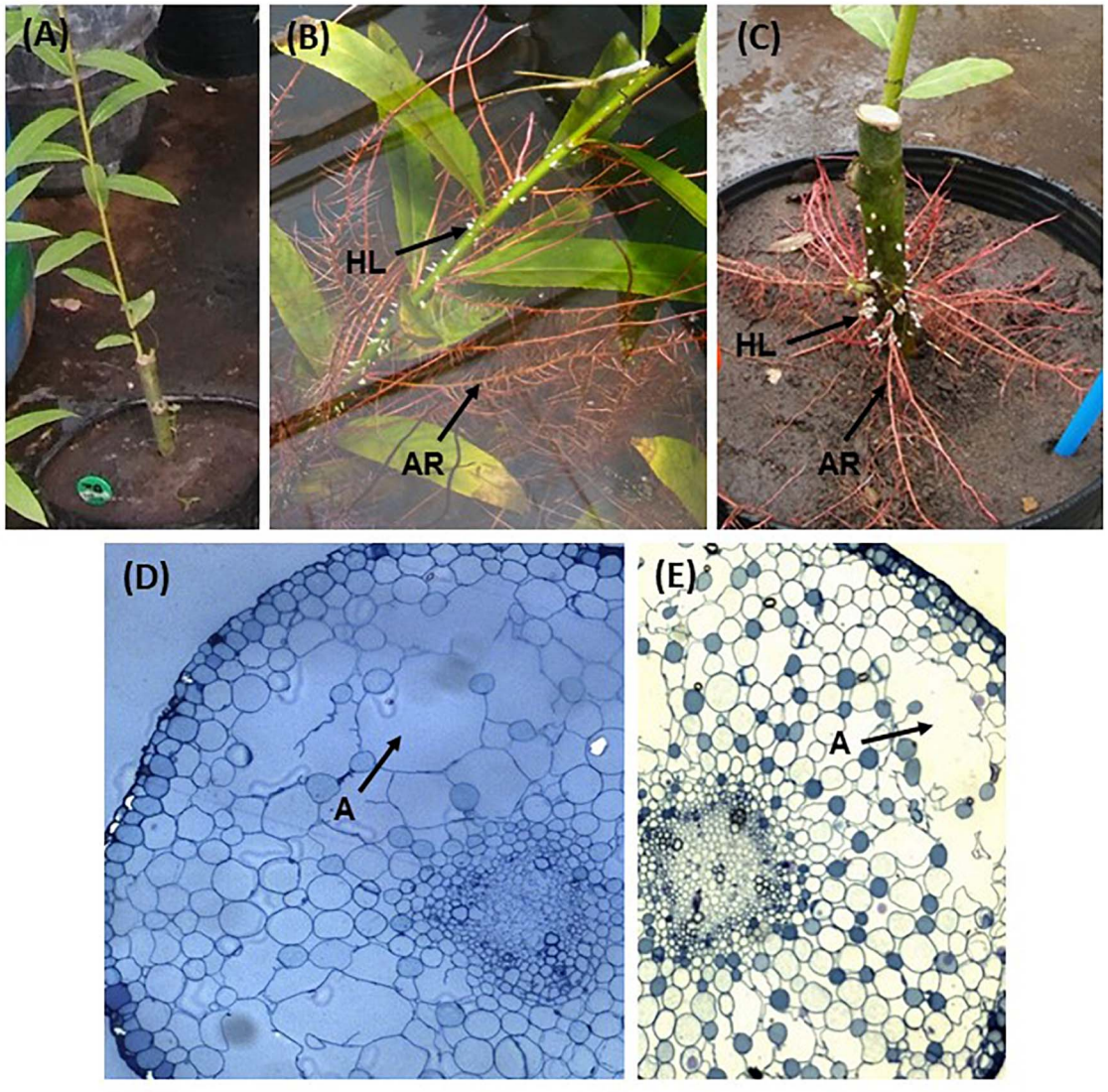

FIGURE 1 | View of the stem of a control plant, without development of hypertrophied lenticels or adventitious roots **(A)**; hypertrophied lenticels (HL) and aquatic roots (AR) in plants of F40 treatment **(B)**; aquatic roots and lenticels outside water in a plant from F10 treatment **(C)**; a transversal view of F40 aquatic roots (**D**, 10×); and a transversal view of an aquatic root in F10 (**E**, 10×). **(A)** aerenchyma lacunae.

biomass. After the flooding period ended, the aquatic roots dried up (**Figures 2A,B**).

At the end of the flooding period (Day 35, **Figure 2C**), F10 plants had a higher total biomass than F40 plants. The difference was due to the increase in shoot biomass (stem plus leaves). For the same reason, the root-to-shoot ratio was significantly lower in F10 compared to Control (C) and F40 treatments. The treatments showed no differences in root biomass as the result of extensive development of aquatic roots in both F10 and F40. The root-to-shoot ratio in both F10 and F40 was calculated including the aquatic root biomass.

At the end of the post-flooding period (Day 63), the treatments showed no differences in the total biomass (**Figure 2C**). However, there were statistically significant differences in root-to-shoot ratio, being significantly lower in F40 than in F10, and in both previously flooded plants compared to Control. The main reason is that root biomass in F40 was significantly lower than in Control plants. The reduction of root biomass in the previously flooded plants (especially F40) was due to the death of the aquatic roots immediately after the end of flooding (**Figure 2B**).

The height and diameter growth were differently affected in the two flooding treatments. At the end of the flooding period (Day 35), F10 showed both a significantly higher height and diameter than Control and F40 (**Figures 3A,C**, respectively). On the same day, F40 had lower values for diameter compared to Control and F10 treatments (**Figure 3C**, day 35). The growth rate in height (GRH) was significantly higher in F10 compared to Control, while F40 did not differ from the other treatments

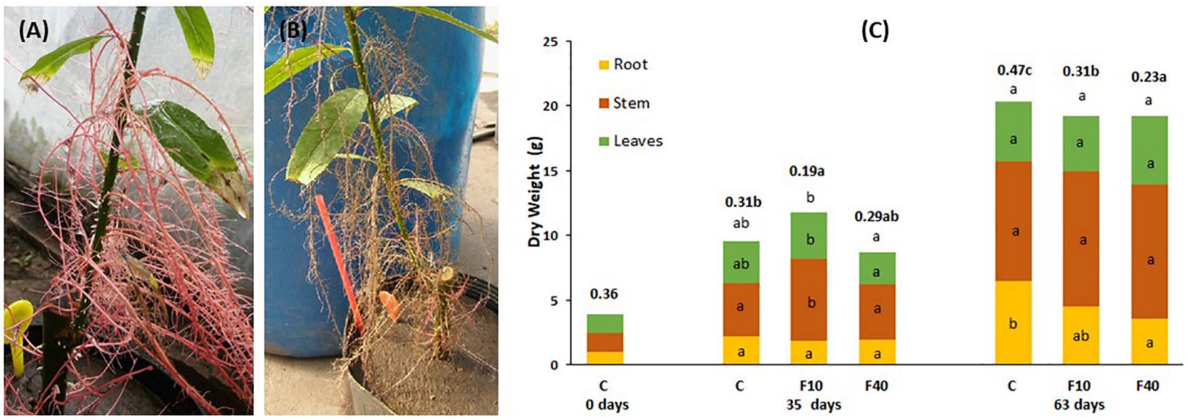

FIGURE 2 | Aquatic roots of a F40 plant immediately after taken out of water **(A)** and 24 h later **(B)**. **(C)** Dry matter partitioning and root-to-shoot ratio (in bold, above the bars) at the beginning of the experiment (day 0), at the end of the flooding period (35 days), and at the end of the post-flooding recovery period (63 days). Means followed by the same letter did not differ according to Tukey's test ($p < 0.05$, $N = 5$). The letters indicate significant differences for each compartment, total biomass (above the bar) and root-to-shoot ratio (next to this value, in bold).

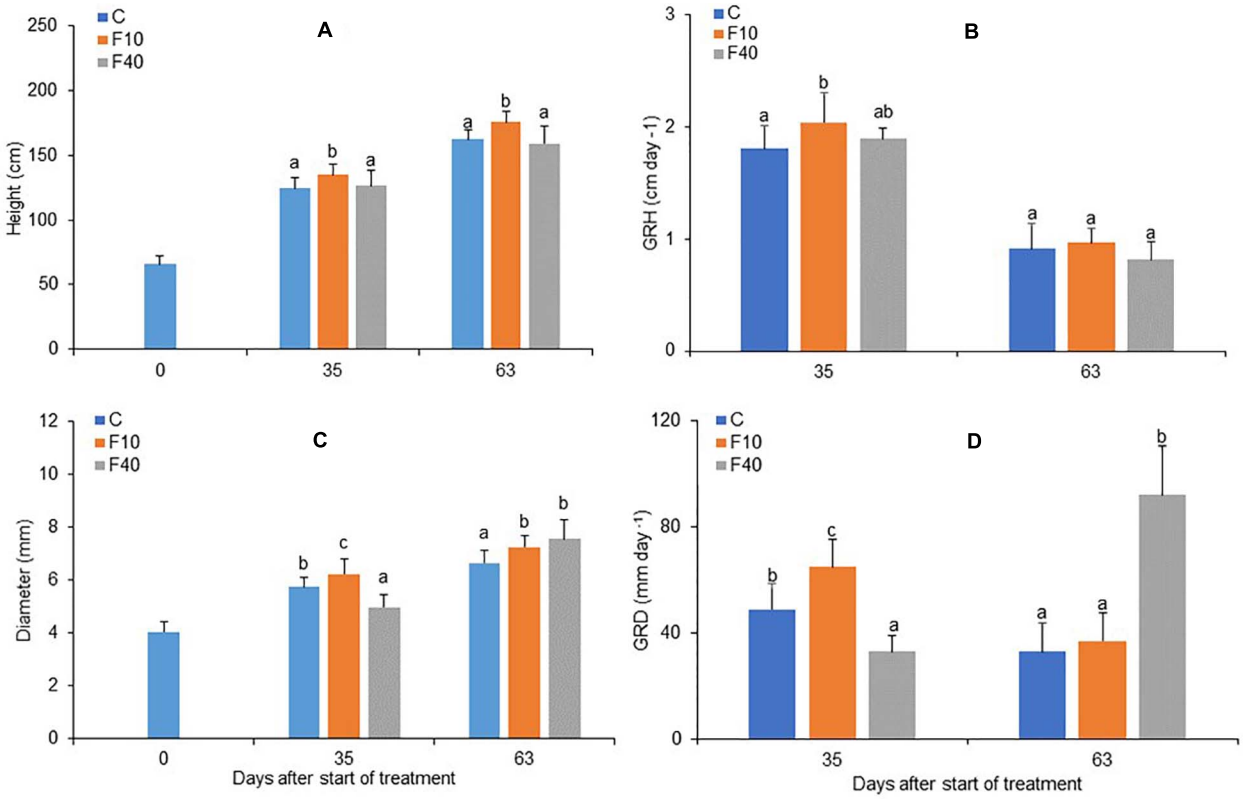

FIGURE 3 | Height **(A)**, growth rate in height **(B)**, diameter **(C)** and growth rate in diameter (**D**, multiplied by 10^3) for Control, F10 and F40 treatments at the beginning of the experiment (Day 0), at the end of the flooding period (Day 35), and at the end of the post-flooding recovery period (Day 63). Growth rates were calculated for the whole flooding and post-flooding periods. Means followed by the same letter did not differ according to Tukey's test ($p < 0.05$, $N = 12$–22). Vertical bar: standard deviation.

(**Figure 3B**, day 35). The growth rate in diameter (GRD) differed significantly among treatments, F40 had the lowest rate, while F10 had the highest (**Figure 3D**, day 35).

At the end of the post-flooding period (Day 63), F10 featured a higher height than Control plants, while F40 did not differ in height from Control (**Figure 3A**). The diameter was higher in

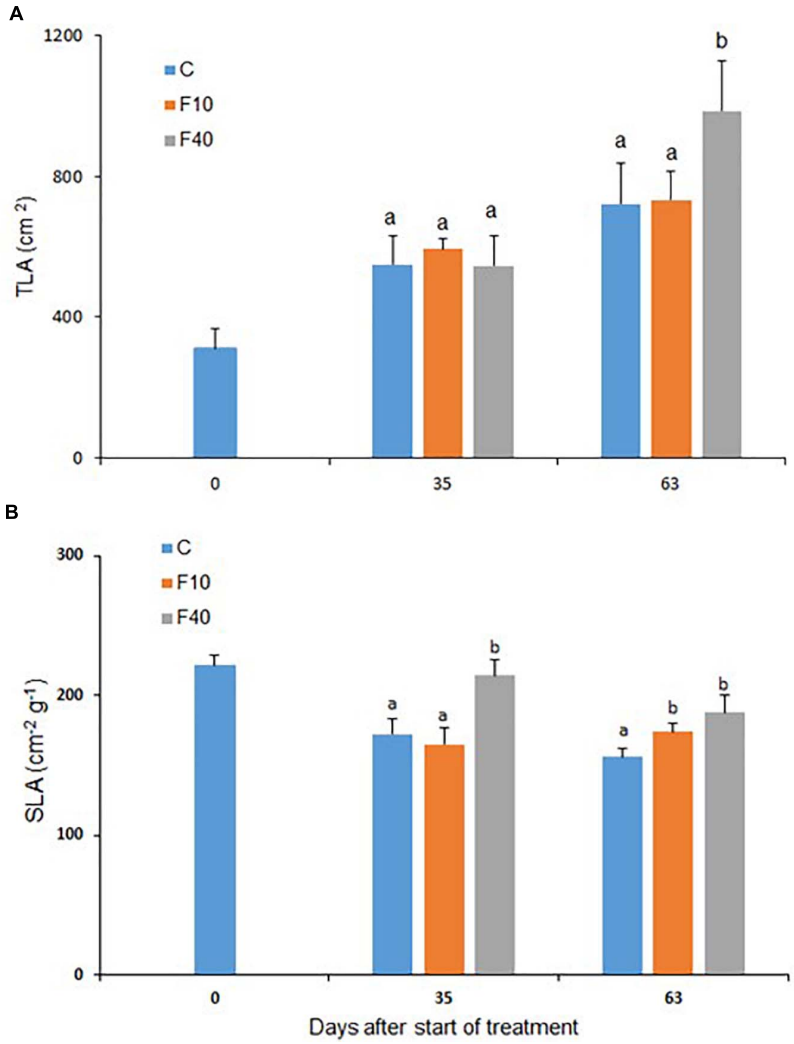

FIGURE 4 | Total leaf area **(A)** and specific leaf area **(B)** for C (Control), F10, and F40 treatments at the beginning of the experiment (Day 0), at the end of the flooding period (Day 35), and at the end of the post-flooding recovery period (Day 63). Means followed by the same letter did not differ according to Tukey's test ($p < 0.05$, $N = 4–8$). Vertical bar: standard deviation.

F10 and F40 than in Control plants, but there were no differences between the previously flooded treatments (**Figure 3B**, day 63). GRH did not differ between the treatments in the post-flooding period (**Figure 3C**, day 63), while GRD was significantly higher in F40 compared to Control and F10 plants (**Figure 3D**, day 63).

The total leaf area (TLA, **Figure 4A**) did not differ between the treatments at the end of the flooding period (Day 35), but after the post-flooding period (Day 63), TLA was significantly higher in F40 than in the other treatments.

The specific leaf area (SLA, **Figure 4B**) on Day 35 was higher in F40 when compared to Control and F10. At the end of the post-flooding period, SLA was significantly higher in both F10 and F40 compared to Control plants.

The stomatal density did not change significantly in the abaxial surface during flooding and post-flooding periods (**Table 1**). At the end of the flooding period (Day 35, **Table 1**) the stomatal density in the adaxial surface was significantly higher in F40 than in F10. At the end of the post-flooding period (Day 63), there were no differences between the treatments for the stomatal density on any leaf surface.

After 35 days of flooding, there were no differences in soluble or insoluble sugar contents of leaves in all treatments (**Figure 5A** and **Supplementary Figure 3**). However, at the end of the post-flooding period, soluble sugars content was significantly higher in the F40 plants when compared to the F10. The Leaf Nitrogen content (**Figure 5B**) was significantly higher in F40 than in control and F10 plants after the end of both flooding and post-flooding periods.

The leaves L1 (expanded during flooding) and L2 (expanded in the post-flooding period) were measured during the post-flooding period (**Table 2**). For L1, the photosynthetic rate (A) was significantly higher in F40 compared to control and F10. For L2,

TABLE 1 | Stomatal density (stomata per mm^{-2}) in fully expanded willow leaves during flooding (Day 35) and post-flooding periods (Day 63).

Treatment	Day 35 (flooding)		Day 63 (post-flooding)	
	Abaxial side	*Adaxial side*	*Abaxial side*	*Adaxial side*
Control	326 (14) a	105 (11) ab	266 (34) a	91 (6) a
F10	320 (12) a	94 (10) a	313 (35) a	111 (16) a
F40	382 (91) a	166 (42) b	334 (56) a	97 (11) a

Days are counted after the start of the flooding treatment. Means followed by the same letter did not differ according to Tukey's test ($p < 0.05$, $N = 3$). Between parenthesis: standard deviation.

A was higher F40 compared to control, but it did not differ from F10. The plant photosynthetic activity was significantly higher in F40 compared to Control and F10 plants (**Supplementary Figure 5**). The stomatal conductance (gs) was significantly higher in F40 and F10 for L1. For L2, gs was significantly higher in F40 than Control plants, while F10 did not differ from the other treatments.

Carbon isotope discrimination (D) was significantly higher for F10 compared to Control in both L1 and L2. F40 did not differ from the other treatments in L1, while for L2 was similar to control and lower than F10.

Chlorophyll content was significantly higher in F40 for both leaves, for chlorophyll a, chlorophyll b, and total chlorophyll. The chlorophyll a/b ratio did not change in any treatment (data not shown).

The results for xylem vessels diameter and area were similar, in consequence only area data are shown. The vessel area (**Figure 6A**, Flooding) did not differ between the treatments at the end of the flooding episode. The vessel number was significantly lower in F40 compared to Control plants, while it did no differ in F10 (**Figure 6B**, Flooding). In the post-flooding period, F40 produced vessels with a larger area than Control plants, while F10 did not differ from Control and F40 (**Figure 6A** Post-flooding). The average for all periods (Total) largely reflects the results of the post-flooding period. The number of vessels (**Figure 6B**) did not differ between Control and F10 plants for any period, while in F40, this trait was significantly lower than in Control plants. We also estimated the lumen fraction (LF, percentage that the vessel lumen area represents of the total stem area, **Figure 6C**). The percentage of vessels formed during the flooding period was similar in Control and F10 plants, while it was significantly lower in F40. During post-flooding it was the

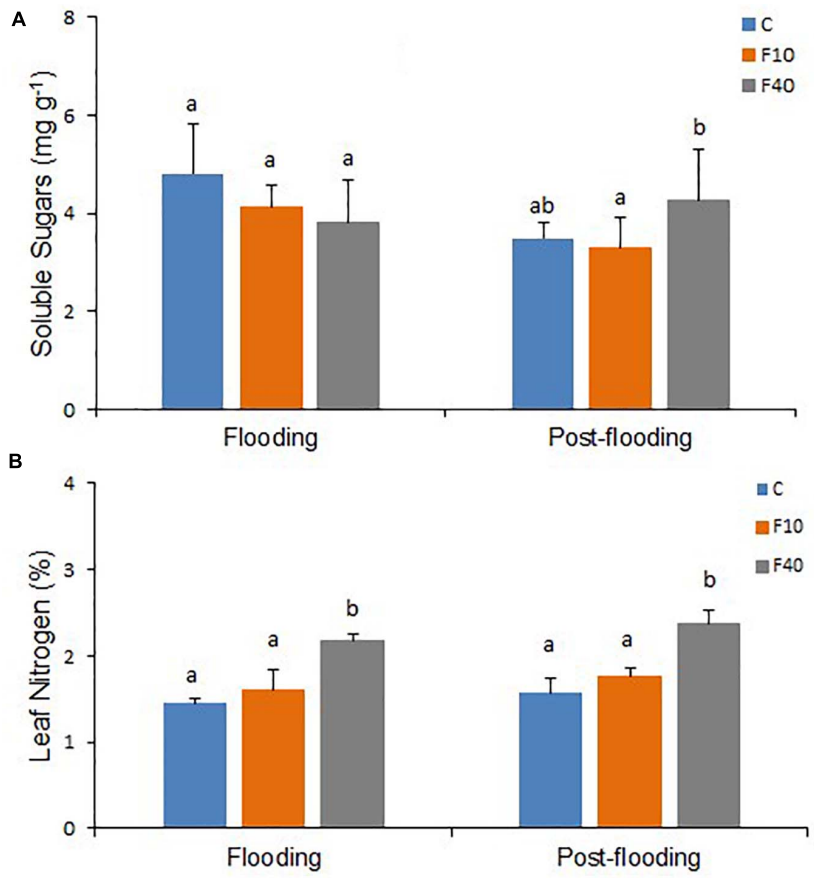

FIGURE 5 | Soluble sugars content (**A**, $N = 5$) and nitrogen content (N, **B**, $N = 3$) on fully expanded leaves after 35 days of flooding, and at the end of the post-flooding recovery period (Day 63). Means followed by the same letter did not differ according to Tukey's test ($p < 0.05$). Vertical bar: standard deviation.

TABLE 2 | Gas exchange and biochemical traits in a leaf expanded during flooding (L1) and a leaf expanded during post-flooding (L2).

Variable	Units	Treatment	L1	L2
Photosynthetic Rate (A)	μmol CO_2 m^{-2} s^{-1}	Control	17.2 (0.4) a	12.7 (3.5) a
		F10	18.2 (2.3) a	18.1 (2.5) ab
		F40	24.7 (3.6) b	20.7 (4) b
Stomatal Conductance (gs)	mmol H_2O m^{-2} s^{-1}	Control	356 (67) a	112 (53) a
		F10	517 (40) b	275 (95) ab
		F40	504 (107) b	315 (139) b
Carbon isotope Discrimination (Δ)	‰	Control	23.1 (0.5) a	22.9 (0.4) a
		F10	23.9 (0.6) b	23.9 (0.4) b
		F40	23.3 (0.5) ab	22.6 (0.6) a
Chlorophyll a	μg cm^{-2}	Control	8.5 (1.5) a	9.6 (0.3) a
		F10	8.7 (1.1) a	9.0 (1) a
		F40	14.4 (2.4) b	15.2 (0.7) b
Chlorophyll b	μg cm^{-2}	Control	2.6 (0.5) a	2.2 (0.4) a
		F10	2.6 (0.4) a	1.9 (0.3) a
		F40	4.4 (0.7) b	3.8 (0.3) b
Total Chlorophyll	μg cm^{-2}	Control	11.2 (2) a	11.72 (0.6) a
		F10	11.3 (1.4) a	10.8 (1.3) a
		F40	18.7 (3.2) b	19 (0.9) b

Determinations were carried out during post-flooding. Means followed by the same letter did not differ significantly according to Tukey's test ($p < 0.05$, $N = 5$). Between parenthesis: standard deviation.

opposite: LF was significantly higher in F40. Taking together all periods (Total), there were no significant differences in LF between the treatments.

The hydraulic conductivity was measured per unit stem length (kh), per unit xylem area (ks) and per unit leaf area (kl) at the end of the post-flooding period (Day 63, **Supplementary Figure 4**). There were no statistically significant differences between the treatments for any of the measurements.

DISCUSSION

Growth Responses to Floodwater Depth

The two flooding treatments had contrasting growth responses, not only during flooding, but also in the post-flooding period. During flooding, leaf area, biomass accumulation, height, diameter and diameter growth rate were higher in F10 than in F40. These results are similar to previous findings that, in willows, the flooding of the root system does not cause significant differences in biomass with control plants (Li et al., 2006; Rodríguez et al., 2018). The results are consistent with previous data that an increased floodwater depth enhances growth reduction (Iwanaga and Yamamoto, 2008; Markus-Michalczyk et al., 2016; Rodríguez et al., 2018). Moreover, during flooding, there was a sharp contrast in dry matter partitioning between the treatments. F10 had a higher total biomass and a lower root-to-shoot ratio than F40. While F10 behavior resembles a LOES escape strategy increasing height growth to avoid submergence (Voesenek and Bailey-Serres, 2015), F40 was neither LOES nor LOQS. Clearly, F40 plants had a reduced growth, but not a quiescent response. On the other hand, both treatments developed hypertrophied lenticels, adventitious roots, and aerenchyma, to enhance ventilation of the submerged organs to avoid the energetic crisis caused by oxygen shortage (Fukao et al., 2019).

In the post-flooding period, several responses were the exact opposite to those during flooding. Most growth variables were higher or similar in F40; while height was significantly lower in F40 than in F10. A possible explanation could be that in the immediate aftermath of flooding, all aquatic roots in F40 dried down (**Figure 2B**), dramatically reducing the root-to-shoot ratio. At the end of the post-flooding period the root-to-shoot ratio was still significantly lower in F40 compared with Control and F10 plants. It is likely that, in the post-flooding period, F40 plants were investing resources in developing new roots to compensate for the losses, instead of increasing the growth in height. This is not only evident in roots, as F40 plants had a higher leaf area and GRD. Clearly, there was a different assignation of growth resources for F10 and F40 in the post-flooding period.

Development of Vessels and Hydraulic Conductivity

Xylem hydraulic conductivity, and vessels number and size are plastic traits regarding flooding. Herrera et al. (2008b) reported that hydraulic conductivity was reduced in early stages of flooding, but increased later with the development of adventitious roots in tropical flood-tolerant tree species. Partial flooding reduced vessel size in stems of *Quercus robur* (Copini et al., 2016) and in two willow genotypes (Doffo et al., 2017).

We found a sharp contrast in the development of xylem vessels in both treatments. During flooding, F40 produced less vessels of similar area than the Control treatment. In the post-flooding period, it was exactly the opposite: F40 produced fewer vessels with a higher area than Control plants. If we consider

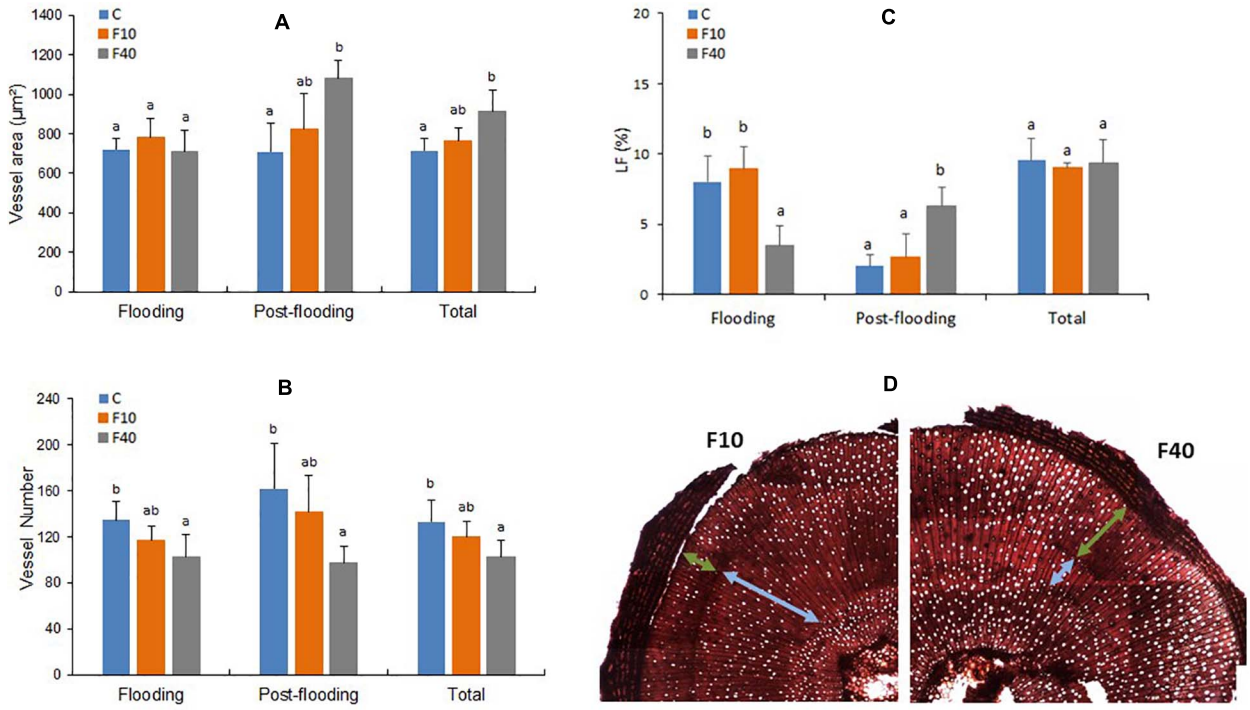

FIGURE 6 | Vessel area **(A)**, vessel number **(B)**, percentage of vessel lumen fraction of the stem (LF, **C**), transversal cut of the stem with light blue arrows indicating the vessels developed during flooding, and green arrows indicating the vessels formed during post-flooding **(D)**. Total refers to the average values of all vessels in the stem (formed during pre-flooding, flooding and post-flooding). Means followed by the same letter did not differ according to Tukey's test ($p < 0.05$, $N = 5$). Vertical bar: standard deviation.

Flooding F10	Flooding F40	Trait	Post-Flooding F10	Post-Flooding F40
		Height		
		Diameter		
		Growth Rate in Diameter		
		Root to Shoot Ratio		
		Total Biomass		
		Plant Leaf Area		
		Vessel Lumen fraction		
		Leaf Nitrogen		
		Leaf Soluble Sugars		
		Specific Leaf Area		
ND	ND	Leaf Chlorophyll*		
ND	ND	Leaf Photosynthetic Rate*		
ND	ND	Carbon Isotopic Discrimination*		

FIGURE 7 | Comparison between the flooding and post-flooding responses among the treatments F10 (plants flooded 10 cm above soil level) and F40 (plants flooded 40 cm above soil level). The change of size of the bars indicates whether a trait increased or diminished compared to the other flooding treatment. Bars of similar size indicates no significant differences between the flooding treatments. The symbol "*" represents an average of L1 and L2 leaves.

the fraction of the lumen area (i.e., the actual water conducting area of the stem), the conducting area was mostly produced during flooding in the plants of Control and F10, but during post-flooding in F40. The plants from F40 compensated the reduction in conducting area producing few bigger vessels in the post-flooding period. Eventually, lumen area was similar in all treatments, which explains the similar values of xylem hydraulic conductivity observed in them (**Supplementary Figure 4**). The increase in vessels size and stem diameter may be associated with the need to increase water transport to supply the higher leaf area developed by F40 in the post-flooding period.

These results are similar to those described for *Quercus robur* (Copini et al., 2016), where flooding reduced early wood vessels size in the submerged parts of the stem (as LF in F40) but not in the non-submerged parts (as LF in Control and F10 plants). This comparison should be considered with caution for the anatomical differences between the two species. Oaks are ring porous species, with big early wood vessels that account for an increased hydraulic conductivity in early season, while willows are diffuse porous species, producing vessels of similar size throughout the growing season (Crang et al., 2018). Anyway, it is interesting to note that flooding of the stem seems to induce the same response in oaks and willows, in spite of the anatomical and functional seasonal differences in the xylem between the two species. The results for F10 are different from the reported in Doffo et al. (2017), where 2 willow genotypes flooded 10 cm above soil level for 45 days had a lower vessel area than Control plants. These differences could be due to the different length of the flooding period, or caused by genetic factors since the genotypes used in that work were different (*S. alba* and a *S. matsudana* × *S. alba* hybrid).

Flooding Depth Effects on Photosynthetic Activity and Other Related Leaf Traits

The acclimation responses to flooding of the photosynthetic machinery are already known. For instance, gray poplar and oak decreased their photosynthetic rate and increased leaf protein content under root flooding, but the chlorophyll content remained unchanged (Kreuzwieser et al., 2002). In several tropical species that acclimate to long-term flooding, there was an increase in leaf protein and chlorophyll content (Herrera, 2014). In some willow genotypes, flooding increased specific leaf area and nitrogen content of leaves, but others did not (Rodríguez et al., 2018). In consequence, we were interested in exploring how changes caused by flooding on leaves affected the photosynthetic responses during post-flooding. The leaves that developed during flooding may have different morphological and biochemical traits that may affect their photosynthetic activity. For this reason, we tagged and compared leaves expanded during flooding and post-flooding periods. The photosynthetic rate was higher in leaves that developed during flooding and post-flooding in F40, when compared to Control treatment. This may partly be the result of an increase in leaves nitrogen content during flooding that persisted into the post-flooding period. More nitrogen implied higher chlorophyll content (and likely leaf protein as well), these traits had shown a strong positive correlation with photosynthesis in a set of 11 willow genotypes (Andralojc et al., 2014). The higher photosynthetic rate in F40 plants may also be the result of an enhanced stomatal conductance. Stomatal conductance increased in F10 plants, and this is likely the reason of the increase in carbon isotopic discrimination, and the decrease in water use efficiency for this treatment. The higher stomatal conductance in previously flooded plants could not be totally accounted for by an increased stomatal density, because the differences between treatments were not always statistically significant. The chlorophyll a/b ratio did not change during flooding or post-flooding periods (data not shown); these results were different from flooded poplar and beech where the ratio increased (Kreuzwieser et al., 2002). During flooding, the deeper flooded plants increased specific leaf area and leaf nitrogen, as described before (Rodríguez et al., 2018), and this higher content was maintained during the post-flooding period for the genotype we used in this study.

Consistently with the higher photosynthetic activity, the F40 leaves showed higher soluble sugar content, but did not increased the non-soluble (starch) sugars. Starch accumulation in leaves has been related to the inhibition of photosynthesis (Rengifo et al., 2005; Andralojc et al., 2014) and clearly this is not the case in previously flooded F40 plants. This scenario is consistent with these leaves producing and exporting more photosynthates to other organs.

Different Responses to Floodwater Depth During Flooding and Post-flooding in Willows

The differences in flooding and post-flooding responses between F10 and F40 treatments are summarized in **Figure 7**. The F40 plants experienced growth reduction in height, diameter and biomass during flooding, but they showed an increased compensatory growth in diameter during post-flooding. This extra growth was sustained by the increased photosynthetic activity, very likely due to higher leaf chlorophyll, nitrogen and stomatal conductance. F40 plants had higher photosynthesis per plant, because they increased leaf area development during post-flooding (**Supplementary Figure 5**). The bigger leaf area is sustained by an increased stem growth in diameter, and the development of xylem vessels with a greater area to compensate for the diminished vessel lumen fraction during flooding. In summary, the plants under deeper floodwater experienced higher growth reduction than the shallow flooded plants, but they showed compensatory responses during post-flooding that made up for the previous losses. Even when plants are only partially flooded, floodwater depth induced different physiological responses that persisted after the end of the flooding episode. In this sense, willow responses are different from *Populus deltoides*, where partial flooding led to a plant leaf area increase in the post-flooding period, but without an increment of the photosynthetic activity per leaf area (Rodríguez et al., 2015). The plastic responses of willow after the stress episode are similar to the growth compensatory responses of young trees of other pioneer riparian species, *Populus fremontii*, *Tamarix ramosisiima,* and *Acer negundo*

(Kui and Stella, 2016). For instance, seedlings that survived partial sediment burial increased their growth in the following season (Kui and Stella, 2016).

CONCLUSION AND PERSPECTIVES

Our first hypothesis was confirmed, since the physiological responses varied during post-flooding according to floodwater depth. Once the flooding episode ended, the deep flooded plants (F40) compensate the greater growth reduction compared with the shallow flooded treatment (F10) by increasing photosynthetic activity, leaf area and xylem lumen fraction in the post-flooding period.

The second hypothesis was also accepted as morphological and biochemical differences were observed between the leaves expanded during and after the flooding episode.

Our results underscore the fact that flooding tolerance of willows is not only caused by the responses during the occurrence of the stress, but also by the compensatory photosynthetic rate and differential growth of organs during post-flooding. Willow resilience is determined by their plasticity to respond to the challenges during the post-flooding period, in addition to what happens during the stress period itself.

DATA AVAILABILITY STATEMENT

The raw data supporting the conclusions of this article will be made available by the authors, without undue reservation.

AUTHOR CONTRIBUTIONS

IM did most experimental work and the statistics. MR collaborated on the experimental work. SM performed the xylem anatomical study and planned the experimental work. VL planned the experiment and wrote the manuscript. All the authors have read and approved the manuscript.

FUNDING

This work was funded by a PUE CONICET 2016 for INFIVE, and grant A343 from UNLP to VL.

ACKNOWLEDGMENTS

We thanks to M. Bartolozzi, S. Martínez Alonso, and L. Wahnan for their technical assistance, to L. Costa for giving advice on biochemical measurements, and to T. Cerrillo for providing the plant material. VL and SM are researchers from CONICET. IM and MR held fellowship from CONICET.

SUPPLEMENTARY MATERIAL

The Supplementary Material for this article can be found online at: https://www.frontiersin.org/articles/10.3389/fpls.2021.575090/full#supplementary-material

REFERENCES

Andralojc, P. J., Bencze, S., Madgwick, P. J., Philippe, H., Powers, S. J., Shield, I., et al. (2014). Photosynthesis and growth in diverse willow genotypes. *Food Energy Secur.* 3, 69–85. doi: 10.1002/fes3.47

Arambarri, A. M. (2018). La "técnica de clarificación 5-5-5", un método natural para el tratamiento de material vegetal. *Bol. Soc. Argent. Bot.* 53, 579–586. doi: 10.31055/1851.2372.v53.n4.21980

Copini, P., den Ouden, J., Robert, E., Tardif, J. C., Loesberg, W., Goudzwaard, L., et al. (2016). Flood-ring formation and root development in response to experimental flooding in young *Quercus robur* trees. *Front. Plant Sci.* 7:775. doi: 10.3389/fpls.2016.00775

Crang, R., Lyons-Sobaski, S., and Wise, R. (2018). *Plant Anatomy*. Cham: Springer.

Cruiziat, P., Cochard, H., and Améglio, T. (2002). Hydraulic architecture of trees: main concepts and results. *Ann. For. Sci.* 59, 723–752.

Doffo, G., Monteoliva, S., Rodríguez, M. E., and Luquez, V. M. C. (2017). Physiological responses to alternative flooding and drought stress episodes in two willow (*Salix* spp.) clones. *Can. J. For. Res.* 47, 174–182. doi: 10.1139/cjfr-2016-0202

Doffo, G., Rodríguez, M. E., Olguín, F., Cerrillo, T., and Luquez, V. M. C. (2018). Resilience of willows (*Salix* spp.) differs between families during and after flooding according to floodwater depth. *Trees* 32, 1779–1788. doi: 10.1007/s00468-018-1751-7

Farquhar, G. D., Ehleringer, J. R., and Hubick, K. T. (1989). Carbon isotope discrimination and photosynthesis. *Ann. Rev. Plant Physiol. Plant Mol. Biol.* 40, 503–537.

Fukao, T., Barrera-Figueroa, B. E., Juntawong, P., and Peña-Castro, J. M. (2019). Submergence and waterlogging stress in plants: a review highlighting research opportunities and understudied aspects. *Front. Plant Sci.* 10:340. doi: 10.3389/fpls.2019.00340

Glenz, C., Schlaepfer, R., Iorgulescu, I., and Kienast, F. (2006). Flooding tolerance of Central European tree and shrub species. *For. Ecol. Manag.* 235, 1–13. doi: 10.1016/j.foreco.2006.05.065

Grièar, J., Zupancic, M., Èufar, K., and Oven, P. (2007). Wood formation in Norway spruce -*Picea abies*- studied by pinning and intact tissue sampling method. *Wood Res.* 52, 1–9.

Herrera, A. (2014). Responses to flooding of plant water relations and leaf gas exchange in tropical tolerant trees of a black-water wetland. *Front. Plant Sci.* 4:106. doi: 10.3389/fpls.2013.00106

Herrera, A., Tezara, W., Marín, O., and Rengifo, E. (2008a). Stomatal and non-stomatal limitations of photosynthesis in trees of a tropical seasonally flooded forest. *Physiol. Plant.* 134, 41–48. doi: 10.1111/j.1399-3054.2008.01099.x

Herrera, A., Tezara, W., Rengifo, E., and Flores, S. (2008b). Changes with seasonal flooding in sap flow of the tropical flood-tolerant tree species, *Campsiandra laurifolia*. *Trees* 22, 551–558. doi: 10.1007/s00468-008-0215-x

Inskeep, W. P., and Bloom, P. R. (1985). Extinction coefficients of chlorophyll a and b in N,N-dimethylformamide and 80% acetone. *Plant Physiol.* 77, 483–485.

Iwanaga, F., Tanaka, K., Nakazato, I., and Yamamoto, F. (2015). Effects of submergence on growth and survival of saplings of three wetland trees differing in adaptive mechanisms for flood tolerance. *For. Syst.* 24:e001. doi: 10.5424/fs/2015241-03010

Iwanaga, F., and Yamamoto, F. (2008). Effects of flooding depth on growth, morphology and photosynthesis in *Alnus japonica* species. *New For.* 35, 1–14. doi: 10.1007/s11056-007-9057-4

Karrenberg, S., Edwards, P. J., and Kollmann, J. (2002). The life history of salicaceae living in the active zone of floodplains. *Freshw. Biol.* 47, 733–748.

Kirk, P. L. (1950). Kjeldahl method for total nitrogen. *Anal. Chem.* 22, 354–358. doi: 10.1021/ac60038a038

Kozlowski, T. T. (1997). Responses of woody plants to flooding and salinity. *Tree Physiol.* 17:490. doi: 10.1093/treephys/17.7.490

Kreuzwieser, J., Fürniss, D., and Rennenberg, H. (2002). Impact of waterlogging on the N-metabolism of flood tolerant and non-tolerant tree species. *Plant Cell Environ.* 25, 1039–1049.

Kreuzwieser, J., and Rennenberg, H. (2014). Molecular and physiological responses of trees to waterlogging stress. *Plant Cell Environ.* 37, 2245–2259. doi: 10.1111/pce.12310

Kui, L., and Stella, J. C. (2016). Fluvial sediment burial increases mortality of young riparian trees but induces compensatory growth response in survivors. *For. Ecol. Manag.* 366, 32–40. doi: 10.1016/j.foreco.2016.02.001

Kuzovkina, Y., and Volk, T. A. (2009). The characterization of willow (*Salix* L.) varieties for use in ecological engineering applications: co-ordination of structure, function and autecology. *Ecol. Eng.* 35, 1178–1189. doi: 10.1016/j.ecoleng.2009.03.010

Li, S., Pezeshki, S. R., Goodwin, S., and Shields, F. D. (2004). Physiological responses of black willow (*Salix nigra*) cuttings to a range of soil moisture regimes. *Photosynthetica* 42, 585–590. doi: 10.1007/S11099-005-0017-y

Li, S., Pezeshki, S. R., and Shields, F. D. Jr. (2006). Partial flooding enhances aeration in adventitious roots of black willow (*Salix nigra*) cuttings. *J. Plant Physiol.* 163, 619–628. doi: 10.1016/j.jplph.2005.06.010

Luquez, V. M. C., Achinelli, F., and Cortizo, S. (2012). Evaluation of flooding tolerance in cuttings of *Populus* clones used for forestation at the Paraná River Delta, Argentina. *South For.* 74, 61–70. doi: 10.2989/20702620.2012.686214

Markus-Michalczyk, H., Hanelt, D., and Jensen, K. (2016). Effects of tidal flooding on juvenile willows. *Estuaries Coast.* 39, 397–405. doi: 10.1007/s12237-015-0014-8

Monteoliva, S., Mozo, I., Rodríguez, M. E., and Luquez, V. (2020). Impacto de la aplicación de una metodología de marcación del cambium en la evaluación de vasos formados exclusivamente en el xilema bajo tratamiento de estrés hídrico. *Rev Fac Agr La Plata* [Epub ahead of print].

Rengifo, E., Tezara, W., and Herrera, A. (2005). Water relations, chlorophyll a fluorescence, and contents of saccharides in tree species of a tropical forest in response to flood. *Photosynthetica* 43, 203–210. doi: 10.1007/s11099-005-0034-x

Rodríguez, M. E., Achinelli, F. G., and Luquez, V. M. C. (2015). Leaf traits related to productivity in *Populus deltoides* during the post-flooding period. *Trees* 29, 953–960. doi: 10.1007/s00468-015-1189-0

Rodríguez, M. E., Doffo, G. N., Cerrillo, T., and Luquez, V. M. C. (2018). Acclimation of cuttings of willow genotypes to flooding depth level. *New For.* 49, 415–427. doi: 10.1007/s11056-018-9627-7

Rodríguez, M. E., Lauff, D., Cortizo, S., and Luquez, V. M. C. (2020). Variability in flooding tolerance, growth and leaf traits in a *Populus deltoides* intraspecific progeny. *Tree Physiol.* 40, 19–29. doi: 10.1093/treephys/tpz128

Southgate, D. A. T. (1976). *Determination of Food Carbohydrates*. London: Applied Science Publication Ltd. 128–129.

Steffens, B., and Rasmussen, A. (2016). The physiology of adventitious roots. *Plant Physiol.* 170, 603–617. doi: 10.1104/pp.15.01360

Voesenek, L. A. C. J., and Bailey-Serres, J. (2015). Flood adaptive traits and processes: an overview. *New Phytol.* 206, 57–73. doi: 10.1111/nph.13209

Voesenek, L. A. C. J., and Sasidharan, R. (2013). Ethylene-and oxygen signaling-drive plant survival during flooding. *Plant Biol.* 15, 426–435. doi: 10.1111/plb.12014

Conflict of Interest: The authors declare that the research was conducted in the absence of any commercial or financial relationships that could be construed as a potential conflict of interest.

frontiers in Plant Science

ORIGINAL RESEARCH
published: 25 May 2021
doi: 10.3389/fpls.2021.670497

Overexpression of a *SOC1*-Related Gene Promotes Bud Break in Ecodormant Poplars

Daniela Gómez-Soto[1†], *José M. Ramos-Sánchez*[1], *Daniel Alique*[1], *Daniel Conde*[1‡], *Paolo M. Triozzi*[1‡], *Mariano Perales*[1,2*†] *and Isabel Allona*[1,2*†]

[1] *Centro de Biotecnología y Genómica de Plantas, Instituto de Investigación y Tecnología Agraria y Alimentaria, Universidad Politécnica de Madrid, Madrid, Spain,* [2] *Departamento de Biotecnología-Biología Vegetal, Escuela Técnica Superior de Ingeniería Agronómica, Alimentaria y de Biosistemas, Universidad Politécnica de Madrid, Madrid, Spain*

Perennial species in the boreal and temperate regions are subject to extreme annual variations in light and temperature. They precisely adapt to seasonal changes by synchronizing cycles of growth and dormancy with external cues. Annual dormancy–growth transitions and flowering involve factors that integrate environmental and endogenous signals. MADS-box transcription factors have been extensively described in the regulation of *Arabidopsis* flowering. However, their participation in annual dormancy–growth transitions in trees is minimal. In this study, we investigate the function of *MADS12*, a *Populus tremula* × *alba SUPPRESSOR OF CONSTANS OVEREXPRESSION 1* (*SOC1*)-related gene. Our gene expression analysis reveals that *MADS12* displays lower mRNA levels during the winter than during early spring and mid-spring. Moreover, *MADS12* activation depends on the fulfillment of the chilling requirement. Hybrid poplars overexpressing *MADS12* show no differences in growth cessation and bud set, while ecodormant plants display an early bud break, indicating that *MADS12* overexpression promotes bud growth reactivation. Comparative expression analysis of available bud break-promoting genes reveals that *MADS12* overexpression downregulates the *GIBBERELLINS 2 OXIDASE 4* (*GA2ox4*), a gene involved in gibberellin catabolism. Moreover, the mid-winter to mid-spring RNAseq profiling indicates that *MADS12* and *GA2ox4* show antagonistic expression during bud dormancy release. Our results support *MADS12* participation in the reactivation of shoot meristem growth during ecodormancy and link *MADS12* activation and *GA2ox4* downregulation within the temporal events that lead to poplar bud break.

Keywords: poplar, MADS-box family transcription factors, dormancy, gibberellins, growth reactivation, SOC1, ecodormancy, bud break

OPEN ACCESS

Edited by:
Amy Brunner,
Virginia Tech, United States

Reviewed by:
Yan Bao,
Shanghai Jiao Tong University, China
Felipe Dos Santos Maraschin,
Federal University of Rio Grande do Sul, Brazil

****Correspondence:***
Mariano Perales
mariano.perales@upm.es
Isabel Allona
isabel.allona@upm.es

†ORCID:
Daniela Gómez-Soto
orcid.org/0000-0003-0318-3079
Mariano Perales
orcid.org/0000-0002-7351-8439
Isabel Allona
orcid.org/0000-0002-7012-2850

‡Present address:
Daniel Conde,
School of Forest, Fisheries and Geomatics Sciences, University of Florida, Gainesville, FL, United States
Paolo M. Triozzi,
School of Forest, Fisheries and Geomatics Sciences, University of Florida, Gainesville, FL, United States

Specialty section:
This article was submitted to Plant Abiotic Stress, a section of the journal Frontiers in Plant Science

Received: *21 February 2021*
Accepted: *06 April 2021*
Published: *25 May 2021*

Citation:
Gómez-Soto D, Ramos-Sánchez JM, Alique D, Conde D, Triozzi PM, Perales M and Allona I (2021) Overexpression of a SOC1-Related Gene Promotes Bud Break in Ecodormant Poplars. Front. Plant Sci. 12:670497. doi: 10.3389/fpls.2021.670497

INTRODUCTION

Woody perennial plants have acquired multiple adaptive mechanisms to coordinate their vegetative and reproductive growth with the seasonal weather changes (Cooke et al., 2012; Brunner et al., 2014). In temperate latitudes, trees switch between growth and dormancy at their shoot apical meristems to survive dehydration and freezing stress during winter months (Yordanov et al., 2014). Deciduous woody plants cease meristem activity to establish a dormant state before winter;

this is called endodormancy. The meristem is rendered insensitive to growth-promoting signals until the chilling requirement fulfillment (Rohde et al., 2007). The inability to initiate growth clearly distinguishes between endodormancy and the subsequent stage, called ecodormancy, when tree buds recover growth capacity in late winter without showing changes in morphology, maintaining plants cold protected (Groover and Cronk, 2017; Maurya and Bhalerao, 2017). During ecodormancy, the tree has the capacity to resume growth and bud break. Cell elongation of preformed leaves inside the buds precedes new cell divisions (Rohde et al., 2007). Photoperiod and temperature are the main regulatory signals of *Populus* dormancy establishment and release (Wareing, 1956; Weiser, 1970; Ding and Nilsson, 2016; Singh et al., 2017). Changes in photoperiod are constant every year in a given location, while the temperature is more variable among the years. This variation in the temperature has been exacerbated by global warming, causing significant ecological and economic detriment. Warmer springs substantially advance leaf unfolding and flowering time in perennials. On the contrary, warmer winters compromise the chilling fulfillment, which results in a delay of bud break (Wang H. et al., 2020). A better understanding of the spring phenology's molecular control in perennials is crucial to avoid global warming damages and help perennials resist future climate.

The photoperiodic pathway drives *Arabidopsis* flowering and poplar shoot growth (Shim et al., 2017; Singh et al., 2017; Triozzi et al., 2018). The CONSTANS/FLOWERING LOCUS T (CO/FT) module conserves the day length measurement function of *Arabidopsis* and poplar (Yanovsky and Kay, 2002; Bohlenius, 2006). Shoot growth resumption after winter correlates with activation of *FT1* and gibberellin (GA) biosynthetic genes (Rinne et al., 2011; Pin and Nilsson, 2012). More specifically, they encode members of the *GA3* and *GA20 oxidases*. GAs correlate with the activation of glucanase *GH17s* gene to reopen the plasmodesmata channels. They reinitiate the symplastic growth-promoting cell-to-cell signaling within the SAM (Rinne et al., 2011; Tylewicz et al., 2018). In poplar, GAs work parallel to the FT pathway controlling shoot elongation since high levels of bioactive GA during short-day (SD) conditions were sufficient to sustain shoot elongation growth (Eriksson et al., 2015; Singh et al., 2018). Furthermore, inactivation of GAs in *GA 2-OXIDASES* (*GA2ox*) overexpressing (OE) poplars produced extreme tree dwarfism (Zawaski et al., 2011). Additionally, the timing of bud break in poplar requires APETALA2/ethylene-like responsive factor, *Early Bud-Break 1* (*EBB1*), which is a positive regulator of bud break (Yordanov et al., 2014). *EBB1* overexpression shows early bud break, and downregulation delayed bud break relative to wild-type (WT) plants (Yordanov et al., 2014). Finally, it is essential to highlight those dynamics in genomic DNA methylation level involved in regulating the dormancy–growth cycle in trees (Santamaría et al., 2009; Conde et al., 2013, 2017a,b). A progressive reduction of genomic DNA methylation in the apex precedes growth in the apical shoot during the bud break. The induction in the apex of a chilling-dependent poplar *DEMETER-LIKE 10* (*DML10*) DNA demethylase causes a global reduction of DNA methylation levels before bud break (Conde et al., 2017a).

Multiple developmental pathways and stress responses in plants include MADS-box transcription factors (TFs), recently reviewed in Castelán-Muñoz et al. (2019). In trees, MADS-box has emerged as a crucial regulator of dormancy–growth transition during vegetative and reproductive development (Rodriguez-A et al., 1994; Hoenicka et al., 2008; Horvath et al., 2010; Leida et al., 2010; Kayal et al., 2011; Klocko et al., 2018; Singh et al., 2018; Falavigna et al., 2019; Wang J. et al., 2020). Genomic study of *Prunus persica evergrowing* (*eve*) mutant revealed a deletion of six *DORMANCY ASSOCIATED MADS-box* (*DAM*) genes essential for endodormancy maintenance (Rodriguez-A et al., 1994). Consistent with this role of DAM, overexpression of *Malus domestica MdDAMb* gene showed delayed bud break (Wu et al., 2017). Endodormancy establishment and maintenance in *Populus* and *M. domestica* require a gene phylogenetically related to *Arabidopsis SHORT VEGETATIVE PHASE* (*SVP*) (Wu et al., 2017; Singh et al., 2018). Opposite to DAM and SVP, heterologous overexpression in poplar of a silver birch *FRUITFUL* homolog, *BpMADS4*, prevented bud dormancy (Hoenicka et al., 2008). Seasonal expression studies identified MADS-box homologs *Arabidopsis SUPPRESSOR OF OVEREXPRESSION OF CO1* (*SOC1*) during winter dormancy (Voogd et al., 2015; Kitamura et al., 2016; Wang J. et al., 2020). *Arabidopsis SOC1* integrates vernalization, photoperiodic, aging, GAs, and flowering signals and promotes meristematic activity-initiated floral meristems (Moon et al., 2003; Andrés and Coupland, 2012; Immink et al., 2012). *SOC1-like* homologs display a seasonal expression pattern and form a heterocomplex with SVP and DAM homologs of *Arabidopsis*, kiwifruit trees, Japanese apricot, and sweet cherry (de Folter et al., 2005; Voogd et al., 2015; Kitamura et al., 2016; Wang J. et al., 2020). Functional analysis of tree *SOC1* homologs during growth dormancy transitions is minimal. Nevertheless, Voogd et al. (2015) studied the phenology of kiwifruit *AcSOC1i-*, *AcSOC1e-*, and *AcSOC1f* OE lines, finding that only *AcSOC1i* presented earlier bud break than control plants. Even though SOC1, SVP, and DAM homologs could coexpress and interact, some members might have unique function during dormancy.

In this study, we investigate the role of the poplar *MADS12* gene in the dormancy–growth transition. Our phylogenetic analysis and protein sequence comparison indicate that MADS12 belongs to the SOC1 clade. Our gene expression analysis demonstrates *MADS12* induction once chilling is fulfilled, showing a peak of expression before bud break. Moreover, we study the performance of *MADS12* OE lines (OE3 and OE5) and WT plants, under phenological assays. Our findings show that hybrid poplar OE *MADS12* downregulates *GA2ox4* gene and promotes early bud break during ecodormancy.

MATERIALS AND METHODS

Plant Material and Growth Conditions

The hybrid poplar *Populus tremula* × *alba* INRA clone 717 1B4 was used as the experimental model. Poplar plantlets were grown *in vitro* in Murashige and Skoog (MS) medium 1B (pH 5.7) supplemented with 2% sucrose and with indole acetic and indole

butyric acids (0.5 mg/L) containing 0.7% (w/v) plant agar under long-day (LD) 16-h light/8-h dark and 22°C conditions.

For the phenological assays, *in vitro*-cultivated poplars of WT and four selected independent *MADS12* OE lines, OE1, OE3, OE5, and OE7, were transferred to pots containing blond peat, pH 4.5, and grown under LD and 22°C conditions for 3 weeks. The plants were fertilized once every 2 weeks with a solution of 1 g/L of Peters Professional 20-20-20 in LD conditions and 20-10-20 in SD conditions (Comercial Química Massó, Barcelona, Spain). Growth cessation and bud set were induced by exposing plants to SD conditions at 22°C (8-h light/16-h dark) during 8 or 10 weeks. Bud set progression was graded by scoring from stage 3 (fully growing apex) to stage 0 (fully formed apical bud) according to Rohde et al. (2010). Winter conditions were emulated by treating plant under SD 4°C for 4 or 6 weeks to fulfill the chilling requirement. Finally, plants were transferred back to LD 22°C to monitor bud break. The regrowth was scored according to the six developmental stages of bud break (stages 0 to 5) according to Johansson et al. (2014). Phenological assays to evaluate bud break of ecodormant plants were performed twice. In the first round, we assayed *MADS12* OE lines OE1, OE5, and OE7 lines and WT. We observed that the highest level of *MADS12* expression correlates with the earliest bud break. In the second round, we assayed only the *MADS12* OE3 and OE5 lines showing the highest *MADS12* expression levels and WT to increase the number of plantlets to make two biological replicates.

Generation of T1 *MADS12* Overexpressing Lines

The *MADS12* coding region (CDS) was amplified from hybrid poplar using gene-specific primers with attB sites (**Supplementary Table 1**). For polymerase chain reaction (PCR), Phusion DNA Polymerase (Thermo Fisher Scientific, Massachusetts, USA) was used, and the PCR products were purified and inserted into pDONR207 (Life Technologies, Carlsbad, CA, USA). Insertions in the resulting entry clones were sequence verified. The Gateway cassettes carrying *MADS12* CDS were then transferred into the destination binary vectors pGWB15 (Nakagawa et al., 2007). These constructs were transferred into *Agrobacterium tumefaciens* strain GV3101/pMP90 (Koncz and Schell, 1986). Hybrid poplar was transformed via an *Agrobacterium*-mediated protocol described previously by Gallardo et al. (1999) with few modifications. Briefly, poplar leaves and stem explants were cultured in minimum inhibitory concentration (MIC) medium, MS medium 1B supplemented with 0.01 mg/L of thidiazuron (TDZ) and 1 mg/L of 2,4-dichlorophenoxyacetic acid in the dark for 48 h. Then explants were placed in an agrobacterium suspension for 15 min and blotted onto sterile filter paper to remove excess bacteria. After 2 days, explants were transferred to MISCT medium composed of MS 1B supplemented with 0.02 mg/L of TDZ, 1 mg/L of 2,4-dichlorophenoxyacetic acid, 250 mg/L of cefotaxime, and 50 mg/mL of kanamycin for 4 weeks in darkness. This medium was used for decontamination and induction of callus growth. After size reached about 0.5 mm^2, calli were moved to MIBS medium supplemented with 0.05 mg/mL of alpha-naphthalene acetic acid (NAA), 0.004 mg/L of TDZ, 250 mg/L of cefotaxime, and 50 mg/L of kanamycin to select transformant calli and induce shoot formation. Once shoots grow, they are transferred to MEMS, MS 1B supplemented with 125 mg/L of cefotaxime, kanamycin (50 mg/L), and 0.5 mg/L of indole-3-acetic acid (IAA) to induce root formation. Regenerated plantlets were propagated in MEMS medium and maintained *in vitro* growth conditions (LD 22°C). *MADS12* expression level of individual T1 OE lines was analyzed by reverse transcription-PCR (qRT-PCR).

Plant Material for Gene Expression Studies

To investigate if *MADS12* activation is dependent on the fulfillment of the chilling requirements, gene expression analysis was performed on RNA obtained from cuttings collected from five 6-year-old hybrid poplars (*P. tremula* × *alba*) growing under natural conditions as reported earlier by Conde et al. (2017a).

Annual expression patterns for poplar *MADS12* were initially determined in 2-year-old poplar branches (*Populus alba*) from adult trees growing under natural conditions in Madrid (Spain) (Conde et al., 2017b).

For comparative gene expression analysis among hybrid poplar *MADS12* OE lines, OE3 and OE5, and WT, RNA was obtained from a pool of six ecodormant apical buds grown for 5 days under LD at 22°C, for each biological sample.

Mid-winter to mid-spring transcriptional profiles, used for making heat maps, were collected from hybrid poplar apical bud samples grown in natural conditions in Madrid (Spain). Normalized expression data are available in the gene atlas from Phytozome https://phytozome.jgi.doe.gov/pz/portal.html (Conde et al., 2019).

RNA Extraction, cDNA Synthesis, and qRT-PCR Analysis

RNA extraction was performed adding to frozen bud cetyltrimethylammonium bromide (CTAB) extraction buffer with 2% β-mercaptoethanol at 65°C for 5–8 min, following by three washes with chloroform. After that, 7.5 M $LiCl_2$:50 mM EDTA was added, and samples were precipitated overnight at 4°C. The next day, RNA was collected by centrifuging at 10,000 RPM for 20 min, the supernatant was discarded, and the pellet was resuspended using NR buffer, and RNA was purified according to the manufacturer's instructions of NZY RNA purification kit (NZYTech, Lisboa, Portugal). A total of 500 ng of RNA was retrotranscribed to cDNA using the Maxima First Strand cDNA Synthesis kit from Thermo Scientific (Thermo Fisher Scientific, Massachusetts, USA), and qRT-PCR was performed as described earlier (Ramos-Sánchez et al., 2019). The gene-specific primers used in these studied are listed in **Supplementary Table 1**.

Phylogenetic Analysis and Sequence Alignment

Arabidopsis protein sequences were obtained from TAIR10 website (www.arabidopsis.org), and *Populus trichocarpa* protein sequences from (Phytozome v10.3, www.phytozome.net). To

construct the phylogenetic tree, protein sequences were aligned with MAFFT E-INS-I algorithm; ProtTest 2.4 was used to select the best evolutionary model (JTT+I+G+F; 5 categories rate; alpha = 1.213); the phylogeny was inferred with RAxML algorithm (perform bootstrap 1000). Tree representation was made using iTol (https://itol.embl.de/) and selecting a bootstrap < 600, and clade coloring was performed according to phylogenetic relationships with *Arabidopsis MADS-box* genes. Multiple sequence alignment was inferred using ClustalW. MADS-box protein domains were annotated as described in Trainin et al. (2013).

In Silico Analysis of *GA2ox4* Promoter

Promoter sequence (2 kb) of *GA2ox4* was obtained from ASPENDB (http://aspendb.uga.edu/) and analyzed using the Plant promoter analysis navigator 3.0 (http://plantpan.itps.ncku.edu.tw/). MADS-box TF binding sides were selected and examined to search putative TFs that were identified using phytozome database (https://phytozome.jgi.doe.gov/pz/portal.html).

MADS12 Coexpression Analysis

Genes coexpressed with *MADS12* were identified using the Pearson Algorithm on bud mid-winter to mid-spring RNAseq dataset applying correlation coefficient higher than 0.9. We identified 258 genes in apical bud dataset coexpressed with *MADS12*. Gene expression values for each gene were normalized being the maximum of gene expression 1. From a total of 258 *MADS12* coexpressed genes, a total of 242 unique homologs to *Arabidopsis* genome were identified.

RESULTS

Poplar SOC1 Clade Displays Seven Members

MADS-box TF gene family displays a large number of uncharacterized members in poplar. We investigated the phylogenetic relationship of *MADS-box* genes in *Arabidopsis thaliana* and *Populus trichocarpa* by generating a maximum likelihood phylogenic tree using all annotated poplar and *Arabidopsis* full-length MADS-box protein sequences. Thirteen major lineages within MIKC-types MADS-box have been resolved and named according to the *Arabidopsis* gene terminology: FLC/MAF, AP1/FUL, SEP, AGL6, SOC1, AG, AGL12, SVP, AGL15, AGL17, AP3, PI, and TT16. Also, we found two clusters that belong to MIKC-type proteins without any *Arabidopsis* orthologous (**Figure 1A**). Even though several *SOC1-like* genes were associated with dormancy release in trees (Voogd et al., 2015; Kitamura et al., 2016; Wang J. et al., 2020), the poplar SOC1-like members remain uncharacterized during dormancy phenology. We performed protein comparison of identified SOC1-like members of *Arabidopsis*, poplar, rice, and maize, revealing a high sequence similarity among MADS-box (M) domain and less conserved intervening (I) and keratin-like (K) domains (**Supplementary Figure 1**). Interestingly, most SOC1-like proteins display conserved C-terminal motif; however, there are members that lack this C-terminal sequence in monocots and dicots (**Figure 1B**). Together, these analyses indicate that SOC1 members might have originated from a common MIKC-type MADS-box ancestor; nevertheless, they have evolved to a novel C-terminal sequence. Since all *Arabidopsis SOC1-like* genes promote flowering transition, the SOC1 C-terminal motif is not critical for flowering (Schonrock, 2006; Lee and Lee, 2010; Dorca-Fornell et al., 2011; Pérez-Ruiz et al., 2015).

MADS12 Activation Occurs Once the Chilling Requirement Has Been Fulfilled

To understand the expression pattern of poplar *SOC1-like* genes during dormancy to growth shift, we studied their temporal expression in the Phytozome public repository, which deposited RNAseq-based gene expression analyses of hybrid poplar apical buds grown under natural conditions (Conde et al., 2019). All these genes display a particular mid-winter to mid-spring pattern of gene expression in shoot apical buds, showing a temporal specialization (**Figure 2A**). We focused on *Potri.012G100200* gene, called *MADS12*, which shows a low expression level during the winter followed by a transitory expression peak with its maximum at Early Spring f2 (**Figure 2A**). *MADS12* is a spring gene activated during the shoot growth resumption period (**Figure 2B**). The repression of *MADS12* observed during the winter suggested that its activation depends on fulfilling the chilling requirement (**Figure 2B**). We investigated *MADS12* expression in dormant buds of pre-chilling and post-chilling cuttings, after moving them to growth-promoting conditions during 0, 6, and 12 days. Our qRT-PCR analysis confirmed that *MADS12* is induced once the chilling requirement has been fulfilled (**Figure 2C**). Moreover, *MADS12* shows its maximal expression at 6 days (83-fold) and decreasing ∼50% at 12 days (**Figure 2C**). However, the expression of *CYCLIN C 6* (*CYC6*) gene, used as marker of cell proliferation (Conde et al., 2017a), peaks at 12 days (**Figure 2D**), suggesting that *MADS12* induction precedes the cell proliferative stage. These results suggest that *MADS12* could be involved in the resumption of growth after chilling period.

MADS12 Overexpression Promotes Shoot Growth Reactivation of Ecodormant Plants

To assess the functional role of *MADS12* during dormancy–growth cycles, we generated 10 independent OE hybrid poplar lines, characterizing their *MADS12* expression levels by qRT-PCR (**Supplementary Figure 2**). Because of the highest *MADS12* expression level, we selected OE3 and OE5 lines to examine the growth and apical bud phenology in growth chambers under photoperiodic and temperature conditions that mimic seasonal transitions autumn–winter–spring (Rohde et al., 2010). Phenology of WT and *MADS12* OE3 and OE5 genotypes did not show any differences in growth cessation and bud set, indicating that *MADS12* overexpression does not impair these transitions (**Supplementary Figures 3A,B**).

To evaluate if *MADS12* OE plants show changes in endodormancy release, we subjected those plants to 8 weeks of SDs at 22°C followed by 4 or 6 weeks of SD at 4°C.

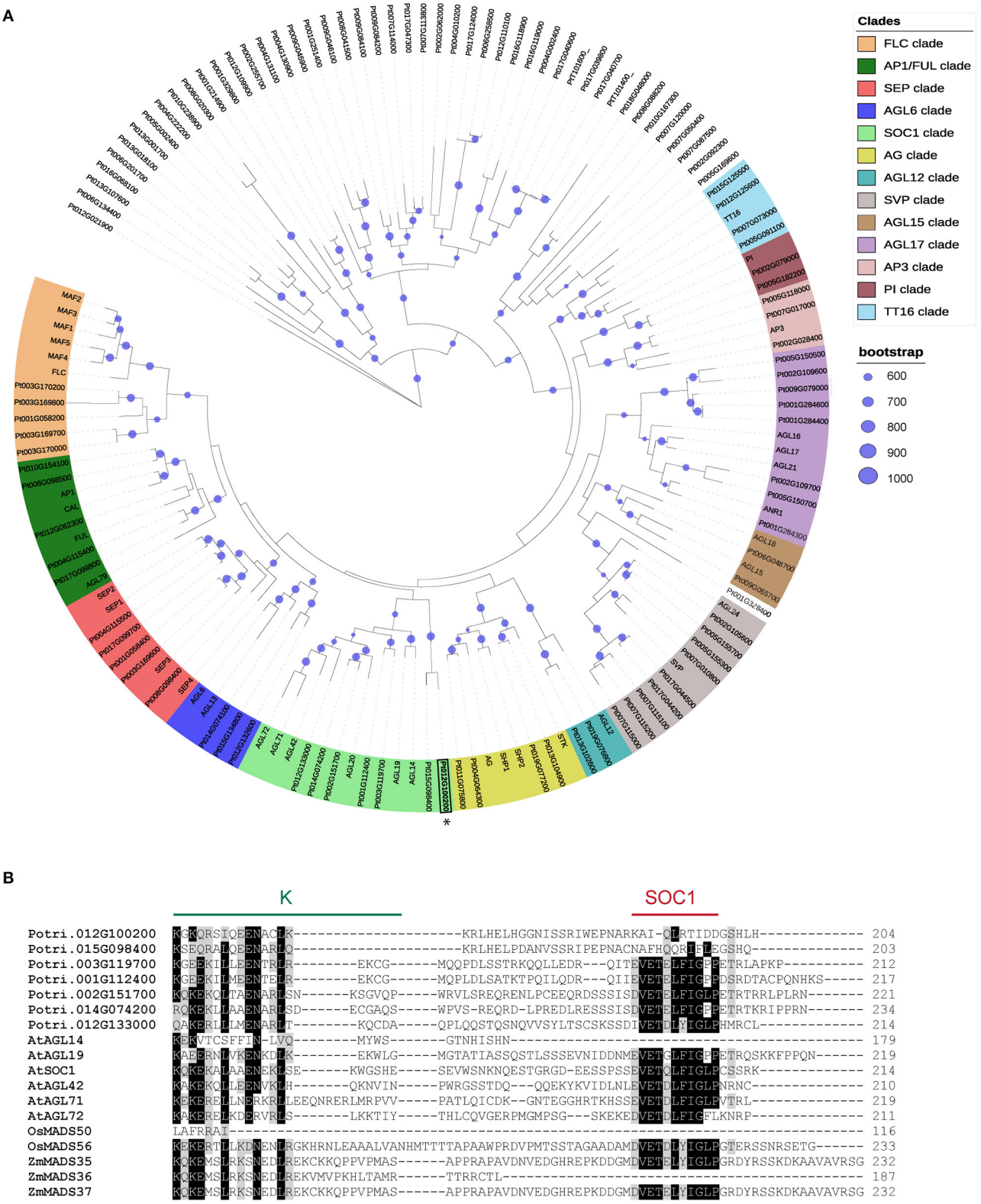

FIGURE 1 | Identification of poplar SOC1-like proteins. **(A)** Phylogenetic tree analyses of MADS-box proteins from *Arabidopsis* and poplar. Maximum likelihood tree obtained using the RAxML tool with 1,000 bootstrap replicates. The right panel indicates the color code of the clades and bootstrap values. Clades are named FLOWERING LOCUS C (FLC), APETALA1/FRUITFUL (AP1/FUL), SEPALLATA (SEP), AGAMOUS-LIKE 6 (AGL6), SOC1, AG, AGL12, SVP, AGL15, AGL17, AP3, PISTILLATA (PI), and TRANSPARENT TESTA16 (TT16). **(B)** MAFF alignment of *Populus*, *Arabidopsis*, rice, and maize SOC1-like proteins. The alignment shows part of the K domain (green ink) and the SOC1 motif (red ink). Black boxes indicate identical amino acids. Gray boxes indicate conservative amino acid substitutions.

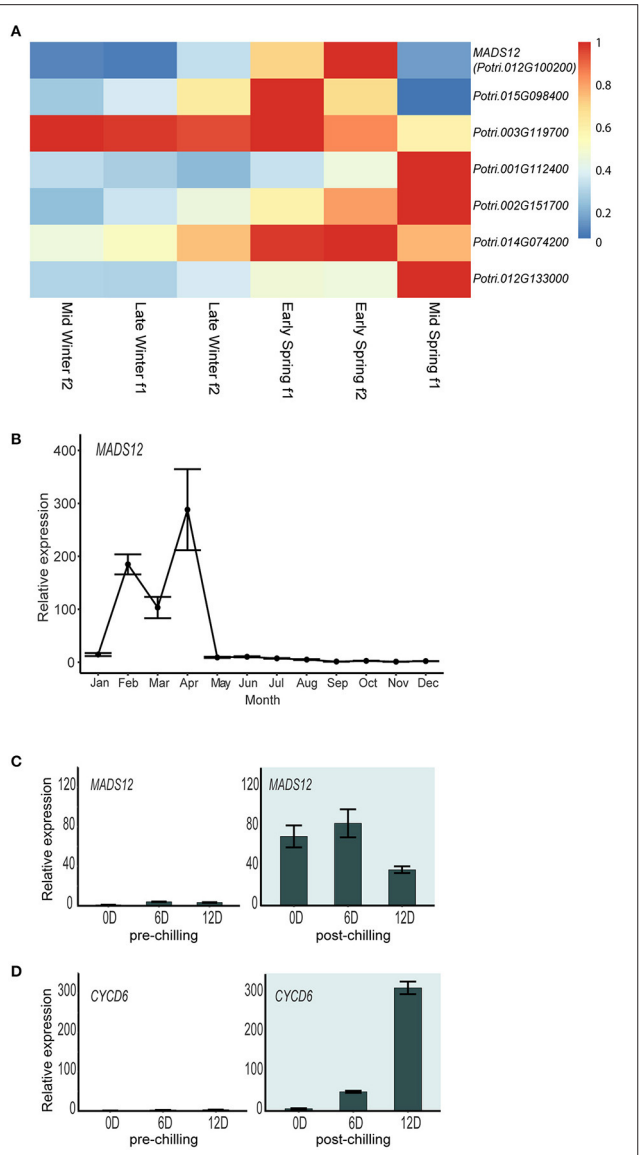

FIGURE 2 | Chilling requirement fulfillment is a prerequisite for *MADS12* activation. **(A)** Heatmap showing normalized expression of hybrid poplar SOC1-like genes from mid-winter to mid-spring in apical buds. Groups are named "early," "mid," or "late" when sampling dates were within the first, second, or third month of each season, respectively, following the Northern Meteorological Seasons dates. "f1" or "f2" mean fortnight-1 and fortnight-2 within the month (Conde et al., 2019). **(B)** *MADS12* annual expression pattern measured by qRT-PCR in 2-year-old poplar branches over 1 year. *Ubiquitin7* is used as the housekeeping gene. Plotted values and error bars are fold-change means ± s.d. of two biological replicates. Note: *MADS12* shows the highest mRNA accumulation during mid-winter–spring period. **(C,D)** qRT-PCR analysis of *MADS12* **(C)** and *CYCD6* **(D)** genes in dormant shoot apex of pre-chilling and post-chilling cuttings grown under LD and 22°C conditions. *Ubiquitin7* is used as the housekeeping gene. Plotted values and error bars are fold-change means ± s.d. of two biological replicates. The x-axis scale is indicated in days. Pre-chilling and post-chilling data are shown in white and green backgrounds, respectively.

Subsequently, we shifted them to LDs at 22°C for monitoring their bud break (Conde et al., 2017a). Noticeably, all genotypes tested remained dormant under growth-promoting conditions after 4 weeks of SD at 4°C, although they resumed growth after 6 weeks of SD at 4°C (**Supplementary Figures 3A,C**). We observed no differences in bud break scores among genotypes, suggesting that chilling requirement fulfillment caused an equal reactivation of shoot growth (**Figures 3A,B**). Once trees entered in endodormancy, WT and OE plants have same chilling requirement, and *MADS12* overexpression does not induce endodormancy release.

Afterward, we tested whether *MADS12* OE could restore growth on plants that had already ceased growing and set buds without any chilling treatment. We arranged a new set of WT, *MADS12* OE3, and OE5 plants in LD at 22°C for 4 weeks and placed them under SD at 22°C for 8 or 10 weeks. Then, plants were subjected again to LD at 22°C, and bud break was monitored (**Figure 3C** and **Supplementary Figure 3D**). After 10 weeks in SD at 22°C, WT and most *MADS12* OE3 and OE5 plants entered endodormancy; therefore, they could not resume growth under favorable environmental conditions without chilling (**Supplementary Figure 3D**). This observation indicates that *MADS12* overexpression does not restrict the plants from reaching the endodormant state and that they could not break endodormancy without chilling. Finally, plants subjected to SD at 22°C conditions for 8 weeks ceased growth and set buds; however, they could not reach the endodormant state since plants resumed total shoot growth under LD at 22°C without chilling (**Figure 3C**). Significantly, the apical shoot of *MADS12* OE3 and OE5 lines restored full growth ∼10 days earlier than WT plants (**Figures 3C,D**). Furthermore, a phenological assay of additional lines confirmed that the lower the *MADS12* overexpression level, the lower the differences in bud break observed (**Supplementary Figure 4**). Collectively, these results indicate that *MADS12* overexpression promotes early bud break of ecodormant plants under favorable environmental conditions.

GA2ox4 Is Downregulated in Ecodormant *MADS12* Overexpressing Plants

Our phenological assays revealed an accelerated shoot growth resumption of *MADS12* OE lines with respect to WT, suggesting an improved growth-stimulating capacity. We hypothesize that MADS12 OE3 and OE5 might differentially express shoot growth-promoting genes with respect to WT. To test this, we collected apical buds of *MADS12* OE3, *MADS12* OE5, and WT plants treated with 8 weeks of SD at 22°C and exposed during 5 days to LD at 22°C conditions, before the observed phenotypic differences (**Figure 3C**). In poplar, one of the main factors involved in shoot growth is FT (Bohlenius, 2006; Hsu et al., 2011). qRT-PCR analysis did not show differences in *FT1* expression in *MADS12* OE3 and *MADS12* OE5 lines with respect to WT (**Figure 4A**). We did not detect *FT2* in these bud tissues (data not shown). This result indicates that an FT-independent pathway controls the activation of shoot growth. Bioactive GAs act as an FT parallel pathway to control poplar shoot growth (Eriksson et al., 2015). *GA2ox* genes cause the inactivation of bioactive GAs (Rieu et al., 2008). Only *GA2ox3*, *GA2ox4*, and *GA2ox5* are expressed in the apical shoot, and RNAi downregulation of *GA2ox4* and *GA2ox5* promotes poplar aerial shoot growth (Gou et al., 2011). Our qRT-PCR analysis showed that *GA2ox4* and *GA2ox5* are downregulated in *MADS12* OE3 and OE5 with

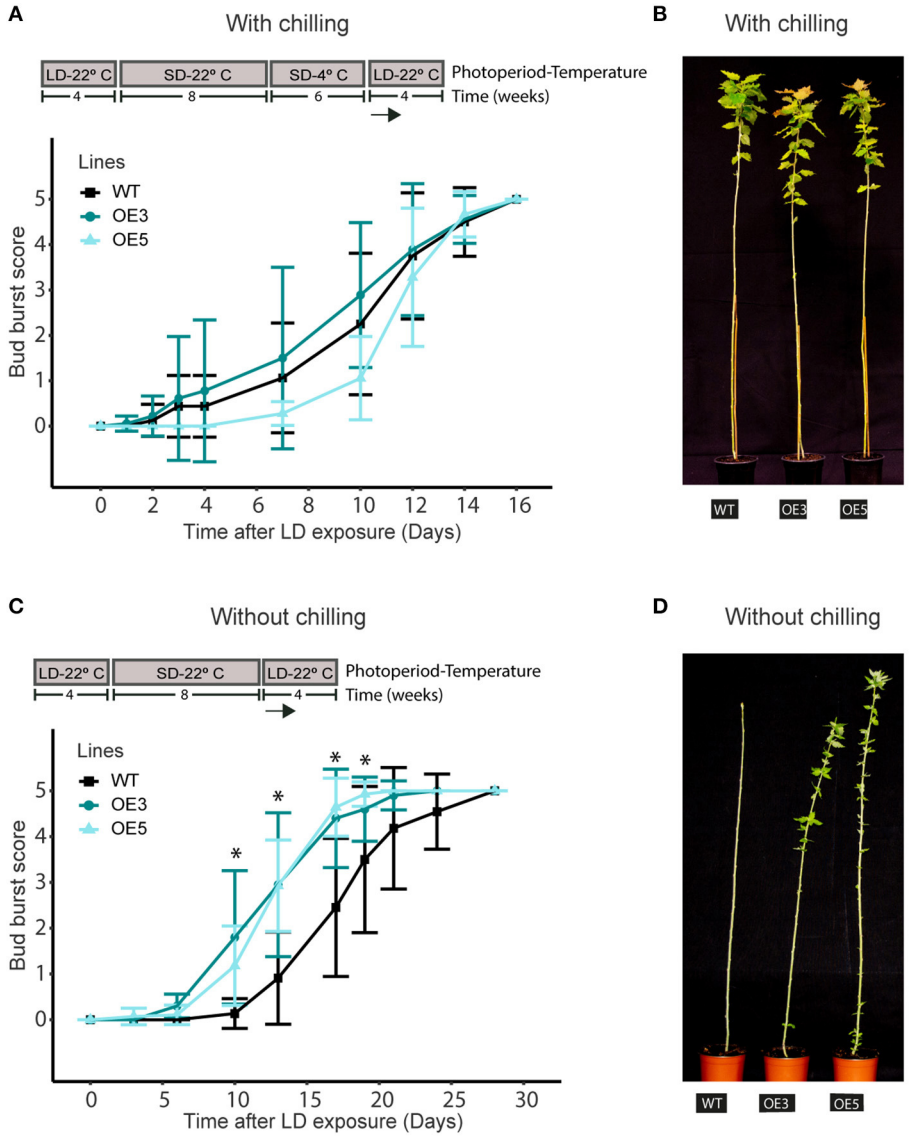

FIGURE 3 | *MADS12* overexpression promotes early bud break of ecodormant poplars. Bud break scoring of hybrid poplar *MADS12* overexpressing OE3 and OE5 lines and wild type after transferring to LD and 22°C conditions **(A,B)** with chilling treatment and **(C,D)** without chilling treatment. **(B,D)** Representative picture of bud break differences in **(B)** plants after 15 days of LD exposure and **(D)** plants after 10 days of LD exposure. Values represent the mean of the bud score measure of $n =$ 10–15 plants. Significant differences between overexpressing (OE) and wild type (WT) were analyzed using Tukey test, $^*p < 0.05$. Top panels indicate photoperiodic and temperature conditions used.

respect to WT, while only *GA2ox4* is found to be significantly repressed (**Figure 4A**). *GA2ox3* shows inconsistent differences in *MADS12* OE3 and OE5 with respect to WT (**Figure 4A**). These results point out that an increase in bioactive GAs could cause the accelerated growth resumption. Accordingly, the mid-winter to mid-spring RNAseq analysis showed an opposite temporal expression pattern, with *GA2ox4* and *GA2ox5* being greatly downregulated when *MADS12* is highly expressed (**Figure 4B**). This result supports the antagonistic role of *MADS12* over *GA2ox4* within the temporal events that lead to poplar bud break.

DISCUSSION

MADS-box homologs to *Arabidopsis* SOC1 have been identified in trees; however, their function remains very little understood. *Arabidopsis SOC1* is expressed in the shoot apical meristem and plays a key role during floral transition, integrating vernalization, photoperiod, GAs, and the aging pathways (Amasino, 2010; Lee and Lee, 2010). Furthermore, *Arabidopsis SOC1*-related genes, *AGL14*, *AGL19*, *AGL42*, *AGL71*, and *AGL72*, are also implicated in the control of the floral transition (Schonrock, 2006; Dorca-Fornell et al., 2011; Pérez-Ruiz et al., 2015). Our phylogenetic

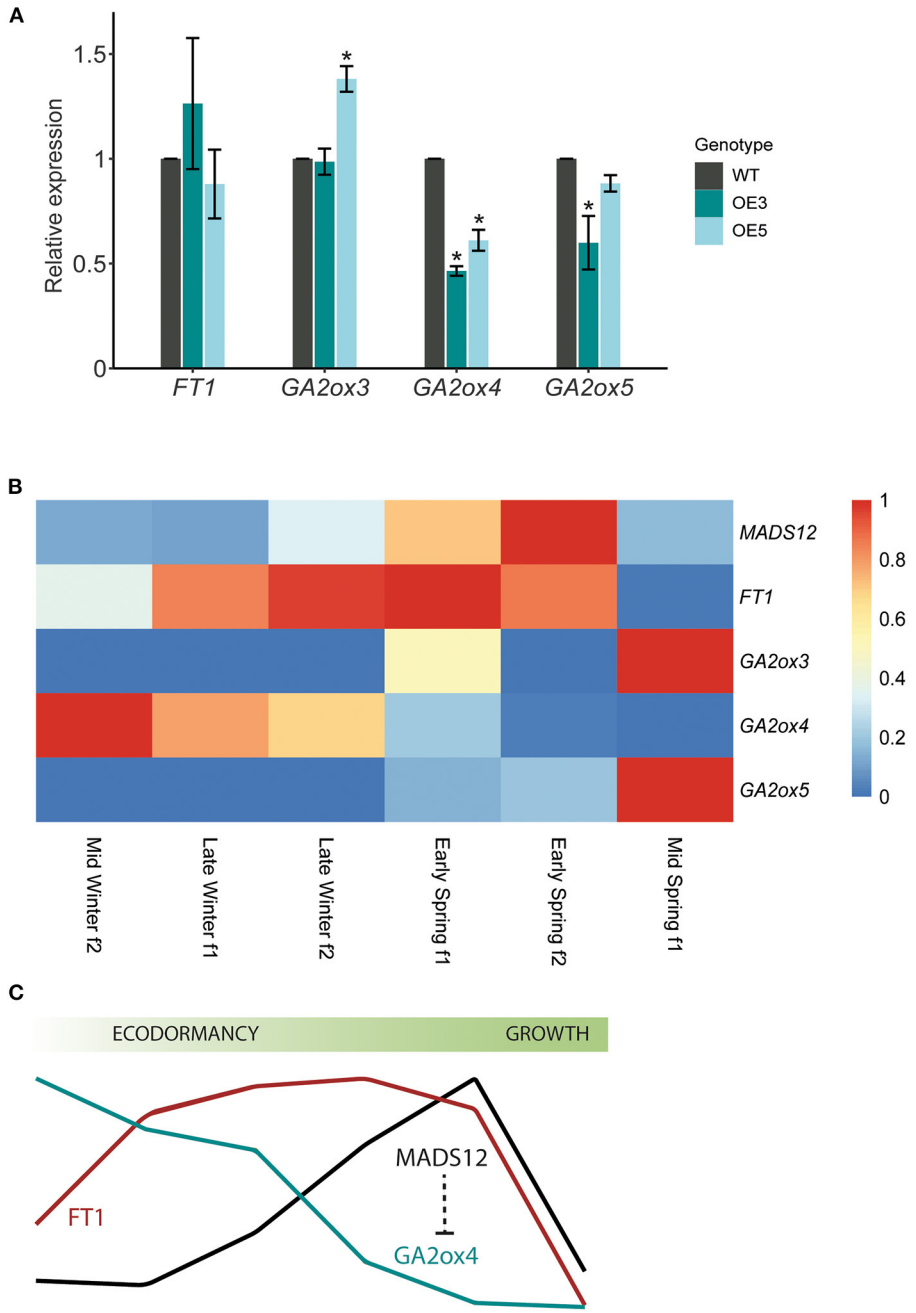

FIGURE 4 | *GA2ox4* is downregulated in *MADS12* overexpressing lines during bud dormancy release. **(A)** qRT-PCR analysis of *FT1*, *GA2ox3*, *GA2ox4*, and *GA2ox5* genes in ecodormant *MADS12* overexpressing OE3 and OE5 and wild-type (WT) apices collected after 5 days in long day (LD) and 22°C treatment. *Ubiquitin7* is used as the housekeeping gene. Plotted values and error bars are fold-change means ± s.d. of two biological replicates. Asterisks (*) represent statistical differences assessed by one-way ANOVA followed by Tukey *post-hoc* test ($p < 0.05$). **(B)** Heatmap showing RNAseq expression data of *MADS12*, *FT1*, *GA2ox3*, *GA2x4*, and *GA2ox5* genes in apical buds from mid-winter f2 to mid-spring f1. **(C)** Schematic representation of *MADS12* and *GA2ox4* antagonist expression pattern during bud dormancy release.

tree of poplar and *Arabidopsis* MADS-box proteins identifies a SOC1 clade including seven poplar SOC1-like family members (**Figure 1A**). These seven poplar *SOC1-like* genes show a specific expression pattern during mid-winter to mid-spring, suggesting their role in dormancy release (**Figure 2A**). Among them, MADS12 and Potri.015G098400 do not conserve a C-terminal SOC1 motif, suggesting that MADS12 C-terminal domain undergoes a divergent evolution (**Figure 1B**). The functional

importance of C-terminal SOC1 motif is still unclear. Structure-function analysis of *Arabidopsis* with intragenic mutations in the *SOC1* gene shows that deletion of C-terminal and part of the K domain renders weak suppression of early flowering of FRIGIDA mutants (Lee et al., 2000, 2008). This observation and the fact that *AGL14*, also lacking the C-terminal SOC1 motif, is required for *Arabidopsis* flowering (Pérez-Ruiz et al., 2015) indicate that the C-terminal SOC1 motif is not essential for SOC1 and its homologs function in flowering.

Functional analyses of three *SOC1* homolog genes in the kiwifruit tree, which exhibited a C-terminal SOC1 motif, resulted in only *AcSOC1i* overexpression that promoted early bud break under ecodormant conditions (Voogd et al., 2015). *MADS12* OE lines also display an accelerated bud break of ecodormant poplars. Moreover, the seasonal expression pattern of *AcSOC1i* resembles one of the *MADS12* showing a seasonal induction at the end of the winter (**Figures 2A,B**; Voogd et al., 2015). These two studies point out that *AcSOC1i* and *MADS12* play identical functions during dormancy phenology, despite C-terminal SOC1 motif differences. Similar to our hybrid poplar *MADS12* OE lines, overexpression of *Arabidopsis SOC1* in poplar did not show phenotypical differences during vegetative shoot growth, but phenological assays were not performed (Bruegmann and Fladung, 2019). Additional functional studies of poplar *SOC1-like* genes are needed.

This work shows that chilling requirement fulfillment is necessary for *MADS12* activation, as it does for *FT1*, *EEB1*, and *DML10*, already described as bud break promoter genes in poplar (Hsu et al., 2011; Yordanov et al., 2014; Conde et al., 2017a). Our results show that *MADS12* participates in ecodormancy release, concurring with a single-nucleotide polymorphism's (SNP's) presence associated with bud flush (Evans et al., 2014). We find that ecodormant *MADS12* OE lines resume growth under LDs and warm temperatures 10 days earlier than WT, consistent with its possible function as a growth inductor during ecodormancy. Our phenological assays indicate that bud break of *MADS12 OE* poplars has no differences to WT after chilling fulfillment. Possibly, *MADS12* OE phenotype would have been masked by the induction of endogenous *MADS12* after chilling. To test this hypothesis, bud break analysis of *MADS12* knockout lines should be performed. Another possibility is that the levels of a transcriptional coregulator limit the activity of *MADS12* OE plants *in vivo*. MADS-box transcriptional regulation operates forming heterocomplexes (de Folter et al., 2005). We found that *AGAMOUS-LIKE MADS-BOX PROTEIN AGL16* (*AGL16-like*) TF coexpressed with *MADS12* (**Supplementary Figures 5**, **6A**, and **Supplementary Table 3**). Moreover, *AGL16-like* expression is not induced in *MADS12* OE lines (**Supplementary Figure 6B**). Thus, we proposed that chilling dependent bud break in *MADS12* OE lines could be conditioned by a limiting factor such as *AGL16-like*. Future protein–protein interaction and coexpression assays in transgenic poplar will sort this out.

During the ecodormancy stage before bud break, reactivation of growth correlates with upregulation of GA biosynthetic genes and simultaneous downregulation of GA catabolic genes, particularly *GA2ox4* (Karlberg et al., 2010). Likewise, bud break correlates with downregulation of GA2 oxidases in *Vitis vinifera* and sweet cherry (Zheng et al., 2018; Vimont et al., 2019). Exogenous addition of GAs to winter buds promoted poplar bud break (Rinne et al., 2011). A functional study demonstrate that the oveexpression of a Gibberellin Oxidase gene caused delayed bud break pointing to GA signaling involvement during bud break (Singh et al., 2018). Recent work showed that *MADS12* activates *PIN5b* in *Populus deltoides* × *euramericana* stem tissue during full-growth conditions (Zheng et al., 2020). Unexpectedly, our qRT-PCR analysis showed that *PIN5b* expression is significantly repressed in both *MADS12* OE3 and OE5 than WT, suggesting an impaired polar auxin efflux in *MADS12* OE ecodormant buds (**Supplementary Figure 7**). The differences in seasonal stages or *Populus* ecotypes might explain this contrasting activity of *MADS12*. *Arabidopsis* PIN5 localizes in endoplasmic reticulum (ER) membrane and mediates polar auxin efflux from the cytosol to ER (Mravec et al., 2009). This intracellular auxin transport plays a role in regulating auxin homeostasis by compartmentalizing cellular auxin pools (Barbez and Kleine-Vehn, 2013). Thus, repression of *PIN5b* in ecodormant buds could increase cytoplasmatic auxin pool. That could contribute to the faster shoot growth resumption capacity observed in MADS12 OE plants, along with GAs. Phenological assays of *PIN5b* RNAi lines are necessary to investigate its role during winter-to-spring transition.

An increasing amount of evidence points out that dormancy and flowering transition sharing conserved regulatory elements (Maurya and Bhalerao, 2017; Triozzi et al., 2018; Falavigna et al., 2019). In *Arabidopsis* shoot apical meristem, SOC1 is the major hub in regulatory networks underlying flowering (Immink et al., 2012). SOC1 antagonizes SVP repressive action over *GA20 oxidases 2* (*GA20ox2*), promoting GA biosynthesis and flowering induction at the shoot apex (Andrés et al., 2014). It is unknown if this model could be conserved during dormancy to growth transition. An inspection of public mid-winter to mid-spring RNAseq data indicates that *SVL* shows an opposite expression pattern with *SOC1*-like genes encoded by *Potri.001G112400* and *Potri.012G13300*, and *GA20 oxidases 3*, *5*, and *6*, but not with *MADS12* (**Supplementary Figure 8**). This observation suggests a possible interplay between *SOC1*-like genes and SVL to modulate GA biosynthesis in poplar during dormancy to growth transition. However, MADS12 might operate in an SVL-independent manner.

Our results revealed that ecodormant *MADS12* OE poplars show accelerated bud break and *GA2ox4* repression. Moreover, the RNAseq mid-winter to mid-spring profiling demonstrates that *MADS12* and *GA2ox4* show opposite expression patterns during dormancy release. *In silico* analysis of *GA2ox4* promoter identified 10 potential MADS-box-binding elements, supporting the idea that *GA2ox4* could be transcriptionally repressed by *MADS12* (**Supplementary Table 2**). Future transactivation assays should test this hypothesis. It has been shown that RNAi downregulation of *GA2ox4* increased shoot growth in poplar; however, it is unknown whether *GA2ox4* RNAi lines could reactivate earlier shoot growth of ecodormant plants (Gou et al., 2011; Singh et al., 2018). Phenological assays of *GA2ox4* RNAi lines are critical to sort the importance of downregulation of GA catabolism during winter-to-spring

transition. We propose that the seasonal function of *MADS12* is to promote growth reactivation during ecodormancy by downregulating *GA2ox4* (**Figure 4C**). Activation of GA signaling promotes reactive oxygen species (ROS) signaling and bud break in Japanese apricot (Zhuang et al., 2013). A transitory activation of oxidative stress has been proposed to play a pivotal role in dormancy in several plant models (Beauvieux et al., 2018). Whether downregulation of *GA2ox4* by *MADS12* promotes GAs and ROS signaling should be explored in poplar.

DATA AVAILABILITY STATEMENT

The original contributions presented in the study are included in the article/**Supplementary Materials**, further inquiries can be directed to the Corresponding authors.

AUTHOR CONTRIBUTIONS

DG-S, JR-S, DA, DC, PT, and MP performed the experiments. All authors participated in the design of the experiments and in the discussions described here. DG-S, MP, and IA wrote the manuscript.

FUNDING

This study was supported by grants AGL2014-53352-R and PGC2018-093922-B-I00, awarded to IA and MP; and SEV-2016-0672 (2017-2021) to the CBGP Severo Ochoa Programme for Centres of Excellence in R&D from the Agencia Estatal de Investigación of Spain. The work of MP was supported by the Ramón y Cajal MINECO program (RYC-2012-10194), of whom DG-S has an FPI fellowship (PRE2019-089312) from Ministerio de Ciencia e Innovacion de España.

SUPPLEMENTARY MATERIAL

The Supplementary Material for this article can be found online at: https://www.frontiersin.org/articles/10.3389/fpls.2021.670497/full#supplementary-material

REFERENCES

Amasino, R. (2010). Seasonal and developmental timing of flowering. *Plant J.* 61, 1001–1013. doi: 10.1111/j.1365-313X.2010.04148.x

Andrés, F., and Coupland, G. (2012). The genetic basis of flowering responses to seasonal cues. *Nat. Rev. Genet.* 13, 627–639. doi: 10.1038/nrg3291

Andrés, F., Porri, A., Torti, S., Mateos, J., Romera-Branchat, M., García-Martínez, J. L., et al. (2014). SHORT VEGETATIVE PHASE reduces gibberellin biosynthesis at the *Arabidopsis* shoot apex to regulate the floral transition. *Proc. Natl. Acad. Sci. U.S.A.* 111, E2760–E2769. doi: 10.1073/pnas.1409567111

Barbez, E., and Kleine-Vehn, J. (2013). Divide et impera—cellular auxin compartmentalization. *Curr. Opin. Plant Biol.* 16, 78–84. doi: 10.1016/j.pbi.2012.10.005

Beauvieux, R., Wenden, B., and Dirlewanger, E. (2018). Bud dormancy in perennial fruit tree species: a pivotal role for oxidative cues. *Front. Plant Sci.* 9:657. doi: 10.3389/fpls.2018.00657

Bohlenius, H. (2006). CO/FT regulatory module controls timing of flowering and seasonal growth cessation in trees. *Science* 312, 1040–1043. doi: 10.1126/science.1126038

Bruegmann, T., and Fladung, M. (2019). Overexpression of both flowering time genes AtSOC1 and SaFUL revealed huge influence onto plant habitus in poplar. *Tree Genet. Genom.* 15:20. doi: 10.1007/s11295-019-1326-9

Brunner, A. M., Evans, L. M., Hsu, C.-Y., and Sheng, X. (2014). Vernalization and the chilling requirement to exit bud dormancy: Shared or separate regulation? *Front. Plant Sci.* 5:732. doi: 10.3389/fpls.2014.00732

Castelán-Muñoz, N., Herrera, J., Cajero-Sánchez, W., Arrizubieta, M., Trejo, C., García-Ponce, B., et al. (2019). MADS-box genes are key components of genetic regulatory networks involved in abiotic stress and plastic developmental responses in plants. *Front. Plant Sci.* 10:853. doi: 10.3389/fpls.2019.00853

Conde, D., González-Melendi, P., and Allona, I. (2013). Poplar stems show opposite epigenetic patterns during winter dormancy and vegetative growth. *Trees* 27, 311–320. doi: 10.1007/s00468-012-0800-x

Conde, D., Le Gac, A.-L., Perales, M., Dervinis, C., Kirst, M., Maury, S., et al. (2017a). Chilling-responsive DEMETER-LIKE DNA demethylase mediates in poplar bud break: Role of active DNA demethylase in trees' bud break. *Plant Cell Environment* 40, 2236–2249. doi: 10.1111/pce.13019

Conde, D., Moreno-Cortés, A., Dervinis, C., Ramos-Sánchez, J. M., Kirst, M., Perales, M., et al. (2017b). Overexpression of DEMETER, a DNA demethylase, promotes early apical bud maturation in poplar. *Plant Cell Environ.* 40, 2806–2819. doi: 10.1111/pce.13056

Conde, D., Perales, M., Sreedasyam, A., Tuskan, G. A., Lloret, A., Badenes, M. L., et al. (2019). Engineering tree seasonal cycles of growth through chromatin modification. *Front. Plant Sci.* 10:412. doi: 10.3389/fpls.2019.00412

Cooke, J. E. K., Eriksson, M. E., and Junttila, O. (2012). The dynamic nature of bud dormancy in trees: Environmental control and molecular mechanisms: bud dormancy in trees. *Plant Cell Environ.* 35, 1707–1728. doi: 10.1111/j.1365-3040.2012.02552.x

de Folter, S., Immink, R. G. H., Kieffer, M., Parenicová, L., Henz, S. R., Weigel, D., et al. (2005). Comprehensive interaction map of the arabidopsis mads box transcription factors. *Plant Cell* 17, 1424–1433. doi: 10.1105/tpc.105.031831

Ding, J., and Nilsson, O. (2016). Molecular regulation of phenology in trees—because the seasons they are a-changin.' *Curr. Opin. Plant Biol.* 29, 73–79. doi: 10.1016/j.pbi.2015.11.007

Dorca-Fornell, C., Gregis, V., Grandi, V., Coupland, G., Colombo, L., and Kater, M. M. (2011). The *Arabidopsis* SOC1-like genes AGL42, AGL71 and AGL72 promote flowering in the shoot apical and axillary meristems: SOC1-like genes control floral transition. *Plant J.* 67, 1006–1017. doi: 10.1111/j.1365-313X.2011.04653.x

Eriksson, M. E., Hoffman, D., Kaduk, M., Mauriat, M., and Moritz, T. (2015). Transgenic hybrid aspen trees with increased gibberellin (GA) concentrations suggest that GA acts in parallel with FLOWERING LOCUS T2 to control shoot elongation. *New Phytol.* 205, 1288–1295. doi: 10.1111/nph.13144

Evans, L. M., Slavov, G. T., Rodgers-Melnick, E., Martin, J., Ranjan, P., Muchero, W., et al. (2014). Population genomics of *Populus trichocarpa* identifies signatures of selection and adaptive trait associations. *Nat. Genet.* 46, 1089–1096. doi: 10.1038/ng.3075

Falavigna, V., da, S., Guitton, B., Costes, E., and Andrés, F. (2019). I want to (Bud) break free: the potential role of DAM and SVP-like genes in regulating dormancy cycle in temperate fruit trees. *Front. Plant Sci.* 9:1990. doi: 10.3389/fpls.2018.01990

Gallardo, F., Fu, J., Cantón, F. R., García-Gutiérrez, A., Cánovas, F. M., and Kirby, E. G. (1999). Expression of a conifer glutamine synthetase gene in transgenic poplar. *Planta* 210, 19–26. doi: 10.1007/s004250050649

Gou, J., Ma, C., Kadmiel, M., Gai, Y., Strauss, S., Jiang, X., et al. (2011). Tissue-specific expression of Populus C19 GA 2-oxidases differentially regulate above- and below-ground biomass growth through

control of bioactive GA concentrations. *New Phytol.* 192, 626–639. doi: 10.1111/j.1469-8137.2011.03837.x

Groover, A., and Cronk, Q. (Eds.). (2017). *Comparative and Evolutionary Genomics of Angiosperm Trees (Vol. 21)*. New York, NY: Springer. doi: 10.1007/978-3-319-49329-9

Hoenicka, H., Nowitzki, O., Hanelt, D., and Fladung, M. (2008). Heterologous overexpression of the birch FRUITFULL-like MADS-box gene BpMADS4 prevents normal senescence and winter dormancy in *Populus tremula* L. *Planta* 227, 1001–1011. doi: 10.1007/s00425-007-0674-0

Horvath, D. P., Sung, S., Kim, D., Chao, W., and Anderson, J. (2010). Characterization, expression and function of DORMANCY ASSOCIATED MADS-BOX genes from leafy spurge. *Plant Mol. Biol.* 73, 169–179. doi: 10.1007/s11103-009-9596-5

Hsu, C.-Y., Adams, J. P., Kim, H., No, K., Ma, C., Strauss, S. H., et al. (2011). FLOWERING LOCUS T duplication coordinates reproductive and vegetative growth in perennial poplar. *Proc. Natl. Acad. Sci. U.S.A.* 108, 10756–10761. doi: 10.1073/pnas.1104713108

Immink, R. G. H., Posé, D., Ferrario, S., Ott, F., Kaufmann, K., Valentim, F. L., et al. (2012). Characterization of SOC1's central role in flowering by the identification of its upstream and downstream regulators. *Plant Physiol.* 160, 433–449. doi: 10.1104/pp.112.202614

Johansson, M., Takata, N., Ibáñez, C., and Eriksson, M. E. (2014). "Monitoring seasonal bud set, bud burst, and cold hardiness in populus," in *Plant Circadian Networks, Vol. 1158*, ed E. D. Staiger (New York, NY: Springer), 313–324. doi: 10.1007/978-1-4939-0700-7_21

Karlberg, A., Englund, M., Petterle, A., Molnar, G., Sjödin, A., Bako, L., et al. (2010). Analysis of global changes in gene expression during activity-dormancy cycle in hybrid aspen apex. *Plant Biotechnol.* 27, 1–16. doi: 10.5511/plantbiotechnology.27.1

Kayal, W. E., Allen, C. C., JU, C. J. T., Adams, E. R. I., King-Jones, S., Zaharia, L. I., et al. (2011). Molecular events of apical bud formation in white spruce, *Picea glauca*. *Plant Cell Environ.* 34, 480–500. doi: 10.1111/j.1365-3040.2010.02257.x

Kitamura, Y., Takeuchi, T., Yamane, H., and Tao, R. (2016). Simultaneous down-regulation of *DORMANCY-ASSOCIATED MADS-box6* and *SOC1* during dormancy release in Japanese apricot (*Prunus mume*) flower buds. *J. Horticult. Sci. Biotechnol.* 91, 476–482. doi: 10.1080/14620316.2016.1173524

Klocko, A. L., Lu, H., Magnuson, A., Brunner, A. M., Ma, C., and Strauss, S. H. (2018). Phenotypic expression and stability in a large-scale field study of genetically engineered poplars containing sexual containment transgenes. *Front. Bioeng. Biotechnol.* 6:100. doi: 10.3389/fbioe.2018.00100

Koncz, C., and Schell, J. (1986). The promoter of TL-DNA gene 5 controls the tissue-specific expression of chimaeric genes carried by a novel type of agrobacterium binary vector. *Mol. Gen. Genet. MGG* 204, 383–396. doi: 10.1007/BF00331014

Lee, H., Suh, S.-S., Park, E., Cho, E., Ahn, J. H., Kim, S.-G., et al. (2000). The AGAMOUS-LIKE 20 MADS domain protein integrates floral inductive pathways in *Arabidopsis*. *Genes Dev.* 14, 2366–2376. doi: 10.1101/gad.813600

Lee, J., and Lee, I. (2010). Regulation and function of SOC1, a flowering pathway integrator. *J. Exp. Bot.* 61, 2247–2254. doi: 10.1093/jxb/erq098

Lee, J., Oh, M., Park, H., and Lee, I. (2008). SOC1 translocated to the nucleus by interaction with AGL24 directly regulates *LEAFY*. *Plant J.* 55, 832–843. doi: 10.1111/j.1365-313X.2008.03552.x

Leida, C., Terol, J., Marti, G., Agusti, M., Llacer, G., Badenes, M. L., et al. (2010). Identification of genes associated with bud dormancy release in *Prunus persica* by suppression subtractive hybridization. *Tree Physiol.* 30, 655–666. doi: 10.1093/treephys/tpq008

Maurya, J. P., and Bhalerao, R. P. (2017). Photoperiod- and temperature-mediated control of growth cessation and dormancy in trees: a molecular perspective. *Ann. Bot.* 120, 351–360. doi: 10.1093/aob/mcx061

Moon, J., Suh, S.-S., Lee, H., Choi, K.-R., Hong, C. B., Paek, N.-C., et al. (2003). The *SOC1* MADS-box gene integrates vernalization and gibberellin signals for flowering in *Arabidopsis*: SOC1 integrates vernalization and GA signals for flowering. *Plant J.* 35, 613–623. doi: 10.1046/j.1365-313X.2003.01833.x

Mravec, J., Skupa, P., Bailly, A., Hoyerová, K., Kreček, P., Bielach, A., et al. (2009). Subcellular homeostasis of phytohormone auxin is mediated by the ER-localized PIN5 transporter. *Nature* 459, 1136–1140. doi: 10.1038/nature08066

Nakagawa, T., Suzuki, T., Murata, S., Nakamura, S., Hino, T., Maeo, K., et al. (2007). Improved gateway binary vectors: high-performance vectors for creation of fusion constructs in transgenic analysis of plants. *Biosci. Biotechnol. Biochem.* 71, 2095–2100. doi: 10.1271/bbb.70216

Pérez-Ruiz, R. V., García-Ponce, B., Marsch-Martínez, N., Ugartechea-Chirino, Y., Villajuana-Bonequi, M., de Folter, S., et al. (2015). XAANTAL2 (AGL14) is an important component of the complex gene regulatory network that underlies arabidopsis shoot apical meristem transitions. *Mol. Plant* 8, 796–813. doi: 10.1016/j.molp.2015.01.017

Pin, P. A., and Nilsson, O. (2012). The multifaceted roles of FLOWERING LOCUS T in plant development: FT, a multifunctional protein. *Plant Cell Environ.* 35, 1742–1755. doi: 10.1111/j.1365-3040.2012.02558.x

Ramos-Sánchez, J. M., Triozzi, P. M., Alique, D., Geng, F., Gao, M., Jaeger, K. E., et al. (2019). LHY2 Integrates night-length information to determine timing of poplar photoperiodic growth. *Curr. Biol.* 29, 2402–2406.e4. doi: 10.1016/j.cub.2019.06.003

Rieu, I., Eriksson, S., Powers, S. J., Gong, F., Griffiths, J., Woolley, L., et al. (2008). Genetic analysis reveals that C $_{19}$ -GA 2-oxidation is a major gibberellin inactivation pathway in *Arabidopsis*. *Plant Cell* 20, 2420–2436. doi: 10.1105/tpc.108.058818

Rinne, P. L. H., Welling, A., Vahala, J., Ripel, L., Ruonala, R., Kangasjärvi, J., et al. (2011). Chilling of dormant buds hyperinduces *FLOWERING LOCUS T* and recruits GA-inducible 1,3-β-glucanases to reopen signal conduits and release dormancy in *Populus*. *Plant Cell* 23, 130–146. doi: 10.1105/tpc.110.081307

Rodriguez-A, J., Sherman, W. B., Scorza, R., Wisniewski, M., and Okie, W. R. (1994). "Evergreen" peach, its inheritance and dormant behavior. *J. Am. Soc. Horticult. Sci.* 119, 789–792. doi: 10.21273/JASHS.119.4.789

Rohde, A., Ruttink, T., Hostyn, V., Sterck, L., Van Driessche, K., and Boerjan, W. (2007). Gene expression during the induction, maintenance, and release of dormancy in apical buds of poplar. *J. Exp. Bot.* 58, 4047–4060. doi: 10.1093/jxb/erm261

Rohde, A., Storme, V., Jorge, V., Gaudet, M., Vitacolonna, N., Fabbrini, F., et al. (2010). Bud set in poplar – genetic dissection of a complex trait in natural and hybrid populations. *New Phytol.* 16, 106–121. doi: 10.1111/j.1469-8137.2010.03469.x

Santamaría, M., Hasbún, R., Valera, M., Meijón, M., Valledor, L., Rodríguez, J. L., et al. (2009). Acetylated H4 histone and genomic DNA methylation patterns during bud set and bud burst in *Castanea sativa*. *J. Plant Physiol.* 166, 1360–1369. doi: 10.1016/j.jplph.2009.02.014

Schonrock, N. (2006). Polycomb-group proteins repressthe floral activator AGL19 in the FLC-independent vernalization pathway. *Genes Dev.* 20, 1667–1678. doi: 10.1101/gad.377206

Shim, J. S., Kubota, A., and Imaizumi, T. (2017). Circadian clock and photoperiodic flowering in *Arabidopsis*: CONSTANS is a hub for signal integration. *Plant Physiol.* 173, 5–15. doi: 10.1104/pp.16.01327

Singh, R. K., Maurya, J. P., Azeez, A., Miskolczi, P., Tylewicz, S., Stojkovič, K., et al. (2018). A genetic network mediating the control of bud break in hybrid aspen. *Nat. Commun.* 9:4173. doi: 10.1038/s41467-018-06696-y

Singh, R. K., Svystun, T., AlDahmash, B., Jönsson, A. M., and Bhalerao, R. P. (2017). Photoperiod- and temperature-mediated control of phenology in trees—A molecular perspective. *New Phytol.* 213, 511–524. doi: 10.1111/nph.14346

Trainin, T., Bar-Ya'akov, I., and Holland, D. (2013). ParSOC1, a MADS-box gene closely related to *Arabidopsis* AGL20/SOC1, is expressed in apricot leaves in a diurnal manner and is linked with chilling requirements for dormancy break. *Tree Genet. Genom.* 9, 753–766. doi: 10.1007/s11295-012-0590-8

Triozzi, P. M., Ramos-Sánchez, J. M., Hernández-Verdeja, T., Moreno-Cortés, A., Allona, I., and Perales, M. (2018). Photoperiodic regulation of shoot apical growth in poplar. *Front. Plant Sci.* 9:1030. doi: 10.3389/fpls.2018.01030

Tylewicz, S., Petterle, A., Marttila, S., Miskolczi, P., Azeez, A., Singh, R. K., et al. (2018). Photoperiodic control of seasonal growth is mediated by ABA acting on cell-cell communication. *Science* 360, 212–215. doi: 10.1126/science.aan8576

Vimont, N., Schwarzenberg, A., Domijan, M., Beauvieux, R., Arkoun, M., Jamois, F., et al. (2019). Hormonal balance finely tunes dormancy status in sweet cherry flower buds. *Tree Physiol.* 4, 544–561. doi: 10.1093/treephys/tpaa122

Voogd, C., Wang, T., and Varkonyi-Gasic, E. (2015). Functional and expression analyses of kiwifruit *SOC1* -like genes suggest that they may not have a role in the transition to flowering but may affect the duration of dormancy. *J. Exp. Bot.* 66, 4699–4710. doi: 10.1093/jxb/erv234

Wang, H., Wu, C., Ciais, P., Peñuelas, J., Dai, J., Fu, Y., et al. (2020). Overestimation of the effect of climatic warming on spring phenology due to misrepresentation of chilling. *Nat. Commun.* 11:4945. doi: 10.1038/s41467-020-18743-8

Wang, J., Gao, Z., Li, H., Jiu, S., Qu, Y., Wang, L., et al. (2020). Dormancy-associated MADS-Box (DAM) genes influence chilling requirement of sweet cherries and co-regulate flower development with SOC1 gene. *Int. J. Mol. Sci.* 21:921. doi: 10.3390/ijms21030921

Wareing, P. F. (1956). Photoperiodism in woody plants. *Annu. Rev. Plant Physiol.* 7, 191–214. doi: 10.1146/annurev.pp.07.060156.001203

Weiser, C. J. (1970). Cold resistance and injury in woody plants: knowledge of hardy plant adaptations to freezing stress may help us to reduce winter damage. *Science* 169, 1269–1278. doi: 10.1126/science.169.3952.1269

Wu, R., Tomes, S., Karunairetnam, S., Tustin, S. D., Hellens, R. P., Allan, A. C., et al. (2017). SVP-like MADS box genes control dormancy and budbreak in apple. *Front. Plant Sci.* 8:477. doi: 10.3389/fpls.2017.00477

Yanovsky, M. J., and Kay, S. A. (2002). Molecular basis of seasonal time measurement in *Arabidopsis*. *Nature* 419, 308–312. doi: 10.1038/nature00996

Yordanov, Y. S., Ma, C., Strauss, S. H., and Busov, V. B. (2014). EARLY BUD-BREAK 1 (*EBB1*) is a regulator of release from seasonal dormancy in poplar trees. *Proc. Natl. Acad. Sci. U.S.A.* 111, 10001–10006. doi: 10.1073/pnas.1405621111

Zawaski, C., Kadmiel, M., Pickens, J., Ma, C., Strauss, S., and Busov, V. (2011). Repression of gibberellin biosynthesis or signaling produces striking alterations in poplar growth, morphology, and flowering. *Planta* 234, 1285–1298. doi: 10.1007/s00425-011-1485-x

Zheng, C., Kwame Acheampong, A., Shi, Z., Halaly, T., Kamiya, Y., Ophir, R., et al. (2018). Distinct gibberellin functions during and after grapevine bud dormancy release. *J. Exp. Bot.* 69, 1635–1648. doi: 10.1093/jxb/ery022

Zheng, S., He, J., Lin, Z., Zhu, Y., Sun, J., and Li, L. (2020). Two MADS-box genes regulate vascular cambium activity and secondary growth by modulating auxin homeostasis in *Populus*. *Plant Commun.* 100134. doi: 10.1016/j.xplc.2020.100134 (in press).

Zhuang, W., Gao, Z., Wang, L., Zhong, W., Ni, Z., and Zhang, Z. (2013). Comparative proteomic and transcriptomic approaches to address the active role of GA4 in Japanese apricot flower bud dormancy release. *J. Exp. Bot.* 64, 4953–4966. doi: 10.1093/jxb/ert284

Conflict of Interest: The authors declare that the research was conducted in the absence of any commercial or financial relationships that could be construed as a potential conflict of interest.

frontiers in Plant Science

ORIGINAL RESEARCH
published: 02 July 2021
doi: 10.3389/fpls.2021.664122

Drought and Nitrogen Application Modulate the Morphological and Physiological Responses of *Dalbergia odorifera* to Different Niche Neighbors

Li-Shan Xiang[1,2], *Ling-Feng Miao*[1,3,4] *and Fan Yang*[1,3,4]*

[1] School of Ecological and Environmental Sciences, Hainan University, Haikou, China, [2] School of Forestry, Hainan University, Haikou, China, [3] Center for Eco-Environmental Restoration Engineering of Hainan Province, Haikou, China, [4] Key Laboratory of Agro-Forestry Environmental Processes and Ecological Regulation of Hainan Province, Haikou, China

Mixed stands can be more productive if growth facilitation via niche segregation occurs. *Dalbergia odorifera* T. Chen, a tropical tree species endemic to Hainan Island with great economic values, belongs to the family Leguminosae. However, selecting mixed species with suitable ecological niches to efficiently construct mixed forests of *D. odorifera* in the context of abiotic stress [drought, nitrogen (N) deposition] remained obscure. In the present study, the target plant *D. odorifera* was planted with the same species *D. odorifera*, heterogeneous but the same family *Delonix regia* and non-Leguminous Family *Swietenia mahagoni* in the root interaction and isolated models under two watering regimes [100% and 30% field capacity (FC)] and two N applications (application, non-application), respectively. Principle component analysis based on the performances of growth, phenotype, and physiology was performed to identify the main factors affected by the treatments and the most discriminatory effects of water, N level, and species interaction models. Both comprehensive evaluation values and comprehensive index values were calculated to evaluate the influences of different niche neighbors on *D. odorifera*. Results showed that *D. odorifera* was benefited from *S. mahagoni* but inhibited from *D. odorifera* in all treatments under root system interaction. Drought stress aggravated the inhibitory effects on *D. odorifera* from *D. odorifera*. N application stimulated the promoted effects on *D. odorifera* from *S. mahagoni* but enhanced competition intensity of *D. odorifera* from *D. regia* under the 100% FC condition. N application alleviated the inhibitory effect of drought stress on *D. odorifera* from *D. odorifera* and *S. mahagoni*. Furthermore, the responses of *D. odorifera* to different niche neighbors were dominated by belowground interaction rather than the negligible aboveground one. Therefore, the feasibility of niche segregation as the criterion for selecting neighbors to construct *D. odorifera* mixed stands was confirmed. In addition, water level and N application could alter responses of *D. odorifera* to different niche neighbors under the root system interaction. Appropriate N application could alleviate the inhibitory effect of drought stress on *D. odorifera* in its mixed forests. A mixture with *S. mahagoni* under appropriate N application could be the optimal planting model.

Keywords: niche difference, biomass accumulation and allocation, root system interaction models, morphological and physiological response, root system isolated model

OPEN ACCESS

Edited by:
Sanushka Naidoo, University of Pretoria, South Africa

Reviewed by:
María Reguera, Autonomous University of Madrid, Spain
Mohammad Nauman Khan, Huazhong Agricultural University, China

***Correspondence:**
Fan Yang
yangfan@hainanu.edu.cn;
fanyangmlf6303@163.com

Specialty section:
This article was submitted to Plant Abiotic Stress, a section of the journal Frontiers in Plant Science

Received: *04 February 2021*
Accepted: *07 June 2021*
Published: *02 July 2021*

Citation:
Xiang L-S, Miao L-F and Yang F (2021) Drought and Nitrogen Application Modulate the Morphological and Physiological Responses of Dalbergia odorifera to Different Niche Neighbors. Front. Plant Sci. 12:664122. doi: 10.3389/fpls.2021.664122

HIGHLIGHTS

- *Dalbergia odorifera* benefitted from *Swietenia mahagoni* but was inhibited by the conspecifics.
- Drought aggravated the inhibitory effects on *D. odorifera* from the conspecifics.
- Nitrogen (N) application stimulated the positive effects on *D. odorifera* from *S. mahagoni* but enhanced competition intensity of *D. odorifera* from *Delonix regia* under well-watered conditions.
- N application alleviated the inhibitory effects of the drought stress on *D. odorifera* from the conspecifics and *S. mahagoni*.
- Negligible aboveground competition occurred in root isolated models.

INTRODUCTION

Interaction among species affects plant growth and community structure (Goisser et al., 2016; Guo et al., 2016). Compared with the traditional pure stands, mixed stands had greater ecological advantages such as higher productivity, biodiversity, and resistance to abiotic stresses in forest management (Richards et al., 2010; Nguyen et al., 2015; Forrester and Bauhus, 2016; Liu et al., 2018). The reduction of competition or facilitation has been proposed to explain the increased productivity from mixed stands (Chomel et al., 2014; Forrester and Bauhus, 2016). Facilitation refers to the fact that a species promotes the growth of its neighboring species by improving the environment [e.g., nitrogen (N) fixation from leguminous species]. Niche segregation is often the basis to select species to reduce competition when constructing mixed stands, such as inter-specific differences in functional traits, resource demand, and absorptive capacity (e.g., shade tolerance, growth rate, root morphology, root structure, nitrogen fixation capacity, nutrient preference) (Forrester and Bauhus, 2016). Also, niche complementarity theory implies that greater niche separation among neighbors may produce more favorable benefits during interaction (File et al., 2012). For example, the interaction among the same species and one among different species belonging to the same genus have different effects on the growth because of different niches in resource utilization (Burns and Strauss, 2011; Bowsher et al., 2017). Thus, niche separation in structural and functional traits via competitive reduction is generally regarded as the primary criteria in selecting neighboring species for mixed forests, and it is widely used to enhance plant growth, productivity, and adaptability to abiotic stresses during plantation forest management (Richards et al., 2010; Pretzsch et al., 2013; Nguyen et al., 2015; Liu et al., 2018).

There is considerable variability during the processes of species interaction in mixed stands along with resource availability or climatic conditions (Forrester, 2014; Goisser et al., 2016; Svanfeldt et al., 2017; Calama et al., 2019). Water deficiency and N deposition are very common with the aggravation of global climate change (Goisser et al., 2016; Liang et al., 2019). It exerted strong impacts on forest ecosystems, individual tree growth, and community composition by species competition (Yi et al., 2015; Aldea et al., 2017; Calama et al., 2019; Helluy et al., 2020). Related studies have confirmed that the interactive relationship among neighboring species can be modified by the variations of abiotic factors, such as belowground resource competition for soil water and nutrient and aboveground competition for light source (Craine et al., 2013; Pierik et al., 2013). For example, the declined growth and death of fir are affected by the increasing competition resulted from abiotic stresses (Linares et al., 2009). Therefore, whether the method of selecting mixed-species based on niche separation will continue to work despite various resource levels (water and N) must be considered.

Water is a key resource that determines individual growth, stand productivity, and dynamics of competition. The low water availability can induce belowground competition for water resources. Related studies have confirmed the adaptive strategy of neighboring species and the outcome of competition would be modified by drought stress in mixed plantations (Wright et al., 2015; Goisser et al., 2016; Aldea et al., 2017; Helluy et al., 2020). For example, in response to drought stress, the plant may maximize root length and root surface area and modify root depth or placement to access more water (Aschehoug et al., 2016); The responses from the same species under a water-limited condition were aggravated because of the similarity of resource utilization (Chen et al., 2014; Calama et al., 2019). The competitive effect of neighbors of *Arrhenatherum elatius* was transformed into a facilitative effect when the plants were exposed to drought (Grant et al., 2014).

Abiotic factors such as water, nutrition, and light may occur simultaneously and interact strongly (Niinemets, 2010). It implies that the species interaction for the combined nutrients and light or the combined nutrients and water has a greater regulatory effect on plant behavior than the single competition (Mittler, 2006; Niinemets, 2010; Forrester, 2014). Light competition causes the increment in aboveground biomass and the reduction in belowground investment, possibly because light requirement affects belowground tissue competition for water and nutrients (Aschehoug et al., 2016). For example, the field experiment on the *Agropyron desertorum* shows that light affects the belowground root structures and resource

Abbreviations: Branch, the number of branch; B/A, the ratio of belowground dry matter to aboveground dry matters; Caro, carotenoid content; CAT, catalase activity; Chl, total chlorophyll content; Chl a, chlorophyll a content; Chl b, chlorophyll b content; *Ci*, intercellular CO_2 concentration; D, stem diameter; *E*, comprehensive evaluation; DD, interaction models between *Dalbergia odorifera* and *D. odorifera*; D/D, interaction models with partition pots between *D. odorifera* and *D. odorifera*; DR, interaction models between *D. odorifera* and *Delonix regia*; D/R, interaction models with partition pots between *D. odorifera* and *D. regia*; DS, interaction models between *D. odorifera* and *Swietenia macrophylla*; D/S, interaction models with partition pots between *D. odorifera* and *S. macrophylla*; FC, field capacity; *Gs*, stomatal conductance; H, height; LA, leaf area; LDM, leaf dry matter; L/S, the ratio of leaf to shoot dry matter; L/R, the ratio of leaf to root dry matter; N, nitrogen; NSC, non-structural carbohydrates; Number (L), the number of leaves; *Pn*, net photosynthesis rate; PNUE, photosynthetic nitrogen-use efficiency; POD, peroxidase; Proline, proline content; RCI, relative competition intensity; RDM, root dry matter; *Tr*, transpiration rate; RWC, relative water content; RWC(L), leaf relative water content; RWC(R), root relative water content; RWC(S), stem relative water content; SDM, stem dry matter; SLW, specific leaf weight; S/R, ratio of shoot to root dry matter; SOD, superoxide dismutase; Soluble sugar/starch, the ratio of soluble sugar to starch content; TDM, total dry matters; WUEi, intrinsic water-use efficiency.

distribution when plants are exposed to compound stresses of both aboveground and belowground competition (Bilbrough and Caldwell, 1995). Accordingly, transformation, synergy, or interaction relationships may be found among aboveground and belowground competition processes. Our study investigated whether the aboveground interaction (e.g., light competition) can affect growth and underground competition via root system isolated experiments.

The previous studies have reported that Leguminous plants have different responses to N addition. Some Leguminous species could keep homeostasis after N addition due to N acquisition via both absorption from the soil and biological N fixation (Markham and Zekveld, 2007; Guo et al., 2017; Wang et al., 2018). However, other Leguminous species are sensitive to N deposition (Hansen et al., 1992) and converted the symbiont N fixation strategy into soil N absorption with sufficient N application (Markham and Zekveld, 2007; Wang et al., 2019). In addition, there are substantial pieces of evidence that N application can modify the N transfer and the interaction in mixed stands, such as non-leguminous *Eucalyptus urophylla* × *Eucalyptus grandis* and leguminous *Dalbergia odorifera* T. Chen (Yao et al., 2019). The related study indicated that Leguminous species play a key role in measuring the impacts of various abiotic environments on the dynamics of forestry systems (Wang et al., 2018). Therefore, under the background of precipitation reduction and N deposition increase, the effects of simulated N deposition increase on the growth and development of Leguminosae Family *D. odorifera* in mixed forests should be further studied.

D. odorifera, a tropical tree species endemic to Hainan Island that has great economic values (Chan et al., 1998; Yu et al., 2007), belongs to the family Leguminosae. At present, *D. odorifera* is widely popularized and cultivated in the subtropical regions in China (Meng et al., 2010; Sun et al., 2015). However, the pure forest of *D. odorifera* does not grow well in these regions because of drought and the lack of suitable neighbors. Therefore, it should be encouraged that an optimal mixed-plantation model of improving growth and development of *D. odorifera* and stimulating N fixation under drought and N deposition. *Delonix regia* and *Swietenia mahagoni* are also tropical woody plants with medical and economic values (Rodan et al., 1992; Guevara et al., 1996; Mishra et al., 2011), which belong to the Leguminosae Family and different family of *D. odorifera*, respectively. Accordingly, the degree of niche differentiation among these three tree species gradually increases with the variation trend of plants from species to family. Collectively, constructing the *D. odorifera* plantation and exploring its optimal plantation models via the combination of abiotic factors (water and N) and species interaction is important.

In the present study, we hypothesized that (1) *D. odorifera* would differentially respond to different niche neighbors under the root system interaction or isolation conditions, (2) the responses of *D. odorifera* to different neighbors would be modulated by the N application and drought stress or combined application, and (3) *D. odorifera* would be influenced by the belowground interaction from different neighbors rather than aboveground interaction.

MATERIALS AND METHODS

Plant Materials and Experimental Designs

In the present study, *D. odorifera* of Family Leguminosae was used as target species, *D. regia* and *S. mahagoni* were used as different related-niche neighbors of *D. odorifera*. Moreover, responses to different niche neighbors and interactions between aboveground and belowground tissues under water deficiency and N application were considered. The whole experiments were conducted in a greenhouse at the Hainan University, Haikou City, China (20° 03′ 33.2″ N, 110° 20′ 16.9″ E), where the climate is characterized by a mean annual temperature, mean annual precipitation, and relative humidity are 24.3°C, 1,684 mm, and 85%, respectively.

A total of 720 1-year-old seedlings (480 *D. odorifera* seedlings, 120 *D. regia* seedlings, and 120 *S. mahagoni* seedlings) were collected from the local nursery garden in Jianfengling (18° 42′ 57.91″ N, 108° 52′ 18.65″ E), Ledong County, Hainan Province, China. All selected healthy seedlings were kept approximately the same basal stem diameter and height (20 cm) to reduce asymmetries in competition caused by differences in plant size. The climatic conditions of Jianfengling are similar to the experimental site.

The experimental layout was completely randomized with three factors (species interaction, water regimes, and N fertilizer application), as shown in **Figure 1**. One *D. odorifera* seedling and one neighboring species seedling were transplanted in a plastic pot (50 × 21 × 16 cm, length × wide × height) at the end of February 2018. Plastic pots filled with 15 kg homogenized soil (red soil: sand = 1:2, v/v). The distance between pots was maintained at 100 cm to ensure that they are not affected by each other. Two individuals (two *D. odorifera* seedlings, one *D. odorifera* seedling and one *D. regia* seedling, or one *D. odorifera* seedling and *S. mahagoni* seedling) per pot were spaced ∼25 cm apart. In order to eliminate the damages to the original root system of seedlings during transplanting, each seedling was transferred with the container soil (about 80 g dry weight) together after removing the plastic bag.

Two kinds of pots were used for the experiment to provide two types of root interaction and isolation: pots were separated into two isolate parts by a plastic partition in the middle of the pot to exclude root interaction between *D. odorifera* and neighboring species, i.e., only aboveground interaction was allowed between them; the other pot was without partition and so belowground root interaction was possible, i.e., where the two species could interact from aboveground parts and belowground roots simultaneously. So, species interaction included three treatments under belowground root system interaction models with no-partition pots (one intra-specific interaction, *D. odorifera* + *D. odorifera*, DD; one inter-specific interaction between species belonging to different genus but the same family, *D. odorifera* + *D. regia*, DR; one inter-specific interaction between species belonging to a different family, *D. odorifera* + *S. mahagoni*, DS). Accordingly, another

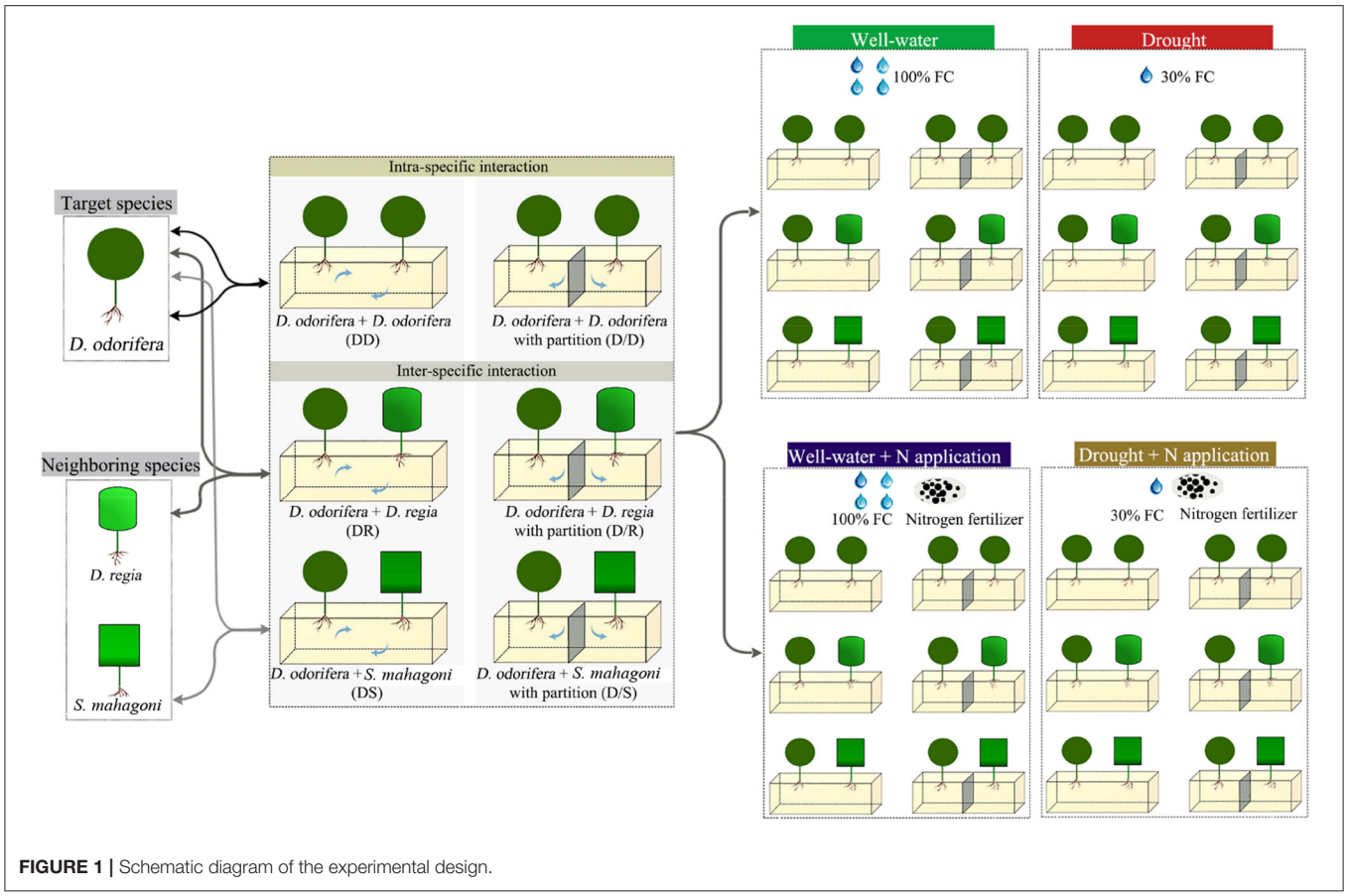

FIGURE 1 | Schematic diagram of the experimental design.

three treatments underground root system isolated models with partition pots (*D. odorifera* + *D. odorifera*, D/D; *D. odorifera* + *D. regia*, D/R; *D. odorifera* + *S. mahagoni*, D/S) were set up.

A full-strength Hoagland's solution was supplemented regularly to ensure the nutrient requirement during the cultivation of *D. odorifera*. After growing steadily for 4 weeks, two watering regimes [well-watered condition, 95–100% field capacity (FC); drought-stressed condition, 25–30% FC] and two N applications (application and non-application) treatments were carried out. N fertilizer was provided as NH_4NO_3 and was dissolved in pure water (the concentration of N solution was 0.64 and 3.2 g/L). The N treatments included no-N application and N application. In the N application treatment, 1,000 mL 0.64 g/L N solution in the well-watered condition and 200 mL 3.2 g/L N solution in the drought condition were poured into each pot, respectively. Accordingly, N solution was replaced by equal volume pure water in the no-N application treatment. N solution was irrigated to the pots once a week during the experiment. The pots were weighed every day to keep 95–100% FC in the well-watered treatments and 25–30% FC in the drought treatments. A total of 24 treatments were performed. Five replications, three pots in each replication, were included in each treatment. After 120 days of treatment, the plants were harvested (**Supplementary Figure 1**).

Determination of Growth and Phenotypic Traits

At the end of the experiment, five pots from each treatment were selected randomly to measure the height (H), stem diameter (D), the number of branches and total leaves, and leaf area (LA). The LA was measured by an LI-3000 area meter (LI-3000C, LI-COR, USA). Then, the selected *D. odorifera* were harvested and divided into leaves, stems, and roots. Biomass samples were dried to a constant weight at 70°C. The leaf dry matters (LDM), shoot dry matters (SDM), and root dry matters (RDM) were then determined. The total dry matter (TDM) was the sum of the LDM, SDM, and RDM. The ratio of leaf to stem dry matters (L/S) was calculated as LDM divided by the SDM. The ratio of leaf to root dry matters (L/R) was calculated as LDM divided by the RDM. The ratio of stem to root dry matters (S/R) was calculated as SDM divided by the RDM. The ratio of belowground to aboveground dry matters (B/A) was calculated as belowground tissue dry matters divided by the aboveground tissue dry matters (the sum of the leaf and stem dry matters); the specific leaf weight (SLW) was calculated as the ratio of leaf weight to LA.

Gas Exchange Measurements

The fourth fully expanded leaf of *D. odorifera* from each replication was used to measure the gas exchange with the LI-6400 portable photosynthesis measuring system (LI-6400XT, Gene Company, USA) according to the methods of Xu et al.

(2008). The net photosynthetic rate (*Pn*), stomatal conductance (*Gs*), intercellular CO_2 concentration (*Ci*), and transpiration rate (*Tr*) were measured in controlled conditions between 08:00 and 11:00. The red and blue light source was used, and light source intensity was set to 1,200 $\mu mol \cdot m^{-2} \cdot s^{-1}$. The intrinsic water-use efficiency (WUEi) was calculated as the ratio of *Pn* to *Tr*. N concentration in the leaves was determined by the semi-micro Kjeldahl method (Mitchell, 1998). Afterward, photosynthetic N-use efficiency (PNUE) was further calculated as *Pn* per leaf N content per area.

Determination of Activities of Catalase (CAT), Superoxide Dismutase (SOD), and Peroxidase (POD), and Proline Content

The fresh leaf samples from five randomly chosen individuals in each treatment were collected for CAT, SOD, and POD analyses at the end of the experiment. The CAT, SOD, and POD activity were measured as described by Yang et al. (2011). A sample of 0.2 g leaves was grounded with liquid N and homogenized in 10 mL of 100 m mol/L universal sodium phosphate extraction buffer. Details of the extraction buffer have been described by Han et al. (2015). After centrifugation, the supernatant was used to determine proline, as Yang et al. (2015) described.

Determination of Photosynthetic Pigment Contents, Relative Water Content, and Leaf Non-Structural Carbohydrate Content

About 0.2 g fresh leaves from each replication were used to determine chlorophyll a, chlorophyll b, and carotenoids contents. These fresh leaves were extracted in 95% (v/v) ethanol. The absorbance values were measured with the spectrophotometer (UV-1800PC, Shanghai Meipda Instrument Co., Ltd, China) at 470, 649, and 665 nm after being placed in the dark box for 24 h. The absorbance values were converted to chlorophyll and carotenoid concentrations described by Zhang et al. (2016a,b). The RWC of the leaves, stems, and roots were calculated by fresh weight and dry weight according to the method of González and González-Vilar (2001). The dried leaves were ground to powder to determine soluble sugar and starch content according to the procedure of the anthrone-sulfuric acid method (Yemm and Willis, 1954) and the anthrone reagent (Yemm and Willis, 1954) using glucose as the standard, respectively. About 50 mg of dry powdered plant samples in 10-mL centrifuge tubes were mixed with 5 mL of 80% (v/v) ethanol, incubated in a water bath at 80°C for 30 min, and centrifuged at 5,000 rpm for 15 min. This procedure was repeated twice, and the supernatants pooled together for the total soluble sugar content measurement. The solid residues left in the centrifuge tubes after soluble sugar extraction were dried in a vacuum drier at 80°C for 24 h to the determination of starch. The reaction in the tubes was accelerated by heating in a boiling water bath for 15 min after adding 4 mL of hot distilled water. Then, the sample was hydrolyzed with 4 mL perchloric acid for 15 min after cooling, followed by centrifugation at 2,500 rpm for 15 min. Samples were then extracted twice with perchloric acid, and the supernatants were combined for starch content measurement by the anthrone reagent. NSC was calculated by the sum of total starch contents and soluble sugar contents.

Data Analysis

The competition index could assess intra-specific and inter-specific relations among three tested species, which could be quantified by relative competition intensity (RCI). The RCI on *D. odorifera* was calculated by the following equation (Jolliffe, 2000):

$$RCI_{ab} = (Y_{ab} - Y_{aa})/Y_{aa},$$

Y_{ab} and Y_{aa} are the average total biomass of *D. odorifera* under inter-specific interaction and total biomass under intra-specific interaction. The growth of *D. odorifera* was considered to be promoted and subjected to positive effects by interaction from neighbors when $RCI_{ab} > 0$ but led to diametrically opposite results when $RCI_{ab} < 0$. In addition, the high value of RCI_{ab} indicated the strong positive effect of inter-specific interaction on the growth of *D. odorifera*.

Principal component analysis (PCA) was used to identify the main factors affecting *D. odorifera* by treatments (water, N application, and species interaction models) and the most discriminatory effects of these treatments. PCA based on trait combinations (growth, phenotypic and physiological indexes (height, stem diameter, the numbers of branches, total leaves, etc.) and Pearson correlation coefficient were conducted using the canoco5.0 (Microcomputer Power, Ithaca, NY). The results were expressed as mean ± standard error. Mean values (height, stem diameter, the numbers of branches, and total leaves. etc.), from each replication were compared using linear mixed models. In addition, mixed models were also conducted to assess the effects of water, N application, species interaction, and their interactions on each trait. The water regimes, N application, and species interaction were used as fixed factors. Linear mixed models were used for all response variables. Tukey's test performed multiple comparison analyses. Before statistical analyses, homoscedasticity of variances and normality of distributions was checked for each variable by Levene's test and Shapiro-Wilk's test, respectively, and log-transformed were applied to correct for deviations from these assumptions when needed. All statistical effects were considered significant at $P < 0.05$. Linear mixed models were implemented using SPSS 19.0 for Windows statistical software package (SPSS, Chicago, IL).

The comprehensive evaluation value (*E*) and comprehensive index value (*C*) were used to evaluate the effects of different neighboring species on the *D. odorifera* in the same water regimes and N application under the root system interaction models. *E* and *C* were calculated based on the phenotypic and physiological traits according to the following equation (Fang et al., 2017):

$$X(\mu) = (C(\mu) - X_{min})/(X_{max} - X_{min}), \quad (1)$$

$$\overline{X_i} = \frac{1}{n} \sum_{j=1}^{n} X_{ji}, \quad (2)$$

$$I_i = \sqrt{\sum_{j=1}^{n} (X_{ji} - \overline{X_i})^2}/\overline{X_i}, \quad (3)$$

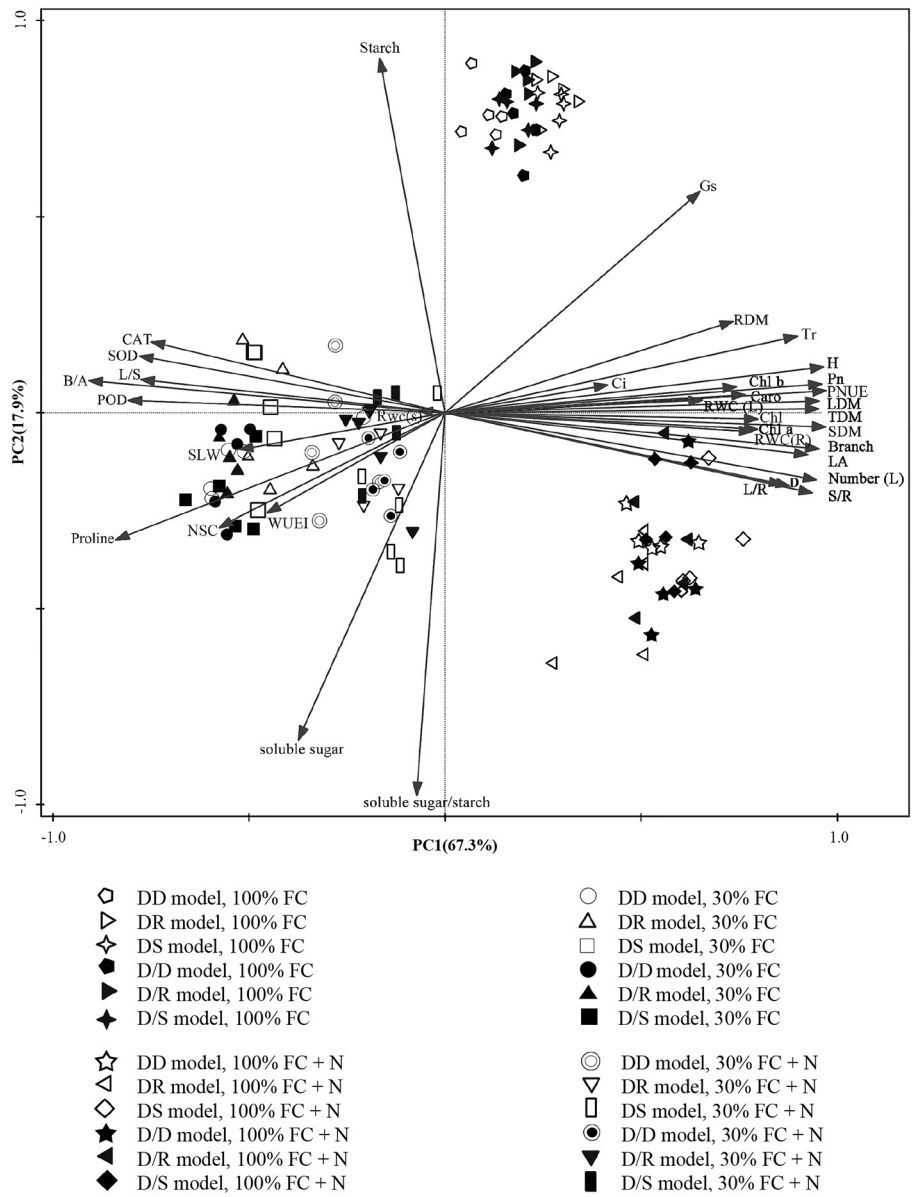

FIGURE 2 | PCA of *Dalbergia odorifera* in different water, nitrogen application, and species interaction according to growth, phenotypic and physiological properties. PC1, the first principal component; PC2, the second principal component; 100% FC, 100% field capacity; 30% FC, 30% field capacity; 100% FC + N, 100% field capacity and N application treatment; 30% FC + N, 30% field capacity and N application treatment; DD, DR, and DS indicated that *D. odorifera* planted with *D. odorifera*, *D. regia*, and *S. mahagoni* under the root system interaction, respectively; D/D, D/R, and D/S indicated that *D. odorifera* planted with *D. odorifera*, *D. regia*, and *S. mahagoni* under the root system isolation, respectively.

$$W_i = I_i / \sum_{i=1}^{m} I_i, \quad (4)$$

$$E = \sum_{i=1}^{n} [X(\mu) \times W_i], \quad (5)$$

where $X(\mu)$, $C(\mu)$, X_{min}, and X_{max} in formula (1) are the subordinate function value, observed value, and the minimum and maximum value of the μth comprehensive indicator, respectively. X_i, n, and X_{ji} in formula (2) represent the mean of the ith evaluation index, the number of interaction models (DD, DR, and DS), and the ith evaluation index of the jth interaction models, respectively. I_i and X_{ji} in formula (3) is the coefficient of the standard deviation of the ith evaluation index and the ith evaluation index of the interaction models. W_i and I_i in formula (4) are the weighted coefficient and contribution rate of the ith comprehensive indexes. The E value in formula (5) indicates the comprehensive evaluation value for response to different neighbors for *D. odorifera* under the same water and N application. A high E value suggested the remarkable promoted effect from a neighbor on *D. odorifera* in a given condition.

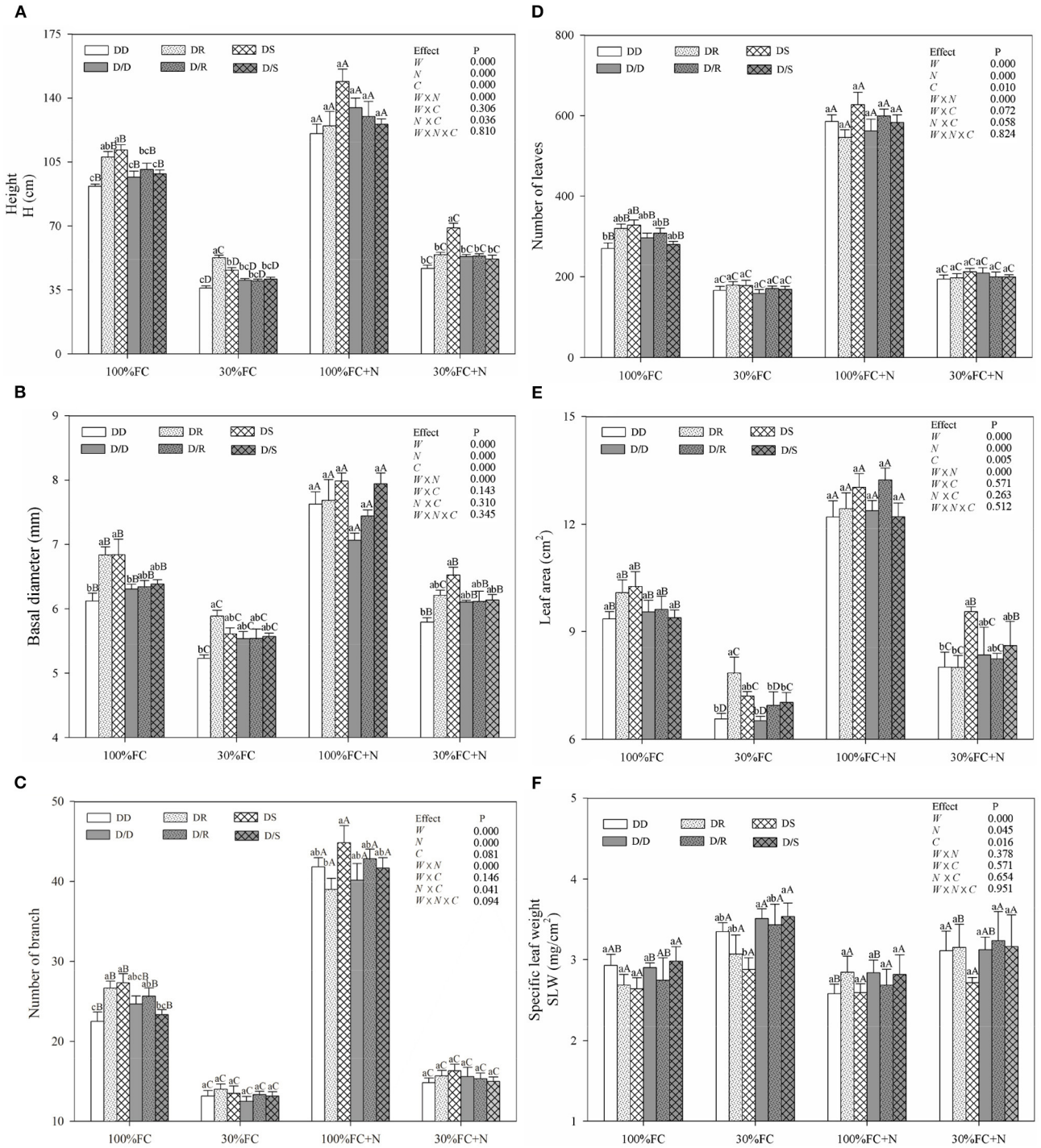

FIGURE 3 | Effects of water, N application, and species interaction on height **(A)**, basal diameter **(B)**, number of branch **(C)**, leaves **(D)**, leaf area **(E)**, and specific leaf weight **(F)** of *D. odorifera*. 100% FC, 100% field capacity; 30% FC, 30% field capacity; 100% FC + N, 100% field capacity and N application treatment; 30% FC + N, 30% field capacity and N application treatment; DD, DR, and DS indicated that *D. odorifera* planted with *D. odorifera*, *D. regia*, and *S. mahagoni* under the root system interaction, respectively; D/D, D/R, and D/S indicated that *D. odorifera* planted with *D. odorifera*, *D. regia*, and *S. mahagoni* under the root system isolation, respectively; *W*, water effect; *N*, nitrogen effect; *C*, species interaction effect; *W* × *N*, the interaction effect of water and nitrogen; *W* × *C*, the interaction effect of water and species interaction; *N* × *C*, the interaction effect of nitrogen and species interaction; *W* × *N* × *C*, the interaction effect of water, nitrogen, and species interaction; Mixed model was conducted to evaluate the influence of different factors and their interaction effects. Values followed by different lowercase above the bars are significantly different at $P < 0.05$ among different species interaction models under the same water and N application; Values followed by different uppercase above the bars are significantly different at $P < 0.05$ among different water and N fertilization application under the same interaction models.

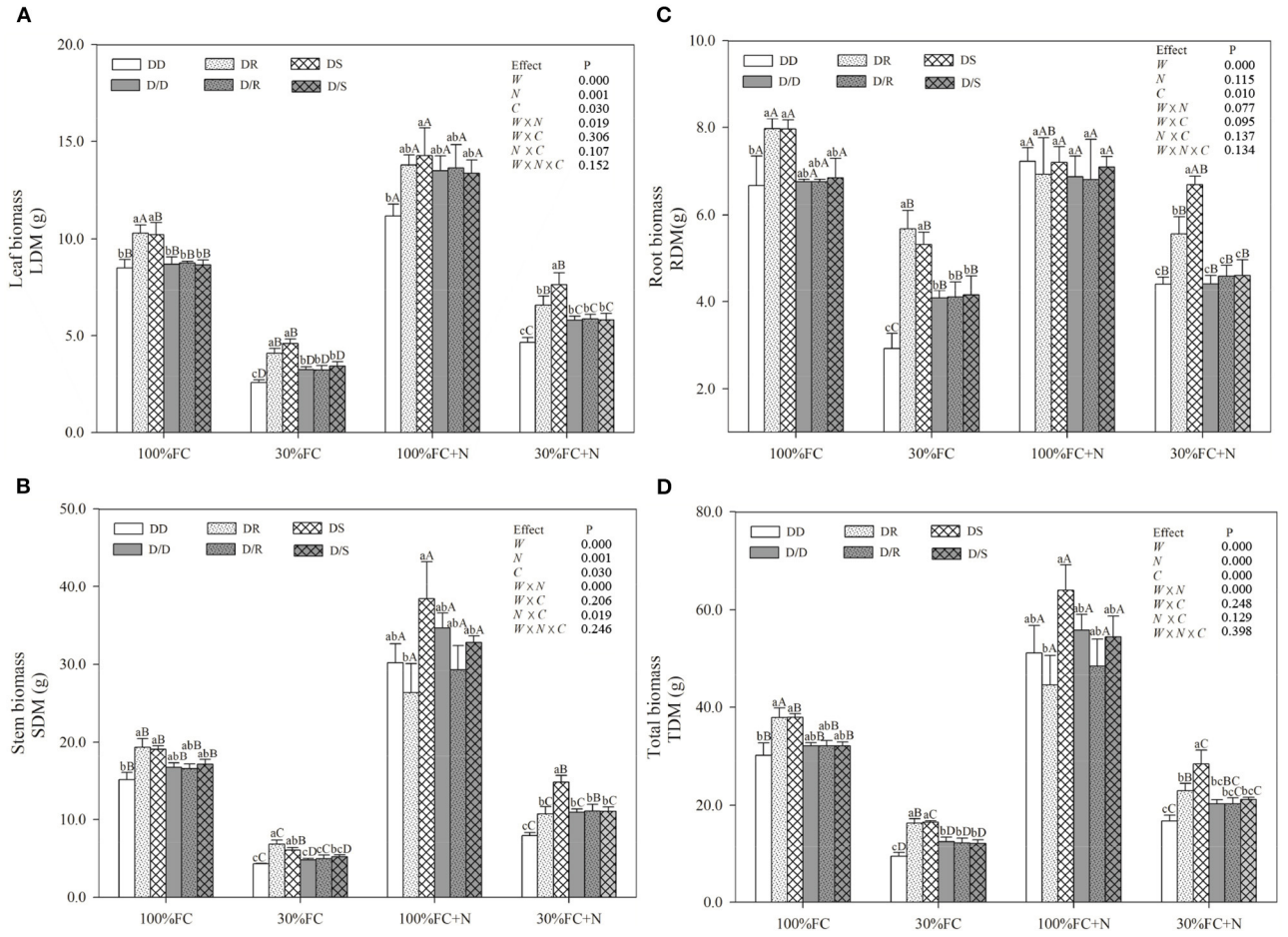

FIGURE 4 | Effects of water, N application, and species interaction on leaf biomass **(A)**, stem biomass **(B)**, root biomass **(C)**, and total biomass **(D)** of *D. odorifera*. Treatments of water, N application, species interaction, data description, and statistics are shown in **Figure 3**.

E values were calculated according to the formulas (1–5) through SPSS 19.0.

RESULT

PCA Analysis

The PCA showed a clear description of the combined phenotypic and physiological properties of *D. odorifera* in different planting models under different water regimes and N application conditions (**Figure 2**). SPSS extracted the two principal components, and the accumulative variance contribution was 85.2%. *D. odorifera* seedlings under 100% FC (in the first quadrant), 100% FC + N (in the fourth quadrant), and 30% FC and 30% FC + N treatments (both treatments were in the second and third quadrants but could be separated from each other) indicated that the seedlings were affected by water and N regime conditions. Under the root system interaction models, *D. odorifera* from DR (*D. odorifera* + *D. regia*) and DS (*D. odorifera* + *S. mahagoni*) models under 100% FC and 30% FC conditions were not separated from each other, whereas *D. odorifera* from these inter-specific interaction models and the intra-specific interaction model (*D. odorifera* + *D. odorifera*, DD) could be distinguished from each other. The majority of *D. odorifera* from the DR model and DS model were separated under N application conditions. However, *D. odorifera* among the interaction models under the root system isolated models (D/D, D/R, and D/S) were hard to distinguish from each other (**Figure 2**), indicating that *D. odorifera* under the root system isolated models could be almost insensitive to neighbors. In addition, the PCA showed that height, leaf number, number of branches, LA, biomass accumulation and allocation, gas exchange, NSC, WUEi, antioxidant enzyme activities, and proline content were the main effects on PC1. PC2 was primarily affected by soluble sugar, starch, and the ratio of soluble sugar to starch. In addition, height, number of leaf and branches, dry matter accumulation, and PNUE showed a positive correlation with *Pn* while had negative correlations with the WUEi, NSC, B/A ratio, antioxidant enzymes activities, and proline content.

TABLE 1 | Biomass allocation of *D. odorifera* when exposed to different water, N application, and species interaction models.

Water and fertilizer level	Species interaction model	L/S ratio (g/g · DW)	L/R ratio (g/g · DW)	S/R ratio (g/g · DW)	B/A ratio (g/g · DW)
100% FC (W)	DD	0.58 ± 0.03Ba	1.31 ± 0.09Ba	2.28 ± 0.12Ba	0.28 ± 0.01Ca
	DR	0.53 ± 0.02Aa	1.29 ± 0.04Ba	2.46 ± 0.13 Ba	0.27 ± 0.01 Ba
	DS	0.53 ± 0.02Ba	1.26 ± 0.05Ba	2.40 ± 0.07Ba	0.27 ± 0.01Ca
	D/D	0.52 ± 0.02Ba	1.29 ± 0.05Ba	2.47 ± 0.04Ba	0.27 ± 0.01Ba
	D/R	0.53 ± 0.01Ba	1.29 ± 0.02Ba	2.44 ± 0.08Ba	0.27 ± 0.01Ba
	D/S	0.51 ± 0.02Ca	1.27 ± 0.02Ba	2.52 ± 0.10Ba	0.27 ± 0.01Ca
30% FC (D)	DD	0.63 ± 0.03Aa	0.86 ± 0.05Da	1.36 ± 0.06Da	0.46 ± 0.03Aa
	DR	0.62 ± 0.03Aa	0.76 ± 0.06Ca	1.23 ± 0.07Ca	0.51 ± 0.02Aa
	DS	0.70 ± 0.02Aa	0.88 ± 0.04Ca	1.26 ± 0.06Ca	0.47 ± 0.02Aa
	D/D	0.67 ± 0.01Aa	0.81 ± 0.01Ca	1.20 ± 0.02Ca	0.50 ± 0.02Aa
	D/R	0.65 ± 0.02Aa	0.80 ± 0.04Ca	1.24 ± 0.06Ca	0.50 ± 0.03Aa
	D/S	0.66 ± 0.02Aa	0.86 ± 0.09Ca	1.31 ± 0.12Ca	0.48 ± 0.03Aa
100% FC + N (WN)	DD	0.38 ± 0.03Cb	1.57 ± 0.06Aa	4.22 ± 0.33Aa	0.18 ± 0.01Da
	DR	0.55 ± 0.06Aa	2.23 ± 0.46Aa	3.97 ± 0.47Aa	0.17 ± 0.02Ca
	DS	0.38 ± 0.03Cb	1.78 ± 0.22Aa	4.72 ± 0.43Aa	0.16 ± 0.02Da
	D/D	0.40 ± 0.04Cb	1.97 ± 0.09Aa	4.90 ± 0.26Aa	0.15 ± 0.01Ca
	D/R	0.47 ± 0.03Bab	2.07 ± 0.17Aa	4.42 ± 0.35Aa	0.16 ± 0.01Ca
	D/S	0.41 ± 0.02Dab	1.89 ± 0.09Aa	4.63 ± 0.14Aa	0.15 ± 0.00Da
30% FC + N (DN)	DD	0.57 ± 0.02Aa	1.02 ± 0.06Cb	1.77 ± 0.08Cc	0.36 ± 0.02Ba
	DR	0.58 ± 0.03Aa	1.09 ± 0.05Bab	1.89 ± 0.08Bbc	0.34 ± 0.01Bab
	DS	0.54 ± 0.04Ba	1.14 ± 0.06BCab	2.17 ± 0.24Babc	0.31 ± 0.03Bab
	D/D	0.53 ± 0.02Ba	1.34 ± 0.09Ba	2.54 ± 0.17Ba	0.26 ± 0.02Bb
	D/R	0.54 ± 0.03ABa	1.29 ± 0.08Bab	2.42 ± 0.13Bab	0.27 ± 0.01Bb
	D/S	0.52 ± 0.02Ba	1.30 ± 0.04Bab	2.50 ± 0.09Bab	0.26 ± 0.01Bb
	P: F_W	**0.000**	**0.000**	**0.000**	**0.000**
	P: F_N	**0.000**	**0.000**	**0.000**	**0.000**
	P: F_C	0.788	**0.003**	**0.045**	**0.037**
	P: $F_{W\times N}$	0.854	**0.000**	**0.000**	**0.000**
	P: $F_{W\times C}$	0.129	0.159	0.681	0.534
	P: $F_{N\times C}$	**0.031**	**0.008**	0.084	**0.025**
	P: $F_{W\times N\times C}$	**0.026**	0.998	0.460	0.060

Values are means ± SE (n = 5). L/S, the ratio of leaf to stem dry matters; L/R, the ratio of leaf to root dry matters; S/R, the ratio of stem to root dry matters; B/A, the ratio of belowground to aboveground dry matters; 100% FC, 100% field capacity; 30% FC, 30% field capacity; DD, DR, and DS indicated that D. odorifera planted with D. odorifera, D. regia, and S. mahagoni under the root system interaction, respectively; D/D, D/R, and D/S indicated D. odorifera planted with D. odorifera, D. regia, and S. mahagoni under the root system isolation, respectively; F_W, water effect; F_N, nitrogen effect; F_C, species interaction effect; $F_{W\times N}$, the interaction effect of water and nitrogen; $F_{W\times C}$, the interaction effect of water and species interaction; $F_{N\times C}$, the interaction effect of nitrogen and species interaction; $F_{W\times N\times C}$, the interaction effect of water, nitrogen, and species interaction. Line mixed model was conducted to evaluate the influence of different factors and their interaction effects. Values followed by different lowercase in the same column are significantly different at $P < 0.05$ among different species interaction models under the same water and N application; Values followed by different uppercase in the same column are significantly different at $P < 0.05$ among different water and N application under the same species interaction model. Significant P values are in bold.

Effects of Water, N Application, and Interaction on the Growth

Under the root system interaction models, drought-stressed *D. odorifera* seedlings showed lower H, the number of branches and total leaves, LA (**Figure 3**), biomass accumulation (**Figure 4**), and S/R (**Table 1**), but higher B/A and RCI values (**Figure 5**) compared with well-watered seedlings. In addition, greater decreases in H, LA, LDM, SDM, RDM, and TDM and less increase in B/A in drought-stressed *D. odorifera* seedlings under the DD model were found compared with those seedlings under DR and DS models (**Table 2**). Moreover, *D. odorifera* under the DR and DS models showed higher values in H, LA, LDM, SDM, and TDM than those under the DD model in 100% and 30% FC conditions. N application caused a significant increase in the H, the number of branches and leaves, LA, LDM, SDM, TDM, and S/R of *D. odorifera* seedlings but decreased B/A under 100% FC condition. Under the 100% FC + N conditions, *D. odorifera* seedlings under the DS model showed the highest values in H, the number of branches and leaves, LDM, SDM, TDM, and RCI in all interaction models under the root system interaction, whereas *D. odorifera* under the DR model showed the lowest SDM, TDM, and RCI (RCI < 0). Under the 30% FC + N conditions, *D. odorifera* seedlings under the DD and DS models showed greater increases in the H, the number of branches, LA, LDM, SDM, RDM, and TDM than that of seedlings under the DR model (**Figures 3A,E**, **4A,C,D**, **Table 2**).

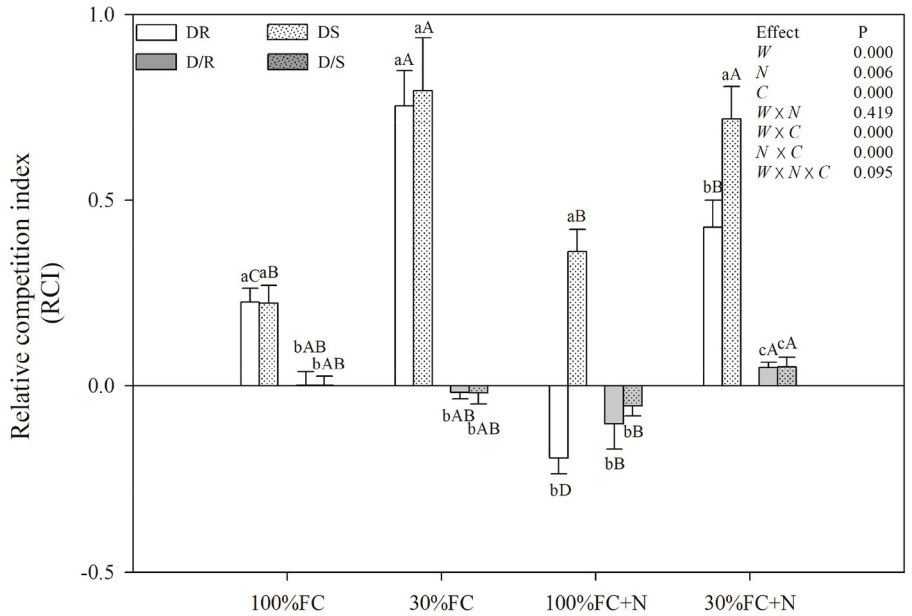

FIGURE 5 | Effects of water and N application on RCI of *D. odorifera* under different species interaction models. DR and DS, *D. odorifera* interaction with *D. regia* (white bars), *S. mahagoni* (white bars with dots) under the root system interaction, respectively; D/R and D/S, *D. odorifera* interaction with *D. regia* (gray bars), *S. mahagoni* (gray bars with dots) under the root system isolation, respectively; other information about treatments, data description, and statistics are shown as in **Figure 3**.

Moreover, H, LA, SDM, LDM, RDM, and TDM of *D. odorifera* increased as the DD, DR, and DS models under the 30% FC + N condition (**Figures 3A,E**, **4**). Collectively, these growth and development characteristics of *D. odorifera* were significantly affected by the interaction of water, N application, and species interaction models.

Under the root system isolated models (i.e., D/D, D/R, and D/S), insignificant differences in H, LA, and the number of branches and leaves (**Figure 3**), LDM, SDM, and TDM (**Figure 4**) among all interaction models were found in all treatments (i.e., 100% FC, 30% FC, 100% FC + N, and 30% FC + N). Under the 100% and 30% FC conditions, the H, SDM, LDM, and TDM of *D. odorifera* seedlings under the D/D models were significantly higher than those under the DD models. In contrast, these parameters showed lower values under D/R and D/S models than under DR and DS models. Under the 100% FC + N condition, H, LA, LDM, SDM, and TDM of *D. odorifera* under the D/S model were lower than that of seedlings under the DS model, whereas *D. odorifera* under the D/R model had higher values than that under the DR model (**Figures 3A,E**, **4A,B,D**, **Table 1**). Under the 30% FC + N condition, the H, LA, LDM, SDM, and TDM of *D. odorifera* under the D/D model were higher than that under the DD model, whereas these parameters of *D. odorifera* under the D/S model were lower than that under the DS model. The root system interaction planting models collectively had more positive effects on the growth and development of *D. odorifera* than the root system isolated models when *D. odorifera* was planted with different niche neighbors.

Effects of Water, N Application, and Species Interaction on Gas Exchange and Photosynthetic Pigment Contents

Under the root system interaction models, *Pn*, *Tr*, PNUE, and photosynthetic pigment contents of *D. odorifera* seedlings under the DD model were slightly or notably lower than that of seedlings under the DR and DS models under the 100% FC condition (**Figures 6**, **7**). Meanwhile, these parameters of *D. odorifera* seedlings under the DD model also showed lower values than those of seedlings under the D/D model. Compared with 100% FC condition, drought stress decreased *Pn*, *Tr*, PNUE, and photosynthetic pigment contents of *D. odorifera* in all interaction models. *Pn* under the DD, DR, and DS model was significantly decreased by 55.79, 45.86, and 46.93%, and PNUE decreased by 59.60, 50.25, and 50.96%, respectively. In addition, *Pn* and PNUE of *D. odorifera* had a higher value under the DR and DS models than under the DD model in 30% FC condition. N application increased *Pn* and PNUE of *D. odorifera* in all interaction models under the 100% and 30% FC conditions (**Figure 6A**). Under the 100% FC + N condition, *Pn* under the DD, DR, and DS model was significantly increased by 31.66, 9.92, and 27.02%. PNUE increased by 40.01, 0.84, and 31.42% compared with 100% FC condition, respectively. *D. odorifera* under the DR and DS models had lower and higher *Pn*, PNUE, and photosynthetic pigment contents than those under the D/R and D/S models (**Figures 6A**, **7**), respectively. Under the 30% FC + N condition, *Pn* and PNUE of *D. odorifera* increased as the DD, DR, and DS models. However, insignificant differences

TABLE 2 | Obtained effects of *D. odorifera* in regard of percent increase or decrease (%) due to drought or nitrogen application when exposed to different species interaction models.

Water and *N* level	Interaction models	H (%)	Branch (%)	LA (%)	LDM (%)	SDM (%)	RDM (%)	TDM (%)	L/R (%)	S/R (%)	B/A (%)	WUEi (%)	CAT (%)	SOD (%)	POD (%)	Proline (%)	NSC (%)	Soluble sugar (%)	Starch (%)
30 VS. 100% FC	DD	−60.44	−41.59	−29.82	−69.58	−72.49	−54.42	−67.67	−34.35	−40.35	64.29	−9.64	43.41	46.52	42.52	202.22	19.29	82.96	−42.78
	DR	−51.85	−47.37	−22.19	−59.01	−64.79	−28.52	−55.58	−41.09	−50.00	88.89	77.29	−7.31	23.89	43.01	163.32	25.51	82.92	−30.41
	DS	−59.57	−50.00	−29.28	−53.85	−65.34	−33.23	−55.33	−30.16	−47.5	74.07	77.02	51.86	30.81	72.37	181.47	31.24	83.57	−23.17
100%FC + N VS. 100%FC	DD	32.46	84.96	29.97	31.35	102.26	6.97	61.09	19.85	85.09	−35.71	0.50	−39.84	−29.73	−36.48	−6.02	3.98	62.88	−53.43
	DR	13.84	45.11	23.24	33.40	34.47	−13.18	24.15	72.87	61.38	−37.04	25.55	−32.38	−32.40	−17.97	5.25	3.38	67.08	−58.68
	DS	32.15	66.18	27.09	36.01	88.51	−0.18	55.22	41.27	96.67	−40.74	8.53	−35.18	−5.63	11.84	21.12	17.73	78.29	−45.23
30%FC + N VS. 30%FC	DD	34.81	12.12	21.9	77.49	94.97	48.52	75.82	18.60	30.15	−21.74	39.59	−13.57	−15.11	−17.08	−31.98	−13.06	−15.73	−4.47
	DR	3.45	11.43	5.58	44.18	52.83	−2.18	32.02	43.42	53.66	−33.33	1.77	−3.57	−21.07	8.43	−25.58	−10.69	−8.20	−17.11
	DS	42.73	19.12	32.48	64.82	122.33	25.80	75.24	29.55	72.22	−34.04	42.28	−40.99	−26.17	−26.25	−37.73	−15.65	−10.78	−27.76

H, height; Branch, the number of branch; LA, leaf area; LDM, leaf dry matter; SDM, stem dry matter; RDM, root dry matter; TDM, total dry matters; L/S, the ratio of leaf to stem dry matter; L/R, the ratio of leaf to root dry matter; S/R, the ratio of stem to root dry matter; B/A, the ratio of belowground to aboveground dry matters; WUEi, water-use efficiency; CAT, catalase activity; SOD, superoxide dismutase; POD, peroxidase; Proline, proline content; NSC, leaf non-structural carbohydrates; Soluble sugar, Soluble sugar content; Starch, starch content. 100% FC, 100% field capacity; 30% FC, 30% field capacity; 100% FC + N, 100% field capacity and N application treatment; 30% FC + N, 30% field capacity and N application treatment. DD, DR, and DS indicated that D. odorifera planted with D. odorifera, D. regia, and S. mahagoni under the root system interaction, respectively.

in gas exchange and photosynthetic pigment contents were observed among the interaction models under the root system isolated planting models (**Figures 6**, **7**). Water, N application, species interaction, and their interaction significantly affected gas exchange parameters of *D. odorifera*.

Effects of Water, N Application, and Species Interaction on WUEi, Leaf NSC, RWC, Antioxidant Enzymes Activities, and Proline Content

Drought stress promoted slightly or notably WUEi under the DR and DS models and increased CAT, SOD, POD, and proline content under all models (**Figures 8A**, **9**). The greater increases in SOD activity and proline content but fewer increases in NSC and WUEi in drought-stressed *D. odorifera* seedlings under the DD model were found compared with those seedlings under DR and DS models (**Table 2**). *D. odorifera* under the DD model possessed lower WUEi, leaf NSC, and starch content but higher activities of SOD and POD, proline content, soluble sugar content, and the ratio of soluble sugar to starch than those seedlings under the DR and DS models in the 30% FC condition (**Figures 9B–D**, **10**). N application in the 100% FC condition increased NSC of *D. odorifera* leaves under the DS model (**Figure 10A**). In addition, *D. odorifera* under the DR model had the lowest NSC among all interaction models. N application under the 30% FC condition significantly increased WUEi of *D. odorifera* under root system interaction models but decreased CAT, POD, and proline content. In addition, a less increase in WUEi and fewer decreases in activities of CAT and POD and proline content of *D. odorifera* were observed in the DR model compared with the DD and DS model (**Table 2**). WUEi of *D. odorifera* increased significantly, and SOD, POD, and proline content decreased as the DD, DR, and DS models (**Figures 8A**, **9**). However, the RWC (**Figures 8B–D**), WUEi, activities of CAT, SOD, and POD, proline content, and leaf NSC of *D. odorifera* among the D/D, D/R, and D/S models, similar to the abovementioned physiological indicators, showed insignificant differences (**Figures 8**–**10**).

Comprehensive Evaluation of *D. odorifera* Response to Different Species Interaction

As shown in **Table 3**, under the 100% and 30% FC conditions, the *E* values of *D. odorifera* under the DR and DS models were significantly higher than that of seedlings under the DD model (the *E* values of *D. odorifera* ranking were as follows: DD < DR, DS). In addition, few differences were found in the *E*-values of *D. odorifera* between the DR and DS models under the 100% FC condition. However, the *E*-values of *D. odorifera* under the DS model were significantly higher than that of other interaction models under the 100% FC + N condition (the *E*-values of *D. odorifera* ranking were as follows: DD, DR < DS). Under the 30% FC + N condition, the *E*-value of *D. odorifera* increased gradually with the DD, DR, and DS models (the *E*-values of *D. odorifera* ranking were as follows: DD < DR < DS).

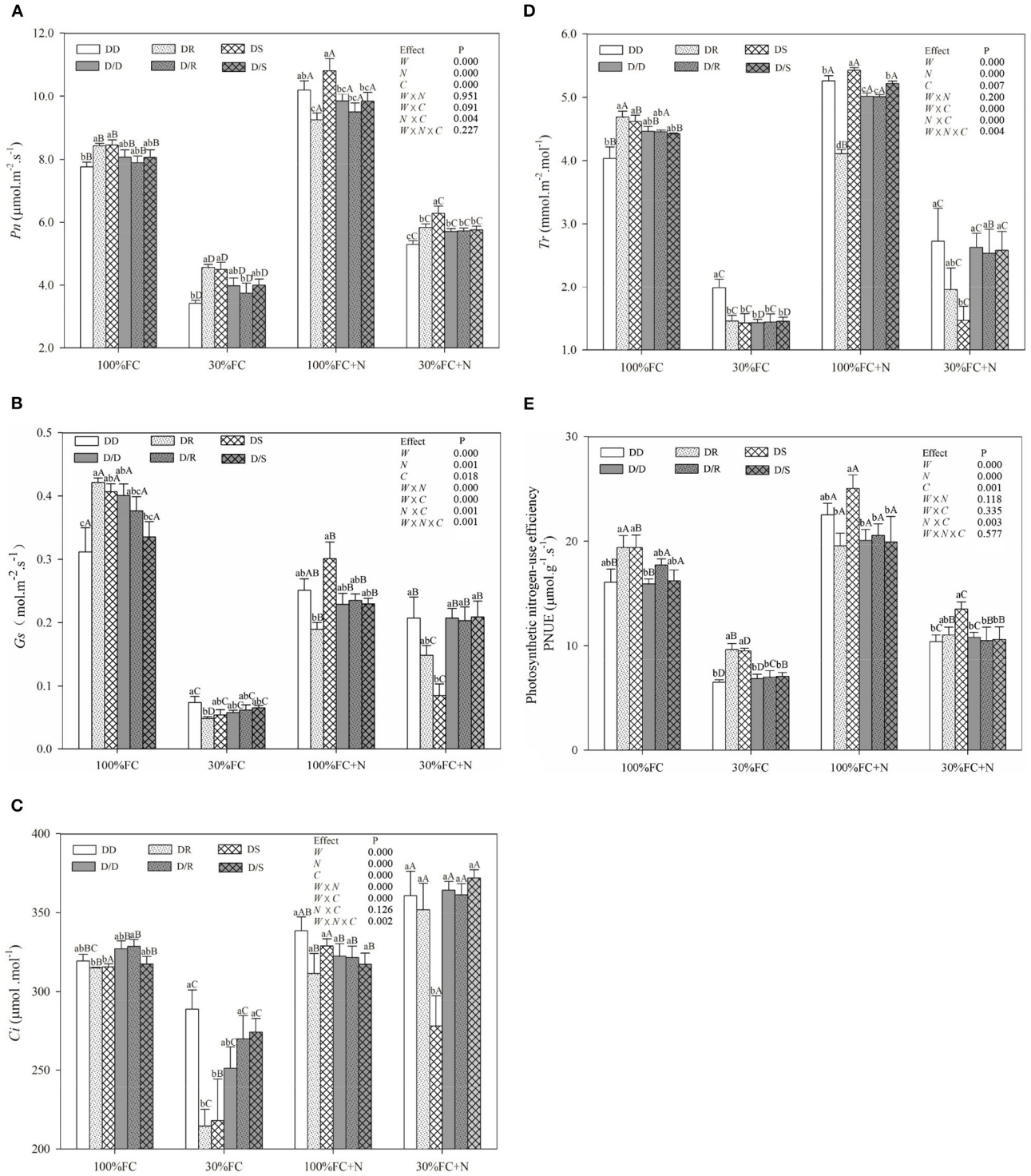

FIGURE 6 | Effects of water, N application, and species interaction on net photosynthetic rates [*Pn*, **(A)**], stomatal conductance [*Gs*, **(B)**], intercellular CO_2 concentration [*Ci*, **(C)**], transpiration rate [*Tr*, **(D)**], and photosynthetic nitrogen-use efficiency [PNUE, **(E)**] of *D. odorifera*. Treatments of water, N application, species interaction, data description, and statistics are shown in **Figure 3**.

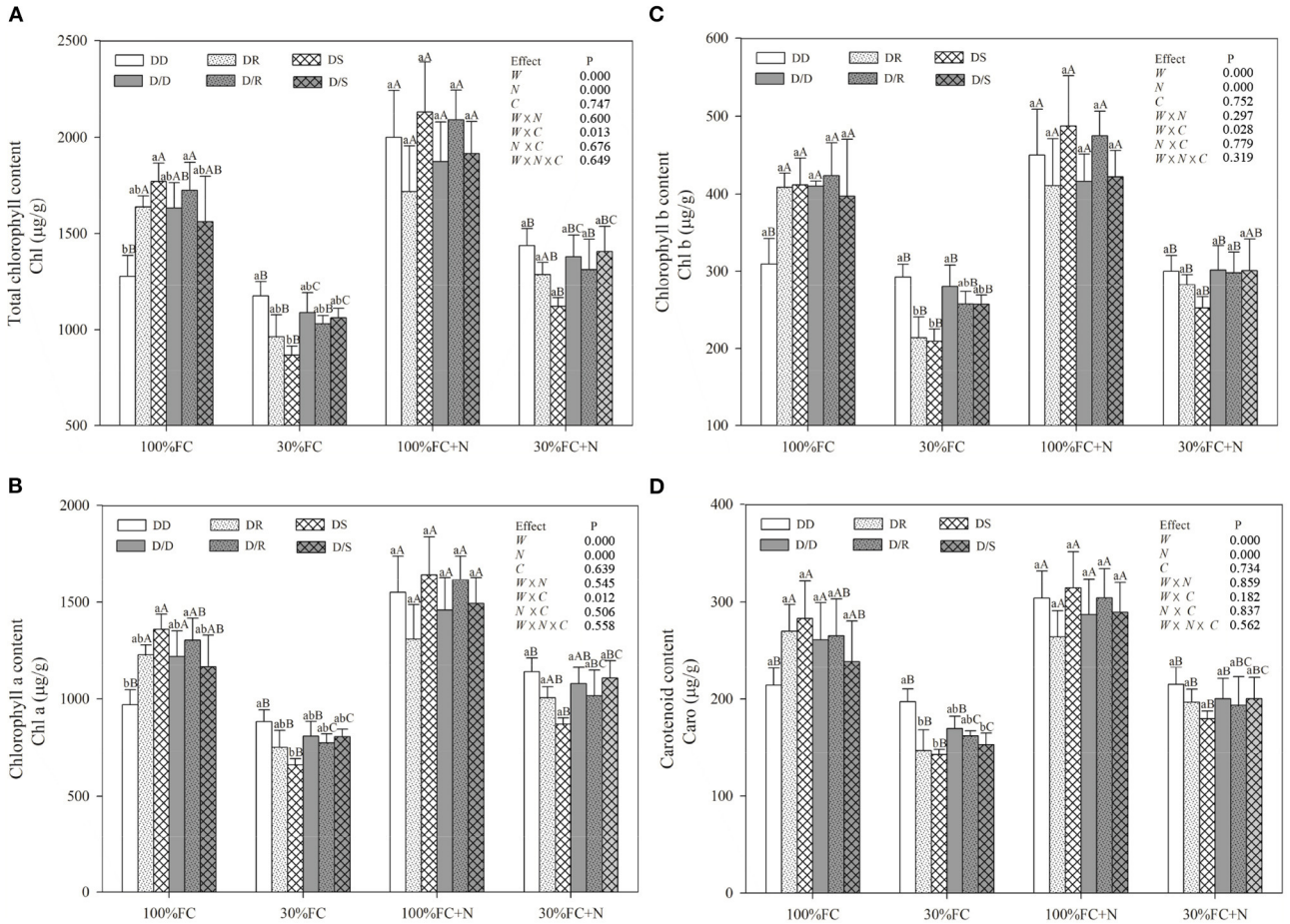

FIGURE 7 | Effects of water, N application, and species interaction on total chlorophyll content **(A)**, chlorophyll a content **(B)**, chlorophyll b content **(C)**, and carotenoid content **(D)** of *D. odorifera*. Treatments of water, N application, species interaction, data description, and statistics are shown as in **Figure 3**.

DISCUSSION

Responses of *D. odorifera* to Different Niche Neighbors Under the Root Interaction Models

The growth and phenotype of plants would be optimized with their social status and neighborhood variation because of resource availability (Duan et al., 2014; Abakumova et al., 2016). The present study revealed that different niche neighbors altered the morphological plasticity of *D. odorifera* under root system interaction models. *D. odorifera* showed better performances in morphology (e.g., H, number of branch and leaves, biomass accumulation, and B/A and RCI > 0) in the inter-specific interaction models (DR and DS) compared with those in the intra-specific interaction models (DD) under the 100% FC and 30% FC conditions (**Figures 3–5**, **Table 1**). These findings indicated that the growth of *D. odorifera* markedly benefited from *D. regia* and *S. mahagoni*, whereas they were inhibited by neighboring *D. odorifera*. It confirmed Hamilton's kin selection theory, which indicated that plants might decrease growth (e.g., reduce input to root) when roots experienced genetically similar or equivalent neighbors (Hamilton, 1964). Previous studies have shown that increased B/A could enhance competitiveness for belowground resources (Bennett et al., 2012). The high biomass allocation in the root system of *D. odorifera* under the inter-specific interaction models might optimize the ability to absorb resources by increasing biomass allocation of the root system in response to different niche neighbors under drought conditions. Different niche neighbors would optimize the ability of *D. odorifera* to absorb resources by increasing root biomass allocation, especially under drought conditions, and thus improved the competitiveness of *D. odorifera*. On the other hand, N-fertilized *D. odorifera* showed the best growth performance (e.g., higher H, branch number, leaf number, LA, and B/A and RCI > 0) under the DS model among all interaction models under the well-watered condition. This finding implied that the presence of non-Leguminous Family *S. mahagoni* promoted the growth and development of Leguminous Family *D. odorifera*. In addition, a previous study suggested that greater niche differentiation would reduce niche overlap and improve resource utilization. Therefore, neighboring *D. regia* and *S. mahagoni* of *D. odorifera* were more beneficial to its growth

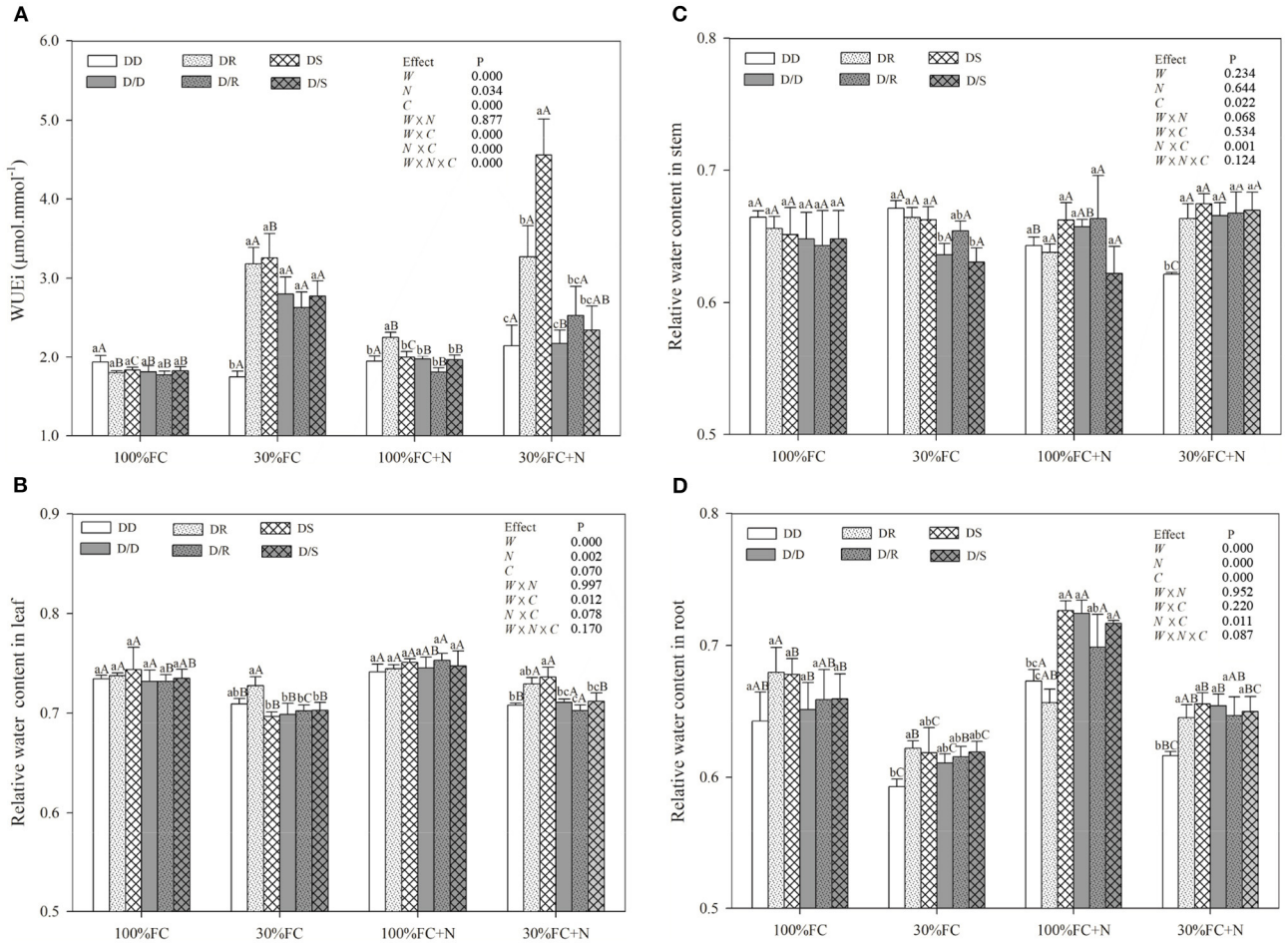

FIGURE 8 | Effects of water, N application, and species interaction on leaf water-use efficiency (WUEi) **(A)**, leaf relative water content **(B)**, stem relative water content **(C)**, and root-relative water content **(D)** of *D. odorifera*. Treatments of water, N application and species interaction, data description, and statistics are shown as in **Figure 3**.

than neighboring *D. odorifera* due to niche complementarity, particularly in restricted and harsh environments (del Río et al., 2014; Zuppinger-Dingley et al., 2014; Cattaneo et al., 2018). Similarly, the growth traits of *D. odorifera* gradually increased slightly or significantly with the DD, DR, and DS models under the 30% FC + N condition, which indicated that distant-stranger neighbors were favorable to the growth of *D. odorifera* in comparison to the close-relative neighbors. Thus, the performance of *D. odorifera* would depend on the degree of niche complementarity among interactive species (Pezzola et al., 2019). Collectively, our results suggested that the growth of *D. odorifera* would respond differentially to different niche neighbors, and PCA confirmed that *D. odorifera* between intra-specific interaction and inter-specific interaction models could be separated from each other.

Previous studies have demonstrated that neighbors could affect the physiological performances and N-use efficiency of the target species, including the chlorophyll (Guo et al., 2018), photosynthetic parameters (Goisser et al., 2016), and PNUE (Duan et al., 2014; Yu et al., 2017). Similarly, the inter-specific interaction between *Populus purdomii* and *Salix rehderiana* improved the photosynthetic capacity of *S. rehderiana* than the intra-specific interaction, indicating that *S. rehderiana* benefited from the presence of *P. purdomii*, particularly under the N-poor condition (Song et al., 2017). Therefore, our studies demonstrated that photosynthetic capacity and N-use efficiency of *D. odorifera* were negatively limited by *D. odorifera* (intra-specific interaction) but positively promoted by the *D. regia* and *S. mahagoni* (inter-specific interaction) under no-N application conditions (**Figure 4**). On the other hand, the height and biomass accumulation could be viewed as indicators of competitiveness, and PCA showed positive correlations between *Pn* and PNUE and these indexes (**Figure 2**). The highest *Pn* and PNUE under the DS model suggested that the neighboring *S. mahagoni* improved the competitiveness of *D. odorifera*. Furthermore, the *Pn* and PNUE of *D. odorifera* seedlings showed remarkable photosynthetic performances and N-use efficiency with the enlarged degree of niche differentiation among neighbors under

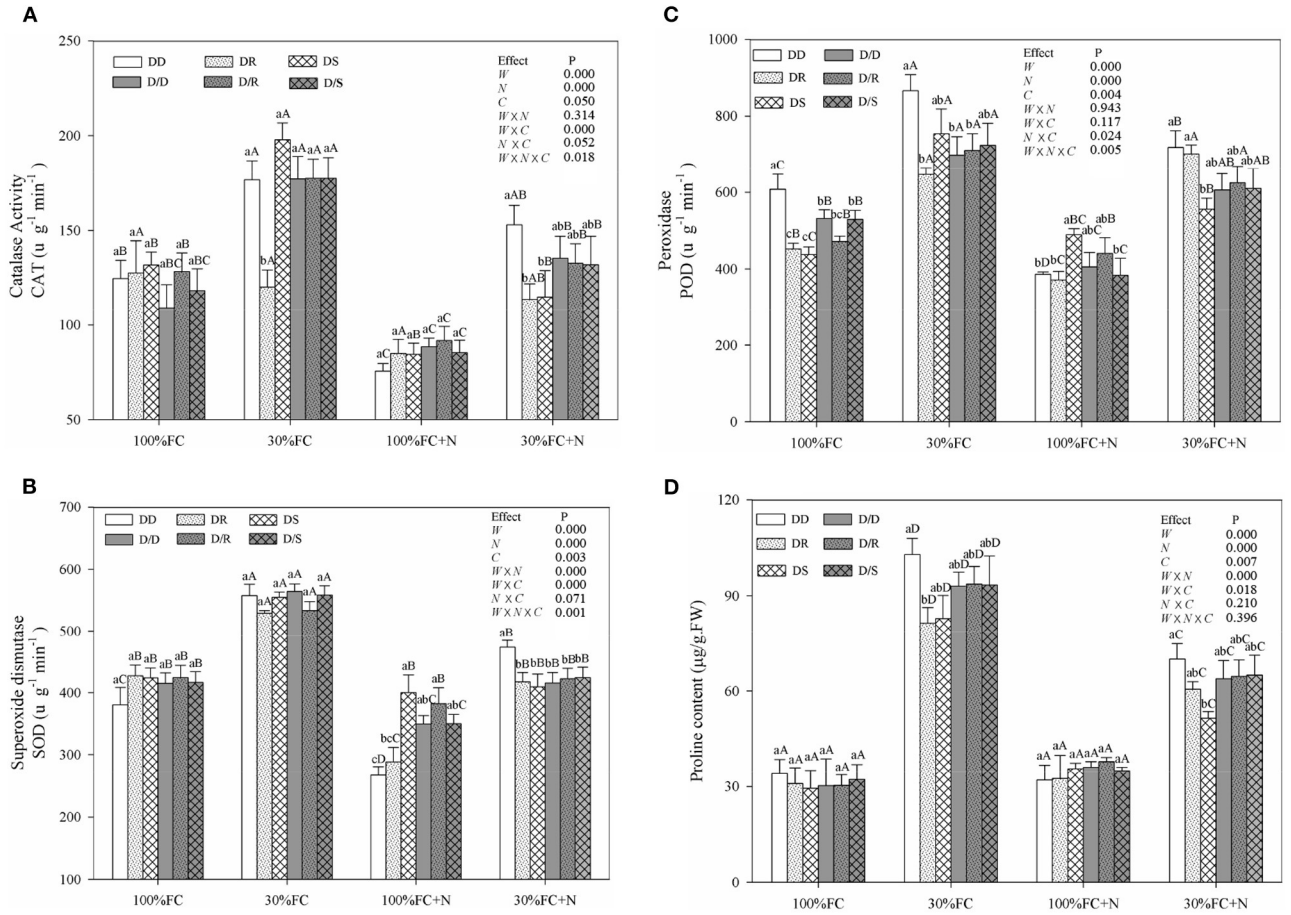

FIGURE 9 | Effects of water, N application, and species interaction on catalase activity (CAT) **(A)**, superoxide dismutase (SOD) **(B)**, peroxidase (POD) **(C)**, and proline content **(D)** of *D. odorifera*. Treatments of water, N application and species interaction, data description, and statistics are shown as in **Figure 3**.

the 30% FC + N condition. The results indicated that *D. odorifera* modulated traits in photosynthetic capacity according to its neighbors, and the responses of *D. odorifera* in photosynthetic capacity were associated with its neighbors and their niche differentiation (Burns and Strauss, 2011).

NSC might be an incentive for increased competitiveness (Duan et al., 2014). The increments of foliar soluble sugars, antioxidant enzymes, and proline content had contributed to maintaining normal cellular turgor and osmoregulation when plants encountered stronger competition for water resources (Zrenner and Stitt, 1991; Zhang et al., 2019; He et al., 2020). Furthermore, plants with higher water-use efficiency had greater advantages in excluding neighbors (Craine et al., 2013). In this study, PCA indicated positive correlations between WUEi and leaf NSC (**Figure 2**). *D. odorifera* exhibited higher WUEi, starch, total NSC, and lower activities of SOD and POD, proline content, soluble sugar, and the ratio of soluble sugar to starch under both DR and DS models than the DD model under the 30% FC condition. This finding suggested that the neighboring *D. regia* and *S. mahagoni* alleviated negative effects caused by drought stress on *D. odorifera*. Therefore, the notable improvement in water utilization of *D. odorifera* under both DR and DS models could help carbon storage (**Figures 8A**, **9A,B**). However, neighboring *D. odorifera* aggravated the intensity of drought stress, then increased ROS, antioxidant enzymes, proline content, and soluble sugar in response to reduce the oxidative damages, and finally blocked the synthesis of NSC starch in *D. odorifera* under the DD model. The results suggested that plants could display different adaptive responses in leaf NSC, antioxidant enzymes, and proline content according to neighbors (Yu et al., 2019).

Taken together, growth and development, physiological, and morphological traits of *D. odorifera* could differentially respond to its neighbors with distinct niche under root system interaction models, particularly under the drought-stressed conditions, which was in agreement with our hypothesis.

Negligible Responses of *D. odorifera* to Different Niche Neighbors Under the Root Isolated Models

Plants altered related traits to improve their competitiveness in response to aboveground and belowground competition

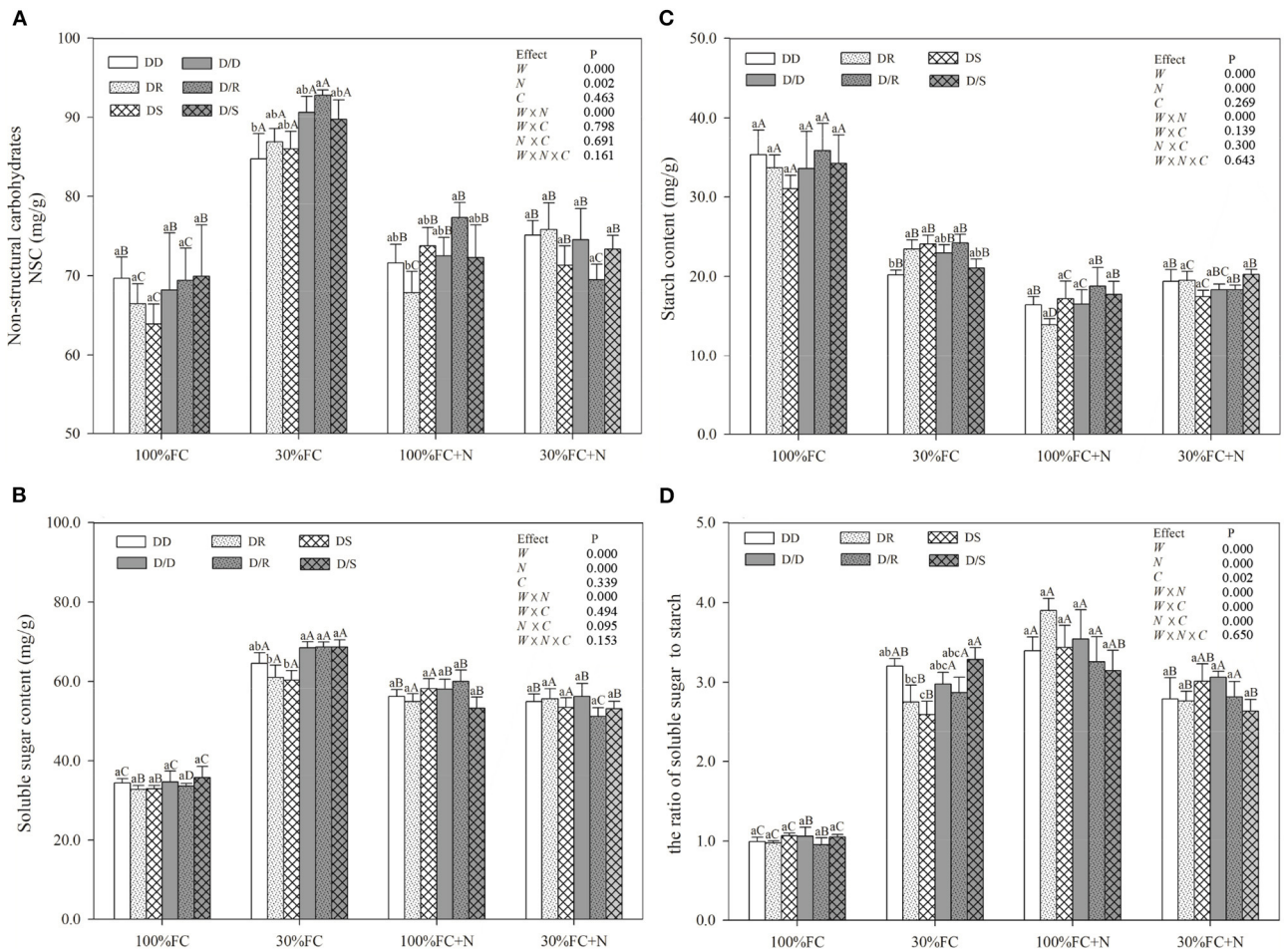

FIGURE 10 | Effects of water, N application, and species interaction on leaf non-structural carbohydrates **(A)**, soluble sugar content **(B)**, starch content **(C)**, and the ratio of soluble sugar content to starch content **(D)** of *D. odorifera*. Treatments of water, N application, species interaction, data description, and statistics are shown as in **Figure 3**.

(Murphy and Dudley, 2007). Compared with the root system isolated models under the 100% and 30% FC conditions, *D. odorifera* from inter-specific interaction models under the root system interaction had better performances in growth, biomass accumulation, RCI, *Pn*, PNUE, POD activity, and proline content. This finding indicated that *D. odorifera* under the root system interaction models had more positive effects from neighbors than those under the root system isolated models. The few or insignificant differences in the growth, morphology, and physiology of *D. odorifera* among the D/D, D/R, and D/S models in majority treatments indicated that the responses of *D. odorifera* to different niche neighbors were dominated by belowground interaction rather than the negligible aboveground interaction. However, studies on the interaction in tropical forests indicated that aboveground competition for light and space exceeded that from the belowground competition for nutrients and water because of the limitation of photosynthetically active radiation (Lewis and Tanner, 2000). The light limitation would occur on the blade, wherein the light available for photosynthesis could not meet the photosynthetic capacity of leaves, which was necessary for plant light competition (Craine et al., 2013). Therefore, based on the negligible responses of *D. odorifera* from the aboveground interaction in our experiment, we supposed that light was not fully saturated to activate the aboveground competition mechanism for light.

Responses of *D. odorifera* to Different Niche Neighbors Were Modified by Drought and N Application Under the Root Interaction Models

Abiotic factors played a key role in the interaction as the primary driving force (Duan et al., 2014; Yu et al., 2019). In the present study, drought-stressed *D. odorifera* seedlings under the DD model showed greater decreases in growth (e.g., H, LA, LDM, SDM, RDM, and TDM) and photosynthetic

TABLE 3 | The value of the comprehensive index [C(μ)], subordinate function value X(μ), and comprehensive evaluation value (*E*) for *D. odorifera* exposed to different species interaction models under various water and *N* application conditions.

Water and fertilizer level	Species interaction	C (*1*)	C (*2*)	X (*1*)	X (*2*)	*E*
100% FC	DD	−5.87	−0.19	0.000	0.430	0.057
	DR	2.53	2.08	0.912	1.000	0.924
	DS	3.34	−1.9	1.000	0.000	0.867
30% FC	DD	−14.75	0.03	0.000	0.526	0.068
	DR	7.76	0.75	1.000	1.000	1.000
	DS	6.99	−0.77	0.966	0.000	0.841
100% FC + N	DD	−0.05	−2.89	0.492	0.000	0.380
	DR	−4.79	1.2	0.000	0.893	0.203
	DS	4.84	1.69	1.000	1.000	1.000
30% FC + N	DD	−4.85	−1.31	0.000	0.000	0.000
	DR	−0.47	2.31	0.431	1.000	0.507
	DS	5.32	−0.99	1.000	0.088	0.878

Treatments of water, N application, and species interaction are shown as in ***Table 1****.*

capacity (*Pn* and PNUE), greater increases in SOD activity and proline content, and fewer increases in NSC and WUEi. These results demonstrated that drought would aggravate the inhibitory effects on *D. odorifera* under the DD model. Similar results have been found in other studies, such that inhibited effects from conspecifics became stronger under drought stress (Chen et al., 2009; Wright et al., 2015; Metz et al., 2016). For example, in one study, the greater inhibition (lower growth and physiological parameters) of *P. cathayana* females was found from intrasexual competition than the intersexual competition when facing variation from well-watered to drought treatment (Chen et al., 2014). These results can be explained by the greater increase in competitive intensity for water that resulted from the similarity of resource utilization, which aided in the capture of a small amount proportion of available water resources (Chen et al., 2014; Calama et al., 2019). Interestingly, the growth and development of *D. odorifera* showed similar performances between the DR and DS models in the 100% FC condition. However, the trend changed by N application, as N fertilized *D. odorifera* under the DS model gained greater positive effects than that under the DR model, and *D. odorifera* under the DR model suffered stronger inhibitory effects (e.g., the value of RCI dropped from positive to negative) under the 100% FC + N condition (**Figure 5**; **Table 2**). A related study reported that nutrient supply could increase the competition intensity between *Eucalyptus* and *Acacia mangium* (Bordron et al., 2021). No positive interaction of N-fixing *Alnus rubra* on the growth of *Pseudotsuga menziesii* could be converted to a strong facilitating effect by high soil N availability (Binkley et al., 2003). These are consistent with the stress-gradient hypothesis that interactions with neighbors could be converted from positive to negative in favorable conditions (N application) (Bertness and Callaway, 1994). Therefore, N application could stimulate the competitiveness of Leguminosae Family *D. odorifera* from non-Leguminosae Family *S. mahagoni* and enhance the competitive intensity of *D. odorifera* from Leguminosae Family *D. regia* under a well-watered condition. However, the N application promoted the performances of *D. odorifera* under the DD and DS models and had little effect on *D. odorifera* under the DR model under drought-stressed conditions. These results are consistent with some previous studies, in which negative effects of competition in low resource environments are converted to the positive effects of facilitation by adding resources (e.g., N application; Forrester et al., 2013; Svanfeldt et al., 2017). For example, growth and complementarity effects between mixed-species stands of *Abies alba* and *Picea abies* improved as growing conditions improved (Forrester et al., 2013). Therefore, N application reduced the inhibitory effect of drought stress on *D. odorifera* under the DD and DS models (Tilman, 1987), and N played a key role in the responses of *D. odorifera* under the root system interaction models (Yu et al., 2017; Guo et al., 2018). Song et al. (2017) considered that N altered the relationships between *S. rehderiana* and *P. purdomii* in a glacier retreat area. Therefore, water level and N application could alter *D. odorifera* to different niche neighbors under the root system interaction models, which was also consistent with our hypothesis.

CONCLUSIONS

In conclusion, Leguminosae Family *D. odorifera* can differentially respond to its different niche neighbors under the root system interaction models, and it can benefit from niche differentiation. It should be encouraged to select different niche mixture species during the construction of the *D. odorifera* forest. The water regime and N application may modulate the interactive effects between neighbors. Appropriate N application maybe alleviate the inhibitory effect of drought stress on *D. odorifera* in its mixed forests. Mixture with *S. mahagoni* or *D. regia* under both the well-watered and drought conditions with root system interaction is the optimal planting model. However, under the condition of N application, a mixture with *S. mahagoni* could be the only optimal planting model.

DATA AVAILABILITY STATEMENT

The original contributions presented in the study are included in the article/**Supplementary Material**, further inquiries can be directed to the corresponding author/s.

AUTHOR CONTRIBUTIONS

L-SX performed the experiment and wrote the draft manuscript. L-FM assisted in carrying out the experiment in the greenhouse. FY designed the experiment, provided funding, and revised the manuscript. All authors were engaged in this present work.

FUNDING

This work was sponsored by the Natural Science Foundation of Hainan Province for High-Level Talent (320RC507 and 317052), National Natural Science Foundation of China (32006240 and 31660165), and Scientific Research Starting Foundation and Young Teachers Foundation of Hainan University to Fan Yang (kyqd1573).

SUPPLEMENTARY MATERIAL

The Supplementary Material for this article can be found online at: https://www.frontiersin.org/articles/10.3389/fpls.2021.664122/full#supplementary-material

REFERENCES

Abakumova, M., Zobel, K., Lepik, A., and Semchenko, M. (2016). Plasticity in plant functional traits is shaped by variability in neighbourhood species composition. *New Phytol.* 211, 455–463. doi: 10.1111/nph.13935

Aldea, J., Bravo, F., Bravo-Oviedo, A., Ruiz-Peinado, R., Rodríguez, F., and Del Río, M. (2017). Thinning enhances the species-specific radial increment response to drought in mediterranean pine-oak stands. *Agr. For. Meteorol.* 237–238, 371–383. doi: 10.1016/j.agrformet.2017.02.009

Aschehoug, E. T., Brooker, R., Atwater, D. Z., Maron, J. L., and Callaway, R. M. (2016). The mechanisms and consequences of interspecific competition among plants. *Annu. Rev. Ecol. Evol. Syst.* 47, 263–281. doi: 10.1146/annurev-ecolsys-121415-032123

Bennett, E., Roberts, J. A., and Wagstaff, C. (2012). Manipulating resource allocation in plants. *J. Exp. Bot.* 63, 3391–3400. doi: 10.1093/jxb/err442

Bertness, M. D., and Callaway, R. (1994). Positive interactions in communities. *Trends Ecol. Evol.* 9, 191–193. doi: 10.1016/0169-5347(94)90088-4

Bilbrough, C. J., and Caldwell, M. M. (1995). The effects of shading and N-status on root proliferation in nutrient patches by the perennial grass. *Oecologia* 103, 10–16. doi: 10.1007/BF00328419

Binkley, D., Senock, R., Bird, S., and Cole, T. G. (2003). Twenty years of stand development in pure and mixed stands of *Eucalyptus saligna* and N-fixing *Facaltaria moluccana*. *For. Ecol. Manage.* 182, 93–102. doi: 10.1016/S0378-1127(03)00028-8

Bordron, B., Germon, A., Laclau, J. P., Oliveira, I. R., Robin, A., Jourdan, C., et al. (2021). Nutrient supply modulates species interactions belowground: dynamics and traits of fine roots in mixed plantations of *Eucalyptus* and *Acacia mangium*. *Plant Soil* 460, 559–577. doi: 10.1007/s11104-020-04755-2

Bowsher, A. W., Shetty, P., Anacker, B. L., Siefert, A., Strauss, S. Y., Friesen, M. L., et al. (2017). Transcriptomic responses to conspecific and congeneric competition in co-occurring *Trifolium*. *J. Ecol.* 105, 602–615. doi: 10.1111/1365-2745.12761

Burns, J. H., and Strauss, S. Y. (2011). More closely related species are more ecologically similar in an experimental test. *Proc. Natl. Acad. Sci. U.S.A.* 108, 5302–5307. doi: 10.1073/pnas.1013003108

Calama, R., Conde, M., de-Dios-García, J., Madrigal, G., Vázquez-Piqu,é, J., Gordo, F. J., et al. (2019). Linking climate, annual growth and competition in a mediterranean forest: *Pinus pinea* in the Spanish Northern Plateau. *Agr. For. Meteorol.* 264, 309–321. doi: 10.1016/j.agrformet.2018.10.017

Cattaneo, N., Bravo-Oviedo, A., and Bravo, F. (2018). Analysis of tree interactions in a mixed Mediterranean pine stand using competition indices. *Eur. J. For. Res.* 137, 109–120. doi: 10.1007/s10342-017-1094-8

Chan, S. C., Chang, Y. S., Wang, J. P., Chen, S. C., and Kuo, S. C. (1998). Three new flavonoids and antiallergic, anti-inflammatory constituents from the heartwood of *Dalbergia odorifera*. *Planta Med.* 64, 153–158. doi: 10.1055/s-2006-957394

Chen, J., Duan, B., Wang, M., Korpelainen, H., Li, C., and Watling, J. (2014). Intra- and inter-sexual competition of *Populus cathayana* under different watering regimes. *Funct. Ecol.* 28, 124–136. doi: 10.1111/1365-2435.12180

Chen, S. Y., Xu, J., Maestre, F. T., Chu, C. J., Wang, G., and Xiao, S. (2009). Beyond dual-lattice models: incorporating plant strategies when modeling the interplay between facilitation and competition along environmental severity gradients. *J. Theor. Biol.* 258, 266–273. doi: 10.1016/j.jtbi.2009.01.011

Chomel, M., DesRochers, A., Baldy, V., Larchevêque, M., and Gauquelin, T. (2014). Non-additive effects of mixing hybrid poplar and white spruce on aboveground and soil carbon storage in boreal plantations. *Forest Ecol. Manage.* 328, 292–299. doi: 10.1016/j.foreco.2014.05.048

Craine, J. M., Dybzinski, R., and Robinson, D. (2013). Mechanisms of plant competition for nutrients, water and light. *Funct. Ecol.* 27, 833–840. doi: 10.111/1365-2435.12081

del Río, M., Condés, S., and Pretzsch, H. (2014). Analyzing size-symmetric vs. size-asymmetric and intra- vs. inter-specific competition in beech (*Fagus sylvatica* L.) mixed stands. *For. Ecol. Manage.* 325, 90–98. doi: 10.1016/j.foreco.2014.03.047

Duan, B., Dong, T., Zhang, X., Zhang, Y., and Chen, J. (2014). Ecophysiological responses of two dominant subalpine tree species *Betula albo-sinensis* and *Abies faxoniana* to intra- and interspecific competition under elevated temperature. *For. Ecol. Manage.* 323, 20–27. doi: 10.1016/j.foreco.2014.03.036

Fang, Z., Hu, Z., Zhao, H., Yang, L., Ding, C., Lou, L., et al. (2017). Screening for cadmium tolerance of 21 cultivars from Italian ryegrass (*Lolium multiflorum* Lam.) during germination. *Grassl. Sci.* 63, 36–45. doi: 10.1111/grs.12138

File, A. L., Murphy, G. P., and Dudley, S. A. (2012). Fitness consequences of plants growing with siblings: reconciling kin selection, niche partitioning and competitive ability. *Proc. Biol. Sci.* 279, 209–218. doi: 10.1098/rspb.2011.1995

Forrester, D. I. (2014). The spatial and temporal dynamics of species interactions in mixed-species forests: from pattern to process. *For. Ecol. Manage.* 312, 282–292. doi: 10.1016/j.foreco.2013.10.003

Forrester, D. I., and Bauhus, J. (2016). A review of processes behind diversity—productivity relationships in forests. *Cur. For. Rep.* 2, 45–61. doi: 10.1007/s40725-016-0031-2

Forrester, D. I., Kohnle, U., Albrecht, A. T., and Bauhus, J. (2013). Complementarity in mixed-species stands of *Abies alba* and *Picea abies* varies with climate, site quality and stand density. *For. Ecol. Manage.* 304, 233–242. doi: 10.1016/j.foreco.2013.04.038

Goisser, M., Geppert, U., Rötzer, T., Paya, A., Huber, A., Kerner, R., et al. (2016). Does belowground interaction with *Fagus sylvatica* increase drought susceptibility of photosynthesis and stem growth in *Picea abies*? *Forest Ecol. Manage.* 375, 268–278. doi: 10.1016/j.foreco.2016.05.032

González, L., and González-Vilar, M. (2001). "Determination of relative water content," in *Handbook of Plant Ecophysiology Techniques*, ed M. J. Reigosa Roger (New York, NY: Kluwer Academic Publishers), 207–212.

Grant, K., Kreyling, J., Heilmeier, H., Beierkuhnlein, C., and Jentsch, A. (2014). Extreme weather events and plant–plant interactions: shifts between competition and facilitation among grassland species in the face of drought and heavy rainfall. *Ecol. Res.* 29, 991–1001. doi: 10.1007/s11284-014-1187-5

Guevara, A. P., Apilado, A., Sakurai, H., and Kozuka, M. (1996). Anti-inflammatory, antimutagenicity, and antitumor-promoting activities of mahogany seeds, *Swietenia macrophylla* (Meliaceae). *Philipp. J. Crop Sci.* 125, 271–278

Guo, Q., Li, J., Zhang, Y., Zhang, J., Lu, D., Korpelainen, H., et al. (2016). Species-specific competition and N fertilization regulate nonstructural carbohydrate contents in two larix species. *Forest Ecol. Manage.* 364, 60–69. doi: 10.1016/j.foreco.2016.01.007

Guo, Q., Song, H., Kang, J., Korpelainen, H., and Li, C. (2018). Different responses in leaf-level physiology to competition and facilitation under different soil types and N fertilization. *Environ. Exp. Bot.* 150, 69–78. doi: 10.1016/j.envexpbot.2018.03.006

Guo, Y., Yang, X., Schob, C., Jiang, Y., and Tang, Z. (2017). Legume shrubs are more nitrogen-homeostatic than non-legume shrubs. *Front. Plant Sci.* 8:1662. doi: 10.3389/fpls.2017.01662

Hamilton, W. D. (1964). The genetical evolution of social behaviour. *J. Theor. Biol.* 7, 1–16. doi: 10.1016/0022-5193(64)90038-4

Han, C.Y., Chan, Z.L., and Yang, F. (2015). Comparative analyses of universal extraction buffers for assay of stress related biochemical and physiological parameters. *Prep. Biochem. Biotech.* 45, 684-695. doi: 10.1080/10826068.2014.940540

Hansen, A. P., Martin, P., and Park, B. S. J. (1992). Nitrate inhibition of N_2 fixation in *Phaseolus vulgaris* L. *cv.* OAC Rico and a supernodulating mutant. *New Phytol.* 122, 611–615. doi: 10.1111/j.1469-8137.1992.tb00088.x

He, W., Liu, H., Qi, Y., Liu, F., and Zhu, X. (2020). Patterns in nonstructural carbohydrate contents at the tree organ level in response to drought duration. *Glob. Chang. Biol.* 26, 3627–3638. doi: 10.1111/gcb.15078

Helluy, M., Prévosto, B., Cailleret, M., Fernandez, C., and Balandier, P. (2020). Competition and water stress indices as predictors of *Pinus halepensis* mill. Radial growth under drought. *Fo. Ecol. Manag.* 460:117877. doi: 10.1016/j.foreco.2020.117877

Jolliffe, P. A. (2000). The replacement series. *J. Ecol.* 88, 371–385. doi: 10.1046/j.1365-2745.2000.00470.x

Lewis, S. L., and Tanner, E. V. J. (2000). Effects of above- and belowground competition on growth and survival of rain forest tree seedlings. *Ecology* 81, 2525–2538. doi: 10.2307/177472

Liang, H., Huang, J. G., Ma, Q., Li, J., Wang, Z., Guo, X., et al. (2019). Contributions of competition and climate on radial growth of *Pinus massoniana* in subtropics of China. *Agr. Forest Meteorol.* 274, 7–17. doi: 10.1016/j.agrformet.2019.04.014

Linares, J. C., Camarero, J. J., and Carreira, J. A. (2009). Interacting effects of changes in climate and forest cover on mortality and growth of the southernmost European fir forests. *Global. Ecol. Biogeogr.* 18, 485–497. doi: 10.1111/j.1466-8238.2009.00465.x

Liu, C. L. C., Kuchma, O., and Krutovsky, K. V. (2018). Mixed-species versus monocultures in plantation forestry: development, benefits, ecosystem services and perspectives for the future. *Glob. Ecol. Conserv.* 15:e00419. doi: 10.1016/j.gecco.2018.e00419

Markham, J. H., and Zekveld, C. (2007). Nitrogen fixation makes biomass allocation to roots independent of soil nitrogen supply. *Can. J. Bot.* 85, 787–793. doi: 10.1139/B07-075

Meng, H., Xie, C., Yang, Y., Wei, J., Feng, J., and Chen, S. (2010). Suitable producing areas of *Dalbergia odorifera* T. Chen. *Lishizhen Med. Mater. Med. Res.* 21, 2304–2306. doi: 10.1080/00949651003724790

Metz, J., Annighofer, P., Schall, P., Zimmermann, J., Kahl, T., Schulze, E., et al. (2016). Site-adapted admixed tree species reduce drought susceptibility of mature european beech. *Glob. Change Biol.* 22, 903–920. doi: 10.1111/gcb.13113

Mishra, S. S., Patel, K. K., Raghuwanshi, N., Pathak, A., Panda, P. P., Girhepunje, K., et al. (2011). Screening of ten indian medicinal plant extracts for antioxidant activity. *Ann. Biol. Res.* 2, 162–170. doi: 10.1016/s0024-3205(03)00259-5

Mitchell, A. K. (1998). Acclimation of pacific yew (*Taxus brevifolia*) foliage to sun and shade. *Tree Physiol.* 18, 749–757. doi: 10.1093/treephys/18.11.749

Mittler, R. (2006). Abiotic stress, the field environment and stress combination. *Trends Plant Sci.* 11, 15–19. doi: 10.1016/j.tplants.2005.11.002

Murphy, G. P., and Dudley, S. A. (2007). Above- and belowground competition cues elicit independent responses. *J. Ecol.* 95, 261–272. doi: 10.1111/j.1365-2745.2007.01217.x

Nguyen, H., Herbohn, J., Clendenning, J., Lamb, D., Dressler, W., Vanclay, J., et al. (2015). What is the available evidence concerning relative performance of different designs of mixed-species plantings for smallholder and community forestry in the tropics? A systematic map protocol. *Environ. Evid.* 4, 1–7. doi: 10.1186/s13750-015-0041-8

Niinemets, Ü. (2010). Responses of forest trees to single and multiple environmental stresses from seedlings to mature plants: past stress history, stress interactions, tolerance and acclimation. *Forest Ecol. Manage.* 260, 1623–1639. doi: 10.1016/j.foreco.2010.07.054

Pezzola, E., Pandolfi, C., and Mancuso, S. (2019). Resource availability affects kin selection in two cultivars of *Pisum sativum*. *Plant Growth Regul.* 90, 321–329. doi: 10.1007/s10725-019-00562-7

Pierik, R., Mommer, L., Voesenek, L. A. C. J., and Robinson, D. (2013). Molecular mechanisms of plant competition: neighbour detection and response strategies. *Funct. Ecol.* 27, 841–853. doi: 10.1111/1365-2435.12010

Pretzsch, H., Bielak, K., Bruchwald, A., Dieler, J., Dudzinska, M., Ehrhart, H. P., et al. (2013). Species mixing and productivity of forests. Results from long-term experiments. *Allg. Forst Jagdztg.* 184, 177–196.

Richards, A. E., Forrester, D. I., Bauhus, J., and Scherer-Lorenzen, M. (2010). The influence of mixed tree plantations on the nutrition of individual species: a review. *Tree Physiol.* 30, 1192–1208. doi: 10.1093/treephys/tpq035

Rodan, B. D., Newton, A. C., and Verissimo, A. (1992). Mahogany conservation: status and policy initiatives. *Environ. Conserv.* 19, 331–338. doi: 10.1017/S0376892900031453

Song, M., Yu, L., Jiang, Y., Lei, Y., Korpelainen, H., Niinemets, U., et al. (2017). Nitrogen-controlled intra- and interspecific competition between *Populus purdomii* and *Salix rehderiana* drive primary succession in the Gongga Mountain glacier retreat area. *Tree Physiol.* 37, 799–814. doi: 10.1093/treephys/tpx017

Sun, S., Zeng, X., Zhang, D., and Guo, S. (2015). Diverse fungi associated with partial irregular heartwood of *Dalbergia odorifera*. *Sci. Rep.* 5:8464. doi: 10.1038/srep08464

Svanfeldt, K., Monro, K., and Marshall, D. J. (2017). Field manipulations of resources mediate the transition from intraspecific competition to facilitation. *J. Anim. Ecol.* 86, 654–661. doi: 10.1111/1365-2656.12644

Tilman, D. (1987). On the neaning of competition and the mechanisms of competitive superiority. *Funct. Ecol.* 1, 304–315. doi: 10.2307/2389785

Wang, X., Gao, Y., Zhang, H., Shao, Z., Sun, B., and Gao, Q. (2019). Enhancement of rhizosphere citric acid and decrease of NO_3^-/NH_4^+ ratio by root interactions facilitate N fixation and transfer. *Plant Soil* 447, 169–182. doi: 10.1007/s11104-018-03918-6

Wang, X., Guo, X., Yu, Y., Cui, H., Wang, R., and Guo, W. (2018). Increased nitrogen supply promoted the growth of non-N-fixing woody legume species but not the growth of N-fixing *Robinia pseudoacacia*. *Sci. Rep.* 8:17896. doi: 10.1038/s41598-018-35972-6

Wright, A., Schnitzer, S. A., Reich, P. B., and Jones, R. (2015). Daily environmental conditions determine the competition-facilitation balance for plant water status. *J. Ecol.* 103, 648–656. doi: 10.1111/1365-2745.12397

Xu, X., Yang, F., Xiao, X., Zhang, S., Korpelainen, H., and Li, C. (2008). Sex-specific responses of *Populus cathayana* to drought and elevated temperatures. *Plant Cell Environ.* 31, 850–860. doi: 10.1111/j.1365-3040.2008.01799.x

Yang, F., Han, C. Y., Li, Z., Guo, Y. N., and Chan, Z. L. (2015). Dissecting tissue-and species-specific responses of two plantago species to waterlogging stress at physiological level. *Environ. Exp. Bot.* 109, 177–185. doi: 10.1016/j.envexpbot.2014.07.011

Yang, F., Wang, Y., Wang, J., Deng, W. Q., Liao, L., and Li, M. (2011). Different eco-physiological responses between male and female *Populus deltoides* clones to waterlogging stress. *For. Ecol. Manage.* 262, 1963–1971. doi: 10.1016/j.foreco.2011.08.039

Yao, X., Li, Y., Liao, L., Sun, G., Wang, H., and Ye, S. (2019). Enhancement of nutrient absorption and interspecific nitrogen transfer in a *Eucalyptus urophylla* × *eucalyptus grandis* and *Dalbergia odorifera* mixed plantation. *Forest Ecol. Manage.* 449:117465. doi: 10.1016/j.foreco.2019.117465

Yemm, E. W., and Willis, A. J. (1954). The estimation of carbohydrates in plant extracts by anthrone. *Biochem. J.* 57, 508–514. doi: 10.1042/bj0570508

Yi, X., Zhang, Y., Wang, X., Wang, Y., and Ji, L. (2015). Effects of nitrogen on the growth and competition between seedlings of two temperate forest tree species. *Scand. J. Forest Res.* 30, 276–282. doi: 10.1080/02827581.2014.1001781

Yu, L., Song, M., Lei, Y., Duan, B., Berninger, F., Korpelainen, H., et al. (2017). Effects of phosphorus availability on later stages of primary succession in gongga mountain glacier retreat area. *Environ. Exp. Bot*. 141, 103–112. doi: 10.1016/j.envexpbot.2017.07.010

Yu, L., Song, M., Xia, Z., Korpelainen, H., and Li, C. (2019). Plant-plant interactions and resource dynamics of *Abies fabri* and *Picea brachytyla* as affected by phosphorus fertilization. *Environ. Exp. Bot*. 168:103893. doi: 10.1016/j.envexpbot.2019.103893

Yu, X., Wang, W., and Yang, M. (2007). Antioxidant activities of compounds isolated from Dalbergia odorifera T. Chen and their inhibition effects on the decrease of glutathione level of rat lens induced by UV irradiation. *Food Chem*. 104, 715–720. doi: 10.1016/j.foodchem.2006.10.081

Zhang, S., Shao, L., Sun, Z., Huang, Y., and Liu, N. (2019). An atmospheric pollutant (inorganic nitrogen) alters the response of evergreen broad-leaved tree species to extreme drought. *Ecotox. Environ. Safe*. 187:109750. doi: 10.1016/j.ecoenv.2019.109750

Zhang, W., Wang, B. J., Gan, Y. W., Duan, Z. P., Hao, X. D., Xu, W. L., et al. (2016b). Competitive interaction in a jujube tree/wheat agroforestry system in northwest China's Xinjiang province. *Agroforest. Syst*. 91: 881–893. doi: 10.1007/s10457-016-9962-7

Zhang, Y., Han, Q., Guo, Q., and Zhang, S. (2016a). Physiological and proteomic analysis reveals the different responses of *Cunninghamia lanceolata* seedlings to nitrogen and phosphorus additions. *J. Proteomics* 146, 109–121. doi: 10.1016/j.jprot.2016.07.001

Zrenner, R., and Stitt, M. (1991). Comparison of the effect of rapidly and gradually developing water-stress on carbohydrate metabolism in spinach leaves. *Plant Cell Environ*. 14, 939–946. doi: 10.1111/j.1365-3040.1991.tb00963.x

Zuppinger-Dingley, D., Schmid, B., Petermann, J. S., Yadav, V., De Deyn, G. B., and Flynn, D. F. (2014). Selection for niche differentiation in plant communities increases biodiversity effects. *Nature* 515, 108–111. doi: 10.1038/nature13869

Conflict of Interest: The authors declare that the research was conducted in the absence of any commercial or financial relationships that could be construed as a potential conflict of interest.

Advantages of publishing in Frontiers

OPEN ACCESS
Articles are free to read for greatest visibility and readership

FAST PUBLICATION
Around 90 days from submission to decision

HIGH QUALITY PEER-REVIEW
Rigorous, collaborative, and constructive peer-review

TRANSPARENT PEER-REVIEW
Editors and reviewers acknowledged by name on published articles

Frontiers
Avenue du Tribunal-Fédéral 34
1005 Lausanne | Switzerland

Visit us: www.frontiersin.org
Contact us: frontiersin.org/about/contact

REPRODUCIBILITY OF RESEARCH
Support open data and methods to enhance research reproducibility

DIGITAL PUBLISHING
Articles designed for optimal readership across devices

FOLLOW US
@frontiersin

IMPACT METRICS
Advanced article metrics track visibility across digital media

EXTENSIVE PROMOTION
Marketing and promotion of impactful research

LOOP RESEARCH NETWORK
Our network increases your article's readership